



MALLA REDDY ENGINEERING COLLEGE

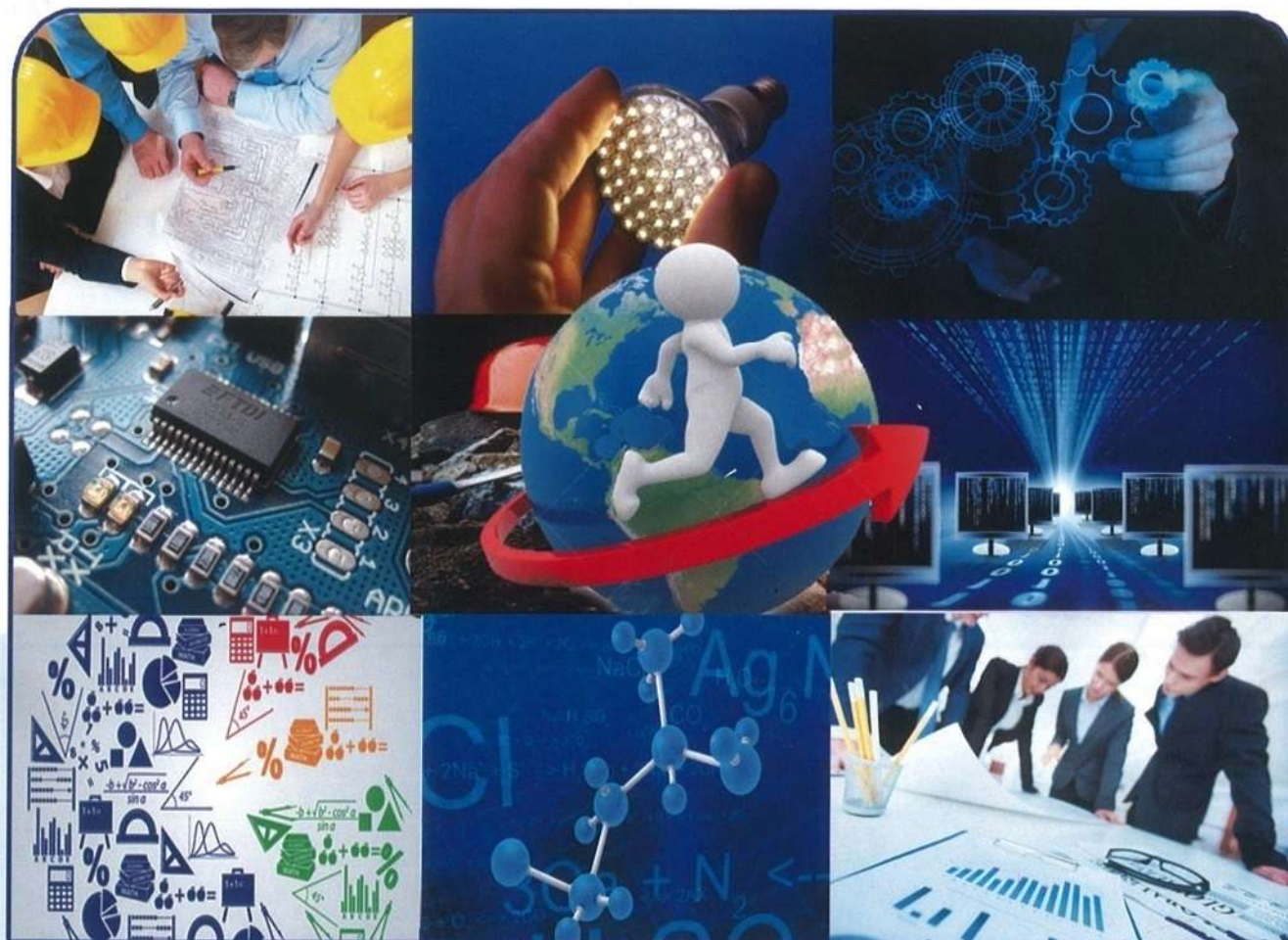
(AUTONOMOUS)

Estd: 2002

(An UGC Autonomous Institute, Approved by AICTE and Affiliated to JNTUH Hyderabad,
Accredited by NBA & NAAC with 'A' Grade and Recipient of World Bank Assistance under TEQIP Phase - II, S.C 1.1)
Maisammaguda, Dhulapally, Secunderabad, Telangana, India - 500 100. Website: www.mrec.ac.in



**Recognised under section 2(f) and
12(B) of UGC Act 1956**



RESEARCH PUBLICATION IN CONFERENCE

Compilation of Research Papers Contributed by Faculty Members of MREC

A.Y. 2016-17



Malla Reddy Engineering College

(AUTONOMOUS)

(An UGC Autonomous Institution Approved by AICTE and Affiliated to JNTU Hyderabad. Accredited by NAAC with 'A' Grade (II - Cycle))

Sri. Ch. Malla Reddy

Founder Chairman, MRGI

Hon'ble MP, Malkajgiri



MESSAGE

It gives me immense pleasure to pen a few words as prologue to our in-house magazine "Research Publications in MREC" with a collection of research papers contributed by the faculty members of our organization.

I believe this will flourish to become very useful source for the researchers, academicians and students who want to further improve their research profile and contribute to the arena of knowledge based wisdom. I hope this magazine will create interest and enhance inspiration of the readers to carry out new research ventures.

I extend my best wishes to bring more challenging research works which is useful to the society from the teaching fraternity with a sense of commitment in the future years to come.

C. H. Malla Reddy
Sri. Ch. Malla Reddy

Maisammaguda, Dhulapally (Post Via Kompally), Secunderabad - 500 100.
Phone: 040-65864982, 65918418, Fax: 040-23792153

Email: principal@mrec.ac.in
www.mrec.ac.in



Malla Reddy Engineering College

(AUTONOMOUS)

(An UGC Autonomous Institution Approved by AICTE and Affiliated to JNTU Hyderabad. Accredited by NAAC with 'A' Grade (II - Cycle))

Sri. Ch. Mahender Reddy
Secretary, MRGI



MESSAGE

I am pleased to know that MREC(A) is bringing out a magazine "Research Publications in MREC" which embrace the research contribution of faculty members of MREC. It is the outcome of our enthusiastic, dedicated and committed faculty members.

I take the pleasure to thank the Principal for providing continuous support and encouragement to the faculty members to publish their papers in Conferences and Journals.

I extend my heartfelt wishes for all to succeed in future endeavors.

Sri. Ch. Mahender Reddy

Maisammaguda, Dhulapally (Post Via Kompally), Secunderabad - 500 100.
Phone: 040-65864982, 65918418, Fax: 040-23792153

Email: principal@mrec.ac.in
www.mrec.ac.in



Malla Reddy Engineering College

(AUTONOMOUS)

(An UGC Autonomous Institution Approved by AICTE and Affiliated to JNTU Hyderabad. Accredited by NAAC with 'A' Grade (II - Cycle))

Dr. S. Sudhakara Reddy

M.Tech, M.B.A., Ph.D., L.M.I.S.T.E.,

F.I.E., M.I.S.M.E

Principal



MESSAGE

It's my pleasure to know that our in-house magazine "Research Publications in MREC" is being brought out with a collection of research contributions by our faculty members. This collection will be an inspiration to upcoming researchers to set new aspirations in research. This edition is an evidence for comfortable environment provided by MREC(A) for teaching and research activities to the faculty members to improve their career.

I wish to express my heartfelt thanks to the Management for their support and encouragement. Also my sincere regards to the HOD's and faculty members for their continuous efforts and contribution in research fields.

I extend my heartfelt wishes for all to succeed in future endeavors.

Dr. S. Sudhakara Reddy

Principal

MALLA REDDY ENGINEERING COLLEGE

(Autonomous)

Faculty Publications in the academic year 2016-2017

S.No	Department	Conferences		International Journals	Total
		International	National		
1	Civil Engineering	09	15	43	67
2	Electrical and Electronics Engineering	Nil	28	16	44
3	Mechanical Engineering	Nil	Nil	22	22
4	Electronics and Communication Engineering	Nil	26	34	60
5	Computer Science and Engineering	01	23	18	42
6	Humanities & Sciences	Nil	02	05	07
TOTAL		10	94	138	242

JOURNALS

MALLA REDDY ENGINEERING COLLEGE(AUTONOMOUS)

Faculty published list of Journal Publications during the Academic year 2016-2017

S.No.	Names of the Authors	Deapartm ent	Title	Journal Name	Volume No	Issue No	Page No's	Year
1	V.Ranjith Kumar and M. Kameswara Rao	Civil	Experimental behaviour of carbon fiber in dense bituminous macadam	International Journal For Technological Research In Engineering	3	6	1212-1216	2016
2	A.Naga Sai Baba and M.Kameswara Rao	Civil	Delay modeling at urban uncontrolled intersection	International Journal of Advance Engineering and Research Development	3	2	112-118	2016
3	M.Kameswara Rao	Civil	A study on permeability charecteristics of phosphogypsum based concrete	IJSER	6	4	116-124	2016
4	M. Kameswara Rao	Civil	Earthquake resistant design of a building using shear wall	IJSRD	4	3	1-9	2016
5	M. Kameswara Rao	Civil	Investigation of flexural strength of Fly Ash and Super Plasticizers Filled Binary Concrete Composites	IJSRST	2	2	49-55	2016
6	M. Kameswara Rao	Civil	Aging characteristics of Binary concrete filled with fly ash/plasticizers on compressive strength	IJSRST	2	1	119-125	2016
7	M. Kameswara Rao	Civil	Utilization of Fly Ash and Super Plasticizers Filled Binary Concrete on Split Tensile Strength	IJSRST	2	1	126-133	2016
8	A. Nagasaibaba , M. Kameswara Rao	Civil	Pedestrian Crossing Behaviour at Suchitra Junction on NH-44 using Discrete & Continuous Model	IJIRST	3	4	7-12	2016
9	A. Nagasaibaba , M. Kameswara Rao	Civil	To Develop A Correlation Between CBR And Dynamic Cone Penetration Value	International Journal For Technological Research In Engineering Volume	4	1	11-16	2016

S.No.	Names of the Authors	Deapartm ent	Title	Journal Name	Volume No	Issue No	Page No's	Year
10	V Ranjith Kumar, M.Kameswara Rao	Civil	Utilization Of Low Cbr Soil For Flexible Pavements For Low Volume Roads With Robo Sand Stabilization	International Journal For Technological Research In Engineering	4	1	1-5	2016
11	V Ranjith Kumar M.Kameswara Rao	Civil	Road Accident Severity Analysis In Cyberabad & Hyderabad Using Ordered Probit Model	International Journal For Technological Research In Engineering	4	1	6-10	2016
12	K. Vamshi Krishna , M. Kameswara Rao	Civil	Design Of Seismic Resistance Reinforced Concrete Structure On A Inclined Ground	IJSRD	4	7	1-6	2016
13	K. Vamshi Krishna , M. Kameswara Rao	Civil	A Comparative Study On Failure Modes Of Anchor Bolt And Mechanical Anchors As Per ACI And European Codes	IJSER	7	9	116-126	2016
14	B.Vamsi Krishna M.Kameswara Rao	Civil	A Study On Mechanical Properties Of Concrete With Addition Of Flyash And Nano-Silica Gel,	International Journal of Engineering Research and Development,	12	9	29-37	2016
15	R. Sumathi,M. Kameswara Rao	Civil	An Experimental Investigation On Self Compacting Concrete By Using L Box, J Ring, V Funnel Apparatus	IJSRD	4	7	16-26	2016
16	M. Kameswararao	Civil	Performance of Concrete Containing Granulated Blast Furnace Slag as a Fine Aggregate	Indian Journal of Science and Technology	9	38	1-5	2016
17	B Vijaybhasker, V Ranjith Kumar Dr.M.Kameswara Rao	Civil	Traffic accident severity analysis on NH-163 using Limdep model	International Journal For Technological Research in Engineering	4	2	392-398	2016
18	A.Naga Saibaba Dr.M.Kameswara Rao	Civil	Traffic calming in hyderabad and secunderabad city perspective	International Journal For Technological Research in Engineering	4	2	399-403	2016
19	Y. Venu, V. Ranjith Kumar Dr.M.Kameswara Rao	Civil	Road Safety Audit For Sagar Intersection To Uppal Intersection	International Journal For Technological Research in Engineering	4	2	404-408	2016
20	A.Naga Saibaba Dr.M.Kameswara Rao	Civil	Intelligent Transportation System In Hyderabad And Secunderabad Along Nh-44, Nh-65	International Journal For Technological Research in Engineering	4	2	409-413	2016

S.No.	Names of the Authors	Deapartm ent	Title	Journal Name	Volume No	Issue No	Page No's	Year
21	A.Naga Saibaba Dr.M.Kameswara Rao	Civil	Influence Of Combined Flakiness & Elongation Indices On Bituminous Mixes	International Journal For Technological Research in Engineering	4	2	414-418	2016
22	Ch.Dilip, V Ranjith Kumar Dr.M.Kameswara Rao	Civil	Road Accident Scenario In Cyberabad And Hyderabad	International Journal For Technological Research in Engineering	4	2	419-423	2016
23	V Ranjith Kumar Dr.M.Kameswara Rao	Civil	Study Of Non-Motorized Transport In Cyberabad And Hyderabad	International Journal For Technological Research in Engineering	4	3	424-428	2016
24	B.Sujay Diwakar, V. Ranjith Kumar Dr.M.Kameswara Rao	Civil	Development Of Delay Model At Median Openings Of Along Nh-44	International Journal For Technological Research in Engineering	4	3	429-433	2016
25	A.NagaSaibaba Dr.M.Kameswara Rao	Civil	Development Of Pavement Management System On Urban Road Network	International Journal For Technological Research in Engineering	4	3	434-438	2016
26	V Sampath Kumar, V. Ranjith Kumar Dr.M.Kameswara Rao	Civil	Preliminary Assessment Of Bus Rapid Transit System For Urban Roads	International Journal For Technological Research in Engineering	4	3	439-443	2016
27	B Arjun, A.Nagasaibaba Dr.M.Kameswara Rao	Civil	Estimation Of Level Of Service At Suchitra And Kukatpally Intersections	International Journal For Technological Research in Engineering	4	3	444-448	2016
28	Bhagawan. D, Saritha Poodari, Chaitanya narala, Ravi surya, Yamuna Rani. M, Vurimindi,Himabindu, S Vidyavathi,	Civil	Industrial solid waste landfill leachate treatment using Electrocoagulation and Biological methods	Desalination and Water Treatment	58	1	137-142	2017

S.No.	Names of the Authors	Deapartment	Title	Journal Name	Volume No	Issue No	Page No's	Year
29	Bhagawan. D, Saritha Poodari, ShankaraiahGolla, Vurimindi Himabindu, S Vidyavathi	Civil	Treatment of the petroleum refinery waste water using combined electrochemical methods	Desalination and Water Treatment	57	8	3387-3394.	2016
30	G. Shankaraiah, P. Saritha, D. Bhagawan, V. Himabindu, S. Vidyavathi	Civil	Degradation of Norfloxacin in aqueous solution using advanced oxidation processes (AOPs). A comparative study	Desalination and Water Treatment	57	12	27804-27815	2016
31	Bhagawan.D, Saritha Poodari, CH. Anand, Shankaraiah.G, V.Himabindu	Civil	Traffic noise level assessment in Rangareddy district, India,	International Journal of Applied Physics (IJAP)	6	1	33-41	2016
32	Bhagawan D, P Saritha, G Shankaraiah, M Elander, Himabindu.V	Civil	Remediation of Contaminated Ground water using sonication: Case study of an industrial area of Hyderabad,India	International Journal of Chemistry and Chemical Engineering	5	1	143-159	2016
33	S M Abdul Mannan Hussain	Civil	Scheduling Of An Residential Building Using Project Management Techniques	International Journal Of Advance Research In Science And Engineering (IJARSE)	6	3	27-33	2017
34	S M Abdul Mannan Hussain	Civil	Study Of Total Quality Management Practices In The Construction Industry	International Journal Of Science Technology And Management(IJSTM)	6	2	378-382	2017
35	S M Abdul Mannan Hussain	Civil	A Study Of Risk Management In The Construction Industry	International Journal Of Advance Research In Science And Engineering (IJARSE)	3	1	317-323	2017

S.No.	Names of the Authors	Deapartment	Title	Journal Name	Volume No	Issue No	Page No's	Year
36	S M Abdul Mannan Hussain	Civil	Importance Of Safety In Indian Construction	International Journal of Innovative Research in Science and Engineering(IJRSE)	2	12	38-45	2016
37	S M Abdul Mannan Hussain	Civil	Improving Construction Work Flow By Implementing Last Planner System On Construction Site	Journal Of Engineering And Applied Sciences	11	10	2209-2212	2016
38	S M Abdul Mannan Hussain	Civil	Barriers To Implement Lean Principles In The Indian Construction Industry	International Journal Of Innovative Research In Advanced Engineering (IJIRAE)	3	1	1-6	2016
39	Kosana Naga Sujatha	Civil	Assessment of Musi River Water and Nearby Ground Water: Impacts on Health of Down Stream Villages of Hyderabad	Indian Journal of Science and Technology	9	34	1-5	Sep-16
40	Kosana Naga Sujatha	Civil	A Statically Study Of Probable Future Water Demand of KOMPALLY	International Research Journal of Engineering and Technology (IRJET)	3	5	1907-1911	May-16
41	Kosana Naga Sujatha	Civil	Assessment of Soil Properties to Improve Water Holding Capacity in Soils”.	International Research Journal of Engineering and Technology (IRJET)	3	3	1777-1783	Mar-16
42	R.Prasanna Kumar	Civil	Corrosion Inhibition Using Water Hyacinth	International Journal Of Chemtech Research	9	5	558-562	2016
43	B Vamshi Krishna	Civil	Settlement Analysis of Piled Raft Foundation System (PRFS) in Soft Clay	IOSR Journal of Mechanical and Civil Engineering	14	2	62-68	2017
44	Gudipally Nithin Krishna Guptha1, K. Chetaswi	EEE	A MPC Integrated E-STATCOM with Adaptive Power Oscillation Damping	IJIT	4	7	1160-1164	June-2016.

S.No.	Names of the Authors	Deapartment	Title	Journal Name	Volume No	Issue No	Page No's	Year
45	T. Suman, Patlola Ramesh	EEE	Single-Phase UPS Inverters with Space Vector PWM Extended Lyapunov-Function Based Control Strategy	International Journal of Innovations Technologies	Vol.04	6	1045-1048	June-2016.
46	Bh Y Anusha, Ch. Narendra Kumar, Dr.M.Lakshmi Swarupa,	EEE	Solar Power Conditioning Systems Evaluation For Photovoltaic Source Simulator With Fast Response Time Related To Mppt	International Journal of Engineering and Computer communication Engineering	3	2	99-105	Mar-17
47	Aditya Bumanapalli, N.Rajeswaran, N.Venkateswaralu, Ch.Narendra Kumar	EEE	Design a Digital Fuel Indicator for Determine the Mileage of Engine	In ternational Journal of Engineering Trends and Technology (IJETT)	37	1	19-21	Jul-16
48	Kota Venkata Padma, Ch.Narendra Kumar	EEE	Analysis of the Performance of the Bidirectional Three-Level and Five Level DC–DC Converter	International Journal of Research	3	14	5105-5112	Oct-16
49	B.Sujatha, Ch.Narender Kumar	EEE	Asymmetrical Multilevel Inverter for Higher Output Voltage Levels	International Journal of Research	3	11	1385-1392	Jul-16
50	S.Divya, S.Sunanda	EEE	Controlling Microgrid System Using Renewable Energy Based Bidirectional PWM Technique with Wireless System and Administered By SCADA	International Research Journal of Engineering and Technology (IRJET)	3	6	2578-2583	Jun-16
51	G.Sumanth, V.Suma Deepthi	EEE	Solar Power Generation Seven Level To Nine Level Inverter	International Journal of Research	3	11	424-431	Jul-16
52	Venkata Ramesh Dongari, P.Ganesh	EEE	Fuzzy Controlled Multilevel Inverter Based MPPT Controlled PV for Grid-Connected Applications	International Journal of Advanced Research in Electrical, Electronics and Instrumentation Engineering	5	6	5466-5476	Jun-16
53	S Baburao, P Ganesh	EEE	Hybrid Fuzzy Control System for Power Control of Grid Connected PV System	In ternational Journal of Research	3	11	634-638	Jul-16

S.No.	Names of the Authors	Deapartment	Title	Journal Name	Volume No	Issue No	Page No's	Year
54	Sarath Baby, Ganesh Pashikanti	EEE	Power Factor Correction of Three Phase I.M Drive using PWM	International Journal of Scientific Engineering and Technology Research	5	51	10500-10504	Dec-17
55	G.Rahul, M.Lakshmi Swarupa,	EEE	An Ultra Capacitor Integrated Power Conditioner For Intermittency Smoothing And Improving Power Quality Of Distribution Grid With Fuzzy System	International Journal Of Global Innovations	5	1	220-224	Jul-16
56	Dr .M. Lakshmi Swarupa, Mr. D. Ramesh	EEE	Load Flow And Contingency Analysis Using Neplan Software	International Journal of Computers Electrical and Advanced Communication Engineering	1	9	126-134	Jul-16
57	Dr .M. Lakshmi Swarupa, Mr. D. Ramesh	EEE	Load Flow, Contingency Analysis, State Estimation And Optimal Operation For Ieee 14-Bus System	International Journal of Research Sciences and Advanced Engineering	2	15	247 - 253	Sep-16
58	T.Suman, K.Ramesh, Dr.M.Lakshmi Swarupa	EEE	Design of a Closed Loop Speed Control for BLDC Motor	International Journal of Advanced Research in Electrical, Electronics and Instrumentation Engineering	5	8	142-147	Nov-16
59	Mr. Desai Feroz, Mrs. M. Lakshmi Swarupa	EEE	A Novel Method of Dynamic Programming for the Adaptive Optimal Control of Nonlinear Systems	International Research Journal of Engineering and Technology	3	5	2282-2287	May-16
60	B. Akshay Kumar, A. Raveendra	Mechanical	Effect of Pulsed and Non-pulsed current on welding characteristics of AA6061 Aluminium alloy welded joints using Tig welding	International Journal of Engineering Research & Science (IJOER)	2	7	93-102	2016
61	Mr. Ch. Prahallad1 & Mr. A. Raveendra	Mechanical	Modeling and Optimization of Cushioning System in Hydraulic Cylinder to achieve Performance Characteristics	Imperial Journal of Interdisciplinary Research (IJIR)	3	1	2122-2128	2017
62	Mr.K prudhvi, Mrs Venkata Vara Lakshmi	Mechanical	Cryogenic Tool Treatment	Imperial Journal of Interdisciplinary Research (IJIR)	2	9	1204-1211	2016

S.No.	Names of the Authors	Deapartm ent	Title	Journal Name	Volume No	Issue No	Page No's	Year
63	J. Padmaja, A. Ravindra	Mechanical	Design and Analysis of a Heat Sink for a High Power LED System	International Journal of Engineering Research & Technology (IJERT)	4	7	975-982	2015
64	Pasula Raju, K. Bharadwaja	Mechanical	Performance Analysis Of I.C Engine Using Diesel And Ethanol Blends	Nternational Journal Of Professional Engineering Studies	6	4	79-85	2016
65	Udutha Raghupathi C.Chandra Sekhara	Mechanical	CFD Analysis of Emission Characteristics of 4-Stroke Single Cylinder SI Engine by Using Eucalyptus Oil and Gasoline Blend	International Journal & Magagine of Engineering ,Technology, Management and research	3	7	516-524	2016
66	K. Shiva Kumar1, A. Ramesh, S. S. Ch. Mouli	Mechanical	Design and Analysis of Composite Disk Brake	International Journal of Scientific Engineering & Technology Research	5	28	5717-5726	2016
67	M. Swamy, D. Suresh Reddy	Mechanical	Design and Analysis of Composite Alloy Wheel	International Journal of Scientific Engineering & Technology Research	5	28	5708-5716	2016
68	K.Aravind Babu K.Srinivasa Rao	Mechanical	Preparation and Testing of a Composite Plate Using Shrimp Shell Filler	International Journal & Magazine of Engineering, Technology, Management and Research	3	6	650-653	2016
69	Kethavath Rajesh , A. Ramesh	Mechanical	Design And Analysis Of Composite Drive Shaft	International Journal of Professional Engineering Studies	6	4	006-018	2016
70	P. Sandeep K.Srinivasa Rao	Mechanical	Preparation and Testing of Metal and Fiber Reinforced Polymer Laminates	International Journal & Magazine of Engineering, Technology, Management and Research	3	6	136-140	2016
71	P.Chandrasekhara Reddy K.Srinivasa Rao	Mechanical	Development and Experimental Characterization of Flexible Joint for Air Borne Propulsion System	International Journal & Magazine of Engineering, Technology, Management and Research	3	6	209-214	2016

S.No.	Names of the Authors	Deapartm ent	Title	Journal Name	Volume No	Issue No	Page No's	Year
72	B. Pavani M.V.Varalakshmi	Mechanical	Mold Flow Analysis on Fan Part using Plastic advisor	International Journal of Engineering Research & Science	2	7	103-108	2016
73	M. Abhinav V. Narasimha Reddy	Mechanical	Computational Investigation of the Effects of Leading-Edge Bluntness on Drag at Supersonic Speeds	International Journal of Engineering Research & Technology	5	6	230-235	2016
74	K. Nagarjuna Reddy N. Srinivasa Rajneesh	Mechanical	Comparative Design And Analysis Of Trinozzle With Convergent-Divergent Nozzle	International Journal of Professional Engineering Studies	6	4	60-69	2016
75	K Abhilash Korvi , A. Raveendra	Mechanical	Improving Productivity And Quality By Changing Feeding System In An Injection Moulding Process	Global Journal of Advanced Engineering Technologies	6	1	001-005	2017
76	Shaik Noor Ahamed, K.Rajesh	Mechanical	Comparing and Optimizing the Process Parameters of two types of AI-MMC's in Turning	International Research Journal of Engineering and Technology	3	8	662-669	2016
77	Ungarala Soma Sekhar , M V Vara Lakshmi	Mechanical	Experimental Investigation To Determine Influence Of Process Parameters On Surface Quality And MRR In Wire Cut Edm	International Journal of Mechanical And Production Engineering	4	12	001-003	2016
78	Venna Swathi , M.V. Varalaxmi	Mechanical	Design And Optimization Of Fixtures To Minimizing Manufacturing Failures Of Turbine Blade: A Finite Element Approach	Anveshana's International Journal of Research In Engineering and Applied Sciences	1	8	015-024	2016
79	K Vishnu Teja, N Srinivasa Rajneesh	Mechanical	Design And Analysis Of A PJ15 Pulse Jet Engine	International Journal of Professional Engineering Studies	6	4	070-078	2016
80	P. Venu Gopal, Shaik Hussain	Mechanical	CFD Simulation of Dual Fuel Natural Gas Based IC Engine Using Ansys ICE Package	International Journal & Magazine of Engineering, Technology, Management and Research	3	7	501-506	2016

S.No.	Names of the Authors	Deapartment	Title	Journal Name	Volume No	Issue No	Page No's	Year
81	Prakash kumar mandal, M V Varalakshmi	Mechanical	Comparisinal Simulational Analysis of Sheet Hydro Forming of a Mechanical Component (Automobile Door)	Imperial Journal of Interdisciplinary Research	2	9	980-984	2016
82	Ingilela Suahsini, K.Rajendra Prasad	ECE	New VLSI Architecture for FM0/Manchester Encoding using SOLS Technique using Wireless Sensor Network	Global Journal of Advanced Engineering Technologies, GJAETS	5	2	1-7	2016
83	Banoth Venkata Sai Kumar, G Prasanna Kumar	ECE	VLSI design of error detection and correction using orthogonal latin square codes	International Journal For Technological Research In Engineering, IJTRE	3	10	2816-2819	2016
84	Madderla Rahul, B. Sagar	ECE	Implementation of Crypto System Based on TEA Cryptography Application	International Journal of Innovative Technologies, Tirumala Publications	4	2	0318-0319	2016
85	V. Datta Kiran, DR. M. J. C. Prasad	ECE	Obstacle Detection in Textured Environment by using Color Coherence	International Journal of Innovative Technologies, Tirumala Publications	4	2	0286-0291	2016
86	Badugu Chaitanya, V.Srinivas	ECE	VLSI design of data encoding schemes for low power	International Journal For Technological Research In Engineering, IJTRE	3	6	1070-1073	2016
87	Varkolu Kiran Varma, A. R. S. Balaji	ECE	Implementation of an Efficient Image Denoising Algorithm on FPGA	International Journal of Scientific Engineering and Technology Research, Innovative Research Publications	5	16	3107-3109	2016
88	Lingam Rajesh, Santosh J	ECE	Design and Power Analysis of 8T SRAM Cell Using Charge Sharing Technique	International Journal o f Innovative Research in Electronics and Communications, Academicians' Research Center	3	1	20-26	2016
89	Balaji Bantupalli	ECE	Time Interleaved Parallel ADC with Efficient Decoder and Improved Sampling Switch	International Journal of Research Studies in Science, Engineering and Technology, IJRSET	3	2	1-7	2016

S.No.	Names of the Authors	Deapartment	Title	Journal Name	Volume No	Issue No	Page No's	Year
90	Amancha Varun Raj, V.Srinivas	ECE	Design and implementation of area efficient fm0/Manchester encoding architectures	International Journal For Technological Research In Engineering, IJTRE	3	7	1310-1314	2016
91	P.Vinod Kumar, K.S.Indrani	ECE	VLSI design of a novel presto with programmable PRPG	International Journal For Technological Research In Engineering, IJTRE	3	8	1610-1613	2016
92	Amtul Shakera, A.Rama Satya Balaji	ECE	Iterative cancellation of non-linear distortion noise in digital communication systems	International journal of electrical electronics and communication, IJEEC	21	7	4181-4191	2016
93	Althaf Pasha Mohammed, N. Pandu Ranga Reddy	ECE	Multi-stream transmission for highly frequency selective channels in mimo-fbmc/oqam systems	International journal of electrical electronics and communication, IJEEC	21	28	4622-4633	2016
94	Gudapati Venkata siva Tejasvi, Murali Krishna	ECE	Region based segmentation in presence of intensity inhomogeneity using legendre polynomials	International journal of electrical electronics and communication, IJEEC	21	28	D5021-D5025	2016
95	Sangepu Rajesh Kumar, Dr.S.Madhu Babu	ECE	Peak-to-average power ratio reduction for ofdm/oqam signals via alternative-signal method	International journal of electrical electronics and communication, IJEEC	21	28	4601 -4608	2016
96	Harith, Dr.M.J.C.Prasad	ECE	ARM Based Smart Cart and Automatic Billing System with Theft Detection	Journal of Computing Technologies, JCT.	5	6	47-51	2016
97	T. Ashwini, Ch. Bhanu Prakash	ECE	Travolution-An embedded system in passenger car for road safety	Journal of Computing Technologies, JCT.	5	8	1-5	2016
98	Bijo Abraham Mathew, Srinivas Vutkuri	ECE	A Raspberry Pi eHealth Smart Monitoring System	International Journal of Advanced Technology and Innovative Research, Semar Groups	8	14	2764-2767	2016
99	B.Vani, P.Ashok Babu	ECE	Implementation of Deep Representations for Iris, Face and Fingerprint Spoofing Detection Using Open Source Platform	International Journal & Magazine of Engineering, Technology, Management and Research, Yuva Engineers, India	3	10	207-214	2016

S.No.	Names of the Authors	Deapartment	Title	Journal Name	Volume No	Issue No	Page No's	Year
100	B. Shylaja, B. Srinivas	ECE	Design and implementation of agricultural automation through wireless Network and GPRS	International journal of professional engineering studies, ijpres	6	5	333-338	2016
101	Chakradhar Chegu, Dr. M.J.C.Prasad	ECE	A Remote Test Platform for Mobile Application	Journal of Computing Technologies, JCT	5	7	40-44	2016
102	CH.Durga Bhavani, M.Murali krishna	ECE	Mobile Environment for Industrial Automation	Journal of Computing Technologies, JCT	5	7	29-32	2016
103	G. Jakeer Hussain, T. Srinivas Reddy	ECE	Advanced Anti-Theft ATM Security using Raspberry Pi	International Research Journal of Engineering and Technology, Fast Track Publication	3	8	183-186	2016
104	Emmanuel Raju Gummadi, CH. Bhanu Prakash	ECE	Web server based efficient water management	International Journal of Science, Engineering and Technology Research, IJSETR	5	7	1-3	2016
105	N.Haritha, Dr.M.J.C.Prasad	ECE	ARM Based Smart Cart and Automatic Billing System with Theft Detection	Journal of Computing Technologies, JCT	5	6	47-51	2016
106	K.Swapna Priya, N.Raju	ECE	RFID- GSM- GPS Imparted School Bus Transportation Management System	International Journal of Research Studies in Science, Engineering and Technology, IJRSET	3	8	12-16	2016
107	Mamidi Dishalini, Mr.Kumaraswamy	ECE	Low Cost Real Time Monitoring Using Raspberrpi	Journal of Computing Technologies, JCT	5	8	13-15	2016
108	V. Mounika, T. Ravi Theja	ECE	Design and development of energy monitoring and automated control system using labview for energy conservation	International journal of professional engineering studies, ijpres	6	5	327-332	2016
109	R.Karan Kumar, Raju.N	ECE	PIBOT: Surveillance & Live Streaming System using Raspberry Pi	International Journal of Science, Engineering and Technology Research, IJSETR	5	8	2735 - 2738	2016

S.No.	Names of the Authors	Deapartment	Title	Journal Name	Volume No	Issue No	Page No's	Year
110	Shaik Mansoor Basha, T. Ravi Theja	ECE	Portable Camera-Based Assistive Text and Product Label Reading from Hand-Held Objects for Blind Persons	International Journal of Advanced Technology and Innovative Research, Semar Groups	8	16	3180-3182	2016
111	A. Srinivas, B. Srinivas	ECE	Camera Based Eye Pupil Controlled Wheelchair System using Raspberry Pi	International Journal of Advanced Technology and Innovative Research, Semar Groups	8	16	2312-2314	2016
112	P.Sai Kumar, Srinivas Bollineni	ECE	Tweeting PI an Household Computerization	International Journal of Advanced Technology and Innovative Research, Semar Groups	8	16	2590-2592	2016
113	K.Ramya	ECE	A Method of Detecting Abnormal Program Behavior on Embedded Devices	International Journal & Magazine of Engineering, Technology, Management and Research, Yuva Engineers, India	3	10	293-299	2016
114	Nekkanti Lakshmi Indira Rani, G.Barathi subhashini	ECE	Design of a JPEG Compressor with an Efficient and Reconfigurable DCT Algorithm	International Journal of Innovative Research in Science, Engineering and Technology, IJSETR	5	9	16624 - 16631	2016
115	S.Reshma, K.Rjendra Prasad	ECE	Area and Power Efficient Booth's Multipliers Based on Non Redundant Radix-4 Signed- Digit Encoding	International Journal of Innovative Research in Science, Engineering and Technology, IJSETR	5	9	16632 - 16639	2016
116	Dr. G. Charles Babu, Mr. K. Rajeshwar Rao	CSE	An Effective Routing for Managing of Critical Issues in Resource Constrained System	International Journal of Computational Intelligence Research	13	3	473-477	2017
117	Dr. G. Charles Babu, Mr. K. Rajeshwar Rao	CSE	Improvisation Of Performance In Cluster Networks	Global Journal Of Engineering Science And Research Management	3	8	87-89	2016

S.No.	Names of the Authors	Deapartment	Title	Journal Name	Volume No	Issue No	Page No's	Year
118	K.Rajeshwar Rao, Dr.G.Charles Babu	CSE	Decision Tree Clustering And Classification Based One-To-Many Data Linkage	International Journal Of Innovative Research In Computer And Communication Engineering	4	4	5278-5283	2016
119	Dr.K.Ratna Babu , Dr.G.Charles Babu	CSE	A Survey On Security Challenges In Cloud Computing	International Journal Of Innovative Research In Science, Engineering And Technology	5	5	7022-7028	2016
120	N.Grace Naomi, G.Charles Babu, Dr. Ch. Ramesh Babu	CSE	Cloud Environment Using Many Phrasal Words Concealment Preserving To Perform Safe Search	International Journal Of Innovative Technology And Research	4	4	3418 – 3420	2016
121	Kesireddy Radhika, G.Charles Babu	CSE	A Healthy Technique For Removing Redundant Copies Of Data	International Journal Of Reviews On Recent Electronics And Computer Science	4	8	5843-5847	2016
122	Dr. Ram Kumar R. P., Ms. Hima Sampathrao, Mr. Vijay Kumar Burugari, Mr.Sanjeeva Polepaka	CSE	Applications Domains Of Internet Of Things: A Survey	International Journal Of Engineering Technology Science And Research	3	10	54-59	2016
123	M.Swami Das, A.Govardhan, D.Vijaya Lakshmi	CSE	Qos Web Service Security Dynamic Intruder Detection System For Http Ssl Services	International Journal Of Computer Science And Information Security	14	1	55-60	2016
124	Ms. Bhagyashri, M. Swami Das	CSE	Multi-Annotator Approach To Automatically Build Theannotation Wrapper	Journal Of Research In Science, Technology, Engineering And Management (Jorstem)	2	4	84-88	2016
125	B. Divya Keerthi, Sanjeeva Polepaka	CSE	Improving Performance In Parallel And Independent Access To Encrypted Cloud Databases	International Journal Of Professional Engineering Studies	6	3	125-129	2016
126	T. Madhukar Reddy, P. Sanjeeva	CSE	Hmac-Sha-1&Proof Of Ownership Protocol On Cloud Data Storage	International Journal Of Research	4	1	144-150	2017

S.No.	Names of the Authors	Deapartment	Title	Journal Name	Volume No	Issue No	Page No's	Year
127	Satrajupalli Naga Lakshmi, Sanjeeva Polepaka	CSE	Unreliable Portrait Information Screening With Contrast Enhancement	International Journal Of Computer Science Information And Engg., Technologies	2	6	001-005	2016
128	Mr. Deverneni Sagar Rao, Mr.B.Vijay Kumar	CSE	Content Caching And Scheduling In Wireless Networks With Elastic And Inelastic Traffic	International Journal Of Innovative Technology And Research	5	1	5492-5494.	2017
129	Tunikapati Kiran Kumar, Mr.B.Vijay Kumar	CSE	Guarantee End-User Routine While Contents Are Gathered From Numerous Facts Hub	International Journal Of Innovative Technology And Research	4	6	5266-5268	2016
130	S.Sandhya Rani, Dr.G.Apparao Naidu, Dr.V. Ushashree	CSE	Survey On Attacks And Security Issues In Mobile Ad Hoc Networks	International Journal Of Computer Science Information And Engg., Technologies	1	6	0001-0008	2016
131	A. Karthik, K. Vijay Krupa Vatsal	CSE	Investigating Of Social Server Scalability Organizing In Mobile Presence Service Applications	International Journal For Research On Electronics And Computer Science	5	3	4543-4549	2016
132	Y.Rokesh, K.Vijay Krupa Vatsal	CSE	A Proposal Towards Effective Image Recovery In Data Hiding Schemes	International Journal Of Innovative Research In Science,	5	10	18091-18093	2016
133	Mr. P.Venkateshwar Rao, Mr. G.Vamshi Krishna, Mr. Y. Rokesh Kumar	CSE	A Novel Technique For Secure Encrypted Messages In Mobile And Pervasive Applications	International Journal Of Engineering Sciences & Research Technology	5	7	1142-1146	2016
134	P Kalyan Kumar & Dr. Shahnaz Bathul	H&S	Creeping flow from Circular Orifice in a Plane wall	International Journal of Mathematical Archive	7	12	49-52	2016
135	Nasreen Begum	H&S	Sweep of Sweet Moments	IJELLH	4	10	475-478	2016

S.No.	Names of the Authors	Deapartment	Title	Journal Name	Volume No	Issue No	Page No's	Year
136	Mopur Vijaya Bhaskar Reddy, Ping-Chung Kuo, Hsin-Yi Hung, Wei-Jern Tsai, and Tian-Shung Wu	H&S	Synthesis and characterization of 3-arylidenechroman-4-ones and their inhibitory effects on platelet aggregation activity	Scholars Research Library	8	20	14-20	2016
137	Mopur Vijaya Bhaskar Reddy , Hsin-Yi Hung	H&S	Synthesis and biological evaluation of chalcone, dihydrochalcone, and 1,3-diarylpropane analogs as anti-inflammatory agents	Elsevier	1	1	1-4	2017
138	Mopur Vijaya Bhaskar Reddy, Tsong-Long Hwang, Tian-Shung Wu	H&S	Inhibitory effects of Bichalcone derivatives on Superoxide anion generation ($O_2^{\bullet-}$) and elastase release by activated human neutrophils in response to FMLP/CB	Scholars Research Library	8	20	172-176	2016

**Department of
Civil Engineering**

EXPERIMENTAL BEHAVIOUR OF CARBON FIBER IN DENSE BITUMINOUS MACADAM

B.Rakesh Kumar¹, V.Ranjith Kumar², M.Kameswara Rao³

¹Research Scholar (M.Tech, T.E), ²Assistant Professor, ³Professor
Malla Reddy Engineering College, (Autonomous) Kompally

Abstract: *In this paper, a brief practical review is presented on the the pavement which is compacted with the conventional compaction has been further compacted due to the movement of traffic and which corresponds to the ultimate density which can be attained on the bituminous pavement called as "Refusal density" of the pavement. Addition of polymers is a common method applied for binder modification, although various types of fibers have also been evaluated. It is widely believed that the addition of fibers to asphalt enhances material strength aswellas fatigue characteristics while at the same time adding ductility. Likewise, carbon fibers may also offer excellent potential for binder modification due to their inherent compatibility with asphalt cement and superior mechanical properties. Secondary compaction has to be studied in detail and it is understood that the 75 blows of the Marshall test does not determine the actual field circumstances. The Marshall design actually in the field will not simulate the field conditions hence there will be a reduction in the air voids at the refusal density. Then due to fineness of the mix, this causes the plastic deformation on the pavement surfaces. Hence an attempt has been made to study the air void content at refusal density. Also the Bulk Density, Air voids (Va), Voids in mineral aggregate (VMA), Voids filled with Bitumen (VFB) of the mix at the refusal density are also studied. For the simulation of the field density in the laboratory a Hugo hammer is used. The usage of the Polymer Modified Bitumen reduces the plastic deformation and other distresses of the pavement.*

Keywords: Road network, urban areas, Gis,Conectivity, behavioral model.

I. INTRODUCTION

During the last decades, there has been a rapid increase in traffic volumes, axle loads and tyre pressure of commercial vehicles on highways. This rapid growth leads to a substantial increment in stresses on to the road surface and has resulted in early failure of asphalt pavements much before their expected design life. In order to improve the performance of the asphalt mixes two solutions are available; firstly, increasing the thickness of asphalt layer which will increase the cost of construction and, secondly making a modified asphalt mixture with the help of additives without increasing the thickness of asphalt layer. At present, there are two research orientations to improve pavement performance of asphalt mixture: one is to better asphalt non-deformability at high temperature, via improving aggregate gradation, which is based on asphalt structure type and design

procedures; the other is to better asphalt mechanical performance & permanent deformation resistance, and decrease temperature susceptibility, via improving asphalt property and quality. For the past few years, more and more new materials are put into the technology field of bituminous pavement. Thus, the third orientation to improve its performance is formed, that is to add fibers to asphalt, as a specific kind of additives, to holistically better its physical mechanical property. At the moment, there are mainly three types of fibers applied in pavement project: cellulose fiber, polyester fiber and mineral fiber. Addition of polymers is a common method applied for binder modification, although various types of fibers have also been evaluated. It is widely believed that the addition of fibers to asphalt enhances material strength aswellas fatigue characteristics while at the same time adding ductility. Likewise, carbon fibers may also offer excellent potential for binder modification due to their inherent compatibility with asphalt cement and superior mechanical properties. With new developments inproduction, carbon modified binder has become cost competitive with polymer modified binders. Further, it was expected that carbon fiber- modified asphalt mixtures would increase stiffness and resistance to permanent deformation and, similarly, that the fatigue characteristics of the mixture would improve with the addition of discrete carbon fibers. Because of the high tensile strength of carbon fibers, cold temperature behaviour of asphalt mixtures was also expected to improve. Finally, carbon fiber modified asphalt could produce a higher quality asphalt mixture for pavements.

II. NEED FOR PRESENT STUDY

Generally we use several kinds of modifications to the bituminous pavements in order to increase the strength and durability of Hot Mix Asphalt. Fibers have been extensively used to increase rheological properties of engineering materials for a long times. The effect of Carbon fiber on asphalt binder investigated in this study. In this paper we are going to see how carbon polymer fibers will show impact on asphalt mixture, fiber improving asphalt behaviour. A previous research paper conveys that by addition or modification of Asphalt mix increases the strength, durability and resistance towards creep, fatigue & rutting condition. In this investigation we are concentrating about the amount of fiber that is added to the bituminous mix design and which will give the optimum fiber content and as a outcome expecting an increase in strength. Dense bituminous concrete Mix is used in our investigation. Fiber content varies between (0.5% - 2.5%). In the present study 60/70

penetration grade bitumen is used as binder.

The whole work is carried out in different stages which are explained below.

- Study on Marshall Properties of DBM mixes using hydrated lime as filler and different percentages of Bitumen content to determine Optimum Bitumen Content.
- Study on Marshall Properties of DBM mixes with different percentages of CARBON fiber added to the weight of the binder in Dry Process.

III. OBJECTIVE AND SCOPE OF THE STUDY

Asphaltic/Bituminous concrete consists of a mixture of aggregates continuously graded from maximum size, typically less than 25 mm, through the fine filler that is smaller than 0.075 mm. Sufficient bitumen is added to the mix so that the compacted mix is effectively impervious and will have acceptable dissipative and elastic properties. The bituminous mix design aims to determine the proportion of bitumen, filler, fine aggregates, and coarse aggregates to produce a mix which is workable, strong, durable and economical. The objective of the mix design is to produce a bituminous mix by proportioning various components so as to have-

1. Sufficient bitumen to ensure a durable pavement
2. Sufficient strength to resist shear deformation under traffic at higher temperature
3. Sufficient air voids in the compacted bitumen to allow for additional compaction by traffic
4. Sufficient workability to permit easy placement without segregation
5. Sufficient resistance to avoid premature cracking due to repeated bending by traffic
6. Sufficient resistance at low temperature to prevent shrinkage cracks

IV. LITERATURE REVIEW

M. AREN CLEVEN (2013) investigated the properties of Carbon Fiber Modified Asphalt Mixtures. Preliminary study used to determine the feasibility of modifying the behaviour of a standard AC mixture through the use of pitch-based carbon fibers. This study focused strictly on the ability of mixing and compacting mixtures made with CFMA to achieve statistically significant improvements in the mechanical properties of the mixture. Carbon fiber modified asphalt mixtures were expected to show increased stiffness and resistance to permanent deformation. Fatigue characteristics of the mixture were expected to improve with the addition of discrete carbon fibers, and because of the high tensile strength of carbon fibers, the cold temperature behaviour of CFMA mixtures was anticipated to improve as well. Carbon fiber modified asphalt was expected to produce a higher quality AC mixture for pavement applications. The addition of carbon fibers improves the high temperature behaviour of the asphalt binder. If the test temperature does not reach the upper binder grade temperature, the effects of the fibers may be masked by binder behaviour. The low temperature behaviour of CFMA mixtures may be dominated

by the binder until it begins to fail, at which time the fibers dominate the behaviour.

Fereidoon Moghadas Nejad, Morteza Vadood & Seeyamak Baeetabar (2013) It is realised that the well-distributed fibers create a network in the internal structure of the composite, resulting in asphalt concrete that is more tightened. In the present paper, an approach was developed to mix carbon fibers and bitumen which guarantees the uniform fiber distribution. Subsequently, to find out the best set of fiber lengths and dose of usage aimed at fortifying asphalt concrete, Marshall's stability and fatigue property of carbon fiber-reinforced asphalt concrete were investigated. Then, indirect tensile stiffness modulus and fatigue properties under different stresses and permanent deformation of modified and unmodified samples at two different temperatures (35°C and 60°C) were studied. To find out the best set of fibre lengths and dose of usage aimed at fortifying asphalt concrete, Marshall's stability and fatigue property of carbon fibre-reinforced asphalt concrete were investigated. Then, indirect tensile stiffness modulus and fatigue properties under different stresses and permanent deformation of modified and unmodified samples at two different temperatures (35°C and 60°C) were studied. Comparing the obtained results indicated that addition of carbon fibres to the asphalt concrete considerably increases the mechanical performance, which benefits all the corresponding fields involved such as repair and maintenance. Based on the investigation, the addition of fibres to asphalt improves the mechanical properties such as strength, fatigue characteristics, Marshall Stability and electrical conductivity. But fibre properties such as length, distribution and content have a great impact on the performance of asphalt. There are hypotheses and limitations in this area, one of which is to use fibres of high flexibility and remarkable thermal resistance against mixing time with high temperature. The main aim of this research is to find the best fibre length and content for reinforcing asphalt concrete. The evaluation of permanent deformation at different temperatures as well as fatigue properties of asphalt concrete modified with optimum values of fibre length and content is another important objective of this research. Fibres are distributed in all directions in the mixture so as to prevent the production and expansion of cracks due to various reasons whether due to tensile stress induced by applied loads or thermal stresses. To this end, carbon fibres with three levels of length and content were selected.

Rebecca Lynn Fitzgerald (2000) researched on the novel application of carbon fiber for hot mix asphalt reinforcement and carbon-carbon pre-forms. The purpose of the research described in this thesis is to explore two new applications for carbon fibers. The first application involves the addition of carbon fiber to asphalt. Preliminary research indicates that carbon fiber modified asphalt may have beneficial properties ranging from improved mechanical properties to reduced electrical resistance. The enhanced mechanical properties should result in longer lasting, more durable pavements. In

addition, carbon fibers are electrically conductive. As an additive to asphalt, they can reduce the electrical resistivity, which may have applications in asphalt stress testing, structural vibration sensing, and eating roads to melt ice and snow. The fibers studied were 2.54cm cut mesophase pitch-based fibers and rolled 5.08cm-7.62cm mesophase pitch-based fibers in random matform. Two different encapsulation methods were investigated: asphalt/water emulsion/carbon fiber and LDPE/carbon fiber.

V. EXPERIMENTAL INVESTIGATIONS

A. Tests on materials used Binder

Here 60/70 penetration grade bitumen is used as binder for preparation of Mix, whose specific gravity was 1.023. Its important properties are given:

Rutting Prevention

In order to resist rutting, an asphalt binder should be stiff (it should not deform too much) and it should be elastic (it should be able to return to its original shape after load deformation). Therefore, the complex shear modulus elastic portion, $G^*/\sin\delta$, should be large. When rutting is of greatest concern (during an HMA pavement's early and mid-life), a minimum value for the elastic component of the complex shear modulus is specified. Intuitively, the higher the G^* value, the stiffer the asphalt binder is (able to resist deformation), and the lower the δ value, the greater the elastic portion of G^* is (able to recover its original shape after being deformed by a load).

Fatigue Cracking Prevention

In order to resist fatigue cracking, an asphalt binder should be elastic (able to dissipate energy by rebounding and not cracking) but not too stiff (excessively stiff substances will crack rather than deform-then-rebound). Therefore, the complex shear modulus viscous portion, $G^*\sin\delta$, should be a minimum. When fatigue cracking is of greatest concern (late in an HMA pavement's life), a maximum value for the viscous component of the complex shear modulus is specified.

Property	Test Method	Value
Penetration at 25°C (mm)	IS : 1203 – 1978	67.7
Softening Point (°C)	IS : 1203 – 1978	48.5
Specific gravity	IS : 1203 – 1978	1.03

Table 5.1 Properties of Binder

Specific gravity and water absorption tests on aggregates
These two tests are conducted

- To measure the strength or quality of the material
- To determine the water absorption of aggregates

The specific gravity of an aggregate is considered to be a measure of strength or quality of the material. Stones having low specific gravity are generally weaker than those with higher specific gravity values.

The size of the aggregate and whether it has been artificially

heated should be indicated. ISI specifies three methods of testing for the determination of the specific gravity of aggregates, according to the size of the aggregates. The three size ranges used are aggregates larger than 10 mm, 40 mm and smaller than 10 mm. The specific gravity of aggregates normally used in road construction ranges from about 2.5 to 3.0 with an average of about 2.68. Though high specific gravity is considered as an indication of high strength, it is not possible to judge the suitability of a sample road aggregate without finding the mechanical properties such as aggregate crushing, impact and abrasion values. Water absorption shall not be more than 0.6 per unit by weight.

Property	Test Method	Test Result
Aggregate Impact Value (%)	IS : 2386 (P IV)	14.3
Aggregate Crushing Value (%)	IS : 2386 (P IV)	13.02
Flakiness Index (%)	IS : 2386 (P IV)	18.03
Elongation Index (%)	IS : 2386 (P I)	21.5
Water Absorption (%)	IS : 2386 (P III)	0.1

Table 5.2 Physical properties of coarse aggregate

VI. ANALYSES OF TEST RESULTS AND DISCUSSIONS

Based on volume considered in evaluating specific gravity of an aggregate, some definitions of specific gravity are proposed. As per Das A. and Chakroborty P. (2010); the definitions and other formulae used in calculations hereafter are as follows:

Theoretical Maximum Specific Gravity

Loose DBM mixtures were prepared to determine their theoretical maximum specific gravity (G_{mm}) values. Test was conducted as per ASTM D 2041.

- The SMA mixture was prepared using oven-dry aggregates, and placed in a pan and the particles of mix were separated by hand, taking care to avoid fracturing the aggregate, so that the fine aggregate portion were not larger than about 6 mm. The sample was cooled to room temperature.
- The sample was placed directly into a cylindrical container and net mass (mass of sample only) weighed and was designated as A.
- Sufficient water was added at a temperature of approximately 25°C to cover the sample completely. The cover was placed on the container.
- The container was placed with the sample and water, and agitation was started immediately to remove entrapped air by gradually increasing the vacuum pressure (by vacuum pump) for 2 min until the residual pressure manometer read $3.7 \pm 0.3\text{kPa}$, vacuum and agitation was continued for 15 ± 2 min.
- The vacuum pressure was gradually released using the bleeder valve and the weighing in water was done. For determining the weight in water, the container and contents were suspended in water for

10 ± 1 min, and then the mass was determined. The mass of the container and sample under water was designated as C.

Specific Gravity of Aggregates

SIZE	BULK SP. Gravity (G _{sb})	Apparent Specific gravity (G _{sa})	Water Absorption (%)
40MM	2.656	2.664	0.1
20MM	2.654	2.661	0.1
10MM	2.656	2.663	0.1

Marshall Stability

It is observed that stability value increases with increase in binder content up to certain binder content; then stability value decreases. Variation of Marshall Stability value with different binder content with different filler is given fig 5.1

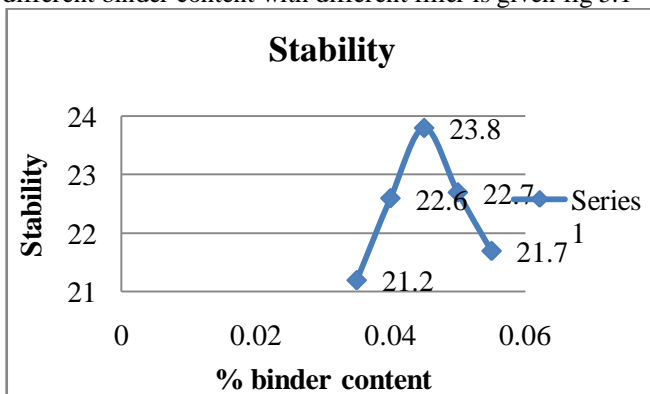


Fig 6.1 Variation of Marshall Stability of BC with different binder content

Flow Value

It is observed that with increase binder content flow value increases. For BC flow value should be within 2 to 4 mm. Variation of flow value with different binder content of BC with different filler is shown in fig 5.2

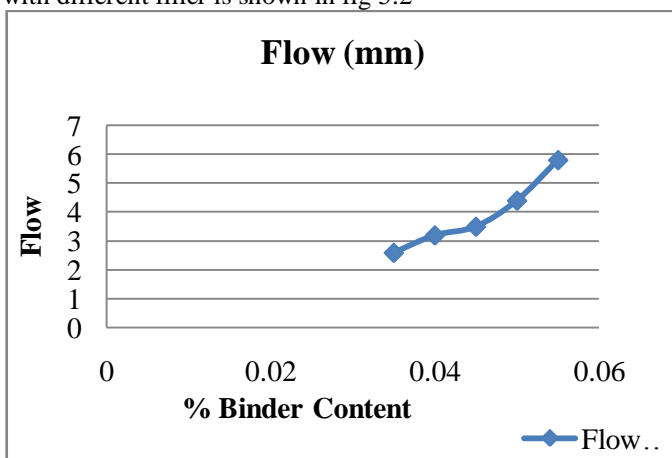


Fig 6.2 Variation of Flow Value of BC with different binder content

Unit weight

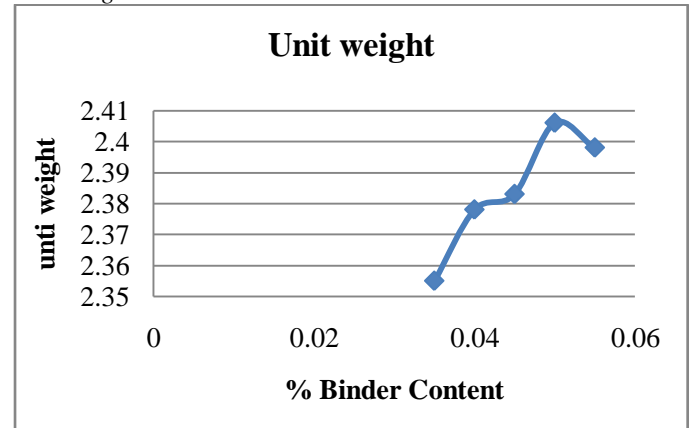


Fig 6.3 Variation of unit weight Value of BC with different binder content

Air Voids (Va) %

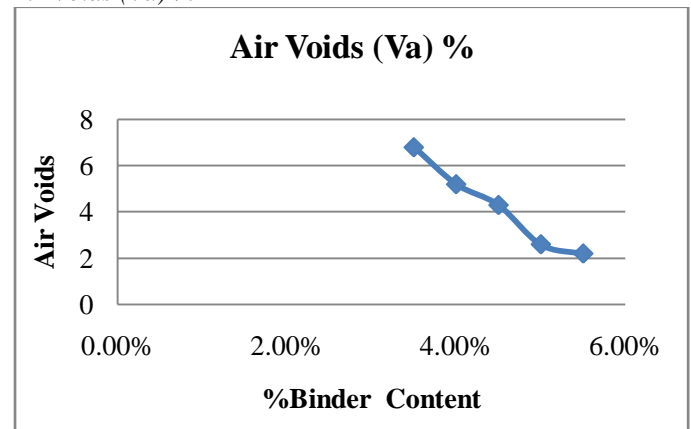


Fig 6.4 Variation of air void of BC with different binder content

VMA (%)

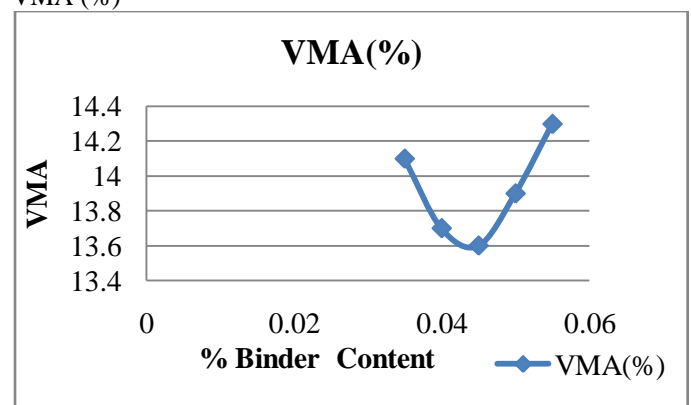


Fig 6.5 Variation of VMA of BC with different binder content

It is observed that stability value increases with increase fiber content and further addition of fiber it decreases. Variation of Marshall Stability value with different fiber content

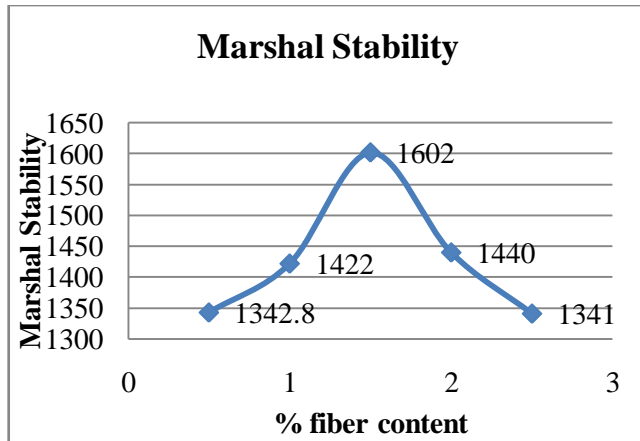


Fig 6.6 Variation of Marshall Stability of DBM With different fiber content

VII. CONCLUSIONS

Based on the results and discussions of experimental investigations carried out on different DBM mixes the following conclusions are drawn.

Marshall Stability

It is observed that with increase in binder content the Marshall Stability value increases upto certain binder content value and then decreases, like conventional bituminous mixes. Highest stability value achieved at 1.5% of fiber modified bituminous mix.

Flow value

The value of flow increases with increasing in fiber content, to bitumen content of 4.5%. The maximum flow value obtained at 2.5% of fiber content.

Unit Weight

The unit weight increases with the increase in binder content upto a certain binder content and their after decreases. The maximum Unit weight is for 2% of fiber modified bituminous mix.

Air voids

The amount of air voids decreases with increase in binder content in the mix. It also increases or decreases depending on the fiber content in the mix. The mix is observed to have the lowest air voids content in the higher fiber mix. Highest air voids have obtained at 2.5% of fiber modified mix.

Optimum Bitumen Content

The optimum bitumen (OBC) of DBM mix based on the marshal test results since, all Marshall Parameters are satisfying the requirement of MoRTH specifications, and the Optimum Binder Content is fixed as 4.5%.

Optimum fiber content

The optimum fiber content is based on the marshal stability test itself which gives the 1.5% of Carbon modified bituminous mix gives the highest stability strength .Anything

above the optimum fiber content, the mix behaved like a less viscous material.

REFERENCES

- [1] Anderson, D.A., and Goetz, W.H. (1973), "Mechanical Behaviour and Reinforcement of Mineral Filler-Asphalt Mixtures", Proceedings of Association of Asphalt Paving Technologists, Volume 42, No. 1, pp. 37-66, USA.
- [2] ASTM D 1559 (1989), "Test Method for Resistance of Plastic Flow of Bituminous Mixtures Using Marshall Apparatus".
- [3] Das A. and Chakroborty P. (2003), "Principles of Transportation Engineering", Prentice Hall of India, New Delhi, pp 294-299.
- [4] IS: 2386 (1963), "Methods of Test for Aggregates for Concrete (P - I): Particle Size and Shape", Bureau of Indian Standards, New Delhi.
- [5] IS: 2386 (1963), "Methods of Test for Aggregates for Concrete (P-III): Specific Gravity, Density, Voids, Absorption, Bulking", Bureau of Indian Standards, New Delhi.
- [6] IS: 1203 (1978), "Methods for Testing Tar and Bituminous Materials: Determination of Penetration", Bureau of Indian Standards, New Delhi.
- [7] IS: 1205 (1978), "Methods for Testing Tar and Bituminous Materials: Determination of Softening Point", Bureau of Indian Standards, New Delhi.
- [8] Ministry of Road Transport and Highways (2001), Manual for Construction and Supervision of Bituminous Works, New Delhi.
- [9] Mix Design Methods for Asphalt Concrete and Other Hot- Mix Types, Asphalt Institute Manual Series NO.2 (MS-2),
- [10] S.K. Khanna and C.E.G Justo "Highway Engineering" 2008.
- [11] Marshall Procedures for Design and Quality Control of Asphalt Mixtures. Asphalt Paving Technology: Proceedings vol. 54. Association of Asphalt Paving Technologists Technical Sessions, 11-13 February 1985. San Antonio, TX. pp. 265-284.
- [12] Goodrich J.L., (1998) "Bitumen and polymer modified Bitumen properties related to the performance of Bitumen concrete mixes", Journal of the Association of Bitumen Pavement Technologists, Volume 57, pp.116-160.
- [13] Xu Q, Chen H, Prozzi JA (2010). Performance of fiber reinforced asphalt concrete under environmental temperature and water effects. J. Constr Build Mater. 24(10): 2003-2010.

**DELAY MODELLING AT URBAN UNCONTROLLED INTERSECTIONS**D.Praveen¹, A.Naga Sai Baba², M.Kameswara Rao³¹Research Scholar (M.Tech, T.E), Malla Reddy Engineering College, (Autonomous) Kompally²Assistant professor, Malla Reddy Engineering College, (Autonomous) Kompally³Professor, Malla Reddy Engineering College, (Autonomous) Kompally

Abstract : Modelling traffic flow through urban uncontrolled intersections in developing countries like India is a complex process because of the high level heterogeneity of traffic and absence of major and minor concepts in traffic regulation schemes. Moreover, Indian codes have not been provided any relation which can be used to directly determine the delay at uncontrolled intersections under Indian traffic conditions.

Uncontrolled intersections are vital points on urban roads, the performance of which will influence the traffic flow on entire network. Delays to vehicles at urban uncontrolled intersections depend upon the several factors, the most important among these being major road approach volume, type of turning movement, and vehicular composition. The average delay caused to vehicles is an important measure to evaluate the performance of uncontrolled intersections. The performance of an uncontrolled intersection is described by the service delay experienced by low priority movements. Under mixed traffic conditions, the traffic compositions, apart from the conflicting traffic volume and proportion of turning traffic are vital factors influencing the service delay. Most of the earlier studies conducted on this subject, pertain to homogeneous traffic environment, and only a few studies with limited scope have been conducted under mixed traffic conditions. In this study, the service delay models have been developed for three uncontrolled intersections located in the city. These models developed were found to be statistically and logically sound. The level of service for the uncontrolled intersections taken under the study has been evaluated using the estimated average service delays from the models developed

Keywords: Delay time, Vehicles, Intersection, Traffic Management

1. INTRODUCTION

Uncontrolled intersections are the intersections which function without any priority assigned to the traffic on any of the intersecting roads, no control (neither STOP signs nor Police-controlled) and the traffic is of heterogeneous nature. These intersections are vital nodal points on urban roads, the performance of which will influence the traffic flow on entire network. Delays to vehicles at urban uncontrolled intersections depend on several factors. The most important among these being the major road approach volume, type of turning movement, and vehicular composition. The extent of intersection of these factors and their collective effect on delay caused to vehicles need to be studied in detailed for better traffic management at these intersections. Field studies due to resources constraint may not include all these, the limited samples that might be obtained will be sufficient to evaluate the effect of various parameters.

At uncontrolled intersections in the absence of indication of specific time intervals to each of the streams of traffic to cross the intersection, the drivers look for gaps and cross the intersections. In developing countries like India, in the absence of the concept of major and minor roads in traffic regulation schemes, vehicles approaching the intersections through all roads, on arrival; assume that equal right to enter the intersection. This has made the traffic situation at the uncontrolled intersection highly complex causing considerable delay to traffic. The delay experienced by vehicles is probably most desirable criteria based on which the performance of the uncontrolled intersection can be evaluated.

The present study was taken up with the following objectives:

1. To establish mathematical relations for service delay to the different types of vehicles for a priority movement at uncontrolled intersections
2. To develop the readily usable mathematical model, to estimate the service delay caused to the subject vehicles at urban uncontrolled intersections, considering interactions of various categories of vehicles under heterogeneous traffic environment.
3. To evaluate the performance of uncontrolled intersections based on the average service delay.

2. LITERATURE REVIEW

Unsignalized intersections make up a great majority of at-grade junctions in any street system. Stop and yield signs are used to assign the right-of-way, but drivers have to use their judgment to select gaps in the major street flow to execute crossings and turn movements at two-way and yield controlled intersections. Two methods are discussed in this section: HCM (2000) Delay method and Blunden's (1961) method.

2.1 HCM (2000) Delay method

The Highway Capacity Manual (HCM) 2000 (TRB, 2000) delay model, is one of the most commonly used time dependent delay models. HCM method involves the calculation of gap times – critical gap and follow-up times.

Critical gap is defined as the minimum time interval in the major-street traffic stream that allows intersection entry for one minor-street vehicle.

$$t_{c,x} = t_{c,base} + t_{c,HV}P_{HV} + t_{c,G}G - t_{c,T} - t_{3,LT} \dots\dots\dots (2.1)$$

Where, $t_{c,x}$ – Critical gap for movement x(s)

$t_{c,base}$ – Base critical gap

$t_{c,HV}$ – Adj. Factor for heavy vehicles

(1.0 for two-lane major streets, 2.0 for four lane major streets)

P_{HV} – Proportion of heavy vehicles for minor movement

$t_{c,G}$ – Adj. Factor for grade

(0.1 for movements 9 and 12 and 0.2 for movements 7,8,10,11)

G – Percent grade divided by 100

$t_{c,T}$ – Adj. Factor for each part of a two-stage gap acceptance process

(1.0 for first or second stage; 0.0 if only one stage)

$t_{3,LT}$ – Adj. Factor for intersection geometry

(0.7 for minor street LT movement at three-leg intersection; 0.0 otherwise)

A driver's critical gap is the **minimum gap** that would be acceptable. A particular driver would

Reject any gaps < critical gap

Accept gaps >= critical gap

Follow-up time is the time between the departure of one vehicle and the next vehicle using the same major-street gap.

$$t_{f,x} = t_{f,base} + t_{f,HV}P_{HV} \dots\dots\dots (2.2)$$

Where, $t_{f,x}$ – Follow-up time for minor movement x

$t_{f,base}$ – Base follow-up time

$t_{f,HV}$ – Adj. Factor for heavy vehicles

(0.9 for two-lane major streets, 1.0 for four lane major streets)

P_{HV} – Proportion of heavy vehicles for minor movement

The gap acceptance method employed in the procedure used in determining the capacity of these intersections computes the potential capacity of each minor traffic stream in accordance with the following equations:

$$c_{p,x} = v_{c,x} \frac{e^{-v_{c,x}t_{c,x}/3600}}{1 - e^{-v_{c,x}t_{f,x}/3600}} \dots\dots\dots (2.3)$$

Where, $c_{p,x}$ – Potential capacity of minor movement x (veh/hr)

$v_{c,x}$ – Conflicting flow rate for movement x (veh/hr)

$t_{c,x}$ – Critical gap for movement x (s)

$t_{f,x}$ – Follow-up time for minor movement x (s)

The movement capacity for the priority movement 'x' can be computed as

$$c_{m,x} = (c_{p,x})f_x \dots\dots\dots (2.4)$$

Where, f_x – Capacity Adj. Factor for rank x movement

Control delay includes initial deceleration delay, queue move-up time, stopped delay, and final acceleration delay. For the purpose of field measurements, control delay is defined as the total elapsed time from the time a vehicle stops at the end of the queue to the time the vehicle departs from the stop line.

Average control delay for any particular minor movement is a function of the capacity of the approach and the degree of saturation.

For a 15-minute analysis period, an estimate of average total delay is given by below equation:

$$d = \frac{3600}{c_{m,x}} + 900T \left[\frac{v_x}{c_{m,x}} - 1 + \sqrt{\left(\frac{v_x}{c_{m,x}} - 1 \right)^2 + \frac{\left(\frac{3600}{c_{m,x}} \right) \left(\frac{v_x}{c_{m,x}} \right)}{450T}} \right] + 5 \dots\dots\dots (2.5)$$

The above equation assumes that the demand is less than capacity for the period of analysis. If demand exceeds capacity during 15-minutes, the period of analysis should be lengthened to include the period of oversaturation. The constant value of 5 sec/veh is included in the above equation to account for the deceleration of vehicles from free-flow speed to the speed of vehicles in queue and the acceleration of vehicles from the stop line to free-flow speed.

Estimation of queue length is an important consideration at unsignalized intersections. Probability distribution of queue lengths for any minor movement is a function of the capacity of the movement and the volume of traffic being served during the analysis period. The following figure-2.4 can be used to estimate the 95 percentile queue length for any minor movement at an unsignalized intersection during the peak 15-minute period. The expected total delay equals the expected number of vehicles in the average queue (numerically identical).

From the queue lengths obtained from the graph shown above, average control delay can be estimated for the each minor movement. The control delay for all the vehicles on a particular approach can be computed as the weighted average of the control delay estimates for each movement on the approach. Level of service (LOS) for an unsignalized intersection (TWSC) is determined by the computed or measured control delay and is defined for each minor movement. LOS is not defined for the intersection as a whole.

The analysis of TWSC intersections is generally applied to existing locations either to evaluate operational conditions under present traffic demand or to estimate the impact of anticipated new demand. The methodology yields a level of service (LOS) and an estimate of average total delay.

HCM (2000) Delay method is based on highly empirical considerations for these types of intersections (TWSC and AWSC) and the Indian conditions at uncontrolled intersections are quite different from those under which these equations were developed.

2.2 Blunden's Method

The analysis of stop and yield-sign controlled approaches has been investigated by a number of researchers, especially Blunden (1961). The capacity of such intersections depends on the traffic flow in the major stream and the confidence of individual drivers to cross this major stream. In formulating an acceptable expression to calculate flow rate, the pattern of gaps in the major stream is assumed to follow a Poisson distribution. In addition, it is assumed that all drivers, on average, will accept a minimum gap. An expression that indicates the number of vehicles per hour that can be "absorbed" by major traffic stream is given by Blunden (1961) as in the following equation-2.4.

$$q_{max} = \frac{V e^{-VT/3600}}{1 - e^{-Vt/3600}} \dots\dots\dots (2.6)$$

Where, q_{max} = Maximum flow rate from the controlled approach

V = Total traffic volumes on the uncontrolled street in both directions

T = Minimum gap acceptable to the first driver on the side street

t = Additional time required for a second driver to follow the first driver into the intersection when a large gap occurs

While comparing the computed maximum flow rate from the above equation with the standard values of maximum flow rates, for the assumed values of T (5 to 8 s) and t (3 to 5 s), given by the Blunden, one could evaluate the performance of stop and yield-sign controlled intersections.

Literature on uncontrolled intersections with mixed traffic where large proportion of the traffic does not follow the rules of the road is extremely limited

Kyte et al. (1991) conducted an empirical study on delay and capacity of the minor approach of two-way stop controlled intersections. They described the capacity and delay characteristics at two-way stop controlled intersections, and concluded that service delay is mainly dependent on the volume of conflicting approaches, and that queue delay is mainly dependent on the volume of the subject approach. They divided total delay into two parts: service delay and queue delay. A linear equation was suggested for minor street service time based upon the volume on the conflicting approaches. However, they did not discuss how this relationship can be used in estimating total delay.

DATA COLLECTION

The data set pertaining to the independent variable and the dependent variable were obtained by conducting the traffic surveys at study intersections. Classified turning movement volume counts of vehicles of each of three groups i.e., light vehicles (two-wheelers, cars, auto-rickshaws, LCVs), heavy vehicles (buses, trucks, tractors, mini-bus/tempo vans) and non-motorized vehicles (cycles, cycle-rickshaws), for each direction of movements (LT, RT, and TH) at each of the approaches (three or four) were done simultaneously for 3hours in the morning session i.e., from 8.30AM to 11.30AM and for 3hours in evening session i.e., from 4.00PM to 7.00PM, on a typical working week day, for each of the intersection. It was observed that the traffic volume and vehicular composition of individual vehicles remained varied slightly during the survey period. For this turning movement volume count study, each enumerator is employed for each turning movement for each of the approaches of the intersections. For a three-legged intersection, 6 enumerators and for four-legged intersection, 12 enumerators are employed.

In order to study the service delay (delay experienced by a vehicle at the reference line), intersections located in city were selected. These intersection sites were in urban areas. But the effect of upstream junctions, on-street parking, or bus stops on arrival rate is negligible. An important traffic feature at all the three intersections was that the queue formation on the minor street approaches was very rare. One of the three intersections is of T-type and the remaining two were four legged.

As a part of delay study, at each intersection, data were collected by video recording technique on a typical weekday. The video camera was placed at a suitable vantage point near the intersection to record an unobstructed view of all approaches and turning movements and data were recorded for about 1hr to 2 hr depending upon the significant sample of vehicle type. The recorded video file was played in the laboratory several times to get the conflicting traffic volume count and the service delay experienced by each subject vehicle. Both crossing and merging types of conflicts were taken into account while noting the conflicting traffic for each maneuver during the data extraction process.

DATA EXTRACTION

Data extraction for the delay study was done using microscopic analysis as described by Kyte et al. (1991). The microscopic analysis requires the definition of the conflicting traffic flow as seen by each subject approach vehicle. Let t_0 = time of arrival of the subject approach vehicle at the reference line; t_d = time of departure of the subject approach vehicle; n = number of observed conflicting vehicles for the subject vehicle, including the conflicting vehicle passing just after departure of the subject approach vehicle; and t_n = time of arrival of n th conflicting vehicle at the reference point.

$$\text{Conflicting flow rate} = \frac{n}{t_n - t_0}$$

$$\text{Service delay} = t_d - t_0$$

The computation of service delay requires the identification of a reference line where the subject approach vehicles would stop. In a homogeneous and lane-disciplined traffic, the stop line is taken as the reference line for measuring the service delay. However, in a mixed traffic flow, the vehicles do not respect the stop line and tend to stop very close to the conflicting area. It was noticed during a preliminary study of recorded data that 50–60% of drivers did not respect the stop line at each of the sites. After observing the behavior of traffic carefully, reference lines where vehicles of each priority movement actually stopped were marked on the screen. The reference line for minor street vehicles was approximately a one-fourth lane width beyond the stop line, i.e., inside the major street.

The equivalent PCUs of different vehicle categories do not remain constant under all circumstances. Rather, these are a function of the physical dimensions and operational speeds of the respective vehicle classes. In urban situations, the speed differential amongst different vehicle classes is generally low, and as such the PCU factors are predominantly a function of the physical dimensions of the various vehicles. Nonetheless, the relative PCU of a particular vehicle type will be affected to a certain extent by increase in its proportion in the total traffic.

PEAK HOUR FLOW RATES

The peak-hour flow rates for different turning movements (TH, LT, and RT) for each approach and total approach flow rates for all the three intersections has been presented through below tables. Vehicular composition of the subject vehicles considered for the delay study at all the low-priority movements (minor RT, major RT, and minor TH) and their variations at different intersections are presented below through pie-charts, as shown in the following figures. The layout of the three intersections has been shown in the figures

Table Peak Hour Flow rates of Ghatkesar Junction

Approach	Movement	Peak Hour Flow Rate		Approach Flow Rate	
		Veh/hr	PCU/hr	Veh/hr	PCU/hr
UPPAL	TH	2140	1693	2741	2459
	LT	241	350		
	RT	360	416		
GANAPUR	TH	218	262	991	1181
	LT	464	574		
	RT	309	345		
BHONGIRI	TH	1400	1751	1696	2149
	LT	149	208		
	RT	147	190		
GHATKESAR Bye-pass	TH	414	572	1209	1586
	LT	315	414		
	RT	480	600		

MODEL DEVELOPMENT

The analysis was done separately for four categories of subject vehicles: 2W, Car, Auto and HV and for two types of movements i.e., right turn from minor (Minor RT) and right turn from major (Major RT) at T-intersection. At four-legged intersections, through traffic from a minor (Minor TH) street was also analyzed in addition to the right turns from major and minor streets.

The regression analysis using “Curve Estimation” between the service delay (T_s , s) (dependent variable) and the corresponding conflicting traffic volume (CT, veh/s) (independent variable), for each subject vehicle for each of the three types of low priority movements (minor RT, major RT, minor TH), was done using the well-known statistical package, IBM® SPSS Statistics V-19. The data points showed an exponential trend and the mathematical equation fitted through the data points for each subject vehicle. The goodness of fit of the model was assessed by the coefficient of determination (R^2) value and the other statistic measures like F-ratio, t-statistic.

Delay is a fundamental parameter in the economic analysis of highway investments. Delay caused to vehicles is important measure to evaluate the performance of urban uncontrolled intersections under mixed traffic conditions. Although the users' perception of quality of service may be difficult to measure, delay is a widely used quality of service measure for intersections. The vehicular composition, apart from traffic volume and proportion of turning traffic, is a vital factor in influencing the extent of delay caused to vehicles. Most of the earlier studies on delay to vehicles at urban uncontrolled intersections have been conducted under homogeneous traffic conditions, and the few studies that have been conducted under mixed traffic conditions being limited in scope. Therefore, there is a need to comprehensively analyse the delay caused to vehicles at urban uncontrolled intersections and develop the appropriate models to estimate the delay.

In this study, curve fitting for the anticipated exponential model has been developed for each subject vehicle (2W, Car, Auto, HV) for all the low priority turning movements (Minor RT, Minor TH, Major RT), taking the three uncontrolled intersections, one three-legged (or T) intersection and two 4-legged intersections, located in Warangal city, as a case study. The models were developed using the well-known statistical package, IBM® SPSS Statistics V-19. The data points showed an exponential trend and the mathematical equation fitted through the data points for each subject vehicle. The goodness of fit of the each model was assessed by the coefficient of determination (R^2) value and the other statistic measures like F-ratio, t-statistic.

CONCLUSIONS

Based on the field studies and the subsequent modelling process, the following conclusions have been drawn:

A simple readily usable mathematical model of service delay, caused to each subject vehicle at an urban uncontrolled intersection under mixed traffic conditions, has been developed.

For each uncontrolled intersection, an aggregate service delay model has been developed, to serve as a useful tool for performance evaluation of such intersections.

Models revealed that with increase in the conflicting flow rate, the service delay was also increased significantly.

Average service delay for Ghatkesar junction was found to be less, as the peak hour conflicting flow rate is less compared to the intersections

Average service delay was found to be more for Heavy vehicles (HV) category, irrespective of the movement, at all the three intersections

REFERENCES

- [1]. Al-Omari, B., and Benekohal, R. (1999), "Hybrid delay models for unsaturated two-way stop-controlled intersections", *J. Transp. Eng.*, 125(3), 291–296.
- [2]. Bonneson, J. A. and Fitts, J. W. (1999). "Delay to major street through vehicles at two-way stop-controlled intersections", *Transportation Research A*, Vol. 33, No. 3, pp. 237-253.
- [3]. Elbermawy and Ayman, E. (2004), "Development of vehicular volume guidelines for two-way versus four-way stop controls", *ITE Journal*, Vol. 74, No. 11, pp. 20-29.
- [4]. Feng Wan, Yunlong Zhang, and Kay Fitzpatrick (2011), "Analysis of Platoon Impacts on Left-Turn Delay at Unsignalized Intersections", *Journal of the Transportation Research Board*, Transportation Research Board, pp. 80-87.
- [5]. Heidemann, D. (1991), "Queue length and waiting time distributions at Priority intersections", *Transp. Res., Part B: Methodol.*, 25 (4), 163–174.
- [6]. Highway Capacity Manual (2000), *Transportation Research Board*, National Research Council, Washington, D.C., 2000.
- [7]. IRC: 106-1990, "Guidelines for Capacity of Urban Roads in Plain areas", *The Indian Roads Congress*, New Delhi.
- [8]. IRC: 93-1985, "Guidelines on Design and Installation of Road Traffic Signals", *The Indian Roads Congress*, New Delhi.
- [9]. IRC: 70-1977, "Guidelines on Regulation and Control of Mixed Traffic in Urban Areas", *The Indian Roads Congress*, New Delhi.
- [10]. IRC: SP: 41-1994, "Guidelines on Design of At-grade intersections in Rural and Urban areas", *The Indian Roads Congress*, New Delhi.
- [11]. Kyte, M., Clemow, C., Mahfood, N., Lall, B. K. and Khisty, C. J. (1991), "Capacity and Delay characteristics of Two-way Stop-controlled intersections", *Transportation Research Record 1320*, TRB, National Research Council, Washington, D.C., pp. 160-167.

- [12]. Kyte, M., and Marek, J. (1989), "Estimating Capacity and Delay at single lane approach, All-way Stop-controlled intersections", *Transportation Research Record* 1225, TRB, National Research Council, Washington, D.C., pp. 73-82.
- [13]. Li, H., Deng, W., Tian, Z., Hu, P. (1996), "Capacities of Unsignalized intersections under mixed vehicular and non-motorized traffic conditions", *Transportation*

Author Profile



D.Praveen was born on 2nd March 1990 in Aushapur, Rangareddy. He has completed his Bachelor of Civil Engineering from Medha College of Engineering, Nalgonda in 2012. Currently he is pursuing his M.Tech (Transportation Engineering) from Malla Reddy Engineering College, Dhulapally, Medchal, Hyderabad.

A STUDY ON PERMEABILITY CHARECTERISTICS OF PHOSPHOGYPSUM BASED CONCRETE

SHAIK IMTHIAZ¹ M. KAMESWARA RAO²

¹M.Tech. Student ² Professor & HOD

^{1,2}, Department of Civil Engineering

^{1,2}, Malla Reddy Engineering College Autonomous), Secunderabad

ABSTRACT

Concrete Permeability may be the most relevant property affecting its durability, especially under exposure to aggressive environment, as a permeability is an aspect of concrete performance that must be specified, designed for an monitored in the production of concrete. To determine the chloride permeability of concrete, many engineers have increasingly been using AASHTO T277, "Rapid determination of the chloride permeability of concrete". Current research studies dealing with normal to moderate concrete strengths have questioned the validity of AASHTO T277, has sole indicator of concrete permeability it has been suggested that for specific concrete mixes AASHTO T277 should not be solely without developing initial correlation data with AASHTO T259 resistance of concrete to chloride penetration.

The main objective of this study is been to evaluate the permeability of concrete with

phosphogypsum as admixture by using the "Rapid chloride chloride ion permeability teat(RCPT)" with all specifications confirming to ASTM C 1202 to evaluate the permeability of concrete with phosphogypsum as admixture a series of tests were planned and performed. Replacement of cement by phosphogypsum as 0%, 10%, 20% and 30% for water / powder ratio 0.50 of M₂₀ grade concrete for every mix 3 cubes of size 150mmX150mmX150mm and 6 cylinders of size 95mm diameter and 50mm height were casted. Cubes were tested at 28 days after casting and the statistical data presented. 3 cylinders were tested at 28 days after casting and remaining 3 cylinders were tested at 90 days after casting. Based on the amount of charge passed in coulombs, Chloride ion permeability of the concrete may be defined as high, moderate, low and very low. The statistical data of chloride ion permeability at 28 days and 90 days is presented.

1. INTRODUCTION

The use of pozzolanic materials in cement concrete paved a solution for

- ❖ Modifying the properties of the concrete
- ❖ Controlling the concrete production cost
- ❖ To overcome the scarcity of cement
- ❖ The economic advantageous disposal of industrial wastes

The most important pozzolanic materials are fly ash, silica fume, metakaolin and Phosphogypsum whose use in cement and concrete is thus likely to be a significant achievement in the development of concrete technology in the coming few decades.

1.1 Phosphogypsum

Phosphogypsum is a by-product in the wet process for manufacture of phosphoric acid (ammonium phosphate fertilizer) by the action of sulphuric acid on the rock phosphate. It is produced by various processes such as dehydrate, hemihydrate or anhydrite processes. In India the majority of phosphogypsum is produced by the dehydrate process due to its simplicity in operation and lower maintenance as compared to other processes. The other sources of phosphogypsum are by-products of hydrofluoric acid and boric acid industries.

Current worldwide production of phosphoric acid yields over 100 million tons of phosphogypsum per year. While most of the rest of the world looked at phosphogypsum as a valuable raw material and developed process to utilize it in chemical manufacture and building products, India blessed with abundant low-cost natural gypsum piled the phosphogypsum up rather than bear the additional expense of utilizing it as a raw material. It should be noted that during most of this time period the primary reason phosphogypsum was not used for construction products in India was because it contained small quantities of silica, fluorine and phosphate (P₂O₅) as impurities and fuel was required to dry it before it could be processed for some applications as a substitute for natural gypsum, which is a material of higher purity. However, these impurities impair the strength development of calcined products. It has only been in recent years that the question of radioactivity has been raised and this question now influences every decision relative to potential use in building products in this country.

2. OBJECTIVE AND SCOPE OF STUDY

The scope of present investigation is to study and evaluate the effect of replacement of cement by various percentages of phosphogypsum (0%, 10%, 20% and 30%) for M₂₀ grade concrete with water binder ratio of 0.50 at 28 days of

compressive strength and permeability characteristics at 28 days and 90 days.

2.1 OBJECTIVES OF THE PRESENT STUDY

The objective of the present study is to investigate the durability characteristics of phosphogypsum based concrete.

- To find out the compressive strength of phosphogypsum based concrete by replacing the cement by various percentages of phosphogypsum (0%,10%,20% and 30%) after 28 days of curing.
- To estimate the permeability of phosphogypsum based concrete by replacing the cement by various percentages of phosphogypsum (0%,10%,20% and 30%) after casting 28 days and 90 days by chloride ion permeability test procedure.

5.3 SCOPE OF STUDY

- The scope of present investigation is limited to find out the compressive strength of phosphogypsum based concrete by replacing the cement by various percentages of phosphogypsum (0%,10%,20% and 30%) after 28 days of curing by compressive strength testing machine.
- Further the scope of present investigation is limited to estimate the permeability of of

phosphogypsum based concrete by replacing the cement by various percentages of phosphogypsum (0%,10%,20% and 30%) after casting 28 days and 90 days by chloride ion permeability test procedure

3. EXPERIMENTAL INVESTIGATIONS

3.1 Cement

The cement used in all mixtures was commercially available Ordinary Portland cement (OPC) of 53 grade manufactured by Ultratech Company confirming to IS: 12269-1987 .

Table 3.1 Physical properties of cement

S. No	Property	Experimental Values	Suggested value as per IS: 12269-1987 code
1.	Specific gravity	3.15	3.14
2.	Normal Consistency	33%	- -
3.	Initial Setting Time	112min	Min 30 minutes

4.	Final Setting Time	238min	Max 10 Hours
----	--------------------	--------	--------------

3.2 Coarse Aggregates

The coarse aggregate from a local crushing unit having 20mm normal size well-graded aggregate according to IS-383 is used in this investigation. The coarse aggregate procured from quarry was sieved through 20mm, 16mm, 12.5mm, 10mm and 4.75mm sieves. The material retained on 12.5mm, 10mm and 4.75mm sieves was filled in bags and stacked separately and used in the production of Self Compacting Concrete.

Table 3.2 Physical properties of coarse aggregate

S. No	Property	Value
1.	Specific gravity	2.67
2.	Bulk density	1239 Kg/m ³
3.	Water Absorption	0.4%
4.	Fineness modulus	7.01

3.3 Fine Aggregates

The fine aggregate that falls in zone-I was obtained from a nearby river course. The sand

obtained was sieved through all the sieves (i.e. 4.75mm, 2.36mm, 1.18mm, 600 μ , 300 μ , 150 μ). Sand retained on each sieve was filled in different bags and stacked separately for use. To obtain zone-I sand correctly, sand retained on each sieve is mixed in appropriate proportion.

Table 3.3 Physical properties of fine aggregate

S. No	Property	Value
1.	Specific gravity	2.61
2.	Fineness modulus	3.06
3.	Bulk Density	1502 Kg/m ³
4.	Grading	Zone-I

Table 3.4 Sieve analysis of fine aggregate

Sieve size (mm)	Weight retained (gms)	% weight retained	Cumulative (%) weight retained (F)	% Weight passing	Cumulative % weight passing
4.75	22	2.2	2.2	97.8	97.8
2.36	38	3.8	6	94	191.8
1.18	221	22.1	28.1	71.9	263.7

600	435	43.5	71.6	28.4	292.1
300	270	27.0	98.6	1.4	293.5
150	12	1.2	99.8	0.2	293.7

3.4 Phosphogypsum

The Phosphogypsum used in the investigation was obtained from Coromandel international Ltd, Ennore, Chennai. The Phosphogypsum passing through 90 μ sieve was used throughout the experiment. The specific gravity of Phosphogypsum was found to be 2.34. The Phosphogypsum used in this study was basically to improve workability and cohesiveness of concrete.

4. CALCULATIONS

Table 4.1 Concrete ingredients by weight for 0% Phosphogypsum (M20mix)

Cement (Kg)	Phosphogypsum (Kg)	Fine aggregate (Kg)	Coarse aggregate (Kg)	W/P ratio	Water in (Litres)
383	0	600.4	1144.3	0.50	197.2
1	0	1.57	2.99	0.5	0.5

Table 4.2 Concrete ingredients by weight for 10% Phosphogypsum (M20mix)

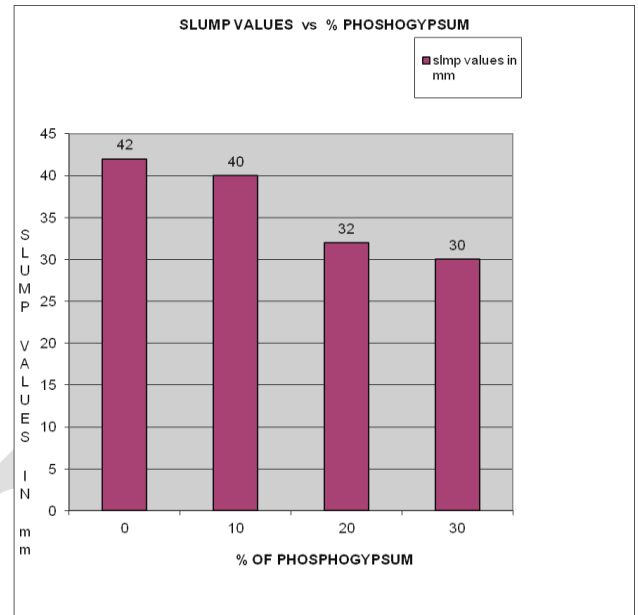
Cement (Kg)	Phosphogypsum (Kg)	Fine aggregate (Kg)	Coarse aggregate (Kg)	W/P ratio	Water in (Litres)
383	38.3	600.4	1144.3	0.50	197.2
1	0.1	1.57	2.99	0.5	0.5

Table 4.3 Concrete ingredients by weight for 20% Phosphogypsum (M20mix)

Cement (Kg)	Phosphogypsum (Kg)	Fine aggregate (Kg)	Coarse aggregate (Kg)	W/P ratio	Water in (Litres)
383	76.6	600.4	1144.33	0.50	197.2
1	0.2	1.57	2.99	0.5	0.5

Table 4.4 Concrete ingredients by weight for 10% Phosphogypsum (M20mix)

Ce men t (Kg)	Phospho gypsum (Kg)	Fine aggrega te(Kg)	Coarse aggrega te(Kg)	W /P ra tio	Wat er in (Lit res)
383	76.6	600.4	1144.3 3	0. 50	197 .2
1	0.2	1.57	2.99	0. 5	0.5



5. TABLES AND GRAPHS OF TEST RESULTS

Table 6.10 Abstract of workability values of fresh phosphogypsum concrete mixes

S.N o.	Replaceme nt of Phosphogy psum	Slu mp valu e (mm)	Compac tion factor value	Vee- Bee degree (secon ds)
1	0%	42	0.891	3.8
2	10%	40	0.885	4.10
3	20%	32	0.872	4.70
4	30%	30	0.867	5.20

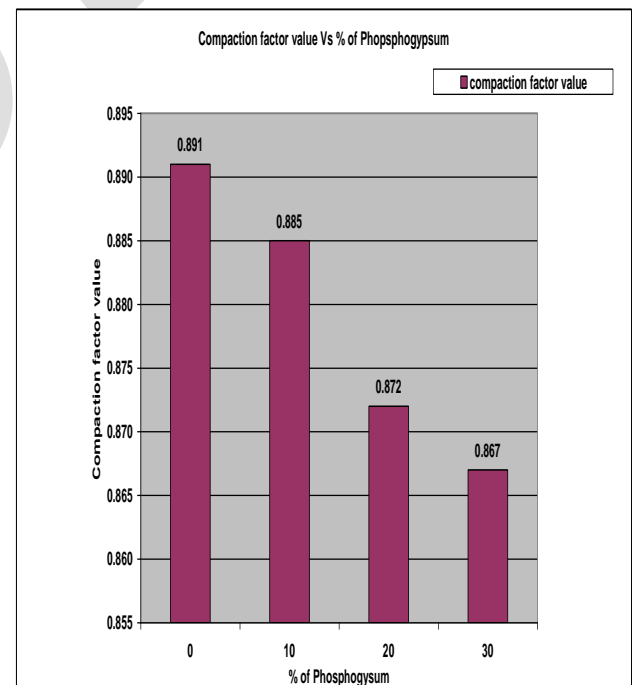


Fig. 6.3 Variation of Compaction Factor with Replacement of Phosphogypsum

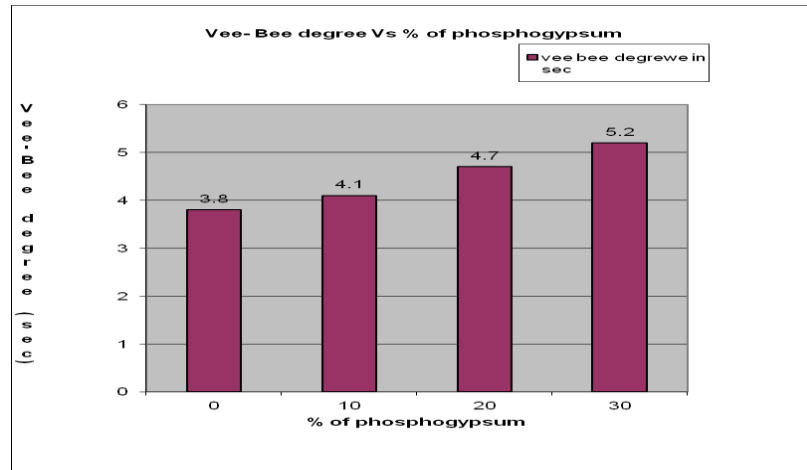


Fig. 6.4 Variation of Vee-Bee Degree with Replacement of Phosphogypsum

Table 6.11 Compressive Strength of Phosphogypsum Mixes

S. No.	% of Phosphogypsum	Mix M20 grade	Compressive strength (MPa) at 28 days	Average Compressive strength (MPa) at 28 days
1	0 percentage	Sample 1	27.9	28.6
		Sample 2	29.3	
		Sample 3	28.7	
2	10 percentage	Sample 1	32	31.1
		Sample 2	30.4	
		Sample 3	30.9	
3	20 percentage	Sample 1	18.7	19.8
		Sample 2	21.1	
		Sample 3	19.6	
4	30 percentage	Sample 1	14.5	15.1
		Sample 2	14.8	
		Sample 3	16	

CONCLUSIONS:

Based on the results obtained from this study, the following Conclusions seems to be valid.

- 1.The increase in percentage replacement of cement with Phoshogypsum from 0% to 30% causes decrease in Slump value and Compaction factor value, but increase Vee-bee degree. This shows workability is reducing as percentage of Phosphogypsum increasing. However at 10% replacement of cement with Phosphogypsum the reduction in workability is very nominal. Hence, 10% replacement of cement with Phosphogypsum is suitable from workability point of view.
- 2.The increase in percentage replacement of cement with Phosphogypsum from 0% to 10% causes increase in compressive strength of concrete from 28.60MPa to 31.10MPa. Further increase in percentage replacement of cement with Phosphogypsum from 10% to 30% causes decrease in the compressive strength from 31.10MPa to 15.10MPa. Hence, 10% replacement of cement with Phosphogypsum is advisable from compressive strength point of view .
- 3.The increase in percentage replacement of cement with Phosphogypsum from 0% to 30% causes reduction in Chloride ion permeability from 3076 Coulombs to 2426

Coulombs, when tested for Chloride ion permeability at the age of 28 days

- 4.The increase in percentage replacement of cement with Phosphogypsum from 0% to 30% causes reduction in Chloride ion permeability from 1879 Coulombs to 1525 Coulombs, when tested for Chloride ion permeability at the age of 90 days.

Finally, it can conclude that though the permeability is reducing even upto 30% replacement of cement with Phosphogypsum , Keeping the workability and compressive strength in mind ,10% replacement of Phosphogypsum is recommended for use in M₂₀ grade concrete.

REFERENCES:

1. Atkins, H. N., "Highway Materials, Soils, and Concretes", 4th Edition, Prentice Hall, pp.277-330(2003).
2. B. Krishna Rao et. al. "steel fiber reinforced Self Compacting concrete incorporating class F fly ash" International Journal of Engineering Science and Technology Vol. 2(9), 2010, 4936-4943
3. Bentz, D. P., "Drying/hydration in cement pastes during curing", Materials and Structures, Vol.34, No. 243, pp.557-565 (2001).
4. Concrete Technology- M.S.Shetty

5. Dodson, V., "Concrete Admixtures", VNR Structural Engineering Series (1990).
6. Duval, R. and E. H. Kadri, "Influence of Silica Fume on the Workability and the Compressive Strength of High-Performance Concretes", Cement and Concrete Research Journal, Vol. 28, Issue 4, pp.533-547 (1998).
7. Ferraris, C. F., "Concrete Mixing Methods and Concrete Mixers: State of the Art", NIST Journal, Vol. 106, No. 2, pp.391-399 (2001).
8. Ferraris, C. F., "Measurement of the Rheological Properties of High-Performance Concrete", J.Res. Natl. Inst. Techn., Vol. 104, No. 5, pp.461-477 (1999).
9. Gebler, S.H. and P. Klieger, "Effect of Fly Ash on Some of the Physical Properties of Concrete", Portland cement Association, R & D Bulletin 089.01T (1986).
10. Gebler, S.H. and P. Klieger, "Effect of Fly Ash on the Air-Void Stability of Concrete", Portland cement Association, R & D Bulletin 085.01T (1983).
11. Gebler, S.H. and P. Klieger, "Effect of Fly Ash on the Durability of Air Entrained Concrete", Portland cement Association, R & D Bulletin 090.01T (1986).
12. Hale, W. M., T. D. Bush, and B. W. Russell, "Interaction of blast furnace slag and Class C Flyash with type I cements", Paper No. 01-045, TRB (2000).
13. Khaloo, A. R. and M. R. Houseinian, "Evaluation of properties of silica fume for use in concrete", International Conference on Concretes, Dundee, Scotland (1999).
14. Khayat, K.H., M.Vachon, and M. C. Lancot, "Use of Blended Silica Fume Cement in Commercial Concrete Mixtures", ACI Materials Journal, pp.183-192 (1997).
15. Kosmatka, S. H., B. Kerkhoff, and W. C. Panarese, "Design and Control of Concrete Mixtures", 14th Edition, Portland cement Association (2002).
16. Lay, M. G., "Handbook of Road Technology", Sec. Ed., Vol. 1, Gordon and Breach Science Publishers (1990).
17. M.A. Taher, "Influence of thermally treated phosphogypsum on the properties of Portland slag cement", Resources, Conservation and Recycling 52 (2007) 28–38
18. Mindess, S., J. F. Young, and D. Darwin, "Concrete", Second Edition, Prentice Hall (2003).

EARTHQUAKE RESISTANT DESIGN OF A BUILDING USING SHEAR WALL

K.S.SAI KARTHIK

M.Tech Research Scholar, Structural Engineering
Malla Reddy Engineering College (Autonomous), Hyderabad, Telangana, India

M. KAMESWARA RAO

Professor, Department of Civil Engineering,
Malla Reddy Engineering College (Autonomous), Hyderabad, Telangana, India

ABSTRACT

Constructions made of shear walls are high in strength ,they majorly resist the seismic force, wind forces and even can be build on soils of weak bases by adopting various ground improvement techniques. Not only the quickness in construction process but the strength parameters and effectiveness to bare horizontal loads are very high. Shear walls generally used in high earth quake prone areas, as they are highly efficient in taking the loads. Not only the earth quake loads but also winds loads which are quite high in some zones can be taken by these shear walls efficiently and effectively. Shear walls have a peculiar behavior towards various types of loads. Calculation of rigidity factor, reactions, shear center, shear force and bending moment is a topic of interest.

To determine the solution for shear wall location in multi-storey building based on its both elastic and elasto -plastic behavior's. The earthquake load is to be calculated and applied to a multistoried building. Model results are calculated and analyzed for the effective location of shear wall. Hence by adopting the shear wall technologies to the college building of VITS block, Deshmukhi Hyderabad city. The building behavior is checked. The design is above verified for this same structure using extended three dimensional analysis of buildings (STAAD Pro V_{8i}) software.

The results are compared. It is found that the provision of shear wall in this building will make this structure completely earth quake resistant in zone II of Hyderabad. Further it is also found that the results of manual and STAAD Pro are almost same, the STAAD Pro giving a little bit of saving in the reinforcement quantity.

Keywords— STAAD.Pro, Earth Quake Loads, Shear Walls, IS: 1893, IS:456-2000.

1. INTRODUCTION

Shear walls are vertical elements of the horizontal force resisting system. Shear walls are constructed to counter the effects of lateral load acting on a structure. In residential construction, shear walls are straight external walls that typically form a box which provides all of the lateral support for the building. When shear walls are designed and constructed properly, they will have the strength and stiffness to resist the horizontal forces. Shear walls are one of the most effective building elements in resisting lateral forces during earthquake. By constructing shear walls damages due to effect of lateral forces due to earthquake and high winds can be minimized. Shear walls construction will provide larger stiffness to the buildings there by reducing the damage to structure and its contents.

In building construction, a rigid vertical diaphragm capable of transferring lateral forces from exterior walls, floors, and roofs to the ground foundation in a direction parallel to their planes. Examples are the reinforced-concrete wall or vertical truss. Lateral forces caused by wind, earthquake, and uneven settlement loads, in addition to the weight of structure and occupants; create powerful twisting (torsion) forces. These forces can literally tear (shear) a building apart. Reinforcing a frame by attaching or placing a rigid wall inside it maintains the shape of the frame and prevents rotation at the joints. Shear walls are especially important in high-rise buildings subjected to lateral wind and seismic forces. In the last two decades, shear walls became

an important part of mid and high-rise residential buildings. As part of an earthquake resistant building design, these walls are placed in building plans reducing lateral displacements under earthquake loads. So shear-wall frame structures are obtained.

Shear wall buildings are usually regular in plan and in elevation. However, in some buildings, lower floors are used for commercial purposes and the buildings are characterized with larger plan dimensions at those floors. In other cases, there are setbacks at higher floor levels. Shear wall buildings are commonly used for residential purposes and can house from 100 to 500 inhabitants per building

2. PURPOSE OF CONSTRUCTING SHEAR WALLS

Shear walls are not only designed to resist gravity / vertical loads (due to its self-weight and other living / moving loads), but they are also designed for lateral loads of earthquakes / wind. The walls are structurally integrated with roofs / floors (diaphragms) and other lateral walls running across at right angles, thereby giving the three dimensional stability for the building structures. Shear wall structural systems are more stable. Because, their supporting area (total cross-sectional area of all shear walls) with reference to total plans area of building, is comparatively more, unlike in the case of RCC framed structures. Walls have to resist the uplift forces caused by the pull of the wind. Walls have to resist the shear forces that try to push the walls over. Walls have to resist the lateral force of

the wind that tries to push the walls in and pull them away from the building.

3. COMPARISONS OF SHEAR WALL WITH CONSTRUCTION OF CONVENTIONAL LOAD BEARING WALLS

Load bearing masonry is very brittle material. Due to different kinds of stresses such as shear, tension, torsion, etc., caused by the earthquakes, the conventional unreinforced brick masonry collapses instantly during the unpredictable and sudden earthquakes.

The RCC framed structures are slender, when compared to shear wall concept of box like three-dimensional structures. Though it is possible to design the earthquake resistant RCC frame, it requires extraordinary skills at design, detailing and construction levels, which cannot be anticipated in all types of construction projects.

On the other hand even moderately designed shear wall structures not only more stable, but also comparatively quite ductile. In safety terms it means that, during very severe earthquakes they will not suddenly collapse causing death of people. They give enough indicative warnings such as widening structural cracks, yielding rods, etc., offering most precious moments for people to run out off structures, before they totally collapse. For structural purposes we consider the exterior walls as the shear-resisting walls. Forces from the ceiling and roof diaphragms make their way to the outside along assumed paths, enter the walls, and exit at the foundation.

4. FORCES ON SHEAR WALL

Shear walls resist two types of forces: shear forces and uplift forces. Shear forces are generated in stationary buildings by accelerations resulting from ground movement and by external forces like wind and waves. This action creates shear forces throughout the height of the wall between the top and bottom shear wall connections.

Uplift forces exist on shear walls because the horizontal forces are applied to the top of the wall. These uplift forces try to lift up one end of the wall and push the other end down. In some cases, the uplift force is large enough to tip the wall over. Uplift forces are greater on tall short walls and less on low long walls. Bearing walls have less uplift than non-bearing walls because gravity loads on shear walls help them resist uplift. Shear walls need hold down devices at each end when the gravity loads cannot resist all of the uplift. The hold down device then provides the necessary uplift resistance.

Shear walls should be located on each level of the structure including the crawl space. To form an effective box structure, equal length shear walls should be placed symmetrically on all four exterior walls of the building. Shear walls should be added to the building interior when the exterior walls cannot provide sufficient strength and stiffness. Shear walls are most efficient when they are aligned vertically and are supported on foundation walls or footings. When exterior shear walls do not provide

sufficient strength, other parts of the building will need additional strengthening. Consider the common case of an interior wall supported by a sub floor over a crawl space and there is no continuous footing beneath the wall. For this wall to be used as shear wall, the sub floor and its connections will have to be strengthened near the wall. For Retrofit work, existing floor construction is not easily changed. That's the reason why most retrofit work uses walls with continuous footings underneath them as shear walls.

5. CLASSIFICATION OF SHEAR WALLS

- Simple rectangular types and flanged walls (bar bell type)
- Coupled shear walls
- Rigid frame shear walls
Framed walls with in filled frames
- Column supported shear walls
- Core type shear walls

5.1 METHODS OF DESIGN OF SHEAR WALL

There are three types of design methods

- (a) Segmented shear wall method
- (b) Force transfer –ground openings method
- (c) Perforated shear wall method

5.2 TYPES OF SHEAR WALLS

1. RC Shear Wall
2. Plywood Shear Wall
3. Midply Shear Wall
4. RC Hollow Concrete Block Masonry Wall
5. Steel Plate Shear Wall

6. DESCRIPTION OF THE BUILDING

The building we considered is C-Block of vignan institute of technology and science, an Engineering college located at desh mukhi village, Rangareddy district, the college offers courses in civil, mechanical ,electronics and communication ,electrical and electronics ,computer sciences engineering with an intake of about 1000 students per year. This block consists of 3 bays of 20m width and 4 m height of 3 floors .the ground floor consists of one laboratory covering an area of 3 bays and the remaining floors G+1 and G+2 consists of 6 Class rooms. And the walls are of 0.3m thick .The walls between central bays are designed as shear walls as shown in figure. It shows the layered structure of the current building.

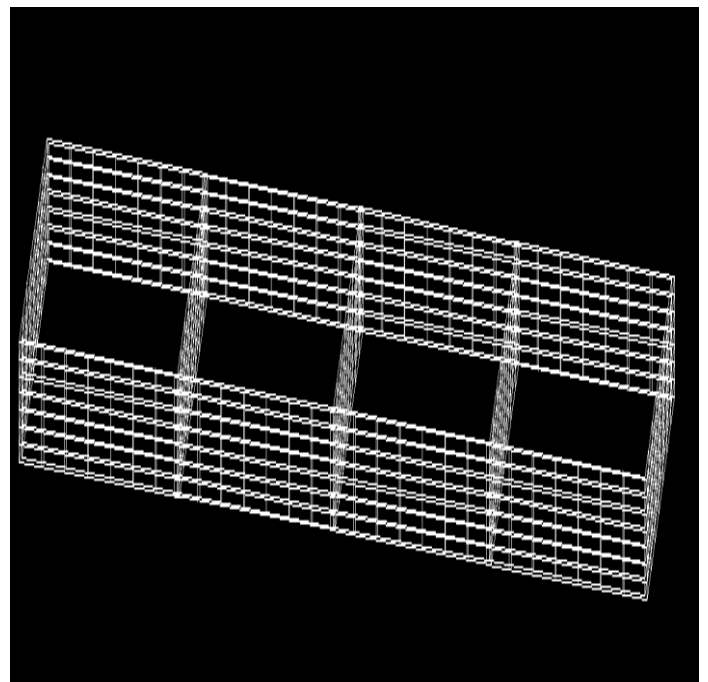


Fig: 1 Layered Structure of Current Building

6.1 SHEAR WALLS

The shear walls are proposed to be inserted in the C-Block Building and the analysis and design of the building with the shear walls is done with staad Pro

and manually .The shear walls will be designed to resist the lateral forces developed due to earthquake and wind loads .The shear walls are proposed to be located at the centre and shear walls are proposed in 8 bays, Each bay 20 m width, 4 m height. Total shear wall Area is 640square meters. Thickness of shear wall is thickness of conventional wall which is 0.3 m. The location of shear walls is shown in Figure.

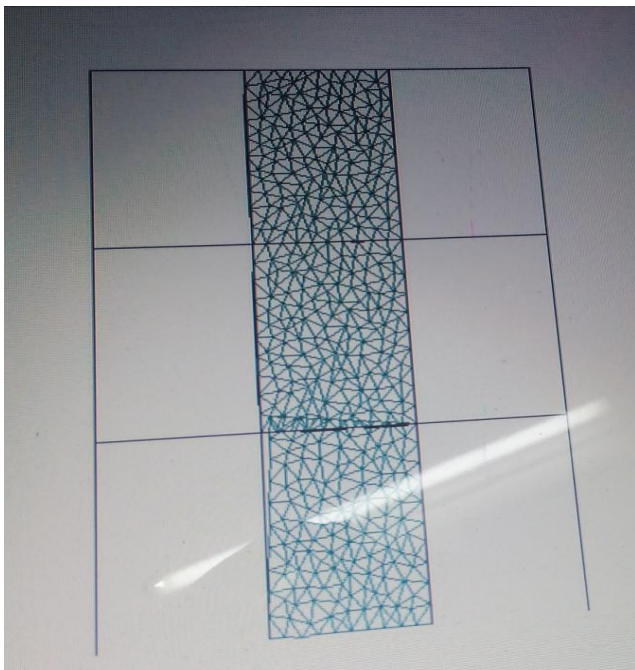


Fig: 2 locations of shear walls

6.2 NECCESSITY OF SHEAR WALLS TO THE PRESENT BUILDING

As already explained the building is often subjected to vibrations produced from the nearby quarrys and moreover it is on hills which are more prone to earthquakes .If at all any earth quake occurs huge life and property loss may occur .So, it is being necessary to take precautions against vibrations

caused due to bomb blasts from the quarry and also against natural disasters .Shear walls are the easiest

ways to provide resistance to vibrations and very easy to design .

Here in our study we are taking the c block of vignan college and locating and designing shear walls for the existing structure. The 3-D view of shear walls in the building is shown in Figure.

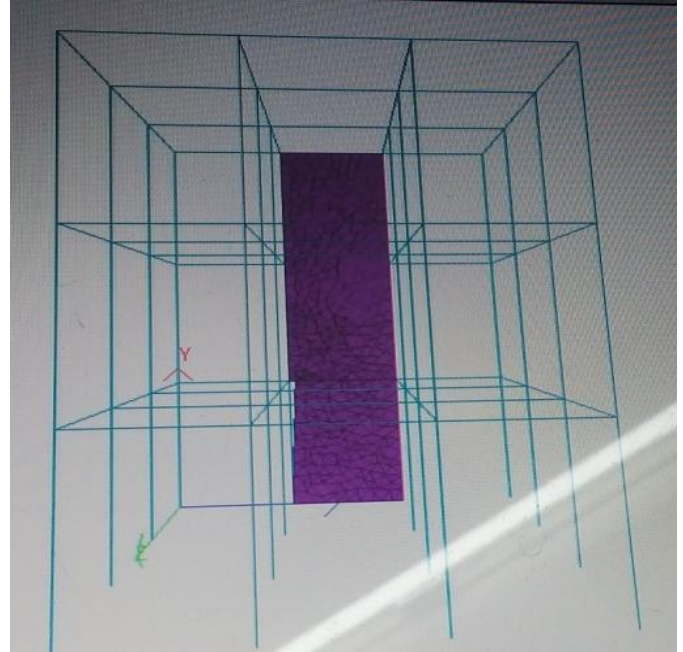


Fig: 3 3D Views of Shear Walls in the Building



Fig: 4 3D Views of Shear Walls in the Building

7. STAAD PRO –AN OVERVIEW

STAAD.Pro V8i is a comprehensive and integrated finite element analysis and design offering, including a state-of-the-art user interface, visualization tools, and international design codes. It is capable of analyzing any structure exposed to static loading, a dynamic response, wind, earthquake, and moving loads. STAAD.Pro V8i is the premier FEM analysis and design tool for any type of project including towers, culverts, plants, bridges, stadiums, and marine structures.

With an array of advanced analysis capabilities including linear static, response spectra, time history, cable, imperfection, pushover and non-linear analyses, STAAD.Pro V8i provides your engineering team with a scalable solution that will meet the demands of your project every time.

in Asia – STAAD.Pro V8i is the perfect workhorse for your

8. RESULTS AND ANALYSIS

The c block in vignan college building is designed using staadpro software. All the columns, beams and shear walls are designed using this software. The shear walls are designed manually also. The block consists of 3 floors and 3 bays in each floor. Shear walls are designed for earthquake loads, dead loads and live load for a college building as per Indian standard code. Wind loads vary with the place, type of soil and type of buildings considering all the conditions appropriate loading is given. The Design and results of the building are detailed in the output obtained from

staadpro software. shear force and bending moment variations and reinforcement details of shear walls for the 8 bays are described here.

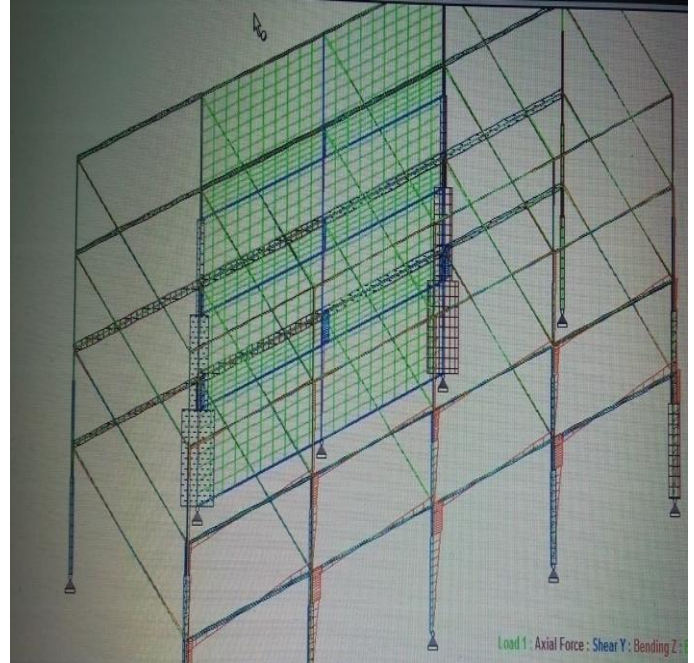


Fig: 5 shows the general dimensions of beams, columns and shear walls

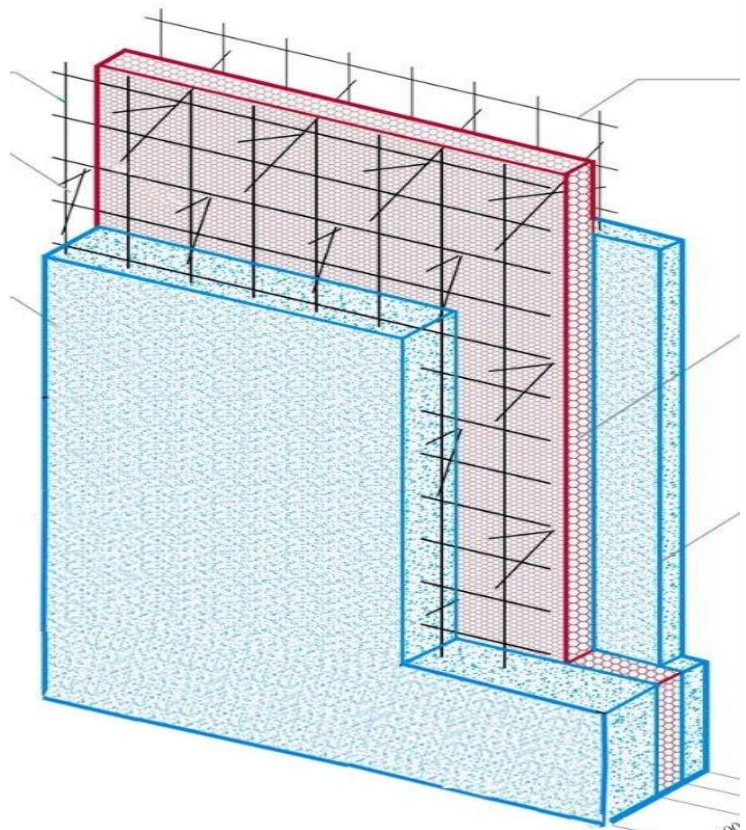
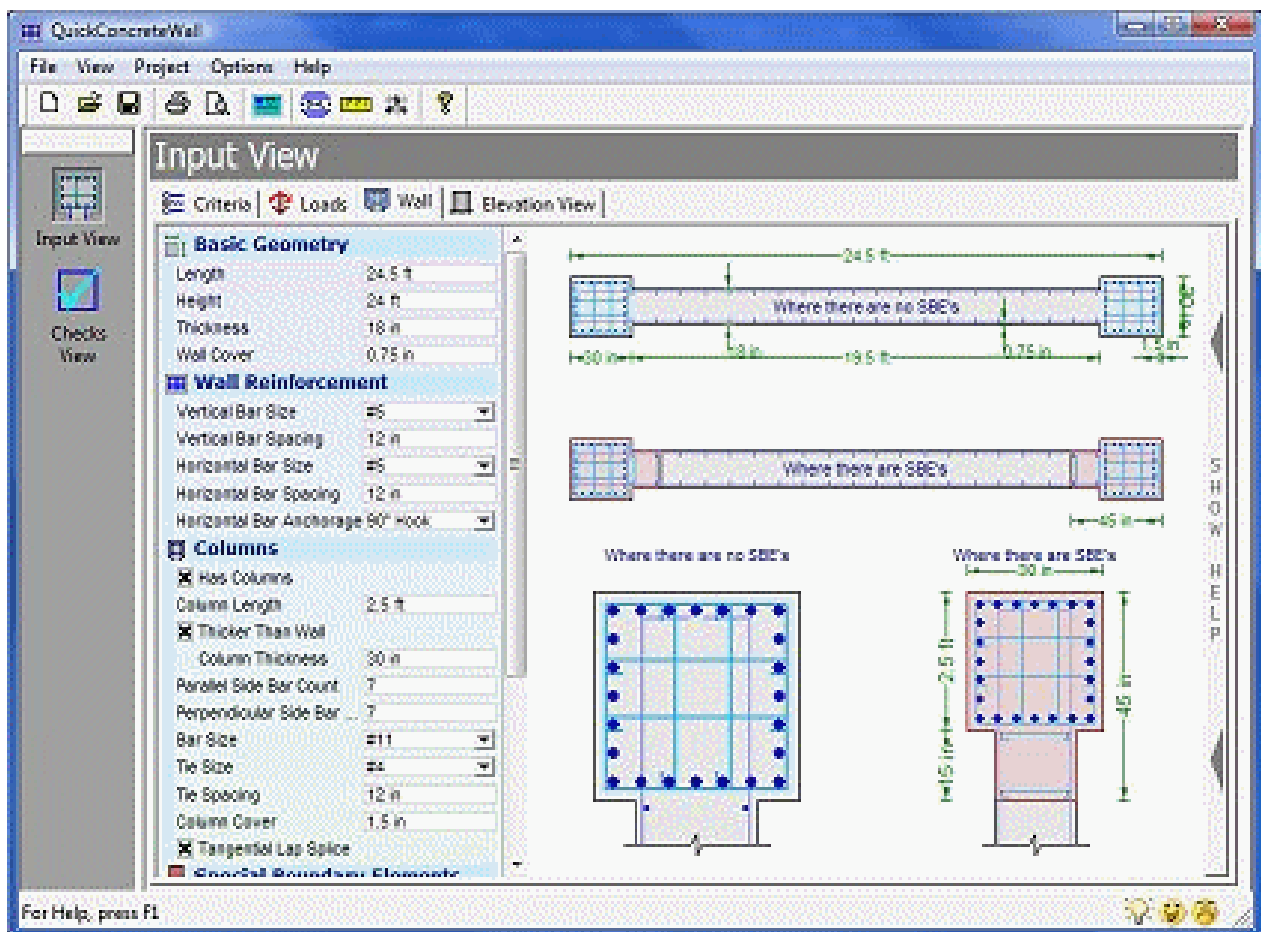


Fig: 6 Figure of Single Shear Wall

8.1 SHEAR FORCES AND BENDING MOMENT VARISTION IN ALL SHEAR WALL SURFACES OBTAINED IN THE RESULTS

Surface number	1	2	3	4	5	6	7	8
Shear force x	1.3672	0.0003	0.0037	1.367	0	0	1.3672	-0.0003
Shear force y	0.0008	0.0038	-0.1229	0	0.0043 -	0.0043 -	0.0008 -	0.0039 -
Shear force z	0.2218	0.0039	2.6438	0	3.8939 -	3.8939 -	0.2218 -	3.8104 -
Bending moment -X	0.0002	0.0003	0.0004	0	0.0038	0.0038	0.0002	0.0038 -
Bending moment -y	0.0006 -	3.8104	0.0375	0.0005 -	0	0	0.0006 -	0.0003
Bending moment -z	0.0009	0	-0.0008	0.001	0	0	0.0009	0

8.2 COMPUTERISED DETAILING OF SHEAR WALL



CONCLUSIONS

The provision of shear walls in C-Block Building of the college in the indicated locations will take care of earth quake load and make the building earth quake resistant

The thickness and the reinforcement considered and provided for the shear walls could be sufficient to take care all types of loads developed due to earthquake.

The columns, Beams, Slabs of the Buildings is also analyzed with Staad Pro and it is found that the existing dimensions and reinforcement are sufficient to take care of the strength requirements developed due to dead load, seismic load and live load.

A comparison of Manual design and computerized design indicates the following

a) As per our **manual design** we used IS code 1893:2000 and the design results for the shear walls are The corner reinforcement of the shear wall of 20 meters is to be provided with 16 mm bars of 20 in numbers, and the middle area is provided with 10 mm bars with 150 mm spacing in vertical direction and 150 mm spacing in horizontal direction for 300 mm wall

b) As per our **computerized design** we used the same code and the results are

The corner reinforcement of the shear wall of 20 meters is to be provided with 16 mm bars of 20 in numbers, and the middle area is provided with 10 mm bars with 140mm spacing in vertical direction and 120 mm spacing in horizontal direction for 300 mm wall

c) The values in the computer design also almost matched the theoretical design the slight variation may be due to accuracy of computerized method. It is estimated that whenever an opening is expected the bar diameter is increased and lateral ties are provided inside the wall to replicate lintel beam in the wall for extra stability

FUTURE SCOPE OF WORK

Construction of shear walls gives all time protection for the building not only while the times of earthquakes but also against vibrations created by blasts in quarry's and also even if the capacity of the building is to be increased shear walls give enough strength and can confidently raise the building to another floor

Shear walls are considered to be a gift to the future construction industry. Scope of shear walls in construction field is immense. It's since their arrival in market there topic was always a topic of interest. Shear walls are the structures usually build to balance lateral loads acting on the structure. Where the lateral loads are most predominantly wind and earth quake loads. And predominantly earthquake loads are more intense in their effect on the building structures. Earthquakes are becoming more intense due to the key reason that is ground water depleasement. Hence in order to overcome the diverse effects of earthquake its always best to save ourselves from future disasters.

Shear walls are quick in construction, as the walls doesn't need any special brick Arrangement or plastering they are very quick in their construction. It just requires an effective form work and very little

skilled labor. It was estimated that a 20 floors building can be built within six months which is most astonishing.

Therefore there is lot of scope for future study in shear walls. The shear walls can be designed and provided for the existing buildings having more than 3 floors. Further various design methods of shear walls can be studied. The various shapes of shear walls can be studied. Different locations can be studied. Provision of shear walls with different materials can be studied.

REFERENCES

1. Khan F.R. and Sbarounis.J.A, "Interaction of shear walls and frames. Journal of the Struct.Div", ASCE, 90(3).1964, 285-335.
2. M. Ashraf, Z.A. Siddiqi, M.A.Javed. "Configuration of a multistory building subjected to lateral forces". Asian journal of civil engineering (building and housing), (2008),vol. 9, no. 5; 525-537.
3. Shahabodin.Zaregarizi. "Comparative investigation on using shear wall and infill to improve seismic performance of existing buildings".The 14th WorldConference on Earthquake Engineering, Beijing, China. October 12-17, 2008.
4. Anshuman. S, Dipendu Bhunia, Bhavin Ramjiyani."Solution of shear wall location in multi-storey building" .International journal of civil and structural engineering, 2011, Vol.02, no 02; 493-506
5. S.V.Venkatesh,H.Sharada bai, "Effect of internal & external shear wall on performance of building frame subjected to lateral load". International Journal of Earth Sciences and Engineering, October 2011, Vol. 04, No 06; 571-576.
6. O.Esmaili,S.Epackachi,M.Samadzaad,S.R.Mirghaderi. "Study of structural RC shears wall system in a 56-story RC tall building". The 14th World Conference on Earthquake Engineering, Beijing, China. October 12-17, 2008.
7. Zhijuan Sun, Jiliang Liu and Mingjin Chu, "Experimental study on behaviours of adaptive slit shear walls" The open civil engineering journal, 2013,7, PP:189-195,2013.
8. Ugale Ashish B. Raut Harshalata R. "Effect of steel plate shear wall on behaviour of structure". International journal of civil engineering research, Vol.5, Number 3, PP-295-300,2014.
9. Venkata Sairam Kumar.N, P.V.S.Maruthi Krishna, "Utilization of reinforced concrete flexural (shear) Walls in multistorey buildings with effect of lateral loads under flat terrain". IJESRT, Vol.2, Issue 9, pp-2467-2471,2013
10. P.P.Chandurkar, Dr.P.S.Pajgade, "Seismic analysis of RCC Building with and without shear wall". IJMER, Vol.3, Issue 3, May-june 2013,pp-1805-1810,2013.
11. Han-Seon Lee, Dong-Woo Ko. "Seismic response characteristics of high-rise RC wall buildings having different irregularities in lower stories". Journal of Structural Engineering, February 1, 2004, Vol. 130, No.2; 2-271-284

Investigation of flexural strength of Fly Ash and Super Plasticizers Filled Binary Concrete Composites

K. Sundeep Kumar^{*1}, P. V. Subba Reddy², Dr. M. K. Rao³

¹CMR TC College, Kandlakoya, Ranga Reddy-Dist, Hyderabad, Andhra Pradesh, India

²N.B.K.R. Institute of Science & Technology, Vidyanagar, SPSR Nellore, Andhra Pradesh, India

³Professor and HOD of Civil Engineering, M.R. Engineering College, Secundrabad, Andhra Pradesh, India

ABSTRACT

In the present research presents the performance of binary concrete when filled with fly ash and plasticizers were discussed based on the soaking water in predetermined no of days such as 3, 7 and 28 days respectively. Flexural strength was evaluated for both fly ash filled concrete and super plasticizers. Hand layup technique was used to prepare the composites. Fly ash filled binary concrete was optimized at 30wt. %. Super plasticizers were proved that when the concrete filled with them with less weight ratio 1.5wt.% itself they showed good results when compared with fly ash filled binary concrete.

Keywords: Concrete, Fly Ash, Super Plasticizers, Flexural Strength

I. INTRODUCTION

It has been above 70 years to research and use fly ash. With its application, the action mechanism of fly ash had been recognized. During the initial stage, only its pozzolanic activity is paid attention. Many researchers devoted themselves to the research of the potential activity of fly ash and the hydration process of fly ash cement. With the deepening of the cognition for fly ash properties, some people found that the particles of fly ash have the morphology that is different to other pozzolanic materials. It is the unique particle morphology to make it have the ability reducing water, which other pozzolanic materials do not have. It influences not only the rheological property of fresh mortar but also the initial structure of hardened cement stone.

Jan de Zeeuw and Abersch in the end of 1970s put forward that the role of fly ash, which its particle size is less than 30 μ m, may be similar to that of the micro-particle of un hydrated cement in cement stone. Danshen et al., in 1981 summarized the previous research results and put forward the hypothesis of "fly ash effects." They

considered that fly ash has three effects in concrete, i.e., morphological, activated and micro aggregate effects. The three effects are relative each other. This shows that the morphological effect is the important aspect of fly ash effects. The morphological effect means that in concrete, mineral-powdered materials produce the effect due to the morphology, structure and surface property of the particle and the particle size distribution. From the influence of fly ash on the properties of cement-based materials, the morphology effect includes three aspects: filling, lubricating and well distributing. These roles depend on the shape, size distribution, etc., of fly ash and influence many properties of concrete. Dayal and Sinha (1999) have reported the specific gravity of Indian coal ashes to range between 1.94 and 2.34 with a mean value of 2.16 and standard deviation of 0.21. The specific gravity of fly ash decreases as the particle size increases. The specific gravity increases when the fly ash particles were crushed. Typical values of the specific surface of Indian fly ashes (3267 to 6842 cm^2/g) were comparable with that of the foreign ashes (2007 to 6073 cm^2/g). Diamond 1986 studied the fly ash contained spherical particles of wide size range about 1 μm to more than 10 μm with smooth surface. Some of the particles were

covered with surface irregularities or deposits. The interior structure of a particle revealed the presence of iron rich magnetic grain on a sphere and in the adjacent sphere needle shaped particles of mullite crystals were present. Garg (1995) studied the morphology of Indian fly ashes. The fly ashes contained angular as well as rounded black particles, spheroid glass, and minute silica grains. Sharma (1993) has classified Indian fly ashes based on the shape of particles as one of the parameters. According to him group-fly ashes contained mainly spherical particles with the size range between 2-25 μ m. The surfaces of glassy spheres in this group are predominantly smooth without any deposit, only some adherence was observed. Poon, C.S., et al. (2002) Low calcium fly ash (ASTM Class F) has been widely used as a replacement of cement in normal and high strength concrete. In normal strength concrete, the replacement level can be more than 50%, while in high strength concrete; the replacement level is usually limited to 15 \pm 25%. According to ASTM C 618-89, fly ash, or pulverized fuel ash (PFA) in the U. K., is a "finely divided residue that results from the combustion of ground or powdered coal." It is primarily the inorganic portion of the source coal in a particulate form. The amount of literature concerning fly ash is considerable, including an ASTM standard (C 311-89) for sampling and testing fly ash for use as an admixture in Portland cement concrete. A number of standards exist which specify the desired properties of the fly ash. In the United States, ASTM C-618 is the standard. The hydraulic behavior of a fly ash is influenced by (1) its carbon content, which should be as low as possible; (2) its silica content, which should be finely divided and as high as possible; and (3) its fineness, which should be as high as possible Orchard 1973b. Fly ash is normally produced by burning coals which have been crushed and ground to a fineness of 70 to 80% passing a 75 μ m sieve. Different types of coal produce different quantities of ash. Depending on the concentration of mineral matter in that type of coal the ash content of the coal used in the western countries is generally less than 20% as the coal is processed prior to delivery at the power point, while in India the ash content of coal used is as high as 50% as the coal contains a higher percentage of rock and soil. Two kinds of fly ash are produced from the combustion of coal are Class C - High, more than 10%, calcium content produced from sub-bituminous coal and Class F - Low, less than 10%, calcium content produced from

bituminous coal. The addition of fly ash to concrete has a considerable effect on the properties of fresh concrete. There is agreement that low calcium ashes show some retarding influence on the mix. This may be due to the fact that the cement is becoming more "diluted." The effects of fly ash on fresh concrete are well known. Workability and pump ability of concrete is improved with the addition of ash because of the increase in paste content, increase in the amount of fines, and the spherical shape of the fly ash particles. Note that this improvement in workability may not be true for coarse, high carbon fly ashes. The use of fly ash may retard the time of setting of concrete. This is especially true of Class F ashes. Class C ash may or may not extend setting time and there are results that show reduction of setting time. Fly ash, in contrast to other pozzolans, reduces the water requirement of a concrete mix. It has been suggested that the major influencing factor in the plasticizing effect of fly ash is the addition of very fine, spherical particles. In fact, it has been shown that as the particle size increases, the plasticizing effect decreases. This indicates that some fly ashes do not improve workability. The rheology of fly ash cement pastes has been shown to behave as a Bingham model. Finally, the inclusion of some fly ashes in a mix reduce bleeding and segregation while improving finishability. This again can be attributed --to the increased amount of fines in the mix and lower water requirement. It is reported that the use of some fly ashes causes an increase in the amount of air entraining admixture required in concrete. It is proposed that carbon in the fly ash absorbs the AEA therefore requiring more to be used as an active role in the mix. In general class C fly ashes require less AEA than class F ashes. Also, there may be an increased rate of air content loss with manipulation if this ash is used. Plasticizers or water reducers, and super plasticizer or high range water reducers, are chemical admixtures that can be added to concrete mixtures to improve workability. In order to produce stronger concrete, less water is added (without "starving" the mix), which makes the concrete mixture less workable and difficult to mix, necessitating the use of plasticizers, water reducers, super plasticizers or dispersants. Plasticizers are also often used when pozzolanic ash is added to concrete to improve strength. This method of mix proportioning is especially popular when producing high-strength concrete and fiber-reinforced concrete. Adding 1-2% plasticizer per unit weight of cement is

usually sufficient. Adding an excessive amount of plasticizer will result in excessive segregation of concrete and is not advisable. Depending on the particular chemical used, use of too much plasticizer may result in a retarding effect. Super plasticizers have generally been manufactured from sulfonated naphthalene condensate or sulfonated melamine formaldehyde, although newer products based on polycarboxylic others [1-14]. The main objectives of using fly ash in high strength concrete are to reduce heat generation and to obtain better durability properties. However, in concrete mixes prepared at a low water-to-binder (w/b) ratio, 20% fly ash content may not be sufficient to suppress the excessive heat of hydration. Manz and others (1982) have suggested that high-calcium fly ashes (Class C ashes) are best distinguished from the low-calcium (Class F) ashes by the incrementing properties. Thus, a general term 'mineral admixtures' has been suggested to describe all classes of slags, ashes, pozzolans and other cement supplements, with a further distinct one being drawn on the basis of their self-cementing capabilities. The above form of classification has been proposed as being preferable to the current division of fly ashes. Ramezani pour, (1994) However the terminology, 'high-calcium' and 'low calcium' have been used in this study, in general, and Class C and Class F, while referring reporting the type of fly ashes actual used by various researchers, in their investigations. Tcnoutasse and Marion (1986) investigated the selective dissolution of different Began low-calcium fly ashes with water, hydrochloric acid solutions by chemical and microscopically techniques. The behavior of fly ashes was also studied in lime-saturated solution. The hydration mechanism was investigated as a function of time, for OPC and OPC' containing 10% to 80% of fly ashes. Cannon (1968) research carried out on the methods of proportioning fly ash concrete mixtures to obtain equal strength to those of conventional control mixtures. Cannon employed Abrams' law and a factor that accounted for the relative costs of fly ash and concrete. Rosen (1976), Gosh (1976) and Popovers (1982) extended the above concept to develop mixture proportions for fly ash concrete. Ghoul (1976) approach, are the standard guidelines available for proportioning pozzolana cements. U.K., Munday and others (1983) proposed a procedure for obtaining any desire strength at 28 days, which requires the collection of data, for a fly

ash source. Brown (1982) found that both slump and vee-see time improved increased substitutions and the changes were found to depend on the level of ash substitution on the water content. He also observed an increase in workability up to 8% replacement of sand or aggregate by ash. Further increase in the percentage replacement caused a rapid decrease in workability. The main objective of thesis is to investigate the strengthen characteristics of the concrete using different proportions of fly ash and super plasticizers. Here fly ash is a product of pulverized coal, considered as a waste by product finding difficulty to be disposed off. Using different proportions of fly ash the maximum strength can be reached in certain proportion of fly ash value. Similarly, super plasticizers are also using different proportions the maximum strength can be reached certain proportion of super plasticizers. The scope of the study is to know the properties of the fly ash and super plasticizers in different proportions. It can be used for find the strength values and find out the maximum strength of the concrete.

II. METHODS AND MATERIAL

Materials used in Binary Concrete concrete are Cement, Fine aggregate, coarse aggregate, water, fly ash, and super plasticizer were used in this project. Zuari 43 grade ordinary Portland cement is used for casting the elements. The following test are conducted such as Fineness test, Standard consistency test, Initial setting time test, Final setting time test, Specific gravity test, Compressive strength test were conducted. In this study we can find out the various tests like compressive strength, split tensile strength and flexural strength are done. The strength properties are done M40 grade concrete mix design. The advantage of binary concrete can be enhanced by substituting some of the cement with other materials, such as fly ash. Fly ash is one of the by-products coal combustion in power generation plants. Large amount of fly ash are discarded each year, increasing costs for disposal. On the other hand, fly ash has been shown to improve the overall performance of concrete, when substituted for a portion of the cement. In same manner super plasticizers is also added different proportions the maximum strength can be reached certain proportion of super plasticizers. Then the maximum strength can be given at a certain proportion

of adding fly ash and super plasticizers at various tests. These tests based on we can identified strength of concrete in addition of fly ash and super plasticizers. Results of the cement are tabulated in the **Table 1** as mentioned below.

Table 1 : Test results on cement

S.NO	TEST NAME	RESULT		
1	sieve test	8 %		
2	standard consistency	29 %		
3	Initial setting time	52 min		
4	Final setting time	480 min		
5	Specific gravity test	3.15		
6	Compressive strength	3 days	7 days	28 days
		N/mm ²	N/mm ²	N/mm ²
		22.12	30.12	44.23

In this investigation fine aggregate is naturally available sand and it is free from dirt, dust and any organic matter. The fine aggregate used for the project was obtained from Penna river .The following tests were conducted on the sand such as Sieve analysis, Bulking of sand by volume method, Specific gravity test. **Table 2** indicates the results of the fine aggregates as mentioned below.

Table 2 Test result on fine aggregates.

S.NO	TEST NAME	RESULT
1	Sieve analysis	Zone III
2	Bulking of sand by volume method	12.5%
3	Specific gravity test	2.51
4	Relative density	45% (medium dense)

In this investigation hard broken granite aggregate is used. The size course aggregate is various from 12 mm to 20 mm. The source the aggregates is Srikalahasti. The following tests like sp. gravity test, fineness modulus test, water absorption test, aggregate impact test, and aggregate crushing strength tests were conducted. The final results thereof as mentioned below in the **Table 3**.

Table 3 Evaluation of course aggregates concrete composites.

S.NO	TEST NAME	RESULT
1	Fineness modulus	7.5
2	Specific gravity	2.33
3	Water absorption	2.1%
4	Crushing strength	22.43%
5	Impact test	28.12%

The following tests of fly ask such as Moisture content, Loss on ignition, Silicon oxide content, Alumina oxide content, Calcium oxide content, Chloride content, Free calcium oxide content, Total alkali oxides content, Particle density determination (by Pycnometer bottle and Le-Chatlier Flask methods), Fineness determination (by dry sieving, wet sieving, Blaine air permeability and laser methods) were conducted. The following tests for fly ash cement pastes, mortars, or concretes are outlined and they are namely Soundness (expansion test), water requirement (expressed as water content of test specimen divided by water content of control specimen to achieve equal specified consistencies), Preparation and curing of specimens, determination of compressive strength (28 days).

III. RESULT AND DISCUSSION

This test was developed by BRAZILAN at Japan in 1943, this is the simplest test and it has been referred in ASTM C78.

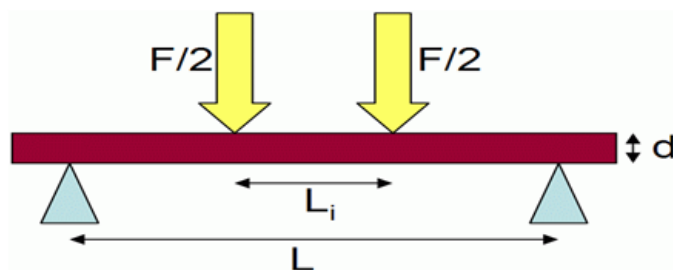


Figure1 Line diagram of flexural strength test using UTM.

This method is used to measure the tensile strength of concrete, and it is a laboratory test. The apparatus for conducting the flexure strength test essentially consists of 4000 kg U.T.M., weighing balance, scale, beam of size 10x10 cm, and length 50 cm, vibrator, measuring jar, pan for mixing cement & sand, trowel, and non porous plate.

Figure 1 shows the line diagram flexural strength testing by UTM. The test specimens are stored in water at a temperature of 24⁰c to 30⁰c for required curing period as per ASTM C 192. They tested immediately on removing from the water whist they are still in a wet condition. The dimension of each specimen should be note down before testing. The specimen is placed in the machine in such manner that the load is applied to the upper surface as in the casting mould. The axis of the specimen is carefully aligned with the axis of the loading device. **Figure 2** shows the photo picture of UTM.



Figure 2 Photo picture of Universal testing machine.

The load is applied without shock and increasing continuously at a rate such that the extreme fibers stress increased approximately 0.7 kg/cm² the load is increased until the specimen fails, and the maximum load is applied to the specimen during. The test recorded. The flexural strength is expressed as *modulus of rupture*. **Figure 3** shows the arrangement of loading below.



Figure 3 Arrangement of loading.

Flexural MR is about 10 to 20 percent of compressive strength depending on type. Size and volume of the coarse aggregate used. Figure 4 shows the Typical fracture failure of the specimen. **Figure 5** shows the variation of flexural strength as a function of fly ash after 3 days soaking in the water conforms that the flexural strength is gradually increases when the fly ash increases on other hand. It was also observed that the when the fly ash was 30wt.% maximum flexural strength was observed as 3.58 N/mm^2 and after that strength was decreased.



Figure 4 Illustration of fracture of failure specimen.

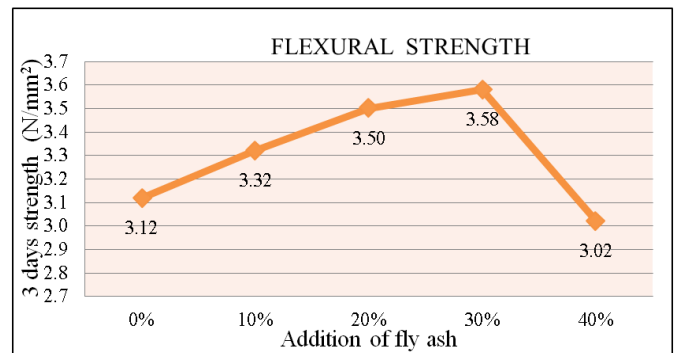


Figure 5 Variation of flexural strength as a function of fly ash after soaking 3 days in water.

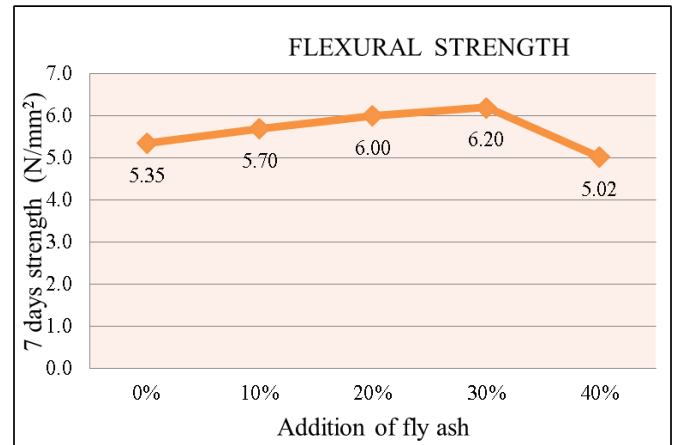


Figure 6 Variation of flexural strength as a function of fly ash after soaking 7 days in water.

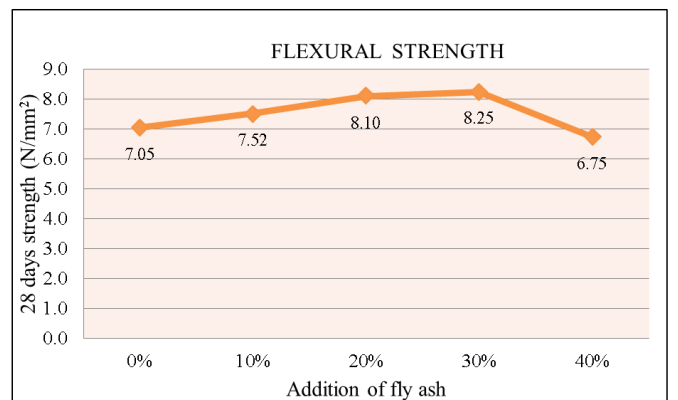


Figure 7 Variation of flexural strength as a function of fly ash after soaking 28 days in water.

Figure 6 shows the variation of flexural strength as a function of fly ash after 7 days soaked in the water was indicates that the flexural strength is gradually increases when the fly ash increases on other hand. It was also observed that the when the fly ash was 30wt.% maximum flexural strength was observe as 6.20 N/mm^2 and after that flexural strength is decreased [2].

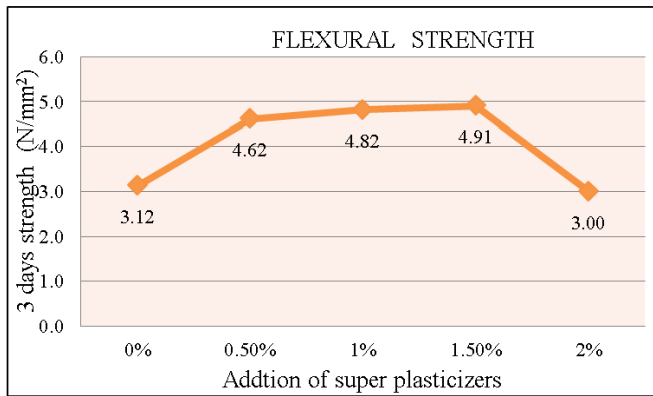


Figure 8 Variation of flexural strength as a function of super plasticizers after soaking 3days in water.

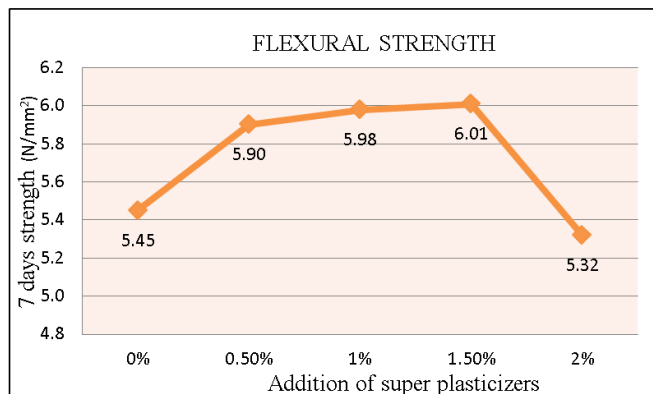


Figure 9 Variation of flexural strength as a function of super plasticizers after soaking 7days in water.

Figure 7 shows the variation of flexural strength as a function of fly ash after 28 days soaked in the water was indicates that the flexural strength is gradually increases when the fly ash increases on other hand. It was also observed that the when the fly ash was 30wt.% maximum flexural strength was observe as 8.25N/mm^2 and after that flexural strength is decreased [13]. **Figure 8** shows the variation of flexural strength as a function of super plasticizers after 3days indicates that the flexural strength is gradually increases when the plasticizers increase on other hand. It was also observed that the when the fly ash was 1.5wt.% maximum flexural strength was observe as 4.91N/mm^2 and after that flexural strength is decreased. When soaking days are increased as a result of that strength is gradually increases.

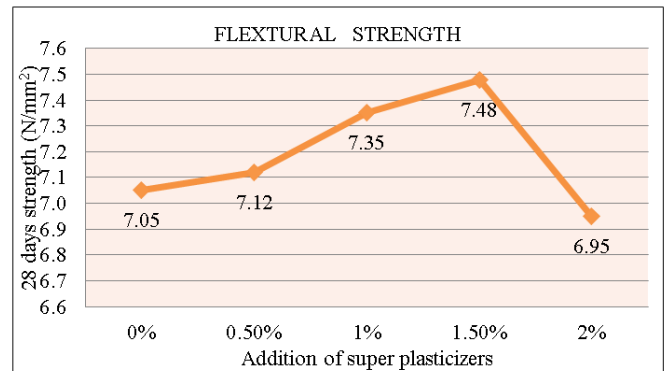


Figure 10 Variation of flexural strength as a function of super plasticizers after soaking 28 days in water.

Figure 9 shows the variation of flexural strength as a function of fly ash after 7days indicates that the flexural strength is gradually increases when the plasticizers increase on other hand. It was also observed that the when the fly ash was 1.5wt.% maximum flexural strength was observe as 6.01N/mm^2 and after that flexural strength is decreased. When soaking days are increased as a result of that strength is gradually increases. **Figure 10** shows the variation of flexural strength as a function of fly ash after 28days indicates that the flexural strength is gradually increases when the plasticizers increase on other hand. It was also observed that the when the fly ash was 1.5wt.% maximum flexural strength was observe as 7.48N/mm^2 and after that flexural strength is decreased. When soaking days are increased as a result of that strength is gradually increases.

IV. CONCLUSION

- Fly ash is added at different proportions namely 0%, 10%, 20%, 30% and 40%.
- For 43 grade cement with M40 mix, by adding up to 30% of fly ash to the cement, the strength is increased and by adding 40% of fly ash the strength is decreasing.
- The test results show that on addition of 30% of fly ash to cement it has gained maximum strength at 28 days period but the rate of strength gain compared to ordinary Portland cement concrete OPCC is at slower rate at initial days.
- The flexural strength increased by 16.18% when compare to normal concrete.

- By use of fly ash as admixture, the cost of construction is also considerably reduced.
- Non-biodegradable fly ash is effectively utilized in Binary concret, so it reduces the disposal problem of fly ash.
- For 43 grade cement with M40 mix, by adding 0%, 0.5%, 1.0%, 1.5% of super plasticizer to the mix prepared the strength is slightly increased and at adding 2.0% of plasticizer to the mix prepared the strength will slightly decreased.
- The test results show that on addition of 1.5% of super plasticizers to concrete it has gained maximum strength at 28 days period.
- The flexural strength increased by 13.46% when compare to normal concrete.
- Super plasticizer may not increase the strength of concrete directly. But it helps in reducing the w/c ratio. Which in turn result in the increase of strength of concrete due to reduction of w/c ratio.
- It is concluded that when compare to super plasticizer, fly ash gives more desirable properties to concrete and ecofriendly.

V. ACKNOWLEDGEMENTS

Authors would like to thank all the professors from the Civil Engineering Department for constant guidance towards the successful completion of this project.

VI. REFERENCES

- [1] A&Court, C. L., "Mix Design and Abrasion Resistance of Concrete," Symposium on Mix Design and Quality Control of Concrete, Cement and Concrete Association, London (1954)
- [2] Abdun-Nur, E. A., Fly Ash in Concrete, Highway Research Board Bulletin 284, Washington, D.C. (1961)
- [3] ASTM Committee C-9, Manual of Concrete Testing, 1976 Annual Book of ASTM Standards, Part 14, Philadelphia (1976)
- [4] ASTM, Manual of Cement Testing, 1988 Annual Book of ASTM Standards, Vol. 04.01 (1988)
- [5] ASTM Committee C-9, Manual of Aggregate and Concrete Testing, 1989 Annual Book of ASTM Standards, Part 14, Philadelphia (1989)
- [6] American Coal Ash Association, Proceeding: Eighth International Ash Utilization Symposium, Vols. 1 and 2. EPRI CS-5362 (1987)
- [7] J. M. Hodgkinson (2000). Mechanical Testing of Advanced Fibre Composites. Cambridge: Woodhead Publishing, Ltd. p. 132–133.
- [8] William D. Callister, Jr. Materials Science and Engineering. Hoken: John Wiley & Sons, Inc., 2003. pegggy carrasquillo, chapter 14, SYM STP 169C, significancies of testing and properties of concrete and concrete making materials, American society for testing and materials west Conshohocken, PA.
- [9] How should strength be measured for concrete paving? Richard c.meininger, NRMCA TIL), and data summary NRMCA TIL 451, NRMCA silver spring, MD.
- [10] "Significance of Tests and Properties of Concrete and Concrete-Making Materials," Chapter 12 on Strength, ASTM STP 169B.
- [11] "Studies of Flexural Strength of Concrete, Part 3, Effects of Variations in Testing Procedures," by Stanton Walker and D.L. Bloem, NRMCA Publication No. 75 (ASTM Proceedings, Volume 57, 1957).
- [12] "Variation of Laboratory Concrete Flexural Strength Tests," by W. Charles Greer, Jr., ASTM, Cement, Concrete and Aggregates, Winter, 1983.
- [13] "Concrete Mixture Evaluation and Acceptance for Air Field Pavements" by Richard O. Meininger and Norman R. Nelson, ASCE Air Field Pavement Conference, September, 1991. NRMCA Publication No. 178.
- [14] ASTM D3967-95a, 1996, Standard test method for splitting tensile strength of rock core specimens

Aging Characteristics of Binary Concrete Filled With Fly Ash/Plasticizers on Compressive Strength

K. Sundeeep Kumar^{*1}, P. V. Subba Reddy², Dr. M. K. Rao³

¹CMR TC College, Kandlakoya, Ranga Reddy-Dist, Hyderabad, Andhra Pradesh, India

²N.B.K.R. Institute of Science & Technology, Vidyanagar, SPSR Nellore, Andhra Pradesh, India

³Professor and HOD of Civil Engineering, M.R. Engineering College, Secundrabad, Andhra Pradesh, India

ABSTRACT

In the present research presents the performance of binary concrete when filled with fly ash and plasticizers were discussed based on the soaking water in predetermined no of days such as 3, 7 and 28 days respectively. Compressive strength was evaluated for both fly ash filled concrete and super plasticizers. Hand layup technique was used to prepare the composites. Super plasticizers were proved that when the concrete filled with them with less weight ratio 1.5wt.% itself they showed good results when compared with fly ash filled binary concrete.

Keywords: Concrete, Fly Ash, Super Plasticizers, Compressive Strength

I. INTRODUCTION

It has been above 70 years to research and use fly ash. With its application, the action mechanism of fly ash had been recognized. During the initial stage, only its pozzolanic activity is paid attention. Many researchers devoted themselves to the research of the potential activity of fly ash and the hydration process of fly ash cement. With the deepening of the cognition for fly ash properties, some people found that the particles of fly ash have the morphology that is different to other pozzolanic materials. It is the unique particle morphology to make it have the ability reducing water, which other pozzolanic materials do not have. It influences not only the rheological property of fresh mortar but also the initial structure of hardened cement stone. Jan de Zeeuw and Abersch in the end of 1970s put forward that the role of fly ash, which its particle size is less than 30 μ m, may be similar to that of the micro-particle of un hydrated cement in cement stone. Danshen et al., were summarized (1981) the previous research results and put forward the hypothesis of "fly ash effects." They considered that fly ash has three effects in concrete, i.e., morphological, activated and micro aggregate effects. The three effects are relative

each other. This shows that the morphological effect is the important aspect of fly ash effects. The morphological effect means that in concrete, mineral-powdered materials produce the effect due to the morphology, structure and surface property of the particle and the particle size distribution. From the influence of fly ash on the properties of cement-based materials, the morphology effect includes three aspects: filling, lubricating and well distributing. These roles depend on the shape, size distribution, etc., of fly ash and influence many properties of concrete. Dayal and Sinha (1999) have reported the specific gravity of Indian coal ashes to range between 1.94 and 2.34 with a mean value of 2.16 and standard deviation of 0.21. The specific gravity of fly ash decreases as the particle size increases. The specific gravity increases when the fly ash particles were crushed. Typical values of the specific surface of Indian fly ashes (3267 to 6842 cm^2/g) were comparable with that of the foreign ashes (2007 to 6073 cm^2/g). Diamond 1986 studied the fly ash contained spherical particles of wide size range about 1 μ m to more than 100 μ m with smooth surface. Some of the particles were covered with surface irregularities or deposits. The interior structure of a particle revealed the presence of iron rich magnetic grain on a sphere and in the adjacent

sphere needle shaped particles of mullite crystals were present. Garg (1995) studied the morphology of Indian fly ashes. The fly ashes contained angular as well as rounded black particles, spheroid glass, and minute silica grains. Sharma (1993) has classified Indian fly ashes based on the shape of particles as one of the parameters. According to him group-fly ashes contained mainly spherical particles with the size range between 2-25 μ m. The surfaces of glassy spheres in this group are predominantly smooth without any deposit, only some adherence was observed. Poon, C.S., et al. (2002) Low calcium fly ash (ASTM Class F) has been widely used as a replacement of cement in normal and high strength concrete. In normal strength concrete, the replacement level can be more than 50%, while in high strength concrete, the replacement level is usually limited to 15 \pm 25%. According to ASTM C 618-89, fly ash, or pulverized fuel ash (PFA) in the U. K., is a "finely divided residue that results from the combustion of ground or powdered coal." It is primarily the inorganic portion of the source coal in a particulate form. The amount of literature concerning fly ash is considerable, including an ASTM standard (C 311-89) for sampling and testing fly ash for use as an admixture in Portland cement concrete. A number of standards exist which specify the desired properties of the fly ash. In the United States, ASTM C-618 is the standard. The hydraulic behavior of a fly ash is influenced by (1) its carbon content, which should be as low as possible; (2) its silica content, which should be finely divided and as high as possible; and (3) its fineness, which should be as high as possible Orchard 1973b. Fly ash is normally produced by burning coals which have been crushed and ground to a fineness of 70 to 80% passing a 75 μ m sieve. Different types of coal produce different quantities of ash. Depending on the concentration of mineral matter in that type of coal the ash content of the coal used in the western countries is generally less than 20% as the coal is processed prior to delivery at the power point, while in India the ash content of coal used is as high as 50% as the coal contains a higher percentage of rock and soil. Two kinds of fly ash are produced from the combustion of coal are Class C - High, more than 10%, calcium content produced from sub-bituminous coal and Class F - Low, less than 10%, calcium content produced from bituminous coal. The addition of fly ash to concrete has a considerable effect on the properties of fresh concrete. There is agreement that low calcium ashes show some

retarding influence on the mix. This may be due to the fact that the cement is becoming more "diluted." The effects of fly ash on fresh concrete are well known. Workability and pump ability of concrete is improved with the addition of ash because of the increase in paste content, increase in the amount of fines, and the spherical shape of the fly ash particles. Note that this improvement in workability may not be true for coarse, high carbon fly ashes. The use of fly ash may retard the time of setting of concrete. This is especially true of Class F ashes. Class C ash may or may not extend setting time and there are results that show reduction of setting time. Fly ash, in contrast to other pozzolans, reduces the water requirement of a concrete mix. It has been suggested that the major influencing factor in the plasticizing effect of fly ash is the addition of very fine, spherical particles. In fact, it has been shown that as the particle size increases, the plasticizing effect decreases. This indicates that some fly ashes do not improve workability. The rheology of fly ash cement pastes has been shown to behave as a Bingham model. Finally, the inclusion of some fly ashes in a mix reduce bleeding and segregation while improving finishability. This again can be attributed --to the increased amount of fines in the mix and lower water requirement. It is reported that the use of some fly ashes causes an increase in the amount of air entraining admixture required in concrete. It is proposed that carbon in the fly ash absorbs the AEA therefore requiring more to be used as an active role in the mix. In general class C fly ashes require less AEA than class F ashes. Also, there may be an increased rate of air content loss with manipulation if this ash is used. Plasticizers or water reducers, and super plasticizer or high range water reducers, are chemical admixtures that can be added to concrete mixtures to improve workability. In order to produce stronger concrete, less water is added (without "starving" the mix), which makes the concrete mixture less workable and difficult to mix, necessitating the use of plasticizers, water reducers, super plasticizers or dispersants. Plasticizers are also often used when pozzolanic ash is added to concrete to improve strength. This method of mix proportioning is especially popular when producing high-strength concrete and fiber-reinforced concrete. Adding 1-2% plasticizer per unit weight of cement is usually sufficient. Adding an excessive amount of plasticizer will result in excessive segregation of concrete and is not advisable. Depending on the

particular chemical used, use of too much plasticizer may result in a retarding effect. Super plasticizers have generally been manufactured from suffocated naphthalene condensate or sulfonated melamine formaldehyde, although newer products based on polycarboxylic others [1-14]. The main objectives of using fly ash in high strength concrete are to reduce heat generation and to obtain better durability properties. However, in concrete mixes prepared at a low water-to-binder (w/b) ratio, 20% fly ash content may not be sufficient to suppress the excessive heat of hydration. Manz and others (1982) have suggested that high-calcium fly ashes (Class C ashes) are best distinguished from the low-calcium (Class F) ashes by the incrementing properties. Thus, a general term 'mineral admixtures' has been suggested to describe all classes of slags, ashes, pozzolans and other cement supplements, with a further distinct one being drawn the basis of their self-cementing capabilities. The above form of classification has been proposed as being preferable to the current division of fly ashes. Ramezani pour, (1994) However the terminology, 'high-calcium' and 'low calcium' have been used in this study, in general, and Class C and Class F, while referring reporting the type of fly ashes actual used by various researchers, in their investigations. Tcnoutasse and Marion (1986) investigated the selective dissolution of different Began low-calcium fly ashes with water, hydrochloric acid solutions by chemical and microscopically techniques. The behavior of fly ashes was also studied in lime-saturated solution. The hydration mechanism was investigated as a function of time, for OPC and OPC' containing 10% to 80% of fly ashes. Cannon (1968) research carried out on the methods of proportioning fly ash concrete mixtures to obtain equal strength to those of conventional control mixtures. Cannon employed Abrams' law and a factor that accounted for the relative costs of fly ash and concrete. Rosen (1976), Gosh (1976) and Popovers (1982) extended the above concept to develop mixture proportions for fly ash concrete. Ghoul (1976) approach, are the standard guidelines available for proportioning pozzolana cements. U.K., Munday and others (1983) proposed a procedure for obtaining any desire strength at 28 days, which requires the collection of data, for a fly ash source. Brown (1982) found that both slump and vee-bee time improved increased substitutions and the changes were found to depend on the level of ash

substitution on the water content. He also observed an increase in workability up to 8% replacement of sand or aggregate by ash. Further increase in the percentage replacement caused a rapid decrease in workability. The main objective of thesis is to investigate the strengthen characteristics of the concrete using different proportions of fly ash and super plasticizers. Here fly ash is a product of pulverized coal, considered as a waste by product finding difficulty to be disposed off. Using different proportions of fly ash the maximum strength can be reached in certain proportion of fly ash value. Similarly, super plasticizers are also using different proportions the maximum strength can be reached certain proportion of super plasticizers. The scope of the study is to know the properties of the fly ash and super plasticizers in different proportions. It can be used for find the strength values and find out the maximum strength of the concrete.

II. METHODS AND MATERIAL

Materials used in Binary Concrete concrete are Cement, Fine aggregate, Coarse aggregate; Water, Fly ash, and Super plasticizer were used. Zuari 43 grade ordinary Portland cement is used for casting the elements. The following test are conducted such as Fineness test, Standard consistency test, Initial setting time test, Final setting time test, Specific gravity test, Compressive strength test were conducted. In this study we can find out the various tests like compressive strength, split tensile strength and flexural strength are done. The strength properties are done M40 grade concrete mix design. The advantage of binary concrete can be enhanced by substituting some of the cement with other materials, such as fly ash. Fly ash is one of the by-products coal combustion in power generation plants. Large amount of fly ash are discarded each year, increasing costs for disposal. On the other hand, fly ash has been shown to improve the overall performance of concrete, when substituted for a portion of the cement. In same manner super plasticizers is also added different proportions the maximum strength can be reached certain proportion of super plasticizers. Then the maximum strength can be given at a certain proportion of adding fly ash and super plasticizers at various tests. These tests based on we can identified strength of concrete in addition of fly ash and super plasticizers.

Results of the cement are tabulated in the **Table 1** as mentioned below.

Table 1 Test Results on Cement

S.NO	TEST NAME	RESULT		
1	sieve test	8 %		
2	standard consistency	29 %		
3	Initial setting time	52 min		
4	Final setting time	480 min		
5	Specific gravity test	3.15		
6	Compressive strength	3 days	7 days	28 days
		N/mm ²	N/mm ²	N/mm ²
		22.12	30.12	44.23

In this investigation fine aggregate is naturally available sand and it is free from dirt, dust and any organic matter. The fine aggregate used for the project was obtained from Penna river .The following tests were conducted on the sand such as Sieve analysis, Bulking of sand by volume method, Specific gravity test. **Table 2** indicates the results of the fine aggregates as mentioned below.

Table 2 Test result on fine aggregate

S.NO	TEST NAME	RESULT
1	Sieve analysis	Zone III
2	Bulking of sand by volume method	12.5%
3	Specific gravity test	2.51
4	Relative density	45% (medium dense)

In this investigation hard broken granite aggregate is used. The size course aggregate is various from 12 mm to 20 mm. The source the aggregates is Srikalahasti. The following tests like sp. gravity test, fineness modulus test, water absorption test, aggregate impact test, and aggregate crushing strength tests were conducted. The final results thereof as mentioned below in the **Table 3**.

Table 3 Results of the course aggregates of the filler.

S.NO	TEST NAME	RESULT
1	Fineness modulus	7.5
2	Specific gravity	2.33
3	Water absorption	2.1%
4	Crushing strength	22.43%
5	Impact test	28.12%

The following tests of fly ash such as Moisture content, Loss on ignition, Silicon oxide content, Alumina oxide content, Calcium oxide content, Chloride content, Free calcium oxide content, Total alkali oxides content, Particle density determination (by Pycnometer bottle and Le-Chatlier Flask methods), Fineness determination (by dry sieving, wet sieving, Blaine air permeability and laser methods) were conducted. The following tests for fly ash cement pastes, mortars, or concretes are outlined and they are namely Soundness (expansion test), water requirement (expressed as water content of test specimen divided by water content of control specimen to achieve equal specified consistencies), Preparation and curing of specimens, determination of compressive strength (28 days).

III. RESULT AND DISCUSSION

The following tests are conducted on binary concrete in this study for different proportions of fly ash and super plasticizer. This test was developed by Chapman at the U.S in 1913, this is the simplest test and that most commonly used in on site testing and it has been referred in B.S 1881. This is used to measure the compressive strength of concrete, and it can be used in laboratory. The apparatus for conducting the compressive strength test essentially consists of 40t U.T.M., weighing balance, scale, cube moulds of 15cms sides, vibrator, pan for mixing cement & sand, measuring jar, trowel, and non-porous plate. Place the green concrete in moulds in equal three layers and with vibrator. Keep the specimens in the moulds at 90% relative humidity. After curing period is completed, moisture around the specimen is wiped-out and weighs the specimen. The non-casting faces are placed in the jaws [10]. Apply the uniaxial load at a rate of 140 kg/cm²/min up to the specimen is crushed. The ultimate load is note down. **Figure 1** shows the variation of compressive strength as a function of fly ash after 3

days indicates that the compressive strength is gradually decreases when the fly ash increases on other hand. It was also observed that the when the fly ash was 0wt.% maximum compressive strength was observed.



Figure 1. Compression testing machine.

Table 4 Test result on compressive strength

Addition of fly ash	Compressive strength(N/mm ²)		
	3 days	7 days	28 days
0%	26.68	29.77	45.77
10%	25.44	32.22	50.44
20%	24.58	34.60	52.33
30%	23.58	35.56	55.56
40%	22.98	28.25	44.23
Super plasticizers			
0%	26.68	29.77	45.77
0.50%	29.11	32.85	54.12
1%	30.01	35.98	54.85
1.50%	30.98	36.01	55.12
2%	25.12	28.12	44.85

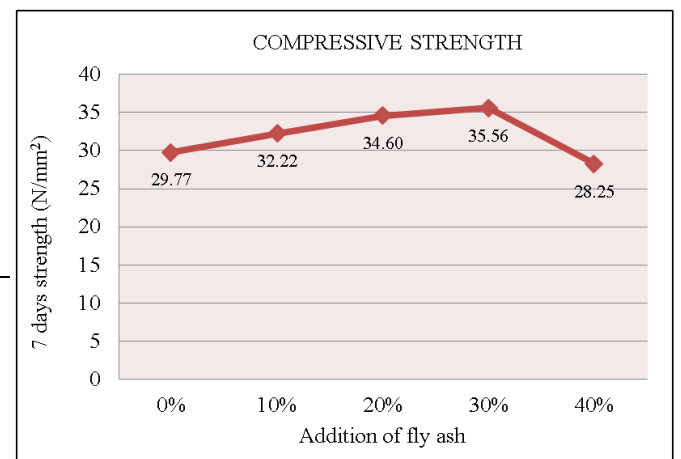
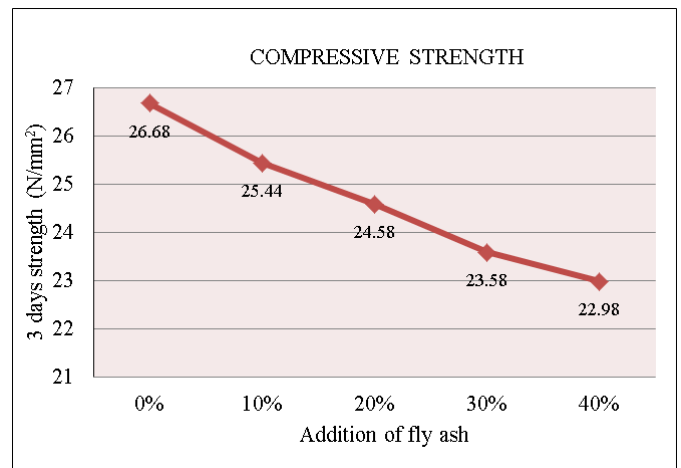


Figure 2 : Variation of compressive strength as a function of fly ash for 3 days.

Figure 2 shows the variation of compressive strength as a function of fly ash after 7days indicates that the compressive strength is gradually increases when the fly ash increases on other hand. It was also observed that the when the fly ash was 30wt.% maximum compressive strength was observe as 35.56 N/mm2 and after that compressive strength is decreased [1]. **Figure 3** shows the variation of compressive strength as a function of fly ash after 7days indicates that the compressive strength is gradually increases when the fly ash increases on other hand. It was also observed that the when the fly ash was 30wt.% maximum compressive strength was observe as

55.56 N/mm² and after that compressive strength is decreased. When soaking days are increased as a results of that strength is gradually increases.

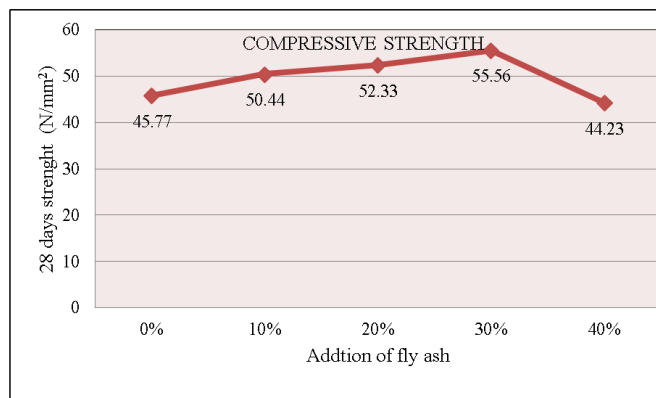


Figure 3 Variation of compressive strength as a function of fly ash for 28 days.

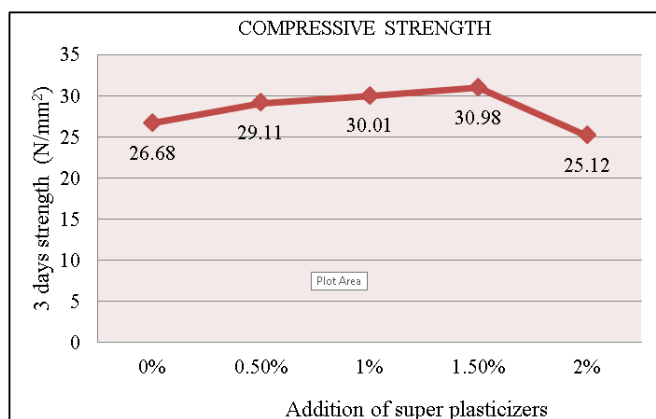


Figure 4 Variation of compressive strength as a function of super plasticizers after soaking 3 days in water.

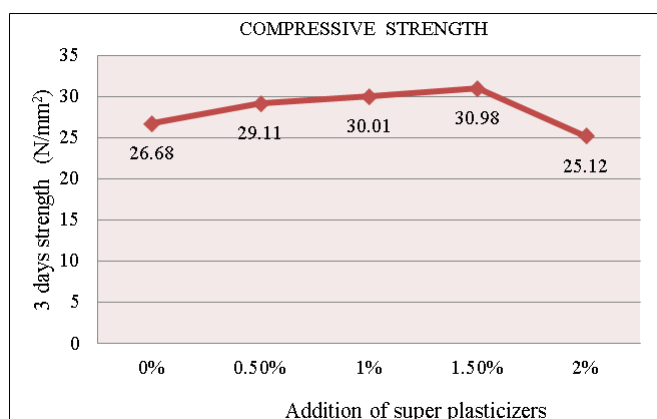


Figure 5 Variation of compressive strength as a function of super plasticizers after soaking 7 days in water.

Figure 4 shows the variation of compressive strength as a function of fly ash after 3days indicates that the

compressive strength is gradually increases when the plasticizers increase on other hand. It was also observed that the when the fly ash was 1.5wt.% maximum compressive strength was observe as 30.98N/mm² and after that compressive strength is decreased. When soaking days are increased as a result of that strength is gradually increases. **Figure 5** shows the variation of compressive strength as a function of fly ash after 7days indicates that the compressive strength is gradually increases when the plasticizers increase on other hand. It was also observed that the when the fly ash was 1.5wt.% maximum compressive strength was observe as 36.01N/mm² and after that compressive strength is decreased. When soaking days are increased as a result of that strength is gradually increases. **Figure 6** shows the variation of compressive strength as a function of fly ash after 28days indicates that the compressive strength is gradually increases when the plasticizers increase on other hand. It was also observed that the when the fly ash was 1.5wt.% maximum compressive strength was observe as 55.12N/mm² and after that compressive strength is decreased. When soaking days are increased as a result of that strength is gradually increases.

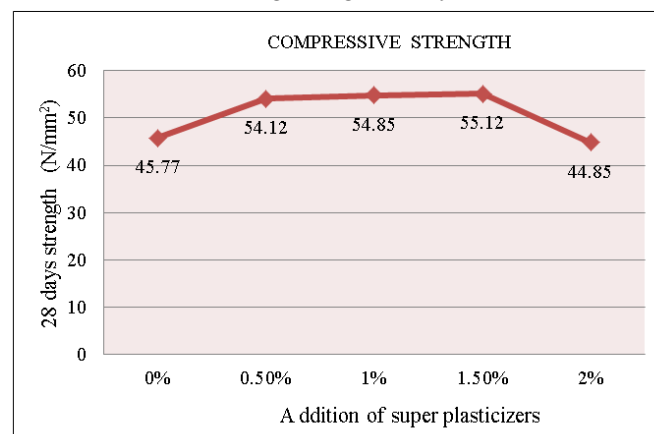


Figure 6 Variation of compressive strength as a function of super plasticizers after soaking 28 days in water.

IV. CONCLUSION

For 43 grade cement with M40 mix, by adding up to 30% of fly ash to the cement, the strength is increased and by adding 40% of fly ash the strength is decreasing. Fly ash is added at different proportions namely 0%, 10%, 20%, 30% and 40%. The test results show that on addition of 30% of fly ash to cement it has gained maximum strength at 28 days period but the rate of strength gain compared to ordinary Portland cement concrete OPCC is

at slower rate at initial days. The compressive strength increased by 22.44% when compare to normal concrete. By use of fly ash as admixture, the cost of construction is also considerably reduced. Non-biodegradable fly ash is effectively utilized in binary concrete, so it reduces the disposal problem of fly ash. For 43 grade cement with M40 mix, by adding 0%, 0.5%, 1.0%, 1.5% of super plasticizer to the mix prepared the strength is slightly increased and at adding 2.0% of plasticizer to the mix prepared the strength will slightly decreased. The test results show that on addition of 1.5% of super plasticizers to concrete it has gained maximum strength at 28 days period. The compressive strength increased by 20.22%, split tensile strength increased by 16.32% when compare to normal concrete. Super plasticizer may not increase the strength of concrete directly. But it helps in reducing the w/c ratio, which in turn result in the increase of strength of concrete due to reduction of w/c ratio. It is concluded that when compare to super plasticizer, fly ash gives more desirable properties to concrete and ecofriendly.

V. ACKNOWLEDGEMENTS

Authors would like to thank all the professors from the Civil Engineering Department for constant guidance towards the successful completion of this project.

VI. REFERENCES

- [1] Court, C. L., "Mix Design and Abrasion Resistance of Concrete," Symposium on Mix Design and Quality Control of Concrete, Cement and Concrete Association, London (1954)
- [2] Abdun-Nur, E. A., Fly Ash in Concrete, Highway Research Board Bulletin 284, Washington, D.C. (1961)
- [3] ASTM Committee C-9, Manual of Concrete Testing, 1976 Annual Book of ASTM Standards, Part 14, Philadelphia (1976)
- [4] ASTM, Manual of Cement Testing, 1988 Annual Book of ASTM Standards, Vol. 04.01 (1988)
- [5] ASTM Committee C-9, Manual of Aggregate and Concrete Testing, 1989 Annual Book of ASTM Standards, Part 14, Philadelphia (1989)
- [6] American Coal Ash Association, Proceeding: Eighth International Ash Utilization Symposium, Vols. 1 and 2. EPRI CS-5362 (1987)
- [7] J. M. Hodgkinson (2000). Mechanical Testing of Advanced Fibre Composites. Cambridge: Woodhead Publishing, Ltd. p. 132–133.
- [8] William D. Callister, Jr. Materials Science and Engineering. Hoken: John Wiley & Sons, Inc., 2003. Peggy Carrasquillo, chapter 14, SYM STP 169C, significancies of testing and properties of concrete and concrete making materials, American society for testing and materials west Conshohocken, PA.
- [9] How should strength be measured for concrete paving? Richard c.meininger, (NRMCA TIL), and data summary NRMCA TIL 451, NRMCA silver spring, MD.
- [10] "Significance of Tests and Properties of Concrete and Concrete-Making Materials," Chapter 12 on Strength, ASTM STP 169B.
- [11] "Studies of Flexural Strength of Concrete, Part 3, Effects of Variations in Testing Procedures," by Stanton Walker and D.L. Bloem, NRMCA Publication No. 75 (ASTM Proceedings, Volume 57, 1957).
- [12] "Variation of Laboratory Concrete Flexural Strength Tests," by W. Charles Greer, Jr., ASTM, Cement, Concrete and Aggregates, Winter, 1983.
- [13] "Concrete Mixture Evaluation and Acceptance for Air Field Pavements" by Richard O. Meininger and Norman R. Nelson, ASCE Air Field Pavement Conference, September, 1991. NRMCA Publication No. 178.
- [14] ASTM D3967-95a, 1996, Standard test method for splitting tensile strength of rock core specimens

Utilization of Fly Ash and Super Plasticizers Filled Binary Concrete on Split Tensile Strength

K. Sundeep Kumar^{*1}, P. V. Subba Reddy², Dr. M. K. Rao³

¹CMR TC College, Kandlakoya, Ranga Reddy-Dist, Hyderabad, Andhra Pradesh, India

²N.B.K.R. Institute of Science & Technology, Vidyanagar, SPSR Nellore, Andhra Pradesh, India

³Professor and HOD of Civil Engineering, M.R. Engineering College, Secundrabad, Andhra Pradesh, India

ABSTRACT

In the present research presents the performance of binary concrete when filled with fly ash and plasticizers were discussed based on the soaking water in predetermined no of days such as 3, 7 and 28 days respectively. Split tensile strength was evaluated for both fly ash filled concrete and super plasticizers. Hand layup technique was used to prepare the composites. Super plasticizers were proved that when the concrete filled with them with less weight ratio 1.5wt.% itself they showed good results when compared with fly ash filled binary concrete.

Keywords: Concrete, Fly Ash, Super Plasticizers, Split Tensile Strength

I. INTRODUCTION

It has been above 70 years to research and use fly ash. With its application, the action mechanism of fly ash had been recognized. During the initial stage, only its pozzolanic activity is paid attention. Many researchers devoted themselves to the research of the potential activity of fly ash and the hydration process of fly ash cement. With the deepening of the cognition for fly ash properties, some people found that the particles of fly ash have the morphology that is different to other pozzolanic materials. It is the unique particle morphology to make it have the ability reducing water, which other pozzolanic materials do not have. It influences not only the rheological property of fresh mortar but also the initial structure of hardened cement stone.

Jan de Zeeuw and Abersch in the end of 1970s put forward that the role of fly ash, which its particle size is less than 30 μ m, may be similar to that of the micro-particle of un hydrated cement in cement stone. Danshen et al., in 1981 summarized the previous research results and put forward the hypothesis of "fly ash effects." They

considered that fly ash has three effects in concrete, i.e., morphological, activated and micro aggregate effects. The three effects are relative each other. This shows that the morphological effect is the important aspect of fly ash effects. The morphological effect means that in concrete, mineral-powdered materials produce the effect due to the morphology, structure and surface property of the particle and the particle size distribution. From the influence of fly ash on the properties of cement-based materials, the morphology effect includes three aspects: filling, lubricating and well distributing. These roles depend on the shape, size distribution, etc., of fly ash and influence many properties of concrete. Dayal and Sinha (1999) have reported the specific gravity of Indian coal ashes to range between 1.94 and 2.34 with a mean value of 2.16 and standard deviation of 0.21. The specific gravity of fly ash decreases as the particle size increases. The specific gravity increases when the fly ash particles were crushed. Typical values of the specific surface of Indian fly ashes (3267 to 6842 cm^2/g) were comparable with that of the foreign ashes (2007 to 6073 cm^2/g). Diamond 1986 studied the fly ash contained spherical particles of wide size range about 1 μ m to more than 100 μ m with smooth surface. Some of the particles were covered with surface irregularities or deposits. The

interior structure of a particle revealed the presence of iron rich magnetic grain on a sphere and in the adjacent sphere needle shaped particles of mullite crystals were present. Garg (1995) studied the morphology of Indian fly ashes. The fly ashes contained angular as well as rounded black particles, spheroid glass, and minute silica grains. Sharma (1993) has classified Indian fly ashes based on the shape of particles as one of the parameters. According to him group-fly ashes contained mainly spherical particles with the size range between 2-25 μ m. The surfaces of glassy spheres in this group are predominantly smooth without any deposit, only some adherence was observed. Poon, C.S., et al. (2002) Low calcium fly ash (ASTM Class F) has been widely used as a replacement of cement in normal and high strength concrete. In normal strength concrete, the replacement level can be more than 50%, while in high strength concrete; the replacement level is usually limited to 15 \pm 25%. According to ASTM C 618-89, fly ash, or pulverized fuel ash (PFA) in the U. K., is a "finely divided residue that results from the combustion of ground or powdered coal." It is primarily the inorganic portion of the source coal in a particulate form. The amount of literature concerning fly ash is considerable, including an ASTM standard (C 311-89) for sampling and testing fly ash for use as an admixture in Portland cement concrete. A number of standards exist which specify the desired properties of the fly ash. In the United States, ASTM C-618 is the standard. The hydraulic behavior of a fly ash is influenced by (1) its carbon content, which should be as low as possible; (2) its silica content, which should be finely divided and as high as possible Orchard 1973b. Fly ash is normally produced by burning coals which have been crushed and ground to a fineness of 70 to 80% passing a 75 μ m sieve. Different types of coal produce different quantities of ash. Depending on the concentration of mineral matter in that type of coal the ash content of the coal used in the western countries is generally less than 20% as the coal is processed prior to delivery at the power point, while in India the ash content of coal used is as high as 50% as the coal contains a higher percentage of rock and soil. Two kinds of fly ash are produced from the combustion of coal are Class C - High, more than 10%, calcium content produced from sub-bituminous coal and Class F - Low, less than 10%, calcium content produced from bituminous coal. The addition of fly ash to concrete has

a considerable effect on the properties of fresh concrete. There is agreement that low calcium ashes show some retarding influence on the mix. This may be due to the fact that the cement is becoming more "diluted." The effects of fly ash on fresh concrete are well known. Workability and pump ability of concrete is improved with the addition of ash because of the increase in paste content, increase in the amount of fines, and the spherical shape of the fly ash particles. Note that this improvement in workability may not be true for coarse, high carbon fly ashes. The use of fly ash may retard the time of setting of concrete. This is especially true of Class F ashes. Class C ash may or may not extend setting time and there are results that show reduction of setting time. Fly ash, in contrast to other pozzolans, reduces the water requirement of a concrete mix. It has been suggested that the major influencing factor in the plasticizing effect of fly ash is the addition of very fine, spherical particles. In fact, it has been shown that as the particle size increases, the plasticizing effect decreases. This indicates that some fly ashes do not improve workability. The rheology of fly ash cement pastes has been shown to behave as a Bingham model. Finally, the inclusion of some fly ashes in a mix reduce bleeding and segregation while improving finishability. This again can be attributed --to the increased amount of fines in the mix and lower water requirement. It is reported that the use of some fly ashes causes an increase in the amount of air entraining admixture required in concrete. It is proposed that carbon in the fly ash absorbs the AEA therefore requiring more to be used as an active role in the mix. In general class C fly ashes require less AEA than class F ashes. Also, there may be an increased rate of air content loss with manipulation if this ash is used. Plasticizers or water reducers, and super plasticizer or high range water reducers, are chemical admixtures that can be added to concrete mixtures to improve workability. In order to produce stronger concrete, less water is added (without "starving" the mix), which makes the concrete mixture less workable and difficult to mix, necessitating the use of plasticizers, water reducers, super plasticizers or dispersants. Plasticizers are also often used when pozzolanic ash is added to concrete to improve strength. This method of mix proportioning is especially popular when producing high-strength concrete and fiber-reinforced concrete. Adding 1-2% plasticizer per unit weight of cement is usually sufficient. Adding an excessive amount of

plasticizer will result in excessive segregation of concrete and is not advisable. Depending on the particular chemical used, use of too much plasticizer may result in a retarding effect. Super plasticizers have generally been manufactured from sulfonated naphthalene condensate or sulfonated melamine formaldehyde, although newer products based on polycarboxylic others [1-14]. The main objectives of using fly ash in high strength concrete are to reduce heat generation and to obtain better durability properties. However, in concrete mixes prepared at a low water-to-binder (w/b) ratio, 20% fly ash content may not be sufficient to suppress the excessive heat of hydration. Manz and others (1982) have suggested that high-calcium fly ashes (Class C ashes) are best distinguished from the low-calcium (Class F) ashes by the incrementing properties. Thus, a general term 'mineral admixtures' has been suggested to describe all classes of slags, ashes, pozzolans and other cement supplements, with a further distinct on being drawn the basis of their self-cementing capabilities. The above form of classification has been proposed as being preferable to the current division of fly ashes. Ramezani pour, (1994) However the terminology, 'high-calcium' and 'low calcium have been used in this study, in general, and Class C and Class F, while referring reporting the type of fly ashes actual used by various researchers, in their investigations. Tcnoutasse and Marion (1986) investigated the selective dissolution of different Began low-calcium fly ashes with water, hydrochloric acid solutions by chemical and microscopically techniques. 'The behavior of fly ashes was also studied in lime-saturated solution. The hydration mechanism was investigated as a function of time, for OPC and OPC' containing 10% to 80% of fly ashes. Cannon (1968) research carried out on the methods of proportioning fly ash concrete mixtures to obtain equal strength to those of conventional control mixtures. Cannon employed Abrams' law and a factor that accounted for the relative costs of fly ash and concrete. Rosen (1976), Gosh (1976) and Popovers (1982) extended the above concept to develop mixture proportions for fly ash concrete. Ghoul (1976) approach, are the standard guidelines available for proportioning pozzolana cements. U.K., Munday and others (1983) proposed a procedure for obtaining any desire strength at 28 days, which requires the collection of data, for a fly ash source. Brown (1982) found that both slump and vee-bee time improved

increased substitutions and the changes were found to depend on the level of ash substitution on the water content. He also observed an increase in workability up to 8% replacement of sand or aggregate by ash. Further increase in the percentage replacement caused a rapid decrease in workability. The main objective of thesis is to investigate the strengthen characteristics of the concrete using different proportions of fly ash and super plasticizers. Here fly ash is a product of pulverized coal, considered as a waste by product finding difficulty to be disposed off. Using different proportions of fly ash the maximum strength can be reached in certain proportion of fly ash value. Similarly, super plasticizers are also using different proportions the maximum strength can be reached certain proportion of super plasticizers. The scope of the study is to know the properties of the fly ash and super plasticizers in different proportions. It can be used for find the strength values and find out the maximum strength of the concrete.

II. METHODS AND MATERIAL

Materials used in Binary Concrete concrete are Cement, Fine aggregate, coarse aggregate, water, fly ash, and super plasticizer were used in this project. Zuari 43 grade ordinary Portland cement is used for casting the elements. The following test are conducted such as Fineness test, Standard consistency test, Initial setting time test, Final setting time test, Specific gravity test, Compressive strength test were conducted. In this study we can find out the various tests like compressive strength, split tensile strength and flexural strength are done. The strength properties are done M40 grade concrete mix design. The advantage of binary concrete can be enhanced by substituting some of the cement with other materials, such as fly ash. Fly ash is one of the by-products coal combustion in power generation plants. Large amount of fly ash are discarded each year, increasing costs for disposal. On the other hand, fly ash has been shown to improve the overall performance of concrete, when substituted for a portion of the cement. In same manner super plasticizers is also added different proportions the maximum strength can be reached certain proportion of super plasticizers. Then the maximum strength can be given at a certain proportion of adding fly ash and super plasticizers at various tests. These tests based on we can identified strength of

concrete in addition of fly ash and super plasticizers. Results of the cement are tabulated in the **Table 1** as mentioned below.

The mathematical editor on which along with text you can also write

Table 1 Test results on cement

S.NO	TEST NAME	RESULT		
1	sieve test	8 %		
2	standard consistency	29 %		
3	Initial setting time	52 min		
4	Final setting time	480 min		
5	Specific gravity test	3.15		
6	Compressive strength	3 days	7 days	28 days
		N/mm ²	N/mm ²	N/mm ²
		22.12	30.12	44.23

In this investigation fine aggregate is naturally available sand and it is free from dirt, dust and any organic matter. The fine aggregate used for the project was obtained from Penna river .The following tests were conducted on the sand such as Sieve analysis, Bulking of sand by volume method, Specific gravity test. **Table 2** indicates the results of the fine aggregates as mentioned below.

Table 2 Test result on fine aggregates

S.NO	TEST NAME	RESULT
1	Sieve analysis	Zone III
2	Bulking of sand by volume method	12.5%
3	Specific gravity test	2.51
4	Relative density	45% (medium dense)

In this investigation hard broken granite aggregate is used. The size course aggregate is various from 12 mm to 20 mm. The source the aggregates is Srikalahasti. The following tests like sp. gravity test, fineness modulus test, water absorption test, aggregate impact test, and aggregate crushing strength tests were conducted. The final results thereof as mentioned below in the **Table 3**.

Table 3 Evaluation of course aggregates concrete composites

S.NO	TEST NAME	RESULT
1	Fineness modulus	7.5
2	Specific gravity	2.33
3	Water absorption	2.1%
4	Crushing strength	22.43%
5	Impact test	28.12%

The following tests of fly ask such as Moisture content, Loss on ignition, Silicon oxide content, Alumina oxide content, Calcium oxide content, Chloride content, Free calcium oxide content, Total alkali oxides content, Particle density determination (by Pycnometer bottle and Le-Chatlier Flask methods), Fineness determination (by dry sieving, wet sieving, Blaine air permeability and laser methods) were conducted. The following tests for fly ash cement pastes, mortars, or concretes are outlined and they are namely Soundness (expansion test), water requirement (expressed as water content of test specimen divided by water content of control specimen to achieve equal specified consistencies), Preparation and curing of specimens, determination of compressive strength (28 days).

III. RESULT AND DISCUSSION

The following tests are conducted on binary concrete in this study for different proportions of fly ash and super plasticizer.

Split Tensile Strength Test:

This test was developed by Chapman at the U.S in 1913, this is the simplest test and that most commonly used in on site testing and it has been referred in B.S 1881. This is used to measure the compressive strength of concrete, and it can be used in laboratory. The apparatus for conducting the compressive strength test essentially consists of 40t U.T.M., weighing balance, scale, cube moulds of 15cms sides, vibrator, pan for mixing cement & sand, measuring jar, trowel, and non-porous plate. Place the green concrete in moulds in equal three layers and with vibrator. Keep the specimens in the moulds at 90% relative humidity. After curing period is completed, moisture around the specimen is wiped-out and weighs the specimen. The non-casting faces are placed in the

jaws [10]. Apply the uniaxial load at a rate of 140 kg/cm²/min up to the specimen is crushed. The ultimate load is note down. **Figure 5** shows the variation of split strength as a function of fly ash after 3 days soaking in the water conforms that the tensile strength is gradually increases when the fly ash increases on other hand. It was also observed that the when the fly ash was 30wt.% maximum tensile strength was observed as 2.75N/mm² and after that strength was decreased. **Figure 6** shows the variation of tensile strength as a function of fly ash after 7days soaked in the water was indicates that the tensile strength is gradually increases when the fly ash increases on other hand. It was also observed that the when the fly ash was 30wt.% maximum tensile strength was observe as 3.08 N/mm² and after that tensile strength is decreased [12].

This test was developed by BRAZILAN at japan in 1943, this is the simplest test and it has been referred in ASTM 496.This method is used to measure the tensile strength of concrete, and it is a laboratory test.

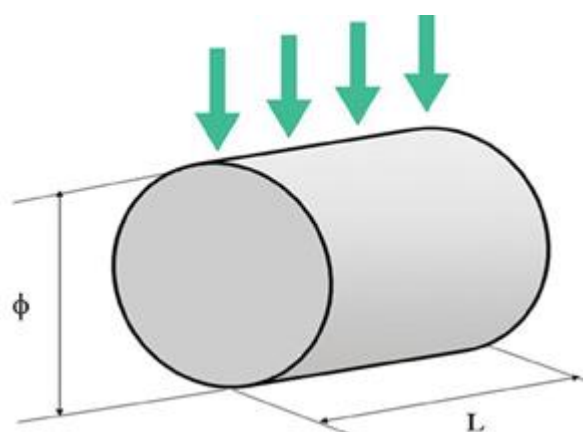


Figure 2. Application of load on cylinder

The apparatus for conducting the split tensile strength test essentially consists of 40t U.T.M., weighing balance, scale, cylinder of size 15 cm diameter and height 30 cm, vibrator, measuring jar, pan for mixing cement & sand, trowel, and non-porous plate. The test is carried out by placing a cylinder specimen horizontally between loading surface of the tensile testing machine. The load is applied till the failure of the specimen. The compressive stress is acting for about 1/6th depth and remaining 5/6th depth is subjected to tension. Metal strip 25 mm wide, 5mm thick and 30 mm long is used as packing to allowing distribution of load over a

reasonable area. This will reduce high compressive stress near the point's application of load.

$$\text{Split tensile strength } f = \frac{2p}{\pi dl}$$

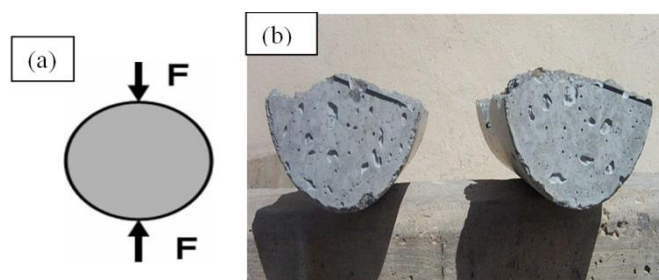


Figure 3 Nature of (a) force applied on the splitted cylinder and (b) fractured cylinder after load is applied.



Figure 4 Illustration of compressive strength testing machine with cylindrical shape binary concrete.

Table 4 Variation of split tensile strength as a function of fillers

Specifications	Split tensile strength (N/mm ²)		
	3 days	7 days	28 days
Addition of fly ash			
0%	2.26	2.50	3.00
10%	2.40	2.68	3.51
20%	2.60	2.90	3.53
30%	2.70	3.08	3.70
40%	2.16	2.55	2.8
Super plasticizers			
0%	2.26	2.67	2.9

0.50%	2.70	3.20	3.54
1.0%	2.87	3.35	3.68
1.50%	2.96	3.45	3.72
2.0%	2.22	2.54	2.85

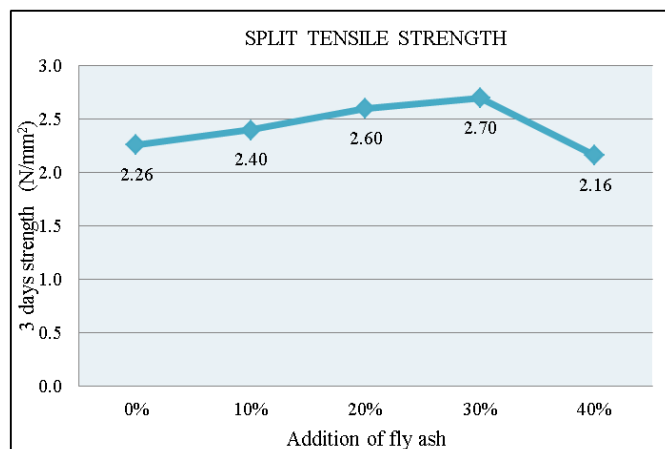


Figure 5 Variation of tensile strength as a function of fly ash when binary concrete soaked in to water for 3 days.

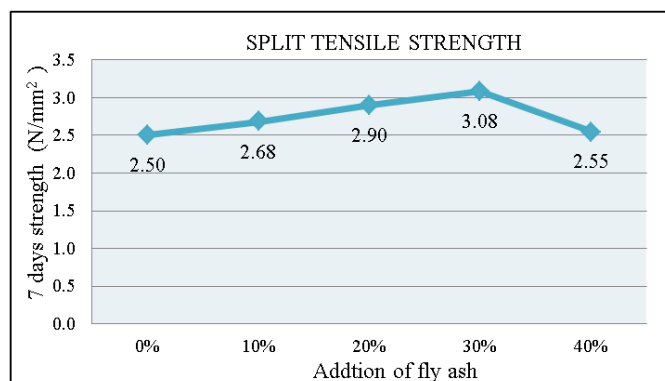


Figure 6 Variation of tensile strength as a function of fly ash when binary concrete soaked in to water for 7 days.

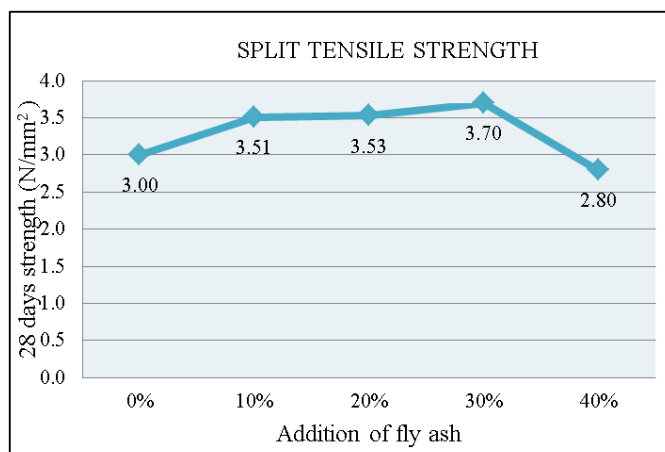


Figure 7 Variation of tensile strength as a function of fly ash when binary concrete soaked in to water for 28 days.

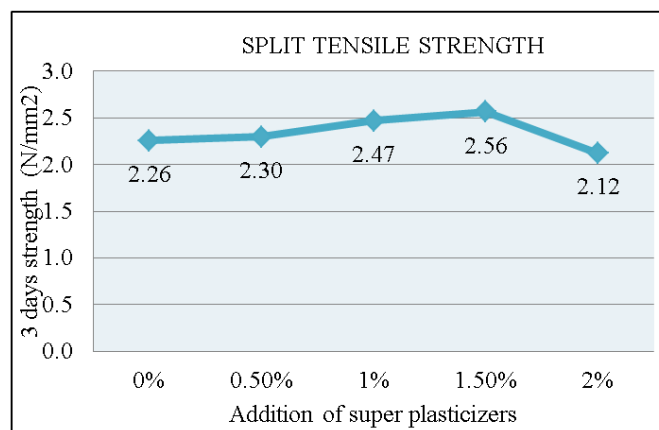


Figure 8 Variation of tensile strength as a function of super plasticizers when binary concrete soaked in to water for 3 days.

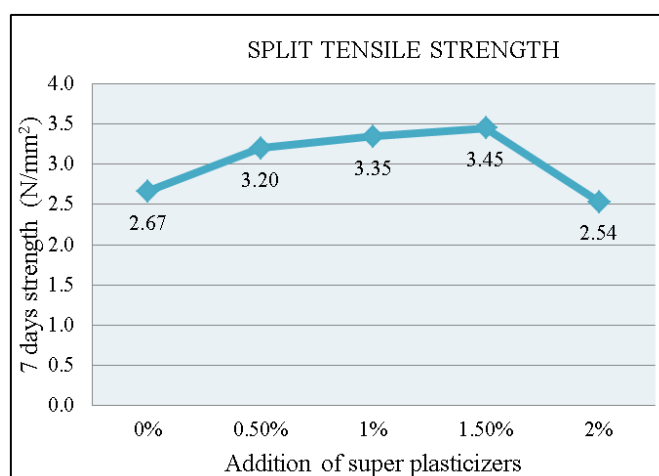


Figure 9 Variation of tensile strength as a function of super plasticizers when binary concrete soaked in to water for 7 days.

Figure 7 shows the variation of tensile strength as a function of fly ash after 28 days soaked in the water was indicates that the tensile strength is gradually increases when the fly ash increases on other hand. It was also observed that the when the fly ash was 30wt.% maximum tensile strength was observe as 3.70 N/mm² and after that tensile strength is decreased [13]. **Figure 8** shows the variation of tensile strength as a function of super plasticizers after 3 days indicates that the tensile strength is gradually increases when the plasticizers increase on other hand. It was also observed that the when the fly ash was 1.5wt.% maximum compressive strength was observe as 2.56/mm² and after that tensile strength is decreased. When soaking days are increased as a result of that strength is gradually increases.

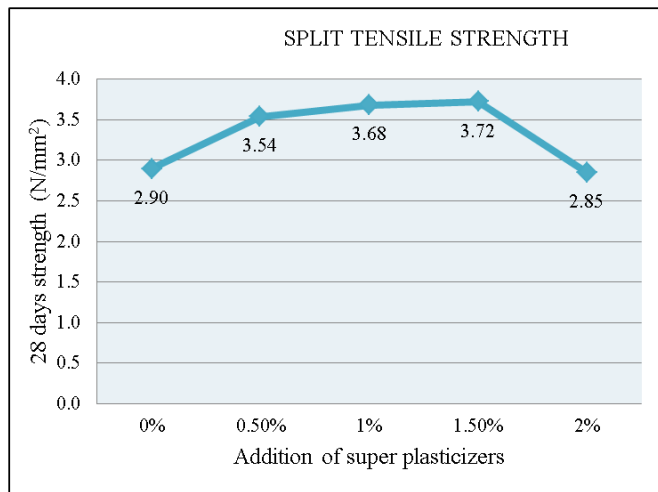


Figure 10 Variation of tensile strength as a function of super plasticizers when binary concrete soaked in to water for 28days.

Figure 9 shows the variation of tensile strength as a function of fly ash after 7days indicates that the tensile strength is gradually increases when the plasticizers increase on other hand. It was also observed that the when the fly ash was 1.5wt.% maximum tensile strength was observe as 3.45N/mm^2 and after that tensile strength is decreased. When soaking days are increased as a result of that strength is gradually increases. **Figure 10** shows the variation of tensile strength as a function of fly ash after 28days indicates that the tensile strength is gradually increases when the plasticizers increase on other hand. It was also observed that the when the fly ash was 1.5wt.% maximum tensile strength was observe as 3.72N/mm^2 and after that tensile strength is decreased. When soaking days are increased as a result of that strength is gradually increases.

IV. CONCLUSION

- Fly ash is added at different proportions namely 0%, 10%, 20%, 30% and 40%.
- For 43 grade cement with M40 mix, by adding up to 30% of fly ash to the cement, the strength is increased and by adding 40% of fly ash the strength is decreasing.
- The test results show that on addition of 30% of fly ash to cement it has gained maximum strength at 28 days period but the rate of strength gain compared to ordinary Portland cement concrete OPCC is at slower rate at initial days.

- Split tensile strength increased by 18.37% and flexural strength increased by 16.18% when compare to normal concrete.
- By use of fly ash as admixture, the cost of construction is also considerably reduced.
- Non-biodegradable fly ash is effectively utilized in Binary concrete, so it reduces the disposal problem of fly ash.
- For 43 grade cement with M40 mix, by adding 0%, 0.5%, 1.0%, 1.5% of super plasticizer to the mix prepared the strength is slightly increased and at adding 2.0% of plasticizer to the mix prepared the strength will slightly decreased.
- The test results show that on addition of 1.5% of super plasticizers to concrete it has gained maximum strength at 28 days period
- Split tensile strength increased by 16.32% and flexural strength increased by 13.46% when compare to normal concrete.
- Super plasticizer may not increase the strength of concrete directly. But it helps in reducing the w/c ratio. Which in turn result in the increase of strength of concrete due to reduction of w/c ratio.
- It is concluded that when compare to super plasticizer, fly ash gives more desirable properties to concrete and ecofriendly.

V. ACKNOWLEDGEMENTS

Authors would like to thank all the professors from the Civil Engineering Department for constant guidance towards the successful completion of this project.

VI. REFERENCES

- [1] A&Court, C. L., "Mix Design and Abrasion Resistance of Concrete," Symposium on Mix Design and Quality Control of Concrete, Cement and Concrete Association, London (1954)
- [2] Abdun-Nur, E. A., Fly Ash in Concrete, Highway Research Board Bulletin 284, Washington, D.C. (1961)
- [3] ASTM Committee C-9, Manual of Concrete Testing, 1976 Annual Book of ASTM Standards, Part 14, Philadelphia (1976)
- [4] ASTM, Manual of Cement Testing, 1988 Annual Book of ASTM Standards, Vol. 04.01 (1988)

- [5] ASTM Committee C-9, Manual of Aggregate and Concrete Testing, 1989 Annual Book of ASTM Standards, Part 14, Philadelphia (1989)
- [6] American Coal Ash Association, Proceeding: Eighth International Ash Utilization Symposium, Vols. 1 and 2. EPRI CS-5362 (1987)
- [7] J. M. Hodgkinson (2000). Mechanical Testing of Advanced Fibre Composites. Cambridge: Woodhead Publishing, Ltd. p. 132–133.
- [8] William D. Callister, Jr. Materials Science and Engineering. Hoken: John Wiley & Sons, Inc., 2003. Peggy Carrasquillo, chapter 14, SYM STP 169C, significances of testing and properties of concrete and concrete making materials, American society for testing and materials west Conshohocken, PA.
- [9] How should strength be measured for concrete paving? Richard c. meininger, NRMCA TIL), and data summary NRMCA TIL 451, NRMCA silver spring, MD.
- [10] “Significance of Tests and Properties of Concrete and Concrete-Making Materials,” Chapter 12 on Strength, ASTM STP 169B.
- [11] “Studies of Flexural Strength of Concrete, Part 3, Effects of Variations in Testing Procedures,” by Stanton Walker and D.L. Bloem, NRMCA Publication No. 75 (ASTM Proceedings, Volume 57, 1957).
- [12] “Variation of Laboratory Concrete Flexural Strength Tests,” by W. Charles Greer, Jr., ASTM, Cement, Concrete and Aggregates, Winter, 1983.
- [13] “Concrete Mixture Evaluation and Acceptance for Air Field Pavements” by Richard O. Meininger and Norman R. Nelson, ASCE Air Field Pavement Conference, September, 1991. NRMCA Publication No. 178.
- [14] ASTM D3967-95a, 1996, Standard test method for splitting tensile strength of rock core specimens

Pedestrian Crossing Behaviour at Suchitra Junction on NH-44 using Discrete & Continuous Model

Venkatesh

M. Tech. Student

Malla Reddy Engineering College, (Autonomous) Kompally

A. Nagasaibaba

Assistant Professor

Malla Reddy Engineering College, (Autonomous) Kompally

Dr. M. Kameswara Rao

Professor

Malla Reddy Engineering College, (Autonomous) Kompally

Abstract

In this paper, a brief practical review is presented on the statistical evidence showing the Pedestrian road safety is a key point of the transport road safety policy in urban areas. Pedestrians are vulnerable road users and despite their limited representation in traffic events, pedestrian involved injuries and fatalities are overrepresented in traffic collisions. This paper presents the findings from the examination of the pedestrian crossing behaviour in signalized crosswalks. The study took place in peak traffic hours, during the summer. The target of the study was to count the pedestrian crossing time and velocity for each crosswalk. Furthermore, the target was to identify the illegal pedestrian crossing with red traffic light, criticize their behaviour and propose remedial actions. The traffic planners mostly give stress on motorized mode of movement. All kinds of steps are taken for development of roads in terms of safety, speed or time interval at intersections in case of motorized vehicle. But in present traffic condition, the non-motorized mode of traffic is also increasing. The pedestrians and bicyclists are occupying the track of motorized vehicle as no separate grades are provided for them. It leads to traffic congestion as well as the safety factor of pedestrian is at stake. According to HCM 2010, for this heterogeneous traffic, we can't just increase the level of service by developing the quality of roads for vehicles. Steps have been taken to reclaim pavement for pedestrians by removing the encroachment on footpath. A study was carried out on Suchitra Junction where about footpath surrounding it and separated from road by divider along road side. The users were asked to answer the questions the quality of service provided by the system in terms of questionnaire formed. The format of questionnaire was based on the factors that user perceive. From the ratings, an analysis was carried out to find the level of service and waiting time of the interviewers. The analysis consisted of five factors as safety, Comfort level vendors encroachment, accessibility and side walk performance, climate condition. The analysis was done on discrete continuous model and the area was categorized to a specific level of service out of 6 degrees of level of service (LOS). It is difficult to have LOS value for an area based on perception as it varies from person to person. So the trail is made to its best possible value of LOS depending on majority of the majority of user's perception.

Keywords: LOS, Pedestrian, Comfort, Pedestrian Safety Urban Roads, Suchitra Junction

I. INTRODUCTION

Pedestrian road safety is a key point of the transport road safety policy in urban areas. Pedestrians are vulnerable road users and despite their limited representation in traffic events, pedestrian involved injuries and fatalities are overrepresented in traffic collisions. Crosswalks are sites where pedestrians face lower levels of road safety, because they have to cross the street and must be aware of the incoming traffic. Intersections with high vehicle flows should be signalized in order to prevent accidents and raise the level of road safety for both pedestrians and vehicle drivers. The pedestrian illegal crossing behaviour is a major fact in the road safety issue. The main concerns are the following: Pedestrians cross the streets without noticing the incoming traffic, usually because their attention is distracted.

- Pedestrians usually miscalculate the traffic gaps.
- Pedestrians walk across the street, usually due to lack of space on sidewalks.
- Pedestrians cross the streets in midblock location or out of designated crosswalks.
- Pedestrians do not follow the indications of the traffic lights.

Due to rapid urbanization in India, the traffic volume is increasing on the roads. The motor vehicle industry is demanding with an annual production rate of 5 million vehicles. This leads to clumsiness on roads giving an unsuitable condition for movement. For some time, transportation engineers and planners have focused on the development vehicular transportation system. Even today, the motorized transportation system receives an overwhelming priority over systems that serve the needs of non-motorized users such as pedestrians and bicyclists. However, in recent years, emphasis has been shifted towards multimodal

approaches for improvement in pedestrian facilities and operations in order to counteract the challenges of congestion, air quality, improving safety and quality of life. The researchers are promoted to step forward in improvements of traffic behavior in all aspects. There has been progress in measuring quality-of-life of pedestrian facilities and in walkability. For example Saelens et al.(2003) mentioned this from the way of users' walking decision and neighboring environmental conditions such as population density, connectivity to different transitions ,land use pattern are also the factor of influence.

II. NEED FOR PRESENT STUDY

Road Safety is a multi-sectoral and multi-dimensional issue. It incorporates the development and management of road infrastructure, provision of safer vehicles, legislation and law enforcement, mobility planning, provision of health and hospital Services, child safety, urban land use planning etc. In other words, its ambit spans engineering aspects of both roads and vehicles on one hand and the provision of health and hospital services for trauma cases (in post-crash scenario) on the other. Road safety is a shared, multi-sectoral, responsibility of the government and a range of civil society stakeholders. The success of road safety strategies in all countries depends upon a broad base of support and common action from all stakeholders.

Pedestrian road safety is a key point of the transport road safety policy in urban areas. Pedestrians are vulnerable road users and despite their limited representation in traffic events, pedestrian involved injuries and fatalities are overrepresented in traffic collisions. Crosswalks are sites where pedestrians face lower levels of road safety, because they have to cross the street and must be aware of the incoming traffic. Intersections with high vehicle flows should be signalized in order to prevent accidents and raise the level of road safety for both pedestrians and vehicle drivers.

The pedestrian illegal crossing behaviour is a major fact in the road safety issue. The main concerns are the following:

- Pedestrians cross the streets without noticing the incoming traffic, usually because their attention is distracted.
- Pedestrians usually miscalculate the traffic gaps.
- Pedestrians walk across the street, usually due to lack of space on sidewalks.
- Pedestrians cross the streets in midblock location or out of designated crosswalks.
- Pedestrians do not follow the indications of the traffic lights.

A. Objective and Scope of the Study

The objective of this study is to develop an instrument for determining factors affecting sidewalk performance based on pedestrian perception. A questionnaire with different items is developed to measure pedestrian perception in five different areas: (a) safety, (b) comfort/convenience, (c) vendors presence, (d) movement easiness and accessibility, (e) environmental condition. It is believed that each item could potentially impact on sidewalk performance. The main objectives are: To provide higher safety to pedestrians without obstructing/hampering the inflow and outflow of traffic.

- How much is the pedestrian crossing time.
- How much is the pedestrian crossing speed.
- Do pedestrians cross the street with red or green traffic light?
- To devise a yardstick for calming the traffic and to design the streets in such a way that it improves the pedestrian walking environment.
- Very little study has been carried out to perk up the pedestrian walking environment and the factors which define it.

III. LITERATURE REVIEW

Earlier studies provide significant facts about pedestrian demographic characteristics (such as age, gender) and how these characteristics influence road crossing behavior. Such studies have focused on detailed experiments to find out the effect of age on road crossing decisions with effect of vehicle distance or speed of vehicle (Oxley et al., 1997; Lobjois and Cavallo, 2007). Most of these studies have been carried out in a virtual environment. Road crossing behavior with respect to gender and baggage held has also been observed in various studies. Males have a tendency to show more hazardous road crossing behavior than females due to less waiting time (Khan et al., 1999; Tiwari et al., 2007).

Few studies have also explored the importance of the pedestrian speed at different locations (Knoblauch et al., 1996; Rastogi et al., 2011), such as the zebra crossing location (Varhelyi, 1998) and signalized intersections (Tarawneh, 2001). Outline of these studies suggest that males walk significantly faster than females while crossing the roads. A recent study was focused on legal versus illegal pedestrian road crossing behavior at mid-block location in China (Cherry et al., 2012). Few studies have identified pedestrian behavior in mixed traffic streets and developed a micro-simulation model in order to find out the fundamental characteristics as well as the conflicts of the pedestrian movement (Shahin, 2006).

A study in Beijing, investigated pedestrian behavior and traffic characteristics at un-signalized midblock crosswalk. Authors have explained the pedestrian speed change condition with pedestrian behavior (Shi et al., 2007). Some studies have also addressed pedestrian road crossing behavior by considering the effectiveness of educational training programs (Dommes et al., 2012). Studies had identified the importance of the environmental characteristics, such as type of crossing facility, traffic volume and roadway geometry on road crossing behavior (Kadali and Vedagiri, 2013). Some studies have also explored the pedestrian road crossing behavior before and after re-construction of traffic facility (Gupta et al., 2010).

Pedestrian crossing behavior is usually get influenced by various factors related to pedestrian characteristics, pedestrian movements, traffic conditions, road conditions and environmental surroundings. Rosenbloom et al. (2008) observed unsafe crossing behavior of children, like not stopping at the curb, not looking before crossing, attempting to cross when a vehicle is nearing and running across the road. Female pedestrians are observed accepting more gaps and less risk compared to male pedestrians. Oxley et al. (2005) have done experimental studies on the effect of age of a pedestrian in gap selection. They reported that, for all age groups, gap selection is primarily based on vehicle distance and speed.

IV. METHODOLOGY

There have been several studies carried out to investigate the pedestrian behavior which is influenced by different factors such as pedestrian perception, roadway, environmental characteristics, etc. Pedestrian crossing behavior is mainly governed by the gap acceptance theory. Each pedestrian has a critical gap to cross the street. Many things correlate the minimum gap from the vehicle that is accepted by pedestrians who intend to cross streets at mid-block. This parameter may be associated with traffic conditions and with vehicle and pedestrian characteristics.

In this study, gap-acceptance theory is used to model pedestrian crossing behavior. An "inconsistent behavior" model is assumed wherein the pedestrian may reject a longer gap before accepting a short one. The critical gap is treated as a random variable at the individual and at the population level. Each gap has a probability of acceptance given by the gap-acceptance function. The gap-acceptance function is assumed to have a multivariate normal distribution, and the parameters are estimated using the maximum-likelihood method.

The major steps involved in this study are: (1) selection of suitable site for field survey (2) field data collection and extraction (3) analysis of pedestrian demographic characteristics and pedestrian behavioural aspects (4) model development for pedestrian road crossing behavior

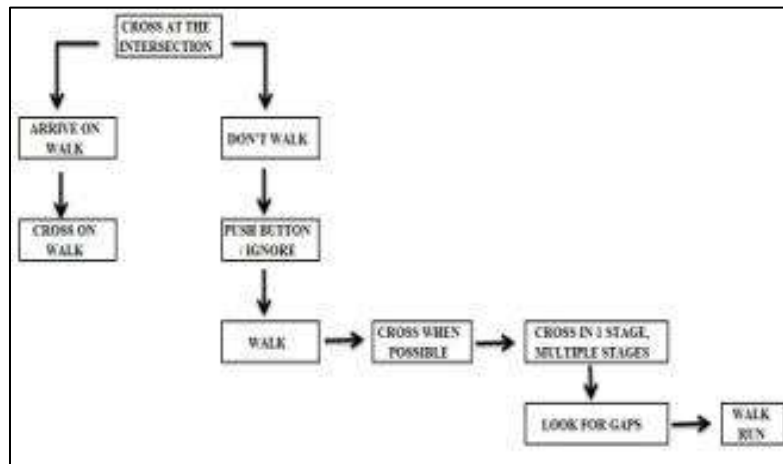


Fig. 1: Methodology

The key step by step procedures for applying methodology for determining performance measures and level of service

B. Questionnaire Formation

A questionnaire with a total of 21 variables is developed to measure pedestrian perception in five different areas: (a) safety, (b) comfort (c) vendors obstruction (d) movement easiness and accessibility (e) environmental condition. It is believed that each variable could potentially impact on sidewalk performance. However, it is unsure which items would contribute the greatest impact and to what degree. In the present study all items are scored on a five-point Likert-type scale with "one" representing strongly disagree, and "five" representing strongly agree. To collect the data, onsite interviews were conducted in the study location. Some interviewers stopped the pedestrians and asked them for possibility to interview. The yes/no type questions were answered as 1(yes)/0(no).

1) Questionnaire Format

- Name
- Age
- Sex

2) Discrete & Continuous Model

As was the case with continuous-continuous data, it is possible to have interrelated variables that are discrete-continuous. An example would be drivers' choice of ITS technology (e.g., visual dashboard display or audio system) and the extent to which it is used (e.g., in minutes per week). To see why this must be considered as part of an interrelated equation system, consider an ITS technology usage equation,

$$U_{kn} = B_k X_{kn} + V_{kn}$$

Where U_{kn} is the minutes of use of technology k by driver n over some time period; X_{kn} is a vector of driver and technology characteristics; B_k is a vector of estimable parameters; and V_{kn} is an error term. In estimating this equation, information on technology use is only available from those people actually observed using the technology. No information is available for drivers that have not yet purchased the technology or have purchased another competing technology. Because the people observed using a particular technology are not likely to be a random sample of the population, a self-selected bias will result

V. ANALYSIS AND RESULTS

A. Introduction

After analyzing by using inverse variance method the results were obtained. From the data the PLOS of the road was determined by suitably determining the range of each LOS. The result obtained can be utilized by a traffic engineer to improve upon the present roads and a better walkable environment can be provided to the pedestrians in future by adopting suitable design methods for the road.

B. Demography and Pedestrian Behavioural Characteristics

The majority of the subjects were male (58%). Respondents grouped in age in under 25 years (31%), from 25 to 30 years (52%), and 31 to 56 years (6%). Walking behavior included 2 persons (46%), walking alone (30%), walking in group with 3 persons (11%), and walking in group with more than 3 persons (18%). About 67 % of respondents stated that walking was their main mode during the survey. Most of the users were using carriage way (40%) rather than footpath due to the preoccupation by vendors.



Fig. 2: Pedestrian rolling gap movement.

Pedestrians' and drivers' behavioural data were extracted from the video. In this study, the pedestrian rolling gap is the one of the important parameter influencing pedestrian behaviour. Pedestrians are rolling over the small vehicular gap which is characterised as rolling gap as depicted as path A-A in Figure 5.1.

C. Pedestrians Count

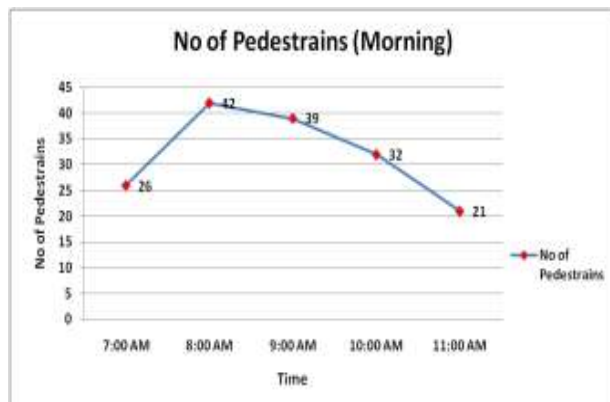


Fig. 3: Pedestrians count on Day 1

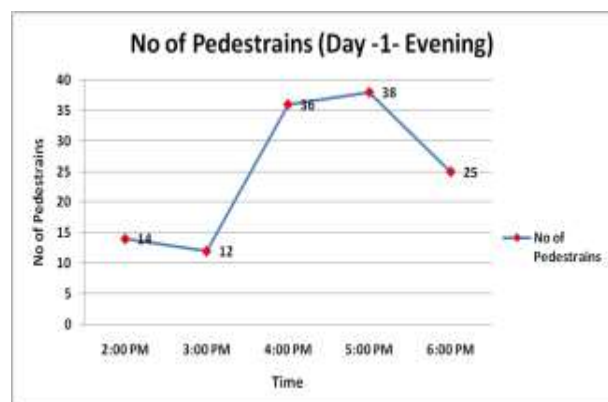


Fig. 4: Pedestrians count on Day 1

D. Factor Determination

Principal component factor analysis with a varimax rotation was conducted on the 21 items. The result for all of the 15 variables was shown in Table.

Intersection		
LOS	Average Pedestrian delay (Sec)	Description
A	<10	very small delay, nobody crossing irregularly
B	10-20	small delay, almost no one crossing irregularly
C	20-30	small delay, very few pedestrian crossing irregularly
D	30-40	big delay, someone start crossing irregularly
E	40-50	very big delay, many pedestrians crossing irregularly
F	>50	very big delay, almost every waiting pedestrian crossing irregularly

VI. INTRODUCTION

This study was carried out the find the LOS qualitatively. The qualitative method is a better method to determine LOS as it inputs the real time response of people thus providing an option of achieving a better and more accurate result. the data was analyzed by using inverse variance method and the LOS score table was obtained by determining the ranges for each level of service which helped in the estimation of the PLOS of the study area.

VII. CONCLUSIONS

This study focused on pedestrian crossing behaviour to examine the pedestrian compliance with signals under different crossing scenarios. The key findings can be summarised as follows:

- The estimated probabilities show a comparatively higher propensity to start crossing during the “blackout/flashing green” phase than during “red”.
- The provision of a “refuge island” gives a perception of safety but at the same time increases the tendency to take a risk by crossing on red.
- There is a higher propensity to cross on red in the following conditions:
 - At non-designated areas
 - In the age group under 30 years old
 - If there are two or more adults in the group
 - When without luggage/children
- Pedestrian compliance is slightly lower at puffin crossing facilities than at any of the other situations considered. This may be due the fact that puffin crossing a relatively recent development compared with existing farside pedestrian facilities, suggesting the need for publicity to raise awareness.

After analyzing the data we arrive at following conclusions:

The LOS score obtained by inverse variance analysis was found out to be 3.62 which was within the range of LOS D i.e. in between 3.435-4.123. This signified that PLOS of the road segments in the study area are providing not good quality of service to the pedestrians in the prevailing geometry and surrounding environmental characteristics.

VIII. SCOPE FOR FURTHER STUDY

Our work leads to a number of recommendations for further study.

First of all, the analyses resulting from this work can feed into the development of a traffic signal control mechanism which takes into account pedestrian crossing behaviour when determining optimum settings.

Some further suggested areas for future work include:

- Further detailed analysis of the video (CCTV) RP data and correlating SP responses to RP data.
- Investigation of the extent to which pedestrians understand the operation/ sequence of different traffic signal types.
- Advice on an education programme on safer crossing and the use of roadside traffic signal infrastructure.
- An awareness programme in schools educating children on puffin crossings.
- Exploration of incentives for compliance.

REFERENCES

- [1] Field, A.: Discovering Statistics Using SPSS, Second Edition, SAGE Publications Ltd., London, 2005.
- [2] Parasuraman, A., Zeithaml, V.A., Berry, L.L.: SERVQUAL: A Multiple-Item Scale for Measuring Consumer Perceptions of Service Quality, Journal of Retailing, Volume 64, Number 1, 1988.
- [3] Tan D, Wang W, Lu J, Bian Y.: Research on Methods of Assessing Pedestrian Level of Service for Sidewalk, Journal of Transportation Systems Engineering and Information Technology, Volume 7, 2007.
- [4] TRB: Highway Capacity Manual, Transportation Research Board, National Research Council, Washington, 2000.

- [5] Zhang, X.: Factor Analysis of Public Clients' Best-Value Objective in Public-Privately Partnered Infrastructure Projects, *Journal Of Construction Engineering And Management ASCE*, pp, 956-965, September 2006.
- [6] Pedestrian's level of service at zebra crossings by Zsuzsanna KOVÁCS IGAZVÖLGYSI from BME Department of Highway and Railway Engineering, e-mail: igazvolgyi@uvt.bme.hu
- [7] Pedestrian crossing behaviour analysis at intersections by Akash Jain¹, Ankit Gupta², Rajat Rastogi³
- [8] Study conducted in cooperation with the U. S. Department of Transportation, Federal Highway Administration Research Study Title: "Pedestrian Signals: Warrants and Effectiveness" Keegan, O., O'Mahony, M. (2003), *Modifying pedestrian behaviour*, Transportation Research Part A, No. 38, pp. 889-901.
- [9] Louviere, J.J., Hensher, D.A. and Swait, J.D. (2000), *Stated Choice Methods: Analysis and Applications*, Cambridge University Press, Cambridge, England.
- [10] McFadden, D. (1981), *Econometric Models of Probabilistic Choice*, Structural Analysis of Discrete Data, C.F. Manski and D. McFadden (Eds.). Cambridge, MA: MIT Press, pp.198-272.
- [11] Rouphail, N. (1984), "Mid-Block Crosswalks: A User Behavior and Preference Study," in *Transportation Research Record* 959, TRB, Washington, D.C., pp. 41-47
- [12] Russell, J. and Hine, J., (1996) "Impact of Traffic on Pedestrian Behaviour; Measuring the Traffic Barrier," *Traffic Engineering and Control*, Vol. 37, No. 1, Jan. 1996, pp. 16-19
- [13] Sisiopiku, V.P., Akin, D. (2003), *Pedestrian behaviour at and perceptions towards various pedestrian facilities: an examination based on observation and survey data*,
- [14] *Transportation Research Part F*, No. F6, pp. 249-274.

TO DEVELOP A CORRELATION BETWEEN CBR AND DYNAMIC CONE PENETRATION VALUE

Ch.Rajasekhar¹, A.Naga Sai baba², Dr.M.Kameswara Rao³

¹Research Scholar (M.Tech, T.E), ²Assistant Professor, ³Professor
Malla Reddy Engineering College, (Autonomous) Kompally

Abstract: *In this paper, a brief practical review is presented on Correlation between CBR and dynamic cone penetration value. In India, California Bearing Ratio (CBR) value of sub grade is used often for design of flexible pavements. In practice, only limited number of such tests could be performed because of high unit cost and time required for such testing. As a result, in many cases, it is difficult to reveal detailed variations in the CBR values, over the length of roads. In such cases if the estimation of the CBR could be done on the basis of some tests which are quick to perform, less time consuming and cheap, then it will be easy to get the information about the strength of subgrade over the length of roads and also will be helpful and important specially for low volume roads being constructed under Pradhan Mantri Gram Sadak Yojana (PMGSY) scheme over different states of India presently, to develop large scale connections of rural India within a short period of time. By considering this aspect, a number of investigators in the past made their investigations in this field and developed different methods for determining the CBR value on the basis of results of low cost, less time consuming and easy to perform tests. The dynamic cone penetrometer (DCP) has been widely used for estimating the strength of soils. Also, the California bearing ratio (CBR) test is the test most widely used in highway pavement design all over the world. An attempt has been made to obtain relationship between DCP and CBR values for fine grained soils. In the first part of the investigation laboratory experiments were carried out by single test method. The purpose of the research was to establish whether any correlation exists between the CBR and penetration depth of the DCP for various types of fine grained soils. In the second part of the investigation field CBR tests were carried out developing a test set-up in the laboratory using five types of soils. The DCP tests were conducted in the same soil to find out the relationship between field DCP value and field CBR value. The results of the research indicate that a good correlation exists between CBR and penetration depth of the DCP for each of the material tested. These relationships are useful to obtain appropriate design inputs for analysis on the basis of field DCP tests conducted during evaluation of in-service pavements.*

Keywords: *CBR, Dynamic Cone penetration, Correlation, investigation.*

I. INTRODUCTION

Traditionally the design of either kind of pavement is based on the strength of the compacted soil in the pavement, called

subgrade. The design of the pavement layers laid over the subgrade soil starts off with the determination of subgrade strength and the traffic volume which is to be carried. The design of pavement is very much dependent on the subgrade strength of soil. Design criteria mainly needs thickness of layers. Weaker subgrade needs thicker layers whereas stronger subgrade needs thinner pavement layers. The Indian Road Congress (IRC) provides the exact procedures for the pavement layers design which based upon the subgrade strength. The strength of a subgrade soil is normally expressed in terms of the California Bearing Ratio (CBR). Due to variable nature of soil, the subgrade strength changes inconsistently, as a result engineers face so many difficulties or challenges during the design of a pavement. The subgrade strength is very much dependent on moisture content. As the subgrade is intended to variation of moisture due to flood, precipitations or all other climatic changes, so it is necessary to enable or understand the subgrade according to the variation of moisture. The CBR is the only test which can figure out the strength of a subgrade. By this test we can compare the strength of different subgrade materials. The CBR test is done in a standard manner by which one can find out or design the strength or thickness of subgrade layer. CBR value is inversely proportional to thickness of the pavement layer. If the subgrade is stronger, the higher is the CBR value, so lesser thickness is required and vice-versa.

II. NEED FOR PRESENT STUDY

Pavement structure design is based on three factors: loading (projected traffic), paving material properties (strength, aging, environmental effects, etc.), and subgrade support. But many uncertainties exist in pavement design. Even after a road is opened to traffic, the engineer cannot verify the accuracy of the traffic projection until the project has been through its design life. During the design stage, the engineer selects a subgrade support value based on a few samples taken from the project site and some engineering assumptions. The engineer controls paving material properties through quality assurance/quality control (QA/QC) programs during construction. Most states use density of the in-place subgrade and unbound base for construction quality control. However, density is not a load-bearing indicator. Also, in most cases, thickness of the unbound base layer is not monitored closely. Experience shows that it is very costly to repair a failed pavement caused by poor base or subgrade quality. Therefore it is very important and beneficial to verify and improve, if needed, the quality of the base and subgrade prior to paving

operations and to provide engineers an opportunity to reevaluate and modify pavement structure design during paving operations. Pavement performance depends greatly upon the quality and uniformity of materials incorporated into the pavement structure. Careful monitoring of material quality and the dimensions of pavement layers during construction improves overall compliance with specifications as well as in-service performance of the pavement. The Dynamic Cone Penetrometer (DCP) provides a quick and simple field test method for evaluating the in-situ stiffness of base and subgrade layers, and DCP testing has been used in many countries and some states for subgrade evaluation. The greatest advantage offered by the DCP is its ability to penetrate underlying layers and accurately locate zones of weakness within the pavement system. This quick and dirty method can measure soil properties to a depth of 3 ft (0.91m).

III. OBJECTIVE AND SCOPE OF THE STUDY

- Develop and implement a procedure for using the DCP as an acceptance criterion for subgrade and unbound base material.
- Develop a threshold, based on DCP readings, for unsuitable material.
- Establish stiffness parameters, based on DCP readings, for pavement design and rehabilitation
- To develop correlation between CBR (California bearing ratio) and DCPT (Dynamic cone penetration test) for different soils (Clayey, silt and Sandy Soil) at different levels of compaction.
- To study the effect of compaction on correlation between CBR and DCPT value
- To compare the results with the correlation given in IRC 37: 2012
- $\text{Log}_{10} \text{ CBR} = 2.465 - 1.12 \text{Log}_{10} N$
- To find out the error percent between the relation developed and the relation given in the IRC 37:2012
- To evaluate the strength of sub-grade in terms of CBR value

IV. LITERATURE REVIEW

Deepika.Chukka, Chakravarthi.V.K conducted an experiment to develop relationship equations between DCPT index to Index and engineering properties of few sub grades with low plasticity characteristics. The tests include determination of DCP index in field and engineering properties in the lab. Studies are extended for both pre monsoon and post monsoon periods to know the effect of moisture on all properties. M. M. E. Zumrawi conducted an experiment to predict the field CBR of different types of soils. Since CBR can't be easily measured in the field, prediction of CBR from other simple tests such as Dynamic Cone Penetration (DCP) and soil properties is a valuable alternative. Various soils have been compacted at different initial state conditions (i.e. water content and dry density) then using laboratory and field equipment to enable the measurement of unsoaked CBR and DCP of these soils. Comparison of the measured and predicted values of unsoaked CBR and DCP using the

developed equation clearly indicates the validity of this equation.

Er Younis Farooq, Prof Ajay K Duggal, Asif Farooq conducted an experiment on the CBR method and with these CBR values which are obtained by conventional method and Dynamic Cone Penetration (DCP) values are correlated to find the conventional CBR value by using DCP in the field. So, with the help of this relationship, it will be easy to get information about the strength of sub grade over the length of road.

Dr. Dilip Kumar Talukdar conducted an experiment to correlate CBR value with other soil parameters. It can also be used for determination of sub grade reaction of soil by using correlation. It is one of the most important engineering properties of soil for design of sub grade of rural roads. CBR value of soil may depends on many factors like maximum dry density (MDD), optimum moisture content (OMC), liquid limit (LL), plastic limit (PL), plasticity index (PI), type of soil, permeability of soil etc.

K.A.K.Karuna Prema and A.G.H.J.Edirisinghe, conducted an experiment to develop relation between dynamic cone penetration(DCP) and other soil parameters that are used in road construction and maintenance work.

In this study, a series of tests were carried out in a laboratory under controlled conditions. The standard proctor compaction test was carried out for each soil sample to find out the dry density/moisture content relationship. Then, DCP test was carried out by varying the moisture content and the dry density. Samples were compacted manually to obtain the pre determined conditions. The unsoaked CBR and soaked CBR tests were also carried out under the same conditions.

V. EXPERIMENTAL INVESTIGATION

5.1 Determination of Liquid and Plastic Limit

To determine the Atterberg's limits (Liquid Limit & Plastic Limit) as per IS 2720 Part 5-1985. The objective of the Atterberg limits test is to obtain basic index information about the soil used to estimate strength and settlement characteristics. It is the primary form of classification for cohesive soils. Fine-grained soil is tested to determine the liquid and plastic limits, which are moisture contents that define boundaries between material consistency states. These standardized tests produce comparable numbers used for soil identification, classification and correlations to strength. The liquid (LL) and plastic (PL) limits define the water content boundaries between non-plastic, plastic and viscous fluid states. The plasticity index (PI) defines the complete range of plastic state. Consistency is meant the relative ease with which soil can be deformed.

Consistency denotes the degree of firmness of the soil which may be termed as soft, firm, stiff or hard. Soil passes through 4 states of consistency. In 1911, Swedish Agriculturist Atterberg divided the entire range from liquid to solid state into 4 stages.

- Liquid state
- Plastic state
- Semi solid state
- Solid state

5.2 Factors Affecting Compaction

Compaction is measured in terms of the dry density achieved. This is found to be a function of (a) the water content (b) the compactive effort applied to the soil, and (c) the nature of the soil. These effects are briefly discussed below

The effect of water content on compaction:

The shearing resistance to relative movement of the soil particles is large at low water contents. As the water content increases, it becomes relatively easier to disturb the soil structure, and the dry density achieved with a given compactive effort increases. However if the dry density is plotted against the water content for a given compactive effort, it will be seen that the dry density reaches a peak, after which any further increase in water content results in a lower dry density. From the dry density / water content curve, we can determine two quantities; the maximum dry density, and the optimum water content at which this maximum dry density is achieved.

The effect of variations in compactive effort:

Both the maximum dry density and the optimum water content are found to depend on the compactive effort used. Increasing the compactive effort increases the maximum dry density, but reduces the optimum water content. The air void ratio at the peak density remains very much the same. It may be seen that, at high water contents, there is little to be gained by increasing the compactive effort beyond a certain point.

The effect of soil type on compaction:

The highest dry densities are produced in well-graded coarse-grained soils, with smooth rounded particles. Uniform sands give a much flatter curve, and a lower maximum dry density. Clayey soils have much higher optimum water contents, and consequently lower maximum dry densities. The effect of increasing the compactive effort is also much greater in the case of clayey soils. Figures 5.1 and 5.2 show typical results of compaction tests for different soils and different moisture contents.

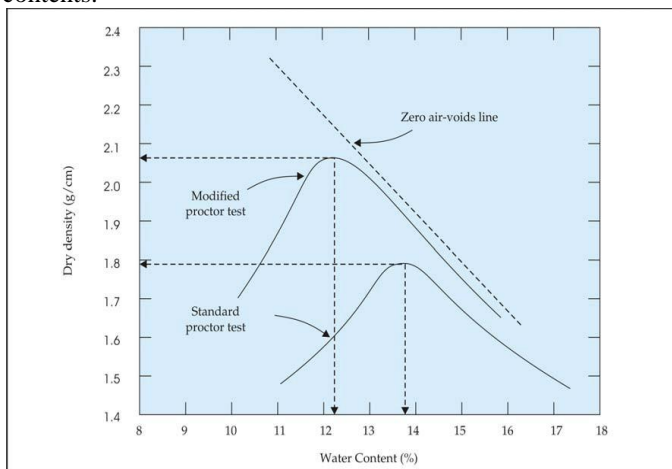


Figure 5.1: Modified Proctor Test Curve (Dry Density vs Moisture Content)

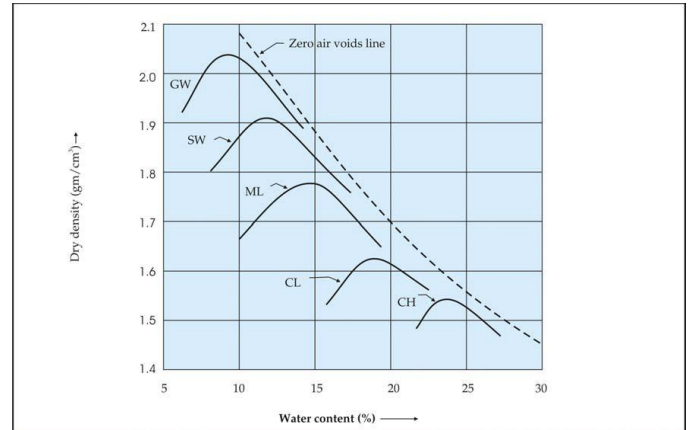


Figure 5.2: Compaction Curve for a Range of Soil Types

Specifications for Granular Sub-Base (GSB)

The material to be used for the sub-base are sand, moorum, gravel crushed stone, crushed slag, granulated slag, crushed concrete, brick metal and kankar, etc. The material shall be free from organic or other deleterious material. The material shall have 9 percent fines value of 50 KN or more (for sample in soaked condition) when tested in compliance with BS: 812. If water absorption value is greater than 2%, the soundness test shall be carried out on the material delivered at the site as per IS: 383-1970. The CBR requirement for sub-base layer should be at least 15% when tested in soaked condition. The material for sub-base shall be preferably non-plastic. Otherwise, the plasticity index (PI) of material passing 425 μ m sieve shall be less than 6 and liquid limit less than 25%. The material shall conform one of the gradations specified in Table 5.1 In case of un-surfaced roads, the PI value of the gravel should not exceed 9%.

Table 5.1: Gradation requirement for coarse graded granular sub-base

Sieve Size (mm)	Percent by weight passing (By wet sieve analysis)		
	Grading – I	Grading – II	Grading – III
75	100	-	-
53	-	100	-
26.5	55-75	50-80	100
4.75	10-30	15-35	25-45
2.36	-	-	-
0.425	-	-	-
0.07	<10	<10	<10

Specifications for base and surface course

As per the MoRD specifications, the gradation requirements for gravel/soil-aggregates in base and surface course of a gravel road were given in Table and Table respectively. Any of the three gradations given in Table for base course can be adopted depending upon the availability of materials. The CBR requirement for base and surface courses is 30% when tested in 4-day soaked condition. These gradations and CBR requirements are recommended in case the gravel surface is sealed by chip sealing or surface dressing

Table 5.2: Grading requirement for surface course

Sieve Size, mm	Percentage passing by Mass
26.5	100
19	97 – 100
4.75	41 – 71
0.425	12 – 28
0.075	9 – 16

Gravel for base courses should have very small portions of fine materials (silt and clay) and a relatively larger top-sized aggregate for strength and durability. Surface-gravel should have a relatively higher percentage of fines (silt and clay) and relatively smaller top sized aggregate, so as to readily shed off water falling on the surface of the gravel road. The percentages of gravel, sand and fines (silt and clay) in the gradations A, B and C were given in Table 5.3.

Table 5.3: Composition of material for base course

Composition	Grading A	Grading B	Grading C
Gravel	53 to 67%	47 to 61 %	41 to 53%
Sand	25 to 43%	31 to 49%	31 to 55%
Silt and Clay	4 to 8%	4 to 8%	4 to 8%

When a single naturally occurring material does not meet any of the specified gradations, 'processing' will have to be resorted to, by blending two or more materials to achieve the required grading. Where gravel meeting the requirements in respect of grading as per the above is not available within economical leads or cannot economically be processed, gravel or soil-aggregate mixtures meeting the following requirements for base and wearing/surfacing course can be used (including processing if required).

Gravel base and surface/wearing courses

Table 5.4 shows the soil specifications for base course and Table 5.5 shows the soil specifications for wearing course.

Table 5.4: Specifications for base course

Composition	Grading A	Grading B	Grading C
Gravel	53 to 67%	47 to 61 %	41 to 53%
Sand	25 to 43%	31 to 49%	31 to 55%
Silt and Clay	4 to 8%	4 to 8%	4 to 8%

Table 5.5: Specifications for wearing/surface course

Percent retained on IS 4.75 mm sieve and passing 80 mm in size (percent gravel)	50-70%
Percent retained on IS 75 μ m sieve and passing 4.75 mm in size (percent sand)	25-40%
Percent passing IS 75 μ m (percent silt and clay)	8-15%

VI. RESULTS AND DISCUSSION

6.1 Properties of different soils

Table 6.1: Comparison of Gravel Content for Different Type of Soils

Type of Soil	Gravel Content
SC	4.9
SC	2.1
SM	38.8
CI	7
CL	0

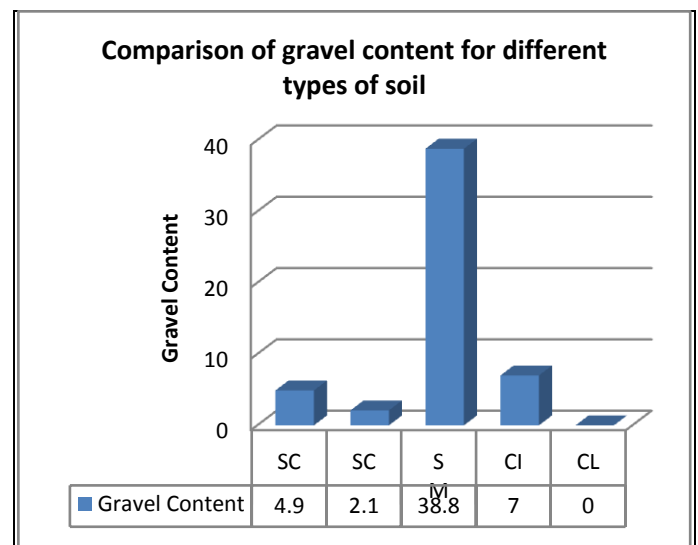


Figure 6.1: Comparison of gravel content for different types of soil

Table 6.2: Comparison of Silt & Clay Content For Different Type of Soils

Type of Soil	Silt & Clay Content
SC	57.5
SC	46.9
SM	6.8
CI	63
CL	55

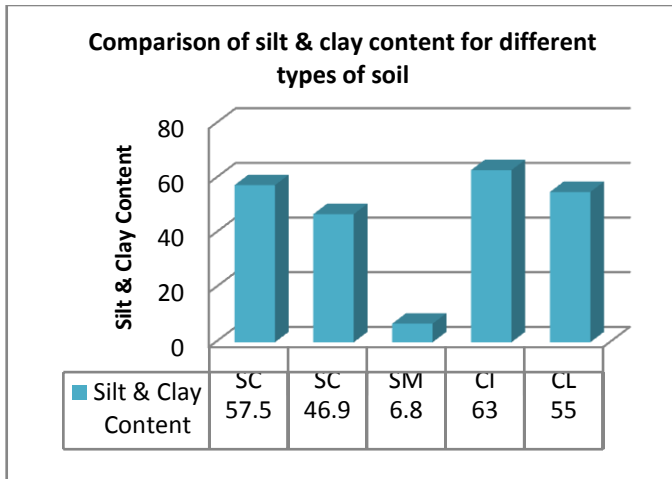
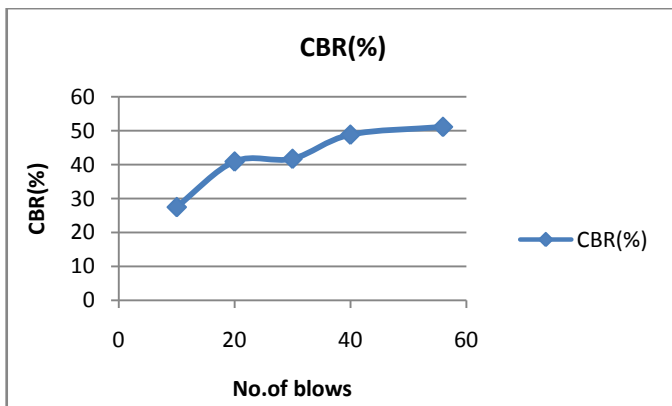


Figure 6.2: Comparison of Silt & Clay Content For Different Type of Soils

Comparison of CBR for different soils at different compaction levels

CBR for SC soil at different compaction levels

No. of blows	CBR (%)
10	27.5
20	40.9
30	41.7
40	48.8
56	51.1



CBR for SC soil at different compaction levels

VII. CONCLUSIONS

- For existing conditions, the in situ DCPT can be conducted for determination of field CBR value for in situ density.
- The logarithmic models are considered to be more suitable for use than any other models.
- As we are expecting that the equation which is given in IRC-37-2012 for finding insuit CBR is not suitable for every type of soil and moisture content. As CBR value may changes with the variation in moisture content and types of soils.

- The analysis of the laboratory work confirmed that a good estimate of CBR could be made from the DCP.
- The CBR value of uniform soils having similar characteristics can be determined quickly and with adequate accuracy using the DCPT results.
- Dynamic Cone Penetration Test can be effectively used to identify number of pavement layers, thickness of each layer and strength of each layer in terms of CBR for rural roads.
- California Bearing Ratio Test results and Penetration resistance observations from DCP test shows that CBR value increase with decrease in DCP values.
- The soaked CBR values of uniform soils which has similar characteristics can be determined quickly and will have adequate accuracy using DCP test results.

REFERENCES

- [1] 20.Varghese George, CH.Nageshwar Rao and R.Shivashankar-"Investigation on Unsoked Bleded Laterite Using DCP and
- [2] CBR test"- Journal of the Indian Roads Congress, October-December 2009, paper No.556
- [3] 21. Bandyopadhyay.K , Bhattacharjee.S-"Comparative Study Between Laboratory and Field CBR by DCP and IS Method"-
- [4] Indian Geotechnical Conference – 2010, GEO trendz December 16-18, 2010 IGS Mumbai Chapter & IIT BOMBAY
- [5] Dar-Hao Chen, Jian-Neng Wang, and John Bilyeu-"Application of Dynamic cone Penetration in Evaluation of Base and
- [6] Subgrade Layers"- Transportation Research Record 1764 Paper No. 01-034
- [7] Harison, J.R. (1983). "Correlation between CBR and DCP strength Measurements of Soils," Proc. Institution of Civil Engineers London, Part-2.
- [8] Harison, J.R. (1987). "Correlation between California Bearing Ratio and Dynamic Cone Penetration Strength Measurement of Soils," Proc. Institution of CivilEngineers, London, Part-2, pp. 83-87.
- [9] Soewignjo Agus N. and Andy, H. (2012)."Correlation Between Index properties And California Bearing Ratio Test of Penkababu Soils with and Without soaked. " Canadian Journal on Environmental, Construction and Civil Engineering Vol. 3, pp. 1-11.
- [10] Felix and Ugbe. (2012)."Predicting Compaction Characteristics of Lateritic Soil of Western Niger delta, Nigeria." Abraka Research Journal of Environmental and Earth Sciences 4(5), pp. 553-559.
- [11] Mohammed, H. and Dahunsi. (2012)." Effects of Natural Moisture content on Selected Engineering Properties of soils." Transnational Journal of

- Science and Technology June 2012 edition Vol. 2, pp. 1-19.
- [12] Rodrigo Salgado Sungmin Yoon (2003), "Dynamic cone penetration Test (DCPT) for Subgrade Assessment." 62-7 02/03 JTRP-2002/30 indot division of Research West Lafayette, IN 47906.
- [13] Talal Al-Refeai and A. Al- Suhaibani. (1996), "The prediction of CBR using DCP", J. King Saud University." Vol. 9, eng.sci. (2), pp. 191-204.
- [14] Mohammadi, S.D. Khamsehchiyan, M. (2004), "The use of Dynamic Cone penetration test (DCP) to determine some useful relationships for sandy and clayey soils", Tarbiat Modares University, Tehran, Iran, pp 1-5.
- [15] Datta, T. (2011). "Correlation between CBR and Index Properties of Soil." Proceedings of Indian Geotechnical Conference, Paper No. A-350, pp. 131-133.
- [16] Farshad Amini (2003). "Toward Potential Applications of the Static and Dynamic Cone Penetrations in Mdot Pavement Design and Construction." Report No. fhwa/ms-dot-rd-03-162.
- [17] Varghese George and Nageswarao. Ch. (2008). "PFWD, DCP AND CBR correlations for evaluation of lateric subgrades Dakshina kannada, India." Proceedings of 12th International Conference of International Association for Computer Methods and Advances in Geomechanics (IACMAG).
- [18] Varghese George and Nageswarao, Ch. (2009). "Investigations on Unsoaked Blended Laterite Using PFWD, CBR and DCP, CBR Tests." Journal of the Indian Roads Congress, No. 556. Pp. 283-293.
- [19] John Siekmeier and Julie Jensen. (2009), "Using the Dynamic Cone Penetration and Light Weight Deflectometer for Construction Quality Assurance." Report No. 2. <http://www.lrrb.org/PDF/200912>, Recipients Accession No. MN/RC 12.
- [20] George. K.P and Waheed Uddin, (2000). "Toward Subgrade Characterization for Highway pavement Design." Technical Report No. fhwa/ms-dot-rd-00-13.

UTILIZATION OF LOW CBR SOIL FOR FLEXIBLE PAVEMENTS FOR LOW VOLUME ROADS WITH ROBO SAND STABILIZATION

H.V.S.N. Murty¹, V Ranjith Kumar², Dr.M.Kameswara Rao³
¹Research Scholar (M.Tech, T.E), ²Assistant Professor, ³Professor
Malla Reddy Engineering College (Autonomous), Kompally

Abstract: Many rural areas in developing countries like India lack adequate and affordable access to transport infrastructure and services. The problem is more persistent in low volume and low CBR value sub-grades. The objective of this project is to evaluate the required flexible pavement for very low volume traffic roads with very low CBR values with practically very low traffic of not more than 30-40 vehicles mostly comprising passenger cars where the level of serviceability is very high. The IRC recommended pavement composition is for unpaved gravel roads in rural areas with low volume traffic. There are various disadvantages associated with construction of the road using gravel like dust generation, and gravel loss over a period of time due to passage of vehicles and inaccessibility during rains and the quality of serviceability is unsatisfactory. Problems with sub grade having low CBR values are stability and large deformations or settlements. A project has been taken up where the CBR of sub grade soil is 1.5 or less, the soil is improved by mechanical stabilization with an additive of stone dust. The emphasis of the project is 'Utilization of low CBR soil for flexible pavements for low volume roads with robosand stabilization'. The addition of robosand has improved the sub soil condition in achieving higher CBR value. Locally available soils mixed with crushed robosand serve as effective reinforcement in soft soils for different sub-grade resulting in technically better sub-grade as well cost economy in savings of aggregate material and also reducing carbon foot print.

Key words: Soil stabilization with robosand, improved sub-grade strength, CBR value, UCS, FSI, etc.

I. INTRODUCTION

Rural road connectivity is a key component of rural development, since it promotes access to economic and social services, thereby generating increased agricultural productivity, non- agriculture employment as well as non-agricultural productivity, which in turn expand rural growth opportunities and real income through which poverty can be reduced. The Ministry of Rural Development (MoRD), Government of India has decided to develop various rural roads under Pradhan Mantri Gram Sadak Yojana (PMGSY). The PMGSY has set up a programme to achieve all weather connectivity to all the habitations with population more than 500 (250 for hilly areas) by the end of tenth five year plan i.e. by 2007. Gravel roads are important components of the road transportation network throughout the world which have not yet been paved. In many developing countries, more than

75% of the road network consists of gravel and earth roads. Aggregate surfaced roads are referred to as unpaved roads. Gravel pavement will not only carry traffic loads but will also be resistant to shear deformation and wear i.e. they have to be of sufficient strength and durable (Cygas and Zilioniene, 2002). The CBR test is a way of putting a figure on the inherent strength, the test is done in a standard manner to compare the strengths of different subgrade materials, and the CBR values are used as a means of designing the road pavement required for a particular strength of subgrade. The stronger the subgrade (the higher the CBR reading) the less thick it is necessary to design and construct the road pavement, this gives a considerable cost saving. Conversely if CBR testing indicates the subgrade is weak (a low CBR reading) a suitable thicker road pavement is to be adopted to spread the wheel load over a greater area of the weak subgrade in order that the weak subgrade material is not deformed, causing the road pavement to fail. The CBR in spite of its limited accuracy still remains the most generally accepted method of determining subgrade strength, and as such this information, along with information on traffic flows and traffic growth is used to design road pavements.

1.2 Pavement Materials

Gravel: Gravel is a naturally occurring material consisting of small pebbles, stones, or fragments of stone intermixed with finer materials such as powdered rock, sand, loam, silt, or clay. Sometimes the term gravel is also meant to represent rounded or water-borne stones or pebbles which have no fine material in them, and is known more popularly as shingle. (IRC: SP: 72:2007)

1.3 Factors Affecting Pavement Performance

In general, pavement performance depends on several factors. These factors can be grouped into following categories.

1. Traffic loading associated factors,
2. Material properties and composition,
3. Environmental associated factors, and
4. Other factors.

1.4 Study Area

The proposed road falls in the proposed campus of College of Engineering at Sulthanpur, JNTUH in Pulkal Mandal, district of Medak in Telangana State. Medak district coordinates are between 17°27' and 17°79' Northern latitude and 78°27' and 79°35' Eastern longitude. Geologically the

District is covered by Classified Granite Rocks, the district has a mean maximum temperature of 40°C and a mean minimum temperature of 26°C. The average annual rain fall is 873 mm. Manjira, a perennial tributary of River Godavari with its tributaries of Haldi (Pasupuyeru) and Kundlair drains the district. The important rock types are Peninsular Gneissic complex, Dharwar supergroup associated with Younger intrusives of Achaean age separated unconformably with overlying Basaltic flows of late Cretaceous to early Eocene age with sub-Recent to Recent alluvium along the stream courses

1.5 Objectives of the Study

The main objectives of the study are listed below:

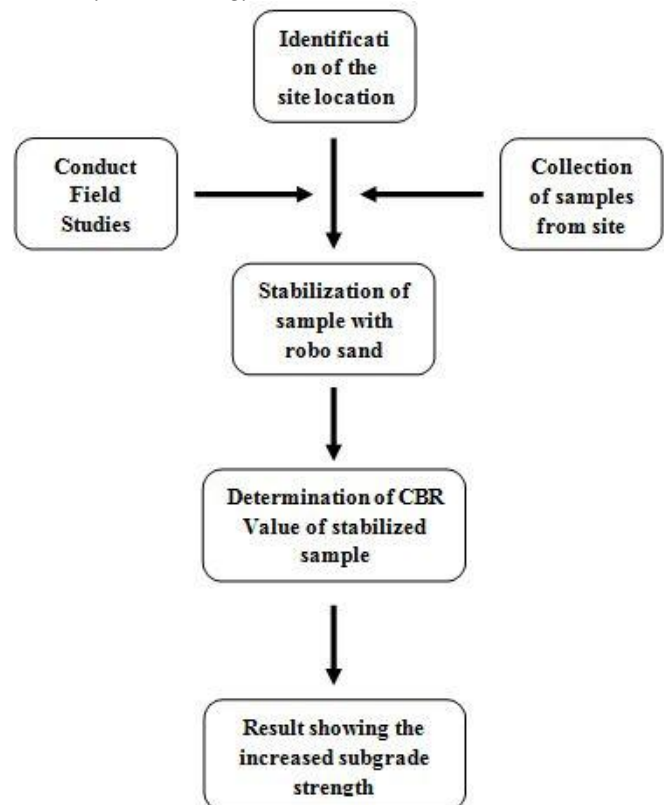
1. To improve the sub-grade strength by stabilizing the sub-soils with soil-robo sand in low CBR conditions.
2. To evaluate and compare the performance of the stabilized sub-grade.

II. REVIEW OF LITERATURE

The rural road connectivity in India, the background information of the gravel roads, types of sealing coat and functions of sealing techniques of the gravel roads have been discussed. In this chapter, attempts have been made to review the literature on gravel roads, various stabilization techniques available for sub-grades, performance evaluation. Sridharan and Soosan et.al (2005) identified that quarry dust manifest high shear strength and is beneficial for its use as a geotechnical material. Sabat et.al (2012) conducted compaction, tri-axial and durability tests on lime stabilized expansive soil-quarry dust mixes. Satyanarayana, et al compacted crusher dust and Crushed Stone mixes through a series of CBR tests by varying the crusher dust. Ramadas and Kumar et.al (2010) reported that the combination of fly ash and stone dust found to be suitable to reduce swelling and increase the strength of expansive soil. Onyelowe Ken et.al (2012) exposes the qualities and applications of quarry dust as admixture during soil improvement and for a more economic approach. Agrawal and Gupta et.al (2011) reported that the potential use of marble dust as stabilizing additive to expansive soil, which involves the determination of the swelling potential of expansive soil in its natural state as well as when mixed with varying proportion of marble dust. Rock flour can be advantageously used in construction of reinforced soil construction such as reinforced earth retaining walls, reinforced soil beds and reinforced flexible pavements as a fill material due to its stability, free draining nature and good frictional characteristics with synthetic reinforcement. Moorthy N.V.R. et al (2002) have studied the interaction of usage of rock flour with Geotextiles and reported the potential areas of application. Soosan et.al (2001) identified that crusher dust exhibits high shear strength and is beneficial for its use as a geotechnical material. Sridharan et.al. (2005) studied the effect of quarry Dust in highway construction that CBR and angle of shearing resistance values are steadily increased with increase the percentage of Quarry Dust. Praveen Kumar et.al(2006) conducted CBR and tri-axial tests on fly ash, coarse sand, stone dust and river bed materials for

their use in the sub base materials of the flexible pavements. Shanker and Ali(1992) have studied engineering properties of rock flour and reported that the rock flour can be used as alternative material in place of sand in concrete based on grain size data. Rao, et al (1996) have reported that sand can be replaced fully with rock flour. Nagaraj T.S and Bhanu et al (2000) have studied the effect of rock dust and pebble as aggregate in cement and concrete. Wood S.A et.al reported that the quality of crushed stone dust depends on the type of parent materials. In this an attempt is made to study the effect of Crusher Dust and Crushed Stone Mixes in studying their Strength, Gradation and Compaction Characteristics.

2.1 Study Methodology – Flow Chart



III. DETERMINATION OF FREE SWELL INDEX OF SOILS

To determine the free swell index of soil as per IS: 2720 (Part XL) – 1977. Free swell or differential free swell, also termed as free swell index, is the increase in volume of soil without any external constraint when subjected to submergence in water. Free swell tests are commonly used for identifying expansive clays and to predict the swelling potential. The free swell test is one of the most commonly used simple tests in the field of geotechnical engineering for getting an estimate of soil swelling potential. This test is performed by pouring 10 cm³ of dry soil through a sieve or aperture size 0.42 mm into a 100 cm³ graduated jar filled with water and noting the swelled volume or the soil after it comes to rest.

Determination of Unconfined Compressive Strength

Determination of the unconfined compressive strength of clayey soils, undisturbed, remoulded or compacted, using controlled rate of strain as per IS 2720 – Part X – 1991. The objective of the unconfined compression test is to determine the UU (unconsolidated, undrained) strength of a cohesive soil in an inexpensive manner. Fine-grained soil is tested in compression. Undisturbed specimens cut from tube samples and disturbed specimens are loaded in compression, recording load and deflection measurements. Laboratory strength tests of soil are similar to testing concrete cylinders, but can be performed with or without lateral confining pressures. The unconfined test uses axial loading without lateral confining pressures, making it the simplest and easiest laboratory method of estimating strength. To more accurately simulate actual loading conditions in the field, lateral confining pressures can be applied using a triaxial test, which is a completely different apparatus.

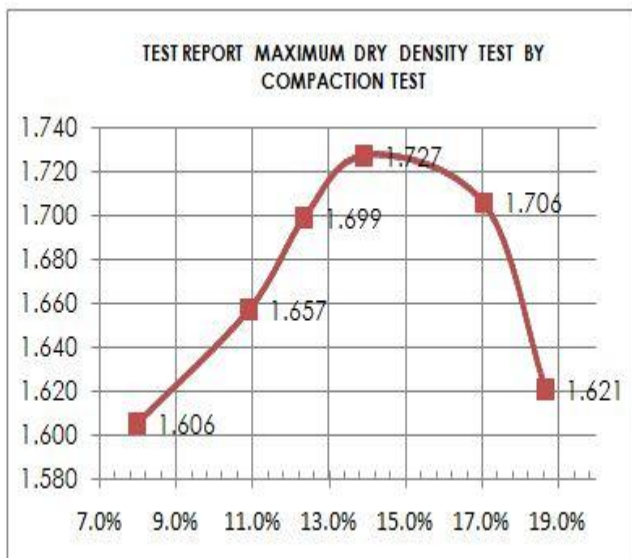
IV. RESULTS AND DISCUSSION

The parameters affecting pavement performance and the methods, equipments used to evaluate the sub-grade strength and other related materials are discussed.

4.1 Compaction Test MDD & OMC

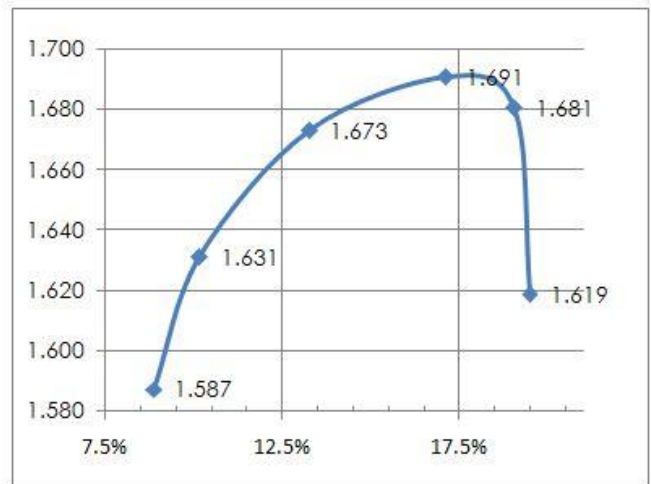
DRY DENSITY	MOISTURE CONTENT
1.606	8.00%
1.657	10.91%
1.699	12.35%
1.727	13.92%
1.706	17.07%
1.621	18.67%

MAXIMUM DRY DENSITY	1.727
OPTIMUM MOISTURE CONTENT	13.924%



COMPACTION TEST MDD & OMC

DRY DENSITY	MOISTURE CONTENT
1.587	8.861%
1.631	10.169%
1.673	13.253%
1.691	17.105%
1.681	19.048%
1.619	19.481%



MAXIMUM DRY DENSITY	1.691
OPTIMUM MOISTURE CONTENT	19.481%

4.2 Determination of Liquid and Plastic Limit

SOIL SAMPLE - LOCATION

	LIQUID LIMIT			PLASTIC LIMIT	
	Test 1	Test 2	Test 3	Test 4	Test 5
Container I.D.	R	24	H	S	A
Mass of Empty Container (grams)	37	32	38	38	39
Mass of Wet Soil + Container (grams)	76	70	77	73	77
Mass of Dry Soil + Container (grams)	66	61	68	68	72
Mass of Water (grams)	10	9	9	5	5
Mass of Dry Soil (grams)	29	29	30	30	33
% Moisture	34.48	31.03	30.00	16.6	15.1
No. of Blows	19	26	30		
Liquid Limit from Flow Curve	31.33				
Plastic Limit	15.91				

Plasticity Index (Liquid Limit - Plastic Limit)	15.42
---	-------

4.3 Determination of Free Swell Index

SOIL SAMPLE - LOCATION

Readings on the Glass Jar	Sample 1	Sample 2	Sample 3
---------------------------	----------	----------	----------

V_d = volume of soil specimen read from the graduated cylinder containing distilled water.	17	18	17
V_k = volume of soil specimen read from the graduated cylinder containing kerosene	10	10	10

Free swell index= $[V_d - V_k] / V_k \times 100\%$	50%	55%	50%
Average Free Swell index	50.25%		

V. SUMMARY

The main objective of this study is to use the locally available gravels/ soils with mixing robosand instead of using borrowed gravels in the sub-grade of internal road at the proposed College of Engineering, Sulthanpur, JNTU and also to check the performance of the sub-grade. Based on the traffic and the CBR value and also in view of the requirement to provide a sub-grade depth of about 0.90 M with good gravel to meet requirement of table 300-2 of MoRT&H, the sub-grade is proposed to be improved by mechanical stabilization with an additive of robosand in the locally available poor black cotton soils which are highly expansive in nature. The reduction in the cost is emphasized below where an overall savings of Rs.42,84,000.00 are projected against the original estimated cost of Rs. 1,94,68,800.00 by using the soil & robosand mixtures in sub-grades. This savings of approximately 22.00% is a commendable savings in the cost of construction. The original estimate is for providing sub-grade with good gravel from an approved quarry located at a lead distance of 8KMS from the work site for a length of 4 KMS and for the entire width of the right of the way. With the advent of the use of the locally available gravels/ soils with mixing robosand and mechanically stabilizing the sub-grade layer over which a capping layer of 150 mm thick good gravel to achieve CBR 10% has been very promising as the savings achieved in terms of money, time reduction, green rating and carbon points etc. The technical parameters and the specification for the sub-grade have been taken care of well in suggesting the usage of mechanically stabilized locally available gravels/ soils with mixing robosand in the sub-grades.

A sample stretch of the road pavement has been proposed with the above methodology where the CBR value is improved from 1.4% to 2.5% by using mechanically stabilized-locally available gravels/ soils mixed with robosand in the sub-grades.

5.1 Conclusions

Following conclusions are drawn from this study:

- To determine the Unconsolidated, Undrained strength of a cohesive soil the Unconfined Compressive Strength test was carried out for all the 5%, 10%, 15% and 20% fraction mixtures of robosand and the strength is ranging between 140.233 KPa to 149.06 KPa.
- The free swell index FSI was determined and found to be ranging between 86.33% to 72.33% for the fractions of robosand mixtures between 10% to 20%.
- Similarly the Optimum Moisture Content and Maximum Dry Density test were carried out to determine the degree of compaction and the results varied between 12.9% - 12.50% and 1.779-1.7142 for the fractions of robosand mixtures between 10% to 20%.
- To assess the sub-grade strength, CBR value of the sub-grade using stabilized soils was tested and found to be ranging between 2.4%-2.6% when tested for a soil & 10% of robosand mixture, which is found to be most economical. However, the stabilized soil mixture was also tested for 10%, 15% and 20% of the robosand fractions mixed in the soil sample, the increase in the CBR is observed, but due to economical criteria 25% fraction of robosand mixture mixed in the local soils was adopted.

5.2 Recommendations for Further Work

- As the proposed road uses only one fraction of robosand mixture i.e., 10% of robosand mixed in the locally available soils is adopted for the road section and the evaluation of the other fractions can be made with respect to the mixes. Distresses like pot holes, corrugations, rutting, ravelling, skid resistance, and roughness in the road sub-grade could not be studied as the road section is not completed in full shape.
- The evaluation of sub-grade strength with the composite mixtures such as fly-ash and robosand in different fractions can be studied in an elaborative manner for more economical and feasible designs.
- This data can be used to develop deterioration models by considering various factors like traffic, pavement distress, and pavement age after continuing this work for few more years. To evaluate the performance of the pavements with proper maintenance, continuous study for successive years is required, for which, this study is to be continued and historical data has to be

generated. To develop various distress progression models, continuous data base is required so that it can be incorporated in the further study.

REFERENCES

- [1] Pradeep Muley, Research Scholar, IIT Roorkee, and P. K. Jain, Professor, MANIT Bhopal, "Betterment and Prediction of CBR of Robosand Mixed Poor Soils" Proceedings of Indian Geotechnical Conference December 22-24, 2013, Roorkee
- [2] Swapan Kumar Bagui "Pavement Design for Rural Low Volume Roads Using Cement and Lime Treatment Base" Jordan Journal of Civil Engineering, Volume 6, No. 3, 2012
- [3] "Quality Assurance Handbook for Rural Roads EQUIPMENT AND TEST PROCEDURES" Ministry of Rural Development Government of India
- [4] V.K. Sinha, H.N. Singh & Saurav Shekhar Paper No. 535 "Rutting In Flexible Pavements – A Case Study"
- [5] Raja J and G.L. Siva Kumar Babu published in VOL.41 NO.6 "Bamboo as Subgrade Reinforcement for Low Volume Roads on Soft Soils" JUNE 2013 INDIAN HIGHWAYS
- [6] IS : 2720 -1977 , Indian Standard methods of test for soils (All parts)
- [7] Lakshmi Keshav, Mangaiarkarasi.V "Effect of Fly Ash on an Expansive Soil for Flexible Pavement Design", International Journal of Engineering and Innovative Technology (IJEIT) Volume 2, Issue 3, September 2012
- [8] K. Suresh, V. Padmavathi, Apsar Sultana, "Experimental Study On Stabilization Of Black Cotton Soil With Robosand And Fibers" IGC 2009, Guntur, INDIA
- [9] Mir Sohail Ali, Shubhada Sunil Koranne, "Performance Analysis of Expansive Soil Treated With Stone dust and Fly Ash" Electronic Journal of Geotechnical Engineering (EJGE)
- [10] Ramadas, T.L. Kumar, N. Darga1 Aparna, G.1 "Swelling and Strength Characteristics of Expansive Soil Treated with Robosand and Fly Ash" IGS Mumbai Chapter & IIT Bombay International Journal of Emerging Technology and Advanced Engineering
- [11] Pardeep Singh1, K.S.Gill2 "CBR Improvement of Clayey Soil with Geo-grid Reinforcement"
- [12] Clemmons, G. H., and Saager, V. (2011). "Financing Low-Volume Road Improvements."
- [13] Transportation Research Record: Journal of the Transportation Research Board, 2203, 143–150.
- [14] Cross, S. A., Voth, M. D., and Shrestha, P. P. (2005). "Guidelines for prime coat usage on low-volume roads." Transportation Research Record: Journal of the Transportation Research Board, 1913, 117–125.
- [15] Dawson, A. R., Kolisoja, P., Vuorimies, N., and Saarenketo, N. (2007). "Design of low- volume pavements against rutting Simplified Approach." Transportation Research Record: Journal of the Transportation Research Board, 1989(1), 165–172.
- [16] Howard, I. L. (2011). "Preservation of low-volume flexible pavement structural capacity by use of seal treatments." Transportation Research Record: Journal of the Transportation Research Board, 2204, 45–53.
- [17] Huntington, G., and Ksaibati, K. (2011). "Improvement recommendations for unsealed gravel roads." Journal of the Transportation Research Board, 2205, 165–172.
- [18] Huntington, G., and Ksaibati, K. (2011). "Implementation Guide for the Management of Unsealed Gravel Roads." Transportation Research Record: Journal of the Transportation Research Board, 2205, 189–197.
- [19] IRC: SP: 77- 2008 "Manual for design, construction and maintenance of gravel roads", Indian Roads Congress, 2008.
- [20] IRC: SP: 20- 2002 "Rural roads manual", Indian Road Congress, New Delhi, 2002.
- [21] IRC: SP: 72- 2007 "Guidelines for the design of flexible pavements for low volume rural roads", Indian Road Congress, New Delhi, 2007.

ROAD ACCIDENT SEVERITY ANALYSIS IN CYBERABAD & HYDERABAD USING ORDERED PROBIT MODEL

Challa Kalyani¹, V Ranjith Kumar², Dr.M.Kameswara Rao³

¹Research Scholar (M.Tech, T.E), ²Assistant Professor, ³Professor
Malla Reddy Engineering College, (Autonomous) Kompally

Abstract: *In this paper, a brief practical review is presented on the statistical evidence showing the Accidents have been a major social problem in the developed countries of world for over fifty years. It is only in the past decade that developing countries like India have began to experience large increase in the number of road accidents taking place and having found it necessary to institute road safety programs. Road accidents in Hyderabad can be studied by identifying the high accidents occurred area having a peak rate. The road accidents study can be done in two areas of Hyderabad city. The project involves identifying of road accidents in seven variations and finally giving solutions. The two areas namely Hayathnagar and Safibabad are the mainly facing alarming road accidents. The road accidents study of two areas is done by conduction two types of data collections. Data collection is done from the police stations of two areas. Based on those data the suitable recommendations and counter measures are given for Hyderabad city and also for Indian cities. By conducting some type of survey in remaining areas of Hyderabad can reduce and prevent road accidents The occurrence and outcome of traffic crashes have long been recognized as complex events involving interactions between many factors, including the roadway, driver, traffic characteristics, and the environment. This study is concerned with the outcome of the crash. Method: Accident injury severity levels are analyzed using the ordered probit modeling methodology. Models showed the significance of victim's gender, vehicle type, type of collision, time of collision, and victim's age on the injury severity level. Results: The results suggest that vehicles involving higher level of severity are unknown vehicles. Pedestrian are more prone to higher severity level. Other conclusions also are presented like hit & run and rear end collisions are associated with more severe injuries*

Keywords: *Accidents, Model, Severity, injuries, Hyderabad, Secunderabad, Probit model.*

I. INTRODUCTION

Traffic safety is a major concern because of the economic and social costs of traffic crashes. The impact that traffic accidents have on society is significant. Individuals injured (or killed) in traffic accidents must deal with pain and suffering, medical costs, wage loss, and vehicle repair costs. For society as a whole, traffic accidents result in enormous costs in terms of lost productivity and property damage. It is assumed that there is total 2% loss of GDP only due to road accident in India. Clearly, efforts to improve our

understanding of the factors that influence accident severity are warranted. So the common practice in transportation engineering is a thorough study of traffic accidents and gets an understanding of the factor affecting them. Severity of injury sustained by victim involved in crashes is of considerable interest to policy makers & safety engineers. Transportation system is meant for movement of people and goods from one place to another place safely. Thus safety is one of the main aspects of the transportation system. Motorization has been happening rapidly throughout the world. This has increased the mobility of the people from one place to other and the accidents also. Road accidents became a serious problem. Accidents are social problems affecting people in many ways. Serious losses caused by road accidents demand the attention of the society and call for the solution of the problem. The prevention of road accidents should not be considered as purely technical exercise. It involves many factors like government, educator, engineers, enforcement, voluntary organizations etc. Investigation of accident severity is one of the important concerns to traffic safety because this is aimed not only at prevention of accidents but also at reduction of their severity. One way to accomplish the aim of the latter is to the identify the most probable factors such as driver and passenger characteristics, seasonal effects, weekly variation, time of day variation, collision type, vehicle type, and traffic and geometric conditions that affect accident severity.

II. NEED FOR PRESENT STUDY

Demand for transport is increasing day by day due to industrialization and urbanization during recent years. But the road infrastructure has not been developed along with the travel demand due to lack of resources. This imbalance is creating problem. Road accidents are not only occurring due to a single factor like driver's negligence or ignorance of traffic rules and regulations, but also due to many other related factors such as changes in road condition, vehicle condition, road user behavior, environment and combinations of other factors. Among the factors responsible for road accidents, the effect of road environment can be reduced if its influence is analyzed. Upgrading the total road network would be time consuming and huge financial resources are required, which may be difficult to implement. The quick and cost effective step in improving road safety may be identifying accident prone locations and improve them instead of improving the complete road network. In this work attention is paid to determine the effects of road environment factors on accidents.

Objective and Scope of the Study

The main objectives of the present study are presented below

- To study the distribution of fatal, non-fatal and vehicle damaged accidents took place during 2013-2015.
- To analyze the cause of accidents during 2013-2015.
- To apprise the hourly incidents of total accidents
- To provide safety measures to reduce pedestrians accidents.
- To study the causes of accidents and to suggest corrective treatment at potential location.
- To evaluate existing designs.
- To support proposed designs.
- To carry out before and after studies and to demonstrate the improvement in the problem.
- To make computations of financial loss.
- To give economic justification for the improvements suggested by the traffic engineer.

III. LITERATURE REVIEW

Gray et al. (2008) observed that young male drivers are over-represented in car accidents in Great Britain. While investigating the factors affecting the severity of these young male drivers they observed that driving in darkness, trips during early morning and towards the end of the week (Friday and Saturday) are related with higher severities. They also observed that carriageway hazards such as passing a site where accident occurred may increase severity of crashes at a site afterwards that specific site. They also observed higher levels of severities during overtaking maneuvers, and on the single carriageway of speed limit 60 mph. Other variables leading to higher severities were driving on main roads, not being at a junction, towing something like a caravan or trailer, young male drivers of age group 20-22, and finally in fine weather condition with no high winds.

Kockelman and Young (2001) applied ordered probit models to examine the risk of different injury levels sustained under all crash types, two-vehicle crashes, and single-vehicle crashes. The results suggest that pickups and sport utility vehicles are less safe than passenger cars under single-vehicle crash conditions. In two-vehicle crashes, however, these vehicle types are associated with less severe injuries for their drivers and more severe injuries for occupants of their collision partners (including drivers and passengers). Crash types such as roll-over and head-on accidents resulted in more severe injuries. Female drivers are also found to be involved with higher crash severities. Pai and Saleh (2007) estimated statistical models to identify whether a specific maneuver by motorcycle or vehicle (e.g., overtaking or changing lanes) is more hazardous to motorcyclists in sideswipe collisions at T-junctions. The modeling results show that injuries to motorcyclists were greatest when an overtaking motorcycle collided with a turning vehicle and such effect appeared to be more severe at unsignalized junctions. Quddus et al. (2002) investigated factors leading to increase in the probability of severe injuries of motorcyclists

and identified that motorcyclist who is not from Singapore experienced higher crash severities compared to Singaporean motorcyclists. , Among other factors they found that increased engine capacity, headlight not turned on during daytime, collisions with pedestrians and stationary objects, driving during early morning hours and motor cycles with pillion passengers experienced higher severities. Additionally they observed that in collisions where the motorcyclists are at fault, they sustained higher levels of injuries than otherwise. Abdel-Aty (2003) applied ordered probit models for analysis of driver injury severity levels at roadway sections, signalized intersections, and toll plazas. He found that older drivers, male drivers, and those not wearing a seat belt will have a higher probability of a severe injury and both signalized intersections and roadway sections models showed higher level of injuries in rural areas, possibly due to higher speeds. He also found that driver's violation was significant in case of signalized intersection. Alcohol, lighting conditions, and the existence of a horizontal curve affected the likelihood of injuries in the roadway sections' model. A variable specific to toll plazas, vehicles equipped with Electronic Toll Collection, had a positive effect on the probability of higher injury severity at toll plazas. Duncan et al. (1998) applied ordered probit model to find injury severity in truck-passenger car rear-end collisions. they investigated that darkness; high speed differentials; high speed limits; grades, especially when they are wet; being in a car struck to the rear (as opposed to being in a car striking a truck to the rear); driving while drunk; and being female are the variables that increase passenger vehicle occupant injury severity. They also found that cars being struck to the rear with high speed differentials and car rollovers are significantly vulnerable. They also indentified variables associated with reduced severity levels and those were snowy or icy roads, congested roads, being in a station wagon struck to the rear (as opposed to a sedan), and using a child restraint. Khattak et al. (2002) reported that alcohol consumption, horizontal curves, higher speed limits, overturning, striking fixed object, accident in rural areas are the factors , which are causing higher level of severity to the older drivers. They also found that crashes involving farm vehicles resulted in significantly higher injury levels as compared with other types of vehicles. They identified that injury level were low on city streets as compared with other classes of road way.

IV. METHODOLOGY

Primary objective of this study is to develop a statistical model that identify the factors that are resulting higher crash severity. Here crash severity is dependent variable and independent variables are those factors affecting crash severity. So selection of an appropriate statistical model that correlates crash severity and factors affecting crash severity in better way was most important step in model development process.

Model Setup

To calibrate the accident severity model, data based on reported accidents in the period from 2013 to 2015 were used

in the study. During this period, there were no of accidents. In the proposed ordered probit model, the dependent variable used is accident severity which may take on one of three values based on the recorded degree of injury involved, viz, fatal, seriously injured and slightly injured. The accident is classified based on the worst condition sustained among the casualties. In the RangaReddy district accident reporting system, a casualty is considered fatal if the person is killed within 30 days of the accident. A seriously-injured casualty is one who had suffered some kind of fracture, concussion, internal lesions, crushing, severe cuts and laceration or severe general shock requiring hospitalization or other forms of bodily pain requiring at least 7 days of medical leave. A person is considered to be slightly injured if the victim had suffered from other forms of injury requiring conveyance from the accident scene to hospital by an ambulance or otherwise, the medical treatment requires medical leave of at least 3 days.

To develop the model for the respective studies of all crash model it is necessary to pre-select various factors consisting of victim, vehicle, crash, road, pedestrian and environmental characteristics that could be reasonably expected to influence accident severity. One way of sorting out these factors is to deliberate upon similar research works where those factors have been used. Also some factors selected are thought to have influence on accident severity in RangaReddy district condition.

Several factors were dropped after correlation test between variables. For example, type of road and speed limit were found strongly correlated. The type of road was a better indicator in predicting injury severity than speed limit; therefore type of road was kept in the model. Some other factors were also excluded because they are found to be statistically insignificant. These include the day of week, gender of driver, surveillance camera, race of driver, central business district area, electronic road pricing hours if in central business district area, area of occurrence and make of vehicle. Eventually 49 variables from 13 factors are retained in the final model. It is noted that a majority of these variables are categorical dummy in nature shows the existence of effect. the independent variables are organized into 5 groups

- General characteristics,
- Vehicle characteristics,
- Road characteristics,
- Driver characteristics and
- Crash characteristics.

Ordered response models recognize the indexed nature of various response variables; in this application, driver injury severities are the ordered response. Underlying the indexing in such models is a latent but continuous descriptor of the response. In an ordered probit model, the random error associated with this continuous descriptor is assumed to follow a normal distribution. In many studies on severity of accidents, discrete models have been used to identify factors affecting the severity.

In contrast to ordered response models, multinomial logit and probit models neglect the data's ordinality, require estimation of more parameters (in the case of three or more alternatives, thus reducing the degrees of freedom available for estimation), and are associated with undesirable properties, such as the independence of irrelevant alternatives (IIA, in the case of a multinomial logit (Ben-Akiva and Lerman, 1985)) or lack of a closed-form likelihood (in the case of a multinomial probit (Greene, 2000)). The ordered probit can be estimated via several commercially available software packages and is theoretically superior to most other models for the data analyzed in this work.

The general specification of each single equation model is:

$$Y_n^* = \beta'x_n + \epsilon_n,$$

Where, Y_n^* is the latent and continuous measure of injury severity faced by the accident victim 'n' in a crash, x_n is a vector of explanatory variables measuring the attributes of accident victim. β' is vector of parameters to be estimated, and ϵ_n is a random error term which assumed to follow a standard normal distribution with mean zero and variance one. The observed and coded discrete injury severity variable, Y_n , is determined from the model as follows:

V. ANALYSIS AND RESULTS

5.1 Introduction

Vanastalipuram division. Three years i.e. 2013-2015 data is collected is collected from Hayathnagar Police Station. The clear data is noted from the Police FIR sheets. Data is separated in to seven categories.

5.2 Total Accidents in Hayathnagar during 2013-2015 Month Wise

Table 5.1 Total Accidents in Hayathnagar Month Wise

Total Accidents in Hayathnagar				
Month wise				
Month	Fatal Accidents	Non-Fatal Accidents	Vehicle Damaged Accidents	Total Accidents
January	18	40	3	61
February	18	33	3	54
March	13	42	3	58
April	20	30	3	53
May	23	32	6	61
June	16	43	4	63
July	17	31	4	52
August	14	33	4	51
September	15	29	4	48
October	13	32	0	45
November	14	38	1	53
December	13	38	4	55
Grand Total	194	421	39	654

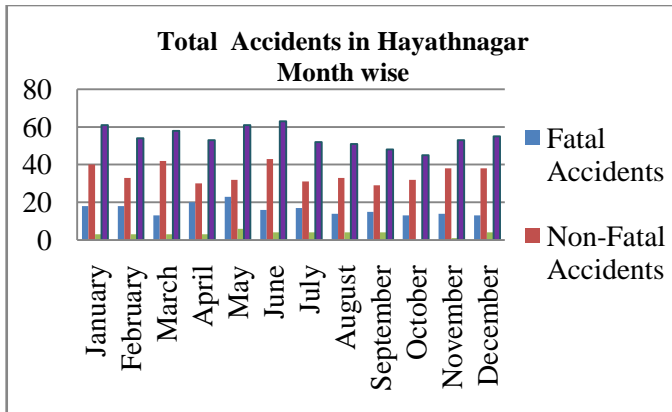


Fig 5.1: No. of Accidents Occurred in Hayathnagar Month Wise

VI. CONCLUSIONS

A safe and efficient transportation system is the primary measure of the quality of service provided by the system. Provision of safe and efficient transportation system is the responsibility of traffic and transportation engineers. The study presented in this thesis work provides methodological as well as empirical knowledge on the effect of several factors affecting crash injury severity. The development of such statistical model helps to gauge the performance of system providing traffic safety professional with information needed for efficient planning and improvement programs as well as strengthening enforcement programs. The primary objective of this study was to identify the factors that are contributing to higher injury severity levels. In order to achieve this objective, various factors such as, seasonal variation, weekly variation, hourly variation, type of vehicle involved in crash, crash location, type of collision, and victim gender have been investigated to find how they influence crash injury severity. Three distinct statistical model, namely all crash model, truck involved crash model, and pedestrian involved crash model have been developed. In order to identify the factors that affect crash injury severity a suitable methodology has been followed. The methodology includes data collection, selection and development of all three models and interpretation of the model findings. Statistical model selected for development of all three cases is ordered probit regression methodology. Recommendations to take precautionary measures for enhancement of traffic safety on national highways are also discussed. Finally future scope of the study is discussed

6.1 Discussions and Recommendation

In this model the developed study on crashes occurring in night, are resulting higher level of crash severity. Particularly accidents occurring between midnight to early morning hours are more sensitive to higher level of crash severity. This may be due to poor illumination and absence of warning measures such as retro-reflective signs which helps in roadway hazard identification. Hence to avoid such crashes proper illumination in night hours on highways along with retro-reflective materials is strongly recommended. For this purpose installation of solar lights may be very effective.

Pedestrians, bicycles, motorcycle and auto-rickshaws are facing higher crash severity. This is mainly because of the discontinuous service roads leading to wrong side movement of traffic in order to avoid long detours. Hence it is logical to provide separate service lane for local traffics. There is lack of proper facilities for vulnerable road users to cross highway forcing them midblock crossing. Therefore, infrastructure and planning such as additional side walk and cross walks that would act to separate vulnerable road users are needed. Educational programs to encourage riders to use helmet will be very effective and is highly recommended.

In accused vehicle categories trucks are resulting higher crash severity. Most of trucks on highways are overloaded and old and also there is absence of safety features in trucks. Also, a high percentage of these vehicle fleets are old, thus improperly maintained and lack safety features such as antilock braking. The crashworthiness of these vehicles is also low. In addition, they are hard to locate at night since they have neither tail lights nor reflective tapes. As a result, they are highly involved in crashes and the chance of survival of the truck users is also very low. Therefore developing stronger enforcement strategies and education programs in order to remove overloading and to improve the safety features in truck is strongly recommended and could only be done through government policies. Hit and run type of crashes is also resulting in higher level of crash severity. There is no remedy for hit and run type of crashes except enforcement and stringent punishment.

Overturning crashes are also resulting higher crash severity. To take care of overturning crashes pavement distress such as potholes and rutting should be removed. Also median openings and turning radius are to be re-designed for better safety..

6.2 Future Scope of Study

This study has a lot of scope for prevention of road accidents in the future. In this study was limited for two areas only but following same kind of work for remaining areas to reduce accidents rate in Cyberabad and Hyderabad.

This kind of study is suitable for any city in India.

REFERENCES

- [1] Amith Gosh and Suman Paul (2014), "Road accident scenario in Kolkata: A spatio-temporal study", European journal of applied Engineering and science research.
- [2] B.Ramakrishnan (1985), "How much safe are our Indian Roads?" journal of transportation Management.
- [3] Dr.M.Kumar and A.Ramesh (2015), "Estimation of influence on type of collection for Road accidents using Logit models in Cyberabad – Hederabad - India", Institute of research Engineers and doctor.
- [4] Guler yalcin (2014), "Non-spatial analysis for the road traffic accidents", Lumen international conference Logos University Mentality education Novelty (LUMEN).
- [5] "Hyderabad Wikipedia"

- [6] "Highway Engineering" by S.K.Khanna and C.E.G.Justo, Nem Chand & Bros (2011).
- [7] Kadiyali, L.R., T.V.Gopalaswami, P.R.Lakshmikantham, U.N.Pathak and A.K.Sood (1983), "Effect of road characteristics on accident rates on rural highways in India", Highway Research Bulletin.
- [8] Liyamal Isen, Shibu A, Saran M.S (2014), "Identification and analysis of accidents black spots using Geographic information system", International journal of innovation research in science Engineering and technology.
- [9] Murat Karacasu, Arzu Er, Safak Bilgic, Hasan B.Barut (2011), "Variations in traffic accidents on Seasonal, Monthly, Daily and Hourly Basis: Eskisehir case", Procedia social and behavioral science.
- [10] Pillai B.B and Joseph.K (2011), "Cause and consequences of road accidents in Kerala", International Journal of Research in IT and management.
- [11] "Traffic Engineering and Transport Planning" by Dr.L.R.Kadiyali, Khanna publishers (2013).
- [12] Gray R. C., Qudus, M. A. and Evans, A. (2008). "Injury severity analysis of accidents involving young male drivers in Great Britain." Journal of Safety Research, 39, 483–495
- [13] Pai, C. and Saleh, W. (2008). "Modelling motorcyclist injury severity resulting from sideswipe collisions at T-junctions in the United Kingdom." International Journal of Crashworthiness, 13(1), 89 —98
- [14] Duncan, C. S., Khattak, A. J. and Council, F. (1998). "Applying the ordered probit model to injury severity in truck-passenger car rear-end collisions." Transportation Research Board, Transportation Research record 1635, Paper no. 98-1237, 63-71.
- [15] Khattak A. J., Pawlovich M. D., Souleyrette R.R., and Hallmark, S.L. (2002). Factors Related to More Severe Older Driver Traffic Crash Injuries. Journal of Transportation Engineering, 128(3).
- [16] Zajac, S.S., and Ivan, J. N. (2003) "Factors influencing injury severity of motor vehicle crossing pedestrian crashes in rural Connecticut." Accident Analysis and Prevention, 35 369–379.
- [17] O'Donnel, C. J., and Connor, D. H. (1996). "Predicting the severity of motor-vehicle accident injuries using models of multiple ordered choice." Accident Analysis and Prevention. 28(6), 739-753.
- [18] Greene, W. H. (2002). LIMDEP Version8.0. New York Econometric Software Inc
- [19] Road accidents in India. (2008). Ministry of Road Transport and Highway, government of India, New Delhi.

DESIGN OF SEISMIC RESISTANCE REINFORCED CONCRETE STRUCTURE ON A INCLINED GROUND

Usha KP ¹ K. Vamshi Krishna ² M. Kameswara Rao ³

M.Tech Research Scholar ¹, Assistant Professor ², Professor ³
Malla Reddy Engineering College (Autonomous), Hyderabad, Telangana, India.

ABSTRACT

This Paper involves the analysis of simple 2-D and 3-D frames of varying floor heights and varying no of bays using a very popular software tool STAAD Pro. Using the analysis results various graphs were drawn between the maximum axial force, maximum shear force and maximum bending moment being developed in the frames on plane ground and sloping ground. The graphs used to drawn comparison between the two cases and the detailed study of “**SHORT COLOUMN EFFECT**” failure was carried up. In addition to that study of seismology was undertaken and the feasibility of the software tool to be used was also checked. Till date many such projects have been undertaken on this very topic but the analysis were generally done for the static loads i.e. dead load, live load etc, but to this the earthquake analysis or seismic analysis is to be incorporated. To create a technical knowhow, two similar categories of structures were analyzed, first on plane ground and another on a sloping ground. Then the results were compared. At last the a structure would be analyzed and designed on sloping ground for all possible load combinations pertaining to IS 456, IS 1893 and IS 13920 manually.

Keywords— STAAD.Pro, Earth Quake Loads, Inclined Ground, IS: 1893, IS: 456-2000, IS:1893, IS:13920.

1. INTRODUCTION

Seismology is the study of vibrations of earth mainly caused by earthquakes. The study of these vibrations by various techniques, understanding the nature and various physical processes that generate them from the major part of the seismology. Elastic

rebound theory is one such theory, which was able to describe the phenomenon of earthquake occurring along the fault lines. Seismology as such is still a very unknown field of study where a lot of things are yet to be discovered.

The following Picture is showing the fault lines and we can see that epicentres are all concentrated all

along the fault lines. The reason for seismic activities occurring at places other than the fault lines are still a big question mark. Also the forecasting of earthquake has not been done yet and would be a landmark if done so. There is general saying that it's not the earthquake which kills people but its the bad engineering which kills people. With industrialization came the demand of high rise building and came dangers with that.

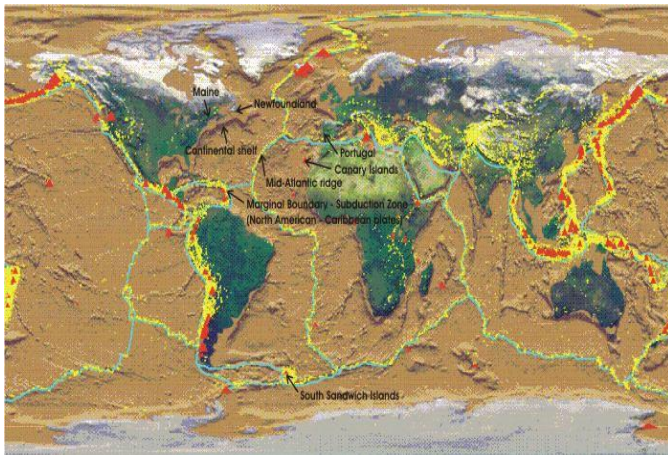


Fig. 1.1 Earth quake fault lines world map

A seismic design of high rise buildings has assumed considerable importance in recent times. In traditional methods adopted based on fundamental mode of the structure and distribution of earthquake forces as static forces at various stories may be adequate for structures of small height subjected to earthquake of very low intensity but as the number of stories increases the seismic design demands more rigorous.

During past earthquakes, reinforced concrete (RC) frame buildings that have columns of different heights within one storey, suffered more damage in the shorter columns as compared to taller columns in the same storey. Two examples of buildings with short columns in buildings on a sloping ground and

buildings with a mezzanine floor can be seen in the figure 1.2.

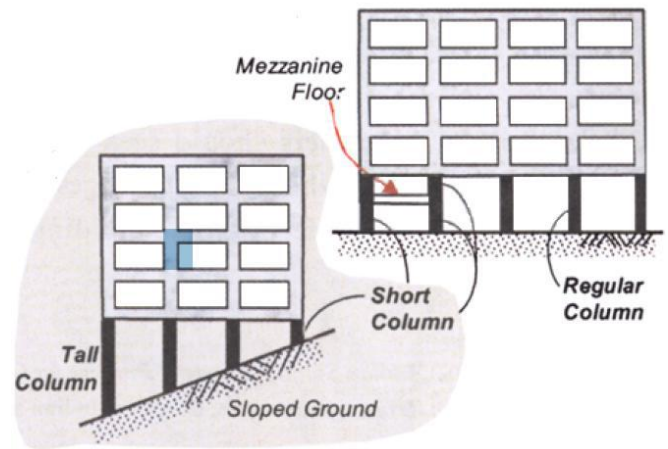


Fig. 1.2 Buildings on a sloping ground and buildings on a plane ground

Poor behaviour of short columns is due to the fact that in an earthquake, a tall column and a short column of same cross section move horizontally by same amount which can be seen from the given figure 1.3.

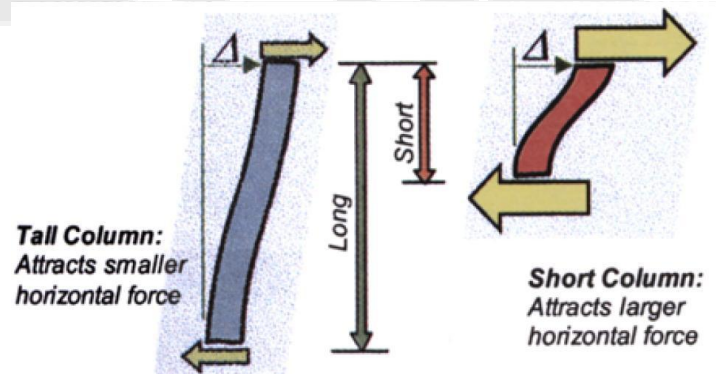


Fig. 1.3 Behaviour of short columns and tall columns of same cross section

2. FEASIBILITY OF STAAD-PRO SOFTWARE TOOL

It is made for providing full seismic safety for the residents inhabiting the most earthquake-prone regions on sloping ground's by providing high quality of construction accordance with related IS

codes and ductility designing and as far as possible avoiding short column effect.

As an example we took up a simple 2 dimensional frame subjected to concentrated loads with un-equal supporting columns. This is for the analogy of the actual problem statement of design of a multi-storied building on a sloping ground

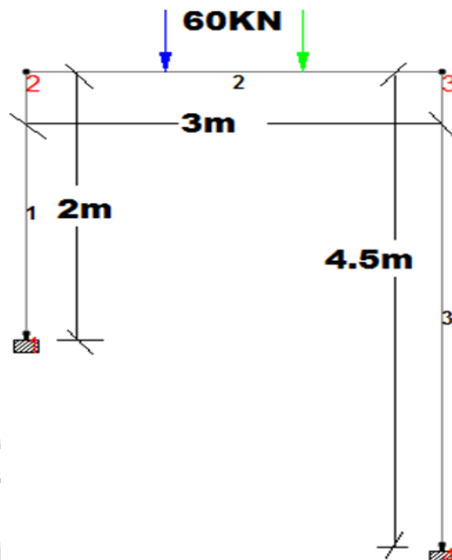


Fig. 2.1 Un-equal 2D frame with 2 concentrated loads

2.1 STAAD Pro RESULTS

Node	L/C	Horizontal		Vertical		Horizontal		Moment		
		Fx kN	Fy kN	Fz kN	Mx kNm	My kNm	Mz kNm			
1	1 LOAD CAS	9.222	58.692	0.000	0.000	0.000	3.480			
4	1 LOAD CAS	-9.222	61.308	0.000	0.000	0.000	15.650			

2.2 REACTIONS

Beam End Forces

Sign convention is as the action of the joint on the beam.

Beam	L/C	Node	Axial			Shear			Torsion			Bending		
			Fx kN	Fy kN	Fz kN	Mx kNm	My kNm	Mz kNm						
1	1 Concentrate	1	58.692	-9.222	0.000	0.000	0.000	3.480						
		2	-58.692	9.222	0.000	0.000	0.000	-21.923						
2	1 Concentrate	2	9.222	58.692	0.000	0.000	0.000	21.923						
		3	-9.222	61.308	0.000	0.000	0.000	-25.847						
3	1 Concentrate	3	61.308	9.222	0.000	0.000	0.000	25.847						
		4	-61.308	-9.222	0.000	0.000	0.000	15.650						

3. ANALYSIS OF SIMPLE 2 AND 3 DIMENSIONAL REINFORCED CONCRETE FRAMES

With full confidence on the STAAD Pro. Design tool, we proceed with the analysis of simple 2 dimensional frames. The analysis was done for both the static load conditions and dynamic load conditions which involves the analysis of frames on a plane ground and then on a sloping ground.

3.1 First start with 2 storey frame. First we went with double bay and up to 4 bays both on a plane ground and on as sloping ground.

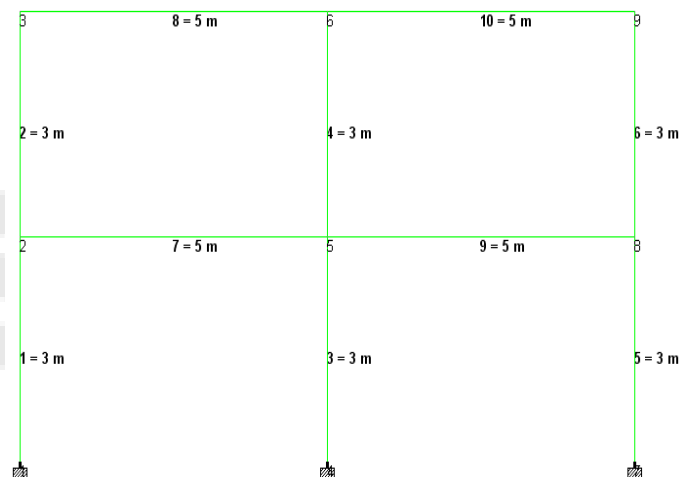


Fig. 3.1.1 Double bay 2 storey frame on a plane ground

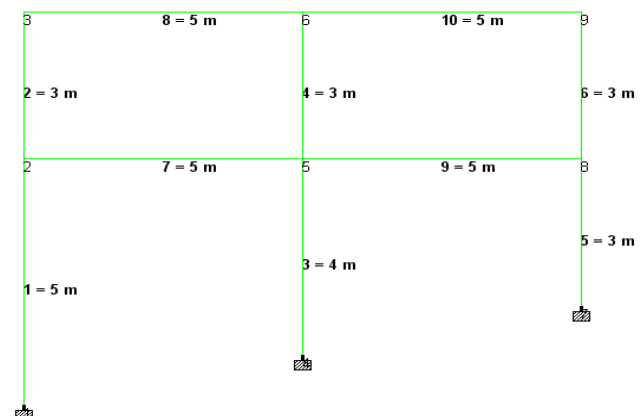
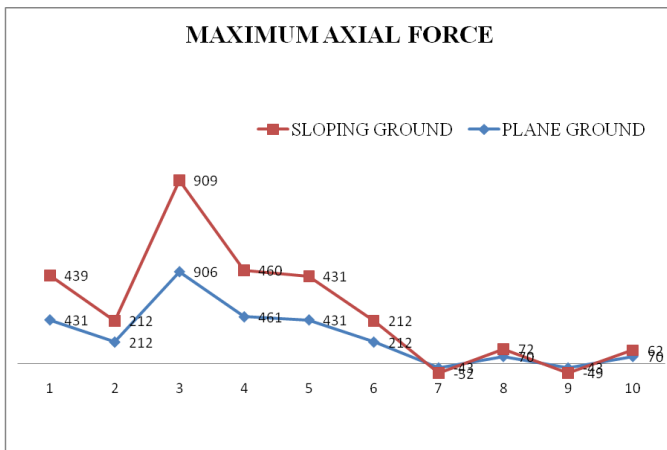
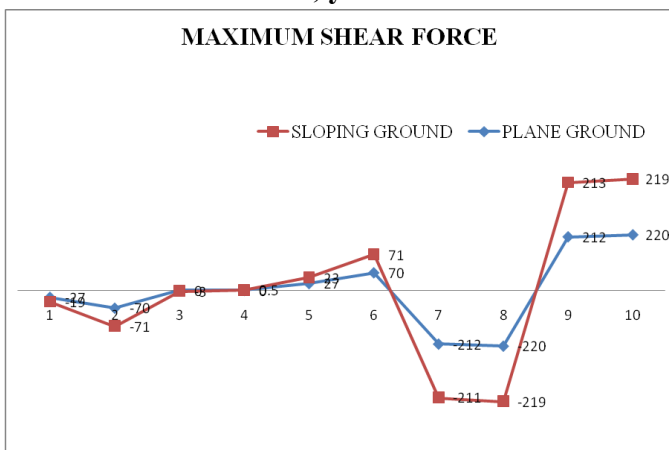


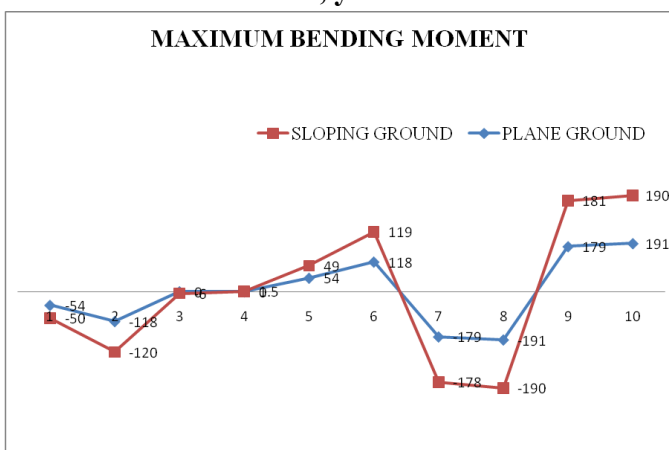
Fig. 3.1.2 Double bay 2 storey frame on a sloping ground



Graph 3.1.1 Variation of maximum axial force on plane ground and on a sloping ground x-axis beam/column no's, y-axis results values.



Graph 3.1.2 Variation of maximum shear force on plane ground and on a sloping ground x-axis beam/column no's, y-axis results values



Graph 3.1.3 Variation of maximum bending moment on plane ground and on a sloping ground x-axis beam/column no's, y-axis results values

3.2) Then go for 4 storey frame. For the same we start with double bay and up to 4 bays both on a plane ground and on a sloping ground.

3.3) Then go for 6 storey frame. For the same we start with double bay in length and width and up to 4 bays both on a plane ground and on a sloping ground.

4. DUCTILITY DESIGN AND DETAILING.

A detailed design of a frame has been carried out with the design aid of IS 456 and IS 13920:1993

4.1) design of an flexural member.

4.2) design of an exterior column.

4.3) design of an interior column.

To illustrate the design of a sub-frame a flexural member with maximum bending moment has been carried out .

General specification

- The member is designed according to IS 456:2000 and IS 13920:1993
- For all building's > 3 storey height minimum grade of concrete M-20 – So we used M-25
- steel reinforcement of FE 415 used.

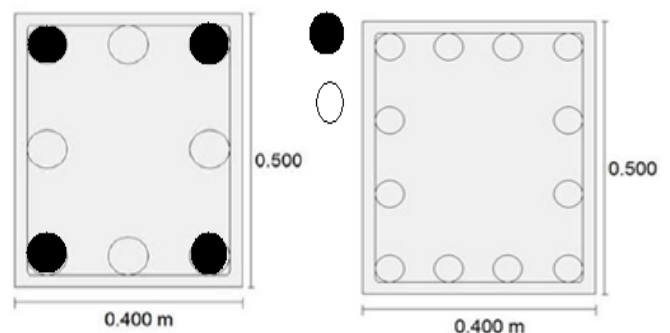


Fig. 4.1 Columns reinforcement cross-section

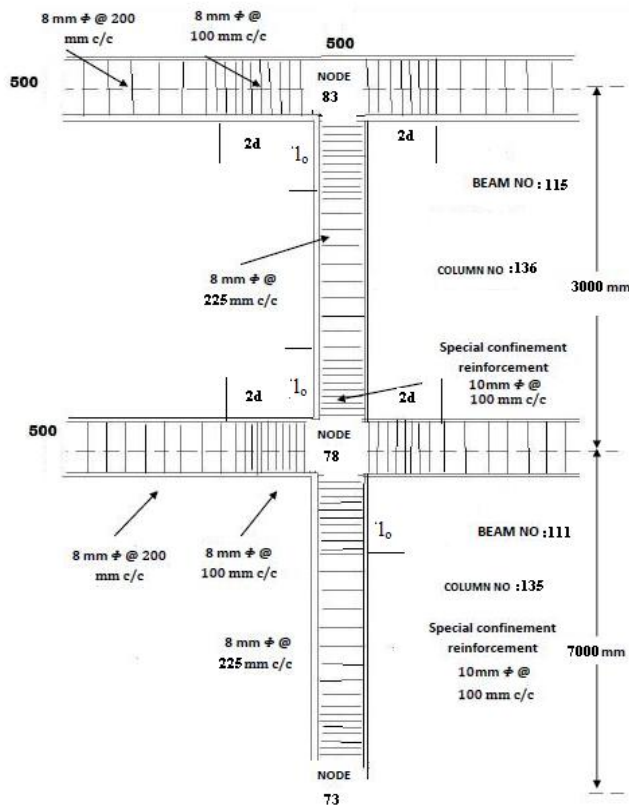


Fig. 5.1 Typical ductility reinforcement detailing in columns

CONCLUSIONS

The tasks of providing full seismic safety for the residents inhabiting the most earthquake-prone regions are far from being solved. However in present time we have new regulations in place for construction that greatly contribute to earthquake disaster mitigation and are being applied in accordance with world practice.

In the regulations adopted for implementation in India the following factors have been found to be critically important in the design and construction of seismic resistant buildings:

- sites selection for construction that are the most favourable in terms of the frequency of occurrence and the likely severity of ground shaking and ground failure;

- high quality of construction to be provided conforming to related IS codes such as IS 1893 , IS 13920 to ensure good performance during future earthquakes.
- To implement the design of building elements and joints between them in accordance with analysis .i.e. ductility design should be done.
- structural-spatial solutions should be applied that provide symmetry and regularity in the distribution of mass and stiffness in plan and in elevation.
- Whereas such the situations demands irregularity maximum effort should be given to done away with the harmful effects like that of “SHORT COLUMN EFFECT”

Researchers indicate that compliance with the above-mentioned requirements will contribute significantly to disaster mitigation, regardless of the intensity of the seismic loads and specific features of the earthquakes. These modifications in construction and design can be introduced which as a result has increase seismic reliability of the buildings and seismic safety for human life.

REFERENCES

- [1] IS:456:2000, Plain and Reinforced code of practice.
- [2] IS:1893(Part-1):2002, Criteria for earth quake resistant design of structure.
- [3] IS:13920:1993, Ductile detailing of RCC structure subjected to earth quake force.

- [4] SP:16, Design Aid for Reinforced concrete to IS:456:2000.
- [5] Ramamurtham, Theory of structures
- [6] STAAD Pro 2007 software from Bentley
- [7] Murthy C.V.R, Learning earthquake design
- [8] Agrawal, Shrikhande Mansih, earth quake resistant design of structures
- [9] Ashimbayev M.U., Itskov I.E., Lobodryga T.D., living with natural and technological hazards, topic a.2: reducing vulnerabilities in existing building and lifelines
- [10] S.S. Nalawade., “ Seismic Analysis of Buildings on Sloping Ground,”
- [11] C.V.R. Murthy, “ Minimising Short-Column Effect In Buildings” Institute Of Technology, Kanpur Courtesy.
- [12] Park, R. (1992). "Capacity design of ductile RC building structures for earthquake resistance."
- [13] Medhekar, M.S., Jain, S.K, and Arya, A.S, "Proposed Draft for IS:4326 on Ductile Detailing of Reinforced Concrete Structures
- [14] Park R., Paulay T., Reinforced Concrete Structures. *John Wiley & Sons*.
- [15] Ashok K. Jain Reinforced concrete (Limit state design)
- [16] Sheikh, S. A., and Uzumeri, S. M. _1982_. “Analytical model for concrete.
- [17] confinement in tied columns.” *J. Struct. Div.*, ASCE, 108_12_, 2703–2722.
- [18] Shetty R.K. and Jain A.K., “Special confinement reinforcement in RC columns and shear walls”, *The Indian Concrete Journal*, Vol. 85, No.6, June 2011, pp. 19-29.
- [19] Watson, S., Zahn, F. A., and Park, R., “Conining Reinforcement for Concrete Columns,” *Journal of Structural Engineering*, Vol. 120, No. 6, June 1994, pp.1798-1824.

A COMPARATIVE STUDY ON FAILURE MODES OF ANCHOR BOLT AND MECHANICAL ANCHORS AS PER ACI AND EUROPEAN CODES

¹K. Srikanth Verma, ²K. Vamshi Krishna, ³M. Kameswara Rao

¹M.Tech. Student ² Assistant Professor, ³Professor

^{1,2,3} Department of Civil Engineering

^{1,2,3} Malla Reddy Engineering College Autonomous), Secunderabad

ABSTRACT

Mechanical anchor are an essential element for nearly all structures and provide the necessary interface between a steel column base plate and a concrete foundation. The design of anchor bolts according to the current concrete code (ACI 318) is a complex and lengthy process that also contains many ambiguities and problems. The current code is investigated for each of the different possible failure modes. These problems are investigated for industrial structures, and recommendations are given to fix each of the different failure modes.

An anchor bolt is used to attach objects or structures to concrete. There are many types of anchor bolts, consisting of designs that are mostly proprietary to the manufacturing companies. All consist of a threaded end, to which a nut and washer can be attached for the external load. Anchor bolts are extensively used on all types of projects, from standard buildings

to dams and nuclear power plants. They can also be used to firmly affix embed plates to a concrete foundation when used with a structural steel element.

The simplest anchor bolt is a cast-in-place anchor. As seen in the figures, most designs consist of a standard bolt with a hexagonal head, which is cast in the wet concrete before it sets. There are other designs, some consisting of a bent bolt with a hook on the end, or some other sort of bending. Cast-in-place anchor bolts are the strongest type of fastener, but the casting is difficult, and they are usually only used for heavy machines mounted on poured concrete floors. Another use of this anchor bolt is to connect the concrete foundation of a building to its wall. With this, the building is more resistant to earthquakes. Currently there are several devices to assist in holding and in placing anchor bolt to set in the concrete. These devices are mostly made from composite plastic. Once

the concrete has been poured and set, the only other types of bolts that can be used are mechanical and epoxy bolts. Epoxy bolts are the strongest, but can be very tricky to install, since the epoxy has to be mixed to exact specifications, the hole must be very clean, and the set time has to be watched. As well, there must be a rigorous testing program. In Boston's Big Dig project, these procedures were not well carried out, which resulted in a large concrete slab crushing a motorist. A concrete screw is another way of attaching things to concrete that has already been poured and set.

Keywords: Anchor Bolt, Mechanical Bolt, American Concrete Institute (ACI) 318 Appendix D, European Code.

1. INTRODUCTION

Anchor fasteners are the world leader on fixings for the construction and have developed the expertise over many years of research and development. Because of the structure of the company, customers can deal directly with anchor fasteners. The company prides itself on the engineering support that is provided to the specifier and the end user of our products.

The design of anchor fasteners has been addressed multiple building codes, yet there have been many ambiguities within these codes.

The IBC (International Building Code) is the standard building code for the United States, and includes provisions for most aspects of the design of a structure. Within the IBC, the design of anchor is largely deferred to ACI 318 Appendix D (American Concrete Institute). The American Society of civil engineers (ASCE) has published a document dealing with the design of anchor for the petrochemical industry that includes some provisions not found within ACI 318 Appendix D. The American Institute of Steel Construction (AISC) has also published many different design guides that deal with many aspects of the construction of steel building, including the anchoring to concrete foundations.

1.1 FRICTION

The applied load, N , is transferred to the base material by friction, R . The expansion force, F_{exp} , is necessary for this to take place.

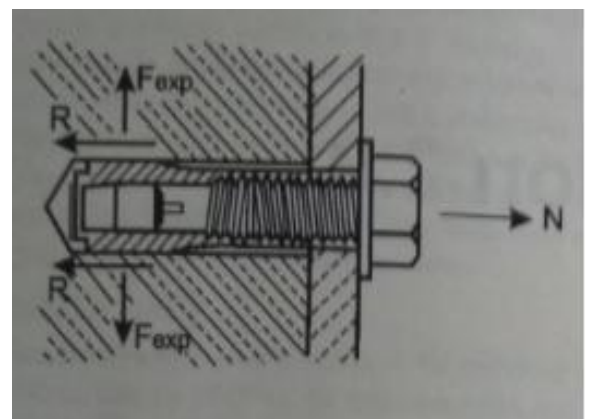


Figure-1.1 Friction Applied Load

1.2 KEYING

The tensile load, N , is in equilibrium with the resisting forces, R , acting on the base material. This creates much lower stresses in the base material than with other mechanical anchors.

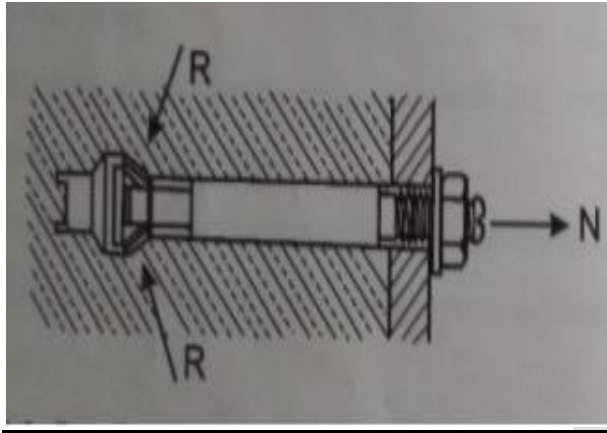


Figure-1.2 Keying

1.3 BONDING

An adhesive bond is produced between the anchor rod and the hole wall by a synthetic resin adhesive. This produces minimal stress in the base material.

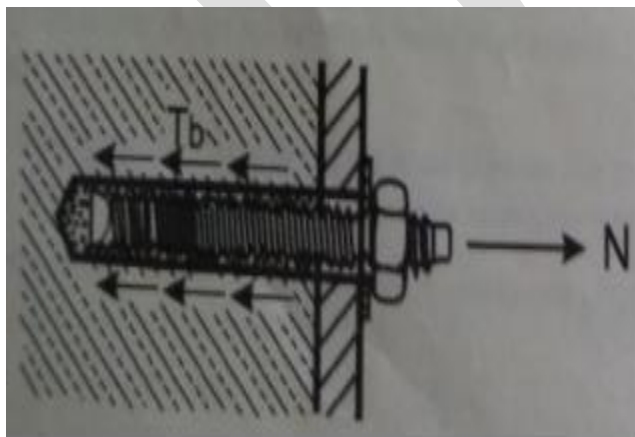


Figure-1.3 Bonding

1.4 COMBINATION OF WORKING PRINCIPLES

Many mechanical anchors obtain their holding strength from a combination of the above principles. When the anchor is expanded and creates the frictional forces, the base material is crushed locally and this produces a keying effect.

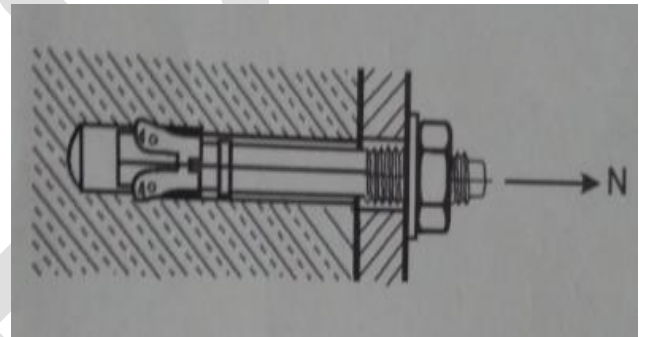


Figure-1.4 combination of working principles

1.5 TYPES OF ANCHORS

They are three major types of anchoring system is

- Cast in Anchors
- Post installed Anchors
- Post installed Rebar Connections

1.5.1 Cast-in Anchor

A headed bolt, anchor rod or hooked bolt that is installed before the concrete is placed. The anchor systems include cast-in channels, T-bolts or hammerhead bolts and all the items necessary to fulfill your project with unmatched quality and in full compliance with safety standards.

Medium to heavy duty, cast-in ferrule. All steel threaded socket for casting into pre-cast concrete and institute concrete elements, giving a prefixed fastening point.

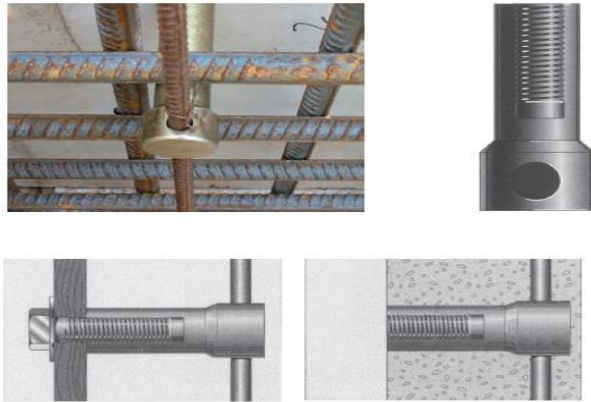


Figure-1.5 Cast in Anchors

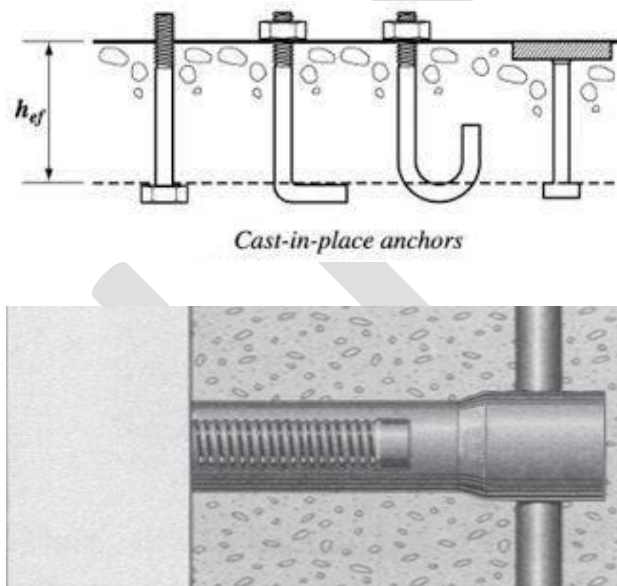


Figure-1.6 Cast Anchors in Place

1.5.2 Post-Installed Anchor

Post installed anchors have been used the early 1900;s secure building components. Originally the anchor hole was manually drilled a star type

drill and a hammer. An anchor consisted of a wood or lead plug which was carved or molded to size and driven into the drilled hole. As a Screw or nail was inserted in the plug, it expanded against the wall of the hole. Commercially manufactured anchored were first made from lead or finer materials in a variety of sizes to match a bolt or screw. The original Raw plug anchor was developed in 1919. As the material and techniques used in building construction changed, new anchors were developed to meet application needs

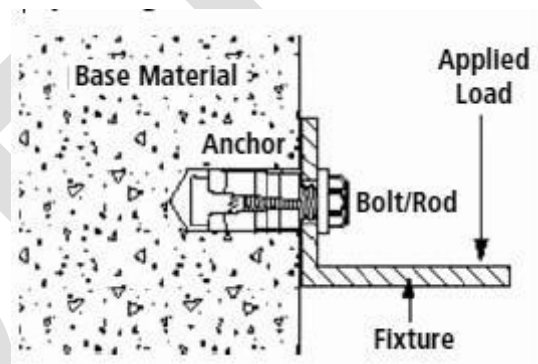


Figure-1.7 Post Install anchors

1.6 AVAILABLE CODES ON ANCHOR DESIGN

Concrete capacity design (CCD) has been a code methodology for anchor design since it was introduced directly into section 1913 of the 2000 international building code (IBC). It was initially a strength design option and was limited to cast.

Design of anchors to refer codes is are:

- ACI 318
- ETAG 001
- CSA A23.3-04

2. FAILURE MODES OF ANCHORS

2.1 Steel Tensile Failure

The tensile behavior of mild steel should be compared with the tensile behavior of high-tensile steel reinforcement.

The test demonstrates:

- The ductile properties of mild steel
- The yield point, working hardening and ductile zones of a mild steel
- The trade-off between increasing strength and reducing ductility

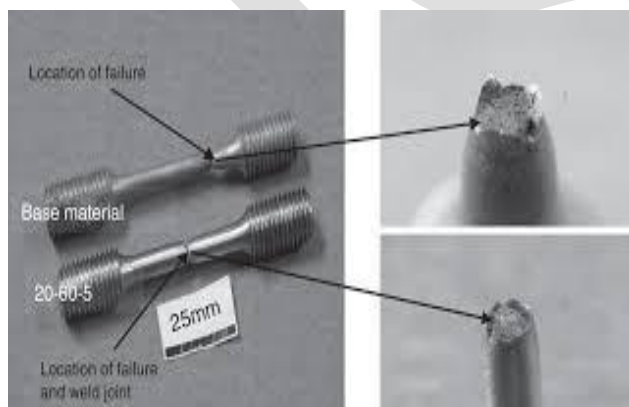


Figure-2.1 Tensile Failure

2.2 Steel Shear Failure

Steel shear failure occurs when the shear force transferred to the anchor is greater than the capacity of the bolt in shear. The anchor

subsequently yields and fails. It is not recommended to transfer the shear forces through the anchors, but to rely on friction, shear lugs, or embedded columns to transfer the shear forces to the base materials. In case of high shear, high uplift, or seismic loadings shear lugs or embedded columns would be required to transfer the shear to the concrete.

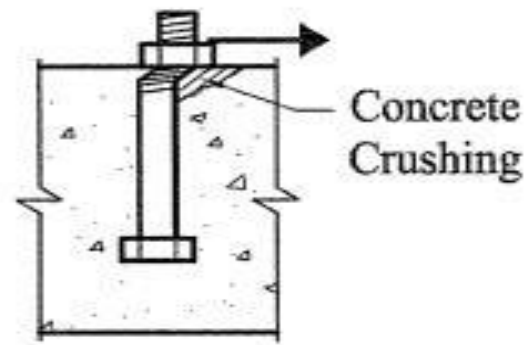


Figure-2.2 Shear Failure

2.3 Concrete Tensile Breakout Failure

Concrete tensile breakout failure occurs when the concrete base material cracks and allows the anchors to breakout along a failure plane of 35 deg. Anchor embedment depth, concrete side cover, or additional reinforcement would need be used to prevent this type of failure. Additional reinforcement can be used to prevent this type of failure by putting adequate reinforcement to prevent the shear plane from forming. The reinforcements would have to be designed to develop the strength on either side of the breakout plane.

2.4 Concrete Shear Breakout Failure

Concrete shear breakout occurs when the concrete cracks and breaks at a 35deg. From the top of the concrete. This occurs when an anchor is near the edge of the concrete base material. To prevent this type of failure, either the base material would have to be designed to have more concrete side cover, or shear reinforcement would need to be provided to prevent breakout.

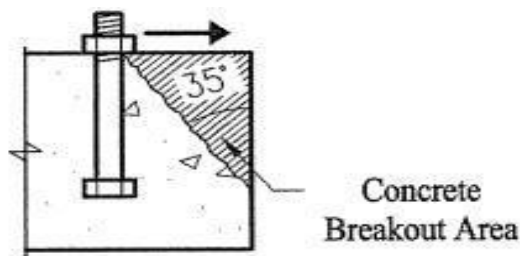


Figure-2.3 Shear Breakout Failure

2.5 Pullout Failure

Pullout failure occurs due to localized failure of concrete at the head of the anchor, when placed in tension. The anchor bolt comes free of the concrete connection and pulls out. This is predominately a problem with post-installed anchor bolts (either adhesive or mechanical), but is also a design consideration for cast-in-place anchors.

Pullout strength typically will only govern when either a low strength concrete, or high-strength bolts are used. In most applications, the pullout strength will be greater than steel tensile

strength if normal weight concrete, and normal strength bolts are used. If pullout strength governs the design.

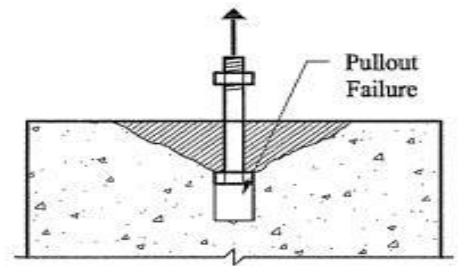


Figure-2.4 Pullout Failure

2.6 Concrete Side-Face Blowout Tensile Failure

Concrete side-face blowout occurs when insufficient side cover is present; the concrete breaks to the side of the anchors due to tensile loads. This occurs when the anchor is embedded relatively deep and is placed near the edge of the base material.

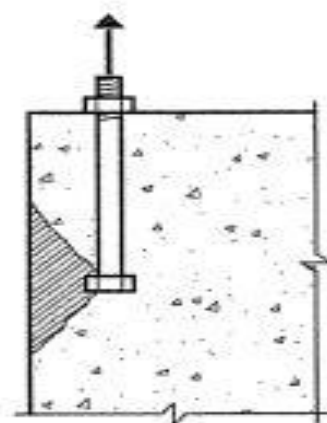


Figure-2.5 Side-Face Blowout Tensile Failure

2.7 Concrete Pryout Shear Failure

Concrete pryout occurs in base material with high shear forces, and the anchors are far from the edge of the base material (e.g. within a mat base material). The shear force causes local concrete failure near the top of the anchor, which in turn creates a moment, and couple force that breaks the concrete out in tension.

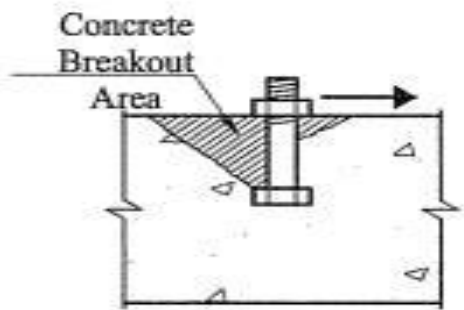


Figure-2.6 PRYOUT Shear failure

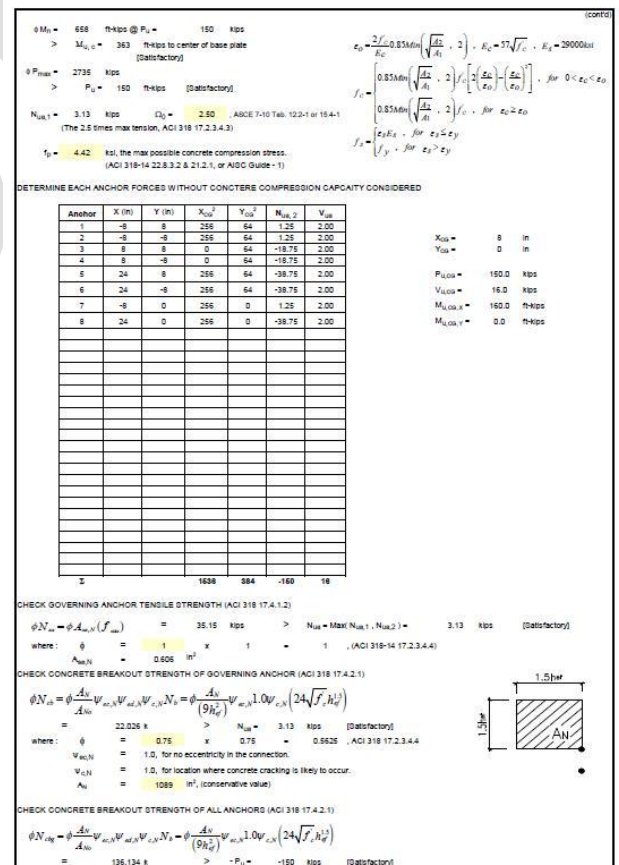
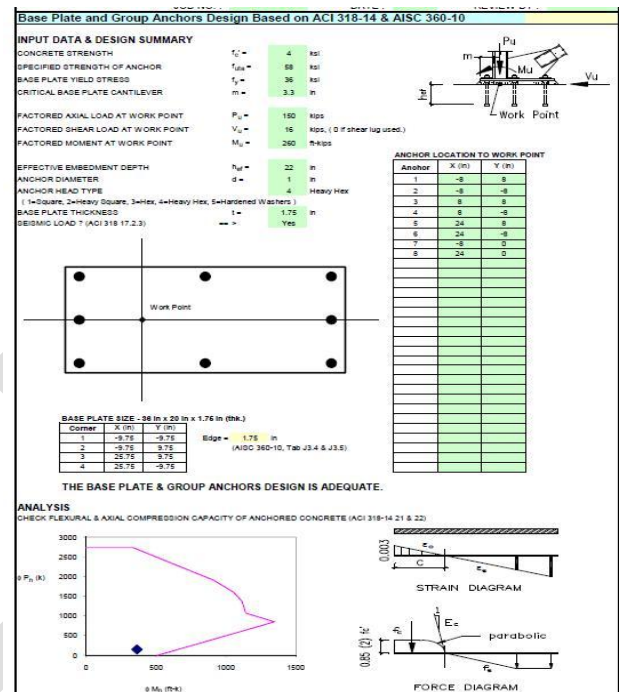
2.8 Concrete Splitting Failure

Concrete splitting failure occurs in thin concrete slabs that have anchors with insufficient edge distances or spacing. If the bolts are placed too close together, the concrete represents a service failure, and could lead to catastrophic failure. Either additional reinforcement is required, or a thicker slab is required to prevent this type of failure. This is predominately a problem in unreinforced concrete slabs.

Unlike the other concrete failure modes, concrete splitting failure is based upon the arrangement of the bolts.

3. DESIGN EXAMPLES

3.1 Cast In Anchors Example



where: $\phi = 0.75$ x $0.75 = 0.5625$ (ACI 318-14 17.2.3.4.4) (cont)

$V_{u,N} = 0.84$ (ACI 318-14 17.4.2.4)

$A_n = 98$ x $82 = 8036$ in²

CHECK PULLOUT STRENGTH OF GOVERNING ANCHOR (ACI 318 17.4.3.1)

$\phi N_{u,N} = \phi V_{u,N} (A_n f_t) = 27.018$ k > $N_{u,N} = 3.13$ kips [Satisfactory]

where: $\phi = 0.75$ x $0.75 = 0.5625$

$A_n = 1.501$ in² (or determined from manufacturer's catalogs)

$V_{u,N} = 1.0$, for location where concrete cracking is likely to occur.

CHECK SIDE-FACE BLOWOUT STRENGTH (ACI 318 17.4.4.1)

$c_{sl} > 0.4$ hef [Satisfactory]

Since this fastener is located far from a free edge of concrete ($c_{sl} > 0.4$ hef) this type of failure mode is not applicable.

DETERMINE DESIGN TENSILE STRENGTH OF GOVERNING ANCHOR

$\phi N_u = \min(\phi N_{u,N}, \phi N_{u,s}, \phi N_{u,t}) = 22.026$ K

CHECK GOVERNING ANCHOR SHEAR STRENGTH (ACI 318 17.5.1.2 & 17.2.3.5.3)

$\phi V_{u,s} = \phi 0.6 A_{n,V} f_v = 13.71$ k > $V_{u,s} = 5.00$ kips [Satisfactory]

where: $\phi = 0.65$ x $1 = 0.65$

$A_{n,V} = 0.606$ in² (for built-up gusset plate, first factor shall be multiplied by 0.8, ACI 318 17.5.1.3)

CHECK CONCRETE BREAKOUT STRENGTH OF GOVERNING ANCHOR FOR SHEAR LOAD (ACI 318 17.5.2.1)

$\phi V_{u,s} = \phi \frac{A_{n,V}}{A_{n,t}} V_{u,t} V_{u,s} V_{u,N} = \phi 1.0 V_{u,t} V_{u,s} V_{u,N} \left(\frac{1}{d} \right)^{1.5} \sqrt{f_c} (1.5 h_{ef})^{1.5}$

$= 95.407$ k > $V_{u,s} = 5.00$ kips [Satisfactory]

where: $\phi = 0.75$ x $1 = 0.75$

$V_{u,t} = 1.0$, for no eccentricity in the connection.

$V_{u,s} = 1.0$, for location where concrete cracking is likely to occur.

l term is load bearing length of the anchor for shear, not to exceed $8d$.

CHECK CONCRETE BREAKOUT STRENGTH OF ALL ANCHOR FOR SHEAR LOAD (ACI 318 17.5.2.1)

$\phi V_{u,s} = \phi \frac{A_{n,V}}{A_{n,t}} V_{u,t} V_{u,s} V_{u,N} = \phi \frac{A_{n,V}}{A_{n,t}} V_{u,t} V_{u,s} V_{u,N} \left(\frac{1}{d} \right)^{1.5} \sqrt{f_c} (1.5 h_{ef})^{1.5}$

$= 103.768$ k > $V_{u,s} = 5.00$ kips [Satisfactory]

where: $\phi = 0.75$ x $1 = 0.75$

CHECK PRYOUT STRENGTH FOR SHEAR LOAD ON GOVERNING ANCHOR (ACI 318 17.5.3.1)

$\phi V_{u,p} = \phi k_{cp} \frac{A_{n,V}}{A_{n,t}} V_{u,t} V_{u,s} N_u = \phi k_{cp} \frac{A_{n,V}}{A_{n,t}} V_{u,t} V_{u,s} N_u (24 \sqrt{f_c} h_{ef}^2)$

$= 58.736$ k > $V_{u,p} = 5.00$ kips [Satisfactory]

where: $\phi = 0.75$ x $1 = 0.75$

$k_{cp} = 2.0$ for $h_{ef} > 2.5$ in.

CHECK PRYOUT STRENGTH FOR SHEAR LOAD ON ALL ANCHOR (ACI 318 17.5.3.1)

$\phi V_{u,p} = \phi k_{cp} \frac{A_{n,V}}{A_{n,t}} V_{u,t} V_{u,s} N_u = \phi k_{cp} \frac{A_{n,V}}{A_{n,t}} V_{u,t} V_{u,s} N_u (24 \sqrt{f_c} h_{ef}^2)$

$= 433.430$ k > $V_{u,p} = 5.00$ kips [Satisfactory]

where: $\phi = 0.75$ x $1 = 0.75$

DETERMINE DESIGN SHEAR STRENGTH OF GOVERNING ANCHOR

$\phi V_u = \min(\phi V_{u,s}, \phi V_{u,p}, \phi V_{u,t}) = 13.708$ K

REQUIRED EDGE DISTANCES AND SPACING TO PRECLUDE SPLITTING FAILURE:

Since headed cast-in-place anchors are not likely to be highly torqued, the minimum cover requirements of ACI 318 20.6.1.3 apply.

Cover (top) > Cover (side) [Satisfactory]

CHECK TENSION AND SHEAR INTERACTION OF GOVERNING ANCHORS (ACI 318 17.6)

Since $N_{u,t} < 0.2 N_u$ and $V_{u,t} < 0.2 V_u$ the full tension design strength is permitted.

The interaction equation may be used

$\frac{N_{u,t}}{\phi N_u} + \frac{V_{u,t}}{\phi V_u} = 0.20 < 1.2$ [Satisfactory]

Summary of Dimensional Properties of Anchors

Anchor Diameter (in)	Gross Area of Anchor (in ²)	Effective Area of Threaded Anchor (in ²)	Bearing Area of Heads, Nuts, and Washers (A _b) (in ²)				
			Square	Heavy Square	Hex	Heavy Hex	Hardened Washers
0.250	0.049	0.032	0.142	0.201	0.117	0.167	0.258
0.375	0.110	0.078	0.280	0.362	0.164	0.299	0.408
0.500	0.196	0.142	0.464	0.569	0.291	0.467	0.690
0.625	0.307	0.228	0.693	0.822	0.454	0.671	1.046
0.750	0.442	0.334	0.824	1.121	0.654	0.911	1.292
0.875	0.601	0.462	1.121	1.465	0.891	1.188	1.804
1.000	0.785	0.606	1.465	1.855	1.163	1.501	2.356
1.125	1.10	0.894	0.763	1.854	2.291	1.472	1.951
1.250	1.14	1.227	0.969	2.298	2.773	1.817	2.237
1.375	1.318	1.485	1.160	2.769	3.300	2.199	2.659
1.500	1.12	1.767	1.410	3.295	3.873	2.617	3.118
1.750	1.314	2.405	1.900	-	-	-	4.144
2.000	2	3.142	2.500	-	-	-	5.316

CHECK BASE PLATE THICKNESS (AISC Guide - I, Eq. 3.3.14a)

$t_{reqd} = 1.5 \sqrt{\frac{V_u}{F_y}} = 1.73$ in < $t = 1.75$ in [Satisfactory]

3.2 Example for Post Installs Anchors

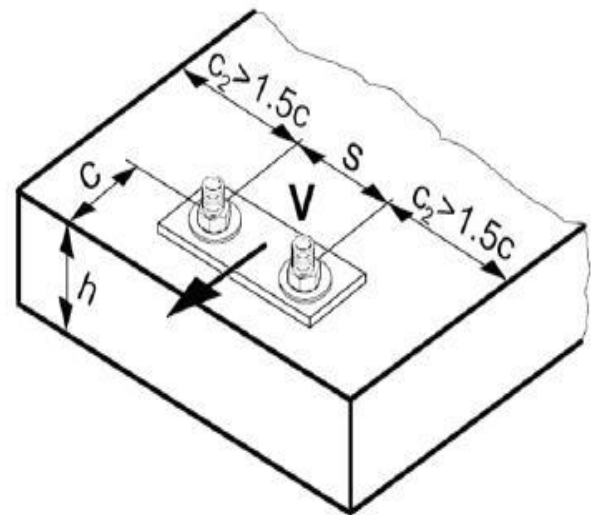
Simplified version of the design method according ETAG 001, Annex C. Design resistance according ETA-11/0374, Issue 2012-07-19.

_ Influence of concrete strength

_ Influence of edge distance

_ Influence of spacing

Valid for a group of two anchors. (The method may also be applied for anchor groups with more than two Anchors or more than one edge. The influencing factors must then be considered for each edge distance and spacing. The calculated design loads are then conservative: They will be lower than the exact values According ETAG 001, Annex C. To avoid this, it is recommended to use the anchor design software PROFIS anchor) the design method is based on the following simplification:



Basic design shear resistance

Design steel resistance $V_{Rd,s}$

Anchor size	M6	M8	M10	M12	M16	M20
$V_{Rd,s}$ HSA, HSA-BW [kN]	5,2	8,5	15,1	23,6	40,8	68,6
HSA-R2, HSA-R [kN]	5,8	9,8	18,1	23,4	45,2	73,5

Tensile Loading

Design concrete pryout resistance $V_{Rd,cp} = k \cdot N_{Rd,c}^{(a)}$

Anchor size	M6			M8			M10		
Effective anchorage depth h_{ef} [mm]	30	40	60	30	40	70	40	50	80
k	1	1	2	1	1,5	2	2,4	2,4	2,4

Anchor size	M12			M16			M20		
Effective anchorage depth h_{ef} [mm]	50	65	100	65	80	120	75	100	115
k	2	2	2	2,9	2,9	2,9	2	3,5	3,5

a) $N_{Rd,c}$: Design concrete cone resistance

Design concrete edge resistance $V_{Rd,c} = V_{Rd,c}^0 \cdot f_b \cdot f_h \cdot f_{d_1} \cdot f_{d_2} \cdot f_{d_3}$

Anchor size	M6			M8			M10		
Effective anchorage depth h_{ef} [mm]	30	40	60	30	40	70	40	50	80
$V_{Rd,c}^0$ [kN]	3,6	3,6	3,7	5,8	5,9	6,0	8,5	8,5	8,6

Anchor size	M12			M16			M20		
Effective anchorage depth h_{ef} [mm]	50	65	100	65	80	120	75	100	115
$V_{Rd,c}^0$ [kN]	11,6	11,6	11,7	18,7	18,8	18,9	27,2	27,3	27,4

a) For anchor groups only the anchors close to the edge must be considered.

Influencing factors

Influence of concrete strength

Concrete strength designation (ENV 206)	C 20/25	C 25/30	C 30/37	C 35/45	C 40/50	C 45/55	C 50/60
$f_b = (f_{ck,cube}/25 \text{ N/mm}^2)^{1/2}$ a)	1	1,1	1,22	1,34	1,41	1,48	1,55

a) $f_{ck,cube}$ = concrete compressive strength, measured on cubes with 150 mm side length

Influence of angle between load applied and the direction perpendicular to the free edge

Angle β	0°	10°	20°	30°	40°	50°	60°	70°	80°	≥ 90°
$f_{\beta} = \frac{1}{\sqrt{(\cos \alpha_{\beta})^2 + \left(\frac{\sin \alpha_{\beta}}{2,5}\right)^2}}$	1	1,01	1,05	1,13	1,24	1,40	1,64	1,97	2,32	2,50

Influence of base material thickness

h/c	0,15	0,3	0,45	0,6	0,75	0,9	1,05	1,2	1,35	≥ 1,5
$f_n = \{n/(1,5 \cdot c)\}^{1/2} \leq 1$	0,32	0,45	0,55	0,63	0,71	0,77	0,84	0,89	0,95	1,00

Pryout Resistance

3.2.2 Combined tension and shear loading

For combined tension and shear loading see section “Anchor Design”.

Recommended loads can be calculated by dividing the design resistance by an overall partial safety factor for action $\gamma = 1,4$. The partial safety factors for action depend on the type of loading and shall be taken from national regulations.

Design resistance

Single anchor, no edge effects

Anchor size	M6			M8			M10		
Effective anchorage depth h_{ef} [mm]	30	40	60	30	40	70	40	50	80
Min. base material thickness h_{min} [mm]	100	100	120	100	100	120	100	120	160

	Tensile N_{Rd}								
HSA, HSA-BW [kN]	4,0	5,0	6,0	5,5	8,5	10,7	8,5	11,9	16,7
HSA-R2, HSA-R [kN]	4,0	5,0	6,0	5,5	8,5	10,7	8,5	11,9	16,7

	Shear V_{Rd}, without lever arm								
HSA, HSA-BW [kN]	5,2	5,2	5,2	5,5	8,5	8,5	15,1	15,1	15,1
HSA-R2, HSA-R [kN]	5,5	5,8	5,8	5,5	9,8	9,8	18,1	18,1	18,1

Anchor size	M12			M16			M20		
Effective anchorage depth h_{ef} [mm]	50	65	100	65	80	120	75	100	115
Min. base material thickness h_{min} [mm]	100	140	180	140	160	180	160	220	220

	Tensile N_{Rd}								
HSA, HSA-BW [kN]	11,9	17,6	23,3	17,6	24,1	33,3	21,9	33,7	41,5
HSA-R2, HSA-R [kN]	11,9	17,6	23,3	17,6	24,1	33,3	21,9	33,7	41,5

	Shear V_{Rd}, without lever arm								
HSA, HSA-BW [kN]	23,6	23,6	23,6	40,8	40,8	40,8	43,7	68,6	68,6
HSA-R2, HSA-R [kN]	23,4	23,4	23,4	45,2	45,2	45,2	43,7	73,5	73,5

Single anchor, min. edge distance ($c = c_{min}$)

Anchor size	M6			M8			M10		
Effective anchorage depth h_{ef} [mm]	30	40	60	30	40	70	40	50	80
Min. base material thickness h_{min} [mm]	100	100	120	100	100	120	100	120	160
Min. edge distance c_{min} [mm]	35	35	35	40	35	35	50	40	40

	Tensile N_{Rd}								
HSA, HSA-BW [kN]	4,0	5,0	6,0	4,0	4,8	10,5	5,6	6,7	12,0
HSA-R2, HSA-R [kN]	4,0	5,0	6,0	4,0	4,8	10,5	5,6	6,7	12,0

	Shear V_{Rd}, without lever arm								
HSA, HSA-BW [kN]	2,5	2,6	2,8	3,1	2,7	3,0	4,5	3,5	3,9
HSA-R2, HSA-R [kN]	2,5	2,6	2,8	3,1	2,7	3,0	4,5	3,5	3,9

Anchor size	M12			M16			M20		
Effective anchorage depth h_{ef} [mm]	50	65	100	65	80	120	75	100	115
Min. base material thickness h_{min} [mm]	100	140	180	140	160	180	160	220	220
Min. edge distance c_{min} [mm]	70	65	55	80	75	70	130	120	120

	Tensile N_{Rd}								
HSA, HSA-BW [kN]	9,2	11,5	18,4	13,6	15,9	24,5	21,9	24,8	29,2
HSA-R2, HSA-R [kN]	9,2	11,5	18,4	13,6	15,9	24,5	21,9	24,8	29,2

	Shear V_{Rd}, without lever arm								
HSA, HSA-BW [kN]	7,4	7,2	6,4	9,9	9,5	9,6	18,1	19,1	19,6
HSA-R2, HSA-R [kN]	7,4	7,2	6,4	9,9	9,5	9,6	18,1	19,1	19,6

4. RESULTS & DISCUSSIONS

It is the restitution of the strength the building had before the damage occurred. This type of action must be undertaken when there is evidence that the structural damage can be attributed to exceptional phenomena that are not likely to happen again and that the original strength provides an adequate level of safety. The main purpose of restoration is to carry out structural repairs to load bearing elements. It may involve cutting portions of the elements and rebuilding them or simply adding more structural material so that the original strength is more or less restored. The process may involve inserting temporary supports, underpinning, etc. Some of the approaches are stated below:

- i) Removal of portions of cracked masonry walls and piers and rebuilding them in richer mortar. Use of non shrinking mortar will be preferable.
- (ii) Addition of reinforcing mesh on both -faces of the cracked wall, holding it to the wall through spikes or bolts and then covering it suitably. Several alternatives have been used.
- (iii) Injecting epoxy like material, which is strong in tension, into the cracks in walls, columns, beams, etc.

Where structural repairs are considered necessary, these should be carried out prior to or simultaneously with the architectural repairs so that total planning of work could be done in a coordinated manner and wastage is avoided.

CONCLUSIONS

- There are many different anchor bolt failures and anchor bolt designs will vary based upon the foundation type and the loading conditions given. There isn't one approach that works for every situation.
- For a ductile anchor bolt design, the concrete failures must be greater than the steel strength, or the anchor bolts must be embedded deep enough to develop with the reinforcement in the concrete. This is required in high seismic areas, but is good practice for all structures.
- For anchor bolts being placed into a pedestal, the base material, the bolts will normally fail due to concrete breakout or side-face blowout, however if adequate reinforcement is used, and adequate anchor bolt embedment is used, then these failures can be neglected. The critical failure mode will then typically be the steel strength of the bolts.
- For a mat foundation, the common failure modes are steel failure, concrete pry out failure, and concrete tensile breakout failure. However, these can be fixed by providing reinforcement in the mat, or by increasing the anchor bolt size or embedment depth.
- For a block foundation, the common failure modes are concrete breakout, and side-face blowout. typically within a block foundation, vertical reinforcement is not

required; hence the bolts cannot be designed to develop with the reinforcement. Either additional reinforcement or a change in concrete layout is needed to compensate for this failure.

- For this failure will be checked before base material property guide lines as per ACI 318. The mainly the anchorage of checks will acceptable & satisfactory within the appendix-D.

REFERENCES

1. **ACI 318-02**, American Concrete Institute, Building Code Requirements for reinforced Concrete
2. **ACI 318-05**, American Concrete Institute, Building Code Requirements for reinforced Concrete
3. **ACI 318-08**, American Concrete Institute, Building Code Requirements for reinforced Concrete
4. **ACI 318-82**, American Concrete Institute, Code Requirements for Nuclear Safety Related Concrete structures.
5. **ACI 318-90**, American Concrete Institute, Code Requirements for Nuclear Safety Related Concrete structures.
6. **IBC 2006**. International Building Code, International Building Code, 2006
7. **ASIC Design Guide 1**, American Institute of Steel Construction, Base Plate and Anchor Rod Design, 2nd edition, 2006
8. **ASIC Design Guide 7**, American Institute of Steel Construction, Industrial Buildings Roofs to Anchor Rods, 2nd edition, 2006
9. Tack Committee on Anchor bolt Design American Society of Civil Engineers, Wind Loads and Anchor Bolts Design for Petrochemical families.
10. ETAG 001:
11. ETAG TR 029:
12. ETAG TR 023:
13. **ACI 318-11**, Anchorage
14. **Manuals:**
15. HILTI: Anchor Fastening Technology Manual
16. Fishers: Fixing Systems-Technical Hand Book EUROPE.

A STUDY ON MECHANICAL PROPERTIES OF CONCRETE WITH ADDITION OF FLYASH AND NANO-SILICA GEL

Charitha.V¹, B.Vamsi Krishna², M.Kameswara Rao³

¹P.G Research Scholar ²Associate Professor ³Professor,
Department of Civil Engineering, Malla Reddy Engineering College (Autonomous), Hyderabad.

Abstract: Concrete is the most common used material for construction and their design consumes almost the total cement production in the world. The use of large quantities of cement produces increasing CO₂ emissions and as a consequence the greenhouse effect. A method to reduce the cement content in concrete mixes is the use of Flyash and silica fines. One of the silica fines with high potential as cement replacement and as concrete additive is nano-silica (NS). This would save not only the natural resources and energy but also protect the environment with the reduction of waste material. The present work deals with addition of Flyash and Nano-silica to concrete as partial replacement to cement in 10%, 20% & 30% and dosages of 1%, 1.5% and 2% respectively by weight of cement. Based on early research M20 grade concrete has been chosen for this work. The mix design was prepared using IS: 10262-2009 Guidelines for concrete mix design proportioning. In the present work 117 numbers of specimens were casted (78 numbers of cube moulds and 39 numbers of cylinder moulds) with addition of Flyash and Nano-silica in different proportions which are tested for compressive strength and split tensile strength. Addition of Nano-silica to normal cement concrete show increase in compressive strength and decrease in splitting tensile strength. SEM (Scanning Electron Microscope) analysis evidence the direct involvement of Flyash and Nano-silica in region of specimen.

Keywords: Nano-silica, Compressive strength, Split tensile strength, SEM (Scanning Electron Microscope)

I. INTRODUCTION

Concrete is the most common material used in the construction. Concrete is a composite material made up of cement, sand, water and sometimes admixtures. Cement is the most active component of concrete usually has the greatest unit cost, its selection and proper use are important in obtaining economical concrete and also concrete of desired properties. The use of large quantities of cement results in increasing CO₂ emissions and as a consequence of the greenhouse effect. One of the methods to reduce the cement content in concrete mixes is the use of nano materials. The properties of concrete in hardened state such as strength is affected by the mix proportions and grading which results in particle packing.

Concrete can be considered as the most widely used in the construction industry. The Indian Standard Code of practice for plain and reinforced concrete recommends the minimum cement content to satisfy the strength. Hence, the utilization of cement is increased. But, the cement production consumes large amount of energy and emits carbon dioxide results in environmental pollution. Hence, one of the solutions to these problems is to reduce the consumption of cement and utilize Pozzolana materials for the preparation of concrete. Previous studies indicate that the use of Fly Ash, Micro Silica, Matakaoline, Ground Granulated Blast Furnace Slag as partial replacement of cement, reduces the cement consumption and also increases the strength. To improve the performance of concrete further, Nano materials are now being introduced as supplementary materials. Recent developments in Nano-technology and the availability of nano-silica made the use of such materials in concrete. Nano-Silica (NS) is a Nano-sized, highly reactive amorphous silica. Due to the smaller particles size and high surface areas compared to the other pozzolanic materials, the use of nano-silica possibly enhances the performance of concrete more effectively. As the nano silica particles are very fine and they tend to agglomerate due to high surface interaction, uniform dispersion of nano-silica is an important issue to get its beneficial effects. The influence of combined application of fly ash and nano-silica is to be investigated.

II. OBJECTIVE

The objective of the present work is to find the influence of the application of Flyash and Nano-Silica on various strength properties of M20 grade of concrete. 10%, 20% and 30% of Flyash and 1%, 1.5% and 2% of Nano-Silica gel are adopted as cement replacement by weight. Specific objectives are

- To find the workability aspect of the Nano-Silica for M20 grade concrete using Flyash.

- To know the strength characteristics of the concrete using Flyash and Nano-Silica.
- To conduct SEM (Scanning Electron Micrograph) investigation on both normal concrete and concrete with Flyash and Nano-Silica.

III. LITERATURE REVIEW

3.1 Flyash

Alvin Harison et.al (2014)¹ The following conclusions were made based on the findings of the study: Compressive strength of fly ash concrete up to 30% replacement level is more or equal to referral concrete at 28 and 56 days. Optimum replacement level of fly ash is 20%. It was observed that at 28 and 56 days in 20% replacement of PPC by fly ash, the strength marginally increased from 1.9% to 3.28%. It was also observed that up to 30% replacement of PPC by fly ash, the strength is almost equal to referral concrete at 56 days. PPC gains strength after the 56 days curing because of slow hydration process.

2.2 Nano-Silica

M. Nazeer et.al (2013)³ Silica fume added mixes shows higher strength values compared to their high volume fly ash counterparts at later ages (after 28 days). A linear logarithmic relation was developed for co-relating the compressive strength with age and silica fume content in various mixes. Using this correlation equation compressive strength values for various mixes are calculated and compared with the experimental results obtained. The addition of supplementary cementitious materials improves the resistance of concrete to chloride penetration. Mathematical models for predicting the diffusion coefficient, total charge passed in 6 hours and carbonation depth by knowing the oxide composition of the binder material for various mixes were developed and compared with the experimental values. The models gave satisfactory results. Equation for predicting the total charge passed in 6 hours knowing the initial current during the beginning of RCPT is formulated to overcome the disadvantage of longer test duration.

2.3 Flyash and Nano-Silica

Dr. D. V. Prasada Rao et.al (2014)⁵ The results of the experimental investigation indicate that the fly ash and nano-silica can be adopted as Ordinary Portland cement replacement for concrete preparation. Using the test results, it can be concluded that with the increase in the percentage of nano-silica the various strength characteristics of concrete increased up to 3%, with further increase in the nano-silica the strength characteristics of concrete are decreased for the given percentages of fly ash. It is very interesting to note that the variation of compressive strength of M25 grade fly ash concrete with nano-silica indicates the similar trend. The increase in various strength characteristics of concrete containing fly ash with increase in the nano-silica content can be due to the availability of additional binder in the presence of nanosilica. Nano silica has high amorphous silicon dioxide content. The Portland cement in concrete releases calcium hydroxide during the hydration process. The nano silica and fly ash reacts with the calcium hydroxide to form additional binder material. The availability of additional binder leads to increase in the paste-aggregate bond, results improved strength properties of the concrete prepared with nano-silica and fly ash combination. The decrease in the strength characteristics of concrete with increase in the nano-silica content beyond 3% is due to the poor quality of binder formed in the presence of high content of nano-silica and fly ash. The various strength characteristics of concrete can be improved by the addition of 3% nano-silica and 20% fly ash content. It can be concluded that the cement content can be reduced without compromising the strength of concrete by the use of fly ash and nano-silica combination at an appropriate proportion.

IV. EXPERIMENTAL PROGRAM

The present method deals with evolution of Mechanical Properties of Concrete Compressive Strength and Split-Tensile Strength. The program involves Casting and Testing of specimens where the standard size of the cube (150mm x 150mm x 150mm) and standard size of cylinder (150mm x 300mm). Cement is partially replaced with Flyash (10%, 20% and 30%) and Nano-Silica Gel of dosages (1%, 1.5% and 2%) in Standard Grade of M20 according to IS: 10262-2009.

Table 4.1 Properties of Cement

S.No	Property	Value
1	Specific Gravity	3.15
2	Normal Consistency	27%
3	Setting Time	
	i) Initial Setting Time	36 Min
	ii) Final Setting Time	390 Min

Table 4.2 Sieve Analysis Results

S.No	Sieve size(mm)	Percent Retained	Cumulative % retained	Percentage Passing
1	4.75	5.20	5.20	94.80
2	2.36	3.00	8.20	91.80
3	1.18	8.60	16.80	83.20
4	600 microns	25.80	42.60	57.40
5	300 microns	32.80	75.40	24.60
6	150 microns	20.70	96.10	3.90

Table 4.3 Properties of Fine Aggregate

S.No	Property	Result
1	Specific Gravity	2.6
2	Fineness Modulus	2.8
3	Bulk Density (Loose)	15.75 kN/m ³
4	Grading of Sand	ZONE-II

Table 4.4 Properties of Coarse Aggregate

S.No	Property	Result
1	Specific Gravity	2.60
2	Bulk Density (Loose)	14.15 kN/m ³
3	Water Absorption	0.5%
4	Fineness Modulus	7.2

Table 4.5 Properties of Flyash

S.No	Ingredient	Value
1	Silica (SiO ₂)	56.88 %
2	Aluminum trioxide (Al ₂ O ₃)	27.65 %
3	Ferric oxide (Fe ₂ O ₃ + Fe ₃ O ₄)	6.28 %
4	Titanium dioxide (TiO ₂)	0.31 %
5	Calcium oxide (CaO)	3.6 %
6	Magnesium oxide (MgO)	0.34 %
7	Sulphate (SO ₄)	0.27 %
8	Loss of ignition (LOI)	4.46 %
9	Specific gravity of Fly Ash	2.12

Table 4.6 Properties of Nano-Silica Gel

S.No	Property	Actual Analysis
1	Active nano Silica Content	35-40%
2	PH	9.3 -9.6
3	Specific Gravity	1.08-1.11
4	Texture	Milky White Liquid
5	Dispersion	Water

Table 4.7 Number of Specimens Casted

S.No	Description	Number of Cubes	Number of Cylinders
1	Control Concrete	6	3
2	10% Flyash replaced with Cement		
	a) 0% Nano Silica Gel	6	3
	b) 1% Nano Silica Gel	6	3
	c) 1.5% Nano Silica Gel	6	3
	d) 2% Nano Silica Gel	6	3
3	20% Flyash replaced with Cement		
	a) 0% Nano Silica Gel	6	3
	b) 1% Nano Silica Gel	6	3
	c) 1.5% Nano Silica Gel	6	3
	d) 2% Nano Silica Gel	6	3
4	30% Flyash replaced with Cement		
	a) 0% Nano Silica Gel	6	3
	b) 1% Nano Silica Gel	6	3
	c) 1.5% Nano Silica Gel	6	3
	d) 2% Nano Silica Gel	6	3
	TOTAL	78	39

4.1 Slump Test

Slump Test is used to determine the consistency of concrete mix of given proportions. Scope and Significance
 Unsupported fresh concrete flows to the sides and a sinking in height takes place. This vertical settlement is known as slump. In this test fresh concrete is filled into a mould of specified shape and dimensions, and the settlement or slump is measured when supporting mould is removed. Slump increases as water-content is increased. For different works different slump values have been recommended. The slump is a measure indicating the consistency or workability of cement concrete. It gives an idea of water content needed for concrete to be used for different works. This results in large voids, less durability and strength. Bleeding of concrete is said to occur when excess water comes up at the surface of concrete. This causes small pores through the mass of concrete and is undesirable. By this test we can determine the water content to give specified slump value. In this test water content is varied and in each case slump value is measured till we arrive at water content giving the required slump value. For example, a harsh mix cannot be said to have same workability as one with a large proportion of sand even though they may have the same slump.



Fig 4.1 Slump Cone Apparatus

Table 4.8 Slump Values

S.No	Description	Slump Value
1	Control Concrete	75mm
2	CF 10%	83mm
3	CF 10% + 1% NS	81mm
4	CF 10% + 1.5% NS	80mm
5	CF 10% + 2% NS	78mm
6	CF 20%	88mm
7	CF 20% + 1% NS	85mm
8	CF 20% + 1.5% NS	82mm
9	CF 20% + 2% NS	79mm
10	CF 30%	96mm
11	CF 30% + 1% NS	93mm
12	CF 30% + 1.5% NS	90mm
13	CF 30% + 2% NS	87mm

4.2 Compressive Test

The dimensions of the specimens to the nearest 0.2 mm and their weight shall be noted before testing. The bearing surfaces of the testing machine shall be wiped clean and any loose sand or other materials removed from the surface of the specimen which are to be in contact with the compression platens. The cube shall be placed in the machine in such a manner that the load shall be applied to opposite sides of the cubes as cast that is not to the top and bottom. The axis of the specimen shall be carefully aligned with the center of the thrust of the spherically seated platen. No packing shall be used between the faces of the test specimen and the steel platen of the testing machine. As the spherically seated block is brought to bear on the specimen, the movable portion shall be rotated gently by hand so that uniform seating may be obtained. The load shall be applied without shock and increased continuously at a rate of approximately 140 kg/sq cm/min until the resistance of the specimen to the increasing load breaks down and no greater load can be sustained.



Fig 4.2 Compressive Test Machine

Table 4.9 Compressive Strength Results

S.No	Specimen Description	Compressive Strength (N/mm ²)	
		7 Days	28 Days
1	Control Concrete	17.51	34.32
2	Flyash 10%	14.98	26.96
3	10% Flyash + 1% NS	15.92	28.59
4	10% Flyash + 1.5% NS	16.78	30.12
5	10% Flyash + 2% NS	17.33	32.45
6	Flyash 20%	14.42	25.13
7	20% Flyash + 1% NS	15.42	26.64
8	20% Flyash + 1.5% NS	16.31	28.85
9	20% Flyash + 2% NS	16.98	31.26
10	Flyash 30%	13.67	24.06
11	30% Flyash + 1% NS	14.96	25.77
12	30% Flyash + 1.5% NS	15.86	28.93
13	30% Flyash + 2% NS	16.45	30.42

4.3 Split-Cylinder Test

It is the standard test, to determine the tensile strength of concrete in an indirect way. This test could be performed in accordance with IS: 5816-1970. A standard test cylinder of concrete specimen (300mm x 150mm diameter) is placed horizontally between the loading surfaces of Compression Testing Machine. The compression load is applied diametrically uniformly along the vertical diameter. Concrete cylinders split into two halves along this vertical plane due to indirect tensile stress generated by poisson's effect.

**Fig 4.3 Compressive Test Machine****Table 4.10 Tensile Strength Results**

S.No	Specimen Description		Tensile Strength (28 Days)
1	CC	NS 0%	3.145
		NS 0%	3.004
2	CF 10%	NS 1%	2.981
		NS 1.5%	2.788
		NS 2%	2.652
		NS 0%	2.916
3	CF 20%	NS 1%	2.862
		NS 1.5%	2.611
		NS 2%	2.643
		NS 0%	2.841
4	CF 30%	NS 1%	2.826

		NS 1.5%	2.584
		NS 2%	2.451

4.4 SEM Analysis

The SEM shows that the micro structure of CFS is denser and more homogenous than conventional concrete because of pozzolanic reaction by consumption of Ca(OH)_2 and formation of additional C-S-H which fill the pores system and causing densification effect which improve the micro structure of concrete.

SEM Pictures

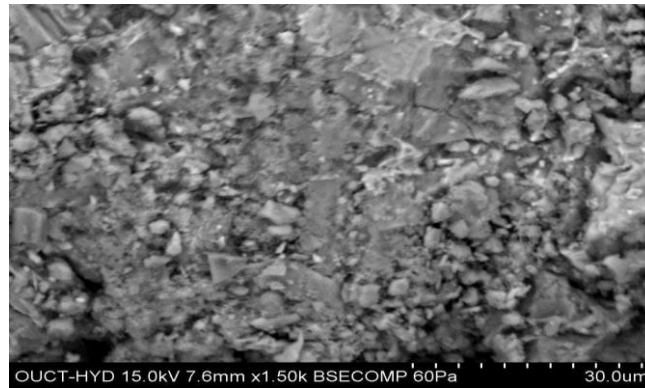


Fig 4.4 Control Concrete (without Flyash and Nano-Silica)

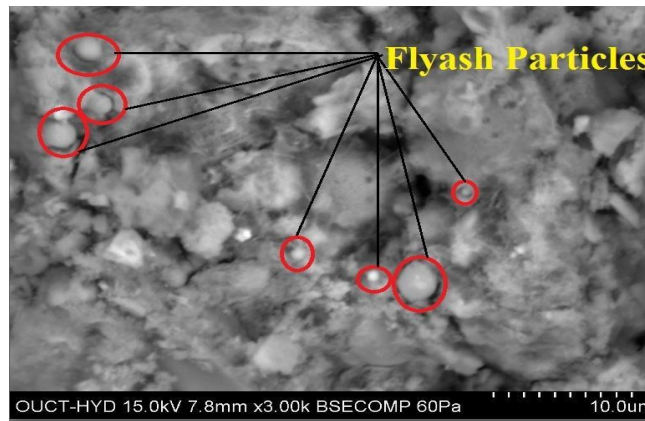


Fig 4.5 Concrete with 30% Flyash

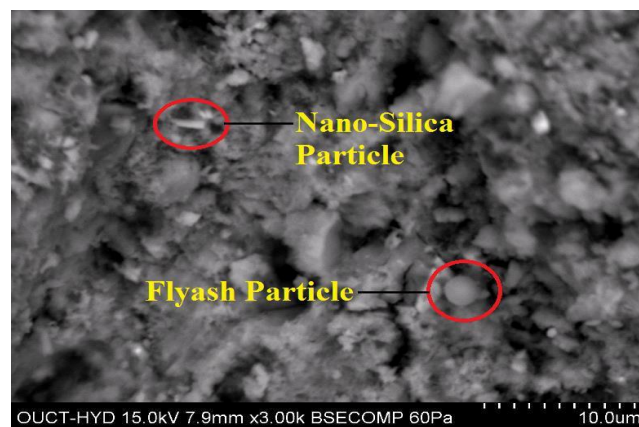


Fig 4.6 Concrete with 10% Flyash and 1% Nano-Silica

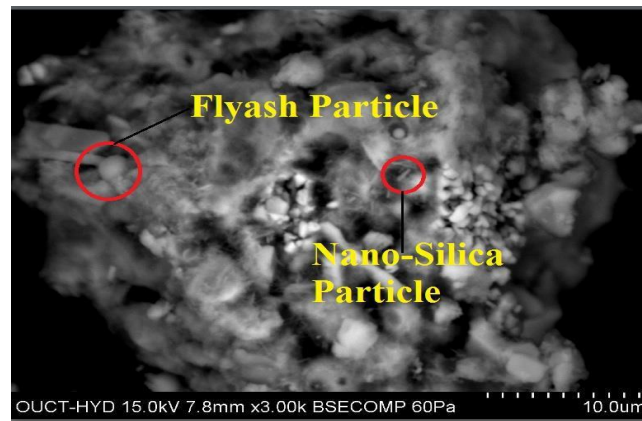


Fig 4.7 Concrete with 20% Flyash and 1.5% Nano-Silica

CONCLUSIONS

1. We observed that when Flyash is added to Concrete, the Workability has increased and when Nano-Silica Gel is added to Flyash Concrete, the Workability has decreased.
2. When compared with Control Concrete, Concrete partially replaced with 10% Flyash has a decrease in 7 days Compressive Strength by 14.48%. When Nano-Silica gel is added to CF10 in dosages of 1%, 1.5% and 2% the Compressive Strength is increased by 6.27%, 12.01% and 15.68% respectively.
3. When compared with Control Concrete, Concrete partially replaced with 20% Flyash has a decrease in 7 days Compressive Strength by 17.64%. When Nano-Silica gel is added to CF20 in dosages of 1%, 1.5% and 2% the Compressive Strength is increased by 6.93%, 13.1% and 17.75% respectively.
4. When compared with Control Concrete, Concrete partially replaced with 30% Flyash has a decrease in 7 days Compressive Strength by 21.93%. When Nano-Silica gel is added to CF30 in dosages of 1%, 1.5% and 2% the Compressive Strength is increased by 9.43%, 16.02% and 20.33% respectively.
5. When compared with Control Concrete, Concrete partially replaced with 10% Flyash has a decrease in 28 days Compressive Strength by 21.44%. When Nano-Silica gel is added to CF10 in dosages of 1%, 1.5% and 2% the Compressive Strength is increased by 6.04%, 12.05% and 20.36% respectively.
6. When compared with Control Concrete, Concrete partially replaced with 20% Flyash has a decrease in 28 days Compressive Strength by 26.77%. When Nano-Silica gel is added to CF20 in dosages of 1%, 1.5% and 2% the Compressive Strength is increased by 6.0%, 14.8% and 24.39% respectively.
7. When compared with Control Concrete, Concrete partially replaced with 30% Flyash has a decrease in 28 days Compressive Strength by 29.89%. When Nano-Silica gel is added to CF30 in dosages of 1%, 1.5% and 2% the Compressive Strength is increased by 7.1%, 20.24% and 26.4% respectively.
8. Due to decrease in the quantity of cement, the concrete becomes economical and eco-friendly.
9. By adding Flyash CO₂ emission is decreased and in presence of NS the compressive strength has been increased.

REFERENCES

- 1) Dr. D. V. Prasada Rao 2.M. Pavan Kumar, Volume 5, Issue 7, July (2014) pp.94-102 "A study on influence of Flyash and Nano-Silica on strength properties of concrete".
- 2) Alvin Harison, Vikas Srivastava and Arpan Herbert, Volume 2, Issue 8, January (2014) "Effect of Flyash on Compressive strength of Portland Pozzolona cement Concrete".
- 3) M. Nazeer, P.S. Anupama, Volume 5, Issue 10, October (2014) "Strength and durability studies on Silica fume modified high-volume Fly ash concrete".
- 4) Abdul Wahab, B. Dean Kumar, M. Bhaskar, S. Vijaya Kumar, B.L.P. Swami, Volume 4, Issue 5, May (2013) "Concrete Composites With Nano Silica, Condensed Silica Fume And Fly Ash – Study of Strength Properties" International Journal Of Scientific & Engineering Research
- 5) YuvarajShanmugaSundaram, , Dr. Sujimohankumar , Volume 1, Issue 1, July-December (2013) "An experimental research on enhancing the strength and its resisting property of Nano-Silica Flyash Concrete "
- 6) S. Yuvaraj, Dr.Sujimohankumar, N.Dinesh, C. Karthic, Volume 2, Issue 6, June (2012) "Experimental research on improvement of concrete strength and enhancing the resisting property of corrosion and permeability by the use of Nano-Silica Flyash concrete"

- 7) C.Marthon*, T.P.Agrawal, Vol. 2, Issue4, July-August (2012), pp.1986-1991 “Effect of Fly Ash Additive on Concrete Properties” G.Quercia,H.J.H.Brouwers, June 20 – 23, (2010)“Application of nano-silica (nS) in concrete mixtures”
- 8) IS : 516-1959, Method of Tests for Strength of Concrete.
- 9) IS : 456-2000, Code of Practice for Plain and Reinforced Concrete.
- 10) IS : 383-1970, Specifications for Coarse and Fine Aggregates from Natural Sources for Concrete
- 11) IS : 10262-2009, Guidelines for Mix Design for Concrete

AN EXPERIMENTAL INVESTIGATION ON SELF COMPACTING CONCRETE BY USING L BOX, J RING, V FUNNEL APPARATUS

Azhar Ali¹ R. Sumathi² M. Kameswara Rao³

M.Tech Research Scholar¹, Assistant Professor², Professor³

Malla Reddy Engineering College (Autonomous), Hyderabad, Telangana, India.

ABSTRACT

Today concrete is most widely used construction material due to its good compressive strength and durability. Depending upon the nature of work cement, fine aggregate, coarse aggregate and water are mixed in specific proportions to produce plain concrete. To make durable concrete structures, sufficient compaction is required. The use of self-compacting concrete (SCC) is spreading worldwide because of its very attractive properties in the fresh state as well as after hardening. The use of SCC will lead to a more industrialized production, reduce the technical costs of in situ concrete constructions, improve the quality, durability and reliability of concrete structures and eliminate potential for human error.

- To develop SCC mix design methodology for mix B (60MPa) and evaluate the fresh properties.
- To study the effect of paraffin wax as a Self Curing compound and its dosage on fresh properties of self-compacting concrete.
- To determine the water retention capacity of all mixes by measuring weight loss of cubes at 3, 7, 14, 21, 28, 56 and 90 days.
- To determine the compressive strength of cubes at 7, 28, 56 and 90 days.

Keywords— Self Compacting Concrete (SCC), Self Curing Concrete (SCC), EFNARC, Liquid Wax.

1. INTRODUCTION

Self-Compacting Concrete (SCC) is a new generation concrete, which has generated tremendous interest since its initial development in Japan by Okamura in the late 1980's in order to reach durable concrete structures. SCC has gained

wide use for placement in congested reinforced concrete structures with difficult casting conditions. For such applications, fresh concrete must possess high fluidity and good cohesiveness. SCC is considered as a concrete which can be placed and compacted under its self-weight with little or no

vibration effort, and which is at the same time, cohesive enough to be handled without segregation or bleeding. It is used to facilitate and ensure proper filling and good structural performance of heavily reinforced structural members. SCC development is a desirable achievement in the construction industry in order to overcome problems associated with cast-in-place concrete. SCC is not affected by the skills of workers, the shape and amount of reinforcing bars or the arrangement of a structure and, due to its high-fluidity and resistance to segregation it can be pumped longer distances. The main advantage of SCC is to shorten construction period and to assure compaction in the structures especially in the confined zones where vibration and compaction is difficult. The other advantages of SCC are

1. It eliminates noise due to vibration.
2. It provides high stability during transport and placement.
3. It provides uniform surface quality and homogenous.
4. It provides greater freedom for design
5. It is useful for casting of underwater structures.

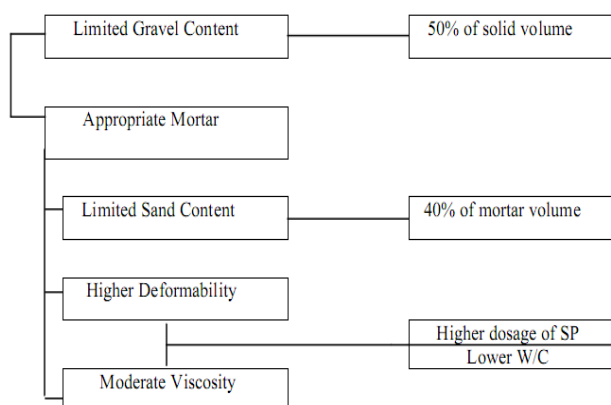


Figure 1.1 Methods for achieving Self Compactability

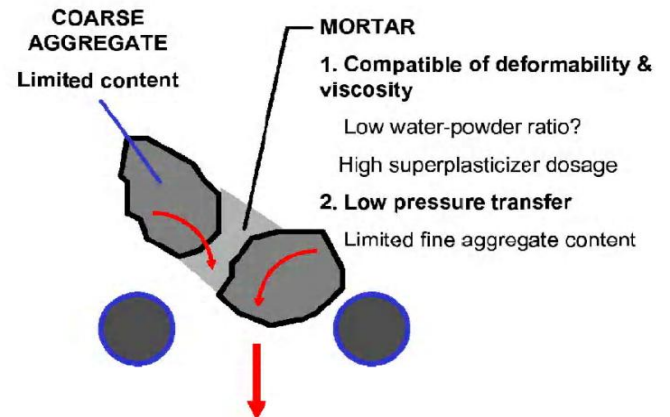


Figure 1.2 Mechanisms for achieving Self Compactability

1.1 MECHANISM OF INTERNAL CURING

According to R.T.Y Liang and R.K Sun, continuous evaporation of moisture takes place from an exposed surface due to the difference in chemical potentials (free energy) between the vapour and liquid phases. The polymers added in the mix mainly form hydrogen bonds with water molecules and reduce the chemical potential of the molecules which in turn reduces the vapour pressure, thus reducing the rate of evaporation from the surface.

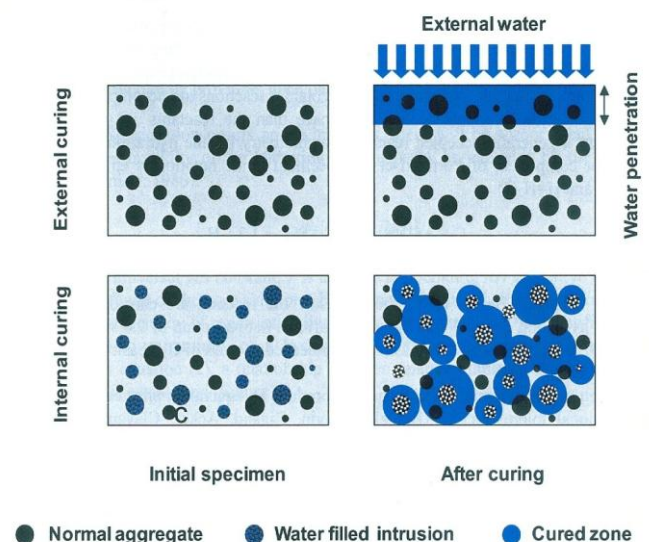


Figure 1.3: Illustrating the concept of External and Internal Curing

This concept of internal curing is compared and contrasted with more conventional (external) curing in Figure. Conventional external curing places water at the surface of the concrete shortly after placement that can be absorbed over time. Because water curing is often difficult to perform, curing membranes or sealers are often used; however, these approaches do not add additional needed water to the system. Further, in lower water to cement ratio systems the external curing, water cannot penetrate much beyond the surface (on the order of 3 mm of movement after 18 hours). Internal curing, however, uses the fine LWA to supply water uniformly across the cross section as shown in Figure. Proportioning procedures exist to determine the amount of lightweight aggregate to use considering both the volume of water that is to be supplied and the spatial distribution of the LWA. The principal contribution of internal curing results in the reduction of permeability that develops from a significant extension in the time of curing.

1.2 LIQUID PARAFFIN WAX

Liquid paraffin is a mixture of hydrocarbons. It is obtained through the petroleum distillation process. It is the clear, light fraction of the distillation process and it can be further purified. It is also known as adepsine oil, glymol, saxol and Vaseline oil.

(i) Physical Properties

Liquid paraffin is an oily, transparent, colorless liquid. At room temperature it is odorless and tasteless. However, when heated it does have a

slightly unpleasant petroleum smell. It does not dissolve in water, glycerol or cold ethanol. It does dissolve in benzene, ether, chloroform and hot ethanol. It has a density of 0.8 gm/cm³.

(ii) Medicinal Properties

Liquid paraffin, as mineral oil, is commonly used to treat constipation. The advantage is that it acts as a stool lubricant and decreases the amount of water removed from stool, and the oil itself is not absorbed into the gastrointestinal system. Liquid paraffin can be used to help treat cradle cap in infants. Cradle cap is a condition resulting in dry scaly skin, most commonly found on the head. When shampooing is not effective in removing the scaly skin, apply liquid paraffin to the scalp area and then wrap in warm cloths. Liquid paraffin can also be used to ease inflammation due to diaper rash or irritation due to eczema, and to soften hardened ear wax.

(iii) Industrial Properties

Liquid paraffin can be used as a non-conductive coolant in electrical systems, such as in transformers. It can also be used as a hydraulic fluid in various types of machinery. It can be used as a lubricant and was commonly used in the textiles industry, but has been replaced with other types of oils since it does not biodegrade as easily. For those who work with abrasive materials, such as cements, tars and industrial paints, liquid paraffin can be used to clean hands. Solvents such as turpentine should be avoided as they are irritating to the skin, but liquid paraffin will not irritate the skin.

(iv) Cautions

Liquid paraffin has the ability to cause a condition known as hydrocarbon pneumonitis, which results when the substance is aspirated into the lungs. This is most commonly seen in fire-eating performers. They use liquid paraffin to coat their mouths, but when inhaled the compound spreads quickly through the bronchial tree, activating macrophages (cells of the immune system) and therefore causing inflammation.

Molecular Formula: $C_nH_{2n+2} = 24 \sim 36$

Figure 1.4 liquid paraffin wax structure

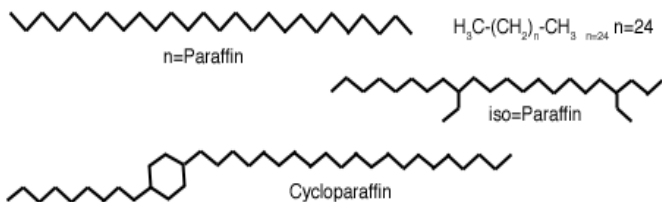


Table 1.3: Physical and Chemical properties of Paraffin Wax

Sr. No.	Characteristics	Liquid Paraffin Light	Heavy Liquid Paraffin
1.	Specific gravity @ 25°C	Between 0.820 to 0.860	Between 0.850 to 0.880
2.	Dynamic viscosity @ 20°C	Between 25 to 80 mpas	Between 110 to 230 mpas
3	Appearance	Clear colour less liquid.	Clear colour less liquid.
3.	Solubility	Passes	Passes
4.	Sulphur compounds	Compiles as per standards	Compiles as per standards

5.	Solid Paraffins	Compiles as per standards	Compiles as per standards
6.	Flash point (PMCC), °c	Min. 150 °c	Min 200 OC
7.	Acidity / alkalinity	Passes	Passes
8.	Light absorption @ 240-280 nm	Less than 0.1	Less than 0.1
9.	Readily carbon sable substances	Passes	Passes

2. EXPERIMENTAL STUDY

The experimental study consisted of arriving at a suitable mix proportions that satisfies the fresh properties of self compacting concrete as per EFNARC specifications. Standard cube moulds of 150mm x 150mm x 150mm made of cast iron were used for casting standard cubes. The standard moulds were fitted such that there are no gaps between the plates of the moulds. Any small gaps were plugged with plaster of Paris. The moulds were then oiled and kept ready for casting. After 24hrs of casting, specimens were demoulded. After cubes were demoulded they were subjected to different curing conditions indoor curing and wet curing. Indoor curing specimens included specimens with no curing compound and also with a definite percentage of curing compound.

The program consisted of casting and testing 60Mpa Self Compacting Concrete without and with Self Curing agents (Liquid Paraffin Wax Light and

Heavy). The parameters in the study include type of curing (I, W, V, P), dosage of Self Curing agent and Age of curing. The dosage Self Curing agent was kept at 0, 0.1%, 0.5% and 1.0%; based on studies available in the literature.

In this part of the work only one concrete (60MPa) was considered. A total of 96 specimens were cast and tested. The casting was done in three batches with specimens each batch belonging to indoor, water curing and paraffin wax based specimens. The cubes were cast and the weight loss was determined at the end of 3, 7, 14, 21, 28, 56 and 90 days.

Table 2.1 Details of specimens cast

Sl.No	Grade of Concrete	Type of Concrete and Designation	% of SCA added	No. of cubes cast 150x150x150 mm
1.	60Mpa (B)	SCC* without SCA** (BI)	0% (wet curing)	12
			0% (indoor curing)	12
		SCC with liquid Paraffin wax light (BV)	0.1%	12
			0.5%	12
			1.0%	12
		SCC with liquid Paraffin wax heavy (BP)	0.1%	12
			0.5%	12
			1.0%	12
		Total Specimens		

*SCC- Self compacting Concrete

**SCA- Self Curing Agent

2.1 SCC MIX DESIGN BASED ON EXACT NAN SU METHOD

Nan SU method of simple mix design for SCC was used to arrive at initial trial mixes and then mixes were modified accordingly as per EFNARC to

achieve optimum mix proportions satisfying fresh properties, hardened properties and also economy.. The proportion arrived for SCC of 60 MPa grade is given in the

Table 2.2 Mix design based on Exact Nan SU Method

Sl.No.	Material	Quantity kg/m ³	Quantity for 9 cubes in Kg	Proportions
I	Cement	430.00	16.50	1.000
ii	Fine Aggregate.	847.10	32.52	1.970
iii	Coarse Aggregate.	782.60	30.00	1.820
iv	Water	194.00	7.44	0.450
v	Flyash	180.00	6.93	0.420
vii	SP	5.16	0.198	0.012
v	Density	2438.86		

2.3 TESTS FOR FRESH PROPERTIES OF SELF COMPACTING CONCRETE

The final selection of recommended test methods was based mainly on their relation to one or more of the key properties of SCC (filling ability, passing ability, and resistance to segregation) as well as on reproducibility and repeatability. The selection process involved consideration of the outcome of an extensive experimental program in laboratory conditions and on site together with the general advantages and disadvantages of each method (cost, portability, simplicity of operation, and other practical aspects).

2.3.1 Slump flow + T50 (Reference method for filling ability)

The slump flow test aims at investigating the filling ability of SCC. It measures two parameters: flow spread and flow time T50 (optional). The former indicates the free, unrestricted deformability and the latter indicates the rate of deformation within a defined flow distance.



Figure 2.1 Abrams Slump flow Equipment

2.3.2 J-ring (Reference method for filling and/or passing ability)

The J-ring test aims at investigating both the filling ability and the passing ability of SCC. It can also be used to investigate the resistance of SCC to segregation by comparing test results from two different portions of sample. The J-ring test measures three parameters: flow spread, flow time T50J (optional) and blocking step. The J-ring flow spread indicates the restricted deformability of SCC due to blocking effect of reinforcement bars and the flow time T50J indicates the rate of deformation within a defined flow distance. The blocking step quantifies the effect of blocking.



Figure 2.2 J-Ring equipment

2.3.3 V-funnel (Alternative method to T50 for filling ability)

The V-funnel flow time is the period of a defined volume of SCC needs to pass a narrow opening and gives an indication of the filling ability of SCC provided that blocking and/or segregation do not take place; the flow time of the V-funnel test is to some degree related to the plastic viscosity.



Figure 2.3 V-Funnel equipment

Table 2.3: Fresh properties

SL. NO.	Plain SCC	Liquid Paraffin wax light			Liquid paraffin wax heavy			EFNARC Specifications
	0%	0.10%	0.50%	1%	0.10%	0.50%	1%	
SLUMP FLOW(mm)	700	730	705	745	760	730	775	550-900
T 50 (sec)	2.5	2.87	3.43	3.26	3.21	3.53	2.27	2-5
J-RING (mm)	7	7	8	7	6	7	5	0-10
L-BOX	0.92	0.88	0.9	0.89	0.84	0.83	0.83	0.8-1.0
V-FUNNEL (Sec)	7.02	8.29	7.67	8.5	7.6	7.44	7.82	6-12
V 5min (sec)	9.54	12	12.9	13.3	11.42	11.4	12	9-15

3. RESULTS AND DISCUSSIONS

The present chapter dealt with the hardened properties of Self Compacting Concrete with different curing compounds. Water retention test and compressive strength tests were carried out on SCC specimens. The aim of experimentation was to evaluate if Paraffin Wax can act as a very good internal curing agent or not. Water retention test, Sorptivity and compressive strength were taken as criteria for comparing the properties.

3.1 Water Retention Test

SCC with Liquid Paraffin Wax Light (V) and Liquid Paraffin Wax Heavy (P) of 0.1%, 0.5%, and 1.0% specimens were cast. Their average weight loss values were taken at 3, 7, 14, 21, 28, 56 and 90 days. The weights were taken with the digital weighting machine with an accuracy of 5 grams.

It is hence, necessary to use self curing compounds, to reduce the weight loss to improve the hydration process. Of all the three dosages 0.1% is the optimum value in case of Liquid Paraffin Wax

Light and 1.0% is optimum in case of Liquid Paraffin Wax Heavy.

Table 3.1 Average weight loss values at different ages in grams

AVG. WEIGHT LOSS OF CUBES AT DIFFERENT AGES IN GRAMS								
Desig	0 days	3 days	7 days	14 days	21 days	28 days	56 days	90 days
BV 0.1	0	70	98	115	126	135	158	163
BV 0.5	0	89	115	134	146	152	176	181
BV 1.0	0	94	117	139	150	156	187	195
BP 0.1	0	93	130	141	155	162	186	193
BP 0.5	0	102	132	152	167	179	191	200
BP 1.0	0	75	101	120	131	140	156	163
BW	0	0	0	0	0	0	0	0

SCC with Liquid Paraffin Wax Light and Heavy at different dosages 0.1%, 0.5% and 1.0% weights were taken and values were noted in Table and

Graphs are plotted for average weight loss Vs dosage of self curing compound, for both Liquid Paraffin Wax Light and Heavy at 7, 28, 56 and 90 days

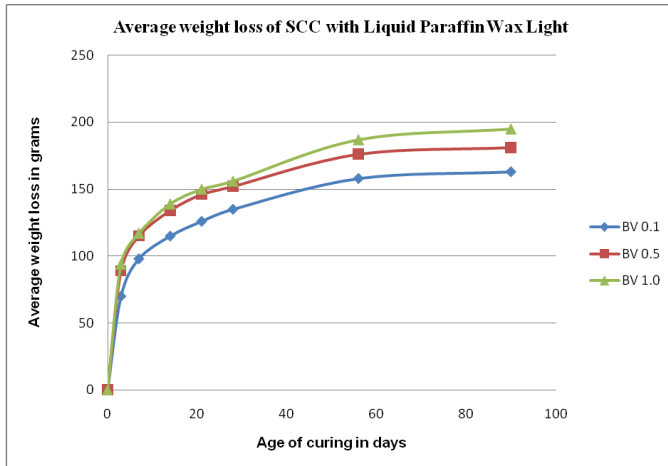


Fig 3.1 Average weight loss Vs Age of curing for LPWL

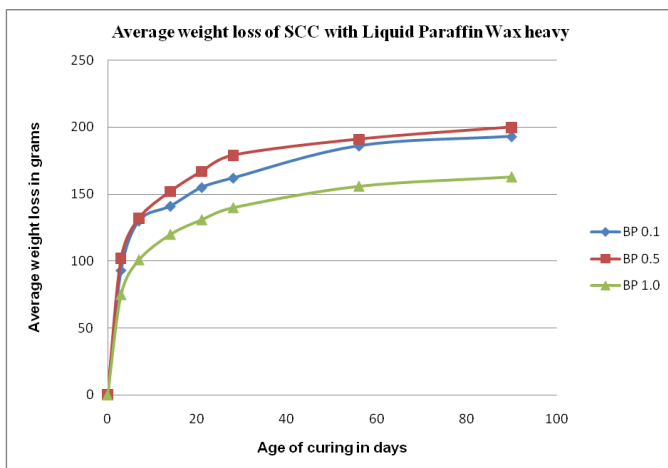


Fig 3.2 Average weight loss Vs Age of curing for LPWH

3.2 Compressive Strength

The strength of concrete depends on the hydration and which in turn depends on the water retention capacity of a certain concrete. While water curing is an ideal condition as explained earlier, may twises water curing is not possible. In the present study Liquid Paraffin Wax Light and Heavy of 0.1%,

0.5% and 1.0% dosage were cast and tested. Two comparative category of specimens Indoor and Wet were also considered. The details of the 7, 28, 56 and 90 days compressive strengths are shown in

Table 5.5: Compressive strength at Different Ages in MPa

Design	0 days	7 days	28 days	56 days	90 days
BW	0	43.29	60.13	64.08	68.03
BI	0	42.52	52.39	53.71	55.03
BV0.1	0	42.18	48.07	52.12	55.57
BV0.5	0	41.33	47.58	49.2	50.83
BV1.0	0	40.48	48.17	48.81	49.44
BP0.1	0	44.68	49.93	53.14	56.34
BP0.5	0	46.89	50.23	52.8	55.38
BP1.0	0	44.93	51.8	55.08	58.35

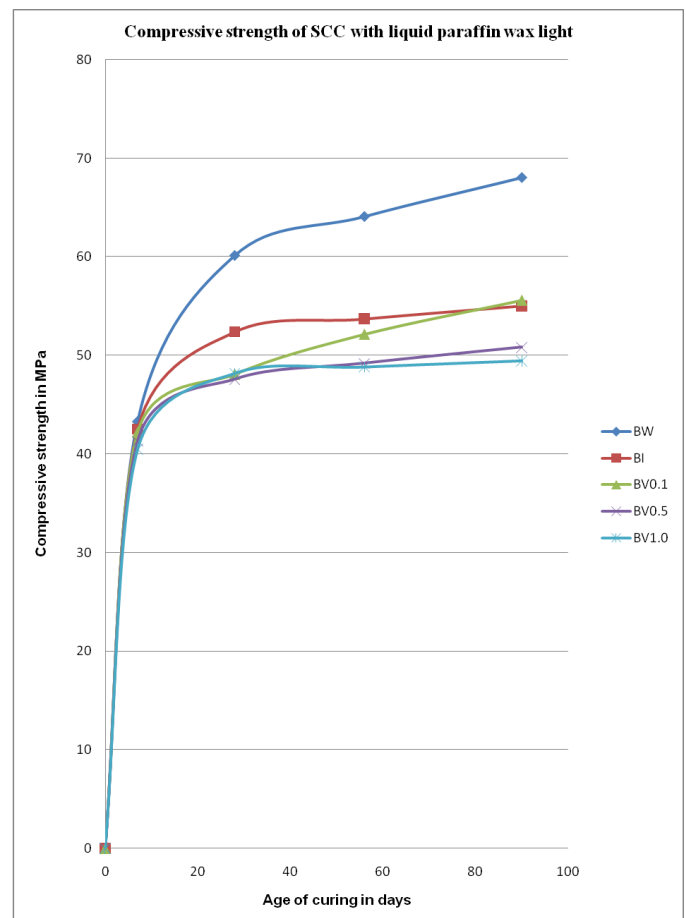


Fig 3.3 Compressive strength Vs Age of curing for LPWL

CONCLUSIONS

- All the mixes fresh properties values are within range of EFNARC specifications.
- After 28 days weight loss rate is considerably decreased in SCC with 0.1% of Liquid Paraffin Wax Light (BV0.1) and SCC with 1% of Liquid Paraffin Wax Heavy (BP1) than other specimens.
- At 56 days curing the weight loss of SCC with 0.1% of Liquid Paraffin Wax Light (BV0.1) and SCC with 1% of Liquid Paraffin Wax Heavy (BP1) are less compared to the other mixes.
- When SCC with 0.1% of Liquid Paraffin Wax Light (BV0.1) and SCC with 1% of Liquid Paraffin Wax Heavy (BP1) weight loss values are compared the weight loss in SCC with Liquid Paraffin Wax Heavy 1% (BP1) is less than the weight loss of SCC with liquid paraffin wax 0.1% (BV0.1). This indicates that SCC with Liquid Paraffin Wax Heavy (BP1) would be given minimum weight loss weight loss than the other mixes in later ages.
- This is attributed due to low water to cement ratio or better sealing capacity of Liquid Paraffin Wax Heavy. So, it is concluded that the optimum dosage for 60MPa concrete with the Liquid Paraffin Wax Light and Liquid Paraffin Wax Heavy of different dosages is 1.0% of Liquid Paraffin Wax Heavy (P).
- Indoor curing specimens have more water absorption than conventional cured specimens.
- The capillary suction of water is increasing with the increase in percentage dosage of Liquid Paraffin Wax Light. Optimum dosage is BV0.1, among BV specimens.
- Hence it is evident that lower percentage dosages of Liquid Paraffin Wax Light impart better sealing properties for the concrete.
- With increase in percentages dosages of Liquid Paraffin Wax Heavy, the water absorption increased up to a dosage of 0.5% and then decreased to 1.0%. Optimum dosage is BP1.0, among BP specimens.
- Among all dosages, 1.0% of Liquid Paraffin Wax Heavy has given better performance.
- At 7 days curing, SCC with Liquid Paraffin Wax Heavy of 0.5% (BP0.5) shown maximum compressive strength compared with other mixes including SCC with wet and Indoor Curing specimens.
- Among SCC Liquid Paraffin Wax Light (BV) mixes, SCC Liquid Paraffin Wax Light of 0.1% (BV0.1) has shown better compressive strength than others. But this compressive strength is less than BW. Whereas in SCC Liquid Paraffin Wax Heavy (BP) mixes, SCC Liquid Paraffin Wax Heavy of 1.0% (BP1.0) has shown better compressive strength than other mixes.
- At 28 days curing, SCC specimens with water curing (BW) have shown better compressive strength than other mixes. Self cured specimens with optimum dosage have also attained almost close compressive strength values as wet cured specimens.
- This behavior is similar for 56 days and 90 days. The increase in the strength percentage for

56 days and 90 days is less compared to 28 days.

- The specimens which have more water retention capacity have shown better superior compressive strength, sorptivity values. Hence, it can be concluded that minimum water loss leads to better gel formation thus increasing strength.
- So, optimum dosage of self curing agent is 0.1% for Liquid Paraffin Wax Light and 1.0% for Liquid Paraffin Wax Heavy in water retention, sorptivity and strength point of view.

REFERENCES

1. Hajime Okamura and Masahiro Ouchi (2003), "Self-Compacting Concrete", Journal of Advanced Concrete Technology Vol.1, No.1, 5-15, April 2003.
2. Ozawa K., Kunishima, M., Maekawa, K. and Ozawa, K, "Development of High Performance Concrete Based on the Durability Design of Concrete Structures". Proceedings of the second East-Asia and Pacific Conference on Structural Engineering and Construction (EASEC-2), Vol. 1, pp. 445-450, January 1989.
3. Domone, P.L. and Jin, J. 'Properties of mortar for self-compacting concrete' Proceedings of RILEM International Symposium on Self-Compacting Concrete, Stockholm, September 1999, RILEM. Paris 109-120
4. Nan Su, Kung-Chung Hsu, His-Wen Chai, "A simple mix design method for self-compacting concrete", Cement and Concrete Research, 6 June 2001, pp1799-1807.
5. H.J.H. Brouwers, H.J. Radix / Cement and Concrete Research 35 (2005) 2116 – 2136
6. "Specifications and guidelines for self-compacting concrete." published by EFNARC in February 2005.
7. Subramanian .S and Chattopadhyay (2002),"Experiments for Mix Proportioning of Self Compacting Concrete", Indian Concrete Journal, January, Vol., PP 13-20.
8. Khayat, k. H. Workability, testing, and performance of self-consolidating concrete. ACI Materials Journal, v. 96, n. 3, p. 346-353
9. Edamastu,Y., Nishida,.n.,Ouchi, M(1999)" a rational mix design method for self-compacting concrete considering interaction between coarse aggregate and mortar particles" proceedings of the first international RILEM symposium on self-compacting concrete, Stockholm, swedon,309-320
10. O Petersson, P Billberg, Buikvan, a model for self-compacting concrete RILEM conference production methods and workability of concrete, paisley, Scotland June 3-5
11. S. Venkateswara Rao, M.V. Seshagiri Rao, P. Rathish Kumar "Effect of Size of Aggregate and Fines on Standard And High Strength Self compacting Concrete", Journal of Applied Sciences Research, 6(5): 433-442, 2010.
12. S Venkateswara Rao, M V Seshagiri Rao, D Ramaseshu international RILEM conference on advances in construction materials through science and engineering-2011. 271-280.

13. I.M. Nikbin et al. / Construction and Building Materials 57 (2014) 69–80
14. T. Ponikiewski , J. gołaszewski archives of civil and mechanical engineering14 (2014) 455 – 465
15. L.A. Pereira-de-Oliveira et al., Construction and Building Materials 51 (2014) 113–120
16. K C Panda and P K Bal , Procedia Engineering 51 (2013) 159 – 164
17. M. Soleymani Ashtiani et al., Construction and Building Materials 47 (2013) 1217–1224
18. Roland Tak Yong Liang, Robert Keith Sun, “Compositions and Methods for Curing Concrete”, Patent No.: US 6,468,344 B1, Date of Patent Oct. 22, 2002.
19. Wen-Chen Jau“Self-curing Concrete”, United States Patent Application Publication, Pub. No: U.S. 2008/0072799 A1, Pub. date: Mar. 27, 2008.
20. R.K. Dhir, P.C. Hewlett and T.D. Dyer,” Durability of ‘Self-Cure’ Concrete”, Cement and Concrete Research, Vol. 25. No. 6, 1153-1158,1995.
21. A.S. El-Dieb / Construction and Building Materials 21 (2007) 1282–1287
22. M. Collepardi, A. Borsoi, S. Collepardi, R. Troli and M. Valente , “Self-Curing, Shrinkage-Free Concrete ”,ACI Material Journal SP 234-47 (2006) 755-764.
23. A.S. El-Dieb, T.A. El-Maaddawy and A.A.M. Mahmoud, “Water-Soluble Polymers as Self-Curing Agent in Silica Fume Portland Cement Mixes”, ACI Material Journal Vol.278 (2011) 1-18.
24. S. Zhutovsky, K. Kovler / Cement and Concrete Research 42 (2012) 20–26
25. M.V. Jagannadha Kumar* Et Al Issn: 2319 - 1163 Volume: 1 Issue: 1 Strength Characteristics Of Self-Curing Concrete Page No: 51 – 57
26. Prof. Nanak J Pamnani1, Dr. A.K. Verma, Dr. D.R. Bhatt International Journal of Engineering Trends and Technology (IJETT) - Volume4Issue5- May 2013
27. A.F. Bingöl, _I. Tohumcu / Materials and Design 51 (2013) 12–18
28. M. Golias et al. / Construction and Building Materials 35 (2012) 52–62
29. El-Dieb, El-Maaddawy and Mahmoud Advances in Cement Research Volume 24 Issue 5
30. R.K. Dhir, P.C. Hewlett and T.D. Dyer, “An investigation into the feasibility of formulating 'self-cure' concrete”, Materials and Structures Vol.27(1994), 606-615.
31. Text book on “ Concrete Technology- “Theory and Practice” by M.S.SHETTY
32. IS: 12269 -1987 "Indian Standard Specification for 53 Grade Ordinary Port land Cement", First Reprint September 1993.
33. IS: 383-1970 "Indian Standard Specification for Coarse and Fine Aggregates from Natural Sources for Concrete (Second Revision)", Ninth Reprint September 1993.

Performance of Concrete Containing Granulated Blast Furnace Slag as a Fine Aggregate

Ch. Srinivasarao^{1*}, S. S. Asadi¹ and M. Kameswararao²

¹KL University, Vaddeswaram - 522502, Andhra Pradesh, India; chraojk@rediffmail.com, asadienviro.asadi@gmail.com

²Mallareddy College of Engineering, Hyderabad - 500043, Telangana, India; rsmarathi2002@yahoo.com

Abstract

The present challenge in front of Civil Engineers is to find alternative materials for fine aggregates in concrete. Since, most of the State Govt. banned the dredging of river sand. The Granulated blast furnace slag is considered as a fine aggregate in concrete. At present, in India Steel Industry produces about 40 Million Tonnes by 2020 it is estimated to 60 million tonnes. The Author has investigated the effect of compressive strength of concrete, when Granulated blast furnace slag is used (GBFS) as a fine aggregate in concrete. The work includes the partially and fully replacement of river sand by granulated slag in M25 Grade of concrete with a constant 0.45 W/C ratio. Slag replacement of 50, 80, 100% are used. It has been observed that concrete made with 50% of river sand and 50% (GBFS) is nearer to Zero percent replacement. **Objectives:** To determine the optimum percentage slag replacement as a fine aggregate in concrete which helps in maintaining sustainability of concrete and balancing between the environmental problems due to construction industry as it is necessary to find out the alternative materials for use as fine aggregates because of restrictions by the local authorities. **Methods:** The experiments are planned to find out the optimum replacement percentage of GBFS against river sand as a fine aggregate in concrete. Mix design for M25 grade of concrete is made with OPC (Ordinary Portland Cement) and PPC (Port land Pozzolana Cement) is considered with a constant 0.45 W/C ratio and slag replacement of 50, 80, 100% are used. 30 Cubes for each cement category of 150 mm size are casted, cured by immersion and tested by CTM. **Findings:** In both the cement category, the compressive strength and slump of concrete is found reducing with the increase in the percentage of slag as a replacement to fine aggregate. In concrete made with OPC when compared with 50%, 80% and 100% replacement with GBFS reduction upto 96.50%, 87% and 77.5% in strength and 84.6%, 53.84% and 34.6% in slump respectively is observed. In concrete made with PPC when compared with 50%, 80% and 100% replacement with GBFS reduction upto 95.30%, 80% and 63% in strength and 82.7%, 51.7% and 34.0% in slump respectively is observed. **Application/Improvements:** This study using alternatives to fine aggregate in concrete will help in making concrete economical, reduction in environmental problems and saving the natural resources. The study may be extended to determine the concrete sustainability in saline conditions also.

Keywords: Compressive Strength, Granulated Blast Furnace Slag, OPC, PPC, River Sand

1. Introduction

The concrete industry is the largest consumer of natural resources like sand, gravel, crushed rock, etc. Sand & crushed stone requirement is about to the tune of 10 billion tonnes per annum. Natural sand obtained from river bed is getting depleted and due to indiscriminate dredging, most of the state Govt.'s imposed a ban on mining of

river sand. Increase in population which causes an acute shortage of building materials and the civil Engineers have been challenged to convert the Industrial by products to useful building and construction materials¹.

Environmental restrictions for the exploitation of sand from riverbeds have resulted in a search for alternative source, particularly near the larger metropolitan areas. The challenge for the government is to reduce the

* Author for correspondence

industrial by products which impacts to both health and environment when not disposed properly². Granulated slag, steel chips are industrial by products in the Iron and steel industry and causes a nuisance.

Thus manufactured fine aggregates and Granulated Blast Furnace Slag appear as an attractive alternative to natural fine aggregates for cement mortars and concrete. Slag is a non-metallic inert by product of steel industry primarily consists of silicates, Alumina silicates, and calcium-alumina silicates. The choice of aggregates is important and their quality plays a key role; they can not only limit the strength of concrete but their characteristics, effects the durability and performance of concrete³.

The inherent benefits of slag play critical part in the preservation of natural resources whilst delivering premium performance. Hence, it could be recommended that slag aggregate could be effectively utilized as fine aggregate in masonry, plastering and all concrete applications.

Recent studies shown that, the natural sand can be replaced by Granulated slag as a fine aggregate in concrete⁴⁻¹⁰.

Keeping in view of the above, the author has tried to conduct a feasibility study on concrete by using Granulated Slag as fine aggregate (GBFS).

The author has presented in this paper that the results from the study carried out in the laboratory on compressive strength and slump of concrete made with slag as a fine aggregate.

2. Study

The primary investigation is to observe the development of the compressive strength of concrete made with Granulated slag as a fine aggregate (GBFS) in M25 grade of concrete in severe condition. The author tested the concrete cubes with Ordinary Portland Cement (OPC) and also with Portland Pozzolana Cement (PPC) for 3 days, 7 days and 28 Days compressive strength.

The concrete cubes are casted with 100% river sand as a reference and replacement of river sand by 50%, 80% and 100% by GBFS for observation. Slump is also recorded at all replacement levels. Finally, based on analysis and discussions of the test results, conclusions are drawn.

3. Materials and its Physical Properties

- Ordinary Portland Cement (OPC), Portland Pozzolana Cement (PPC)
- Granulated Blast Furnace Slag (GBFS)
- River sand
- Coarse aggregates (20 mm & 12 mm)
- Chemical admixture used is Mid PCE Ecmas 92SP
- Water

The properties arrived at laboratory for OPC and PPC are shown in Table 1 and Table 2.

Table 1. Physical properties of X(OPC 53Gr.) and Y(PPC)Cement

Cement	Sp. Gravity (Sq.M/Kg)	IST (Minutes)	FST (Minutes)	Compressive strength (MPa.)			Fineness Sqm/Kg.
				3 Days	7 Days	28 Days	
OPC 53Gr. (X) as per IS:12269	3.15	145	240	42	52	63	311.90
PPC (Y) - as per IS:1489	2.91	166	260	25	33	57	346.40

Table 2. Chemical properties of OPC (X) and PPC(Y) cement

Element	OPC	PPC
1. Silica(SiO ₂)	21.20	36.40
2. Alumina(Al ₂ O ₃)	6.20	11.04
3. Iron Oxide(Fe ₂ O ₃)	4.75	4.68
4. Calcium Oxide(CaO)	62.05	42.29
5. Magnesium Oxide(MgO)	1.26	1.0
6. Sulphur Trioxide (SO ₃)	0.67	2.10
7. Sodium Oxide(Na ₂ O)	0.13	0.18
8. Potassium Oxide(K ₂ O)	0.34	0.40
9 Insoluble Residue (IR)	0.93	28.02
10 Loss on ignition	2.01	2.66

The laboratory results of GBFS are shown in Table 3 and Table 4.

The laboratory results of river sand and coarse aggregates are shown in Table 5 and Table 6.

Table 3. Chemical properties of GBFS

S.No	Element	%Present in GBFS
1.	CaO	35.60
2.	SiO ₂	28.90
3.	Al ₂ O ₃	17.12
4.	Fe ₂ O ₃	0.75
5.	MgO	6.05
6.	MnO	0.30
7.	SO ₃	-
8.	S	1.35

Table 4. Physical properties of GBFS

SNo:	Element	Results
1	Sp.Gravity	2.85
2	Loose bulk Density	1.20
3	Silt(wet Sieving)	<1.5%
4.	Particle Shape	Sub angular to sub round.
5.	Water Absorption	1%

Table 5. Sieve analysis of GBFS -(conforming to Zone -II) as fine aggregate and coarse aggregate (Tested as per IS 2386)

IS Sieve Size, mm	Cumulative percentage of material passing fine Aggregate (GBS)	Cumulative percentage of material passing coarse Aggregate	
		20 – 10 mm	< 10 mm
40	100	100	100
20	100	99.09	100
10	100	4.62	98.46
4.75	99.50	3.03	12.88
2.36	94.75	0	0
1.18	70.20	0	0
0.6	39.70	0	0
0.3	7.0	0	0
0.15	1.95	0	0

Table 6. Sieve analysis of combined grading of coarse aggregate (Tested as per IS 383) To meet IS specification for combined grading of coarse aggregate, the following proportions are used. Coarse aggregate (20mm) = 60% Coarse aggregate (<12.5mm)= 40%

IS Sieve Size, mm	Cumulative percentage of material passing 20mm (60%)	Cumulative percentage of material passing <12.5mm (40%)	Combined Grading	Limits as per IS:383
40	60	40	100	100
20	59.45	40	99.45	95 - 100
10	2.77	39.38	42.15	25 - 55
4.75	1.82	5.15	6.97	0 - 10

4. Design Mix for M25 as per IS 10262-2009

The concrete mix design is carried out as per IS code and the quantities of materials required are given in Table 7.

Table 7. Required quantities of materials for M25 grade concrete

Cement (Kg/Cum)	River Sand per Kg/Cum	Coarse Aggregate per Cum	Total Water required in Lts	Chemical Admixture in Lts
		20 mm 12.5mm	0.45 W/c	
372.40	660	699.60 572.40	172.70	1.70

5. Experimental Programme

Materials used in the study are OPC 53Gr. and PPC cement confirming IS 12269 and IS 1489. Fine and coarse aggregates, GBFS are confirming to IS 383-1970.

Design mix is carried out as per IS 10262:2000 for M 25 concrete in severe condition. The design mix done with 100% natural sand as reference and the natural sand has been replaced with GBFS by 50, 80 and 100% for comparison and to draw the conclusions. Concrete cubes are casted for 3, 7 and 28 days and kept for curing.

Concrete cubes were tested on compression testing machine. Workability is also measured by using slump cone apparatus.

6. Test Results

The test results of compressive strengths of concrete made with OPC, PPC, coarse aggregate, river sand varying with different proportion of GBFS are depicted in Table 8 to Table 15.

Table 8. Compressive strength (MPa) of concrete cubes with OPC and 100% river sand

Sample No:	3 Days (Mpa)	7 Days (Mpa)	28 Days (Mpa)	Slump (mm)@1 hr
Cube 1A	38.8	44.0	52.3	130mm
Cube 1B	40.0	43.8	51.9	
Cube 1C	39.0	42.6	50.7	
Avg.	39.2	43.5	51.6	

Table 9. Compressive strength (MPa) of concrete cubes with OPC and 50% GBFS

Sample No:	3 Days (Mpa)	7 Days (Mpa)	28 Days (Mpa)	Slump (mm) @1 hr
Cube 2A	36.6	42.0	49.8	110
Cube 2B	38.3	41.3	48.6	
Cube 2C	37.2	40.8	50.1	
Avg.	37.3	41.3	49.5	

Table 10. Compressive strength (MPa) of concrete cubes with OPC and 80% GBFS

Sample No:	3 Days (Mpa)	7 Days (Mpa)	28 Days (Mpa)	Slump (mm) 1 hr
Cube 3A	34.0	38.02	45.0	70
Cube 3B	33.8	38.6	45.8	
Cube 3C	31.2	40.1	43.0	
Avg.	33.0	38.8	44.6	

Table 11. Compressive strength (MPa) of concrete cubes with OPC and 100% GBFS

Sample No:	3 Days (Mpa)	7 Days (Mpa)	28 Days (Mpa)	Slump (mm) @1 hr
Cube 4A	30.2	31.0	40.1	45
Cube 4B	29.8	32.8	40.8	
Cube 4C	29.0	34.3	38.6	
Avg.	29.60	32.36	39.80	

Table 12. Compressive strength (MPa) of concrete cubes with PPC and 100% River Sand

Sample No:	3 Days (Mpa)	7 Days (Mpa)	28 Days (Mpa)	Slump (mm) @1 hr
Cube 1P	28.6	38.0	48.9	145
Cube 1P	27.3	37.4	50.0	
Cube 1P	26.2	38.2	48.2	
Avg.	27.3	37.8	49.0	

Table 13. Compressive strength (MPa) of concrete cubes with PPC and 50% GBFS

Sample No:	3 Days (Mpa)	7 Days (Mpa)	28 Days (Mpa)	Slump (mm) @1 hr
Cube 2P	26.8	37.1	47.2	120
Cube 2P	27.2	36.8	46.8	
Cube 2P	26.0	35.4	46.2	
Avg.	26.6	36.4	46.7	

Table 14. Compressive strength (MPa) of concrete cubes with PPC and 80% GBFS

Sample No:	3 Days (Mpa)	7 Days (Mpa)	28 Days (Mpa)	Slump (mm) @1 hr
Cube 3P	22.8	29.9	38.6	75
Cube 3P	21.6	28.2	39.2	
Cube 3P	23.1	30.1	40.8	
Avg.	22.56	29.4	39.53	

Table 15. Compressive strength (MPa) of concrete cubes with PPC and 100% GBFS

Sample No:	3 Days (Mpa)	7 Days (Mpa)	28 Days (Mpa)	Slump (mm) @1 hr
Cube 4P	20.1	25.6	31.3	50
Cube 4P	19.4	23.4	30.1	
Cube 4P	20.8	26.2	32.4	
Avg.	19.9	25.0	31.2	

7. Results and Discussions

In OPC and PPC concrete, the natural river sand was replaced by Granulated blast furnace slag at 50, 80 and 100%. The compressive strength of concrete made with OPC with 100% natural river sand as a reference and compared with the replacement of natural sand by 50%,

80% and 100% GBFS. Concrete cube with 100% got 51.60Mpa at 28 days when, natural sand was replaced by 50% the compressive strength achieved at 49.5Mpa. At 80 % and 100% replacement levels, the compressive strength achieved at 44.6 and 39.8 as furnished in Table 8 – 11. The concrete made with PPC with 100% natural sand got the compressive strength of 49.0Mpa at 28 days and 46.7MPa, 39.5Mpa and 31.2 Mpa at replacement of natural river sand by GBFS by 50, 80 &100% respectively as shown in Table 12-15.

The workability also noted for concrete made with OPC and PPC with 100% natural sand given at 130mm and 145mm respectively. The slump measured at replacement of natural sand by GBFS at 50, 80 and 100% were 110, 70, 45mm and 120, 75 and 55mm respectively.

Based on the test results, we have observed that the GBFS percentage is increased towards 100% in concrete, there a decrease in compressive strength as well as workability in OPC and PPC concrete.

8. Conclusion

It is recommended that 50% natural sand can be replaced by GBFS to get the optimum compressive strength and workability as compared with 100% natural river sand concrete made with OPC and PPC.

9. References

1. Turgut P, Algin HM. Limestone dust and wood saw dust as brick material. *Build Environ.* 2007; 42(9):3399–403.
2. Alwaell A, Nadziakiewicz MJ. Recycling of scale and steel chips waste as a partial replacement of sand in concrete. *Construct Build Mate.* 2012; 28(1):157–63.
3. Neville MA. *Proprieties Des betons.* Edition Eyrolles, Paris. 1998; 35(12):1239–308.
4. Zeghichi L. The effect of replacement of natural aggregates by slag products on the strength of the concrete. *Asian J Civ Eng.* 2006; 7(1):27–35.
5. Sudavizhi M, llangovan SR. Performance of copper slag and ferrous slag as partial replacement of sand in concrete. *Int J Civ Struct Eng.* 2011; 1(4):1–10.
6. Alnuaimi AS. Effects of copper slag as a replacement for fine aggregate on the behaviour and ultimate strength of reinforced concrete slender columns. *TJER.* 2012; 9(2):90–102.
7. Priyadharshini E, Veerakumar R, Selvamani P, Kaveri S. An experimental study on strengthening of reinforced concrete beam using glass fiber reinforced polymer composites. *Indian Journal of Science and Technology.* 2016 Jan; 9(2). Doi: 10.17485/ijst/2016/v9i2 /86358.
8. Raghavendra DS, Sivakumar A. Compressive strength index of different types of light weight plastic aggregate concrete. *Indian Journal of Science and Technology.* 2015 Jan; 8(S2). Doi: 10.17485/ijst/2015/v8iS2/59087.
9. Kumar D, Pourush PKS. Strength and workability of low lime fly-ash based geopolymer concrete. *Indian Journal of Science and Technology.* 2010 Dec; 3(12). Doi: 10.17485/ijst/2010/v3i12/29859.
10. Felixkala T, Partheeban P. Granite powder concrete. *Indian Journal of Science and Technology.* 2010 Mar; 3(3). Doi: 10.17485/ijst/2010/v3i3/29706.

1. Turgut P, Algin HM. Limestone dust and wood saw dust as

TRAFFIC ACCIDENT SEVERITY ANALYSIS ON NH-163 USING LIMDEP MODEL

B Vijaybhasker¹, V Ranjith Kumar², Dr.M.Kameswara Rao³

¹Research Scholar (M.Tech, T.E), ²Assistant Professor, ³Professor

Malla Reddy Engineering College (Autonomous), Kompally

Abstract — In this paper, a brief practical review is presented on the statistical evidence showing the model indicate that factors such as location of the crash, time of occurrence of the accident, the vehicles involved in the accidents as well as the maneuver of collisions are the four most important attributes that are found to be consistently significant. For example, the accidents occurring in day light are resulting in lower injury severity level than accidents occurring at night time. It has also been observed that accidents occurring near intersections are relatively less severe than accident occurring on roadway segments. Lorry's and unknown vehicles (in hit and run accidents) have been identified as accused vehicle in more cases than motorcycles & autos. Results also indicating that all the single vehicle collision are less severe than crashes involving SUVs and cars. Pedestrians, motorcycles, bicycle and autos are observed to sustain higher levels of injury severity than other users. Analysis of crash maneuver also shows that hit and run type of accident is very high and often results in higher levels of severities than even a head-on collision.

Keywords—Accidents, severity, ranga reddy, NH-163, probit Modeling,

1. Introduction

Throughout the world, the growth of the transport system has been and continues to be a key element in economic development. Increase in gross national product is associated with greater movement of people and goods and greater investment in both vehicles and transport infrastructure. In the developing world, current trends in population growth, industrialization and urbanization are causing heavy pressure on the transport network in general and on road network in particular. Most unwanted side-effect of this growth in traffic is growing numbers of deaths and injuries from road traffic accidents resulting in enormous cost in terms of lost productivity of the society. This also includes personal losses due to injuries (or fatalities) in traffic accidents as the victims must deal with pain and suffering, medical costs, wage loss, and vehicle repair costs. As a result traffic safety issues had attracted much attention of traffic engineers and planners to do effective research and get better understanding of the problem that provides the framework against which effective policies and counter-measures could be developed.

Traffic safety is a major concern because of the economic and social costs of traffic crashes. The impact that traffic

accidents have on society is significant. Individuals injured (or killed) in traffic accidents must deal with pain and suffering, medical costs, wage loss, and vehicle repair costs. For society as a whole, traffic accidents result in enormous costs in terms of lost productivity and property damage. It is assumed that there is total 2% loss of GDP only due to road accident in India. Clearly, efforts to improve our understanding of the factors that influence accident severity are warranted. So the common practice in transportation engineering is a thorough study of traffic accidents and gets an understanding of the factor affecting them. Severity of injury sustained by victim involved in crashes is of considerable interest to policy makers & safety engineers. The relationship between the injury severity of traffic crashes and factors such as driver and passenger characteristics, vehicle type, and traffic and geometric conditions has attracted much attention. Better understanding of this relationship is necessary and very important for improving vehicle and roadway designs such that severe injuries can be reduced. Numerous studies have applied statistical models for crash injury severity study.

Recent years have witnessed rapid motorization, urbanization, industrialization, migration and other changes related to globalization and economic policies of successive governments in India. An accompanying effect of these changes is the increasing road crashes and deaths due to lack of safety policies and program.

The total number of accidents reported by Ministry of road transport and highways in the year 2012 were 4,84,704 of which 1,06,591 or 22.0% of total accidents were fatal; the number of persons killed in the accidents were 1,19,860 (i.e. an average of one fatality per 4.0 accidents) and the number of persons injured at 5,23,193 exceeded total number of accidents (4,84,704) in 2012. The proportion of fatal accidents in the total road accidents has consistently increased since 2001 as reflected in Table-1.1 The severity of road accidents measured in terms of persons killed per 100 accidents is observed to have increased from less than 20 in 2001 to 24.7 in 2012. India has a rural road network of over 3,300,000 km, and urban roads total more than 250,000 km. The national highways (NH), with a total length of 70934 km, serve as the arterial network across the country (NHAI). Roads carry about 61% of the freight and 85% of the passenger traffic. National

Highways total about 71000 km (2% of all roads) and carry 40 % of the road. Highways permit greater speed resulting in relatively greater number of road accidents with higher severities.

Among the various accidents it has been observed that national highways accounted for 29% in total road accidents and 36% in total number of persons killed in 2012. The accident figures are not in proportion to the highway network since national highways are only 2% of all roads. Hence the accidents involvement rate on national highway is extremely high.

2. NEED FOR THE PRESENT STUDY

Initial investigation of collected sample data on National Highway-163 (NH-163) of Rangareddy District as shown in the figure-2.1 and last three years i.e. 2012-2014 accident data of Rangareddy district that in 2010, 53 % of total crashes on NH-163 were fatal and 39 % were major injury crashes. While in 2013 major injury and fatal crashes were 51% and 44% and in 2012 it was 49% and 40% respectively as shown in figure-2.2. This clearly shows that crashes occurring on NH-163 rarely result in minor or no injury crashes, probably due to higher average speed of these facilities. A further investigation on share of crashes on various roadways in RangaReddy district shows that, 54% of the total people died in the district due to road traffic crashes occurred on NH-163 only, compared to other state and district roadways. These statistics clearly shows that the accident situation on NH-163 is worsening.

The present study was conducted to understand the contributing factors affecting severity of road crashes in RangaReddy with a broad consideration of driver characteristics, roadway features, vehicle types and environmental factors. For this purpose, the type of accident severity analyses have been incorporated, i.e. all vehicle crash severity to get an overview of the factors affecting the severity throughout the RangaReddy district. The reason behind choosing this type of accident in severity analysis is that they constitute about the accidents that occurred in RangaReddy district from 2012 to 2014.



Figure-2.1 Map of NH-163 in Ranga Reddy district.

3. LITERATURE REVIEW

Gray et al. (2012) observed that young male drivers are over-represented in car accidents in Great Britain. While investigating the factors affecting the severity of these young male drivers they observed that driving in darkness, trips during early morning and towards the end of the week (Friday and Saturday) are related with higher severities. They also observed that carriageway hazards such as passing a site where accident occurred may increase severity of crashes at a site afterwards that specific site. They also observed higher levels of severities during overtaking maneuvers, and on the single carriageway of speed limit 60 mph. Other variables leading to higher severities were driving on main roads, not being at a junction, towing something like a caravan or trailer, young male drivers of age group 20-22, and finally in fine weather condition with no high winds.

Kockelman and Young (2001) applied ordered probit models to examine the risk of different injury levels sustained under all crash types, two-vehicle crashes, and single-vehicle crashes. The results suggest that pickups and sport utility vehicles are less safe than passenger cars under single-vehicle crash conditions. In two-vehicle crashes, however, these vehicle types are associated with less severe injuries for their drivers and more severe injuries for occupants of their collision partners (including drivers and passengers). Crash types such as roll-over and head-on accidents resulted in more severe injuries. Female drivers are also found to be involved with higher crash severities.

Pai and Saleh (2007) estimated statistical models to identify whether a specific maneuver by motorcycle or vehicle (e.g., overtaking or changing lanes) is more hazardous to motorcyclists in sideswipe collisions at T-junctions. The modeling results show that injuries to motorcyclists were greatest when an overtaking motorcycle collided with a turning vehicle and such effect appeared to be more severe at unsignalized junctions.

Quddus et al. (2002) investigated factors leading to increase in the probability of severe injuries of motorcyclists and identified that motorcyclist who is not from Singapore experienced higher crash severities compared to Singaporean motorcyclists. , Among other factors they found that increased engine capacity, headlight not turned on during daytime, collisions with pedestrians and stationary objects, driving during early morning hours and motor cycles with pillion passengers experienced higher severities. Additionally they observed that in collisions where the motorcyclists are at fault, they sustained higher levels of injuries than otherwise.

Abdel-Aty (2003) applied ordered probit models for analysis of driver injury severity levels at roadway sections, signalized intersections, and toll plazas. He found that older drivers, male drivers, and those not wearing a seat belt will have a higher

probability of a severe injury and both signalized intersections and roadway sections models showed higher level of injuries in rural areas, possibly due to higher speeds. He also found that driver's violation was significant in case of signalized intersection. Alcohol, lighting conditions, and the existence of a horizontal curve affected the likelihood of injuries in the roadway sections' model. A variable specific to toll plazas, vehicles equipped with Electronic Toll Collection, had a positive effect on the probability of higher injury severity at toll plazas.

4.0 OBJECTIVE AND SCOPE OF STUDY

The principal objective of this study is to investigate how various factors such as the seasonal variation, weekly variation, time of day variation, collision type, victim gender, crash location, and vehicle type can lead to variations in the probabilities of sustaining different levels of injury severity in motor vehicle accidents on NH-163.

To do so injury severity levels had been categorized into three levels. Three levels are minor injury, major injury and death. Data have been collected from different police stations of RangaReddy district along NH-163. Then after initial investigations of primary data has been done. From those analyses it was found that there were over-representation of pedestrian and truck involved crashes. So three distinct model, all crash model, truck involved crash model, and model for all pedestrian involved crashes have been developed to get clear understanding of the factors influencing higher level of severities. Finally the probability of occurring different levels of injury severity associated with different factors such as collision type, vehicle type, time of day variation have been estimated.

In all the above studies environmental factors such as climatic condition, roadway geometry like horizontal curve, vertical curve are not taken into account due to lack of accident data. Victim's age have not been considered into model due to insufficient data and has been separately investigated.

To achieve the above mentioned objective ordered probit model have been applied to real accident data. Ordered probit model is a widely used statistical tool which is generally used for analysis of ordinal data. Here injury severities are ordinal data type. The models are analyzed to find the factors causing higher level of severities in traffic crash.

5.0 METHODOLOGY

The methodology implemented to analyze police-reported crash data on national highway-163 to identify possible factors that cause these crashes and to understand their effect on injury severity using statistical modeling techniques. The method and procedures adopted for this study can be divided into three steps-

- a. Collection of accident data,

- b. Variable selection and development of statistical model and
- c. Analysis and interpretation of model findings. A detailed description of the above mentioned steps is presented in the following sections.

5.1 DATA COLLECTION

As mentioned in Section 1.4 of Chapter one above, since the objective of the study was to understand the effects of various factors such as the seasonal variation, weekly variation, time of day variation, collision type, victim gender, crash location, and vehicle type on injury severity of crashes on NH-163, several data sources have to be used to obtain all the data necessary to carry out the study. In order to meet this objective of the research, which specifically is attempting to create a better understanding the effects of these factors believed to possibly influence injury severity, collection of accurate and representative data was the most critical and of course lengthiest part of the research.

5.2 COLLECTION AND PROCESSING OF ACCIDENT DATA

Due to lack of any standard traffic crash data reporting system a field survey have been done to collect all police-reported crash data on NH-163. Since the study area was NH-163 in RangaReddy district all the police station that were reporting any crash occurred on national highway have been taken into consideration. Unfortunately, police reports at accident sites do not describe injuries in much detail because of the lack of police qualifications and training as well as facilities needed to perform complex examinations. All these police station having theses crash data in form of FIR sheets and complaint lodged by victim or else one. All the reported crashes occurring in last three years i.e. from 2008 to 2010 were collected. From these FIR sheets and complain letter a data set have been prepared. Preparation of data set was the most time consuming part of the study.

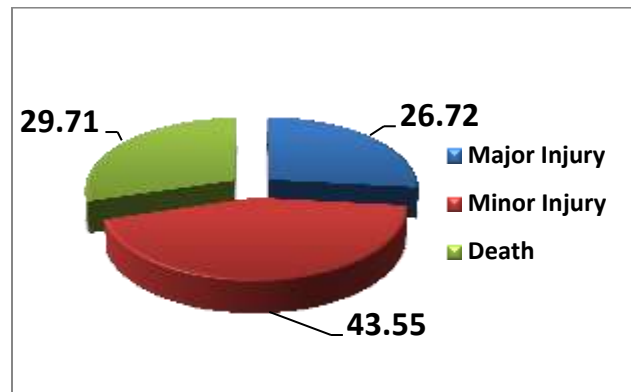


Fig 1 Percent share of crash severity on NH-163 in RangaReddy district

Monthly distribution of crash injury severity:

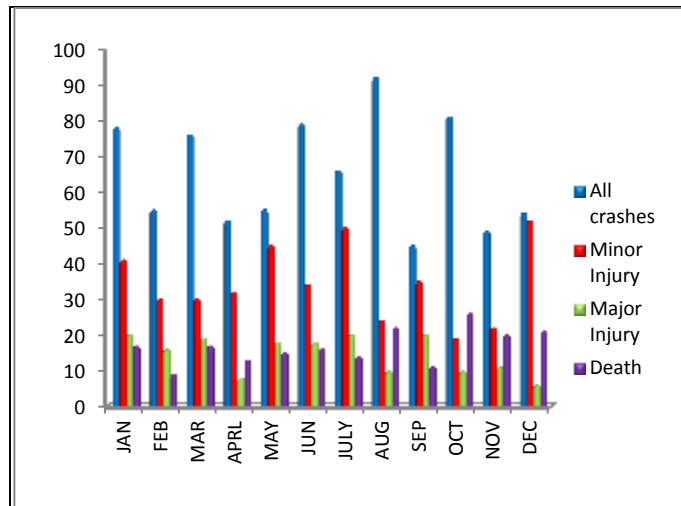


Fig 2 Monthly variation of crash Severity on NH-163 during 2012-2014

Weekly distribution of crash severity:

Days	Minor injury	Major injury	Death
MON	19.31	11.88	16.12
TUE	17.16	13.98	20.64
WED	13.3	22.37	10.96
THR	17.16	13.98	6.45
FRI	18.88	11.18	19.35
SAT	12.44	12.58	8.38
SUN	12.87	13.98	18.6

Weekly distribution of crash severity:

Through-out the week no major variation have found. All crashes are between 1% to 4 %, minor injury crashes are between 4% to 8 % whereas major injury and fatal crashes are always greater than 20%.

Hourly variation of crash injury severity

Hourly variation of crash severity is estimated with four hours of interval throughout the day by plotting percent distribution of crash severity on Y-axis. Table 4.1 show that between night 00:00 hrs to morning 03:59 hrs percentage of occurring fatal crashes are higher which is 31.20% of total crash occurring between that hours.

Also, medical reports were hard to obtain because police accident data and medical data are not kept together. Consequently, it was impossible to obtain details on the degree of accident severity. All that can be learned from the police records is that the accident is a fatal accident, minor injury, severe injury on accident. Each observation in this data set is a record of the level of injury severity sustained by crash victim, Vehicle type involved in crash, location of the accident, type of collision, year, month, day, date, and time of the collision, victim gender, victim age, and lane direction.

PRIMARY INVESTIGATION OF ACCIDENT DATA.

A total of 10 major factors contributing to higher crash severity were summarized from those 535 crash counts. A preliminary investigation of these factors was done so that their impacts on injury severity could be estimated. Detailed discussion of these major variables is given in following paragraphs.

Monthly distribution of crash injury severity:

As illustrated in figure-4.2 highest accidents are occurring in month of August. It is 11.76% of all accident occurring during 2008-2010.

About 12.93 % of all fatal crashes are occurring in August and October each. In August highest major injury has been observed which is about 11 % of all major injury occurred during 2008-2010.

Model Selection

The crash injury severity is a typical ordered variable which could be categorized at different levels from the least severe level to the most severe. In this study crash injury severity is ordinal variable categorized as “no injury = 0,” “minor injury = 1,” “major injury = 2,” and “fatal = 3”. As ordered response models are capable of recognizing the indexed nature of various response variables so it is commonly used for analyzing the data sets that include categorical and ordered dependent variable. Among ordered response model ordered probit/logit are the most often used models



Model Specification

The general specification of each single equation model is:

$$Y_n^* = \beta'x_n + \varepsilon_n,$$

Where, Y_n^* is the latent and continuous measure of injury severity faced by the accident victim 'n' in a crash, x_n is a vector of explanatory variables measuring the attributes of accident victim. β' is vector of parameters to be estimated, and ε_n is a random error term which assumed to follow a standard normal distribution with mean zero and variance one.

The observed and coded discrete injury severity variable, Y_n , is determined from the model as follows:

$$Y_n = \begin{cases} 0 & \text{if } -\infty \leq Y_n^* \leq \mu_1 \text{ (no injury),} \\ 1 & \text{if } \mu_1 < Y_n^* < \mu_2 \text{ (not severe injury),} \\ 2 & \text{if } \mu_2 < Y_n^* < \mu_3 \text{ (severe injury),} \\ 3 & \text{if } \mu_3 < Y_n^* < \infty \text{ (fatal),} \end{cases}$$

Where, the μ_i represents thresholds to be estimated along with the parameter vector β .

The probabilities associated with the coded responses of an ordered probit model are as follows:

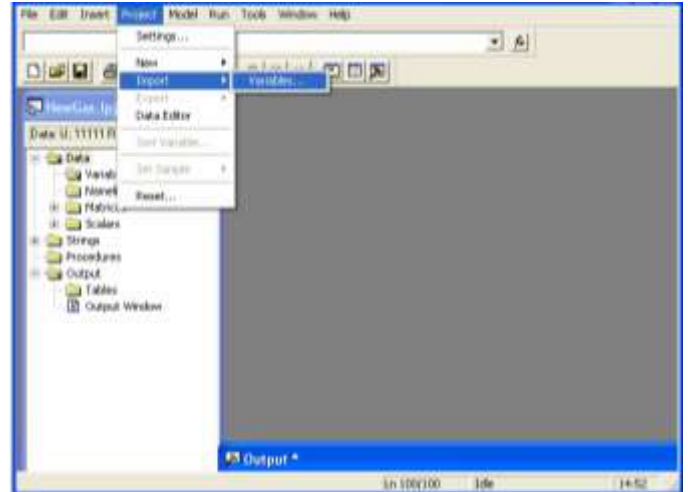
$$P_n(0) = \Pr(Y_n = 0) = \Pr(Y_n^* \leq \mu_1) = \Pr(\beta'x_n + \varepsilon_n \leq \mu_1) \\ = \Pr(\varepsilon_n \leq \mu_1 - \beta'x_n) = \Phi(\mu_1 - \beta'x_n)$$

$$P_n(1) = \Pr(Y_n = 1) = \Pr(\mu_1 < Y_n^* \leq \mu_2) \\ = \Pr(\varepsilon_n \leq \mu_2 - \beta'x_n) - \Pr(\varepsilon_n \leq \mu_1 - \beta'x_n) \\ = \Phi(\mu_2 - \beta'x_n) - \Phi(\mu_1 - \beta'x_n)$$

$$P_n(k) = \Pr(Y_n = k) = \Pr(\mu_k < Y_n^* \leq \mu_{k+1}) \\ = \Phi(\mu_{k+1} - \beta'x_n) - \Phi(\mu_k - \beta'x_n)$$

$$P_n(K) = \Pr(Y_n = K) = \Pr(\mu_k < Y_n^*) \\ = 1 - \Phi(\mu_k - \beta'x_n)$$

Where, n is an individual, k is a response alternative ($Y_n=k$) is the probability that individual n responds in manner k , and $\Phi(\cdot)$ is the standard normal cumulative distribution function. The model is usually identified by setting $\mu_0=0$. So the unknown parameters needing to estimate then become β and $(\mu_1, \mu_2, \mu_3, \dots, \mu_k)$.



The parameters of ordered multiple choice models are estimated by the method of maximum likelihood (ML). In very simple terms, the method of ML is a method for choosing parameter estimates in order to maximize the probability, or likelihood, of observing given data. A likelihood function is an equation expressing this probability/likelihood as a function of the data and the unknown parameters, and ML estimation involves the systematic evaluation of this function at different points (i.e. sets of parameter values) in order to find the point at which the function is maximized. This set of parameter values then becomes set of ML estimates.

For a sample of N accident victims, the log-likelihood function (i.e. the logarithm of the likelihood function) for ordered probit models can be written as

$$\log(L) = \sum_{n=1}^N \sum_{k=1}^K d_{nk} \log[P_n(k)]$$

Where d_{nk} is a dummy variable which takes the value one if individual n chose alternative k and $d_{nk} = 0$ otherwise.

Table-3 Description of all Variables Used in This Study

Explanatory variable	Description
Dependent variable	

CRASH SEVERITY	Injury severity level: Property damage only = 0, Minor injury = 1, Major Injury = 2, Fatal = 3
Seasonal effects	
JAN	If accident occurs in January = 1, otherwise = 0
FEB	If accident occurs in February = 1, otherwise = 0
MAR	If accident occurs in March = 1, otherwise = 0
APR	If accident occurs in April = 1, otherwise = 0
MAY	If accident occurs in May = 1, otherwise = 0
JUN	If accident occurs in June = 1, otherwise = 0
JUL	If accident occurs in July = 1, otherwise = 0
AUG	If accident occurs in August = 1, otherwise = 0
SEP	If accident occurs in September = 1, otherwise = 0
OCT	If accident occurs in October = 1, otherwise = 0
NOV	If accident occurs in November = 1, otherwise = 0
DEC	If accident occurs in December = 1, otherwise = 0
Day of Week	
MON	If accident occurs on Monday = 1, otherwise = 0
TUE	If accident occurs on Tuesday = 1, otherwise = 0
WED	If accident occurs on Wednesday = 1, otherwise = 0
THU	If accident occurs on Thursday = 1, otherwise = 0
FRI	If accident occurs on Friday = 1, otherwise = 0
SAT	If accident occurs on Saturday = 1, otherwise = 0
SUN	If accident occurs on Sunday = 1, otherwise = 0
Time of the Day	
TIME1 (00:00 hrs to 03:59 hrs)	If accident occurs during this time = 1, otherwise = 0
TIME2 (04:00 hrs to 07:59 hrs)	If accident occurs during this time = 1, otherwise = 0
TIME3 (08:00 hrs to 11:59 hrs)	If accident occurs during this time = 1, otherwise = 0
TIME4 (12:00 hrs to 15:59 hrs)	If accident occurs during this time = 1, otherwise = 0
TIME5 (16:00 hrs to 19:59 hrs)	If accident occurs during this time = 1, otherwise = 0

TIME6 (20:00 hrs to 23:59 hrs)	If accident occurs during this time = 1, otherwise = 0
Accused vehicle	
LORRY	If accused vehicle is lorry = 1, otherwise = 0
BUS	If accused vehicle is bus = 1, otherwise = 0
AUTO	If accused vehicle is minilorry or pickup vans = 1, otherwise = 0
CAR	If accused vehicle is SUV or car = 1, otherwise = 0
MOTORCYCLE	If accused vehicle is motorcycle = 1, otherwise = 0
UNKNOWN	If accused vehicle is unknown = 1, otherwise = 0
OTHERS	If accused vehicle is other type (tanker, trailer, any other vehicle) = 1, otherwise = 0
Victim Vehicle	
PEDESTRN	If victim is pedestrian = 1, otherwise = 0
MOTORCYCLE	If victim vehicle is motorcycle = 1, otherwise = 0
LORRY	If victim vehicle is lorry = 1, otherwise = 0
SUVCAR	If victim vehicle is SUV or car = 1, otherwise = 0
Vitim Gender	
VICTIMGE	If gender of victim is male = 1, otherwise = 0
VICTIM AGE	
0-10	If victim age is 0-10=1, otherwise=0
11-20	If victim age is 11-20=1, otherwise=0
21-30	If victim age is 21-30=1, otherwise=0
31-40	If victim age is 31-40=1, otherwise=0
41-50	If victim age is 41-50=1, otherwise=0
51-60	If victim age is 51-60=1, otherwise=0
61-90	If victim age is 61-90=1, otherwise=0

DISCUSSION AND RECOMMENDATION

In this model the developed study on crashes occurring in night, are resulting higher level of crash severity. Particularly accidents occurring between midnight to early morning hours are more sensitive to higher level of crash severity. This may be due to poor illumination and absence of warning measures such as retro-reflective signs which helps in roadway hazard

identification. Hence to avoid such crashes proper illumination in night hours on highways along with retro-reflective materials is strongly recommended. For this purpose installation of solar lights may be very effective.

Seasonal variation

Seasonal variation was estimated using month of the year as dummy variable considering January as a reference month. Results show that accidents occurring in month of August ($\beta = 0.4004$, $t = 2.13$, $p < 0.05$) and October ($\beta = 0.3469$, $t = 21.817$, $p = 0.0692$) are resulting higher level of crash severity than month of January.

Victim Age

Effects of age on crash injury severity have been measured with reference of 0-10 age. 21-30 ($p < 0.05$, $t = 3.239$) and 31-40 ($p < 0.05$, $t = 2.239$) types of ages are resulting higher level of crash severity in comparison of crashes.

Type of collision

Effect of types of collision on injury severities were estimated with a reference of head-on collisions. Results associated with higher level of crash severity are conflicting with previous result of all single vehicle crash of trucks resulting in as lower crash injury severity.

Hourly variation

Time of day effects in model were measured with dummy variable at four hour interval with respect to midnight 00:00 hrs to morning 03:59 hrs same as of all crash model. Result is quite interesting. Coefficients of TIME2 ($p < 0.05$, $t = 2.178$) showing that with respect to reference time interval accident occurring in morning 04:00 hrs to 7:59 hrs are resulting higher severity.

Weekly variation

Effects of day of week have been estimated with reference to Monday. Result is consistent with result of all crash model. Statistical significance levels of variable coefficient are showing that there is no variation in injury severity level.

CONCLUSIONS

This study highlights factors that are responsible for higher level of crash severity on national highway-163. Ordered probit regression methodology has been used to develop statistical models that were able to recognize those factors. To get clear understanding of those factors affecting higher crash severity three distinct models- all crash model, truck involved

crash model and pedestrian involved crash model, have been developed. Finding of all this study may be concluded as follows:

- Accidents occurring during night time are more severe than accidents occurring in day light. In case of trucks, the early morning time crashes between 4 and 8 am resulted in higher severity than other time of the day.
- Accidents occurring at intersections are less severe than other roadway sections.
- Pedestrians, bicycle, motorcycle, and auto-rickshaws are always facing higher level of crash severity.
- Unknown vehicles and trucks are responsible for high crash severity on national highway.
- Both all crash model and lorry involved crash model show that hit and run and overturning crashes are more severe than head-on collision.

REFERENCES

- Kockelman, K. M., and Kweon, Y. J. (2002). "Driver injury severity: an application of ordered probit models." *Accident Analysis and Prevention*, 34, 313–321.
- Abdel, M. A. (2003). "Analysis of driver injury severity levels at multiple locations using ordered probit models." *Journal of Safety Research*, 34, 597–603.
- Qudus, M. A., Noland, R. B., and Chin H. C. (2002). "An analysis of motorcycle injury and vehicle damage severity using ordered probit models." *Journal of Safety Research*, 33, 445–462.
- Gray R. C., Qudus, M. A. and Evans, A. (2008). "Injury severity analysis of accidents involving young male drivers in Great Britain." *Journal of Safety Research*, 39, 483–495
- Duncan, C. S., Khattak, A. J. and Council, F. (1998).
- "Applying the ordered probit model to injury severity in truck-passenger car rear-end collisions." *Transportation Research Board, Transportation Research record 1635*, Paper no. 98-1237, 63-71.
- Khattak A. J., Pawlovich M. D., Souleyrette R.R., and Hallmark, S.L. (2002). Factors Related to More Severe Older Driver Traffic Crash Injuries. *Journal of Transportation Engineering*, 128(3).
- Zajac, S.S., and Ivan, J. N. (2003) "Factors influencing injury severity of motor vehicle crossing pedestrian crashes in rural Connecticut." *Accident Analysis and Prevention*, 35 369–379.

TRAFFIC CALMING IN HYDERABAD AND SECUNDERABAD CITY PERSPECTIVE

V Kranthi Naik¹, A.Naga Saibaba², Dr.M.Kameswara Rao³

¹Research Scholar (M.Tech, T.E), ²Assistant Professor, ³Professor

Malla Reddy Engineering College (Autonomous), Kompally

Abstract---

Traffic calming has become one of the most popular subjects in the Transportation Engineering field over the last ten years. In India it is in nascent stage and held a lot of potential for future. The aim of the study is to see the various traffic calming measures in other countries, its relevancy and application in Indian condition. Cities and towns play a vital role in promoting economic growth and prosperity. Although less than one-third of India's people live in cities and towns, these areas generate over two-third of the country's income and account for 90% of government revenues. In the coming years, as India becomes more and more urbanized, urban areas will play a critical role in sustaining high rates of economic growth. Although Indian cities have lower vehicle ownership rate, number of vehicles per capita, than their counterparts in developed countries, they suffer from worse congestion, delay, pollution, and accidents than cities in the industrialized world. Traffic calming is coined as the best technique to overcome traffic congestions and accidents. Traffic calming is the combination of mainly physical measures that reduce the negative effects of motor vehicle use, alter driver behaviour and improve conditions for non-motorized street users. The concept of traffic calming is fundamentally concerned with reducing the adverse impact of motor vehicles on built up areas. This usually involves reducing vehicle speeds, providing more space for pedestrians and cyclists, and improving the local environment. It includes change in street alignment, installation of barrier and other physical measures to reduce traffic speed and /or volume in the interest of safety and liveability. The main objective of this study is to reduce the high frequency of collision and the need for police enforcement. It aims at achieving slow speeds for motor vehicles and enhancement of safety for non motorized users. A junction in Hyderabad which is subjected to congestion and high frequency of collision is considered for study and requirements of traffic calming in the junction have been analysed.

Key words: Traffic Calming; congestion; slow speeds

1.INTRODUCTION

The rapid growth of India's urban population has put enormous strains on all transport systems. Its urban population is growing at an average rate of around 3% per year.. Assuming decadal increase of around 32%, India's

urban population is expected to increase from 377 million in 2011 to 500 million in 2021. In terms of percentage of total population, the urban population has gone up from 17% in 1951 to 31.8% in 2011 and is expected to increase up to around 35% by the year 2021. During the 2000s, 91 million people joined the ranks of urban dwellers – which implies that the growth rate in urban areas remains almost the same during the last twenty years; urban population increased by 31.5% from 1991 to 2001 and 31.8% from 2001 to 2011[1]. From 35 in 2001, the number of metropolitan cities rose to 50 according to the Census of India, 2011. Out of these 50, eight cities – Mumbai, Delhi, Kolkata, Chennai, Hyderabad, Bangalore, Ahmedabad, and Pune – have population more than 5 million. India's big cities now account for a larger share of total urban population – a trend that has been observed since independence. In 2011, the share of metropolitan cities was 42.3%, up from 37.8% in 2001 and 27.7% in 1991[6].

Hyderabad is well connected to many other locations in India, such as Bangalore, Mumbai, Delhi, Kolkata, Nagpur, Chennai, Pune, Vishakapatnam and Vijayawada, either through directly or through intermediary locations.

The highway (express way) network linking Hyderabad to various parts of the country is very good. Three National Highways (NH) pass through the city—NH-7, NH-9 and NH-202. Five state highways—SH-1, SH-2, SH-4, SH-5 and SH-6 begin from Hyderabad [7]. As a growing city, regular multiple development projects, around the city had made traffic congestion a common issue. In Hyderabad the roads occupy 10% of the total city area. Traffic calming is the name for road design strategies to reduce vehicle speeds and volumes[2]. Traffic calming encompasses a series of physical treatments that are meant to lower vehicle speeds and volumes by creating the visual impression that certain streets are not intended for high-speed or cut-through traffic [10]. Thus, traffic calming can improve safety for pedestrians and reduce noise and pollution levels. Examples of these measures include Bulbouts, speed humps, chicanes, and traffic circles. Traffic

Calming techniques have emerged primarily as a society's response to concern for safety. Traffic Calming in the Western Nations have been implemented in residential areas, neighbourhoods and cities because inter-city highways and freeways are relatively safer [10]. It is well accepted by the experts that differences and variations in the speed, direction, and/or mass of vehicles usually determine the severity of road accidents [10]. Traffic Calming Techniques have played an important role in achieving safety by ensuring low driving speeds and smaller speed differences between different road users [8]. Traffic calming is defined by Institute of Traffic Engineers as, "The combination of mainly physical measures that reduce the negative effects of motor vehicle use, alter driver behaviour and improve conditions for non-motorized street users." It involves physical alterations to a road or street which cause or invite motorists to decrease driving speed and increase his attention to driving task. It includes change in street alignment, installation of barrier and other physical measures to reduce traffic speed and /or volume in the interest of safety and liveability [3]. Traffic calming techniques can be classified based on speed control measures and volume control measures. Various speed control measures that are intended to reduce speed and improve the conditions for non-motorists are

- Speed humps
- Speed tables
- Raised crosswalks
- Raised intersection
- Traffic circles
- Roundabouts

Various volume control measures that are intended to reduce the cut-through traffic by obstructing traffic movements in one or more directions are (1) Full closures (2) Half closures (3) Diagonal closures (4) Median barriers [4]. The main advantage of traffic calming is speed and volume control can be obtained at an effective cost but measures when implemented leads to rough drive for huge vehicles and impact to drainage needs have to be considered. The definition of Traffic Calming varies but the aim of it is to reduce the speed and in some cases the volume of traffic, providing a safer environment for non-motorized road users. The definitions obtained are as follows:

a) ITE's (Institute of Transportation Engineers): "Traffic calming involves changes in street alignment, installation of barriers, and other physical measures to reduce traffic

speeds and/or cut-through volumes, in the interest of street safety, livability, and other public purposes."

b) NYSDOT Design Definition (New York State Department of Transportation): "The combination of mainly physical measures that reduce the negative effects of motor vehicle use, alter driver behavior, and improve conditions for non motorized street users"

c) Municipal Government of City of Vancouver, Canada: The practice of using physical techniques to influence traffic movements in neighborhoods. Objectives of traffic calming vary from improving safety through speed reduction measures such as traffic circles to discouraging traffic from entering an area through diversion measures such as "right-in, right-out" intersections.

To summarize we can say that traffic calming is a mean of designing roads using physical measures to encourage people to drive slowly and carefully and enhance the safety of walking and bicycling. The main advantage of traffic calming is that it is self enforcing and does not normally require any complication traffic control devices and is usually highly cost-effective; achieving benefits with a value far greater than the costs.

II. STUDY AREA

The study area for understanding traffic calming in Hyderabad city is Begumpet stretch. The reasons behind selecting this stretch for study are poor road condition and regular traffic congestion in Begumpet stretch. The study area is shown in fig 1.



Fig 1: Begumpet Stretch



Fig 2 :Bowenpally-Balanagar Stretch

Observed problems



Fig 3: Footpath at Bowenpally



Fig 3: Footpath occupied by local vendors

III. METHODOLOGY

The methodology followed to understand traffic calming in Hyderabad city is as shown in fig 2

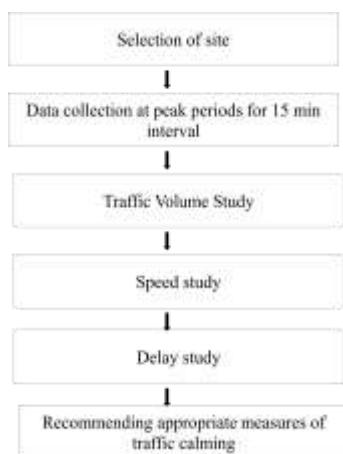


Fig 2: Methodology involved

A. Data Collection

Traffic flow study which includes study of movement of all types of vehicles through particular junction for a period of 15 min was made at regular interval of one hour from 8:00 am to 11:00 am in the morning and 4:00pm to 7:00pm in the evening. Signal timing was also noted down in these areas [10]

B. Traffic Volume Count

Traffic volume studies are conducted to collect data on the number of vehicles and/or pedestrians that pass a point on a highway facility during a specified time period. This time period varies from as little as 15 minutes to as much as a year depending on the anticipated use of the data [5]. Traffic volume studies are usually conducted when certain volume characteristics are needed, some of which follow[10]:

1. Average Annual Daily Traffic (AADT) is the average of 24-hour counts collected every day of the year.
2. Average Daily Traffic (ADT) is the average of 24-hour counts collected over a number of days greater than one but less than a year.
3. Peak Hour Volume (PHV) is the maximum number of vehicles that pass a point on a highway during a period of 60 consecutive minutes.
4. Vehicle Classification (VC) records volume with respect to the type of vehicles.

5. Vehicle Miles of Travel (VMT) is a measure of travel along a section of road. It is the product of the traffic volume (that is, average weekday volume or ADT) and the length of roadway in miles to which the volume is applicable.

C Speed Studies

Speed studies are conducted to estimate the distribution of speeds of vehicles in a stream of traffic at a particular location on a highway [5]. The speed of a vehicle is defined as the rate of movement of the vehicle; it is usually expressed in miles per hour (mi/h) or kilometres per hour (km/h). A spot speed study is carried out by recording the speeds of a sample of vehicles at a specified location. Speed characteristics identified by such a study will be valid only for the traffic and environmental conditions that exist at the time of the study [12].

D Delay Studies

A travel time study determines the amount of time required to travel from one point to another on a given route. In conducting such a study, information may also be collected on the locations, durations, and causes of delays [5]. When this is done, the study is known as a travel time and delay study. Data obtained from travel time and delay studies give a good indication of the level of service on the study section. These data also aid the traffic engineer in identifying problem locations, which may require special attention in order to improve the overall flow of traffic on the route [13].

IV. RESULTS

From table 1 and 2 it is evident that traffic flow at Paradise junction is more during 9:00am to 10:00am in the morning. Number of two wheelers crossing the junction is more in both the cases. On an average traffic flow during 9:00am to 10:00 am is 36% of total traffic flow. Nearly 50% of traffic flow occurs during 5.00pm to 6.00pm.

From table 5 it can be said that speed of two wheelers at Bowenpally-Balanagar and Begumpet stretch is 13 Km/hr and 10 Km/hr respectively. According to IRC speed on district roads is 18-20 Km/hr. Reduction in speed is due to poor road condition and increased traffic volume count. From table 5 it can be said that speed of three wheelers at Bowenpally-Balanagar and Begumpet stretch is 11 Km/hr and 9 Km/hr respectively. According to IRC speed of three wheelers on district roads is 12-15 Km/hr. Reduction in speed is due to and increased traffic volume count at Begumpet. From table 5 it can be said that speed of four wheelers at Bowenpally-Balanagar and Begumpet stretch is 9 Km/hr and 8 Km/hr respectively. According to IRC speed of four wheelers on district roads is 8-10 Km/hr. Speed of four wheelers is in IRC standards.

V. RECOMMENDATIONS

- Speed has been reduced at both the locations because of damaged overlays. Removal of the existing road and laying new road would improve the speed at the junctions.
- From the tables it can be observed that traffic volume count has drastically increased in the past 5 years. Best way to reduce traffic volume count is to provide traffic circles at places where vehicles move with low speed.
- Level separated intersection at Begumpet area would help in easy movement of traffic.

- Median barrier if provided at Bowenpally-Balanagar junction would reduce traffic congestion because of movement of different type of vehicles at a time.
- Fly over also would serve the purpose of reducing the traffic volume count and would help to provide faster travel for multi axle vehicles.
- Separate lanes for heavy vehicles and multi axle vehicles help to reduce traffic volume count and increase in speed.
- Speed humps have to be provided on the path from Begumpet to NTR circle to reduce abrupt speed of two wheelers.
- From the pictures shown above, it can be said that there is misuse of foot paths at various places of study. This problem can be solved by providing raised crosswalks. Raised crosswalks can give elegant appearance as well as reduce traffic congestion.
- Footpaths have to be raised so that vehicles won't pass on footpath and cause inconvenience to pedestrians.
- Another problem that can be observed from the pictures is poor maintenance of roads which leads to storage of water during rainy season. Proper camber has to be provided in roadways.

TABLE 1 Vehicular Statistics of Begumpet Stretch

Time Type of vehicle	Number of vehicles that cross the junction in an interval of one hour		
	8:00 to 9:00	9:00 to 10:00	10:00 to 11:00
2-wheelers	8012	12686	8925
3-wheelers	1237	1949	1300
4-wheelers	3074	4781	3242
Heavy vehicles	480	712	507

TABLE 2 Speed Study

Type of vehicle	Begumpet Stretch (Speed in Km/hr)
2-wheelers	10.28
3-wheelers	9.48
4-wheelers	8.89
Heavy vehicles	6.26

REFERENCES

- [1] Reid Ewing, PH.D., Steven J. Brown, P.E. and Aaron Hoyt, "Traffic Calming Practice Revisited", ITE Journal, November 2005.

[2]C. Edward Walter, “*Sub urban Residential Traffic Calming*”, ITE Journal, September 1995.

[3] Doug Brown, “Effective Application of Traffic Calming Techniques”, Preliminary Investigation Caltrans Division of Research and Innovation, September 2011.

[4] Joseph E.Womble, P.E. and W.Martin Bretherton Jr., P.E., “*Traffic Calming Design Standards for New Residential Streets: A Proactive Approach*”, ITE Journal, March 2003.

[5] Saad Yousif, Mohammed Alterawi and Ralph R. Henson, “*Effect of Road Narrowing on Junction Capacity Using Micro simulation*”, Journal of Transportation Engineering, Vol. 139, No. 6, June 1, 2013.

[6] Jeff Gulden, P.E. and Reid Ewing, PH.D., “*New Traffic Calming Device of Choice*”, ITE Journal, December 2009.

[7] Jing and Glen Koorey, “*Investigating And Modeling The Effects Of Traffic Calming Devices*”, IPENZ Transportation Group Conference Christchurch March, 2010

[8] John D.Leonard 11 and W.Jeffrey Davis, “*Urban Traffic Calming Treatments: Performance Measures and Design Conformance*”, ITE Journal, August 1997.

[9] Michael Skene, “*Traffic Calming on arterial roadways*”, ITE Journal, August 2000.

[10] P.Teja Abhilash, K.Jaya Sunder, K.Tharani, “Traffic Calming in Hyderabad City”, *International Journal on Engineering Research and Management*, Vol.2 (06), pp: 152-155

[11] Todd Litman, “*Traffic Calming Benefits, Costs and Equity Impacts*”, Victoria Transport Policy Institute, December 1999.

[12] Tolley, R., *Calming Traffic in Residential Areas*, Brefi Press, Brefi, England, 1990.

[13] Topp, H.H., “Traffic Safety, Usability, and Streetscape Effects of New Design Principles for Major Urban Roads,” *Transportation*, Vol. 16, 1990, pp. 297–310.

ROAD SAFETY AUDIT FOR SAGAR INTERSECTION TO UPPAL INTERSECTION

Y. Venu¹, V. Ranjith Kumar², Dr.M.Kameswara Rao³

¹Research Scholar (M.Tech, T.E), ²Assistant Professor, ³Professor
Malla Reddy Engineering College (Autonomous), Kompally

Abstract: --Road Accidents are increasing at a high rate all around the world day by day due to spectacular growth of the road transportation sector. Millions of people are injured and killed during years all over the world due to road accidents. The accidents in the Hyderabad and Cyberabad areas are increasing simultaneously. In order to reduce the accidents and their effects in a stretch a Post Construction Road Safety Audit is performed. This paper is an attempt to analyze the traffic safety situation of a stretch from Sagar Intersection to Uppal Intersection (Inner Ring roads) of Hyderabad and identifies the elements causing accidents in the stretch. The main purpose of this paper is to set out the safety assessment for road users in the stretch. This emphasis on the reduction of potential crashes and suggesting safety measures in the stretch.

This is an important tool for assessing accident potential of a specific design. Analysis of major accident in the recent decades has concluded that driver's errors are the major concern for the occurrence of road accident. This project represents Road Safety Audit of selected stretch from Uppal Ring road to Sagar Cross road, Hyderabad, Telangana. It will focus on evaluating the benefits of the proposed actions that have emanated from deficiencies identified through the audit process. The selected stretch of 7 km consists of various junctions and Intersection. The Audit report is prepared for the selected stretch showing various deficiencies and suggesting remedial measures.

Keywords --Deficiencies, Fatalities, Road Traffic accidents, Road safety, Road safety Audit.

1.INTRODUCTION

Rapid Rise in population along with increased and versatile land use patterns and increase in vehicle ownership have generated considerable traffic demand in the major cities in India. Road Traffic accidents have now become a great social concern in India and the situation is deteriorating. Millions of people are injured and killed during years all over the world due to road accidents. Huge amount of socio-economic cost incurred due to accidents. Accidents rates are increasing despite of many preventive measures applied to improve road conditions and traffic laws. Due to increase in vehicles and constant road width with changing environment scenario, the rates of accidents are increasing drastically. Road safety is the main concern to reduce accidents. For road user safety, the analysis of accident is primary requirement for road design.

Road safety Audit is a systematic, proactive and formal procedure for assessing accident potential and safety performance of new or existing roads. It is a formal examination of a future traffic project, or an existing road, in which an independent and qualified team looks at the project's crash potential and safety performance. RSAs can be viewed as a proactive low-cost approach to improve safety. Road Safety Audits form an important role in diagnosing the safety of the road network, both as far as existing roads and upgrading projects on the road and transport network are concerned.

Road accidents have been increasing in the world due to the rapid growth of population, motor vehicles and usage of the transportation sector. These road accidents results in the loss of lives and socioeconomic cost. In order to reduce this effects road safety has to be implemented. Road safety Audit is a best and emerging tool for improvement of road safety and the assessing accident potential in developed and developing countries.

Road safety Audit is a systematic, proactive approach for assessing accident potential and safety performance of new or existing roads. It is a formal examination of a future traffic project, or an existing road, in which an independent and qualified team looks at the project's crash potential and safety performance.

Post Construction Safety Audits are performed on existing facilities to ensure that the safety needs of road users are being served. Post construction stage audits may be performed on a road section newly opened to traffic to evaluate its performance or it can be used to identify safety deficiencies on existing roads. Intersections, roadway segments and road side features are some elements that may be examined in an audit of an existing roadway.

Safety audit stages and study points

As per IRC: SP: 88-2010 the safety audits are conducted in various stages in India. They are:

- Feasibility stage
- Preliminary stage
- Detailed stage
- Pre-opening stage

- Post construction stage.

II ROAD SAFETY CONCERN IN INDIA

Road accidents in India are high due to heterogeneous traffic conditions. The Enormous growth in population, motor vehicles and the movement of all types of vehicles on the same road in India cause congestion, delays, inadequate parking and safety issues which results in accidents. Thousands of lives are lost and millions of people are injured in India in road accidents in the past years. In order to reduce these road accidents Road Safety Audits (RSA) have been implemented by National Highway Authority of India (NHAI) on existing and on proposed new highway projects.

This paper is aimed to evaluate road safety concern for an existing road in Hyderabad, Telangana. For evaluating road safety in the stretch a Post construction safety audit is performed.

III. NEED FOR THE STUDY

The main objective of the study is

- 1.To curtail unsustainable losses to health and economy.
- 2.To identify the causes of Accidents and to ensure safety for road users.
- 3.To check consistency of the road features.
- 4.To identify problems in the routine maintenance procedures.

Objectives of a Road Safety Audit:

The objectives of the road safety auditing process are:

- To minimize the severity and crash risk of road traffic crashes that may be influenced by the road facility or adjacent environment;
- To create and maintain an awareness of safe design practice during all stages of a road project
- To identify and report on the crash potential and safety problems of a road project;
- To ensure that road elements with an increased risk potential are removed or that measures are identified to reduce the risk.
- To avoid the possibility of the scheme giving rise to accidents elsewhere in the road network; and
- To enable all kinds of users of the new or modified road to perceive clearly how to use it safely.

IV. STUDY AREA

The Stretch selected for the study is the points on two major National highways in Hyderabad. The two distinct points in the study area are Sagar Intersection (an

intersection on NH-19) and Uppal Intersection (an intersection on NH-163) in Hyderabad, Telangana, India.

These two points are connected by an Inner ring road service and intersecting other National highway NH-9 at LB Nagar. The length of stretch is 7 Kms.

The study area consists of signalized At-grade intersections, various T & Y Junctions and a rotary.

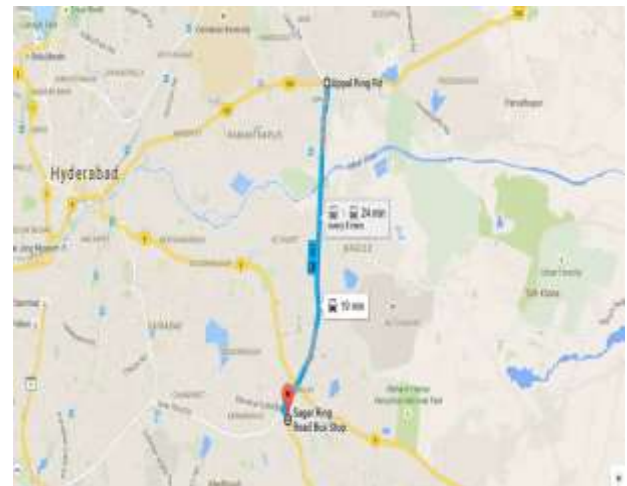


Figure 4.1: Selected stretch for Audit

V. Scope of study

The scope of this thesis is to carry out a road safety audit in a selected stretch to evaluate different road safety auditing techniques on the road selected. Throughout the implementation and reporting at this study, the present safety situation of Inner ring road (IRR) service road, Hyderabad will be evaluated.

- To identify and report on the crash potential and safety problems of a road project;
- To ensure that road elements with an increased risk potential are removed or that measures are identified to reduce the risk.
- To minimize the severity and crash risk of road traffic crashes that may be influenced by the road facility or adjacent environment;
- To complement a program of accident black spot treatment
- To specifically address safety, rather than relying completely on routine maintenance
- To identify problems in routine maintenance procedures

The main motto of Post-construction safety Audit is

- To check a road or a network for consistency, to make sure that a road user does not encounter unexpected road safety issues.

VI. SAFETY AUDIT FOR THE STRETCH

This post construction safety audit mainly concentrated on safety issues like road profile, road markings, road signage, width of shoulder and lightings throughout the stretch for the safety of road users as per IRC:SP:88:2010.

VII. DATA COLLECTION AND INVENTORIES

Following data of the corridor were collected:

- A. Road Inventory and Surrounding Land use type.
- B. Accident data from police stations

A. Road Inventory and Surrounding Land use type

Road inventory surveys are carried out to identify road profile like road width, No. of lanes, shoulder width, road alignment. People living nearby study area corridor use their personal vehicles for making trips. The land use pattern surrounding the study area is Residential, Commercial, Industrial and Institutional type. The land use pattern data is obtained from Municipal office.

B. Accident data from police Stations

Road accident data is collected from two police stations in the stretch i.e. from LB Nagar and Uppal police station under various sections of IPC 338,337,304a.

VIII. ANALYSIS AND INTERPRETATION OF ACCIDENT DATA

A total of 987 accident cases were registered in the police stations from the year 2009 – September 2014 in the stretch. The accident data is analyzed in the following groups.

Classification of accidents according to

- A. Year
- B. Month
- C. Time
- D. Nature of Accident
- E. Cause of Accident.
- F. Accident spots in the stretch

A. Yearly Variation of Accidents (2009-2014)

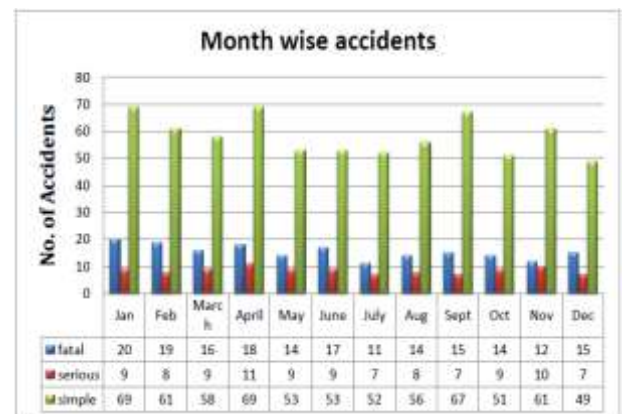
Table II: Yearly Distribution of Accident Data



The data from Table II represents the accidents in the stretch from the year 2009-2014 September. There is an increase in the rate of accidents for the year 2009 to 2011 and decreased from the year 2011-2014 September. The decrease in the rate of accidents from a couple of years in the stretch is mainly due to the installation of traffic signals and road signs.

B. Monthly variation of Accidents

Table III: Monthly Classification of Accidents



The data from table III represents the accidents are more in the month of January and April due to temperature effects.

C. Accidents classified according to Time

Table IV: Accidents as Per Time

Time	Fatal	Serious	Simple
0:00-1:00	13	2	22
1:00-2:00	4	1	17
2:00-3:00	8	2	11
3:00-4:00	3	2	8
4:00-5:00	1	1	8
5:00-6:00	2	2	15
6:00-7:00	8	2	17
7:00-8:00	7	3	24
8:00-9:00	5	7	28
9:00-10:00	5	3	35
10:00-11:00	8	3	35
11:00-12:00	8	3	32
12:00-13:00	9	5	34
13:00-14:00	5	8	28
14:00-15:00	11	6	33

15:00-16:00	5	3	31
16:00-17:00	11	3	27
17:00-18:00	9	5	36
18:00-19:00	5	7	50
19:00-20:00	8	8	45
20:00-21:00	15	6	45
21:00-22:00	10	8	44
22:00-23:00	13	7	38
23:00-24:00	12	6	36

The data from table IV represents the rate of fatal accidents. These are high during night time due to poor lighting system and visibility. The fatal accidents are more from 20:00 - 1:00.

D. Nature of Accidents

Table V: Nature of Accidents

Collision type	Fatal	Serious	Simple
Head on	12	6	10
Rear End	36	26	174
Hit pedestrians	29	7	41
Hit fixed objects	24	9	118
Hit pedal cyclist	10	8	32
Right angle collision	9	5	25
Side swipe	40	24	223
Others	25	18	74

The data from table V represents the Rear end collision and side swipe collisions are more common in Hyderabad due to heterogeneous and mixed traffic conditions. 57% of simple accidents are due to rear end and sideswipe collisions.

E. Cause of Accidents

Table VI: Cause of Accidents

Cause of Accident	No. of accidents	% of Accidents
Negligence and rash driving	642	65
Mechanical failure of Vehicles	25	2.53
Pedestrians	30	3.0
Drunk & drive	178	18.0
Animal on roads	10	1.0
Others	102	10.33

The accidents caused in the stretch are mainly due to human errors. 65% of accidents are caused due to human negligence.

F. Accident spots in the stretch

Table VII: Accidents Spots in the Stretch

Place	Fatal	Serious	Simple
-------	-------	---------	--------

Near Sagar X Road	23	13	95
Near LB Nagar rotary	49	25	210
Near Kamineni Intersection	15	12	61
At Rajeev Gandhi Nagar	13	3	58
Near Alkapuri Junction	21	20	81
At Snehapuri Junction	9	8	24
Nagole Intersection	22	11	82
Nagole Bridge	7	3	34
Near Uppal	17	6	63

There are several accident spots in the stretch. Traffic Police have identified some of the accident prone points and installed sign boards for the safety of road users.

XI. OBSERVATIONS

Various deficiencies and elements causing the accidents were observed during the survey.

- 1) Misleading sign boards in the stretch are more, which results in chance of accident.
- 2) Pedestrian crossings are missing at the junctions and school areas.
- 3) Traffic signal system with time display has more chances of causing accidents in the stretch.
- 4) Proper signs and markings are missing in the stretch.
- 5) Improper design of bus bays and absence of bus bay markings.
- 6) Kilometer and hectometer stones were missing in the stretch.
- 7) Water accumulates on roads during rainy seasons causing congestions and resulting in accidents.
- 8) Inadequate Curb height at medians and pavement edges were observed.
- 9) Damaged flexes were hanged to hoarding boards were observed.

X. CONCLUSIONS

Following conclusions were drawn from present study and accident data.

- 1) The accidents in the stretch are more during day time than nights.
- 2) Rear end type and side swipe collisions are more when compared with others.
- 3) Overall accidents in the stretch are more during daytime than in nights.
- 4) Accidents caused due to human negligence are more in the stretch.
- 5) The accidents are more from 18:00- 00:00 in the stretch.
- 6) The accident rate has increased from 2009-2011 and decreased from 2012 -2014 due to the

application of traffic signaling system in major junctions in the stretch.

XI. RECOMMENDATIONS

Road Safety Audits are being considered as more and more important and widely used tools/applications to increase the road and the road environment safety. These surveys should be done for short intervals to observe changes in the road structure and equipment as well as the road environment.

The following countermeasures are to be implemented in the stretch to reduce the accident level and to increase the safety concern.

- 1) Curb height has to be increased at medians and at pavement edges.
- 2) Worn signs should be renewed or removed.
- 3) Warning signs should be installed at required sections of the route.
- 4) Markings & signs should be installed wherever it is necessary.
- 5) Detectable Warning Tiles are to be installed at sidewalks at pedestrian crossings.
- 6) Bus lay-bys are to be provided.
- 7) Reflectors or raised pavement markers (Road Studs) are to be installed on pedestrian crossings.
- 8) Movements of vehicles at unauthorized medians are to be regulated.
- 9) Damaged Hoardings are to be removed.

REFERENCES

- [1] IRC: SP 88-2010, "Manual for the road Safety Audit", Indian Road Congress, New Delhi.
- [2] Road safety Audits and Inspections by statens vegvesen (Manual V720E).
- [3] MIROS Road Safety Audit Report MRSA 01/2012.
- [4] International Journal of Science and Modern Engineering (IJISME) ISSN: 2319-6386, Volume-1, Issue-6, May 2013.
- [5] Road safety Audit Guidelines by Massachusetts Department of Transportation, Highway Division.
- [6] Road Traffic Management Corporation South Africa "Road Safety Audit Manual" 2012.
- [7] Hiderbrand, E. And Wilson, F., "Road Safety Audit Guidelines", UNB Transportation Group, 1999.
- [8] Eugene M. Wilson "Application of Road Safety Audit To Urban Streets".
- [9] Devang G Patel, F.S. Umrigar, C.B. Mishra, Amit A Vankar "Road Safety Audit of Selected Stretch from Umreth Junction to Vasad Junction" IJISME ISSN: 2319-6386, Volume-1, Issue-6, May 2013.

INTELLIGENT TRANSPORTATION SYSTEM IN HYDERABAD AND SECUNDERABAD ALONG NH-44, NH-65

T. Manasa Reddy¹, A.Naga Saibaba², Dr.M.Kameswara Rao³
¹Research Scholar (M.Tech, T.E), ²Assistant Professor, ³Professor
Malla Reddy Engineering College (Autonomous), Kompally

Abstract---

The road traffic is a regular problem of the any developed cities. India is the fast growing country and the Indian cities are having a lot of traffic congestion. To improve the traffic management the road infrastructure improvement is required. One kind of the infrastructure of the road contains the Intelligent Transport Systems (ITS). Intelligent Transport Systems (ITS), used for efficient traffic management in developed countries, that cannot be proper using in India. ITS techniques have to undergo adaptation and innovation to suit the different traffic characteristics of Indian roads. Intelligent transport systems in Hyderabad can be studied about the two main road lines in the city. The project involves the all the (ITS) technologies in the city. The two main road lines are the National Highway-65 and National Highway-44. In this position paper, I present a comprehensive study of all available ITS systems, including both research prototypes and deployed systems. We next pose a set of interesting open research problems in the context of Hyderabad ITS. Though our paper focuses on the Hyderabad traffic scenario because of our hands-on experience of working with it, many of the problems and solutions outlined in this paper are relevant for other developing countries as well

Key words: Intelligent Transport Systems, GPS, GSM, VMS, ITS.

1.INTRODUCTION

Intelligent transport systems ITS is the application of modern information and communication technologies in roads and vehicles to promote safer travel, reduce the congestion, and maximize the capacity of existing infrastructure. Intelligent transport systems vary in technologies applied, from basic management systems such as traffic signal control systems, container management systems, speed cameras to monitor applications like

security CCTV systems, car navigation, automatic number plate recognition, variable message signs, speed cameras to monitor applications, and to more advanced applications that integrate live data and feedback from a number of other sources, such as parking guidance and information systems, weather information systems. India, the second most populous country in the world, and a fast growing economy, is seeing terrible road congestion problems in its cities. Building infrastructure, levying proper taxes to curb private vehicle growth and improving public transport facilities are long-term solutions to this problem. These permanent solution approaches need government intervention. The Government of India has committed Rs.234,000 crores in the urban infrastructure sector [5]. Bus Rapid Transit (BRT), metro rails and mono rails are being built in different cities to encourage the use of public transport. But still there is a steep growth of private vehicles [6]. Some cities like Bengaluru, Pune, Hyderabad and Delhi-NCR, with their sudden growths in the IT sector, also have a steep growth in population, further increasing transportation needs. Meeting such growth with infrastructure growth is seemingly infeasible, primarily because of space and cost constraints. Intelligent management of traffic flows and making commuters more informed about traffic and road status, can reduce the negative impact of congestion, though cannot solve it altogether. This is the idea behind Intelligent Transport Systems (ITS). ITS in India, however, cannot be a mere replication of deployed and tested ITS in the developed countries. The non-lane based disorderly traffic with high heterogeneity of vehicles, need the existing techniques to be adapted to the Indian scenario, before they can be used. Thus ITS in the Indian context needs significant R&D efforts. ITS is an interdisciplinary research area. Building road sensors need embedded systems background. Using mobile phones for sensing need mobile computing background. Analyzing sensed data needs signal processing or computer vision background. Communication among sensors and traffic control authorities need wired or

wireless networking background. The traffic classification and prediction algorithms need machine learning or statistics background. Applications like traffic signal management need transportation engineering background. So the ITS literature is very widespread with papers appearing in seemingly unrelated venues. In this paper, we make a comprehensive list of ITS literature, to give an overview of all existing techniques. We follow it up with a set of open research questions in the context of Indian roads and traffic. Finally, we list a set of public and private sector organizations and academic institutions, who are active in research or application in this field, as meaningful collaborations and technology transfer should happen if research has to make any practical impact.

II. NEED FOR THE STUDY

In any development country economy will mostly based on transportation. The new technologies are used to decrease the congestion of traffic, travel time, air pollution, to improve the emergency management, toll pricing, and to detect the vehicles. The ITS is essential part in transportation of the developing city. Demand for transport is increasing day by day due to industrialization and urbanization during recent years. But the road infrastructure has not been developed along with the travel demand due to lack of resources. This imbalance is creating problem. To improve the modern technologies is necessary in transportation net works to improve the city as a free of traffic congestion, travel time, parking management etc.

III. STUDY AREA

The Hyderabad is a huge developed city. One such an metropolitan city is Hyderabad. It is a 5th largest city in India, and it is the capital of both Telangana and Andhra Pradesh states. In Hyderabad the population is more than 12 lacks Million & agglomerated area is 727 sq.kms on the Deccan plateau. In Hyderabad city having an high traffic congestion, incident managements, to erect these problems the ITS implementation is necessary. The Hyderabad metropolitan development authority (HMDA) is decided to implement the ITS technologies in the city. The implementation of ITS will ensure the city with proper facilities and information systems.

Objectives of the study

The major objectives of this study are

- To relieve the traffic congestion in Hyderabad.
- To improve traffic safety.
- To reduce air pollution.
- To increase the energy efficiency.

- To promote the development of related industries.
- To suggest the ITS technologies to the HMDA.

Literature review

Intelligent transportation systems by Roger R. Stough and Guang Yang, school of public policy, George Mason University, USA. In this paper is examines the concept of intelligent transportation systems ITS as a method of improving the productivity of existing transportation systems.

The goals of this paper are to explain what ITS is and how it is or is not contributing to improved transportation facilities. The ITS is the application of computer and information technology to transportation systems in the hope of making them more efficient and productive.

In these paper indicates and examines in some detail a broad range of ITS technologies and the benefits. This benefit includes improved mobility, travel time, throughput, cost savings, improved safety, air quality and economic development. In this part of the paper the benefits of ITS is accessed. The assessment is organized around four category synthesis of the list of user services are Advanced Traveler Information Systems (ATIS), Advanced Traffic Management Systems (ATMS), Advanced Public Transportation Systems (APTS), and Advanced Commercial Vehicle Operations (CVO). In ATIS collect and synthesize traffic information from a number of sources like video surveillance and disseminate it to travelers via radio telephone/ mobile phones, television, and the internet. ATMS is the mobility by improving the flow of traffic during non incident conditions, Improved communications and better sensor supported traffic information enable traffic managers to adjust traffic control devices like dynamic signal timings, variable message signs which in turns the improves flow conditions in both congested and uncongested conditions. APTS is like other transportation modes can improve travel time by more efficient vehicle operation and by improving transportation networks by using automatic vehicle location (AVL) systems based on GPS. CVO is reducing the time of involved in transporting cargo in an important competitiveness. The ITS and CVO services can be expected to reduce the commercial vehicle travel time.

How rapidly should developing countries implement intelligent transportation systems (ITS) to solve the growing urban traffic congestion problem, by Mandar Khanal, Boise State University. This paper examines how to implement the intelligent transportation systems to develop the countries like India to reduce the traffic congestion problem in urban cities.

Many newly developing countries are growing rapidly. One example is India, currently the second most populous country in the world. According to the Indian Ministry of Urban Development, from 1981 to 2001, the population in six major Indian cities increased twofold while motor vehicles increased eightfold. Such rapid growth in vehicles without a comparable growth in transportation infrastructure leads to increasing traffic congestion. Cities in India are already considered congested today, and are going to be even more congested in the coming years since the rate of urbanization in India in 2006 was only 29% and is expected to grow to 41% by 2030. The corresponding rates for the world and Asia as a whole are projected to be 61% and 55%, respectively.

SURVEY AND DATA COLLECTION

Initially Primary and secondary survey was conducted for identification of areas facing transportation problem and partitions of each area. Based on the survey finally I have taken two stretches in two different area namely crowded and wider areas. For those two survey stretches I have done two different types of surveys and results also showed.

IV. RESULTS

The results and observations are shown for along the NH-65 and NH-44 throughout the Hyderabad areas with seven variations of categories for both the areas.

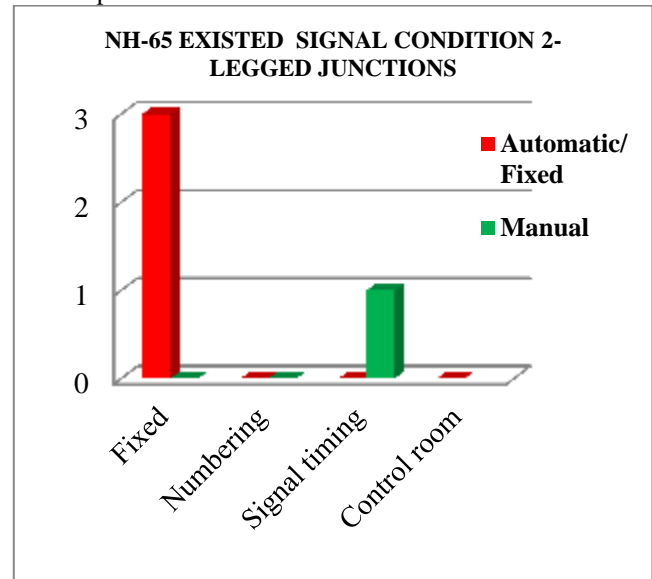
In Hyderabad ITS developed now a days. The ITS is installed mostly the congestion places to control the traffic. The data will be collected along the stretch of NH-65, NH-44 throughout the Hyderabad.

The following ITS observations are made in Hyderabad:

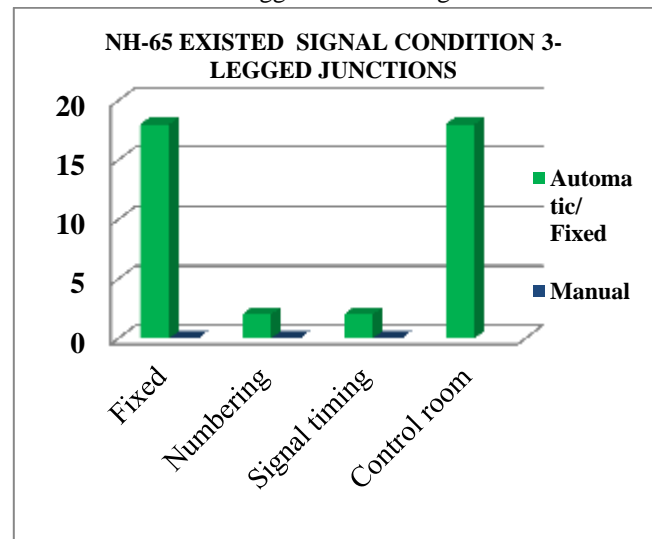
Advanced Traffic Management Systems (ATMS) are

- Traffic signals,
- Variable message signs.

- Vehicle detectors.
- Speed detectors



Stretch of NH-65 2-Legged Junction Signal Condition



Observations:

The signals are the two types operating are there in the city traffic. The signals are actuated and fixed type signals are using in Telangana. I have observed Type of Signals-SOLAR & AUTOMATIC, Some places Virtual loop cameras used for presence or absence of vehicles, these cameras changes the signals time depends on vehicles volume, time. In some signals having a control room. The signals are actuated and fixed type signals are using in Telangana. Signal timing also some of the signal having a fixed time signals are used.

Automatic vehicle location based on GPS:

Public transportation ITS technologies are using Automatic vehicle location based on GPS and GSM in Hyderabad. The system consists of four modules: BUS Station Module, In-BUS Module, BASE Station Module and BUS Stop Module. Equipped with PC and GSM modem, BUS Station Module sends the initialization information containing the bus number and license plate number to In-BUS Module and BASE Station Module using SMS. The microcontroller based In-BUS Module consisting mainly of a GPS receiver and GSM modem then starts transmitting its location and number of passengers to BASE Station Module. BASE Station Module equipped with a microcontroller unit and GSM modems interfaced to PCs is designed to keep track record of every bus, processes user request about a particular bus location out of BUS Station and updates buses location on bus stops. BUS Stop Module is installed at every bus stop and consists of a GSM modem, memory unit and dot matrix display all interfaced to a microcontroller. This module receives buses location information coming towards that stop from BASE Station module and displays the information on a dot matrix display. The results have shown that the developed system is useful for facilitating people using public transportation services.

V. RECOMMENDATIONS

The recommendations are given to the not only the stretch it applies along the city of the Hyderabad. The recommendations are given based on types of ITS technologies.

Signals

Total 122 junctions are there in NH-44, NH-65&Major junctions in Hyderabad

- 37 junctions are having fixed signals, 14 junctions are having solar signal. We have to implement the 37 fixed signal junctions are replacing with solar signals. Solar signals mainly implemented in 2 legged & 3 legged junctions.
Ex: Dhullapally X-road, Kompally, Jeedimetla.
- 11 junctions are having manual signals, 36 junctions are having Automatic signals. We have to implement the 11 manual signal junctions are replacing with Automatic signals, by operating the Control room.

Automatic signals mainly implemented in 3-legged & 4-legged junctions.

- Density control room using IR sensors and microcontroller & Sydney coordinated adaptive traffic system. We have to implement the major 4-way & 5-way junctions
Ex: Khairathabad, LB Nagar, Dilsuknagar etc...
- We can reduce the traffic congestion, accidents, delay of time& money.

CONCLUSIONS

Following conclusions are drawn from this study: Signals: total 122 junctions are there in the stretch of NH-44, NH-65.in this 2-legged, 3-legged, 4-legged junctions are there in NH-44, in NH-65 2-legged, 3-legged, 4-legged and 5-legged junctions are present.

- In the Stretch of national high way-65 along the city .the signals solar automatic signals are used in the junctions.
- The signals are the two types operating are there in the city traffic. The signals are actuated and fixed type signals are using in Hyderabad.
- Some places Virtual loop cameras used for presence or absence of vehicles, these cameras changes the signals time depends on vehicles volume, time. In some signals having a control room. The signals are actuated and fixed type signals are using in Hyderabad. Signal timing also some of the signal having a fixed time signals are used.
- Stretches of national highway-44 the signals are mostly manual type of signals are used.
- Signal timing also some of the signal having a fixed time signals are used.
- The signals are actuated and fixed type signals are using in Hyderabad. Signal timing also some of the signal having a fixed time signals are used.
- The variable message sign at tank band is not working in the city.
- The variable message sign is not using properly throughout the city.
- The CCTV cams are will detect the vehicles in the NH-44 the CCTV cams are installed high traffic junctions only

REFERENCES

- Roger r. Stough and Guang Yang, “intelligent transportation systems”, school of public policy, George mason university, USA
- Dinesh Mohan, “Intelligent Transportation Systems (ITS) And The Transportation System” Transportation research and injury prevention programme, Indian Institute of Technology Delhi, India.
- Rijurekha Sen and Bhaskaran Raman “Intelligent Transport Systems For Indian Cities” Department of Computer Science and Engineering, Indian Institute of Technology, Bombay.
- Praveen Kumar, Varun Singh, Student Member, IEEE, and Dhanunjaya Reddy, “Advanced Traveler Information System For Hyderabad City”, Department of Civil Engineering, Indian Institute of Technology, Roorkee, India .
- Hyderabad Traffic Integrated Management System(HTRIMS),HYDERABAD
- “Hyderabad Wikipedia”
- “The Hindu news paper”
- “Times of India News Paper”
- “Traffic Engineering and Transport Planning” by Dr.L.R.Kadiyali, Khanna publishers (2012).
- “Fundamentals of Intelligent Transportation systems planning”. M A Chowdhary and A Sadek Artech House Inc., US, 2003.

INFLUENCE OF COMBINED FLAKINESS & ELONGATION INDICES ON BITUMINOUS MIXES

K Kirankanth Reddy¹, A.Naga Saibaba², Dr.M.Kameswara Rao³

¹Research Scholar (M.Tech, T.E), ²Assistant Professor, ³Professor

Malla Reddy Engineering College (Autonomous), Kompally

Abstract-- Flakiness & Elongation index is one of the most prominent criteria that govern behavior and performance of aggregate in the bituminous mixes. The strength and serviceability requirements of bituminous mixture such as Stability, Flow, Voids in Total mix (VTM), Voids Filled with Bitumen and (VFB) highly depend on the physical properties of aggregates. This study conducted by observing the effect of flakiness & elongated index by adding different percentages from 0% to 50% of flaky & elongated aggregates of different sieve with required quantity to the bituminous mixes. The method of Marshall Mix design is adopted for this purpose. The change in rotation angle of coarse aggregate was found to correlate well with the internal resistance of a HMA mix. The particle shape determines how aggregate was packed into a dense configuration and also determines the internal resistance of a mix. Cubical particles were desirable for increased aggregate internal friction and improved rutting resistance. Also the Particle index (PI) value correlated well to aggregate geometric characteristics. The more cubical the aggregate, the higher the PI value is obtained.

Keywords: Asphalt Concrete, Elongation index, Flakiness index (F.I), Flow, Stability flow, Volumetric Characteristics (VFB, VTM)

I. INTRODUCTION

Road transport provides greater utility in transport over short and long hauls of lighter weight commodities and of lesser volumes as also for passenger transport for short and medium hauls. Road transport has shown immense potential in highly advanced countries, especially for passenger transport due to flexibility in operation and door to door service. Development in road network is regarded as a social, commercial and economic progress of a country. No region or country can flourish, if it lacks adequate transport facilities and mainly in road network. Road as one of land transportation infrastructure is very important in supporting the economic for both regional and national

development. The quality of material for road construction will also influence the road performance. Bituminous concrete as one of road surface material is mainly influenced by the quality of aggregates. Aggregates are the principal material in pavement, since aggregate occupies 95% by weight in total mixture. Various shapes of aggregates might be occurred during crushing in the crushing plant starting from rounded to flaky and elongated aggregates. Some tests on aggregates have to be done prior its use in asphalt mixture such as gradation, toughness, durability, shape, surface texture, specific gravity, micro texture, etc. The engineering properties of aggregates, including aggregate shape are therefore very important in having satisfied performance of asphalt concrete mixture including the workability index and stiffness modulus. One of the aggregate properties is called as 'flaky' measured as a Flakiness Index (FI) and 'elongated' measured as a Elongation Index (EI) and it is suspected to influence the performance of B.C mixture. Flakiness index of an aggregate can be defined as a percentage by weight of particles whose least Dimension (Thickness) is less than 0.6 of their mean dimension. Elongation index of an aggregate can be defined as a percentage by weight of particles whose greatest dimension (Length) is greater than one and four fifth times or 1.8 times of their mean dimension. Physical shape of coarse aggregate is a very important property in performance of the bituminous mixes in the highway pavements. Existence of flaky & elongated materials in the bituminous mixes is an undesirable and a dangerous phenomenon because of their tendency to break under wheel load either during compaction in construction stage or in service life of the pavement. The flaky & elongated aggregates will also cause problem in achieving the required degree of compaction.

II. OBJECTIVE OF STUDY

To study the effect of different proportions of flaky & elongated particles (0 %, 10%, 20%, 30%, 40%, and 50%) taking 5.2% as constant bitumen content of CRMB.

- To study the basic properties of CRMB.

- To study the properties of stability, flow by varying the percentages of elongated aggregates using Marshall stability test
- To study the bulk density and volumetric properties (VTM, VFB, VMA) Of Marshall Specimen's.

III. EXPERIMENTAL INVESTIGATIONS

Basically the materials that are used in this study include aggregate components such as stone dust and flaky & elongated aggregates. Second important item is Base bitumen. The most important tests which are carried out along this thesis are sieve analysis, flakiness & elongation index test and Mix design by using Marshall Mix design method.

Aggregate

Impact Test
Los Angeles abrasion Test
Aggregate crushing value Test
Stripping Test of aggregate
Flakiness & Elongation index Test of aggregate
Specific gravity of aggregate

Bitumen

Penetration Test
Softening point Test
Ductility Test
Viscosity Test
Specific gravity of bitumen

Mix Design

Specimen preparation
Properties of the Mix
Theoretical specific gravity of the mix G_t
Bulk specific gravity of mix G_{mb}
Air voids percent V_v or VTM
Percent volume of bitumen V_b
Voids in mineral aggregate VMA
Voids filled with bitumen VFB
Marshall Testing

IV. DISCUSSION OF RESULTS

A. Aggregate test

A number of tests have been discussed for both aggregate and bitumen, in order to insure that their physical property is suitable according to the given criteria. The test results of aggregate and bitumen are given in Annexure1 and Annexure 2.

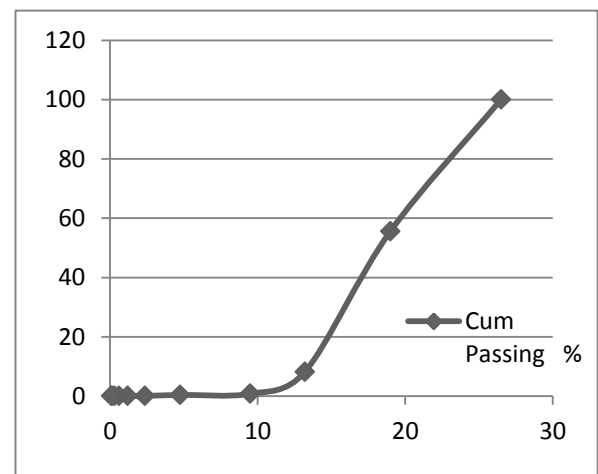
The individual results of sieve analysis are shown with their respective graphs. Sieve analysis result of coarse aggregate as shown in table I and graph II.

20 mm size aggregate weight = 5.457k

Table I sieve analysis of coarse Aggregates

Is sieve (mm)	Cum Passing %
26.5	100
19	55.58
13.2	8.145
9.5	0.807
4.75	0.44
2.36	0.102
1.18	0.1
0.6	0.1
0.3	0.1
0.15	0.1
0.075	0.1

Graph I



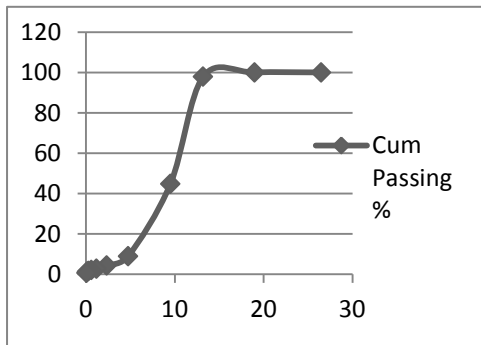
Sieve analysis result of fine aggregate as shown in table II and graph II.

12mm size aggregate weight = 4.447kg

Table II sieve analysis of fine Aggregates

Is sieve (mm)	Cum Passing %
26.5	100
19	100
13.2	98
9.5	44.774
4.75	9
2.36	4.346
1.18	2.8
0.6	2.2
0.3	1.7
0.15	1.3
0.075	0.8

Graph II



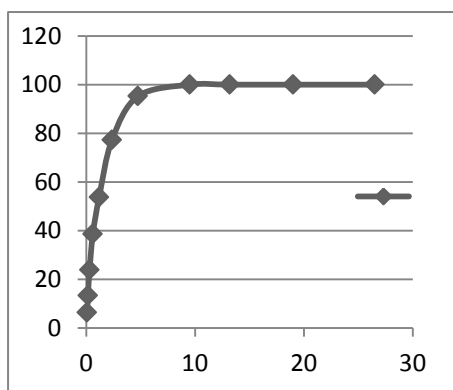
Sieve analysis result of stone dust as shown in table III and graph III.

Stone dust weight = 2.504kg

Table III represents sieve analysis of fine Aggregates

Is sieve (mm)	Cum Passing %
26.5	100
19	100
13.2	100
9.5	100
4.75	95.248
2.36	77.277
1.18	53.755
0.6	38.58
0.3	23.924
0.15	100
0.075	100

Graph III



The combined Sieve analysis results of coarse aggregate, fine aggregate and dust are shown in Annexure 3.

B. Bitumen Tests

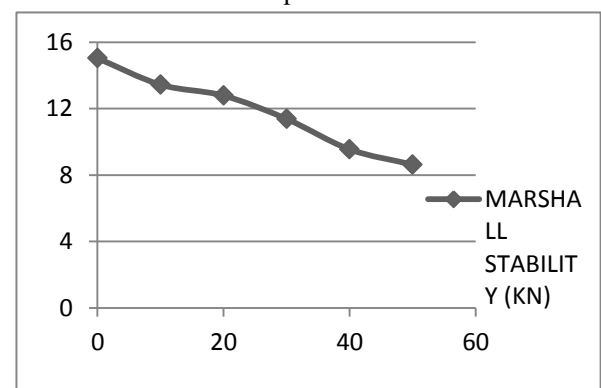
1. Stability

It's the property of strength and performance of the bituminous mixes against wheel loads and traffic intensity.

Table IV stability test results

Flaky & Elongated %	MARSHALL STABILITY (KN)
0	15.03
10	13.44
20	12.78
30	11.38
40	9.55
50	8.63

Graph IV



It was observed that it has been observed that with increasing flakiness & elongation index, stability decreased by 42.58%. The maximum stability is 15.03 KN and sharply decreased to 8.63 KN at 50% flakiness & elongation index.

2. Flow

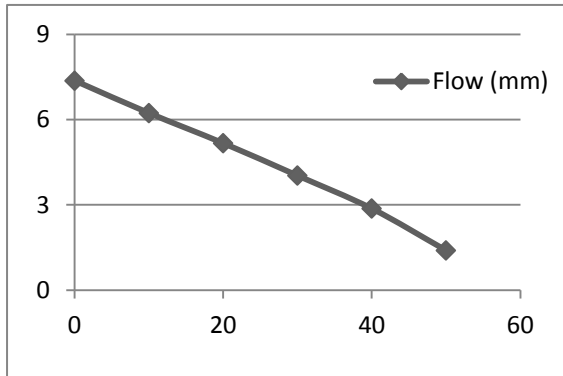
Flow is the deformation of the bituminous mixes under a certain applied load. In this study we observe that the value of flow decreases with increasing elongation index.

Table V represents flow results

Flaky & Elongated %	Flow (mm)
0	7.37
10	6.23
20	5.17
30	4.03
40	2.87
50	1.40

It was observed that the value of flow decreases with increasing elongation index by 81%. The maximum value of flow is 7.37 mm at non-flaky mix and its 1.40 mm at 50% elongation index. The acceptable flow limit is between 2-4 mm.

Graph V

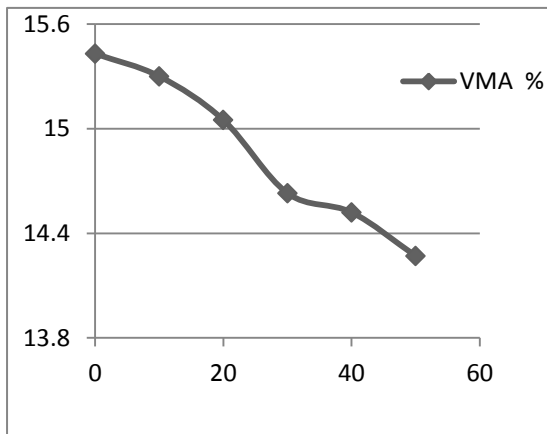


3. Void in mineral aggregate (VMA)

Table VI VMA Results

Elongated Index	VMA %
0	15.43
10	15.3
20	15.05
30	14.63
40	14.52
50	14.27

Graph 6



From the results it was observed that the value of VMA is decreasing with increasing of flakiness & elongation index by 7.51%. VMA value is 15.43 % at 0% flakiness & elongation index and 14.27 % at 50 % flakiness & elongation index.

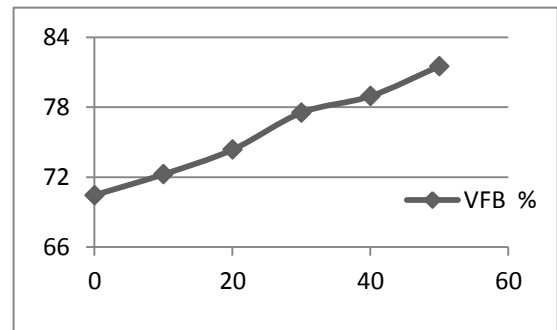
The VMA limit is between 12-14% for nominal maximum size of aggregate 19 mm.

4 Void filled with bitumen (VFB)

Table VII VFB results

Flaky & Elongated %	VFB%
0	70.45
10	72.24
20	74.35
30	77.52
40	78.94
50	81.51

Graph VII



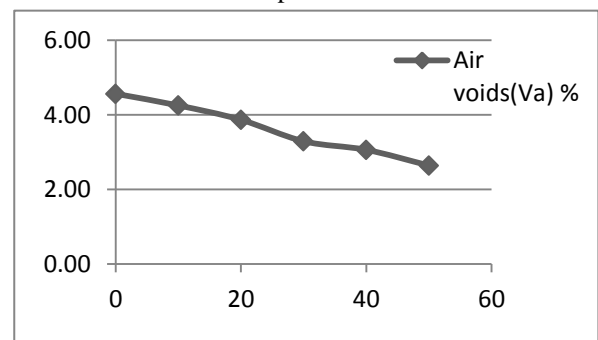
From the results it was observed that the value of VFB is increased by 13.57% from 70.45 % at 0% flaky & elongation index to 81.51% at 50% flakiness & elongation index. The standard limit for VFB is between 65-75%.

5. Void in total mix (VTM)

Table VIII represents VTM results

Flaky & Elongated %	VTM%
0	4.56
10	4.25
20	3.86
30	3.29
40	3.06
50	2.64

Graph VIII



It was observed that VTM is decreasing with increasing of elongation index by 34.19 %. The value of VTM is decreased from 4.56% at 0% flakiness & elongation index to 2.64 % at 50% flakiness & elongation index, while its limit is between 3-6 %.

V. CONCLUSION

- 1) With increasing flakiness & elongation index, stability decreases.
- 2) Increase of flaky & elongation index decreases the stability due to negative performance of flaky & elongated aggregates in the mix.
- 3) The value of flow decreases with increasing elongation index.
- 4) Flow is decreasing with increase in flakiness & elongation index in the mix, because due to lack of degree of interlocking.
- 5) Void filled with bitumen (VFB) is a property that is highly related to VTM. The more void percentage in the mix, decreases the strength and the more voids are filled by bitumen. So they are inversely proportional.
- 6) The value of VMA is decreasing with increasing of flakiness & elongation index.
- 7) VTM is decreasing with increasing of elongation index.
- 8) The value of density is decreasing with increasing of flakiness & elongation index.

REFERENCES

- [1] Herrain, M. and Goetz, W. H. "Effect of aggregate shape on stability of bituminous mixes", HRB Proc., Vol. 33, 1954, pp.293-308.
- [2] IS 2386(I), Indian standard methods of test for aggregates for concrete, Part-I: particle size and shape, The Bureau of Indian Standards, New Delhi, 12th reprint, 1999.
- [3] Bachtiar, Z. (2000) *Kajian Batasan Jumlah Agregat Pipih untuk Campuran Beton Aspal*, Thesis, Magister Program on Highway and Development, Bandung Institute of Technology.
- [4] Li M.C., and Kett.I. (1967), "Influence of coarse aggregate shape on the strength of asphalt concrete mixtures", Highway Research Record 178, pp 93-106.
- [5] JKR (2008), Standard Specification for Road Work, Jabatan Kerja Raya Malaysia, Kuala Lumpur.
- [6] Huber, G.A., and Heiman, G.H. (1987) "Effect of asphalt concrete parameters on rutting performance" a field investigation. Proceedings

of Association of Asphalt Paving Technologists, 56, 33-61.

- [7] Zhang, Y., Luo, R. and Lytton, R. L., "Microstructure-based inherent anisotropy of asphalt mixtures", Journal of Materials in Civil Engineering, Vol. 23, No. 10, (2011), 1473-1482.
- [8] Stephens, J.E., and Sinha, K.C. (1978) "Influence of aggregate shape on bituminous mix character". Journal of Association of Asphalt Paving Technologists, 47, 434-456.
- [9] Indian standard IS: 2386 part 2, 4 and 7 and IS: 6241.1997
- [10] Ishai, I. and Gelber, H., "Effect of geometric irregularity of aggregates on the properties and behavior of bituminous concrete", Proc. of AAPT, Vol. 51, 1982.
- [11] Kalcheff, I. V. and Tunnicliff, D. G., "Effects of crushed stone aggregate size and shape on properties of asphalt concrete", Proc. of AAPT, Vol. 51, 1982.
- [12] Kandhal, P.S., Khatri, M.A., and Motter, J.B. (1992) "Evaluation of particle shape and texture of mineral aggregates and their blends". Journal of Association of Asphalt Paving Technologists, 61, 217-240.

ROAD ACCIDENT SCENARIO IN CYBERABAD AND HYDERABAD

Ch.Dilip¹, V Ranjith Kumar², Dr.M.Kameswara Rao³

¹Research Scholar (M.Tech, T.E), ²Assistant Professor, ³Professor
Malla Reddy Engineering College (Autonomous), Kompally

Abstract-- In developed countries Road accidents has been a major social problem. Developing countries like India have started facing large number of road traffic accidents. Road traffic accidents in Hyderabad city are alarming rate and Proper preventive measures are need to taken .The road accidents study is done for outside the city and within the city. This paper presents various aspects of Road traffic accidents in LB nagar and Saifabad. Three years (i.e.2012-2014) police stations data is used. Nature of accident in both the areas is Hit from Back and Hit pedestrian .The data analysis is done in various categories. Accidents have been a major social problem in the developed countries of world for over fifty years. It is only in the past decade that developing countries like India have began to experience large increase in the number of road accidents taking place and having found it necessary to institute road safety programs. Road accidents in Hyderabad can be studied by identifying the high accidents occurred area having a peak rate. The road accidents study can be done in two areas of Hyderabad city. The project involves identifying of road accidents in seven variations and finally giving solutions. The two areas namely Hayathnagar and Safibabad are the mainly facing alarming road accidents. The road accidents study of two areas is done by conduction two types of data collections. Data collection is done from the police stations of two areas. Based on

those data the suitable recommendations are given for Hyderabad city and also for Indian cities. By conducting some type of survey in remaining areas of Hyderabad can reduce and prevent road accidents.

Keywords: *Analysis, preventive Safety measure, road traffic Accidents, Hit from Back, Hit pedestrian.*

I. INTRODUCTION

India is said to be heart of south asia. India is undergoing mJOR financial and demographic transition coupled with increasing urbanization and motorization. In seven metropolitan cities in India namely Ahmadabad, Bangalor, Mumbai, Kolkata, Delhi, Chennai and Hyderabad. In India, 16% of deaths due to non-communicable diseases are due to injuries 80% of injuries death is due to road traffic accidents in the year 2013.)

Transportation system is meant for movement of people and goods from one place to another place safely. Thus safety is one of the main aspects of the transportation system. Motorization has been happening rapidly throughout the world. This has increased the mobility of the people from one place to other and the accidents also. Road accidents became a serious problem. Accidents are social problems affecting people in many ways. Serious losses caused by road accidents demand the attention of the society and call for the solution of the problem. The prevention of road accidents should not be considered as purely technical exercise. It involves many factors like government, educator, engineers, enforcement, voluntary organizations etc.

A multi-disciplinary approach is needed in understanding the problem. The road safety problem has been analyzed in many different ways. Prominent among them are in four 'C' element forms.

- i. Carriageway (Road)
- ii. Carriers (Vehicles)
- iii. Captain of the carrier (Driver)

iv. Climate (Environment)

Similarly the approach of the road safety has taken a three 'E' element form.

- i. Engineering
- ii. Enforcement
- iii. Education

There are four opportunities for the application of road safety engineering.

1. Safety conscious planning of new road network and new developments
2. Incorporation of safety features in the design of new road
3. Improvement of safety aspects of existing roads to avoid future problems
4. Implementation of known hazardous locations on the road network

1.1 Accident Scenario in India

Indian road traffic condition is of Heterogeneous with more presence of two wheelers. This imbalance traffic conditions make the safety situation worse. The accidents rate is alarming and the accident rate increased around from the 406000 to 500000 during 2001-2014 and 138,268 were killed. In India, 65% of total accidents take place during night through the night traffic is hardly 20 % of 24hours volume which means that the accident in India during night is eight times greater than the day traffic.

1.2 Study Area

Hyderabad is the capital city of the state of "Telangana" in South India. Hyderabad occupies 650square kilometers (250sqmi).The Hyderabad is one of the Metropolitan cities in India greater hub for Administrative, Financial, Industrial, Educational, Medical, Cultural activities resulting high growth rate. There are three National High- ways and five State Highways

II. OBJECTIVE OF STUDY

The main objectives of this study are-

- To analyze the distribution of fatal, non-fatal accidents took place.
- To apprise the causes of accidents.
- To study hourly incidents of total accidents.
- To provide safety preventive measures to reduce pedestrian's accidents.

II. LITERATURE REVIEW

General

Road accidents are not intentionally caused but occurs due to complex reason of induced conditions due to

- Geometrical and surface conditions of the road
- Dynamic road worthy conditions of vehicle
- Physical and psychological condition of the drivers
- Environmental conditions

These literatures are considered because by using only police station data they have given some counter measures to reduce road accident.

Road Accident Scenario in Kolkata: A spatio temporal study by Amith Ghosh and Suman Paul, (2009).Kolkata is a metropolitan city ,the traffic accident situation in Kolkata police station is really alarming and the loss of lives are property damages are expressed. In this city has high population density and huge pressure of vehicles on road. Data on accidents were collected from Lal Bazar, Police Head Quarters in the city from three years (i.e. 2007-2009).In this study they have taken only police station data, It was found that a total 7217 accidents occurred during this period. Accident data analysis is done. From the data they have concluded that 25% victims are between ages 18 to 30 years, 82% victims are the pedestrians only,21% bus and truck are mostly involved in accidents. To minimize the accidents at greater extent by providing round hump to slow down the fast moving vehicles, installing good signal system, preventing the U-turn, eliminating the irregular stopping of auto-rickshaw at intersections and installing road divider to prevent lane changing activities, introducing raised hump with vertical post, side walk for pedestrians and control of road side parking. Identification and analysis of accident black spots using Geographic information System by Liyamol isen, Shibu A and Saran M.S,(2013).the Kerala Road Safety Authority(KRSA) found that maximum number of accidents black spots are in Alappuzha and Erankulam districts. Data collection is done in two types primary data and secondary data. Three years data is collected (i.e. 2010-2012).The primary data collected from field road inventory survey, traffic volume count, speed and delay study. The secondary data is collected from State Crime Records Bureau (SCRB), Trivandrum. From the data using GIS the black spots are identified developing weighted severity index method (WSI).From that six black spots are identified in Alappuzha district and 10 black spots are identified in Ernakulam were done using ARCGIS. Some suggestions are given for Alappuzha

district like to increase the number of lanes from two lanes to four lanes, provide footpath on both sides of the road for pedestrians, provide adequate drainages, provide separate bus bays for avoiding delay of other vehicles at the bus stops, take suitable geometric modifications to reduce speed of vehicle and repair pot holes for the safety of vehicle users. Similarly for Ernakulam district like to provide necessary road signs and markings, provide sufficient road way width, remove illegal construction from the road, provide adequate sight distances. Estimation of influence on type of collision for road accidents using logits models in Cyberabad-Hderabad-India by Dr.M.Kumar and A.Ramesh, (2014).Hyderabad is a metropolitan city mixed traffic conditions. In Hyderabad Accident rate is really alarming. Data collection is done from the various police stations. Three years data is collected (i.e. 2009-2011) From the data yearly comparison, monthly variation of accidents during (2010 to 2011), Nature of accidents occurred and causes of accidents is done. From the data analysis Logistic Regression is used for development of models based on severity and chi-square test results for severity and type of collision (fatal) are developed. Conclusion of the study is observed that day time accidents are marginally lesser than night time accidents. More number of accidents occurred in Balanagar division, the Rear end Severity (fatal) in accidents seem to be very less with a odds ratio of -0.022 and not much during 2009-2011.

III. EXPERIMENTAL INVESTIGATIONS

The case study involves accident data analysis for Cyberabad and Hyderabad. The field survey is performed for study areas namely LB nagar and Saifabad These include selected areas police station accident data.

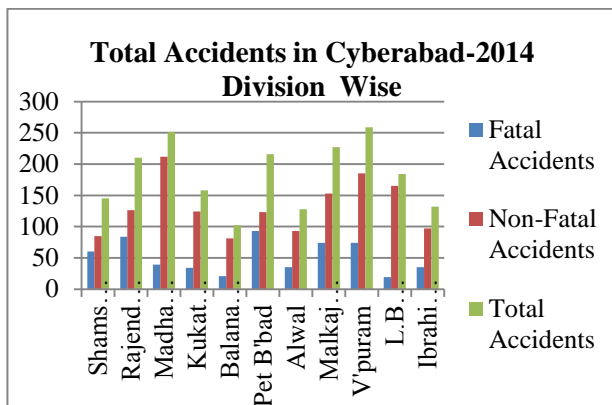


Fig1: Total no. of Accidents Occurred in Cyberabad Division Wise

Total Accidents in Cyberabad-2014			
Month wise			
Month	Fatal	Non-fatal	Total accidents
January	91	212	303
February	65	184	249
March	83	203	286
April	82	176	258
May	97	186	283
June	79	207	286
July	71	185	256
August	83	178	261
September	`	173	250
October	77	204	281
November	91	217	308
December	90	185	275
Grand Total	986	2310	3296

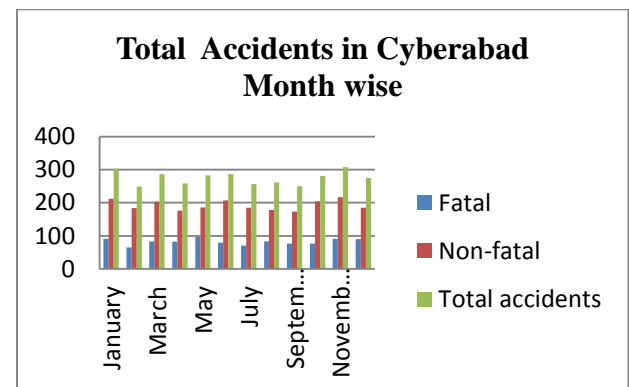


Fig 3: No. of Accidents Occurred in Cyberabad Month Wise

Total Accidents in Hyderabad-2014	
Day wise	
Day	Total Accidents
Sunday	369
Monday	343
Tuesday	372
Wednesday	349
Thursday	369
Friday	368
Saturday	415
Grand total	2585

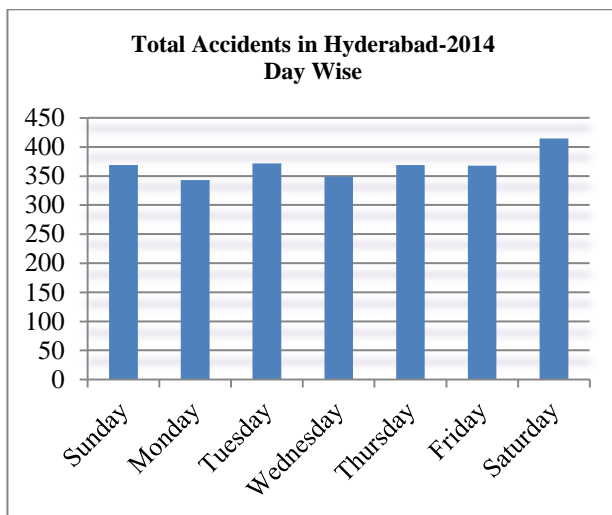


Fig 4: No. of Accidents Occurred in Hyderabad Day Wise

IV. CONCLUSION

In Monthly wise Accident Report the Non-fatal accidents rate is peak in the month of November, Fatal accidents are is peak in the month of December. In Hourly wise Accident Report high number of accidents occurred during 12am-2am duration time with two hours interwell. In Yearly wise Accident Report the variations in Non-fatal accidents increased and Fatal accidents rate is decreased. Nature of Accident Report shows Hit from Back cases are high and Hit pedestrian are in peak levels. In victim vehicles profile Accident Report 2wheelers, cars and LCV are highly involved in road accidents. In accused vehicles profile Accident Report Cars, 2wheelers, Buses and LCV are highly .

V RECOMMENDATIONS

Common Recommendations for both areas:

- According to the favorable weather conditions speed limits are need to maintain.
- Every year after rainy season road conditions are need to check because of rainfalls roads may get damaged. So road repairs are need to done. vehicle tyres are also need to check.
- ITS technology system is to be introduced in city outskirts also. Because to create a better awareness and to control road accidents upto some extent.
- Need to check traffic signal system is properly implemented are not.
- Proper street lights and traffic indicators are needed to provide in city outskirts during night times.
- During peak period duration temporary traffic

barriers are provided for free left and right.

- Pavement Geometric modification is needed to do according to its road traffic conditions.
- Traffic rules are to be following very strictly .If not the fine amount should be increase and the license should be canceled.
- Raised humps are needed to provide with marking to slowdown the fast moving vehicles.
- Interceptors are to be fixed to monitor speed limits of moving vehicles.
- Make a note that the vehicle is regularly checked and maintained.
- 2Wheelers vehicles count is increasing day by day due to this traffic volume is also reaching peak levels. So need to provide private buses for offices to reduce 2Wheelers count on roads.
- Pedestrians signals are to be introduced in city outskirts also for good visibility
- Cross walks tracks are provided for both sides of the road.
- Need to introduce raised hump with vertical post for pedestrians crossing. For good visibility during night time.
- Separate lane is provided for 2Wheelers and Cars.
- Ensure sure that vehicle headlights and taillights are in working condition or not.
- Speed control is maintained according to the present traffic conditions.
- Limit and control self night driving.
- Eliminate Irregular stopping of auto-rickshaws are to be needed.
- Control Road side parking according to traffic conditions.
- Provide Proper free left

VI REFERENCES

1. Amith Gosh and Suman Paul (2013), "Road Accident Acenario in Kolkata: A spatio-temporal Study", European journal of applied Engineering and science research.
2. Basri Lenjani, Salih Krasniqi, Njlazi Gashi, Ilaz Bunjaku and Thaxhedin Zaim (2012), "Frequency of Road Accidents in Prishtina in the Period 2007-2010"
3. Dr.M.Kumar and A.Ramesh (2014), "Estimation of Influence on type of Collection for Road Accidents using Logit models in Cyberabad – Hederabad - India", Institute of research Engineers and doctor.
4. G.Kondal Rao (2013), "Road Traffic Safety Mangement in India-analysis-Exploring

Solutions”International Journal pr Application or
Innovation in Engineering &
Management(IJAIEM)

5. Guler yalcin (2013), “Non-spatial analysis for the road traffic accidents”, Lumen international conference Logos University Mentality education Novelty (LUMEN).
6. “Highway Engineering” by S.K.Khanna and C.E.G.Justo, Nem Chand & Bros (2011).
7. “Hyderabad Wikipedia”
8. IRC:53-(2012) Road Accident recording forms A1 and A4
9. Mark Richmund DE LEON , Nelson DOROY , Hussein LIDASAN and Jun CASTRO(2013), “Black spots Cluster Analysis of Motorcycle Accidents”
10. Mohamad Ghazali Masuri,Khairil Anuar MD Isa & Mohd Tahir (2012), “Children,Young and Road Environment:Road Traffic Accident” in Kuching,Malayasia.Procedia-Social and Behavioral Science
11. YU Qing-yuan(2013), “Causes and Prevention Measures of Secondary Rear-end Accidents in the Rescue of Highway Traffic Accidents.

STUDY OF NON-MOTORIZED TRANSPORT IN CYBERABAD AND HYDERABAD

Hyderabad Shahabaz¹, V. Ranjith Kumar², Dr.M.Kameswara Rao³

¹Research Scholar (M.Tech, T.E), ²Assistant Professor, ³Professor
Malla Reddy Engineering College (Autonomous), Kompally

Abstract: --Economic and Industrial growth is a positive sign for a developing country like India. But all this growth is coming along with some new challenges to the environment and public which is creating an artificial disaster in urban areas as Traffic jams and creating much of noise and pollution. Even more deaths are caused by the road accidents more than any other natural disaster or terrorist activities like 9/11. Unfortunately what happens on our urban transportation is more vehicles move rather than more people, Which is the source of the problem. The present study is to identify the reasons for this problem and working out a methodology to develop Non-Motorized Transport (NMT) model for cyberabad region in Hyderabad city. A detailed study is done to understand the problems of pedestrians, who are mostly killed and injured on roads. Methodologies and measure are to be taken to make the road safer for pedestrians which by adopting the best practices of NMT policies of various developed countries where the importance is understand for the safe roads and green public transport are recommend. The benefits of NMT and the cost of the components are also worked out to develop NMT infrastructure for cyberabad region of Hyderabad city where more private vehicles are used for commute

Keywords -- NMT, Pedestrians, Road accidents, Cycling, Public Transportation

I.INTRODUCTION

Non-Motorized Transport modes (NMT) include walking, bicycle and cycle rickshaw. Earlier days Cycle Rickshaw was a mode of most of middle class public transport. With the economic, social technological growth there is a drastic shift in mode of public

transport. In India the urban road infrastructure is mainly favoring only the use of motorized vehicles. No where in the country we can find a pedestrian friendly road infrastructure in India. The present situation itself is very pathetic and dangerous for non motorists on Indian roads. Now it's the peak time to make some measure s and corrective actions to make our roads safer for now and future. From the statistic it can be understood that every month there is a 9/11 happening on Indian roads taking more live than that of a terrorist attack. UNEP Study on fatalities on urban roads tells the dirty picture of Indian Roads. The reason for this is the importance given in spending for motorized vehicles is not overlooked by the policies and officials.

Urban road infrastructure in India is biased in favour of motorised vehicles. This is on account of lack of a reaction to extremely high growth in motorized vehicles in urban India in the last two decades. While the population of India's six major metropolises increased by about 1.9 times during 1981 to 2001, the number of motor vehicles went up by over 7.75 times during the same period (Ministry of Urban Development, 2007, pp. 1-2). From the population census of 2010, at least 35 per cent (27.76 million) urban households had a motorized two wheeler and 9.7 per cent (7.65 million) urban households had a motorized four-wheeler. While, on the whole, the registered motor vehicles increased by 2.4 times during 2002-2011 period or at the rate of 10.2 per cent per annum, in 19 metropolitan cities for which the two time point data is available, registered an increase at 8.8 per cent per annum in the decade (Transport Research Wing, 2012, pp. 3-4).

This has created congestion on the roads, resulting in road widening exercises and construction of flyovers. These two infrastructures have also become symbols of world class cities. Many cities are aspiring to become world class to attract investments. Car usage has become a status symbol, and car buying is termed by the government as contributing to economic growth. This in turn has made car-users a group which is set to de-rail any equitable road development exercises in a city,

claiming every inch of road space for their own rightful consumption.

II LITERATURE REVIEW

Vasconcellos (2001) argues that transport is not an end in itself. The 'end' has to be the equitable appropriation of space and the corresponding access to social and economic life. It is quite clear that road infrastructure in India completely ignores facilities for pedestrians and bicyclists, and hence is not equitable. The National Urban Transport Policy (NUTP) 2007 has also acknowledged that there is a need for bringing about a more equitable allocation of road space with people, rather than vehicles. This inherent inequity in distribution of road space has also resulted in a rampant growth in number of accidents. As per Transport Research Wing & Ministry of Road and Transport (2011), 497,686 accidents occurred on Indian roads in 2011 alone, of which 24.4 per cent were fatal accidents in which 142,485 persons were killed. Accident severity³ has increased from 20.8 in 2002 to 28.6 persons.

Non-Motorised Transport is a sustainable mode of transport (Massink et al., 2011). This is primarily due to the reduced external costs and higher value of benefits (Litman, 2007; Sinnett et al., 2011). The range of benefits of Non-Motorised Transport is also wider than the benefits that can be obtained through motorised transport, especially on an individual level (Pucher and Buehler, 2010).

Whether the Non-Motorised Transport mode is used for only a part of the entire journey or for the whole journey, it helps reduce the number of motorised trips and distance. Hence, reducing motorised trips is an important element in lowering the amount of non-renewable resources used and the external costs that are generated by motorised transport trips (Pucher and Buehler, 2010; Murguía, 2004; Elvik, 1999).

However, despite the various benefits and the value NMT has for both people and the environment, it is often not prioritized (Hüging et al., 2014). This is partly due to the conventional focus on motorised transport modes in policy and practice (Macmillan, 2014; Litman, 2007).

Another important issue that hinders the implementation of NMT projects is the lack of adequate tools to assess these types of projects (Hüging et al., 2014; Sinnett et al., 2011, Litman, 2007). Due to the lack of information regarding the potential impact that NMT projects or single NMT measures can have, decision makers often overlook them in favour of initiatives that come with

more information and/or evidence (Litman, 2007; Pucher and Buehler, 2010).

Motorised transport projects generally are easier to cost and the benefits thereof are normally easier to quantify both ex-ante and ex-post to the implementation. All these factors have contributed to NMT projects being overlooked and undervalued in developing countries (Pucher and Buehler, 2010; Litman, 2007).

III. NEED FOR THE STUDY

The main objective of the study is

1. To curtail unsustainable losses to health and economy.
2. To identify the causes of Accidents and to ensure safety for road users.
3. To check consistency of the road features.
4. To identify problems in the routine maintenance procedures.

PUBLIC TRANSPORTATION IN HYDERABAD

As a fast growing IT hub and metropolitan city with vast population adding **everyday** to the city as migrants for better education or employment adds to the demand to the existing public transportation facilities. Modes of Public Transport in HMA are

- (i) Multi-Modal Transport System (MMTS) rail with 43 Km network running in 3 routes having a ridership of 1,70,000 commuters daily using the facility travelling to and from home to work and vice versa.
- (ii) City Buses operated by Road Transport Corporation serves more than 1 million commuters with 3700 buses plying all across the city.
- (iii) Autos are also considered to be private owned public transport which serves more than 0.5 million commuters with 1,60,000 auto rickshaws.
- (iv) Taxis/cabs serves near about 2lakh commuters with 40,000 plus vehicles.
- (v) Institutional transport facilities provided for self use to commute own stake holders. Eg – Colleges buses transporting students, office buses transporting employees etc.,
- (vi) As the last option commuters use their own vehicles primarily 2 wheelers occupying most of the roads with 3.6 million followed by four wheelers which are 4, 00,000 plus moving on the roads of city.
- (vii) Metro Rail which is to be commissioned by March 2017 is expected to make the real difference in the

travel pattern of the commuters which may reduce the private vehicles usage.

Planning of NMT Facility:

It is important to have the NMT network well integrated with the other road network within the study area. The integrated network should strive for the following Goals:



INFRASTRUCTURE FACILITIES

HMA is totally having a road network of 17000 kms including all the major and minors roads together. To park all the vehicles GHMC has estimated that a land of 4000 acres would be required. Huge crisis of parking spaces in the city greats and adds a problem to the increasing number of vehicles to the city. Daily 600 plus vehicles are registered by Road transport authorities adding to intensify the problem. But the crisis of parking is managed by occupying the road space creating chaos and traffic jams.

Out of the total road network in the city, not even 5% of the roads are having foot paths and wherever the footpaths are made available that is for the benefit of the street hawkers and not for the use of pedestrians. Very poor infrastructure facility is developed and no plans were made to develop cycle tracks and footpaths. As per IRC the width of footpaths based on the number of pedestrians are given as below.

Table 1.Capacity of side Walks

(in meters)	Width of side walk	
	All in one direction	In both direction
1.50	1,200	800
2.00	2,400	1,600
3.00	4,800	3,200
4.00	6,000	4,000

With the existing infrastructure facility which is not at all useful for cyclists or walkers make HMA as unfriendly city for NMT. There is huge scope and need

to develop large Infrastructure facilities for safe travel of NMT users who make a great difference in protecting city and environment by sacrificing their own comfort and which is also a risky affair to get on road without motorized vehicle.



N.B. : Year 2015 (upto 31st August- 2015) figures

Accidents in Hyderabad City Year on Year

From the above bar charts of the Hyderabad, it can be understood that walking on roads is fatal. So to make NMT a safe mode of transportation in Hyderabad, a proposal is made for Cyberabad region to develop NMT infrastructure for pedestrians and bicyclist. People are much empowered with many organizations coming up with campaigns and activities to promote walk to work, Cycle to work, car pool, special buses for making people to shift in mode of transport. Few organization working in for the rights of pedestrians and Right to Walk foundation, CPIP of ASCI, Roadkraft etc., raising the problems and advocating with local governments for a safe road for cyclists and pedestrians. HYSEA, a software employees association had also made campaigns like Carfree Thrusday, Special buses for work and many other initiatives. To promote cycling Hyderabad Cycling Club (HBC) made bicycles available for rent.

Even after many such initiatives and efforts due to lacks of suitable infrastructure challenges are faced by green commuters. So, in this study a techno economic proposal for developing NMT is studied and derived an approximate budget required for developing a 56 km stretch of with 2 meter width of cycle track will cost only Rs 47 million for Cyberabad region. This region is primarily with IT employees which the awareness and adoption is easy and even the demand for the same is raised in various forums to have a better NMT infrastructure.

IV BENEFITS OF USING NMT

Better planning leads to better(more integrated) put-system and NMT-Facilites, which result in better accessibility, conservation of energy and improved of the traffic flow for causing of traffic congestion and by using the NMT services for the Shorter distance it leads

to the travel time saving and improving the saving in fuel consumption and improves in atmosphere in less air pollution and helps lead to the improving of the health of individual and also saves the environment by reducing the consumption of fossil fuels.

With the increase in vehicular growth, commuter's value of time, tendency to fast modes of travel, NMT in spite of its health benefits has been put away from regular travel mode. But in most of countries NMT has developed tends to be retrofitted to existing infrastructure, and to concentrate on minimizing the disturbance that it causes to the flow of motorized traffic. For various reasons, people are now trending to walk, bicycle.

V CONCLUSION:

A well-functioning road infrastructure must fulfill the requirements of all road users. In the context of the present socio-economic realities pedestrians cannot be ignored from the urban landscape. It is true that all the investment plan focus more on cars but congestion seems to worsen along with lesser pedestrians. Given that there is not much space available to expand existing roads. Future mobility needs are best met by increasing the capacity of the existing road network. This can only be achieved by encouraging modes which are more efficient in terms of space utilization. If pedestrian paths are constructed together with dedicated public transport corridors, will ease of congestion on roads as well as it will make the travel safer. To achieve the sustainability goals of the transport sector, it is necessary to promote use of NMT in Hyderabad. Cost for developing NMT infrastructure would be less than 1 million per km for Cyberabad region for a stretch of 56 kilometers, approximate cost is Rs 47 million. A single project, Hyderabad Metro is expected to spend 150 billion just for a stretch of 72 km. if atleast 0.5% of amount is spend the same length NMT infrastructure could be developed. So, hereafter for any infrastructure development it should be made as a policy that 1 % is to be kept for NMT. Always every Urban Local Body (ULB) need to have a policy for green commutation to promote NMT,

Plan for implementing the policy with proper fund allocation and monitoring the service levels regularly.

REFERENCES

1. Ministry of Urban Development. (2007). *National Urban Transport Policy*. Retrieved May 25, 2010, from <http://www.urbanindia.nic.in/policies/Transportpolicy.pdf>
2. Our Inclusive Ahmedabad. (2010, October). *Report of Public Hearing on Habitat and Livelihood Displacements*. Retrieved March 12, 2011, from <http://www.spcept.ac.in/download/cuemisc/Public-Hearing-Report-2010.pdf>
3. Shastri, P. (2012). Where is the walker's paradise of the city? *Times of India*, January 6.
4. Singh, A., & Gadgil, R. (2011). *Comprehensive Assessment of Cycle Tracks in Pune*. Pune: Parisar & Centre for Policy Research.
5. TRIPP. (2005). *First Delhi BRT Corridor-A Design Summary*. Retrieved May 11, 2011, from <http://tripp.iitd.ernet.in/delhibrts/brts/hcbs/hcbs/BR Tdesignsum.pdf>
6. Tiwari, G. and Jain, H. (2008). Bicycles in Urban India, *Institute of Urban Transport (IUT) Journal*, December, pp. 59-68. Retrieved December 13, 2008, from <http://tripp.iitd.ernet.in/publications/paper/planning/bicle%20in%20india-IUT-himani.o.pdf>
7. UTTIPEC. (2010, November). *Street Design Guidelines-for Equitable Distribution of Road Space*. Retrieved June 12, 2012, from <http://www.uttipecc.nic.in/StreetGuidelines-R1-Feb2011-UTTPECC-DDA.pdf>
8. Wilbur Smith & Associates and IL&FS Urban Infrastructure Services Ltd. (2008).
9. *Comprehensive Mobility Plan for Pune City*. Pune: Pune Municipal Corporation.
10. Wilbur Smith Associates and Ministry of Urban Development. (2008). *Study on Traffic and Transportation-Policies and Strategies in Urban Areas in India*. Retrieved June 23, 2011, from http://www.urbanindia.nic.in/programme/ut/final_report.pdf
11. Gurung, M. (2006). *Delhi's graveyard of rickshaws*. Retrieved April 2012, from <http://infochangeindia.org/livelihoods/features/delhi-s-graveyard-of-rickshaws.html>
12. India, Ministry of Housing and Urban Poverty Alleviation. (2009). *National Policy on Urban Street Vendors-2009*, Retrieved November 1,2012

-
- from Ministry of Housing and Urban Poverty Alleviation:
<http://mhupa.gov.in/policies/StreetPolicy09.pdf>
13. IRC:103-1988. (1989). *Guidelines for Pedestrian Facilities*. New Delhi: The Indian Roads Congress.
 14. Indian Road Congress (1990). *Guidelines for Capacity of Urban Roads in Plain Areas*, New Delhi: IRC.
 15. ITDP. (2009). *Designing for Cyclists*, Retrieved November 1, 2012 from Embarq India: http://embarqindia.org/sites/default/files/Chris-Bicycle%20infrastructure_0.pdf
 16. Mahadevia, D. (2011). Branded and renewed? Policies, politics and processes of urban development in the reform era. *Economic and Political Weekly*, 46 (31), pp 56-64.
 17. Mahadevia, D., Joshi, R., & Datey, A. (2012). *Low Carban Mobility in India and the Challenges of Social Inclusion: (BRT) Bus Rapit Transit Case Studies in India* UNEP Risoe Centre .
 18. Mahapatra, D. (2010). SC refuses to cap number of rickshaws in Delhi, *The Times of India*, August 6, 2010; Retrieved on December 13, 2012 from http://articles.timesofindia.indiatimes.com/2010-08-06/delhi/28661100_1_cycle-rickshawscap- number-licenses.

DEVELOPMENT OF DELAY MODEL AT MEDIAN OPENINGS OF ALONG NH-44

B.Sujay Diwakar¹, V. Ranjith Kumar², Dr.M.Kameswara Rao³

¹Research Scholar (M.Tech, T.E), ²Assistant Professor, ³Professor
Malla Reddy Engineering College (Autonomous), Kompally

Abstract: -- A U-turning vehicle, during merging at an uncontrolled median opening creates the possibility of conflict with approaching through traffic movement and causes traffic congestion which reduces the roadway capacity. The effect of conflicting traffic volume on the U-turning maneuver was also investigated by collecting placement data extremely congested traffic conditions. Compared with turning movements at intersections, U-turn movement at median openings is highly complex and risky. Normally, the speed of conflicting traffic stream is relatively high and the turning vehicle must wait for accepted gap and then turn under low speed level. Therefore, the turning vehicle needs large gap in the conflicting stream before performing the U-turn. In fact, the little studies which contain procedures and models for estimating capacity and delay for different movements at unsignalized intersections do not provide specific guidelines for estimating capacity and delay of U-turn movement at median openings. For this reason, an effort was made to estimate capacity and delay at U-turn median openings.

In this study, empirical approach is used to estimate capacity of U-turn movement at median openings of divided arterials. The empirical approach using regression analysis was adopted to estimate the best form of the predictive equation for the U-turn capacity and investigate the effect of different relevant factors that might affect the estimated capacity. The results of the approach are presented in this study. A linear model was also recommended as a relationship between the average total delay of the U- turning vehicles and the conflicting traffic flow.

Keywords -- Traffic engineering, Capacity, Delay, Conflicting Traffic Flow.

I.INTRODUCTION

The major purpose of capacity modeling of U-turn median opening is to develop useful relationship between capacity and set of traffic and geometric characteristics. The developed model should be easy for practical applications and predictive under different traffic conditions. It should be mentioned that intersections are provided to facilitate traffic turning movements. As part of traffic management to improve intersection operation, some traffic movements are not permitted at some intersection locations, especially along

divided arterial. In most cases, such minor movements are accommodated at separate U-turn median openings. Compared with turning movements at intersections, U-turn movement at median openings is highly complex and risky. Normally, the speed of conflicting traffic stream is relatively high and the turning vehicle must wait for accepted gap and then turn under low speed level. Therefore, the turning vehicle needs large gap in the conflicting stream before performing the U-turn. In fact, the little studies which contain procedures and models for estimating capacity and delay for different movements at unsignalized intersections do not provide specific guidelines for estimating capacity and delay of U-turn movement at median openings. For this reason, an effort was made to estimate capacity and delay at U-turn median openings.

However, the operation can be considered as an interaction of drivers on the minor or stop-controlled turn with drivers on the oncoming approach of the major street in two directions simultaneously. Although the U-turn movement is more complex than right-or left-turning movements at unsignalized intersections, the general concepts and procedures developed for analyzing capacity at priority unsignalized intersections are very crucial in this respect.

The purpose of capacity analysis is to insure that planned highway network could deal with the present and future traffic flows with satisfying quality; Since unsignalized intersections and Median openings are the most common type, their functionality has a great impact on the quality of traffic flows on the urban street network and especially on the suburban and rural highway network (at connections of state and county roads). In the following chapters of this paper, first the development of available capacity methodologies is presented followed by the summary results of conducted capacity modeling using regression analysis.

Problems of U-Turns at Median Openings

In India Due to the wide variation in the operating and performance characteristics of the Vehicles mixed traffic systems operate very much differently as compared to the homogeneous traffic

condition. The traffic in mixed flow is comprised of fast and slow moving vehicles or motorized and non-motorized vehicles. The vehicles also vary in size, maneuverability, control, and static and dynamic characteristics. In the absence of lane discipline and wide variation in sizes of different types of vehicles, they are found to move side by side on the road. Vehicular traffic is increasing very rapidly in recent times giving burden on transportation infrastructure. To meet the demand of vehicular traffic most of the roads now constructed as multilane roads or two lane roads are being widened to multilane roads. Multilane roads are generally constructed with raised median in order to segregate the opposing traffic movements. Median-separated highways provide distinct benefit over undivided roadways (two-lane or multilane roads without medians). Medians segregate opposing traffic, allow space for speed changes and storage of U-turning vehicles, minimize headlight glare, and provide width for future lanes. Median openings are provided at various locations along divided multilane roads to permit vehicles to reach abutting property or reverse their direction of travel. The U-turn movement at a median opening is highly complex and risky compared with turning movements at intersections, firstly because of the high speed and traffic volume and secondly because the turning vehicle has to make a 180° movement and merge the traffic stream in which it is seeking an acceptable gap. The turning vehicle must wait and then turn under low speed conditions in the face of oncoming traffic and may need to accelerate rapidly to reach the speed of the traffic stream. If there are many turning vehicles that have to wait, then a long queue in the stream cannot be avoided and queue spill-back to block through traffic is possible. This can lead to traffic problems, mainly reduced capacity and level of safety. At these median openings vehicles take U-turn to merge with the approaching traffic.

Concept of Level of Service at Median openings

LOS category	Service Delay range (s/Vehicle)	Control Delay ranges (s/Vehicle) for TWSC (hcm-2010)
A	0-5	0-5
B	>5-8	>10-15
C	>8-13	>15-25
D	>13-20	>25-35
E	>20-33	>35-50
F	>33	>50

Delay ranges for LOS categories of uncontrolled median openings

Objectives of the Study

The objectives of the present study are mentioned below

- To develop a model for estimating the capacity and Delay at U-turn median opening.
- To evaluate the effect of U-turning vehicles on the capacity of a stretch.
- To evaluate the relation between capacity and conflicting traffic flow.
- To evaluate the relation between delay and conflicting traffic flow.

LITERATURE REVIEW

Location of median openings

The growing number of multilane highways with raised or depressed medians and without access control has created the need to provide median openings, or crossovers, at various locations along such facilities to permit vehicles to reach abutting property or reverse their direction of travel. Median openings, however, may also become points of increased congestion and accident exposure.

A committee of the Institute of Transportation Engineers developed a list of factors to consider in locating median openings. These included the potential number of left turns into driveways, length of frontage along the street right-of-way line of the property proposed to be served, distance of proposed opening from adjacent intersections or other openings, length and width of the left-turn storage lane as functions of the estimated maximum number of vehicles to be in the lane during peak hours, and traffic control. The committee noted the need to consider circuitous routing and added intersection turns that may be caused by closing a median opening.

Kimber et al. (1980) using the empirical approach, concluded that the capacities of the non-priority streams at T-intersections depend linearly on the flow in the relevant priority streams.

AL-Masaeid (1999) identified specific guidelines for estimating capacity and delay models of U-turn movements at median openings. He found that, the capacity and delay were significantly influenced by the conflicting traffic flow, that the predictive capacity model had linear form, while the delay relationship had an exponential form. A wide difference obtained by AL-Masaeid between the gap acceptance and the empirical approaches for capacity estimation.

Kyte et al. (2003) listed the three main causes of difference, including headway distribution of major stream, usage of gaps of minor stream, and driver behavior. The arrival of conflicting vehicles on urban arterial sometimes does not follow the random process. In other words, the headways are not negatively exponential distributed. This affects the availability of gaps for the u-turn vehicles. This research considered the headway distribution.

Liu et al. (2007; 2008a; 2008b; 2009) have conducted a series of research relating to capacity of U-turn at median opening. They estimated the parameters (critical headway and follow-up headway) of U-turn movements from the field data. They validated the capacity estimation from the model with the field capacity. The model provides reasonable estimated capacity for U-turn movement at median openings. The HCM 2010 utilizes the values of these parameters of U-turn movement for the capacity analysis in the US. Nevertheless, the critical headway and the follow-up headway need local calibration due to differences in driving style (Vasconcelos et al., 2012). Those parameters also vary according to physical geometry characteristics of the junction (Weinert, 2000). The model capacity can differ from field capacity.

Zhou et al. (2009) studied the gap acceptance behavior of left turning drivers at six unsignalized intersections. Logit models were used for estimating the probability of accepting a given gap. Results showed that the number of lanes on the major road, the presence of left turn lanes and the gender of the driver explained the variation in the gap acceptance probability. It was also found that older drivers generally tended to accept longer gaps.

Tupper et al. (2011) studied the factors that influenced the driver's gap acceptance behavior and had clear impact on safety. Different driver's age and gender groups were found to have different gap acceptance behaviors. Factors that had the greatest effect on gap acceptance behavior were found to be the presence of a queue behind the driver, the driver's waiting time and the number of the rejected gaps.

STUDY AREA AND METHODOLOGY

Today the city of Hyderabad, India cover an area of 650 square kilometers (250 sq mi), has a population of 6,809,970 making it the fourth most populous city in India. There are 3,500,802 male and 3,309,168 female citizens. The area under the municipality increased from 170 square kilometers (66 sq mi) to 650 square kilometers (250 sq mi) in 2007 when the Greater Hyderabad Municipal Corporation was created. As a

consequence, the total population leaped from 3,637,483 in 2001 census to 6,809,970 in 2014 census, an increase of over 87%. Migrants from rest of India constitute 24% of the city population. Hyderabad city is governed by Greater Hyderabad Municipal Corporation that comes under the Hyderabad Urban Agglomeration, which has a population of 12 million the fourth most populous urban agglomeration in the country, with 3,985,240 males and 3,764,094 are females. A proposal to expand the area covered by the city to make it 721 square kilometers (278 sq mi) by merging the surrounding gram panchayats and around 30 villages is being considered, as of 2009.

Study Area

Hyderabad city is the sixth largest metropolitan city in India. The phenomenal increase in population coupled with growth of road vehicles has created considerable traffic problems. It is facing a peculiar problem of combined traffic conditions, where cars, scooters, autos, buses, trucks etc., are operating together. In addition to this the city is facing with the problems of narrow streets and choked intersections. Compared with turning movements at intersections, U-turn movement at median openings is highly complex and risky. Normally, the speed of conflicting traffic stream is relatively high and the turning vehicle must wait for accepted gap and then turn under low speed level. Therefore, the turning vehicle needs large gap in the conflicting stream before performing the U-turn. So for the modeling of capacity and delay three median openings were chosen in the present study.

To accomplish the objective of this study, three median openings located in Hyderabad City were selected.

- Balaji Hosital
- Kompally
- Bowenpally



Median opening at Bowenpally stretch



Median opening at Balaji Hospital

Methodology

The study methodology consists of Five phases, through which the corridor management study would be completed for the selected corridor. The Five phases are listed as below:

- Identification of the study Area
- Traffic data collection
- Developing Capacity model for heterogeneous traffic flow
- Developing Delay model for heterogeneous traffic flow
- Evaluation of LOS

To accomplish the objective of this study, Six median openings located in Hyderabad City were selected. These median openings are located along divided suburban arterials and operated at capacity during peak periods. At capacity condition is defined, as the condition in which there is continuous queue of turning vehicles in the approach of the turning lane.

DATA COLLECTION AND ANALYSIS

The data collected at a median opening at Bowenpally and Kompally stretch is shown in the following table

Data collected at a median opening

Capacity of U-turning vehicles (veh/min)	Capacity of U-turning vehicles (veh/hr)	Conflicting Traffic Flow (veh/min)	Conflicting Traffic Flow (veh/hr)	Average Total Delay (sec/veh)

10	600	23	1380	5.9
2	120	70	4200	23.3
4	240	50	3000	13.2
3	180	60	3600	18.1
6	360	36	2160	7.7
4	240	52	3120	13.5
3	180	61	3660	17.37
5	300	43	2580	10.9
2	120	71	4260	24

Development of capacity model

The capacity of U-turning Vehicles is denoted by 'C', Conflicting Traffic is represented as 'q' and the Delay is represented as 'D'.

From the above table

$$\Sigma C = 9260$$

$$\Sigma C^2 = 772400$$

Mean of capacity

$$= \frac{\Sigma C}{\text{no. of observations}}$$

$$= \frac{9260}{50}$$

$$\bar{C} = 221 \text{ veh/hr.}$$

Standard Deviation

$$= \sqrt{\frac{\Sigma C^2}{\text{no. of observations}} - (\text{mean}^2)}$$

$$= \sqrt{\frac{772400}{50} - (221^2)}$$

$$= \sqrt{15448 - 48841}$$

$$S.D = \sigma_c = 182.73$$

CONCLUSIONS

Based on the results of this study, the following points were concluded:

- Capacity and average total delay models for U-turn movements at median openings were found to be significantly influenced by the conflicting traffic flow.
- For Bowenpally and Kompally stretch, Capacity of the U-turning vehicles is inversely proportional to the Conflicting Traffic Flow.
- Capacity model at Bowenpally and Kompally stretch has an R^2 value of 0.9239 i.e., it explains a high percentage of relation between Capacity of U-turning vehicles and conflicting traffic flow.
- The Delay model has linear relationship obtained between the average total delay and the conflicting traffic flow at U-turn median openings.
- Delay model has an R^2 value of 0.924 i.e., it explains a high percentage of relation between Delay and conflicting traffic flow..
- Capacity model at Bowenpally stretch has an R^2 value of 0.911 i.e., the capacity is 91.1% correlated with conflicting traffic flow.
- Delay model has an R^2 value of 0.914 i.e., delay is 91.4% correlated with conflicting traffic flow.
- Capacity model at Kompally stretch has an R^2 value of 0.9014 i.e., the capacity is 90.14% correlated with conflicting traffic flow.
- Delay model has an R^2 value of 0.9066 i.e., delay is 90.66% correlated with conflicting traffic flow.
- Abou-Henaidy, M., Teply, S. and Hunt, J.D. (1994), "Gap acceptance investigations in Canada".
- R. Akcelik (ed.), Proceedings of the Second International Symposium on Highway Capacity, Vol. 1, Australian Road Research Board, Melbourne, Australia, 1-19.
- Al-Azzawi, M. (1997), "An evaluation of current traffic models used to design priority junctions", Traffic Engineering and Control, Vol. 38, No. 5, 267-275.
- Al-Masaeid, I.R. (1995), "Capacity of one-way yield-controlled intersections". Transportation Research Record, Vol. 1484, 9-15.
- Austroads (1991), "Roadway capacity. Part 2 of Guide to Traffic Engineering Practice", Austroads, Sydney. Bennett.
- Kyte, M., Kittelson, W., Zongzhong, T., Brilon, W., Troutbeck, R.J. and Mir, Z. (1994), "New measurements for saturation headways and critical gaps at stop-controlled intersections".
- Hussein Kariem Mohammed. (2008), "Model Development of U-turn Capacity Using Simulation and Empirical Approaches" The 1st Regional Conference of Eng. Sci. NUCEJ Spatial ISSUE vol.11, No.1, 2008 pp189-193.

REFERENCES

- AL-Masaeid. H.R. (1999), "Capacity of U-turn at Median Openings", ITE Journal, vol69, no.6, June 1999: pp. 28-34.
- HCM, Transportation Research Board. Highway Capacity Manual. Special Report 209. National Research Council 2000.
- Kimber, R. and Coombe. (1980), "The Traffic Capacity of Major/Minor Priority Junctions", TRRL Report SR 582, 1980.
- Kariem H. (2001), "Development of Simulation Model for Traffic Performance at U-Turn Median Openings", Proceedings of the fourth Scientific conference organized by Ministry of Housing and Construction, Baghdad, 2001, vol. 1, pp. 171-197.
- Kyte, M., Clemow, C., Mahfood, N. and Kent, B. (1991), "Capacity and Delay Characteristics of Two-Way Stop-Controlled Intersections", Transportation Research Record, and No. 1320, 1991: pp. 160-167.

DEVELOPMENT OF PAVEMENT MANAGEMENT SYSTEM ON URBAN ROAD NETWORK

D.Prachallaja¹, A.NagaSaibaba², Dr.M.Kameswara Rao³

¹Research Scholar (M.Tech, T.E), ²Assistant Professor, ³Professor
Malla Reddy Engineering College (Autonomous), Kompally

Abstract: --Pavements are major assets of urban infra-structure. Maintenance and rehabilitation of these pavements to the desired level of serviceability is one of the challenging problems faced by pavement engineers. The evaluation of pavement performance using pavement condition is a basic component of any Pavement Management system. (PMS) is a planning tool used to aid pavement management decisions, pavement deterioration due to traffic and weather, and recommend maintenance and repairs to the road's pavement based on the type and age of the pavement and various measures of existing pavement quality. It represents an effort in the similar direction, to develop a combined Overall pavement Condition Rating (OPCR) for the selected network of Hyderabad City Roads. The study area consists of urban road sections constituting 39.9 km of Hyderabad city. The methodology includes the identification of urban road sections, pavement distress data collection, Pavement condition Distress, Quality control analysis and finally developing Overall Pavement Condition Ratings (OPCR). The proposed rating is expected to be a good indicative of pavement condition and performance. The Ratings was used to select the maintenance strategy for the pavement section. It is far less expensive to keep a road in good condition than it is to repair it once it has deteriorated. This is why pavement management systems place the priority on preventive maintenance of roads in good

condition, rather than reconstructing roads in poor condition. In terms of life time cost and long term pavement conditions, this will result in better system performance

Keywords -- Pavement, PMS , OPCR, Overlay.

1. INTRODUCTION

India is said to be the fastest developing countries today. Although India is doing exceptionally well in industrialization there are still certain areas where the country is lagging behind. India's road network is gigantic. But one of the striking underlying facts is the condition of the roads. Since roads indirectly contribute to the economic growth of the country it is extremely essential that the roads are well laid out and strong. India is home to several bad roads be it the metropolitans, the cities or the villages. Bad road conditions are nothing new to India and the problem. Since India is a developing nation there is a constant demand for good quality infrastructure, transportation and services. But since India is a huge country with quite a sizable population this problem still has not been addressed in totality. In order to improve the conditions of roads efforts began way back in the 1980s. It is during this time that roads were built to link major highways, to expand the width of existing roads and to construct important bridges. India has a total of about 2 million kilometers of roads out of which 960,000 kilometers are surfaced roads and about 1 million kilometers of roads in India are the poorly constructed ones. India is also home to Fifty-three National highways which carry about 40 percent of the total road traffic. Although the figures look pretty impressive but the underlying fact is that 25 percent of villages in India still having poor road links. The other problems faced by the Indian roads are; bad riding quality, poor geometrics, and insufficient pavement thickness. In India the responsibilities for road building and maintenance lies with the Central and state government. The administration of the national highway system is vested with the Ministry of State for Surface Transport in India and other state roads are preserved by the state public works departments. As far as the minor roads in the country are concerned they are up kept by the various districts, municipalities, and villages

Need For Study

In India, due to the large scale industrialization and commercial activities, there has been an unprecedented traffic growth during the last four decades. The high volume of vehicular traffic and increasingly heavy axle loads witnessed on Indian highways have brought the existing arterial road network to such a crippling stage that heavy investments are needed for restoring it to a desired serviceability level. This is a particular difficult situation, because pavements often are deteriorating faster than they are being corrected. Effective management of pavements is essential in these challenging times. Therefore, there is a need to link together explicitly the activities of planning, design, construction and maintenance of pavements.

The Road User Cost Study in India has established that due to improper maintenance and poor surface condition of road pavements, there is a considerable economic loss to the country due to increase in vehicle operation costs. If the road pavements are maintained to the desired level at an appropriate time, it is possible to save the losses in road user cost. In view of the budgetary constraints and the need for judicious spending of available resources, the maintenance planning and budgeting are required to be done based on scientific methods.

Pavement management System

General

A pavement management system (PMS) is a planning tool used to aid pavement management decisions. PMS software programs model future pavement deterioration due to traffic and weather, and recommend maintenance and repairs to the road's pavement based on the type and age of the pavement and various measures of existing pavement quality.

Measurements can be made by persons on the ground, visually from a moving vehicle, or using automated sensors mounted to a vehicle. PMS software often helps the user create composite pavement quality rankings based on pavement quality measures on roads or road sections. Recommendations are usually biased towards preventive maintenance, rather than allowing a road to deteriorate until it needs more extensive reconstruction.

Pavement Deterioration- Pavements tend to deteriorate very slowly during the first few years after placement and very rapidly when they are aged. Even though pavement designs and materials varied widely, the deterioration of pavements followed a standard curve.

This curve, pavement condition vs. age, is shown in the figure 1.1



Pavement Deterioration Curve

Objective of Study:

The aim of this study is to suggest establishment of a new system of pavement management in Hyderabad City. The basic purpose of pavement management system is to achieve best value possible for the available public funds and to provide safe, comfortable and economic transportation. The function of management at all levels involves comparing alternatives, coordinating activities, making decisions and seeing that they are implemented in an efficient and economical manner.

The intent of this Thesis is to present the development of a PMS for use with Hyderabad city roads in the state of Telangana.

LITERATURE REVIEW

The present paper is an effort in the similar direction, to develop a combined Overall Pavement Condition Index (OPCI) [1] for the selected network of Noida urban roads. The study area consists of 10 urban road sections constituting 29.92 km of Noida city near New Delhi, capital of India. The condition indicator used to represent the pavement condition [2] of selected urban road sections is, combined Overall Pavement Condition Index (OPCI). These indices were developed individually and were then combined together to form an OPCI giving importance of each indicator. The pavement condition data was collected in the year 2012. All the individual condition indices and the combined index ranged from the value 0 to 100

[7] The pavement condition was rated based these values as 0-10: Failed; 10-25: Very Poor; 25-40: Poor; 40-55: Fair; 55-70: Good; 70-85: Very Good; 85-100: Excellent. [8] [9] [10]

The minimum and maximum range of various pavement performance indicators observed on the study sections

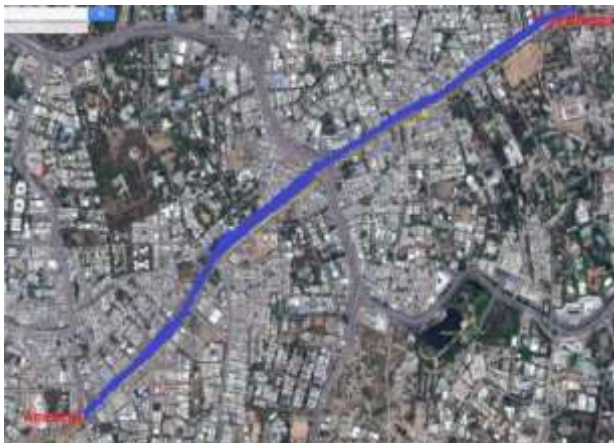
are: longitudinal cracking: 8.3% & 11.86%; transverse cracking: 2.23% & 6.61%; alligator cracking: 11.44% & 16.16%; patching: 43.78% & 12.0%, raveling: 9.58% & 29.24%; potholes: 1 & 6 nos.; IRI: 2.08 m/km & 5.41 m/km; deflection: 1 mm to 1.82 mm & SRV: 48 & 75 respectively.

Primary Survey

In this identification of pavement stretch in HYDERABAD was done by conducting field trips in Hyderabad and Cyberabad regions. Field Trips means direct on-fields observations to find the distress problems in each place. For this survey the following data was utilized:



Hyderabad Road Plan



Selected stretch from Ameerpet to Khairathabad Data collection & Analysis

Visual Rating Survey & Distress Evaluation:

The form used for noting location, degree and extent of the distresses in this survey is given in the end in Annexure-2.

There were three types of distresses observed in the study area:

- Ravelling
- Rutting
- Pot-holes

Pavement Excavation



Shows cross section of Pavement-Ameerpet to Punjagutta

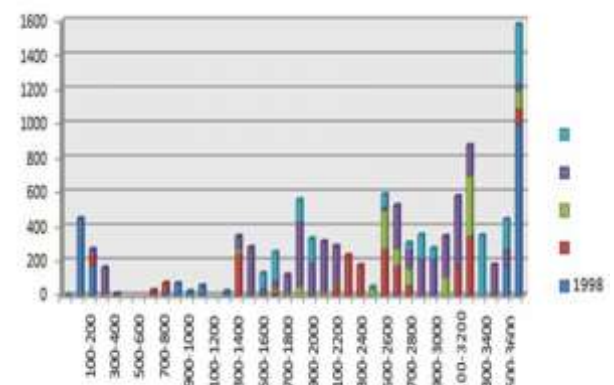
RESULTS

oad Inventory Data

Section	Carriageway Width		Shoulder Width		Median Width
	L.H.S	R.H.S	L.H.S	R.H.S	
Ameertpet	12.3m	10.62m	0.22m	0.33m	0.5m
Punjagutta	11.71m	11.69m	0.18m	0.27m	0.5m
Irrumanzil	8.1m	8.72m	0.1m	0.22m	0.5m
Khairathabad	14.81m	15.7m	0.31m	0.27m	0.5m

Visual Survey Raveling

As per the survey results the data is enclosed in the form of graph as shown below which reveals that severity levels verses chainage length of every 100.



Area of raveling of different severity levels Vs chainage

Cost of Repair works and Rehabilitation:

The cost of repair works is generally taken as 10% - 15% of the cost of new construction. As seen above, the expenditure required for repairing 1 Km road of width 7.5 m is Rs.8167750. Therefore the cost of repairing of 3.8 km long study area is about Rs 3103650. To sum up: Cost of reconstructing the study area: Rs. 26898300; and Cost of Repairing the study area: Rs. 3103650

Other than these direct costs, there are several indirect benefits, like vehicle maintenance costs, accident costs, etc. that are gained when the functional efficiency of road is improved. In order to optimize the funds, the MPI values should be followed to see which section needs to be repaired first. If these steps are followed carefully, we can get an efficient road network with optimum use of resources

5. CONCLUSIONS

- The minimum and maximum range of various pavement performance indicators are observed on the study sections are: longitudinal cracking: 8.3% & 11.86%; transverse cracking: 2.23% & 6.61%; alligator cracking: 11.44% & 16.16%; patching: 43.78% & 12.0%, Raveling: 9.58% & 29.24%, Deflection: 1mm to 1.82mm.
- Based on the survey Maintenance of pavements is not done regularly, overlays of pavements are going on without testing (i.e. Deflection testing). Continuous Overlays are done without reconstruction of Stretch.
- Quality reveals that Quality of materials also not up to the mark. Traffic growth is in high rate while design of overlays is not considering.
- Due to growth of traffic more considerations are taking into account for overlays. Thickness of Overlays also neglected.
- For Stretch One OPCI/R Reconstruction should do, if not maintenance cost will be too high.
- Width of the road is also varying from place to place due to this vehicular load is more at particular stretch and causes deterioration, due to improper drainage facility water get staged on roads and causes damage to roads, In rainy seasons its effect is severe.
- Pavement structural strength was found to be a crucial pavement condition indicator for changing the pavement performance and deciding the M&R strategy for selected urban pavement sections.

RECOMMENDATIONS

- Proper supervision to be taken on Entire Hyderabad City Road Network

- Quality of Materials Used In the Pavement is not up to the mark, GHMC has to control the Quality related Issues as per MORTH.
- Required Testing's to be done as per IRC before going for Overlays of Pavement
- Road widening to be done to control the Heavy traffic as per Standards, As Hyderabad Roads Consists of Narrow Roads.
- After completion Of Overlays drainage lids to be brought into the same level of pavement, due to this traffic flow is obstructed.
- For further Extension of this project by maintaining the data in software to implement maintenance periodically, Skid resistance and roughness also plays an key role ,so we can apply this get a good result.

REFERENCES

- Principles and practices of Highway engineering By Dr.L.R.Kadyali, Dr.N.B.Lal.Khanna Publications.
- U.S, Army (1982). Pavement Maintenance Management, Technical Manual TM 5-623.
- Zhang, Z., Singh, N. and Hudson, W. R. (1993b). Comprehensive ranking index for flexible pavement using fuzzy sets model. Transportation
- Optimum analysis of pavement maintenance using multi-objective genetic algorithms Author: Hakan Sahin, Paul Narciso, and Narain Hariharan
- Incorporation of Surface Texture, Skid Resistance and Noise into PMS
- Author: Alauddin, Mohammad Ahammed, M.A.Sc., P.Eng., Ph.D. Candidate Department of Civil and Environmental Engineering University of Waterloo
- IRC:37-2001 "Guide lines for the design of flexible pavements" (second revision) Indian Road Congress
- Morth 5th revision, for pavement design.
- Carey, W.N. and Irick, P.E. (1960). Pavement serviceability-performance concept.
- AASHO Road Test, Highway Research Board, 250, 40-58.
- FHWA (1990). An advanced course in pavement management systems, Course notes, Federal Highway Administration, Washington, D.C.
- Gharaibeh, N.A., Zou. Y. and Saliminejad, S. (2010). Assessing the agreement among pavement condition indexes. Journal of Transportation Engineering, ASCE, 136 (8), 765-772.
- Huang, Y.H. (1993). Pavement Analysis and Design. Prentice-Hall, Inc. a Paramount

Communication Company, Englewood, New Jersey, USA.

- Juang, C.H. and Amirkhanian, S.N. (1992). Unified pavement distress index for managing flexible pavements, *Journal of Transportation Engineering*, ASCE, 118 (5), 686-699.
- India, Highway Research Bulletin, Indian Roads Congress, 76, 55-69.
- U.S, Army (1982). Pavement Maintenance Management, Technical Manual TM 5-623.
- Zhang, Z., Singh, N. and Hudson, W. R. (1993b). Comprehensive ranking index for flexible pavement using fuzzy sets model. *Transportation Research Board*, TRR 1397, 96-102.
- Reddy, B.B. (1996). Development of failure criteria for flexible pavements, Ph. D.Thesis, Bangalore University, Bangalore.
- ❖ Noyce, D. A., H. U. Bahia, J. M. Yambo, and G. Kim. Incorporating Road Safety into Pavement Management: Maximizing Asphalt Pavement Surface Friction for Road Safety Improvements. Draft Literature Review and State Surveys. Midwest Regional University Transportation Center Traffic Operations and Safety (TOPS) Laboratory, April 29, 2005.
- *International Journal of Pavement Engineering*, <http://www.tandfonline.com/doi/full/10.1080/10298436.2012.657798>.
- Transport Canada. Canadian Motor Vehicle Traffic Collision Statistics 2004 and Road Safety in Canada: An Overview. Transport Canada Website <http://www.tc.gc.ca/> (Accessed on November 07, 2006).

PRELIMINARY ASSESSMENT OF BUS RAPID TRANSIT SYSTEM FOR URBAN ROADS

V Sampath Kumar¹, V. Ranjith Kumar², Dr.M.Kameswara Rao³

¹Research Scholar (M.Tech, T.E), ²Assistant Professor, ³Professor
Malla Reddy Engineering College (Autonomous), Kompally

Abstract: -- Bus rapid transit is applied to a variety of public transportation systems using buses to provide faster, more efficient service than an ordinary bus line. The goal of these systems is to approach the service quality of rail transit while still enjoying the cost savings and flexibility of bus transit. Those are Alignment in the center of the road to avoid typical curb-side delays, Stations with off-board fare collection to reduce boarding and alighting delay related to paying the driver. Station platforms level with the bus floor will reduce a boarding and alighting delay caused by steps and Bus priority at intersections to avoid intersection signal delay. In Hyderabad one of the most hectic Problems is traffic. Even though we have many roads, but do not have a proper traffic system. The rapid growth in the number of Motor vehicles has resulted in severe traffic congestions and air pollution not only in Hyderabad but also many cities of the country. To have traffic less end to reduce pollution, the BRT System should come in to the implementation. So, study has been made to make a project on BRTS to develop the BRT System in Hyderabad.

Keywords -- BRTS, Traffic congestion, Transportation, Level of Service.

I.INTRODUCTION

India is one of the largest and fastest growing economies in Asia and the entire world especially in transport. The transport is important for the development of a country. Growth of urban population has created serious challenges and imposed greater demand on the resources of municipal governments in India. The public transport remains the primary mode of transport for most of the population, and India's public transport systems are among the most heavily used in the world. The present transport system of India comprises several modes of transport including rail, road, coastal shipping, air transport, etc. Traffic in Indian cities generally moves slowly, where traffic jams and accidents are very

common. India population is more so where two wheeler and four wheeler vehicles are increase day by day, it causes to the traffic congestion and delays. It is seen not only one place, all over India.

Problems of public transport occur within the broader context of demoralizing urban transport problems in general. Air pollution, noise, congestion, and traffic fatality levels are often much more severe than those experienced in the developed countries. Transportation and basic infrastructure systems have not kept pace with urban growth, further disadvantaging the poor. Road systems are piecemeal, grossly overloaded and under maintained, while the number of motorized vehicles increased at extraordinary rate (World Bank, 2001; Figueroa, 1996). Public transportation, which tends to be fragmented between public authorities and a myriad of private carriers, cannot extend too many of improvised settlements because the quality of roads is bad.

National Urban Transport Policy has emphasized on more equitable allocation of road space to people, rather than vehicles, greater use of public transport and non-motorized modes and reserving lanes and corridors exclusively for public transport and non-motorized modes of travel.

Bus rapid transit (BRT, BRTS) is a bus-based mass transit system. A true BRT system generally has specialized design, services and infrastructure to improve system quality and remove the typical causes of delay. Sometimes described as a "surface subway", BRT aims to combine the capacity and speed of light rail or metro with the flexibility, lower cost and simplicity of a bus system.

2 Need for the Study

In India, the growing trend toward private transportation increases congestion. With the phenomenal increase in the personalized motor vehicles, one of the major problems confronted by the motorist is the occurrence of traffic delay. Roads are getting congested. Indian government should pass legislation to control vehicles on roads and enforce tougher environmental regulations. With the majority of World Bank funds allocated toward transportation and highways, the government should adopt the latest technology and introduce metro rail, monorail to reduce congestion and accidents on roads. But still road users have face traffic problem like congestion, predictable travel-time delays and road

accidents are taking a serious shape. The study of BRT system helps to reduce the wastage of time, increase the economic health, to reduce the pollutants released from

vehicles, to reduce frustration developed in drivers. The best example is Ahmedabad bus rapid transport system.

3. Objectives of the Study

The main objectives of the present study are presented below

- To relieve the traffic congestion.
- To analyze the present traffic condition.
- To provide good level of service during the peak hours.
- To encourage people to opt for public transportation for the welfare of government.
- To present BRTS as a clean, modern, fast, safe, and reliable transportation solution to the public.
- Better quality, better service and providing value for the investment.

4 Bus Rapid Transit System (BRTS):

Bus rapid transit system is a “bus based mass transit system that delivers fast, comfortable, and cost effective urban mobility” this system have separate lane for buses. The ‘Rapid Transit’, which describes a high- capacity transport system with its own right-of-way, implemented using buses through infrastructural and scheduling improvements, to provide a high level of service. It incorporates most of the high quality aspects of metropolitan systems without the high investments, it uses available space on arterial roads of cities with dedicated bus ways and it utilizes modern technologies for optimizing flow, passenger movement, ticketing, bus scheduling, and traffic signal priority. Bus Rapid Transit system as an approach to providing superior transit service with buses that integrate technology, an operating plan (or service design), and a customer interface.

Historical Development of BRTS

BRT has now become a worldwide phenomenon; its current operation area around the world.

BRTS in World: The first wide scale development of Bus Rapid Transits started in Curitiba, Brazil in 1974, although there were several smaller scale projects prior to its development. Since then, Curitiba’s experience has inspired other cities to develop similar systems. In the 1990s, the replication of the BRTS concept gained

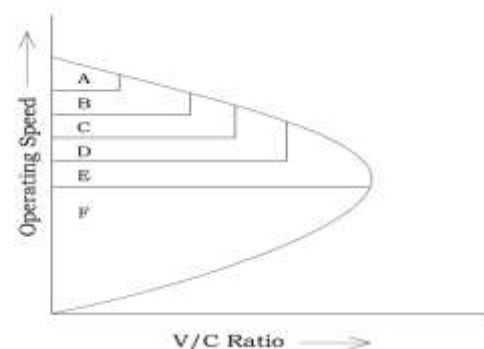
momentum and BRTS were opened in Quito, Ecuador (1996), Los Angeles, USA (1999) .in year 2000 the Transmilenio system in Bogotá, Colombia was opened and get a grand success, after the successes of

Transmilenio system Bogotá the concept of BRTS is adopted worldwide. Moreover 100 BRT systems was running success fully around the world & approximately 150 series are under construction.

BRTS in India: In India, it has become operational so far in cities like Delhi, Ahmadabad, Jaipur, Indore, Pune, Bhopal Vijayawada and Rajkot, covering a total network of over 120 km. The investment involved till now in the development of BRTS in these cities would come upto more than Rs.13.6 billion. Expansions of the BRTS network in these six cities are either already in progress or are being planned. Moreover, six new BRTS projects are already underway in cities like Kolkata, Hubli-Dharwar, Surat, Visakhapatnam, Naya Raipur and Pimpri-Chinchwad.

Level of service

Level-of-Service (LOS) of a traffic facility is a concept introduced to relate the quality of traffic service to a given flow rate. Level-of-Service is introduced by HCM to denote the level of quality one can derive from a local under different operation characteristics and traffic volume. HCM proposes LOS as a letter that designates a range of operating conditions on a particular type of facility. Six LOS letters are defined by HCM, namely A, B, C, D, E, and F, where A denote the best quality of service and F denote the worst. These definitions are based on Measures of Effectiveness (MoE) of that facility. Typical measure of effectiveness includes speed, travel-time, density, delay etc. There will be an associated service volume for each of the LOS levels. A service volume or service flow rate is the maximum number of vehicles, passengers, or the like, which can be accommodated by a given facility or system under given conditions at a given LOS.



Level of service A to F

5 LITERATURE REVIEW

Agarwal P K, Sharma Anupama, Singh A. P (2010), “An Overview on Bus Rapid Transit System”. An important advantage of BRTS is its flexibility. This

approach lends itself to incremental learning of the problem, and eliminating mistakes as the development proceeds. The relatively low implementation costs also don't leave taxpayers tied to one particular technology or solution. The commuters prefer to board/alight at intersections, thus creating informal bus stops which cause hazardous Traffic conditions; it is advisable to plan the facilities as per the commuters' requirements. Kerbs dividing the lanes may lead to accidents without physical kerbs but the lane segregation will not be possible without the kerb stones these can be suitably redesigned to take care of safety aspect. The signal system should be resorted to at the junctions to minimize the merging/ weaving of the traffic.

Anuj Jaiswal, K. K. Dhote, R. Yadu Krishnan, Devansh Jain (2012). Bus rapid transit system: a milestone for sustainable transport: a case study of janmarg BRTS, Ahmedabad, India. BRTS Ahmedabad has improved access for local riders and advanced public transportation systems while reducing the environmental impacts of transportation. Under the 'Regular bus operations' the quality of bus services tends to deteriorate after certain level of operations. BRTS will also improve operating conditions for personalized vehicles. The various contributing factors towards this are: segregated traffic, improved road surface quality, better lighting, and junction improvements and shifting a part of heavy traffic to outer ring road. Some of the BRT corridors are presently highly accident prone. With traffic segregation, exclusive pedestrian and bicycle facilities, better illumination, effective regulation, training and public education, accidents on these roads are likely to come down by 75 to 90%.

Tuhin Subhra Maparu and Debapratim Pandit (2010). A Methodology for Selection of Bus Rapid Transit Corridors: A Case Study of Kolkata. The paper aims at formulation of a methodology for selection of corridors for introduction of BRTS in urban areas in India and Kolkata in particular in the context of present challenges like increasing traffic congestion and car ownership, lack of road and transport infrastructure and gradual deterioration of LOS of bus transit system. A methodology and planning framework for selection of BRT corridors for bus transit reform and redesign in urban areas in India and Kolkata in particular in the context of the present challenges of increasing traffic

congestion, car ownership, and lack of road and transport infrastructure and gradual deterioration of LOS of bus transit system. Incorporation of feasibility constraints both for selection and phasing of BRT corridors would enable planners and decision makers to

make more informed decisions about implementing BRTS in Indian cities.

Study Area

Primarily the corridor selection is made on the basis of the traffic volume in the city, the people in the corridor suffering from heavy traffic, traffic jams and traffic congestions may make use of BRTS. The Selected corridor is from Panjagutta to Miyapur (via Kukatpally) is shown in Fig.3.10 which has NH9. The total distance of this stretch is 14km. This is completely commercial area with 15 stops. These are Panjagutta, Ameerpet, Mitrivanam, S.R nagar, E.S.I, Erragadda, Bharath nagar, Moosapet, Kukatpalli, KPHB, JNTU, Nijampet cross road, Hider Nagar, Calvary Temple and Miyapur cross road. This corridor consists of 5 junctions they are,

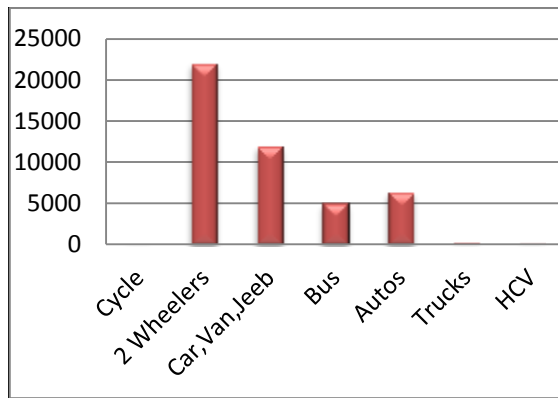
1. Panjagutta
2. Mitrivanam
3. Moosapet Y-Junction
4. JNTU
5. Miyapur.



Map of selected corridor in Hyderabad

In areas of Panjagutta, Ameerpet, Kukatpalli and KPHB, there is more shopping complex. Mitrivanam, S.R Nagar areas have educational areas and Jawaharlal Nehru Technology University is located in JNTU area, E.S.I Hospital is located in E.S.I stop, Raithubazar and Fruit market are there in Erragadda stop. People who are going to BELL, Patancheru and ligampalli areas, they use the way on JNTU, Miyapur Cross roads only and this stretch connects to the industrial areas like Balanagar, Bell. Because of these conditions, this stretch is having more traffic jams and delays.

Observations and results on traffic in Panjagutta to Miyapur



Traffic volume at Panjagutta

PEAK HOURS	BUS	AUTOS	TRUKS	HCV
MORNING				
7.30-7.45	88	68	13	15
7.45-8.00	84	72	7	12
8.00-8.15	122	94	8	11
8.15-8.30	131	115	0	2
8.30-8.45	196	168	6	9
8.45-9.00	232	183	4	18
9.00-9.15	228	214	12	4
9.15-9.30	247	311	15	3
9.30-9.45	253	380	11	5
9.45-10.00	189	360	8	9
10.00-10.15	208	340	12	12
10.15-10.30	193	296	3	14
SUM	2171	2601	99	114

PEAK HOURS	BUS	AUTOS	TRUKS	HCV
EVENING				
4.00-4.15	191	230	8	0
4.15-4.30	195	245	12	15
4.30-4.45	184	265	5	7
4.45-5.00	169	298	15	6
5.00-5.15	191	315	18	0
5.15-5.30	238	324	23	0
5.30-5.45	222	272	9	7
5.45-6.00	346	351	5	4
6.00-6.15	289	395	0	1

6.15-6.30	334	410	0	0
6.30-6.45	249	381	15	0
6.45-7.00	278	344	5	0
SUM	2886	3830	115	40

CONCLUSIONS

1. As there is heavy traffic in the stretch from Panjagutta to Miyapur. The level of service is F condition in Panjagutta, Ameerpet, Mitrivanam areas which is known to be Fully Congested. After applying BRTS, the condition will change from F to B or C condition.
2. Level of service is E condition in Bharath nagar, Moosapet areas which is known to be congested. After applying BRTS, the condition will change from F to B or C condition.
3. Level of service is D condition in SR Nagar, Erragadda, JNTU, Miyapur areas which is known to be unstable flow. After applying BRTS the condition will change from D to B condition.
4. Where provide good level of service during the peak hours, it provides good level of service during the peak hours.
5. It gives the better quality, better service and providing value for the investment.
6. It presents as a clean, modern, fast, safe, and reliable transportation solution to the public.
7. Increasing ridership attraction.

RECOMMENDATIONS

1. Construct foot over bridge to reduce pedestrian crossing on road, which increases the moving time of traffic.
2. Elevated BRT System is suitable for areas having 2, 3 lanes and lesser road width with highly traffic.
3. Provide footpath for pedestrians.
4. No permission should be given to road side vendors and stalls.
5. Market should be allotted a place far away from the road side.
6. RTO should give limited permission to two wheelers per house.
7. Different timings should be allotted for opening and closing of different public, private and educational centers.

FUTURE SCOPE

At present Hyderabad has more traffic related problem. This study has a lot of scope to prevent traffic delays and

road accidents in future. This study was limited for Panjagutta to Miyapure area but same kind of work is recommended to remaining areas to reduce traffic delays and rate of road accidents. This kind of study is suitable for any area in the Hyderabad and any city in India.

REFERENCES

1. Agarwal P K, Sharma Anupama and Singh A. P (2010), "An Overview on Bus Rapid Transit System", Journal of Engineering Research and Studies.
2. Anuj Jaiswal, K. K. Dhote, R. Yadu Krishnan and Devansh Jain (2012). Bus rapid transit system: A mile stone For Sustainable Transport: A Case
3. Study of Janmarg Brts, Ahmedabad, India, OIDA International Journal of Sustainable Development.
4. Tuhin Subhra Maparu and Debapratim Pandit (2010), "A Methodology for Selection of Bus Rapid Transit Corridors: A Case Study of Kolkata", Institute of Town Planners, India Journal.
5. Madhuri Jain, Arti Saxena, Preetvanti Singh and P.K. Saxena. "Developing bus rapid transit system in India".
6. Devarshi Chaurasia (2014). "Bus Rapid Transit System (BRTS): A Sustainable Way of City Transport (Case Study of Bhopal BRTS)", International Journal of Engineering and Advanced Technology.
7. Geetam Tiwari, Dinesh Mohan, Sandeep Gandhi, B. Sriram, Sonia Kapoor, Ruchi Verma, Dheeraj Gupta, Mahesh Gaur (2005), "First Delhi brt corridor, A design summary Ambedkar nagar to Delhi gate". Transportation Research and Injury Prevention Programme.
8. Bhanu Kireeti Chanda & Addali Sai Satya Goutham (2014), "Introduction to corridor selection & assessment for Bus Rapid Transit System (BRTS) in Hyderabad, American Journal of Engineering Research (AJER).
9. H.S. Kumara (2009), "Planning for Bus Rapid Transit System in Indian Metropolitan Cities: Challenges and options", Institute of Town Planners, India.
10. Ajay Mishra, Saxena Anil Kumar, Purohit Pradee, "Study of Bus Rapid Transit system In Respect to Growing Cities of India", International Journal of Engineering Research & Technology.
11. "Hyderabad Wikipedia".
12. "Hyderabad Google Map".
13. "Principles and Practice of Highway Engineering" by Dr.L.R.Kadiyali, Dr.N.B. Lal, Khanna publishers Delhi-6.
14. S.C.Wirasinghe, L. Kattan, M.M. Rahman, J. Hubbell, R. Thilakaratne and S. Anowar, "Bus rapid transit – a review", International Journal of Urban Sciences, 2013.
15. Darshit M. Shah, Deepa Akshay Patel, "Impact of Brts on Urban Traffic a Case Study of Ahmedabad" GRA – Global Research Analysis.

ESTIMATION OF LEVEL OF SERVICE AT SUCHITRA AND KUKATPALLY INTERSECTIONS

B Arjun¹, A.Nagasaibaba², Dr.M.Kameswara Rao³

¹Research Scholar (M.Tech, T.E), ²Assistant Professor, ³Professor
Malla Reddy Engineering College (Autonomous), Kompally

Abstract: -- Delay is one of the principal measures of performance used to determine the level of service (LOS) at signalized intersections and several methods have been widely used to estimate vehicular delay. Very few studies only have been carried out to estimate delay at signalized intersections under mixed traffic conditions prevailing in developing countries like India. In the present study various problems associated with delay estimation under mixed traffic conditions in a developing country (India) and the methods to overcome them were discussed and an attempt was made to improve the accuracy estimating the same.

Uncontrolled intersections are vital points on urban roads, the performance of which will influence the traffic flow on entire network. Delays to vehicles at urban uncontrolled intersections depend upon the several factors, the most important among these being major road approach volume, type of turning movement, and vehicular composition. The average delay caused to vehicles is an important measure to evaluate the performance of uncontrolled intersections. The performance of an uncontrolled intersection is described by the service delay experienced by low priority movements. Under mixed traffic conditions, the traffic compositions, apart from the conflicting traffic volume and proportion of turning traffic are vital factors influencing the service delay. Most of the earlier studies conducted on this subject, pertain to homogeneous traffic environment, and only a few studies with limited scope have been

conducted under mixed traffic conditions. In this study, the service delay models have been developed for three uncontrolled intersections located in the city. These models developed were found to be statistically and logically sound. The level of service for the uncontrolled intersections taken under the study has been evaluated using the estimated average service delays from the models developed

Keywords -- Delay, Signalized intersections, Mixed Traffic, Saturation Flow, LOS.

I.INTRODUCTION

Uncontrolled intersections are the intersections which function without any priority assigned to the traffic on any of the intersecting roads, no control (neither STOP signs nor Police-controlled) and the traffic is of heterogeneous nature. These intersections are vital nodal points on urban roads, the performance of which will influence the traffic flow on entire network. Delays to vehicles at urban uncontrolled intersections depend on several factors. The most important among these being the major road approach volume, type of turning movement, and vehicular composition. The extent of intersection of these factors and their collective effect on delay caused to vehicles need to be studied in detailed for better traffic management at these intersections. Field studies due to resources constraint may not include all these, the limited samples that might be obtained will be sufficient to evaluate the effect of various parameters.

At uncontrolled intersections in the absence of indication of specific time intervals to each of the streams of traffic to cross the intersection, the drivers look for gaps and cross the intersections. In developing countries like India, in the absence of the concept of major and minor roads in traffic regulation schemes, vehicles approaching the intersections through all roads, on arrival; assume that equal right to enter the intersection. This has made the traffic situation at the uncontrolled intersection highly complex causing considerable delay to traffic. The delay experienced by vehicles is probably most

desirable criteria based on which the performance of the uncontrolled intersection can be evaluated.

Objectives of the Study:

- To establish mathematical relations for service delay to the different types of vehicles for a priority movement at uncontrolled intersections
- To develop the readily usable mathematical model, to estimate the service delay caused to the subject vehicles at urban uncontrolled intersections, considering interactions of various categories of vehicles under heterogeneous traffic environment.
- To evaluate the performance of uncontrolled intersections based on the average service delay.
- To conduct the traffic and delay studies at signalized intersections to evaluate the performance of the signalized intersection
- To determine the aggregate delay of the intersection.
- To establish the level of service (LOS) of the Signalized intersection.
- To analyze the delays and draw meaningful inferences.

LITERATURE REVIEW

Unsignalized intersections make up a great majority of at-grade junctions in any street system. Stop and yield signs are used to assign the right-of-way, but drivers have to use their judgment to select gaps in the major street flow to execute crossings and turn movements at two-way and yield controlled intersections. Two methods are discussed in this section: HCM (2000) Delay method and Blunden's (1961) method.

William (1977) presented a simple and accurate technique for measuring vehicular delay on an approach to a signalized intersection. Precise definitions were established for four measures of performance: stopped delay, time-in-queue delay, approach delay and percentage of vehicles stopping and interrelationships among the four measure of performance were established.

Ternus et al. (1977) developed a procedure for measuring load factor and to determine relationship between load factor, peak hour factor and delay. In this study three locations are considered, volume counts are measured by two methods, one is manual and another is by traffic flow analyzer. A manual counter was used for comparison with the manual volume counts and also to compute peak hour factors. The traffic flow analyzer is used to measure the delay more accurately than with traditional methods with less difficulty and expense. The relation among load factor, constant split ratio and constant flow was calculated from the graph drawn

between constant split ratio, constant flow and load factor.

Sosin (1980) has done empirical investigations of delays at some chosen intersections in Poland using time lapse photography technique. The effect of composition of traffic upon delays was also studied and passenger car units estimated using simulation along with the delay observations. The results of the study were compared with the delay models such as Webster and Miller's approach.

Hurdle (1984) presented a paper to serve as a primer for traffic engineers who are familiar with capacity estimation techniques but have not made much use of delay equations. It was noted that the methods available at that time either ignore the way in which the delay vary with the time or try to cope with the variation in ways that are more mathematical application of common sense than mathematical models of traffic signal system. He found that none of the models examined can be expected to give really consistent and accurate results. To obtain such results, one would not need just better models but better information about traffic patterns.

DATA COLLECTION

In order to study the service delay (delay experienced by a vehicle at the reference line), intersections located in city were selected. These intersection sites were in urban areas. But the effect of upstream junctions, on-street parking, or bus stops on arrival rate is negligible. An important traffic feature at all the three intersections was that the queue formation on the minor street approaches was very rare. One of the three intersections is of T-type and the remaining two were four legged.

As a part of delay study, at each intersection, data were collected by video recording technique on a typical weekday. The video camera was placed at a suitable vantage point near the intersection to record an unobstructed view of all approaches and turning movements and data were recorded for about 1hr to 2 hr depending upon the significant sample of vehicle type. The recorded video file was played in the laboratory several times to get the conflicting traffic volume count and the service delay experienced by each subject vehicle. Both crossing and merging types of conflicts were taken into account while noting the conflicting traffic for each maneuver during the data extraction process.

Methodology

Two signalized intersections located in an industrially fast developing city located in Hyderabad, India were chosen for the present study. All of them are four legged isolated type, provided with pre timed signal control operating in four phases with permitted left turns. These study intersections were selected in such a way that they have fair geometry (level gradient on all the approaches) and there is least interference to traffic by pedestrians, bus stops and parked vehicles etc. Average driving behavior was assumed and the condition of vehicles was assumed to be moderate. The traffic is highly heterogeneous in nature with poor observance of lane discipline. The composition of traffic consists of a large proportion of motorized two wheelers, a small percentage of auto rickshaws, cars and very smaller proportion of heavy vehicles. Layout of all the five study intersections showing the geometry.

Analysis of Suchitra Junction Data

➤ Measurement of Saturation Flow

$$\text{saturation headway} = \frac{\text{total saturation green time}}{\text{no. of vehicles}}$$

$$\text{Saturation Flow} = \frac{3600}{\text{Saturation Headway}}$$

➤ East Bound:

Total saturation green time = 285 sec

No. of vehicles = 561

Saturation headway = (285/561)

= 0.5

Saturation flow = (3600/0.5)

= 7086 veh/hr.

➤ West Bound

Total saturation green time = 265 sec

No. of vehicles = 457

Saturation headway = (265/457)

= 0.58

Saturation flow = (3600/0.58)

= 6208 veh/hr.

➤ North Bound

Total saturation green time = 275 sec

No. of vehicles = 482

Saturation headway = (275/482)

= 0.571

Saturation flow = (3600/0.571)

= 6304 veh/hr.

➤ South Bound

Total saturation green time = 282 sec

No. of vehicles = 542

Saturation headway = (282/542)

= 0.52

Saturation flow = (3600/0.52)

= 6923 veh/hr.

Time-in-Queue Calculation

➤ East Bound:

Vehicles in Queue for East Bound

No. of cycles	Time interval	No. of vehicles in queue
1	20	94
2	20	96
3	20	98
4	20	112
5	20	108
6	20	98
7	20	105

Total no. of vehicles in queue =

$$\sum V_{iq} = 94 + 96 + 98 + 112 + 108 + 98 + 105 = 711$$

Total vehicles passing through the approach = V_{tot}
= 615

$$\text{Time-in-queue per vehicle} = I_s * \frac{\sum V_{iq}}{V_{tot}} * 0.9$$

Therefore

$$\text{Time-in-queue} = diq = 0.9 \times [20 \times (711/615)] = 20.8 \text{ sec.}$$

No. of vehicles stopped = $V_{stop} = 346$

$$FVS = (346/615) = 0.562$$

No. of vehicles stopping per lane each cycle = $\frac{V_{stop}}{N_c \cdot N}$

$$= \frac{346}{7 \times 2} = 24.71$$

$$\text{Acceleration-deceleration delay} = 0.562 \times 2$$

$$= 1.12 \text{ sec}$$

$$\text{Therefore control delay} = \text{time-in-queue} + \text{acceleration-deceleration delay}$$

$$= 20.8 + 1.12$$

$$= 22 \text{ sec/veh.}$$

➤ West Bound

Vehicles in Queue for West Bound

No. of cycles	Time interval	No. of vehicles in queue
1	20	75
2	20	76
3	20	78
4	20	77
5	20	69
6	20	83
7	20	74

$$\begin{aligned} \text{Total no. of vehicles in queue} &= \sum V_{iq} \\ &= 75+76+77+69+83+74 \\ &= 532 \end{aligned}$$

$$\begin{aligned} \text{Total vehicles passing through the approach} &= V_{tot} \\ &= 506 \end{aligned}$$

$$\text{Time-in-queue per vehicle} = I_s * \frac{\sum V_{iq}}{V_{tot}} * 0.9$$

Therefore

$$\begin{aligned} \text{Time-in-queue} &= diq = 0.9 \times [20 \times (532/506)] \\ &= 18.91 \text{ sec.} \end{aligned}$$

$$\text{No. of vehicles stopped} = V_{stop} = 296$$

$$FVS = (296/506) = 0.585$$

$$\text{No. of vehicles stopping per lane each cycle} = \frac{V_{stop}}{N_c \cdot N}$$

$$\begin{aligned} &= \frac{296}{7 \times 2} \\ &= 21.14 \end{aligned}$$

$$\text{Acceleration-deceleration delay} = 0.585 \times 2$$

$$= 1.2 \text{ sec}$$

$$\text{Therefore control delay} = \text{time-in-queue} + \text{acceleration-deceleration delay}$$

$$= 18.91 + 1.2$$

$$= 20.07 \text{ sec/veh.}$$

Conclusions

From analysis of results and observation of traffic characteristics the following conclusions are drawn.

- Following the above mentioned criteria study intersection 1 i.e., Suchitra Junction has an aggregate delay of 21.2 sec/veh.
- Based on the aggregate delay the Level of Service at the intersection 1 i.e., Suchitra Junction is LOS "C".
- Following the above mentioned criteria study intersection 2 i.e., Kukatpally Junction has an aggregate delay of 35.62 sec/veh.
- Based on the aggregate delay the Level of Service at the intersection 2 i.e., Kukatpally Junction is LOS "D".

Scope for Further Work

For better understanding of the methodology, the data should be considered from morning to evening. The acceleration and deceleration delay can be measured directly from the field. By using HCM methodology in this present study reliable results are obtained. Besides HCM methodology, other delay models should also be modified under the heterogeneous road traffic condition to estimate delays for oversaturated conditions. Moreover by considering the variability of delay, more reliable signal control strategies may be generated resulting in improved level of service.

REFERENCES

- SU Yuelong, WEI Zheng, CHENG Sihan, YAO Danya, ZHANG Yi and LILi (2009), "Delay Estimates of Mixed Traffic Flow at Signalized Intersections in China" Tsinghua Science and Technology, Volume 14, Number 2, April 2009.
- YusriaDarma, Mohamed Rehan Karim, Jamilah Mohamad andSulaiman Abdullah (2005)," Control Delay Variability at SignalizedIntersection based on HCM Method", Proceedings of theEastern Asia Society for Transportation Studies, Vol. 5, pp. 945-958, 2005.
- Reilly, W. R. and Gardner, C. C. (1977), "Technique forMeasurement of Delay at Intersections", TransportationResearch Record 644,

- TRB, National Research Council, Washington, D.C., pp. 1-7.
- Hurdle VF, (1984) "Signalized intersection delay models – Aprimer for the uninitiated", Transportation Research Record 971. pp 96-105.
 - Lin, Feng-Bor (1989), "Application of 1985 Highway Capacity Manual for Estimating Delay at Signalized Intersections", Transportation Research Record 1225, TRB, National Research Council, Washington, D.C., pp. 18 -23.
 - Teply, S. (1989), "Accuracy of Delay Surveys at Signalized Intersections", Transportation Research Record 1225, TRB, National Research Council, Washington, D.C., pp. 24-32.
 - Dowling, R. G. (1994), "Use of Default Parameters for Estimating Signalized Intersection Level of Service", Transportation Research Record 1457, TRB, National Research Council, Washington, D.C., pp. 82-95.
 - Arasan, T. V. and Jagadish, K. (1995), "Effect of Heterogeneity of Traffic on Delay at Signalized Intersections", Journal of Transportation Engineering, ASCE, Volume 121, No.4. pp. 397-404.
 - Braun, S. M. and Ivan, J. N. (1996), "Estimating Approach Delay Using 1985 and 1994 Highway Capacity Manual Procedures", Transportation Research Record 1555, TRB, National Research Council, Washington, D.C., pp. 23-32.
 - Ko J, Hunter M, and Guensler R. (2007), "Measuring Control Delay Using second-by-Second GPS Speed Data", Transportation Research Board 86th Annual meeting compendium of papers TRB 2007.
 - Maini P and Khan S. (2000), "Discharge characteristics of heterogeneous traffic at signalized intersections". Proceedings of fourth International Symposium on Highway Capacity 2000; 258–270.
 - Chandra, S and Kumar, U. (2003) "Effect of Lane Width on Capacity under Mixed Traffic Conditions in India", Journal of Transportation engineering ASCE, Volume 129, No.2, pp.155-160.
 - Md Hadiuzzaman, Md Mizanur Rahman and Md Ahsanul Karim. (2008), "Saturation Flow Model at Signalized Intersection for Non-lane Based Traffic" Canadian Journal of Transportation volume 2, Part 1. pp.78-90
 - Jenish Joseph and Gang-Len Chang. (2005), "Saturation Flow Rates and Maximum Critical Lane Volumes for Planning Applications in Maryland" Journal of Transportation engineering ASCE, Volume 131, No.12. Pp.946-952. Highway Capacity Manual. Transportation Research Board 2000.
 - Bhuyan, P.K and Krishna Rao, K.V. (2011), "Application of GPS and Clustering Techniques in defining LOS Criteria of Signalized Intersections for Indian Cities" Highway Research journal, Indian Roads Congress, New Delhi. Volume 4. No.1. Pp.69-75.
 - Aloysius Tjan and Ria Sujoto (2008), "Verification of HCM2000 Delay Equation on a Ideal Signalized Junction in Bandung" (Junction of Asia Afrika And Tamblong) Proceedings of the Eastern Asia Society for Transportation Studies, Vol.4, October, 2003. pp.583-595.
 - R. Prasanna Kumar and G. Dhinakaran (2012), "Estimation of delay at signalized intersections for mixed traffic conditions of a developing country" International Journal of Civil Engineering, Vol. 11.



Industrial solid waste landfill leachate treatment using electrocoagulation and biological methods

Dheeravath Bhagawan^a, Saritha Poodari^b, Narala Chaitanya^a, Surya Ravi^a, Yamuna M. Rani^a, Vurimindi Himabindu^{a,*}, S. Vidyavathi^c

^aCentre for Environment, Institute of Science and Technology, Jawaharlal Nehru Technological University, Hyderabad, India -500 085, Tel. 9441184024, email: bhagawanist@gmail.com (D. Bhagawan), Tel. 9441184024, email: naralachaitanya.biotech@gmail.com (N. Chaitanya), ravisurya1990@gmail.com (S. Ravi), Tel. 9030918640, email: Yamuna.m218@gmail.com (Y.M. Rani), Tel. +91 9849693828, email: drohimabindu@gmail.com, bhagawanist@gmail.com (V. Himabindu)

^bCivil Engineering Department, Malla Reddy Engineering College (A), Hyderabad, India -500 085, Tel. 9849332474, email: cesarithap@mrec.ac.in

^cDepartment of Civil Engineering, JNTUH College of Engineering Hyderabad, Jawaharlal Nehru Technological University, Hyderabad, India - 500 085, Tel. 9392493533, email: vidyasom@yahoo.co.in

Received 23 March 2016; Accepted 1 November 2016

ABSTRACT

This paper aims to provide a treatment approach to the landfill leachate using electrochemical (EC) method and bio gas generation. The study mainly focused on the affecting parameters of the EC process, such as electrode material, initial pH, applied voltage, inter electrode distance, electrode reactive surface and insituperoxi-EC. The pH-7 has been observed to be the best for the removal of metals. Fe–Fe electrode pair with 1cm inter-electrode distance and electrode surface area of 40 cm² at an applied voltage of 7 V has been observed to be more efficient in the metal removal. The maximum removal percentage of the Ni, Zn, Pb, Cu, Fe and COD have been observed to be 95, 99.6, 98, 97.2, 73 and 60% respectively along with 13.4% of bio-hydrogen. Treatment cost also evaluated. This method has been observed to be very effective for the of landfill leachate.

Keywords: Land fill; Leachate; Electrocoagulation; Heavy metal; Bio-fermentation; Hydrogen

1. Introduction

Growing trend in global population, urbanization and industrialization towards achieving high quality of life and well-being of the population has resulted high amount of solid wastes being generated. The developing country like India has to develop the sustainable technology to manage industrial solid waste. The current solid waste disposal method is secure land filling. However, leachate is a promising problem from that land filling site, which has serious than that of industrial wastewater to the ecosystem [1] and contains both biodegradable

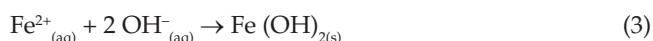
and resistant organic compounds, heavy metals, suspended solids, chlorinated compounds and inorganic salts and exhibiting acute and chronic toxicity [2]. Some of the treatment methods such as biological treatment methods [3], membrane processes [4], advanced oxidation techniques [5], coagulation–flocculation methods [6], lagoon and wetland applications [7] have been examined in the literature. Because its characteristics change with advancing years of the landfill, these test methods have troubles such as decreasing treatment efficiencies and increasing cost [5,8]. Therefore, the implementation of a joint treatment comprising of a few treatment steps has been used to solve the problem. The electrochemical method followed by biological expected to be sufficient to treat such type of complex liquids.

*Corresponding author.

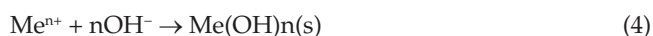
Electrocoagulation (EC) presents a robust novel and innovative alternative in which a sacrificial metal anode doses water electrochemically, which is applied for the treatment of many type of industrial wastewaters [8].

The reactions occurring in an electrochemical cell involving Iron (Fe) electrodes are as follows:

Reactions:



Fe metal ions immediately form hydroxides and/or poly hydroxides that finally transform into $\text{Fe}(\text{OH})_2$ (S), as shown in Eqs. (1) and (3) (electrocoagulation). Hydroxides have strong affinity to capture the pollutants in the waste water, causing more pollutant removal than those conventional methods. Eq. (2) involves electro oxidation phenomena [9,10].



The metal hydroxide floc formed from Fe electrode normally acts as adsorbents and/or traps for metal ions. Therefore, they would eliminate them from the solution. Simultaneously, the hydroxyl ions produced at the cathode increase the pH in the electrolyte and may induce co-precipitation of Fe, Cu, Pb, Ni, and Zn in the form of their corresponding hydroxides [Eqns. (3), (4)][9,11].

The organics present in the leachate will not be completely removed with single electrocoagulation method, however, addition of oxidizing agents can enhance the removal of organics. Hydrogen peroxide is most often used as chemical oxidant to improve the radical formation to degrade the organic pollutants.



With peroxide dosage the enhanced production of hydroxyl radicals [Eq. (5)] would degrade organic matter in the landfill leachate effectively [12].

Further, a combined electrocoagulation-biological treatment system results in high organic matter removal efficiency since it reduces the processing time and supply of water for dilution. Moreover, biological fermentation of organics with mixed consortia is also advantageous as it generates clean and renewable energy carrier gas at low-cost, thus attracting worldwide attention to sustain the future energy resources.

In the present study, the efficiency of electrocoagulation for the treatment of land fill leachate has been reported. The effect of electrode material, initial pH, applied voltage, inter electrode distance, reactive electrode area and insituperoxi EC on the treatment efficiency has been explored and discussed to determine the optimum operational conditions. Biological treatment has also been applied to enhance the COD removal at optimized electrocoagulation. The operating cost of treatment is also investigated, by considering the cost of consumption of electric power and electrode.

2. Material and methods

2.1. Electroplating wastewater

Leachate has been collected from land filling site in Hyderabad, India. The initial characterization of the sample has been given in Table 1.

2.2. Methodology

Batch mode experiments have been carried in a 250 ml beaker with the working volume of 200 ml at room temperature (27°C). The three electrode materials (Fe, Al and stainless steel) have been used as anode and cathode with dimensions of 100 mm × 50 mm × 2mm. The pH of the leachate varied from 5–11 (4, 6 and 8), effective reactive surface area studied between 10–40 cm² (10, 20 and 40 cm²), distance between electrodes studied between 1–4 cm (1, 2 and 4 cm) and effect of applied voltage had been studied at 4 and 7 V, respectively. The adjustment of pH is made with 0.1 N/1.0 N solution of HCl or 0.1 N/1.0 N NaOH. Working electrodes are connected to a DC power supply (APLAB regulated DC power supply L6403) unit with 0–84 V voltage supply capacity. Hydrogen peroxide is added to the electrocoagulation unit at above optimized conditions dosages with variation of peroxide from 250–1250 ppm. The samples are collected at an interval of 10 min for 30 min and analyzed for pollutant content.

To enhance the organic matter removal, anaerobic biological fermentation in batch mode is combined with EC. The 320 ml batch reactor with working volume of 250 ml used for biological treatment of the leachate at room temperature under anaerobic conditions.

The active microbial inoculum is introduced in to the leachate and kept it for acclimatization for 20 d. The acclimatized mixed consortium is used for further treatment studies, where simultaneous biogas production is observed and analyzed using gas chromatography.

Table 1
Initial characterization of the landfill leachate

Parameters	Initial characterization
pH	5.1
Electrical conductivity (EC) (ms/cm)	44.7
Total dissolved solids (TDS) (g/l)	26.84
Alkalinity (mg/l)	3750
Total hardness as CaCO ₃ (mg/l)	100
Calcium hardness as Ca (mg/l)	50
Chlorides as Cl (mg/l)	7090
Chemical oxygen demand (COD) (mg/l)	14420
Nickel Ni (mg/l)	75.4
Copper as Cu (mg/l)	25
Zinc as Zn (mg/l)	707
Iron as Fe (mg/l)	92
Lead as Pb (mg/l)	52

2.3. Analytical instruments

Physicochemical parameters such as pH, electrical conductivity, alkalinity, total hardness, calcium hardness, chlorides and chemical oxygen demand (COD) are determined accordance to standard methods (APHA 2005). The physico chemical instrumental analysis has been carried using double beam Shimadzu UV 2450 UV-Visible Spectrophotometer, and metal analysis using Atomic absorption SensAA Spectrometer.

Hydrogen gas analysis carried using Gas Chromatography Agilent-6890 equipped with a thermal conductivity detector (TCD) and a 2 m column packed with 5A molecular sieves. Nitrogen gas is used as the carrying gas at the flow rate of 30 ml/min. The operating temperatures of the column, detector and injector were 80, 100 and 100°C, respectively.

The pollutant removal percentage (%) is calculated as follows:

$$\text{Removal of the pollutant (\%)} = \frac{C_i - C_f}{C_i} \times 100 \quad (6)$$

where C_i is the initial pollutant concentration (mg L^{-1}) and C_f is the final pollutant concentration (mg L^{-1}).

The hydrogen % present in the produced gas is calculated using the following formulae:

$$\% H_2 = \frac{A}{SA} \times \% S \quad (7)$$

where A = sample area; SA = standard area; S = Purity of the standard.

2.4. Operation cost evaluation (OC)

One of the most important parameter affecting the application of any method is operating cost, which heavily determines cost of the treatment process. The OC of the EC is calculated [Eq. (8)] by including the material cost (mainly electrodes), utility cost (mainly electrical energy) and chemicals fixed costs [6,9].

$$OC = aC \text{ energy} + bC \text{ electrode} + cC \text{ chemicals} \quad (8)$$

where 'a' is the electricity consumed (kWh/m^3), 'b' is the electrode material consumed (kg/m^3) and 'c' chemicals is consumption quantities of chemicals (kg/m^3) of the wastewater treated. The cost values (\$) of a, b and c calculated according to the Indian market (January, 2015). It is the energy price as 0.1 \$/kWh (6.40 Rs/kWh), electrodes price as Fe-1.61\$/kg; Al-3.27\$/kg (97 Rs/kg and 197 Rs/kg) and chemical cost (H_2O_2) as 9.07\$/kg (572 Rs/l).

The electrode and energy consumption were calculated using the following equations:

$$C \text{ energy} = \frac{UIt_{EC}}{V} \quad (9)$$

$$C \text{ electrode} = \frac{It_{EC}M}{ZFV} \quad (10)$$

where U is cell voltage(V), I is the current (A), t_{EC} is the operating time (h), V volume of the sample (m^3), M is the

molecular weight of electrode (for Fe-55.84 g/mol, Al-26.98 g/mol), Z is number of electrons transferred ($Z = 3$ for Al and 2 for Fe), F is the Faraday constant (96487C/mol).

3. Results and discussion

3.1. Effect of reaction time on leachate treatment by EC

The reaction time for metal removal from leachate has been investigated at different reaction time intervals (10–30 min) with Fe–Fe electrodes. From the results it is observed that, a maximum of 24% COD removal has been achieved at 30 min while the maximum removal of metal has been observed (Fig. 1) to be 53, 53, 73, 95 and 50% of Ni, Zn, Pb, Cu and Fe respectively at the reaction time of 20 min. After 20 min, removal rate has not increased to a considerable range, which might be due to passivation layer on the electrode material. Similar results have been also observed by Bazafshan et al., [13] and Sepideh et al., [14]. Therefore, to avoid excess operational cost, the reaction time has been optimized to 20 min.

3.2. Effect of electrode metal on leachate treatment by EC

The identification of the electrode material is also an important parameter to know the coagulant affinity. The materials most widely tested for their effectiveness are iron, aluminum and stainless steel as they are cheap and readily available. The maximum metal removal has been achieved with the Fe–Fe electrodes and hence considered as the optimum choice. Moreover, the settle ability of particle formed by Fe–Fe electrode combination by $\text{Fe}(\text{OH})_3$ is better than that formed by $\text{Al}(\text{OH})_3$. Similar results were observed by Li et al., [15]. The COD removal has been observed to be better with the SS electrode, which is of 40% (Fig. 2). This might be due to the OH radicals released from the SS surface.

3.3. Effect of applied voltage on leachate treatment by EC

Applied voltage is one of the operating parameters directly affecting the performance and the operating cost.

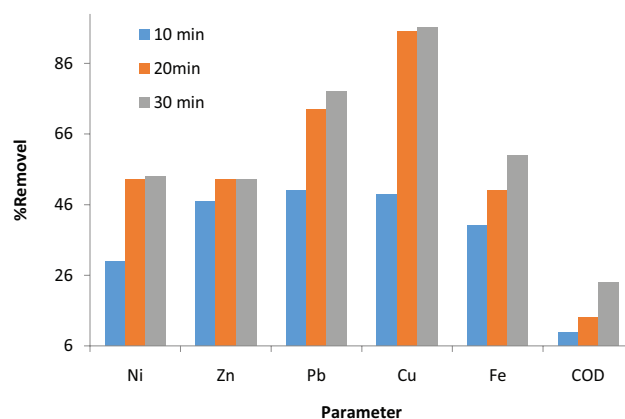


Fig. 1. Effect of reaction time on leachate treatment by EC. Experimental conditions: electrode material: Fe; applied voltage: 6V; pH: 6; area of the electrode: 40 cm^2 ; volume of the sample: 200 ml; inter electrode distance: 2 cm; reaction time 10, 20, 30 min.

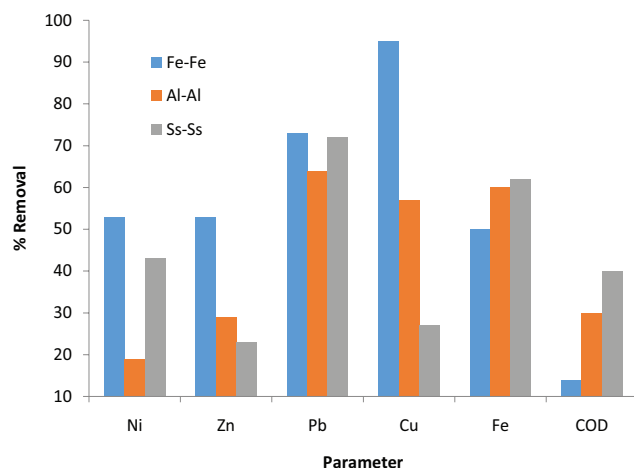


Fig. 2. Effect of electrode metal on leachate treatment by EC. Experimental conditions: electrode material: Fe, Al, Ss; applied voltage: 6 V; pH: 6; area of the electrode: 40 cm²; volume of the sample: 200 ml; inter electrode distance: 2 cm; reaction time: 20 min.

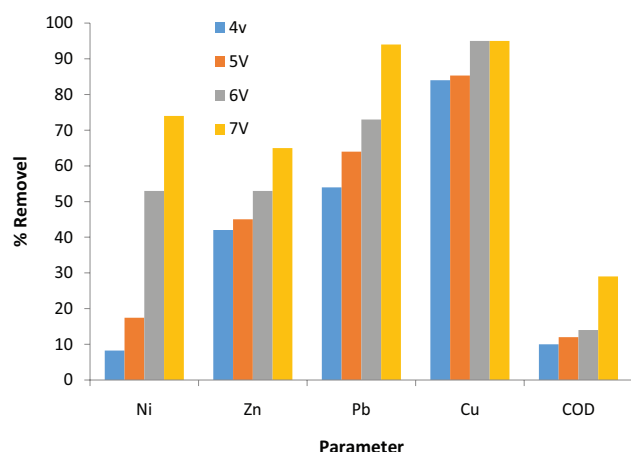


Fig. 3. Effect of applied voltage on leachate treatment by EC. Experimental conditions: electrode material: Fe; applied voltage: 4 V, 5 V, 6 V, 7 V; pH: 6; area of the electrode: 40 cm²; volume of the sample: 200 ml; inter electrode distance: 2 cm; reaction time: 20 min.

EC experiments have been carried out at 4 V, 5 V, 6 V and 7 V (Fig. 3). At 7 V the maximum removal of metals had been found to be 74, 65, 94, 95, 62 and 29% of Ni, Zn, Pb, Cu, Fe and COD respectively. With increase in voltage, treatment efficiency also increased which might be attributed to increase in both the coagulant dose and bubble generation rate [16]. Akbal et al., [17] also observed the same order of removal while treating the metal plating wastewater.

3.4. Effect of initial pH on leachate treatment by EC

The initial pH of the solution shows considerable effect on the removal efficiency of the electrocoagulation process. In the present study, it has been observed (Fig. 4) that metal removal efficiency is optimum at neutral conditions. At pH 7 the maximum removal was observed to be 95, 99.4,

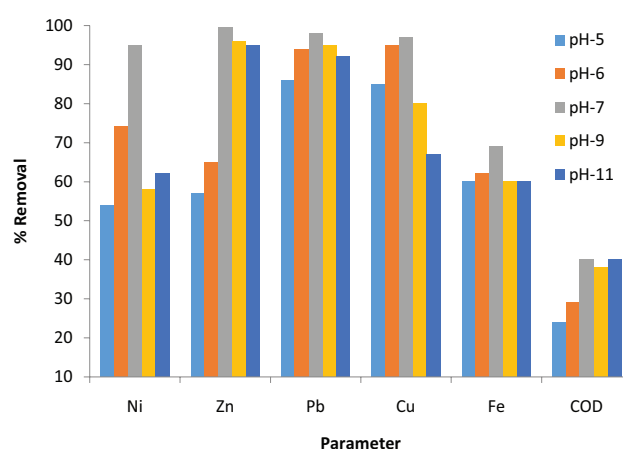


Fig. 4. Effect of initial pH on leachate treatment by EC. Experimental conditions: electrode material: Fe; applied voltage: 7V; pH: 5, 6, 7, 9, 11; area of the electrode: 40 cm²; volume of the sample: 200 ml; inter electrode distance: 2 cm; reaction time: 20 min.

98, 97, 69 and 40% of Ni, Zn, Pb, Cu, Fe and COD respectively. However, with increase or decrease in pH from 7, the removal rate decreased which might be due to the solubility of discharged metal ions [18]. Same trend has been observed by Liet al., [15].

3.5. Effect of Inter electrode distance on leachate treatment by EC

The inter-electrode distance has been studied as a parameter to minimize electricity consumption for the treatment of leachate. Inter-electrode distance varied at 1 cm, 2 cm and 4 cm. The removal percentage of metals has been observed to be decrease with increase in inter-electrode distance from 1 to 4 cm (Fig. 5). The maximum removal achieved were Ni (95%), Zn (99.4 %), Pb (98 %), Cu (97 %), Fe (69%) and COD (40%) at the shortest distance (1 cm) between the electrodes with electrode area of 40 cm². Similar observations have also been reported by Ashok Kumaret al., [19] and Ghosh et al., [20]. That removal efficiency increase might be due to the faster anion discharge at the anode and improved oxidation. It also reduces resistance, the electricity consumption and consequently, the cost of the wastewater treatment [9,21].

3.6. Effect of reaction area on leachate treatment by EC

Reaction surface area has been studied at 10, 20 and 40 cm² to minimize reactive surface area and electrode consumption for the treatment. The metal removal efficiency decreased with decrease in electrode reaction area from 40 cm² to 10 cm². The maximum % removal efficiency of Ni, Zn, Cu, Pb, Cu, Fe and COD were observed (Fig. 6) to be 95, 99.4, 98, 95, 69 and 40%, respectively. This might be attributed to a greater electrode area that produced larger amounts of anions and cations from the electrodes. The larger the electrode surface, the increased rate of floc's formation, which in turn influenced the removal efficiency. Similar results were observed by Ashok Kumar et al., and Ghosh, et al., [19,20].

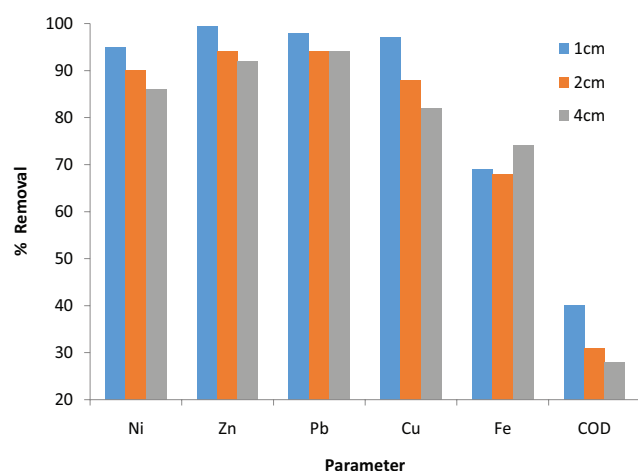


Fig. 5. Effect of inter electrode distance on leachate treatment by EC. Experimental conditions: electrode material: Fe; applied voltage: 7 V; pH: 7; area of the electrode: 40 cm²; volume of the sample: 200 ml; inter electrode distance: 1 cm, 2 cm, 4 cm; reaction time: 20 min.

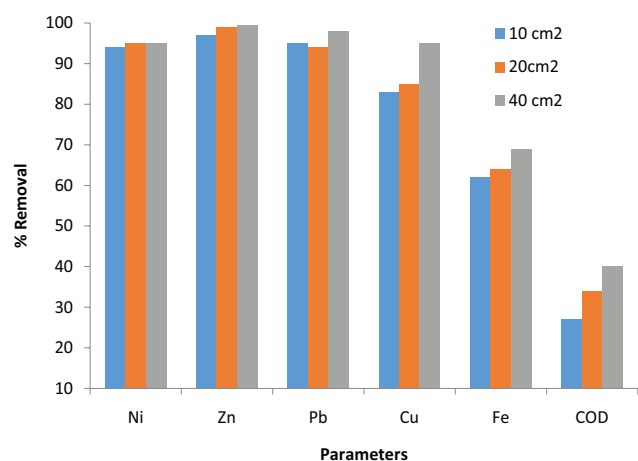


Fig. 6. Effect of reaction area on leachate treatment by EC. Experimental conditions: electrode material: Fe; applied voltage: 7 V; pH: 7; area of the electrode: 10 cm², 20 cm², 40 cm²; volume of the sample: 200 ml; inter electrode distance: 1 cm; reaction time: 20 min.

3.7. Effect of insitu- peroxide EC on leachate treatment

The effect of different hydrogen peroxide dosages (250 ppm–1250 ppm) on the treatment efficiency has been shown in Fig. 7. The metal removal has not been significantly influenced by the addition of peroxide. However, the COD removal efficiency increased with increased hydrogen peroxide dosage, where maximum COD removal efficiency of 56% at 750 ppm peroxide dosage was observed. Similar results were observed by Merve Oya Orkun [21]. Addition of excess peroxide above 750 ppm of the dosage did not increase the removal rate which might be attributed to the formation of hydroperoxyl radical HO₂[•], a much weaker oxidizing radical than hydroxyl radical [Eq. (11)] [22,23].

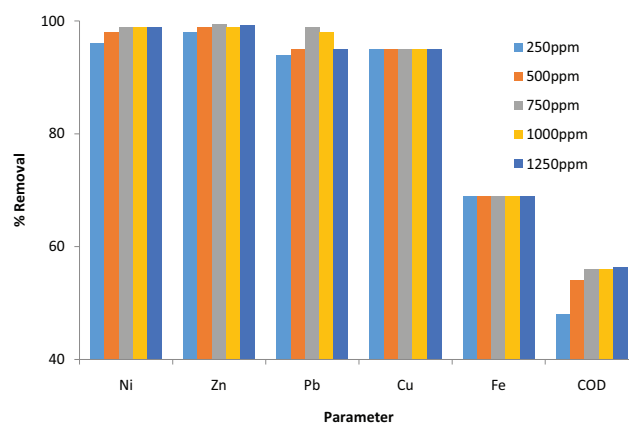


Fig. 7. Effect of insitu- peroxide EC on leach at treatment. Experimental conditions: electrode material: Fe; applied voltage: 7 V; pH: 7; area of the electrode: 40 cm²; volume of the sample: 200 ml; inter electrode distance: 1 cm; reaction time: 20 min, hydrogen peroxide dosage: 250, 500, 750, 1000, 1250 ppm.

Table 2
Operational cost for the treatment of leachate

Process	Cost US\$/m ³
Electrode material	
Fe–Fe	4.52
Al–Al	3.14
Applied voltage	
4 V	2.50
5 V	3.81
6 V	6.41
7 V	9.80
Initial pH	
pH 5	9.43
pH 6	11.2
pH 7	9.77
pH 9	11.1
pH 11	12.0
Reaction area	
40 cm ²	11.3
20 cm ²	9.47
10 cm ²	6.90
Inter electrode distance	
4 cm	10.4
2 cm	13.2
1 cm	16.2
Peroxide dosage	
H ₂ O ₂ 250 ppm	17.2
H ₂ O ₂ 500 ppm	17.8
H ₂ O ₂ 750 ppm	18.3
H ₂ O ₂ 1000 ppm	18.9
H ₂ O ₂ 1250 ppm	19.4



The treatment cost for the leachate at optimum condition has been observed to be 10.4 US\$/m³ (Table 2).

3.8. Biogas production and treatment of leachate

In the biological treatment of leachate samples, the degradation of organic matter has been observed to be 20%, where hydrogen production of 13.4% has been achieved at room temperature. The peak area for the standard hydrogen, acclimatization stage and fermentation of leachate has been observed to be 265, 2.3 and 36.5 respectively. During acclimatization studies only 2.3% of hydrogen has been observed. However with leachate fermentation process the production of hydrogen of 134 ml out of 1000 ml biogas has been observed. After biological treatment, pollutant removal carried with EC and the removal of Ni, Zn, Cu, Pb, Cu, Fe and COD observed to be 95, 99.6, 98, 97.2, 73 and 60% respectively.

4. Conclusions

This study concluded that biological fermentation followed by EC is efficient and effective for the removal of pollutants from industrial solid waste landfill leachate. The maximum removal of metal is observed at a reaction time of 20 min, initial pH of 7, electrode material as Fe–Fe, electrode reaction area of 40 cm², applied voltage of 7 V and electrode spacing of 1 cm. Iron electrodes are found to be most ideal electrodes, compared to aluminum and SS electrodes. Metal removal rate increased with increasing current applied voltage and electrode surface area. However, it decreased with increasing inter-electrode distance. Under optimum treatment conditions % removal of metal has been found to be 95, 99.6, 98, 97.2, 73 and 60% of Ni, Zn, Cu, Pb, Cu, Fe and COD respectively along with 13.4% of bio hydrogen.

References

- [1] R. Jotin, S. Ibrahim, N. Halimoon, Electro coagulation for removal of chemical oxygen demand in sanitary landfill leachate, *Int. J. Environ. Sci.*, 3(2012) 921–930.
- [2] T. Elisabetta, G. Apostolos, C. Raffaello, E. Gidarakos, D. Mantzavinos, K. Alexandros, Electrochemical oxidation of stabilized landfill leachate on DSA electrodes, *J. Hazard. Mater.*, 190 (2011) 460–465.
- [3] U. Welander, T. Henrysson, T. Welander, Biological nitrogen removal from municipal landfill leachate in a pilot scale suspended carrier biofilm process, *Water Res.*, 32 (1998) 1564–1570.
- [4] K. Tabet, Moulin Ph, J.D. Vilomet, A. Amberto, F. Charbit, Purification of landfill leachate eighth membrane processes, Preliminary studies for an industrial plant, *Separ. Sci. Technol.*, 37 (2002) 1041–1063.
- [5] J.J. Wu, C.C. Wu, H.W. Ma, C.C. Chang, Treatment of landfill leachate by ozone-based advanced oxidation processes, *Chemosphere*, 54 (2004) 997–1003.
- [6] A. Amokrane, C. Comel, J. Veron, Landfill leachate pretreatment by coagulation-flocculation, *Water Res.*, 31 (1997) 2775–2782.
- [7] T. Mæhlum, Treatment of landfill leachate in on-site lagoons and constructed wetlands. *Water Sci. Technol.*, 32 (1995) 129–135.
- [8] L. Etiegni, B.O. Orori, K. Senelwa, M.M. Mwamburi, Bekuta K. Balozi, K. Justin, Maghang, Ash leachate used as supporting electrolyte during wastewater treatment by electrocoagulation, *Geophys. Res. Abstr.*, 13 (2011) 1–2.
- [9] D. Bhagawan, P. Saritha, G. Shankaraiah, V. Himabindu, S. Vidyavathi, Treatment of the petroleum refinery wastewater using combined electrochemical methods, *Desal. Wat. Treat.*, 57 (2016) 3387–3394.
- [10] D. Norma, A. Fernandes, M.J. Pacheco, L. Ciriacoand, A. Lopes, Electrocoagulation and anodic oxidation integrated process to treat leachate from a Portuguese sanitary landfill, Portugal. *Electrochim. Acta*, 30 (2012) 221–234.
- [11] D. Bhagawan, P. Saritha, P. Tulasiram, D. Srinivasulu, G. Shankaraiah, M. Yamuna Rani, V. Himabindu, S. Vidyavathi, Effect of operational parameters on heavy metal removal by electrocoagulation, *Environ. Sci. Pollut. Res.*, 21 14166–14173. DOI 10.1007/s11356-014-3331-8.
- [12] H. Zhang, D. Zhang, J. Zhou, Removal of COD from landfill leachate by electro-Fenton method. *J. Hazard. Mater.*, B135 (2005) 106–111.
- [13] E. Bazafshan, A.H. Mahvim, S. Nasser, A.R. Mesdaghinia, F. Vaezi, S.H. Nazmara, Removal of cadmium from industrial effluents by electrocoagulation process using iron electrodes, *Iran. J. Environ. Health. Sci. Eng.*, 3 (2006) 261–266.
- [14] S. Sadeghi, M. Reza Alavi Moghaddam, M. Arami, Improvement of electrocoagulation process on hexavalent chromium removal with the use of polyaluminum chloride as coagulant, *Desal. Wat. Treat.*, 52 (2014) 4818–4829.
- [15] X. Li, J. Song, J. Guo, Z. Wang, Q. Feng, Landfill leachate treatment using electrocoagulation, *Procedia Environ. Sci.*, 10 (2011) 1159–1164.
- [16] A.K. Golder, A.N. Samanta, S. Ray, Removal of trivalent chromium by electrocoagulation, *Separat. Sci. Technol.*, 53 (2007) 33–41.
- [17] F. Akbal, S. Camci, Copper, chromium and nickel removal from metal plating wastewater by electrocoagulation, *Desalination*, 269 (2011) 214–222.
- [18] X. Zhao, B. Zhang, H. Liu, J. Qu, Simultaneous removal of arsenite and fluoride via an integrated electro-oxidation and electrocoagulation process, *Chemosphere*, 83 (2011) 726–729.
- [19] C. Ashok Kumar, A.K. Sharma, Removal of turbidity, COD and BOD from secondarily treated sewage water by electrolytic treatment, *Appl Water Sci.*, 3 (2013) 125–132.
- [20] D. Ghosh, C.R. Medhi, H. Solanki, M.K. Purkait, Copper, chromium and nickel removal from metal plating wastewater by electrocoagulation, *J. Environ. Prot. Sci.*, 2 (2008) 25–35.
- [21] M.O. Orkun, A. Kuleyin, Treatment performance evaluation of chemical oxygen demand from landfill leachate by electrocoagulation and electro-Fenton technique, *Environ. Prog. Sus. Ener.*, 31 (2010) 59–67.
- [22] D. Venu, R. Gandhimathi, P.V. Nidheesh, S.T. Ramesh, Treatment of stabilized landfill leachate using peroxicoagulation process, *Separat. Sci. Technol.*, 129 (2014) 64–70.
- [23] M.L. Singh, Z.A. Wahid, Treatment of sewage by electrocoagulation and the effect of high current density, *Ener. Environ. Eng. J.*, 1 (2012) 27–31.



Desalination and Water Treatment

Publication details, including instructions for authors and subscription information:

<http://www.tandfonline.com/loi/tdwt20>

Treatment of the petroleum refinery wastewater using combined electrochemical methods

D. Bhagawan^a, Saritha Poodari^b, Shankaraiah Golla^a, Vurimindi Himabindu^a & S. Vidyavathi^c

^a Centre for Environment, Institute of Science and Technology, Jawaharlal Nehru Technological University, Hyderabad 500 085, India, Tel. +91 9441184024, Tel. +91 9912297832, Tel. +91 9849693828

^b Civil Department, Malla Reddy Engineering College, Hyderabad 500 085, India, Tel. +91 9849332474

^c Department of Civil Engineering, JNTUH College of Engineering Hyderabad, Jawaharlal Nehru Technological University, Hyderabad 500 085, India, Tel. +91 9392493533

Published online: 20 Dec 2014.



[Click for updates](#)

To cite this article: D. Bhagawan, Saritha Poodari, Shankaraiah Golla, Vurimindi Himabindu & S. Vidyavathi (2014): Treatment of the petroleum refinery wastewater using combined electrochemical methods, Desalination and Water Treatment, DOI: [10.1080/19443994.2014.987175](https://doi.org/10.1080/19443994.2014.987175)

To link to this article: <http://dx.doi.org/10.1080/19443994.2014.987175>

PLEASE SCROLL DOWN FOR ARTICLE

Taylor & Francis makes every effort to ensure the accuracy of all the information (the "Content") contained in the publications on our platform. However, Taylor & Francis, our agents, and our licensors make no representations or warranties whatsoever as to the accuracy, completeness, or suitability for any purpose of the Content. Any opinions and views expressed in this publication are the opinions and views of the authors, and are not the views of or endorsed by Taylor & Francis. The accuracy of the Content should not be relied upon and should be independently verified with primary sources of information. Taylor and Francis shall not be liable for any losses, actions, claims, proceedings, demands, costs, expenses, damages, and other liabilities whatsoever or howsoever caused arising directly or indirectly in connection with, in relation to or arising out of the use of the Content.

This article may be used for research, teaching, and private study purposes. Any substantial or systematic reproduction, redistribution, reselling, loan, sub-licensing, systematic supply, or distribution in any form to anyone is expressly forbidden. Terms & Conditions of access and use can be found at <http://www.tandfonline.com/page/terms-and-conditions>



Treatment of the petroleum refinery wastewater using combined electrochemical methods

D. Bhagawan^a, Saritha Poodari^b, Shankaraiah Golla^a, Vurimindi Himabindu^{a,*}, S. Vidyavathi^c

^aCentre for Environment, Institute of Science and Technology, Jawaharlal Nehru Technological University, Hyderabad 500 085, India, Tel. +91 9441184024; email: bhagawanist@gmail.com (D. Bhagawan), Tel. +91 9912297832;

email: shankar_cool2008@yahoo.com (S. Golla), Tel. +91 9849693828; email: drvhimabindu@gmail.com (V. Himabindu)

^bCivil Department, Malla Reddy Engineering College, Hyderabad 500 085, India, Tel. +91 9849332474;

email: poodarisaritha@gmail.com

^cDepartment of Civil Engineering, JNTUH College of Engineering Hyderabad, Jawaharlal Nehru Technological University, Hyderabad 500 085, India, Tel. +91 9392493533; email: gollashankar11@gmail.com

Received 15 April 2014; Accepted 4 November 2014

ABSTRACT

This study explores the performance of electrochemical and combined oxidation methods for the treatment of petroleum refinery wastewater (PRW). The electrocoagulation operating parameters studied includes reaction time and applied voltage. *In situ* hydrogen peroxide treatments at different dosages and hybrid electrochemical systems (ECEO, ECS₂₅, ECS₃₃, ECEO + US₃₃) have been studied. The efficacy of the treatment system has been evaluated in terms of reduction of phenols, COD, TOC, oil, and grease. The most effective method for PRW treatment is ECEO + US₃₃ where the maximum % removal of phenols, TOC, COD, oil, and grease are reported to be 98, 92, 92, and 92%, respectively. The results demonstrate the technical feasibility of using hybrid electrochemical process as a possible and reliable methods for the treatment of PRW.

Keywords: Refinery; Electrocoagulation; Electrooxidation; Peroxidation; Ultrasonication

1. Introduction

Petrochemical industries cause considerable water pollution by discharging their effluents into the surrounding aquatic environment. Large amount of wastewater is produced from petrochemical manufacturing processes like distillation, cracking, treating, and reforming. Petroleum refinery industrial processes occupied the first place in releasing high volumes of oily wastewater compared to any other industrial

processes. The average release of the wastewater is 0.4–1.6 times to the volume of the processed crude oil. Consequently, a wide variety of pollutants including refractory organics are usually encountered in petrochemical wastewater [1,2]. The chemical composition of petroleum refinery wastewater (PRW) effluent is very complex and contains several inorganic substances, such as Mg²⁺, Ca²⁺, S²⁻, Cl⁻, and SO₄²⁻ that upgrade the mineralization of water, emulsified oil, phenols, and sulfides. This wastewater must be treated before being released into the freshwater [3].

*Corresponding author.

Conventional wastewater treatment methods, including gravity separation and skimming, air flotation, coagulation, de-emulsification, and flocculation, have intrinsic disadvantages such as low efficiency, high operation cost, and corrosion and generates a considerable quantity of secondary pollutants (chloride, sulfate in the coagulation–precipitation) and large volumes of sludge or waste which pose serious environmental problems [4,5]. Evaporation of these solutions in ponds is impractical due to their high salt concentration [6]. Even the biological processes are also inefficient in treating PRW, because the partial inhibition of biodegradation is observed. It might be due to the presence of the sulfide which affects the oxygen transfer of the biosystems [7]. Nevertheless, these processes present limitations which can be accomplished by electrochemical methods.

Electrochemical process is advantageous over the conventional coagulation process, in which the reactants are generated *in situ* through the dissolution of a sacrificial anode by applied current with simultaneous evolution of hydrogen at the cathode. This method has been shown as an efficient and promising technique in treating various wastewater contaminants such as reactive dyes [8], azo dyes [9], metal cutting [10], oily bilge water [11], industrial wastewater [12], poultry slaughter house [13], fluoride [14], pulp and paper mill wastewater [15], phosphate, zinc [14], and textile wastewaters [16]. In hybrid electrochemical methods there are combined reaction possibilities such as electrocoagulation (EC), electrooxidation (EO), and electroflotation along with other treat systems (ultrasonication, photocatalysis, ozonation, and other oxidation applications). Electrochemical methods are efficient in removing soluble inorganic solids, suspended solids as well as oil and grease. It has also the advantage of producing a relatively low amount of sludge [5]. The reactions occurring in an electrochemical cell involving aluminum electrodes are as follows:

Reactions at the anodes:



Reactions at the cathodes:

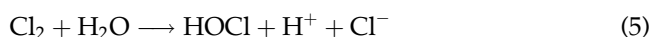


Al metal ions immediately form hydroxides and/or poly hydroxides that finally transform into $\text{Al}(\text{OH})_3$ (s), as shown in Eqs. (1) and (2) (electrocoagulation). Hydroxides have strong affinity to capture the pollutants in the

waste water, causing more pollutant removal than those conventional methods. Eq. (3) involves electrooxidation phenomena [17,18].

Along with anodic dissolution of the coagulant, hydrogen bubbles are released from the cathode due to water splitting. Gas evolution during electrochemical treatment wastewaters has been termed electroflotation [19]. This process might be responsible for the removal of oil and grease from the oily waters [17,20].

The organic recalcitrant compounds could also be effectively oxidized by oxidizing agents such as hypochlorite and peroxide. Hypochlorite formation might be due to the presence of NaCl which is readily available in the PRW (Eqs. (4)–(6)). This might be responsible for the indirect oxidation of organics in the solution and/or near the anode surface [17,21,22].



Hydrogen peroxide is most often used as chemical oxidant to improve the radical formation to degrade the organic pollutants. Specifically, peroxide is more effective in the removal of sulfide and H_2S from PRW. This might be due to the conversion of sulfide in sulfate which can be easily removed from solution by electrochemical methods [23].

Sometimes it may become necessary to use two or more methods of treatments, i.e. hybrid processes, to ensure efficient treatment of wastewater. Removal of coloring materials from dye stuffs using electrochemical methods has been reported by Akyol [5], Lin and Peng [24], Pouet and Grasmick [25], and Mahesh et al. [15]. Combined electrochemical oxidation, coagulation, and activated sludge have been reported by Lin and Peng [24]. EC has also been used in conjunction with filtration to remove silica and suspended solids that tend to foul reverse osmosis membranes [25,26].

However, no attempt has been made so far in the usage of combined technique (*in situ* electrocoagulation–ultrasonication) for the treatment of PRW. Hence, the present paper discusses the treatment of PRW using EC and hybrid techniques.

2. Materials and methods

2.1. Petroleum refinery wastewater

The PRW is provided by refinery processing industry, India. Initial characteristics of the wastewater are represented in Table 1.

2.2. Experimental setup and methodology

The initial characterization of the sample has been carried according to “standard methods for examination of water and wastewater 21th addition-2005, APHA” [27]. In electrocoagulation method, the operational parameters like reaction time (10–40 min) and current voltage (10–30 V) are investigated. The above EC experiments are carried in a 250 mL glass beaker having a working capacity of 200 mL as shown in Fig. 1(A). Al Electrodes are connected to the respective anode and cathode leading to the DC rectifier (AP lab, L 6403(1–84 V, 0–3 A)). The active surface area of the each electrode is 12.6 cm² and the inter-electrode distance between the anode and cathode rods is 3.5 cm. Before each run, aluminum electrodes are washed with tap water and then again rinsed with distilled water.

To increase the organic removal from PRW, the peroxi-electrocoagulation, EC followed by electro oxidation (ECEO) and *in situ* EC ultra sonication (US) are studied.

In peroxi-EC experiment, peroxide dosages are varied from 50 to 400 ppm. The *In situ* EC ultrasono-EC (25 kHz (ECS₂₅), 33 kHz (ECS₃₃)) are carried as

shown in Fig. 1(B) where EC reactor is placed in the sonicator bath which is constituted of a 3.3 L ultrasonic bath (Model No. EN-30-US, Enertech Electronics Pvt Ltd, Bombay, India) with a selective- frequency-based electronic ultrasound generator. The ultrasonic bath has a two piezo-ceramic transducers bonded to the bottom of a stainless steel tank with the option of operating at 25 or 33 kHz in a continuous or pulse (5 s on and 1 s off) mode.

Finally, ECEO followed by ultrasonication at 33 kHz (ECEO + US₃₃) has been studied. All the experiments are performed at room temperature (27 ± 2°C). The samples are collected at an interval of 10 min and are analyzed for reduction of phenol, COD, TOC, oil, and grease content.

2.3. Analytical instruments

The instrumental analysis is carried using Double beam Shimadzu UV 2450 UV-visible Spectrophotometer and TOC-L CPH E 200.

The pollutant removal percentage (%) is calculated as follows:

$$\text{Removal of the pollutant (\%)} = \frac{C_i - C_f}{C_i} \times 100 \quad (7)$$

where, C_i is the initial pollutant concentration (mg L⁻¹) and C_f is the final pollutant concentration (mg L⁻¹).

3. Results and discussion

The initial characterization of the PRW is given in Table 1.

3.1. Factors affecting the performance of electrocoagulation

3.1.1. Effect of reaction time on the performance of electrocoagulation

Operating time is an important parameter for economic applicability of the EC process. In the present study, the time course of EC has been observed at time intervals of 10, 20, 30, and 40 min. During initial stages of the treatment, the % removal efficiency was observed to increase up to 20 min after which the removal rate was observed to be constant. So 20 min has been chosen as the optimal reaction time for EC of the PRW sample. At this reaction time, 84, 85, 84, and 66% of the phenol, COD, TOC, oil, and grease % reduction have been observed (Fig. 2). The decrease in removal rate after 20 min might be due to the

Table 1
Initial characterization of the effluent sample

S.No	Name of the parameters	Initial (mg L ⁻¹)
1	pH	7.92
2	EC (microsiemens/cm)	2,084
3	Total dissolved solids (TDS)	1,550
4	Total solids(TS)	2,000
5	Total suspended solids (TSS)	450
6	Phenols	79
7	Biological oxygen demand (BOD)	195
8	Total hardness(TH)	200
9	Chemical oxygen demand (COD)	760
10	Alkalinity as CaCO ₃	515
11	Calcium hardness as CaCO ₃	110
12	Magnesium hardness as CaCO ₃	90
13	Chlorides as Cl ⁻	600
14	Sulfates as SO ₄	116
15	Nitrates as NO ₃ ⁻	146
16	Phosphates as PO ₄	1.43
17	Sodium as Na	380
18	Potassium as K	22
19	Fluoride as F	0.25
20	Turbidity (NTU)	130.4
21	Sulfides SO ₃	14.4
22	Oil and grease	150
23	Total organic carbon	620

Note: All the parameters are expressed in mg L⁻¹ except pH, EC, and Turbidity.

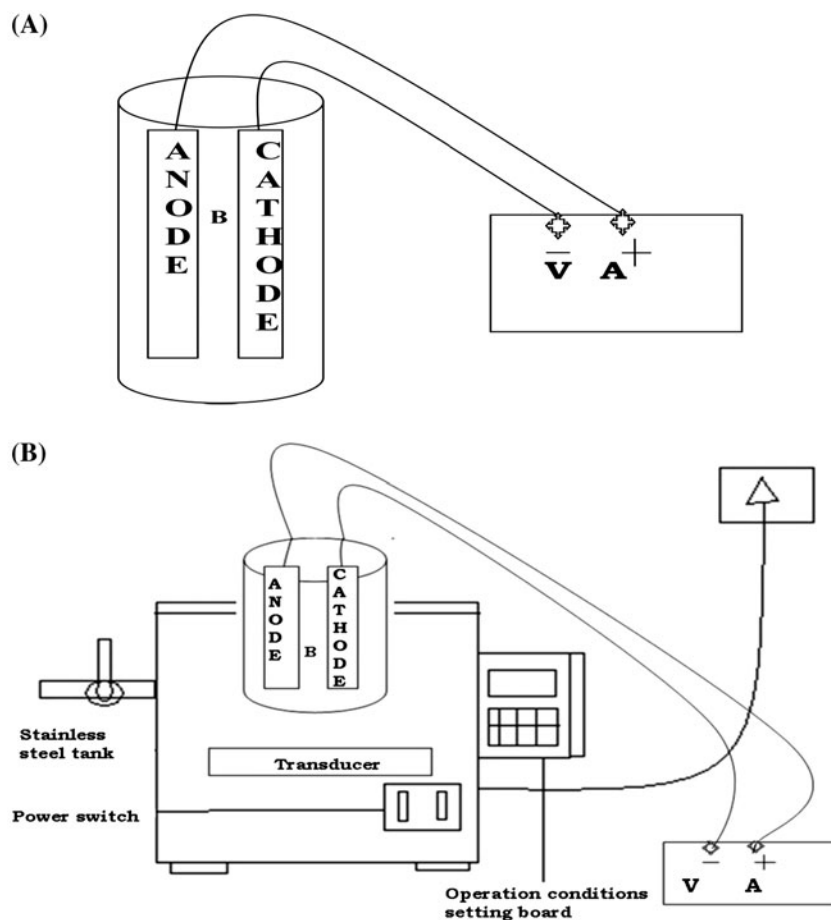


Fig. 1. (A) Systematic design of electrocoagulation setup. (B) Schematic design of sonicator with electrocoagulation. Note: B-Beaker, V-DC Voltage, and A-DC Ampere.

decreased extent of cathodic reduction (passivation) and formation of monomeric electrocoagulants [5]; this monomeric hydrolysis products includes $\text{Al}(\text{OH})_2^+$, $\text{Al}(\text{OH})_2^+$, and $\text{Al}_2(\text{OH})_2^{4+}$ [26,28]. The same results also observed by Mollah et al. [26] and Ahmadi et al. [29] in terms of oil and grease, Akyol in terms of TOC [5] and Ugurlu in case of the paper mill effluent treatment [30]. According to Zhao et al. [31], dissolved substances are difficult to remove only by individual electrocoagulation process even with the reaction time was increased [28,31,32].

3.1.2. Effect of applied voltage on the performance of electrocoagulation

Among the various operating parameters in all the electrochemical processes, the applied voltage is an important factor which strongly influences the performance of electrocoagulation. The effects of applied voltage on the pollutants removal efficiency from

PRW have been investigated at voltages of 10, 15, 20, 25, and 30 V, and corresponding current density of 6.3, 9.4, 16.6, 21.3, and 28.4 mA/cm^2 (Fig. 3) had observed, respectively. The maximum % removal (Fig. 4) of the phenol, COD, TOC, oil, and grease has been observed to be 89, 84, 84, and 67%, respectively, at an applied voltage of 20 V. The results showed that the removal efficiency increased with increasing voltage up to 20 V. Further, increase in the voltage leads to a constant or slight decrease in the removal efficiency.

Generally with an increase in the current density, the dissolution of anode and generation of bubbles at cathode increases. This improves the degree of mixing of $\text{Al}(\text{OH})_3$ which further enhances floatation ability of the cell, thus, increasing the pollutant removal efficiency [5,33]. However, an excessive increase in the current voltage causes a reduction in the production of the flocs. This had also been previously observed by Adhoum and Monser [34], according to whom this

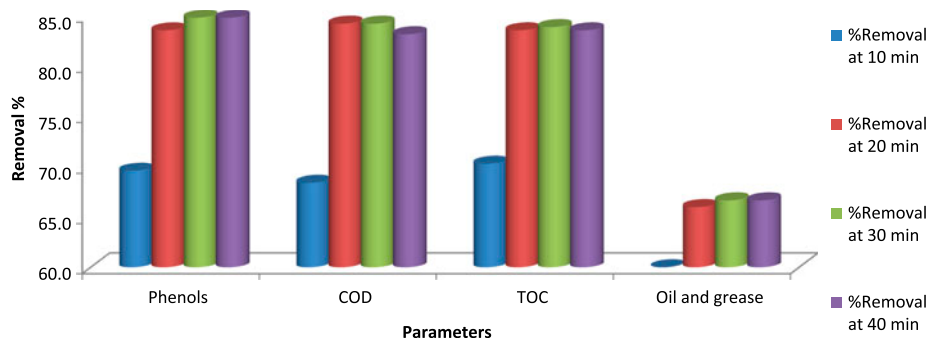


Fig. 2. Effect of electrocoagulation time for the treatment PRW.

Note: Conditions: volume of the sample: 200 mL, electrode: Al/Al, voltage: 10 V, reaction time 10–40 min, surface area of electrode: 25.3 cm², and current density: 6.32 mA/cm².

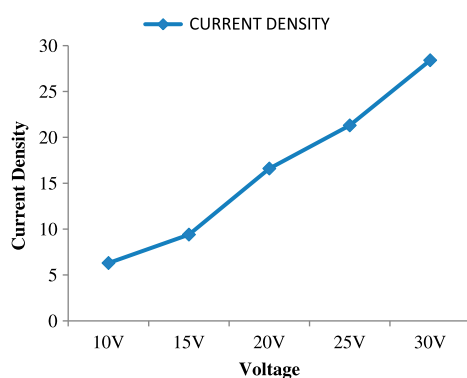


Fig. 3. Applied voltages with respective current density.

might be due the faster generation of gas bubbles, which are responsible for removal of aluminum hydroxide from solution by flotation further leading to a reduction in the probability of collision between the pollutant and coagulant. Thus, despite the high removal efficiency obtained, high current density has been observed to be not beneficial for the maximum use of the flocs [5,17,26].

3.2. Effect of hydrogen peroxide on the performance of electrocoagulation

Peroxide is a strong oxidizing agent and it doesn't pollute the water. The treatment of PRW is performed at peroxi-electrochemical process by varying H₂O₂ dosages (50–400 ppm). It has been observed that from the Fig. 5, with an increase in the addition of H₂O₂, the percentage removal of pollutants has also increased till 300 mg L⁻¹ dosage. At this point maximum of % removal of 91.9, 92, 92, and 92% of phenol, COD, TOC, oil, and grease has been achieved. Above which (>300 mg L⁻¹) no significant increase in the % removal of the pollutants has been observed. Increased H₂O₂ dosage increases the ·OH radicals generation which further enhances the oxidation ability of treatment process. However, the decessive trend indicated that the over-abundant H₂O₂ could also consume ·OH and eliminate the hydroxyl radical generating oxygen (Reactions 8 and 9) [29,30,34]. It is clearly observed from Fig. 5 that maximum removal of phenol is achieved at a dosage of 200 mg L⁻¹ of peroxide. This variation between COD and phenol

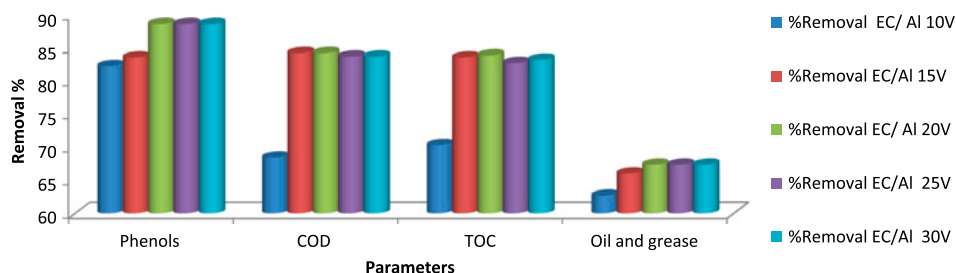


Fig. 4. Effect of applied voltage for the treatment of PRW.

Notes: Conditions: volume of the sample: 200 mL, electrode: Al/Al, voltage: 20 V, reaction time 20 min, surface area of electrode: 25.3 cm², current density for 10 V: 6.32 mA/cm², current density for 15 V: 11.7 mA/cm², current density for 20 V: 16.6 mA/cm², current density for 25 V: 21.3 mA/cm², and current density for 30 V: 28.4 mA/cm².

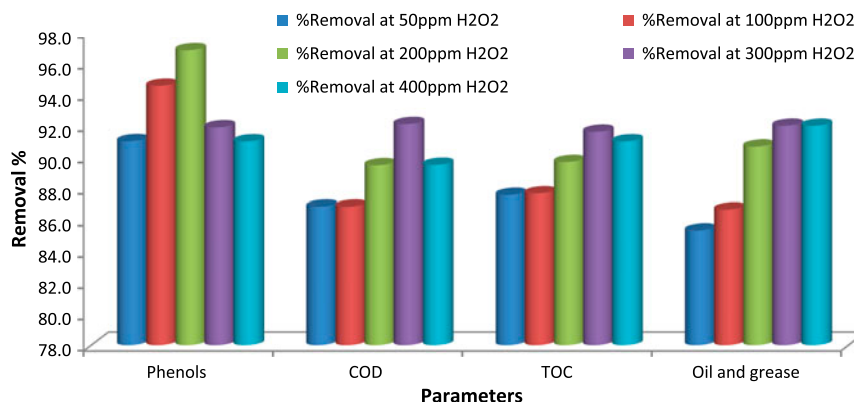
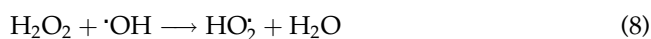


Fig. 5. Effect of *in situ* peroxi-electrocoagulation for the treatment of PRW.

Note: Conditions: volume of the sample: 200 mL, electrode: Al/Al, voltage: 20 V, reaction time 20 min, surface area of electrode: 25.3 cm², current density for 20 V: 16.6 mA/cm², peroxide concentration: 50–400 ppm.

removal pattern might be due to the presence of complex structure of phenols [35,36].



3.3. Comparison between different treatment processes for PRW treatment

The results shown that the % reduction of COD in ECS₃₃ is observed to be more, while compared with ECS₂₅ treatment process (Fig. 6). This might be due to generation of more OH radicals at higher frequencies [31,32]. Oxidation efficiency of the ECS₃₃, ECEO, and ECEO + US₃₃ is observed to be same in case of COD and TOC. The percentage removal of phenol, oil, and grease under different treatment processes is found to

be in the order of ECS₂₅ < ECS₃₃ < ECEO < ECEO + US₃₃ which is of 91, 96, 97, and 98% of phenols, and 74, 83, 90, and 92% of oil and grease, respectively.

The pollutant removal by hybrid electrochemical techniques might be due to the direct anodic oxidation and indirect oxidation species (Reactions 4–6). The presence of sufficiently high chloride ion concentrations (concentrations greater than 300 mg L⁻¹) is sufficient for the formation of HOCl at certain pH values and potentials. Typically, chloride is regenerated; however, depending on the parameters of the electrochemical process some chloride can also escape from the solution in the form of gaseous chlorine [17,21,31]. Moreover, phenol and COD removal might also involve electrochemical oxidation and adsorption by electrostatic attraction and physical entrapment [20,34,36–38]. Electrochemical techniques combination with ultrasonication had shown the remarkable increment in % removal of the pollutants from PRW.

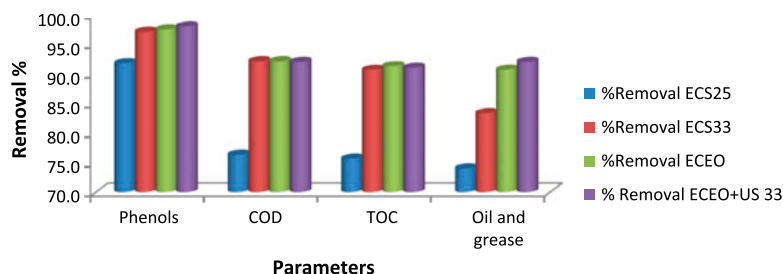


Fig. 6. Electrocoagulation combined with other techniques.

Note: Conditions: ECS₂₅: volume of the sample: 200 mL, electrode: Al/Al, voltage: 20 V, reaction time 20 min, surface area of electrode: 25.3 cm², current density for 20 V: 16.6 mA/cm², ultrasonication at 25 kHz. ECS₃₃: volume of the sample: 200 mL, electrode: Al/Al, voltage: 20 V, reaction time 20 min, surface area of electrode: 25.3 cm², current density for 20 V: 16.6 mA/cm², ultrasonication at 33 kHz. ECEO: volume of the sample: 200 mL, electrode: Al/Al (EC), & SS/SS (EO), voltage: 20 V, reaction time 20 min, surface area of electrode: 25.3 cm², current density for 20 V: 16.6 mA/cm². ECEO + US₃₃: ECEO followed by ultrasonication at 33 kHz.

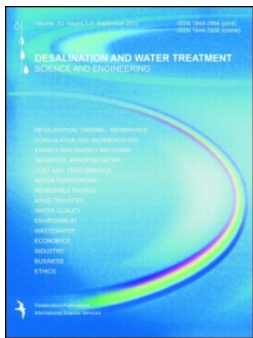
4. Conclusions

- (1) The application of hydrogen peroxide for enhancing the oxidative process of the PRW is observed to be beneficial.
- (2) EC alone is not suitable for treatment of the refinery waste waters, because PRW is very complex in composition.
- (3) PRW treatment needs collaborative treatment processes like electrochemical methods and/or ultrasonication.
- (4) From this study, the maximum % removal of 98, 92, 92, and 92% of phenols, TOC, COD, oil, and grease is observed in ECEO + US₃₃ process.

References

- [1] S. Ahmadi, E. Sardari, H.R. Javadian, R. Katal, M.V. Sefti, Removal of oil from biodiesel wastewater by electrocoagulation method, *Korean J. Chem. Eng.* 30 (2013) 634–641.
- [2] A. Coelho, A.V. Castro, M. Dezotti, G.L. Sant'Anna Jr., Treatment of petroleum refinery sourwater by advanced oxidation processes, *J. Hazard. Mater.* 137 (2006) 178–184.
- [3] L. Yan, H. Ma, B. Wang, W. Mao, Y. Chen, Advanced purification of petroleum refinery wastewater by catalytic vacuum distillation, *J. Hazard. Mater.* 178 (2010) 1120–1124.
- [4] G. Moussavi, R. Khosravi, M. Farzadkia, Removal of petroleum hydrocarbons from contaminated groundwater using an electrocoagulation process: Batch and continuous experiments, *Desalination* 278 (2011) 288–294.
- [5] A. Akyol, Treatment of paint manufacturing wastewater by electrocoagulation, *Desalination* 285 (2012) 91–99.
- [6] U. Daiminger, W. Nitsch, P. Plucinski, S. Hoffmann, Novel techniques for oil/water separation, *J. Membr. Sci.* 99 (1995) 197–203.
- [7] S.A. Martinez-Delgadillo, M.A. Morales-Mora, I.D. Barcelo-Quintal, Electrocoagulation treatment to remove pollutants from petroleum refinery wastewater, *Sustain. Environ. Res.* 20 (2010) 227–231 (Formerly, *J. Environ. Eng. Manage.*).
- [8] T.H. Kim, Ch. Park, E.B. Shin, S. Kim, Decolorization of disperse and reactive dyes by continuous electrocoagulation process, *Desalination* 150 (2002) 165–175.
- [9] M.Y.A. Mollah, S.R. Pathak, P.K. Patil, M. Vayuvegula, T.S. Agrawal, J.A. Gomes, M. Kesmez, D.L. Cocke, Treatment of orange II azo-dye by electrocoagulation (EC) technique in a continuous flow cell using sacrificial iron electrodes, *J. Hazard. Mater.* 109 (2004) 165–171.
- [10] M. Koby, E. Demirbas, M. Bayramoglu, M.T. Sensoy, Optimization of electrocoagulation process for the treatment of metal cutting wastewaters with response surface methodology, *Water Air Soil Pollut.* 215 (2011) 399–410.
- [11] M. Asselin, P. Drogui, S.K. Brar, H. Benmoussa, J.F. Blais, Organics removal in oily bilgewater by electrocoagulation process, *J. Hazard. Mater.* 151 (2008) 446–455.
- [12] M.Y.A. Mollah, P. Morkovsky, J.A.G. Gomes, M. Kesmez, J. Parga, D.L. Cocke, Fundamentals, present and future perspectives of electrocoagulation, *J. Hazard. Mater.* 114 (2004) 199–210.
- [13] M. Bayramoglu, M. Koby, M. Eyvaz, E. Senturk, Technical and economic analysis of electrocoagulation for the treatment of poultry slaughterhouse wastewater, *Sep. Purif. Technol.* 51 (2006) 404–408.
- [14] M. Koby, E. Demirbas, A. Dedeli, M.T. Sensoy, Treatment of rinse water from zinc phosphate coating by batch and continuous electrocoagulation processes, *J. Hazard. Mater.* 173 (2010) 326–334.
- [15] S. Mahesh, B. Prasad, I.D. Mall, I.M. Mishra, Electrochemical degradation of pulp and paper mill wastewater. Part 1. COD and color removal, *Ind. Eng. Chem. Res.* 45 (2006) 2830–2839.
- [16] O.T. Can, M. Koby, E. Demirbas, M. Bayramoglu, Treatment of the textile wastewater by combined electrocoagulation, *Chemosphere* 62 (2006) 181–187.
- [17] I.B. Hariz, A. Halleb, N. Adhoum, L. Monser, Treatment of petroleum refinery sulfidic spent caustic wastes by electrocoagulation, *Sep. Purif. Technol.* 107 (2013) 150–157.
- [18] Ch.T. Wang, W.L. Chou, Y.M. Kuo, Removal of COD from laundry wastewater by electrocoagulation/electroflotation, *J. Hazard. Mater.* 164 (2009) 81–86.
- [19] N.P. Gamage, J.D. Rimer, S. Chellam, Improvements in permeate flux by aluminum electroflotation pretreatment during microfiltration of surface water, *J. Membr. Sci.* 411–412 (2012) 45–53.
- [20] S. Farhadi, B. Aminzadeh, A. Torabian, V. Khatibikamal, M.A. Alizadeh Fard, Comparison of COD removal from pharmaceutical wastewater by electrocoagulation, photoelectrocoagulation, peroxi-electrocoagulation and peroxi-photoelectrocoagulation processes, *J. Hazard. Mater.* 219–220 (2012) 35–42.
- [21] P.G. Garcia, A.L. Lopez, J.M.M. Baquero, A.G. Fernandez, Treatment of wastewaters from the green table olive packaging industry using electro-coagulation, *Chem. Eng. J.* 170 (2011) 59–66.
- [22] J. Ge, J. Qu, P. Lei, H. Liu, New bipolar electrocoagulation–electroflotation process for the treatment of laundry wastewater, *Sep. Purif. Technol.* 36 (2004) 33–39.
- [23] K. Waterston, D. Bejan, N.J. Bunce, Electrochemical oxidation of sulfide ion at a boron-doped diamond anode, *J. Appl. Electrochem.* 37 (2007) 367–373.
- [24] S.H. Lin, C.F. Peng, Continuous treatment of textile wastewater by combined coagulation, electrochemical oxidation and activated sludge, *Water Res.* 30 (1996) 587–592.
- [25] M.F. Pouet, A. Grasmick, Urban wastewater treatment by electrocoagulation and flotation, *Water Sci. Technol.* 31(3–4) (1995) 275–283.
- [26] M.Y.A. Mollah, R. Schennach, J.R. Parga, D.L. Cocke, Electrocoagulation (EC)—Science and applications, *J. Hazard. Mater.* 84 (2001) 29–41.

- [27] L.S. Clesceri, A.E. Greenberg, A.D. Eaton, Standard Methods for the Examination of Water and Wastewater, twenty-first ed., American Public Health Association, Washington, DC, 2005.
- [28] A. Gürses, M. Yalçın, C. Doğar, Electrocoagulation of some reactive dyes: A statistical investigation of some electrochemical variables, *Waste Manage.* 22 (2002) 491–499.
- [29] S. Ahmadi, E. Sardari, H.R. Javadian, R. Katal, M.V. Sefti, Removal of oil from biodiesel wastewater by electrocoagulation method, *Korean J. Chem. Eng.* 30 (2013) 634–641.
- [30] M. Uğurlu, A. Gürses, Ç. Doğar, M. Yalçın, The removal of lignin and phenol from paper mill effluents by electrocoagulation, *J. Environ. Manage.* 87 (2008) 420–428.
- [31] X. Zhao, B. Zhang, H. Liu, F. Chen, A. Li, J. Qu, Transformation characteristics of refractory pollutants in plugboard wastewater by an optimal electrocoagulation and electro-Fenton process, *Chemosphere* 87 (2012) 631–636.
- [32] O. Abdelwahab, N.K. Amin, E.S.Z. El-Ashtouky, Electrochemical removal of phenol from oil refinery wastewater, *J. Hazard. Mater.* 163 (2009) 711–716.
- [33] P.K. Holt, G.W. Barton, C.A. Mitchell, The future for electrocoagulation as a localised water treatment technology, *Chemosphere* 59 (2005) 355–367.
- [34] N. Adhoum, L. Monser, Decolourization and removal of phenolic compounds from olive mill wastewater by electrocoagulation, *Chem. Eng. Process.* 43 (2004) 1281–1287.
- [35] R. Portela, S. Suárez, S.B. Rasmussen, N. Arconada, Y. Castro, A. Durán, P. Ávila, J.M. Coronado, B. Sánchez, Photocatalytic-based strategies for H₂S elimination, *Catal. Today* 151 (2010) 64–70.
- [36] Y. Yavuz, A.S. Koparal, U.B. Ögütveren, Treatment of petroleum refinery wastewater by electrochemical methods, *Desalination* 258 (2010) 201–205.
- [37] M. Ashokkumar, J. Lee, S. Kentish, F. Grieser, Bubbles in an acoustic field: An overview, *Ultrason. Sonochem.* 14(4) (2007) 470–475.
- [38] M.H. Ortega, T. Ponziak, C.B. Diaz, M.A. Rodrigo, G.R. Morales, B. Bilyeu, Use of a combined electrocoagulation–ozone process as a pre-treatment for industrial wastewater, *Desalination* 250(1) (2010) 144–149.



Degradation of antibiotic norfloxacin in aqueous solution using advanced oxidation processes (AOPs)—A comparative study

G. Shankaraiah, Saritha Poodari, D. Bhagawan, Vurimindi Himabindu & S. Vidyavathi

To cite this article: G. Shankaraiah, Saritha Poodari, D. Bhagawan, Vurimindi Himabindu & S. Vidyavathi (2016) Degradation of antibiotic norfloxacin in aqueous solution using advanced oxidation processes (AOPs)—A comparative study, *Desalination and Water Treatment*, 57:57, 27804-27815, DOI: [10.1080/19443994.2016.1176960](https://doi.org/10.1080/19443994.2016.1176960)

To link to this article: <http://dx.doi.org/10.1080/19443994.2016.1176960>



Published online: 29 Apr 2016.



Submit your article to this journal [↗](#)



Article views: 77



View related articles [↗](#)



View Crossmark data [↗](#)



Degradation of antibiotic norfloxacin in aqueous solution using advanced oxidation processes (AOPs)—A comparative study

G. Shankaraiah^a, Saritha Poodari^b, D. Bhagawan^a, Vurimindi Himabindu^{a,*}, S. Vidyavathi^c

^aCentre for Environment, Institute of Science and Technology, Jawaharlal Nehru Technological University, Hyderabad 500 085, India, Tel. +91 9912297832; email: shankar_cool2008@yahoo.com (G. Shankaraiah), Tel. +91 9441184024;

email: bhagawanist@gmail.com (D. Bhagawan), Tel. +91 9849693828; email: drvhimabindu@gmail.com (V. Himabindu)

^bCivil Department, Malla Reddy Engineering College, Hyderabad 500 085, India, Tel. +91 9849332474;

email: poodarisaritha@gmail.com

^cDepartment of Civil Engineering, JNTUH College of Engineering Hyderabad, Jawaharlal Nehru Technological University, Hyderabad 500 085, India, Tel. +91 9392493533; email: vidyasom@yahoo.co.in

Received 8 July 2015; Accepted 24 March 2016

ABSTRACT

The consumption of antibiotics in today's world has increased tremendously and as such they are frequently found in effluents, sewage treatment plants, hospital waste water and surface water like lakes and rivers. The aquatic organisms are severely affected due to the presence of these antibiotics. Moreover, as these antibiotics are mostly recalcitrant, biological treatment methods are not feasible. Hence, the present study is focused on the treatment of one such antibiotic called norfloxacin using advanced oxidation processes (AOPs). The parameters considered in this study include the effect of UV, initial pH of the recalcitrant solution, UV/H₂O₂, Fenton, photo-Fenton process, UV/TiO₂ and UV/TiO₂ immobilization with glass beads. Among all the processes studied, photo-Fenton process has found to be effective and removed 96% of the norfloxacin. The optimum conditions obtained for the maximum degradation with photo-Fenton process are: pH 3, H₂O₂ concentration of 200 mg/L and iron concentration of 30 mg/L, for an initial drug concentration of 150 ppm.

Keywords: Antibiotics; Pharmaceuticals; Norfloxacin; Photocatalysis; Non-biodegradable; TiO₂ immobilization glass beads

1. Introduction

Several pharmaceuticals have been detected in aquatic environment such as treated drinking water, surface water, groundwater, wastewater treatment plants (WWTPs) effluents and sludge [1]. Release of these chemicals in the environment can be of high concern for public health, and may have undesirable

health effects on humans, animals and ecosystem. Antibiotics are such materials that can reach the environment via different routes like: human or animal excretions, pharmaceutical manufacturing plants effluents, medical wastes, municipal WWTPs and hospital wastewater [2]. Antibiotics in the environment has been reported worldwide, such as in rivers of Europe [3,4], surface water of America [5,6], rivers of Australia [7] and seas and rivers of Asia [8,9].

*Corresponding author.

The presence of antibiotics in environmentally relevant levels has been associated with chronic toxicity to some non-target organisms and evolution of antibiotic-resistant bacteria [10]. Thus, the antibiotics in wastewater are of particular concern, as they can induce bacterial resistance, even at low concentrations [11].

The fluoroquinolone group (ciprofloxacin, norfloxacin and enrofloxacin) is one of the most important pharmaceuticals used worldwide for humans and veterinary purposes. Norfloxacin is a synthetic antibacterial agent occasionally used to treat common as well as complicated urinary tract infections. The presence of such broad-spectrum antibiotics in aquatic environments may pose serious threat to the ecosystem and human health by inducing proliferation of bacterial drug resistance [12]. To avoid the dangerous accumulation of antibiotics in the aquatic environment, research efforts are underway to develop powerful treatment. Although different physical, biological and chemical methods are available for the treatment of waste water and as since antibiotics are non-biodegradable, physical and biological treatment methods are not applicable for degradation of antibiotics. Hence, advanced oxidation processes (AOPs) technique is chosen in the present study. AOPs are based on the generation of hydroxyl radical (OH) as oxidant. AOPs are very efficient methods for destruction and mineralization of recalcitrant organic compounds in pharmaceutical effluents.

Recent studies show that AOP can be successfully applied for the treatment of drug wastewater [13,14]. Degradation of amoxicillin by ozonation and photo-Fenton has also been reported [15,16]. UV/H₂O₂ process also could degrade carbamazepine very effectively [17]. UV/TiO₂ immobilization glass beads process is used effectively for decolourization of an Azo Dye C.I. Direct Red 23 [18]. Photoreactors used for liquid-phase oxidation are typically based on the slurry system, in which TiO₂ particles are suspended in an aqueous solution. The immobilized TiO₂ glass beads under UV light are configured more effective towards the treatment of recalcitrant organic pollutants. Moreover, release of TiO₂ particles into the environment leads to potential adverse effects on human and ecological health. Interactions of TiO₂ particles with exposed cells and organic pollutants disrupt cellular energy metabolism and increase intra-cellular oxidative stress, DNA double-strand breaks and chromosomal damage, although nano-TiO₂ alone shows no significant cytotoxicity or genotoxicity [19,20]. Norfloxacin was selected as the model pollutant in this paper since it had been widely detected in aqueous environment and it is known to cause severe

pollution problems to the aquatic environments. The different UV combination methods such as UV/H₂O₂, Fenton process, photo-Fenton, UV/ TiO₂ and UV/ IGBT were applied for the degradation of norfloxacin.

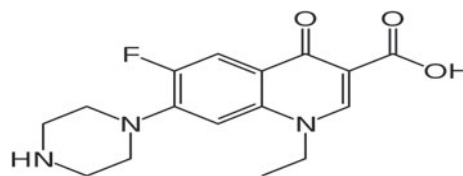
2. Materials and methods

2.1. Chemicals and reagents

Norfloxacin is procured from one of the reputed pharma laboratory with purity of 99%. Degussa P₂₅ titanium dioxide is obtained from Degussa Corporation, Pune, India. H₂O₂ solution (30%, reagent grade) is procured from Lobacheme. FeSO₄·7H₂O (ferrous sulphate) as the source of Fe(II), H₂SO₄ (sulphuric acid) and NaOH (sodium hydroxide) are purchased from Merck. All the chemicals used in the present study are of analytical grade. Distilled water is used for the entire study. Chemical structure of norfloxacin is shown in Fig. 1.

2.2. Reactor set-up

All the experiments are performed in a cylindrical photoreactor (Fig. 2) with a total volume of 1.0 L (diameter 12 cm and height 13.3 cm). The UV lamp is encased in a quartz tube to protect it from direct contact with an aqueous solution flowing through an annulus between the inner surface of the vessel and the outer surface of the quartz tube, located at the axis of the vessel. The reactor is provided with inlets for feeding reactants, and ports for measuring temperature and withdrawing samples. The reactor is open to air with Teflon coating. A magnetic stirrer is placed at the bottom for homogenization. The UV irradiation sources is 250-W low-pressure mercury vapour lamp (maximum emission at 365 nm) encased in the quartz tube. The lamp was axially centred and immersed in the solution containing the respective norfloxacin. A gas tight syringe is used to collect the sample at regular intervals from the sample-port of the reactor.



1-ethyl-6-fluoro-4-oxo-7-piperazin-1-yl-1H-quinoline-3-carboxylic acid

Fig. 1. Structure of norfloxacin.

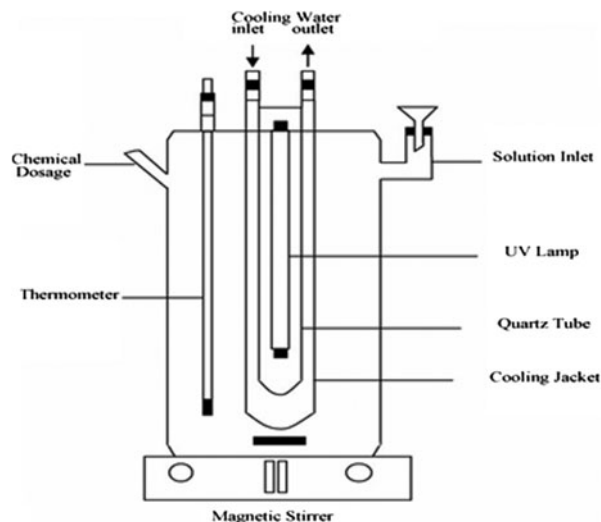


Fig. 2. The schematic of the laboratory-scale photochemical reactor.

2.3. Experimental set-up

Desired quantities of substituted norfloxacin is weighed and dissolved in distilled water to prepare 1,000 ppm stock solution. The shelf life of the stock solutions was maintained for 1 week. Further dilutions are made from stock solution. All the stock solutions, standards and pure compounds are stored in dark below room temperature. The samples are brought to room temperature before experimentation. Control samples are run for every experiment to validate the degradation and also check for any loss on volatilization. Norfloxacin solutions are treated at different pH values. The adjustment of pH is made with 0.1 N/1.0 N solution of H_2SO_4 or 0.1 N/1.0 N NaOH.

Experiments are carried out in batch mode. Different concentrations of H_2O_2 and Fe^{2+} in the ratio of 10:1 are used in photo-Fenton experiments. In case of UV/ H_2O_2 , different concentrations of hydrogen peroxide (50, 100, 150, 200 and 250 ppm) are used to observe norfloxacin degradation. Initial concentration of norfloxacin is 150 mg/L. In Photocatalytic experiments with TiO_2 , the dosage of TiO_2 is varied from 0.1 to 0.5 g. The reaction mixture is homogenized by magnetic agitation for 15 min before introducing into the photoreactor. Samples are withdrawn at regular intervals and centrifuged, followed by filtration through 0.25- μm membrane disc filters (MDI, India type SY25NN). The filtrate is stored at 4°C and further analysed for compound degradation and COD reduction. The samples containing H_2O_2 are treated with MnO_2 powder to decompose the residual H_2O_2 since it interferes with the COD and absorbance measurements [21]. In order to arrest oxidation after

treatment time, the filtered samples are quenched by adding 10% Na_2SO_3 aqueous solution [22].

2.4. Preparation of Immobilization of TiO_2 on Glass Beads

TiO_2 is supported on glass beads by heat attachment method as follows. Glass beads are etched with dilute hydrofluoric acid (5% v/v) for 24 h and washed thoroughly with distilled water, making a rough surface for better contact of TiO_2 on the glass beads surface. TiO_2 slurry is prepared with a known amount of TiO_2 (2 g) in 200 mL distilled water and continuously mixed for 24 h. The glass beads are immersed in the slurry of TiO_2 and were thoroughly mixed for 20 min. It is then removed from the suspension and placed in an oven for 1.5 h at 150°C. It is subsequently placed in the furnace for 2 h at 500°C. The samples are thoroughly washed with doubly distilled water for the removal of free TiO_2 particles [23–26].

2.5. Analytical procedure

Norfloxacin concentration is measured by Shimadzu-2450 UV-vis Spectrophotometer at a wavelength of 272 nm and TOC measured by Shimadzu TOC-L CPH E 200. COD analysed as per the standard method No. 5220 C, from STANDARD METHODS for the examination of Water and Wastewater 20th addition 1998, APHA.

The norfloxacin removal percentage (%) is calculated as follows:

$$\text{Removal of the norfloxacin (\%)} = \frac{C_i - C_f}{C_i} \times 100 \quad (1)$$

where C_i is the initial pollutant concentration (mg/L) and C_f is the final pollutant concentration (mg/L).

3. Results and discussion

3.1. UV Photolysis

3.1.1. Effect of pH on the degradation of norfloxacin

To study the effect of pH on norfloxacin degradation, a series of experiments are carried at different pH values ranging from 3 to 11 with initial concentration of norfloxacin 150 mg/L, and COD reduction, the results of which are illustrated in Figs. 3 and 4. It has been observed that the photodegradation of norfloxacin is influenced by the pH value, and the maximum compound degradation % and COD reduction of norfloxacin (49 and 46%) is achieved at pH 7 after 180-min irradiation. The compound degradation

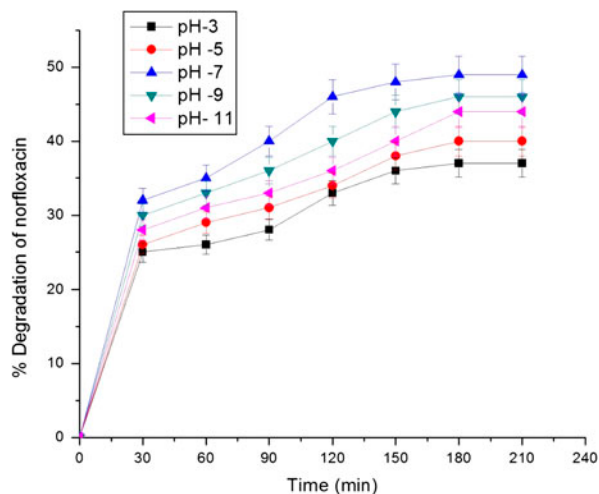


Fig. 3. Variation in initial pH on the degradation of norfloxacin and initial drug concentration of 150 ppm.

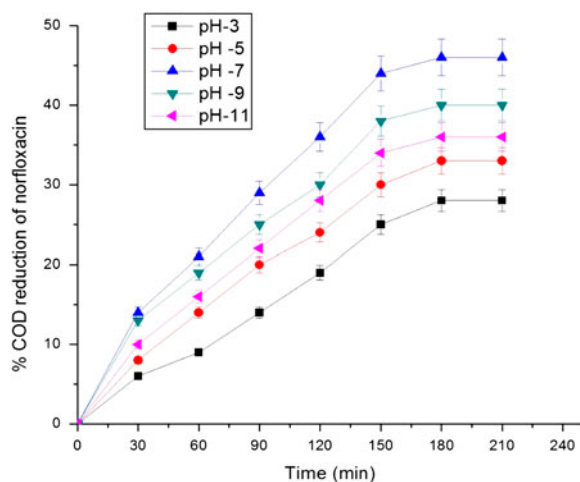


Fig. 4. Variation in initial pH on the COD reduction of norfloxacin and initial drug concentration of 150 ppm.

decreased from 49 to 37% with increasing pH from 7 to 11. This is in agreement with the observation of Stefan et al. [27] that direct photolysis contributions decreased when the pH is increased from 3 to 7. pH may affect the formation of active substance in the generation of hydroxyl radical. Effect of pH on the photodegradation of norfloxacin demonstrates that pH plays an important role in the photochemical degradation of norfloxacin in aqueous solution.

3.2. Effect of Initial concentration on the degradation of norfloxacin

Optimization experiments on direct photolysis of norfloxacin are first carried out by irradiating the

aqueous solution to determine the effect of initial concentration with 250-W UV lamp. Photolysis is a common method for generating free radicals through sigma bond cleavage. These radicals are most often the precursors that generate other free radicals [28]. The first step in a photochemical reaction is the excitation of a molecule through absorption of one photon. The excited molecule leads to a chemical reaction. Thus, the organic substrate is progressively degraded. In order to choose the effective concentration of norfloxacin, studies are conducted in the range of 50–250 ppm of norfloxacin at pH 7 (Figs. 5 and 6). From the concentration screening experiments, it has been observed that 150 mg/L of the norfloxacin compound concentration is efficiently degraded with maximum COD % reduction (45 and 40%). And above 150 mg/L, the degradability diminished and COD reduction diminished. For all further experiments, 150 ppm of the norfloxacin is considered as optimum concentration.

3.3. Peroxide with UV process

The effect of initial H_2O_2 concentration on the degradation of norfloxacin and COD reduction is illustrated in Figs. 7 and 8. Hydrogen peroxide doses are varied from 50 to 250 ppm. In the presence of UV/ H_2O_2 process, the norfloxacin photodegradation increased when compared to direct photolysis even at low initial H_2O_2 concentrations. The efficiency increased with increasing H_2O_2 concentration. However, increasing the initial hydrogen peroxide concentration enhanced the oxidation up to a certain level. On further increase in concentration, hydrogen peroxide inhibition on the photolytic degradation of the drug is observed. From these experiments, it has been observed that the optimum H_2O_2 concentration is 200 ppm at which 72% compound removal and 66% COD reduction has achieved. Further addition of H_2O_2 did not improve the degradation rate due to self-decomposition of H_2O_2 . Moreover, at higher concentrations, hydrogen peroxide acted as a free-radical scavenger itself, thereby decreasing the hydroxyl radical concentration and reducing compound elimination efficiency [29–32]. From all these experiments, it is concluded that the optimum H_2O_2 concentration is 200 ppm at which 72% of norfloxacin degradation is absorbed from the suspension at pH 7 after 180-min irradiation.

The following reactions are observed in peroxide-mediated photo-oxidation. The photolysis of hydrogen peroxide leads to the formation of $\cdot OH$ radicals [33].

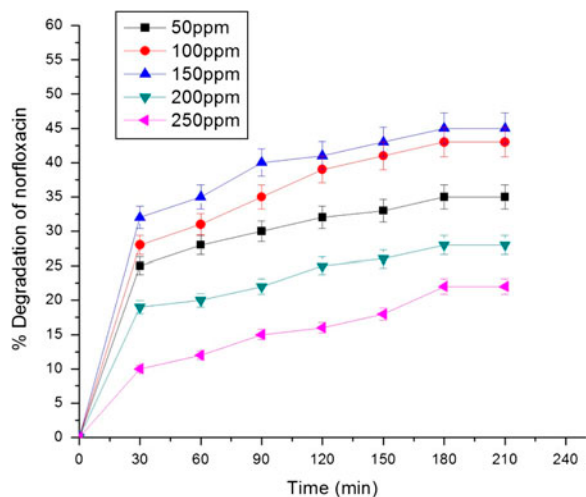


Fig. 5. Variation in initial norfloxacin concentration.

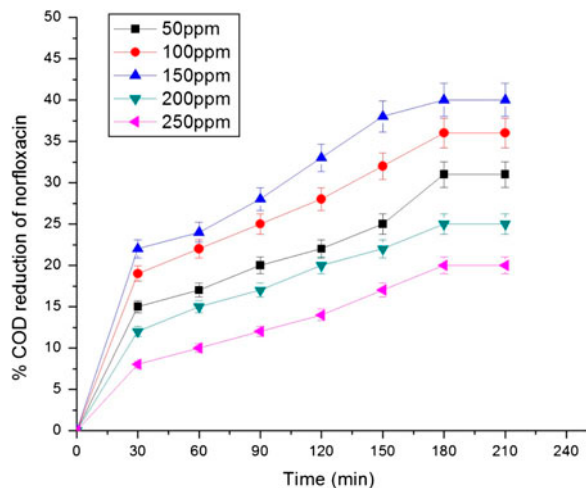


Fig. 6. Variation in initial norfloxacin concentration of the COD reduction.

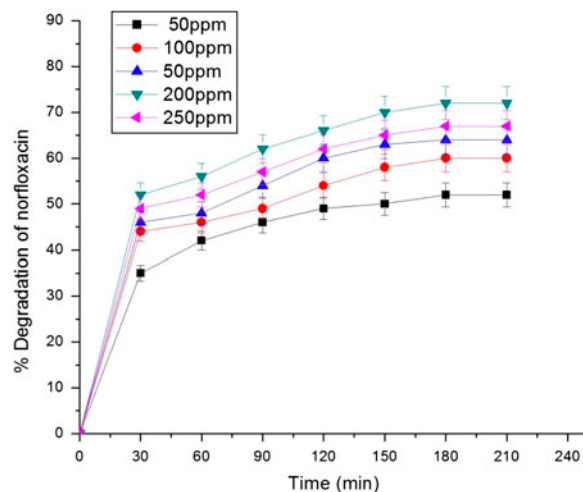
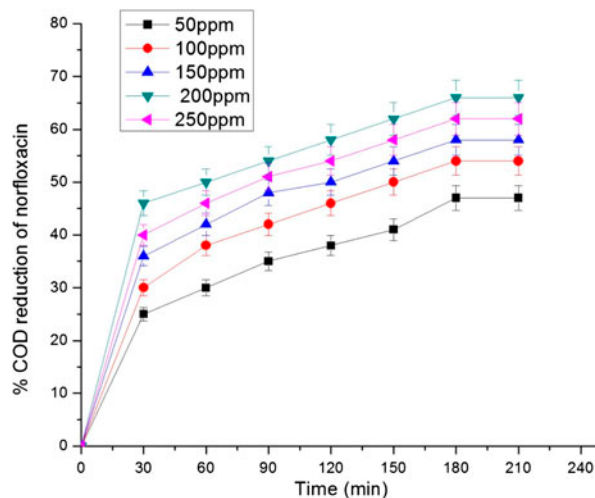


Also, HO_2^- , which is in acid and base equilibrium with H_2O_2 , absorbs the UV radiation of the wavelength at 365 nm and releases $\cdot\text{OH}$ radicals which are responsible for the oxidation of norfloxacin.



3.4. Fenton and photo-Fenton oxidation

Results reported in the relevant literature clearly indicate that the operation pH determines the degree

Fig. 7. Effect of initial H_2O_2 concentration on the degradation of 150 ppm of norfloxacin in peroxide with UV at pH 7.Fig. 8. Effect of initial H_2O_2 concentration on the COD reduction of 150 ppm of norfloxacin in peroxide with UV at pH 7.

of oxidation reached in the treatment, with pH 3.0 being the most effective value [34] (Kang et al.). The efficiency of the treatment experiencing strong reductions as the pH is set out of this interval [35,36]. At higher pH levels, iron precipitates as hydroxide, and at lower levels, self-decomposition of hydrogen peroxide is promoted [37]. Hence, in the present study, the Fenton and photo-Fenton experiments are performed at an acidic pH of 3.0 ± 0.1 with an initial H_2O_2 concentration of 200 ppm.

3.4.1. Effect of initial Fe^{2+} concentrations on the degradation of norfloxacin

The effect of initial Fe^{2+} concentrations on the degradation of the drug in Fenton and photo-Fenton processes is presented in Figs. 9–12 by varying Fe^{2+} concentration from 10 to 50 ppm. The degradation rate of the drug increased with an increase in iron concentration. With Fenton reagent (Fe^{2+}), only 38 and 36% of compound degradation and COD reduction has been achieved. While with photo-Fenton (Fe^{2+} concentration 30 ppm), the maximum compound and COD%

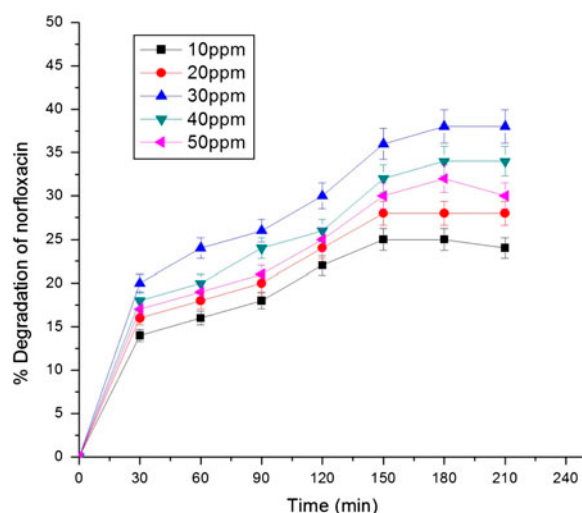


Fig. 9. Effect of initial Fe^{2+} concentrations on the degradation of 150 ppm norfloxacin in Fenton process.

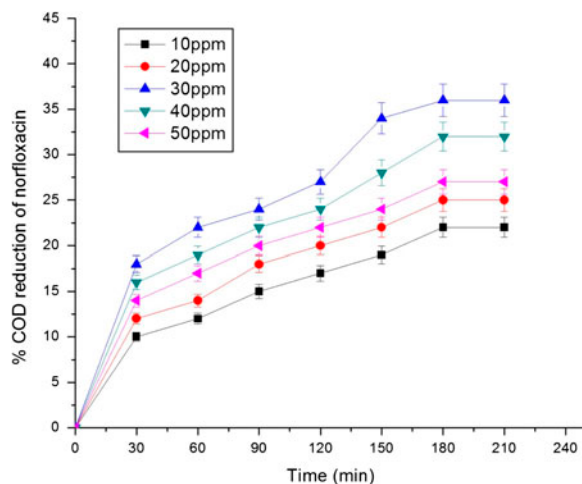


Fig. 10. Effect of initial Fe^{2+} concentrations on the COD reduction of 150 ppm norfloxacin in Fenton process.

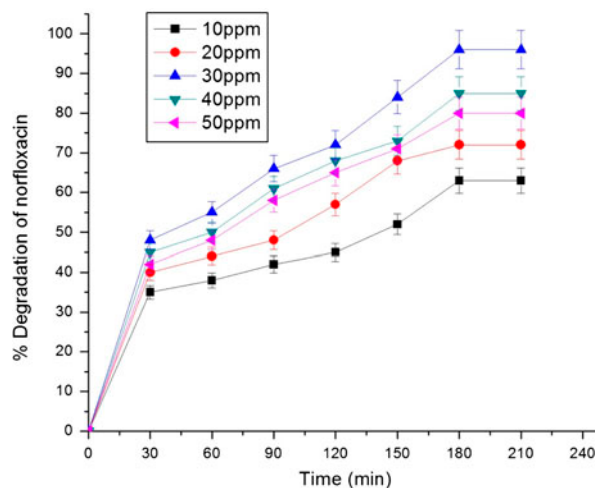


Fig. 11. Effect of initial Fe^{2+} concentrations on the degradation of 150 ppm norfloxacin in photo-Fenton process.

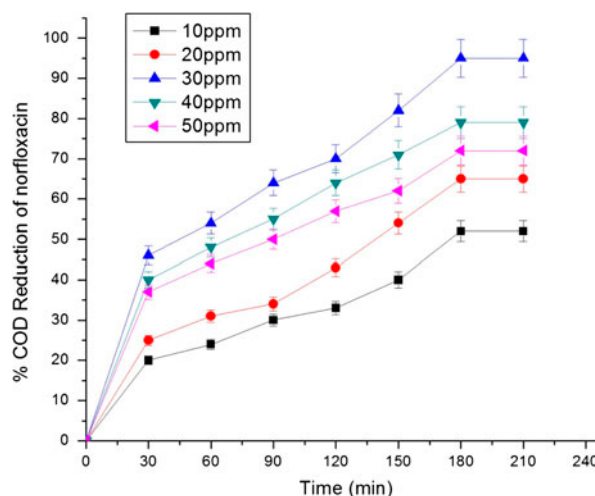


Fig. 12. Effect of initial Fe^{2+} concentrations on the COD reduction of 150 ppm norfloxacin in photo-Fenton process.

reduction observed to be 96 and 93%, respectively. Further increase in iron concentration did not show any change in the degradation rate [38]. This is due to the fact that at a Fe(II) concentration higher than the optimum, most of the hydroxyl radicals are consumed by the side reactions before they could be utilized effectively for the removal of the compound [39]. Moreover, it resulted in brown turbidity that hindered the absorption of the UV light required for photolysis and caused the recombination of OH radicals [40]. The following reactions occur in photo-Fenton process when Fe^{3+} ions are added to the $\text{H}_2\text{O}_2/\text{UV}$.

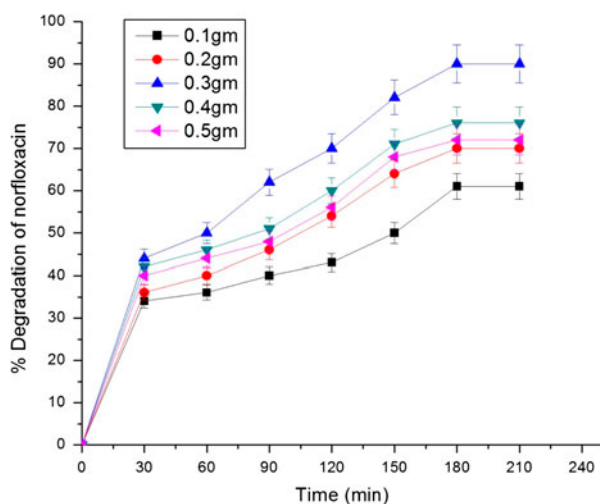
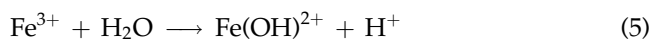
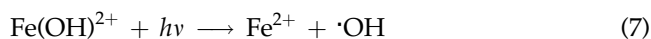


Fig. 13. Effect of TiO_2 dosage on the degradation of 150 ppm norfloxacin at pH 7.



In reaction (7), $\text{Fe}(\text{OH})^{2+}$ complex is formed at pH 3 which when exposed to UV irradiation, the complex is further subjected to decomposition and will produce $\cdot\text{OH}$ and Fe^{2+} ions:



3.5. TiO_2 -mediated photooxidation (UV/ TiO_2)

The effect of different TiO_2 dosages on the degradation COD reduction of norfloxacin is illustrated in Figs. 13 and 14 by varying the dosages from 0.1 to 0.5 g. UV/ TiO_2 results observed that the degradation of norfloxacin is influenced by the pH 7 [41]. Therefore, the surface of the TiO_2 is positively charged under acidic conditions and negatively charged under alkaline conditions. The maximum oxidizing capacity of the TiO_2 is at lower pH; however, the reaction rate is known to decrease at low pH due to excess H^+ [42]. In the presence of TiO_2 process, the efficiency increased with increasing TiO_2 dosage. However, increased initial TiO_2 dosage enhanced the oxidation only up to a certain level. On further increase in the dosage of the catalyst, TiO_2 inhibition on the photolytic degradation of the norfloxacin is observed. Figs. 13 and 14 show 61, 70, 90, 76 and 72% of

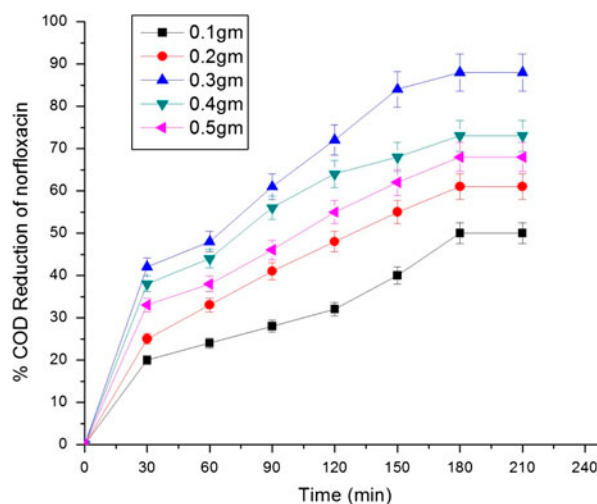
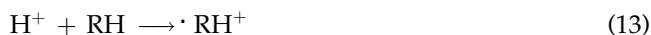


Fig. 14. Effect of TiO_2 dosage on the COD reduction of 150 ppm norfloxacin at pH 7.

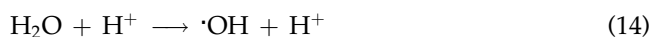
compound degradation and 50, 61, 88, 73 and 68% of COD reduction at 0.1, 0.2, 0.3, 0.4 and 0.5 g dosage of TiO_2 , respectively. From these experiments, it is concluded that the optimum TiO_2 dosage is 0.3 g at which 90 and 88% compound removal and COD reduction is achieved after 180-min irradiation.

The basis of photocatalysis is the photo-excitation of a semiconductor that is solid as a result of the absorption of electromagnetic radiation, often, but not exclusively, in the near-UV spectrum. Under near-UV irradiation, a suitable semiconductor material may be excited by photons possessing energies of sufficient magnitude to produce conduction band electrons and valence band holes [40]. These charge carriers are able to induce reduction or oxidation, respectively. At the surface of the TiO_2 particle, these may react with absorbed species.



Holes possess an extremely positive oxidation potential and should thus be able to oxidize almost all chemicals. Even the one-electron oxidation of water

resulting in the formation of hydroxyl radicals should be energetically feasible.



3.6. UV/TiO₂-immobilized glass beads

The effect of TiO₂-immobilized glass beads (IGBT) on the degradation of norfloxacin and COD reduction has been illustrated in Figs. 15 and 16. The TiO₂ IGBT dosage varied from 2 to 12 g [41]. In the presence of TiO₂ process, the efficiency increased with increasing IGBT. From the results (Figs. 15 and 16), it has been observed that 45, 56, 63, 67, 78 and 70% norfloxacin degradation and 42, 48, 57, 62, 74 and 68% of COD reduction % at 2, 4, 6, 8, 10 and 12 g of IGBT, respectively. However, increased initial IGBT enhanced the oxidation only up to a certain level (10 g) and further increase in the IGBT dose, TiO₂ inhibition on the photolytic degradation and COD reduction of the norfloxacin is observed. From these experiments, it is concluded that the optimum IGBT is 10 g at which 78 and 74% of norfloxacin degradation and COD reduction has been observed at 180-min irradiation, respectively.

3.7. Comparison of various AOPs

3.7.1. COD and TOC reduction

A comparison of UV, UV/H₂O₂, Fenton processes, photo-Fenton, UV/TiO₂ and UV/IGBT in terms of

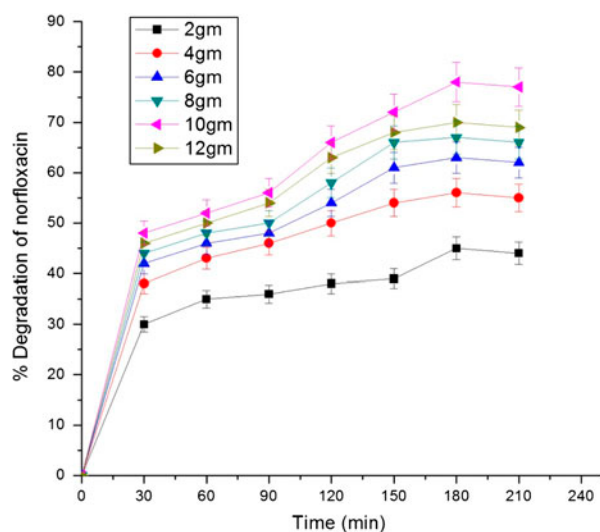


Fig. 15. Effect of TiO₂ IGBT on the degradation of 150 ppm norfloxacin at pH 7.

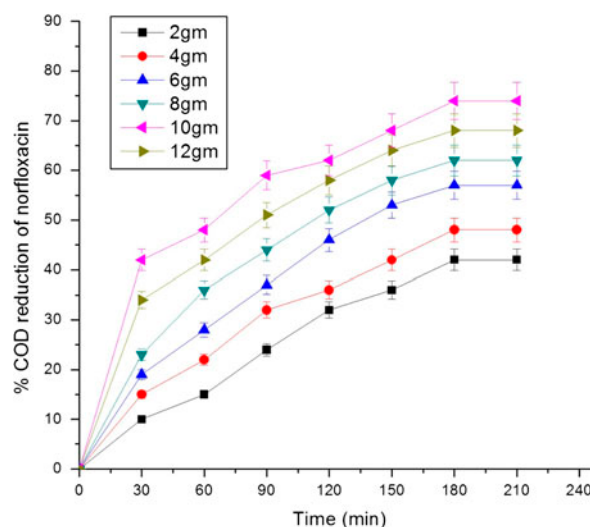


Fig. 16. Effect of TiO₂ IGBT on the COD reduction of 150 ppm norfloxacin at pH 7.

COD and TOC reduction is determined to find the efficacy of the treatment systems. Initial COD and TOC of the norfloxacin are 610 and 495 mg/L, respectively. Percentage reduction of COD and TOC with different AOPs is shown in Figs. 17 and 18. UV alone, Fenton process, UV/H₂O₂, UV/TiO₂ and UV/IGBT could not totally remove COD and TOC in Table 1. Hence, it is observed that the photo-Fenton process is increased; reduction in COD and TOC is found to be 95 and 93%, respectively (Figs. 19 and 20).

3.8. Cost estimation

Cost evaluation is one of the important aspects in the treatment of waste. Cost estimates are developed to allow direct comparison among the various AOPs studied. The costs for AOPs are highly dependent on the quality of the source water to be treated and effluent treatment goals.

Hence, in the present section, an attempt is made on the estimation of operating costs for the treatment processes used considering norfloxacin as the model compound. The cost of reagents is given in Table 2.

Cost evaluation for UV processes was based on electrical energy per order (EE/O) [43] using the following formula:

$$\text{EE/O (kWh/m}^3\text{)} = \frac{Pt \times 1000}{V \times 60 \log(C_{\text{in}}/C_{\text{fin}})}$$

where P is the rated power (kW), V is the volume (in litres) of water treated, t is the time (min), C_{ini} and C_{fin}

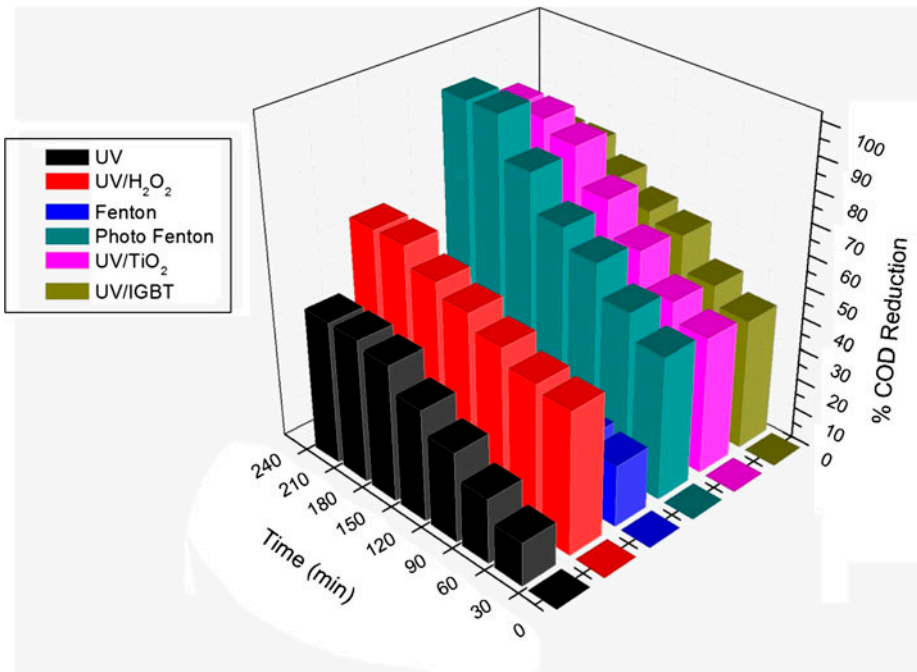


Fig. 17. COD reduction in norfloxacin using various (AOPs).

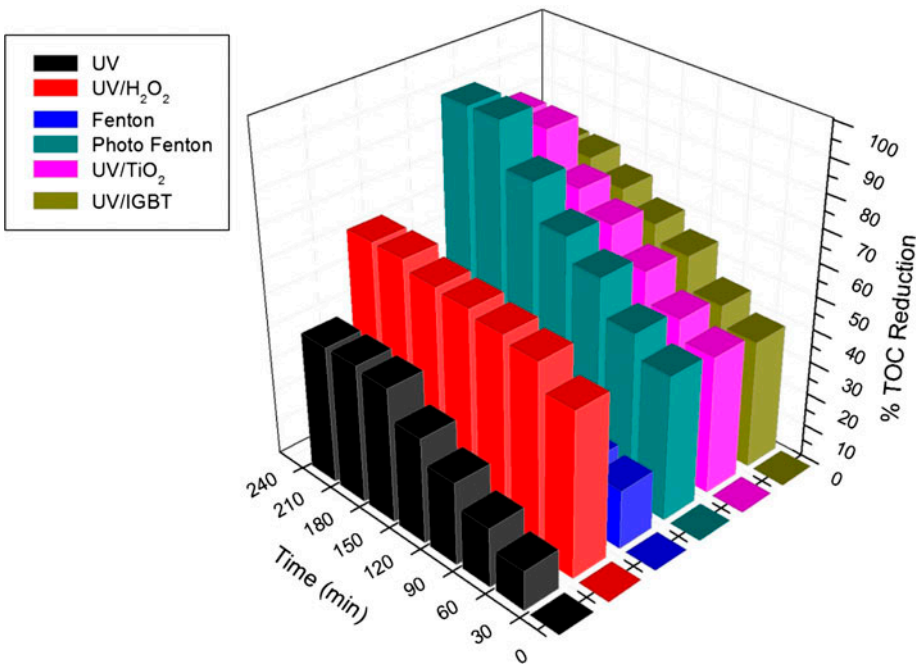


Fig. 18. TOC reduction in norfloxacin using various (AOPs).

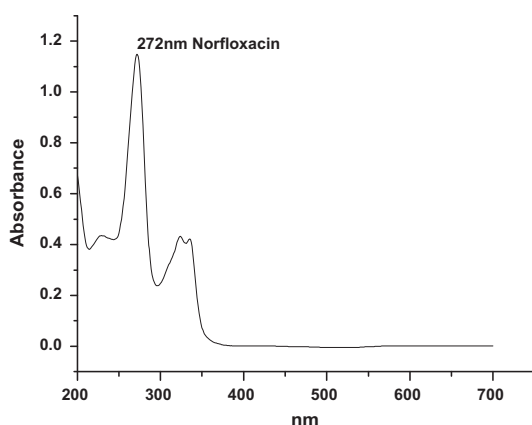


Fig. 19. Initial norfloxacin UV-vis spectrum.

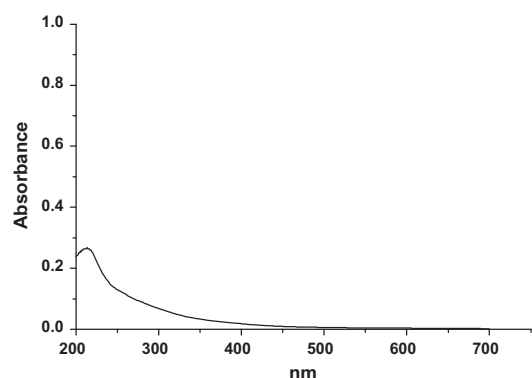


Fig. 20. Final spectrum of norfloxacin After treating with US/Fenton.

are the initial and final concentrations of the compound to be treated. The operating costs of the treatment processes used in the degradation of norfloxacin are given in Table 3.

Table 1

Several AOPs for norfloxacin degradation expressed % and mg/L (Initial concentration of norfloxacin 150 mg/L)

S. no.	Different AOPs	Norfloxacin degradation (%)	Norfloxacin degradation (mg/L)
1	UV	45	67.5
2	UV/H ₂ O ₂	72	108
3	Fenton processes	38	57
4	Photo-Fenton	96	144
5	UV/TiO ₂	90	135
6	UV/IGBT	78	117

Table 2

Cost of the reagents

S. no.	Reagent	Basis	Cost (\$)
1	H ₂ O ₂	kg	6.17
2	FeSO ₄ ·7H ₂ O	kg	4.76
3	TiO ₂	kg	33.98
4	HF	kg	10.58
4	Glass beads	kg	17.95
5	Electricity	KW h	0.088

Table 3

Operating costs of the treatment methods used in the degradation of norfloxacin

S. no.	Process	Treatment cost (\$/m ³)	Norfloxacin degradation (%)
1	UV	2.94	45
2	UV/H ₂ O ₂	9.98	72
3	Fenton	8.82	38
4	UV/Fenton	18.35	96
5	UV/TiO ₂	21.80	90
6	UV/IGBT	6.99	78

4. Conclusions

- (1) The results of this study showed that the degradation of norfloxacin is strongly accelerated by the oxidation process.
- (2) pH 7 is found to be considerable for the degradation of norfloxacin in UV irradiation.
- (3) The rate of degradation of norfloxacin by photo-Fenton process is greater than that which can be achieved by either UV alone, Fenton process, photo-Fenton, UV/H₂O₂, UV/TiO₂ and UV/IGBT or in combination with any other chemical or reagent used in the present study.
- (4) The optimum conditions obtained for the best degradation with photo-Fenton process were pH 3, iron concentration of 30 ppm and 200 mg/L H₂O₂ for an initial antibiotic concentration of 150 mg/L.
- (5) It was found that the TiO₂ suspension had better degradation than that of IGBT.

References

- [1] T. Heberer, Occurrence, fate, and removal of pharmaceutical residues in the aquatic environment: A review of recent research data, *Toxicol. Lett.* 131(1–2) (2002) 5–17.

- [2] B. Pauwels, W. Verstraete, The treatment of hospital wastewater: An appraisal, *J. Water Health* 4 (2006) 405–416.
- [3] Q.T. Dinh, F. Alliot, E. Moreau-Guigon, J. Eurin, M. Chevreuil, P. Labadie, Measurement of trace levels of antibiotics in river water using on-line enrichment and triple-quadrupole LC–MS/MS, *Talanta* 85 (2011) 1238–1245.
- [4] M. Al Aukidy, P. Verlicchi, A. Jelic, M. Petrovic, D. Barcelò, Monitoring release of pharmaceutical compounds: Occurrence and environmental risk assessment of two WWTP effluents and their receiving bodies in the Po Valley, Italy, *Sci. Total Environ.* 438 (2012) 15–25.
- [5] J.M. Cha, S. Yang, K.H. Carlson, Trace determination of β -lactam antibiotics in surface water and urban wastewater using liquid chromatography combined with electrospray tandem mass spectrometry, *J. Chromatogr. A* 1115 (2006) 46–57.
- [6] C. Wang, H. Shi, C.D. Adams, S. Gamagedara, I. Stayton, T. Timmons, Y. Ma, Investigation of pharmaceuticals in Missouri natural and drinking water using high performance liquid chromatography–tandem mass spectrometry, *Water Res.* 45 (2011) 1818–1828.
- [7] A.J. Watkinson, E.J. Murby, D.W. Kolpin, S.D. Costanzo, The occurrence of antibiotics in an urban watershed: From wastewater to drinking water, *Sci. Total Environ.* 407 (2009) 2711–2723.
- [8] S. Zou, W. Xu, R. Zhang, J. Tang, Y. Chen, G. Zhang, Occurrence and distribution of antibiotics in coastal water of the Bohai Bay, China: Impacts of river discharge and aquaculture activities, *Environ. Pollut.* 159 (2011) 2913–2920.
- [9] A. Shimizu, H. Takada, T. Koike, A. Takeshita, M. Saha, Rinawati, N. Nakada, A. Murata, T. Suzuki, S. Suzuki, S.X. Chiem, B.C. Tuyen, P.H. Viet, M.A. Siringan, C. Kwan, M.P. Zakaria, A. Reungsang, Ubiquitous occurrence of sulfonamides in tropical Asian waters, *Sci. Total Environ.* 452–453 (2013) 108–115.
- [10] K. Kümmerer, Antibiotics in the aquatic environment—A review—Part II, *Chemosphere* 75 (2009) 435–441, doi: 10.1016/j.chemosphere.2008.12.006.
- [11] F. Hernandez, J.V. Sancho, M. Ibanez, C. Guerrero, Antibiotic residue determination in environmental waters by LC-MS, *TrAC, Trends Anal. Chem.* 26 (2007) 466–485.
- [12] A.J. Watkinson, E.J. Murby, S.D. Costanzo, Removal of antibiotics in conventional and advanced wastewater treatment: Implications for environmental discharge and wastewater recycling, *Water Res.* 41 (2007) 4164–4176, doi: 10.1016/j.watres.2007.04.005.
- [13] G. Zhang, S. Ji, B. Xi, Feasibility study of treatment of amoxillin wastewater with a combination of extraction, Fenton oxidation and reverse osmosis, *Desalination* 196 (2006) 32–42, doi: 10.1016/j.desal.2005.11.018.
- [14] I. Arslan-Alaton, S. Dogruel, Pre-treatment of penicillin formulation effluent by advanced oxidation processes, *J. Hazard. Mater.* 112 (2004) 105–113, doi: 10.1016/j.jhazmat.2004.04.009.
- [15] R. Andreozzi, M. Canterino, R. Marotta, N. Paxeus, Antibiotic removal from wastewaters: The ozonation of amoxicillin, *J. Hazard. Mater.* 122 (2005) 243–250, doi: 10.1016/j.jhazmat.2005.03.004.
- [16] E.S. Elmolla, M. Chaudhuri, Improvement of biodegradability of antibiotics wastewater by photo Fenton process, *World Appl. Sci. J.* 5 (2009) 53–58.
- [17] D. Vogna, R. Marotta, A. Napolitano, R. Andreozzi, M.d. Ischia, Advanced oxidation of the pharmaceutical drug diclofenac with UV/H₂O₂ and ozone, *Water Res.* 38 (2004) 414–422, doi: 10.1016/j.watres.2003.09.028.
- [18] N. Daneshvar, D. Salari, A. Niaei, M.H. Rasoulifard, A.R. Khataee, Immobilization of TiO₂ nanopowder on glass beads for the photocatalytic decolorization of an azo dye C.I. Direct Red 23, *J. Environ. Sci. Health, Part A* 40 (2005) 1605–1617.
- [19] D. Zheng, N. Wang, X.M. Wang, Y. Tang, L.H. Zhu, Z. Huang, H.Q. Tang, Y. Shi, Y.T. Wu, M. Zhang, B. Lu, Effects of the interaction of TiO₂ nano particles with bisphenol A on their physicochemical properties and *in vitro* toxicity, *J. Hazard. Mater.* 199–200 (2012) 426–432.
- [20] M.H. Li, K.J. Czymmek, C.P. Huang, Responses of *Ceriodaphnia dubia* to TiO₂ and Al₂O₃ nanoparticles: A dynamic nano-toxicity assessment of energy budget distribution, *J. Hazard. Mater.* 187 (2011) 502–508.
- [21] P. Saritha, C. Aparna, V. Himabindu, Y. Anjaneyulu, Comparison of various advanced oxidation processes for the degradation of 4-chloro-2 nitrophenol, *J. Hazard. Mater.* 149 (2007) 609–614, doi: 10.1016/j.jhazmat.06.111.
- [22] M. Trapido, J. Kallas, Advanced oxidation process for the degradation and detoxification of 4-nitrophenol, *Environ. Technol.* 21 (2000) 799–808, doi: 10.1080/09593330.2000.9618966.
- [23] M. Bideau, B. Claudel, C. Dubien, L. Faure, H. Kazouan, On the “immobilization” of titanium dioxide in the photocatalytic oxidation of spent waters, *J. Photochem. Photobiol. A: Chem.* 91 (1995) 137–144.
- [24] J.C. Lee, M.S. Kim, B.W. Kim, Removal of paraquat dissolved in a photoreactor with TiO₂ immobilized on the glass-tubes of UV lamps, *Water Res.* 36 (2002) 1776–1782.
- [25] S. Sakthivel, M.V. Shankar, M. Palanichamy, B. Arabinthoo, V. Murguesan, Photocatalytic decomposition of leather dye comparative study of TiO₂ supported on alumina and glass beads, *J. Photochem. Photobiol. A* 148 (2001) 153–159.
- [26] J.A. Byrne, B.R. Eggins, N.M.D. Brown, B. McKinney, M. Rouse, Immobilization of TiO₂ powder for the treatment of polluted water, *Appl. Catal. B: Environ.* 17 (1998) 25–36.
- [27] M.I. Stefan, A.R. Hoy, J.R. Bolton, Kinetics and mechanism of the degradation and mineralization of acetone in dilute aqueous solution sensitized by the UV photolysis of hydrogen peroxide, *Environ. Sci. Technol.* 30 (1996) 2382–2390, doi: 10.1021/es950866i.
- [28] J. Giménez, D. Curcó, M.A. Queral, Photocatalytic treatment of phenol and 2,4-dichlorophenol in a solar plant in the way to scaling-up, *Catal. Today* 54 (1999) 229–243.
- [29] U. Bali, E. Catalkaya, F. Sengul, Photodegradation of reactive black 5, direct red 28 and direct yellow 12 using UV, UV/H₂O₂ and UV/H₂O₂/Fe²⁺: A comparative study, *J. Hazard. Mater.* 114 (2004) 159–166, doi: 10.1016/j.jhazmat.2004.08.013.

- [30] C. Galindo, P. Jacques, A. Kalt, Photochemical and photocatalytic degradation of an indigoid dye: A case study of acid blue 74 (AB74), *J. Photochem. Photobiol. A: Chem.* 141 (2001) 47–56, doi: [10.1016/S1010-6030\(01\)00435-X](https://doi.org/10.1016/S1010-6030(01)00435-X).
- [31] I.A. Alaton, I.A. Balcioglu, Photochemical and heterogeneous photocatalytic degradation of waste vinylsulphone dyes: A case study with hydrolyzed Reactive Black 5, *J. Photochem. Photobiol. A: Chem.* 141 (2001) 247–254, doi: [10.1016/S1010-6030\(01\)00440-3](https://doi.org/10.1016/S1010-6030(01)00440-3).
- [32] A. Aleboyeh, Y. Moussa, H. Aleboyeh, Kinetics of oxidative decolourisation of Acid Orange 7 in water by ultraviolet radiation in the presence of hydrogen peroxide, *Sep. Purif. Technol.* 43 (2005) 143–148, doi: [10.1016/j.seppur.2004.10.014](https://doi.org/10.1016/j.seppur.2004.10.014).
- [33] C. Tizaoui, K. Mezughi, R. Bickley, Heterogeneous photocatalytic removal of the herbicide clopyralid and its comparison with UV/H₂O₂ and ozone oxidation techniques, *Desalination* 273 (2011) 197–204.
- [34] N. Kang, D. Soo Lee, J. Yoon, Kinetic modeling of Fenton oxidation of phenol and monochlorophenols, *Chemosphere* 47 (2002) 915–924, doi: [10.1016/S0045-6535\(02\)00067-X](https://doi.org/10.1016/S0045-6535(02)00067-X).
- [35] V. Kavitha, K. Palanivelu, Degradation of nitrophenols by Fenton and photo-Fenton processes, *J. Photochem. Photobiol. A: Chem.* 170 (2005) 83–95, doi: [10.1016/j.jphotochem.2004.08.003](https://doi.org/10.1016/j.jphotochem.2004.08.003).
- [36] M. Federico, V. Fernando, V. Natalia, Changes in solution color during phenol oxidation by Fenton reagent, *Environ. Sci. Technol. A* 40 (2006) 5538–5543, doi: [10.1021/es060866q](https://doi.org/10.1021/es060866q).
- [37] S. Meriç, D. Kaptan, T. Ölmez, Color and COD removal from wastewater containing Reactive Black 5 using Fenton's oxidation process, *Chemosphere* 54 (2004) 435–441, doi: [10.1016/j.chemosphere.2003.08.010](https://doi.org/10.1016/j.chemosphere.2003.08.010).
- [38] A. Durán, J.M. Monteagudo, A. Carnicer, M. Ruiz-Murillo, Photo-Fenton mineralization of synthetic municipal wastewater effluent containing acetaminophen in a pilot plant, *Desalination* 270 (2011) 124–129.
- [39] A. Yamila, F. Liendo, O. Nunez, On the Fenton degradation mechanism-The role of oxalic acid, *Arkivoc x* (2003) 538–549. Available from: <http://dx.doi.org/10.3998/ark.5550190.0004.a49>.
- [40] M.Y. Ghaly, G. Hartel, R. Mayer, R. Haseneder, Photochemical oxidation of P-chlorophenol by UV/H₂O₂ and photofenton process—A comparative study, *Water Manage.* 21 (2001) 41–47.
- [41] W.Y. Wang, Y. Ku, Effect of solution pH on the adsorption and photocatalytic reaction behaviors of dyes using TiO₂ and Nafion-coated TiO₂, *Colloids Surf. A Physicochem. Eng. Aspects* 302 (2007) 261–268.
- [42] M. Kosmulski, pH-dependent surface charging and points of zero charge, *J. Colloid Interface Sci.* 298 (2006) 730–741.
- [43] M.A. Rodrigo, P.A. Michaud, I. Duo, M. Panizza, G. Cerisola, Ch Comninellis, Oxidation of 4-chlorophenol at boron-doped diamond electrode for wastewater treatment, *J. Electrochem. Soc.* 148 (2001) D60–D64.

See discussions, stats, and author profiles for this publication at: <https://www.researchgate.net/publication/303638382>

Traffic noise level assessment in Ranga reddy district

Article · May 2016

CITATIONS

0

READS

12

1 author:



Dr Bhagawan DS

Jawaharlal Nehru Technological University, Hyderabad

23 PUBLICATIONS 10 CITATIONS

SEE PROFILE

All content following this page was uploaded by [Dr Bhagawan DS](#) on 18 January 2017.

The user has requested enhancement of the downloaded file. All in-text references [underlined in blue](#) are added to the original document and are linked to publications on ResearchGate, letting you access and read them immediately.

Traffic Noise level assessment in Ranga Reddy district, India

Bhagawan D¹, Saritha Poodari², Ch. Anand³,
Shankaraiah G⁴, and V. Himabindu^{5*}

¹Doctoral student, Center for Environment, Institute of Science and Technology,
Jawaharlal Nehru Technological University, Hyderabad, India 500 085

²Post Doctoral Research Associate, Center for Environment, Institute of Science and
Technology, Jawaharlal Nehru Technological University, Hyderabad, India 500 085

³Research Scholar, Center for Environment, Institute of Science and Technology,
Jawaharlal Nehru Technological University, Hyderabad, India 500 085

⁴Doctoral student, Center for Environment, Institute of Science and Technology,
Jawaharlal Nehru Technological University, Hyderabad, India 500 085

^{5*}Associate Professor, Center for Environment, Institute of Science and Technology,
Jawaharlal Nehru Technological University, Hyderabad, India 500 085

Abstract

Noise is an inevitable consequence of today's society, acoustic noise beyond a level is harmful. It is a significant environmental problem in many rapidly urbanizing areas. Most of the cities in India being alarming noise pollution, the main thrust of this investigation was to estimate the noise level in Rangareddy (R.R. Dist) city. Assessed noise level was represented in terms of L_{max}, L_{min}, Leq, L₁₀, L₅₀, L₉₀, TNI and L_{NP}. It was observed that noise levels were more than that of the prescribed limits of y Central Pollution Control Board (CPCB) and The National Institute for Occupational Safety and Health (NIOSH). Most of the Leq values were found in the range of 76.2+10dB. The L_{max} is approximately 1.2 folds higher than the prescribed levels. Vehicular load at each station per day was calculated, among commercial zone facing more vehicle load than industrial zones. Highest noise levels during day times was ranged between 71.7 -109.2dB, during night times was ranged in between 54.9 – 101.9 dB in commercial locations. Day time highest noise was ranged from 76 to 105.1 dB and during night times ranged between 71.5 - 97 dB in industrial zone. Remedial measures were suggested.

Keywords: Traffic, Noise, Industrial sector, Vehicle, Urban.

INTRODUCTION

Noise pollution is a significant environmental problem in many rapidly urbanizing areas. Which effects the human health and contributes deterioration of the environmental quality. Noise pollution was of two categories, they were indoor and outdoor [8]. Indoor is due to playing of loudspeakers and industrial machinery movements, where as outdoor noise pollution is mainly contributed by the transportation sector and is identified as the most common forms of community annoyance [6]. The increase in the number of vehicles was aggravating the situation day by day, therefore noise level also accelerating [5]. High exposure to noise level can causes feeling of annoyance and irritation, damage to auditory mechanisms, number of health related effects like physiological disorders, psychological disorders, disturbances of daily activities and performances, hypertension and rheumatic heart diseases [11]. According to National Institute for Occupational Safety and Health, human exposure time to noise level of 100dB is approximately 15minutes only. These permissible sound levels and exposure time are given in table: 1. Standard safe time limit has been set for the exposure to noise levels. Beyond this 'safe' time, exposure might lead to loss hearing.

Table 1: Noise Limits According NIOSH

Sound Pressure Level	Permissible Exposure Time
115 dB	~30 sec
112 dB	~1 min
109 dB	< 2 min
106 dB	3.75 minutes
103 dB	7.5 minutes
100 dB	15 minutes
97 dB	30 minutes
94 dB	1 hour
91 dB	2 hours
88 dB	4 hours
85 dB	8 hours
82 dB	16 hours

Traffic related noise pollution accounts for nearly two-third of the total noise pollution in an urban area. Traffic noise on existing urban road-ways lowers the quality of life and property values for person residing in vicinity of these urban corridors. Due to limited availability of land resources and finances, many highways and important roads were in the residential and commercial areas. Hence there will be some adverse and environmental effects including psychological and physiological effects to those living to proximity of these corridors.

The assessment of the existing or envisaged changes in traffic noise condition might give a definite solution to noise pollution. In present paper we reported the noise levels of the busy traffic junctions in the areas of Rangareddy District, India.

STUDY AREA

R.R.Dist. is located at the heart of the Deccan Plateau of the Indian sub continent and lies between 17° 20' North latitude and 78°28' East by longitude. This area was undergone rapid industrialization and rapid undergoing urbanization. It covers an area of 7662.71sq.kms with average density of 707 per sq. km. Due to explosion of population and rapid industrialization, the transportation in the city increased to unimaginable heights. The required efficient mass transit systems, individual vehicular growth also touched the heights. A mixed population right from elite urban to the downtrodden and poverty driven rural population, it may be witnessed a mixed cosmopolitan culture in urban areas due to the migrant of people. In the recent days, there was a tremendous development in the sub-urban of R.R district due to establishment of Hi-Tech city, Universities, Hardware and chemical industries, Engineering & Medical Colleges, Software Companies, and IIIT etc. In Ranga Reddy dist., the traffic was usually heterogeneous and the condition of traffic interrupts very frequently to vehicular passage. Further, heavy traffic volumes and higher speed increased the loudness of traffic noise. It created deceleration and acceleration of noises as vehicles approach and depart from each of the signal. The monitored stations basic information was given in table 2

Table 2: Details of the noise monitoring locations

S.No	Name of the location	Nature of Land use	Traffic characteristics	Type of junction
1	Balanagar	Commercial	Heavy traffic flow	X-type
2	Bowenpally	Commercial	Heavy traffic flow with frequent traffic jams	X-type
3	ECIL	Commercial	Medium traffic flow	T-type
4	Hi-Tech city	Commercial	Heavy traffic flow	X-type
5	Bollaram	Industrial	Medium traffic flow	T-type
6	Jeedimetla	Industrial	Continues traffic flow	T-type
7	JNTU	Commercial and Institutional	Heavy traffic flow with continues traffic jams	X-type
8	Miyapur	Commercial	Heavy traffic flow with frequent traffic jams	T-type
9	Near WIPRO	Commercial	Heavy traffic flow	T-type
10	Y-junction	Commercial	Heavy traffic flow with frequent traffic jams	Y-type

METHODOLOGY

Road traffic noise level is monitored in the day (6:30am-10:00pm) and night (10:30pm) (sampath, 2004) by a digital sound level meter (CESVA make, Model-160, Type-II). The monitoring programme was carried out in the month of March 2012 for two consecutive days and nights with five sampling stations per day. Sound level readings were collected for every 30 min over a period of 10min and were analyzed for most

commonly adopted noise rating methods in environmental noise studies which are L_{max} , L_{min} , L_{eq} , L_{10} , L_{50} , L_{90} , TNI and L_{NP} where:

1. L_{max} is the Maximum Noise Level in dBA
2. L_{min} is the Minimum Noise Level in dBA
3. L_{eq} is the Equivalent Sound Level in dBA
4. L_{10} are the noise level in dBA exceeded only 10% of the time or Peak Sound Level.
5. L_{50} is the noise level in dBA exceeded only 50% of the time or Mean Sound Level.
6. L_{90} is the noise level in dBA exceeded only 90% of the time or Background or Residual Noise Level.
7. TNI is the Traffic Noise Index calculated by the equation:

$$TNI = 4 \times (L_{10} - L_{90}) + L_{90} - 30 \text{Db}$$
8. L_{NP} is the Noise Pollution level calculated by the equation:

$$L_{NP} = L_{aeq} + (L_{10} - L_{90})$$

Care was taken to retain a distance between the instrument and the surrounding building walls or other obstacles which might intensify or reduce the received noise.

RESULTS AND DISCUSSION

The noise sampling locations are categorized into 2 zones based on guidelines of CPCB. The temporal analysis is done at the study area and noise indexes are represented in table 2.

Table 3 Ambient Air Quality Standards in respect of Noise

S.No	Category of Area/Zone	Limits in dB(A) L_{eq}	
		Day Time	Night Time
1	Industrial Area	75	70
2	Commercial Area	65	55
3	Residential Area	55	45
4	Silence Zone	50	40

(Source: The Noise Pollution (Regulation and Control) Rules, 2000)

Table 4: Noise Index values of the study area

Sampling locations	TIME	Lmax	Lmin	Leq (dB)	L50(dB)	L10(dB)	L90(dB)	TNI(dB)	LNP
Balanagar	Day	107.1	75.8	92	91.5	107.1	95	113.4	104.1
	Night	97.6	76.2	84.3	83.3	97.6	87.3	98.5	94.6
Bowenpally	Day	103.1	74	85.8	83.7	103.1	88.8	116.1	100.1
	Night	90.5	55	68.6	68.3	90.5	71.6	117.1	87.5
Ecil	Day	101.5	84.4	93.4	94.1	101.5	96.4	86.8	98.5
	Night	101.9	65.2	83.8	82.3	101.9	86.8	117.4	98.9
Hitech City	Day	99.3	84.3	92.1	93.1	99.3	95.1	81.9	96.3
	Night	97.8	78.8	88.6	88.7	97.8	91.6	86.6	94.8
Bollaram	Day	102.6	76.1	91.2	91.8	102.6	94.2	97.7	99.6
	Night	93	76.8	85	85.3	93	88	78	90
Jeedimetla	Day	105.1	76	90.7	91.5	105.1	93.7	109.5	102.1
	Night	97	71.5	83.8	82.2	97	86.8	97.7	94
Jntu	Day	105.4	79.5	95.8	96.9	105.4	98.8	95.1	102.4
	Night	97.3	86.8	91.5	91.5	97.3	94.5	75.8	94.3
Miyapur	Day	109.2	74.7	90.4	90.5	106.8	93.4	117	103.8
	Night	97.4	61.9	83.4	81.4	109.2	86.4	147.6	106.2
Wipro	Day	96.9	71.7	84.8	84.5	96.9	87.8	94.2	93.9
	Night	89.8	49.8	68.7	64.7	89.8	71.7	114.1	86.8
Kukatpally Y- Junction	Day	103.3	74.2	86.7	86.2	103.3	89.7	114.2	100.3
	Night	98.6	76.1	86.9	85.8	98.6	89.9	94.7	95.6

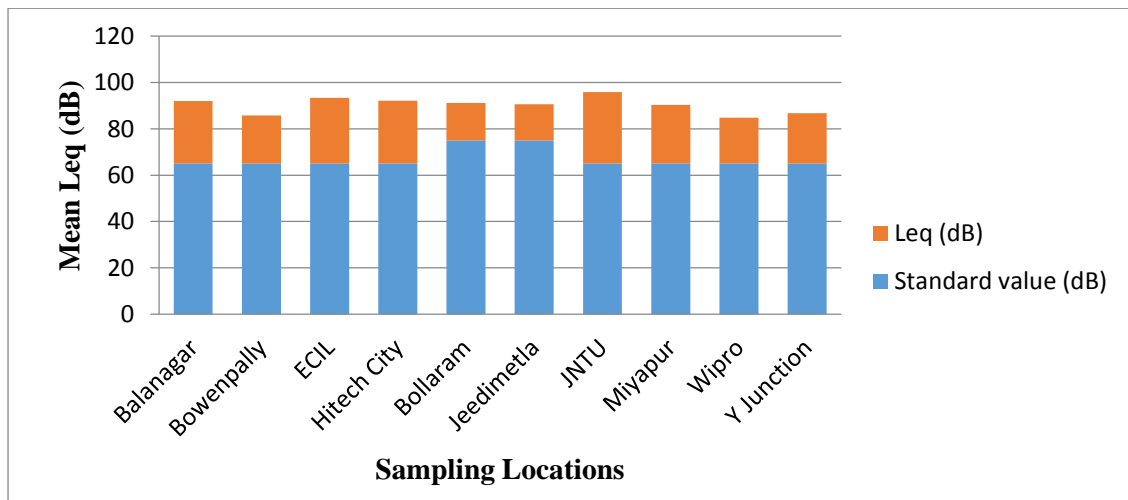


Figure 1: The mean value of Leq in sampling locations in comparison with the standard value during day

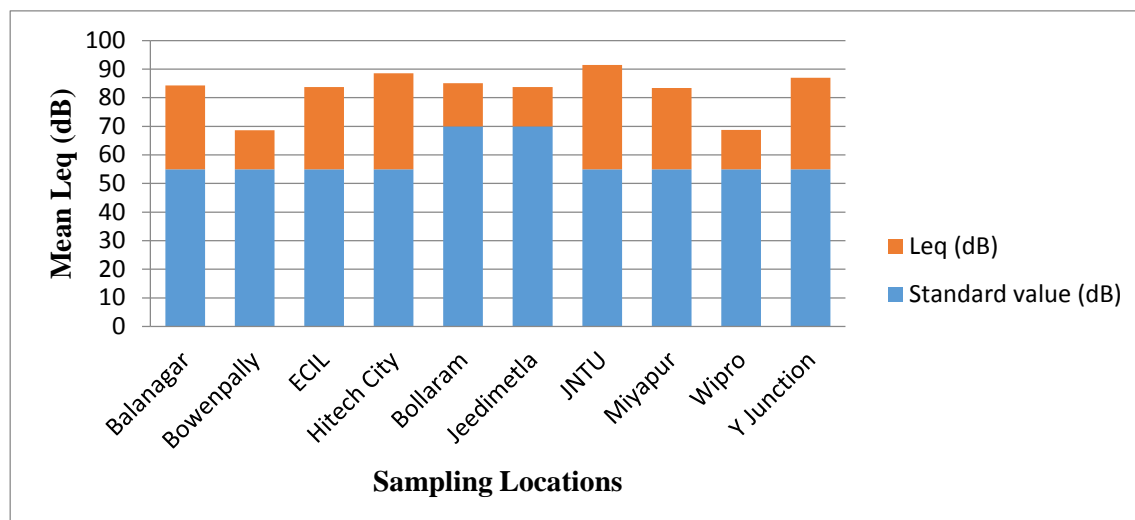


Figure 2: The mean value of Leq in sampling locations in comparison with the standard value during night

Industrial Zones

The monitoring locations were selected based on proximity of roadways to industrial units. The noise level in this zones were varied between 76 - 105.1 dB(A) during day time, 71.5 - 97 dB(A) during night time. The Day time Leq was ranged between 90.7 - 91.2 dB(A) , night time equivalent noise level was varied between 83.8- 85 dB(A), being higher that to the prescribed limits by CPCB.

Commercial Zone

Being an urban area, commercial establishments were numerous, varying between isolated ones to clusters of shops in the form of markets, shopping complexes, etc. Commercial establishments were present alongside to all the roadways and in the absence of proper footpaths they tend to sprawl on the roads, which cause frequent traffic congestions and noise hot spots. The shop owners and customers were generally exposed to high noise level throughout the day. The noise level varied from 71.7 to 109.2 dB(A) during daytime, while it during night time ranged between 54.9 - 101.9 dB(A). All the locations having noise level above than the prescribed limits during the 24 hours. The people using the period for shopping irrespective to time lines and the movement of heavy trucks during night time was the causes for high noise level. The Leq values ranged from 84.8 to 95.8 dB during the day time, where in night time ranged between 68.6 - 91.5 dB during monitoring period.

In all the locations surveyed, the night-time noise levels were very comparable to those reported for the day-time noise levels.

Attempts were also made to measure the traffic flow at the monitoring points, which contributes the environmental noise on roads. Future increase in traffic volume on these roadways may result in heavy congestions as well as increase in noise level.

Table 5: Traffic Noise Index Noise deviation during Day and Night times

PLACE	Day Time Noise	Night Time Noise	Standard Deviation in TNI
Balanagar	104.1	94.6	6.71
Bowenpally	100.1	87.5	8.90
ECIL	98.5	98.9	0.28
Hi-Tech city	96.3	94.8	1.06
Bollaram	99.6	90	6.78
Jeedimetla	102.1	94	5.72
JNTU	102.4	94.3	5.72
Miyapur	103.8	106.2	1.69
WIPRO	93.9	86.8	5.02
Y-junction:	100.3	95.6	3.32

The day time mean noise levels were observed between 84.9-93.4dB, where night time noise levels were ranged between 73.8-95.2dB. Deviation of the noise level to day and night hours be represented in Table 3, the variation was ranged between 0.4-9.4dB. Highest noise deviation was reported at Bowenpally followed by Wipro, ECIL, Bollaram, Y- junction, Hi-tech city, Miyapur, JNTU, Jeedimetla, and Balanagar were 9.4 dB, 7.9 dB, 5.1 dB, 4.4 dB, 2.5 dB, 1.9 dB, 1.4 dB, 1.2 dB, 1.2 dB, 0.4dB respectively.

It was observed in Table 4, except Hi-Tech city and WIPRO, the % of the two wheelers were at first place. At Hi-Tech city and WIPRO the % cars were at first place. It might be due to allocation of the soft ware parks and residency to the rich families. As earlier we discussed Bollaram was an industrial carder, so % of trucks were occupied the first place.

Table 6: Vehicular % per day

S.No	PLACE	% of Two wheelers	% of Autos	% of Cars	% of Busses	% of Trucks
1	Balanagar	49.0	17.4	17.9	7.9	7.6
2	Bowenpally	44.6	11.8	27.0	8.8	7.5
3	ECIL	48.8	12.0	19.1	9.2	11.0
4	Hi-Tech city	39.9	14.7	41.2	2.5	1.5
5	Bollaram	31.5	14.4	19.0	8.4	26.4
6	Jeedimetla	53.8	17.9	13.8	8.0	6.3
7	JNTU	43.3	17.2	18.7	11.3	9.3
8	Miyapur	39.9	16.6	17.1	10.7	15.4
9	WIPRO	36.7	14.6	43.3	3.2	2.0
10	Y-junction:	50.2	14.1	21.9	8.87	4.7

Future increase in traffic volume on these roadways may result in heavy congestions during the daily peak hours.

CONCLUSION AND SUGGESTIONS:

- Based on the noise survey, it was observed that immediate mitigatory measures were required to control the high road traffic noise emission. Because the traffic noise was higher than the limits set up by Central Pollution Control Board of India.
- Among all the places, noise levels were observed to be high in commercial zones rather than in industrial zones. Since, commercial establishments such as markets, shopping complexes etc., were present along road side and, in the absence of proper footpaths, they tend to sprawl on the roads, which cause frequent traffic congestions and noise hot spots.
- The Leq at JNTU junction is higher compared to all other stations. During day and night times it was 95.8dB and 91.5 respectively. Since this was a commercial as well as an institutional zone.
- Control in the transmission path by installation of barriers between noise source and receiver can attenuate the noise levels: the barrier may be either close to the source or receiver
- The development of Green belt can attenuate the sound levels
- A comprehensive urban land use planning and management

REFERENCES

- [1] Environmental criteria for road traffic noise, Noise Policy Section Environmental Policy Branch Environment Protection Authority, *October 1999*.
- [2] F.J. Langdon and W.E. Scholes, *The Traffic Noise Index: A Method of*
- [3] *Controlling Noise Nuisance*, Building Research Station Current Papers 38168,
- [4] April 1968, pp. 2-3.
- [5] G.Benedetto and R. Spagnolo, Traffic noise survey of Turin, Italy. Applied acoustics printed in great Britain.pg 202-222.
- [6] [H.K.Sy, P.P.Ong, Tang and K.L.Tan., Traffic noise survey and analysis in Singapore. applied acoustics. Pg 115-125.](#)
- [7] [Nayef Al-Mutairi, Assessment of Traffic Noise Pollution Impact of Residential/Commercial Development.Civil Engineering Department, College of Engineering and Petroleum, Kuwait University, Kuwait. J Civil Environment Engg 2012, 2:1](#)
- [8] Shing Tet Leong and Preecha Laortanakul Monitoring and assessment of daily exposure of Roadside workers to traffic noise levels in an asian City: a case study of bangkok streets., *Environmental Monitoring and Assessment* **85**: 69–85, 2003.
- [9] S.SamPATH, S. Murali and Sasi Kumar, Ambient Noise Levels in Major Cities in Kerala; Atmospheric division, Centre for Earth Science Studies, Akkulam Trivandram-695031.j.ind. geophys.union(oct.2004) vol-8,no-4,pp-293-298.

- [10] [T. Vidya sagar and G. Nageswara, Noise Pollution Levels in Visakhapatnam City \(India\), journal of environ. Science engg.vol.48, no.2,p.139-142,aprial2006.](#)
- [11] [National Instruments Corporation, 12/12/2008.](#)
- [12] [Oyedepo S. Olayinka and Saadu A. Abdullahi, 2008. A Statistical Analysis of the Day-time and Night-time Noise Levels in Ilorin Metropolis, Nigeria. *Trends in Applied Sciences Research*, 3: 253-266.](#)
- [13] [Wazir Alam,GIS based Assessment of Noise Pollution in Guwahati City of Assam, India, INTERNATIONAL JOURNAL OF ENVIRONMENTAL SCIENCES Volume 2, No 2, 2011 Received on September 2011 Published on November 2011 731](#)

See discussions, stats, and author profiles for this publication at: <https://www.researchgate.net/publication/303638647>

Remediation of Contaminated Ground water using sonication: Case study of an industrial area of Hyderabad; India

Article in *IRANIAN JOURNAL OF CHEMISTRY & CHEMICAL ENGINEERING-INTERNATIONAL ENGLISH EDITION* · May 2016

CITATIONS

0

READS

29

5 authors, including:



Dr Bhagawan DS

Jawaharlal Nehru Technological University, ...

23 PUBLICATIONS 10 CITATIONS

[SEE PROFILE](#)



Golla Shankar

Jawaharlal Nehru Technological University, ...

6 PUBLICATIONS 6 CITATIONS

[SEE PROFILE](#)

Remediation of Industrially Contaminated Ground Water Using Sonication: Case Study

Bhagawan. D¹, P.Saritha¹, [G.Shankaraiah](#)¹, M. Elander¹ & V.Himabindu^{1*}

¹*Centre for Environment, Institute of Science and Technology, Jawaharlal Nehru Technological University, Kukatpally, Hyderabad-500 085*

Abstract

Water pollution is a serious problem throughout the world. Although, different physico-chemical and biological methods are available for the treatment, the most promising techniques are the so called advanced oxidation processes which are based on the generation of hydroxyl radicals that strongly oxidize the organic matter. Hence in the present study, an attempt is made to remediate ground water samples contaminated with industrial effluents using ultra sonication as one of the advanced oxidation process. Three ground water samples collected from potential industrial zones (Bollaram Anjaneya Temple Sample (BAS), Patancheru Bandlaguda Sample (PBS), Isnapur Sample (IS)) in Hyderabad, the capital of Andhra Pradesh, Southern state of India, were studied for treatment using sonication. It is observed that among the studied ground water samples, a maximum remediation of 91% in Chemical Oxygen Demand (COD) is observed in the sample BAS, while 76% and 60% reduction is observed in IS and PBS samples.

Keywords: Sonication; Advanced Oxidation Processes; Effluents; Hydroxyl Radicals; Ground water sample.

* Corresponding Author:

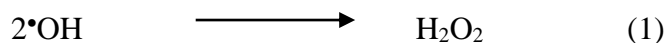
Dr. V.Himabindu, Associate Professor & Head - Centre for Environment Institute of Science and Technology, Jawaharlal Nehru Technological University Hyderabad, Kukatpally, Hyderabad-500085, Andhra Pradesh, India.
E-Mail: drvhimabindu@gmail.com (or) bhagawanist@gmail.com

1. INTRODUCTION

Ground water pollution is a serious problem through out the world. Chemical industry is at the fore front of the water management challenge, due to increasing government pressure on effluent discharge, raw water usage, increasing process water costs and in many locations, general lack of available water. Most ground water is clean, but groundwater can become polluted or contaminated as a result of human activities or as a result of natural conditions. Before the 1980's the regulation of these wastes is less stringent, and waste materials are often disposed of or stored on land surfaces where they percolated into the underlying soil and eventually are carried downward, contaminating the underlying ground water and therefore jeopardizing the natural quality of it. As a result, contaminated ground water became unsuitable for use. Current practices can still impact ground water, such as the over application of fertilizers or pesticides, spills from industrial operations (bulk drugs, pesticides, pharmaceuticals, plastics, ceramics and paints), infiltration from urban runoff, and leaking from landfills. Using contaminated ground water causes hazards to public health through poisoning or the spread of disease and hence the practice of ground water remediation has been developed to address these issues.

Conventional treatments like biological treatments (Sathish kumar.S et al., 2011; Charlespijls, 2010; Albertutier, 2009), chemical treatments (Mirapetrovio et al ., 2011; Michele mascia et al ., 2010) are found to be inefficient . Biological techniques needs maintenance of controlled conditions and much time to remediate (Ghosh,et, al, Alvarez et, al.,2001, [Ibbini et,al,. 2010](#)). While chemical treatment gives rise to additional hazards due to addition of chemicals and denatures its origin (Mirapetrovio et al., 2011; Michele mascia et al ., 2010; [Mark H. Stenzel et al ., 2006](#)). Under such conditions the emerging wastewater treatments like Advanced Oxidation Processes (AOP's) , especially sonochemical methods are gaining popularity since they are more efficient in converting harmful organic pollutants into innocuous compounds such as carbon dioxide and water (Yean ling pang et al ., 2011).

Ultrasonic irradiation has received considerable interest as an AOP because it leads to rapid degradation of chemical contaminants in water. Sonolysis has a distinct advantage over ultraviolet light mediated AOPs since ultrasound is readily transmitted even through opaque systems. Ultrasonic irradiation of liquid reaction mixtures induces cavitations, a process during which the radii of pre-existing gas cavities in the liquid oscillate in a periodically changing pressure field created by the ultrasonic waves (Kejzhang et a.l, 2011; Petrier et al. 1994; R.J. Emery). Ultrasonic waves in water provoke the collapse of cavitation bubbles and induce the formation of reactive chemical species such as H^\bullet , $\bullet\text{OH}$, O^\bullet . H_2O_2 will be formed outside the hot bubble or at the cooler interface as a consequence of $\bullet\text{OH}$ and $\bullet\text{OOH}$ recombination (Reaction 1 and 2) (Yean ling pang et al., 2011). These reactive species are responsible for the destruction of the chemical contaminants in solution. (Suslick, 1989).



Sonolysis alone is not generally deemed to be attractive for application in large-scale chemical process because it requires costly equipment and consumes high amount of energy. However the organics which are non-biodegradable can be de-toxified efficiently using this method.

The present study aims at remediating ground water contaminated with effluent of industrial zones of Bollaram, Patancheru and Isnapur using sono-chemical oxidation. The study stresses the effect of process parameters like frequency, pH, power and Peroxide concentrations. The efficiency of treatment process is evaluated in terms of COD reduction.

2. MATERIALS

2.1 Chemicals

All the chemicals used are of AR grade, which includes pH tablets 4,7,9.2 ;Potassium chloride, Ammonium chloride, Ammonia solution, Sodium hydroxide, EDTA, EB-T indicator, Muroxide indicator, Sulphuric acid, Phenolphthalein solution, Methyl orange indicator, Silver nitrate, Potassium chromate, Potassium nitrate, Hydrochloric acid, Sodium chloride, Sodium sulphate, Glycerol, Isopropyl alcohol ,Barium chloride, Potassium dihydrogen phosphate ,Ammonium molybdate, Stannous chloride ,Sodium fluoride, Spadns reagent , Zirconyl chloride, Nitric acid, Mercuric sulphate, Potassium hydrogen phthalate, Potassium dichromate, Ferrous ammonium sulphate, 1,10-phenanthroline monohydrate, Ferrous sulphate heptahydrate, Silver sulphate, Hydrogen peroxide, Sodium hydroxides. Glass distilled water is used throughout the experiments.

2.2 Reactor setup

The experimental setup consisted of a 3.3 L ultrasonic bath (Model No. EN-30-US, Enertech Electronics Pvt Ltd., Bombay, India, Figure 1) with a high-frequency Mosfet based electronic ultrasound generator. The ultrasonic bath has a two piezo-ceramic transducers bonded to the bottom of a stainless steel tank, with the option of operating at 25 or 33 kHz in a continuous or pulse (5 s on and 1 s off) mode. The ultrasonicator could be operated at three different power outputs, 500 W, 880 W, and 1255 W (power calculated by calorimetric method).

$$\text{Power} = (d_T/d_t) C_p M$$

C_p is the Specific heat of water (4.2J/gK), M is mass of water, d_T/d_t Temperature increment per second.

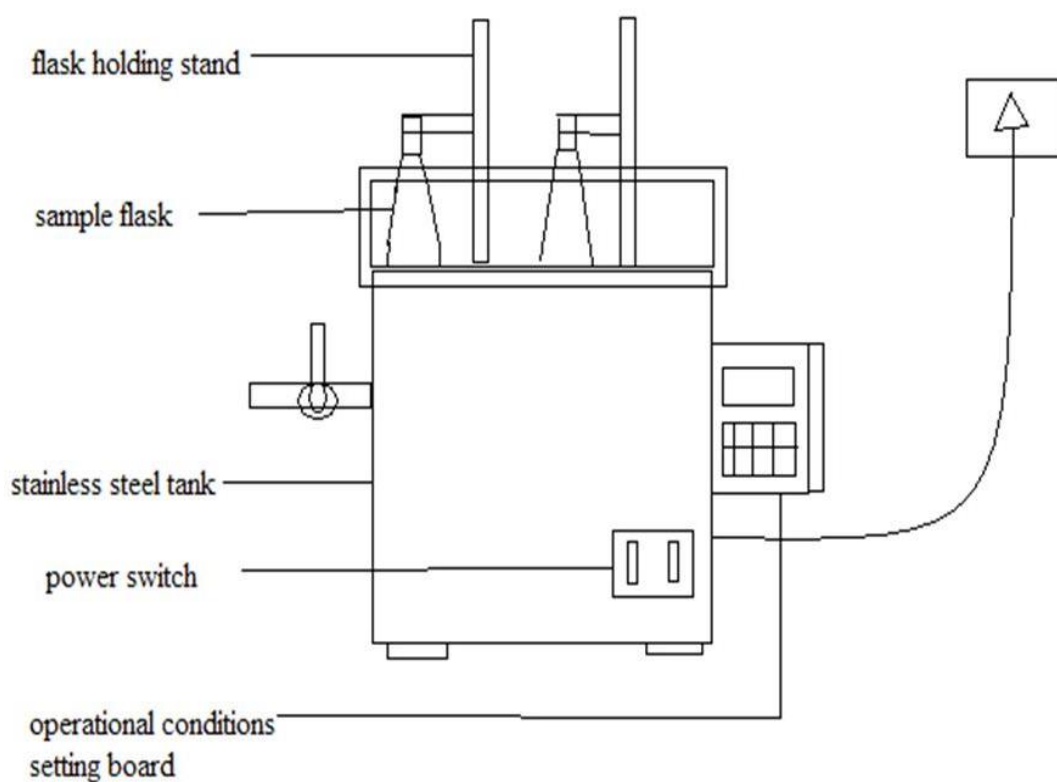


Figure 1: Schematic representation of Ultrasonicator

2.3 Study area

The ground water samples are collected from the area which is contaminated with industrial effluents. Since the last decade, Hyderabad, the capital of Telangana, Southern state of India, has become a hub for pharmaceutical industries. The ground water has been severely contaminated with the effluents released from these industries. Bollaram ($17^{\circ}33'13.46''\text{N}$, $78^{\circ}21'14.64''\text{E}$), Patancheru ($17^{\circ}31'41.70''\text{N}$, $78^{\circ}16'32.1''\text{E}$) and Isnapur ($17^{\circ}32'33.56''\text{N}$, $78^{\circ}10'49.46''\text{E}$) are the three major suburbs of Hyderabad; where about more than 300 industries are located. These industries include bulk drugs, pesticides, pharmaceuticals, plastics, ceramics and paints. The ground water in these areas is highly contaminated with the organics released from these industries.

2.3.1 Initial characterization of the samples

Table: 1: List of Initial Characteristics of the studied samples

S.No	Parameters	BAS	IS	PBS
1	pH	7.54	6.92	5.72
2	Electrical Conductivity	2.11	2.48	3.94
3	Total Dissolved Solids	3530	5160	1970
4	Total Hardness	940	2000	2100
5	Calcium Hardness	600	1125	1000
6	Calcium Hardness as	240	450	400
7	ca	580	1540	1795
8	Non-carbonate Hardness	360	460	305
9	Alkalinity	974.87	1435.72	1152.1
10	Chlorides	241.52	134.28	251.76
11	Sulphates	54.93	27.67	7.017
12	Nitrates	156.9	120.3	141.2
13	Sodium	5.8	1.0	4.1
14	Potassium	0.66	1.22	1.40
15	Fluorides	0.98	2.24	4.69
16	Fe	0.47	5.01	0.45
17	Zn	0.47	0.02	0.43
18	Ni	0.15	0.11	0.01
19	Ba	229.75	245.9	38.35
20	Ca	0.02	0.006	0.03
21	Co	0.01	0.01	0.01
22	Cr	0.05	0.001	0.01
23	Cu	0.007	3.09	2.7
24	Mn	0.08	0.07	0.02
25	Pb	120	140	80
	COD			

**Note: All the parameters are expressed as mg/l except for pH and EC.*

2.4. Experimental methodology

The ground water samples are initially characterized according to “**Standard Methods for Examination of the Water and Waste water 20th addition 1998 APHA**”. According to the experimental plan, each water sample remediation is initiated with power variations of 500W, 880W and 1255W which are measured using calorimetry method. Ultrasono-oxidation of ground water samples are carried out using a constant sample volume of 100ml. Before starting the experiment the initial organic content in the water sample is measured. Then Ultrasono-oxidation was carried out at two different frequencies (25 kHz, 33 kHz) which are available in the equipment and three different power variations (500W, 880W, 1255W) are applied to each ground water samples. The effective conditions (power & Frequency) to reduce COD content of ground water samples are all studied. Optimum pH required for treatment of ground water samples is studied by varying the pH from 3 to 11 (3, 5, 7, 9 and 11). At regular intervals, 5-10ml of sample is withdrawn and analyzed for COD content in the ground water sample. pH adjustments are carried out by using 0.1N H₂SO₄, 0.1N NaOH. The optimum peroxide dosage is identified by adding different concentrations of H₂O₂ (10ppm to 900ppm) to the ground water sample.

3. RESULTS AND DISCUSSION

In this chapter results obtained during the remediation of ground water samples are presented and discussed in detail. The rate of remediation of ground water samples are investigated as a function of H₂O₂ concentration, pH variation, COD reduction, Ultra sonic power and frequency.

3.1 Effect of frequency of Sonicator on COD reduction of ground water samples at 1255W power

Experimental Conditions: Volume of the sample: 100ml; Power: 1255w; Frequencies: 25 and 33 kHz.

The sonochemical remediation of polluted ground water samples is studied under two different frequencies 25 kHz and 33 kHz. Figure 2 shows the percentage reduction of organics in ground water with frequency variation. From the figure, it is observed that higher frequency increased the COD reduction i.e., it showed a maximum COD reduction of 56% and 34% for samples BAS & IS at a frequency of 33 kHz. The low efficiency at 25 kHz can be explained by the fact that the lifetime of the bubbles produced at low frequencies is longer and the production of radicals is slower, compared to higher frequencies. Moreover, the extent of recombination would be higher at low frequencies as the radicals will have enough time to recombine inside the bubble.

However, a sample PBS showed reverse result i.e., in this sample maximum COD reduction of 45% was observed at 25 kHz while only 25% reduction in COD was

observed at 33 kHz. This might be due to the degradation of organics mostly inside the bubble phase (Muthupandian, 2007, Goel et al., 2004). On the other hand, frequency of ultrasound has two counteracting effects on the generation of hydrogen radicals. At very low frequency, although more hydroxyl radicals are generated inside the bubble, chances of recombination of the OH radicals inside the bubble are higher due to the higher temperature inside the bubble. As the frequency increases, the pulsation and collapse of the bubble occur more rapidly causing more radicals to escape from the bubble. However, at very high frequency, the acoustic period is much shorter, thus decreasing the size of the cavitation bubble. As a result, the cavitation intensity decreases, subsequently decreases the amount of OH radicals in the solution. The existence of an optimum frequency with respect to generation of OH radicals was reported earlier in the literature Petrier and Francony 1997 and Kang et al., (1999).

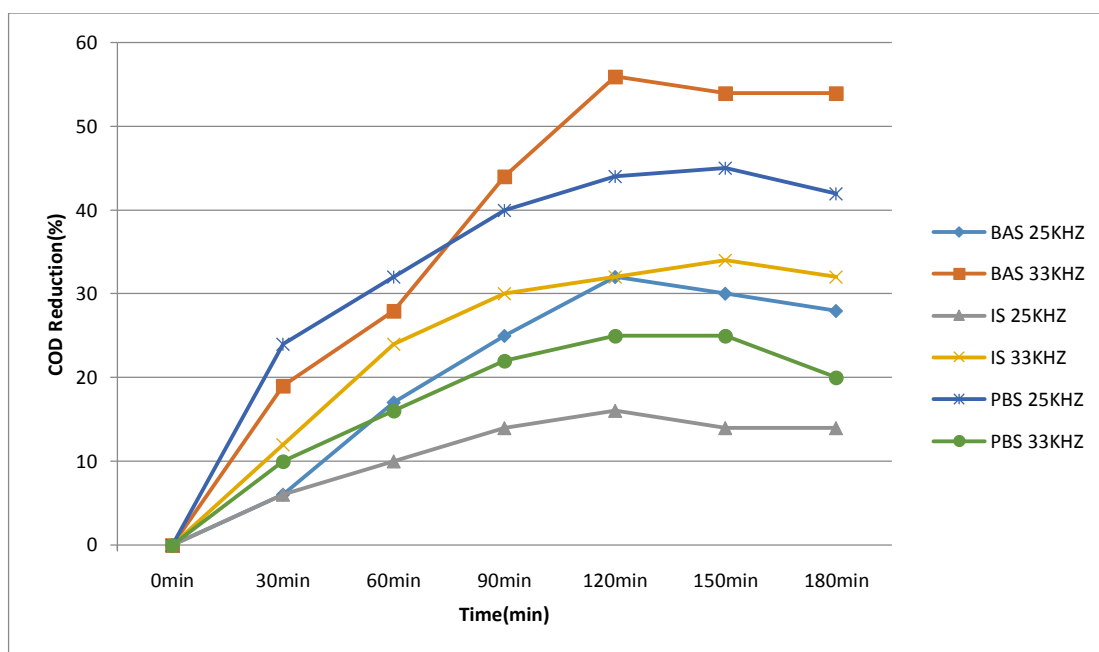


Figure 2: Effect of Frequency on COD Reduction (%).

3.2 Effect of power on COD reduction of ground water samples

Experimental Conditions: volume of sample= 100ml; Frequency =33 kHz (BAS, IS), 25 kHz (PBS); pH=7; Power variation: 500W (40%), 880W (70%), 1255(100%).

Sonochemical degradation of polluted ground water is studied at different powers of 500W, 880W and 1255W. From Figure 3 it is clearly observed that percentage COD reduction increased with increasing applied power. The percentage COD reduction is observed to be 34%, 24%, & 20% for BAS, IS, and PBS samples at 500W power. As

the power is increased to 1255W, COD reduction also increased, in case of BAS, COD reduction is observed to be 56%, for IS - 34% and for PBS-45%. The results observed in this study are comparable with that reported by Kang et al. whose observations indicate enhanced degradation of organics present in the ground water samples with increased power intensity. The beneficial effect of power on increased COD reduction is attributed to increase in cavitation activity. With an increase in the power the number of collapsing bubbles also increases, thus leading to enhanced reduction levels. In addition, applying more power not only enlarges cavitating bubbles, but also generates higher temperature and pressures during bubble collapse, which further enhances sonolytic degradation.(Y.L Pang et al., 2011).

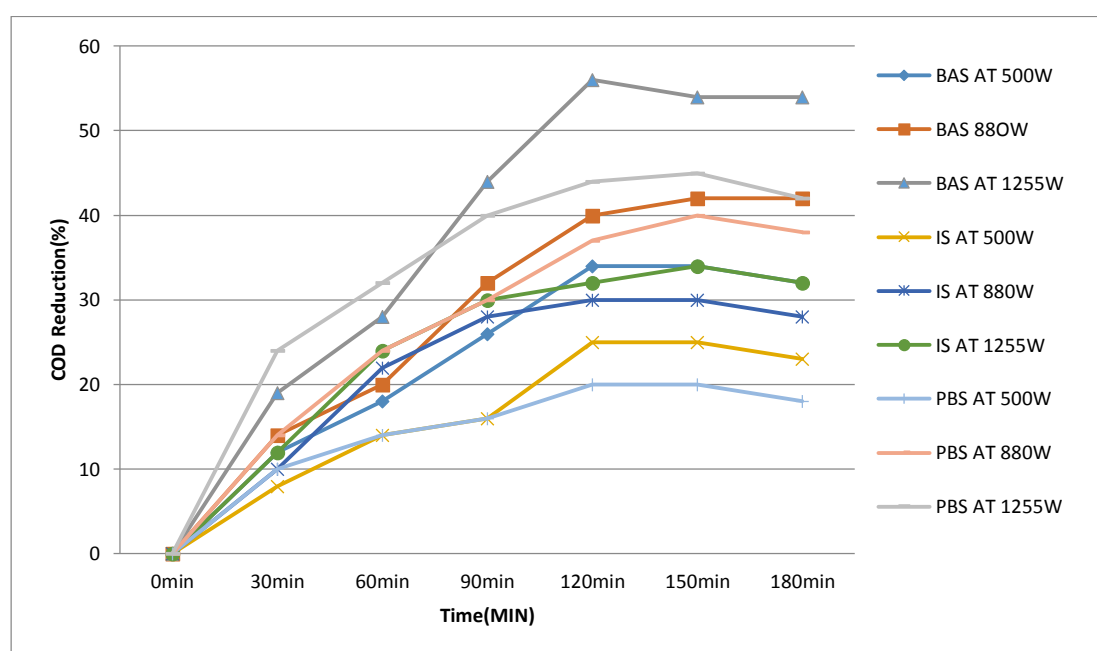


Figure 3: Effect of Power on COD Reduction (%).

3.3 Effect of pH on COD reduction of ground water samples

Experimental Conditions: volume of sample= 100ml; Frequency =33 kHz (BAS, IS), 25 kHz (PBS); pH=3, 5, 7, 9, 11; Power: 1255(100%).

Solution pH is an important factor in determining the physical and chemical properties of the solution which in turn affects the bubble dynamics. The effect of pH on percentage degradation of COD in sonication process is investigated by varying the pH from 3-11. COD reduction of all the three samples is found to be higher at neutral conditions (pH-7) than under acidic and basic conditions which might be caused by the physico-chemical properties of organics present in the samples. A maximum reduction

of COD at pH 7 is observed (Figure 4) to be 56%, 34% and 45% for samples BAS, IS and PBS. A gradual decrease in COD reduction is observed when the pH is increased above pH 7.0. This observed decrease is probably due to the fast decomposition of hydroxyl radicals. Below pH 7.0 the released OH radicals combined with the H ions present in the ground water sample and thus decreased the reduction rate (Yean ling pang et al., 2011).

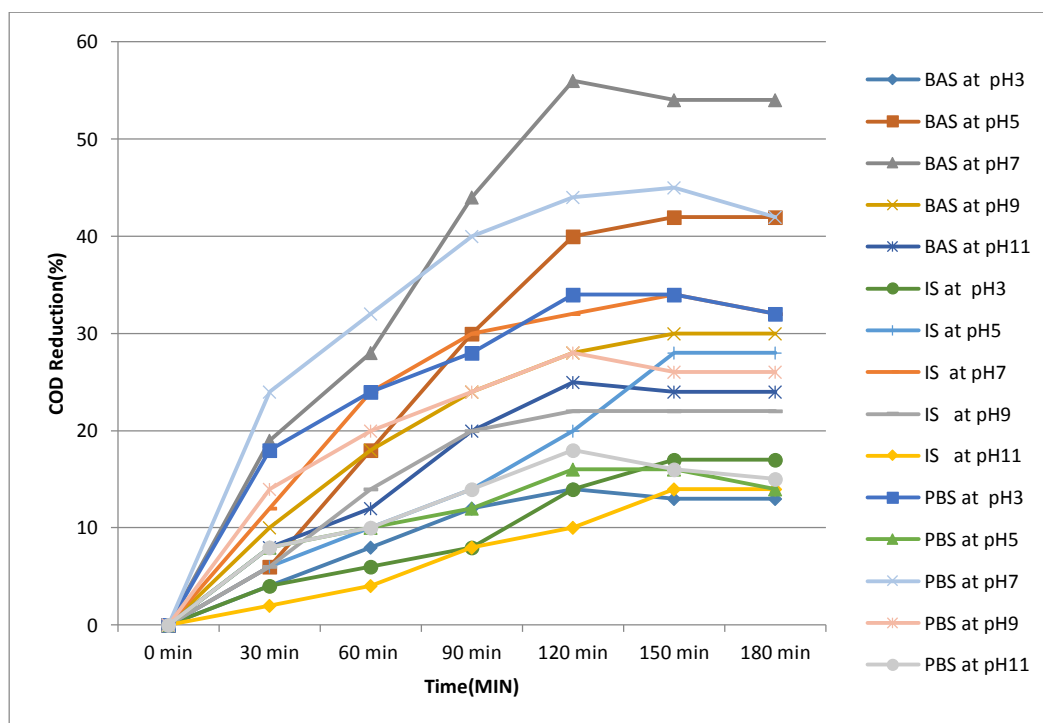


Figure 4: Effect of pH on COD Reduction (%).

3.4 Effect of peroxide on COD reduction of ground water samples

Experimental Conditions:

volume of sample= 100ml; Frequency =33 kHz (BAS, IS), 25 kHz

(PBS); PH= 7; power: 1255(100%); H₂O₂ concentration variations: 10- 900ppm.

Initially experiments are carried with H₂O₂ alone. But negligible reduction in COD is observed. However, when H₂O₂ is combined with ultra-sonication an increase in the COD reduction is observed. There by, the degradation of organics present in the ground water sample using sonooxidation is investigated in presence of H₂O₂ with varying

concentrations of H_2O_2 from 10 ppm to 900 ppm (Figure 5, Figure 6, Figure 7). From the graph, it is clearly observed that with an increase in peroxide concentration, COD reduction also increased. A maximum of 91% reduction in COD is observed for sample BAS with a peroxide concentration of 500 ppm. In case of ground water sample IS, 76% COD reduction is observed with an increased peroxide concentration of 800 ppm while for PBS, 60% reduction in COD is observed with the addition of 40ppm hydrogen peroxide. However, addition of excess peroxide above the optimum did not increase the COD reduction since, at very high load of H_2O_2 , detrimental effects are observed due to the recombination reaction of hydroxide radicals. Also, H_2O_2 acts as a scavenger for hydroxide radicals, thereby decreasing the COD reduction efficiency of the treatment system. Moreover, the presence of higher concentration of H_2O_2 results in lower intensity of cavitation due to the generation of vaporous cavities. (Jose Gonzalez Garcia et al., 2010).

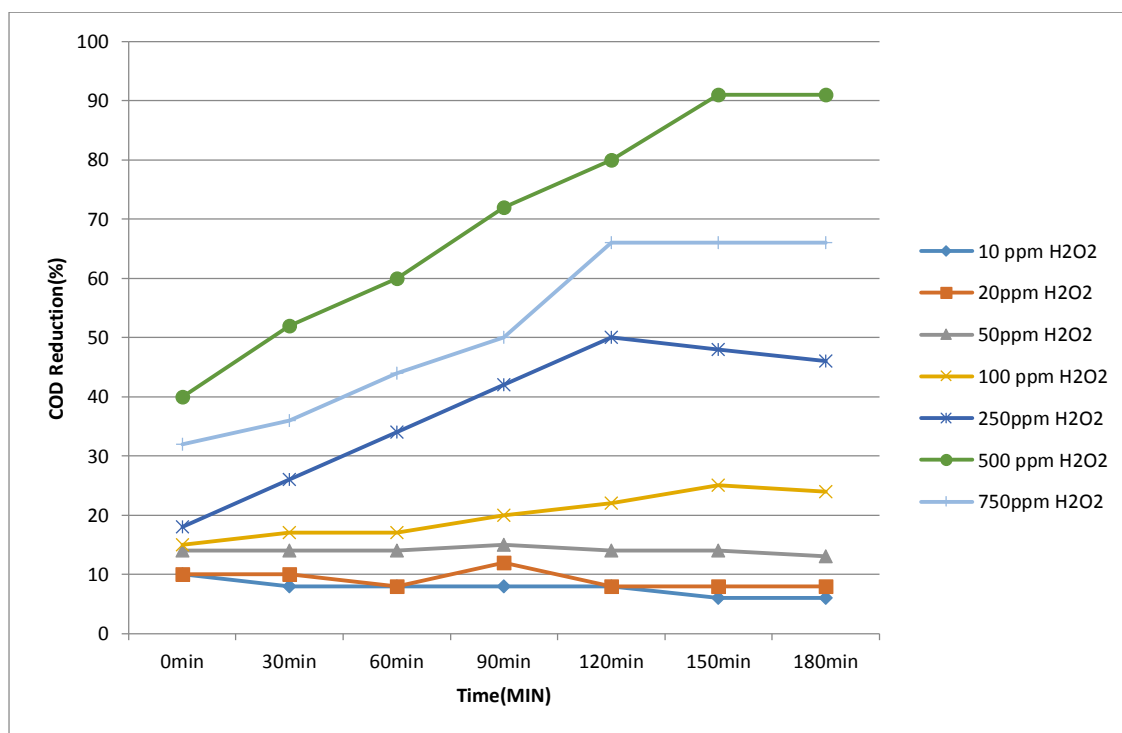


Figure 5: Effect of H_2O_2 on COD Reduction (%) for BAS.

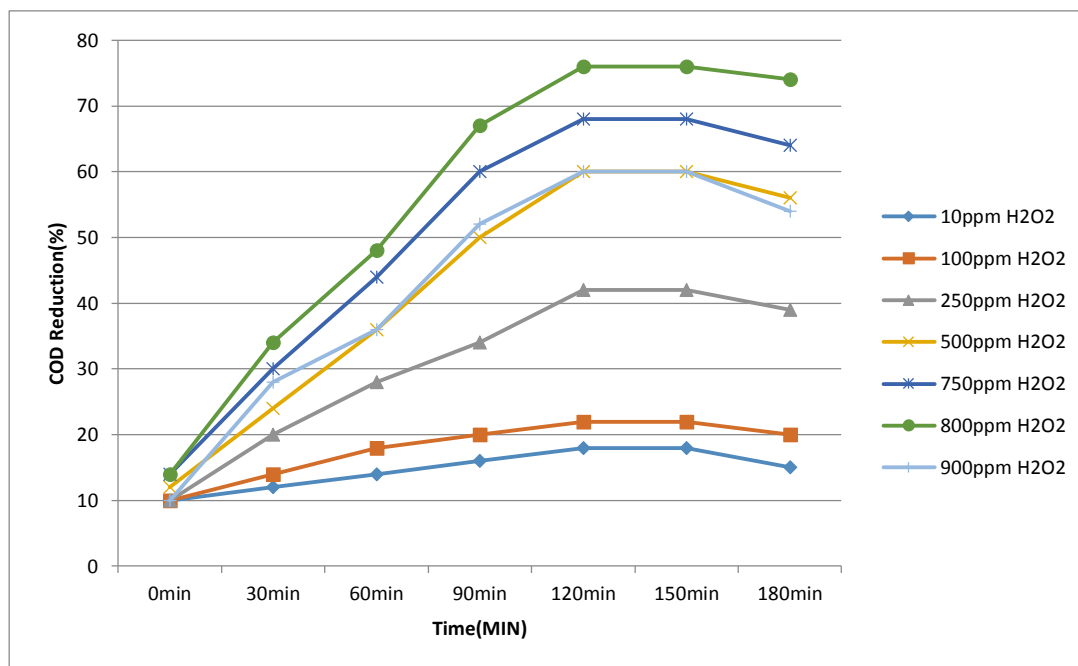


Figure 6: Effect of H₂O₂ on COD Reduction (%) for IS

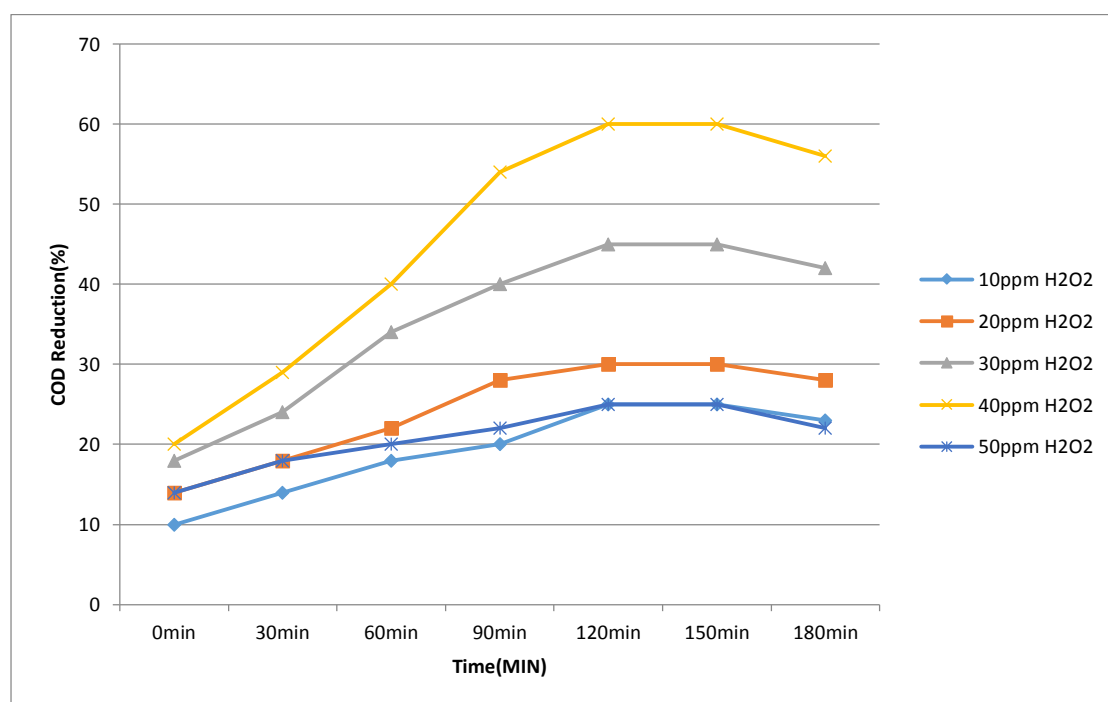


Figure 7: Effect of H₂O₂ on COD Reduction (%) for PBS

3.5 Effect of pH on Sonochemical COD Reduction (%) In Presence of H_2O_2 :

Experimental Conditions: volume of sample=100ml; Frequency =33 kHz (BAS, IS), 25 kHz (PBS); pH=7; Power: 1255(100%).

The effect of pH on the sonochemical remediation of ground water samples in the presence of peroxide is studied by varying the pH from 3-11 (Figure 8). A maximum reduction in COD is observed at neutral pH compared to acidic or basic conditions. From the graph it is concluded that a maximum of COD reduced is 91%, 76% and 60% for samples BAS, IS & PBS. A gradual decrease in COD reduction is observed when the pH is increased above pH 7.0. This observed decrease is probably due to the fast decomposition of hydroxyl radicals. Below pH 7.0 the released OH radicals combined with the H ions present in the ground water sample and thus decreased the reduction rate (R.J. EMERY et al., 2003).

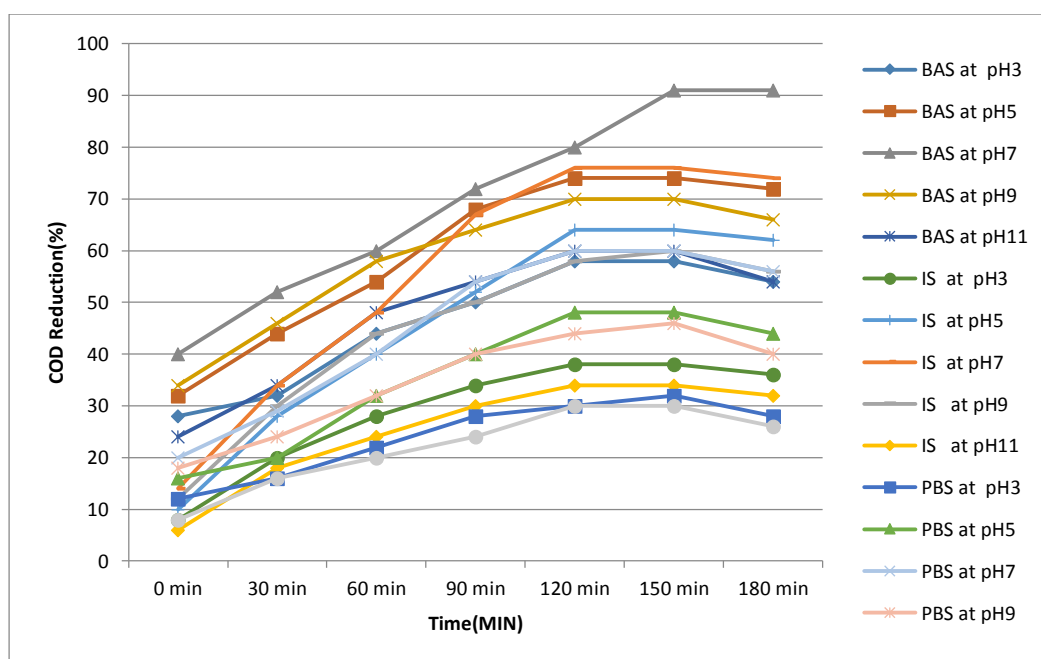


Figure 8: Effect of pH on COD reduction (%) in presence of H_2O_2 .

3.6 Comparative study of various systems for remediation of ground water samples

In this section of results, a comparative study of the treatment systems is evaluated for the ground water samples (Figure 9 (**Experimental Conditions:** volume of sample=100ml; Frequency =33 kHz (BAS, IS), 25 kHz (PBS); pH= 7; Power: 1255(100%))) With Ultrasonication alone, 56%, 34%, 45% of COD reduction is observed for samples BAS, IS & PBS. With peroxide alone, almost negligible reduction

in COD is observed. However, when peroxide is combined with ultrasonication, there is a tremendous increase in COD reduction (Figure 10 (**Experimental Conditions:** volume of sample=100ml; Frequency =33 kHz (BAS, IS), 25 kHz (PBS); pH=7; Power: 1255(100%); peroxide concentration=500ppm (BAS), 800ppm (IS), 40ppm (PBS))). A maximum of 91%, 76%, 60% of COD reduction is observed for samples BAS, IS & PBS in peroxide mediated ultrasonication. The increase in COD reduction in US/H₂O₂ system is due to increase in the formation of increased OH radicals by peroxide.

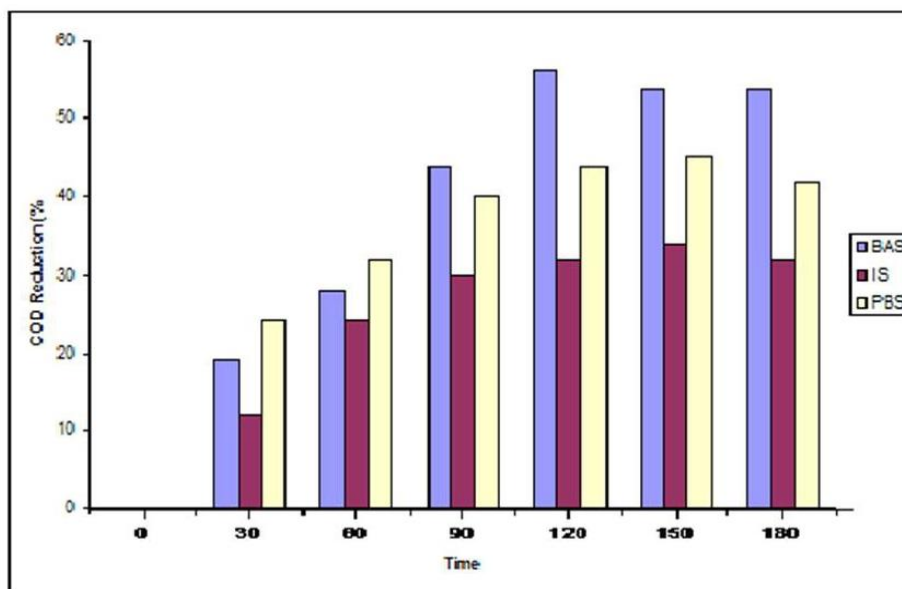


Figure 9: Comparative study of Treatment of ground water with Sonication alone

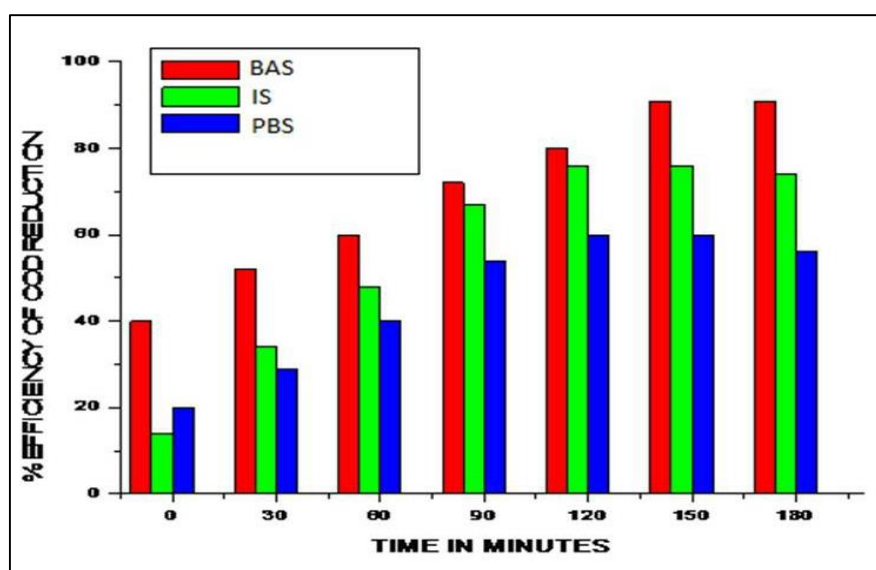


Figure 10: Comparative study of Treatment of ground water with Peroxy mediated sonication

4. CONCLUSIONS

This study concludes that the reduction of organics in ground water is strongly affected by the sonochemical oxidation process. A combination of hydrodynamic cavitation and peroxide oxidation can be efficiently used for treatment of real pollutants, which are causing ground water pollution. The reduction in COD is strongly dependent on certain process parameters like pH, initial peroxide concentration and organic type and concentration.

The following conclusions can be drawn from the study

- Among the treatment processes studied, US/H₂O₂ system is found to be more efficient in remediating the ground water samples.
- The optimal experimental conditions obtained are frequency of 33 kHz for BAS & IS; 25 kHz for PBS at power input of 1255W.
- The optimum concentration of H₂O₂ for BAS, IS and PBS was found to be 500ppm, 800ppm and 40ppm.
- Thus, Sonochemical process in combination with peroxide could be used as an effective treatment system for the maximum mineralization of recalcitrants present in ground waters.

REFERENCES

- [1] Adewuyi, Y.G., (2001). Sonochemistry: Environmental Science and Engineering Applications. *Ind. Eng. Chem. Res.*, 41, 4681.
- [2] Albertutier., (2010). Soil and Ground Water Remediation Guidelines Alberta Environment. ISBN: 978-0-7785-9949-4, <http://environment.gov.ab.ca/info>.
- [3] Arie.; Grostach.; Elizabeth A, Edwards., (2006). A1, 1, 1-trichloroethane-degrading Anaerobic Mixed Microbial Culture Enhances Bio Transformation of Mixtures of Chlorinated Ethenes & Ethanes. *Applied microbial*. 72(12): 7849-7856.
- [4] Barth, J. and Hahne, W., (2002). Review article. *Aliment. Pharmacol. Ther.* 16:suppl. 1, pp. 31-33.
- [5] Butler, R.; Ehrenberg, S.; Godley, A R.; Lake, R., Lytton, L.; Cartmell, E., (2006). Remediation of bromate-contaminated groundwater in an ex situ fixed-film bioreactor. *Science of The Total Environment* Volume: 366, Issue: 1, Pages: 12-20.
- [6] Charlespijls., and Diepak Mohan (2010). Cost Effective Biological Remediation of a Large Soil Contamination at a Gasoil Terminal. Master

- dissertation, Tauw bv, industries, soil and ground water department, Deventer, Netherlands.
- [7] Cheng, J.; C.D.Vecitis.; H.park.; B.T.marder.; M.R.Haffmann., (2009). Degradation of PFOS and PFOA in land fill ground water: Environmental matrix effects. *Environmental Science and Technology*, 42 (21), pp 8057–8063.
 - [8] Emery, R J.; Papadaki, M.; Mantzavinos, D., (2003). Sonochemical degradation of phenolic pollutants in aqueous solutions. *Environmental Technology* Volume: 24, Issue: 12, Pages: 1491-1500.
 - [9] Ghosh, S.; Liu, T.; and Fukushi,K., (2009). Anaerobic Biodegradation of Toluene in a Plugflow Reactor. Ksu.edu. web. <http://www.engg.ksu.edu/HSRC/96Proceed/ghosh.pdf>.
 - [10] Gondrexon, N.; Renaudin, V.; Boldo, P.; Gonthier, Y.; Bernis, A.; Petrier, C., (1997). Degassing effect and gas–liquid transfer in a high frequency sonochemical reactor. *Chem. Eng. J.* 66, 21–26.
 - [11] Hector M, Alvarez a.; Maria F. Souto .; Alberto Viale .; Oscar H. Pucci .,(2001). Bio-synthesis of fatty acids and triacylglycerols by 2,6,10,14-tetramethyl pentadecane-grown cells of *Nocardia globerula* 432. *FEMS Microbiology Letters* 200 195-200.
 - [12] Hua and Hoffmann,M. R.,(1997). Optimization of Ultrasonic Irradiation as an Advanced Oxidation Technology. *Environ. Sci. Technol.*, 31, 2237-2243.
 - [13] Ibbini,J. ; Santharam , S.; L. C. Davis and Erickson , L. E.,(2010). Laboratory and Field Scale Bioremediation of Tetrachloroethene (PCE) Contaminated Groundwater. *Jordan journal of mechanical and industrial engineering*, 4(1), Pages 35 – 44.
 - [14] Jose Gonzalez-Garcia .; Veronica Saez .; Ignacio Tudela .; Maria Isabel Diez-Garcia .; Maria Deseada Esclapez and Olivier Louisnard .,(2010). Sonochemical Treatment of Water Polluted by Chlorinated Organocompounds. A Review. *Water*, 2, 28-74.
 - [15] Kandasamy Thangavadivel.; Mallavarapu Megharaj.; Roger St C Smart.; Peter J Lesniewski.; Ravi Naidu., (2010). Sonochemical destruction of chloroform by using low frequency ultrasound in batch and flow cell. *Environmental science and health Part a Toxic hazardous substances environmental engineering*, 45(4), 483-489.
 - [16] Kao, CM.; Chen, CY.; Chen, SC.; Chien, H Y.; chen, YL., (2008). Application Of In Situ Biosparging to Remediate A Petroleum-Hydrocarbon Spill Site: Field And Microbial Evaluatio. *Chemosphere*, Volume: 70, Issue: 8, Pages: 1492-1499.
 - [17] Kejia Zhang.; Naiyun Gao.; Yang Deng.; Tsair Fuh Lin.; Yan Ma.; Lei Li.; Minghao Sui ., (2011). Degradation of bisphenol-A using ultrasonic irradiation

- assisted by low-concentration hydrogen peroxide. *Journal of environmental sciences (China)* 23 (1):31-6.
- [18] Lawton E. Shaw.; Dana Lee., (2009). Sonication of pulp and paper effluent *Ultrasonics Sonochemistry* .Volume 16, Issue 3, Pages 321-324
 - [19] Mark H. Stenzel.; William J. Merz .,(2006). Use of carbon adsorption processes in groundwater treatment. *Environmental Progress*, 8(4), 257–264.
 - [20] Mason, T.; and Lorimer, J.,(1988). *Sonochemistry: Theory, Applications, and Uses of Ultrasound in Chemistry*. Ellis Norwood Ltd., Chichester, NY.
 - [21] Michele Mascia.; Annalisa Vacca.; Polcara, Palmas& Pozzo., (2011). Electro Chemical Treatment of Simulated Ground Water Containing MTBE& BTEX with Bdd Anodes. *J Chem Technol Biotechnol*; 86: 128–137. Mikolaj Owsianiak.; Arnaud Dechesne.; Philip J. Binning.; Julie C. Chambon.; Sebastian R. Sørensen; and Barth F. Smets ., (2010). Evaluation of Bioaugmentation with Entrapped Degrading Cells as a Soil Remediation Technology. *Environ. Sci. Technol.*, 44 (19), 7622–7627.
 - [23] Mirapetrovi.; Jelena Radjenovic.; Damiabarielo., (2011). Advanced oxidation processes (AOP's) Applied For Waste Water & Drinking Water Treatment: Elimination of Pharmaceuticals. *The Holistic Approach to Environment*, 1(2), 63-74.
 - [24] Mohammad Shafeeq. ; D, Kokub .; Z, M, Khalid.; A, M, Khan .; and Kauser A. Malik, (1989). Degradation of different hydrocarbons and production of biosurfactant by *Pseudomonas aeruginosa* isolated from Coastal waters. *MIRCEN Journal*, 5, 505 -510.
 - [25] Muthupandian Ashokkumar.; Judy Lee.; Sandra Kentish.; Franz Grieser.,(2007). Bubbles in an acoustic field: an overview. *Ultrasonics Sonochemistry*, 14(4), 470-475.
 - [26] Petrier C, Jiang, Y.; Lamy, MF., (1998). Ultrasound and environment: Sonochemical destruction of chloroaromatic derivatives. *EnvironSci Technol* 9:1316 –1318.
 - [27] Pratap S. Bapat, Parag R. Gogate, Aniruddha B. Pandit.,2008. Theoretical analysis of sonochemical degradation of phenol and its chloro-derivatives. *Ultrasonics Sonochemistry*, 15(4), 564-570.
 - [28] Sathishkumar Santharam.; Jwan Ibbini.; Lawrence C. Davis.; Larry E. Erickson., (2011). Field Study of Biostimulation and Bioaugmentation for Remediation of Tetrachloroethene in Groundwater. *Remediation Journal*. 21(2), 51–68.
 - [29] Suslick.K.S., (1989).The Chemical Effects of Ultrasound. *Scientific American*. <http://www.scs.illinois.edu/suslick/documents/sciamer8980.pdf>.
 - [30] Suslick, K.S.; Choe, S.B.; Cichowlas, A.A.; and Grinstaff, M.W., (1991). Sonochemical Synthesis of Amorphous Iron. *Nature*, vol 353 p 414.

- [31] [Vilensky, Y.; Brian Berkowitz; Abraham Warshawsky.,\(2002\). In situ remediation of groundwater contaminated by heavy- and transition-metal ions by selective ion-exchange methods” Environmental science technology, 36\(8\), 1851-1855.](#)
- [32] [Yean-Ling Pang.; Ahmad Zuhairi Abdullah and Subhash Bhatia.,\(2011\). Review on sonochemical methods in the presence of catalysts and chemical additives for treatment of organic pollutants in wastewater, *Desalination*, 277, 1-14.](#)
- [33] [Zhang, Y.; and R M Miller., \(1994\). Effect of a Pseudomonas rhamnolipid biosurfactant on cell hydrophobicity and biodegradation of octadecane. *Appl. Environ. Microbiol.* 60\(6\):2101.](#)

SCHEDULING OF AN RESIDENTIAL BUILDING USING PROJECT MANAGEMENT TECHNIQUES

**S M Abdul Mannan Hussain¹, Madamachi Mani Chakravarthy² ,
Asra Fatima³**

¹Associate Professor ²B.Tech Final Year Student , Civil Eng. Department

Malla Reddy Engineering College (A)

³Assistant Professor. Civil Eng. Department , Muffakham Jah Engineering College

ABSTRACT

Resource management is one of the most important aspects of construction project management in today's economy because the construction industry is resource-intensive and the costs of construction resources have steadily risen over the last several decades. Thus general schedule control techniques are useful in optimizing resource scheduling and project duration. These techniques help to reduce project duration use of unlimited availability of resources for completion of a project. Through it is observed that resources are limited in real project scenario. It has been observed that the project delays occur due to insufficient supply of resources. In large scale projects, preparing an accurate and workable plan is very difficult. Computer packages like MS Project and Primavera project planner are used in construction industry. Primavera is an amazing project management software tool which is not just used by project managers. Designed to make managing large or complex projects a piece of cake, Primavera is the ideal tool for anyone who is involved in planning, monitoring and reporting on the progress of any big task, development or venture. Project management techniques can be used to resolve resource conflicts and also useful in minimizing the project duration within limited availability of resources to make the project profitable. The main aim of this study is to analyze the schedule control techniques by constraints and activity types is done using primavera P6 software for an apartment building. The project schedule control decreases the duration due to apply of constraints, level of effort, resource dependent it has an effect on the project duration.

Keywords; Schedule Control, Constraints, Activity Types, Level Of Effort, Resource Dependent, Primavera.

1. INTRODUCTION

A resource can be defined as an entity that is assigned to an activity and is required to accomplish the task. It is recommended to create and assign the minimum number of resources to activities. A resource is any

quantifiable item in limited supply and of sufficient value to justify tracking and assigning of specific activities for a project. Every project schedule has its own precedence constraints, which means that each activity can be processed when all its predecessors are finished. In general the purpose of project scheduler is to minimize its completion time, subject to precedence constraints. A more general version assumes that to develop one or more activities, resources such as tools, equipment, machines, or human resources are needed.

Construction industry is an integral component of a nation's infrastructure and industrial growth. Construction industry is the second largest industry in India still it's growth has been differential across the nation. There is a vast difference of development in the rural and urban areas. To cope up with the status of development in urban areas the rural regions need tools for economic development, land use and environment planning.

Each resource has limited capacity; consequently at a certain moments one activity may not begin their processing due to resource constraints even if all their predecessors are finished. This type of problems is called Resource-constrained project scheduling problem (RCPSP) which involves assigning jobs or tasks to a resource or a set of resources with limited capacity in order to meet some predefined objective. Project Monitoring acts like a warning mechanism; it is the process of recording, collecting and reporting information regarding project performance that the project manager and others wish to know.

Monitoring includes watching the progress of the project against time, performance schedule and resources during actual execution of the project and it identified the lagging areas which require timely attention and actions.

II OBJECTIVE OF STUDY

The objectives of this study are:

- 1 To identify construction sequence for a residential building construction.
- 2 To work out the practical durations required to carry out the activities.
- 3 To identify scheduling technique used by the organization in developing plan and scheduling.
- 4 To develop scheduling using Primavera project planner's software.
- 5 To track the project and analyze the reasons for delays, and increase in estimated budget etc.
- 6 To investigate defects in the planning and scheduling procedure of the organization, and suggest suitable improvements in their methods.

III PROJECT MANAGEMENT

Primavera Systems, Inc was a private company providing Project Portfolio Management (PPM) software to help project-intensive organizations identify, prioritize, and select project investments and plan, manage, and control projects and project portfolios of all sizes. On January 1, 2009 Oracle Corporation took legal ownership of Primavera. Primavera Systems, Inc. was founded on May 1, 1983 by Joel Koppelman and Dick Faris. It traded as a private company based in Pennsylvania (USA), developing software for the Project Portfolio Management market. To help expand its product capabilities, Primavera acquired Eagle Ray Software Systems in 1999, Evolve Technologies (a professional services automation vendor) in 2003, Pro Sight (an IT

portfolio management software vendor) in 2006, and, in the same year, Pert master (a project risk management software vendor).

3.1 Planning, Controlling, and Managing Projects

Before implementing Primavera to schedule projects, team members and other project participants should understand the processes involved in project management and the associated recommendations that help smooth the Primavera implementation that supports your corporate mission. If you were driving to a place you had never seen, would you get in the car without directions or a map probably not. More than likely you'd take the time to plan your trip, consider alternate routes, and estimate your time of arrival. Planning the drive before you even left would help your trip be more successful. And, along the way, should you encounter road blocks or traffic delays, you would have already identified alternate ways to reach your destination.

3.2 Construction, Planning and Scheduling Tracking

3.2.1 Construction Planning

Construction planning is a fundamental and challenging activity in management and execution of construction projects. It includes the selection of technology, the definition of work task, the estimation of required durations and resources of individual task, and identify the interactions between different work tasks.

A good construction plan is the base for developing the schedule and the budget for work. Developing the construction plan is a critical task in construction management, even if the plan is not written or else formally recorded. During planning a planner begins with a result (a design) and he must synthesize the steps required to yield this result. The necessary aspects of construction planning include the generation of required activities, analysis of the implications of these activities and the choice among various alternatives methods of performing these activities. A planner must imagine the final design and describe it in plans and specifications.

In developing a construction plan the importance is given either cost or schedule. Some projects a primarily divided into expense categories with associated cost in these cases planning is cost oriented. In this category, a distinction is made between cost incurred directly in the performance of the activity and indirectly for the accomplishment of the project. For other projects where time is a critical or the planner ensures that proper precedence among activities is maintained and that efficient scheduling of the available resource prevails. In such cases a critical path scheduling procedure is followed. Finally most of the complex projects require considerations of both cost and schedule over time, so that planning; monitoring and record keeping must be considered in both dimensions. In these cases integration of budget and scheduling information is a major concern.

3.2.2 Scheduling

Scheduling is determination the timing of events in the project that is when and which task will be performed? Putting it in simple words it is a reflection of plan. In other words we can say, planning is How, What and Who whereas scheduling is when and why. Scheduling can be also defined as the detailed plan of the project work tasks with respect to time. A schedule is also a good communication tool between all the stakeholders of the project. Schedule gives an overall sense of expected progress of the project without schedule it is very difficult to explain someone unfamiliar with the project what is going on and what is expected to take place.

3.2.3 Tracking

Tracking is the process of collecting, entering and analyzing of actual project performance values, such as work on tasks and actual durations. Tracking is the second major phase of project management. The main thing to focus on project planning is developing and communicating the details of project plan before actual work starts. When work begins, the next phase of project management is tracking progress. Tracking means recording project details such as what work did by whom, when the work was done, and at what costs these details are called as actual. Properly tracking actual work and comparing it's against original plan is useful to identify the difference in actual and planned and it enables to adjust incomplete task of the plan.

Primavera P6 : RIVERA01-2 (Materials Original)

File Edit View Project Enterprise Tools Admin Help

Activities

Layout: Tracking layout

Filter: All Activities

Auto Compute Actuals

Activity ID

Activity Name

Original Duration

Start

Finish

Schedule % Complete

Planned Value Cost

BL Project Total Cost

Building B

No

1

Building B

255

01-Dec-12 09:00 AM

24-Sep-13 06:00 PM

0%

Rs0.00

Rs13,395,100.00

Milestones for Payments

207

26-Jan-13 09:00 AM

24-Sep-13 06:00 PM

0%

Rs0.00

Rs0.00

EARTH WORK

45

01-Dec-12 09:00 AM

22-Jan-13 06:00 PM

0%

Rs0.00

Rs503,844.33

CONCRETE & REINFORCEMENT WORK

No

CONC LABOUR1

CONCRETE & REINFORCEMENT WORK

169

07-Dec-12 09:00 AM

21-Jun-13 06:00 PM

0%

Rs0.00

Rs15,268,701.21

PCC (Plain Cement Concrete)

No

PCC1

PCC Below footing & Lift Raft

2

07-Dec-12 09:00 AM

08-Dec-12 06:00 PM

0%

Rs0.00

Rs67,427.85

No

PCC2

PCC Below plinth beam

1

11-Jan-13 09:00 AM

11-Jan-13 06:00 PM

0%

Rs0.00

Rs39,753.28

No

PCC3

PCC -Below Parking Flooring

3

23-Jan-13 09:00 AM

25-Jan-13 06:00 PM

0%

Rs0.00

Rs167,668.90

RCC (Reinforcement Cement Concrete)

164

13-Dec-12 09:00 AM

21-Jun-13 06:00 PM

0%

Rs0.00

Rs12,309,011.17

PLINTH WORK

No

RCC PL1

RCC Footings

14

13-Dec-12 09:00 AM

28-Dec-12 06:00 PM

0%

Rs0.00

Rs309,609.32

No

RCC PL2

RCC Lift Raft

4

13-Dec-12 09:00 AM

17-Dec-12 06:00 PM

0%

Rs0.00

Rs166,869.52

No

RCC PL3

Lift Paradi - Raft Top to Plinth Top

3

18-Dec-12 09:00 AM

20-Dec-12 06:00 PM

0%

Rs0.00

Rs270,036.74

No

RCC PL4

Columns - footing to Plinth Top

5

29-Dec-12 09:00 AM

03-Jan-13 06:00 PM

0%

Rs0.00

Rs416,297.76

No

RCC PL5

RCC Beam - Plinth Beam

5

15-Jan-13 09:00 AM

19-Jan-13 06:00 PM

0%

Rs0.00

Rs243,311.59

PARKING FLOOR / 1ST SLAB

No

RCC PARK1

Columns - 1st slab

7

26-Jan-13 09:00 AM

02-Feb-13 06:00 PM

0%

Rs0.00

Rs431,453.83

No

RCC PARK2

Lift Paradi_1st slab

3

28-Jan-13 09:00 AM

30-Jan-13 06:00 PM

0%

Rs0.00

Rs170,265.93

No

RCC PARK3

Staircase - 1st slab (Building)

3

29-Jan-13 09:00 AM

31-Jan-13 06:00 PM

0%

Rs0.00

Rs48,667.17

No

RCC PARK4

RCC Beam - 1st Slab

7

04-Feb-13 09:00 AM

11-Feb-13 06:00 PM

0%

Rs0.00

Rs349,727.87

No

RCC PARK5

RCC Slab - 1st Slab

7

04-Feb-13 09:00 AM

11-Feb-13 06:00 PM

0%

Rs0.00

Rs339,292.71

1ST FLOOR / 2ND SLAB

14

12-Feb-13 09:00 AM

27-Feb-13 06:00 PM

0%

Rs0.00

Rs1,300,494.09

General

Status

Resources

Relationships

Codes

Notebook

Steps

Feedback

WPs & Docs

Expenses

Summary

Activity

Project

Resource ID Name

C | C

Remaining Units / Time

Price / Unit

Budgeted Units

1st This Period Units

Actual Units

Completion Units

Portfolio: All Projects

User: admin

Data Date: 01-Dec-12 09:00 AM

Access Mode: Shared

Baseline: Current Project

FIGURE I: Activities entered in Primavera software

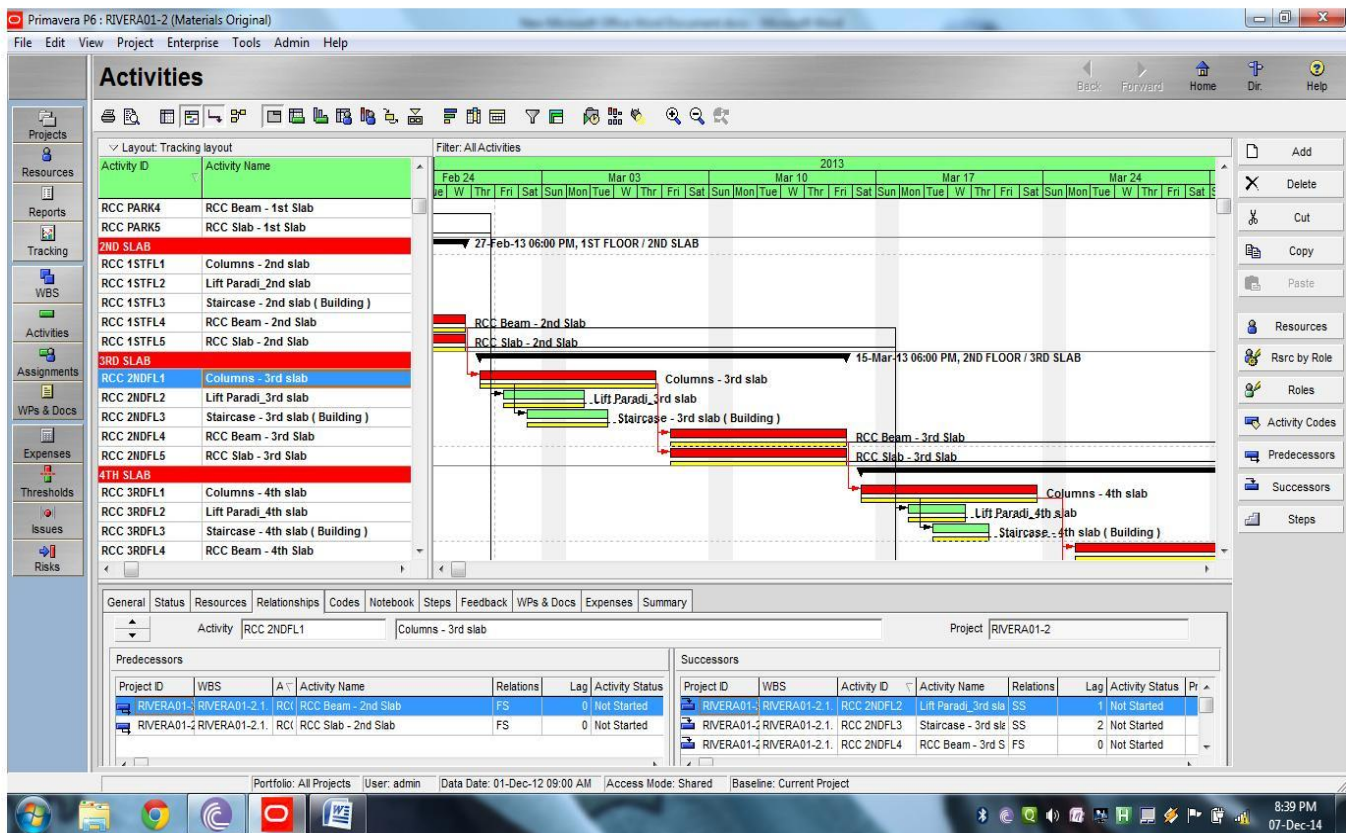


FIGURE 2: Activities linked in Primavera software

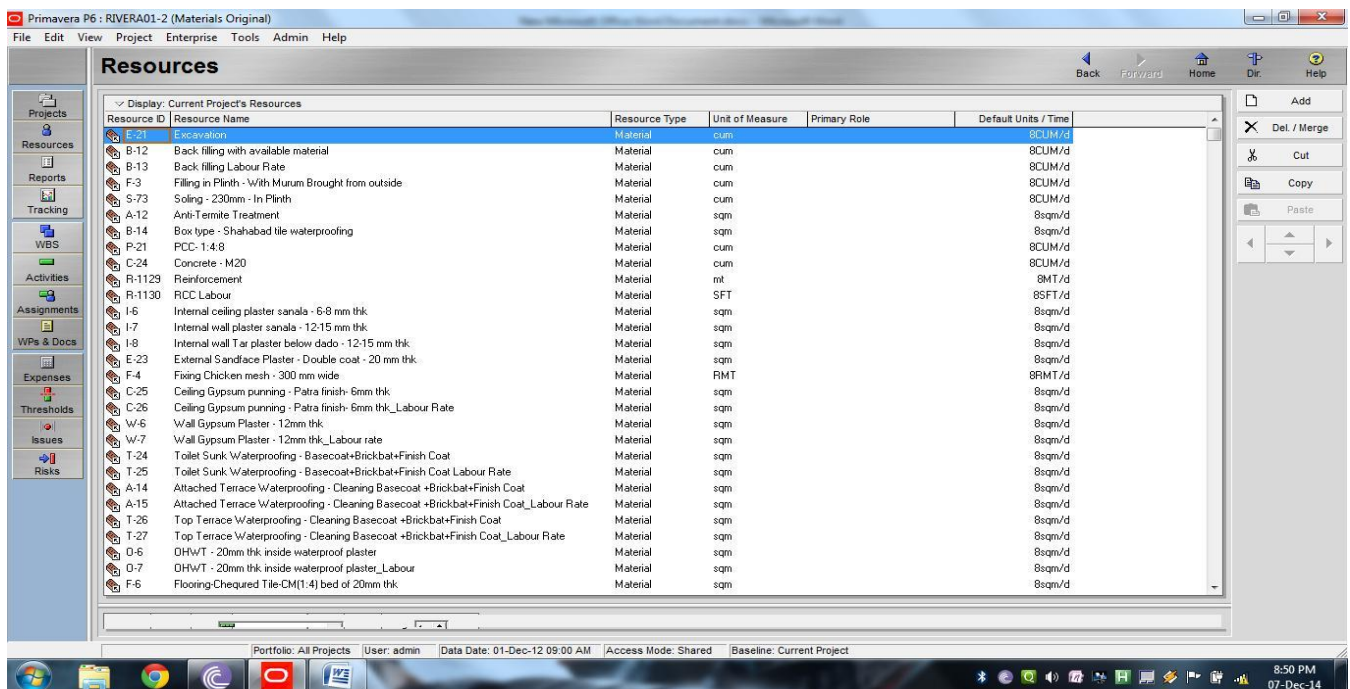


FIGURE 3: Resources entered in primavera

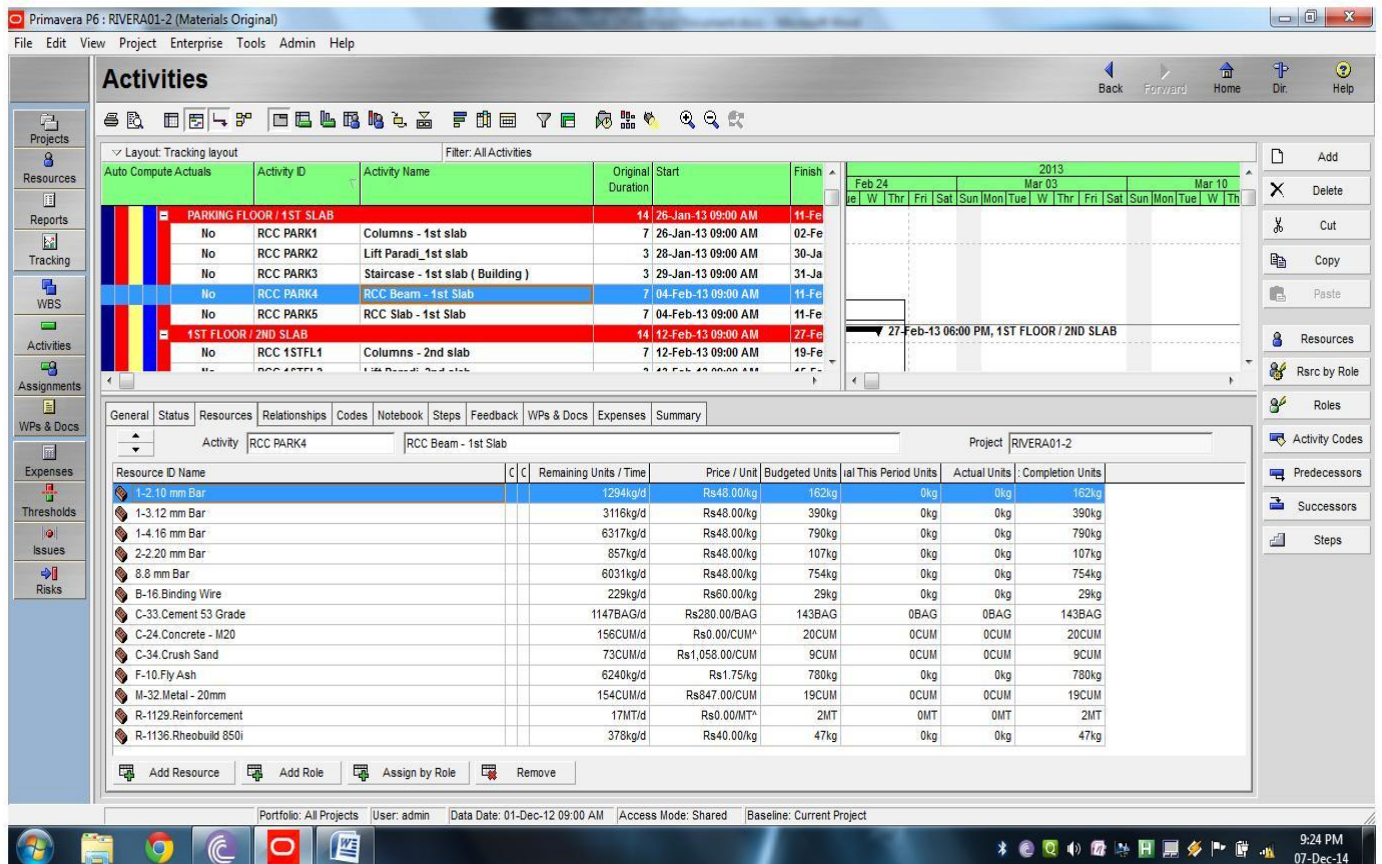


FIGURE 4: Resources allocated to activities in Primavera software.

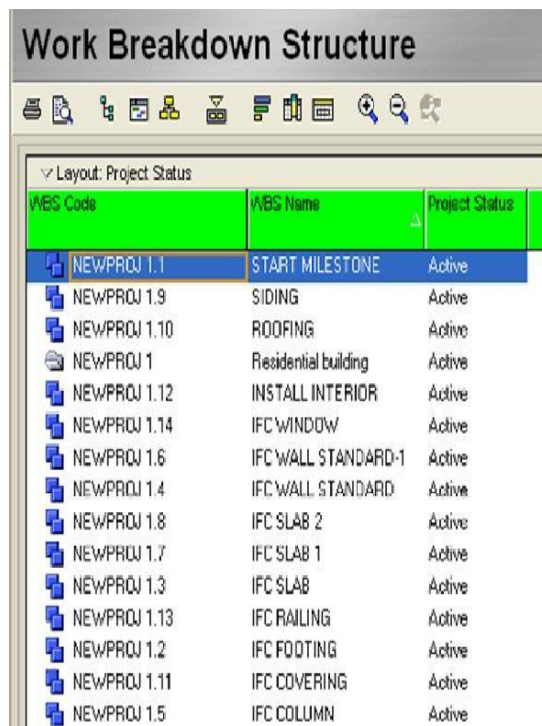


Figure. 5 WBS Window

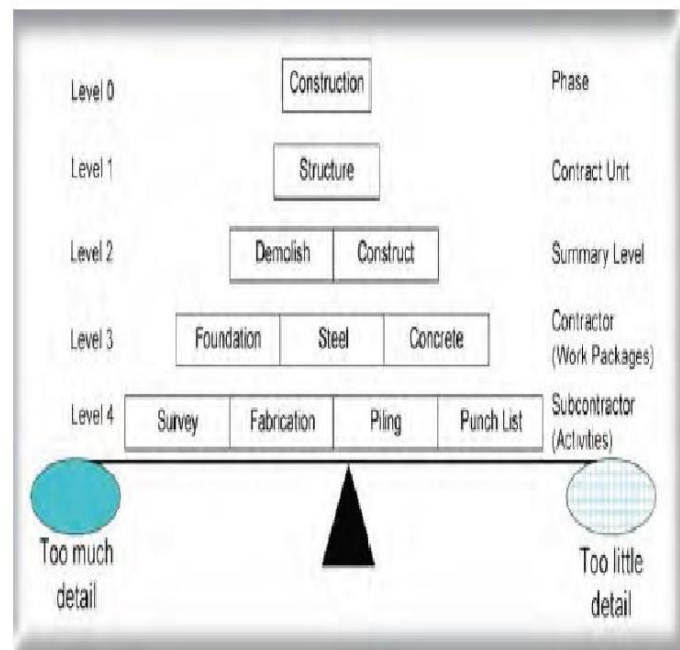


Figure.6 WBS Level of Detail

IV CONCLUSION

This study compared time performance of the conventional method of construction for high- rise residential and Industrial Building System (IBS) method by formulate benchmark measures of industry norms for overall construction period using scheduling simulation modeling. The positive changes include creating a healthy working environment among those involved directly in the construction industry. Better Efficiency in Delivering Services: Project management provides a “roadmap” that is easily followed and leads to project completion. Once you know where to avoid the bumps and potholes, it stands to reason that you’re going to be working smarter and not harder and longer. Improved Customer Satisfaction Whenever you get a project done on time and under budget, the client walks away happy. And a happy client is one you’ll see again. Smart project management provides the tools that enable this client/manager relationship to continue. Enhanced Effectiveness in Delivering Services The same strategies that allowed you to successfully complete one project will serve you many times over and also reduced risk and cost of schedule overrun. It helps easily plan and manage project activities, It optimizes management of all resources, It gives clear visibility of what’s going on in the project, It allows quick and easy forecasting of WBS’s, activities or projects.

REFERENCES

- [1] Devikamalam.J.Jane Helena. 2013 “Resource Scheduling Of Construction Projects Using Genetic Algorithm” International Journal of Advanced Engineering Technology
- [2] Ahamed E. Haroun, Adil H.A. Loghman, And Salam Y. M. Mahmoud..Etc (2012) “Scheduling Problem under Constrained Resource: A Historical Review of Solution Methods And Computer Application” Journal of Science and Technology
- [3] Milos Seda (2008) “A Construction to Shift Algorithms for Resource-Constrained Scheduling With Dynamic Changes” International Journal of Advanced Engineering Technology
- [4] Kastor And K. Sriakoulis (2010) “Effectiveness Of Resource Leveling Tools For Resource Constraint Project Scheduling Problem” International Journal of Project Management
- [5] Francois Berthaut..etc (2011) “Optimal Resource Constrain Project Scheduling With Overlapping Modes” International Journal of Advanced Engineering Technology
- [6] T.Subramani, K.Chinnadurai (2015) “Construction Management And Scheduling of Residential Building Using Primavera” International Journal of Application or Innovation in Engineering & Management
- [7] Rhuta Joshil, Pros. V. Z. Patil (2013) “Resource Scheduling Of Construction Project: Case Study” International Journal of Science and Research
- [8] B. S. K. Reddy, S K. Nagaraju, M D Salman (2015) “A Study on Optimisation of Resources for Multiple Projects By Using Primavera” Journal of Engineering Science and Technology
- [9] Jin-Lee Kim and Ralph D. Ellis Jr.(2008) “Permutation-Based Elitist Genetic Algorithm for Optimization of Large- Sized Resource Project Scheduling”, Journal of Construction Engineering and Management
- [10] Andrew Fernans Tom, Sachin Paul (2013) “Project Monitoring And Control Using Primavera” International Journal of Innovative Research in Science, Engineering and Technology

STUDY OF TOTAL QUALITY MANAGEMENT PRACTICES IN THE CONSTRUCTION INDUSTRY

S M Abdul Mannan Hussain¹, Gangaraju Ravi Teja², Asra Fatima³

¹Associate Professor, Civil Eng. Department, Malla Reddy Engineering College (A) (India)

²B.Tech Final Year Student, Civil Eng. Department, Malla Reddy Engineering College (A) (India)

³Assistant Professor, Muffakham Jah Engineering College, Secunderabad. (India)

ABSTRACT

Globally, maintenance of quality is an important consideration in modern construction. This is evident by clients' increasing use of companies' reputations for good quality work as a basis for choosing prospective contractors. The aim of this research is to empirically examine the extent to which TQM practices are associated with Construction project quality performance (CPQP). The study examines the influence of factors leading to implementation of TQM practices in building industry. In this paper we discuss the problems of defining quality in the construction industry, examine possible benefits of implementing quality, and look at barriers to quality implementation in construction. A conceptual framework and hypotheses is also developed. The Total Quality Management is one of the main association approaches, so that can be used to achieve continuous quality improvement of the products. From after that, quality management has emerge through quality examination (QI), to quality control (QC), to quality assurance (QA) then to the current Total quality management (TQM)

Keywords: *Total Quality Management, Quality Management; Construction Industry, Implementation*

I INTRODUCTION

Quality administration essentially is the course of assuring that a good or service continuously meet and need to exceed customer needs and can be generally looked at as a business management way that attempts to maximize organizational rewards throughout continuous process up gradation of its products, services, manpower in company, processes improvement, and environment. Ever since it is a management based approach it can be achieved all the way through total involvement and participation of everybody in the association led by the management people (Kasongo & Moono, 2010). The researcher Zakuan et al. (2012) measured teaching as a significant factor that boosts employee's hard work towards development. To him, quality preparation includes humanizing and training of workers at all levels in the association with a meaning of expansion their

information on quality issues and programs and as long as them with in sequence about the organization's quality assignment, visualization and general wanted way.

A critical winning implementation of TQM factors is connected to monetary and presentation achievement of every association. The benefits and improvements are come in the areas of fewer faults and errors, decreased waste, increased disposal, increased quantity, increased profit, market share, stronger relationships with suppliers increased employee, customer satisfaction, consistency, reduced manufacture time, drop in the quantity of goods damaged in transit, Improvement in customer perceptions of the organization, decrease in costs

II LITERATURE SURVEY

Muatafa Maher Altayeb (2014) has exposed that the building industry has been one of the most important for initial infrastructure and financial system of the Palestinian. In this revise the author establish that sensational factors essential for the functioning of TQM at various parts of the project planning, design, and construction in the Gaza strip. The investigation resolute that 7 significant success factors with 38 sub factors out of 8 major factors and 81 sub factors. It was proven that continuous improvement is the most critical factor for the successful implementation of TQM in Gaza strip organization.

Customer focus can be defined as the degree to which a firm continuously satisfies customer needs (Gherbal et al., 2012). The key to the quality management is maintaining a closer relationship with the customer in order to fully determine the customer's need, so the customer should be closely involved in the product design and development with valuable input to every stage (Saylor 1996 as cited in Gherbalet al., 2012). The customer allows an organization to exist, for every organization, profit or non profitable, partnerships, departments, functions, groups, or teams, therefore customer focus is very critical in TQM. Impliedly, in construction industry, quality should be customer driven. Employers should be well aware of the concept of internal and external customers. They should care about meeting and exceeding the customer expectations. There must be a focus on customer feedback and accordingly the process should be driven.

According to Hoonakker (2010) most of the research concludes that it is necessary to transpose and translate the principles, practices and techniques used for TQM in manufacturing to construction. In line with this suggestion, TQM elements that past researchers have identified as applicable to the construction industry include; top management commitment and leadership, human resource management, customer focus, planning, process management, supplier management, continuous improvement, information analysis and evaluation, teamwork and quality culture.

The researcher Ross Chapman (2002) has identified the degree of appliance of TQM principles and then investigated the association between TQM implementation and labor productivity in manufacturing company.

This research also identified the relationship between all the probable fundamentals of TQM and labor productivity throughout functioning. The study establishes that average labor productivity dimensions for high-TQM companies were appreciably higher than for low-TQM firms. So it shows that if the organization has higher level of TQM implementation having higher level of labor productivity, if the organization has lower level of TQM implementation having lower level of labor productivity. The final results of regression analysis and factor analysis demonstrate that there is a linear association between TQM and labor productivity. This connection showed a high positive gradient in organizations with ISO 9000 certification, and significantly lower but still positive gradient in organization without ISO 9000 certification.

III CONCEPTUAL FRAMEWORK OF TQM

The interrelationships of the aspects of TQM are represented in the conceptual framework represented by Figure 1. The framework consists of three parts; TQM elements, project quality performance and barriers to the implementation of TQM and project quality performance. The TQM comprises seven elements namely; top management commitment and leadership, employee relations, customer focus management, supplier quality management, process management, teamwork and information analysis and evaluation.

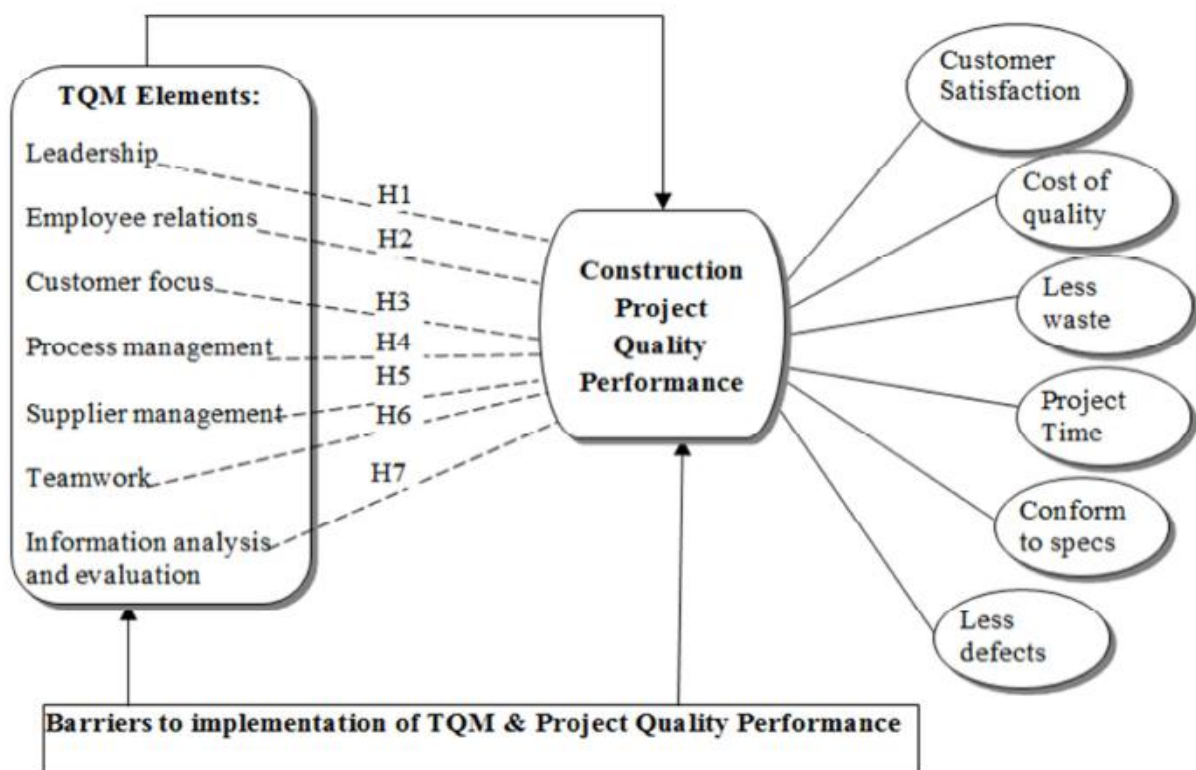


Figure 1. Framework of TQM

3.1 Hypotheses

The hypothesized relationships of interest are represented by H1 to H7 in Figure 1 and summarized below:

- H1: Top-management commitment and Leadership for TQM practices is positively correlated with quality performance of construction project.
- H2: Employee Relations for TQM practices is positively correlated with quality performance of construction project
- H3: Customer focus for TQM practices is significant, positively correlated with quality performance of construction project
- H4: Supplier management in relation to TQM practices is positively correlated with quality performance of construction project
- H5: Process management in relation to TQM practices is positively correlated with quality performance of construction project
- H6: Teamwork in relation to TQM practices is positively correlated with quality performance of construction project.
- H7: Information Analysis and Evaluation in relation to TQM practices is positively correlated with project quality performance.

IV PROJECT RESEARCH MODEL

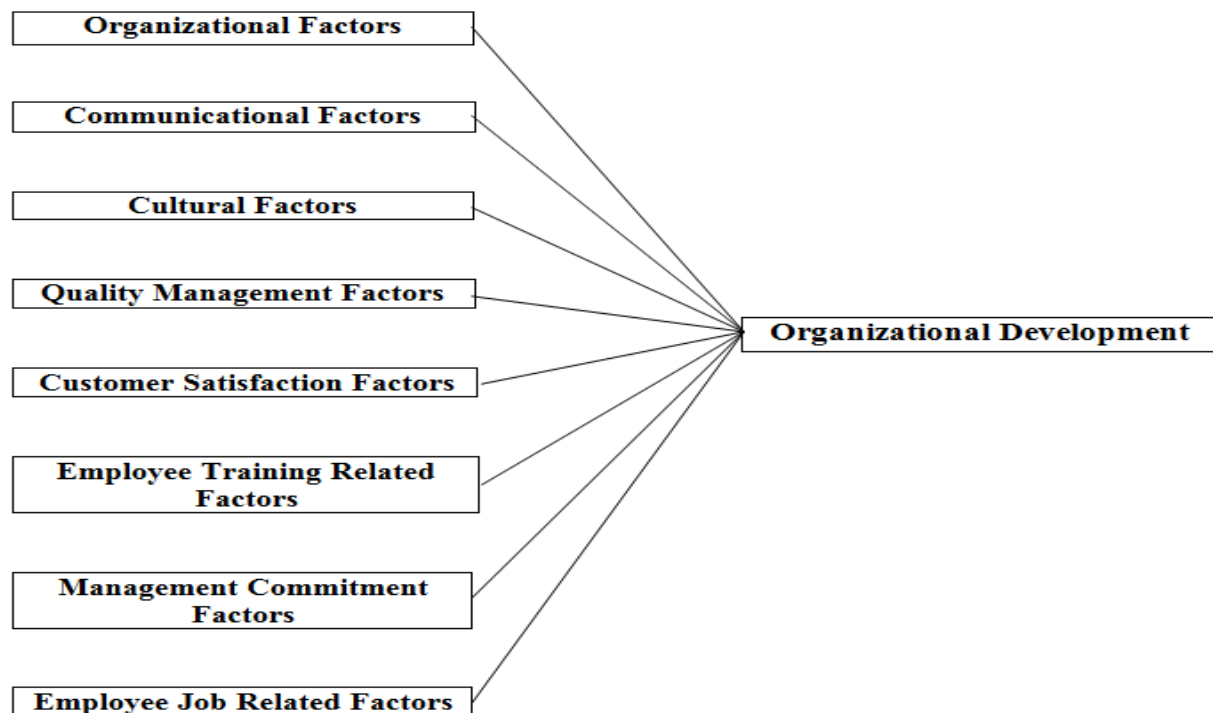


Figure 2. Organizational Development model

V CONCLUSIONS

In spite of the different approaches to address Total Quality Management (TQM) implementations and applications, researchers insist that to achieve excellence, top management should be involved in the application of quality. The study found that the identified TQM practices had positive effects on construction project quality performance of the respondents. Thus, TQM practices can enhance the quality performance of construction project by reducing the cost of poor quality, delivery time, waste, defects, rework, non-conformities and increasing the quality of project implementation. They strongly believe that all functions, all employees should participate in the improvement process. They reveal the importance of evaluation to achieve continuous improvement. Theories and models in the field of Total Quality Management start from the same base of principles and end to same results (the importance of teamwork and continuous improvement...etc) but in different approaches.

REFERENCES

1. Hoonakker, P., Carayon, P., & Loushine, T. (2010). Barriers and Benefits of Quality Management in the Construction Industry. *Total Quality Management – Routledge*, 21 (9), 953-969.
2. Gherbal, N., Shibani, A., Saidani, M., & Sagoo, A. (2012). Critical Success Factors of Implementing Total Quality Management in Libyan Organisations. *Proceedings of the 2012 International Conference on Industrial Engineering and Operations Management. Istanbul, Turkey*.
3. Ali Mohammad Mosadeghrad, "Why TQM programmes fail? A pathology approach", *The TQM Journal*, Vol. 26, Pp. 160 – 187, 2014.
4. Andrew W.T. Lau and Tang S.L, "A survey on the advancement of QA (quality assurance) to TQM (total quality management) for construction contractors in Hong Kong", *International Journal of Quality & Reliability Management*, Vol.26, Pp.410 – 425, 2009.
5. Anupam Das and Vinod Kumar and Uma Kumar, "The role of leadership competencies for implementing TQM", *International Journal of Quality & Reliability Management*, Vol. 28, Pp. 195 – 219, 2011.
6. Khan, H. J. (2003). Impact of Total Quality Management on Productivity. *The TQM Magazine*, 15 (6): 374 – 380.

A STUDY OF RISK MANAGEMENT IN THE CONSTRUCTION INDUSTRY

S M Abdul Mannan Hussain¹, E.Sanjay², N.Jaswanth³

¹Associate Professor, ^{2,3}B.Tech, Student, Malla Reddy Engineering College(A), Secunderabad.

ABSTRACT

Economic growth and socio-economic development are particularly important for developing countries; and the construction industry plays a central role in driving both of these. The general situation observed currently in building construction in a developing country such as India is that the output of a construction company is usually characterized by poor quality work, cost and time overruns. Construction projects are initiated in complex and dynamic environments resulting in circumstances of high uncertainty and risk, which are compounded by demanding time constraints. Construction industry has changed significantly over the past several years. Risk management is thus in direct relation to the successful project completion. Project management literature describes a detailed and widely accepted risk management process, which is constructed basically from four iterative phases: risk identification, risk estimation, risk response planning and execution, often managing the risk management process is included. Construction project planning is an essential element in the management and execution of construction projects which involves the definition of work tasks and their interactions, as well as the assessment of required resources and expected activity durations.

Keywords: Risk Assessment, Risk Management, Construction

I. INTRODUCTION

Buildings have been considered as one of the most valuable assets of a nation to provide people with shelter and facilities for work and leisure. Building construction projects have been identified as one of the most dynamic, risky and complex endeavors. An overview of the traditional construction process can be explained in four simple stages: conceptual design, construction, operation and maintenance. However, the passage from one stage to another is not all “smooth- sailing”, but fraught with problems. The cost of risk is a concept many construction companies have never thought about despite the fact that it is one of the largest expense items. Risk can be managed, minimized, shared, transferred or accepted. It cannot be ignored. Risk management helps the key project participants - client, contractor or developer, consultant, and supplier - to meet their commitments and minimize negative impacts on construction project performance in relation to cost, time and quality objectives.

Construction projects are initiated in complex and dynamic environments resulting in circumstances of high uncertainty and risk, which are compounded by demanding time constraints. Construction industry has changed significantly over the past several years. It is an industry driven primarily by private investors; the presence of

securitized real estate has increased considerably. It is vulnerable to the numerous technical & business risks that often represent greater exposures than those that are traditional. Thus risk assessment need arises. Risk assessment is a tool to identify those risks in a project and manage it accordingly with proper treatment. Risk assessment is defined in this study as a technique that aims to identify and estimate risks to personnel and property impacted upon by a project.

II. CONSTRUCTION PROJECT RISK

Risk is a complex phenomenon that has physical, monetary, cultural and social dimension. Risk is the probability of occurrence of uncertain, unpredictable and even undesirable events that would change the prospects for the profitability on a given investment. Managing risk is to minimize, control and share risk and not just pass them off unto another party. Project in controlled environment describes risk as the chance of exposure to the adverse consequences of future events. Consequently, Smith et al states that risk exists when a decision is expressed in terms of a range of possible outcomes and when known probabilities can be attached to the outcomes. A construction risk is a variable in the process of construction, whose occurrence results in uncertainty as to the final cost, duration and/or the quality of the project.

However, the environment in which decision- making takes place can be described in three methods, which include certainty, risk and uncertainty. Certainty exist only when one can specify exactly what will happen during the period of time covered by the decision and conform to the specific requirements of certainty. However, this does not happen in the construction industry. Making a distinction between uncertainty and risk is necessary in order to be able to explain the influence of these on project performance.

Risks can be viewed as business, technical, or operational. A technical risk is the inability to build the product that will satisfy requirements. An operational risk is the inability of the customer to work with core team members. Risks are either acceptable or unacceptable. An acceptable risk is one that negatively affects a task on the non-critical path. An unacceptable risk is one that negatively affects the critical path. Risks are either short or long term. A short-term risk has an immediate impact, such as changing the requirements for a deliverable. A long-term risk has an impact sometime in the distant future, such as releasing a product without adequate testing. Risks are viewed as either manageable or unmanageable. A manageable risk is one you can live with, such as a minor requirement change. An unmanageable risk is impossible to accommodate, such as a huge turnover of core team members. Risk factors for this study are classified into eight categories namely.

- ☐ Construction risk
- ☐ Design risk
- ☐ Environmental risk
- ☐ Financial risk
- ☐ Management risk
- ☐ Political risk
- ☐ Procurement risk
- ☐ Sub-Contractors risk
- ☐ Technology risk

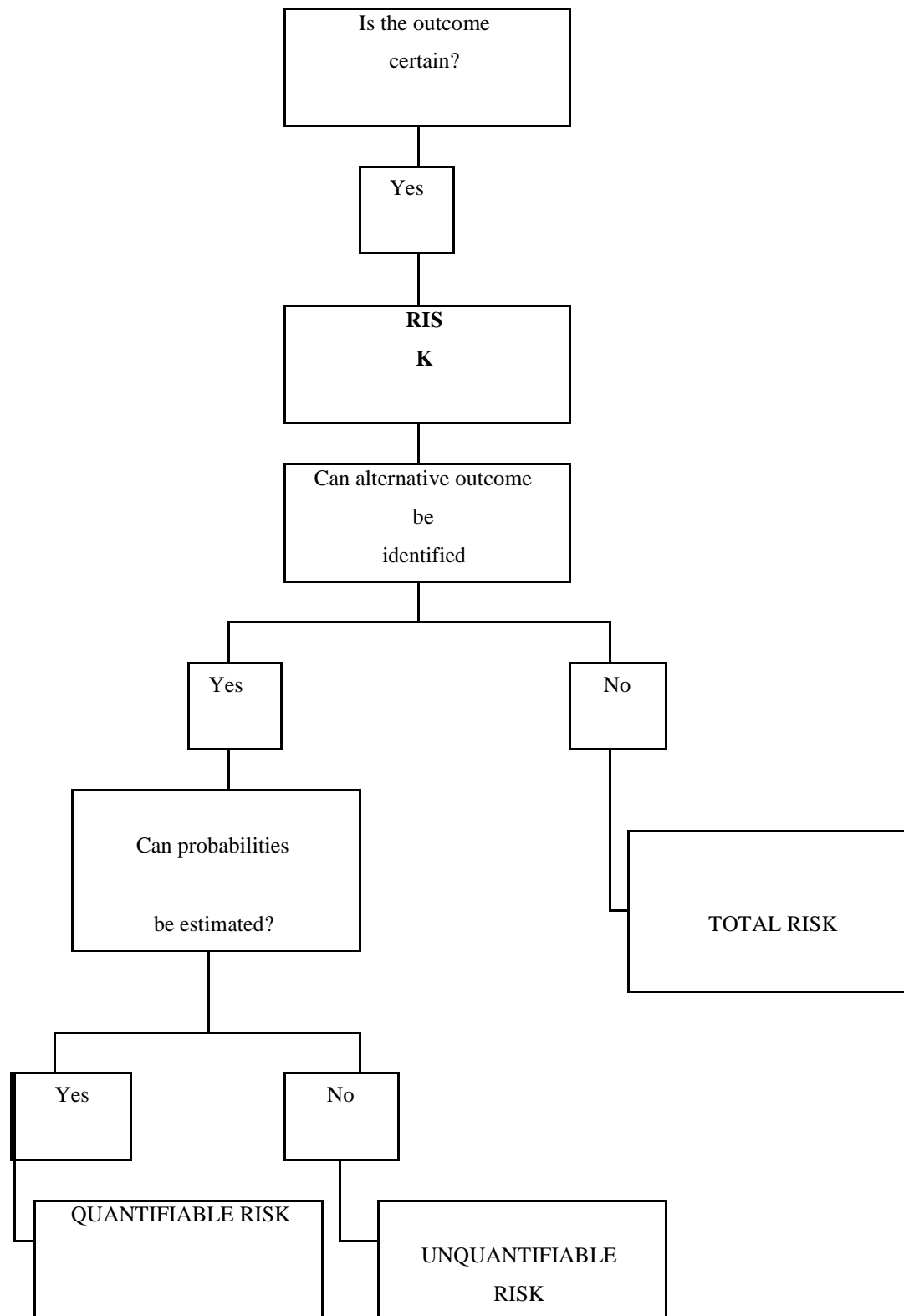


Figure 1. A holistic view of project risk

III. RISK MANAGEMENT PROCESS FOR BUILDING CONSTRUCTION PROJECTS

Building projects in developing countries have constantly faced great difficulty in controlling time and cost overruns. An example of poor construction performance can be found in the Indian construction industry. The research conducted shows that the performance of the building construction industry in India has consistently been a source of concern to both public and private sector clients. The study conducted on some 12 building projects executed by the federal government of India through the federal housing authority, state housing corporation, Oyo state ministry of works and housing, and Lagos state property development corporation (LSDPC) concludes that the performance of building projects in terms of cost and time parameters is least satisfactory.

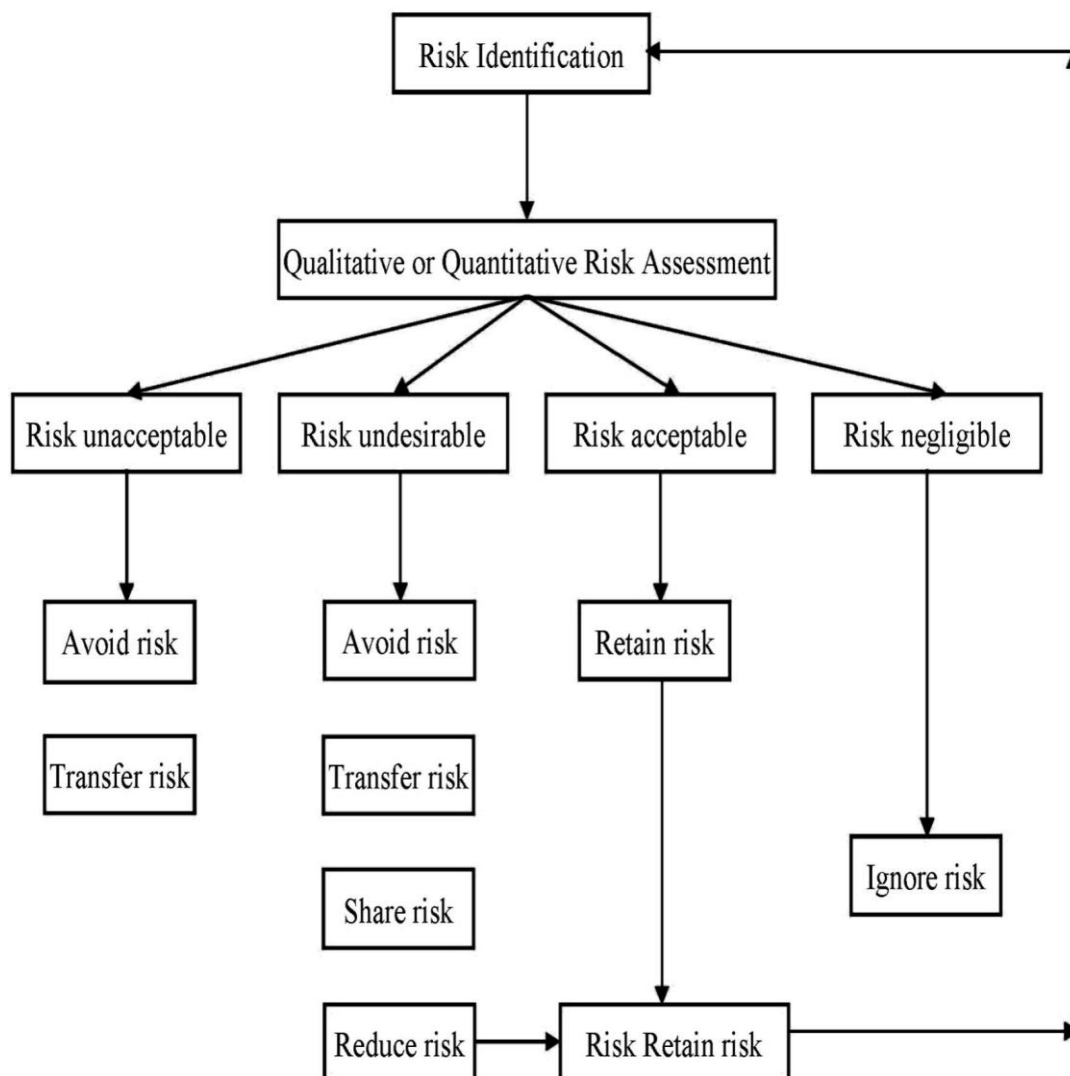


Figure 2. Cycle of risk management process

IV. RISK MANAGEMENT AND ITS TYPE'S **Table 1.** Risks Factors of Building Construction projects

Risk group	Risk factors
Physical risk	Occurrence of accident because of poor safety procedures Supplies of defective materials Varied labour and equipment productivity
Design risk	Defective design (incorrect) Not coordinated design (structural, mechanical, electrical, etc.) Inaccurate quantities
Logistics risk	Unavailable labour, materials and equipment Undefined scope of working High competition in bids Inaccurate project program Poor communication between the home and field officers (contractors side)
Financial risk	Inflation Delayed payment in contracts Financial failure of the contractor
Legal risk	Difficulty to get permit Ambiguity to work legislations Legal disputes during the construction phase among the parties of the contract Delayed dispute resolutions No specialized arbitrators to help settle fast
Construction risk	Rush bidding Gaps between the implementation and the specification due to misunderstanding and specification Undocumented change orders Lower work quality in presence of time constraints Design changes Actual quantities differ from the contract quantities
	Segmentation of construction process

Political risk	Working at hot (dangerous) areas New governmental acts or legislations Unstable security circumstances (invasion) closure
Management risk	Ambiguous planning due to project complexity Resource management Changes in management ways Information unavailability (include uncertainty) Poor communication between involved parties

Risk management is a management discipline whose goal is to protect the asset, reputation, and profits an organization by reducing the possible losses or damages before they occur. Risk management is one of the nine knowledge areas (i.e., integration management, scope management, time management, cost management, quality management, human resource management, communications management, risk management, and procurement management) propagated by the Project Management Institute. Zou et al describe risk management in the construction project management context as a systematic way of identifying, analyzing and dealing with risk as associated with a project with an aim to achieve the project objectives while Williams describe project risk management as an integrated process which includes activities to identify project uncertainty, estimate their impact, analyze their interactions, control them in the execution stage, and even provide feedback to the maintenance of collective knowledge asset.

V. CONCLUSIONS

As far as India is concerned risk management is still a new word in the construction sector and this should be changed as soon as possible. Currently the Government of India has proposed a risk rating system will help the developers to develop projects at a faster pace by taking quick decisions. Each rating agency will have its own methodology to rate projects. Construction projects are unique in terms of design, construction methods, personnel, location, etc. Variations in these factors will induce different types of risk factors into construction projects. In addition, risk factors could come from many different directions, such as social, legal, economic, environmental, political, logistic, management and technological sources.

The system will help government to develop a strategy to mitigating risk. This will encourage more response from developers and investors for public-private partnerships projects. It could make the bidding projects more competitive. The construction companies need to include risk as an integral part of their project management. Decision making such as risk assessment in construction projects is very important in the construction management. The identification and assessment of project risk are the critical procedures for projecting success. This study determines the key factors of risk in construction industry.

REFERENCES

- [1.] O. O. Odimabo, C. F. Oduoza. 2013. Risk Assessment Framework for Building Construction Projects' in Developing Countries. International Journal of Construction Engineering and Management. p-ISSN: 2326-1080 ISSN: 2326-1102, 2(5): 143-154.
- [2.] Kinnaresh Patel. 2013. A study on risk assessment and its management in India. American Journal of Civil Engineering. 1(2): 64-67.
- [3.] Cheng Siew Goh and Hamzah Abdul-Rahman¹. 2013. The Identification and Management of Major Risks in the Malaysian Construction Industry. Journal of Construction in Developing Countries. 18(1): 19-32.
- [4.] Babak A. Samani, 2012, "A Fuzzy Systematic Approach to Construction Risk Analysis" Journal of Risk Analysis and Crisis Response, Vol. 2, No. 4 (December 2012), 275-284.
- [5.] Dr. R. K. Kansal, Manoj Sharma. 2012. Risk Assessment Methods and Application in the Construction Projects. International Journal of Modern Engineering Research (IJMER). 2(3): 1081-1085, ISSN: 2249-6645
- [6.] Lam E.W.M, Chan P.C.A, and Chan W.M.D., 2010, Qualitative survey on managing building maintenance projects; world academy of science, engineering and technology; Vol. 65, pp. 232-236.
- [7.] Abujnah M and Eaton, 2010, Towards a risk management framework for Libyan house-building projects; the research institute for the building and human environment, University of Salford; pp. 346-353
- [8.] Adnan Enshassi and Jaser Abu Mos. 2008. Risk Management in Building Projects: Owners Perspective. The Islamic University Journal. 16(1): 95-123, ISSN 1726-6807.

IMPORTANCE OF SAFETY IN INDIAN CONSTRUCTION

Chandan Mehra¹, S M Abdul Mannan hussain², Asra fatima³

¹B.Tech Final Year Student, Dept. of Civil Engineering,

Malla Reddy Engineering College, Secunderabad, (India)

²Phd Research Scholar, GITAM University, Hyd., Associate Professor, Dept. Of civil Engineering,

Malla Reddy Engineering College, Secunderabad, (India)

³Phd Research Scholar, GITAM University, Hyd., Assistant Professor, Civil Engg. Dept.,

Muffakham Jah Engg. College, Banjara Hills, Hyderabad, (India)

ABSTRACT

This research paper illustrates the present scenario of the labours working in the construction firms with respect to health and safety issues. It gives the information about safety principles compared to the construction field ground reality based on daily routines at site. Lucidly, the safety professionals are required at site to take responsibility in getting acknowledge the discrete safety and health rules, regulations, acts and principle simultaneously creating attention among each other and entourage the industry for the advancement of the project and mankind.

Keywords: *Construction, Safety, Injury, Accidents, Workers*

I INTRODUCTION

Construction in developing countries such as India is more labour-intensive than that in the developed areas of the globe. In numerous developing countries such as India, there is a significant difference between large and small contractors. Most large firms do have a safety policy, on paper, but employees generally are not aware of its existence. Nevertheless, a number of major constructors exhibit a concern for safety and have established various safety procedures. They also provide training for workers and maintain safety personnel at the job site. Construction Industry in India is highly prone to hazards related to site activities and construction projects engage large number of contractual workers. These workers come from varied trades especially from rural areas and agricultural background who do not have proper training in construction safety also are not literate enough to forecast the unknown dangers. During execution at site, these workers are exposed to various risks involved in construction works and other occupational diseases and health hazards which cause injuries and illnesses. As a result, the construction projects get delayed due to loss of working hours and other legal hassles. This ultimately accounts for cost and time overrun. Therefore, it is essential for any construction project to have

certain safety guidelines and procedure to be followed for site activities and to create awareness among the workers, site supervisor and engineers.

II OBJECTIVE OF STUDY

The objective of study are the following:-

- a) To determine the various facades of construction safety
- b) To get information about health and safety act and regulations
- c) To know causes of a major injury
- d) Efforts put in practice in India

III RESEARCH METHODOLOGY

Research Methodology is designed in such a way that it depends on four factors which are taken into consideration:-

- i. Health and safety issues for construction workers
- ii. Safety principles v/s ground reality
- iii. Construction accidents
- iv. Foundation of major and minor injury
- v. Efforts put in practice in India
- vi. To conclude the implementation of zero injury environment



Figure 3.1. Representation of unique methodology for Safety in Indian Construction

IV HEALTH AND SAFETY ISSUES FOR CONSTRUCTION WORKERS

Majority of the health issues that labours are facing in construction field are the following:-

- a) Pain or injury from overexertion.
- b) Repetitive manual tasks, or working in uncooperative postures.
- c) Exposure to moulds, fungi or rodent droppings.
- d) Exposure to paints, lead, wood dust, asbestos and/or toxic chemical solutions.
- e) Working in extreme conditions like high temperatures and under UV radiations.
- f) Working with hand tools, powered tools and heavy machinery equipments.
- g) Excessive vibration of hands, arms or body from powered tools or equipments.
- h) Extension of work days, stress or Shift work hours.
- i) During night, working in low lightening or poor visibility

The best way to protect workers against hazards is to control problems at the source. OSHA stated that workers must have PPE (Personal Protective equipment) that fits properly. Poorly fitted PPE may cause additional hazards. Construction safety (the intermediate phase between a finished design and a completed building) is largely the responsibility of the contractors and other site professionals. Hazard can be defined as a physical or chemical characteristic that has the potential to cause harm to people, property and to the environment. To prevent health hazards at work, all possible sources should be identified before commencement of construction work. Hazards at a construction site may come from hazardous substances used on site, and/ also environmental variables may create additional risks as heat and noise. Most construction accidents result from basic root causes such as lack of proper training, deficient enforcement of safety, unsafe equipment, unsafe methods or sequencing, unsafe site conditions, not using the safety equipment that was provided, and a poor attitude towards safety.

V SAFETY PRINCIPLES V/S GROUND REALITY

Safety Principle: Ensuring safety at construction sites is mandatory requirement as it is directly related to welfare of staffs and contractors' workers.

Ground Reality: Many sites don't have the necessary safety equipment such as safety harness vest while working at heights.

Safety Principle: All accidents and occurrences of near-misses can be avoided by proper planning and thorough implementation of safe practices at work place.

Ground Reality: Planning is generally done by the labors or less experience supervisors as per their suitability and ease, without considering the risk involved.

Safety Principle: To increase the safety consciousness of the workforce and the supervisory staffs through continuous training and motivation towards safe practices.

Ground Reality: It is only reputed builders and contractors that have adopted such practices.

Safety Principle: Regular monitoring, inspections and safety audits will form an integral part of the safety programs at the worksite.

Ground Reality: Many sites do not follow such audits and monitoring to avoid the extra cost and effort.

VI HEALTH AND SAFETY RULES AND REGULATIONS

There are two major pieces of legislation governing health and safety law. These are:

- Building and Other Construction Workers (Regulation of Employment and Condition of Services) Act 1996
- Building and Other Construction Workers (Regulation of Employment and Condition of Services) Central Rules 1998

Allied to these are several statutory instruments governing safety. These are:

- Factories Act 1948

- The Delhi Building and Other Constructions Workers (Regulation of Employment and Condition of Services) Rules 2002
- Indian Electricity Act 1948
- Indian Electricity Regulations 1956
- Motor Vehicle Act 1998

Construction safety in India is still in its early years because safety laws are not strictly enforced. The contractors ignore many basic safety rules and regulations from the start of any work. However, to improve working conditions, the government has enacted specific legislations like the Minimum Wages Act, the Workmen's Compensation Act of 1923 (modified in 1962), and the Contract Labour (Regulation and abolition) Act of 1970, of which only a small amount scope and procedures are put into practice. National Building Code of India, 2005 provides guidelines for regulating construction activities for a building; across the country along with many IS codes of Bureau of Indian Standards (BIS), such as, SP70-Handbook on Construction Safety Practices for site engineers, Project Managers, and engineers-in-charge of buildings and civil works. Even then, worker's safety in the Indian construction industry is frequently pushed to the bottom in the priority list of most of the builders, contractors, and engineers while many are unaware of any such norms and regulation

In developing countries like India. Bangladesh.etc., safety rules usually do not exist, even if it exists; regulatory authorities are unable to implement such rules effectively. Therefore, it is up to the construction professional to inculcate and concrete these safety norms in their working and ultimately setting up a desired standard. This can definitely reduce accidents that directly or indirectly reduce project cost and ultimately the delays. In India efforts should be made to raise the level of awareness among the workers and the employers about the importance of health and safety-related issues.

VII FOUNDATION OF MAJOR INJURY

The recognition that any unintended occurrence is an accident is the first requirement of hazard control. It is altogether a different matter whether such accidents results in injury or not. It can be observed that on many occasions the accidents do not cause any injury due to a number of reasons. In construction, for instance, objects falling from height may miss a person by a whisker. Such instances are also known as near misses and they are as important as accidents involving injuries.

According to a study conducted by **Heinrich(1959)**, the ratio of 'no injury' to 'minor injury' to 'major injury' is **300:29:1** (see Figure 7.1). Underlying these minor injuries are numerous unsafe practices and unsafe conditions that, fortunately, may not result in any accident. **Bird and Loftus (1982)** have updated this ratio with further information on property damage accidents. According to this study, the ratio of 'near miss accidents' to 'property damaging accidents' to 'accidents involving minor injuries' to 'accidents involving serious or disabling injuries' is **600:30:10:1** (see figure 7.2). The moral of these ratio studies is that accident prevention must start with prevention of unsafe practices and unsafe conditions as well as of minor injuries.

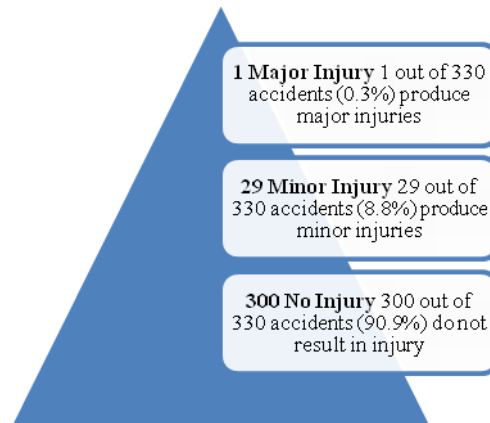


Figure 7.1 Foundation of major injuries (Heinrich 1959)

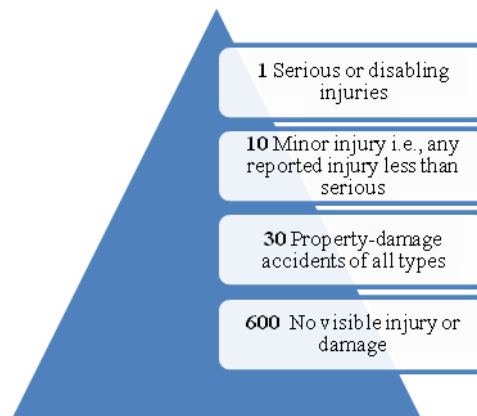


Figure 7.2 Foundation of major accidents/injuries (Bird and Loftus 1982, cited in Mining Safety Handbook)

VIII CONSTRUCTION ACCIDENTS

Accidents in the construction industry are costly in human and financial terms. The economic cost is not the only basis on which a contractor should consider construction safety. The reasons for considering safety are humanitarian concerns, economic reasons, laws and regulations, and organizational image. Cost of safety is paid by the organization either through the uncontrolled cost of accidents or through the controlled cost of safety program. The uncontrolled cost of accidents includes the loss of productivity, administrative time for investigations, disruption of schedules, wages paid to the injured workers, adverse publicity, liability claims, and equipment damage. The controlled cost of safety program consists of salaries of safety, medical, and clinical personnel, expenses for safety meetings, inspections of tools and equipment, orientation sessions, site inspections, personal protective equipment, and health programs. The identification of root causes of accidents is a complex process. Accident mitigation requires a comprehensive understanding of construction process. With increasing population and expansion of urbanization, many projects are therefore, carried in congested

spaces of cities, like Mumbai, Pune, Delhi, Chennai, etc., where, not only the safety of the workers inside the site needs to be ensured but also the safety of people passing and residing in the adjacent. Still every month accidents, such as, adjoining residents being killed in mishaps, pieces of reinforcement falling and piercing in someone's body, dusty environments as a result of construction activities resulting health hazards, etc., come up which can bring a legal stay over the project and thus making errands of walks to court which instead could have been prevented if precautionary measures would have been taken.

A. Accident statistics

In the economic point of view, the construction industry plays a vital role as it typically contributes 10 per cent of a developing country's GNP. It is also very hazardous with almost six times as many fatalities and twice as many injuries per hour worked relative to a manufacturing industry. Helander analyze 739 construction fatalities that occurred in the UK. He found that fifty two per cent occurred due to falls from roofs, scaffolds and ladders. Falling objects and material were involved in 19.4 per cent of the deaths, and transportation equipment, (e.g. excavators and dumpers) were involved in 18.5 per cent. Helander also found that 5 per cent of construction accidents occur during excavation work. The categories used for classifying fatal accidents were:

- a) Falls
- b) Falling material and objects
- c) Electrical hazards
- d) Transport and mobile plants
- e) Other

Most of the accidents that involved falls occur during work on roofs, scaffolds and ladders. Moreover, collapses of structures and falling materials also contribute for a large proportion of victims. Many of the safety hazards are particular to the different trades, and usually construction workers underestimate the hazards in their own work which affects the motivation for adopting safe work procedures. The establishment and use of procedures and regulations to enhance safety can avoid a large proportion of these accidents. There are also forceful monetary incentives in construction safety as it is estimated that construction accidents amount to about six per cent of total building costs; this should encourage the industry as well as the regulatory agencies to invest in construction safety.

IX EFFORTS IN INDIA

Efforts are taken by government by setting up, National Safety Council (NSC) which generates, develops and sustains a voluntary movement on Safety, Health and Environment (SHE) at the national level. It carries out various activities such as specialized training courses, conferences, seminars & workshops; conducting consultancy services such as safety audits, hazard evaluation & risk assessment; designing and developing HSE promotional materials & publications; facilitating organizations in celebrating various campaigns e.g. Safety Day, Fire Service Week, World Environment Day i.e. 4th March, in India, is celebrated as National Safety Day/Week every year, during which various campaigns are organized in promotion of Safety, Health and Environment (SHE) movement to different parts of the country. Apart from this, the BIS (Bureau of Indian

Standards) have taken intensive researches and studies to publish many SP and IS codes, for bringing standardization, marking and quality certification of goods and for matters connected therewith or incidental thereto, acting as guidelines for construction, manufacturing, processing etc.

With increase in market competition, many construction giants are taking up modern trends and technique, such as, ISO certification, under which they are to undertake the safety of their workers, set up safety organization, issue safety policy, safety checklist, safety manuals, etc. These giants have understood the importance of safety after having gone through the adverse side effects of non-safe acts. The cost of accidents can go anywhere from low cost to tremendous high cost, which not only affects the current projects but also the upcoming project of the company. Now companies define standards for every project, for health and safety guideline. Regular health and fitness checkup for every member is carried out. Gammon India holds the record of *Twelve Million* hours of accident-free work at Kalpakkam.

X CONCLUSION

Owing to increase in complexity of operations, the construction industry has become more dangerous than ever before. Construction organizations are faced with the challenge of having to closely monitor their safety management systems to minimize occupational hazards, while simultaneously trying to sustain profits in a competitive marketplace. In the United States, government agencies such as Occupational Safety and Health Administration (OSHA) have done their part to promote a ZERO injury environment. However, in India effective safety construction management is not available. Moreover, the key to proper safety execution is not necessarily through strict guidelines and standards, but through an effective total safety management initiative, first supported by an organizations senior management, then integrated via specific safety management implementation tools/ systems, and finally by continuous follow up and monitoring to ensure quality and continuous improvement. It is the attitude of the senior management and proprietary contractors to take the initiative and start giving importance to health & safety of workers and engineers at site. Construction organizations interested in maximizing safety and competitiveness must look to Total Quality Management (TQM) initiatives for inspiration. Quality focus, total commitment, and continual improvement must be the mantra of choice. Only those companies that take on an aggressive safety management approach will sustain profit margins and achieve world-class competitiveness.

REFERENCES

Journals

- [1] "Safety health and welfare on construction sites A Training Manual", International Labour Office, Geneva.
- [2] Pratibha Joshi, Promila Sharma, T.C. Thakur, and Amit Khatter, "Safety in Construction Line: Important issue for Risk Identification", International Journal of Advanced Engineering Research and Studies, IJAERS/Vol. I/ Issue III/April-June, 2012/30-34.

- [3] “SP70:2001, Handbook on Construction Safety Practices”, (Reprint 2007)”, Published by Bureau of Indian Standards, New Delhi 110002.
- [4] The Building and Other Construction Workers Act, 1996, Commercial Law Publishers(India) Pvt. Ltd. , 2007 , New Delhi
- [5] Heinrich H.W.,1959, Industrial Accident Prevention: A Scientific Approach, McGraw-Hill, USA.
- [6] Heinrich h.w. , 1980, Industrial Accident Prevention, New York: McGraw-Hill.
- [7] Bird, F. And Loftus, R., 1976, Loss Control Management, Loganville, Ga: Institute Press.
- [8] Kaushik Kayal, B. Srinivas, G.L.N. Padmavathi, and Praveen Dubey,”Construction Safety Manual for Works Contract”, BARC/2011/E/006.
- [9] Heinze J, Wiegand F. Role of designers in construction worker safety, Journal of Construction Engineering and Management, ASCE, 118(1992) 677-84.
- [10] Gammon India Limited, e-reference. <http://www.gammonindia.com/about-sgammon-india/health-safetygammon-india.htm>.1566

Improving Construction Work Flow by Implementing Last Planner System on Construction Site

¹S.M. Abdul Mannan Hussain, ²T. Seshadri Sekhar and ³Asra Fatima

¹Department of Civil Engineering, Malla Reddy Engineering College,
GITAM University, Secunderabad, Hyderabad, India

²Department of Civil Engineering, NICMAR, Hyderabad Campus,
Taangana, India

³Department of Civil Engineering, MuffakhmJah Engineering College,
Banjara Hills, Hyderabad, India

Abstract: As part of an improving planning assessment procedure at the construction site, a questionnaire survey has been undertaken among all employees. Questionnaire surveys were administered to the project participants to evaluate the Last Planner System implementation process. The case study was carried out in Reserve Bank Officer's Quarters, Ameerpet, Hyderabad located in Southern region of India. It entailed the construction of one prototype residential building and one community centre building. The project is located at Reserve Bank of India's permanent site which is located 6 km from the Reserve Bank of India's Hyderabad office (Saifabad). The contract value of the project is approximately INR 12.5 Crores with estimated project duration of 18 months (24th July, 2014-23rd January, 2016). The project location is having direct access to the main road and is located in the core hub of the city. The questionnaire was divided into four sections (Section A-D). The first section (i.e., Section A) focused on getting an overview of the outcome of the implementation. Whereas the second section (i.e., Section B) focused primarily on the barriers of the implementation process. The third section (i.e., Section C) gave attention to the critical success factors of the implementation process. Furthermore, the last section (i.e., Section D) dwelt on the benefits perceived on implementing Last Planner System on the case project. The respondents for the questionnaire comprised of the contractor's team, the employer's and the suppliers. A percentage breakdown of the respondents is shown in Table 1 and the details of the questionnaires and their corresponding responses are discussed below. Out of the 25 employees involved in the survey 24 (96%) provided responses accordingly. Out of the respondent, 13 (54.17%), 4 (16.67%), 4 (16.67%) and 3 (12.50%) are respectively contractor's team, client's team, sub-contractor's team and the supplier's team.

Key words: Continous improvement system, design science, lean construction, last planner system, weekly work plan, percent planned complete, make work ready planning

INTRODUCTION

Questionnaires surveys were utilized at the tail end of the implementation. The questionnaire was to provide a feedback on the implementation process. The questionnaire was divided into four sections. The first two sections were to establish the profile of the respondents and that of his organization. Subsequently, the next section reviewed the benefits recorded in the implementation of LPS while the last section dwelt with the critical success factors of the implementation. The

questions for the case studies focused on the barriers, benefits and critical success factors of the implementation. However, the questionnaires for the current case study focused on the performance of the project in relation to the current construction practices of the project.

MATERIALS AND METHODS

Questionnaire design and analysis: Properly designing and formatting questionnaires plays a huge role in

achieving a high response rate (Salem *et al.*, 2006). The questions were both closed and open-ended and formatted using a 5 point likert scale for each attribute of question. The first section focused on the overview of the implementation, with four different questions being asked on; the effectiveness of the LPS implementation; the fulfillment of results obtained; the usefulness of the Weekly Work Plans (WWP) and the Percentages of Plans Completed (PPC); the degree of difficulty experienced while implementing the LPS. The second section on the other hand, centered on the barriers faced during the implementation process. Six possible barriers derived from the literature search and the other research processes were identified. The respondents were asked to determine the frequency of occurrences of these barriers. Similarly, the third section dwelt on the critical success factors of LPS. Different factors were identified from literature reviews and respondents were asked to determine their frequency of occurrence. Conversely, the fourth section focused on the perceived benefits of implementing LPS. The researcher also identified from literature reviews 10 possible benefits of implementing LPS within the case studies and respondents were asked to determine their frequency of occurrence.

RESULTS AND DISCUSSION

Data analysis: Data analysis is the process of bringing meaning and interpretation to mass data collected. Amaratunga *et al.* (2002) identified that data analysis, forms a major part of any research. It consists of examining, categorising and tabulating data obtained. In this research, a structured literature review was first conducted and it served as the foundation for the research. The empirical data gathered was both qualitative and quantitative in nature and they were used to establish the link between the literature reviews. Questions were asked using questionnaires and interviews. For the questionnaires, a Likert scale was used to access the views of the participants. Sacks and Goldin (2007) indicated that Likert scales fall within the ordinal level of measurement which means that the responses are categorized and ranked into the following categories; never, rare, seldom, frequent and very frequent. The categorization and ranking enables priorities to be allocated (Ballard and Howell, 2004).

In carrying out this research, the Ranking Indices of Importance (RII) was used. RII is commonly used to measure the extent to which the occurrence of an outcome exists. The following formula was used to calculate RII.

$$RII = \frac{\sum x}{K}$$

Where:

$$\sum x = \text{mean} = \frac{\sum fx}{\sum f}$$

Where:

k = Maximum point on likert scale (k = 5)

x = Points on the Likert scale (1, 2, 3, 4)

f = Frequency of respondents choice

For the interpretation of the RII values, RII is ranked from the highest to the lowest. If $RII < 0.60$ item has low rating $0.60 < RII < 0.8$ item has high rating $RII = 0.8$ item has very high rating. Other statistical analysis were also employed using simple Microsoft excel and word to present a visual representation of the patterns and trends of the data, especially for the PPC presentations and the reasons for incomplete assignment calculations.

Post implementation process: The respondents for the questionnaire comprised of the contractor's team, the employer's and the suppliers. A percentage breakdown of the respondents is shown in Table 1 and the details of the questionnaires and their corresponding responses are discussed below. Out of the 25 employees involved in the survey 24 (96%) provided responses accordingly. Out of the respondent, 13 (54.17%), 4 (16.67%), 4 (16.67%) and 3 (12.50%) are respectively contractor's team, client's team, sub-contractor's team and the supplier's team (Table 2-6).

The question asked that whether Last Planner System is effective within the project or not, was examined by the 24 respondents under the Five Point Likert Scale. The percentage of those accepting the effectiveness of Last Planner System within the project is 76%, against 24% that neither agreed nor disagreed. Furthermore, it was identified that 56% of the respondents agreed to the statement that as compared to their previous projects, the results were quite satisfactory this time. In the same way, the question that whether the weekly work plans or PPC's were useful to the implementation was carefully examined, 48% respondents agreed on the usefulness of weekly plans and PPC while the remaining 52% respondents were indifferent or disagreed. Additionally, from the survey results, 64% of the respondents felt that the process of implementing Last Planner System was difficult. However, the remaining 36% felt it was easy to carry out the implementation of Last Planner System. In summary of the section A and judging from the proportion of responses

Table 1: Respondents of the questionnaire for the case study

Parameters	Frequency	Percentage
Contractor's team	13	54.17
Client's team	4	16.67
Subcontractor's team	4	16.67
Supplier's team	3	12.50
Respondents total	24	100.0

Table 2: Overview of the implementation (Section A) case study

Reasons	Weighting frequency (f)					Σf	\bar{x}	RII	Rank	Rating	Rating (%)
	1	2	3	4	5						
LPS was very effective within this project.	0	1	5	12	7	25	4.00	0.80	1	Very high	76.00
The results obtained from the implementation were satisfactory as compared to the previous projects	5	6	0		6	25	3.16	0.63	3	High	56.00
The weekly work plans and PPC were very useful	5	3	5	12	0	25	2.96	0.59	4	Low	48.00
Difficulty to carry out the implementation	4	0	5	9	7	25	3.60	0.72	2	High	64.00

Table 3: Barriers during the implementation (Section B) case study

Barries	Weighting frequency (f)					Σf	\bar{x}	RII	Rank	Rating	Rating (%)
	1	2	3	4	5						
Poor Supervision and quality control	5	5	3	10	2	25	2.96	0.59	3	Low	48.00
Fluctuations and variations	6	7	2	10	0	25	2.64	0.53	6	Low	40.00
Employer's involvement	0	8	8	7	2	25	3.12	0.62	2	Low	36.00
Resistance to change	7	5	2	7	4	25	2.84	0.57	4	Low	44.00
Cultural issues	4	4	2	15	0	25	3.12	0.62	1	High	60.00
Length approval issues by client	9	0	5	11	0	25	2.72	0.54	5	Low	44.00

Table 4: Critical success factors to the Implementation (Section C) case study

Factors	Weighting frequency (f)					Σf	\bar{x}	RII	Rank	Rating	Rating (%)
	1	2	3	4	5						
Training and empowering last planners	0	3	2	11	9	25	4.04	0.81	3	Very high	80.00
Involvement of all stake holders (team work)	0	0	8	9	8	25	4.00	0.80	4	High	68.00
Motivating people to make changes	3	4	0	10	8	25	3.64	0.73	6	Very high	72.00
Having the appropriate human capital	0	5	5	9	6	25	3.64	0.73	7	High	60.00
Top management support	0	3	0	15	7	25	4.04	0.81	2	Very high	88.00
Manage resistance to change.	2	1	4	7	11	25	3.96	0.79	5	High	72.00
Close relations with suppliers	0	1	0	13	11	25	4.36	0.87	1	Very high	96.00

Table 5: Benefits of the implementation (Section D) case study

Benifits	Weighting frequency (f)					Σf	\bar{x}	RII	Rank	Rating	Rating (%)
	1	2	3	4	5						
Solve Problems on time.	2	0	7	9	7	25	3.76	0.75	3	High	64.00
Reducing the incidence of bad news and to get what bad news there is early	0	0	7	9	9	25	4.08	0.82	2	Very high	72.00
Developing supervisory skills and reducing the load on management	2	5	6	7	5	25	3.32	0.66	7	Low	48.00
Creating a more predictable and reliable production program	0	0	7	8	10	25	4.12	0.82	2	Very high	72.00
Delivering projects more safely, faster and at reduced costs	5	5	4	5	6	25	3.08	0.62	8	Low	44.00
Stabilize projects and support other lean actions	0	1	5	8	11	25	4.16	0.83	1	Very high	76.00
Improving construction logistics on projects	0	8	0	8	9	25	3.72	0.74	4	High	68.00
Improving predictions of labour required	3	0	8	9	5	25	3.52	0.70	5	High	56.00
Reduces the risk of catastrophic loss	4	1	6	7	7	25	3.48	0.70	5	High	56.00
Completes projects on schedule	0	3	9	13	0	25	3.40	0.68	6	High	52.00

Table 6: Benefits of last planner system (Section E) case study

Reasons	Weighting frequency (f)					Σf	\bar{x}	RII	Rank	Rating	Rating (%)
	1	2	3	4	5						
Increased work flow reliability	0	1	1	13	10	25	4.28	0.86	1	Very high	92.00
Improved supply chain integration	5	0	4	10	6	25	3.48	0.70	10	High	64.00
Reduced production time	0	1	3	9	12	25	4.28	0.86	2	Very high	84.00

Table 6: Continue

Reasons	Weighting frequency (f)					Σf	\bar{x}	RII	Rank	Rating	Rating (%)
	1	2	3	4	5						
Improved communication.	0	0	8	13	4	25	3.84	0.77	6	High	68.00
Improvement in quality of work	2	0	8	6	9	25	3.84	0.77	7	High	60.00
Improved collaboration	0	3	9	13	0	25	3.40	0.68	11	High	52.00
Greater customer satisfaction	1	1	9	10	4	25	3.60	0.72	8	High	56.00
Improved safety	0	0	6	15	4	25	3.92	0.78	4	Very high	76.00
Commitment	1	1	9	11	3	25	3.56	0.71	9	High	56.00
Improved project delivery time	0	0	5	13	7	25	4.08	0.82	3	Very high	80.00
Less stress	1	0	6	12	6	25	3.88	0.77	5	Very high	72.00

obtained from each question, we can conclude that a large proportion of the respondents agreed to the effectiveness of the Last Planner System and the results obtained from the implementations were satisfactory. Similarly, a large proportion of respondents also attested to the usefulness of WWP and PPC. However, a significant proportion agreed that it was difficult to implement Last Planner System on this project.

Summary: This chapter presents in substantial detail the process of implementing “last planner system” in the construction of reserve bank officer’s quarters in Ameerpet, Hyderabad. The chapter described the phases of Last Planner System implementation; these phases comprised of Pre-implementation, Implementation and Post-implementation phases. The chapter also highlights the Barriers, Critical success factors and the perceived benefits recorded from the responses of the survey questionnaire completed by the project participants. From the PPC data recorded in this chapter, it was also revealed that material unavailability, pre-requisite work, labour supply, submittals, poor weather, rework, equipment breakdown and incomplete design information were all constraints faced within the project. However, implementing last planner system by the contractor was able to identify these constraints on time and it minimised the effect on the project.

CONCLUSION

It was observed that contractor produced substantial results in terms of time cost and quality performances.

The contractor completed the construction project two months before than the actual completion date allocated to the project, even though the project kicked off three months late. The contractor had a better allocation of resources, an organized flow and access of materials and this reduced interference amongst working teams by making all the team members aware of what to do and when to do each assignment. Although the project suffered from shortage of materials, the problem of material shortage was overcome by engaging in short term and look ahead planning together with regularly doing a constraint analysis to envisage possible constraints to the project before they occur. Thus, implementation of Last Planner System helped the project team to receive information regularly of the project success and failures during weekly meetings.

REFERENCES

- Amaratunga, D., D. Baldry, M. Sarshar and R. Newton, 2002. Quantitative and qualitative research in the built environment: Application of mixed research approach. *Work Study*, 51: 17-31.
- Ballard, G. and G. Howell, 2004. Competing construction management paradigms. *Lean Constr. J.*, 1: 38-45.
- Sacks, R. and M. Goldin, 2007. Lean management model for construction of high-rise apartment buildings. *J. Constr. Eng. Manage.*, 133: 374-384.
- Salem, O., J. Solomon, A. Genaidy and I. Minkarah, 2006. Lean construction: From theory to implementation. *J. Manage. Eng.*, 22: 168-175.

Barriers to Implement Lean Principles in the Indian Construction Industry

S M Abdul Mannan Hussain¹

Research Scholar, GITAM University, Hyd
Assistant Professor, Dept. of Civil Engg
Malla Reddy Engineering College
Autonomous Campus, Secundrabad.

Apoorva Mercy Nama²

B.Tech Final Year Student
Malla Reddy Engineering College
Department of Civil Engineering
Autonomous Campus, Secundrabad

Asra Fatima³

Research Scholar, GITAM University
Assistant Professor, Civil Eng. Dept
Muffakham Jah Engineering College
Banjara Hills, Hyderabad

Abstract— *Lean construction emerged from attempts of transferring and applying the Japanese Lean production philosophy to the construction industry. Lean construction is a confluence of ideas including continuous improvement, flattened organization structure, efficient usage of resources, elimination of waste, and cooperative supply chain. Based on the success of Lean Production in manufacturing and the development of Lean Construction in countries such as Brazil, Denmark and the USA, the application of Lean Construction is currently debated in India. The aim of the study is identification of barriers to successful implementation of lean construction in the Indian construction sector. The data was collected by questionnaire survey of project managers of building construction organizations and senior consultants of architectural and project management firms. The data collected was then analyzed to rank the main barriers and lean principles are suggested to overcome these barriers*

Keywords—*Lean construction; waste; barriers; management; project*

INTRODUCTION

Toyota was the first to bring the Lean principles into limelight. Toyota created a focus on eliminating waste and grew to be the world's largest automotive industry by adopting seven principles of reducing waste. It believed in preserving value with less work and also improvement in efficiency by improving the workflow. Today Lean manufacturing is practiced by many leading auto makers.

Lean principles have slowly made inroads into the construction industry because of its approach to waste elimination and providing value with less effort and time. Construction management is defined as the judicious allocation of resources to finish a project on time, at budget and at desired quality [1]. The biggest cost impact of the construction today is the way the whole process is managed and not the cost of labor and materials. Construction process consists of countless activities that add no value to the product. According to Hines and Rich, these non value adding activities (e.g. waiting time, double handling, searching for material etc) are pure waste and should be eliminated completely [2]. In a study conducted by Josephson and Saukkorippi, a group of workers were followed around for 22 working days and it was noted that 33.4% of their time was waste [3].

I. NEED FOR STUDY

India's rapid economic growth over the past few decades has placed a tremendous stress on its limited infrastructure. Construction industry is one of the largest industries which support the economy of a country. Since construction has a major and direct influence on many other industries reducing waste in construction can go a long way in helping the economy of the world.

II. LITERATURE REVIEW

Existing data and literature on lean principles and its applications in construction industry around the world was collected. This formed the reference for framing the questionnaire for survey.

A. Lean construction

According to Chick G. et al, waste is more than the physical wastes that are the focus of construction site activity [4]. In fact waste is any activity (or inactivity) that does not add value to the product or service. Waste can be

- Value-adding (VA): is the work that the customer is willing to pay for.
- Essential non-value adding: these are the tasks that must be completed to enable the value-adding activity to be completed, but do not add value. For example, inspection is not that the customer pays for but is necessary.
- Waste: Waste can be of two types. Waste in the work itself (e.g. excessive walking, looking for tools and materials, poor quality). Introduced or enforced waste (e.g. waiting for information, materials not supplied), which has prevented work activity from being carried out.

According to Koskela and Howell, Lean Construction is a way to design to minimize waste of materials, time, and effort in order to generate the maximum possible amount of value [5] According to Dulaimi and Tanamas, managing construction under lean construction is different from typical contemporary practice [6] because it:

- Has a clear set of objectives for the delivery process
- Is aimed at maximizing performance for the customer at the project level
- Designs concurrently product and process
- Applies production control throughout the life of the project

B. Lean principles

Womack and Jones describe Lean thinking as a cycle of five guiding principles where the implementation of the first four lead to achieving the fifth [7]. The ultimate goal is the elimination of waste. The principles are described below:

- **Specify value**
Only what the customer considers as value should be taken into consideration, —*nothing more, and nothing less*”. In construction activities can be classified as 3 types:
 1. Value Adding (VA)
 2. Non-value Adding (NVA)
 3. Necessary Waste (NW)
- **Identify the value stream**
This is about identifying all the steps in the value stream in order to determine activities that do not add value and seek for their elimination.
- **Make value flow without interruption**
This is done by minimizing delays, inventories, defects and downtime.
- **Use pull logistics**
All components and information are made and supplied at the necessary time to deliver the product or service to the customer at exactly the time the customer wants it.
- **Pursue perfection**
Lean consists of continuously improving through collaboratively identifying and removing wastes to provide the desired results.

C. Lean Project Delivery System (LPDS)

According to Ballard, the Lean Project Delivery System (LPDS) [8] consists of the following phases:

- project definition
- lean design
- lean supply
- lean assembly
- Use

Essential features of LPDS include:

- the project is structured and managed as a value generating process
- downstream stakeholders are involved in front end planning and design through cross functional teams
- project control has the job of execution as opposed to reliance on after-the-fact variance detection
- optimization efforts are focused on making work flow reliable as opposed to improving productivity
- pull techniques are used to govern the flow of materials and information through networks of cooperating specialists
- feedback loops are incorporated at every level, dedicated to rapid system adjustment; i.e., learning.

IV. METHODOLOGY

The main tool for the collection of data includes questionnaires. The target population for the data collection includes project managers of building construction organizations.

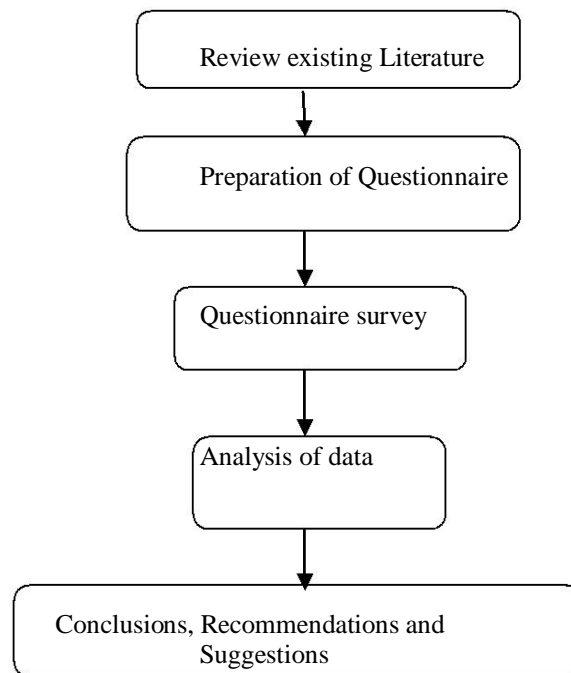


Fig. 1 Proposed methodology for the project

The questionnaire was uploaded to Google drive in the form of Google docs so that the survey details could be collected online. The questionnaire was circulated as a link to the architects, civil engineers and project managers of construction firms through emails. The questionnaire was circulated to about 50 companies. The representatives were to fill the questionnaire and submit the data online. The questionnaire when submitted collects the data in an excel sheet real- time in the Google drive database.

V. RESULTS AND DISCUSSIONS

To identify the barriers for successful implementation of lean construction, a questionnaire was prepared after thorough literature study of barriers faced in other countries. Table 1 lists out the mean score of various barriers to implementation of lean principles in India.

The main barriers to applying Lean principles in Construction industry in India have been identified as

- Lack of exposure on the need to adopt lean construction
- Uncertainty in the supply chain
- The tendency to apply traditional management
- Culture & human attitudinal issues (Mindset issues)
- Lack of commitment from top management
- Non-participative management style for workforce

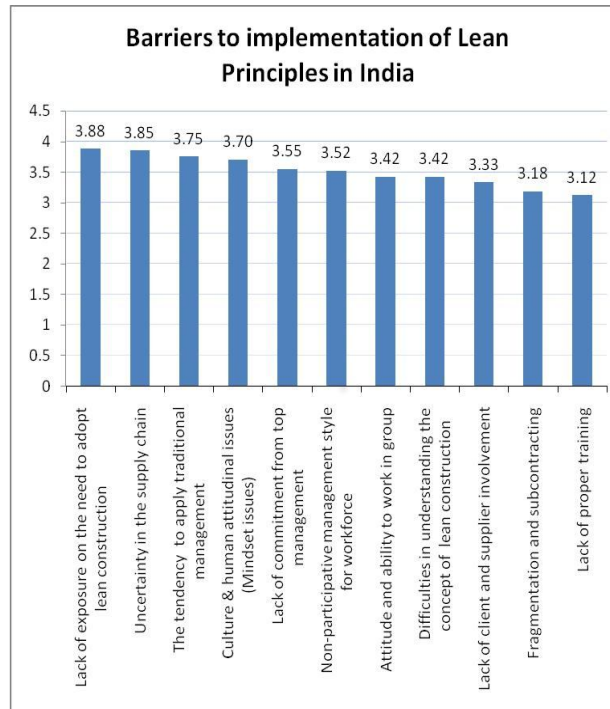


Fig. 2 Barriers To Implementation Of Lean Principles In India

TABLE 1. MEAN SCORE OF BARRIERS TO IMPLEMENTATION OF LEAN PRINCIPLES IN INDIA

BARRIERS TO IMPLEMENTATION OF LEAN PRINCIPLES IN INDIA	MEAN SCORE
Lack of exposure on the need for lean Construction	3.88
Uncertainty in the supply chain	3.85
The tendency to apply traditional management	3.75
Culture & human attitudinal issues (Mindset issues)	3.70
Lack of commitment from top management	3.55
Non-participative management style for workforce	3.52
Attitude and ability to work in group	3.42
Difficulties in understanding the concept of lean construction	3.42
Lack of client and supplier involvement	3.33
Fragmentation and subcontracting	3.18
Lack of proper training	3.12

Lean construction principles are still a new concept in Indian construction sector. The benefits of lean construction has been recognized by some of the leading construction firms like Larsen and Toubro, Tata Realty & Infrastructure, Shapoorji Pallonji & Co., GMR Group and other such organizations, but it is yet to percolate down to the medium and smaller construction firms. —Lack of exposure on the benefits of adopting Lean construction is one of the main barriers identified in the survey.

The next important barrier identified in the survey is the Uncertainty in the supply chain. The Lean Construction principles stress on waste minimization. This can be achieved through maintaining the right inventory; there should be no over-ordering or under-ordering of materials. Lean principles also stress on just-in-time supply. This does minimize waste but the risk involved is also high. Therefore the uncertainties in the supply chain can prove to be a big risk and a barrier which can prevent the practitioners from adopting the Lean principles.

The third barrier identified is the —Human attitudinal issues and cultural mindset and the tendency to apply the traditional concepts of project management. Human beings are people of habits and there is a general tendency to resist change. Construction industry is a huge and old industry. People are used to and are comfortable with the traditional style of management and so do not want to disturb what is already working. But with the construction sector on the boom and resources depleting at a fast pace, it is high time that the construction industry which has a big role in waste generation and environment pollution, changes and adopts principles which will result in waste minimization and prevention of environment pollution.

Lack of commitment from the top management and the Non-participative style of management is also a barrier in implementing Lean concepts in construction. Indian construction industry is used to working as a bureaucratic style of management, where orders are given by the managers and they are executed by the workers. Managers are resistant to change, as they feel that workers would not work properly if they are included in the decision making process. Previously workers in the construction sector were illiterate and learnt on the job, but with technological advances in construction, at present the workforce consists of engineers and other educated and experienced personnel, who if given responsibility, will be motivated and assume responsibility to provide better and faster results.

VI. CONCLUSION AND RECOMMENDATION

Most of the respondents who have not heard about lean management principles are from the public sector executing huge projects along with big firms. Though the big firms are using lean principles, people from the government sector should also be educated about the savings due to adopting lean principles, so that they can mandate it on all government sponsored projects.

Individual practitioners can also be made aware of lean concepts by workshops, conferences, journals, and business magazines.

Lack of exposure on the need to adopt lean construction can be overcome by communicating the benefits of Lean construction through seminars and conferences to the construction practitioners. Also the government should enact policies which appreciate the effort by firms which adopt Lean principles. Recommendation is to take companywide initiative to apply Lean principles and it is not enough to send a few managers or personnel for workshops and seminars. This way of working should eventually percolate to the lower levels. The sub contractors and suppliers should also be made to attend these workshops and take initiatives to implement Lean management principles.

Barriers in uncertainty in the supply chain can be overcome by choosing proper suppliers who not quote less price, but deliver good quality and who also have a proven track record. By working closely with suppliers and subcontractors, problematic issues can be minimized by participative style of managing projects and establishing strategic alliances with them. This can be done effectively if one works with the same supplier again and again

There is a tendency to apply traditional management principles. People generally do not want to disturb processes which have been going on since a long time, but now with so much construction boom, it is high time the construction industry gives cognizance to the fact that waste produced by industry is high and needs to be minimized. This can be achieved by training all managers and workers in the firm on the benefits of Lean construction. Workshops on the comparisons on Lean and traditional methods of construction, and how Lean is better should be conducted. Suitable metrics should be developed so that practitioners apply Lean management principles.

Managers should promote lean construction, as it can bring considerable revenue savings for the firm. Managers should change with times and new technology. This can be done by bringing about a change in organization culture by making the adoption of lean principles mandatory, by enacting new policies for waste minimization, and by partnering with suppliers and subcontractors to ensure that they follow Lean construction methods.

ACKNOWLEDGMENT

The authors record their appreciation for the time and effort taken by the project managers to complete the questionnaire survey, in spite of their hectic schedule.

REFERENCES

- [1]. Clough, R.H. & Sears, G.A. (1994) Construction Contracting. (6th edition) John Wiley & Sons Inc., New York.
- [2]. Hines, P., Jones, D. and Rich, N. (1998), Lean Logistics, Pergamon, London.
- [3]. Josephson, P-E., and Saukkoriipi, L. (2005). Waste in construction projects. Call for a new approach. Report 0507. The centre for Management of the Built Environment, Building Economics and Management, Chalmers University of Technology, Gøteborg.
- [4]. Chick, G., Corfe, C., Dave, B., Fraser, N., Kiviniemi, A., Koskela, L.,
- [5]. O'Connor, R., Owen, R., Smith, S., Swain, B. and Patricia



- [6]. Tzortzopoulous (2013), Implementing lean in construction, CIRIA, London, United Kingdom.
- [7]. Koskela, L., Ballard, G., Howell, G., and Iris D. Tommelein (2002),
- [8]. ‘The foundations of lean construction’, Design and construction: building in value, Butterworth Heinemann, Oxford, UK, pp. 211-226.
- [9]. Dulaimi, M. F., and Tanamas, C. (2001), ‘The principles and application of lean construction in Singapore’, Proceedings of the 9th Annual
- [10]. Conference of the International Group for Lean Construction, Singapore.
- [11]. Womack, J. P. and Jones, D. T. (1996), Lean Thinking: Banish waste and create wealth in your corporation, Simon and Schuster, New York, USA.
- [12]. Ballard, G. (2000), Lean Project Delivery System, LCI White Paper – 8, Lean Construction Institute.

Assessment of Musi River Water and Nearby Ground Water: Impacts on Health of Down Stream Villages of Hyderabad

K. N. Sujatha*

Civil Engineering Department, Malla Reddy Engineering College (A), Hyderabad - 500100, Telangana, India;
suji.nissi07@gmail.com

Abstract

Objective: The present study focused on the MUSI River contamination and its impacts on health of downstream villages of MUSI in Hyderabad city. These pollutants are responsible for the degradation of aquatic ecosystems and groundwater resources.

Methods and Analysis: The areas from PEERIZADIGUDA to PRATAPASINGARAM selected for analysis which are located at down streams of MUSI River. Ground water samples are collected from each location and Physical, chemical and biological parameters are analyzed by using suitable methodologies of P^H , Total dissolved salts, Turbidity, Total Hardness, chlorides sulphates and Biological oxygen demand water quality parameters are assessed. A study has made on these selected areas of population for health hazards due water born diseases by sampling method. **Finding:** This paper discuss about Environmental sanitation, water pollution constitutes a serious problem particularly in the mega cities. City like Hyderabad has seen rapid economic development and urbanization which lead to the burden of illness and severity of skin and communicable diseases in and around MUSI River due to its worst contamination in recent days due to poor hygienic and to explore the importance of treated water supply. **Novelty/Improvement:** Poor hygiene and polluted ground waters interventions are causing health hazards in these of areas. So, safe treatment of wastewater before disposal may sustain its natural environment and which can improve the self-purification of river and help in sustain river ecology.

Keywords: Health Problems, Hygiene and Sanitary, Water Pollution, Waste Water Treatment

1. Introduction

Water is a key source to sustain life on earth. The expansion of industrial development and urbanization in two last decades of Hyderabad city has not only increased water consumption considerably but also affected water quality³. The city has no outlet source to dispose the waste water produced except to discharge into musu, which is an only source to discharge. Hence musu in this city has drastically changed its river ecology, which Even contaminated the ground water sources⁴.

Musi River which is a tributary of River Krishna passes through Telangana state has good discharge and quality in the upstream. But when it reaches to down streams of Hyderabad city this river is within to be a sewerage drain.

This is due to high sewerage disposal and pollutant from nearby industries. The Hyderabad city discharges about 600 million liters per day untreated sewerage water into Musi River. Even ground water sources are contaminated, the drinking water in entire area is brought from distant places; they were spending lots of money². The people who are residing in downstream are low economic standard. So they are force to consume these contaminated waters. The quality of water in Musi is degradation considerably. Hence the health problems in the downstream villages are witnessed. Health problems can because of pathogenic bacteria, viruses and parasites present in the wastewater. Hookworm infections are more common in agricultural workers who go barefoot in wastewater- irrigated fields⁸.

*Author for correspondence

This review was done to explore the impact of poor water treatment, hygiene, and sanitary interventions on health conditions, to diagnose the severity and ways to find out better solution to reduce health problems in downstream villagers. In this research a systematic study has carried out on surface and ground waters pollution in the Musi River Basin, to evaluate its contamination, and causes. Samples of water were obtained from individual water sources (wells) from villages and from surface water sources⁵. Contamination from various sources pollutes ground water through leaching of organic and inorganic contaminates animal waste, domestic effluents and industry. The untreated municipal sewage and solid waste into water bodies increases nitrogen concentrations and sometimes can reach more than 60mg/l⁶. The present study is an attempt to report a comparative account of health effects due to untreated municipal sewages, untreated effluent and water quality of the River Musi surrounding water ground⁷.

People of downstream depend on ground water resources due to their low economic standards, Groundwater quality in these areas are degraded considerably. Ground water in these areas is used for various purposes¹. Groundwater pollution has been reported in many aquifers because of high concentration of organic and inorganic compounds in groundwater. These contamination lead too many diseases especially skin disorders, gastric disorders and allergies. More Health problems are witnessed in these areas, which priorities for the treatment and provision of drinking water. May reduce the health problems¹¹ due to high dumping of sewerage and solid waste in the river Musi has led to Microbial con-

tamination of drinking water remains a significant threat and constant vigilance is essential⁶ untreated waste from different sources may alter the ecosystems and degrade them¹².

2. Study Area

The study area is located in the Hyderabad city of Telangana state, India, which is a downstream of Musi River in Hyderabad.

The area falls in the Survey of India Topographic map number 56K/10 to a scale of 1:50,000. The area lies between to 17° 22' 58.8"N latitude and to 78° 39' 39.276" E longitude. The area is located between PEERIZADIGUDA, PRATAPASINGARM the groundwater and river water samples are analyzed for physical, chemical and parameters. These samples are collected from bore wells of five locations:

PEERIZADIGUDA, RTC-COLONY,
PARVATHAPURAM, MUTHYLAGUDA,
PRATAPASIGARAM. Samples are analyzed for various parameters to diagnose the concentrations present in the samples.

3. Methodology

Ground water samples are collected from each location and Physical Properties and chemical properties and biological parameters are analyzed by using suitable methodologies for, PH, TDS, Turbidity, Alkalinity, Total Hardness, chlorides sulphates, Nitrates BOD and COD water quality parameters are assessed.

Table 1. Ground water quality parameters of the study area

LOCATION/ PARAMETERS	PEERIZADI GUDA	RTC COLONY	PARVATHA PURAM	MUTHYLA GUDA	PRATAP SINGARAM	INDIAN STANDARD OF DRINKING WATER
P ^H	7.97	7.83	8.23	7.89	8.51	6-8
TDS mg/l	1250	1820	2410	2175	2250	500
Turbidity NTU	8 NTU	7	7.3	7.56	8.2	10
Alkalinity (mg/l)	259	246	288	302	259	300
Total hardness mg/l	340	355	328	329	342	100
Chlorides mg/l	140	138	135	209	202	250
Sulphates mg/l	345	231	246	302	359	250
Nitrates (mg/l)	3.8	5.1	4.7	5.7	4.3	45
BOD (mg/l)	2.2	1.2	2.4 mg/l	2.3	2.6	3
COD ppm	69.3	120	87.2	112.3	102	250

A study has made on these selected areas of population for health hazards due water born diseases by sampling method

4. Results and Interpretation

pH of the study samples is in the range

8.51 to 7.81 PARVATHAPURAM and PRATAPSINGARAM ground water samples are beyond normal range of drinking waters 6-8 pH this may be due to the industrial effluents, sewerage discharges Results of various pH in the study areas is shown in the below. From Table 1.

Total Dissolved Solids, the presence of dissolved salts in the water samples collected from various locations of study area are shown in Table 1 range from 1250 to 2410, the results of shows very high amount of TDS which indicates that the water is contaminated with high amounts of inorganic matters which are either from commercial, industrial or domestic waste. This water may not suitable for direct consumption; these may create various health hazards like diarrhea, joint pains, skin allergies, gastrointestinal disturbances, and vomiting. The study areas are witnessed with more amounts of TDS mainly downstream areas PARVATHAPURAM, MUTHYLAGUDA, PRATAPASIGARAM has high TDS.

Turbidity and Color some samples are witnessed with slightly non transparent in color. Study area, results shows slight variations in turbidity From Table 1 ranges from 7 to 8.2 Areas PEERIZADIGUDA, PRATAPASIGARAM shows high turbidity. It is due to leaching of Musi River to ground water aquifer which contain high amount of organic and inorganic wastes. It may create health problems like diarrhea, gastrointestinal disturbances, and vomiting.

Alkalinity samples of study areas shows slightly high amount alkalinity which is beyond the limit of drinking

water. Ranges from 246 mg/l to 302 mg/l. high alkalinity in RTCCOLONY, MUTHYLAGUDA Excess Alkalinity in water is not good to consume and relatively not better and can cause Gastrointestinal problems.

Total hardness of the study samples is in the range 328 mg/l-355 mg/l ground water samples are beyond normal range of drinking waters Areas RTC-COLONY, PRATAPASIGARAM shows high limits of hardness. Results are shown in Table 1.

Chlorides: Chloride levels in the study area are within the limits, results shown in Table 1 ranges from 136 mg/l to 209 mg/l. More levels are shown in areas MUTHYLAGUDA, PRATAPASIGARAM.

Sulphates: Study area shows high amounts of sulphates results are shown in Table 1 ranges from 231 mg/l to 359 mg/l PEERIZADIGUDA, PRATAPASIGARAM shows high amounts of sulphates it is due high discharge of domestic sewage which contain detergents, Sulphates induces the formation of sulphuric acid, Hydrogen sulphate and its man may be a cause for the gastrointestinal and skin allergies.

Nitrates Study area shows nitrates ranges from 3.8 mg/l to 5.7 mg/l results are shown in Table 1. Areas RTC-COLONY, PRATAPASIGARAM results are within the limit.

Biological Oxygen Demand (BOD): Study area shows BOD from 1.2 mg/l to 2.6 mg/l which is within the limits more BOD in PARVATHAPURAM, PRATAPASIGARM in Table 1.

Chemical Oxygen Demand (COD) Study area shows COD ranges from 69.3 ppm to 120 ppm more concentration is found in areas RTC-COLONY, MUTHYLAGUDA results are within the limit. These concentrations in ground water are due to contamination of MUSI which is near to these downstream areas.

A random study has made for the analysis of health problems in the downstream villagers of MUSI to identify

Table 2. Field survey conducted randomly on Jan15 to April-15 in the study area for health hazards

Study Areas	Sample distribution	Skin diseases %	Diarrheic %	Arthis %	Gastero intestinal problems%	Skin allergies %	Malaria %
PEERIZADIGUDA	57	55	35	45	45	65	35
RTC COLONY	63	68	46	52	50	75	45
PARVATHAPURAM	43	46	32	56	44	68	48
MUTHYLAGUDA	65	54	37	55	34	85	55
PRATAPSINGARAM	85	86	52	65	48	83	58

the problems and impact of MUSI River on downstream villagers. Results or observations are tabulated in the Table 2. Results shows number of health problems like skin diseases, allergies and gastric disorders and parasitic fever like malaria. Arthis and other pediatric problems are also witnessed. People of these areas are less economic standards. So, they have satisfy with available ground waters and impact of pollution of Musi River surrounding ground water which lead to health problems in down streams villagers of MUSI River.

5. Conclusions

Due to rapid development from last two decades in Hyderabad, large quantities of waste waters produced in the city, as there are no other outlet sources to dispose the wastewater. When untreated domestic sewage, Industrial Effluents are discharge into the dry bed of the Musi River adversely impacting on the river ecology and on downstream villagers. Poor water quality had a negative impact on farmer health and undesirable for drinking purposes. Ground water is the primary source of water used in these areas, thus knowledge about its availability and sustainability are essential for the successful

Management and future development of this limited resource. Ground-water availability and sustainability are influenced by many factors, one of which is water quality. Water quality generally has been over looked in these because the primary focus has been on obtaining a sufficient water supply.

The areas from PEERIZADIGUDA to PRATAPSINGARAM selected for analysis are located at down streams of Musi and the Musi conditions in these regions made worst due to heavy dumping of the organic waste, sewage from various sources from industrial and municipal waste. And the safe water supply for these areas is very less and people of these areas depend on ground water and poor hygiene, sanitary and polluted ground waters, interventions are causing health hazards in these of regions. Thus, anthropogenic activity is a source of contaminants to the water table.

Untreated waste water at each sources level, treated before disposal can reduce pollutants, so safe treatment using advance scientific technology can reduce the load of pollution and accumulation of pollutants at the downstream. it also improves water quality and thus protects

River ecology and thus minimizes health impacts on downstream villagers.

Sustainable developments like waste water treatment systems and natural techniques of filtration methods can sustain or help the environment surrounding of Musi, and from various skin and health hazards through water pollution.

6. References

1. Packialakshmi S, Deb M, Chakraborty H. Assessment of groundwater quality index in and around Sholinganallur area, Tamil Nadu. *Indian Journal of Science and Technology*. 2015 Dec; 8(36). DOI: 10.17485/ijst/2015/v8i36/87645.
2. Pullaiahcheepi. Impact of pollution of Musi River water in downstream villages-A study. *IOSR Journal of Environmental Science, Toxicology and Food Technology*. 2012 Sep-Oct; 1(4):40–51. ISSN: 2319-2402, ISBN: 2319-2399.
3. Salve VB, Hiware CJ. Study of water quality of Wanparakalpa reservoir Nagpur, near Parli Vajinath, district Beed, Marathwada region. *J Aqua Biol*. 2008; 21(2):113–7.
4. Hujare MS. Seasonal variation of physico-chemical parameters in the perennial tank of Talsande, Maharashtra. *Ecotoxicol Environ Monitor*. 2008; 18(3):233–42.
5. Ensink JHJ, Scott CA, Brooker S, Cairncross S. Sewage disposal in the Musi-River, India: Water quality remediation through irrigation infrastructure. *Irrig Drainage Sys*, Springer. 2009; 24(1):65–77. DOI: 10.1007/s10795-009-9088-4.
6. Kumar RM. Predatory industrialisation and environmental degradation: A case study of Musi-river. *Telangana: Dimensions of underdevelopment*. Center for Telangana studies Hyderabad; 2003. P. 203–12.
7. Van der Hoek, Mehmood, et al. Urban Waster water: A valuable resource for agriculture- A case study from Haroonabad, Pakistan. *IWMI –Research Report*; 2002.
8. Ayres RM, Mara DD. APHA-WWE-WEF. Standard methods for the examination of water and wastewater. *American Public Health Association*, Washington DC; 1996.
9. Swaranlatha S, Narsingrao A. Ecological studies of Banjara lake with reference to water pollution. *J Envi Biol*. 1998; 19(2):179–86.
10. Rao R. Physico-chemical and biological characteristics of Husain sagar, an industrially polluted lake, Hyderabad. *Environ Biol*; 1993.
11. Krishnamurthy R. Hydro-biological studies of Wohar reservoir Aurangabad (Maharashtra State) India. *J Environ Biol*. 1990; 11(3):335–43.

12. Karanth KR, Groundwater assessment development and management. New Delhi: Tata McGraw Hill Publishing Company Ltd; 1987. p. 725.
13. Venkateswarlu V. Sponge city: Water balance of mega-city water use and wastewater use in Hyderabad. India Irrig and Drain. 1969; 54:S81–9. An ecological study of algae of the river Moosi, Hyderabad (India) with special reference to water pollution I. Physico-Chemical Complexes. Hydrobiologica. 1969; 33:117–43

A Statically Study Of Probable Future Water Demand of KOMPALLY

K. N. Sujatha

Assistant Professor, Dept. of Civil Engineering, Malla Reddy Engineering College,

-----****-----

Abstract: Population projections are key elements of many planning and policy studies, the future development of the town mostly depends on water, while the designing the water supply scheme for a town or city, it is necessary to determine the total quantity of water required for various purpose in city and present population for design of water supply project like storage reservoir and other can be conveniently used.

This paper discuss about the population forecast for next 3decades based on past data to a small town KOMPALLY in TELANGANA and also estimation of present water requirement in the town based on the census A satisfactory study to measure the probable estimation of water demand in future for KOMPALLY town in TELANGANA .

Key words: population forecasting, water demand, geometric estimation, cumulative demand, mass curve method

1. INTRODUCTION

Water is required for multiple uses such as agricultural, domestic, community or industrial use in our life and for each use quality of water differs. To make water available for various purposes we have to know the requirement then quantity and then the quality. Two main challenges related to water are affecting the sustainability of human urban settlements: the lack of access to safe water and sanitation, and increasing water-related disasters such as floods and droughts. As the water resources are not evenly distributed, across different continents, some countries have surplus water while many other countries are facing scarcity of water. Likewise, there is skewed growth of population in different continents, resulting in a wide mismatch between the existing population and water availability. Among various continents, Asia has 36% of the available fresh water reserves, with over 60% of the world population where water is a scarce commodity.

India is most vulnerable because of the growing demand and in-disciplined lifestyle. This calls for immediate attention by the stakeholders to make sustainable use of the available when the concentration of the population increases; it becomes very difficult to locate wells. In addition to the sources of water having good quality of water, are less readily available to the individuals. It also

becomes compulsory to protect the community from the danger of fire, which is not possible through private source of water. These all situations led to the development, of public water supply schemes water resources to ensure better quality of lives.

While designing the water supply schemes for a town or city, it is to determine the total quantity of water required for various purposes by the city. A matter of fact the first duty of the engineer is to be determining the water demand of the town and then to find out the suitable water sources from where the demand can be meet. These results indicated that NWP-based analogs showed promising features for advancing the accuracy of short-term urban water demand forecasts Reference [2]

Population growth has long been a concern of the government, and India has a lengthy history of explicit population policy. The periodic census enumeration obtains data on the size and composition of the population at the time census was taken. But for many purposes, it is important to know the number and characteristics of the people at different dates between the two censuses. With the Government's commitment to stabilizing the population of India by 2045 as stated in the National.

2. STUDY AREA

KOMPALLY is one of the fastest growing suburbs of Hyderabad, India which is located in the QUTUBULLAPUR Mandal of RANGA REDDY District. The main approach to KOMPALLY is the 250 feet, 6 Lane, NH 7 towards Nagpur and KOMPALLY is just 10 km from Paradise, SECUNDERABAD. There is lot of green everywhere in KOMPALLY making it the best place for a home.

2.1 Colonies in and around Kompally

The main colonies are Royal Meadows near to Cine Planet, a prime villas ranging between 1.4 cores to Rs.2.00 cores .Sachet Bhu : Sattva, ARMSBURG MY SPACE BEHIND DEEWAN DHABA LANE,Prajay Jamuna Gruhatara Apartments, NCL North Avenue, Satyam Enclave, BHEL R&D co-op society, Laxmi Ganga Enclave, Palm Springs, NCL Colony, Meenakshi Estates, Palm Meadows,Prestige Park, Maa Laxmi Residency, Sree Vishnu Enclave(Behind Chandra Reddy Gardens), Nagarjuna Dreamlands, Vitis Villa,

Shanthiniketan, Ashoka-Ala-Maison,Vitis Villa, Aparna Canopy, Sri Sai Krupa Apartments,Tanusha Residency,

Population year	Population (as per census)
1991	6591
2001	8035
2011	11193

Prestige Park, Casa Estebana, Gangasthan, Gurusai Residency, Sree Vensai Projects, canton Park, Devender Colony, ELA Projects, Panchsheel Enclave, Patel's Landmark, Durga Vihar, Diamond Residency, Sriram Residency, Spring Field Colony,Angadi Pet, Anthem Vistas, Anthem Ambience & Neighborhood, Trident Grande,Oorjitha Grand Vie, Srinivas Nagar Colony, Godavari Homes, Gayatri Nagar Colony, Bank Colony & Jayabheri Park. The largest among being Jayabheri Park next to which is Devender Colony followed by Central Park, Bank Colony and SN colony,HI-VISION Residency,ncl north, Jayadarsini Enclave, Siri Sampadha Residency gated community.

3. METHODOLOGY

3.1 Water demand

Whenever an engineer is given the duty to design a water supply scheme for a particular section of community, it becomes imperative upon him,to first of all, evaluate the amount of water available and the amount of water demanded by the public. In fact the first study is to consider the demand, and then the second requirement is to find sources to fulfil the demand. The various types of water demands, which a city may have,may be broken in to the following cases.

Data collection:

The statistically water data of Kompally area collected from the Gramapanchayat and the peoples.

Mass curve method is adopted for the calculations of water demand, Source of water: Area of the Kompally is 2272 acres and the house holders are 7700, others are commercial. The data of Kompally can be collected from the Gramapanchayat they are

- 1) **Bore wells:** Bore wells in kompally are 88. In these 50 bore wells are dry up. The remaining 38 are in working condition. In these 21 are seasonal and 17 are in working condition.
- 2) **Sumps:** The sumps present in Kompally are 10. In these four are under Gramapanchayat and remaining six under private sector. The daily supply of water from these four sumps is 8 Kl*4

- 3) **Tanks:** The tanks present in Kompally are 11. In this five tanks are under Gramapanchayat and remaining six are under private sector.

The storage capacity of each tanks are described in below table

TABLE 3: 1 Capacity of water tanks present in Komapally

3.2 Population forecasting:

Data collection:

The statistical population data of Kompally collected from the Gramapanchayat and from the peoples. Geometric Increase method is adopted for the calculation of population, To forecasting the population for next three decades is can be worked out by using geometric method. The collected past population data from the Grampanchayat

The collected population data is used to compute the growth rate (%) for an each decade by Geometric Mean Method

S.NO	Number of tanks	Storage capacity (kl)
1	3	90 kl
2	1	60 kl
3	3	100 kl

TABLE 3:2 last three decade populations

3.3 METHODOLOGY TO ADOPT FOR FORECASTING THE WATER DEMAND:

The forecasting the requirement of water for the future generations is needed to calculate the total storage capacity of distribution reservoir. The total storage capacity of distribution reservoir is the summation of

- a) Balancing storage (or equalizing or operating storage)
- b) Breakdown storage
- c) Fire storage

The main and primary function of distribution reservoir is to meet the fluctuating demand with a constant rate of supply from the treatment plant. The quantity of water required to store in the reservoir for balancing or equalizing this variable demand against the constant supply

is known as the balance reserve or the storage capacity of a balancing reservoir. The balancing storage can be worked out by utilizing the hydrographs of inflow or outflow, either by mass curve method or by using an analytical tubular solution.

Mass - curve method:

A mass diagram is the plot of accumulated inflow (i.e. supply) or outflow (i.e. demand) versus time. The mass curve of supply (i.e. supply line) is, therefore, first drawn and is superimposed by the demand curve. The procedure to construct such diagram is as follows: From the past records, determine the hourly demand for all 24 hours for typical days (maximum, average and minimum). Calculate and plot the cumulative demand against time, and thus plot the mass curve of demand. Read the storage required as the sum of the two maximum ordinates between demand and supply line as shown in fig. Repeat the procedure for all the typical days (maximum, average and minimum), and determine the maximum storage required for the worst day.

4. RESULTS AND INTERPRETATION

4.1 Geometric mean method:

Population year (1)	Population (2)	Increase in population in each decade (3)	Growth rate (%) Col (3)/(2)x100 (4)
1991	6591	-	-
2001	8035	1444	$1444/6591 \times 100 = 21.90$
2011	11193	3158	$3158/8035 \times 100 = 39.30$
		Average = 2301	Average = 30

TABLE: 4.1 forecasting of population for next three decades

The average of increase in population is $= 1444 + 3158/2 = 2301$

Similarly,

The average or geometric mean of growth rate (r) is $= (21.90 \% + 39.30 \%) / 2 = 30.60 \%$

(30 %)

Now, assuming that the future population increases at this constant rate (30%), we have $P_n = PO (1 + r / 100)^n$

As per census, using $n = 1, 2, 3$ decades

1. The population after first decade for the year 2021 is

$$P_{2021} = 11193 + 30.60/100 \times 11193 = 14168$$

2. The population after second decade for the year 2031 is

$$P_{2031} = 14168 + 30.60 / 100 \times 14168 = 19091$$

Similarly,

3. The population after third decade for the year 2041 is

$$P_{2041} = 19091 + 30.60 / 100 \times 19091 = 24932$$

Therefore the forecasting population for next three decades is 24932.

4.3 Interpretation of water demand by using mass curve method:

As per the present population required water demand for 135 liters/day/head is 15, 11055 liters. But the present supply of water in Kompally is 30 liters/day/head and the deficiency of water is 615615 liters.

Now, as per the forecasted population for next three decades is 24932, the requirement of water for the next three decades at 135 liters/day/head is

$$\begin{aligned} \text{Total daily supply} &= \text{Rate of supply} \times \text{Population} = 24932 \times 135 = 3365820 \text{ liter} \\ &= (33, 66,000 \text{ liters}) \end{aligned}$$

For the water supply of a small town

(Kompally) with the daily requirement of 33,66,000 liters, it is proposed to construct a distribution reservoir.

\The pattern of draw off or maximum peak hours are as follows

7:00 A.M – 8:00 A.M 30% of days supply

8:00 A.M - 5:00 P.M 35% of days supply

5:00 P.M – 6: 30 P.M 30% of days supply

6:30 P.M – 7:00 A. 5% of days supply

The pumping is to be done at constant rate of 8 hours per day (8 A.M to 4 P.M)

Then the total daily requirement is $= 3365820$ liters/ day or

Approximately $= (33, 66,000 \text{ liters/day})$ is required during peak hours.

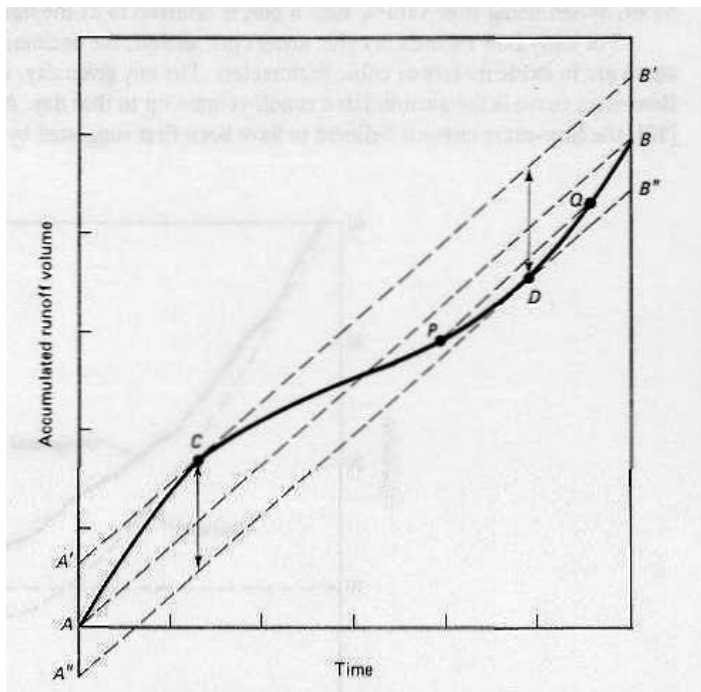
An Average water supply/ water demand is required for the population of Komapally for next decades

Period (1)	Rate of demand (2)	Demand in liters $\text{Col}(2) \times (3366 \times 10^3)$ (3)	Cumulative demand in 10^3 liters (4)
7:00AM–8:00AM	30% of total	$0.3 \times (3366 \times 10^3)$ $= 1009.8 \times 10^3$	1009.80
8:00AM–5:00PM	35% of total	$3.5 \times (3366 \times 10^3)$ $= 2187.9 \times 10^3$	2187.9
5:00AM–6:30PM	30% of total	$0.3 \times (3366 \times 10^3)$ $= 3297.7 \times 10^3$	3297.7
6:30PM–7:00AM	5% of total	$0.05 \times (3366 \times 10^3)$ $= 168.30 \times 10^3$	3466.0

TABLE: 4:2 cumulative water demands

The total supply is obtained in 8 hours at rate = $3366 \times 10^3 / 8$ liters/hour

$$= 420.750 \times 10^3 \text{ liters /hour}$$



An Average demand is converted in to cumulative demand as shown in table

Graph: 1 Mass diagram for during 24 hours pumping

The supply line on the mass diagram will, therefore be a straight line with its slope as 420.750×10^3 liters per hour, as shown by the dotted line. From the graph the two maximum ordinates A and B enclosed between the demand and supply lines are read out from the graph.

$$\text{Maximum ordinate A} = 1009.8 \times 10^3 \text{ liters}$$

$$\text{Maximum ordinate B} = 1366 \times 10^3 \text{ liters}$$

$$\text{The total storage required is } (A + B) = (1009.8 \times 10^3 + 1366 \times 10^3) \text{ liters} = 2375.8 \times 10^3 \text{ liters}$$

$$\text{Hence, Per capita demand} = 3366 \times 10^3 / 365 \times 24 \times 32 = 0.3698 \text{ liter/person/hour}$$

As for the above collected data and its calculations, we have concluded that the design for the storage capacity of water reservoir for Kompally is 2375.8×10^3 liters.

Thus, the per capita demand is 0.3698 liters /person/hour is recommended for future next three decades.

5. CONCLUSION

The population of Kompally for the next three decades and water demand of Kompally calculated.

For the present population of Kompally the water deficiency is 615615 liters, if there is no proper supply of water, possible of increase of water demand. Hence, it may lead to scarcity of water in this region. In this region content has less ground water resources.

As above collected data and its calculations, we have concluded that the design for the storage capacity of water reservoir for Kompally is 2375.8×10^3 liters.

Thus, the per capita demand is 0.3698 liters /person/hour is recommended for future next three decades.

REFERENCES

Alvisi, S., Franchini, M., and Marinelli, A. (2007). "A short-term, pattern-based model for water-demand forecasting". *Journal of Hydroinformatics*.

Babel, M.S., and Shinde, V.R. (2011). "Identifying Prominent Explanatory Variables for Water Demand Prediction Using

Artificial Neural Networks: A Case Study of Bangkok". *Water Resources Management*.

Bakker, M., Vreeburg, J.H.G., Palmen, L.J., Sperber, V., Bakker, G., and Rietveld, L.C. (2013). "Better water quality and higher energy efficiency by using model predictive flow control at water supply systems". *Journal of Water Supply: Research and Technology*.

Bakker, M., Vreeburg, J.H.G., Van Schagen, K.M., and Rietveld, L.C. (2013). (Submitted). "A fully adaptive forecasting model for short-term drinking water demand". *Journal of Environmental Modeling and Software*

Box, G.E.P., and Jenkins, G.M. 1976. *Time Series Analysis: Forecasting and Control*. 2 nd ed. San Francisco: Holden-Day.

Bunn, S.M., and Reynolds, L. (2009). "The energy-efficiency benefits of pump scheduling optimization for potable water supplies". *IBM Journal of Research and Development*.

Caiado, J. (2010). "Performance of combined double seasonal univariate time series models for forecasting water demand". *Journal of Hydrologic Engineering*.

Grillenzoni, C. (2000). "Time-varying parameters prediction". *Annals of the Institute of Statistical Mathematics*.

House-Peters, L.A., and Chang, H. (2011). "Urban water demand modeling: Review of concepts, methods, and organizing principles". *Water Resources Research*.

Jain, A., Varshney, A.K., and Joshi, U.C. (2001). "Short-term water demand forecast modeling at IIT Kanpur using artificial neural networks". *Water Resources Management*.

Joo, C.N., Koo, J.Y., and Yu, M.J. (2002). "Application of short-term water demand prediction model to Seoul". *Water Science and Technology*. 46 (6-7): 255-261.

Jowitt, P.W., and Chengchao, X. (1992). "Demand forecasting for water distribution systems". *Civil Engineering Systems*.

Lertpalangsunti, N., Chan, C.W., Mason, R., and Tontiwachwuthikul, P. (1999). "Toolset for construction of hybrid intelligent forecasting systems: Application for water demand prediction". *Artificial Intelligence in Engineering*.

Odan, F.K., and Reis, L.F.R. (2012). "Hybrid Water Demand Forecasting Model Associating Artificial Neural Network with Fourier Series". *Journal of Water Resources Planning and Management*

PWN. (2006). "Automated Water System Control". *Control Engineering*.

Worm, G.I.M., van der Helm, A.W.C., Lapikas, T., van Schagen, K.M., and Rietveld, L.C. (2010). "Integration of models, data management, interfaces and training support in a drinking water treatment plant simulator". *Environmental Modelling and Software*.

Zhou, S.L., McMahon, T.A., Walton, A., and Lewis, J. (2000). "Forecasting daily urban water demand: A case study of Melbourne". *Journal of Hydrology*. 236 (3-4): 153-164.

Zhou, S.L., McMahon, T.A., Walton, A., and Lewis, J. (2002). "Forecasting operational demand for an urban water supply zone". *Journal of Hydrology*. 259 (1-4): 189-202.

Arandia, E., Ba, A., Eck, B., and McKenna, S. (2015). "Tailoring Seasonal Time Series Models to Forecast Short-Term Water Demand." *Journal of Water Resources Plan*

Tian, D., Martinez, C., and Asefa, T. (2016). "Improving Short-Term Urban Water Demand Forecasts with Reforecast Analog Ensembles." *Journal of Water Resources Planning and Management*,

Brauman, K., Freyberg, D., and Daily, G. (2014). "Impacts of Land-Use Change on Groundwater Supply: Ecosystem Services Assessment in Kona, Hawaii." *Journal of Water Resources Planning and Management*,

Steinschneider, S., McCrary, R., Wi, S., Mulligan, K., Mearns, L., and Brown, C. (2015). "Expanded Decision-Scaling Framework to Select Robust Long-Term Water-System Plans under Hydroclimatic Uncertainties." *Journal of Water Resources Planning and Management*,

Assessment of Soil Properties to Improve Water Holding Capacity in Soils

K. N. Sujatha¹, G. Kavya², P. Manasa³, K. Divya⁴

¹K. N. Sujatha: Assistant Professor, Dept. of Civil Engineering, Malla Reddy Engineering College,

²G. Kavya, UG student, Malla Reddy Engineering College, Hyderabad

³P. Manasa, UG student, Malla Reddy Engineering College, Hyderabad

⁴K. Divya UG student, Malla Reddy Engineering College, Hyderabad, Telangana state, India

Abstract : The cultivated and non cultivated land is about 114.84 lakh hectares in Telangana in which 43.2% i.e. 49.61 lakh hectares land is cultivated and the remaining are fallow lands. Most of the land is kept fallow may be due to deficiency in soil moisture or water holding capacity of soils. This deficiency is mainly due to insufficient rainfall and lack of natural water resources in Telangana region.

The present research paper discusses about the physio-chemical properties of some cultivated and non cultivated soils in Telangana to evaluate the deficiency of soil moisture and soil holding capacity of soils with the help of nutrients and analysis is carried out to improve the soil properties by addition of required amount of biomass and nutrients to improve the deficiency of soil moisture and water holding capacity. The paper discusses about the assessment of the soil properties of the cultivated and non cultivated soils and by improvement techniques soil moisture, water holding deficiency may be reduced.

Keywords: Soil properties, water holding capacity Organic manure, Clay, soil moisture, Permeability,

1. INTRODUCTION

Water holding capacity designates the ability of a soil to hold water. It is useful information for irrigation scheduling, crop selection, groundwater contamination considerations, estimating runoff and determining when plants will become stressed. By understanding some physical characteristics of the soil, you can better define the strengths and weaknesses of different soil types. Soil moisture limits forage production potential the most in semiarid regions. Estimated water use efficiency for irrigated and dry-land crop production systems is 50 percent, and available soil water has a large impact on management decisions producers make throughout the year.

Soil moisture available for plant growth makes up approximately 0.01 percent of the world's stored water. Soil texture and structure greatly influence water infiltration, permeability, and water-holding capacity Reference [1, 2].

Soil texture refers to the composition of the soil in terms of the proportion of small, medium, and large particles (clay, silt, and sand, respectively) in a specific soil mass. For example, a coarse soil is sand or loamy sand, a medium soil is a loam, silt loam, or silt, and a fine soil is a sandy clay, silt clay, or clay. Water holding capacity varies by soil texture Reference [1]. Permeability refers to the movement of air and water through the soil, which is important because it affects the supply of root-zone air, moisture, and nutrients available for plant uptake. A soil's permeability is determined by the relative rate of moisture and air movement through the most restrictive layer within the upper 40 inches of the effective root zone. Water-holding capacity is controlled primarily by soil texture and organic matter Reference [3, 5]. Soils with smaller particles (silt and clay) have a larger surface area than those with larger sand particles, and a large surface area allows a soil to hold more water. In other words a soil with a high percentage of silt and clay particles. Which Reference [3] describes fine soil, has a higher water-holding capacity. The table illustrates water-holding-capacity differences as influenced by texture. Organic matter percentage also influences water-holding capacity. As the percentage increases, the water-holding capacity increases because of the affinity organic matter has for water Reference [9].

2. STUDY AREA

The total land area of the State is 114.84 lakh hectares, out of which the area under forest cover is 27.43 lakh hectares, constituting 23.89 percent of the geographic area. Nearly, 43.20 percent area is under cultivation (49.61 lakh hectares), 8.36 percent is Current Fallow Lands (9.60 lakh hectares), 7.79 percent Land is put to non-agricultural uses (8.95 lakh hectares), 5.36 percent is barren and uncultivable (6.15 lakh hectares)

and 6.24 percent falls under other fallows (7.17 lakh hectares). The remaining 5.16 percent is under culturable waste, permanent pastures and other grazing lands, and land under miscellaneous tree crops and groves are not included in the net area sown (5.93 lakh hectares).

Soil samples were collected from three different locations of komapally area, in Telangana state for investigation for determining the physiochemical properties and to assess the relationship between moisture content and infiltration rate.

Three Soil samples are collected from three different places with GPS technique which are shown below:

Table 1: sample collection

Maisammaguda	Latitude: 17°33'47.19" N Longitude: 78°27'19.08" E
HMT	Latitude: 17°33'48.35" N Longitude: 78°27'39.56" E
Badurpally	Latitude: 17°33'48.35" N Longitude: 78°27'39.56" E

3. MATERIALS AND METHODS

Disturbed Soil samples were collected from various locations is analyzed for different physiochemical properties.

3.1 Sampling Depth

Sample number one: to a depth of 15-30 cm

Sample number two: to the depth that of 15-30 cm

Sample number three: sample is collected at depth of 15-30 cm

3.2 Sampling Equipment

A soil-sampling probe, an auger, a spade or shovel is used for cutting the soil sample at site

Sample collection

The sample should represent the area it is taken from. A soil sample must be taken at the right time and in the right way.

3.3 Methods for Determination of properties of soil samples

3.3.1 Determination of moisture content

The moisture content was determined by drying a known weight of the soil sample in an electric oven at 105°C for about 15 minutes. The moisture bottle and the stopper is removed and placed in desiccators

3.3.2 Bulk density of soil

The soil bulk density (BD), also known as dry bulk density, is the weight of dry soil (M_{solids}) divided by the total soil volume (S_{oil}). The total soil volume is the combined volume of solids and pores which may contain air (V_{air}) or water (V_{water}), or both.

3.3.3 Specific gravity

The value of specific gravity helps up to save extent in identification and classification of soils. It gives an idea about the suitability of the soil as a construction material. Higher value of specific gravity gives more strength for roads and foundations.

3.3.4 Sieve analysis

A sieve of set of sizes 4.75, 2.36, 1.18, 0.6, 0.3, 0.15, 0.075 mm including lid and collecting pan are placed on mechanical sieve shaker. Allow to shake for ten minutes. Retained material on each pan is weighed and results are tabulated and a grain size distribution curve is drawn. Coarse grained soils are classified mainly by sieve analysis. The grain size distribution curve gives an idea regarding the gradation of the soil.

3.3.5 Liquid limit

About 120 gm. of air dried soil from thoroughly mixed portion of material passing 425 micron IS sieve is obtained. Distilled water is mixed to the soil thus obtained in a mixing disc to form uniform paste. The paste shall have a consistency that would require 30 to 35 drops of cup to cause closer of standard groove for sufficient length. A portion of the paste is placed in the cup of casagrande device and spread into portion with few strokes of spatula. It is trimmed to a depth of 1 cm. at the point of maximum thickness and excess of soil is returned to the dish. The soil in the cup is divided by the firm strokes of the grooving tool along the diameter through the centre line of the follower so that clean sharp groove of proper dimension is formed. Then the cup is dropped by turning crank at the rate of two revolutions per second until two halves of the soil cake come in contact with each other for a length of about 12 mm. by flow only. The number of blows required to cause the groove close for about 12 mm. is recorded.

3.3.6 Plastic limit

Take out 30g of air-dried soil from a thoroughly mixed sample of the soil passing through 425µm IS Sieve. Mix the soil with distilled water in an evaporating dish. Take about 8g of the soil and roll it with fingers on a glass plate. The rate of rolling should be between 80 to 90 strokes per minute to form a 3mm dia.

3.3.7 Compaction

Take a representative oven-dried sample, approximately 5 kg in the given pan. Thoroughly mix the sample with sufficient water to dampen it to approximately four to six percentage points below optimum moisture content.

3.3.8 Permeability

Water flowing through soil exerts considerable seepage forces which have direct effect on the safety of hydraulic structures. The rate of settlement of compressible clay layer under load depends on its permeability. The quantity of water escaping through and beneath and earthen dam depends on the permeability of the embankment and the foundation soils respectively. Shear strength of soils depends indirectly on its permeability, because dissipation of pore pressure is controlled by its permeability.

4. RESULTS AND DISCUSSIONS

Results are obtained from the laboratory tests conducted on the soil samples. These tests are conducted to evaluate the

Soil physiochemical properties. Chemical tests i.e., N, P, K tests are conducted at soil laboratories outside the college. Soil sample is given to laboratory technician and values of NPK are collected. Bulk density, specific

gravity, Atterburg limits, compaction, tests are conducted to find out the moisture content in the soil sample, that optimum moisture content is used in permeability test and the foundation soils respectively. Shear strength of soils depends indirectly on its permeability, because dissipation of pore pressure is controlled by its permeability.

Table: 3 Results of soil properties

For sample one: The soil which is collected from the Maisamaguda has the moisture content value 0.961

For sample two: The soil which is collected from the HMT has the moisture content value 0.90

For sample one: soil is black in colour. These soils are often associated with high levels of organic matter (peats). Soil has more water logging, low pH and high denitrification

Types of sample	Depth Cms	Physical properties	
		Color	Texture
Sample 1 (Maisammaguda)	30	Black	Clay
Sample 2 (HMT)	30	Red	Red soil
Sample 3 (Badharpally)	30	Red	Loamy sand

(variable head method) are analyzed in college laboratory are discussed in this chapter.

4.1 Soil moisture content:

Table: 2 Results of moisture content

Types of sample	Wet wt of soil (gm)	Dry wt of soil (gm)	Moisture content (%)
Sample 1 (Maisammaguda)	55	30	0.961
Sample 2 (HMT)	52	50	0.90
Sample 3 (Badharpally)	62	54	0.909

The moisture content was determined by drying a known weight of the soil sample in an electric oven at 105°C for about 15 minutes. The moisture content was calculated by the loss in weight of the soil and in weight of the soil and expressed in oven dry basis-

For sample three: The soil which is collected from the Badurpally has the moisture content value Is0.909.

Color of soil:

Discussion

For sample two: soil is Red in color. This color indicates good drainage. Iron found within the soil is oxidized more readily due to the higher oxygen content. This causes the

Types of sample	Bulk density g/cm ³	Specific gravity	Liquid limit	Plastic Limit	Compaction	Permeability
Sample 1 (Maisam maguda)	0.961	2.093	36%	83.3	11%	7.17x10 ⁻³
Sample 2 (HMT)	0.9	2.60	28%	83.3	13%	8.25x10 ⁻³
Sample 3 (Badharp ally)	0.909	2.73	28%	150	11%	-

soil to develop a 'rusty' color. The color can be darker due to organic matter. It has low plant availability of water

For sample three: soil is yellow in color. These soils often have poorer drainage than red soils. The iron compounds in these soils are in a hydrated form and therefore do not produce the 'rusty' color. It has low plant availability of water

Texture of soil

For sample one: Soils with the finest texture are called clay soils, Hence the soils texture is clay

For sample two: Soil that has a relatively even mixture of sand, silt, and clay and exhibits the properties from each separate is called a loam. Hence the soils texture is silty loam soil.

For sample three: Soils with the coarsest texture are called sands. Hence the soils texture is loamy sand soil.

Table 4 Results of soil properties

Types of sample	pH	Chemical properties		
		N	P	K
Sample 1 (Maisammaguda)		2.4	1.5	1.3
Sample 2 (HMT)		1.2	0.8	1.0
Sample 3 (Badharpally)		0.7	0.5	0.8

4.2 pH

Discussion:

For sample one: The soil which is collected from the Maisamaguda has the PH value of 6 is in between the standard value between 6-7. Soil contains alkaline this is because of using fertilizers for growing the crops

For sample two: The soil which is collected from the HMT has the PH value of 7.1 is exceeded the standard value, hence soil exceeding the ph range above 7 is alkaline soil, this soil has so because it is industrial soil

For sample three: The soil which is collected from the Badharpally has the PH value of 6.2 is in between the standard value between 6-7. Soil contains alkaline this is because of using fertilizers for growing the crops, Soil contains all types of grain sizes

Table: 5 soil characteristics

4.3 Bulk density of soil:

Discussion:

For sample one: Bulk density of the soil sample is 0.961 g/cm³ are medium due to medium coarse fraction of soils.

For sample two: Bulk density of the soil samples is 0.9 g/cm³ are lower.

For sample three: Bulk density of the soil samples is 0.909 g/cm³

4.4 Specific gravity

Discussion:

For sample one: Hence the soil sample is found as organic soil because of its specific gravity 2.093.

For sample two: Hence the soil sample is found as fine grained soil because of its specific gravity 2.73.

For sample three: Hence the soil sample is found as coarse grained soil because of its specific gravity 2.64.

4.5 Sieve analysis

For sample one: This curve represents a soil which contains the particles of different sizes in good proportion. Such soil is called a well graded or uniformly graded soil

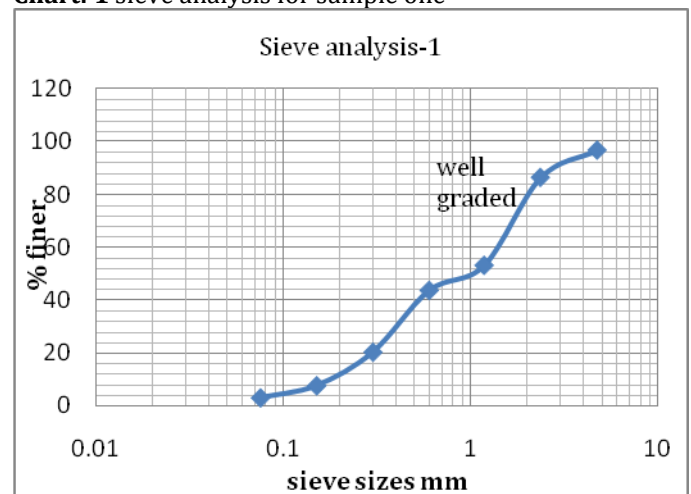
Uniformity of soil $C_u = D_{60}/D_{10}$

$C_u > 4$ gravels; $C_u > 6$ for sands; $C_u > 5$ for well graded gravel:

$C_u > 3$ for uniform soil

$C_u = 10.34$ hence soil is well graded

Chart: 1 sieve analysis for sample one



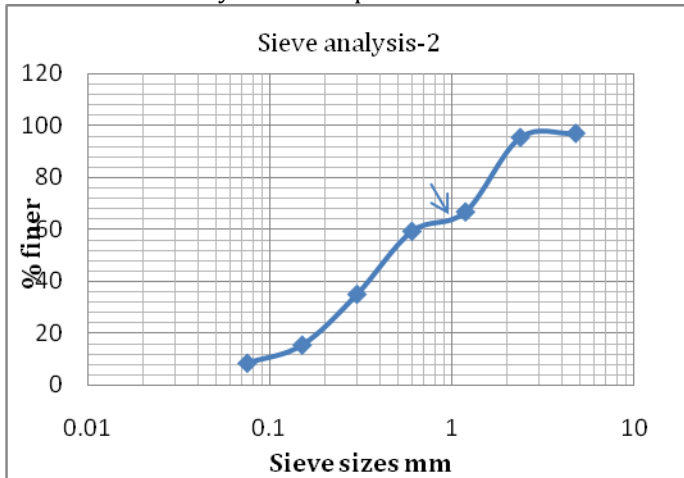
Discussion

For sample two: This curve represents a soil which contains the particles of different sizes in good proportion. Such soil is called a well graded or uniformly graded soil

Uniformity of soil $C_u = D_{60}/D_{10}$

$C_u = 7.5$ hence soil is well graded

Chart: 2 sieve analysis for sample two

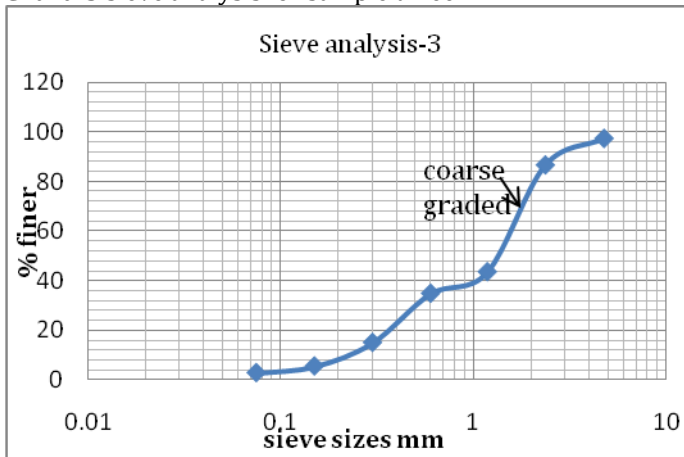


This curve represents a soil which contains the particles of different sizes in good proportion. Such soil is called a well graded or coarse graded soil

Uniformity of soil $C_u = D_{60}/D_{10}$

$C_u = 7.4$ hence soil is coarse graded

Chart: 3 sieve analysis for sample three



4.6 Liquid limit

Discussion

For sample one: The liquid limit value of soil is 36% is obtained at standard 25 blows from the graph. The value of liquid limit if in between 35-50 then soil indicates Medium compressibility soil. So the amount of water which is responsible for this state of consistency of soil is called liquid limit of soil.

For sample two: The liquid limit value of soil is 28% is obtained at standard 25 blows from the graph. The value of liquid limit if in between 0-35 then soil indicates low compressibility soil.

For sample three: The liquid limit value of soil is 28% the value of liquid limit if in between 0-35 then soil indicates low compressibility soil.

4.6 Plastic limit

Discussion

For sample one: The average plastic limit $W_p = 83.3$ for the soil sample

For sample two: The average plastic limit $W_p = 150$ for the soil sample

For sample three: The average plastic limit $W_p = 83.3$

4.7 Compaction

Discussion:

For sample one: The dry density is maximum at the optimum water content. A curve is drawn between the moisture content and the dry density to obtain the maximum dry density and the optimum water content. From the above graph the Maximum dry density: 2.45 g/cm^3 Optimum moisture content: 11% are obtained

For sample two: A curve is drawn between the moisture content and the dry density to obtain the maximum dry density and the optimum water content. From the above graph the Maximum dry density: 2.8 g/cm^3 Optimum moisture content: 7% are obtained

For sample three: A curve is drawn between the moisture content and the dry density to obtain the maximum dry density and the optimum water content. From the above graph the Maximum dry density: 2.38 g/cm^3 Optimum moisture content is 11%

4.6 Permeability

Discussion

For Sample one the coefficient of permeability $= 7.17 \times 10^{-3} \text{ mm/s}$

Soil sample having maximum water holding capacity that the water can permit easily.

The permeability test is a measure of the rate of the flow of water through soil. In this test, water is forced by a known constant pressure through a soil specimen of known dimensions and the rate of flow is determined.

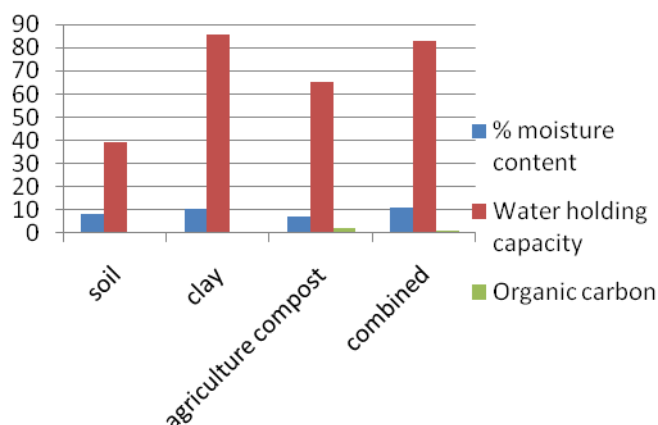
For sample two: The coefficient of permeability $= 8.12 \times 10^{-3} \text{ mm/s}$. The soil bought from HMT area is having enough water holding capacity to irrigate the crops.

For sample three: The soil of badurpally did not permit the water into it, hence to increase the soils water holding capacity Organic matter is added in percentages thus water holding capacity may increase, the main aim of the project i.e., water holding capacity may increase in the soil which gives more crop yield

4.7 RESULTS OBTAINED WHEN SOILS TREATED SOIL WITH ORGANIC MANURE AND CLAY

Table: 6 Changes in physiochemical properties of sample soil (Badurpally)

Chart: 4 showing Changes in physiochemical properties of sample soil (Badurpally)



Discussion:

The different physicochemical properties such as soil pH, percentage moisture content, water holding capacity, organic carbon, were estimated (Table 5.23). The soil moisture content was found to be increased from 8.3% in soil to 10.3, 7.2% and 10.94% in soil, clay agricultural compost (manure) and combined treatment respectively. The incorporation of organic residue also leads to reduction of evaporation of the soil water (Mandal et al., 2004). The water holding capacity in the untreated soil was very low and treated soil (combined treatment) 82.69%. The central role of soil organic carbon in maintaining soil function and plant productivity in agro-ecosystem has long been recognized. The results in the combined treatment of organic residue were extremely good in comparison to other and in untreated soil it was least.

IMPROVEMENT TECHNIQUE ADOPTED FOR WATER RETENTION CAPACITY IN SOIL COLLECTED IN BADHURAPALLY AREA

From the above Results and Discussion it is has revealed that the soil sample collected in Badurpally has very less Water retention and Water holding capacity ,it has varied soil structure and it has very least permeability factor. As permeability factor is very important factor for conduction of water in soils and this property helps in water holding and water retention capacity in soils. And this water which is available is very important for plant growth.

To Rectification this soil from all the above deficiencies, we have adopted an improvement technique for water holding capacity in soil and this technique also improves the binding nature.

Table: 6 Changes in physiochemical properties of sample soil (Badurpally)

Physiochemical properties	Soil	Clay	Agriculture compost (manure)	Combined
Soil pH	6.2	7.1	6.5	7.0
% moisture content	8.3	10.3	7.2	10.94
Water holding capacity	39.25	85.5	65.3	82.69
Organic carbon	0.52	0.63	2.1	1.28
% Mix	1Kg	2%	2%	2:2
Coefficient of permeability at T_k	7.17×10^{-3}	8.12×10^{-3}	8.25×10^{-3}	8.65×10^{-3}

Experiment has been conducted by adding different proportions of clay and manure equally to the soil sample and water holding and enrich of fertility has been analyzed.

5. CONCLUSION

The present study with respect to reclaiming the Badhurpally soil sample soil by using the organic manure and clay shows increase in water holding capacity and also shows improves characteristics of fertility. And after the treatment it increased. Through this experiment it is clear that the incorporation of waste organic residues in Badhurpally soil can convert it into a fertile soil as these treatments were able to increase the range of all the required nutrients and were also successful to fulfill the physical, chemical and biological requirements needed in a healthy soil.

Organic matter behaves somewhat like a sponge, with the ability to absorb and hold up to 90 percent of its weight in water. A great advantage of the water-holding capacity of organic matter is that the matter will release most of the water that it absorbs to plants. In contrast, clay holds great quantities of water, but much of it is unavailable to plants.

Thus a good supply of soil organic matter is beneficial in crop or forage production. Consider the benefits of this valuable resource and how you can manage your operation to build, or at least maintain, the organic matter in your soil. Of all the components of soil, organic matter is probably the most important and most misunderstood. Organic matter serves as a reservoir of nutrients and water in the soil, aids

in reducing compaction and surface crusting, and increases water infiltration into the soil.

REFERENCES

Vega Dhrmana, A, and Jashothan,J. *Nat. Prod. Plant Resour.*, 2012, 2012 Effect of organic fertilizers on the water holding capacity of the soils in different terrians. 2 (4):500-503.

Mbah C.N., Nenneji R.K. 2010 Effect of different crop residues management techniques on selected soil properties and grain production Vol. 6(17), pp. 4149-4152, 5 September, 2011

Hedley, C,B And Yule, I,J, 2009 Soil water status mapping and two variable rate irrigation, Volume 10, Issue 4, pp 342-355

Seenarious. Lawes, R.A 2009 Integrating effects of climate and plant available soil water holding capacity. Volume 113, Issue 3, Pages 297–305

Reynolds, W.D. and Top 2008 soil water analysis, principles and parameters soil samples and methods of analysis

Kemka, H.O, Rebecca, 2007 Influence of temperature and pH bio resource and protein bio synthesis.

Litter M.M, 2006 Nutrient manipulation methods are coral reef studies. *Journal of Experimental Marine Biology and Ecology*. Volume 336, Issue 2, 5 September 2006, Pages 242–253

Grace, Chart, M, 2006 laboratory manual of the soil microbial biomass group.

Das T.H. Sarkar etal. 2005 Water retention characteristics of some typical soil

Singh R. and Kundu D.K., 2005 Prediction of profile water storage capacity for major soil groups. Volume 36: issue: 3 pages 169-171

Iyenger,S.R, Bhav, 2005 composting of house hold waste.

Havlin, J.L., S.L. Tisdale, 2005 Soil fertility and fertilizer.

Board, N. 2004 the complete Technology Book on *Biofertilizer and organic Farming*, New Delhi

Mishra upasana, 2004 A potential bio fertilizer for crops.

Malik F.R, Ahmeds. Riziki Y.M, 2001 Utilization of lignocellulosic waste for the preparation of nitrogenous fertilizer.

Martens Dean, 2000A Plant residue bio chemistry regulates soil carbon cycling and carbon sequestration.

Adetunji MT (1997). Organic residue management, soil nutrient changes and maize yield on a humid Ultisol. *Nutr.Cycl. Agro Ecosyst*, 47: 181-188

Plaster, E. J. 1996. *Soil Science and Management*. 3rd ed. Albany: Delmar Publishers,

Maheshwari BL etal 1992 Infiltration characteristics of some clayey soil measured during boarder irrigation *Agricultural Water Management* Volume 21, Issue 4, September 1992, Pages 265-279



ChemTech

International Journal of ChemTech Research

CODEN (USA): IJCRGG, ISSN: 0974-4290, ISSN(Online):2455-9555
Vol.9, No.05 pp 558-562, 2016

Corrosion Inhibition Using Water Hyacinth

B.Subramanyam and R.Prasanna Kumar*

School of Civil Engineering.SASTRA University, Thanjavur -613401, India.

Abstract : Corrosion can also occur in materials other than metals, such as ceramics or polymers, and it degrades the useful properties of materials and structures including strength, appearance and permeability to liquids and gases. Corrosion from civil engineering point of view is wearing of metals due to chemical changes. Due to the gradual wearing away of material, the resistance capacity of materials decreases. In many structures the effects of corrosion are seen clearly. In case of offshore structures this effect is predominant. The adverse effects of corrosion increase with the increase in number of days of exposure of materials to the environment. Generally these effects of corrosion are controlled by painting, plating, galvanization, anodization, bio-film coatings, etc. In the present work an attempt was made to study the corrosion inhibition property by using a material called water hyacinth.

Key words: Water Hyacinth, Multimeter, Weight loss method, Inhibition efficiency, resistance.

Introduction

Corrosion of steel is a predominant phenomenon in many structures and more specifically in offshore structures. Due to this there is a rapid deterioration of materials and development of cracks in the structures, ultimately affecting the stability of the structures. The popular cases are bridges, buildings etc. which have been affected by corrosion due to the sea water environment. This sea water environment may be either a direct contact with the surface of the structures or with the medium of air and water to corrode the structures. The main reason for corrosion⁷⁻²⁰ is that the steel bars which we use as reinforcement is made of iron or steel. These easily react with the sea water and form iron oxides that cause a gradual deterioration of materials and eventually leading to loss of strength. In the present study it is proposed to use water hyacinth plant powder mixed with water as an alternative to various conventional anti corrosion coatings.

Objectives of the Study

To study the effect of water hyacinth plant powder in resisting corrosion.

To compare the changes taking place in steel bars by using this material as an alternative to conventional anti corrosion coatings.

Review of Literature

A study was conducted to understand the inhibitive effect of an aqueous extract of naval leaves¹ on the corrosion of carbon steel in dam water using weight loss method. It was found from the results obtained from this method that there is an increase in inhibition efficiency with increasing inhibitor concentration to a particular extent and then it decreases. Another study was conducted² by making use of natural products as corrosion inhibitors for metals and found that these compounds come out as effective inhibitors of corrosion in

the years to come because of their biodegradability, easy availability and non-toxic nature. The corrosion inhibition characteristics of water hyacinth extract of varying concentrations was studied³ on 1014 steel in a chloride environment and found that there was considerable reduction in the metallic ions in the elemental composition of water hyacinth after thirty days. The effect of naturally occurring Emilia Sonchifolia was investigated⁴ as a corrosion inhibitor for mild steel by using gravimetric measurements at different temperatures and observed that corrosion rate was retarding.

Experimental Study

Materials used in this study are Water hyacinth plant, Steel bars of 12 mm diameter and sea water. The characteristics of sea water were presented in Table 1 below. After collecting these materials the plant was dried for seven days and crushed into powder and then mixed with water in different concentrations. The mixture was then coated over the steel bar of 8 mm diameter uniformly and a standard electrode and testing bar was placed inside the sea water sample. The resistance is measured using the multimeter instrument and weight loss using a digital balance.

Table 1: Characteristics of Sea Water (Nagapattinam, Tamil Nadu, India)

Parameters	Result
pH	7.91
Total dissolved salts(mg/l)	41881
Total Hardness (CaCO ₃ equivalent)(mg/l)	6099
Chloride as Cl (mg/L)	19353
Potassium as K (mg/L)	1323
Sulphate as SO ₄ (mg/L)	1542
Electrical conductivity (micro mhos/cm)	60998

Measuring Resistance Using Multimeter

In this method resistance of the metals was found with standard electrode. It was found that the resistance of uncoated metals keeps on decreasing but in case of coated metals; the resistances first keep increasing to some extent, till the coated material sticks with the bar. But after it loses its sticking property with the metal then the material/ metal loses its resistance and keep decreasing. This was shown in a graph, where in the graph is plotted with time in x- axis and resistance in y-axis. For uncoated bar, the graph decreases and moves downwards but in coated bar, the graph keeps increasing to some extent and forms a heap like shape. From this the corrosion rate happening in the steel bars under different corrosive environment can be understood. Resolution is also related with sensitivity of multimeter. Greater is the sensitivity higher is the resolution. It has one more advantage: it has very high input resistance. The main part of most of the Digital Multi Meter (DMMs) is the analog to digital converter (A/D) which converts an analog input signal into a digital output. While specifications may vary, virtually such multimeters were developed around the same block diagram.

Visual Observation

From the name implies, through visual observation the happenings are judged. In this method, the two metals are placed in sea water having same concentration, one with coating and other with plain surface. It was found that the coated bar dint have any bubbles sticking around the surface of the bars. But in the uncoated bar, reddish brown bubbles were sticking to the surface and also the ribs were turned into red color even after the bar has been taken out from the sea water environment, which reveals that uncoated bar cannot withstand if sea water concentration is more.

The readings obtained from weight loss method were presented in the following Table 2 below.

Table 2 Data for mild Steel bar immersed in sea water with hyacinth extracts

Exposure Time (Days)	Weight (g)	Weight Loss (g)	Cumulative Weight loss(g)	Corrosion rate (mm/yr)	Inhibitor Efficiency (%)
0	189.675	-			
7	188.922	0.753	0.753	0.039	27.10
13	188.592	0.330	1.083	0.009	84.69
21	188.364	0.226	1.311	0.003	92.20
30	188.233	0.131	1.442	0.001	96.05

These readings were taken on the 13th day of the observation. Both the coated and uncoated bar were having the same dimensions including the weight. But on 13th day the increase in the decrease of the weight of the uncoated bar is more, while the coated bar is just slowly starting to lose its weight. These were the observations made on the bars while working out the process

Inhibition Efficiency (IE)

The corrosion IE was then calculated using the equation.

$$IE^5 = 100 [1 - (W_2/W_1)] \%, \text{----- (1)}$$

Where W_1 is the weight loss value in the absence of inhibitor, W_2 is the weight loss value in the presence of inhibitor, Corrosion rate was calculated using the formula ,

$$\text{Corrosion rate}^6 (\text{mm/year}) = 87.6 W / DAT \text{----- (2)}$$

Where W = weight loss in milligram, D = density of specimen g/cm^3 , A = area of specimen in square cm, T =exposure time in hours.

Since the rate of corrosion is more for uncoated which means that uncoated bar will easily fail due corrosion. The resistance values coated and uncoated bars were presented in Table 3 below.

Table 3: Resistance Values of Coated and Uncoated Steel bars

Day	Resistance in 20 K	Resistance in 20 K
1	3.1	3.1
2	3.1	3.4
3	3.1	3.5
4	3	3.7
5	3	3.8
6	3	4
7	3	4.2
8	2.9	4.3
9	2.9	4.6
10	2.8	4.8
11	2.8	5
12	2.7	5.1
13	2.7	5.3
14	2.6	5.5
15	2.5	5.6
16	2.4	5.9
17	2.3	6.1
18	2.1	6.3
19	1.8	6.5
20	1.5	6.6
21	1.1	6.7

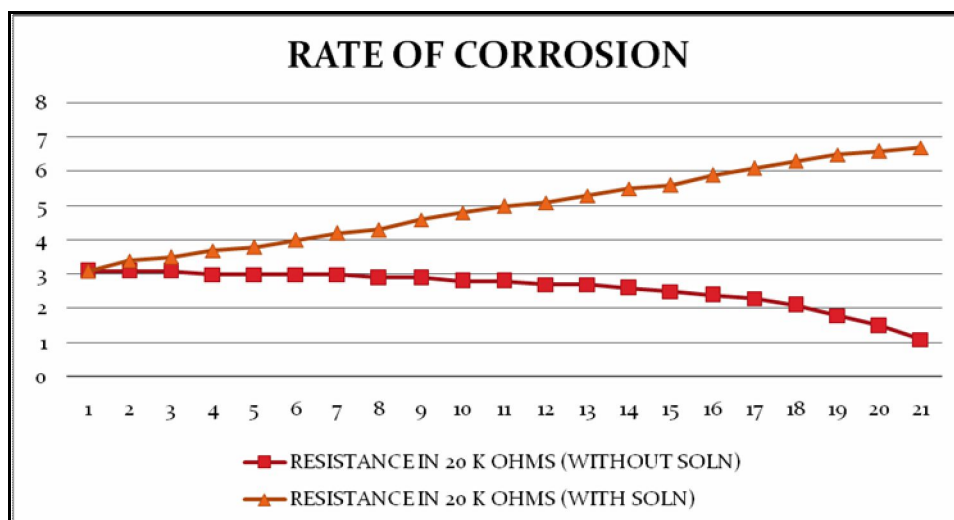


Fig 1 Resistance vs Rate of corrosion

Discussion of Test Results

From the results obtained from digital balance, it can be said that the uncoated bar has been exposed to a larger amount of the concentration of the sea water in any medium. So the weight initially decreases lightly and after that it starts decreasing more and more until the bar got completely corroded. The bar which was coated and also exposed to the larger amount of the concentration of the sea water doesn't lose its weight like the uncoated bar. Its weight decreased slightly throughout the observation period.

From the multi meter readings it can be observed that the uncoated bar's resistance is decreasing more and more due to which it may completely fail. This failure may cause the whole structure to fail. But in the coated bar, the resistance is increasing drastically initially and after some days its incremental increase in resistance is decreasing. So from the Fig 1 also, it can be understood that the coated bar keep on increasing or increases up to a point and can decrease afterwards. This may happen. There may be this critical point. So this can be of more help in the increasing the life of the structure. From the Visual method it was observed that the bubbles were coming from the uncoated bar. This means that the uncoated bar is getting corroded and is forming cracks in between. This causes the formation of bubbles as the sea water enters the bar. While in the coated bar, the water hyacinth solution is protecting the bar as a layer and is preventing the bar from corrosion. There is no/less anode mud formed when compared to the uncoated bar.

Conclusion

From the results of the experiments conducted and from visual observations it can be concluded that the material water hyacinth is a cheap, highly efficient, eco-friendly and anti corrosive. Since the resistance values of coated bars were increasing, this material will be very much useful in reducing corrosion of reinforcement.

References

1. Abdulrahman, A.S. and Mohammad, I. (2011). Eco-friendly green inhibitor to improve the strength of concrete contaminated by chloride and sulphate, IJRRAS, 9(3), 355 – 360.
2. Raja, P. B. and Sethuraman, M. G. (2008). Natural products as corrosion inhibitor for metals in corrosive media – A review' Materials letters, 62(1), 113-116.
3. Oloruntoba, D.T. (2013). Corrosion Inhibition of Water Hyacinth on 1014 Steel in a Chloride Environment, Cjasr, 2(2), 6-16. Available online at <http://www.cjasr.com>.
4. Shanab, S. M. M. and Shalaby, E. A. (2012). Biological activities and anticorrosion efficiency of water hyacinth (*Eichhornia crassipes*). Journal of Medicinal Plants Research, 6(23), 3950-3962.
5. Wranglen G., Synergistic effect of 2-chloroethyl phosphonic acid and Zn²⁺ Introduction to Corrosion and protection of Metals (Chapman & Hall, London) 236 (1985).

6. Fontana Mars G., Corrosion Engineering, TATA McGrawHill publishing company Limited, New Delhi, Third edition, 171 (2006).
7. Mary Anbarasi C and Jerli Auxilia A, Surface Modification of Carbon Steel by Hexanesulphonic Acid- Ni^{2+} System and its Corrosion Study, International Journal of ChemTech Research,2016, Vol.9, No.01 pp 218-225.
8. P.R.Thyla, N. Tiruvenkadam, M. Senthil Kumar; Investigation of Corrosion Behavior of Light Weight NanoHybrid Al 6061-ZrO₂ -SiC- Gr Composites; International Journal of ChemTech Research;
9. Sravani Pappu, Vamsi Kamal, M. K. Mohan; Effect of Heat Treatment on the Electrochemical Corrosion Behavior of Ti- 15 V- 3 Al- 3 Cr- 3 Sn Alloy in HCl and NaCl Media; International Journal of ChemTech Research;2015, Vol.8, No.1, pp 155-163.
10. G. Kavitha, S. Jegannathan, and C. Vedhi; Inhibition of corrosion of mild steel in sulphuric acid by 2-Picoline N-Oxide and 4-Picoline N-Oxide; 2015, Vol.7, No.4, pp 1693-1701.
11. S.Karthikeyan, P.A.Jeeva; Hydrogen permeation analysis of corrosion of stainless steel in pickling solution; International Journal of ChemTech Research;2015, Vol.8, No.7, pp 335-339.
12. Ashish Kumar, Sumayah Bashir; Review on Corrosion inhibition of Steel in Acidic media; International Journal of ChemTech Research;2015, Vol.8, No.7, pp 391-396.
13. Charitha B.P., and Padmalatha Rao; Ecofriendly biopolymer as green inhibitor for corrosion control of 6061-aluminium alloy in hydrochloric acid medium; International Journal of ChemTech Research;2015, Vol.8, No.11 pp 330-342.
15. V.Saravanan, P.R. Thyla, N. Nirmal, S.R. Balakrishnan; Corrosion Behavior of Cenosphere - Aluminium Metal Matrix Composite in Seawater Condition; International Journal of ChemTech Research;2015, Vol.8, No.2, pp 726-731.
16. J. Yamuna, Noreen Anthony; Corrosion Protection of Carbon Steel in Neutral Medium using Citrus medica [CM] leaf as an Inhibitor; International Journal of ChemTech Research;2015, Vol.8, No.7, pp 318-325.
17. S.Karthikeyan, M.Anthony Xavier, P.A.Jeeva, K.Raja; A green approach on the corrosion studies of Al-SiC composites in Sea water; International Journal of ChemTech Research;2015, Vol.8, No.3, pp 1109-1113.
18. A.V.Balan, T.Kannan; Effect Of Heat Input On Pitting Corrosion Resistance Of Super Duplex Stainless Steel Weld Claddings; International Journal of ChemTech Research;2016, Vol.9, No.03 pp 358-362.
19. M. Gnanasekaran, A. Kumaravel, S. Jerome; Effect of oxide layer and activating flux on corrosion behavior of TIG welding of 304 austenitic stainless steel weldments; International Journal of ChemTech Research;2016, Vol.9, No.04 pp 350-356.
20. R. Ganapathi Sundaram, and M. Sundaravadivelu; Electrochemical and Surface Investigation of Quinoline-8-sulphonyl chloride as Corrosion Inhibitor for Mild Steel in Acidic Medium; International Journal of ChemTech Research;2016, Vol.9, No.03 pp 527-539.
21. Mary Anbarasi C and Jerli Auxilia A; Surface Modification of Carbon Steel by Hexanesulphonic Acid- Ni^{2+} System and its Corrosion Study; International Journal of ChemTech Research;2016, Vol.9, No.01 pp 218-225.

Settlement Analysis of Piled Raft Foundation System (PRFS) in Soft Clay

SrinivasaReddy Ayuluri¹, B. Vamsi Krishna², D. Sidhu Ramulu³

¹(PG Scholar, Civil Engineering Department, MallaReddy Engineering College, Hyderabad, Telangana, India)

²(Assistant Professor, Civil Engineering Department, MallaReddy Engineering College, Hyderabad, Telangana, India)

³(Assistant Professor, Civil Engineering Department, Gokaraju Rangaraju Institute of Engineering & Technology, Hyderabad, Telangana, India)

Abstract : The piled raft foundation allows the high load bearing capacity and reduces the settlements in soils at very economic way as compared with the conventional foundation designs. This paper presents combinations of 3-D numerical analysis (by Plaxis 3D Foundation v 1.1) of piled raft foundation on clayey soil to investigate the behaviour of piled raft system in soils under different loading conditions. The settlement was measured at the centre of the models of pile raft with (single, two, three & four) piles. Finally, the behaviour of piled raft foundation w.r.t effect of number of piles, spacing between piles, elastic of modulus and raft size on the load carrying capacity of piled raft foundation system (PRFS) are assessed and conclusions are made.

Keywords: Plaxis 3D Foundation, Pile raft foundation System (PRFS), Settlements, Soil.

I. Introduction

To carry the excessive loads that come from the superstructures like high-rise buildings, bridges, power plants or other civil structures and to prevent excessive settlements, piled foundations have been developed and widely used in recent decades. However, it is observed that the design of foundations considering only pile or raft is not a feasible solution because of the load sharing mechanism of the pile-raft-soil. Therefore, the combination of two separate systems, namely “Piled Raft Foundation systems” has been developed (Clancy and Randolph (1993)) [1].

Piled raft foundation system is verified to be an economical foundation type comparing the conventional piled foundations, where, only piles are used for the reducing both total and differential settlements and the contribution of the raft is generally disregarded.

In this study, behavior of the piled raft foundation systems under axial loads has been investigated by comparing the traditional design approaches and the current design approaches by parametric analyses. In the literature, there are plenty of researches focusing of these parameters, like; the number of piles, length of piles, diameter of piles, pile spacing ratio, location of piles, stiffness of piles, distribution of load, level of load, raft thickness, raft dimensions and type of soil. However, through these parameters, the number of piles, length of piles and level of load are emphasized in this study. Effects of these parameters are discussed with the solutions of finite element models. To this end, parametric analyses are conducted via the software Plaxis 3D and compared with the experimental results done by (Mr. Mudhafar Kareem Hameedi) – Thesis, experimental and theoretical for piled raft foundation system in soft clay (2011) [2].

1.1 Aim of the Thesis:

This study aims to describe and clarify the load sharing mechanism between the un-piled & of piled raft foundation systems (PRFS) by considering the ratio of raft /pile load sharing under variable conditions (load levels, pile lengths, spacing and number of piles). The finite element method through Plaxis 3D Foundation software is adopted to evaluate the effect of parameter on the load-settlement behaviour of the PRFS and compared with the available experimental results. This parameter is the scale factor effect on the load-settlement behaviour of PRFS.

II. Literature Review

2.1 Introduction

In the design of foundations, shallow foundation is the first option where the top soil has sufficient bearing strength to carry the superstructure load without any significant total and differential settlements to prevent damage of infrastructure and superstructure. However, in the last decades the need for high-rise buildings and high-loaded superstructures has been increased rapidly, even in the lands with poor subsoil conditions. Therefore, the need for foundations with high bearing capacity and showing low settlement values,

both total and differential, has also been increased. These types of foundations can be constructed as a shallow foundation after the application of ground improvement techniques or as a piled foundation which transfers the excessive load to a deeper and stiffer stratum through the piles and reduces the settlements.

This chapter presents a brief review of previous researches on piles, rafts, pile groups and piled raft foundations. However, the main attention is on design methods and analyses of piled raft foundations. Chapter may be outlined as;

- a. Single Piles
- b. Pile Groups
- c. Raft Foundations
- d. Piled Raft Foundations
- e. Finite Element Programs: Plaxis 3D

2.2 Piled Raft Foundations

Piled raft foundations are the composite structures which consist of three elements; piles, raft and the subsoil. Applied loads are transferred to the subsoil both through the raft and the piles. This load transfer mechanism can be simply shown in Fig. 1. Load sharing between raft and piles is the main distinctive feature that diversifies this type of foundation from other type of piled foundations' design.

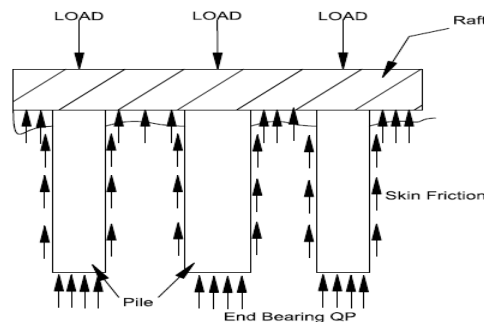


Fig.1. Simplified load transfer mechanism of piled raft foundation.

Randolph (1994) has presented three design approaches for the piled raft foundations in his state-of-the-art report as:

1. The Conventional Approach: Piles are designed to carry the majority of the load.
2. Differential Settlement Control: Piles are located in order to reduce the differential settlement, rather than the overall average settlement.
3. Creep Piling: Piles are designed to operate at a working load (70-80% of the ultimate capacity) at which significant creep occurs.

In conventional design approach, loads are assumed to be carried only by the piles or by the raft. However, in the design of piled raft foundations, the load sharing between piles and the raft is taken into account. Naturally, this load sharing improves the underestimated load capacity of the foundation comparing with the conventional approach, considering the properties of the piles and the raft remain unchanged. In addition, the piles may be used to control the settlement rather than carry the entire load in the piled rafts. Tan and Chow (2004) [3] illustrated the usage benefit of piles and raft together in the design of foundations in Fig. 2.

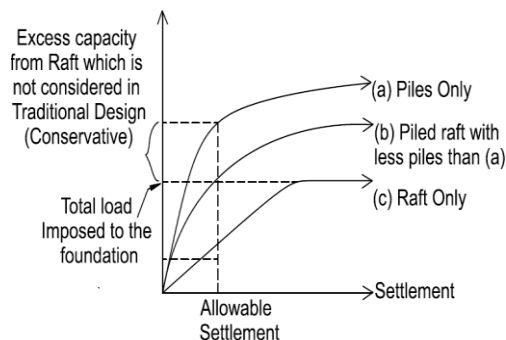


Fig.2. Concept of piled raft (Tan and Chow, 2004) [3]

III. Methodology

3.1 Finite Element Program: Plaxis 3D

Plaxis is a company based in the Netherlands, developing software under the same brand name; Plaxis. The Plaxis 3D program is a three-dimensional finite element program used to make deformation and stability analysis for various types of geotechnical applications (Reference Manual, Plaxis). The user interface of the Plaxis 3D consists of two sub-programs as Input and Output. Properties of soil and other elements (boreholes, embedded piles, plates etc.) are assigned to the elements by using material data sets by the Input interface. The basic soil elements of the 3D finite element mesh are the 10-node tetrahedral elements (Fig. 3).

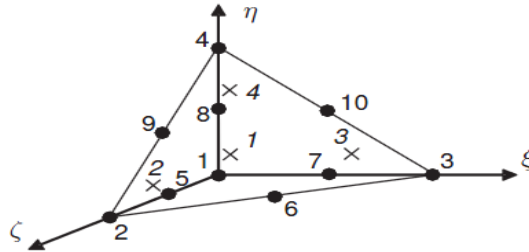


Fig.3. 3D soil elements (10-node tetrahedrons) zone (Reference Manual, Plaxis)

3.2 Modeling of Pile Raft

The model of pile raft foundation with different configurations has been done by considering the raft (steel plate) and the pile is of concrete and with constant diameter and length.

Table I: Properties of Pile & Raft

S. No	Material	Properties	Value	Raft Thickness (cm)
1	Raft (Steel Plate)	Elastic Modulus, E^* (kN/m ²)	2×10^8	1.2
		Poisson's Ratio, ν^*	0.33	0.6
2	Pile (Concrete Pile)	Elastic Modulus, E^{**} (kN/m ²)	2.9×10^5	
		Poisson's Ratio, ν^*	0.15	

The properties values of the pile and raft (Table 1), given by *Bowles (1997) [4] and **Mudhafar Kareem (2011) [2], are used.

Table II: Material properties and pile model used for the numerical model.

Material Properties	Type of Layer	Unsaturated & saturated Unit (kN/m ³)	Elastic Modulus, E (kN/m ²)	Poisson's Ratio, ν	Undrained cohesion, C_u	Angle of Shearing Resistance, ϕ (°)
	Soft Clay	18.6	15000	0.35	25	0
Pile Model	Pile Diameter, D_p (cm)	Pile length, L (cm)	Raft size, $L_r \times B_r$ (cm)	L/D_p	L/B_r	Spacing (cm)
	1.0	40	6 x 6	16	6.67	7.5 cm
	2.5	40	15 x 15	16	2.67	

The embedment length ration $L/D_p = 16$, the spacing between piles are kept constant about 3 times the diameter of pile for large and small scale models. Table (1) shows the material parameters of the raft and pile.

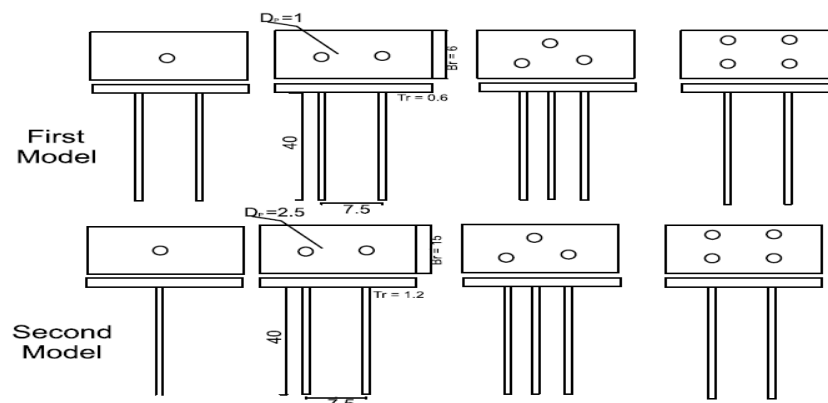


Fig. 4 Models of Piled raft for Numerical Analysis

3.3 PLAXIS 3D Foundation Program

The computer oriented finite element method has become one of the most powerful tools in the analyses of engineering problems. In the present work, the PLAXIS Structural Static Analysis has been adopted for numerical modeling of the structural response.

PLAXIS 3D Foundation is finite element analysis software. The flexibility, capabilities, and options have been developed over many years, at the request of a worldwide user community, such that the PLAXIS program can be applied to a wide variety of engineering applications.

There are two types of structural analyses in the PLAXIS family of products, which are explained below (Vermeer and Brinkgreve, 2004) [5]: 1. Static Analysis: It is used to determine displacements, stresses effect under static loading conditions. Linear and non-linear static analyses. Nonlinearities can include plasticity, stress stiffening, large deflection, large strain, hyper elasticity, contact surface and creep. 2. Modal Analysis: It is used to calculate the natural frequencies and mode shapes of structure. Different mode extraction methods are available. Finite Element Mesh When the full geometry model has been defined and all geometry components have their initial properties, the finite element mesh can be generated. From the geometry model, a 2D mesh is generated first. The basic soil elements used for 2D and 3D finite element mesh are the 15-node wedge elements. These elements are generated from the 6-node triangular elements. The accuracy of the 15-node wedge element and the compatible structural elements are comparable with the 6-node triangular element and compatibles in a 2D PLAXIS analysis. Higher order element types, for example comparable with the 15-node triangle in a 2D analysis, are not considered for a 3D foundation analysis because this will lead to large memory consumption and unacceptable calculation times (Vermeer and Brinkgreve, 2004) [5].

After reviewing the results of the analysis (Fig. 6), it can be concluded that the results obtained from the experimental study and theoretical study are close indicating that PLAXIS results are accurate and can be adopted practically. Besides, the program is specified for geotechnical Engineering. The models which are performed by the finite element program with different configuration of piles are shown in Fig. 4. Six models are analyzed by the finite element program, these are:

- a. Raft with single pile.
- b. Raft with two piles (2×1).
- c. Raft with three piles (triangular shape).
- d. Raft with four piles (2×2).

The soil is modeled as elastic-perfectly plastic solid. One layer of soft clay is used. The material properties and pile model for the numerical model are shown in Table - II. Material Model The solution theory is based on the material. Material model is described by a set of mathematical equations that give a relationship between stress and strain. Material models are often expressed in a form in which infinitesimal increments of stress (or 'stress rates') are related to infinitesimal increments of strain (or 'strain rates'). All material models implemented in PLAXIS are based on a relationship between the effective stress rates σ' , and the strain rates ϵ . The program can account for three types of material model (Vermeer and Brinkgreve, 2004) [5]: 1. The Mohr-Coulomb model (Elastic-perfectly plastic). 2. The hardening-soil model (Isotropic hardening). 3. Linear and non-linear behavior models for structural elements. The Mohr-Coulomb Model Plasticity is associated with the development of irreversible strains. In order to evaluate whether or not plasticity occurs in a calculation, a yield function, f , is introduced as a function of stress and strain. A yield function can often be presented as a surface in principal stress space. A perfectly plastic model is a constitutive model with a fixed yield surface, i.e. a yield surface that is fully defined by model parameters and not affected by (plastic) straining. For stress states represented by points within the yield surface, the behavior is purely elastic and all strains are reversible (Vermeer and Brinkgreve, 2004) [5].

This classical form of the theory is referred to as associated plasticity. For Mohr-Coulomb yield functions, the theory of the associated plasticity overestimates dilatancy. The Mohr-Coulomb model requires a total of five parameters, which are generally familiar to most geotechnical engineers and which can be obtained from basic tests on soil samples. These parameters are: Young's modulus, E (15000 kN/m²); Poisson's ratio, ν (0.35); friction angle, (0°) ; cohesion, C (25 kN/m²); and dilatancy angle, ψ (0°).

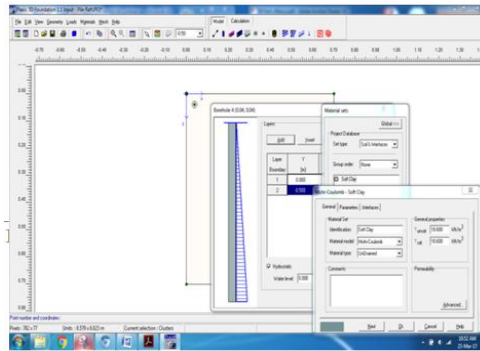


Fig. 5 Bore log data Modelled

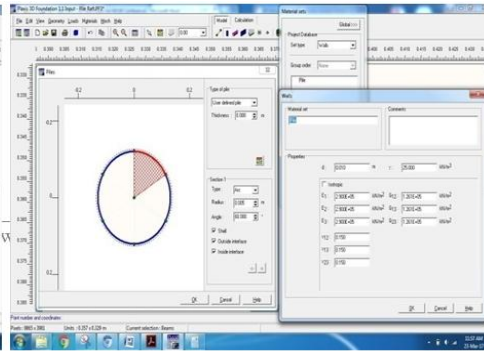


Fig. 6 Massive circular pile properties

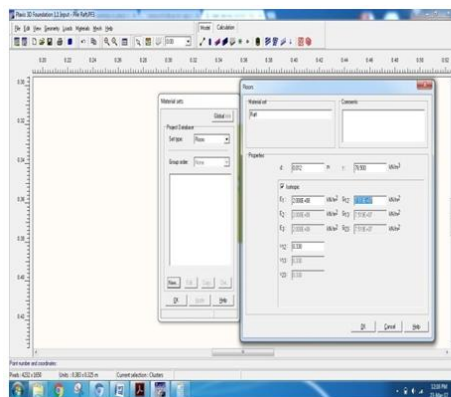


Fig. 7 Raft properties

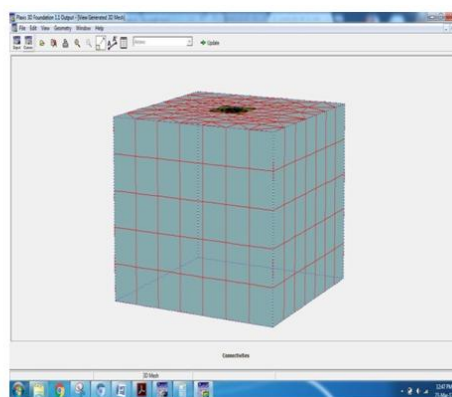


Fig. 8 Generated 3D Mesh

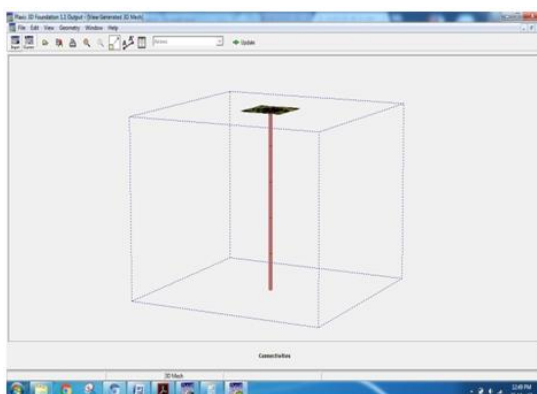


Fig.9 Single piled Raft Model

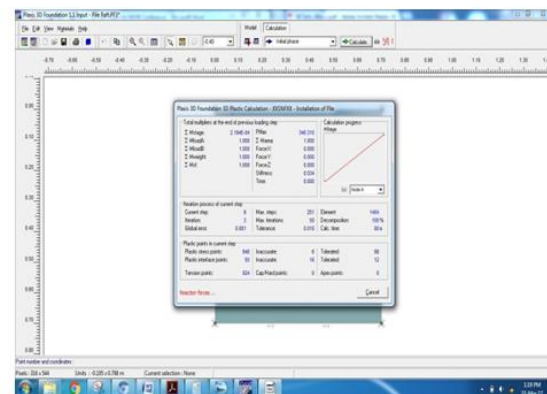


Fig.10 Calculation Phases

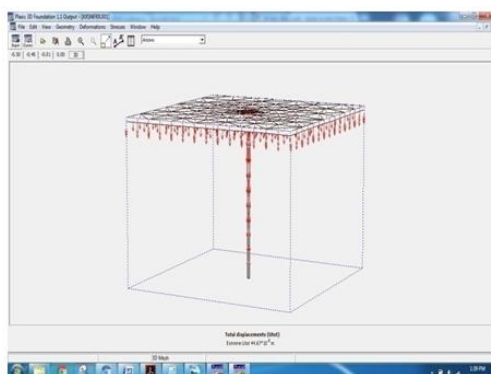


Fig.11 Total Displacement (U_{tot})

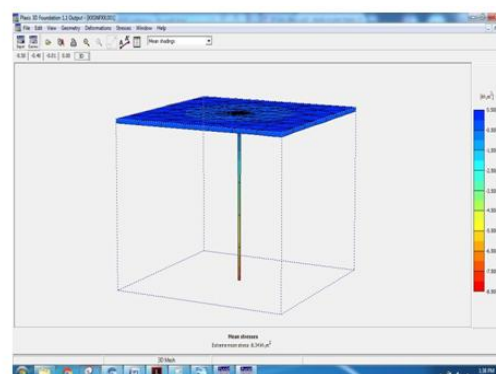


Fig.12 Mean stress for single piled raft foundation

IV. RESULTS AND DISCUSSION

One of the most challenging problems in soil-structure interaction is the piled raft. Piled-raft foundations have proved to be a viable alternative to conventional pile foundations or mat foundations. The load carrying capacity for the numerical model of one layer of soft clay, the settlement is plotted with the vertical applied load. Fig. 13 to 16 shows the load-settlement behavior of piled rafts of the same size of (15 cm × 15 cm) and thickness 1.2 cm as well as the load carried on piled raft with 1, 2, 3 and 4. The aforementioned Fig. 13 to 16 shows that the shape of load settlement indicates the local shear failures which are controlled. In addition, it is found that the tangent proposal can be adopted in specifying the ultimate piled raft capacity.

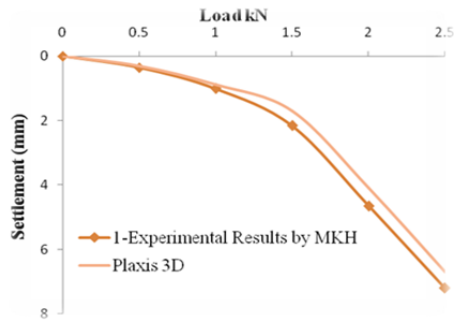


Fig.13. Load-Settlement Curve for Single Piled raft.

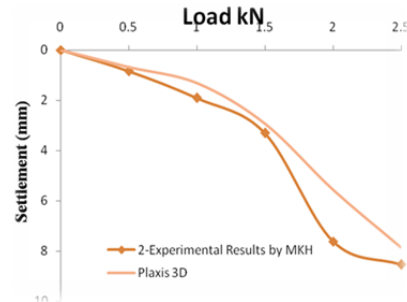


Fig.14. Load-Settlement Curve for two Piled raft.

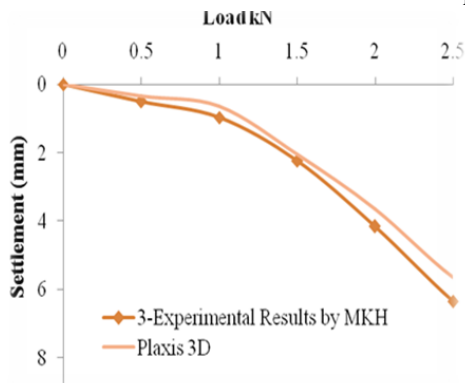


Fig.15. Load-Settlement Curve for three Piled raft.

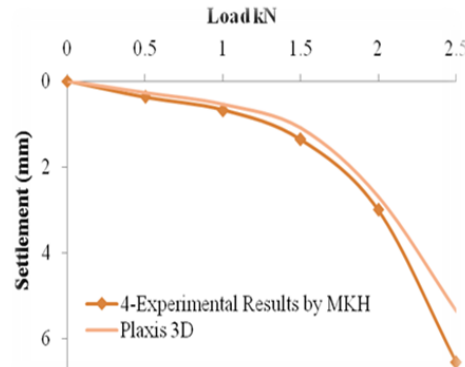


Fig.16. Load-Settlement Curve for four Piled raft.

Fig. 17 to 20 shows the load – settlement behaviour of piled rafts of the second model. The raft size is (6 cm x 6 cm) and thickness of 0.6 cm as well as the load is carried on these configurations of the model. The pile diameter is (1 cm) and length 16 cm with ratio $L/D_p = 16$.

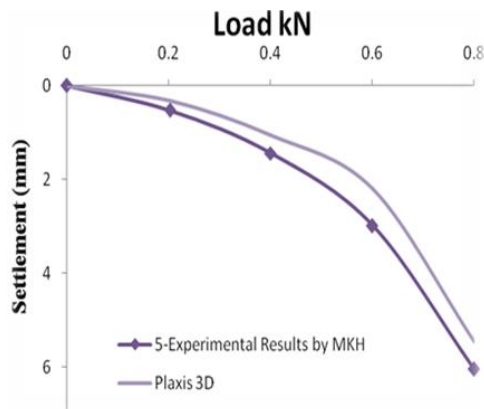


Fig.17. Load-Settlement Curve for Single Piled raft.

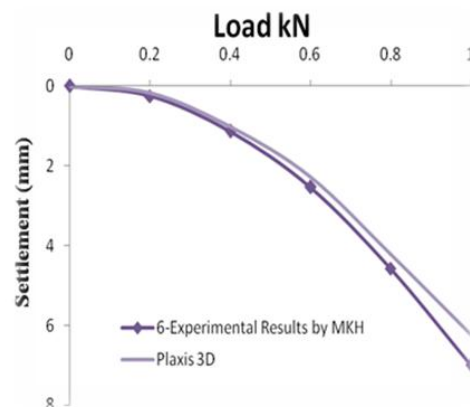


Fig.18. Load-Settlement Curve for two Piled raft.

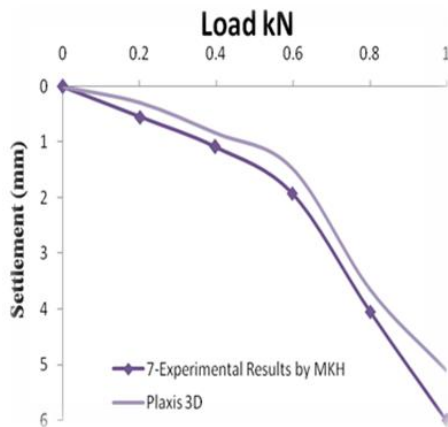


Fig.19. Load–Settlement Curve for Three Piled raft.

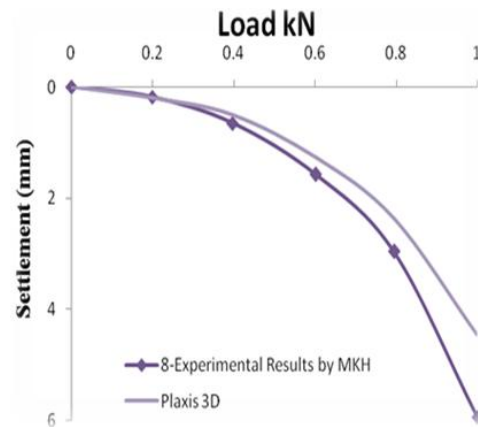


Fig.20. Load–Settlement Curve for four Piled raft.

V. Conclusion

This paper summarizes the comparison between two models of the experimental work; it is found that the effect of scale factor on load carrying capacity of piled raft increases when increasing number of piles. The numerical modeling of the piled raft problem considering the load effect using the finite element method through the program PLAXIS reveals the following conclusions:

1. The load bearing capacity of piled raft increases as the number of piles beneath the raft increases.
2. The percentage of the load carried by piles to the total applied load from the numerical model for the case of four piles with raft is around 38% & 46%, while from experimental work it is 61% & 65% for the 1st & 2nd cases of piled raft foundation system respectively.
3. In comparison to shallow (raft) foundations, piled rafts reduce effectively the settlements.

Analysis using PLAXIS 3D compares well with the experimental values and hence it can be used for studies on piled raft foundation systems of other configurations.

References

- [1]. Clancy, P. and Randolph, M. F. (1993), an approximate analysis procedure for piled raft foundations. *Int. J. Numer. Anal. Meth. Geomech.* 17: 849–869. doi:10.1002/nag.1610171203.
- [2]. Hameedi, M. K., “Experimental and Theoretical Study for Piled Raft Foundation in Soft Clay”, Unpublished M.Sc. Thesis, Building and Construction Engineering Department, University of Technology, Baghdad, Iraq, 2011.
- [3]. Y.C. Tan and C.M. Chow, “Design of Piled Raft foundation on soft Ground”, 2004.
- [4]. Bowles, J.E., “foundation Analysis and Design”, Fifth edition, McGraw-Hill”, 1997.
- [5]. Vermeer, P.A., and Brinkgreve, R.B.J., “PLAXIS 3D User’s Manual, Version 1.1”, Balkema, Rotterdam, The Netherlands, 2004.

**Department of
Electrical and Electronics
Engineering**

A MPC Integrated E-STATCOM with Adaptive Power Oscillation Damping

GUDIPALLY NITHIN KRISHNA GUPTHA¹, K. CHETASWI²

¹PG Scholar, Malla Reddy Engineering College (Autonomous), India, E-mail: gudipallynithin@gmail.com.

²Assistant Professor, Malla Reddy Engineering College (Autonomous), India, E-mail: chetaswi@mrec.ac.in.

Abstract: In this paper we introduce E-STATCOM (Energy Storage Static Synchronous Compensator) with MPC(Model Predictive Control) compensating the grid system with adaptive power oscillation damping. We consider a 11-bus system with four conventional sources connected through a two line transmission system. Transfer of active power and reactive power through the bus is been observed with E-STATCOM connected at different locations and compared with RLS (recursive least square) controller and MPC controller. Analysis of the design is carried out in Matlab Simulink software with all graphical representations.

Keywords: E-Statcom, MPC, RLS.

I. INTRODUCTION

To have sustainable growth and social progress, it is necessary to meet the energy need by utilizing the renewable energy resources like wind, biomass, hydro, co-generation, etc In sustainable energy system, energy conservation and the use of renewable source are the key paradigm. The need to integrate the renewable energy like wind energy into power system is to make it possible to minimize the environmental impact on conventional plant[1]. The integration of wind energy into existing power system presents a technical challenges and that requires consideration of voltage regulation, stability, power quality problems. The power quality is an essential customer-focused measure and is greatly affected by the operation of a distribution and transmission network. The issue of power quality is of great importance to the wind turbine [2]. There has been an extensive growth and quick development in the exploitation of wind energy in recent years. The individual units can be of large capacity up to 2 MW, feeding into distribution network, particularly with customers connected in close proximity [3]. Today, more than 28 000 wind generating turbine are successfully operating all over the world. In the fixed-speed wind turbine operation, all the fluctuation in the wind speed are transmitted as fluctuations in the mechanical torque, electrical power on the grid and leads to large voltage fluctuations. During the normal operation, wind turbine produces a continuous variable output power. These power variations are mainly caused by the effect of turbulence, wind shear, and tower-shadow and of control system in the power system. Thus, the network needs to manage for such fluctuations.

The power quality issues can be viewed with respect to the wind generation, transmission and distribution network, such as voltage sag, swells, flickers, harmonics etc. However the wind generator introduces disturbances into the distribution network. One of the simple methods of running a wind generating system is to use the induction generator connected directly to the grid system. The induction generator has inherent advantages of cost effectiveness and robustness. However; induction generators require reactive power for magnetization. When the generated active power of an induction generator is varied due to wind, absorbed reactive power and terminal voltage of an induction generator can be significantly affected. A proper control scheme in wind energy generation system is required under normal operating condition to allow the proper control over the active power production. In the event of increasing grid disturbance, a battery energy storage system for wind energy generating system is generally required to compensate the fluctuation generated by wind turbine. A STATCOM-based control technology has been proposed for improving the power quality which can technically manages the power level associates with the commercial wind turbines. The proposed STATCOM control scheme for grid connected wind energy generation for power quality improvement has following objectives.

- Unity power factor at the source side.
- Reactive power support only from STATCOM to wind Generator and Load.
- Simple bang-bang controller for STATCOM to achieve fast dynamic response.

The considered test system is shown below in fig. 1

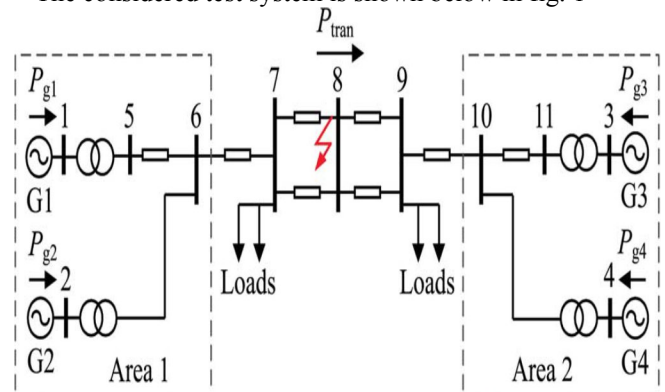


Fig.1. 11-bus test system.

II. PWM INVERTER

The pulse width modulation technique is generally used for the conversion of DC to AC waveforms. A full bridge inverter with six IGBTs can be used to convert DC to three phase AC. Each phase has to be phase shifted to each other by 120° and has to be in synchronization with the grid to which it is being connected. The pulses are to be given to the IGBTs are generated with a reference or fundamental waveform compared with a triangular waveform. The fundamental waveform has the frequency of the grid and the triangular or carrier waveform has higher frequency to create a modulation signal. The diagram of the fundamental and the carrier waveform are shown below in fig. 3. Six pulses are formed by applying NOT gates to the three pulses produced by the comparison of the fundamental and carrier waveforms. The generated pulses are fed to the VSI (Voltage source Inverter) with G1 G2 G3 G4 G5 and G6 switches. A simple construction of VSI is shown in fig. 2.

The rating of IGBT is taken as
 Internal resistance $R_{on} = 0.001$ ohms
 Snubber resistance $R_s = 100$ kohms
 Snubber capacitance $C_s = 1F$

Due to the impedance load the load current gets ceased during sudden switch OFF of the IGBT switch and generate high voltage peaks in the output voltage. To avoid this an anti parallel diode is attached to the switch (IGBT) so that the inductor current from the impedance load can pass through the diode.

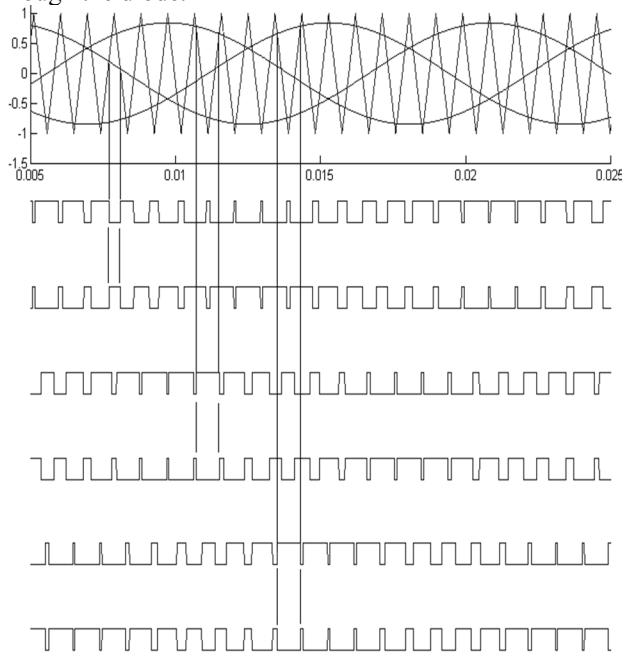


Fig.2. Generation of pulses with respect to reference fundamental waveforms.

The higher the carrier frequency the lower the harmonics developed by the inverter. To eliminate the minimum harmonics we also use LC filter to filter the higher order

harmonics from the three phase AC voltage waveforms. The three sinusoidal fundamental waveforms are generated as

$$V_a = V_m \sin(\omega t) \quad (1)$$

$$V_b = V_m \sin(\omega t + 2\pi/3) \quad (2)$$

$$V_c = V_m \sin(\omega t - 2\pi/3) \quad (3)$$

Where V_m = maximum voltage i.e., amplitude of sinusoidal waveform which is '1'

The modulation index in PWM waveform is controlled by controlling the amplitude of the fundamental waveform. By reducing amplitude of the sinusoidal wave the space between the pulse is increased reducing the amplitude of the PWM waveform. The phase of the reference wave considered decides the phase of the PWM waveform.

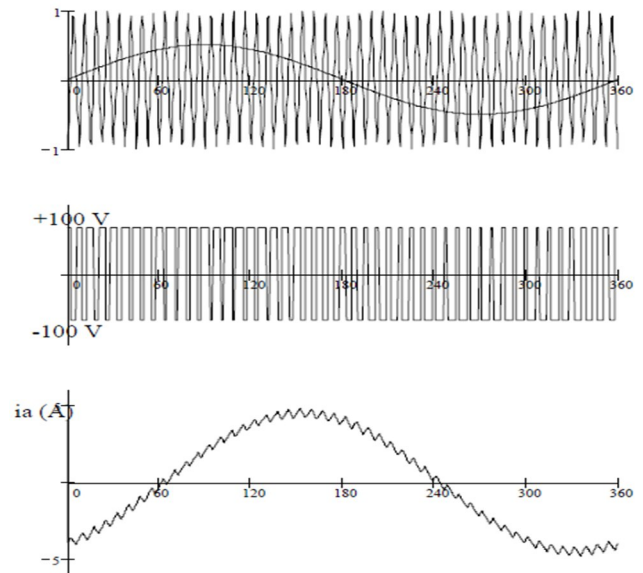


Fig. 3. Effect of change in amplitude of sinusoidal waveform.

III. RLS ALGORITHM

The selection is a tradeoff between a good selectivity for the estimator and its speed of response. A high forgetting factor results in low estimation speed with good frequency selectivity. With increasing estimation speed (decreasing), the frequency selectivity of the algorithm reduces. For this reason, the conventional RLS algorithm must be modified in order to achieve fast transient estimation without compromising its steady-state selectivity. In this paper, this is achieved with the use of variable forgetting factor as described in [13].

$$\begin{aligned} y(t) &= Y_{avg}(t) + \sum_{i=1}^N Y_{osc,i} \\ &= Y_{avg}(t) + \sum_{i=1}^N Y_{ph,i}(t) \cos[\omega_{osc,i}t + \varphi_i(t)] \end{aligned} \quad (4)$$

When the RLS algorithm is in steady-state, its bandwidth is determined by the steady-state forgetting factor f a rapid change is detected in the input. This frequency is dependent

A MPC Integrated E-STATCOM with Adaptive Power Oscillation Damping

on the system parameters and its operating conditions. If the frequency content of the input changes, the estimator will give rise to a phase and amplitude error in the estimated quantities. Therefore, a frequency adaptation mechanism as described in [14] is implemented to track the true oscillation frequency of the input from the estimate of the oscillatory component.

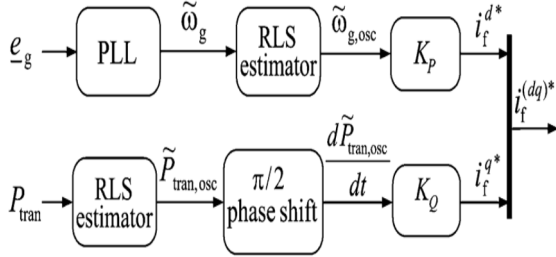


Fig. 4. Control structure of E-STATCOM.

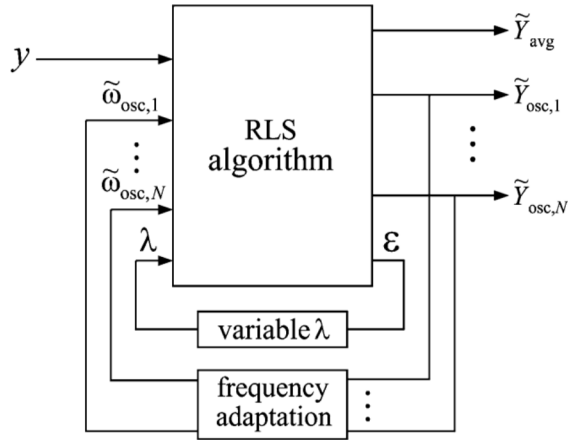


Fig. 5. Internal modeling of RLS control.

The mathematical model of the system in Fig. 5 is developed in this section to investigate the performance of the POD controller using active and reactive power injection. Using the expressions in (6)–(7) for

$$\begin{aligned} i_f^d &\approx K_P \omega_{g0} [\Gamma_P \Delta \omega_{g1} + (1 - \Gamma_P) \Delta \omega_{g2}] \\ i_f^q &\approx K_Q \omega_{g0} \left\{ \frac{V_{g1} V_{g2} \cos(\delta_{g10} - \delta_{g20})}{X_1 + X_2} \right\} [\Delta \omega_{g1} - \Delta \omega_{g2}] \end{aligned} \quad (5)$$

Linearizing around an initial steady-state operating point, the small-signal dynamic model of the two-machine system with the E-STATCOM in per unit is developed as in

$$\begin{aligned} \frac{d}{dt} \begin{bmatrix} \Delta \omega_{g1} \\ \Delta \delta_{g12} \\ \Delta \omega_{g2} \end{bmatrix} &= \begin{bmatrix} \beta_{11} & \beta_{12} & \beta_{13} \\ \omega_{g0} & 0 & -\omega_{g0} \\ \beta_{31} & \beta_{32} & \beta_{33} \end{bmatrix} \begin{bmatrix} \Delta \omega_{g1} \\ \Delta \delta_{g12} \\ \Delta \omega_{g2} \end{bmatrix} \\ &+ \begin{bmatrix} \frac{1}{2H_{g1}} & 0 \\ 0 & 0 \\ 0 & \frac{1}{2H_{g2}} \end{bmatrix} \begin{bmatrix} \Delta T_{m1} \\ \Delta T_{m2} \end{bmatrix} \end{aligned}$$

This represents the rotor angle difference between the two generators and other signals as defined previously. Assuming

no mechanical damping and the initial steady-state speed of the generators set to

$$\begin{bmatrix} \beta_{11} \\ \beta_{12} \\ \beta_{13} \\ \beta_{31} \\ \beta_{32} \\ \beta_{33} \end{bmatrix} = \begin{bmatrix} \frac{\omega_{g0} (K_P E_{g0} \Gamma_P^2 + K_Q \Gamma_Q)}{2H_{g1}} \\ -\frac{V_{g1} V_{g2} \cos(\delta_{g10} - \delta_{g20})}{2H_{g1} (X_1 + X_2)} \\ \frac{\omega_{g0} (K_P E_{g0} \Gamma_P (1 - \Gamma_P) - K_Q \Gamma_Q)}{2H_{g1}} \\ \frac{\omega_{g0} (K_P E_{g0} \Gamma_P (1 - \Gamma_P) - K_Q \Gamma_Q)}{2H_{g2}} \\ \frac{V_{g1} V_{g2} \cos(\delta_{g10} - \delta_{g20})}{2H_{g2} (X_1 + X_2)} \\ \frac{\omega_{g0} (K_P E_{g0} (1 - \Gamma_P)^2 + K_Q \Gamma_Q)}{2H_{g2}} \end{bmatrix}$$

IV. SIMULINK MODEL AND RESULTS

As an example for the analysis in this section, a hypothetical 20/230 kV, 900 MVA transmission system similar to the one in Fig. 6 with a total series reactance of 1.665 p.u. and inertia constant of the generators are considered. The leakage reactance of the transformers and transient impedance of the generators are 0.15 p.u. and 0.3 p.u., respectively. The movement of the poles for the system as a function of the E-STATCOM location is shown in Fig. 7. With the described control strategy, injected active power is zero at the point where the effect of active power injection on damping is zero. This is at the electrical midpoint of the line. On the other hand, at the same location damping by reactive power injection is maximum. The reverse happens at either end of the generators. Thanks to a good control of P & Q it is also possible to see from Fig. 6 that a more uniform damping along the line is obtained by using injection of both active and reactive power.

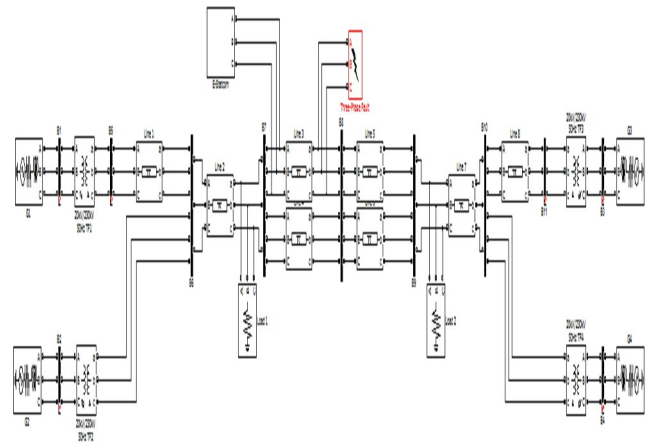


Fig. 6. Simulink design of 11bus test system.

With the POD controller structure described in Fig. 4, the performance of the E-STATCOM following the fault at three different locations is shown in Fig. 8. As described in the small-signal analysis for two-machine system in Section IV, when moving closer to the generator units, a better damping is achieved by active power injection (see Fig. 8, black solid

Fig. 7. E-Statcom.

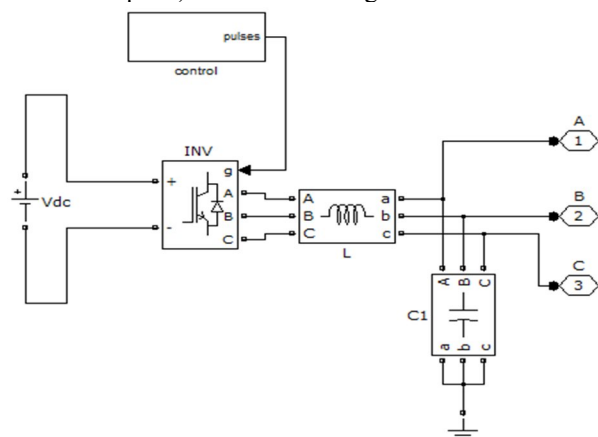


Fig. 7. E-Statcom.

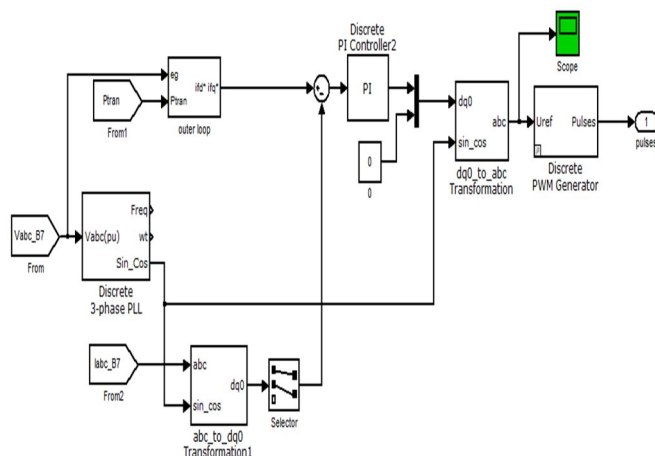


Fig. 8. Control design.

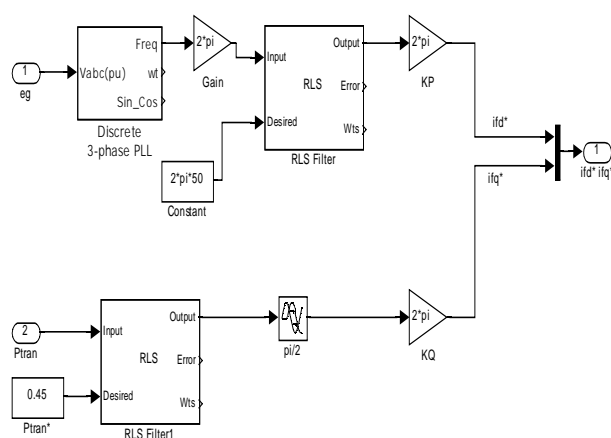


Fig. 9. RLS control.

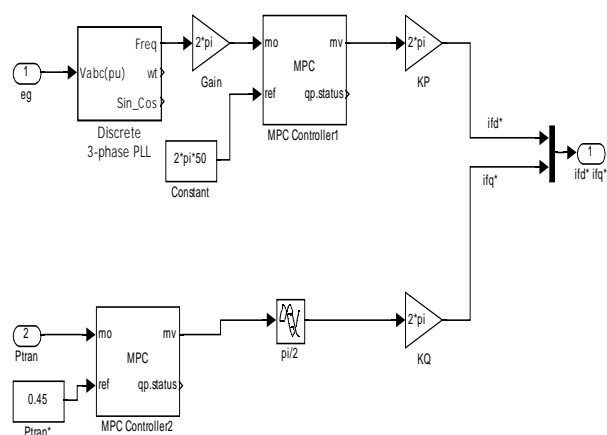


Fig. 10. MPC control.

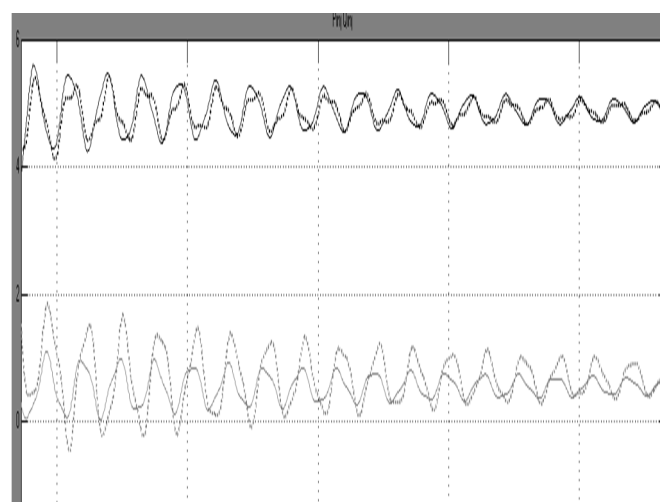


Fig. 11. Comparison of Pinj and Qinj with RLS and MPC controllers.

V. CONCLUSION

With the above comparison results with RLS and MPC controllers of P_{inj} and Q_{inj} at bus 8 of the test system when E-Statcom is connected at bus 7. A balanced fault is given at bus 8 for 0.012sec from 0.05 to 0.062 secs and the damping of P_{inj} and Q_{inj} is observed. From fig. 11 it can be observed that the P_{inj} and Q_{inj} (dotted waveforms) with RLS algorithm has more damping than P_{inj} and Q_{inj} (solid waveforms) with MPC controller.

VI. REFERENCES

- [1] N. G. Hingorani and L. Gyugyi, Understanding FACTS. Concepts and Technology of Flexible AC Transmission Systems. New York, NY, USA: IEEE, 2000.
- [2] G.Cao, Z.Y.Dong, Y.Wang, P. Zhang, and Y.T. Oh, "VSC based STATCOM controller for damping multi-mode oscillations," in Proc. IEEE Power and Energy Soc. General Meeting—Conversion and Delivery of Electrical Energy in the 21st Century, Jul. 2008, pp. 1–8.
- [3] M. Zarghami and M. L. Crow, "Damping inter-area oscillations in power systems by STATCOMs," in Proc. 40th North Amer. Power Symp., Sep. 2008, pp. 1–6.

- [4] Z. Yang, C. Shen, L. Zhang, M. L. Crow, and S. Atcitty, "Integration of a statcom and battery energy storage," IEEE Trans. Power Syst., vol. 16, no. 2, pp. 254–260, May 2001.
- [5] A. Arulampalam, J. B. Ekanayake, and N. Jenkins, "Application study of a STATCOM with energy storage," Proc. Inst. Electr. Eng.—Gener., Transm. and Distrib., vol. 150, pp. 373–384, July 2003.
- [6] N. Wade, P. Taylor, P. Lang, and J. Svensson, "Energy storage for power flow management and voltage control on an 11 kV UK distribution network," Prague, Czech Republic, CIRED paper 0824, Jun. 2009.
- [7] A. Adamczyk, R. Teodorescu, and P. Rodriguez, "Control of full-scale converter based wind power plants for damping of low frequency system oscillations," in Proc. IEEE PowerTech, Trondheim, Norway, Jun. 2011, pp. 1–7.
- [8] H.Xie, "On power-system benefits, main-circuit design, control of Statcoms with energy storage," Ph.D. dissertation, Dept. Electr. Energy Conversion, Royal Inst. Technol., Stockholm, Sweden, 2009.
- [9] P. Kundur, Power System Stability and Control. New York, NY, USA: McGraw-Hill, 1994.
- [10] K. Kobayashi, M. Goto, K. Wu, Y. Yokomizu, and T. Matsumura, "Power system stability improvement by energy storage type STATCOM," in Proc. IEEE Power Tech Conf., Bologna, Italy, Jun. 2003, vol. 2, DOI 10.1109/ PTC. 2003.1304302.
- [11] L. Zhang and Y. Liu, "Bulk power system low frequency oscillation suppression by FACTS/ESS," in Proc. IEEE PES Power Syst. Conf. Exp., Oct. 2004, pp. 219–226.

Single-Phase UPS Inverters with Space Vector PWM Extended Lyapunov-Function Based Control Strategy

T. SUMAN¹, PATLOLA RAMESH²

¹Associate Professor, Dept of EEE, Malla Reddy Engineering College, TS, India, E-mail: sumankumar2k@gmail.com.

²PG Scholar, Dept of EEE, Malla Reddy Engineering College, TS, India, E-mail: p.ramesh224@gmail.com.

Abstract: Many UPS inverters used in today's technology are more efficient and reliable. In this paper we propose a UPS inverter controlled by space vector PWM technique with extended Lyapunov function control strategy which is formed by the energy storage in inductor and capacitor making the system to converge at an equilibrium point when the energy is continuously dissipated. Therefore, an extended Lyapunov function based control strategy is proposed, which eliminates the steady-state error without destroying the global stability of the closed-loop system. The steady state and dynamic performance of the proposed control strategy has been tested by simulations in MATLAB software with complete results and discussion.

Keywords: PWM, IGBTs, VSI (Voltage source Inverter), UPS.

I. INTRODUCTION

A. Sinusoidal PWM Technique

The pulse width modulation technique is generally used for the conversion of DC to AC waveforms. A full bridge inverter with six IGBTs can be used to convert DC to three phase AC. Each phase has to be phase shifted to each other by 120° and has to be in synchronization with the grid to which it is being connected. The pulses are to be given to the IGBTs are generated with a reference or fundamental waveform compared with a triangular waveform. The fundamental waveform has the frequency of the grid and the triangular or carrier waveform has higher frequency to create a modulation signal. The diagram of the fundamental and the carrier waveform are shown below in fig.1. Six pulses are formed by applying NOT gates to the three pulses produced by the comparison of the fundamental and carrier waveforms. The generated pulses are fed to the VSI (Voltage source Inverter) with G1 G2 G3 G4 G5 and G6 switches. A simple construction of VSI is shown in fig. 2. The rating of IGBT is taken as

Internal resistance $R_{on} = 0.001 \text{ ohms}$

Snubber resistance $R_s = 100 \text{ kohms}$

Snubber capacitance $C_s = 1F$

Due to the impedance load the load current gets ceased during sudden switch OFF of the IGBT switch and generate high voltage peaks in the output voltage. To avoid this an anti parallel diode is attached to the switch (IGBT) so that

the inductor current from the impedance load can pass through the diode.

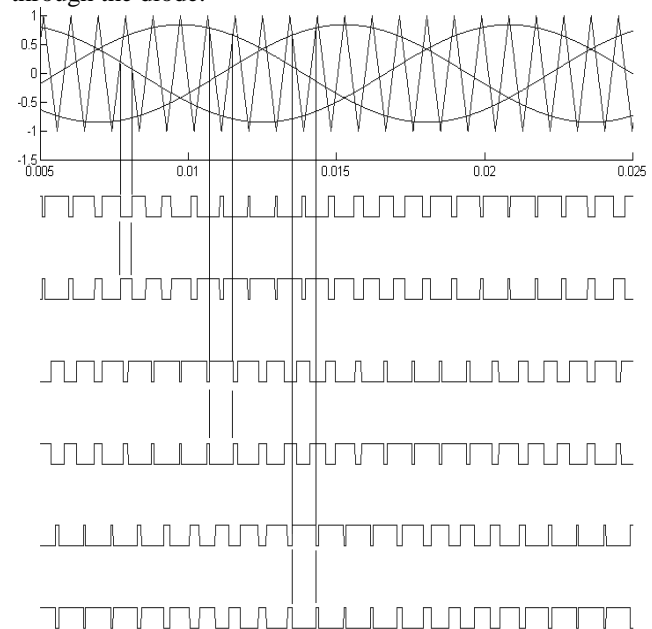


Fig. 1. Generation of pulses with respect to reference fundamental waveforms.

The higher the carrier frequency the lower the harmonics developed by the inverter. To eliminate the minimum harmonics we also use LC filter to filter the higher order harmonics from the three phase AC voltage waveforms. The three sinusoidal fundamental waveforms are generated as

$$V_a = V_m \sin(\omega t) \quad (1)$$

$$V_b = V_m \sin(\omega t + 2\pi/3) \quad (2)$$

$$V_c = V_m \sin(\omega t - 2\pi/3) \quad (3)$$

Where V_m = maximum voltage i.e., amplitude of sinusoidal waveform which is '1'. The modulation index in PWM waveform is controlled by controlling the amplitude of the fundamental waveform. By reducing amplitude of the sinusoidal wave the space between the pulse is increased reducing the amplitude of the PWM waveform. The phase of the reference wave considered decides the phase of the PWM waveform.

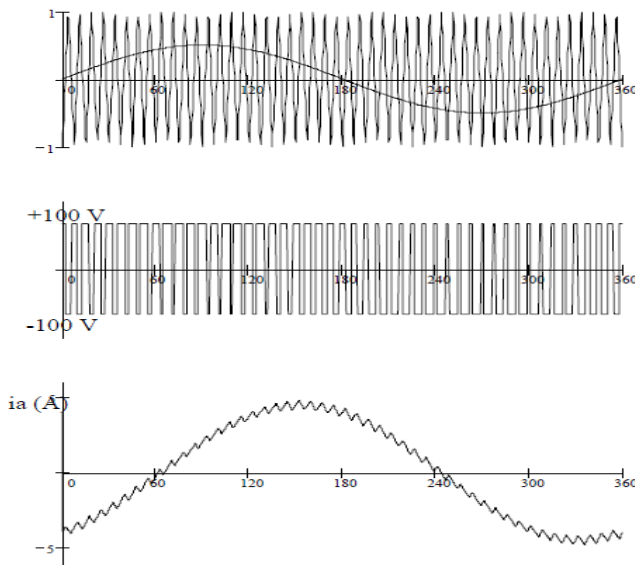


Fig. 2. Effect of change in amplitude of sinusoidal waveform.

B. Space vector PWM Technique

Space vector PWM technique is an advancement of sinusoidal PWM as the pulses produced by digital switching of the fundamental waveform as shown in Fig.3. Considering six switch operation we divide the VSI into two parts as upper part and lower part. The upper part contain the switches S1 S3 & S5 leaving the lower part of the VSI with S2 S4 & S6.

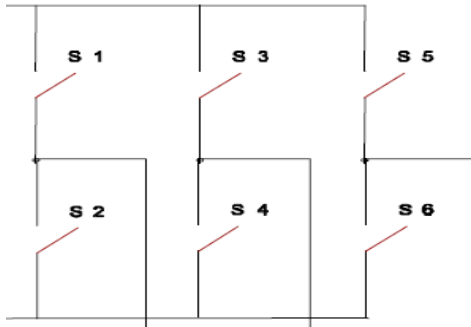


Fig. 3. switch assigning of VSI.

The state of the switches are either to be ON or OFF i.e., two states. The number of possible switching states are given as $2^3 = 8$. The 8 switching states are given below.

TABLE I: Switching States

SWITCH	S1	S3	S5
1 ST MODE	0	0	0
2 ND MODE	0	0	1
3 RD MODE	0	1	0
4 TH MODE	0	1	1
5 TH MODE	1	0	0
6 TH MODE	1	0	1
7 TH MODE	1	1	0
8 TH MODE	1	1	1

In the above mentioned 8 switching modes the first and the last are completely OFF and ON which is not applicable. We only consider the six states from 1st to 6th eliminating 0 and 7th mode as shown in Fig.4. The last three switching states are the complement of first three switching states, which concludes that we have to only generate the three switching states i.e., 1st, 2nd and 3rd. The other switching states i.e., 4th, 5th and 6th are generated by applying a NOT gate to the previous modes. A simple hexagonal representation of switching pattern is shown below which can be called as Space vector Trajectory.

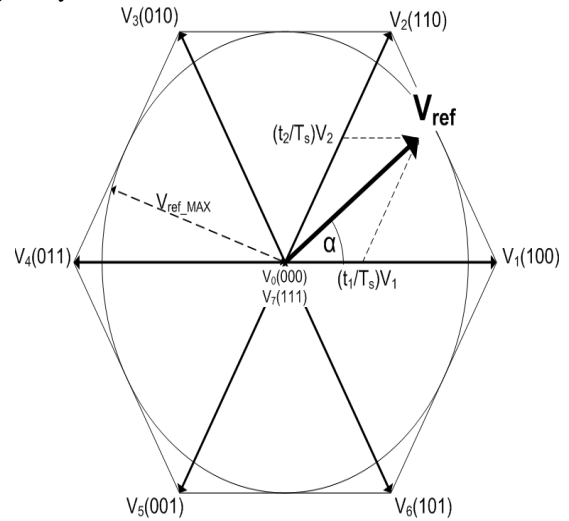


Fig. 4. Space vector trajectory.

The signal generation of space vector is compared to the triangular waveform to generate three PWM pulses to which NOT gates are given to get the other three pulses. The control signal of space vector PWM is given below Fig.5.

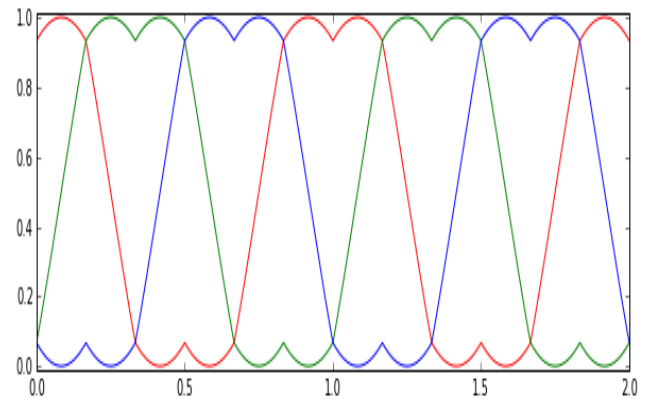


Fig. 5. Control signals of Space vector PWM.

II. EXTENDED LYAPUNOV-FUNCTION-BASED CONTROL STRATEGY

It is well known that the behavior of a system about its equilibrium point of interest can be investigated by using Lyapunov's stability theorem [21]. In the case of single-phase inverter, the equilibrium point of interest is ($x_1 = 0$, $x_2 = 0$). In this study, we are interested in studying inverter's global asymptotic stability around this equilibrium point.

Single-Phase UPS Inverters with Space Vector PWM Extended Lyapunov-Function Based Control Strategy

rather than its local stability. The former can be accomplished by using Lyapunov's direct method with the fact that the inverter system states converge to the equilibrium point if the total energy is continuously dissipated. When the state trajectory reach to the equilibrium point ($x_1 = 0$, $x_2 = 0$), then the energy dissipation converges to zero. The typical energy distribution of the single-phase inverter is depicted in Fig. 2. The total (input) energy, which is delivered by the dc power supply is denoted by E_{in} . Part of the input energy is dissipated by the resistance of inductor (E_r) and the switching devices of inverter (E_{sw}). The rest energy is transferred to the load (E_{out}). Since the inductor and capacitor do not dissipate energy, all the energy stored in the inverter is distributed in these components. Therefore, part of the input energy is exchanged by the energy stored (ΔEL and ΔEC) in these components in a bidirectional manner until the whole energy dissipation settles down to the equilibrium point of the inverter. Lyapunov's stability theorem allows us to determine the stability for the inverter system by studying a scalar energy function, which is usually called as the Lyapunov function $V(x)$. According to Lyapunov's direct method, the equilibrium point is globally asymptotically stable if $V(x)$ satisfies the following properties:

- $V(0) = 0$;
- $V(x) > 0$ for all $x \neq 0$;
- $V(x) \rightarrow \infty$ as $x \rightarrow \infty$;
- $\dot{V}(x) < 0$ for all $x \neq 0$.

In order to reduce the steady-state error in the output voltage, we modify the control strategy by adding an outer voltage loop together with a suitable gain in (11) as follows:

$$\Delta u = K_i V_{sx1} - K_v x_2. \quad (4)$$

Now, substituting (13) into (10) gives

$$\dot{V}(x) = K_i V_{2sx21} - r x_2^2 - K_v V_{sx1x2}. \quad (5)$$

III. SIMULATION RESULTS AND OUTPUTS

Simulation results of this paper is as shown in bellow Figs.6 to 8.

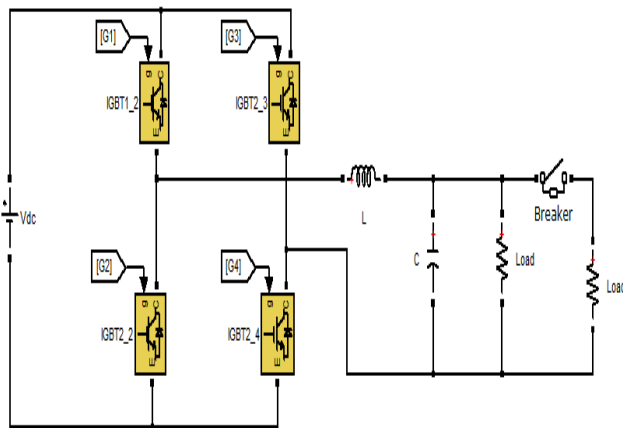


Fig. 6. Proposed circuit topology.

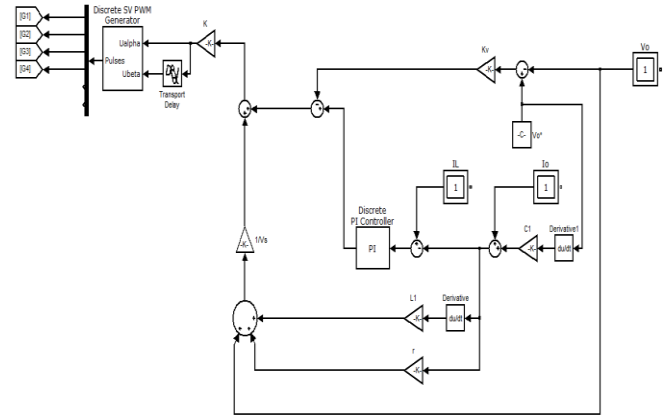


Fig.7. Space vector PWM with Lyapunov control strategy.

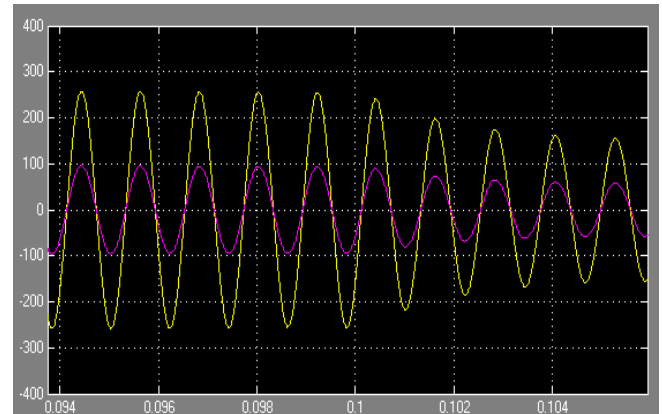


Fig. 8. Voltage and current output of inverter.

IV. CONCLUSION

With the above design and results of the UPS inverter with space vector PWM Lyapunov control strategy it can be observed that the voltage and current are in same phase with power factor maintaining at unity. With dynamic load the change of resistance at 0.1 sec is reduced with change in the voltage and current waveforms. Therefore, the classical Lyapunov-function-based control approach was then modified by adding the outer voltage loop into the control input such that the steady-state error in the output voltage is eliminated without degrading the global stability of the closed-loop system.

V. REFERENCES

- [1] F. J. Chang, E. C. Chang, T. J. Liang, and J. F. Chen, "Digital-signal-processor-based DC/AC inverter with integral-compensation terminal sliding-mode control," IET Power Electron., vol. 4, no. 1, pp. 159–167, Jan. 2011.
- [2] A. Abrishamifar, A. A. Ahmad, and M. Mohamadian, "Fixed switching frequency sliding mode control for single-phase unipolar inverters," IEEE Trans. Power Electron., vol. 27, no. 5, pp. 2507–2514, May 2012.
- [3] J. Y. C. Chiu, K. K. S. Leung, and H. S. H. Chung, "High-order switching surface in boundary control of inverters," IEEE Trans. Power Electron., vol. 22, no. 5, pp. 1753–1765, Sep. 2007.

- [4] M. Ordonez, J. E. Quaicoe, and M. T. Iqbal, "Advanced boundary control of inverters using the natural switching surface: Normalized geometrical derivation," *IEEE Trans. Power Electron.*, vol. 23, no. 6, pp. 2915–2930, Nov. 2008.
- [5] S. Chen, Y. M. Lai, S. C. Tan, and C. K. Tse, "Boundary control with ripple-derived switching surface for DC-AC inverters," *IEEE Trans. Power Electron.*, vol. 24, no. 12, pp. 2873–2885, Dec. 2009.
- [6] N. M. Abdel-Rahim and J. E. Quaicoe, "Analysis and design of multiple feedback loop control strategy for single-phase voltage-source UPS inverter," *IEEE Trans. Power Electron.*, vol. 11, no. 4, pp. 532–541, Jul. 1996.
- [7] M. J. Ryan, E. W. Brumsickle, and R. D. Lorenz, "Control topology options for single-phase UPS inverters," *IEEE Trans. Ind. Appl.*, vol. 33, no. 2, pp. 493–501, Mar./Apr. 1997.
- [8] O. Kukrer, H. Komurcugil, and N. S. Bayindir, "Control strategy for single-phase UPS inverters," *Proc. IEE*, vol. 150, no. 6, pp. 743–746, Nov. 2003.
- [9] L. Padmavathi and P. A. Janakiraman, "Self-tuned feed-forward compensation for harmonic reduction in single-phase low-voltage inverters," *IEEE Trans. Ind. Electron.*, vol. 58, no. 10, pp. 4753–4762, Oct. 2011.
- [10] S. Xu, J. Wang, and J. Xu, "A current decoupling parallel control strategy of single-phase inverter with voltage and current dual closed-loop feedback," *IEEE Trans. Ind. Electron.*, vol. 60, no. 4, pp. 1306–1313, Apr. 2013.
- [11] M. Monfared, S. Golestan, and J. M. Guerrero, "Analysis, design, and experimental verification of a synchronous reference frame voltage control for single-phase inverters," *IEEE Trans. Ind. Electron.*, vol. 61, no. 1, pp. 258–269, Jan. 2014.

SOLAR POWER CONDITIONING SYSTEMS EVALUATION FOR PHOTOVOLTAIC SOURCE SIMULATOR WITH FAST RESPONSE TIME RELATED TO MPPT

#1BH Y ANUSHA, PG STUDENT

#2CH. NARENDRA KUMAR, ASSOCIATE PROFESSOR

#3DR.M.LAKSHMI SWARUPA, PROFESSOR

DEPT OF EEE

MALLAREDDY COLLEGE OF ENGINEERING COLLEGE (ATONOMOUS), Dhulapally, Secundrabad.

Abstract—Photovoltaic (PV) source simulators serve as a convenient tool for the dynamic evaluation of solar power conditioning systems and maximum power point tracking algorithms. High efficiency and fast transient response time are essential features any PV source simulator. This paper proposes a new type of PV source simulator that incorporates the advantages of both analog and digital-based simulators. The proposed system includes a three-phase ac–dc dual boost rectifier cascaded with a three phase dc–dc interleaved buck converter. The selected power stage topology is highly reliable and efficient. Moreover, the multiphase converter helps improve system transient response though producing low output ripple which makes it adequate for PV source simulators. The simulator circuitry emulates precisely the static and the dynamic characteristics of actual PV generators under different load and environmental conditions. Additionally, the system allows the creation of the partial shading and bypass diodes effect on PV characteristics. The paper investigates the dynamic performance of a commercial solar power inverter using the proposed PVsource simulator in steady-state and transient conditions. Closed-loop output impedance of the proposed PV source simulator has been measured and verified at different operating regions. The impedance profile—magnitude and phase—matches the output impedance of actual PV generators.

I. INTRODUCTION

RENEWABLE energy sources are becoming increasingly important recently with focus turning toward clean electricity generation. In particular, photovoltaic (PV) or solar power systems are one of the most promising and attractive renewable energy sources due to their low operational and maintenance costs, pollution free power generation, long life cycles, and noise-free operation [1], [2]. Prior to installation, performance and efficiency of solar power conditioning systems have to be evaluated.

Moreover, experimental validation and verification of solar power conditioning systems under a wide range of different environmental and load conditions have to be done [3], [4]. Solar or PV cells are used to directly convert sunlight into dc power. Solar cells exhibit nonlinear output current–voltage characteristics. This current–voltage curve is characterized with a unique maximum power point (MPP) and depends on environmental conditions (solar irradiance, cell temperature, wind speed, etc.) and PV cell fabrication material [5]–[7]. Accordingly, a maximum power point tracking (MPPT) algorithm is required in solar power conditioning systems in order to maximize the generated output power [8]–[10]. Testing medium and high-power solar power conditioning systems with actual solar cells along with direct solar irradiance or an artificial light source is costly, bulky, and highly dependent on weather conditions. Furthermore, evaluation and comparison of different MPPT techniques requires repeatable weather and load conditions that are impractical. To overcome these difficulties, PV source simulators have been introduced. A PV source simulator is a power electronics circuit able to reproduce the static and the dynamic output characteristics of an actual solar cell or arrays of cells over a wide range of environmental and load conditions. PV source simulators can be cost-effective, compact, and flexible [10]. A well-designed PV source simulator should adopt the following features: 1) Accurately predict the static characteristics of solar cells and arrays under different environmental and load conditions. 2) Match the frequency response of the output impedance of actual PV cell in high- and low-frequency ranges and at different operating regions including constant current and constant voltage. 3) Simulate the PV characteristics under partial shading conditions with multiple peaks and steps. 4) Emulate the effect of bypass and blocking diodes on PV output characteristics.

- 5) Reflect the effect of different PV configurations on PV output characteristics.
- 6) Evaluate different MPPT algorithms performance with reasonable response time.
- 7) Achieve high power stage efficiency to be adequate for operations over a long period of equipment testing.
- 8) Interface capability with other power electronics circuits and solar power conditioning systems.
- 9) Evaluate solar power conditioning systems performance in steady-state and transient-state under different load and environmental conditions. PV source simulators can be used to assess the PV energy production, experimentally investigate the dynamic performance of PV systems including stand-alone and grid-connected inverters regardless of environmental conditions, and evaluate different MPPT algorithms' response and efficiency.

PV source simulators can be classified into different categories based on the design of power stage, control system, and reference generation technique. Power stage design can be configured with a linear or a switching power stage. Linear PV source simulators are excellent in dynamic response but are limited to low power applications. Low efficiency, high heat generation, and bulky size are serious concerns at high power applications where switching power stages are more attractive. To replicate the current-voltage characteristics of a PV cell, the switching power stage should operate in buck mode. Different switching power stages have been reported as PV source simulators such as, single-phase dc-dc buck converter [16], three-phase ac-dc voltage source and current source rectifier [17], half- and-full bridge dc-dc converter [18], [19], and an LLC resonant dc-dc converter [20]. Other power stages have been used such as a dc programmable power supply with a current limit, dc power supply with a variable resistor [21] or controlled switch resistor [22], and active power load [23]. The reference current-voltage generation techniques can be either analog [24]–[26] or digital based [27]–[29]. The analog-based simulators are distinguished with simplicity and low cost implementation. Their current-voltage reference curves can be employed in one of three ways: 1) using a small PV cell with a light source [30]; 2) using a photodiode with a light-emitting diode [31]; and 3) using a PV cell diode model with current source [32], [33]. The first approach is a real-time simulator [34] and, hence, is the most accurate among other approaches. The second approach is flexible and can be used to emulate shading conditions effectively [35]. The implementation of

the last approach is simple where the current source represents the sunlight illumination. Digital reference generation based PV source simulators are flexible, reliable, and less sensitive to high-frequency switching noise. However, the digital time delay may affect the performance and design of control loops. The current-voltage digital reference curve can be generated using one of two techniques. The first technique is to store premeasured current-voltage curves in a data memory at different environmental and load conditions. The more data points stored, the higher the resolution and accuracy needs to be of the pregenerated characteristics. The second technique is the digital implementation of the mathematical model of PV cells. A high-speed digital signal processor (DSP) is required due to the execution of sophisticated mathematical semiconductor equations. Two PV models have been widely used: 1) the parametric model and 2) the interpolation model. The parametric model is used when all PV cell parameters (from manufacturer's data sheets) are known, whereas the interpolation model.

II. PHOTOVOLTAIC INVERTER

The basic block diagram of grid connected PV power generation system is shown in Fig. 2.1.

The PV power generation system consists of following major blocks:

1. PV unit
2. Inverter
3. Grid
4. MPPT

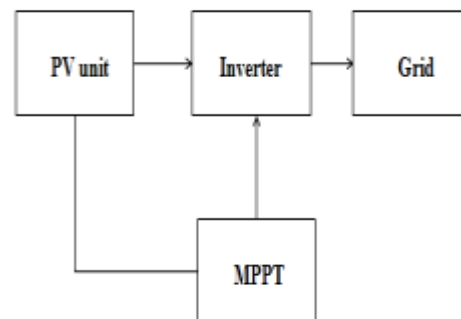


Fig. 3 Schematic diagram of PV system

1. **PV unit** : A PV unit consists of number of PV cells that converts the energy of light directly into electricity (DC) using photovoltaic effect.
2. **Inverter** : Inverter is used to convert DC output of PV unit to AC power.

3. Grid : The output power of inverter is given to the nearby electrical grid for the power generation.
4. MPPT : In order to utilize the maximum power produced by the PV modules, the power conversion equipment has to be equipped with a maximum power point tracker (MPPT). It is a device which tracks the voltage at where the maximum power is utilized at all times.

For the design of PV generation system, the specifications of considered PV system are shown in below Table 2.1

2.1.1 Photovoltaic Cell and Array Modeling

A PV cell is a simple p-n junction diode that converts the irradiation into electricity. Fig.3.1 illustrates a simple equivalent circuit diagram of a PV cell. This model consists of a current source which represents the generated current from PV cell, a diode in parallel with the current source, a shunt resistance, and a series resistance.

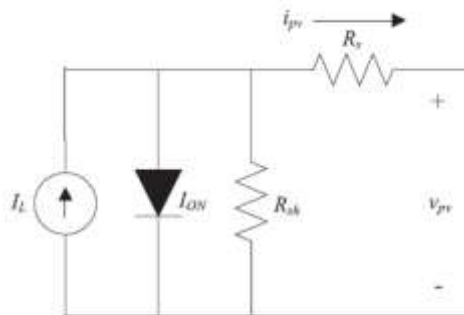


Fig.4 Equivalent circuit diagram of the PV cell

III.DC-DC CONVERTER BASICS

A DC-to-DC converter is a gadget that acknowledges a DC info voltage and produces a DC yield voltage. Normally the yield delivered is at an alternate voltage level than the info. Also, DC-to-DC converters are utilized to give clamor confinement, force transport regulation, and so on. This is a synopsis of a portion of the prevalent DC-to-DC converter topologies.

3.1 BUCK CONVERTER

In this circuit the transistor turning ON will put voltage V_{in} toward one side of the inductor. This voltage will tend to bring about the inductor current

to rise. At the point when the transistor is OFF, the present will keep coursing through the inductor however now moving through the diode.

We at first accept that the current through the inductor does not achieve zero, in this way the voltage at V_x will now be just the voltage over the leading diode amid the full OFF time. The normal voltage at V_x will rely on upon the normal ON time of the transistor gave the inductor current is persistent.

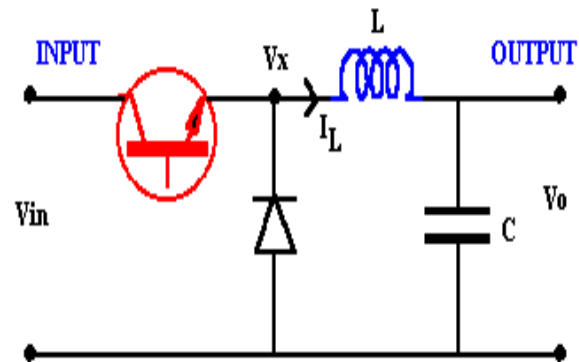


Fig 5 Buck Converter

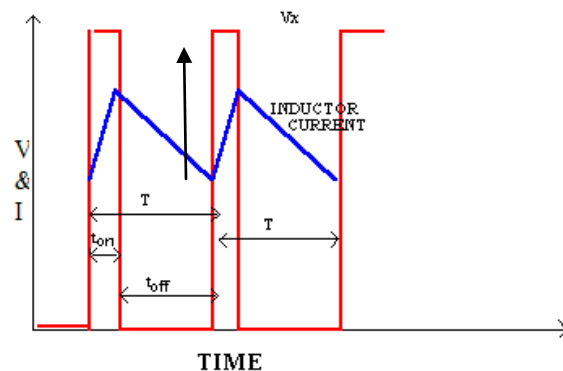


Fig6: Voltage and current changes

IV. SYSTEM DESCRIPTION AND CONTROL STRATEGY

The basic structure of the proposed PV source simulator is composed of three main circuit: 1) power stage circuit, 2) digital control circuit, and 3) analog reference-generation circuit. The power stage is a three-phase ac-dc rectifier cascaded with a

multiphase dc–dc converter. The three-phase ac–dc rectifier is a new type of dual boost topology [51], [52]. Fig. 1 presents the circuit diagram of the proposed ac–dc dual boost rectifier. For each phase, the upper and lower switch duty cycles are determined by the direction of its input phase reference current and its calculated ac reference duty cycle, described as follows:

$$\left. \begin{aligned} i_{a_{ref}} &\leq 0 \\ d_{aU} &= 1/2 - 1/2 d_a \\ d_{aL} &= 0 \end{aligned} \right\} \quad (1)$$

$$\left. \begin{aligned} i_{a_{ref}} &\geq 0 \\ d_{aV} &= 0 \\ d_{aL} &= 1/2 + 1/2 d_a \end{aligned} \right\} \quad (2)$$

where i_{ref} is the phase a reference current, d_a is the phase a reference duty cycle, and d_{aU} , d_{aL} are the phase a upper and lower switch duty cycles, respectively, with no dead time required. The dual boost circuit integrates two active switches per phase or six active switches for a three-phase system without having two switches in series for each phase leg; in consequence, the shoot-through failure is avoided. This distinguished feature makes the dual boost topologies attractive due to their high reliability. Generally, a hard-switched conventional three-phase circuit utilizes the insulated gate bipolar transistors (IGBTs) rather than the metal–oxide–semiconductor field-effect transistors (MOSFETs) as the main switch because of poor reverse recovery characteristics of their body diodes. However, in dual boost circuit, the MOSFETs can be employed with three-phase circuits as their body diodes do not conduct current. The use of MOSFETs allows higher switching frequencies where the size of the passive components can be significantly reduced. Furthermore, the turn-off and conduction losses can be substantially reduced with proper switch selection. Fig. 2 illustrates the proposed control strategy of the threephase dual boost rectifier. This digital control system is based on the $dq0$ synchronous rotating reference frame that is referenced to the grid phase-to-neutral voltage v_{an} through a phase-locked loop (PLL). The PLL circuit is designed in the $dq0$ synchronous frame as shown in Fig. 3 along with its designed parameters. The voltage reference of the PLL control loop $v^*_{d\text{PLL}}$ is set to zero and an angle offset (30°) has been added to compensate for the phase difference between line-to-line and phase-to-neutral grid voltages. The control system incorporates two decoupled inner current loops (d-axis and q-axis)

to control the ac input current and a superimposed outer voltage loop to control the dc

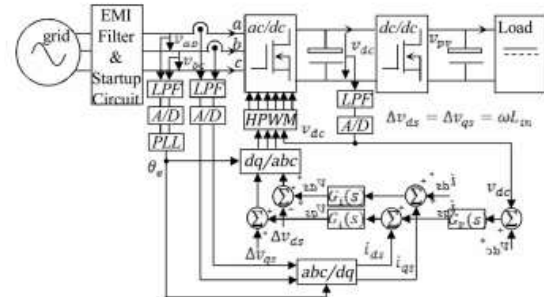


Fig7: Control strategy block diagram for the three-phase ac–dc rectifier

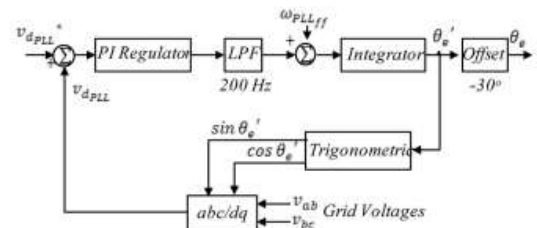


Fig8: Circuit diagram of the digital PLL.

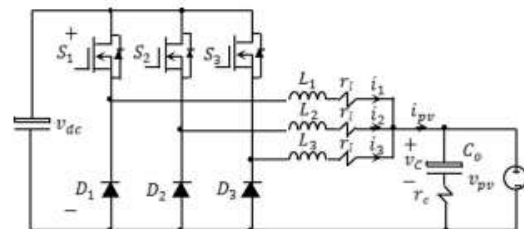


Fig9: Circuit diagram of the proposed three-phase dc-dc interleaved buck converter.

V.SIMULATION RESULTS:

The proposed PV source simulator was simulation implemented and tested to verify its steady-state and dynamic performance based on the methodology described earlier. Fig. 12 shows the proposed simulator. Two simulator setups were conducted: 1) the PV source simulator connected to an electronic load (resistive mode) to reproduce the PV characteristics at different load and environmental conditions and 2) the PV source simulator connected to a commercial solar power microinverter to evaluate the dynamic performance of the solar power conditioning system and to optimize the PV source simulator control loop bandwidth. Moreover, the microinverter is tested with actual PV generators to justify the validity of the PV source simulator as a replacement for actual PV systems. The electrical specifications and components parameters of the proposed PV source

simulator and the solar microinverter are summarized in Table II.

TABLE II
SYSTEM TECHNICAL SPECIFICATIONS

ac-dc Rectifier Stage (Boost)			
Electrical Specifications		Component Parameters	
Input Voltage	120 V (RMS)	Inductance	950 μ H
Output Voltage	375 V	Capacitance	2.35 mF
Power Factor	1.0	Main Switch	FCA76N60
Sampling Time	30 μ s	Main Diode	STTH6004W
dc-dc Converter Stage (Buck)			
Electrical Specifications		Component Parameters	
Input Voltage	375 V	Inductance	450 μ H
Output Voltage	(0-200) V	Capacitance	100 μ F
Output Current	(0-20) A	Main Switch	IPW60R045CP
Sampling Time	30 μ s	Main Diode	STTH6004W
ac-dc Inverter Stage (Enphase)			
Electrical Specifications		Electrical Specifications	
Input Voltage	56 V (MAX)	Input Power	230 W
Output Voltage	240 V	Output Power	190 W
Input Current	10 A (MAX)	Power Factor	> 0.95
MPPT Range	22 V – 40 V	Peak Efficiency	95.5 %

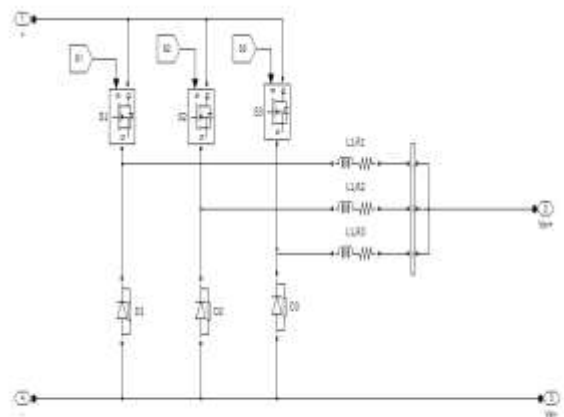


Fig12: Interleaved DC-DC Converter

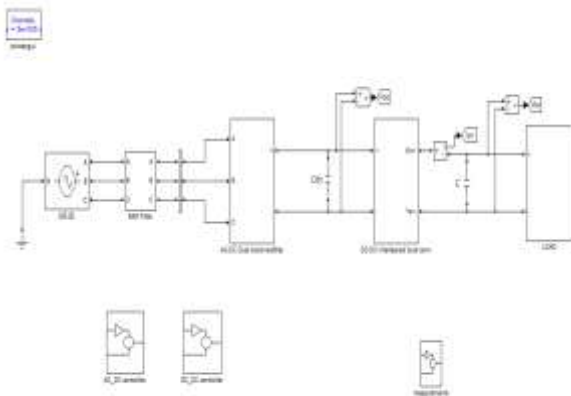


Fig10: Proposed simulation diagram

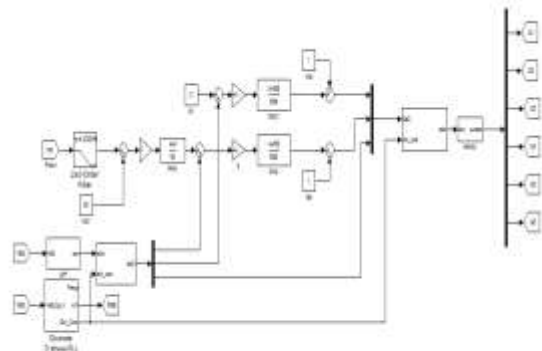


Fig13: Control diagram of AC-DC Converter

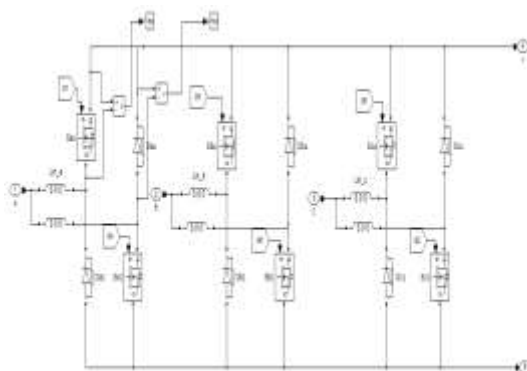


Fig11: AC-DC Boost rectifier

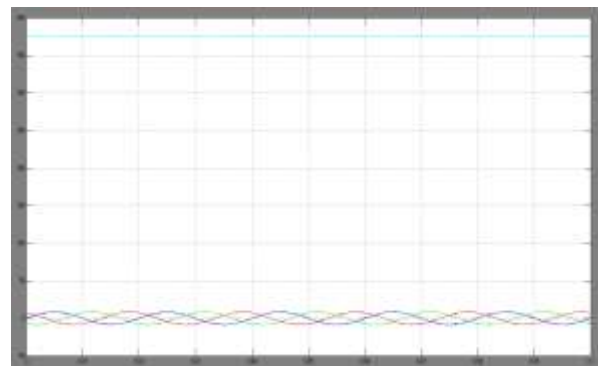
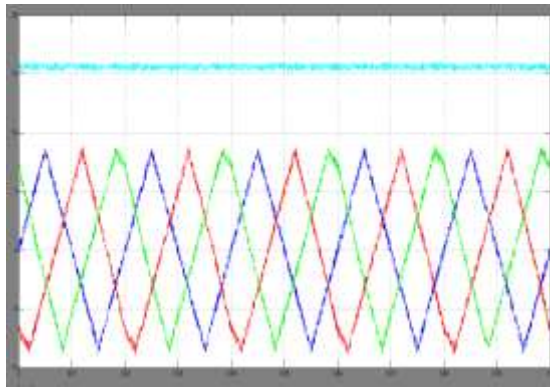


Fig14: Simulation waveforms of the proposed PV source simulator: rectifier input currents and dc-link voltage



X-axis: Time, Y-axis: Amplitude

Fig15: converter output currents and total output current

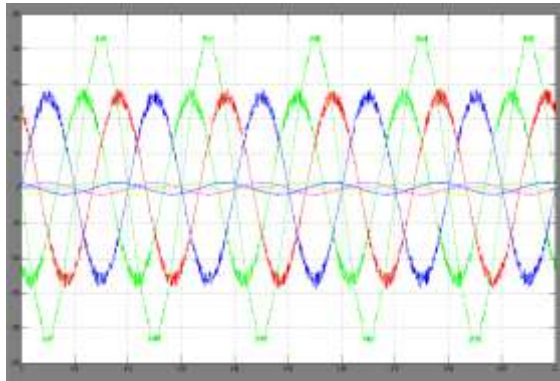


Fig16: rectifier input phase voltage, input phase current, duty cycle, and electrical angle

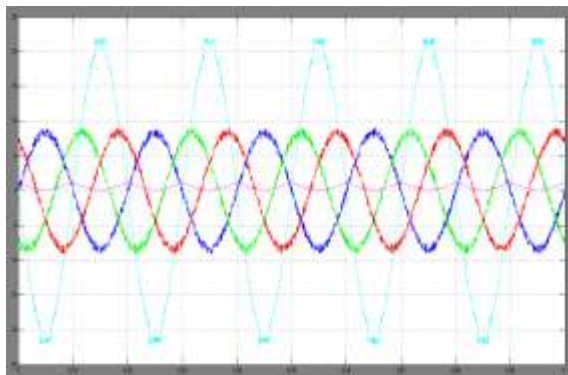


Fig: rectifier duty cycle, upper duty cycle, lower duty cycle, and input phase current.

VI.CONCLUSION:

A new type of PV source simulator has been proposed and thoroughly described. The proposed simulator has been used to precisely emulate the static and the dynamic characteristics of actual PV systems at different load and environmental conditions including the effect of partial shading. The simulator uses a real-time analog reference circuit to extract the reference curves which are then digitally processed to emulate the characteristics of a high power system. The proposed simulator has been successfully used to evaluate the dynamic performance of a commercial solar power inverter and its MPPT algorithm in steady-state and transient conditions. The measured closed-loop output impedance has been verified at different operating regions including, constant current and constant voltage. The impedance profile of the proposed simulator matches the impedance of actual PV generator. The proposed PV source simulator consists of two power switching stages. The three-phase ac-dc rectifier stage is a new dual boost topology that is reliable and highly efficient, whereas the second-stage, the three-phase dc-dc converter helps improve system transient response though producing low output voltage and current ripples. The Simulation results illustrate the proposed system has achieved high two-stage efficiency and fast transient response time relative to MPPT algorithms. With a potential of high reliability, high efficiency, and fast transient response, the proposed system architecture is well suited for high-power PV source simulator. Further improvement of the simulator response can be obtained with the increase of the number of phases of the output dc-dc stage.

REFERENCES

- [1] Q. Li and P. Wolfs, "A review of the single phase photovoltaic module integrated converter topologies with three different dc link configurations," IEEE Trans. Power Electron., vol. 23, no. 3, pp. 1320–1333, May 2008.
- [2] E. Koutroulis, K. Kalaitzakis, and N. Voulgaris, "Development of a microcontroller-based photovoltaic maximum power point tracking control system," IEEE Trans. Power Electron., vol. 16, no. 1, pp. 46–54, Jan. 2001.
- [3] M. C. Di Piazza, M. Pucci, A. Ragusa, and G. Vitale, "A grid-connected system based on a real time PV emulator: design and experimental set-up,"

in Proc. 36th Annu. IEEE IECON Conf., 2010, pp. 3237–3243.

[4] L. Zhang, K. Sun, L. Feng, H. Wu, and Y. Xing, “A family of neutral point clamped full-bridge topologies for transformerless photovoltaic grid-tied inverters,” *IEEE Trans. Power Electron.*, vol. 28, no. 2, pp. 730–739, Feb. 2013.

[5] G. Vachtsevanos and K. Kalaitzakis, “A hybrid photovoltaic simulator for utility interactive studies,” *IEEE Trans. Energy Convers.*, vol. EC-2, no. 2, pp. 227–231, Jun. 1987.

[6] S. Jiang, D. Cao, Y. Li, and F. Peng, “Grid-connected boost-half-bridge photovoltaic microinverter system using repetitive current control and maximum power point tracking,” *IEEE Trans. Power Electron.*, vol. 27, no. 11, pp. 4711–4722, Nov. 2012.

[7] Y. Chen and M. Smedley, “A const-effective single-stage inverter with maximum power point tracking,” *IEEE Trans. Power Electron.*, vol. 19, no. 5, pp. 1289–1294, Sep. 2004.

[8] T. Esum and P. Chapman, “Comparison of photovoltaic array maximum power point tracking techniques,” *IEEE Trans. Power Electron.*, vol. 22, no. 2, pp. 439–449, Jun. 2007.

[9] N. Femia, G. Petrone, G. Spagnuolo, and M. Vitelli, “Optimization of perturb and observe maximum power point tracking method,” *IEEE Trans. Power Electron.*, vol. 20, no. 4, pp. 963–973, Jul. 2005.

[10] Y. Kuo, T. Liang, and J. Chen, “Novel maximum-power-point-tracking controller for photovoltaic energy conversion system,” *IEEE Trans. Power Electron.*, vol. 48, no. 3, pp. 594–601, Jun. 2001.

Design a Digital Fuel Indicator for Determine the Mileage of Engine

Aditya Bumanapalli^{*1}, N.Rajeswaran^{#2}, N.Venkateswaralu^{#3}, Ch.Narendra kumar^{#4}

^{1*}Department ECE, VNR VJIET, Hyderabad, India

^{2,3,4#}Department EEE, Malla Reddy Engineering College,
Secunderabad, India

Abstract: Nowadays because of the increase in fuel cost throughout the country, there has been a big problem of mileage; sometimes the user gets stuck in an unknown zone since they forget to check the fuel level. By indicating mileage to user the excessive usage of fuel can be controlled and the problem can be minimized. The design proposed in this paper will be helpful for controlling the fuel flow in vehicles, also continuously displaying the fuel left indicating the kilometers it can cover; with this controlling the fuel can be done by units placed in the fuel tank and when the fuel tank is empty an indication for the driver will be given that the fuel is empty and automatically the vehicle will turn off. This proposed design is developed on the basis of PIC 16F877A, used to identify the fuel level in the vehicle. For indication fuel present in the vehicle LCD display is an output unit. Fuel level for the user and how much distance it can cover is shown. So, the user can drive at the level of the fuel. The system is effective and efficient, can be easily debugged and mostly cost efficient.

Keywords — Controller, LCD Interfacing, Monitoring system and Digital Design.

I. INTRODUCTION

The existing fuel indicating system in vehicle uses analog and digital visuals for showing approximate status of fuel level, not presenting the quantity in numerical [1]. This system referred shows the fuel level in numerical form by using LCD. In India, mileage problem has emerged to be a big problem leading to users getting stuck in unknown zone since they forget to check the fuel level. This proposed design can provide a way to stop this problem and control the excessive usage of the fuel to the user by indicating mileage [2-3].

This proposed design will be helpful to control the flow of the fuel in the vehicle, also continuously displays the fuel left and the kilometer it can cover. This is done by controlling the fuel usage with the help of units placed in the fuel tank and when the fuel tank gets empty an indication is given for the driver that the fuel is empty and the vehicle will turn off. On the basis of PIC 16F877A development of this design is done and to indicate the fuel that is present in the vehicle LCD display is used as output unit [4]. The Characters received from the controller unit is just displayed as well as the fuel level and the distance it can travel, so that the user can drive at the

level of the fuel. The system is effective at all times, debugged farther and mostly cost effective [5].

II. PROPOSED DESIGN

A. Level Sensing Section

In Fig.1 Fuel level sensor is designed for precision fuel level measurement in all kinds of vehicles tanks and it is used as a standard fuel level sensor.



Fig. 1 Block diagram of level sensing unit

To obtain the reliable information about current fuel volume in vehicle tank and define the vehicle fuelling volume we used this sensor. This interface unit is used to detect the fuel theft from the tank and also carry out the remote tank monitoring for determine the fuel consumption and possibility of sealing [6].

B. RPM Sensing Section

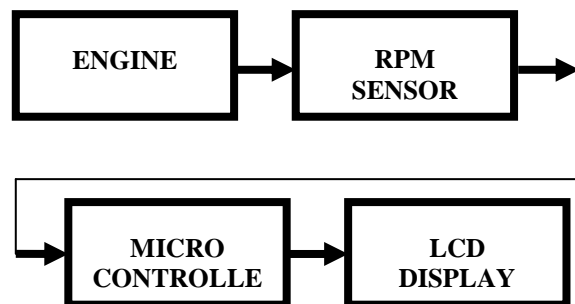


Fig. 1 RPM Block

In Fig.2 RPM Meter used to feed continuous data of RPM status to Controller for Speed Calculation. LCD display is an output unit which displays received character from Controller unit. In vehicle Engine RPM is using the electric signal from the ignition or engine management system [7-8].

C. LCD Section

A Liquid Crystal Display (LCD) is an output unit. In Fig.3 displays the Fuel Capacity in Numerical Value and it displays the distance we can cover.

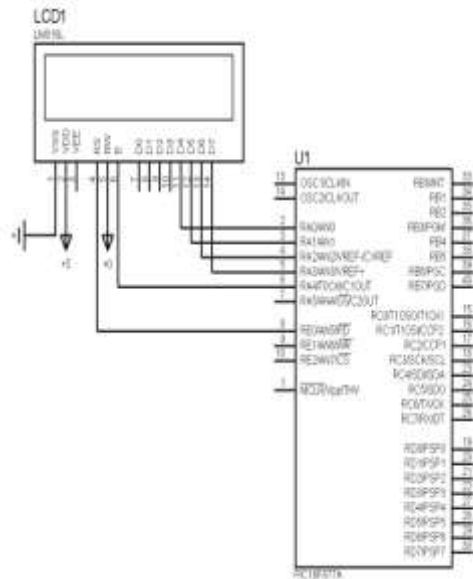


Fig. 3 LCD Interfacing with controller

D. Keyboard Section

In Fig.4 3x4 Matrix Keyboard is used to give the Set Speed, Run Speed, Total mileage to be covered and to set the reserve capacity.

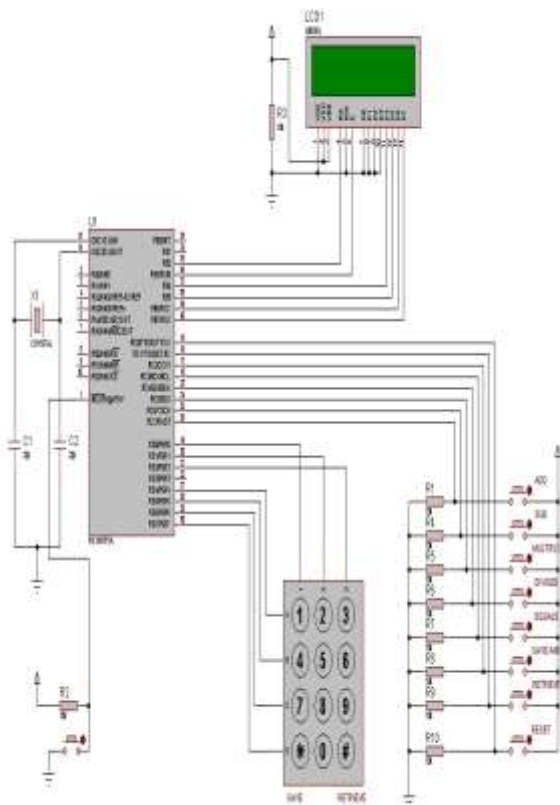


Fig. 4 Keyboard Interfacing with controller

III.HARDWARE UNIT

In Fig.5, microcontroller that has been used for this design. PIC microcontroller is the first RISC based microcontroller fabricated in CMOS (Complementary Metal Oxide Semiconductor) that uses separate bus for instruction and data allowing simultaneous access of program and data memory. The main advantage of CMOS and RISC combination is low power consumption resulting in a very small chip size with a small pin count.

A. Core Features

- High-performance RISC CPU
- Only 35 single word instructions to learn
- All single cycle instructions except for program branches which are two cycle
- Operating speed: DC - 20 MHz clock input
DC - 200 ns instruction cycle
- Up to 8K x 14 words of Flash Program Memory,
Up to 368 x 8 bytes of Data Memory (RAM)
Up to 256 x 8 bytes of EEPROM data memory
- Pin out compatible to the PIC16C73/74/76/77
- Interrupt capability (up to 14 internal/external
- Eight level deep hardware stack
- Direct, indirect, and relative addressing modes
- Power-on Reset (POR)

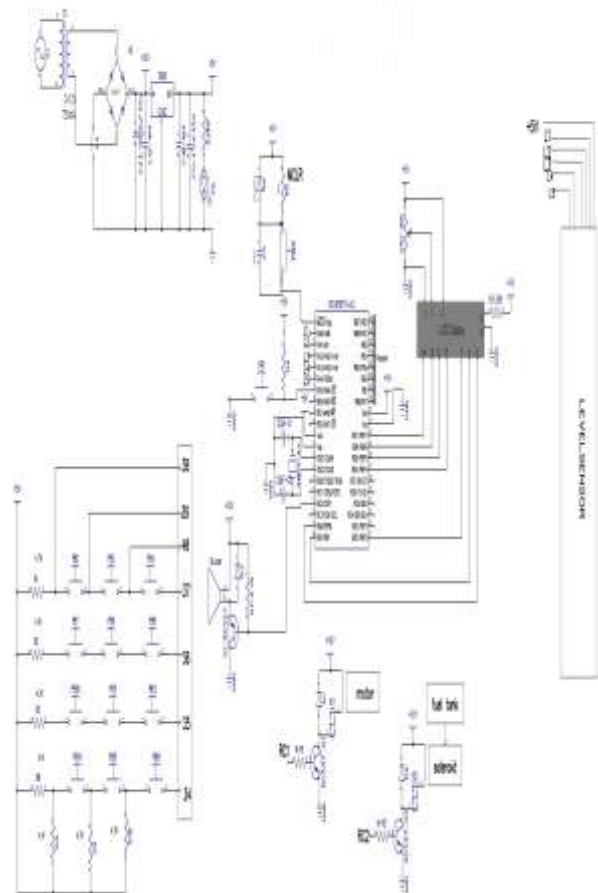


Fig. 5 Proposed design unit

- Power-up Timer (PWRT) and Oscillator Start-up Timer (OST)
- Watchdog Timer (WDT) with its own on-chip RC Oscillator for reliable operation
- Programmable code-protection
- Power saving SLEEP mode
- Selectable oscillator options
- Low-power, high-speed CMOS EPROM/EEPROM technology
- In-Circuit Serial Programming (ICSP) via two pins
- Only single 5V source needed for programming capability
- In-Circuit Debugging via two pins
- Processor read/write access to program memory
- Wide operating voltage range: 2.5V to 5.5V
- High Sink/Source Current: 25 mA

IV. RESULTS

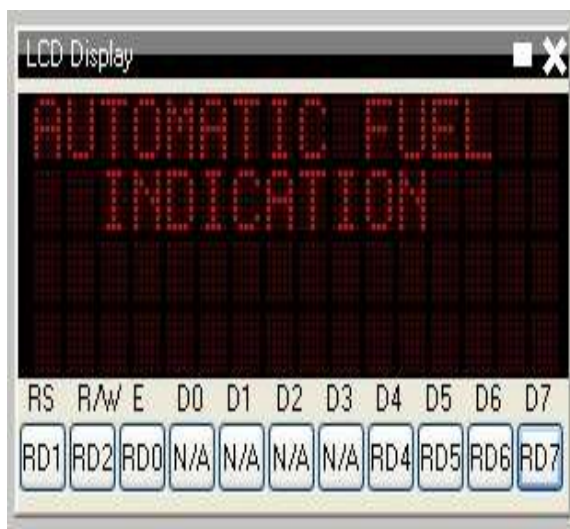


Fig. 6 LCD Output of proposed unit

Various microcontrollers offer different kinds of memories. EEPROM, EPROM, FLASH etc. are some of the memories of which FLASH is the most recently developed. Technology that is used in PIC16F877 is flash technology, so that data is retained even when the power is switched off. Easy Programming and Erasing are other features of PIC16F877. CCS COMPILER is integrated C

development environment gives developers the capability to quickly produce very efficient code from an easily maintainable high level language.

V. CONCLUSIONS

In order to overcome such difficulties, this proposal can be used to control the excessive consumption of fuel in vehicle by indicating mileage. Here we conclude that the system is used to identify the level of the fuel present in the fuel tank also the system predict the mileage of the vehicle and further some vehicles didn't have reserve capacity, for such case this proposal might be very useful.

REFERENCES

- [1]. B. Naresh Kumar Reddy; M. Naraimhulu; S. V. Sai Prasad; K. Khaja Babu; S. V. Jagadeesh Chandra, "An Efficient Online Mileage Indicator by Using Sensors for New Generation Automobiles", 2013 2nd International Conference on Advanced Computing, Networking and Security, pp. 199 - 203, 2013.
- [2]. K. Burak Dalci, Kayhan Gulez, T. Veli Mumcu (2004), "The Design of the Measurement Circuit using Ultrasonic Sound Waves for Fuel Level of Automobile Tanks and the Detection of Bad Sectors of Tank by Neural Networks" Yildiz Technical University, Istanbul, Turkey.
- [3]. Terzic, Nagarajah, R. Alamgir (2012), "A Neural Network Approach to Fluid Quantity Measurement in Dynamic Environments-Capacitive Sensing Technology" Springer, XI, 138p, 95 illus, 19 illus. in color, ISBN: 978-1-4471-4059-7.
- [4]. Suresh Babu C. S, Shashidhar Y M (2006), "An Intelligent Online Mileage Indicator for new generation Automobiles", Malnad College of Engineering, Hassan, Karnataka.
- [5]. Jay J. Ely, Truong X. Nguyen, Kenneth L. Dudley, Stephen Scarce, Fred Beck, Manohar D (2000), "An investigation of EME as a potential cause of fuel tank || NASA Langley Research Center, Hampton, Virginia.
- [6]. Wang S ujing, Wang Lide, Shen Ping, Liu Biao, Nie Xiaobo (2008), "Research on Electronically Controlled Fuel Injection System" Department of Electrical Engineering, University of Beijing Jiaotong, Beijing, China.
- [7]. U. Schmid and H. Seidel (2005), "An Injection Quantity Sensor for Automotive Applications" Saarland University, Faculty of Natural Sciences and Technology, Saarbruecken, Germany
- [8]. Claire D'Agostino; Alexandre Saidi; Gilles Scourarnec; Liming Chen, "Rational truck driving and its correlated driving features in extra-urban areas", 2014 IEEE Intelligent Vehicles Symposium Proceedings , pp. 1199 - 1204, 2014.

Analysis of the Performance of the Bidirectional Three-Level and Five Level DC–DC Converter

KOTA VENKATA PADMA

M-tech Scholar

Department of Electrical & Electronics Engineering,
Mallareddy Engineering College(Autonomous),
Maissammaguda,Secundrabad 50010;
Telangana, India.
Email:padma.appireddy@gmail.com

CH.NARENDRA KUMAR

Assistant Professor

Department of Electrical & Electronics Engineering,
Mallareddy Engineering College(Autonomous),
Maissammaguda,Secundrabad 50010;
Telangana, India.
Email:chnk.eee@gmail.com

Abstract—In this paper Bidirectional Five-Level DC–DC Converter is implemented for automotive applications. Bidirectional dc/dc converter is used in battery/ultra-capacitor electric vehicles. a three-level non-isolated bidirectional dc/dc converter (TLC) as the power electronics interface between the battery and the UC, instead of a conventional two-quadrant buck/ boost converter (CBC), which would increase the conversion efficiency and reduce the size of the magnetic components. In this regard, the Five-level converter was analyzed and comprehensively compared with three level CBC and interleaved bidirectional converter in terms of magnetic component size and efficiency considering a UDDS drive cycle where the battery and UC power are split using three-level converter. Particularly in higher switching frequencies, the efficiency of this converter decreases due to increased switching losses. This paper has proposed using a five-level non-isolated bidirectional dc/dc converter (TLC) as the power electronics interface between the battery and the UC, instead of a conventional three level buck/ boost converter (CBC). The simulation results are presented by using Matlab/Simulink software.

Index Terms—Electric vehicles (EVs), interleaved converter, non-isolated dc–dc converter, three-level converter, Ultra capacitor (UC).

I. INTRODUCTION

Electrochemical double layer capacitors (EDLC), well known as the ultra-capacitors, have received lot of attention in power conversion application. They have been used in controlled industrial electric drives, traction and automotive drives; uninterruptible power supplies (UPS) and active filters. Fig.1 shows simplified block diagram of a controlled electric drive equipped with an ultra-capacitor. The ultra-capacitor is used to store the drive braking energy when the drive is braking. The stored energy is recovered when the drive operates in motoring mode [1]. Moreover, the ultra-capacitor powers the drive when the power supply is not available, for example the mains short interruptions.

Nowadays' ultra-capacitors are composed of two electrodes separated by a porous membrane, so-called a separator, and impregnated by a solvent electrolyte [2]. The electrodes are made of porous conducting material such as activated carbon. Specific surface area of the electrode is as high as 2000m²/g. Such a large surface area and very thin layer of the charges (in order of nm)

gives specific capacitance up to 250F/g. Rated voltage of the ultra-capacitor cell is determined by the decomposition voltage of the electrolyte [3]. Typical cell voltage is 1 to 2.8V, depending on the electrolyte technology. To obtain higher working voltage that is determined by the application, elementary cells are series connected into one capacitor module. Ultra-capacitors as energy storage devices have found very wide application in power conversion due to their advantages over the conventional capacitors and electro-chemical batteries; high energy and power density, high efficiency, high cycling capability and long life. To achieve the drive system flexibility and high efficiency, a switching mode power converter is used as a link between the ultra-capacitor and the drive dc bus. The converter is controlled in the way depending on the system requirements; control of the dc bus voltage, the ultra-capacitor state of charge, active sharing of the energy between the drive and ultra-capacitor and so on [4-6].

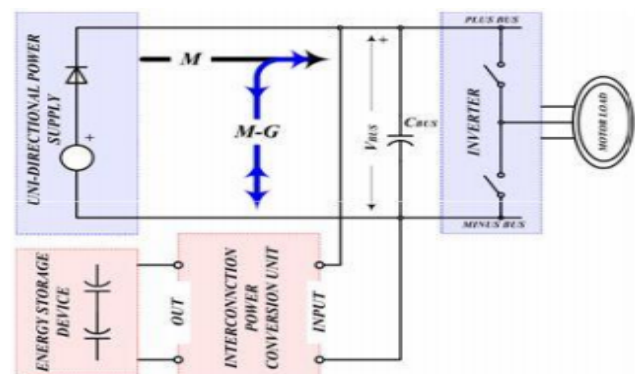


Fig.1. Controlled electric drive system with energy storage device.

Most of dc-dc converter topologies are based on ordinary two-level single-phase or multiphase interleaved topologies. The main drawback of these topologies is the fact that the switches are rated on the full dc bus voltage. As the dc bus voltage may go up to 800V, even more, the switches are rated on 1200V. This becomes an issue if the converter switching frequency is quite high; let us say above 20kHz. Two-level dc-dc converter with soft switching has been presented. This solution offers lower switching losses. However, since the converter operates in discontinuous conduction mode (DCM), the peak current

and ripple current are quite greater than of that one operates in continuous conduction mode (CCM) [7-8]. This causes problem of the inductor losses, particularly the core losses. Isolated dc-dc converter topologies with soft switching have been analyzed. These topologies are attractive solution when ratio between the dc bus voltage and the ultra-capacitor voltage is high, greater than 2. If the ratio is lower than 2, the efficiency is lower than that of a non-isolated topology. Three-level converters are well adopted solution in applications with high input voltage and high switching frequency. The switches are stressed on half of the total dc bus voltage. This allow us to use lower voltage rated switches having better switching and conduction performance compared to the switches rated on the full blocking voltage.

Power converters synthesizing more than two voltage levels, such as the neutral point clamped (NPC), cascaded H-bridge (CHB) and flying capacitor (FC), are traditionally known as multilevel converters. Usually, the multilevel topology is used in medium or high voltage inverter applications [9]. The CHB topology is typically used with multiple cascaded DABs to achieve higher voltages. In the CHB topology, a DAB module itself does not synthesize multilevel (e.g., 3L, 5L, and so on) voltages, like

NPC or FC. Because of the simple control and modulation scheme along with the simpler circuit structure, the 3L NPC is ahead of others in various industrial applications [10]. Very few works have been published on ML-DAB. A silicon carbide junction gate field-effect transistor (SiC-JFET) based 25-kW, high switching frequency DAB has been proposed in [11], where both primary and secondary bridges produce two-level voltages, although the secondary side bridge is formed in the NPC configuration. A detailed analysis on a semi-dual active bridge (S-DAB) has been presented, where the primary and secondary bridges produce 2L and 3L voltage waveforms, respectively, which are phase-shifted to control the power flow. The concept of symmetric modulation for 2L-to-5L bridge voltages with an NPC-based secondary bridge has been introduced by the authors in [12], which has the advantage of having simple mathematical representation and a minimum number of parameters to define the voltage waveforms and to control the power flow through the ML-DAB. In [13], an NPC-based multilevel DAB is reported with capacitor voltage balancing.

II. DC-DC CONVERTER

Basic dc-dc converters such as buck and boost converters (and their derivatives) do not have bidirectional power flow capability. This limitation is due to the presence of diodes in their structure which prevents reverse current flow. In general, a unidirectional dc-dc converter can be turned into a bidirectional converter by replacing the diodes with a controllable switch in its structure. The

bidirectional dc-dc converter along with energy storage has become a promising option for many power related systems, including hybrid vehicle, fuel cell vehicle, renewable energy system and so forth. It not only reduces the cost and improves efficiency, but also improves the performance of the system. In the electric vehicle applications, an auxiliary energy storage battery absorbs the regenerated energy fed back by the electric machine. In addition, bidirectional dc-dc converter is also required to draw power from the auxiliary battery to boost the high-voltage bus during vehicle starting, accelerate and hill climbing. With its ability to reverse the direction of the current flow, and thereby power, the bidirectional dc-dc converters are being increasingly used to achieve power transfer between two dc power sources in either direction. In renewable energy applications, the multiple-input bidirectional dc-dc converter can be used to combine different types of energy sources. This bidirectional dc-dc converter features galvanic isolation between the load and the fuel cell, bidirectional power flow, capability to match different voltage levels, fast response to the transient load demand, etc. Recently, clean energy resources such as photovoltaic arrays and wind turbines have been exploited for developing renewable electric power generation systems. The bidirectional dc-dc converter is often used to transfer the solar energy to the capacitive energy source during the sunny time, while to deliver energy to the load when the dc bus voltage is low. Most of the existing bidirectional dc-dc converters fall into the generic circuit structure illustrated in Figure .2. , which is characterized by a current fed or voltage fed on one side. Based on the placement of the auxiliary energy storage, the bidirectional dc-dc converter can be categorized into buck and boost type. The buck type is to have energy storage placed on the high voltage side, and the boost type is to have it placed on the low voltage side. To realize the double sided power flow in bidirectional dc-dc converters, the switch cell should carry the current on both directions. It is usually implemented with a unidirectional semiconductor power switch such as power MOSFET (Metal-Oxide-Semiconductor-Field-Effect-Transistor) or IGBT (Insulated Gate Bipolar Transistor) in parallel with a diode; because the double sided current flow power switch is not available.

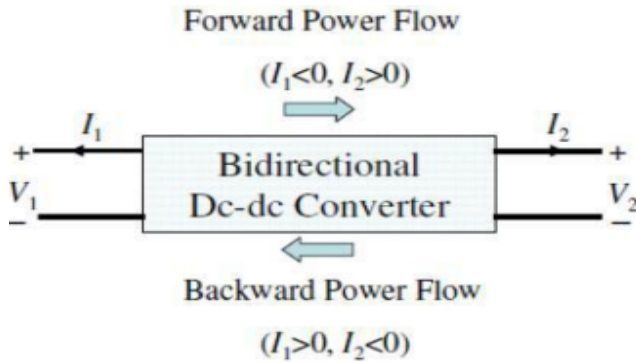


Figure 2. Illustration of bidirectional power flow.

III. BIDIRECTIONAL THREE-LEVEL DC-DC CONVERTER

In a battery/UC-powered drivetrain, where the battery is connected to the high-voltage dc link via a bidirectional converter, the converter is “power controlled” through stepping-up the battery voltage during propulsion and stepping-down the high voltage dc link to the battery voltage during regenerative braking. A majority of the studies in the literature use the conventional two-level buck/boost converter (CBC) due to its simple structure and control [24]–[31]. However, in high-power applications, the boost inductor becomes the major component that increases the volume, weight, and cost of the system. Moreover, high-voltage switches must be used, which, in turn, causes higher losses. By using TLC, significant improvements can be achieved over the CBC.

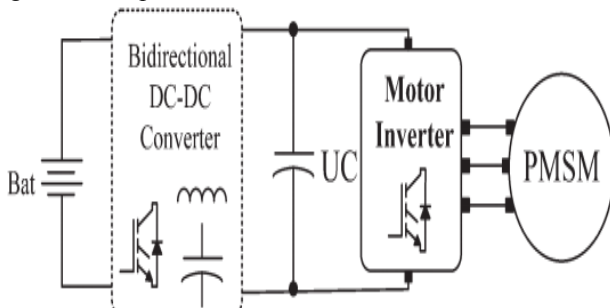


Fig. 3. Drivetrain of the battery/UC vehicle with a bidirectional converter.

The switching scheme for the TLC converter is given in Fig. 5. The switch turn-on times are phase-shifted, resulting in an effective inductor current ripple frequency that is equal to twice the switching frequency. This effective period is shown as T_{seff} in Fig. 5. The boost and buck operation modes of the TLC are shown in Figs. 6 and 7, respectively. Since operations of the buck and boost modes are similar, only boost mode is explained. The operation of the circuit can be divided into four modes. Based on the duty cycle value, the sequence of the equivalent circuits is separated into two. The climax value of the duty cycle of the switches, i.e., d , is 0.5. Basically, if $d < 0.5$, the sequence of equivalent circuits is IV–II–IV–III and keeps repeating. Since the control signals of each switch is displaced by 180° , as the duty cycle gets

higher than 0.5, the control signals begin to overlap. This overlap causes a new equivalent circuit to emerge. The new equivalent circuit sequence becomes I–II–I–III. The output-voltage-to-input-voltage ratio for continuous conduction mode (CCM) operation can be found through analyzing the inductor current ripple within one cycle of the effective switching period. When $d > 0.5$, the voltage conversion ratio can be expressed as

$$\frac{V_{UC}}{V_B} = \frac{2}{1 - d_{\text{eff}}} \quad (1)$$

Where d_{eff} is

$$d_{\text{eff}} = (d_{s2} - 0.5) + (d_{s3} - 0.5) \quad (2)$$

Here, d_{s2} and d_{s3} denote the duty cycles of switches S_2 and S_3 . It is worth mentioning that the duty cycles of S_2 and S_3 are the same; hence, the effective duty cycle can be rewritten as

$$d_{\text{eff}} = 2d - 1 \quad (3)$$

Where $d = d_{s2} = d_{s3}$. The output-voltage-to-input-voltage ratio, when $d < 0.5$, can be found by equalizing mode II or III and mode IV, i.e.,

$$\frac{V_{UC}}{V_B} = \frac{2}{2 - d_{\text{eff}}} \quad (4)$$

The effective duty cycle for this mode is the sum of the individual duty cycles

$$d_{\text{eff}} = d_{s2} + d_{s3} = 2d \quad (5)$$

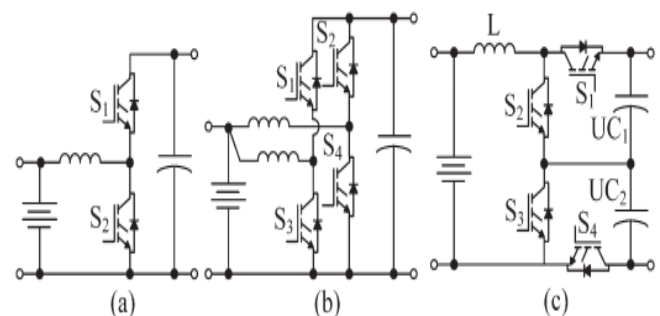


Fig. 4. Non isolated bidirectional buck/boost converters. (a) Two-level (CBC). (b) Interleaved (BIC). (c) Three-level (TLC).

IV. COMPARISON OF THREE-LEVEL CONVERTER WITH THE STATE-OF-THE-ART CONVERTERS

TLC provides several advantages over the state-of-the-art CBC and BIC converters. Switching losses highly depend on the voltage applied across the switch. Particularly, even without soft switching, the switching loss of the parasitic capacitance can be significantly reduced in comparison to CBC as the switches are subjected to half

the output voltage. In fact, the parasitic capacitance losses are expected to be even lower as low-voltage switches are used. On the passive component side, the diode reverse recovery losses are lower as reverse voltage is only half the output voltage, and low-voltage diodes typically recover faster. This section compares bidirectional buck/boost dc-dc converter topologies, given in Fig. 2, in terms of magnetic component size and efficiency over the full drive cycle range, considering the dynamic variations of the battery and UC voltages as well as the power processed by the converter.

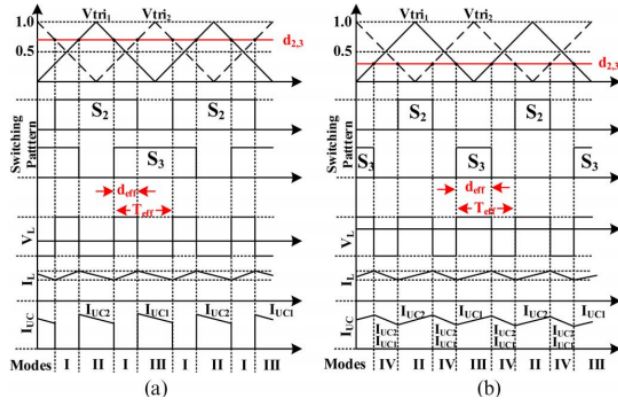


Fig. 5. Switching scheme of the three-level converter for boost mode. (a) $d > 0.5$. (b) $d < 0.5$.

A. Drive Cycle Characteristic

The efficiency of the bidirectional converter varies to a great extent with respect to the load power and dynamic voltage variations of the energy sources. In the drivetrain configuration in Fig. 1, the power of the converter is equal to the power requested from/to the battery. The sizing and power/energy management of energy storage systems are important for the efficiency of the system, as it impacts the voltages of the energy sources and the battery power. In this study, the UDDS drive cycle, which simulates an urban route of 7.5 mi with frequent stops, is chosen. The maximum and average speeds are 56.7 and 19.6 mi/h. It is assumed that daily commute consists of four UDDS drive cycles, corresponding to 30 mi. A 15.8-kWh Li-ion battery pack with a nominal voltage of 350 V, which goes up to 407 V at a fully charged state, is considered. The battery voltage varies between 380 and 350 V in the linear operation region. The UC voltage is limited by the minimum operation voltage of the inverter and set to 350 V as it is connected to the dc link directly, whereas the upper voltage limit is set to 600 V. As energy stored in the UC is proportional to the square

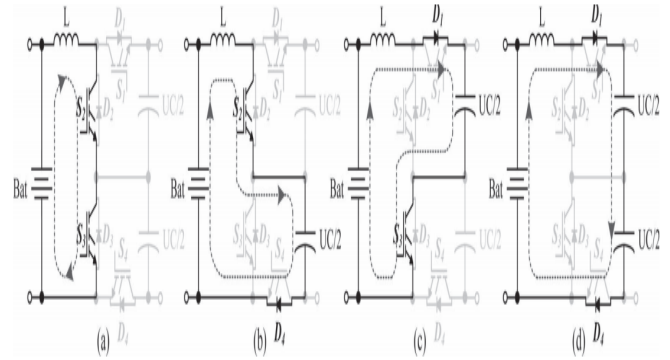


Fig. 6. Boost-mode operation. (a) Mode I (S2 and S3 are on). (b) Mode II (S2 and D4 are on). (c) Mode III (D1 and S3 are on). (d) Mode IV (D1 and D4 are on).

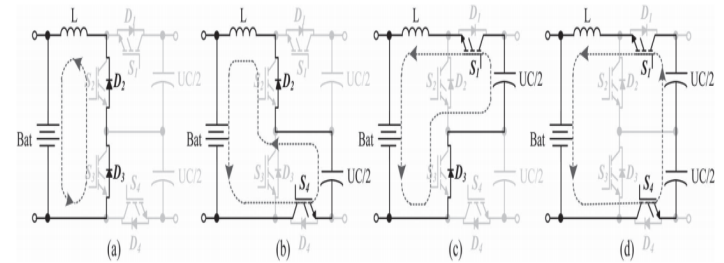


Fig. 7. Buck-mode operation. (a) Mode I (D2 and D3 are on). (b) Mode II (D2 and S4 are on). (c) Mode III (S1 and D3 are on). (d) Mode IV (S1 and S4 are on).

B. Magnetic Component Size

The size of the magnetic component is related to the peak flux density, which, in turn, is related to the peak current passing through the core. In CBC, the current ripple of the battery can be expressed as

$$\Delta i_{\text{bat_boost}}(d) = \frac{V_o}{Lf_s} d(1-d) \quad (6)$$

The battery current ripple for TLC is

$$\Delta i_{\text{bat_TL}}(d) = \frac{V_o}{2Lf_s} d_{\text{eff}}(1-d_{\text{eff}}) \quad (7)$$

For the TLC converter, the relation between the current ripple and duty cycle of a switch can be found by substituting the effective duty cycles given in (3) and (5), i.e.,

$$\Delta i_{\text{bat_TL}}(d) = \begin{cases} \frac{V_o}{Lf_s} d(1-2d) & |_{d \leq 0.5} \\ \frac{V_o}{Lf_s} (1-d)(2d-1) & |_{d > 0.5} \end{cases} \quad (8)$$

The input current of the BIC converter is the sum of two inductor currents. When the duty cycles of the switches are less than 50%, the input current ripple becomes

$$\Delta i_{\text{bat_Interleaved}}(d) = \frac{2V_{\text{in}} - V_o}{Lf_s} \left(1 - \frac{V_{\text{in}}}{V_o}\right) \quad (9)$$

When the duty cycle is greater than 50%, the input current ripple is expressed as

$$\Delta i_{\text{bat_Interleaved}}(d) = \frac{V_o - 2V_{\text{in}}}{Lf_s} \left(\frac{V_{\text{in}}}{V_o} \right) \quad (10)$$

Where the current ripple of each interleaving inductor is the same as (6), i.e.,

$$\Delta i_{L_Interleaved}(d) = \frac{V_o}{Lf_s} d(1-d) \quad (11)$$

The maximum input ripple current for BIC and TLC occur at 25% and 75% duty cycles, where for CBC, it occurs at 50%. For the same maximum battery current ripple, CBC requires four times larger inductance compared with TLC.

To calculate the approximate size of the magnetic component, the core geometry approach is utilized. To estimate the core size, several parameters such as peak current (I_{peak}), rms current (I_{rms}), maximum flux density (B_{max}), regulation (α), maximum output power ($P_{o,\text{max}}$), required inductance (L), and window utilization factor (K_u) should be determined. α is defined as the ratio of the voltage drop across the inductor to the output voltage and is related with the copper losses. The energy handling capability, i.e., E , is a function of α , core geometry coefficient K_g , and an electrical coefficient K_e , which is determined by the magnetic and electrical conditions. Thus

$$E^2 = K_g \cdot K_e \cdot \alpha \quad (12)$$

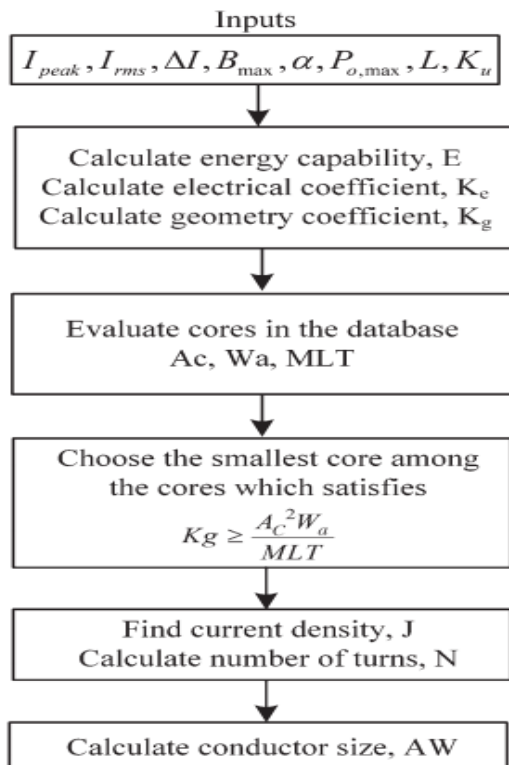


Fig. 8. Flowchart of the inductor design algorithm based on the core geometry estimation approach.

Where E is 0.5LI 2peak. The electrical coefficient is a function of the magnetic and electrical quantities as

$$K_g = 0.145 \cdot P_o \cdot B_{\text{max}}^2 \cdot 10^{-4} \quad (13)$$

The estimation approach is based on finding and evaluating K_g . Some core manufacturers directly provide the $K_g[\text{cm}^5]$ value for each core, whereas most of the manufacturers just provide area product $A_c W_a[\text{cm}^4]$, where A_c and W_a denote cross-sectional and winding areas, respectively. The relation between the area product and K_g can be expressed as

$$K_g \geq \frac{A_c^2 \cdot W_a}{MLT} \quad (14)$$

Where MLT is the mean length per turn. The current density can be extracted from the maximum flux density and area product as

$$J = \frac{2 \cdot E \cdot 10^4}{B_{\text{max}} \cdot A_c \cdot W_a \cdot K_u} \quad (15)$$

The current density dictates the wire size, which is

$$A_w = \frac{I_{\text{rms}}}{J} \quad (16)$$

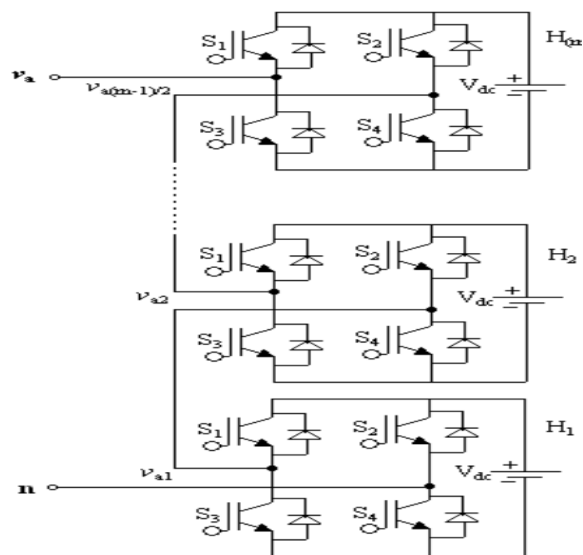
Based on the given wire size and winding area, the number of turns can be calculated as

$$N = \frac{W_a \cdot K_u}{A_w} \quad (17)$$

The flowchart of the inductor core selection is presented in

MULTILEVEL INVERTER

The cascade multilevel inverter consists of a number of H-bridge inverter units with separate dc source for each unit and is connected in cascade or series. Each H-bridge can produce three different voltage levels: $+V_{dc}$, 0 and $-V_{dc}$ by connecting the dc source to ac output side by different combinations of the four switches S_1 , S_2 , S_3 , and S_4 . The ac output of each H-bridge is connected in series such that the synthesized output voltage waveform is the sum of all of the individual H-bridge outputs. By connecting sufficient number of H-bridges in cascade and using proper modulation scheme, a nearly sinusoidal output voltage waveform can be synthesized.



Single-phase cascade multilevel inverter topology.

The number of levels in the output phase voltage and line voltage are $2s+1$ and $4s+1$ respectively, where s is the number of H-bridges used per phase. For example, three H-bridges, five H-bridges and seven H-bridges per phase are required for 5-level, 7-level and multilevel inverter respectively. A typical waveform produced by 5-level CMLI. The magnitude of the ac output phase voltage is the sum of the voltages produced by H-bridges.

INDUCTION MOTOR (IM)

An induction motor is an example of asynchronous AC machine, which consists of a stator and a rotor. This motor is widely used because of its strong features and reasonable cost. A sinusoidal voltage is applied to the stator, in the induction motor, which results in an induced electromagnetic field. A current in the rotor is induced due to this field, which creates another field that tries to align with the stator field, causing the rotor to spin. A slip is created between these fields, when a load is applied to the motor. Compared to the synchronous speed, the rotor speed decreases, at higher slip values. The frequency of the stator voltage controls the synchronous speed. The frequency of the voltage is applied to the stator through power electronic devices, which allows the control of the speed of the motor. The research is using techniques, which implement a constant voltage to frequency ratio. Finally, the torque begins to fall when the motor reaches the synchronous speed. Thus, induction motor synchronous speed is defined by following equation,

$$n_s = \frac{120f}{P}$$

Where f is the frequency of AC supply, n_s is the speed of rotor; p is the number of poles per phase of the motor. By

varying the frequency of control circuit through AC supply, the rotor speed will change.

A. Control Strategy of Induction Motor

Power electronics interface such as three-phase SPWM inverter using constant closed loop Volts / Hertz control scheme is used to control the motor. According to the desired output speed, the amplitude and frequency of the reference (sinusoidal) signals will change. In order to maintain constant magnetic flux in the motor, the ratio of the voltage amplitude to voltage frequency will be kept constant. Hence a closed loop Proportional Integral (PI) controller is implemented to regulate the motor speed to the desired set point. The closed loop speed control is characterized by the measurement of the actual motor speed, which is compared to the reference speed while the error signal is generated. The magnitude and polarity of the error signal correspond to the difference between the actual and required speed. The PI controller generates the corrected motor stator frequency to compensate for the error, based on the speed error.

V.MATLAB/SIMULATION RESULTS

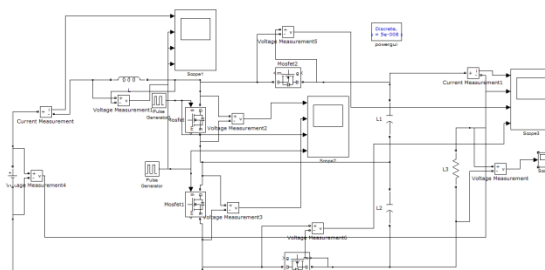
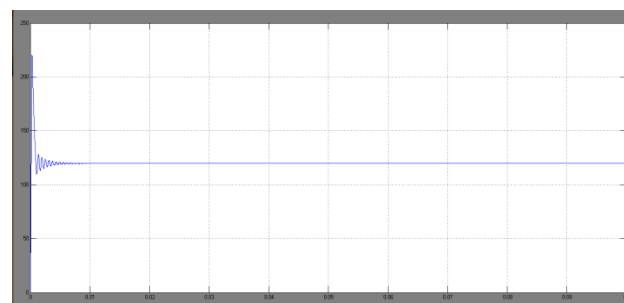
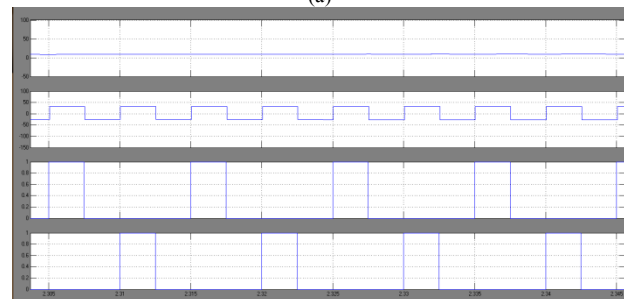


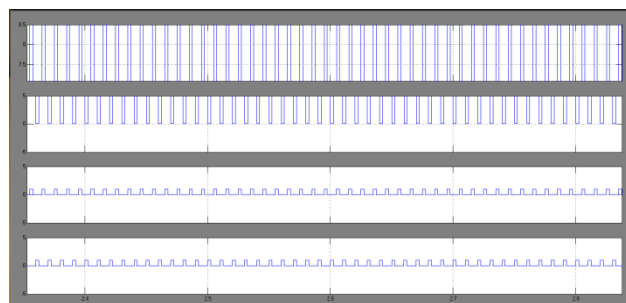
Fig 9 Matlab/simulation circuit if none isolated bidirectional buck/boost converters.



(a)



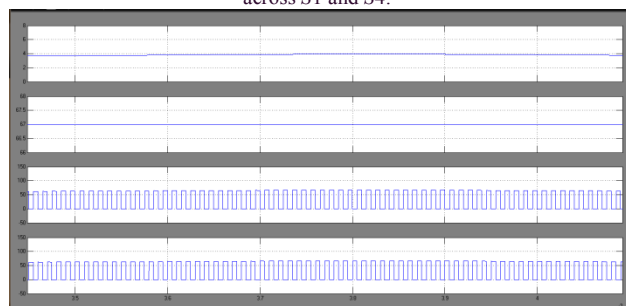
(b)



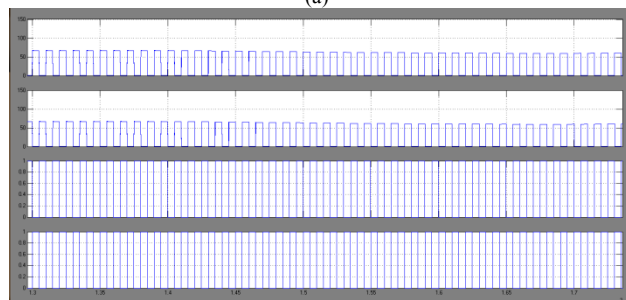
(c)

Fig 10 simulation waveforms for TLC boost mode when $d = 0.25$ ($V_{in} = 90$ V, $V_o = 120$ V, $P_o = 700$ W). (a) Inductor voltage and current.

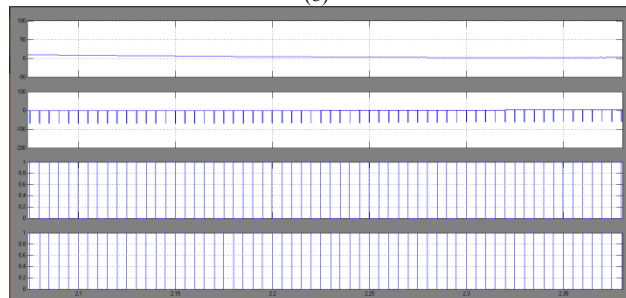
(b) Voltages across S_2 and S_3 . (c) Input voltage, output current, voltages across S_1 and S_4 .



(a)



(b)



(c)

Fig 11 simulation waveforms for TLC boost mode when $d = 0.48$ ($V_{in} = 67$ V, $V_o = 130$ V, $P_o = 500$ W). (a) Inductor voltage and current.

(b) Voltages across S_2 and S_3 . (c) Input voltage, output current, voltages across S_1 and S_4

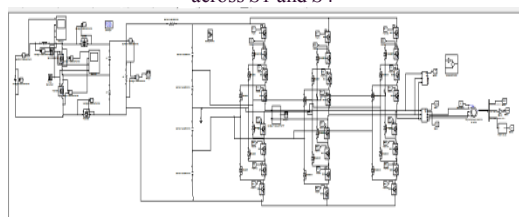


Fig 12 Matlab/simulation circuit if none isolated bidirectional buck/boost converters with three phase five level Induction Motor

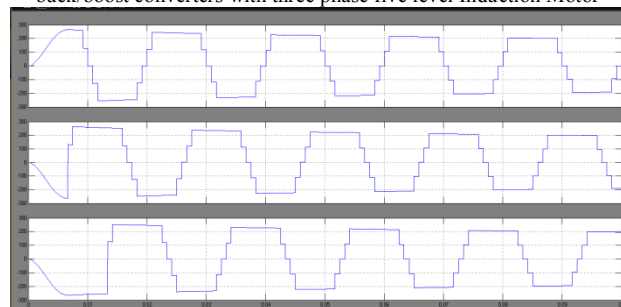


Fig 13 simulation wave form of three phase five level induction motor phase voltage

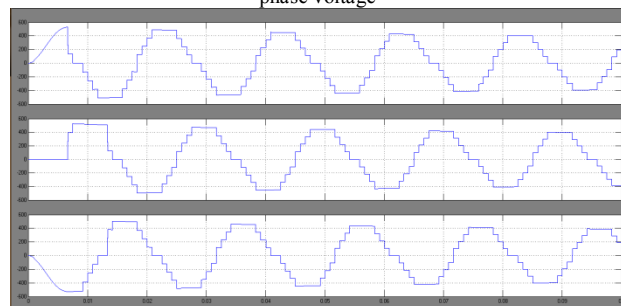


Fig 14 simulation wave form of three phase five level induction motor line current

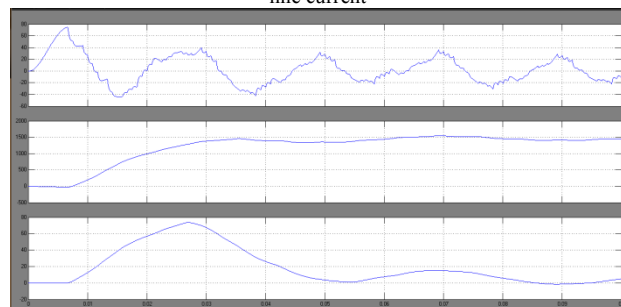


Fig 15 simulation wave form of three phase five level induction motor stator current, speed and torque

VI.CONCLUSION

In battery/UC hybrid EVs, the selection of the bidirectional dc/dc converter topology, which processes the battery power, is of great importance as it is one of the major factors contributing to the size and efficiency of the system. Particularly in higher switching frequencies, the efficiency of this converter decreases due to increased switching losses. This paper has proposed using a three-level non-isolated bidirectional dc/dc converter (TLC) as the power electronics interface between the battery and the UC, instead of a conventional two-quadrant buck/boost converter (CBC), which would increase the conversion efficiency and reduce the size of the magnetic components. The results prove the effective integrated operation of input sources with bidirectional three-level and five level dc/dstructure, through operating four switches in a phase-shifted manner without introducing control complexity and application to the Induction Motor and study the characteristics of Induction Motor.



REFERENCES

- [1]. Serkan Dusmez, Student Member, IEEE, Amin Hasanzadeh, Member, IEEE, and Alireza Khaligh, Senior Member, IEEE” Comparative Analysis of Bidirectional Three-Level DC–DC Converter for Automotive Applications” IEEE Transactions On Industrial Electronics, Vol. 62, No. 5, May 2015
- [2] M. Ortuzar, J. Moreno, and J. Dixon, “Ultra capacitor-based auxiliary energy system for an electric vehicle: Implementation and evaluation,” IEEE Trans. Ind. Electron., vol. 54, no. 4, pp. 2147–2156, Aug. 2007.
- [3] O. Laldin, M. Moshirvaziri, and O. Trescases, “Predictive algorithm for optimizing power flow in hybrid ultra capacitor/battery storage systems for light electric vehicles,” IEEE Trans. Power Electron., vol. 28, no. 12, pp. 3882–3895, Aug. 2013.[4] I. Aharon and A. Kuperman, “Topological overview of powertrains for battery-powered vehicles with range extenders,” IEEE Trans. Power Electron., vol. 26, no. 3, pp. 868–876, Mar. 2011.
- [5] A. Khaligh and Z. Li, “Battery, ultracapacitor, fuel-cell, hybrid energy storage systems for electric, hybrid electric, fuel cell, plug-in hybrid electric vehicles: State-of-art,” IEEE Trans. Veh. Technol., vol. 59, no. 6, pp. 2806–2814, Jul. 2010.
- [6] D. Rotenberg, A. Vahidi, and I. Kolmanovsky, “Ultracapacitor assisted powertrains: Modeling, control, sizing, the impact on fuel economy,” IEEE Trans. Control Syst. Technol., vol. 19, no. 3, pp. 576–589, May 2011.
- [7] W.-S. Liu, J.-F. Chen, T.-J. Liang, R.-L. Lin, and C.-H. Liu, “Analysis, design, control of bidirectional cascaded configuration for a fuel cell hybrid power system,” IEEE Trans. Power Electron., vol. 25, no. 6, pp. 1565–1575, Jun. 2010.
- [8] J. Jia, G. Wang, Y. T. Cham, Y. Wang, and M. Han, “Electrical characteristic study of a hybrid PEMFC and ultra capacitor system,” IEEE Trans. Ind. Electron., vol. 57, no. 6, pp. 1945–1953, Jun. 2010.
- [9] M. H. Todorovic, L. Palma, and P. N. Enjeti, “Design of a wide input range DC–DC converter with a robust power control scheme suitable for fuel cell power conversion,” IEEE Trans. Ind. Electron., vol. 55, no. 3, pp. 1247–1255, Mar. 2008.
- [10] A. Emadi, K. Rajashekara, S. S. Williamson, and S. M. Lukic, “Topological overview of hybrid electric and fuel cell vehicular power system architectures and configurations,” IEEE Trans. Veh. Technol., vol. 54, no. 3, pp. 763–770, May 2005.
- [11] J. Bauman and M. Kazerani, “A comparative study of fuel-cell–battery fuel-cell–ultra capacitor and fuel-cell–battery–ultra capacitor vehicles,” IEEE Trans. Veh. Technol., vol. 57, no. 2, pp. 760–769, Mar. 2008.
- [12] P. Thounthong, V. Chunkag, P. Sethakul, B. Davat, and M. Hinaje, “Comparative study of fuel-cell vehicle hybridization with battery or super capacitor storage device,” IEEE Trans. Veh. Technol., vol. 58, no. 8, pp. 3892–3904, Oct. 2009.
- [13] U. R. Prasanna and A. K. Rathore, “Extended range ZVS active-clamped current-fed full-bridge isolated DC/DC converter for fuel cell applications: Analysis, design, experimental results,” IEEE Trans. Ind. Electron., vol. 60, no. 7, pp. 2661–2672, Jul. 2013.

Asymmetrical Multilevel Inverter for Higher Output Voltage Levels

B.SUJATHA

M-tech Student Scholar

Department of Electrical & Electronics Engineering,

Malla reddy Engineering College, (autonomous);

Ranga reddy secunderbad (Dt); Telangana, India.

Email:m.sujatha.mt@gmail.com

Abstract: Now a days the growth of interest in multilevel inverters has been increasing because there are enormous applications of there in FACTS and industrial drives etc., Although there are many topologies of multilevel inverters in literature, popular among them are cascaded H-bridge. In general the control methods of these cascaded inverters are designed an assumption of having all dc source voltages same for all H-bridges. This paper discusses the abilities of cascaded multilevel inverter to produce more output voltage levels with same number of H-bridges, but with different input voltage ratios. The ideal nature of input dc voltage sources is shown as an advantage in this paper. The proposed inverter is then used to feed an induction motor drive and the simulation results are shown.

Keywords: Asymmetrical cascaded multilevel inverter, induction motor, pulse width modulation technique, v/f control method, synchronous speed.

I. INTRODUCTION

An induction motor is a paradigm of asynchronous AC machine, which consists of a stator and a rotor [1]. This motor is extensively used because of its well-built features and sensible cost. Induction motors are used in many industrial applications such as heating, ventilation, air conditioning systems, waste water treatment plants, blowers, fans, textile mills, and in rolling mills, etc. An electromagnetic field is generated

CH.NARENDER KUMAR

Associate Professor

Department of Electrical & Electronics Engineering,

Malla reddy Engineering College, (autonomous);

Ranga reddy secunderbad (Dt); Telangana, India.

Email.chnk.eee@gmail.com

when sinusoidal voltage is applied to the stator, in the induction motor. A current in the rotor is induced due to this field, which creates an added field that tries to align with the stator field, causing the rotor to revolve. When a load is applied to the motor a slip is formed between these fields. Compared to the synchronous speed, the rotor speed diminishes, at advanced slip values. The frequency of the stator voltage controls the synchronous speed [2]-[3]. The frequency of the voltage is applied to the stator through power electronic devices, which permits the control of the speed of the motor. Finally, the torque begins to fall when the motor reaches the synchronous speed. Thus, induction motor synchronous speed is defined by following equation,

$$N_s = 120f/p$$

Where f is the frequency of AC supply, n, is the speed of rotor; p is the number of poles per phase of the motor. By altering the frequency of control circuit throughout AC supply, the rotor speed will alter. The induction motor speed variation can be effortlessly achieved for a short variety by either stator voltage control or rotor resistance control. But together of these schemes result in very low efficiencies at lesser speeds. On the whole competent design for speed control of induction motor is by altering supply frequency. This not only results in design with wide speed range but also advances the starting performance. If the machine is functioning at speed under base speed, then v/f ratio is to be set aside, so that flux remains stable. This

retains the torque capability of the machine at the same value. But at lesser frequencies, the torque capability reduces and this drop in torque has to be compensated for increasing the applied voltage.

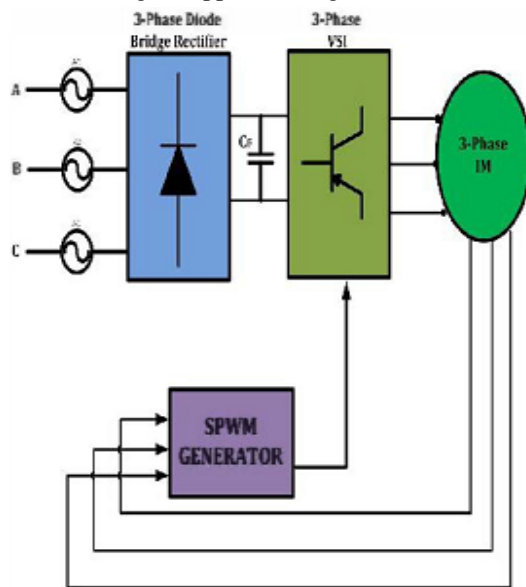


Fig. 1. Block Diagram Schematic of V/f control of YSI fed 3- phase Induction Motor Drive

List of benefits of V/f Control are as follows:

- It provides good range of speed.
- It provides superior operation and momentary concert.
- It has low starting current requirement.
- It has a wider stable operating region.
- Voltage and frequencies reach rated values at base speed.
- The speeding up can be inhibited by controlling the rate of change of supply frequency.
- It is cheap and easy to implement.

Synchronous speed can be controlled by varying the supply frequency. Voltage induced in the stator is $E \propto \phi \omega$ where ϕ is the air-gap flux and ω is the supply frequency. As we can ignore the stator voltage drop we obtain terminal voltage $V \propto \phi$. Thus reducing the frequency without varying the

supply voltage will direct to a raise in the air-gap flux which is undesirable. Hence whenever frequency is diverse in order to control speed, the terminal voltage is also varied so as to maintain the V/f ratio stable. Thus by maintaining a steady V/f ratio, the maximum torque of the motor becomes constant for changing speed. Since voltage and frequency are the significant parameters to be considered for control the speed of induction motor, hence inverters are selected as the front end converters for induction motor, which can controlled together voltage and frequency.

A. Multilevel Inverters: Multilevel inverters have received added awareness for their ability on high-power and medium voltage function and because of former compensation such as high power quality, lower order harmonics, switching losses and improved electromagnetic interference [4], [5]. And also multilevel inverters are promising; they have virtually sinusoidal output-voltage wave forms, Output current with improved harmonic profile, a lesser amount of stressing of electronic components owing to decreased voltages, switching losses that are inferior than those of predictable two-level inverters, a slighter filter size, and worse EMI, all of which make them cheaper, lighter, and more compact. Multilevel inverters make small Common mode voltage; consequently the stress in the bearings of a motor allied to a multilevel motor drive can be condensed. In addition CM voltages can be eliminated by using advanced modulation technique.

Multilevel inverters can draw input current with low distortion. These inverters can operate at equally fundamental frequency and high switching frequency PWM. It should be noted that lower switching frequency means lower switching loss and higher efficiency. These inverters make a stepped voltage waveform by means of a number of dc voltage sources as the input and a suitable arrangement of the power-semiconductor-based devices [6]. Three major structures of the multilevel inverters have been presented: "diode clamped multilevel inverter," "flying capacitor

multilevel inverter," and "cascaded multilevel inverter" [7].

The cascaded multilevel inverter is collected of a number of single-phase H-bridge inverters and is classified into symmetric and asymmetric groups based on the magnitude of dc voltage sources. In the symmetric types, all the dc voltage sources of cascaded H-bridges are having equal magnitudes, whereas in the asymmetric types, the values of the dc voltage sources of all H-bridges are dissimilar. In topical years, a number of topologies with various control techniques have been presented for cascaded multilevel inverters [8]-[9]. In [7] and, diverse symmetric cascaded multilevel inverters have been presented.

The foremost advantage of all these structures is the short variety of dc voltage sources, which is one of the most significant features in determining the cost of the inverter. On the other hand, because some of them utilize an elevated number of bidirectional power switches, a high number of insulated gate bipolar transistors (IGBTs) are necessary, which is the major drawback of these topologies. Consequently, it increases control complexity, circuit size and cost. The major advantage of this asymmetric topology and its algorithms is associated to its ability to create a substantial number of output voltage levels by using a low number of dc voltage sources and power switches but the high diversity in the magnitude of dc voltage sources is their most outstanding disadvantage. Recently, asymmetrical and hybrid multistage topologies are becoming one of the most fascinated research area. In the asymmetrical configurations, the magnitudes of dc voltage supplies are uneven. These topologies diminish the cost and size of the inverter and get better reliability since lesser number of power electronic components capacitors, and dc supplies are used.

The hybrid multistage converters consist of dissimilar multilevel configurations with uneven dc voltage supplies. Bidirectional switches with an suitable control technique can enhance the performance of multilevel inverters in terms of

falling the number of semiconductor components, minimizing the withstanding voltage and achieving the required output voltage with higher levels [10]-[11]. The magnitudes of the utilized dc voltage supplies have been selected in a way that brings the elevated number of voltage levels with an effective application of a fundamental frequency staircase modulation technique. For a single-phase seven-level inverter, 12 power electronic switches are required in both the diode-clamped and the flying-capacitor topologies. Asymmetric voltage technology is used in the cascade H-bridge multilevel inverter to allow more levels of output voltage [12], so the cascade H-bridge multilevel inverter is suitable for applications with increased voltage levels. Two H-bridge inverters with a dc bus voltage of multiple relationships can be connected in cascade to produce a single phase seven-level inverter and eight power electronic switches are used. In this paper a new asymmetric Bi-directional converter topology which uses contradictory ratios of dc voltage sources.

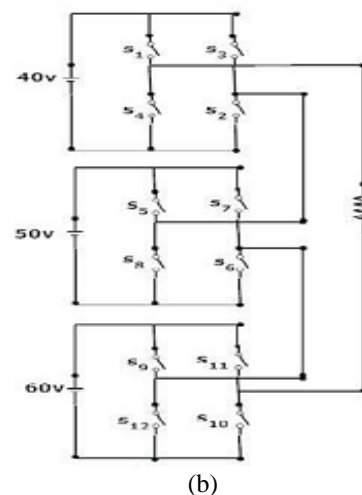
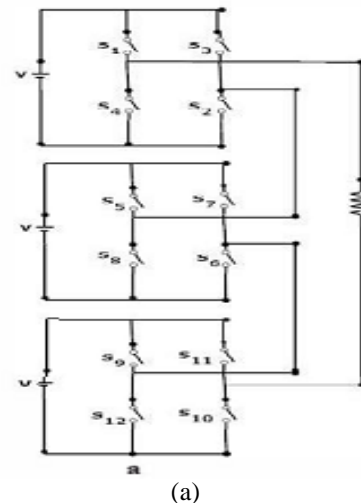
II. PROPOSED CONCEPT

Hybrid Multilevel Inverter was introduced by means of all $3M$ possible output voltages, where M is the number of modules allied in series. Though this inverter uses extremely different DC voltage sources in the relation of 1:3:9 etc. In distinguish, the DC voltage sources consider in this paper are still exceptionally close to each other, they fluctuate only by $\pm 20\%$. The quantity of cells in sequence determines the number of output levels. $3M = 27$ switching states SI , when $M = 3$ cells. With similar DC voltages, there are numerous switching states that create the same output voltages, resulting in $2.M + 1 = 7$ different phase output voltage levels. Uneven DC source voltages direct to an improved number of different output voltage levels. The maximum number of levels is $3M = 27$. With the DC source voltages distributed as $V_{i12} : V_{i13} = 1V_{oc} : 3V_{oc} : 9V_{oc}$, all the dissimilar output voltage levels are consistently spaced. The aim of such an inverter (Hybrid

Multilevel Inverter) has the disadvantage that the preliminary modularity is vanished. Each module must be intended for the equivalent voltage class. When the DC source voltages are uneven but only $\pm 20\%$ unlike from each other, the number of different output voltage levels is also superior. As an instance, we believe a case where one cell has 100 % of its nominal DC voltage, other has 120% and the third one has 80%.

The DC source voltages are in relation of 4:5:6 in this scheme. As can be seen, the voltage levels are approximately the same as in the 1:3:9 case, apart from some levels not there at high complete values of output voltage. In order to consider the possible benefits of using unlike DC voltages, the 4:5:6 relation is used as an instance in the following part. For a first estimation it is abandoned if these differences are introduced by the moment behavior of the DC voltages, or if they are introduced by design and thus can be supposed to be stable. The second case is considered at this time for the sake of simplicity.

The below figure shows the output wave forms the proposed asymmetrical converter. It is clearly seen that the level of inverter varies with the change in the ratios of input voltage. The inverter gives 7 level output voltage when the ratio is 1: 1:1, while it gives 23 level output voltage when the ratio is 4:5:6 and it gives 27 level output voltage when the ratio is 1:3:9. This inverter having 3 bridges connected in series gives different levels of output voltages without changing the circuit except the ratios of input voltages. Switching of the converter is done by following the staircase control technique. Pulse width Modulation technique can also be applied by appropriate calculation of the switching time period.



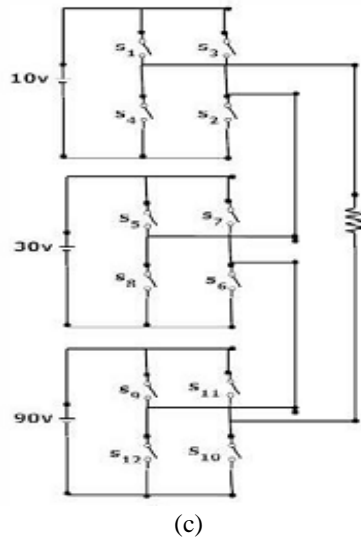


Fig. 2. Proposed asymmetrical cascaded multilevel inverter with different voltage ratios

III. CONTROL SCHEME

This section will discuss in detail a converter consisting of three modules with a DC voltage ratio of $V_{i11}:V_{i12}:V_{i13} = 4V_{oc} : 5V_{oc} : 6V_{oc}$. As can be seen in Fig. 3, this results in a huge number of diverse output voltage levels with an incredibly good voltage resolution. This composition will be compared with the predictable approach with identical DC voltage sources, and with the Hybrid Multilevel Inverter using a 1:3:9 voltage relation. Two different control methods for a single phase converter are offered. Both algorithms imagine a steady sampling interval of the control, T_s . The first one uses a stable switching state during a full sampling interval (step or staircase method), whereas the second one is implemented with a Pulse Width Modulation (PWM method). Both methods receive that the DC source voltages are not steady but variable in time. The definite voltages on the capacitors are therefore calculated, and the phase voltage vector V_{ii} is created. In order to compute all attainable output voltages V_{ol} , the phase voltage vector is multiplied with all 311 possible switching states S_i . This results in an unsorted vector containing all feasible output voltages.

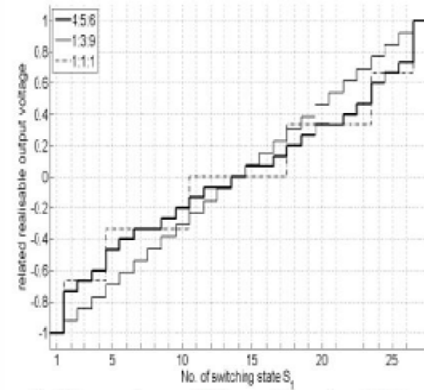


Fig.3. Output voltages of different voltage ratios of CHB

TABLE I. SWITCHING SEQUENCE OF 23-LEVEL CHB INVERTER

Switches Voltage Levels	S1	S2	S3	S4	S5	S6	S7	S8	S9	S10	S11	S12
V_{dc}	1	0	1	0	0	0	1	1	1	1	0	0
$2V_{dc}$	0	0	1	1	1	0	1	0	1	1	0	0
$3V_{dc}$	1	1	0	0	1	1	0	0	0	0	1	1
$4V_{dc}$	1	1	0	0	1	0	1	0	1	0	1	0
$5V_{dc}$	1	0	1	0	1	1	0	0	1	0	1	0
$6V_{dc}$	1	0	1	0	1	0	1	0	1	1	0	0
$7V_{dc}$	0	0	1	1	1	1	0	0	1	1	0	0
$8V_{dc}$	1	1	0	0	1	1	0	0	1	0	1	0
$9V_{dc}$	1	1	0	0	1	0	1	0	1	1	0	0
$10V_{dc}$	1	1	0	0	1	0	1	0	1	1	0	0
$11V_{dc}$	1	0	1	0	1	1	0	0	1	1	0	0
$12V_{dc}$	1	1	0	0	1	1	0	0	1	1	0	0
$13V_{dc}$	1	1	0	0	1	1	0	0	1	1	0	0
$0V_{dc}$	0	1	0	1	0	1	0	1	0	1	0	1
$-V_{dc}$	0	0	1	1	0	1	0	1	0	1	0	1
$-2V_{dc}$	1	1	0	0	0	0	1	1	0	1	0	1
$-3V_{dc}$	0	1	0	1	0	0	1	1	0	1	0	1
$-4V_{dc}$	0	0	1	1	0	0	1	1	0	1	0	1
$-5V_{dc}$	1	1	0	0	1	1	0	0	0	0	1	1
$-6V_{dc}$	0	1	0	1	1	1	0	0	0	0	1	1
$-7V_{dc}$	0	0	1	1	1	1	0	0	0	0	1	1
$-8V_{dc}$	1	1	0	0	0	1	0	1	0	0	1	1
$-9V_{dc}$	0	1	0	1	0	1	0	1	0	0	1	1
$-10V_{dc}$	0	0	1	1	0	1	0	1	0	0	1	1
$-11V_{dc}$	1	1	0	0	0	0	1	1	0	0	1	1
$-12V_{dc}$	0	1	0	1	0	0	1	1	0	0	1	1
$-13V_{dc}$	0	0	1	1	0	0	1	1	0	0	1	1

TABLE II. SWITCHING SEQUENCE OF 27-LEVEL CHB INVERTER

Switches Voltage Levels	S1	S2	S3	S4	S5	S6	S7	S8	S9	S10	S11	S12
V_{dc}	1	1	0	0	0	1	0	1	0	1	0	1
$2V_{dc}$	0	0	1	1	1	1	0	0	0	1	0	1
$3V_{dc}$	0	1	0	1	1	1	0	0	0	1	0	1
$4V_{dc}$	1	1	0	0	1	1	0	0	0	1	0	1
$5V_{dc}$	0	0	1	1	0	0	1	1	1	1	0	0
$6V_{dc}$	0	1	0	1	0	0	1	1	1	1	0	0
$7V_{dc}$	1	1	0	0	0	0	1	1	1	1	0	0
$8V_{dc}$	0	0	1	1	0	1	0	1	1	1	0	0
$9V_{dc}$	0	1	0	1	0	1	0	1	1	1	0	0
$10V_{dc}$	1	1	0	0	0	1	0	1	1	1	0	0
$11V_{dc}$	0	0	1	1	1	1	0	0	1	1	0	0
$12V_{dc}$	0	1	0	1	1	1	0	0	1	1	0	0
$13V_{dc}$	1	1	0	0	1	1	0	0	1	1	0	0
$0V_{dc}$	0	1	0	1	0	1	0	1	0	1	0	1
$-V_{dc}$	0	0	1	1	0	1	0	1	0	1	0	1
$-2V_{dc}$	1	1	0	0	0	0	1	1	0	1	0	1
$-3V_{dc}$	0	1	0	1	0	0	1	1	0	1	0	1
$-4V_{dc}$	0	0	1	1	0	0	1	1	0	1	0	1
$-5V_{dc}$	1	1	0	0	1	1	0	0	0	0	1	1
$-6V_{dc}$	0	1	0	1	1	1	0	0	0	0	1	1
$-7V_{dc}$	0	0	1	1	1	1	0	0	0	0	1	1
$-8V_{dc}$	1	1	0	0	0	1	0	1	0	0	1	1
$-9V_{dc}$	0	1	0	1	0	1	0	1	0	0	1	1
$-10V_{dc}$	0	0	1	1	0	1	0	1	0	0	1	1
$-11V_{dc}$	1	1	0	0	0	0	1	1	0	0	1	1
$-12V_{dc}$	0	1	0	1	0	0	1	1	0	0	1	1
$-13V_{dc}$	0	0	1	1	0	0	1	1	0	0	1	1

IV. MATLAB/SIMULATION RESULTS

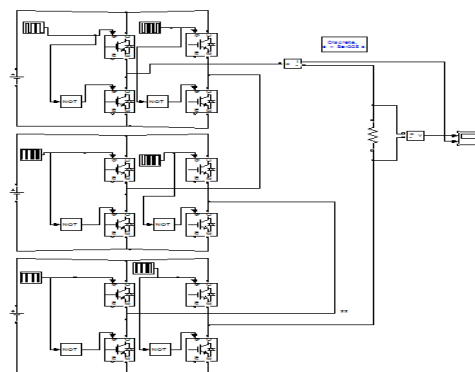


Fig 4 Matlab/simulation circuit of symmetrical cascaded multilevel inverter

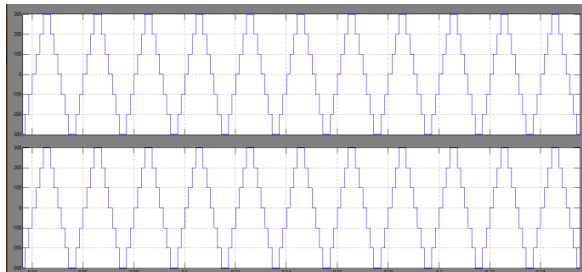


Fig 5 Output wave form of 7-level inverter

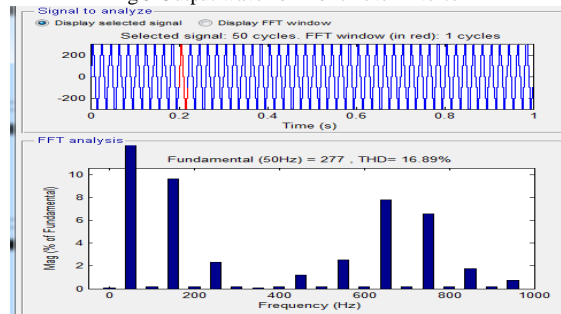


Fig 6 THD of the 7-level cascaded inverter

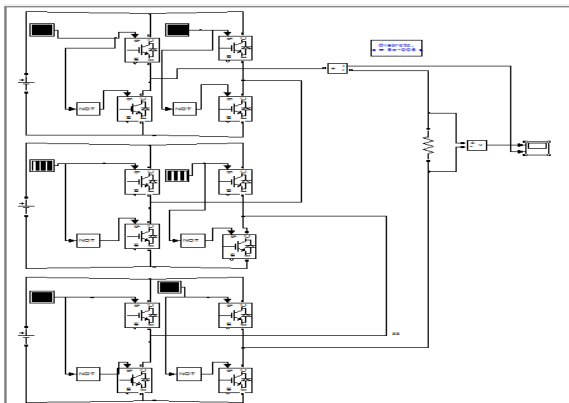


Fig 7 Proposed asymmetrical cascaded multilevel inverter

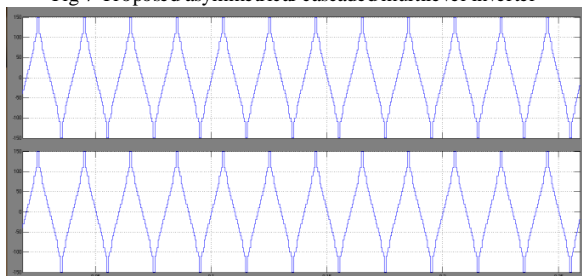


Fig 8 Output wave form of 23-level inverter

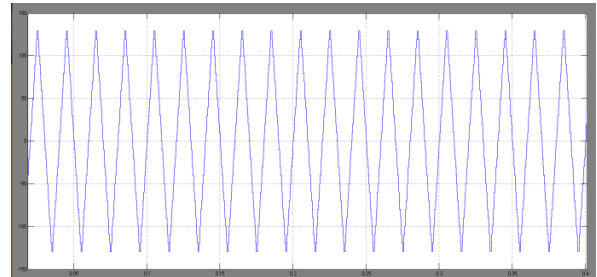


Fig 9 Output wave form of 27-level inverter

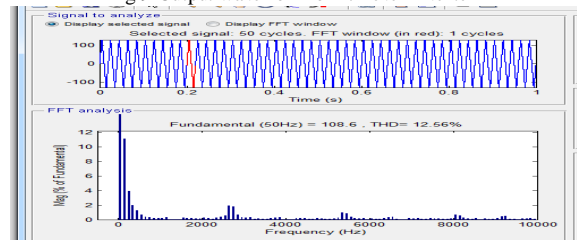


Fig 10 THD of the 27-level cascaded inverter

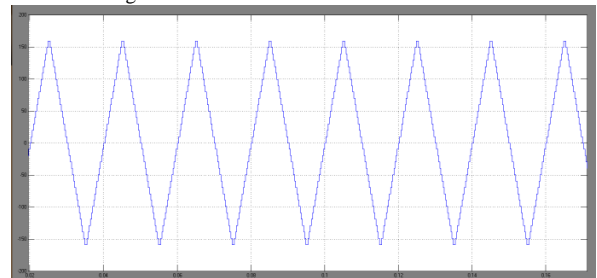


Fig 11 Output wave form of 33-level inverter

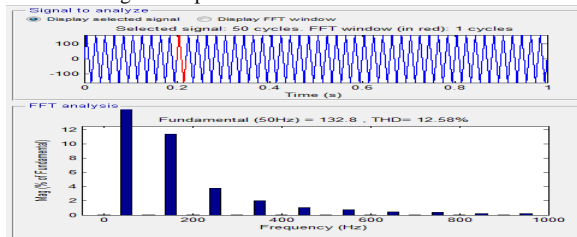


Fig 12 THD of the 33-level cascaded inverter

V.CONCLUSION

The simulation results show that in this paper 3-phase 23-level and 27-level asymmetrical cascaded H-bridge inverter are studied. The output voltage of three phase Asymmetrical 23-level CHB gives 16.59% THD, whereas 27-level asymmetrical CHB gives 12.56% THD without PWM technique. Hence compared to 23-level CHB, 27-level and 33-level CHB unequal de voltage ratios consists of minute number of harmonics and increased output voltage quality. Finally the proposed system is

connected to induction motor for future industrial and automotive applications and the simulation results are shown.

REFERENCES

- [1] 1. A Santiago-Gonzalez, 1.Cruz-Colon, R. otero-De-leon, V. lopezSantiago, E.I. Ortiz-Rivera, "Thre phase induction motor drive using flyback converter and PWM inverter fed from a single photovoltaic panel," Proc. IEEE PES General Meeting, pp. 1-6, 2011.
- [2] M. A Vitorino et al. , "An efficient induction motor control for photovoltaic pumping," IEEE Trans. Industrial Electron., vol. 54, no.4, pp. 1162-1170, April. 2011.
- [3] ADiaz, R. Saltares, C. Rodriguez, R. F. Nunez, E.I. OrtizRivera, and 1. Gonzalez-Llorente, "Induction motor equivalent circuit for dynamic simulation," Proc. IEEE Electric Machines and Drive Conference, (IEMDC), May 2009.
- [4] E. Babaei and S. H. Hosseini, "Charge balance control methods for asymmetrical cascade multilevel converters," in Proc. ICEMS, Seoul, Korea, 2007, pp. 74-79.
- [5] K. Wang, Y. Li, Z. Zheng, and L. Xu, "Voltage balancing and fluctuation suppression methods of floating capacitors in a new modular multilevel converter," IEEE Trans. Ind. Electron., vol. 60, no. 5, pp. 1943-1954, May 2013.
- [6] L.M Tolbert, F. Z.Peng and T.G Habelter, "Multilevel Converter for large electric drives," IEEE trans. Ind. Appl. Vol. 35, no. 1, pp. 36-44, Jan/Feb. 1999.
- [7] K. Nakata, K. Nakamura, S. Ito and K. Jinbo, "A three level traction inverter with IGBTs for EMU", in Conf. Rec. IEEE IAS Annu. meeting, 1994, vol. 1, pp. 667- 672.

Controlling Microgrid System Using Renewable Energy Based Bidirectional PWM Technique with Wireless System and Administered By SCADA

S.Divya¹, S.Sunanda²

¹S.Divya, PG Scholar, EEE (control systems), Mallareddy engineering college (A), Dullapally, Hyderabad.

²S.Sunanda, Asst.Professor (EEE), Mallareddy engineering college (A), Dullapally, Hyderabad.

Abstract - A microgrid is a local distribution system connecting local renewable energy sources and loads. A smart grid is a national electricity network that uses digital and other advanced technologies to monitor and manage the transport of electricity from all generation sources and loads, including the microgrids, to meet the varying electricity demands of end users. This paper deals with the control of microgrid system by using bidirectional PWM (Pulse Width Modulation) technique by utilizing renewable energy resources wirelessly through mobile phone using Bluetooth. All the wired and wireless devices of the system is controlled by a microcontroller, ARM 7 (LPC2148). The result of the designed converter is verified using the hardware. Assuming for an industrial control system, the design is simulated in the SCADA software and results are observed.

Key Words: Microgrid, PWM, Wireless control, SCADA, Renewable energy,

1. INTRODUCTION

A grid remarkable in its intelligence and impressive in its scope which offers valuable technologies that can be developed within the very near future or are already developed today[1]. It simply means a "smarter" power grid. Smart grids co-ordinate the needs and capabilities of all generators, grid operators, end-users and electricity market stakeholders to operate all parts of the system as efficiently as possible, minimizing costs and environmental impacts while maximizing system reliability, resilience and stability.

Smart grid establishes a two-way communication between the utilities and the customer and reduces the stress on the power system infrastructure. Smart grid integrates all sources of energy, mainly renewable energy.

2. MICROGRID

Microgrids are electricity distribution systems containing loads and distributed energy sources (such as distributed generators, storage devices or controllable loads) that can be operated in a controlled, coordinated way either as local islanded network or as connected to the main power network.

From a grid perspective, the microgrid concept is attractive because it recognizes the reality that the nation's distribution system is old, and will change only very slowly. The microgrid concept enables high penetration of **Distributed Generation** without requiring re-design or re-engineering of the national distribution system itself.

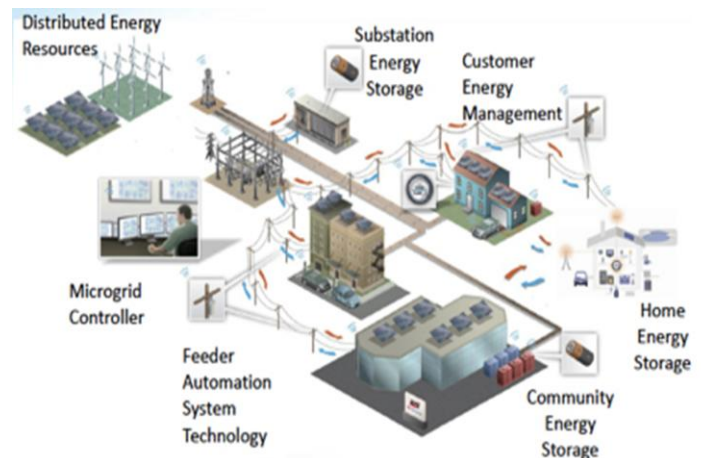


Fig -1: Microgrid

The benefits of using microgrids are improved energy efficiency, minimization of overall energy consumption, reduced environmental impact, and improvement of reliability of supply and network operational benefits such as loss reduction, congestion relief, voltage control and security of supply [2].

Solar energy is often heralded as a clean alternative to fossil energy, a way to save the planet from global warming while still ensuring everyone's electrical needs are met. The technology is still progressing and people are finding new ways to make use of it. One idea is for communities to create their own Microgrids and here's why Microgrids are a great way for communities to generate their own solar electricity.

Single phase Bidirectional PWM converter is an important component in Microgrid system that connects ac and dc subsystem. It has to operate in Inverter mode as well as Rectifier mode by utilizing dc and ac renewable energy sources [3].

3. RENEWABLE ENERGY

Renewable energy is generally defined as energy that is collected from resources which are naturally replenished on a human timescale, such as sunlight, wind, rain, tides, waves, and geothermal heat.[4] Renewable energy often provides energy in four important areas: electricity generation, air and water heating/cooling, transportation, and rural (off-grid) energy services.

Solar energy is the ultimate source of energy from millions of years and it is a renewable energy. This energy consists of radiant light and heat energy from the sun. Out of all energy emitted by sun only a small fraction of energy is absorbed by the earth. Just this tiny fraction of the sun's energy that hits the earth is enough to meet all our power needs[5]. We can use solar energy by converting it to electrical energy. So we must use a device called solar panels which can convert the light energy into electrical energy. Solar panel is a group of solar cells. Solar cells work on the principle of photoelectric effect.

4. CONTROLLER

ARM-Advanced RISC Machine is a 32-bit RISC (Reduced Instruction Set Computer) processor architecture developed by ARM Holdings. ARM7 is most successful and widely used processor family in embedded system application. So we have decided to choose ARM7 TDMI based NXP controller LPC2148.

Also ARM is balance between classic microcontroller and new Cortex series. ARM7 is excellent to get start with in terms of resources available on internet

and quality documentation provided by NXP. It suits perfectly for beginners to get in-depth idea about hardware and software implementation. LPC2148 is manufactured by NXP Semiconductor (Phillips) and it is preloaded with many in-build features and peripherals. The main advantages of using ARM7 LPC2148 is it is a 32 bit processor with High speed and Low power consumption and it has Internal ESD Protection

The PWM is based on the standard timer block and inherits all of its features, although only the PWM function is pinned out on the LPC2148. The timer is designed to count cycles of the peripheral clock (PCLK) and optionally generate interrupts or perform other actions when specified timer values occur, based on seven match registers. The PWM function is also based on match register events [13]. The ability to separately control rising and falling edge locations allow the PWM to be used for more applications. It can be used as a standard timer if the PWM mode is not enabled.

5. HARDWARE DESIGN

5.1 Block Diagram

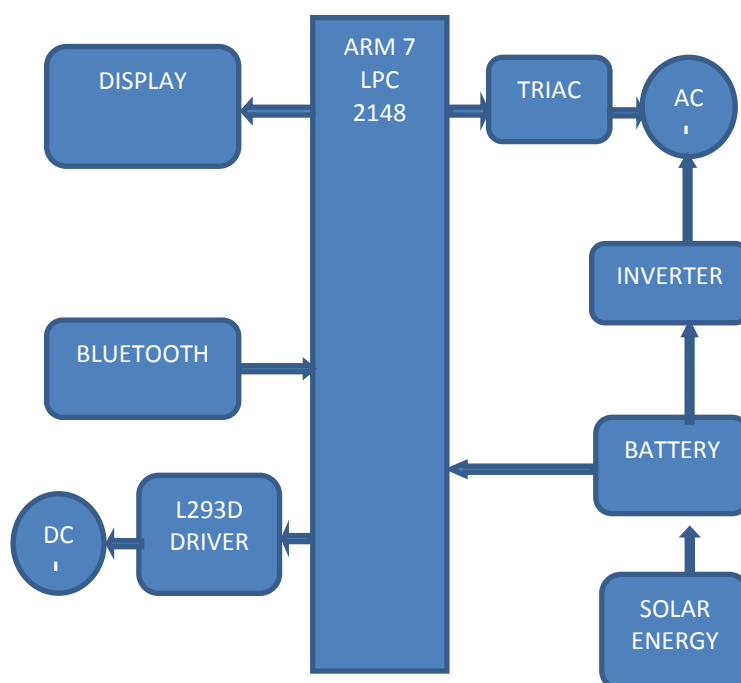


Fig -2: Basic Block Diagram

5.2 Schematic Diagram

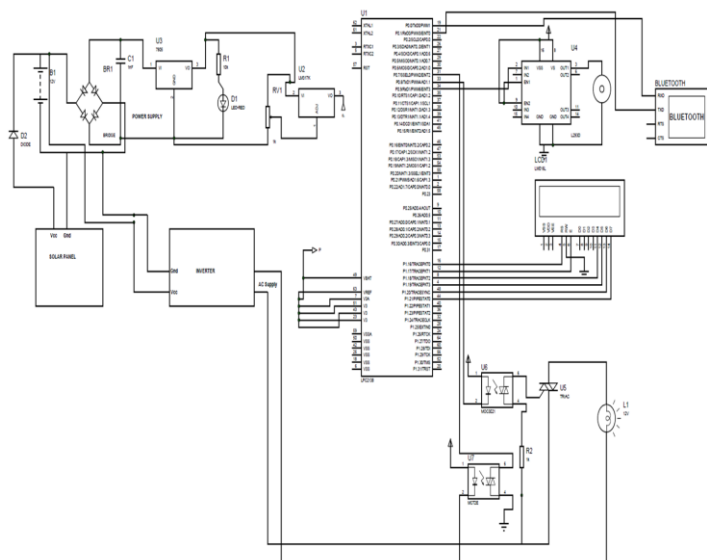


Fig -3: Schematic Diagram

5.3 Design

The bidirectional converter is designed using the optocoupler (MOC3021) and microcontroller LPC2148 is used to control the switches in the converter and driver L293D is used to drive the DC motor. Triac BT136 is used as a switch for AC bulb. Bluetooth HC05 is connected to the controller to control wirelessly. The power supply is taken from the solar panel. In order to avoid device failure and safety, the fabrication and the experiments were done as a scaled down voltage level

6. EXPERIMENTAL RESULTS

Serial controller application from the Google play store is installed our android mobile phone. The required buttons are set, for e.g. AC LOW, DC MID and so on. The phone is now paired to the setup using Bluetooth. The output on the hardware is controlled wirelessly through the mobile phone and it is tabulated.

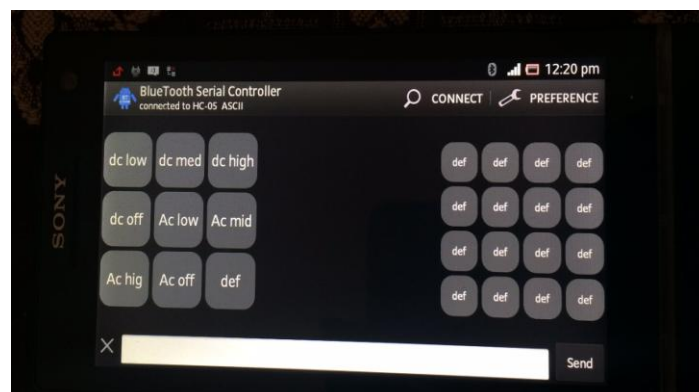


Fig -4: Bluetooth serial controller

Table -1

Input on the phone	CD motor	AC Bulb
AC low		Intensity is low
AC high		Intensity is high
AC Off		OFF
DC high	Motor in max speed	
DC low	Speed is decreased	
DC off	OFF	

7. SIMULATION ON SCADA

SCADA (Supervisory Control and Data Acquisition) is a system for remote monitoring and control that operates with coded signals over communication channels (using typically one communication channel per remote station). The control system may be combined with a data acquisition system by adding the use of coded signals over communication channels to acquire information about the status of the remote equipment for display or for recording functions. It is a type of industrial control system (ICS). Industrial control systems are computer-based systems that monitor and control industrial processes that exist in the physical world. Most control actions are performed by PLC because they are more economical, versatile, flexible and configurable [19]. Hence PLC is to control the process and SCADA allow the operator to change the set points for

the process and the process can be displayed and recorded.

The main advantages of using SCADA are, it minimizes the fault response time and reduce failure or unplanned downtimes.

For an industrial control system, the design is designed using SCADA software and the simulations are observed. The software used for PLC is CODESYS which is a software platform especially designed to fulfill the different requirement of modern industrial automation projects. The software used for SCADA is Intouch from wonderware by Schneider Electric.



Fig -5: On SCADA

8. SIMULATION OBSERVATION

Fig -6-8 shows the control panel of the SCADA simulation. ON and OFF button for AC load and DC load is used. Regulator is used to control the AC and DC load. The graph shows the performance of the load. Green line in the graph shows the speed of the DC load which is assumed to be the fan and the red line indicates the intensity of the AC load which is assumed to be a bulb.

The simulation results are observed as, when speed of the AC load is increased, the frequency changes and when intensity on the bulb is increased the amplitude is increased.

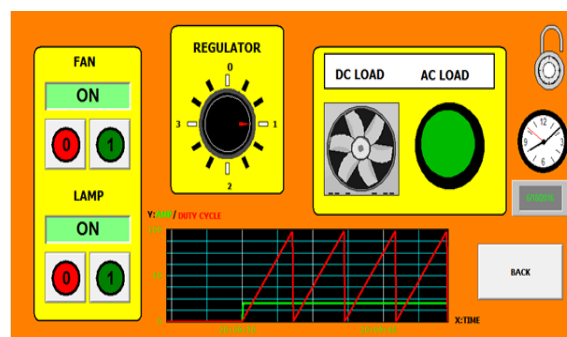


Fig -6: LOW

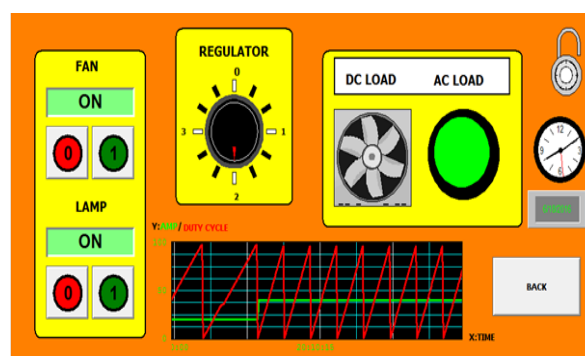


Fig -7: MEDIUM

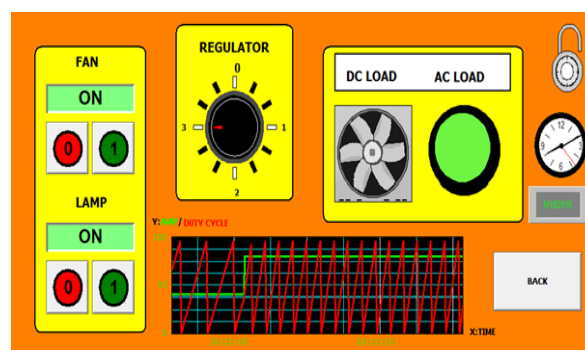


Fig -8: HIGH

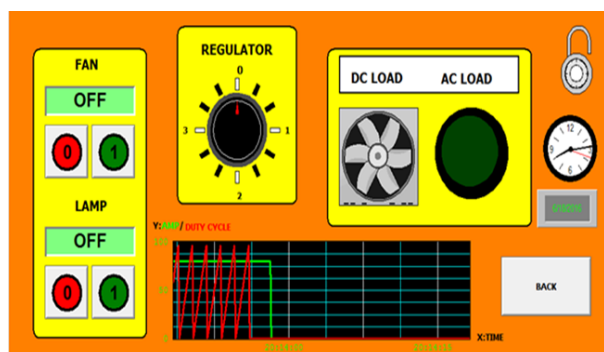


Fig -9: OFF

9. CONCLUSION

With world's enhanced focus on renewable energy resources the growth of microgrids is imminent for the efficient distribution of electricity. The success of microgrids depends on their seamless two-way integration with national smart grids. This paper shows how bidirectional PWM (Pulse Width Modulation) technique and SCADA system can be used to achieve this integration.

REFERENCES

- [1] Single Phase Bidirectional PWM Converter for Microgrid System C.Kalavalli et al / International Journal of Engineering and Technology (IJET)
- [2] Cvetkovice et al. "Future home uninterruptible renewable energy system with vehicle-to-Grid technology," in Proc. 2009 IEEE Energy Conv. Congr. Expo., pp. 2675-2681
- [3] Naser M. Abdel-Rahim, et al., "Analysis and design of a multiple feedback loop control strategy for single-phase voltage-source UPS inverter", IEEE Trans. Power Electron. vol. 11, July 1996, pp. 532-541
- [4] Different aspects of Solar PV integrations into power grid by Prajnasmitha Mohapatra and C.K. Panigrahi, Novus International Journal of Engineering & Technology, 2012, Vol. 1, No. 1, 20-27.
- [5] The Electric Power Transmission and Distribution Industry by A publication of the Indiana Business Research Center at IU's Kelley School of Business on July-Aug 2010
- [6] H. Gu, Z. Yang, D. Wang, and W. Wu, "Research on control method of double-mode inverter with grid-connection and stand-alone," in Proc. 2006 IEEE Power Electron. Motion Control Conf., pp. 1-5
- [7] N. Mohan, T. M. Undeland, W. P. Robbins, "Power Electronics, Converters, Applications, and Design", 3th edition, John Wiley & Sons, New York, 2003.
- [8] D. Dong, T. Thacker, R. Burgos, D. Boroyevich, F. Wang, and B. Giewont, "Control design and experimental of a multi-function single phase bidirectional PWM converter for renewable energy systems," in Proc. 2009 Eur. Conf. Power Electron. Appl., pp. 1-10.
- [9] Borrego Springs Microgrid Project by green energy corp
- [10] Nagalingam Rajeshwaran, Tenneti MADHU, and Munagala SURYAKALAVATHI, "Improved Switching Performance Analysis of Space Vector Pulse Width Modulation on Field Programmable Gate Array", Leonardo El J Pract Technol 2014; 13(24):83-96. ICID: 1089090.
- [11] N. Rajeswaran, T. Madhu, and M. Suryakalavathi, "Design of Optimized controller for fault diagnosis of Three Phase Induction Motor using Genetic Algorithm", Applied Mechanics and Materials Vols. 496-500 (2014) pp 1732-1735 © (2014) Trans Tech Publications, Switzerland doi:10.4028/www.scientific.net/AMM.496-500.
- [12] Tzou Y.Y., Hsu H.J., FPGA realization of space vector PWM control IC for three-phase PWM inverters, IEEE Trans. Power Electron., 1997, 12(6), p. 953-963.
- [13] International Journal of Advanced Research in Computer Science and Software Engineering Research Paper on ARM-7 Development Board by Brijesh Pate, Ravindra Mankar, Vinay Sigedar Volume 3, Issue 11, November 2013
- [14] Celanovic N., Boroyevich D., A fast space-vector modulation algorithm for multilevel three-phase converters, IEEE Trans. on Industry Applications, 2001, 37(L293D Motor Driver IC details on ron robotics Submitted by Rakesh Ron on Fri, 08/16/2013
- [15] Integration of Renewable Energy Resources in Microgrid by Manzar Ahmed, Uzma Amin, Suhail Aftab, Zaki Ahmed Published Online January 2015 in SciRes
- [16] Farret, F.A. and Simoes, M.G. (2006) Integration of Alternative Sources of Energy. John Wiley & Sons, Hoboken.
- [17] Mehrotra, P. (2011) Nanotechnology Applications in Energy Sector. Reinste Nano Ventures Nano Science and Technology.
- [18] DOE's Office of Energy Efficiency and Renewable Energy (2004) Solar Energy Technologies Program Multi-Year Technical Plan 2003-2007.
- [19] IMPLEMENTATION OF MICROCONTROLLER BASED WIRELESS SCADA SYSTEM by Kandhare Pooja, Jadhavar Santosh,

PatilPratish,International Journal of Science, Engineering and Technology Research (IJSETR), Volume 3, Issue 4, April 2014

- [20] F. Katiraei, R. Iravani, N. Hatziargyriou, and A. Dimeas, "MicrogridsManagement. Controls and Operation Aspects of Microgrids", IEEE Power & Energy Magazine, May/June 2008, pp. 56.
- [21] Experience on the Implementation of aMicrogrid Project in Barcelona by Manuel Roman-Barri, Ignasi Cairo-Molins, Andreas Sumper, and AntoniSudria-AndreuCatalonia Institute for Energy Research (IREC)

BIOGRAPHIES



S.Divya received B.Tech. in Electronics and instrumentation from National Engineering college, Kovilpatti, Tamilnadu in 2006 and worked as an Order Entry Administrator (Fisher control valves) for Emerson Process Management, Dubai. Currently she is pursuing M.Tech in control system from Malla Reddy Engineering College (A), Dullapally, Hyderabad.
E-mail: sdivya1985@gmail.com



S.Sunanda received BE from OU College of Engineering, Hyderabad in 2001 and received M.Tech in Control system from JNTU, Anaparthi in 2005. Currently she is working as an assistant professor in Malla Reddy Engineering College (A), Dullapally, Hyderabad.
E-mail: sunandav2015@gmail.com

SOLAR POWER GENERATION SEVEN LEVEL TO NINE LEVEL INVERTER

G.Sumanth
M-tech Student

Department of Electrical & Electronics Engineering,
Mallareddy Engineering College (Autonomous)

V.Suma Deepthi
Assistant Professor

Department of Electrical & Electronics Engineering,
Mallareddy Engineering College (Autonomous)

Abstract- Solar energy is becoming more important since it produces less pollution and the cost of fossil fuel energy is rising, while the cost of solar arrays is decreasing. The proposed solar power generation system generates a sinusoidal output current that is in phase with the utility voltage and is fed into the utility. The power conversion interface is important to grid connected solar power generation systems because it converts the dc power generated by a solar cell array into ac power and feeds this ac power into the utility grid. An inverter is necessary in the power conversion interface to convert the dc power to ac power. the output voltage of a solar cell array is low, a dc-dc power converter is used in a small-capacity solar power generation system to boost the output voltage, so it can match the dc bus voltage of the inverter. In this proposed inverter have eight switches and their switches operate with fundamental frequency. a new solar power generation system, which is composed of a dc/dc power converter and a new seven-level inverter. The dc/dc power converter integrates a dc-dc boost converter and a transformer to convert the output voltage of the solar cell array into two independent voltage sources with multiple relationships. The proposed inverter produced seven level output voltage from two input voltage sources. The proposed inverter reduced the switching losses (because of all switches operate with fundamental frequency), complexity, control circuit and place requirement. This new seven-level inverter is configured using a capacitor selection circuit and a full-bridge power converter, connected in cascade. The capacitor selection circuit converts the two output voltage sources of dc-dc power converter into a three-level dc voltage, and the full-bridge power converter further converts this three-level dc voltage into a seven-level ac voltage. The performance of this proposed solar power generation system. The proposed concept can be implemented with PV based system using MATLAB/SIMULINK software.

Keywords— DC/DC boost converter, Nine level inverter, Multilevel inverter, Pulse width modulated (PWM), Solar panel

I. INTRODUCTION

In numerous rural areas uninterrupted electricity is not accessible from grid. Mostly the grid gets power from hydro power station as well as from thermal power station. As the conservative energy sources are

diminishing hasty, in the midst of consequent mount in cost, solar and wind energy offers a superior substitute resource along with free from pollution. The renewable energy resources are profitable and they will not cause any detrimental effects on the surroundings. With the latest investigate, results the expenditure of photovoltaic cells are likely to go down in future. Each cell having 0.7V and that are allied in series or parallel and form solar array. A single phase PV based seven-level inverter is discussed in paper [9]. The PV power generation is a budding modern trend owing to its various advantages resembling inexpensive, ecological responsive power generation. Multilevel inverter possibly will generate almost sinusoidal output voltage waveform along with output current which will compress the harmonic distortion furthermore improve its power quality [12].

Multilevel Inverters (MLI) began with the neutral point clamped inverter topology proposed by Nabae et al. [1]. Recently, multilevel inverters have become more attractive for researchers due to their advantages over conventional three-level pulse width-modulated (PWM) inverters. MLI has two main advantages compared with the conventional H-bridge inverters, the higher voltage capability and the reduced harmonic content in the output waveform due to the multiple dc levels. MLI is now preferred in high power medium voltage applications due to the reduced voltage stresses on the devices. MLI incorporates a topological structure that allows a desired output voltage to be synthesized among a set of isolated or interconnected distinct voltage sources. Numerous topologies realize this connectivity, and can be generally divided into three major categories, namely, diode clamped MLI, flying capacitor MLI, and separated dc sources (cascaded voltages) MLI.

The planned nine level controlled solar power generation system consisting of dc/dc boost converter, capacitor selection circuit and seven-level inverter. This method plays a crucial task in reducing the amount of switches designed for generating seven level of output. It

consisting of no more than six power electronic switches moreover only one switch will activate at high frequency at any instant. The solar panel dc outputs are boost up by means of boost converter along with its switches are embarrassed through the maximum power point technique (MPPT) [2]. In favour of supplying power towards the utility, the dc power is rehabilitated to ac by means of single H-bridge inverter combined in the company of the capacitor selection circuit.

Recently, many topologies of the MLI and its control techniques have been published. The MLI technique is implemented by adding one switch and four power diodes to the H-bridge single phase inverter. Another solution can be found by using two switches and two power diodes with the H-bridge single phase inverter. Those two systems can generate only five levels in the output voltage with less harmonic contents. The other solution is a modular inverter that can reach to any required voltage levels. But these inverters topologies can be improved by reducing their switches without affecting their performances.

The modular multilevel inverter is similar to the cascade H-bridge type. For this, a new modulation method is proposed to achieve dynamic capacitor voltage balance. A multilevel dc-link inverter is presented to overcome the problem of partial shading of individual photovoltaic sources that are connected in series. The dc bus of a full-bridge inverter is configured by several individual dc blocks, where each dc block is composed of a solar cell, a power electronic switch, and a diode. Controlling the power electronics of the dc blocks will result in a multilevel dc-link voltage to supply a full-bridge inverter and to simultaneously overcome the problems of partial shading of individual photovoltaic sources.

This paper proposes a new solar power generation system. The proposed solar power generation system is composed of a dc/dc power converter and a seven-level inverter. The seven level inverter is configured using a capacitor selection circuit and a full-bridge power converter, connected in cascade. The seven-level inverter contains only six power electronic switches, which simplifies the circuit configuration. Since only one power electronic switch is switched at high frequency at any time to generate the seven-level output voltage, the switching power loss is reduced, and the power efficiency is improved. The inductance of the filter inductor is also reduced because there is a seven level output voltage. In this topology nine level inverters are used to produce pulse width modulated signals. Conventional PI inverter has some disadvantage i.e large steady state error and more settling time.

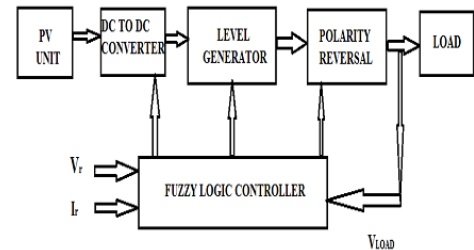


Fig.1. Block Diagram of Proposed Solar Power Generation System

II. CIRCUIT CONFIGURATION

Fig 1 shows the configuration of the proposed solar power generation system.

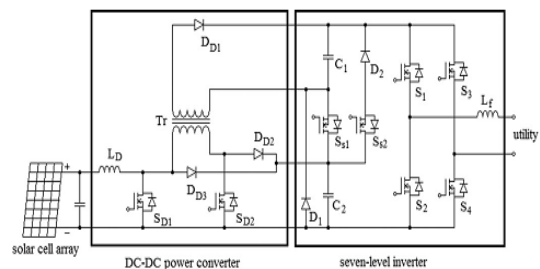


Fig. 2 Configuration of the proposed solar power generation system.

The proposed solar power generation system is composed of a solar cell array, a dc–dc power converter, and a new seven-level inverter. The solar cell array is connected to the dc–dc power converter, and the dc–dc power converter is a boost converter that incorporates a transformer with a turn ratio of 2:1. The dc–dc power converter converts the output power of the solar cell array into two independent voltage sources with multiple relationships, which are supplied to the seven-level inverter. This new seven-level inverter is composed of a capacitor selection circuit and a full-bridge power converter, connected in a cascade. The power electronic switches of capacitor selection circuit determine the discharge of the two capacitors while the two capacitors are being discharged individually or in series. Because of the multiple relationships between the voltages of the dc capacitors, the capacitor selection circuit outputs a three-level dc voltage. The full-bridge power converter further converts this three-level dc voltage to a seven-level ac voltage that is synchronized with the utility voltage. In this way, the proposed solar power generation system generates a sinusoidal output current that is in phase with the utility voltage and is fed into the utility, which produces a unity power factor. As can be seen, this new seven-level inverter contains only six power electronic switches, so the power circuit is simplified.

III. DC–DC POWER CONVERTER

As seen in Fig.1, the DC–DC power converter incorporates a boost converter and a current-fed forward converter. The boost converter is composed of an inductor L_D , a power electronic switch SD_1 , and a diode, DD_3 . The boost converter charges capacitor C_2 of the seven-level inverter. The current-fed forward converter is composed of an inductor L_D , power electronic switches SD_1 and SD_2 , a transformer, and diodes DD_1 and DD_2 . The current-fed forward converter charges capacitor C_1 of the seven-level inverter. The inductor L_D and the power electronic switch SD_1 of the current-fed forward converter are also used in the boost converter. Fig 3(a) shows the operating circuit of the dc–dc power converter when SD_1 is turned ON. The solar cell array supplies energy to the inductor L_D . When SD_1 is turned OFF and SD_2 is turned ON, its operating circuit is shown in Fig 3(b). Accordingly, capacitor C_1 is connected to capacitor C_2 in parallel through the transformer, so the energy of inductor L_D and the solar cell array charge capacitor C_2 through DD_3 and charge capacitor C_1 through the transformer and DD_1 during the off state of SD_1 . Since capacitors C_1 and C_2 are charged in parallel by using the transformer, the voltage ratio of capacitors C_1 and C_2 is the same as the turn ratio (2:1) of the transformer. Therefore, the voltages of C_1 and C_2 have multiple relationships. The boost converter is operated in the continuous conduction mode (CCM). The voltage of C_2 can be represented as

$$V_{c2} = \frac{1}{1-D} V_s \quad (1)$$

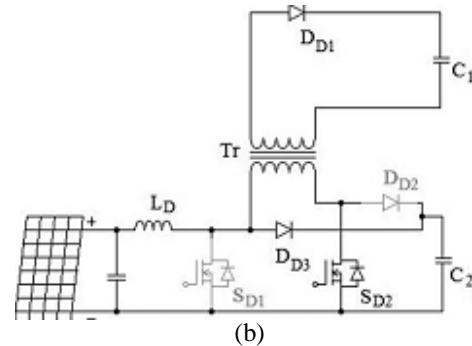
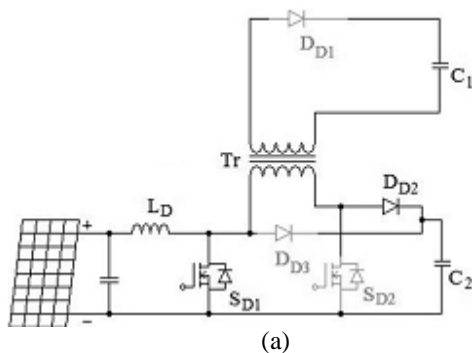


Fig.3 Operation of dc–dc power converter: (a) SD_1 is on and (b) SD_1 is off.

Where V_S is the output voltage of solar cell array and D is the duty ratio of SD_1 . The voltage of capacitor C_1 can be represented as

$$V_{c1} = \frac{1}{2(1-D)} V_s. \quad (2)$$

It should be noted that the current of the magnetizing inductance of the transformer increases when SD_2 is in the ON state. Conventionally, the forward converter needs a third demagnetizing winding in order to release the energy stored in the magnetizing inductance back to the power source. However, in the proposed dc–dc power converter, the energy stored in the magnetizing inductance is delivered to capacitor C_2 through DD_2 and SD_1 when SD_2 is turned OFF. Since the energy stored in the magnetizing inductance is transferred forward to the output capacitor C_2 and not back to the dc source, the power efficiency is improved. In addition, the power circuit is simplified because the charging circuits for capacitors C_1 and C_2 are integrated. Capacitors C_1 and C_2 are charged in parallel by using the transformer, so their voltages automatically have multiple relationships. The control circuit is also simplified.

IV. SEVEN-LEVEL INVERTER

As seen in Fig1, the seven-level inverter is composed of a capacitor selection circuit and a full-bridge power converter, which are connected in cascade. The operation of the seven level inverter can be divided into the positive half cycle and the negative half cycle of the utility. For ease of analysis, the power electronic switches and diodes are assumed to be ideal, while the voltages of both capacitors C_1 and C_2 in the capacitor selection circuit are constant and equal to $V_{dc}/3$ and $2V_{dc}/3$, respectively. Since the output current of the solar power generation system will be controlled to be sinusoidal and in phase with the utility voltage, the output current of the seven-level inverter is also positive in the positive half cycle of the utility. The operation of the seven-level inverter in the

positive half cycle of the utility can be further divided into four modes, as shown in Fig 3.

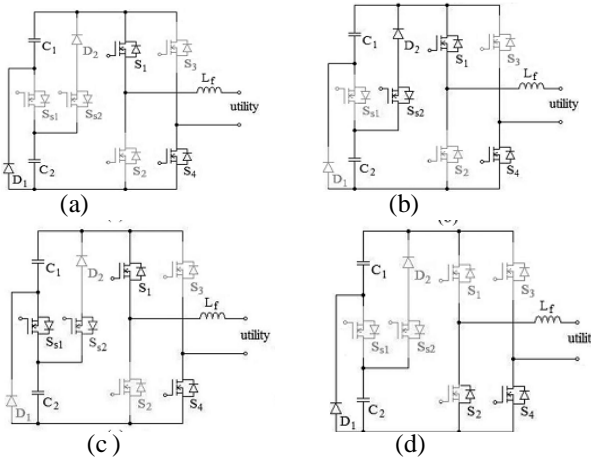


Fig 4 Operation of the seven-level inverter in the positive half cycle, (a) Mode 1, (b) mode 2, (c) mode 3, and (d) mode 4.

Mode 1: The operation of mode 1 is shown in Fig 4(a). Both SS1 and SS2 of the capacitor selection circuit are OFF, so C1 is discharged through D1 and the output voltage of the capacitor selection circuit is $V_{dc}/3$. S1 and S4 of the full-bridge power converters are ON. At this point, the output voltage of the seven-level inverter is directly equal to the output voltage of the capacitor selection circuit, which means the output voltage of the seven-level inverter is $V_{dc}/3$.

Mode 2: The operation of mode 2 is shown in Fig 4(b). In the capacitor selection circuit, SS1 is OFF and SS2 is ON, so C2 is discharged through SS2 and D2 and the output voltage of the capacitor selection circuit is $2V_{dc}/3$. S1 and S4 of the full-bridge power converter are ON. At this point, the output voltage of the seven-level inverter is $2V_{dc}/3$.

Mode 3: The operation of mode 3 is shown in Fig 4(c). In the capacitor selection circuit, SS1 is ON. Since D2 has a reverse bias when SS1 is ON, the state of SS2 cannot affect the current flow. Therefore, SS2 may be ON or OFF, to avoiding switching of SS2. Both C1 and C2 are discharged in series and the output voltage of the capacitor selection circuit is V_{dc} . S1 and S4 of the full-bridge power converter are ON. At this point, the output voltage of the seven-level inverter is V_{dc} .

Mode 4: The operation of mode 4 is shown in Fig 4(d). Both SS1 and SS2 of the capacitor selection circuit are OFF. The output voltage of the capacitor selection circuit is $V_{dc}/3$. Only S4 of the full-bridge power converter is ON. Since the output current of the seven-level inverter is positive and passes through the filter inductor, it forces the anti parallel diode of S2 to be switched ON for

continuous conduction of the filter inductor current. At this point, the output voltage of the seven level inverter is zero. Therefore, in the positive half cycle, the output voltage of the seven-level inverter has four levels: $V_{dc}, 2V_{dc}/3, V_{dc}/3$, and 0.

In the negative half cycle, the output current of the seven-level inverter is negative. The operation of the seven-level inverter can also be further divided into four modes, as shown in Fig 5. A comparison with Fig 4 shows that the operation of the capacitor selection circuit in the negative half cycle is the same as that in the positive half cycle. The difference is that S2 and S3 of the full-bridge power converter are ON during modes 5, 6, and 7, and S2 is also ON during mode 8 of the negative half cycle. Accordingly, the output voltage of the capacitor selection circuit is inverted by the full-bridge power converter, so the output voltage of the seven-level inverter also has four levels: $-V_{dc}, -2V_{dc}/3, -V_{dc}/3$, and 0. In summary, the output voltage of the seven-level inverter has the voltage levels: $V_{dc}, 2V_{dc}/3, V_{dc}/3, 0, -V_{dc}/3, -2V_{dc}/3$, and $-V_{dc}$. The seven-level inverter is controlled by the current-mode control, and pulse-width modulation (PWM) is used to generate the control signals for the power electronic switches. The output voltage of the seven-level inverter must be switched in two levels, according to the utility voltage. One level of the output voltage is higher than the utility voltage in order to increase the filter inductor current, and the other level of the output voltage is lower than the utility voltage, in order to decrease the filter inductor current. In this way, the output current of the seven-level inverter can be controlled to trace a reference current.

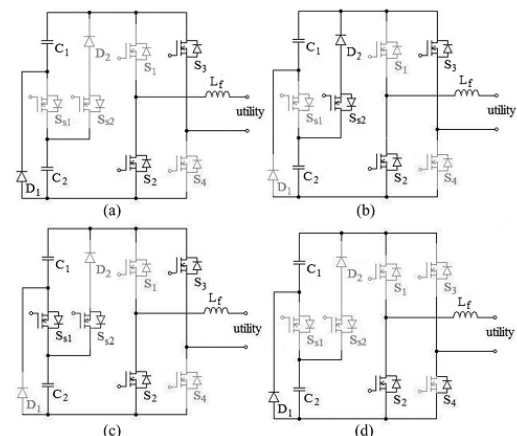


Fig 5 Operation of the seven-level inverter in the negative half cycle: (a) Mode 5, (b) mode 6, (c) mode 7, and (d) mode 8.

Accordingly, the output voltage of the seven-level inverter must be changed in accordance with the utility voltage. In the positive half cycle, when the utility voltage is smaller than $V_{dc}/3$, the seven-level inverter must be

switched between modes 1 and 4 to output a voltage of $V_{dc}/3$ or 0. Within this voltage range, S1 is switched in PWM. The duty ratio d of S1 can be represented as

$$d = v_m / V_{tri} \quad (3)$$

Where V_m and V_{tri} are the modulation signal and the amplitude of carrier signal in the PWM circuit, respectively. The output voltage of the seven-level inverter can be written as

$$v_o = d \cdot V_{dc}/3 = k_{pwm} v_m \quad (4)$$

Where k_{pwm} is the gain of inverter, which can be written as

$$k_{pwm} = V_{dc}/3V_{tri} \quad (5)$$

Fig .5(a) shows the simplified model for the seven-level inverter when the utility voltage is smaller than $V_{dc}/3$. The closed loop transfer function can be derived as

$$I_o = \frac{k_{pwm} G_c / L_f}{s + k_i k_{pwm} G_c / L_f} I_o^* - \frac{1/L_f}{s + k_i k_{pwm} G_c / L_f} V_u \quad (6)$$

Where G_c is the current inverter and k_i is the gain of the current detector. The seven-level inverter is switched between modes 2 and 1, in order to output a voltage of $2V_{dc}/3$ or $V_{dc}/3$ when the utility voltage is in the range ($V_{dc}/3, 2V_{dc}/3$). Within this voltage range, SS2 is switched in PWM. The duty ratio of SS2 is the same as (3). However, the output voltage of seven-level inverter can be written as

$$v_o = d \cdot V_{dc}/3 + V_{dc}/3 = k_{pwm} v_m + V_{dc}/3. \quad (7)$$

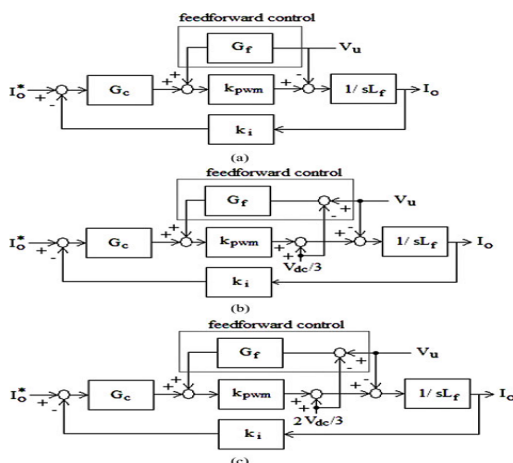


Fig 6. Model of the seven-level inverter under different range of utility voltage, (a) in the range of smaller than $V_{dc}/3$, (b) in the range of ($V_{dc}/3, 2V_{dc}/3$), (c) in the range of higher than $2V_{dc}/3$

Fig 6(b) shows the simplified model for the seven-level inverter when the utility voltage is within this voltage range. The closed-loop transfer function can be derived as

$$I_o = \frac{k_{pwm} G_c / L_f}{s + k_i k_{pwm} G_c / L_f} I_o^* - \frac{1/L_f}{s + k_i k_{pwm} G_c / L_f} (V_u - V_{dc}/3). \quad (8)$$

The seven-level inverter is switched between modes 3 and 2 in order to output a voltage of V_{dc} or $2V_{dc}/3$, when the utility voltage is in the range ($2V_{dc}/3, V_{dc}$). Within this voltage range, SS1 is switched in PWM and SS2 remains in the ON state to avoid switching of SS2. The duty ratio of SS1 is the same as (3). However, the output voltage of seven-level inverter can be written as

$$v_o = d \cdot V_{dc}/3 + 2V_{dc}/3 = k_{pwm} v_m + 2V_{dc}/3. \quad (9)$$

Fig.5(c) shows the simplified model for the seven-level inverter when the utility voltage is within this voltage range. The closed-loop transfer function can be derived as

$$I_o = \frac{k_{pwm} G_c / L_f}{s + k_i k_{pwm} G_c / L_f} I_o^* - \frac{1/L_f}{s + k_i k_{pwm} G_c / L_f} (V_u - 2V_{dc}/3). \quad (10)$$

TABLE I
STATES OF POWER ELECTRONIC SWITCHES FOR A SEVEN-LEVEL INVERTER

positive half cycle						
	SS1	SS2	S1	S2	S3	S4
$ v_u < V_{dc}/3$	off	off	PWM	off	off	on
$2V_{dc}/3 > v_u > V_{dc}/3$	off	PWM	on	off	off	on
$ v_u > 2V_{dc}/3$	PWM	on	on	off	off	on
negative half cycle						
$ v_u < V_{dc}/3$	off	off	off	on	PWM	off
$2V_{dc}/3 > v_u > V_{dc}/3$	off	PWM	off	on	on	off
$ v_u > 2V_{dc}/3$	PWM	on	off	on	on	off

As seen in (6), (8), and (10), the second term is the disturbance. Hence, a feed forward control, which is also shown in Fig5, should be used to eliminate the disturbance, and the gain G_f should be $1/k_{pwm}$. In the negative half cycle, the seven-level inverter is switched between modes 5 and 8, in order to output a voltage of $-V_{dc}/3$ or 0, when the absolute value of the utility voltage is smaller than $V_{dc}/3$. Accordingly, S3 is switched in PWM. The seven level inverter is switched in modes 6 and 5 to output a voltage of $-2V_{dc}/3$ or $-V_{dc}/3$ when the utility voltage is in the range ($-V_{dc}/3, -2V_{dc}/3$). Within this voltage range, SS2 is switched in PWM. The seven-level inverter is switched in modes 7 and 6 to output a voltage of $-V_{dc}$ or $-2V_{dc}/3$, when the utility voltage is in the range ($-2V_{dc}/3, -V_{dc}$). At this voltage range, SS1 is switched in PWM and SS2 remains in the ON state to avoid switching of SS2. The simplified model for the seven-level inverter in the negative half cycle is the similar to that for the positive half cycle. Since only six power electronic switches are used in the proposed seven-level inverter, the power circuit is

significantly simplified compared with a conventional seven-level inverter. The states of the power electronic switches of the seven-level inverter, as detailed previously, are summarized in Table I. It can be seen that only one power electronic switch is switched in PWM within each voltage range and the change in the output voltage of the seven-level inverter for each switching operation is $V_{dc}/3$, so switching power loss is reduced. Figs 3 and 4 show that only three semiconductor devices are conducting in series in modes 1, 3, 4, 5, 7, and 8 and four semiconductor devices are conducting in series in modes 2 and 6. This is superior to the conventional multilevel inverter topologies, in which at least four semiconductor devices are conducting in series. Therefore, the conduction loss of the proposed seven-level inverter is also reduced slightly. The drawback of the proposed seven-level inverter is that the voltage rating of the full-bridge converter is higher than that of conventional multilevel inverter topologies. The leakage current is an important parameter in a solar power generation system for transformer less operation. The leakage current is dependent on the parasitic capacitance and the negative terminal voltage of the solar cell array respect to ground. To reduce the leakage current, the filter inductor L_f should be replaced by a symmetric topology and the

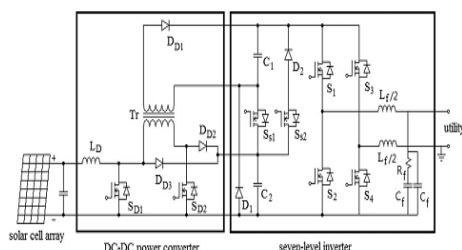


Fig 6 Configuration of the proposed solar power generation system for suppressing the leakage current.

A. Seven-Level Inverter

Fig.7(a) shows the control block diagram for the seven-level inverter. The control object of the seven-level inverter is its output current, which should be sinusoidal and in phase with the utility voltage. The utility voltage is detected by a voltage detector, and then sent to a phase-lock loop (PLL) circuit in order to generate a sinusoidal signal with unity amplitude. The voltage of capacitor C_2 is detected and then compared with a setting voltage. The compared result is sent to a PI inverter. Then, the outputs of the PLL circuit and the PI inverter are sent to a multiplier to produce the reference signal, while the output current of the seven-level inverter is detected by a current detector. The reference signal and the detected output current are sent to absolute circuits and then sent to

subtract or, and the output of the subtract or is sent to a current inverter. The detected utility voltage is also sent to an absolute circuit and then sent to a comparator circuit, where the absolute utility voltage is compared with both half and whole of the detected voltage of capacitor C_2 , in order to determine the range of the operating voltage. The comparator circuit has three output signals, which correspond to the operation voltage ranges, $(0, V_{dc}/3)$, $(V_{dc}/3, 2V_{dc}/3)$, and $(2V_{dc}/3, V_{dc})$. The feed-forward control eliminates the disturbances of the utility voltage, $V_{dc}/3$ and $2V_{dc}/3$, as shown in (6), (8), and (10). The absolute value of the utility voltage and the outputs of the compared circuit are sent to a feed-forward inverter to generate the feed-forward signal. Then, the output of the current inverter and the feed-forward signal are summed and sent to a PWM circuit to produce the PWM signal. The detected utility voltage is also compared with zero, in order to obtain a square signal that is synchronized with the utility voltage. Finally, the PWM signal, the square signal, and the outputs of the compared circuit are sent to the switching signal processing circuit to generate the control signals for the power electronic switches of the seven-level inverter, according to Table I. The current inverter controls the output current of the seven level inverter, which is a sinusoidal signal of 60 Hz. Since the feed-forward control is used in the control circuit, the current inverter can be a simple amplifier, which gives good tracking performance. As can be seen in (6), (8), and (10), the gain of the current inverter determines the bandwidth and the steady state error. The gain of the current inverter must be as large as possible in order to ensure a fast response and a low steady-state error. But the gain of the current inverter is limited because the bandwidth of the power converter is limited by the switching frequency.

B. DC-DC Power Converter

Fig.7(b) shows the control block diagram for the dc-dc power converter. The input for the DC-DC power converter is the output of the solar cell array. A ripple voltage with a frequency that is double that of the utility appears in the voltages of C_1 and C_2 , when the seven-level inverter feeds real power into the utility. The MPPT function is degraded if the output voltage of solar cell array contains a ripple voltage. Therefore, the ripple voltages in C_1 and C_2 must be blocked by the dc-dc power converter to provide improved MPPT. Accordingly, dual control loops, an outer voltage control loop and an inner current control loop, are used to control the dc-dc power converter. Since the output voltages of the DC-DC power converter comprises the voltages of C_1 and C_2 , which are controlled by the seven-level inverter,

the outer voltage control loop is used to regulate the output voltage of the solar cell array. The inner current control loop controls the inductor current so that it approaches a constant current and blocks the ripple voltages in C1 and C2. The perturbation and observation method is used to provide MPPT. The output voltage of the solar cell array and the inductor current are detected and sent to a MPPT inverter to determine the desired output voltage for the solar cell array. Then the detected output voltage and the desired output voltage of the solar cell array are sent to a subtract or and the difference is sent to a PI inverter. The output of the PI inverter is the reference signal of the inner current control loop. The reference signal and the detected inductor current are sent to a subtract or and the difference is sent to an amplifier to complete the inner current control loop. The output of the amplifier is sent to the PWM circuit. The PWM circuit generates a set of complementary signals that control the power electronic switches of the dc-dc power converter.

VI. MATLAB/SIMULINK RESULTS

Case I. Seven level inverter for RES by using PI inverter

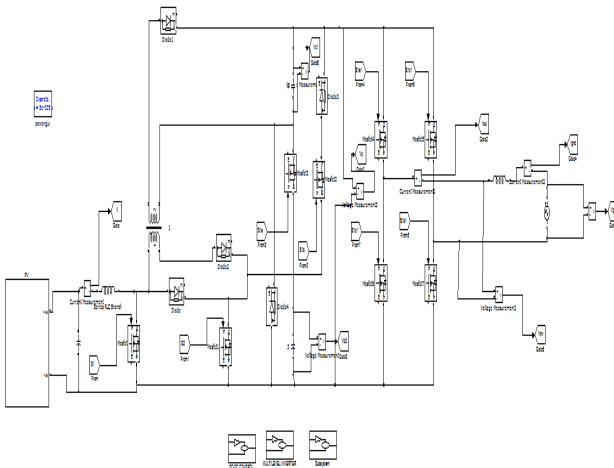


Fig.8. Simulink circuit for proposed seven level inverter using PI Inverter.

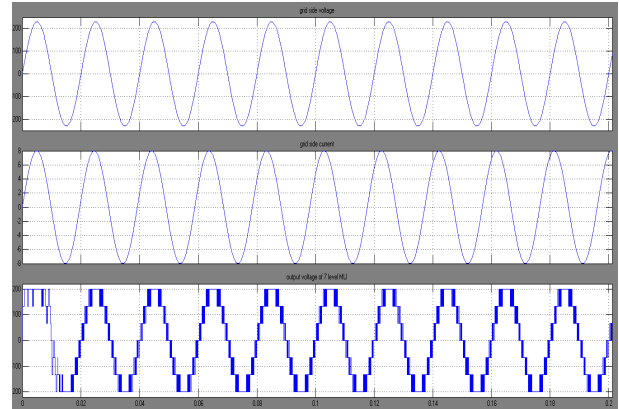


Fig.9. simulation results for the ac side of the seven-level inverter: (a) grid voltage, (b) inverter current (c) output voltage of seven-level inverter.

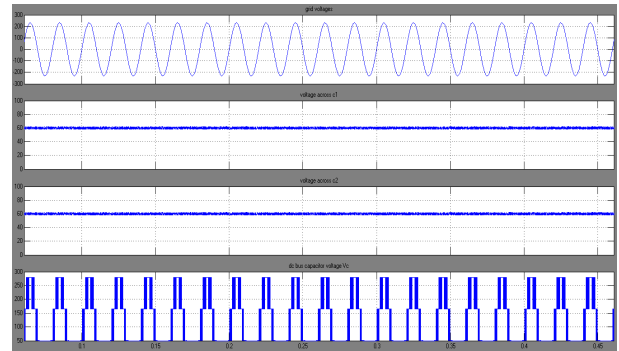


Fig.10. simulation results for (a) grid voltage, (b) voltage of capacitor C1, (c) voltage of capacitor C2, and (d) output voltage of the capacitor selection circuit.

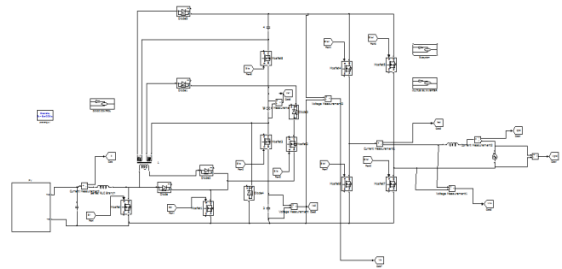


Fig 11 Simulink circuit for proposed nine level inverter using PV

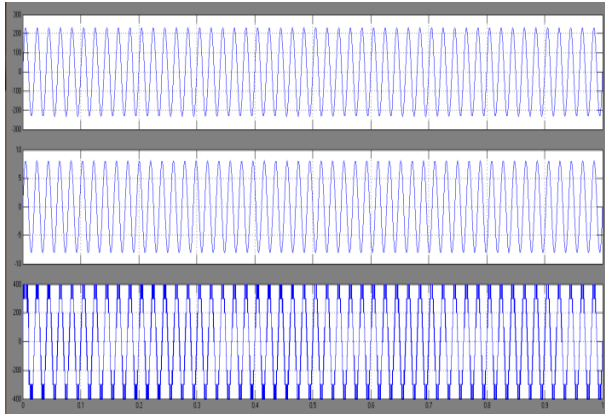


Fig 12 simulation results for the ac side of the nine-level inverter: (a) grid voltage, (b) inverter current (c) output voltage of nine-level inverter

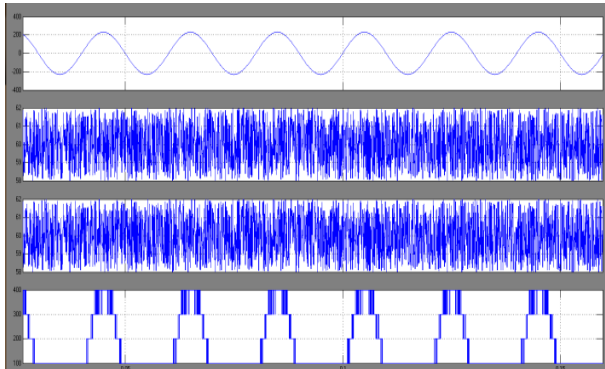


Fig 13 simulation results for (a) grid voltage, (b) voltage of capacitor C1, (c) voltage of capacitor C2, and (d) output voltage of the capacitor selection circuit

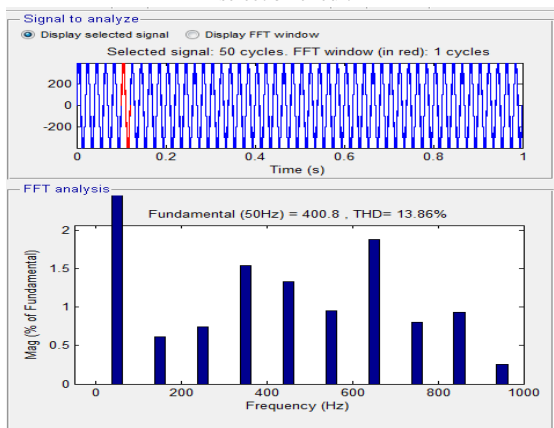


Fig 14 FFT analysis for inverter current

VII. CONCLUSION

The proposed technique has some features such as it reduces the cost of the overall system, compact size as well as an increased efficiency. With the help of lower number of switches, seven-level of output voltages are generated and thus it reduces the switching loss and conduction losses. The THD of seven-level inverter

is less compare to the five-level and three-level inverter. The fuzzy logic inverter could control the switches present in the boost converter and H-bridge inverter. For the seven level of output, only six power electronic switches are used and only one switch will operate at high frequency at any time. For further implementation, the inverter level can extend by cascading additional H-bridge inverter. There may be some loss due to the transformer and this can also overcome by providing transformer less connection with its replacement. As the inverter level increases, the filter requirements and harmonic content decreases.

REFERENCES

- [1] Jinn-Chang Wu, Member, IEEE, and Chia-Wei Chou, —A Solar Power Generation System With a Seven-Level Inverter, *IEEE Trans. Power Electron.*, vol. 29, no. 7, pp. 3454–3462, July. 2014.
- [2] Fan Zhang, Kary Thanapalan, Andrew Procter, Stephen Carr, and Jon Maddy, —Adaptive Hybrid Maximum Power Point Tracking Method for a Photovoltaic System, *IEEE Trans. Energy Conversion*, vol. 28, no. 2, pp.353-360, June. 2013.
- [3] J. D. Barros, J. F. A. Silva, and E.G.A Jesus, —Fast-predictive optimal control of NPC multilevel converters, *IEEE Trans. Ind. Electron.*, vol. 60, no. 2, pp. 619–627, Feb. 2013.
- [4] J. Chavarria, D. Biel, F. Guinjoan, C.Meza, and J. J. Negroni, —Energy balance control of PV cascaded multilevel grid-connected inverters under level-shifted and phase-shifted PWMs, *IEEE Trans. Electron.*, vol. 60, no. 1, pp. 98–111, Jan. 2013.
- [5] X. She, A. Q. Huang, T. Zhao, and G. Wang, —Coupling effect reduction of a voltage-balancing inverter in single-phase cascaded multilevel converters, *IEEE Trans. Power Electron.*, vol. 27, no. 8, pp. 3530–3543, Aug. 2012.
- [6] S. Choi and M. Saeedifard, —Capacitor voltage balancing of flying capacitor multilevel converters by space vector PWM, *IEEE Trans. Power Delivery*, vol. 27, no. 3, pp. 1154–1161, Jul. 2012.
- [7] R. A. Mastromauro, M. Liserre, and A. Dell'Aquila, —Control issues in single-stage photovoltaic systems: MPPT, current and voltage control, *IEEE Trans. Ind. Informat.*, vol. 8, no. 2, pp. 241–254, May. 2012.
- [8] L. Maharjan, T. Yamagishi, and H. Akagi, —Active-power control of individual converter cells for a battery energy storage system based on a multilevel cascade PWM converter, *IEEE Trans. Power Electron.*, vol. 27, no. 3, pp. 1099–1107, Mar. 2012.
- [9] N. A. Rahim, K. Chaniago, and J. Selvaraj, —Single-phase seven-level grid-connected inverter for photovoltaic system, *IEEE Trans. Ind. Electr.*, vol. 58, no. 6, pp. 2435–2443, Jun. 2011.
- [10] Huan-Liang Tsai, Ci-Siang Tu, and Yi-Jie Su, Member, —Development of Generalized Photovoltaic Model Using MATLAB/SIMULINK, *IAENG, WCECS*, San Francisco, USA October 22 - 24, 2008.
- [11] Ravi, A., Manoharan, P.S., Vijay Anand, J.: 'Modeling and simulation of three phase multilevel inverter for grid connected photovoltaic systems', *Solar Energy*, 2011, 85, pp. 2811–2818.
- [12] A Ravi, PS Manoharan, M Valan Rajkumar Harmonic Reduction of Three-Phase Multilevel Inverter for Grid Connected Photovoltaic System Using Closed Loop Switching Control' 2012, *International Review on Modelling & Simulations* 5 (5), pp.1934-1942.



ISSN (Print) : 2320 – 3765
ISSN (Online): 2278 – 8875

International Journal of Advanced Research in Electrical, Electronics and Instrumentation Engineering

(An ISO 3297: 2007 Certified Organization)

Vol. 5, Issue 6, June 2016

Fuzzy Controlled Multilevel Inverter Based MPPT Controlled PV for Grid-Connected Applications

Venkata Ramesh Dongari, P.Ganesh

M. Tech Student Scholar, Department of EEE, Malla Reddy Engineering College (Autonomous), Hyderabad,
Telangana, India

Assistant Professor, Department of EEE, Malla Reddy Engineering College (Autonomous), Hyderabad, Telangana,
India

ABSTRACT: The inverters are categorized according to the configuration of the PV system, the configuration of the conversion stages within the inverter and whether they use transformers. After the introduction of the state of the art of inverters for PV systems with and without transformers, the paper focuses on some known problems and challenges for transformer less inverters. Topologies without transformers have big advantages like low weight, volume and cost. In addition they often reach higher efficiencies than topologies with transformers. Eliminating the leakage current is one of the most important issues for transformer less inverters in grid-connected photovoltaic system applications, where the technical challenge is how to keep the system common-mode voltage constant to reduce the leakage current. To realize better utilization of PV modules and maximize the solar energy extraction, a distributed maximum power point tracking control scheme is applied to both single- and three-phase multilevel inverters, which allows independent control of each dc-link voltage. For three-phase grid-connected applications, PV mismatches may introduce unbalanced supplied power, leading to unbalanced grid current.

KEYWORDS: cascaded multilevel inverter, distributed maximum power point (MPP) tracking (MPPT), Fuzzy logic, modular, modulation Compensation.

I. INTRODUCTION

In recent years, the efforts to spread the use of renewable energy resources instead of pollutant fossil fuels and other forms have increased. Photovoltaic systems offer the possibility of converting sunlight into electricity. The transformation of electricity through photovoltaic provides ease of installation, maintenance and become more affordable. One of the most common control strategies structures applied to decentralized power generator is based on power direct control employing a controller for the dc link voltage and a controller to regulate the injected current to the utility network. The system components and power control scheme are modeled in terms of dynamic behaviors. An improved MPPT converter with current compensation method for small-scaled PV-applications is presented in [1]. The proposed method implements maximum power point tracking (MPPT) by variable reference current which is continuously changed during one sampling period. Lot of research has been done on maximum power point tracking [3] of Photovoltaic cell. A new maximum power point tracking algorithm for photovoltaic arrays is proposed in [4]. The algorithm detects the maximum power point of the PV. The computed maximum power is used as a reference value of the control system. The proposed MPPT has several advantages: simplicity, high convergence speed, and independent on PV array characteristics. The many different techniques for maximum power point tracking of photovoltaic (PV) arrays are discussed in [5]. Paper should serve as a convenient reference for future work in PV power generation in [6].

The modular cascaded H-bridge multilevel inverter, which requires an isolated dc source for each H-bridge, is one dc/ac cascaded inverter topology. The separate dc links in the multilevel inverter make independent voltage control



International Journal of Advanced Research in Electrical, Electronics and Instrumentation Engineering

(An ISO 3297: 2007 Certified Organization)

Vol. 5, Issue 6, June 2016

possible. As a result, individual MPPT control in each PV module can be achieved, and the energy harvested from PV panels can be maximized. Meanwhile, the modularity and low cost of multilevel converters would position them as a prime candidate for the next generation of efficient, robust, and reliable grid connected solar power electronics. A modular cascaded H-bridge multilevel inverter topology for single- or three-phase grid-connected PV systems is presented in this paper. The panel mismatch issues are addressed to show the necessity of individual MPPT control, and a control scheme with distributed MPPT control is then proposed. The distributed MPPT control scheme can be applied to both single and three-phase systems [7].

In addition, for the presented three-phase grid-connected PV system, if each PV module is operated at its own MPP, PV mismatches may introduce unbalanced power supplied to the three-phase multilevel inverter, leading to unbalanced injected grid current. To balance the three-phase grid current, modulation compensation is also added to the control system.

An improved perturbation and observation maximum power point tracking algorithm for PV arrays. Improved perturbation and observation method of Maximum Power Point Tracking control for photovoltaic power systems in [10]. He explained about the perturbation observation method. Maximum photovoltaic power tracking an algorithm for rapidly changing atmospheric conditions explained in [11]. Evaluation of maximum power point tracking methods for grid connected photovoltaic systems discussed in [12]. In the maximum power point tracking method so many methods are available but he used the suitable tracker. The fuzzy inference is carried out by using Sugeno's . So this is Sugeno, or TakagiSugeno-Kang, method of fuzzy inference. Introduced in 1985[9], it is similar to the Mamdani method in many respects. Hardware Implementation of Fuzzy Logic based Maximum Power Point Tracking Controller for PV System. The electric power supplied by a photovoltaic power generation systems depends on the solar irradiation and temperature. A Rule-Based Fuzzy Logic Controller for a PWM Inverter in Photo-voltaic Energy Conversion Scheme discussed in . The modeling and simulation of the electric part of a grid connected photovoltaic generation system explained. This work proposed a fuzzy logic based controller to track MPPT in photovoltaic cell.

II. SYSTEM DESCRIPTION

Modular cascaded H-bridge multilevel inverters for single and three-phase grid-connected PV systems are shown in Fig.1. Each phase consists of n H-bridge converters connected in series, and the dc link of each H-bridge can be fed by a PV panel or a short string of PV panels. The cascaded multilevel inverter is connected to the grid through L filters, which are used to reduce the switching harmonics in the current.

By different combinations of the four switches in each H-bridge module, three output voltage levels can be generated: $-V_{dc}$, 0, or $+V_{dc}$. A cascaded multilevel inverter with n input sources will provide $2n + 1$ levels to synthesize the ac output waveform. This $(2n + 1)$ -level voltage waveform enables the reduction of harmonics in the synthesized current, reducing the size of the needed output filters. Multilevel inverters also have other advantages such as reduced voltage stresses on the semiconductor switches and having higher efficiency when compared to other converter topologies.

III. PANEL MISMATCHES

PV mismatch is an important issue in the PV system. Due to the unequal received irradiance, different temperatures, and aging of the PV panels, the MPP of each PV module may be different. If each PV module is not controlled independently, the efficiency of the overall PV system will be decreased.

To show the necessity of individual MPPT control, a five-level two-H-bridge single-phase inverter is simulated in MATLAB/SIMULINK. Each H-bridge has its own 185-W PV panel connected as an isolated dc source. The PV panel is modeled according to the specification of the commercial PV panel from Astronergy CHSM-5612M.

Consider an operating condition that each panel has a different irradiation from the sun; panel 1 has irradiance $S = 1000$ W/m², and panel 2 has $S = 600$ W/m². If only panel 1 is tracked and its MPPT controller determines the average voltage of the two panels, the power extracted from panel 1 would be 133 W, and the power from panel 2 would be 70 W, as can be seen. Without individual MPPT control, the total power harvested from the PV system is 203 W.

However, the MPPs of the PV panels under the different irradiance. The maximum output power values will be 185 and 108.5 W when the S values are 1000 and 600 W/m², respectively, which means that the total power harvested from

International Journal of Advanced Research in Electrical, Electronics and Instrumentation Engineering

(An ISO 3297: 2007 Certified Organization)

Vol. 5, Issue 6, June 2016

the PV system would be 293.5 W if individual MPPT can be achieved. This higher value is about 1.45 times of the one before. Thus, individual MPPT control in each PV module is required to increase the efficiency of the PV system. In a three-phase grid-connected PV system, a PV mismatch may cause more problems. Aside from decreasing the overall efficiency, this could even introduce unbalanced power supplied to the three-phase grid-connected system. If there are PV mismatches between phases, the input power of each phase would be different. Since the grid voltage is balanced, this difference in input power will cause unbalanced current to the grid, which is not allowed by grid standards. For example, to unbalance the current per phase more than 10% is not allowed for some utilities, where the percentage imbalance is calculated by taking the maximum deviation from the average current and dividing it by the average current.

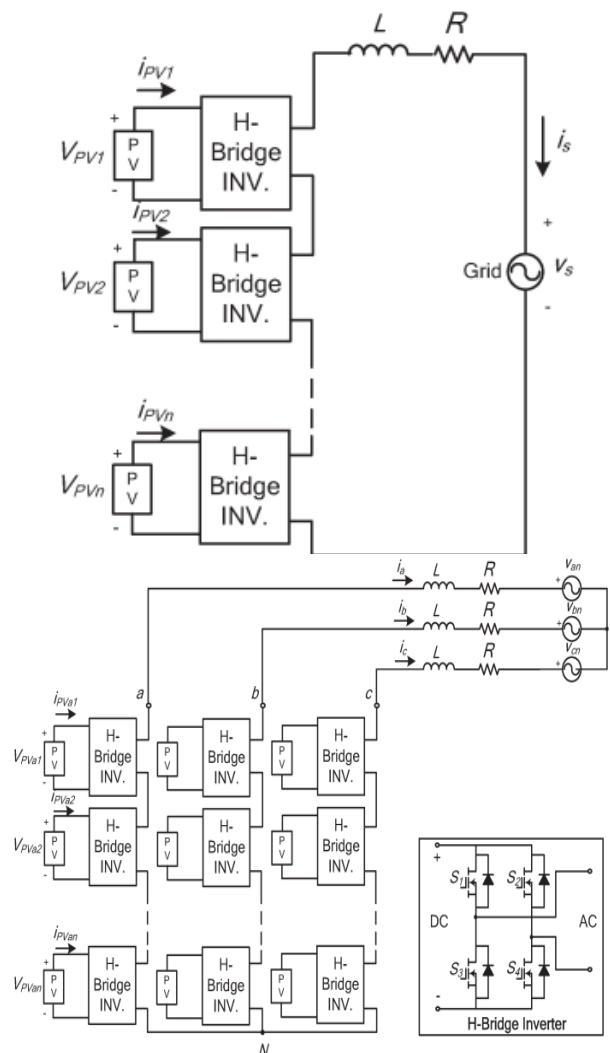


Fig. 1. Topology of the modular cascaded H-bridge multilevel inverter for grid-connected PV systems.

To solve the PV mismatch issue, a control scheme with individual MPPT control and modulation compensation is proposed. The details of the control scheme will be discussed in the next section.



IV. CONTROL SCHEME

A. Distributed MPPT Control

In order to eliminate the adverse effect of the mismatches and increase the efficiency of the PV system, the PV modules need to operate at different voltages to improve the utilization per PV module. The separate dc links in the cascaded H-bridge multilevel inverter make independent voltage control possible. To realize individual MPPT control in each PV module, the control scheme proposed is updated for this application.

The distributed MPPT control of the three-phase cascaded H-bridge inverter is shown in Fig.2. In each H-bridge module, an MPPT controller is added to generate the dc-link voltage reference. Each dc-link voltage is compared to the corresponding voltage reference, and the sum of all errors is controlled through a total voltage controller that determines the current reference I_{dref} . The reactive current reference I_{qref} can be set to zero, or if reactive power compensation is required, I_{qref} can also be given by a reactive current calculator. The synchronous reference frame phase-locked loop (PLL) has been used to find the phase angle of the grid voltage. As the classic control scheme in three-phase systems, the grid currents in abc coordinates are converted to d_q coordinates and regulated through proportional-integral (PI) controllers to generate the modulation index in the d_q coordinates, which is then converted back to three phases.

The distributed MPPT control scheme for the single-phase system is nearly the same. The total voltage controller gives the magnitude of the active current reference, and a PLL provides the frequency and phase angle of the active current reference. The current loop then gives the modulation index.

To make each PV module operate at its own MPP, take phase a as an example; the voltages v_{dca2} to v_{dcan} are controlled individually through $n - 1$ loops. Each voltage controller gives the modulation index proportion of one H-bridge module in phase a . After multiplied by the modulation index of phase a , $n - 1$ modulation indices can be obtained. Also, the modulation index for the first H-bridge can be obtained by subtraction. The control schemes in phases b and c are almost the same. The only difference is that all dc-link voltages are regulated through PI controllers, and n modulation index proportions are obtained for each phase.

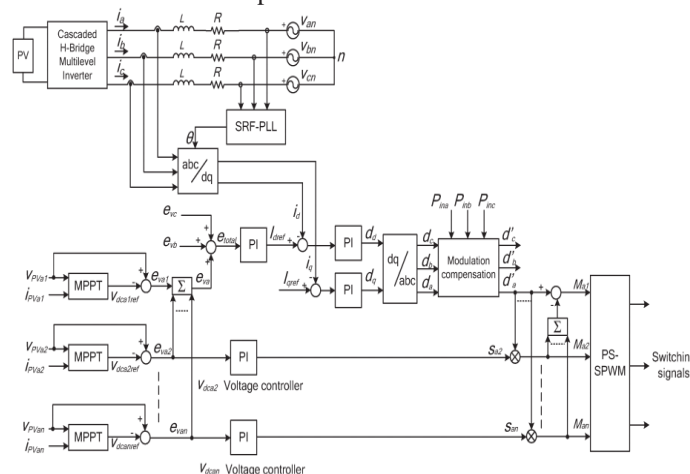


Fig.2. Control scheme for three-phase modular cascaded H-bridge multilevel PV inverter.

A phase-shifted sinusoidal pulse width modulation switching scheme is then applied to control the switching devices of each H-bridge.

It can be seen that there is one H-bridge module out of N modules whose modulation index is obtained by subtraction. For single-phase systems, $N = n$, and for three-phase systems, $N = 3n$, where n is the number of H-bridge modules per phase. The reason is that N voltage loops are necessary to manage different voltage levels on N H-bridges, and one is the total voltage loop, which gives the current reference. So, only $N - 1$ modulation indices can be determined by the last $N - 1$ voltage loops, and one modulation index has to be obtained by subtraction.

Many MPPT methods have been developed and implemented. The incremental conductance method has been used in this paper. It lends itself well to digital control, which can easily keep track of previous values of voltage and current and make all decisions.

International Journal of Advanced Research in Electrical, Electronics and Instrumentation Engineering

(An ISO 3297: 2007 Certified Organization)

Vol. 5, Issue 6, June 2016

B. Modulation Compensation

As mentioned earlier, a PV mismatch may cause more problems to a three-phase modular cascaded H-bridge multilevel PV inverter. With the individual MPPT control in each H-bridge module, the input solar power of each phase would be different, which introduces unbalanced current to the grid. To solve the issue, a zero sequence voltage can be imposed upon the phase legs in order to affect the current flowing into each phase. If the updated inverter output phase voltage is proportional to the unbalanced power, the current will be balanced.

Thus, the modulation compensation block, as shown in Fig. 3, is added to the control system of three-phase modular cascaded multilevel PV inverters. The key is how to update the modulation index of each phase without increasing the complexity of the control system. First, the unbalanced power is weighted by ratio r_j , which is calculated as

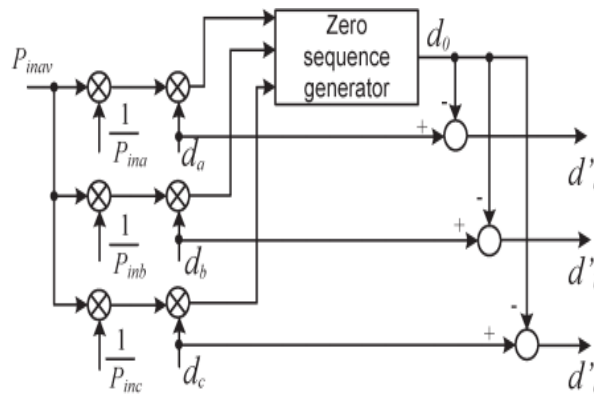


Fig. 3. Modulation compensation scheme.

$$r_j = \frac{P_{inav}}{P_{inj}} \quad (1)$$

Where P_{inj} is the input power of phase j ($j = a, b, c$), and P_{inav} is the average input power.

Then, the injected zero sequence modulation index can be generated as

$$d_0 = \frac{1}{2} [\min(r_a \cdot d_a, r_b \cdot d_b, r_c \cdot d_c) + \max(r_a \cdot d_a, r_b \cdot d_b, r_c \cdot d_c)] \quad (2)$$

Where d_j is the modulation index of phase j ($j = a, b, c$) and is determined by the current loop controller.

The modulation index of each phase is updated by

$$d'_j = d_j - d_0. \quad (3)$$

Only simple calculations are needed in the scheme, which will not increase the complexity of the control system. An example is presented to show the modulation compensation scheme more clearly. Assume that the input power of each phase is unequal

$$P_{ina} = 0.8 \quad P_{inb} = 1 \quad P_{inc} = 1 \quad (4)$$

International Journal of Advanced Research in Electrical, Electronics and Instrumentation Engineering

(An ISO 3297: 2007 Certified Organization)

Vol. 5, Issue 6, June 2016

V. FUZZY LOGIC CONTROLLER

Fuzzy logic is all about the relative importance of precision: use as Fuzzy Logic Toolbox software with MATLAB technical computing software as a tool for solving problems with fuzzy logic. Fuzzy logic is a fascinating area of research because it does a good job of trading off between significance and precision something that humans have been managing for a very long time.

In this sense, fuzzy logic is both old and new because, although the modern and methodical science of fuzzy logic is still young, the concept of fuzzy logic relies on age-old skills of human reasoning.

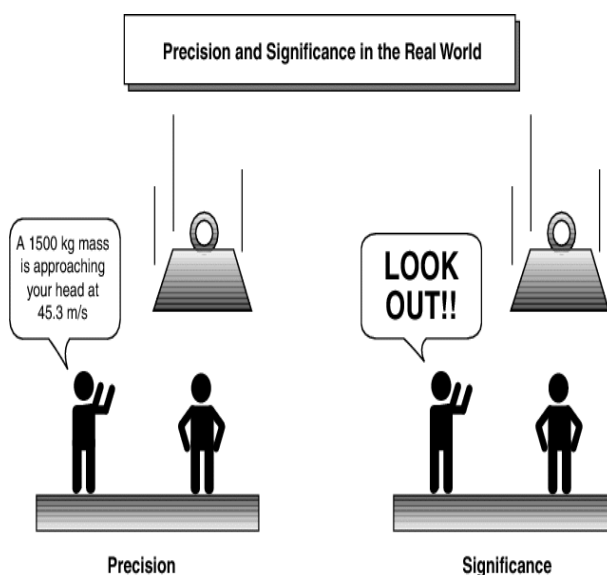


Fig 4 Fuzzy Description

Fuzzy logic is a convenient way to map an input space to an output space. Mapping input to output is the starting point for everything. Consider the following examples:

- With information about how good your service was at a restaurant, a fuzzy logic system can tell you what the tip should be.
- With your specification of how hot you want the water, a fuzzy logic system can adjust the faucet valve to the right setting.
- With information about how far away the subject of your photograph is, a fuzzy logic system can focus the lens for you.
- With information about how fast the car is going and how hard the motor is working, a fuzzy logic system can shift gears for you.

To determine the appropriate amount of tip requires mapping inputs to the appropriate outputs. Between the input and the output, the preceding figure shows a black box that can contain any number of things: fuzzy systems, linear systems, expert systems, neural networks, differential equations, interpolated multi dimensional lookup tables, or even a spiritual advisor, just to name a few of the possible options. Clearly the list could go on and on. Of the dozens of ways to make the black box work, it turns out that fuzzy is often the very best way. As Lotfi Zadeh, who is considered to be the father of fuzzy logic, once remarked: "In almost every case you can build the same product without fuzzy logic, but fuzzy is faster and cheaper".



International Journal of Advanced Research in Electrical, Electronics and Instrumentation Engineering

(An ISO 3297: 2007 Certified Organization)

Vol. 5, Issue 6, June 2016

Fuzzy logic is not a cure-all. When should you not use fuzzy logic? The safest statement is the first one made in this introduction: fuzzy logic is a convenient way to map an input space to an output space. Fuzzy logic is the codification of common sense — use common senses when you implement it and which will probably make the right decision. Many controllers, for example, do a fine job without using fuzzy logic. However, it takes the time to become familiar with fuzzy logic, it can be a very powerful tool for dealing quickly and efficiently with imprecision and nonlinearity.

Fuzzy logic arose from a desire to incorporate logical reasoning and the intuitive decision making of an expert operator into an automated system [14]. The aim is to make decisions based on a number of learned or predefined rules, rather than numerical calculations. Fuzzy logic incorporates a rule-based structure in attempting to make decisions. However, before the rule-base can be used, the input data should be represented in such a way as to retain meaning, while still allowing for manipulation. Fuzzy logic is an aggregation of rules, based on the input state variables condition with a corresponding desired output. A mechanism must exist to decide on which output, or combination of different outputs, will be used since each rule could conceivably result in a different output action.

Fuzzy logic can be viewed as an alternative form of input=output mapping. Consider the input premise, x , and a particular qualification of the input x represented by A_i . Additionally, the corresponding output, y , can be qualified by expression C_i . Thus, a fuzzy logic representation of the relationship between the input x and the output y could be described by the following:

R1: IF x is A_1 THEN y is C_1

R2: IF x is A_2 THEN y is C_2

.....

.....

.....

R $_n$: IF x is A_n THEN y is C_n

Where x is the input (state variable), y is the output of the system, A_i are the different fuzzy variables used to classify the input x and C_i are the different fuzzy variables used to classify the output y . The fuzzy rule representation is linguistically based. Thus, the input x is a linguistic variable that corresponds to the state variable under consideration. Furthermore, the elements A_i are fuzzy variables that describe the input x . correspondingly, the elements C_i are the fuzzy variables used to describe the output y . In fuzzy logic control, the term “linguistic variable” refers to whatever state variables the system designer is interested in. Linguistic variables that are often used in control applications include Speed, Speed Error, Position, and Derivative of Position Error. The fuzzy variable is perhaps better described as a fuzzy linguistic qualifier. Thus the fuzzy qualifier performs classification (qualification) of the linguistic variables. The fuzzy variables frequently employed include Negative Large, Positive Small and Zero. Several papers in the literature use the term “fuzzy set” instead of “fuzzy variable”, however; the concept remains the same. Table 30.1 illustrates the difference between fuzzy variables and linguistic variables. Once the linguistic and fuzzy variables have been specified, the complete inference system can be defined. The fuzzy linguistic universe, U , is defined as the collection of all the fuzzy variables used to describe the linguistic variables. i.e. the set U for a particular system could be comprised of Negative Small (NS), Zero (ZE) and Positive Small (PS). Thus, in this case the set U is equal to the set of [NS, ZE, PS]. For the system described by Eq. (30.1), the linguistic universe for the input x would be the set U_x . $A_1 A_2 \dots A_n$. Similarly,



International Journal of Advanced Research in Electrical, Electronics and Instrumentation Engineering

(An ISO 3297: 2007 Certified Organization)

Vol. 5, Issue 6, June 2016

TABLE Fuzzy and linguistic variables

Linguistic Variables		Fuzzy Variables (Linguistic Qualifiers)	
Speed error	(SE)	Negative large	(NL)
Position error	(PE)	Zero	(ZE)
Acceleration	(AC)	Positive medium	(PM)
Derivative of position error	(DPE)	Positive very small	(PVS)
Speed	(SP)	Negative medium small	(NMS)

the linguistic universe for the output y would be the set $U_y = \{C_1, C_2, \dots, C_n\}$. The Fuzzy Inference System (FIS) The basic fuzzy inference system (FIS) can be classified as: Type 1 Fuzzy Input Fuzzy Output (FIFO)
Type 2 Fuzzy Input Crisp Output (FICO)

Type 2 differs from the first in that the crisp output values are predefined and, thus, built into the inference engine of the FIS. In contrast, type 1 produces linguistic outputs. Type 1 is more general than type 2 as it allows redefinition of the response without having to redesign the entire inference engine. One drawback is the additional step required, converting the fuzzy output of the FIS to a crisp output. Developing a FIS and applying it to a control problem involves several steps:

1. fuzzification
2. fuzzy rule evaluation (fuzzy inference engine)
3. defuzzification.

The total fuzzy inference system is a mechanism that relates the inputs to a specific output or set of outputs. First, the inputs are categorized linguistically (fuzzification), then the linguistic inputs are related to outputs (fuzzy inference) and, finally, all the different outputs are combined to produce a single output (defuzzification). Figure 30.1 shows a block diagram of the fuzzy inference system.

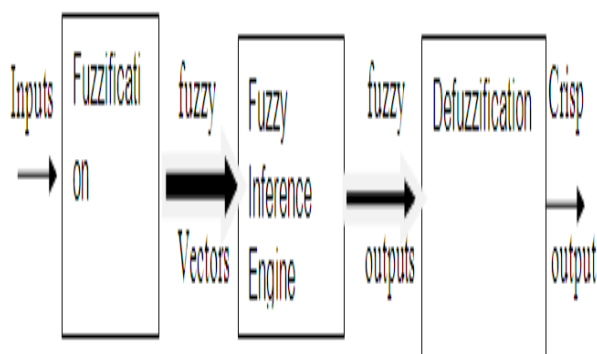


Fig 5 Fuzzy inference system.

Fuzzification: Fuzzy logic uses linguistic variables instead of numerical variables. In a control system, error between reference signal and output signal can be assigned as Negative Big (NB), Negative Medium (NM), Negative Small (NS), Zero (ZE), Positive small (PS), Positive Medium (PM), Positive Big (PB). The triangular membership function

International Journal of Advanced Research in Electrical, Electronics and Instrumentation Engineering

(An ISO 3297: 2007 Certified Organization)

Vol. 5, Issue 6, June 2016

is used for fuzzifications. The process of fuzzification convert numerical variable (real number) to a linguistic variable (fuzzy number).

Defuzzification: The rules of fuzzy logic controller generate required output in a linguistic variable (Fuzzy Number), according to real world requirements; linguistic variables have to be transformed to crisp output (Real number). This selection of strategy is a compromise between accuracy and computational intensity.

V. MATLAB/SIMULATION RESULTS

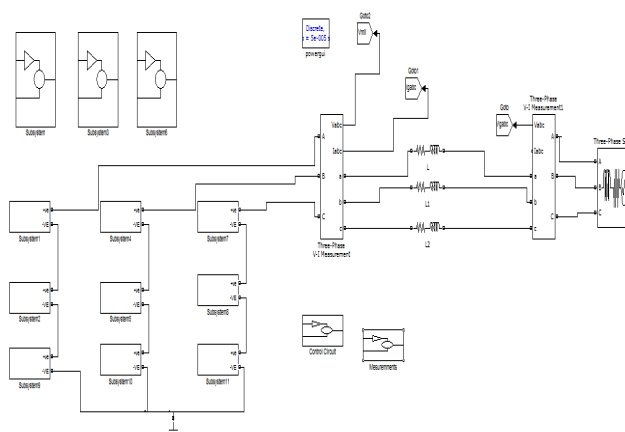


Fig 6 Basic simulation diagram

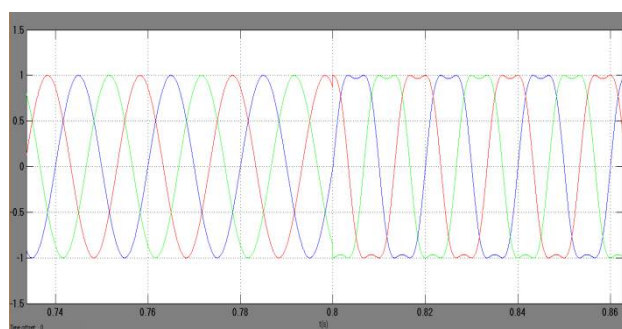


Fig 7 Modulation indices before and after modulation compensation

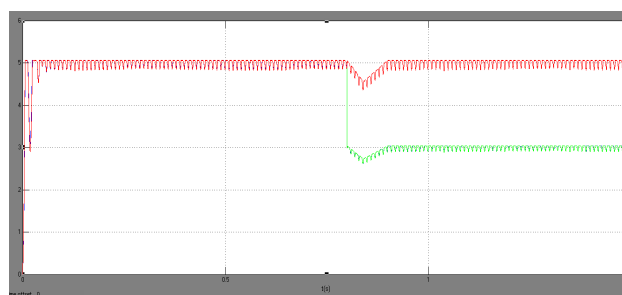


Fig 8 PV currents of phases with distributed MPPT



International Journal of Advanced Research in Electrical, Electronics and Instrumentation Engineering

(An ISO 3297: 2007 Certified Organization)

Vol. 5, Issue 6, June 2016

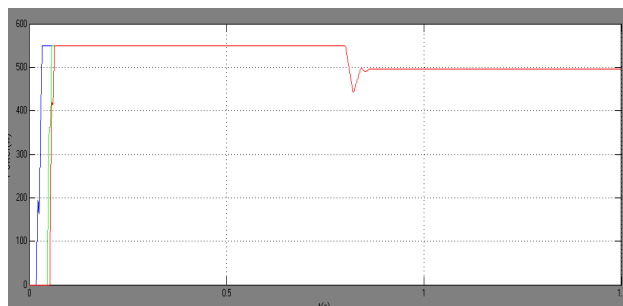


Fig 9 Power injected to the grid with modulation compensation

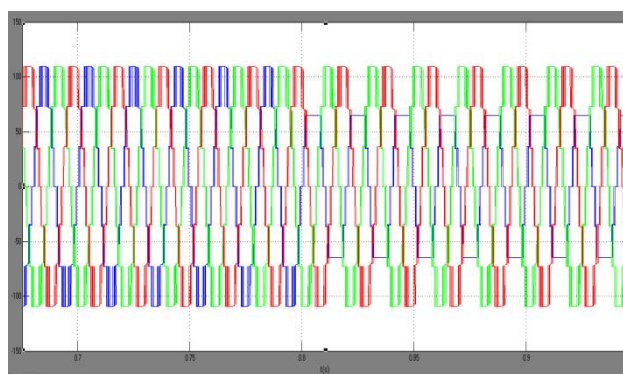


Fig 10 Three phase inverter output voltage waveforms with modulation compensation

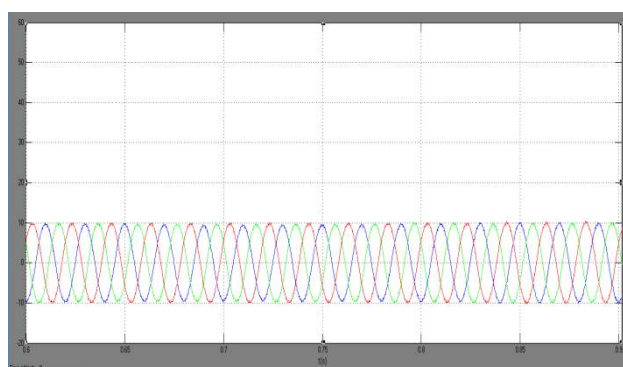


Fig 11 Three phase grid current waveforms with modulation compensation

VI.CONCLUSION

The purpose of this paper is to study the harmonic profile of Grid connected PV system for different MPPT methods including perturbation & observation incremental conductance and Fuzzy logic controller. The PV simulation system used in this paper is set up under Matlab/Simulink environment. After accomplishing the model of PV modules, the models of Multi level inverter and MPPT systems are combined with it to complete the PV simulation system with the MPPT functions. The proposed fuzzy MPPT sets the optimum DC bus voltage reference for the inverter without the need for a dc-dc converter. The control of the active and reactive power is done using a PI controller. Fuzzy based three phase single stage grid connected PV system has been proposed. The harmonics are eliminated by the double



ISSN (Print) : 2320 – 3765
ISSN (Online): 2278 – 8875

International Journal of Advanced Research in Electrical, Electronics and Instrumentation Engineering

(An ISO 3297: 2007 Certified Organization)

Vol. 5, Issue 6, June 2016

tuned resonant filter. The power extracted from the PV array increased by the fuzzy based MPPT which develop the system performance in varying weather condition.

REFERENCES

- [1] J. M. Carrasco et al., "Power-electronic systems for the grid integration of renewable energy sources: A survey," IEEE Trans. Ind. Electron., vol. 53, no. 4, pp. 1002–1016, Jun. 2006.
- [2] S. B. Kjaer, J. K. Pedersen, and F. Blaabjerg, "A review of single-phase grid connected inverters for photovoltaic modules," IEEE Trans. Ind. Appl., vol. 41, no. 5, pp. 1292–1306, Sep./Oct. 2005.
- [3] M. Meinhardt and G. Cramer, "Past, present and future of grid connected photovoltaic- and hybrid power systems," in Proc. IEEE PES Summer Meet., 2000, vol. 2, pp. 1283–1288.
- [4] M. Calais, J. Myrzik, T. Spooner, and V. G. Agelidis, "Inverter for singlephase grid connected photovoltaic systems—An overview," in Proc. IEEE PESC, 2002, vol. 2, pp. 1995–2000.
- [5] J. M. A. Myrzik and M. Calais, "String and module integrated inverters for single-phase grid connected photovoltaic systems—A review," in Proc. IEEE Bologna Power Tech Conf., 2003, vol. 2, pp. 1–8.
- [6] F. Schimpf and L. Norum, "Grid connected converters for photovoltaic, state of the art, ideas for improvement of transformer less inverters," in Proc. NORPIE, Espoo, Finland, Jun. 2008, pp. 1–6.
- [7] B. Liu, S. Duan, and T. Cai, "Photovoltaic DC-building-module-based BIPV system—Concept and design considerations," IEEE Trans. Power Electron., vol. 26, no. 5, pp. 1418–1429, May 2011.
- [8] L. M. Tolbert and F. Z. Peng, "Multilevel converters as a utility interface for renewable energy systems," in Proc. IEEE Power Eng. Soc. Summer Meet., Seattle, WA, USA, Jul. 2000, pp. 1271–1274.
- [9] H. Ertl, J. Kolar, and F. Zach, "A novel multicell DC–AC converter for applications in renewable energy systems," IEEE Trans. Ind. Electron., vol. 49, no. 5, pp. 1048–1057, Oct. 2002.
- [10] S. Daher, J. Schmid, and F. L. M. Antunes, "Multilevel inverter topologies for stand-alone PV systems," IEEE Trans. Ind. Electron., vol. 55, no. 7, pp. 2703–2712, Jul. 2008.
- [11] G. R. Walker and P. C. Sernia, "Cascaded DC–DC converter connection of photovoltaic modules," IEEE Trans. Power Electron., vol. 19, no. 4, pp. 1130–1139, Jul. 2004.
- [12] E. Roman, R. Alonso, P. Ibanez, S. Elorduizaparietxe, and D. Goitia, "Intelligent PV module for grid-connected PV systems," IEEE Trans. Ind. Electron., vol. 53, no. 4, pp. 1066–1073, Jun. 2006.

BIOGRAPHY



Venkata Ramesh Dongari received M.Tech degree from Mallareddy Engineering College (Autonomous) in the year 2016 and pursuing M.Tech in the stream of Electrical Power Systems. He received B-tech from Dr. Samuel George Institute of Engineering & Technology in the year 2012. His areas of interest are Power systems, Electrical Circuits, Control Systems and Power electronics drives.



Ganesh Pashikanti received M.Tech degree from Vathsalya Institute of Science Technology in the year 2014 and received M.Tech in the stream of Power Electronics. Received B-tech from Vidya Bharathi Institute of Technology in the year 2009. Currently working as a Assistant Professor in Mallareddy Engineering college since 3 years and he is also the member of IJEEEE. And his areas of interest are Electrical machines, Electrical Circuits, Control Systems and Electrical drives.

Hybrid Fuzzy Control System for Power Control of Grid Connected PV System

S BABURAO

M-tech Student Scholar

Department of Electrical & Electronics Engineering,
Mallareddy Engineering College, maisammaguda ;
Hyderabad (Dt); Telangana, India.

P GANESH

Assistant Professor

Department of Electrical & Electronics Engineering,
Mallareddy, Engineering College, maisammaguda ;
Hyderabad (Dt); Telangana, India.

Abstract- The penetration of renewable energy in modern power system, Microgrid has become a popular application worldwide. In this concept bidirectional converters for AC and DC hybrid Microgrid application are proposed as an efficient interface. To reach the goal of bidirectional power conversion, both rectifier and inverter modes are analyzed. In order to achieve high performance operation and single-phase bi-directional inverter with dc-bus voltage regulation and power compensation in dc-Microgrid applications. This concept proposes a control design methodology for a multi functional single-phase bidirectional PWM converter in renewable energy systems. There is a generic current loop for different modes of operation to ease the transition between different modes, including stand-alone inverter mode, grid-tied inverter mode, ac voltage regulation is of importance because of the sensitive loads In dc-Microgrid applications, a power distribution system requires a bi-directional inverter to control the power flow between dc bus and ac grid, and to regulate the dc bus to a certain range of voltages, in which dc load may change abruptly. This will result in high dc-bus voltage variations; the bi-directional inverter can shift its current commands according to the specified power factor at ac grid side. Parallel-connected bidirectional converters for AC and DC hybrid Microgrid application are proposed as an efficient interface. To reach the goal of bidirectional power conversion, both rectifier and inverter modes are analyzed. The proposed concept can be implemented by hybrid fuzzy controller by using Matlab/Simulink software.

Keywords—Microgrid, Grid-tie Inverter, Voltage control, Automatic power control.

I. INTRODUCTION

Microgrids are the networks comprising of various generators, storage devices, and controllable loads that can operate either grid connected or islanded mode as a controlled entity. Suitable micro-grid control strategy design is the key for stability of the microgrid under different operation mode, especially when changing from the grid connected operation to the islanding operation. Operation of micro-grid in grid connected mode demands control of power flow from micro-grid to utility grid. Photovoltaic generation on DC bus is highly intermittent.

Therefore, it is required to regulate the power flow between DC bus and AC bus which is achieved by phase angle control. Voltage and frequency control formulate the control system for synchronization. This paper describes design, simulation and practical implementation of the control strategy for grid tie inverter.

II. GRID TIE-INVERTER CONTROL PROBLEM

Synchronization of inverter with grid requires inverter frequency to be equal to that of grid. Grid has almost constant frequency, however difference in frequency of inverter output and grid results in high power imbalance. Phase difference is key factor which determines the active and reactive power flow to and from grid [1]. A varying phase difference can cause varying power flow in the circuit. With inverter frequency at 49 Hz and grid frequency at 50 Hz the variations in power flow can be seen in fig 1.[6]

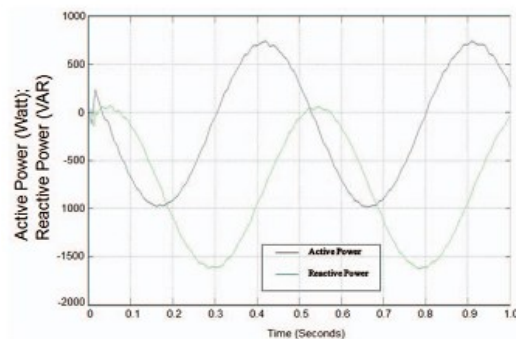


Fig. 1: Power flow due to frequency variations

Voltage of inverter governs the reactive power flow and needs to be regulated. Difference in inverter terminal voltage and grid voltage results in reactive power flow[1]. Control System is required to maintain required voltage and frequency in islanded condition. Control System needs to be robust and have quick response time. Delays in response time

can lead to failure of synchronization of inverter with grid and lead to varying power flow and can damage inverter power circuit [2].

III. PROPOSED SOLUTION

To deal with the problem statement mentioned above, various control strategies are incorporated.

A. Power Control System To throw constant power into the grid, the capacitor voltage must be maintained constant. As the power generated on DC bus increases capacitor gets over-charged. Voltage of capacitor is compared with a reference value and using PID control system the power angle of inverter is changed to control the power flow into the grid (fig. 2). The capacitor voltage is maintained at such a value so as to reduce reactive power demand of inverter.

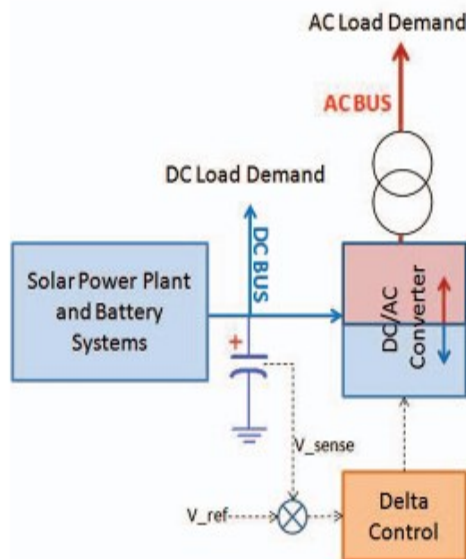


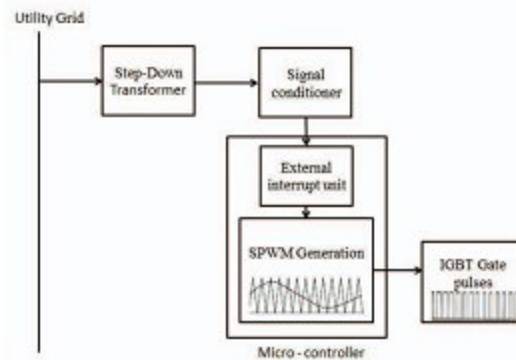
Fig. 2: Control System for Power flow

Discrete PID control [3] is applied for active and reactive power control. PID control is implemented to maintain the voltage of capacitor same as that of reference voltage. The power transfer from DC side to AC side is governed by phase angle (power angle), given by equation

$$P_{active} = \frac{EV \sin(\delta)}{X}$$

As the Capacitor voltage increases phase angle is increased to alter the power flow from Inverter to Grid.

B. Frequency Control System The feedback obtained from the grid is stepped down to 5 Volts. The grid waveform is converted to square wave using sine to square wave converter. Obtained square wave is used to measure frequency of the grid. The square wave acts as input to external interrupt hardware of micro-controller which measures the frequency of interrupts received (fig. 3). The frequency of inverter output is related to frequency of SPWM used to drive inverter bridges. Thus the frequency of inverter can be changed to frequency of grid measured using external interrupt hardware and frequency of grid is synchronized with frequency of inverter. Frequency control system has improved response time due to analog external interrupt hardware.



C. Phase Control System Phase control system maintains the phase difference between inverter generated wave and grid voltage wave constant. The sinusoidal wave of grid is stepped down using a transformer and converted to corresponding square wave. Square wave acts as an external interrupt to processor/ microcontroller generating SPWM. Phase of generated SPWM can be adjusted according to the external interrupt received and power angle predefined as per power flow required. PID controller[3] is used to give perfect matching of phase angle after the filter and phase angle of grid wave. The PID controller is necessary because the filter gives some additional phase shift to inverter generated voltage wave.

D. Voltage Control System Micro-Grid has limited generation and in islanded mode as the load on inverter increases the voltage regulation of inverter increases. The Voltage of inverter falls below rated terminal voltage. Voltage Control System involves regulation of terminal voltage. It involves feedback from inverter terminal which is given to PID control which changes the modulation index of SPWM waveforms and alters the terminal voltage of inverter.

E. Design of Discrete PID Controller

The Transfer function of discrete PID Controller[5] is shown in fig 4.

$$\frac{U[z]}{E[z]} = Kp + Ki * \frac{Ts}{2} * \frac{z+1}{z-1} + Kd * \frac{z-1}{zTs} \quad (1)$$

$$\frac{U[z]}{E[z]} = \frac{(Kp + Ki * \frac{Ts}{2} + \frac{Kd}{Ts})z^2 + (-Kp + Ki * \frac{Ts}{2} + \frac{Kd}{Ts})z + \frac{Kd}{s}}{z^2 - z} \quad (2)$$

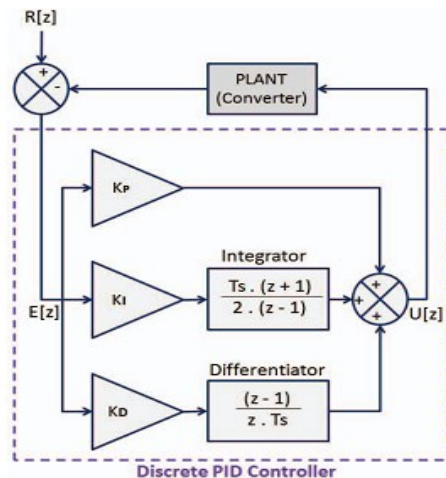


Fig. 4: PID Control System for Power Angle Control

$$U[z] = z^{-1}U[z] + aE[z] + bz^{-1}E[z] + cz^{-2}E[z] \quad (3)$$

$$u[k] = u[k-1] + ae[k] + be[k-1] + ce[k-2] \quad (4)$$

$$a = Kp + Ki * \frac{Ts}{2} + \frac{Kd}{s} \quad (5)$$

$$b = -Kp + Ki * \frac{Ts}{2} - \frac{2Kd}{s} \quad (6)$$

$$c = \frac{Kd}{Ts} \quad (7)$$

Ts = Sampling time of the discrete system

Kp = Proportional gain

KI = Integral gain

KD = Differential gain

U[z] = input to the plant

R[z] = reference to controller

E[z] = error sequence [4]

Trade-off between overshoot and settling time is achieved by proper tuning of Kp, Ki, Kd values used above. Discrete PID controller developed maintains the capacitor voltage to the reference value and controls the reactive power flow from the inverter by variations in power angle of inverter. Active Power is proportional to sine of the power angle. PID controller works best in linear range. Therefore saturation block is introduced after the PID controller to limit the output from $-\pi/2$ to $\pi/2$. The DC Bus voltage of microgrid is 48V which is reference voltage for PID controller.

HYBRID FUZZY:

This paper investigates two fuzzy logic controllers that use simplified design schemes. Fuzzy logic PD and PI controllers are effective for many control problems but lack the advantages of the fuzzy controller. Design methodologies are in their infancy and still somewhat intuitive. Fuzzy controllers use a rule base to describe relationships between the input variables. Implementation of a detailed rule base increases in complexity as the number of input variables grow and the ranges of operation for the variables become more defined. We propose a hybrid fuzzy controller which takes advantage of the properties of the fuzzy PI and PD controllers and a second method which adds the fuzzy PD control action to the integral control action.

The effectiveness of the two PID fuzzy controller implementations, PD and PI fuzzy controllers have the same design disadvantages as their classical

counterparts. Therefore, in some cases a fuzzy PID controller maybe required. The fuzzy PID controller entails a large rule base

which presents design and implementation problems. First, a reduced rule fuzzy PID scheme was implemented to take advantage of both PD and PI control actions. Some further research is required for the process of switching between the control actions. The second fuzzy PID control scheme used only the PD portion with an integral term added to eliminate steady-state error. Results from simulations of both control schemes demonstrate the effectiveness of the PID controller

IV. SIMULATIONS AND RESULTS

The Grid-tie inverter was simulated in MATLAB. The SPWM generator block has input of phase angle (power angle) and modulation index for the SPWM waves. The terminals DC4 and DC4 are connected to PV system. The terminals AC1, AC3, AC5 are AC output terminals. The LCL filter is connected between inverter and power measurement unit. The LCL filter filters the output voltage waveform of inverter. The PID controller is discrete type, and controls the phase angle so as to maintain DC link voltage constant. The model is simulated in discrete mode. Ode 45 equation solver is used and the sampling time is of 5e-6 sec.

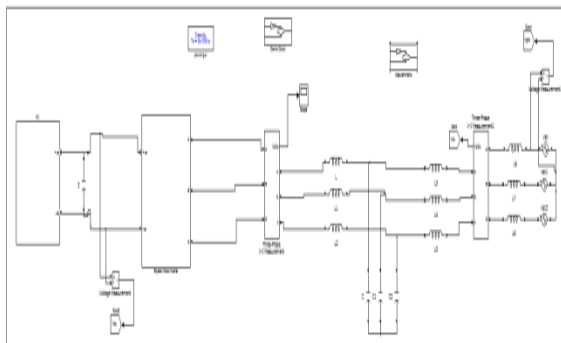


Fig. 5: Simulated Control System DC-AC Converter

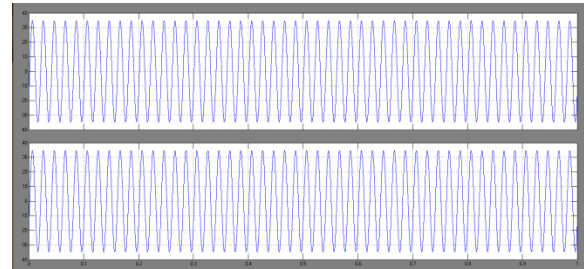


Fig 6 simulation wave form of input and grid voltage

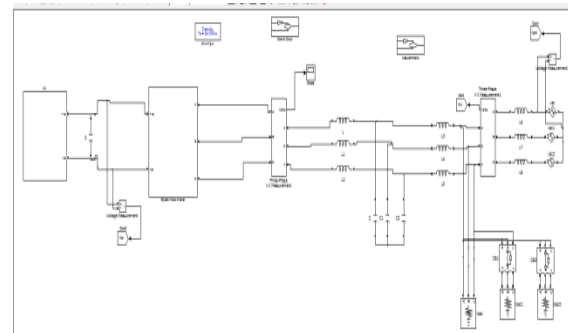


Fig 7 Simulated Control System for Grid Connected DC-AC Converter

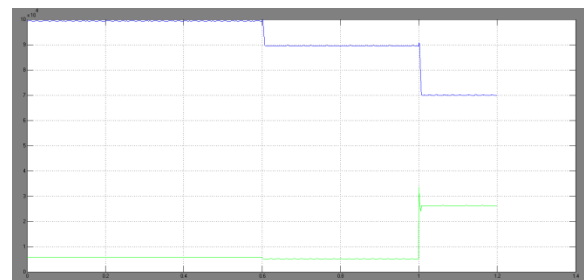


Fig 8 Manual control of active power transfer

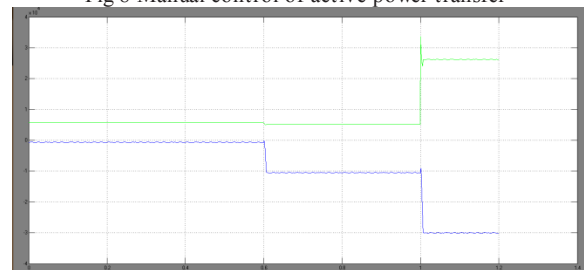


Fig 9 Automatic control of active power and DC link voltage

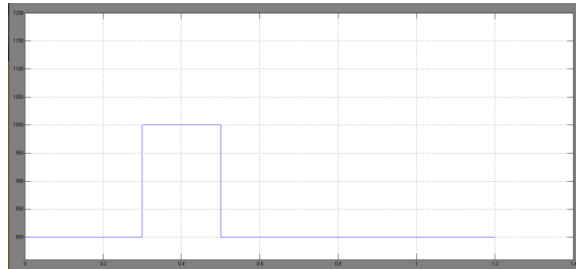


Fig 10 simulation wave form of DC link voltage PV

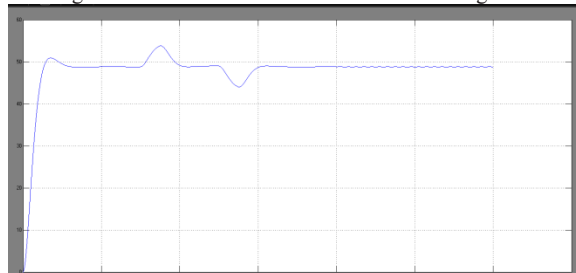


Fig 11 simulation wave form of DC link voltage

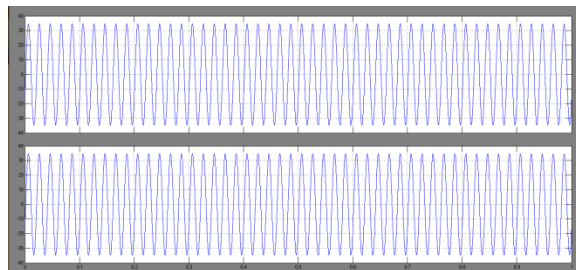


Fig 12 simulation wave form of input and grid voltage with hybrid fuzzy controller

VII. CONCLUSION

This paper gives description about implementation of hybrid fuzzy control system for grid-tie inverter. The control system developed has better response time due to external interrupt hardware. The frequency control system and phase control system keep the inverter in exact synchronization and provide desirable phase angle between inverter voltage wave and grid voltage wave. Control system is able to regulate the power flow into AC bus and maintain the DC link voltage constant through control action. Power flow variations due to increase in generation on DC bus causes fluctuations in DC link capacitor voltage which cannot be restricted beyond certain extent due to limitations of PID control and hybrid fuzzy controller can be implemented.

REFERENCES

- [1] Zia, F.B., Salim, K.M. , Venus, S., "Experiment with a locally developed single phase grid tie inverter" *Proc. of IEEE Informatics, Electronics & Vision (ICIEV)* , 2012 , Dhaka.
- [2] Sung-Yeul Park, "An easy, simple, and flexible control scheme for a threephase grid-tie inverter system"
- [3] Ang K.H., Chong G., Li Y., "PID control system analysis, design, and technology" *IEEE Trans. Control Syst. Technol.* 13(4), 559–576 (2005)"
- [4] L. A. Serpa, et al., "A Modified Direct Power Control Strategy Allowing the Connection of Three-Phase Inverters to the Grid Through LCL Filters," *IEEE Trans on Industry Applications*, vol. 43, pp. 1388-1400, Sep/Oct. 2007. (Pubitemid 47570239)
- [5] Ibrahim A. El-Sharif, Fathi O. Hareb and Amer R. Zerek, "Design of Discrete time PID controller", *International Conference on Control, Engineering and Information Technology*, 2014.
- [6] Prabha Kundur, Neal J. Balu, Mark G. Lauby, "Power System Stability and Control", McGraw-Hill Education, 1994

Power Factor Correction of Three Phase I.M Drive using PWM Boost Inverter

SARATH BABY¹, GANESH PASHIKANTI²

¹PG Scholar, Dept of EEE, Malla Reddy Engineering College, Hyderabad, R. R(Dt), TS, India.

²Assistant Professor, Dept of EEE, Malla Reddy Engineering College, Hyderabad, R. R(Dt), TS, India.

Abstract: Induction motor are used approximately 85% of the industrial applications, due to their high reliability. When it goes to high speed the induction motor will be the better choice compared to the PMSM because we can easily control the field/flux building current. They are used vastly in HVAC, industrial, manufacturing plants, pumps in sewage and irrigation. They are also used in ceiling fan, mixer, pump, compressor, hydraulic power pack, drilling machine etc. They work mainly on the principle of induction. The boost inverters are applied in DC grid. They can also be inculcated in circuits which supply to both AC and DC loads. The boost inverters convert the low dc input signal into high ac output signal. The boost inverters are also applied in automobiles, buses, forklifts, motorcycles and bicycles, airplanes, boats, sub-marines etc. The boost-inverter topology is used as a building block for a single-phase grid-connected system offering low cost and compactness.

Keywords: HVAC, PMSM, VFDs, DC Grid.

I. INTRODUCTION

Induction motor is an AC electronic motor in which the electric current in the rotor needed to produce torque is obtained by electromagnetic induction from the magnetic field of the stator winding. An induction motor can therefore be made without electrical connections to the rotor as are found in universal, dc and synchronous motors. An asynchronous motors rotor can be either wound type or squirrel-cage type. Three phase induction motors are widely used in industrial drives because they are rugged, reliable and economical. Although traditionally used in fixed-speed service, induction motors are increasingly being used with variable-frequency drives in variable speed service. VFDs offer especially important energy savings opportunities for existing and prospective induction motors in variable torque centrifugal fan, pump and compressor load applications. In electrical engineering, the power factor of an AC electrical power system is defined as the ratio of the real power flowing to the load to the apparent power in the circuit, and is a dimensionless number in the closed interval of -1 to +1. A power factor of less than one means that the voltage and current waveforms are not in phase, reducing the instantaneous product of the two waveforms. Boost inverter is a system which converts a low level input signal into a high level output signal. Inverter is relevant because many equipments work on AC voltage and they are not able to work on DC voltage. They even include many domestic appliances like mixer, refrigerator etc.

II. POWER FACTOR

The power factor of an AC electrical power system is defined as the ratio of the real power flowing to the load to

the apparent power in the circuit, and is a dimensionless number in the closed interval of -1 to +1. A power factor of less than one means that the voltage and current waveforms are not in phase, reducing the instantaneous product of the two waveforms. Real power is the circuit for performing work in a particular time. Apparent power is the product of the current and voltage of the circuit. Due to energy stored in the load and returned to the source, or due to a non-linear load that distorts the wave shape of the current drawn from the source, which is normally considered the generator. In an electric power system, a load with a low power factor draws more current than a load with a high power factor for the same amount of useful power transferred.

III. POWER FACTOR CORRECTION

Power factor is decreased mainly due to the presence of the Total Harmonic Distortion in an AC to DC converter. But when we connect an Induction Motor, the readings are taken of the speed and the torque as shown in Fig.1. When they do not reach the required speed or torque, values are added or subtracted (adjusted) to the dc rectifiers. These values are of voltage and frequency. The voltage and frequency producing a good speed and less torque as the time progress will be taken into consideration as shown in Fig.2.

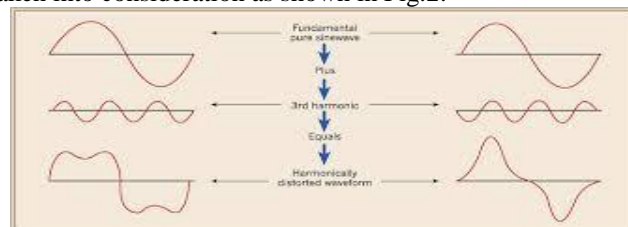


Fig.1. Total Harmonic Distortion.

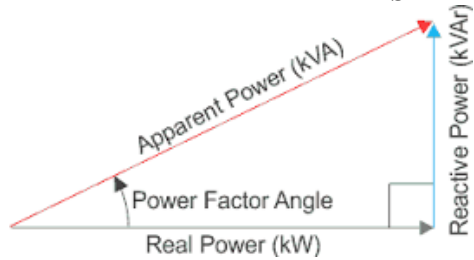


Fig.2. Power triangle.

IV. RECTIFIER

Rectifier is the device which converts an input ac signal into an output dc signal. The ac signal is passed to the rectifier. A rectifier consists of four thyristors, a capacitor, an inductor and a resistor. During the positive half cycle of the signal, T1 and T4 are on and T2 and T3 are off. So a signal of positive half cycle appears on the load resistor. During the negative half cycle, the thyristors T2 and T3 will be on and T1 and T4 will be off. So this will also lead to the positive signal on resistor load. Now the output will be a pulsating dc. To avoid this, we put a capacitor in parallel to the load. So whenever there is a lowering signal at output, the capacitor produces the sufficient voltage to level the dc output. This voltage is already stored by the capacitor during the ac supply as shown in Fig.3.

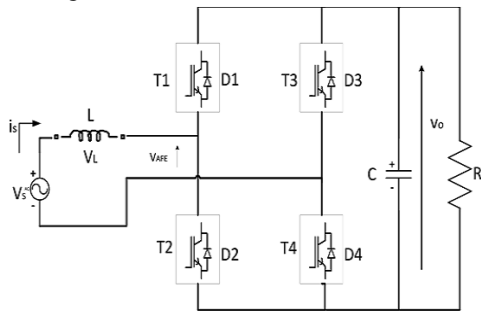


Fig.3.PWM Rectifier.

V. INVERTER

Inverter is an electronic device or circuitry that changes direct current into alternating current. The inverter does not produce any power, the power is provided by the DC source. A power inverter can be entirely electronic or may be a combination of mechanical effects or electronic circuitry. Static inverters do not use moving parts in the conversion process. An inverter can produce a square wave, modified sine wave, pulse width modulated wave or sine wave depending on circuit design as shown in Fig.4.

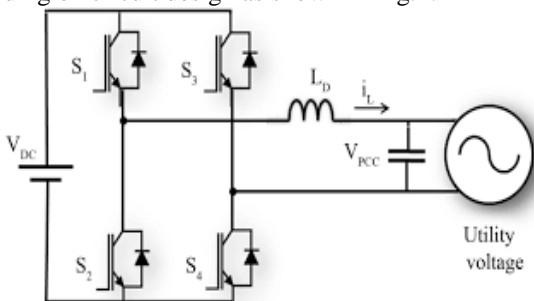


Fig.4. Inverter.

VI. INDUCTION MOTOR

An induction motor is an example of asynchronous AC machine, which consists of a stator and a rotor. This motor is widely used because of its strong features and reasonable cost. A sinusoidal voltage is applied to the stator, in the induction motor, which results in an induced electromagnetic field. A current in the rotor is induced due to this field, which creates another field that tries to align with the stator field, causing the rotor to spin. A slip is created between these fields, when a load is applied to the motor. Compared to synchronous speed, the rotor speed decreases at higher slip values. The frequency of the stator voltage controls the synchronous speed. The frequency of the voltage also controls the synchronous speed. The frequency of the voltage is applied to the stator through power electronic devices, which allows the control of the speed of the motor. The research is using techniques, which implement a constant voltage to frequency ratio. Finally, the torque begins to fall when the motor reaches the synchronous speed. Thus, induction motor synchronous speed is defined by following equation,

$$N_s = 120f/P \quad (1)$$

Where f is the frequency of AC supply, N is the speed of rotor; P is the number of poles per phase of the motor. By varying the frequency of control circuit through AC supply, the rotor speed will change as shown in Fig.5.

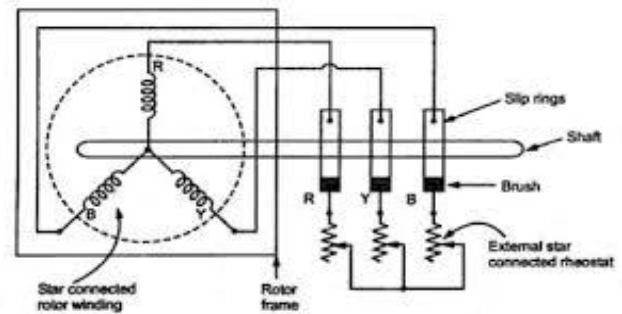


Fig.5. Induction motor.

VII. CONTROL STRATEGY OF SINGLE PHASE PWM RECTIFIER

The input AC voltage is applied to the controlled rectifier and the output must be DC voltage. The basic operation of voltage source rectifier consist of keeping the dc link voltage desired reference value V_{ref} . The output of DC link voltage is measured and compared with the generate reference voltage. This voltage error signal generated by comparison is used to switch ON and OFF the values of the voltage source rectifier. The control includes a voltage controller, typically a proportional integrative controller which controls the amount of power required to maintain the DC link voltage constant. The voltage controller is given the amplitude of the source current. For this reason, the voltage controller output is multiplied by a sinusoidal signal with the same phase and frequency than V_s , in order to obtain the input current reference as shown in Fig.6. The fast current controller controls the input current, so the high input power factor is

Power Factor Correction of Three Phase IM Drive using PWM Boost Inverter

achieved. This controller is used for hysteresis with a PWM modulator.

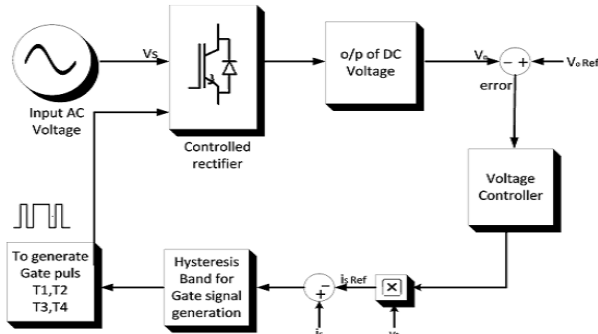


Fig.6. Block diagram of single phase PWM rectifier.

VIII. PULSE WIDTH MODULATION

It is a modulation technique used to encode a message into a pulsating signal. Its main use is to allow the control of power supply to the electrical devices. The average value of voltage fed to the load is controlled by turning the switch between supply and load on and off at a fast rate. The longer the switch is on compared to the off period, the larger the power supplied to the load. The PWM switching frequency has to be much higher than that would affect the load, which is to say that the resultant waveform perceived by the load must be as smooth as possible. The frequency at which the power supply must switch can vary greatly depending on load and application as shown in Fig.7. Pulse Width Modulation play a very important role in saving the power in a system. They also help in changing the reactive power into active power thus reducing the power factor to a greater extend.

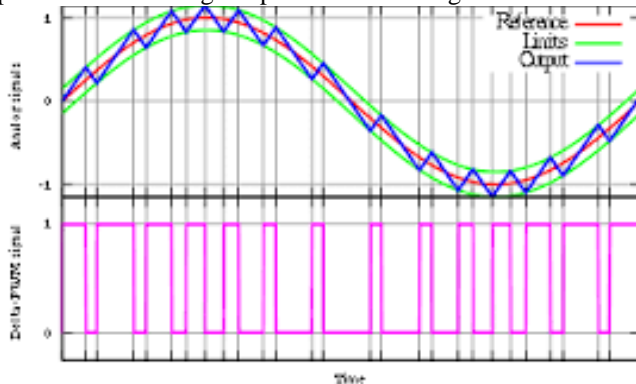


Fig.7. Pulse Width Modulation.

IX. CONTROL STRATEGY OF INDUCTION MOTOR

A. Open Loop

In this type of control, the desired value of speed and torque are set. When the original value of the speed and torque do not reach the desired value, there is some decrease in power factor due to the presence of Total Harmonic Distortion, Eddy current etc. To decrease the closeness of speed and torque to the desired value, we need to provide a voltage and frequency which uplifts the power factor to maximum. So we test different frequency and voltage. From the output values of different speed and torque we get the most suitable input voltage and frequency. Then we apply them as inputs.

B. Closed Loop

Power electronics interface such as three phase SPWM interface using constant voltage loop volts/hertz control scheme is used to control the motor. According to the desired output speed, the amplitude and frequency of the reference (sinusoidal) signals will change. In order to maintain constant magnetic flux in the motor, the ratio of the voltage amplitude to voltage frequency will be kept constant. Hence a closed loop proportional integral controller is implemented to regulate the motor speed to the desired set point. The closed loop speed control is characterized by the measurement of the actual motor speed, which is compared to the reference speed while the error signal is generated. The magnitude and polarity of the error signal correspond to the difference between the actual and required speed. The PI controller generates the corrected motor stator frequency to compensate for the error, based on the speed error.

IX. MATLAB/SIMULATION RESULT

Simulation results of this paper is as shown in bellow Figs.8. to 14.

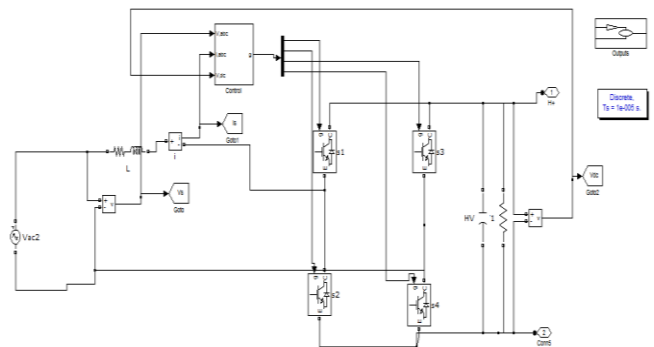
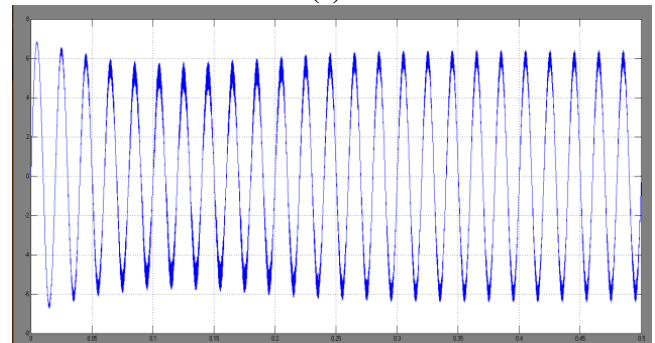


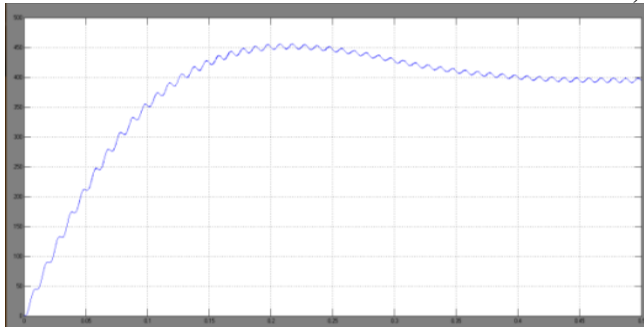
Fig.8. Matlab/simulation circuit of Single phase Rectifier.



(a)



(b)



(c)

Fig.9. Simulation result of single phase PWM rectifier. (a) Result of source voltage and source current, (b) Result of source current, (c) Result of DC link voltage.

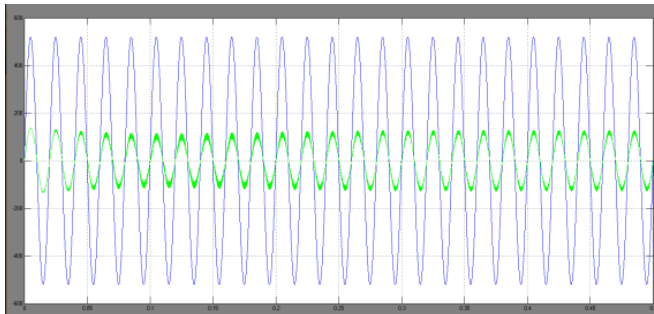


Fig.10. Simulation waveform of power factor.

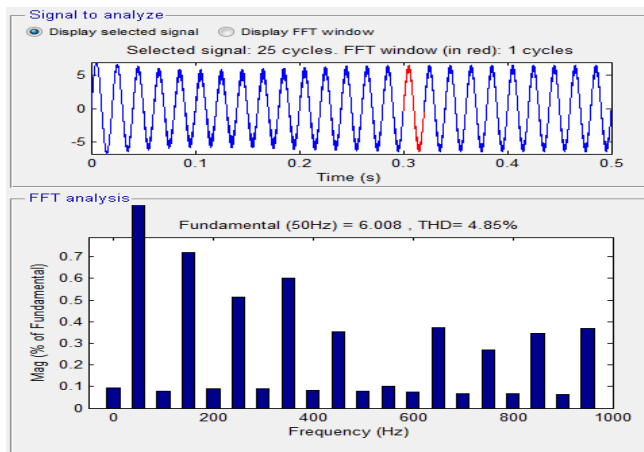


Fig.11. Input current THD result.

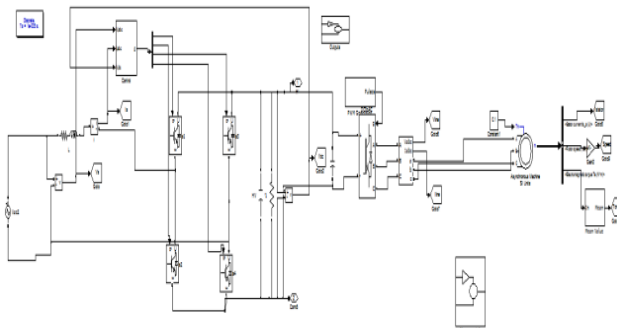


Fig.12. Matlab/Simulation circuit for single phase inverter.

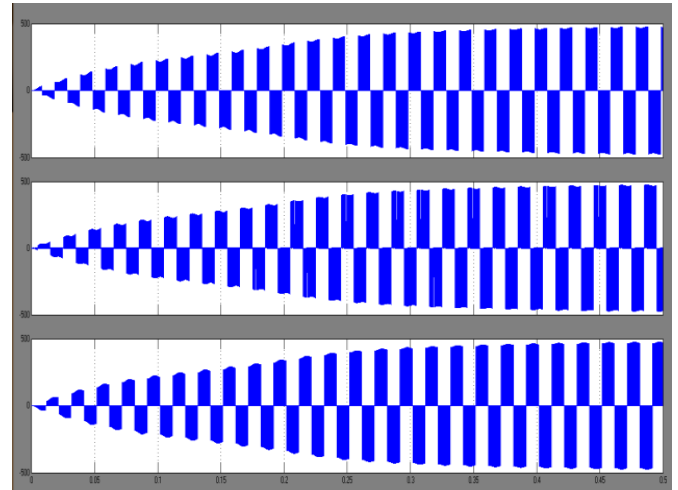


Fig.13. Simulation waveform of line voltage.

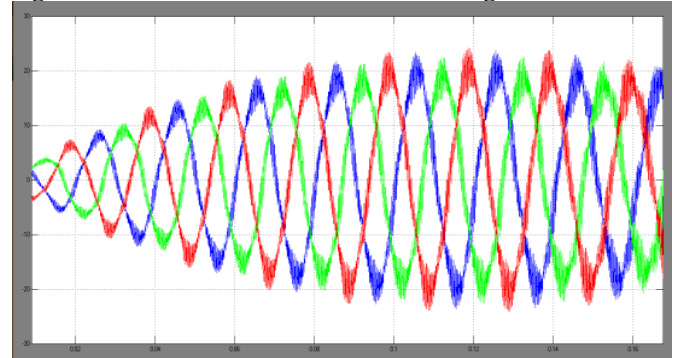


Fig.14. Simulation waveform of line current.

X. CONCLUSION

The study of the power factor is done by connecting an induction motor at the load terminal. The power factor is corrected with the help of the open loop system. From the study of power factor, error signals are analyzed. The apt input voltage and frequency are taken for the apt speed and torque output. The THD and the eddy current are also studied from the output.

XI. REFERENCES

- [1] N. Mohan, T. Undeland, W. Robbins, "Power Electronics converters applications and design"
- [2] J. Rodriguez, J. Dixon, J.E Spinoza and P. Lezana, "PWM Regenerative Rectifier: state of the art", IEEE Trans. Ind. Electron volume 52, No 1, Feb 2005
- [3] H. Azizi and A. Vahedi, "Performance analysis of direct power controlled PWM rectifier under disturbed AC line voltages"
- [4] IEEE recommended practices and requirement for harmonics control in electrical power system, IEEE, 1992
- [5] Limits for Harmonic current emission, International standard, 2000
- [6] Huai Wei, Issa BATERSEH, Guangyong Zhu and Peter Cornetzy, "A Single Switch AC to DC Converter with Power Factor Correction", IEEE transaction on Power Electronics, May 2000.
- [7] O. Stihl and B. Ooi, "A single phase controlled current PWM rectifier", IEEE transaction on power electronics, October 1998.

AN ULTRA CAPACITOR INTEGRATED POWER CONDITIONER FOR INTERMITTENCY SMOOTHING AND IMPROVING POWER QUALITY OF DISTRIBUTION GRID WITH FUZZY SYSTEM

^{#1}G.RAHUL, M.Tech Student,

^{#2} M.LAKSHMI SWARUPA, Associate Professor,

Department Of EEE,

MALLAREDDY ENGINEERING COLLEGE, DHULAPALLY, SECUNDERABAD, TS, INDIA.

ABSTRACT: Penetration of various types of distributed energy resources (DERs) like solar, wind, and plug-in hybrid electric vehicles (PHEVs) onto the distribution grid is on the rise. There is a corresponding increase in power quality problems and intermittencies on the distribution grid. In order to reduce the intermittencies and improve the power quality of the distribution grid, an ultra capacitor (UCAP) integrated power conditioner is proposed in this paper. UCAP integration gives the power conditioner active power capability, which is useful in tackling the grid intermittencies and in improving the voltage sag and swell compensation. UCAPs have low energy density, high-power density, and fast charge/discharge rates, which are all ideal characteristics for meeting high-power low-energy events like grid intermittencies, sags/swells. In this paper, UCAP is integrated into dc-link of the power conditioner through a bidirectional dc–dc converter that helps in providing a stiff dc-link voltage. The integration helps in providing active/reactive power support, intermittency smoothing, and sag/swell compensation. Design and control of both the dc ac inverters and the dc–dc converter are discussed. The simulation model of the overall system is developed and compared with the fuzzy logic controller system.

I.INTRODUCTION

In the last few years the pollution problems and the increase of the cost of fossil energy (oil, gas) have become planetary problems. The car manufacturers started to react to the urban pollution problems in nineties by commercializing the electric vehicle. But the battery weight and cost problems were not solved. The batteries must provide energy and peaks power during the transient states. These conditions are severe for the batteries. To decrease these severe conditions, the super capacitors and batteries associate with a good power management present a promising solution.

Super capacitors are storage devices which enable to supply the peaks of power to hybrid vehicle during the transient states. During the steady states, batteries will provide the energy requested. This methodology enables to decrease the weight and increases the lifespan of the batteries. Hybridization using batteries and super capacitors for transport applications is needed when energy and power management are requested during the transient states and steady states.

The multi boost and multi full bridge converters will be investigated because of the high power. For range problems, traction batteries used until now cannot satisfy the energy needed for future vehicles. To ensure a good power management in hybrid vehicle, the multi boost and multi full bridge converters topologies and their control are developed. Two topologies proposed for the power management in ECCE Hybrid Vehicle are presented.

Most of the appliances today are powered by electricity and electrical power is transmitted over long distance stop over the appliances. During the initial days of commercialization and mass-production of electricity, Nikola Tesla proved to the world that electrical power can be transmitted over long distances in a much more efficient way if poly phase alternating current transmission is used instead of direct current transmission. Since then most of the electrical energy is transmitted over long distances using 3phase alternating current. One of the major draw backs of electrical energy in a current system is that it cannot be stored electrically.

II. POWER QUALITY

Power quality is a major cause of concern in the industry and it is important to maintain good power quality on the grid. Therefore, there is renewed interest in power quality products like the dynamic voltage restorer (DVR) and the active power filter (APF).

The DVR prevent sensitive loads from experiencing voltage sags/swells and the active power filter (APF) prevents the grid from supplying non-sinusoidal currents when the load is non-linear. The concept of integrating the dynamic voltage restorer (DVR) and active power filter (APF) through a back-back inverter topology was first introduced and the topology was called a unified power quality conditioner (UPQC). The design goal of the UPQC was to improve the power quality of the distribution grid by being able to provide sag, swell and harmonic current compensation. With the increase in penetration of the

distributed energy resources (DERs) such as wind, solar and PHEVs, there is a corresponding increase in grid intermittencies and power quality problems on the distribution grid in the seconds to minutes time scale. Integration of energy storage in to the distribution grid is a potential solution which helps in addressing various power quality problems and problems related to grid intermittencies. Applications where energy storage integration is needed are being identified and efforts are being made to make energy storage integration commercially viable on a large scale.

Renewable intermittency smoothing is one application which requires active power support from energy storage in the seconds to minutes time scale. Different types of optimal controls are being explored to provide smoothing of DERs.

In a super capacitor and flow battery hybrid energy storage system is integrated into the wind turbine generator to provide wind power smoothing and the system is tested using a real time simulator. In a super capacitor is used as auxiliary energy storage for PV/fuel cell and a model based controller is developed for providing optimal control. In battery energy storage system based control to mitigate wind/PV fluctuations is proposed. In a multi-objective optimization method to integrate battery storage for improving PV integration in to the distribution grid is proposed. In a rule based control is proposed to optimize the battery discharge while dispatching intermittent renewable resources. In optimal sizing of zinc bromine based battery for reducing the intermittencies in wind power is proposed.

III. ULTRA CAPACITOR (OR) SUPER CAPACITORS

Capacitors store electric charge. Because the charge is stored physically, with no chemical or phase changes taking place, the process is highly reversible and the discharge-charge cycle can be repeated over and over again, virtually without limit. Electrochemical capacitors (ECs), variously referred to by manufacturers in promotional literature as Super capacitors also called ultra capacitors and electric double layer capacitors (EDLC) are capacitors with capacitance values greater than any other capacitor type available today. Capacitance values reaching up to 400 Farads in a single standard case size are available. Super capacitors have the highest capacitive density available today with densities so high that these capacitors can be used to applications normally reserved for batteries. Super capacitors are not as volumetrically efficient and are more expensive than batteries but they do have other advantages over batteries making the preferred choice in applications requiring a large amount of energy storage to be stored and delivered in bursts repeatedly.

The most significant advantage super capacitors have over batteries is their ability to be charged and discharged continuously without degrading like batteries do. This is why batteries and super capacitors are used in conjunction with each other. The super capacitors will supply power to the system when there are surges or energy bursts since super capacitors can be charged and discharged quickly while the batteries can supply the bulk energy since they can store and deliver larger amount energy over a longer slower period of time.

Controller Implementation:

$$\begin{bmatrix} V_{sa} \\ V_{sb} \\ V_{sc} \end{bmatrix} = \begin{bmatrix} 1 & 0 \\ -\frac{1}{2} & \frac{\sqrt{3}}{2} \\ -\frac{1}{2} & -\frac{\sqrt{3}}{2} \end{bmatrix} \begin{bmatrix} \cos(\theta - \frac{\pi}{6}) & \sin(\theta - \frac{\pi}{6}) \\ -\sin(\theta - \frac{\pi}{6}) & \cos(\theta - \frac{\pi}{6}) \end{bmatrix} \begin{bmatrix} \frac{V_m}{\sqrt{3}} \\ \frac{V_m}{\sqrt{3}} \\ \frac{V_m}{\sqrt{3}} \end{bmatrix} \quad (1)$$

$$\begin{bmatrix} V_{refa} \\ V_{refb} \\ V_{refc} \end{bmatrix} = m * \begin{bmatrix} \sin(\theta - \frac{\pi}{6}) - \frac{V_{inj2}}{100.7} \\ \sin(\theta - \frac{2\pi}{3}) - \frac{V_{inj2}}{100.7} \\ \sin(\theta + \frac{2\pi}{3}) - \frac{V_{inj2}}{100.7} \end{bmatrix} \quad (2)$$

$$\begin{aligned} P_{dvr} &= 3V_{inj2a}(rms) I_{La}(rms) \cos \varphi \\ Q_{dvr} &= 3V_{inj2a}(rms) I_{La}(rms) \sin \varphi. \end{aligned} \quad (3)$$

$$P_{ref} = -\frac{3}{2} v_{sq} i_{qref}$$

$$Q_{ref} = -\frac{3}{2} v_{sq} i_{dref}$$

$$\begin{bmatrix} i_{refa} \\ i_{refb} \\ i_{refc} \end{bmatrix} = \begin{bmatrix} 1 & 0 \\ -\frac{1}{2} & \frac{\sqrt{3}}{2} \\ -\frac{1}{2} & -\frac{\sqrt{3}}{2} \end{bmatrix} \begin{bmatrix} \cos \theta & \sin \theta \\ -\sin \theta & \cos \theta \end{bmatrix} \begin{bmatrix} i_{dref} \\ i_{qref} \end{bmatrix}$$

The series inverter controller implementation is based on the in-phase compensation method that requires PLL for estimating θ , and this has been implemented using the fictitious power method described in [4].

Based on the estimated θ and the line-line source, voltages V_{ab} , V_{bc} , V_{ca} (which are available for this delta-sourced system) are transformed into the d-q domain and the line-neutral components of the source voltage V_{sa} , V_{sb} , and V_{sc} which are not available can then be estimated using above equations. These voltages are normalized to unit sine waves using line-neutral system voltage of 120 Vrms as reference and compared with unit sine waves in-phase with actual system voltages V_s from (2) to find the injected voltage references V_{ref} necessary to maintain a constant voltage at the load terminals, where m is the modulation index, which is 0.45 for this case. Therefore, whenever there is a voltage sag or swell on the source side, a corresponding voltage V_{inj2} is injected in-phase by the DVR and UCAP system to negate the effect and retain a constant voltage V_L at the load end. The actual active and reactive power supplied by the series inverter can be computed using (3) from the rms values of injected voltage V_{inj2a} and load current I_{La} and ϕ is the phase difference between the two waveforms.

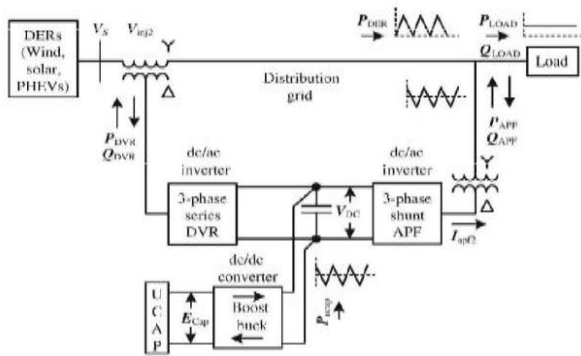


Fig. 1. One-line diagram of power conditioner with UCAP energy storage

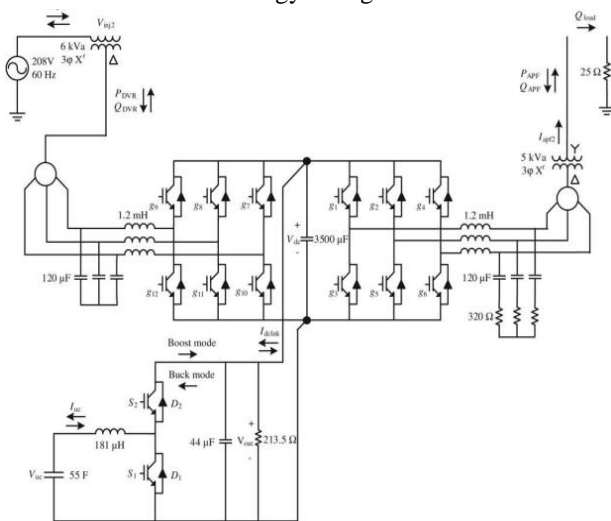


Fig. 2. Model of power conditioner with UCAP energy storage

IV. UCAP AND BIDIRECTIONAL DC-DC CONVERTER

UCAP Bank Hardware Setup:

UCAPs can deliver very high power in a short time span; they have higher power density and lower energy density when compared to Li-ion batteries. The major advantage UCAPs have over batteries is their power density characteristics, high number of charge-discharge cycles over their life time and higher terminal voltage per module. These are ideal characteristics for providing active/reactive power support and intermittency smoothing to the distribution grid on a short term basis. It is proposed that UCAPs are currently viable as short term energy storage for bridging power link range in the seconds to few minutes time scale. The choice of the number of UCAPs necessary for providing grid support depends on the amount of support needed, terminal voltage of the UCAP, dc-link voltage and distribution grid voltages. In the present case the choice was made based on the following parameters. It is clear that the dc-link voltage needs to be 260V for the 208V distribution grid for optimal performance of the inverter. The terminal

voltage of each BMOD0165P048 module is 48V which means connecting three modules in series would bring the initial voltage of the UCAP bank to 144V and connecting four modules in series would bring the initial voltage of the UCAP bank to 192V. For a 260V dc-link voltage these two options are ideal for integrating the UCAP bank through the dc-dc converter since the duty ratio of the converter would be either too high for other cases. It is cost effective as well to use 3 modules in the UCAP bank when compared to 4 modules. In this paper, the experimental setup consists of three 48V, 165F UCAPs (BMOD0165P048) manufactured by Maxwell Technologies which are connected in series.

V. FUZZY LOGIC CONTROLLER:

L. A. Zadeh presented the first paper on fuzzy set theory in 1965. Since then, a new language was developed to describe the fuzzy properties of reality, which are very difficult and sometime even impossible to be described using conventional methods. Fuzzy set theory has been widely used in the control area with some application to dc-to dc Cuk converter system. A simple fuzzy logic control is built up by a group of rules based on the human knowledge of system behavior. Matlab/Simulink simulation model is built to study the dynamic behavior of dc-to-dc Cuk converter and performance of proposed controllers. Furthermore, design of fuzzy logic controller can provide desirable both small signal and large signal dynamic performance at same time, which is not possible with linear control technique. Thus, fuzzy logic controller has been potential ability to improve the robustness of dc-to-dc Cuk converters. The basic scheme of a fuzzy logic controller is shown in Fig 4 and consists of four principal components such as: a fuzzy fication interface, which converts input data into suitable linguistic values; a knowledge base, which consists of a data base with the necessary linguistic definitions and the control rule set; a decision-making logic which, simulating a human decision process, infer the fuzzy control action from the knowledge of the control rules and linguistic variable definitions; a de-fuzzification interface which yields non fuzzy control action from an inferred fuzzy control action [10].

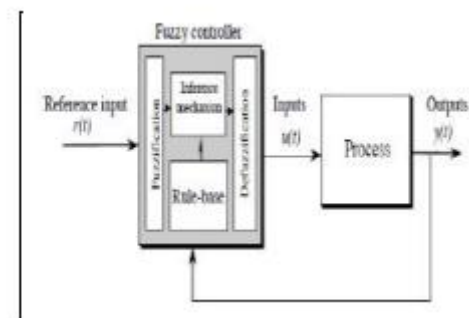


Fig5.1: General structure of the fuzzy logic controller on closed-loop system

The fuzzy control systems are based on expert knowledge that converts the human linguistic concepts into an automatic control strategy without any complicated mathematical model [10]. Simulation is performed in buck converter to verify the proposed fuzzy logic controllers.

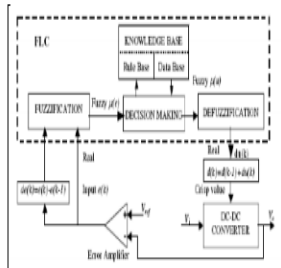


Figure 5: Block diagram of the Fuzzy Logic Controller (FLC) for dc-dc converters

5.1. Fuzzy Logic Membership Functions

The dc-dc Cuk converter is a nonlinear function of the duty cycle because of the small signal model and its control method was applied to the control of boost converters. Fuzzy controllers do not require an exact mathematical model. Instead, they are designed based on general knowledge of the plant. Fuzzy controllers are designed to adapt to varying operating points. Fuzzy Logic Controller is designed to control the output of boost dc-dc converter using Mamdani style fuzzy inference system. Two input variables, error (e) and change of error (de) are used in this fuzzy logic system. The single output variable (u) is duty cycle of PWM output.

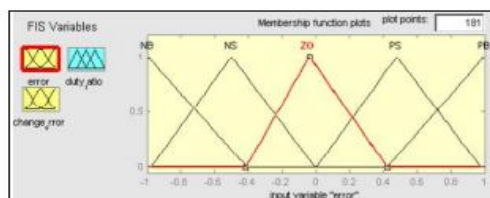


Figure 4: The Membership Function plots of error

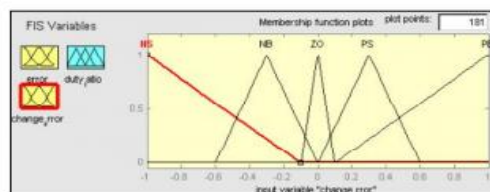


Figure 5: The Membership Function plots of change error

5.2. Fuzzy Logic Rules

The objective of this dissertation is to control the output voltage of the boost converter. The error and change of error of the output voltage will be the inputs of fuzzy logic controller. These 2 inputs are divided into five groups; NB: Negative Big, NS: Negative Small, ZO: Zero Area, PS: Positive small and PB: Positive Big and its parameter [10].

These fuzzy control rules for error and change of error can be referred in the table that is shown in Table I as per below:

(de) \ (e)	NB	NS	ZO	PS	PB
NB	NB	NB	NB	NS	ZO
NS	NB	NB	NS	ZO	PS
ZO	NB	NS	ZO	PS	PB
PS	NS	ZO	PS	PB	PB
PB	ZO	PS	PB	PB	PB

Table 1: Table rules for error and change of error

VI. SIMULATION RESULTS:

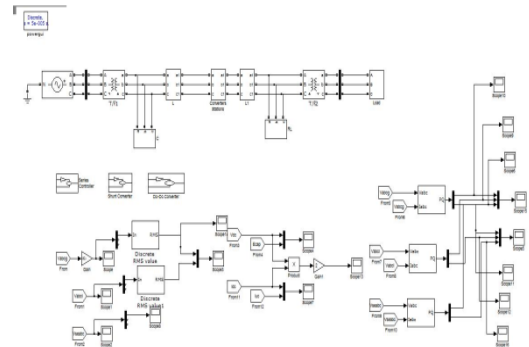


Fig.3 Simulink circuit of Proposed Model

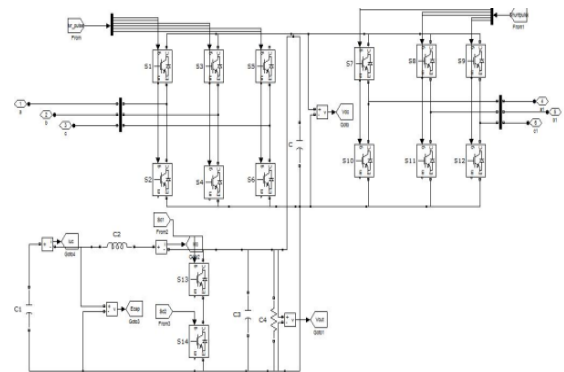


Fig.4 Simulink circuit of Converter Station

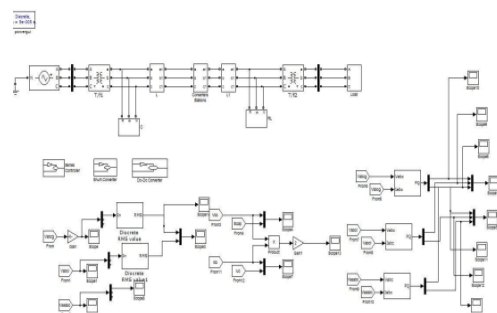


Fig.5 Simulink circuit of proposed model using fuzzy controller

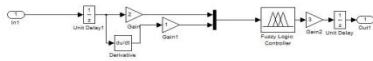


Fig.6 Simulink circuit of dc-dc converter using Fuzzy controller

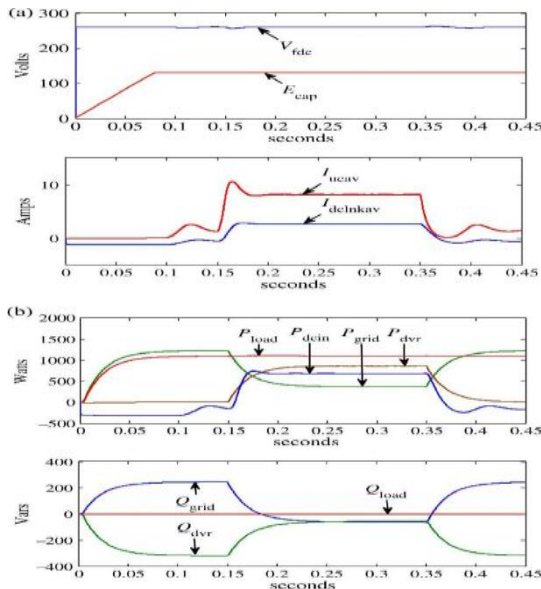


Fig. 7 (a) Currents and voltages of dc-dc converter. (b) Active and reactive power of grid, load, and inverter During voltage sag

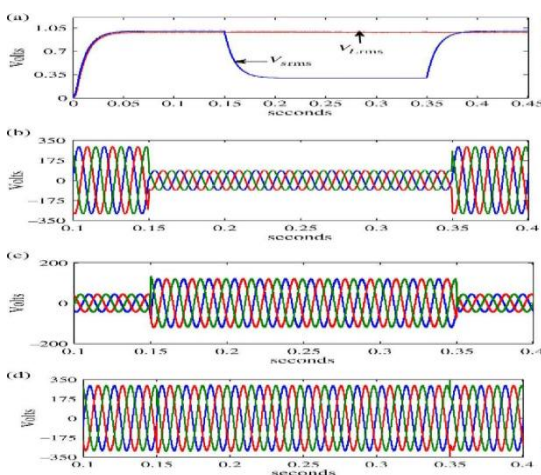


Fig8: output wave forms

VII.CONCLUSION

In this paper, the concept of integrating UCAP-based rechargeable energy storage to a power conditioner system to improve the power quality of the distribution grid is presented. With this integration, the DVR portion of the power conditioner will be able to independently compensate voltage sags and swells and the APF portion of the power conditioner will be able to provide active/reactive power support and renewable intermittency smoothing to the distribution grid. UCAP integration through a bidirectional

dc-dc converter at the dc-link of the power conditioner is proposed. The control strategy of the series inverter (DVR) is based on in phase compensation

and the control strategy of the shunt inverter (APF) is based on $i_d - i_q$ method. Designs of major components in the power stage of the bidirectional dc-dc converter are discussed. Average current mode control is used to regulate the output voltage of the dc-dc converter. results are observed for both the converters that is PI and neuro fuzzy controllers.

REFERENCES

- [1] N. H. Woodley, L. Morgan, and A. Sundaram, "Experience with an inverter-based dynamic voltage restorer," IEEE Trans. Power Del., vol. 14, no. 3, pp. 1181–1186, Jul. 1999.
- [2] J. G. Nielsen, M. Newman, H. Nielsen, and F. Blaabjerg, "Control and testing of a dynamic voltage restorer (DVR) at medium voltage level," IEEE Trans. Power Electron., vol. 19, no. 3, pp. 806–813, May 2004.
- [3] V. Soares, P. Verdelho, and G. D. Marques, "An instantaneous active and reactive current component method for active filters," IEEE Trans. Power Electron., vol. 15, no. 4, pp. 660–669, Jul. 2000.
- [4] H. Akagi, E. H. Watanabe, and M. Aredes, Instantaneous Reactive Power Theory and Applications to Power Conditioning, 1st ed. Hoboken, NJ, USA: Wiley/IEEE Press, 2007.
- [5] K. Sahay and B. Dwivedi, "Super capacitors energy storage system for power quality improvement: An overview," J. Energy Sources, vol. 10, no. 10, pp. 1–8, 2009.
- [6] B. M. Han and B. Bae, "Unified power quality conditioner with super-capacitor for energy storage," Eur. Trans. Elect. Power, vol. 18, pp. 327–343, Apr. 2007.
- [7] P. F. Ribeiro, B. K. Johnson, M. L. Crow, A. Arsoy, and Y. Liu, "Energy storage systems for advanced power applications," Proc. IEEE, vol. 89, no. 12, pp. 1744–1756, Dec. 2001.
- [8] A. B. Arsoy, Y. Liu, P. F. Ribeiro, and F. Wang, "StatCom-SMES," IEEE Ind. Appl. Mag., vol. 9, no. 2, pp. 21–28, Mar. 2003.
- [9] J. Rittershausen and M. McDonagh, Moving Energy Storage from Concept to Reality: Southern California Edison's Approach to Evaluating Energy Storage [Online].
- [10] M. Branda, H. Johal, and L. Ion, "Energy storage for LV grid support in Australia," in Proc. IEEE Innov. Smart Grid Tech. Asia (ISGT), Nov. 13–16, 2011, pp. 1–8.

LOAD FLOW AND CONTINGENCY ANALYSIS USING NEPLAN SOFTWARE

Dr .M. LAKSHMISWARUPA 1*, Mr. D. RAMESH 2*

1. Professor -Dept of EEE, Malla Reddy Engg. College (AUTONOMOUS), Hyderabad, India.
2. Asst. Prof- Dept of EEE, Malla Reddy Engg. College (AUTONOMOUS), Hyderabad, India.

Abstract— Load flow analysis is an important method for the power system analysis and designing. This analysis is carried out at each and every state of planning, operation, control and economic scheduling. In this project, firstly we have analyzed IEEE-14 bus system under the standard test data & after that we have increased load data in step of 5%. For finding a most sensitive node, the results are compared with the original power flow results of IEEE-14 bus system. According to the reasons that are mentioned, the prediction and recognition of voltage instability in power system has particular importance and it makes the network security stronger. In this paper, we have focus on the finding of most sensitive node in IEEE-14 bus systems. Simulation is carried out at NEPLAN software which includes a complete set of user-friendly graphical interface for voltage stability analysis and sensitive nodes determination. This project also includes power system contingencies based on the maximum loading parameter point in order to analyze the voltage stability using continuation power flow method.

Index Terms— IEEE-14 Bus, System, Sensitive Node, Contingency ranking, Continuation Power Flow, Voltage Stability.

I. INTRODUCTION

The voltage stability is the capability of a power system to maintain steady state voltage at all buses in the system at normal values and after being subjected to a disturbance [1]. A power system becomes unstable, when voltages uncontrollably changes due to the disbalance between load and generation, outage of equipment & lines and failure of voltage control mechanism in the system. The problem of voltage instability occurs mainly due to deficient supply of the reactive power or by an unnecessary absorption of reactive power. Continuous monitoring of the system status is required because the voltage instability affects the satisfactory operation of power system. Voltage stability assessment [1,2] is becoming an essential task for power system planning and operation. Power system security analysis [3] forms an integral part of modern energy management system. Security is a term used to reflect a power system's ability to meets its load without unduly stressing its apparatus or allowing variables to stray from prescribed range under the apparatus or allowing variables to stray from prescribed range under certain pre-specified credible contingencies. The contingencies [4,5] are in the form of network outage such as line or transformer outage or in the form of equipment outage e.g. a generator outage. The outages, which are important from limit violation viewpoint, are branch flow for line security or MW security and bus voltage magnitude for voltage security. Voltage stability has become a very important limit in assessing voltage security.

The importance of voltage stability in determining system security and performance will continue to increase due to the increased loadings and interconnections brought about by economic and environmental pressures which have let to increasingly complex power systems that must operate closer to their stability limits.

II. METHODOLOGY

A. Contingency Analysis Studies

The most difficult methodological problem to cope within contingency analysis is the accuracy of the method and the speed of solution of the model used. The operator usually needs to know if the present operation of the system is secure and what will happen if a particular outage occurs. Operations personnel must recognize which line or generator outages will cause power flows or voltages to go out of their limits. In order to predict the effects of outages, contingency analysis technique is used. Contingency analysis procedures model a single equipment failure event, that is one line or one generator outage, or multiple equipment failure events, that is two transmission lines, a transmission line and a generator; one after another in sequence until all credible outages have been studied. For each outage tested, the contingency analysis procedure checks all power flows and voltage levels in the network against their respective limits [3].

B. Methods of Contingency Analysis

Methods based on AC power flow calculations are considered to be deterministic methods which are accurate compared to DC power flow methods.[1] The methods used for analyzing the contingencies are based on full AC load flow analysis are faster and accurate. And therefore the wide use of the network control center. Because the contingency alarms came too late for operators to act, they are worthless. Most operations control centers that use an AC power flow program for contingency analysis use either a Newton-Raphson or the decoupled power flow. An algorithm under the AC load flow method will be used to ensure higher accuracy [2]. Since these algorithms has a good performance in terms of convergence speed and reliability in unfavorable conditions. Below is a brief description of these methods.

C. Equations

The programming of the above procedure for contingency analysis has been implemented in NEPLAN is fast decoupled load flow. And more a set of single and multiple contingencies are performed on Azerbaijan power network using full AC load flow analysis applying the simulation of lines and generator's outage. The simulation of transmission line outage is carried out by the formulation of the corresponding admittance matrix. Assume that the line connected between buses m and n will be outage. The elements of the admittance [Y] matrix that will be affected are Y_{mm} and Y_{nn} , and the new values of those admittances for the (π) mode of representation of transmission lines will be given by:

$$Y'_{mm} = Y_{mm} - \frac{1}{(R_{mn} + jX_{mn})} - \frac{jB_{mn}}{2}$$

$$Y'_{nn} = Y_{nn} - \frac{1}{(R_{nm} + jX_{nm})} - \frac{jB_{nm}}{2}$$

$$Y'_{mn} = Y_{mn} - \frac{1}{(R_{mn} + jX_{mn})} = 0$$

$$Y'_{nm} = Y_{nm} - \frac{1}{(R_{nm} + jX_{nm})} = 0$$

III. SOFTWARE DESCRIPTION

MATLAB is a programming language developed by MathWorks. It started out as a matrix programming language where linear algebra programming was simple. It can be run both under interactive sessions and as a batch job. This tutorial gives you aggressively a gentle introduction of MATLAB programming language. It is designed to give students fluency in MATLAB programming language. Problem-based MATLAB examples have been given in simple and easy way to make your learning fast and effective.

NEPLAN software is the best software of this feature because its Background is based on the power market. The characteristic of voltage stability are illustrated with IEEE 14-bus system. The generator produces active power, which is transferred through a transmission line to load. The reactive power capability of the generator is infinite. Thus the generator terminal voltage V_1 is constant.

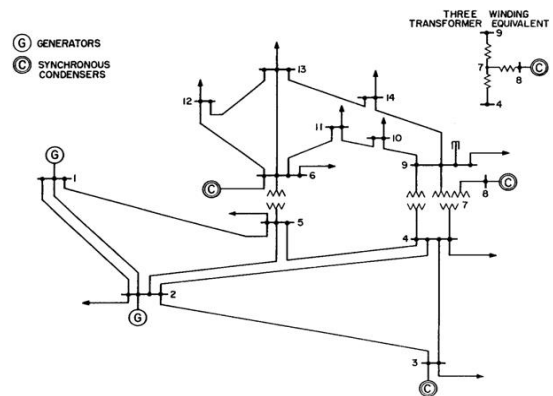


Fig 1: Line diagram of IEEE bus test system

$$V_2 = \sqrt{((V_1^2 - 2QX) \pm \sqrt{(V_1^4 - 4QXV_1^2 - 4PX^2)})^2}$$

Voltage at
buses (P.u)

$$P_i = \sum V_i V_j Y_{ij} \cos(\delta_i - \delta_j Y_{ij})$$

$$Q_i = \sum V_i V_j Y_{ij} \sin(\delta_i - \delta_j Y_{ij})$$

For $i, j = 1$ to n

Where P_i and Q_i are active and reactive powers injected at load.

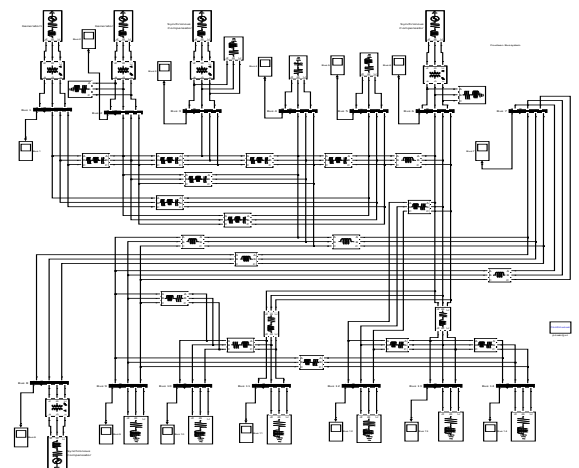


Fig 2. Simulation Model for IEEE 14-BUS system (Healthy condition)

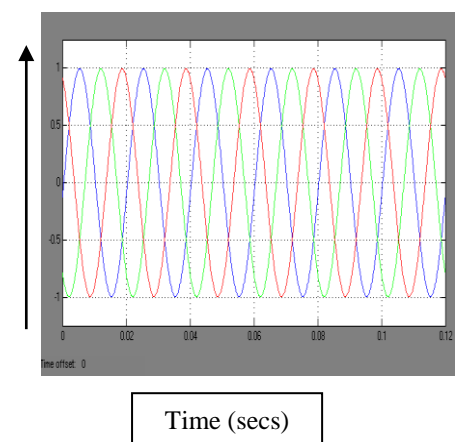


Fig 3. Results of Three –Phase Voltages for Healthy condition

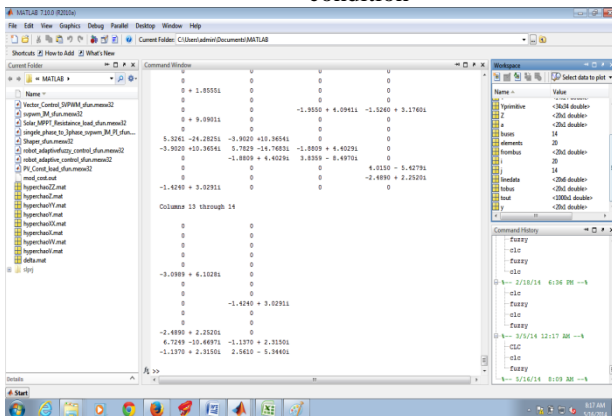


Fig 6 Eigen values of the reduced Jacobian matrix against load multiplication factor, K.

Table 1.1: Transmission lines data (R, X and B in Pu on 100MVA base) for the 14-bus test system

End buses	R	X	B/2
1-2	0.01938	0.05917	0.0264
2-4	0.05811	0.17632	0.0170
12-13	0.22092	0.19988	0
13-14	0.17093	0.34802	0

Table 1.2: Transformer data (R, X in pu on 100 MVA base) for the 14-bus test system

End buses	R	X
3-8	0.0671	0.17173
7-9	0	0.11001
6-7	0	0.2522

Table 1.3: Shunt capacitor(R, X in pu on 100 MVA base) for the 14-bus test system

End buses	MVAR(pu)
4	0.191
5	0.016

Table 1.4: Base case load data (Pu on 100 MVA base) for the 14-bus test system

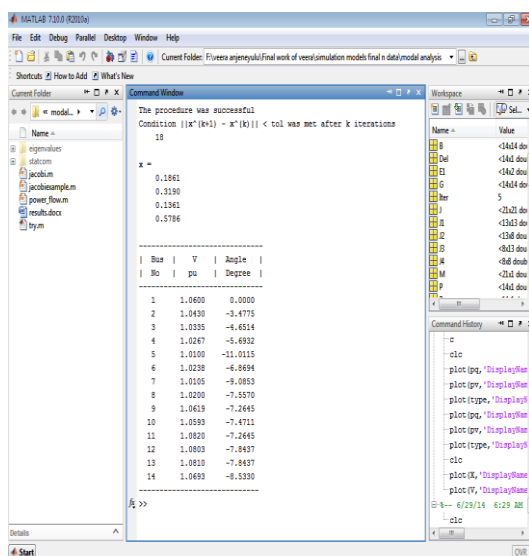
bus	P(MW)	QMVAR(pu)
3	0.217	0.127
4	0.942	0.191
7	0.112	0.075
8	0.050	0
9	0.295	0.166
10	0.09	0.058
11	0.035	0.018
12	0.061	0.016
13	0.135	0.058
14	0.1499	0.050

Table 1.5: Base case generator data (Pu on 100 MVA base) for the 14-bus test system

Fig 4. Ybus formation

	From	To	R	X	B/2	X'
%	Bus	Bus	pu	pu	pu	TAP (a)
linedata =	[1	2	0.01938	0.05917	0.0264	1
	1	5	0.05403	0.22304	0.0246	1
	2	3	0.04699	0.19797	0.0219	1
	2	4	0.05811	0.17632	0.0170	1
	2	5	0.05695	0.17388	0.0173	1
	3	4	0.06701	0.17103	0.0064	1
	4	5	0.01335	0.04211	0.0	1
	4	7	0.0	0.20912	0.0	0.978
	4	9	0.0	0.55618	0.0	0.969
	5	6	0.0	0.25202	0.0	0.932
	6	11	0.09498	0.19890	0.0	1
	6	12	0.12291	0.25581	0.0	1
	6	13	0.06615	0.13027	0.0	1
	7	8	0.0	0.17615	0.0	1
	7	9	0.0	0.11001	0.0	1
	9	10	0.03181	0.08450	0.0	1
	9	14	0.12711	0.27038	0.0	1
	10	11	0.08205	0.19207	0.0	1
	12	13	0.22092	0.19988	0.0	1
	13	14	0.17093	0.34802	0.0	1];

Fig 5. Line data of IEEE 14-bus system



Bus	V(pu)
1	1.06
2	1.045

Table 1.6:
Eigen values of reduced Jacobian matrix (Pu on 100 MVA base) for the 14-bus test system

K	E1	E2	E3	E4
1.124	0.1861	0.3190	0.1361	0.5786

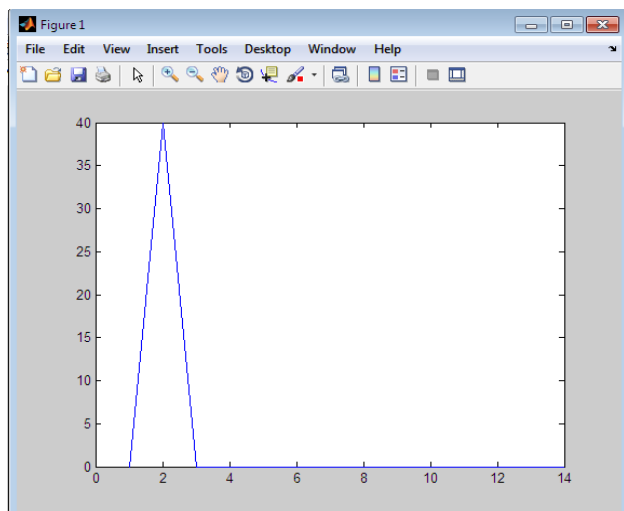


Fig.7 Power Generation versus bus number

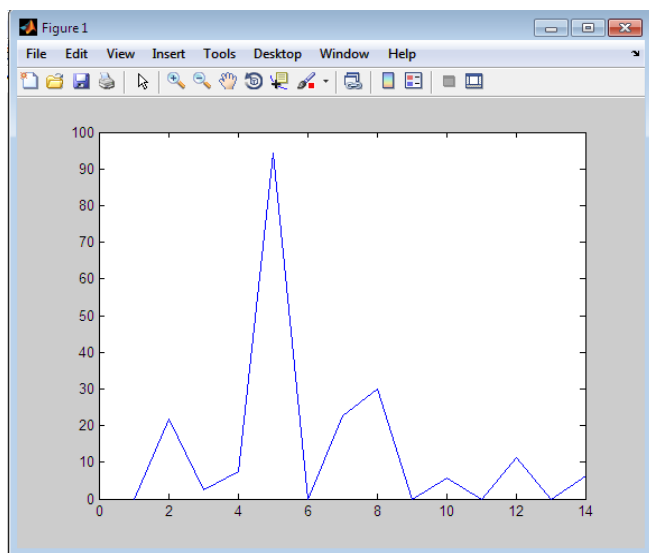


Fig.8 Power load versus bus number

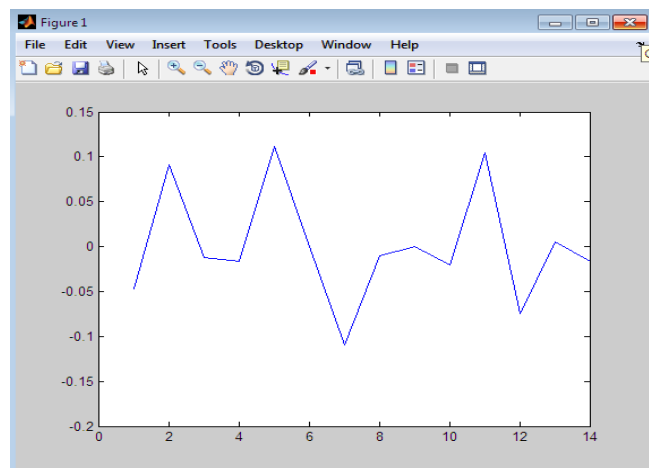


Fig.9 Reactive power versus bus number

Bus No	V(pu)	Angle(rad)	Pgen(Pu)	Qgen(Pu)	Pload(Pu)	Qload(Pu)
1	1.06	-0.52	Generator			
2	1.045	-0.52	Generator			
3	1.01	-0.52	Synchronous Compensator		0.217	0.127
4	1	0	Load		0.942	0.191
5	1	0	Load		0.478	0
6	1.07	-0.52	Synchronous Compensator		0.076	0.016
7	1	0	Load		0.112	0.075
8	1.09	-0.52	Synchronous Compensator		0.050	0
9	1	0	Load		0.295	0.166
10	1	0	Load		0.09	0.058
11	1	0	Load		0.035	0.018
12	1	0	Load		0.061	0.016
13	1	0	Load		0.135	0.058
14	1	0	Load		0.149	0.050

Fig.10 Line data with both generation and load powers

Linear Regression Modeling:

- Data set collected for 22 iterations:

S.No	Pr	V5	V6
1	0	1.0733	0
2	.1	1.0730	.0259
3	.2	1.0721	.0518
4	.3	1.0705	.0778
5	.4	1.0683	.1040
6	.5	1.0654	.1303
7	.6	1.0618	.1569
8	.7	1.0575	.1838
9	.8	1.0524	.2111
10	.9	1.0464	.2388
11	1.0	1.0396	.2671

12	1.1	1.0317	.2961
13	1.2	1.0227	.3258
14	1.3	1.0124	.3566
15	1.4	1.0005	.3885
16	1.5	.9868	.4576
17	1.6	.9769	.4220
18	1.7	.9519	.4959
19	1.8	.9286	.5382
20	1.9	.8984	.5872
21	2.0	.8538	.6504
22	2.1	.7613	.7613

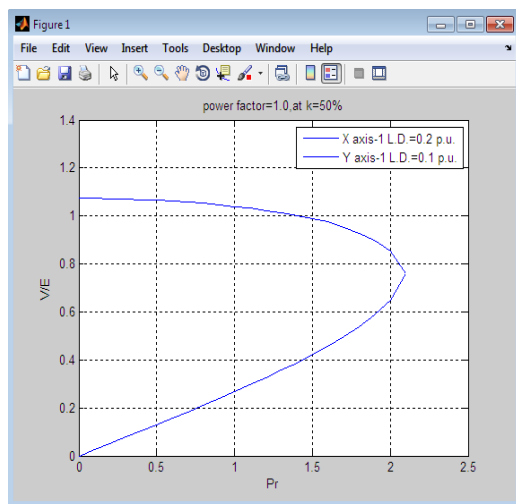


Fig.11: Loading Factor K=0.5

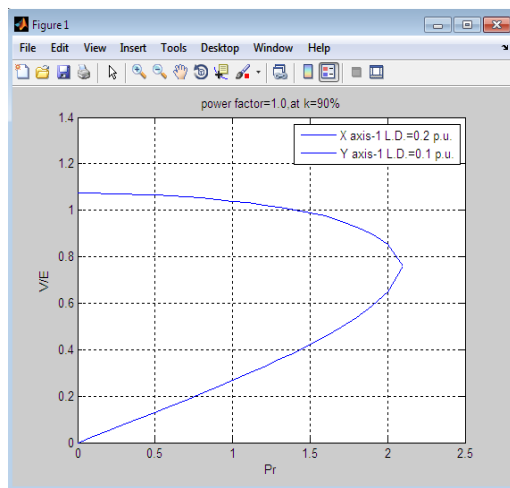


Fig.12. Loading factor K= 0.9

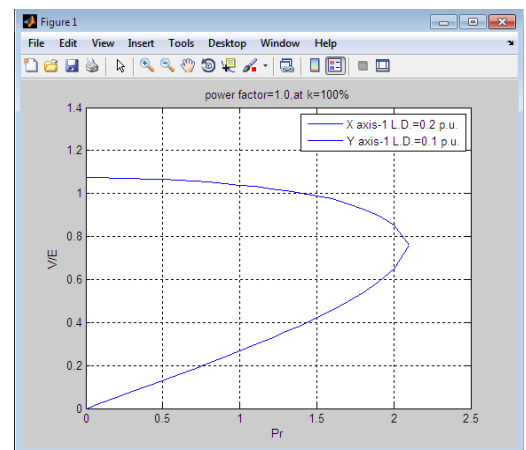


Fig. 13: Loading Factor K=1

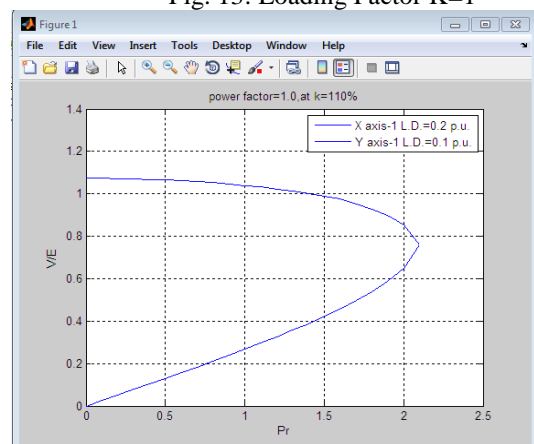


Fig.14. Loading Factor K=1.1

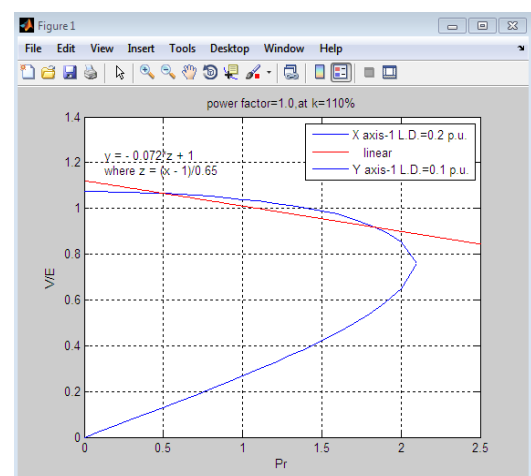


Fig.15. P-V curve at weakest buses for different iterations

Fitness Equation:

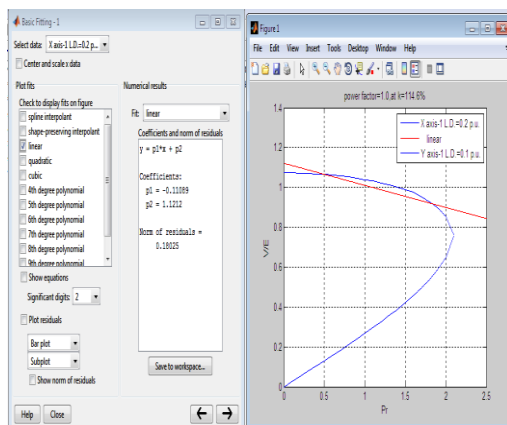


Fig.16. Linear regression (Basic fitting) Analysis
(K=1.146)

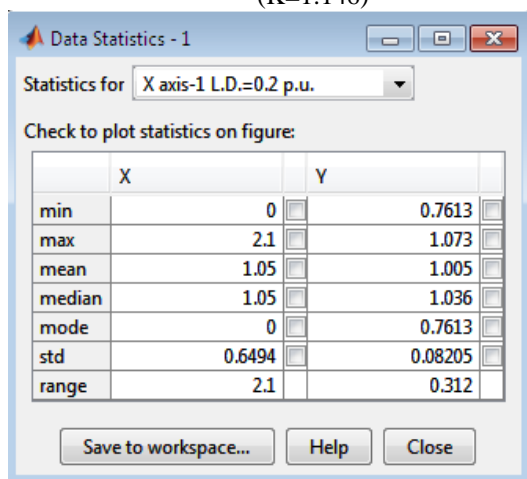


Fig.17 Data statistics of mean, standard deviation

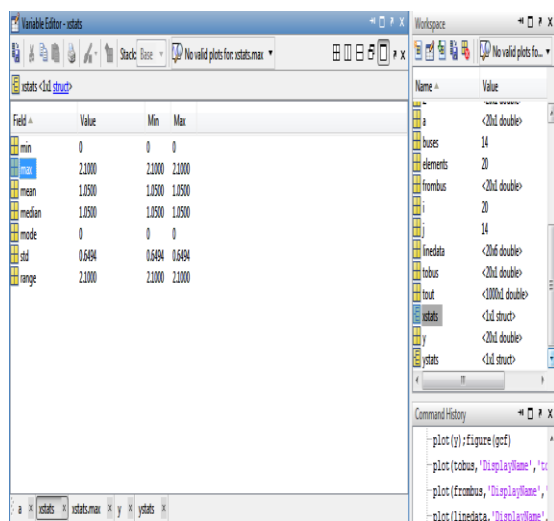


Fig.18. Data Statistics for Input

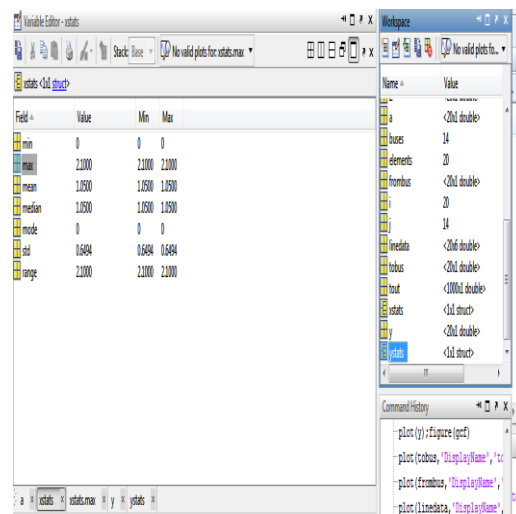


Fig. 19. Data Statistics for Output

Simulation model in NEPLAN Software:

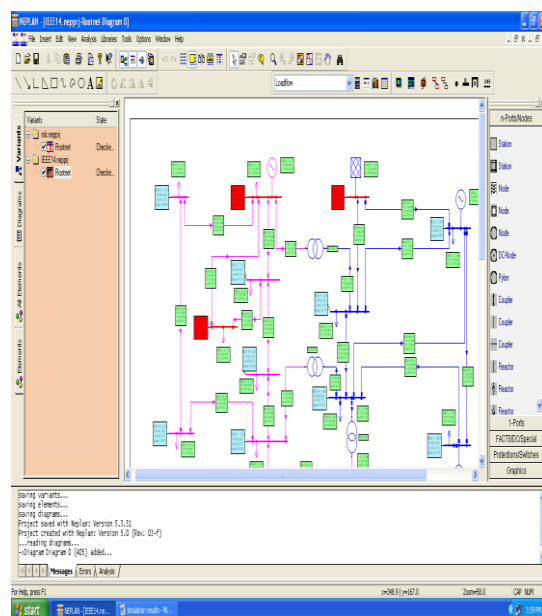


Fig.20: Selection of Method for Load Flow

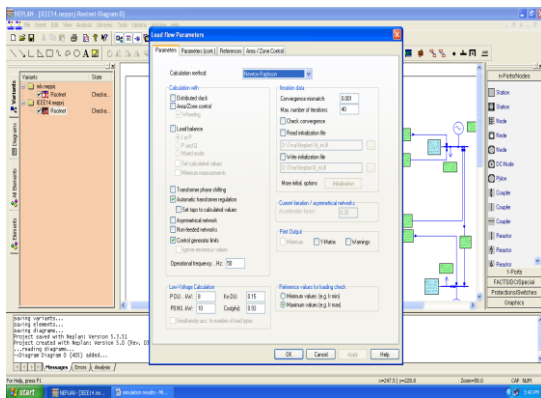


Fig 21: Analysis for Load Flow

Start Analysis...

...Check Network Connectivity...

--> Number of isolated Nodes.....0

--> Number of not feeded Networks.....0

--> Number of partial Networks to calculate....1

--> Number of isolated Nodes.....0

--> Number of not feeded Networks.....0

--> Number of partial Networks to calculate....1

Load flow calculation:

Iteration progress:

1 . 2.547775e+000

2 . 2.186047e-001

3 . 1.493830e-003

Qmin. Change of node type from PV to PQ. Generator:

GNBUS_8 18.0 (ID=617)

4 . 5.813800e-003

5 . 1.834669e-005

6 . 1.554407e-010

Node-mismatches:

Regulated transformers:

Tapcal Tapact Tapmin Tapmax Reg.node:

...Assign Results...

Violated Lower Voltage Limits

Violated Upper Voltage Limits

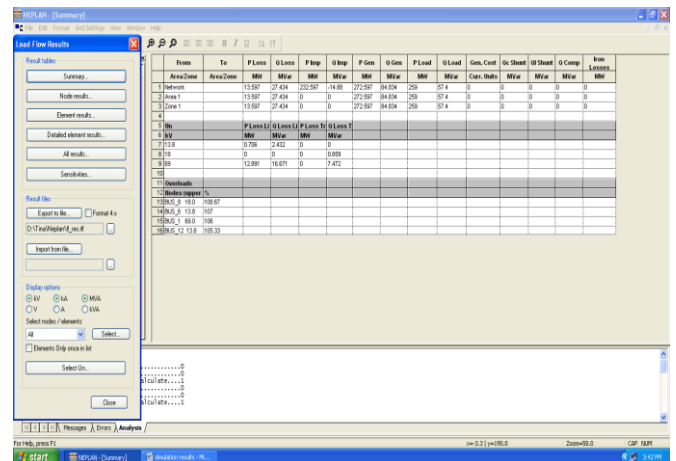


Fig 22: Selection Over loaded elements

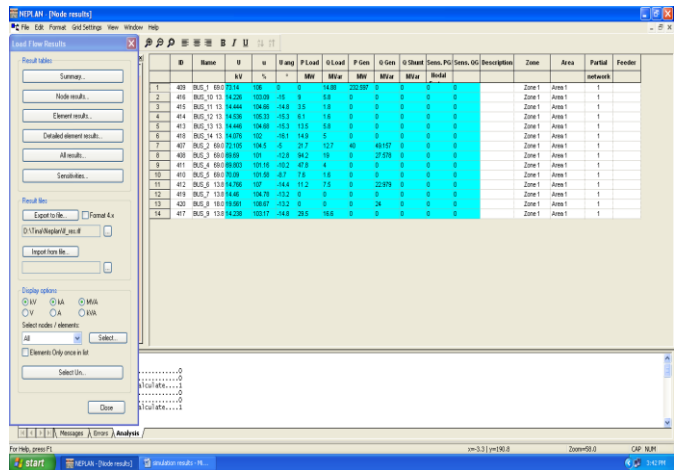


Fig 23: Selection Under loaded elements

BUS_1 69.0 (ID=409)	Zone 1	u% = 106.00	Area 1
BUS_6 13.8 (ID=412)	Zone 1	u% = 107.00	Area 1
BUS_12 13.8 (ID=414)	Zone 1	u% = 105.33	Area 1
BUS_8 18.0 (ID=420)	Zone 1	u% = 108.67	Area 1

Overloaded Elements

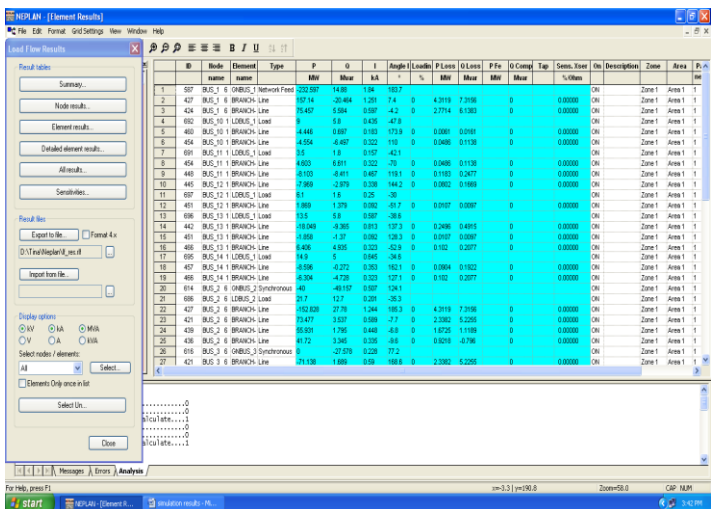


Fig 24: Selection of all elements

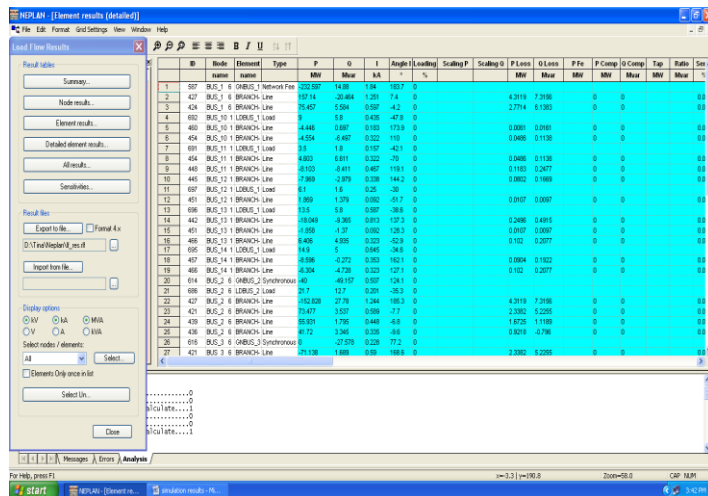


Fig 25: Selection of elements with their voltage profile, powers

Building Network Started...

...Check Network Connectivity...

...Update partial Networks...

--> Number of isolated Nodes.....0

--> Number of not feeded Networks.....0

--> Number of partial Networks to calculate....1

--Building Network Completed

Optimal Power Flow calculation...

Call: 1 - Feas./Opt. error = 7.868067e-001/3.228385e-002

Call: 2 - Feas./Opt. error = 6.911282e-001/2.689883e-002

Call: 3 - Feas./Opt. error = 6.341681e-001/2.159601e-002

Call: 4 - Feas./Opt. error = 4.118766e-001/3.352933e-002

Call: 5 - Feas./Opt. error = 3.874682e-001/3.685130e-002

Call: 6 - Feas./Opt. error = 3.825234e-001/3.760764e-002

--- Value of Objective function = 1.381108e-002

Call: 11 - Feas./Opt. error = 3.823726e-001/3.758300e-002

Call: 12 - Feas./Opt. error = 3.823727e-001/3.758288e-002

Call: 13 - Feas./Opt. error = 3.823727e-001/3.758283e-002

Call: 14 - Feas./Opt. error = 3.823727e-001/3.758281e-002

Call: 15 - Feas./Opt. error = 3.823727e-001/3.758280e-002

Call: 16 - Feas./Opt. error = 3.823727e-001/3.758279e-002

Call: 17 - Feas./Opt. error = 3.823727e-001/3.758279e-002

Call: 18 - Feas./Opt. error = 3.823727e-001/3.758279e-002

Call: 19 - Feas./Opt. error = 3.823727e-001/3.758279e-002

Call: 20 - Feas./Opt. error = 3.823727e-001/3.758279e-002

--- Value of Objective function = 1.381188e-002

Call: 21 - Feas./Opt. error = 3.823727e-001/3.758279e-002

Call: 22 - Feas./Opt. error = 3.823727e-001/3.758279e-002

Call: 23 - Feas./Opt. error = 3.823727e-001/3.758279e-002

Call: 24 - Feas./Opt. error = 2.663489e-001/1.278532e-002

Call: 25 - Feas./Opt. error = 2.492371e-001/1.385230e-002

Call: 26 - Feas./Opt. error = 4.536324e-003/1.340660e-002

Call: 27 - Feas./Opt. error = 6.245372e-004/6.502549e-003

Call: 28 - Feas./Opt. error = 4.867740e-004/1.363297e-003

Call: 29 - Feas./Opt. error = 6.010717e-005/1.332051e-004

Call: 30 - Feas./Opt. error = 4.334158e-007/4.148780e-005

--- Value of Objective function = 2.381972e-002

Call: 31 - Feas./Opt. error = 7.876568e-008/8.374479e-006

Call: 32 - Feas./Opt. error = 4.960229e-009/1.033526e-007

Call: 33 - Feas./Opt. error = 5.943024e-013/1.003407e-009

EXIT OPF: *** LOCALLY OPTIMAL SOLUTION FOUND

Obj. = 2.37387966

Network MW losses = 2.37387966

Network Mvar losses = -16.06956110

Network Total Gen.Cost (CurrU/h) = 0.00000000

Voltage Deviation^2 (%) = 0.00000000

Discretizing variables..

...Assign Results....

Violated Lower Voltage Limits

Violated Upper Voltage Limits

Overloaded Elements

Completed

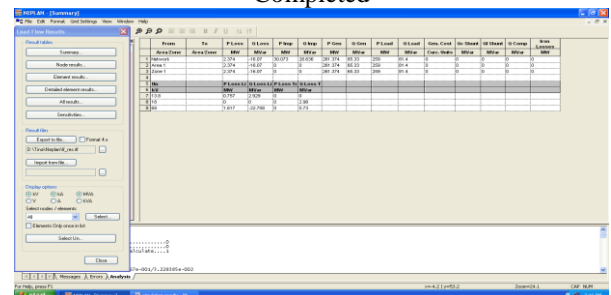


Fig 26: Load flow, state estimation and contingency analysis completed

IV. CONCLUSIONS

In this paper, the method for load flow, state estimation and contingency analysis was done using NEPLAN software was proposed. The proposed algorithm has been applied to practical IEEE 14-Bus system. The study of contingency ranking and analysis is very important from the view point of power system security. Here obtained results lead the contingency ranking for IEEE 14 Bus system. For IEEE-14 Bus system line number 10 connected between Bus 7 to Bus 9 is most severe line among all 20 lines. This identification being able to significantly improve the secure performance of

power systems and to reduce the chances of failure of system. Good planning helps to ensure that reliability and security of the system. Contingency ranking analysis helps the power system engineer to give the most priority to notice or monitoring the line flows to which line and monitoring other lines flow in descending order. The fitness value of the objective function is obtained in more optimized way in NEPLAN software than compared to MATLAB software.

V. REFERENCES

- [1]. A.J. Wood and Wollenberg, "Power generation, operation and control," 2nd Edition, John and Wiley & Sons Ltd, 2009.
- [2] B. Scott, O. Alsac and A.J. Monticelli, "Security analysis and optimization," Proceedings of the IEEE, Vol. 75, No. 12, Dec 1987, pp. 1623-1644.
- [3] N.M. Peterson W.F. Tinney and D.W. Bree, "Iterative linear AC power flow for fast approximate outage studies," IEEE Transactions on Power Apparatus and Systems, Vol. 91, No. 5, October 1972, pp. 2048-2058.
- [4] Ching-Yin Lee and Nanming Chen, "Distribution factors of reactive power flow in transmission line and transformer outage studies," IEEE Transactions on Power Systems, Vol. 7, No. 1, February 1992, pp. 194-200. M. Young, The Technical Writer's Handbook. Mill Valley, CA: University Science, 1989.
- [5] S.N. Singh and S.C. Srivastava, "Improved voltage and reactive power distribution for outage studies," IEEE Transactions on Power Systems, Vol. 12, No. 3, August 1997, pp. 1085-1093.
- [6] J. Zaborsky, K.W. Whang, K. Prasad, "Fast contingency evaluation using concentric relaxation," IEEE Transactions on Power Apparatus and Systems, Vol. PAS-99, No. 1, January 1980, pp. 28-36.
- [7] R. Bacher, W.F. Tinney, "Faster local power flow solutions: the zero mismatch approach," IEEE Transactions on Power Systems, Vol. 4, No. 4, October 1989, pp. 1345-1354.
- [8] P. Marannino, A. Berizzi, M. Merlo, G. Demartini, "A Rule-based Fuzzy Logic Approach for the Voltage collapse Risk Classification," IEEE Power Engineering Society Winter Meeting, Vol. 2, pp. 876-881, 2002.
- [9] Tarlochan S. Sindhu and Lan Chui, "Contingency Screening for Steady State Security Analysis by using FFT and Artificial Neural Networks," IEEE Transactions on Power Systems, Vol. 15, No. 1, February 2000.

LOAD FLOW, CONTINGENCY ANALYSIS, STATE ESTIMATION AND OPTIMAL OPERATION FOR IEEE 14-BUS SYSTEM

Dr .M. LAKSHMISWARUPA 1*, Mr. D. RAMESH 2*

1. Professor -Dept of EEE, Malla Reddy Engg. College (AUTONOMOUS), Hyderabad, India.
2. Asst. Prof- Dept of EEE, Malla Reddy Engg. College (AUTONOMOUS), Hyderabad, India.

Abstract— In this paper the work is divided into two main parts. The first part provides further improvements in power system state estimation and the second part implements Contingency Constrained Optimal Power Flow (CCOPF) in a multiple contingency framework. The demand of the energy management systems (EMS) set forth by modern power systems requires fast energy management systems. Contingency analysis is among the functions in EMS which is time consuming. In order to handle this limitation, this paper introduces agent based technology in the contingency analysis. The main function of agents is to speed up the performance. Negotiations process in decision making is explained and the issue set forth is the minimization of the operating costs. The IEEE 14 bus system and its line outage have been used in the research and simulation results are presented.

Index Terms— model, negotiation, optimal dispatch, power systems.

I. INTRODUCTION

It is well known that power system is a complex network consisting of numerous equipments like generators, transformers, transmission lines, circuit breakers etc. Failure of any of these equipments during its operation harms the reliability of the system and hence leading to outages. Whenever the pre specified operating limits of the power system gets violated the system is said to be in emergency condition. These violations of the limits result from contingencies occurring in the system. Thus, an important part of the security analysis revolves around the power system to withstand the effect of contingencies. The contingency analysis is time consuming as it involves the computation of complete AC load flow calculations following every possible outage events like outages occurring at various generators and transmission lines. This makes the list of various contingency cases very lengthy and the process very tedious. In order to mitigate the above problem, automatic contingency screening approach is being adopted which identifies and ranks only those outages which actually causes the limit violation on power flow or voltages in the lines. The contingencies are screened according to the severity index or performance index where a higher value of these indices denotes a higher degree of severity. The importance of power system security assessment for prediction of line flows and bus voltages following a contingency has been presented in [1-2]. The paper also details the challenges faced for the practical implementation of security analysis algorithms. The approximate changes in the line flow due to an outage in generator or transmission line is predicted based on distribution factors [3-4]. The use of AC power flow solution in outage studies has been dealt in [5]. Contingency screening or contingency selection is an essential task in contingency analysis. This helps to reduce the numerous computations; the bounding method [6] reduces the number of branch flow computation by using a bounding criterion that helps in reducing the number of buses for analysis and is based on

incremental angle criterion. The 1P-1Q method for contingency selection has been presented in [7]. In this method the solution procedure is interrupted after an iteration of fast decoupled load flow. Zaborzky et al. introduced the concentric relaxation method for contingency evaluation [8] utilizing the benefit of the fact that an outage occurring on the power system has a limited geographical effect. The use of fast decoupled load flow [9] proves to be very suitable for contingency analysis. Contingency selection criterion based on the calculation of performance indices has been first introduced by Ejebe and Wollenberg [10] where the contingencies are sorted in descending order of the values of performance index (PI) reflecting their severity. The practical implementation of contingency screening can be done by installing the phasor measurement units which are being used to capture the online values of bus voltages and angles [11]. The fast estimation of voltages in power system is essential for contingency analysis and this was proposed in [12]. Apart from performance index other index like voltage stability criteria index can also be chosen contingency ranking [13]. Multiple contingency can occur in the power system at the same time, hence its identification and analysis is a more complicated task, the multiple contingency screening in power system has been illustrated in [14]. The analysis of power system contingency becomes more challenging when the system is connected to a variable generation units like wind or solar systems, where the firm capacity is variable. In [15] the contingency analysis by incorporating sampling of Injected powers has been done. In this paper, the values of active power performance index (PIP) and reactive power performance index (PIV) have been calculated for 5-bus, IEEE-14 bus and IEEE-30 bus systems using the algorithm implemented in MATLAB software. Based on the values of PIV, contingencies have been ranked where a transmission line contingency leading to high value of PIV has been ranked 1 and a least value of PIV have been ranked last. The load flow analysis following the most severe transmission line contingency has been simulated and the results of active

power flow in various transmission lines and the bus voltages has been analyzed.

II. CONTINGENCY ANALYSIS USING LOAD FLOW SOLUTION

Load flow analysis performs static security analysis for a given system so that the system is operated defensively. Due to contingency, the system may enter an emergency state, wherein the operator has to take fast actions to restore the system back to normal. Here the status of all the elements selected as contingency cases under contingency analysis section are made and outage study is performed. The output of the program alarms the user of any potential overloads or out of limit voltages.

Contingency Selection Since contingency analysis process involves the prediction of the effect of individual contingency cases, the above process becomes very tedious and time consuming when the power system network is large. In order to alleviate the above problem contingency screening or contingency selection process is used. Practically it is found that all the possible outages does not cause the overloads or under voltage in the other power system equipments. The process of identifying the contingencies that actually leads to the violation of the operational limits is known as contingency selection. The contingencies are selected by calculating a kind of severity indices known as Performance Indices (PI) [1]. These indices are calculated using the conventional power flow algorithms for individual contingencies in an off line mode. Based on the values obtained the contingencies are ranked in a manner where the highest value of PI is ranked first. The analysis is then done starting from the contingency that is ranked one and is continued till no severe contingencies are found. There are two kind of performance index which are of great use, these are active power performance index (PIP) and reactive power performance index (PIV). PIP reflects the violation of line active power flow and is given by (1)

$$PIP = \sum (P_i P_{imax}) L 2n \quad i=1 \quad (1)$$

where, P_i = Active Power flow in line i , P_{imax} = Maximum active power flow in line i , n is the specified exponent, L is the total number of transmission lines in the system.

If n is a large number, the PI will be a small number if all flows are within limit, and it will be large if one or more lines are overloaded, here the value of n has been kept unity. The value of maximum power flow in each line is calculated using the formula $P_{imax} = V_i V_j / X$ (2) where, V_i = Voltage at bus i obtained from FDLF solution V_j = Voltage at bus j obtained from FDLF solution X = Reactance of the line connecting bus 'i' and bus 'j'. Another performance index parameter which is used is reactive power performance index corresponding to bus voltage magnitude violations. It mathematically given by (3) $PIV = \sum [2(V_i - V_{inom}) / (V_{imax} - V_{imin})]^2 Npq \quad i=1 \quad (3)$ where, V_i = Voltage of bus i , V_{imax} and V_{imin} are maximum and minimum voltage limits, V_{inom} is average of V_{imax} and V_{imin} , Npq is total number of load buses in the system.

Any power system operates on satisfying the demand from the generation. And also on the contingency state the power system should operate by giving alarm or to inform the insecurity to the operator, also to diagnose the faulty bus and preventive measures should be taken to handle the contingency. There for contingency study is very important in the load-flow analysis. The performance index is calculated for every line outage for IEEE 14-bus test system to implement the module for power system static security assessment. The security classification, contingency selection and ranking are done based on the performance index which is capable of accurately differentiating the secure and non-secure cases. Here in this project for IEEE-14 bus and load flow analysis and performance index is done in MiPower software.

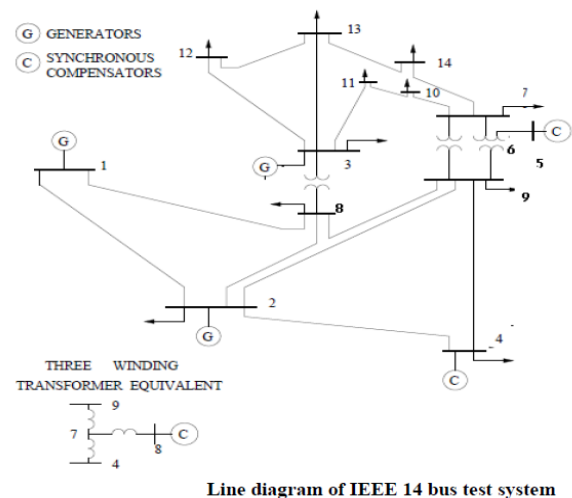


Fig 1 Line Diagram of IEEE 14 bus test system

III. LOAD FLOW METHODS

The objective of power flow study is to determine the voltage and its angle at each bus, real and reactive power flow in each line and line losses in the power system for specified bus or terminal conditions. Power flow studies are conducted for the purpose of planning (viz. short, medium and long range planning), operation and control. The other purpose of the study is to compute steady state operating point of the power system, that is voltage magnitudes and phase angles at the buses. By knowing these quantities, the other quantities like line flow (MW and MVAR) real and reactive power supplied by the generators and loading of the transformers can also be calculated. The conditions of over loads and under or over voltages existing in the parts of the system can also be detected from this study.

The different mathematical techniques used for load flow study are 1. Gauss Seidel method 2. Newton Raphson method 3. Fast Decoupled method 4. Stott's fast decoupled method III. Performance index A. Voltage performance index:

$$PIV = \left[\sum_{i=0}^{nb} W_i \frac{|V_i^{new} - V_i^{spec}|}{V_i^{max}} \right]^2 \quad (1)$$

Where, nb: Number of buses, Wi: Weightage factor for bus i, |V i| new: post outage voltage magnitude at bus i, |V i| spec: Specified voltage magnitude at bus i (1.0 p.u.) Vi max: Maximum allowable voltage change, which is computed as the difference between maximum voltage and difference between minimum voltage and specified voltage, if the voltage magnitude is less than the specified voltage. The significance of the weightage is to give lower ranking (higher severity) for poor voltage at specific buses. B. Lineflow performance index

$$PIF = \sum_{i=0}^{nl} W_i \left[\frac{P_{i\text{ new}}}{P_{i\text{ limit}}} \right]^2 \quad (2)$$

(2) Where, nl: Total number of series equipment, Wi: Weightage factor for series element I, Pi new: New real powerflow in the line, Pi limit: Real power flow limit of the line. The contingency can be ranked depending on the importance of a line. If it is desired not to overload a particular line,

SE is a very useful tool for the economic and secure operation of transmission networks. From early days of Scheweppe [3]–[5], developments of SE are done as a notion of robust estimation, hierarchical estimation, with and without the inclusion of current measurements, etc. The SE uses only voltage magnitude, real and reactive power injections and flows of SCADA measurements. The inclusion of branch currents measurements in SE deteriorates the performance of estimators. It also leads to non uniquely observable which produces more than one state for the given one set of measurements [6], [7]. Distributed SE for very large power system has been taken for study since the very beginning. The computational procedure involved in SE is an optimization function. The optimization function can be first order or second order of the derivative. The first order methods are the classical weighted least squares [8], the iteratively reweighted least squares [9] and the linear programming based on least absolute value estimator. The second order method involves the evaluation of the Lagrangian Hessian matrix. The primal-dual interior-point method and Huber M estimator are the solution methodologies available in literature to solve the second order method. The system states are evaluated either by statically or dynamically. The above methods mentioned are static state estimators. At the given point of time, the set of measurements are used to estimate the system state at that instant of time. The common method used to solve the static SE is weighted least square and weighted least absolute value methods. The heuristic methods are also applied to find the states. In the dynamic state estimation, the system states are continuously monitored at the regular intervals. The DSE uses the Kalman filter, Leapfrog algorithm, non-linear observer technique and invariant imbedding method to estimate the system states dynamically.

A. Weighted Least Square (WLS) Method In the WLS method, the objective is to minimize the sum of the squares of the weighted deviations of the estimated measurements from the actual measurements. The system states are estimated from the

available measurements. The objective function is expressed as follows, (1) where $f_i(x)$ and σ^2 is the system equation and the variance of the i th measurement respectively. $J(x)$ is the weighted residuals. m is the number of measurements and z_i is the i th measured quantity. If $f_i(x)$ is the linear function then the solution of eqn. (1) is a closed form. Usually, the power flow and power injection equations are described by nonlinear function. Hence the solution leads iterative procedure to determine the state of the system. Solved in WLS are (1) to find the gradient of $J(x)$ and (2) force it into zero and solved by Newton's method. The optimal state estimate is found using eqn. (2). (2) (3) where R Measurement error covariance matrix x System state vector H Jacobian matrix z Measurement vector The covariance matrix R reflects the relative relation between the measurements. If there is no interaction between the various measurements then R will be a diagonal matrix. The diagonal elements are the variances of the individual measurements ($r_i = \sigma^2$). Recently the SE with measurement dependencies is solved with WLS technique [10].

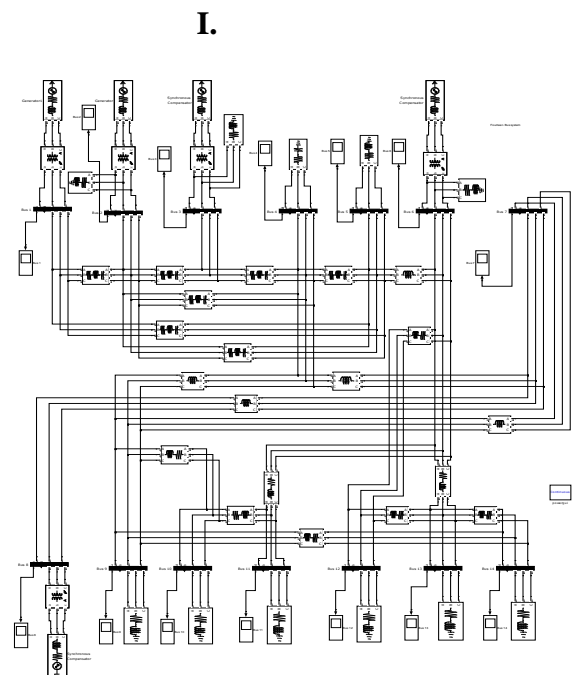
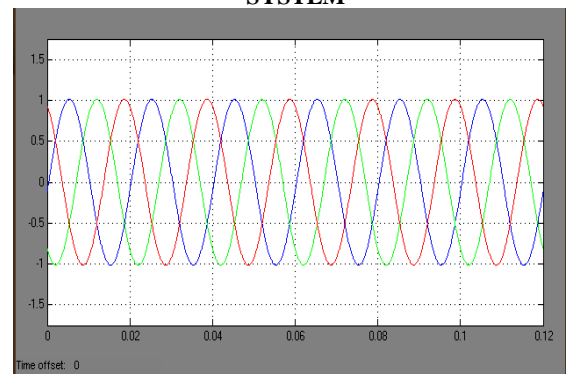


Fig 1. SIMULATION MODEL FOR IEEE 14-BUS SYSTEM



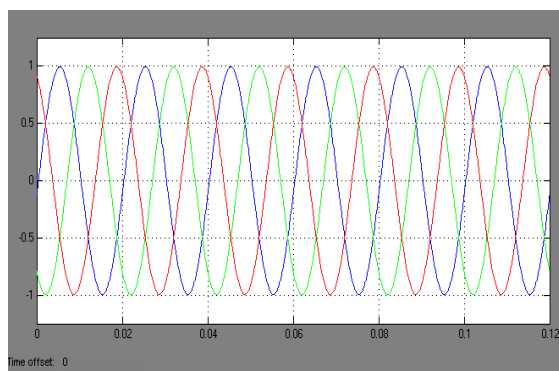
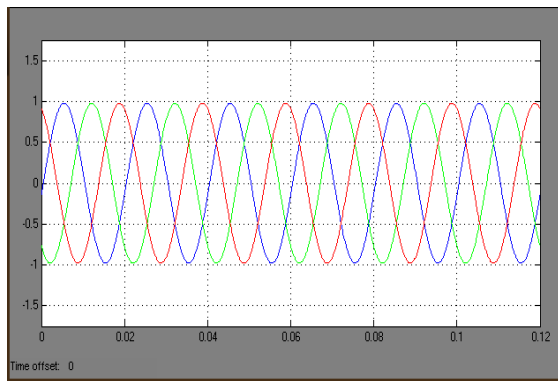


Fig 2. RESULTS OF BUS VOLTAGES ACROSS EACH BUS (example 1,3,7 taken)

%	From	To	R	X	B/2	X'
%	Bus	Bus	pu	pu	pu	TAP (a)
linedata =	[1	2	0.01938	0.05917	0.0264	1
	1	5	0.05403	0.22304	0.0246	1
	2	3	0.04699	0.19797	0.0219	1
	2	4	0.05811	0.17632	0.0170	1
	2	5	0.05695	0.17388	0.0173	1
	3	4	0.06701	0.17103	0.0064	1
	4	5	0.01335	0.04211	0.0	1
	4	7	0.0	0.20912	0.0	0.978
	4	9	0.0	0.55618	0.0	0.969
	5	6	0.0	0.25202	0.0	0.932
	6	11	0.09498	0.19890	0.0	1
	6	12	0.12291	0.25581	0.0	1
	6	13	0.06615	0.13027	0.0	1
	7	8	0.0	0.17615	0.0	1
	7	9	0.0	0.11001	0.0	1
	9	10	0.03181	0.08450	0.0	1
	9	14	0.12711	0.27038	0.0	1
	10	11	0.08205	0.19207	0.0	1
	12	13	0.22092	0.19988	0.0	1
	13	14	0.17093	0.34802	0.0	1

Fig 4. LINE DATA OF IEEE 14-BUS SYSTEM

a. Modal Analysis

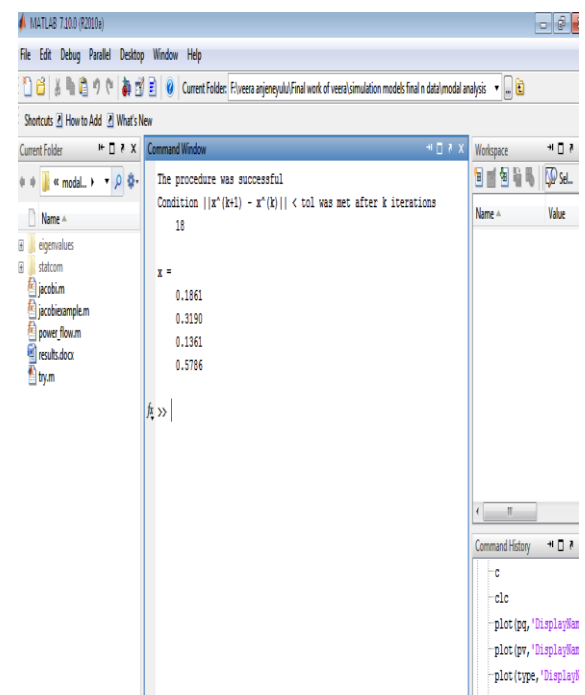


Fig5 Eigen values of the reduced Jacobian matrix against load multiplication factor, K.

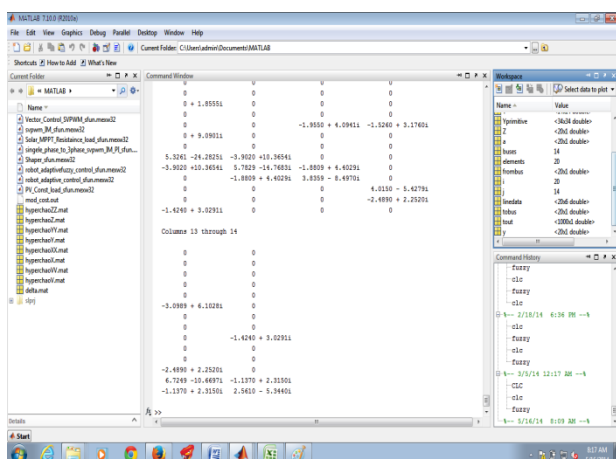
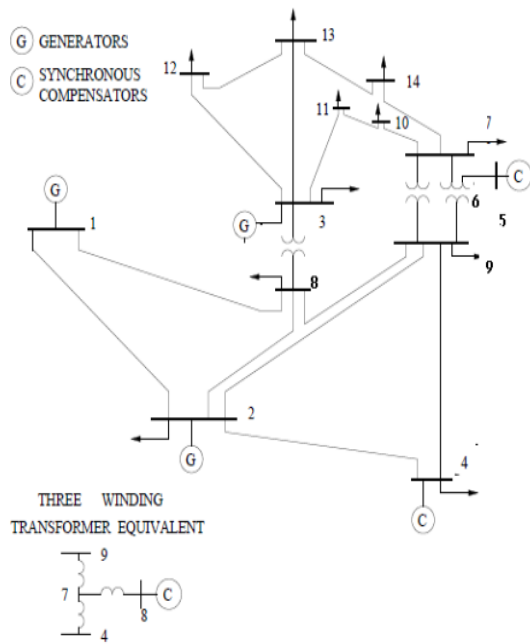


Fig 3. Ybus formation



Line diagram of IEEE 14 bus test system

Fig 6 Line Diagram of IEEE 14 bus test system

Table 1.1: Transmission lines data (R, X and B in Pu on 100MVA base) for the 14-bus test system

End buses	R	X	B/2
1-2	0.01938	0.05917	0.0264
2-4	0.05811	0.17632	0.0170

End buses	MVAR(pu)
4	0.191
5	0.016

12-13	0.22092	0.19988	0
13-14	0.17093	0.34802	0

Table 1.2: Transformer data (R, X in pu on 100 MVA base) for the 14-bus test system

End buses	R	X
3-8	0.0671	0.17173
7-9	0	0.11001
6-7	0	0.2522

End buses	R	X	Tap setting
9-10	0.03181	0.08450	1
			0.978
			0.969
			0.932

Table 1.3: Shunt capacitor(R, X in pu on 100 MVA base) for the 14-bus test system

Table 1.4: Base case load data (Pu on 100 MVA base) for

bus	P(MW)	QMVAR(pu)
3	0.217	0.127
4	0.942	0.191
7	0.112	0.075
8	0.050	0
9	0.295	0.166
10	0.09	0.058
11	0.035	0.018
12	0.061	0.016
13	0.135	0.058
14	0.1499	0.050

the 14-bus test system

Table 1.5: Base case generator data (Pu on 100 MVA base) for the 14-bus test system

Bus	V(pu)
1	1.06
2	1.045

Table 1.6: Eigen values of reduced Jacobian matrix (Pu on 100 MVA base) for the 14-bus test system

K	E1	E2	E3	E4
1.124	0.1861	0.3190	0.1361	0.5786

Table 1.7: Transformer data for different load levels (Pu on 100 MVA base) for the 14-bus test system

Table 1.8: Load data for different load levels (Pu on 100 MVA base) for the 14-bus test system

Bus	P(pu)	Q(pu)	Load level
4	0.942	0.191	1
	0.931	0.185	0.978
	0.928	0.189	0.969
	0.940	0.172	0.932
5	0.478	0.197	1
	0.435	0.192	0.978
	0.241	0.188	0.969
	0.448	0.179	0.932
9	0.295	0.166	1

	0.285	0.164	0.978
	0.274	0.158	0.969
	0.286	0.149	0.932

Table 1.9: Generator data for different load levels (Pu on 100 MVA base) for the 14-bus test system

Bus	P(pu)	Voltage(pu)	Load level
4	0.035	1.06	1
	0.061		0.978
	0.135		0.969
	0.1499		0.932
5	0.050	1.045	1
	0.295		0.978
	0.09		0.969
	0.217		0.932
9	0.242	1.01	1
	0.112		0.978
	0.235		0.969
	0.241		0.932

Table 1.10: Load voltages and reactive power outputs of generator 2 and 3 at load level 1 (Pu on 100 MVA base) for the 14-bus test system

Contingency	V5	V6	QG3	QG2
Without outage, fixed tap	0.96	1.11	290	-83
Without outage, LTC active	0.99	1.08	227	144
Line outage, fixed tap	0.91	1.00	200	224
Line outage, LTC active	1.01	1.09	243	146

Table 1.11: Load voltages and reactive power outputs of generator 2 and 3 at load level 2 (Pu on 100 MVA base) for the 14-bus test system

Contingency	V5	V6	QG3	QG2
Without outage, fixed tap	1.03	1.11	290	-83
Without outage, LTC active	0.99	1.08	227	164

Table 1.12: Load voltages and reactive power outputs of generator 2 and 3 at load level 3 (Pu on 100 MVA base) for the 14-bus test system

Contingency	V5	V6	QG3	QG2
Without outage, fixed tap	1.02	1.11	401	-81
Without outage, LTC active	0.98	1.07	700	249

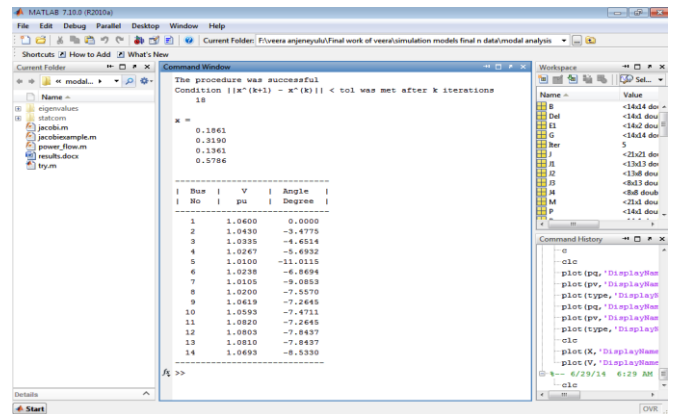


Fig 7 Voltages in magnitude and angle, Eigen values after modal analysis applied

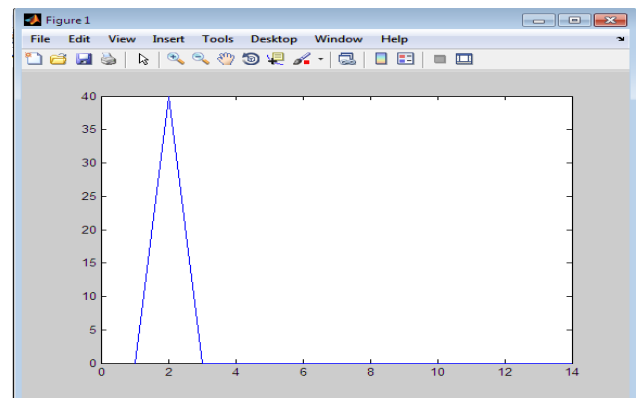


Fig 9 Power Generation versus bus number

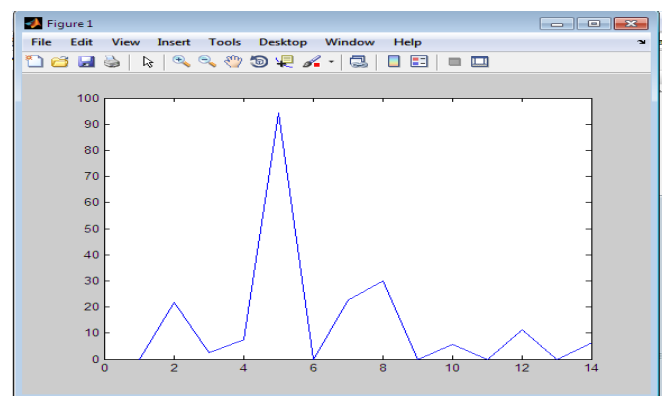


Fig 10 Power load versus bus number

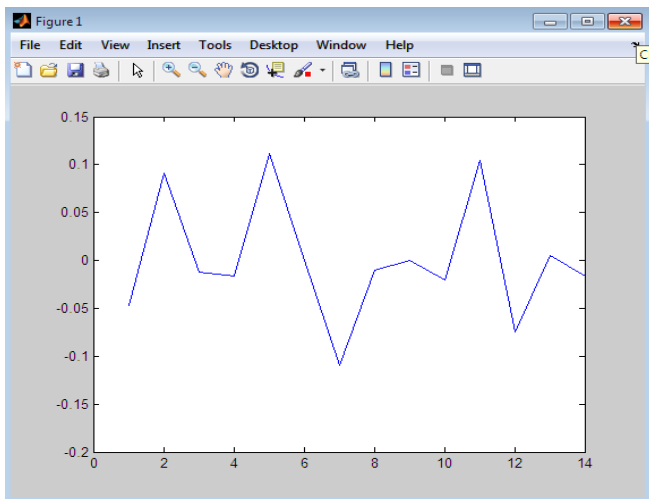


Fig 11 Reactive power versus bus number

Bus No	V(pu)	Angle(rad)	Pgen(Pu)	Qgen(Pu)	Pload(Pu)	Qload(Pu)
1	1.06	-0.52	Generator			NIL
2	1.045	-0.52	Generator			NIL
3	1.01	-0.52	Synchronous Compensator		0.217	0.127
4	1	0	Load		0.942	0.191
5	1	0	Load		0.478	0
6	1.07	-0.52	Synchronous Compensator		0.076	0.016
7	1	0	Load		0.112	0.075
8	1.09	-0.52	Synchronous Compensator		0.050	0
9	1	0	Load		0.295	0.166
10	1	0	Load		0.09	0.058
11	1	0	Load		0.035	0.018
12	1	0	Load		0.061	0.016
13	1	0	Load		0.135	0.058
14	1	0	Load		0.149	0.050

REFERENCES

- [1] Wood A.J and Wollenberg B.F., "Power generation, operation and control", John Wiley & Sons Inc., 1996.
- [2] Stott B, Alsac O and Monticelli A.J, "Security Analysis and Optimization", Proc. IEEE, vol. 75, No. 12, pp. 1623-1644, Dec 1987.
- [3] Lee C.Y and Chen N, "Distribution factors and reactive power flow in transmission line and transformer outage studies", IEEE Transactions on Power systems, Vol. 7, No. 1, pp. 194-200, February 1992.
- [4] Singh S.N and Srivastava S.C, "Improved voltage and reactive distribution factor for outage studies", IEEE Transactions on Power systems, Vol. 12, No.3, pp.1085-1093, August 1997
- [5] Peterson N.M, Tinney W.F and Bree D.W, "Iterative linear AC power flow solution for fast approximate outage studies", IEEE Transactions on Power Apparatus and Systems, Vol. PAS-91, No. 5, pp. 2048-2058, October 1972.
- [6] Brandwijn V and Lauby M.G, "Complete bounding method for A.C contingency screening", IEEE Transactions on Power systems, Vol. 4, No. 2, pp. 724-729, May 1989.
- [7] Albuyeh F, Bose A and Heath B, "Reactive power consideration in automatic contingency selection", IEEE Transactions on Power systems, Vol. PAS-101, No. 1, pp. 107-112, January 1982.
- [8] Zaborzky J, Whang K.W and Prasad K, "Fast contingency evaluation using concentric relaxation", IEEE Transactions on Power systems, Vol. PAS-99, No. 1, pp. 28-36, February 1980.
- [9] Stott B and Alsac O, "Fast decoupled load flow", IEEE Transactions on Power Apparatus and Systems, Vol. PAS-91, No. 5, pp. 859-869, May 1974.
- [10] Ejebe G.C and Wollenberg B.F, "Automatic Contingency Selection", IEEE Transactions on Power Apparatus and Systems, Vol. PAS-98, No. 1, pp. 97-109, January 1979.
- [11] Innocent Kamwa, Robert Grondin and Lester Loud, "Time-Varying Contingency Screening for Dynamic Security Assessment Using Intelligent-Systems Techniques", IEEE Transactions on Power Systems, Vol. 16, No. 3, pp. 526-537, August 2001
- [12] T.Jain, L.Srivastava, S.N. Singh and Arvind Jain, "Parallel Radial Basis Function Neural Network Based Fast Voltage Estimation for Contingency Analysis", IEEE International Conference on Electric Utility Deregulation, Restructuring and Power Technologies, Hong Kong, April 2004.
- [13] F. Fatehi, M.Rashidinejad and A.A Gharaveisi, "Contingency Ranking Based on a Voltage Stability Criteria Index", IEEE Transactions in Power System, 2007
- [14] Vaibhav Donde, Vanessa Lopex, Bernard Lesieutre, Ali Pinar, Chao Yang and Juan Meza, "Severe Multiple Contingency Screening in Electric Power Systems", IEEE Transactions on Power Systems, Vol.23, No.2, pp. 406-417, May 2008.
- [15] Magnus Perninge, Flip Linskog and Lennart Soder, "Importance Sampling of Injected Powers for Electric Power System Security Analysis", IEEE Transactions on Power Systems, Vol.27, No.1, February 2012..

Design of a Closed Loop Speed Control for BLDC Motor

T.Suman, K.Ramesh, Dr.M.Lakshmiswarupa,

Associate Professor, Dept. of EEE, MREC (A), Hyderabad, Telangana, India

Asst. Professor, Dept. of EEE, MREC (A), Hyderabad, Telangana, India

Associate Professor, Dept. of EEE, MREC (A), Hyderabad, Telangana, India

ABSTRACT: The present work deals with speed control of BLDC motor in which an Inverter is controlled using PWM techniques and checked the performance of sinusoidal PWM and Space Vector PWM schemes and simulated to produce the desired dynamic and static speed-torque characteristics. The speed can be controlled in a closed loop by measuring the actual speed of the motor. The error in the set speed and actual speed is calculated. A Proportional plus Integral plus derivative (P.I.D) controller can be used to amplify the speed error and dynamically adjust the PWM duty cycle. The developed speed control scheme is verified through Matlab/simulink

KEYWORDS: Speed controller, feedback loop, Brushless dc (BLDC) motor drive, SPWM, SVPWM, Hysteresis current control

I. INTRODUCTION

The construction of BLDC appears like inside –out Permanent Magnet DC motor (PMDC) .In a PMDC motor the stator is a permanent magnet and the rotor has the windings, which are excited with a dc current. The current in the rotor winding is reversed to create a rotating or moving electric field by means of a mechanical commutator and brushes. On the other hand, in a BLDC motor the three phase windings are on the stator and the rotor is a permanent magnet. Hence it is inside-out PMDC motor.

The Brushless DC motor (BLDC motor) drive is a combination of an ac machine, a solid state inverter, and electronic control circuitry and rotor position sensors. The speed –torque characteristics of this drive is drooping nature just similar to a conventional dc motor.

The PMSM has a sinusoidal back-EMF and requires sinusoidal stator currents to produce constant torque while the BDCM has a trapezoidal back-EMF and requires rectangular stator currents to produce constant torque. There is a slight variation among the modeling of PMSM and BLDC motors. The PMSM is very similar to the standard wound rotor synchronous machine except that it has no damper windings and field excitation is no required as they are permanent magnets. Hence the d-q model of the PMSM can be derived from the well-known [4] model of the synchronous machine with the equations of the damper windings and field current dynamics removed and it is well known that the transformation will make.

In the present paper implemented the state space model of BLDC motor in a-b-c reference frame and performed detailed examination of torque behavior and speed control. Firstly the modeling is done by developing suitable blocks in MATLAB/Simulink and various blocks like torque, rotor position, speed, trapezoidal induced back EMF, phase currents, phase voltages are obtained.

The Speed control of BLDC motor is carried out in a closed loop by measuring the actual speed of the motor. The error in the set speed and actual speed is calculated. A Proportional plus Integral plus derivative (P.I.D) controller can be used to amplify the speed error and dynamically adjust the PWM duty cycle.

International Journal of Advanced Research in Electrical, Electronics and Instrumentation Engineering

(An ISO 3297: 2007 Certified Organization)

Vol. 5, Special Issue 8, November 2016

II. PRINCIPLE OF OPERATION

To understand the operation of BLDC motor, consider a three-phase BLDC motor with only three coils. To make the motor to rotate the coils are excited (or energized) in a predetermined sequence to get uniform torque. The direction of current in stator coils determines the orientation of magnetic field and based on current direction, the magnetic field attracts and rejects the permanent magnets of rotor. The method of reversing current flow in stator coils and thereby the magnetic field at right point of time and in right sequence to rotate the rotor is known as commutation. In three-phase BLDC motor, there are six commutation states and they have been repeated in a sequence for every mechanical rotation of rotor. One sequence (i.e. six states) for every electrical cycle of rotation. A four-pole BLDC motor consisting two electrical cycles of rotation [1]-[3].

The inverter, rotor position sensors and electronic control circuitry imitates the commutation in a conventional dc motor therefore; this method of commutation is called as electronic commutation

III. MODELING OF BLDC MOTOR

The BLDC motor has been modeled using stator phase currents, phase voltages, speed, and rotor position as state variables of drive system. The following model of BLDC motor is based on a few assumptions, such as iron and stray losses are neglected and induced currents in the rotor due to stator harmonic fields are being neglected.

First model equation from Phase-A of stator winding is

$$\frac{di_a}{dt} = \frac{1}{L-M} [v_a - R_s i_a - k_p \omega_m \theta_a(\theta_r)]$$

In the above equation L, M are self inductance and mutual inductance of stator winding respectively. Where R_s is stator resistance per phase. Similarly for Phase –B and C are as below

$$\frac{di_b}{dt} = \frac{1}{L-M} [v_b - R_s i_b - k_p \omega_m \theta_b(\theta_r)]$$

$$\frac{di_c}{dt} = \frac{1}{L-M} [v_c - R_s i_c - k_p \omega_m \theta_c(\theta_r)]$$

Now model equation contributing electromechanical energy conversion in the motor is as follows,

$$\frac{d\omega_m}{dt} = \frac{-B}{J} (\omega_m) - \frac{1}{J} (T_e - T_l)$$

Hence

$$T_e = \frac{P}{\omega_m} = \frac{e_a i_a + e_b i_b + e_c i_c}{\omega_m} = T_a + T_b + T_c$$

$$T_e = \frac{2(k_p \omega_m)I}{\omega_m} = 2 * k_p * I$$

This equation further modified as

$$T_e = k_t * I$$

Where k_t is called as torque constant and the equation is just similar to separately excited brushed dc motor when flux is constant.

Now governing equation of rotor position is as follows

$$\frac{d\theta_r}{dt} = \frac{P}{2} [\omega_m]$$

Where P is the number of poles.

The variation of back EMF values with respect to rotor position is as shown below

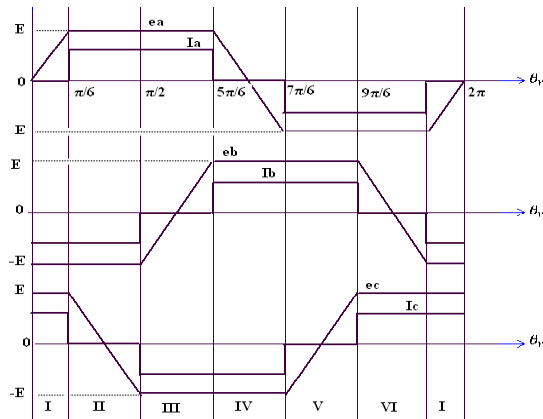


Fig.1 back-EMF variation with rotor position

IV. DYNAMIC SIMULATION

The overall block diagram implemented in MATLAB is described in Fig.2 and it consisting various functional blocks such as back-EMF, speed-torque, hysteresis block and inverter blocks etc with Sinusoidal PWM and Space Vector PWM techniques [1],[2].

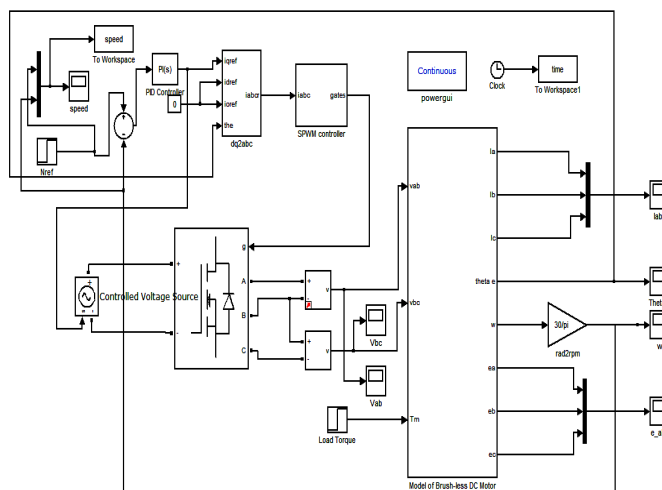


Fig.2 (a) Sinusoidal PWM technique.

International Journal of Advanced Research in Electrical, Electronics and Instrumentation Engineering

(An ISO 3297: 2007 Certified Organization)

Vol. 5, Special Issue 8, November 2016

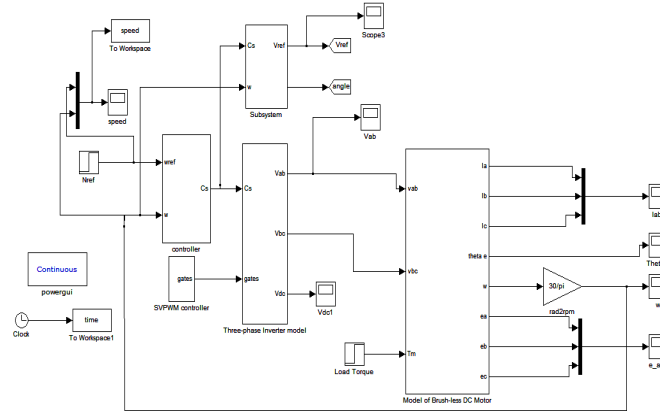


Fig.2 (b) Sinusoidal PWM technique

V. SIMULATION RESULTS

The following figures representing simulation results for sinusoidal PWM technique and Space Vector PWM technique.

Fig.3 (a) (b) and (c) shows the speed performance, torque wave form and Back –emf of SPWM scheme and Fig.4 (a) (b) and (c) shows the speed performance, torque wave form and Back –emf of Space Vector PWM technique.

Torque ripples very high at dynamic conditions for BDLDC motor when it is run by using Sinusoidal PWM technique as

Compared to Space Vector PWM and similarly the same is happening with regard to speed performance.

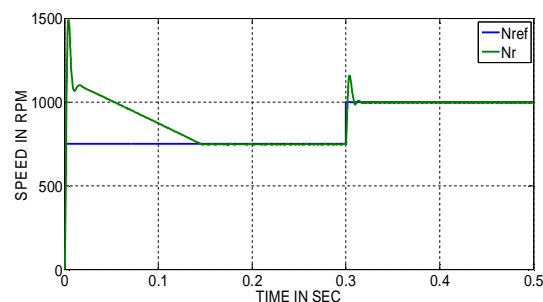


Fig.3 (a) speed versus time

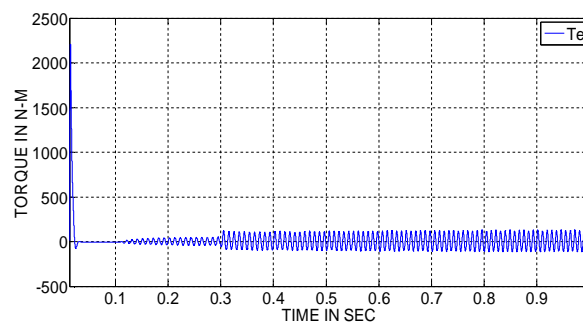


Fig.3 (b) torque versus time

International Journal of Advanced Research in Electrical, Electronics and Instrumentation Engineering

(An ISO 3297: 2007 Certified Organization)

Vol. 5, Special Issue 8, November 2016

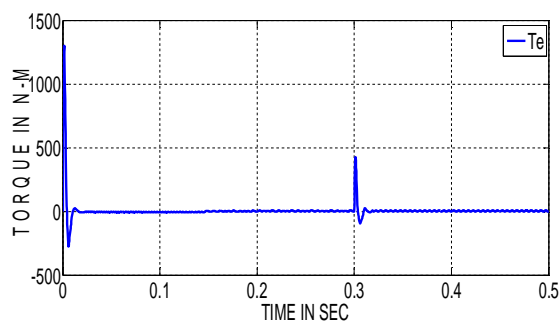


Fig.3 (c) Back-emf wave form

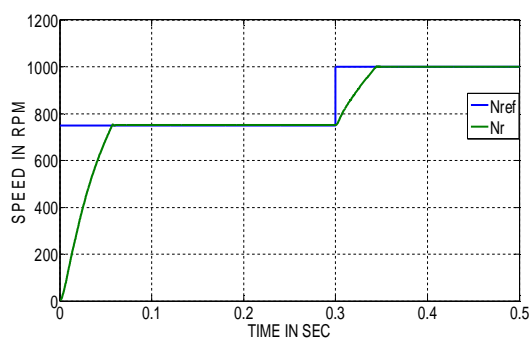


Fig.4 (a) speed versus time

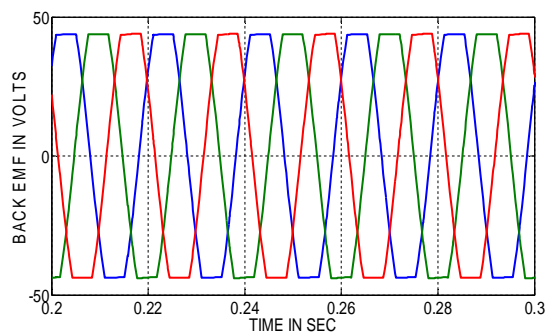


Fig.4 (b) Torque versus time

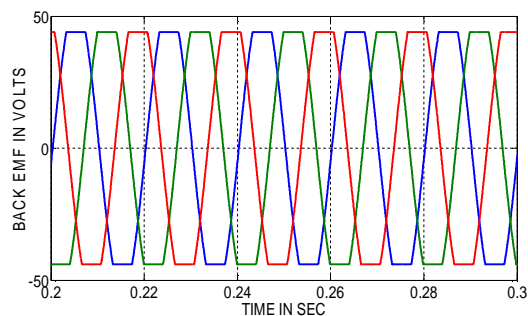


Fig.4 (c) Back-emf wave form



ISSN (Print) : 2320 – 3765
ISSN (Online): 2278 – 8875

International Journal of Advanced Research in Electrical, Electronics and Instrumentation Engineering

(An ISO 3297: 2007 Certified Organization)

Vol. 5, Special Issue 8, November 2016

VI. CONCLUSION

The simulation results reveal that the fluctuations in speed and torque are less when the Space Vector Modulation strategy is implemented in the BLDC motor. Thus it can be concluded that the overall performance of a motor drive system is improved when Space Vector Modulation technique is used in the drive system.

REFERENCES

- [1] R. Krishnan, "Electric Motor Drives Modeling, Analysis and Control," Prentice Hall 2001.
- [2] Bimal K. Bose, Modern Power Electronics and AC Drivers. Penitence.
- [3] J. Fang, H. Li, And B. Han, "Torque Ripple Reduction In BLDC Torque Motor With Nonideal Back Emf," *IEEE Trans. Power Electron.*, Vol. 27, No. 11, Pp. 4630-4637, November 2012.
- [4] T.H. Kim And M.Ehsani, "Sensorless Control Of The BLDC Motors From Near-Zero To High Speeds," *IEEE Trans. Power Electron.*, Vol. 19, No. 6, Pp. 1635–1645, Nov. 2004.
- [5] "A Novel Microcontroller-Based Sensorless Brushless Dc (BLDC) Motor Drive For Automotive Fuel Pumps," *IEEE Trans. Ind.Appl.*, Vol. 39, No. 6, November/December 2003
- [6] D. Chen and J. C. Fang, "Commutation torque ripple reduction in PM brushless DC motor with Nonideal trapezoidal back EMF," in Proc. CSEE, Oct. 2008, vol. 28, no. 30, pp. 79–83.
- [7] J. H. Song and I. Choy, "Commutation torque ripple reduction in brushless DC motor drives using a single DC current sensor," *IEEE Trans. Power Electron.*, vol. 19, no. 2, pp. 312–319, Mar. 2004.
- [8] X. F. Zhang and Z. Y. Lu, "A new BLDC motor drives method based on BUCK converter for torque ripple reduction," in Proc. IEEE Power Electron. Motion Control, Conf., 2006, pp. 1–4.
- [9] W. Chen, C. L. Xia, and M. Xue, "A torque ripple suppression circuit for brushless DC motors based on power DC/DC converters," in Proc. IEEE Ind. Electron. Appl. Conf., 2006, pp. 1–4.
- [10] T. N. Shi, Y.T. Guo, P. Song, and C.L.Xia, "A new approach of minimizing commutation torque ripple for brushless DC motor based on DC-DC converter," *IEEE Trans. Ind. Electron.*, vol. PP, no. 99, pp. 1–9, 2010.
- [11] K. Wei, C. S. Hu, and Z. C. Zhang, "A novel commutation torque ripple suppression scheme in BLDCM by sensing the DC current," in 36th IEEE Power Electron. Spec. Conf., 2005, pp. 1259–1263.
- [12] G.W. Meng, X. Hao, and H. S. Li, "Commutation torque ripple reduction in BLDC motor using PWM_ON_PWM mode," in Proc. Int. Conf. Electr.Mach. Syst. Conf., 2009, pp. 1–6.

A Novel Method of Dynamic Programming for the Adaptive Optimal Control of Nonlinear Systems

Mr. Desai Feroz¹, Mrs. M. Lakshmi Swarupa².

¹Mr. Desai Feroz, P.G. Scholar, EEE, MREC(Autonomous), Telangana, India

²Mrs. M. Lakshmi Swarupa, Assoc. Professor & HOD, EEE, MREC (Autonomous), Telangana, India

Abstract - Dynamic programming offers a theoretical way to solve optimal control problems. However, it suffers from the inherent computational complexity, also known as the curse of dimensionality. To achieve online approximation of the cost function and the control policy, neural networks are widely used in the previous ADP architecture. The main purpose of this paper is to develop a novel dynamic programming methodology to achieve global and adaptive suboptimal stabilization of uncertain nonlinear systems via online learning. In this paper an optimization problem, of which the solutions can be easily parameterized, is proposed to relax the problem of solving the Hamilton-Jacobi-Bellman (HJB) equation. This approach is inspired from the relaxation method used in approximate dynamic programming. It is also proposed that a relaxed policy iteration method is different for the inverse optimal control design and the results are obtained by M-file programming.

Key Words: Global adaptive dynamic programming, Approximate Dynamic programming, Nonlinear Systems, Adaptive optimal control, Semi-definite programming (SDP), Sum of squares (SOS).

1.INTRODUCTION

The main purpose of this paper is to develop a novel method to achieve adaptive optimal stabilization of nonlinear system via online learning. As the first contribution of this paper, an optimization problem is proposed to relax the Hamilton-Jacobi-Bellman (HJB) equation. The second contribution of the paper is an online learning method that implements the proposed iterative schemes using only the real-time online measurements, when the perfect system knowledge is not available. The final contribution of this paper is the Robust Design of the approximate suboptimal control policy, such that the overall system can be globally asymptotically stable in the presence of dynamic uncertainties.

2. PROBLEM FORMULATION AND PRELIMINARIES

In this section, we first formulate the control problem [16][17]. Then, we introduce conventional policy iteration algorithm.

2.1 Problem formulation

Consider the nonlinear system

$$\dot{x}/dt = f(x) + g(x)u \quad (1.1)$$

where,

x is the system state,

u is the control input,

$f(x)$ and $g(x)$ are locally Lipschitz functions with $f(0) = 0$.

In conventional optimal control theory [1], the common objective is to find a control policy u that minimizes certain performance index. In this chapter, it is specified as follows.

$$J(x_0; u) = \int_0^\infty r(x(t), u(t))dt; \quad x(0) = x_0 \quad (1.2)$$

where,

$r(x, u) = Q(x) + u^T R u$, with $Q(x)$ a positive definite function, and R is a symmetric positive definite matrix.

2.2 Optimality and stability

Here, we recall a basic result connecting optimality and global asymptotic stability in nonlinear systems [2]. To begin with, let us give the following assumption.

Assumption 2.1.2. There exists $V^0 \in P$, such that the Hamilton-Jacobi-Bellman (HJB) equation holds [16]

$$H(V^0) = 0 \quad (1.3)$$

Where,

$$H(V) = \nabla V^T(x)f(x) + Q(x) - (1/4)\nabla V^T(x)g(x)R^{-1}g^T(x)\nabla V(x)$$

Under Assumption 2.1.2, it is easy to see that V^0 is a well-defined Lyapunov function for the closed-loop system comprised of (1.1) and

$$u^0(x) = -\frac{1}{2}R^{-1}g^T(x)\nabla V^0(x) \quad (1.4)$$

Hence, this closed-loop system is globally asymptotically stable at $x = 0$ [3]. Then, according to [2], u^0 is the optimal control policy, and the value function $V^0(x_0)$ gives the optimal cost at the initial condition $x(0) = x_0$, i.e.,

$$V^0(x_0) = \min_u J(x_0, u) = J(x_0, u^0), \quad \forall x_0 \in \mathbb{R}^n \quad (1.5)$$

By Theorem 3.19 in [2], along the solutions of the closed-loop system composed of (1.1) and $u = \hat{u} = -\frac{1}{2}R^{-1}g^T\nabla\hat{V}$, it follows that $\hat{V}(x_0) = V^0(x_0) - \int_0^\infty \|u^0 - \hat{u}\|_R^2 dt$, $\forall x_0 \in \mathbb{R}^n$ (1.6)

Finally, comparing (1.5) and (1.6), we conclude that $V^0 = \hat{V}$.

Algorithm 2.1.1 Conventional policy iteration:

1. Policy evaluation: For $i = 1; 2; \dots$, solve for the cost function $V_i(x) \in \mathbb{C}^1$, with $V_i(0) = 0$, from the following partial differential equation.

$$\mathcal{L}(V_i(x), u_i(x)) = 0. \quad (1.7)$$

2. Policy improvement: Update the control policy by

$$u_{i+1}(x) = -\frac{1}{2} R^{-1} g^T(x) \nabla V_i(x) \quad (1.8)$$

The following result is a trivial extension of [4, Theorem 4], in which $g(x)$ is a constant matrix and only stabilization over compact set is considered.

Notice that finding the analytical solution to (1.7) is still non-trivial. Hence, in practice, the solution is approximated using, for example, neural networks or Galerkin's method [5]. When the precise knowledge of f or g is not available, ADP based online approximation method can be applied to compute numerically the cost functions via online data [6], [7].

In general, approximation methods can only give acceptable results on some compact set in the state space, but cannot be used to achieve global stabilization. In addition, in order to reduce the approximation error, huge computational complexity is almost inevitable. These facts may affect the effectiveness of the previously developed ADP-based online learning methods.

2.3. Semidefinite Programming (SDP)

According to the equivalence between SOS programs and SDPs, the SOS-based policy iteration can be reformulated as SDPs [16] [17]. Notice that we can always find two linear mappings $\mathbf{u} : \mathbb{R}^{n_{2r}} \times \mathbb{R}^{m \times n_r} \rightarrow \mathbb{R}^{n_{2d}}$ and $\mathbf{x} : \mathbb{R}^{n_{2r}} \rightarrow \mathbb{R}^{m \times n_r}$, such that given $p \in \mathbb{R}^{n_{2r}}$ and $k \in \mathbb{R}^{m \times n_r}$,

$$\mathbf{u}(p, k)^T [x]_{2,2d} = \mathcal{L}(p^T [x]_{2,2r}, k [x]_{1,2r-1}) \quad (1.9)$$

$$\mathbf{x}(p, k)^T [x]_{1,2r-1} = -\frac{1}{2} R^{-1} g^T \nabla (p^T [x]_{2,2r}) \quad (1.10)$$

Then, by properties of SOS constraints [8], the polynomial $\mathbf{u}(p, k)^T [x]_{2,2d}$ is SOS if and only if there exists a symmetric and positive semidefinite matrix $L \in \mathbb{R}^{n_d \times n_d}$, such that

$$\mathbf{u}(p, k)^T [x]_{2,2d} = [x]_{1,d}^T L [x]_{1,d} \quad (1.11)$$

Furthermore, there exist linear mappings $M_P : \mathbb{R}^{n_r \times n_r} \rightarrow \mathbb{R}^{n_{2r}}$ and $M_L : \mathbb{R}^{n_d \times n_d} \rightarrow \mathbb{R}^{n_{2d}}$, such that, for any vectors $p \in \mathbb{R}^{n_{2r}}$, $l \in \mathbb{R}^{n_{2d}}$, and symmetric matrices $P \in \mathbb{R}^{n_r \times n_r}$ and $L \in \mathbb{R}^{n_d \times n_d}$, the following implications are true.

$$p^T [x]_{2,2r} = [x]_{1,r}^T P [x]_{1,r} \Leftrightarrow p = M_P(P) \quad (1.12)$$

$$l^T [x]_{2,2d} = [x]_{1,d}^T L [x]_{1,d} \Leftrightarrow l = M_L(L) \quad (1.13)$$

using above assumptions policy iteration can be reformulated as follows.

Algorithm 2.2.1 SDP-based policy iteration:

1. Let $i = 1$. Let $p_0 \in \mathbb{R}^{n_{2r}}$ and $K_1 \in \mathbb{R}^{m \times n_d}$ satisfy $V_0 = p_0^T [x]_{2,2r}$ and $u_1 = K_1 [x]_{1,d}$.

2. Solve for an optimal solution $(p_i; P_i; L_i) \in \mathbb{R}^{n_{2r}} \times \mathbb{R}^{n_r \times n_r} \times \mathbb{R}^{n_d \times n_d}$ to the following problem.

$$\min_{p, P, L} c^T p \quad (1.14)$$

$$\text{s.t. } \mathbf{u}(p, k_i) = M_L(L) \quad (1.15)$$

$$p_{i-1} - p = M_P(P) \quad (1.16)$$

$$P = P^T \geq 0 \quad (1.17)$$

$$L = L^T \geq 0 \quad (1.18)$$

where $c = \int s(x) [x]_{2,2r} dx$.

3: Go to Step 2 with $k_{i+1} = \mathbf{x}(p_i)$ and i replaced by $i+1$.

3. ONLINE LEARNING VIA GLOBAL ADAPTIVE DYNAMIC PROGRAMMING

The proposed policy iteration method requires the perfect knowledge of the mappings \mathbf{u} and \mathbf{x} , which can be determined if f and g are known exactly. In practice, precise system knowledge may be difficult to obtain. Hence, in this section, we develop an online learning method based on the idea of ADP to implement the iterative scheme with real-time data, instead of identifying the system dynamics. To begin with, consider the system

$$\dot{\mathbf{x}} = f + g(u_i + e) \quad (1.19)$$

where u_i is a feedback control policy and e is a bounded time-varying function, known as the exploration noise, added for the learning purpose.

Lemma 3.1.1. Consider system (1.19). Suppose u_i is a globally stabilizing control policy and there exists $V_{i-1} \in \mathcal{P}$, such that

$$\nabla V_{i-1}(f + gu_i) + u_i^T R u_i \leq 0.$$

Then, by completing the squares, it follows that

$$\nabla V_{i-1}(f + gu_i + ge) \leq -u_i^T R u_i - 2u_i^T R e$$

$$= -|u_i + e|_R^2 + |e|_R^2$$

$$\leq |e|_R^2$$

$$\leq |e|_R^2 + V_{i-1}$$

Suppose there exist $p \in \mathbb{R}^{n_{2r}}$ and $k_i \in \mathbb{R}^{m \times n_r}$ such that $V = p^T [x]_{2,2r}$ and $u_i = k_i [x]_{1,d}$. Then, along the solutions of the system (1.19), it follows that

$$\begin{aligned} \dot{V} &= \nabla V^T (f + gu_i) + \nabla V^T B e \\ &= -r(x, u_i) - \mathcal{L}(V, u_i) + \nabla V^T g e \\ &= -r(x, u_i) - \mathcal{L}(V, u_i) + 2(1/2 R^{-1} g^T \nabla V)^T R e \\ &= -r(x, u_i) - \mathbf{u}(p, k_i)^T [x]_{2,2d} - 2[x]_{1,d}^T \mathbf{x}(p)^T R e \end{aligned} \quad (1.20)$$

where the last row is obtained by (1.9) and (1.10).

Now, integrating the terms in (1.52) over the interval $[t, t + \delta t]$, we have

$$\begin{aligned} p^T ([x(t)]_{2,2r} - [x(t + \delta t)]_{2,2r}) \\ = \int_t^{t+\delta t} [r(x, u_i) + \mathbf{u}(p, k_i)^T [x] + 2[x]_{1,d}^T \mathbf{x}(p)^T R e] dt \end{aligned} \quad (1.21)$$

Eq. (1.21) implies that, given $p \in \mathbb{R}^{n_{2r}}$, $\mathbf{u}(p, k_i)$ and $\mathbf{x}(p)$ can be directly calculated by using real-time online data, without knowing the precise knowledge of f and g .

Indeed, define

$$\sigma_e = -[[x]_{2,2d}^T \quad 2[x]_{1,d}^T e^T R]^T \in \mathbb{R}^{n_{2d} + mn_d},$$

$$\Phi_i = [\int_{t_0,i}^{t_{1,i}} \sigma_e dt \int_{t_{1,i}}^{t_{2,i}} \sigma_e dt \dots \int_{t_{q_i-1,i}}^{t_{q_i,i}} \sigma_e dt]^T \in \mathbb{R}^{q_i(n_{2d} + mn_d)}$$

$$\Xi_i = [\int_{t_0,i}^{t_{1,i}} r(x, u_i) dt \int_{t_{1,i}}^{t_{2,i}} r(x, u_i) dt \dots \int_{t_{q_i-1,i}}^{t_{q_i,i}} r(x, u_i) dt]^T \in \mathbb{R}^{q_i},$$

$$\Theta_i = [[x]_{2,2r} |_{t_0,i}^{t_{1,i}} \dots [x]_{2,2r} |_{t_{q_i-1,i}}^{t_{q_i,i}}]^T \in \mathbb{R}^{q_i \times n_{2r}};$$

Then, (1.21) implies

$$\Phi_i \begin{bmatrix} i(p, k_i) \\ \text{vec}(x(p)) \end{bmatrix} = \Xi_i + \Theta_i p. \quad (1.22)$$

Assumption 3.1.2. For each $i = 1; 2; \dots$, there exists an integer q_{i0} , such that when $q_i \geq q_{i0}$ the following rank condition holds.

$$\text{rank}(\Phi_i) = n_{2d} + m n_d. \quad (1.23)$$

Remark 3.1.2. Such a rank condition (1.23) is in the spirit of persistency of excitation (PE) in adaptive control and is a necessary condition for parameter convergence.

Given $p \in \mathbb{R}^{n_{2r}}$ and $k_i \in \mathbb{R}^{m \times n_d}$, suppose Assumption 3.1.2. is satisfied and $q_i \geq q_{i0}$ for all $i = 1, 2, \dots$. Then, it is easy to see that the values of $i(p, k_i)$ and $x(p)$ can be uniquely determined from

$$\begin{bmatrix} i(p, k_i) \\ \text{vec}(x(p)) \end{bmatrix} = (\Phi_i^T \Phi_i)^{-1} \Phi_i^T (\Xi_i + \Theta_i p) \quad (1.24)$$

Now, we are ready to develop the ADP-based online implementation algorithm for the proposed policy iteration method.

Algorithm 3.1.4. Global adaptive dynamic programming algorithm

1: Initialization: Let p_0 be the constant vector such that $V_0 = p_0^T [x]_{2,2r}$, and let $i = 1$.

2: Collect online data: Apply $u = u_i + e$ to the system and compute the data matrices Φ_i , Ξ_i , and Θ_i , until the rank condition (1.23) in Assumption 3.1.2 is satisfied.

3: Policy evaluation and improvement: Find an optimal solution (p_i, k_{i+1}, P_i, L_i) to the following optimization problem

$$\min_{p, k, P, L} c^T p \quad (1.25)$$

$$\text{s.t: } \begin{bmatrix} ML(L) \\ \text{vec}(k) \end{bmatrix} = (\Phi_i^T \Phi_i)^{-1} \Phi_i^T (\Xi_i + \Theta_i p) \quad (1.26)$$

$$p_{i-1} - p = M_P(P) \quad (1.27)$$

$$P = P^T \geq 0 \quad (1.28)$$

$$L = L^T \geq 0 \quad (1.29)$$

Then, denote $V_i = p_i^T [x]_{2,2r}$, $u_{i+1} = k_{i+1} [x]_{1,d}$, and go to Step 2) with $i \leftarrow i + 1$.

4. ONLINE IMPLEMENTATION VIA GLOBAL ADAPTIVE DYNAMIC PROGRAMMING

Let $V = p^T \bar{\mathcal{O}}$. Similar as in Section above, over the interval $[t, t + \delta t]$, we have

$$p^T [\bar{\mathcal{O}}(x(t)) - \bar{\mathcal{O}}(x(t + \delta t))] = \int_t^{t+\delta t} [r(x, u_i) + \bar{i}(p, k_i)^T \bar{\sigma} + 2\bar{\sigma} \bar{x}(p)^T \text{Re}] dt \quad (1.30)$$

Therefore, (1.30) shows that, given $p \in \mathbb{R}^{n_1}$, $\bar{i}(p, k_i)$ and $\bar{x}(p)$ can be directly obtained by using real-time online data, without knowing the precise knowledge of f and g .

Indeed, define [17]

$$\bar{\sigma}_e = -[\bar{\sigma}^T 2\sigma^T \otimes e^T R]^T \in \mathbb{R}^{l_1+m_l},$$

$$\bar{\Phi}_i = [\int_{t_{0,i}}^{t_{1,i}} \bar{\sigma}_e dt \int_{t_{1,i}}^{t_{2,i}} \bar{\sigma}_e dt \dots \int_{t_{q_i-1,i}}^{t_{q_i,i}} \bar{\sigma}_e dt]^T \in \mathbb{R}^{q_i \times (l_1+m_l)},$$

$$\bar{\Xi}_i = [\int_{t_{0,i}}^{t_{1,i}} r(x, u_i) dt \int_{t_{1,i}}^{t_{2,i}} r(x, u_i) dt \dots \int_{t_{q_i-1,i}}^{t_{q_i,i}} r(x, u_i) dt]^T \in \mathbb{R}^{q_i},$$

$$\bar{\Theta}_i = [\bar{\mathcal{O}}(x) | t_{1,i,t_{0,i}} [\bar{\mathcal{O}}(x) | t_{2,i,t_{1,i}} \dots]^T \in \mathbb{R}^{q_i \times N_1}$$

Then, (1.30) implies

$$\bar{\Phi}_i \begin{bmatrix} \bar{i}(p, k_i) \\ \text{vec}(\bar{x}(p)) \end{bmatrix} = \bar{\Xi}_i + \bar{\Theta}_i p. \quad (1.31)$$

Assumption 4.1.1. For each $i = 1; 2; \dots$, there exists an integer q_{i0} , such that, when $q_i \geq q_{i0}$, the following rank condition holds.

$$\text{rank}(\bar{\Phi}_i) = l_1 + m_l. \quad (1.32)$$

Let $p \in \mathbb{R}^{N_1}$ and $k_i \in \mathbb{R}^{m \times l}$. Suppose Assumption 4.1.1 holds and assume $q_i \geq q_{i0}$, for $i = 1, 2, \dots$. Then, $\bar{i}(p, k_i)$ and $\bar{x}(p)$ can be uniquely determined by

$$\begin{bmatrix} h \\ \text{vec}(k) \end{bmatrix} = (\bar{\Phi}_i^T \bar{\Phi}_i)^{-1} \bar{\Phi}_i^T (\bar{\Xi}_i + \bar{\Theta}_i p) \quad (1.33)$$

Now, we are ready to develop the ADP-based online implementation algorithm for the proposed policy iteration method.

Algorithm 4.1.2 Global adaptive dynamic programming algorithm for non-polynomial systems

1: Initialization: Let p_0 and k_1 satisfying $V_0 = p_0^T \bar{\mathcal{O}}$, $u_1 = k_1 \sigma$, and $\mathcal{L}(V_0, u_1)$ and let $i = 1$.

2: Collect online data: Apply $u = u_i + e$ to the system and compute the data matrices $\bar{\Phi}_i$, $\bar{\Xi}_i$, and $\bar{\Theta}_i$, until the rank condition (1.32) is satisfied.

3: Policy evaluation and improvement: Find an optimal solution (p_i, h_i, K_{i+1}) to the following optimization problem

$$\min_{p, h, k} c^T p \quad (1.34)$$

$$\text{s.t: } \begin{bmatrix} h \\ \text{vec}(k) \end{bmatrix} = (\bar{\Phi}_i^T \bar{\Phi}_i)^{-1} \bar{\Phi}_i^T (\bar{\Xi}_i + \bar{\Theta}_i p) \quad (1.35)$$

$$h \in S^+ \sigma \quad (1.36)$$

$$p_{i-1} - p \in S^+ \bar{\mathcal{O}} \quad (1.37)$$

Then, denote $V_i = p_i \bar{\mathcal{O}}$ and $u_{i+1} = k_{i+1} \bar{\sigma}$.

4: Go to Step 2) with $i \leftarrow i + 1$.

5. ROBUST REDESIGN

Consider nonlinear system with dynamic uncertainties as follows [17]

$$\dot{w} = q(w, x) \quad (1.38)$$

$$\dot{x} = f(x) + g(x) [u + \Delta(w, x)] \quad (1.39)$$

where $x \in \mathbb{R}^n$ is the system state, $w \in \mathbb{R}^{n_w}$ is the state of the dynamic uncertainty, $u \in \mathbb{R}^m$ is the control input, $f: \mathbb{R}^n \rightarrow \mathbb{R}^n$ and $g: \mathbb{R}^n \rightarrow \mathbb{R}^{n \times m}$ are unknown polynomial mappings with $f(0) = 0$.

Again, in the presence of the dynamic uncertainty, i.e. the w -subsystem, Algorithm 4.1.2. may not lead to an optimal or suboptimal control policy, since u_i obtained in Algorithm 4.1.2. may not be stabilizing for the overall system (1.38)-(1.39). Therefore, to balance the tradeoff between global

robust stability and optimality, here we develop a method to redesign the control policy. Similarly as in the previous chapter, the idea is inspired from the work by [9, 10].

To begin with, we define the cost functional as

$$\min J(x_0, u) = \int_0^\infty [Q(x) + u^T R u] dt, \quad (1.40)$$

where $Q(x) = Q_0(x) + \varepsilon \|x\|^2$, with $Q_0(x)$ is a positive definite function, $\varepsilon > 0$ is a constant, R is a symmetric and positive definite matrix.

Our design objective is twofold. First, we intend to minimize the cost (1.40) for the nominal system

$$\dot{x} = f(x) + g(x)u, \quad (1.41)$$

by finding online an optimal control policy u_0 . Second, we want to guarantee the stability of the system comprised of (1.38) and (1.39) by redesigning the optimal control policy. To this end, let us introduce the following Assumption.

Assumption 5.1.1. Consider the system comprised of (1.38) and (1.39).

There exist functions $\underline{\lambda}, \bar{\lambda} \in \mathcal{K}\infty$, $\kappa_1, \kappa_2, \kappa_3 \in \mathcal{K}$, and positive definite functions W and κ_4 , such that for all $w \in \mathbb{R}^p$ and $x \in \mathbb{R}^n$, we have

$$\underline{\lambda}(\|w\|) \leq W(w) \leq \bar{\lambda}(\|w\|), \quad (1.42)$$

$$\|\Delta(w, x)\| \leq \kappa_1(\|w\|) + \kappa_2(\|x\|), \quad (1.43)$$

together with the following implication:

$$W(w) \geq \kappa_3(\|x\|) \Rightarrow \nabla W(w)^T q(w, x) \leq -\kappa_4(w). \quad (1.44)$$

Assumption 5.1.1 implies that the w -system (1.38) is input-to-state stable (ISS) [11, 12] when x is considered as the input.

Let $V_i \in \mathcal{P}$ and u_i be the cost function and the control policy obtained from Algorithm 4.1.2. Then, we know that $\mathcal{L}(V_i, u_i) \geq 0$. Also, there exist $\underline{\alpha}, \bar{\alpha} \in \mathcal{K}\infty$, such that the following inequalities hold:

$$\underline{\alpha}(\|x\|) \leq V^0(x) \leq V_i(x) \leq V_0(x) \leq \bar{\alpha}(\|x\|), \forall x_0 \in \mathbb{R}^n; \quad (1.45)$$

The robustly redesigned control policy is given below:

$$u_{r,i} = \rho^2(\|x\|)u_i + e \quad (1.46)$$

where $\rho(\cdot)$ is a smooth and no decreasing function with $\rho(s) \geq 1, \forall s > 0$, e denotes the time varying exploration noise added for the purpose of online learning.

Theorem 5.1.2. Consider the closed-loop system comprised of (1.38), (1.39), and (1.46). Let $V_i \in \mathcal{P}$ and u_i be the cost function and the control policy obtained from Algorithm 4.1.2 at the i -th iteration step. Then, the closed-loop system is ISS with respect to e as the input, if the following gain condition holds:

$$\gamma > \kappa_1 \circ \underline{\lambda}^{-1} \circ \kappa_3 \circ \underline{\alpha}^{-1} \circ \bar{\alpha} + \kappa_2, \quad (1.47)$$

where is defined by

$$\gamma(s) = \varepsilon s \sqrt{\frac{\frac{1}{2} + \frac{1}{2}\rho^2(s^2)}{\lambda_{\min}(R)}} \quad (1.48)$$

Proof. Let $\chi_1 = \kappa_3 \circ \underline{\alpha}^{-1}$. Then, under Assumption 5.1.1, we immediately have the following implications

$$W(w) \geq \chi_1(V_i(x))$$

$$\Rightarrow W(w) \geq \kappa_3(\underline{\alpha}^{-1}(V_i(x))) \geq \kappa_3(\|x\|)$$

$$\Rightarrow \nabla W(w)^T q(w, x) \leq -\kappa_4(w) \quad (1.49)$$

Define $\bar{\rho}(x) = \sqrt{\frac{\frac{1}{2} + \frac{1}{2}\rho^2(s^2)}{\lambda_{\min}(R)}}$. Then, along solutions of the system

comprised of (1.39), it follows that

$$\nabla V_i^T [f + g(u_{r,i} + \Delta)]$$

$$\leq -Q(x) - \|u_i\|_R^2 + \nabla V_i^T g[(\rho^2(\|x\|)^2 - 1)u_i + \Delta + e]$$

$$\leq -Q(x) - \bar{\rho}^2 \|g^T \nabla V_i\|^2 + \nabla V_i^T g(\Delta + e)$$

$$\leq -Q(x) - \|\bar{\rho} g^T \nabla V_i - \frac{1}{2} \bar{\rho}^{-1} \Delta\|^2 n + \frac{1}{4} \bar{\rho}^{-2} \|\Delta + e\|^2$$

$$\leq -Q_0(x) - \varepsilon^2 \|x\|^2 + \bar{\rho}^2 \Delta \max\{\|\Delta\|^2, \|e\|^2\}$$

$$\leq -Q_0(x) - \bar{\rho}^{-2} (\gamma^2 - \max\{\|\Delta\|^2, \|e\|^2\})$$

Hence, by defining $\chi_2 = \bar{\alpha} \circ (\gamma - \kappa_2)^{-1} \circ \kappa_1 \circ \underline{\lambda}^{-1}$, it follows that

$$V_i(x) \geq \max\{\chi_2(W(w)), \bar{\alpha} \circ (\gamma - \kappa_2)^{-1}(\|e\|)\},$$

$$\Leftrightarrow V_i(x) \geq \bar{\alpha} \circ (\gamma - \kappa_2)^{-1} \circ \max\{\kappa_1 \circ \underline{\lambda}^{-1}(W(w)), \|e\|\}$$

$$\Rightarrow (\gamma - \kappa_2) \circ \bar{\alpha}^{-1}(V_i(x)) \geq \max\{\kappa_1 \circ \underline{\lambda}^{-1}(W(w)), \|e\|\}$$

$$\Rightarrow \gamma(\|x\|) - \kappa_2 \|x\| \geq \max\{\kappa_1 \circ \underline{\lambda}^{-1}(W(w)), \|e\|\}$$

$$\Rightarrow \gamma(\|x\|) - \kappa_2 \|x\| \geq \max\{\kappa_1 \|w\|, \|e\|\}$$

$$\Rightarrow \gamma(\|x\|) \geq \max\{\|\Delta(w, x)\|, \|e\|\}$$

$$\Rightarrow \nabla V_i^T [f + g(u_{r,i+1}, \Delta)] \leq -Q_0(x) \quad (1.50)$$

Finally, by the gain condition, we have

$$\gamma > \kappa_1 \circ \underline{\lambda}^{-1} \circ \kappa_3 \circ \underline{\alpha}^{-1} \circ \bar{\alpha} + \kappa_2$$

$$\Rightarrow Id > (\gamma - \kappa_2)^{-1} \circ \kappa_1 \circ \underline{\lambda}^{-1} \circ \kappa_3 \circ \underline{\alpha}^{-1} \circ \bar{\alpha}$$

$$\Rightarrow Id > \bar{\alpha} \circ (\gamma - \kappa_2)^{-1} \circ \kappa_1 \circ \underline{\lambda}^{-1} \circ \kappa_3 \circ \underline{\alpha}^{-1} \circ \bar{\alpha}$$

$$\Rightarrow Id > \chi_2 \circ \chi_1 \quad (1.51)$$

The proof is thus completed by the small-gain theorem [13].

Similarly as in the previous section, along the solution of the system (1.39) and (1.46), it follows that

$$\begin{aligned} \dot{V} &= \nabla V^T (f + g u_{r,i}) \\ &= \nabla V^T (f + g u_i) + \nabla V^T g \tilde{e} \\ &= -r(x, u_i) - \mathcal{L}(V, u_i) + \nabla V^T g \tilde{e} \\ &= -r(x, u_i) - \mathcal{L}(V, u_i) + 2 \left(\frac{1}{2} R^{-1} g^T \beta \nabla V \right)^T R \tilde{e} \\ &= -r(x, u_i) - \iota(p, k_i)^T [x]_{2,2d} - 2 [x]_{1,d}^T \kappa(p)^T R \tilde{e} \end{aligned} \quad (1.52)$$

where $\tilde{e} = \rho^2(\|x\|)^{-1}$.

Therefore, we can redefine the data matrices as follows. Indeed, define

$$\bar{\sigma}_e = -[\bar{\sigma}^T 2\sigma^T \otimes e^T R]^T \in \mathbb{R}^{l_1 + ml},$$

$$\bar{\Phi}_i = [\int_{t_0,i}^{t_{1,i}} \bar{\sigma}_e dt \int_{t_{1,i}}^{t_{2,i}} \bar{\sigma}_e dt \dots \int_{t_{q_i-1,i}}^{t_{q_i,i}} \bar{\sigma}_e dt]^T \in \mathbb{R}^{q_i \times (l_1 + ml)},$$

$$\bar{\Xi}_i = [\int_{t_0,i}^{t_{1,i}} r(x, u_i) dt \int_{t_{1,i}}^{t_{2,i}} r(x, u_i) dt \dots \int_{t_{q_i-1,i}}^{t_{q_i,i}} r(x, u_i) dt]^T \in \mathbb{R}^{q_i},$$

$$\bar{\Theta}_i = [\bar{\Theta}(x) |_{t_0,i} \bar{\Theta}(x) |_{t_{1,i}} \dots]^T \in \mathbb{R}^{q_i \times N_1}$$

Then, the global robust adaptive dynamic programming algorithm is given below.

Algorithm 5.1.3. The global robust adaptive dynamic programming algorithm

1: Initialization: Let p_0 and k_1 satisfying $V_0 = p_0^T \bar{\theta}$, $u_1 = k_1 \sigma$, and $\mathcal{L}(V_0, u_1)$, and let $i = 1$.

2: Collect online data: Apply $u = u_{r,i} = \rho^2(|x|^2)u_i + e$ to the system and compute the data matrices Φ_i , Ξ_i , and Θ_i until the rank condition in Assumption 4.1.1, is satisfied.

3: Policy evaluation and improvement: Find an optimal solution (p_i, h_i, k_{i+1}) to the following optimization problem

$$\min_{p, h, k} c^T p \quad (1.53)$$

$$\text{s.t: } \begin{bmatrix} h \\ \text{vec}(k) \end{bmatrix} = (\bar{\Phi}_i^T \bar{\Phi}_i)^{-1} \bar{\Phi}_i^T (\bar{\Xi}_i + \bar{\Theta}_i p) \quad (1.54)$$

$$h \in S^+ \sigma \quad (1.55)$$

$$p_{i-1} - p \in S^+ \bar{\theta} \quad (1.56)$$

Then, denote $V_i = p_i^T \bar{\theta}$ and $u_{i+1} = k_{i+1} \bar{\sigma}$.

4: Go to Step 2) with $i \leftarrow i + 1$.

6. NUMERICAL EXAMPLE

This section provides a numerical example to illustrate the effectiveness of the proposed algorithms[17].

6.1 Jet engine dynamics

Consider the following system, which is inspired by the jet engine surge and stall dynamics in [14, 15]

$$\dot{x} = -ax^2 - ax(2y + y^2) \quad (1.57)$$

$$\dot{y} = -by^2 - cy^3 - (u + 3xy + 3x) \quad (1.58)$$

where $x > 0$ is the normalized rotating stall amplitude, y is the deviation of the scaled annulus-averaged flow, u is the deviation of the plenum pressure rise and is treated as the control input, $a \in [0.2, 0.5]$, $b \in [1.2, 1.6]$, $c \in [0.3, 0.7]$ are uncertain constants.

In this example, we assume the variable x is not available for real-time feedback control due to a 0.2s time-delay in measuring it. Hence, the objective is to find a control policy that only relies on y . The cost function we used here is

$$J = \int_0^\infty (5y^2 + u^2) dt \quad (1.59)$$

and an initial control policy is chosen as

$$u_{r,1} = \frac{1}{2} \rho^2(y^2)(2p - 1.47p^2 - 0.45x^3) \quad (1.60)$$

with $\rho(s) = \sqrt{2}$.

Only for the purpose of simulation, we set $a = 0.3$, $b = 1.5$, and $c = 0.5$. The control policy is updated every 0.25s. The simulation results are provided in Chart 1 and chart 2. It can be seen that the system performance has been improved via online learning.

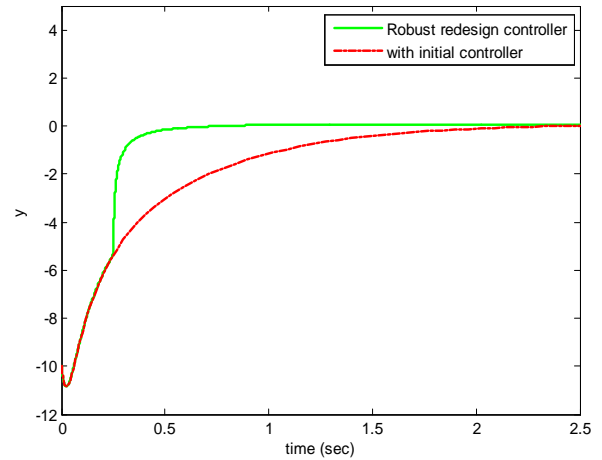


Chart -1: Simulation of the jet engine: Trajectories of y

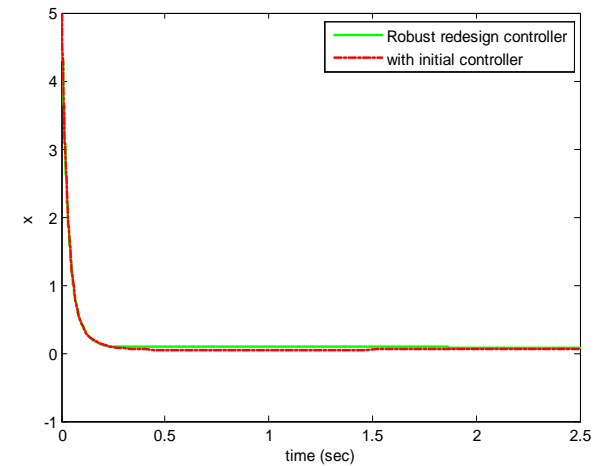


Chart -2: Simulation of the jet engine: Trajectories of x

8. CONCLUSIONS

This paper has proposed a Novel method of dynamic programming for the adaptive optimal control of nonlinear systems. In particular, a new policy iteration scheme has been developed. Different from conventional policy iteration, the new iterative technique does not attempt to solve a partial differential equation but a convex optimization problem at each iteration step.

It has been shown that, this method can find a suboptimal solution to continuous-time nonlinear optimal control problems [1]. In addition, the resultant control policy is globally stabilizing. In the presence of dynamic uncertainties, robustification of the proposed algorithms and their online implementations has been addressed, by integration with the ISS property [11, 12] and the nonlinear small-gain theorem [9, 13]. When the system parameters are unknown, conventional ADP methods utilize neural networks to approximate online the optimal solution, and a large number of basis functions are required to assure high approximation accuracy on some compact sets. Thus, neural-network-based

ADP schemes may result in slow convergence and loss of global asymptotic stability for the closed-loop system. Here, the proposed method has overcome the two above-mentioned shortcomings, and it yields computational benefits.

REFERENCES

- [1] F.L. Lewis, D. Vrabie, and V.L.Syrmos. Optimal Control, 3rd ed. Wiley, New York, 2012.
- [2] R. Sepulchre, M. Jankovic, and P. Kokotovic. Constructive Nonlinear Control. Springer Verlag, New York, 1997.
- [3] H. K. Khalil. Nonlinear Systems, 3rd Edition. Prentice Hall, Upper Saddle River, NJ, 2002.
- [4] G.N. Saridis and C. S. G. Lee. An approximation theory of optimal control for trainable manipulators. IEEE Transactions on Systems, Man and Cybernetics, 9(3):152-159, 1979.
- [5] R. W. Beard, G. N. Saridis, and J. T. Wen. Galerkin approximations of the generalized Hamilton-Jacobi-Bellman equation. Automatica, 33(12):2159-2177, 1997.
- [6] D. Vrabie and F.L. Lewis. Neural network approach to continuous-time direct adaptive optimal control for partially unknown nonlinear systems. Neural Networks, 22(3):237-246, 2009.
- [7] Y. Jiang and Z. P. Jiang. Robust adaptive dynamic programming and feedback stabilization of nonlinear systems. IEEE Transactions on Neural Networks and Learning Systems, 25(5):882-893, 2014
- [8] G. Blekherman, P. A. Parrilo, and R. R. Thomas, editors. Semidefinite Optimization and Convex Algebraic Geometry. SIAM, Philadelphia, PA, 2013.
- [9] Z. P. Jiang, A. R. Teel, and L. Praly. Small-gain theorem for ISS systems and applications. Mathematics of Control, Signals and Systems, 7(2):95-120, 1994.
- [10] L. Praly and Y. Wang. Stabilization in spite of matched unmodeled dynamics and an equivalent definition of input-to-state stability. Mathematics of Control, Signals and Systems, 9(1):1-33, 1996.
- [11] E. D. Sontag. Smooth stabilization implies coprime factorization. IEEE Transactions on Automatic Control, 35(4):473-476, 1990.
- [12] E. D. Sontag and Y. Wang. On characterizations of the input-to-state stability property. Systems and Control Letters, 24(5):351-359, 1995.
- [13] Z. P. Jiang, I. M. Mareels, and Y. Wang. A Lyapunov formulation of the nonlinear small-gain theorem for interconnected ISS systems. Automatica, 32(8):1211-1215, 1996.
- [14] M. Krstic, D. Fontaine, P. V. Kokotovic, and J. D. Paduano. Useful nonlinearities and global stabilization of bifurcations in a model of jet engine surge and stall. IEEE Transactions on Automatic Control, 43(12):1739-1745, 1998.
- [15] F. Moore and E. Greitzer. A theory of post-stall transients in axial compression systems: Part 1 development of equations. Journal of engineering for gas turbine and power, 108(1):68-76, 1986.
- [16] Y. Jiang and Z. P. Jiang. Global adaptive dynamic programming for continuous time nonlinear systems.

IEEE Transactions on Automatic Control, vol 60, No. 11, November 2015.

- [17] Y. Jiang. Robust Adaptive Dynamic Programming for Continuous-Time Linear and Nonlinear Systems. Phd Thesis, UMI Dissertation Publishing, ProQuest CSA, 789 E. Eisenhower Parkway.



“Mr. Desai Feroz was born in India, in 1989. He obtained the BTech degree in EIE from JNTU, Hyderabad. Currently, he is a final year MTech candidate working in Control and Simulation Lab (CS lab) at Mallareddy Engineering College, Hyderabad, Telangana, India.”



“Mrs. M. Lakshmiswarupa, Associate Professor & HOD, M.Tech (Phd), LMISTE, MIEEE, currently is the HOD of EEE department in Mallareddy engineering college. She has published 10 papers in international journals and 15 papers in international conferences.”

**Department of
Mechanical Engineering**

Effect of Pulsed and Non-pulsed current on welding characteristics of AA6061 Aluminium alloy welded joints using Tig welding

B. Akshay Kumar¹, A. Raveendra²

¹M.Tech Scholar, Department of Mechanical Engineering, Mallareddy Engineering College (Autonomous), Secunderabad, India

²Associate Professor, Department of Mechanical Engineering, Mallareddy Engineering College (Autonomous), Secunderabad, India

Abstract— In this experimental work tests were conducted on the weldments of AA6061 aluminium alloy using TIG/GTAW with pulsed current at constant frequency of 6HZ and non-pulsed current on 3mm thick sheets. Destructive and non-destructive tests like Hardness test, tensile test, microstructure, radiography and liquid penetrate tests conducted, evaluated and compared with pulsed and non-pulsed current welding. Aim of the experimental work is to see the effect of pulsed current on characteristics of weldments. The experimental results pertaining to different welding parameters for the above material using pulsed and non-pulsed current GTAW are discussed and compared.

Keywords— AA6061, Tungsten Inert Gas Welding/Gas Tungsten Arc Welding, Pulsed current, Non-pulsed current, Heat Affected Zone

I. INTRODUCTION

Reduction of mass is a prime concern for many industries like the automobile industry, aerospace applications; hence the focus on light materials like aluminium has become predominant. The demand is increasing for aluminium alloy welded products where high quality is required. Aluminium alloy can be welded easily by conventional arc welding methods like Metal Inert Gas Welding (MIGW) and Tungsten Inert Gas Welding (TIGW/GTAW). Among these two methods, The Gas Tungsten Arc Welding (GTAW) process has proved for many years to be suitable for welding aluminum alloy since it gives best quality welds. GTAW process (AC) is used in this study for welding of AA6061 aluminium alloy.

Further development has been Pulsed current GTA welding, developed in 1950s, is a variation of GTA welding which involves cycling of the welding current from a high level to a low level at a selected regular frequency. The high level of peak current is generally selected to give adequate penetration and bead contour, while the low level of background current is set at a level sufficient to maintain stable arc. Pulsed current welding process has many advantages over non-pulsed current (constant current) welding, including enhanced arc stability, increased weld depth/width ratio, narrower HAZ range, reduced hot cracking sensitivity, refined grain size, reduced porosity, low heat input, lower distortion of gas by weld pool and better control of the fusion zone. All these factors will help to improve mechanical properties. Pulsed current welding technology has been widely used in Fabrication of high pressure air bottles, high pressure gas storage tanks, rocket motors, structures in aerospace applications such as aircrafts, rockets and missiles. Switching between predetermined high and low level of welding current can be used to produce pulsed current gas tungsten arc welds.

Some progress is done on pulsed current GTAW of aluminium alloy. So far the pulsed current welding is used to study the effect of pulse current, shielding gas composition, weld speed and bead shape, the incidence of welding defects, joint strength, using alloy sheets of 5083 type, angular distortion in SS310 type, to study the microstructure and weld bead geometry. Usually the pulsed waves are in rectangular shape and the parameters used for pulsed GTA welding are in shown in figure 1. The main characteristics of Pulsed Current Welding are determined by peak current I_p , base current I_b , peak time t_p and base time t_b . The present study was carried out to understand the effect of pulsed current welding technique on the hardness, the microstructure and the tensile properties of gas tungsten arc welded AA6061 aluminium joints.

II. EXPERIMENTAL PROCEDURE

In this investigation, AA6061 aluminium alloy plates with 3mm in thickness were used as the base materials. The chemical compositions and mechanical properties of base metal are presented in Table 1 and 2. These plates of aluminum alloy were cut to required size (150mm × 150mm) by power hacksaw cutting and grinding. High purity (99.999%) argon gas was used as shielding gas. The plates were welded with pulsed and non-pulsed current GTAW process.

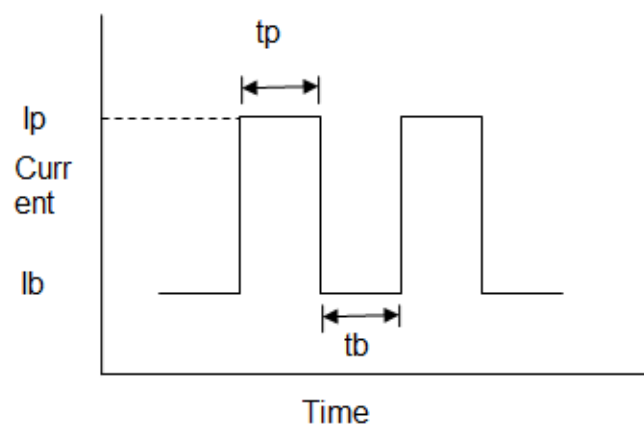


FIG. 1 PARAMETERS USED FOR PULSED GTAW: PEAK CURRENT I_p , BASE CURRENT I_b , PEAK TIME t_p , BASE TIME t_b

Filler wire material of ER4043 with 2mm diameter was used during the welding, which reduced the weld cracks and produced the good strength and ductility than other filler metals. These filler metals melt at a temperature lower than that of the base metal, for this reason it yields during cooling, since it remains more plastic than the base metal and relieves the contraction stresses that might cause cracking.

The aluminium alloy work pieces were chemically cleaned in hot Sodium Hydroxide for 10 minutes followed by dipping in Nitric Acid solution for about 15 minutes and then washed in water. A Master TIG AC/DC 3500W GTAW machine with AC was used for welding of AA6061 aluminium alloy test specimens. The choice of tungsten electrode depends upon the type of welding current selected for the application. Zirconated tungsten (EWZr) electrodes are best suited for AC wherein they keep hemispherical shape. This welding process was conducted with 2.4 mm diameter 2% Zirconated tungsten electrode. The welding parameters used for this welding process both in pulsed current and non-pulsed current of the above material are given in Tables 4 and 5. The edge preparation of the tested AA6061 aluminum alloy specimens are shown in fig.2.

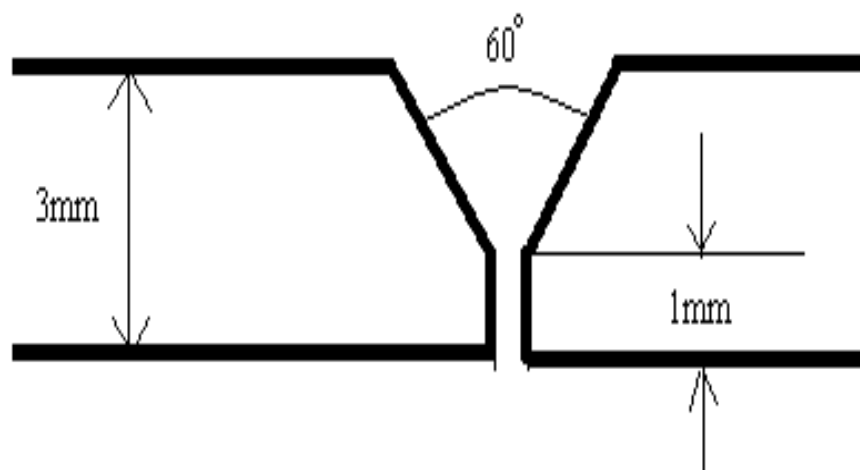


FIG. 2 EDGE PREPARATION OF WELD SPECIMENS

After welding process is over, the radiography, liquid penetrant test were carried out on the weldments according to the ASTM standards, Section IX, Division 2 for radiography and ASTM E-1417 for liquid penetrant test. The parameters used in the non-destructive testing are given in the Tables 6 and 7.

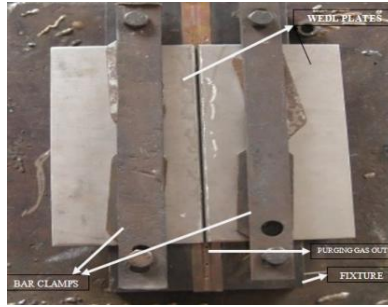
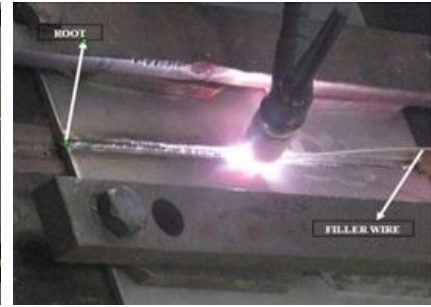
**FIG. 3 ALUMINIUM PLATES****FIG. 4 FIXTURES****FIG. 5 ROOT OF WELDING****FIG. 6 ARC GUN****FIG. 7 GTAW MACHINE****FIG. 8 AC/DC PULSED PANEL**

TABLE 1
CHEMICAL COMPOSITION OF WORK MATERIAL AA6061

Material	Chemical Composition % wt								
	Si	Fe	Cu	Mn	Mg	Zn	Ti	Cr	Al
AA 6061	0.40-0.80	0-0.70	0.15-0.40	0-0.15	0.80-1.20	0-0.25	0-0.15	0.04-0.35	Balanced

TABLE 2
MECHANICAL PROPERTIES OF WORK MATERIAL AA6061

Material	UTS(MPa)	YS(MPa)	% Elongation
AA6061	310 MPa	145 MPa	22%

TABLE 3
CHEMICAL COMPOSITION OF FILLER WIRE ER4043

Material	Chemical Composition % wt							
	Cu	Si	Mn	Mg	Fe	Cr	Ti	Al
ER4043	0.17	4.5-6.0	0.24	0.05	0.05	0.05	0.05	Balanced

TABLE 4
WELDING PARAMETERS FOR PULSED CURRENT WELDING OF AA6061

Exp No.	Weld layer	Peak Current/ A	Base Current/ A	Voltage/ V	Pulse on time/ %	Frequency/ HZ	Welding speed (mm /sec)
1	Root	100	50	14.4 -15.2	50	6	2.66
	1 st layer	100	50	12.9-14.3	50	6	2.40
2	Root	110	55	14.2-15.3	50	6	2.88
	1 st layer	110	55	13.9-15.0	50	6	2.41
3	Root	120	60	12.6-14.2	50	6	4.03
	1 st layer	120	60	14.7-16.1	50	6	3.70
4	Root	130	65	14.5-18.3	50	6	3.91
	1 st layer	130	65	14.9-16.1	50	6	3.87

TABLE 5
WELDING PARAMETERS FOR NON-PULSED CURRENT WELDING OF AA6061

Exp No.	Weld layer	Current/ A	Voltage/ V	Welding speed (mm/sec)
1	Root	100	14.4 – 15.2	2.02
	1 st layer	100	14.3 – 15.3	2.84
2	Root	110	12.9 – 14.1	3.01
	1 st layer	110	15.9 – 16.9	3.26
3	Root	120	13.9 – 15.1	2.78
	1 st layer	120	15.1 – 16.0	3.14
4	Root	130	12.9 – 14.1	3.32
	1 st layer	130	15.2 – 16.4	1.72

Images of pulsed current welded Aluminium plates

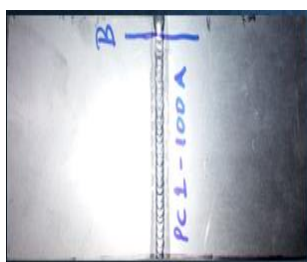


FIG. 9



FIG. 10

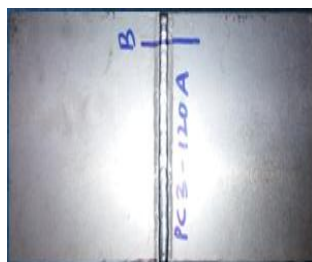


FIG. 11

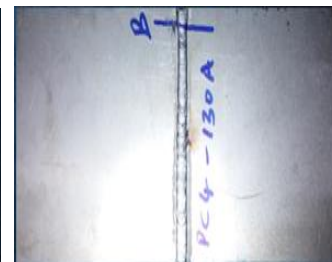


FIG. 12

PULSED CURRENT (100A) PULSED CURRENT (110A) PULSED CURRENT (120A) PULSED CURRENT (130A)

Images of non-pulsed current welded Aluminium plates

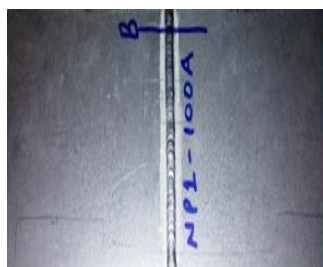


FIG. 13

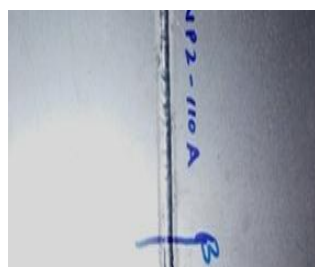


FIG. 14

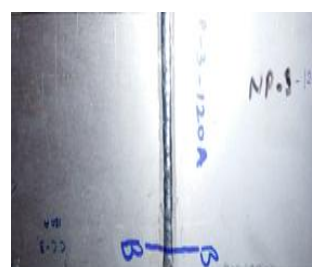


FIG. 15

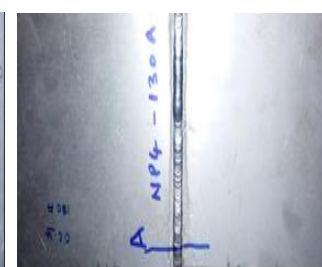


FIG. 16

NON-PULSED CURRENT (100A) NON-PULSED CURRENT (110A) NON-PULSED CURRENT (120A) NON-PULSED CURRENT (130A)

TABLE 6
LIQUID PENETRANT TEST PARAMETERS OF AA6061

Aluminum Alloy 6061	
DP DIT	MAGNA FLUX
Penetrant Used	SKL-SP
Cleaner Used	SKC-1
Developer Used	SKD-S2
Dwell time (at room temp)	10 Min
Viewing Media	Normal light
Sensitivity	30 micron

TABLE 7
RADIOGRAPHY TEST PARAMETERS OF AA6061

Exposure parameters	Technique	Single wall single image
	Source	X-Ray
	Voltage (Kv)	150 KV
	Current (mA)	5 mA
	Exposer Time	1 min
	Film type	KODAK - DY
	S.F.D./F.F.D. (mm)	1000 mm
	I.Q.I.	DIN-AL10-16
Processing parameters	Developer Time (min)	5.0
	Stop Bath Time (min)	1.0
	Fixer Time (min)	10
	Sensitivity	2%

III. RESULTS AND DISCUSSION

TABLE 8
LIQUID PENETRANT TEST RESULTS OF AA6061

S.no.	Material thickness (mm)	Pulsed/non-pulsed welding	Frequency (HZ)	Observations
1	3	Pulsed 100A	6	No defect observed on welded area
2	3	Non-Pulsed 100A	-	No defect observed on welded area
3	3	Pulsed 110A	6	No defect observed on welded area
4	3	Non-Pulsed 110A	-	No defect observed on welded area
5	3	Pulsed 120A	6	No defect observed on welded area
6	3	Non-Pulsed 120A	-	No defect observed on welded area
7	3	Pulsed 130A	6	No defect observed on welded area
8	3	Non-Pulsed 130A	-	No defect observed on welded area

TABLE 9
RADIOGRAPHY TEST RESULTS OF AA6061

S.no.	Material thickness (mm)	Pulsed/non-pulsed welding	Frequency (HZ)	Observations
1	3	Pulsed 100A	6	No significance defect
2	3	Non-Pulsed 100A	-	No significance defect
3	3	Pulsed 110A	6	No significance defect
4	3	Non-Pulsed 110A	-	No significance defect
5	3	Pulsed 120A	6	No significance defect
6	3	Non-Pulsed 120A	-	No significance defect
7	3	Pulsed 130A	6	No significance defect
8	3	Non-Pulsed 130A	-	No significance defect

Radiography images of AA6061 aluminium alloy



FIG. 17 PULSED CURRENT (100A)



FIG. 18 PULSED CURRENT (110A)

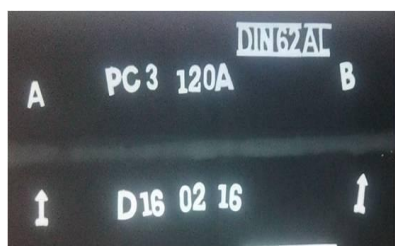


FIG. 19
PULSED CURRENT (120A)

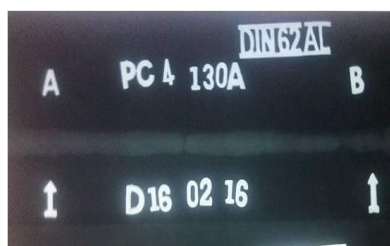


FIG. 20
PULSED CURRENT (130A)



FIG. 21
NON-PULSED CURRENT (100A)

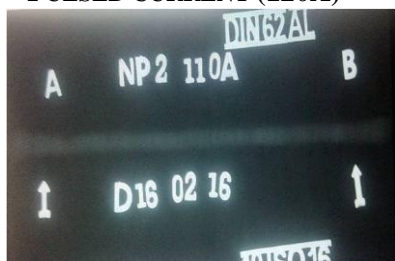


FIG. 22
NON-PULSED CURRENT (110)



FIG. 23
NON-PULSED CURRENT (120)

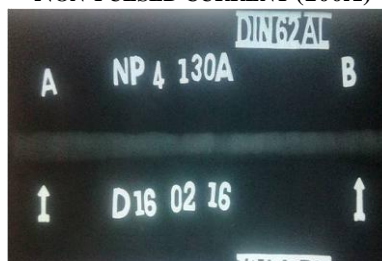


FIG. 24
NON-PULSED CURRENT (130)

Images of tensile strength test work pieces



FIG. 25 WORK PIECES BEFORE TEST

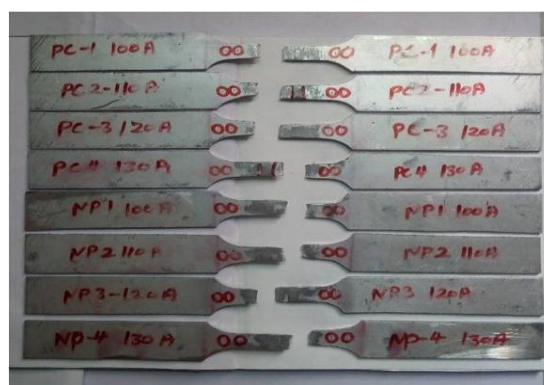
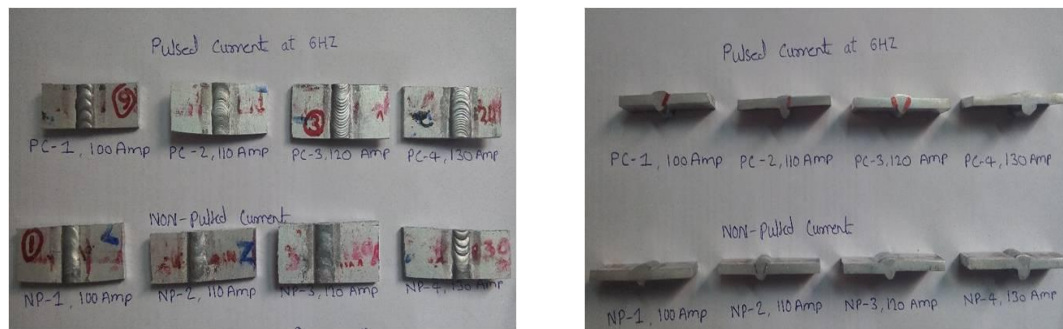


FIG. 26 WORK PIECES AFTER TEST

TABLE 10
TENSILE STRENGTH TEST RESULTS OF AA6061

S.no.	Process	Frequency (HZ)	Thickness	Ultimate Tensile Strength (MPa)	0.2% Proof stress (MPa)
1	Pulsed 100 A	6	3	152.290	149.893
2	Non-Pulsed 100 A	-	3	158.300	137.848
3	Pulsed 110 A	6	3	167.341	114.440
4	Non-Pulsed 110 A	-	3	158.470	106.256
5	Pulsed 120 A	6	3	170.370	127.671
6	Non-Pulsed 120 A	-	3	158.912	121.251
7	Pulsed 130 A	6	3	158.983	136.989
8	Non-pulsed 130 A	-	3	154.915	94.150

Images of welded samples used for hardness test and microstructure test

**FIG. 27 SAMPLES USED FOR HARDNESS TEST AND MICROSTRUCTURE****TABLE 11****OBSERVED HARDNESS RESULTS FOR WELDMENT WELDED WITH PULSED CURRENT 100A**

S.no.	Location	Observed values in HV			
		Impression 1	Impression 2	Impression 3	Average
1	WELD ZONE	70.8	70.4	71.2	70.80
2	HAZ	72.0	72.4	72.0	72.13
3	FUSION ZONE	76.1	76.3	77.0	76.47
4	BASE METAL	67.0	67.5	67.2	67.23

TABLE 12**OBSERVED HARDNESS RESULTS FOR WELDMENT WELDED WITH PULSED CURRENT 110A**

S.no.	Location	Observed values in HV			
		Impression 1	Impression 2	Impression 3	Average
1	WELD ZONE	70.4	70.8	71.2	70.80
2	HAZ	71.6	71.2	71.6	71.47
3	FUSION ZONE	76.9	77.1	76.9	76.97
4	BASE METAL	67.2	67.4	67.0	67.2

TABLE 13**OBSERVED HARDNESS RESULTS FOR WELDMENT WELDED WITH PULSED CURRENT 120A**

S.no.	Location	Observed values in HV			
		Impression 1	Impression 2	Impression 3	Average
1	WELD ZONE	72.0	72.8	71.6	72.13
2	HAZ	73.2	73.6	74.0	73.60
3	FUSION ZONE	74.4	75.3	75.7	75.13
4	BASE METAL	67.5	67.2	67.1	67.26

TABLE 14**OBSERVED HARDNESS RESULTS FOR WELDMENT WELDED WITH PULSED CURRENT 130A**

S.no.	Location	Observed values in HV			
		Impression 1	Impression 2	Impression 3	Average
1	WELD ZONE	69.2	68.8	69.2	69.07
2	HAZ	71.2	70.8	71.2	71.07
3	FUSION ZONE	71.6	71.6	71.2	71.47
4	BASE METAL	67.0	67.7	67.0	67.23

TABLE 15**OBSERVED HARDNESS RESULTS FOR WELDMENT WELDED WITH NON-PULSED CURRENT 100A**

S.no.	Location	Observed values in HV			
		Impression 1	Impression 2	Impression 3	Average
1	WELD ZONE	70.4	70.0	69.6	70.00
2	HAZ	71.6	70.4	70.8	70.93
3	FUSION ZONE	72.4	72.0	72.8	72.40
4	BASE METAL	67.2	67.2	67.3	67.23

TABLE 16
OBSERVED HARDNESS RESULTS FOR WELDMENT WELDED WITH NON-PULSED CURRENT 110A

S.no.	Location	Observed values in HV			
		Impression 1	Impression 2	Impression 3	Average
1	WELD ZONE	70.8	70.0	70.4	70.49
2	HAZ	70.8	71.2	70.4	70.80
3	FUSION ZONE	71.2	72.8	72.0	72.00
4	BASE METAL	67.1	67.4	67.2	67.23

TABLE 17
OBSERVED HARDNESS RESULTS FOR WELDMENT WELDED WITH NON-PULSED CURRENT 120A

S.no.	Location	Observed values in HV			
		Impression 1	Impression 2	Impression 3	Average
1	WELD ZONE	71.6	71.2	70.8	71.20
2	HAZ	71.6	71.6	71.8	71.67
3	FUSION ZONE	73.2	74.0	73.2	73.47
4	BASE METAL	67.1	67.3	67.4	67.26

TABLE 18
OBSERVED HARDNESS RESULTS FOR WELDMENT WELDED WITH NON-PULSED CURRENT 130A

S.no.	Location	Observed values in HV			
		Impression 1	Impression 2	Impression 3	Average
1	WELD ZONE	66.6	66.0	67.4	66.57
2	HAZ	71.2	70.8	70.4	70.80
3	FUSION ZONE	71.6	71.2	70.8	71.20
4	BASE METAL	67.0	67.7	67.0	67.23

Images of microstructure at Heat Affected Zone (HAZ)



FIG. 28 PULSED 100A (HAZ)

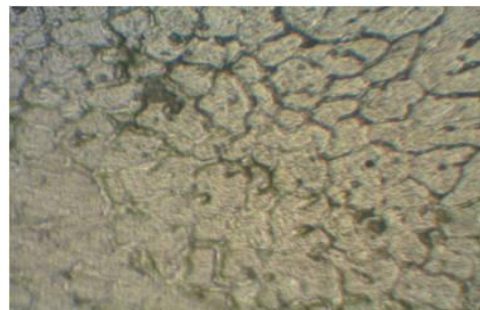


FIG. 29 PULSED 110A (HAZ)

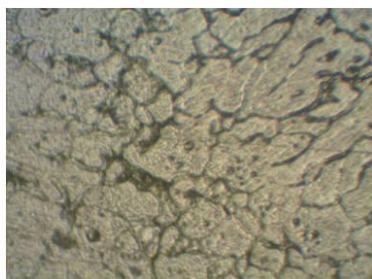


FIG. 30 PULSED 120A (HAZ)



FIG. 31 PULSED 130A (HAZ)

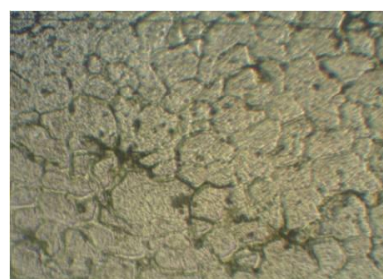
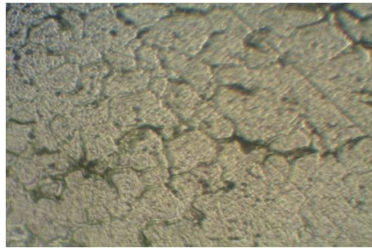
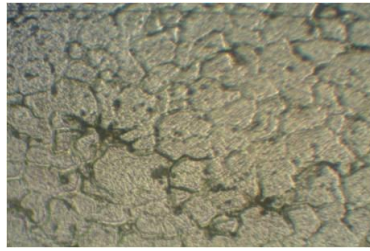


FIG. 32 NON-PULSED 100A (HAZ)



**FIG. 33 NON-PULSED 110A
(HAZ)**



**FIG. 34 NON-PULSED 120A
(HAZ)**

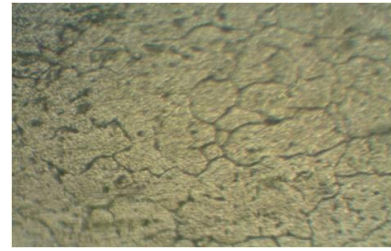


**FIG. 35 NON-PULSED 130A
(HAZ)**

1. Liquid penetrant tests were conducted upon these weldments to know the effect of Pulsed current and Non-pulsed current on the welding characteristics of these metal alloys. No defect was observed during liquid penetrant test.
2. Radiography tests were conducted on these weldments, no significant defects were found on weldments. No porosity was observed in pulsed current and non-pulsed current welded weldments.
3. Tests were conducted on all the weldments and observed more Tensile strength values in all Pulsed current weldments done at (100A, 110A, 120A, 130A) compared to Non-pulsed current weldments done at (100A, 110A, 120A, 130A). Among all pulsed current weldments, observed more tensile strength i.e. "170.370 MPa" in weldment done at 120Amp.
4. A load of 5kgs was applied to obtain Vickers hardness HV. Tables 11-18 lists the Vickers hardness values for all weldments at weld zone, heat affected zone, base metal and fusion zone for pulsed and non-pulsed current. It was observed that the values of hardness are less in the Non-pulsed current joints compared with the Pulsed current ones in all the locations. The reason for the decrease in the hardness can be attributed to the variation in the temperatures attained and also the pulsing of current in the joint fabricated by the pulsed current. Hence the higher hardness is attributed to the joints fabricated by pulsed current.
5. The strength of the weld metal is characterized by the grain size and the phase present in the microstructure. The phase formation and grain growth are highly influenced by the thermal cycle of the welding process. The interesting region of would be the weld metal and the interface zones because at the weld metal the temperature goes to the peak and cools rapidly thus formation of finer grain sizes. The welded specimen was prepared using the standard metallographic procedure, and the polished surfaces were itched with aqua-reagent to get the clear microscopic view of the weldments. The results of the microstructure of all weldments at the heat affected zone (HAZ) are presented in fig.28-35.

IV. CONCLUSION

The main conclusions of the present study can be summarized as follows,

- 1) The pulsed current welding technique records lower peak temperatures and lower magnitude of residual stresses compared with non-pulsed current welding, which is highly preferable for thin sheet welding.
- 2) The tungsten inert gas or gas tungsten arc welded aluminium alloy joint fabricated by pulsed current welding technique exhibits superior tensile properties compared with non-pulsed current welding technique.
- 3) The formation of finer grains caused by pulsed current is the main reason for enhanced tensile and hardness properties of the joints.

REFERENCES

- [1] Troyer, W., Tomsic, M., and Barhotst, R, "Welding characteristics of Aluminium alloy" welding journal, 56(1), 1977, 26-32.
- [2] Becker, D.W. and Adams, C.M., "The role of pulsed GTA welding variables in solidification and grain refinement" welding journal, 58(5) 1979, 134s-152s.
- [3] Becker, D.W. and Adams, C.M., "Investigation of Pulsed GTA Welding parameters" welding journal, 57(5) 1978, 134s-138s.
- [4] Omar, A.A., and Lundin, C.D., "welding journal", 58(4), 1970, 97s-104s.
- [5] Tseng, C.F. and Savage, W.F., "The effect of oscillation" welding journal, 50(11) 1971, 777-786.
- [6] Sharir, Y., Peiieg, J. and grill, "Metallurgical Technology", 5, 1978, 190-196.
- [7] Tsai, C.L., and Hou, C.A., "Theoretical Analysis of Weld Pool Behaviour in the Pulsed Current GTAW Process", Heat Transfer, 110, 1988, 160165.

- [8] Kate, S and Tanabe, S, "High speed welding of 0.5mm thickness alloy sheets using pulsed TIG welding", welding International 7, 1988, 602608.
- [9] Tsen, K.H. and Chou, C.P, "Effect of pulsed gas tungsten arc welding on angular distortion in austenitic stainless steel weldments", science and Technology of welding and joining 6,(3),2001,149-153.
- [10] Reddy,G.M.,Gokhale,A,A.and Prasad Rao K, "Effect of filler metal composition on weldability of Al-Li alloy 1441",Material Science&Technology,14,1998,61-66.
- [11] Giridharam, P.K and Muragan, N, "Sensitivity Analysis of pulsed current GTA welding process parameters on weldbead geometry", National conference in advances in joining Technology 2004.
- [12] Mohandas T, MadhusudhanReddy G (1996) Effect of frequency of pulsing in gas tungsten arc welding on the microstructure and mechanical properties of titanium alloy welds, J Mater Sci Lett 15:625-628.
- [13] Shelwatker DA, Madhusudhan Reddy G, GokhaleAA (2002) Gas tungsten arc welding studies on similar and dissimilar combinations of AlZn-Mg alloy RDE 40 and Al-Li alloy 1441. SciTechnol weld Join 352-361.
- [14] VahidNazarpoor,Abdoreza,Soltanipoor,KhosrowFarmanesh"Effect of current on Mechanical, Metallurgical and Corrosion Properties of AA 5083 Aluminium Alloy Pulse TIG Welding Joints "Journal of Materials Science, vol.2,2010,54-67.
- [15] Ramulu, M and Rubbert,M.P, "Gas Tungsten Arc welding of al-li-cu alloy 2090", Welding Research Supplement, 109s-114s. 16Parmar, R.S., "Welding Engineering and Technology" p623.
- [16] Mohamed, "Optimization of Weld Bead Dimensions in GTAW of Al-Mg Alloy," Materials and Manufacturing Processes, Vol. 16, No. 5, 2001, pp. 725-736.

Modeling and Optimization of Cushioning System in Hydraulic Cylinder to achieve Performance Characteristics

Mr. Ch. Prahallad¹ & Mr. A. Raveendra²

¹M. Tech Student, Mechanical Dept., Malla Reddy Engineering College, Hyderabad
²Mr. A. Raveendra, Associate Professor, Mechanical, Dept., Malla Reddy Engineering College, Hyderabad

ABSTRACT: Hydraulic Operating system technology is wide spread into all sectors of manufacturing, agriculture and construction, aerospace and in marine industries where precision and accuracy play a key role in the quality of the work output. As hydraulic systems are more integrated into automated systems it is important to maintain precise control of hydraulic cylinders which can be achieved by assisting the deceleration response of piston due to the pressure generated when fluid passes through the cushion orifice. Dynamic models are developed for describing the cylinder cushioning Systems that when solved numerically predicts the pressure and velocity responses of the cylinder with time. The study includes modeling of cushion profiles and performing analytical analysis for achieving a constant deceleration during cushioning phase. It has been observed that performance of cushion is highly sensitive to variations in the spear shape profile. analytical analysis produced a profile leading to nearly constant deceleration with an RMSE of 1.4×10^{-3} m/s (0.29 feet per minute; fpm) when simulated by the dynamic model. The parabolic and linear regression curves producing RMSE values of 14.9×10^{-3} and 21.7×10^{-3} m/s (2.94 and 4.28 fpm) respectively. This means the performance of the cushion is highly sensitive to variations in the spear shape profile. the analytically developed spear profile was simulated with viscous effects the RMSE value increased to 40.7×10^{-3} m/s (8.01 fpm) therefore an optimization procedure was developed to select the ideal cushion dimensions with viscous effects included. The optimization procedure produced a consistent family of results for each spear with an average standard deviation of 2.6×10^{-3} m/s (0.51 fpm). This dynamic modelling approach has potential to assist designers in cushioning spear development that meets customer cushion response specifications.

1. Introduction

The modern day technology advancements in hydraulic industry have revolutionized our ability to

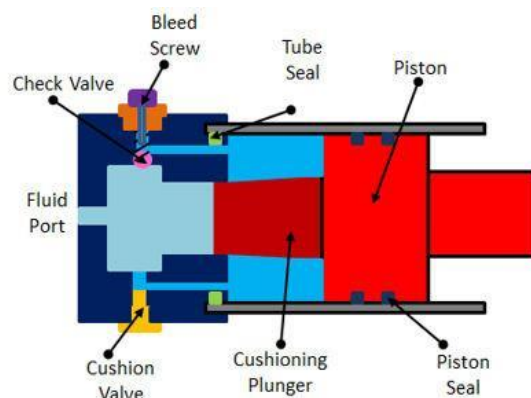
automate the process in manufacturing and construction sectors through the application of automation technology. The advances are achieved by making automated machines with hydraulic systems that has both rotational and linear motions. The focus of the study is to analyze cushioning component within cylinders to understand the dynamic relationship with in the cylinders to predict and optimize the deceleration performance of cylinder. Hydraulic cylinders operating under high loads experiences high impact on end caps due to the high piston velocity at stroke end.

The cushion technology is developed to decelerate the cylinder piston and reducing the speed before the piston rod assembly reaches the end of stroke. Cushion system works by metering the fluid flow through cylinder case when piston rod nears the end stroke. When the fluid flow is restricted, an increase in the cylinder end pressure observed at both ends retraction and extension strokes. The pressure developed is exerting the force upon the cylinder piston resulting in its deceleration. The rate of deceleration is dependent on the rate of fluid flowing out of the cylinder. The Cushioning mechanism is based on energy conservation and dynamic relationship. The main objective of this research is to compare the cushioning velocity profile produced by the analytically developed spear shape design with the standard spear shapes used in industries.

2. Hydraulic Cylinder Cushion System

The cushioning effect in hydraulic cylinders mainly act as a force damping system at the end of the piston stroke by decelerates the piston moving with high velocity at the cap end. The cushioning effect is generated by building a high fluid pressure in the cylinder at the retrieving stroke by restricting the out flow of the fluid through the cylinder. This effect is generated by developing a spear that obstructs the free flow of the fluid through orifice by entering into the cushion orifice. In this case the a analytical and dynamic analysis is performed on standard cushion models and developed models to

compare and generate a generic model that is more useful for the manufactures in achieving the **customer's specifications** as per the applications. In this case four cushion spears stepped, tapered, parabolic and piccolo models are developed considering the length of the spear, cylinder diameter, cushion cavity length, orifice diameter and viscosity of the fluid. As the friction generated is minimal it is neglected for the better results. The other factors that are considered in this analysis are the fluid pressure, velocity, acceleration and deceleration with respect to the time factor.



3. Cylinder Cushion Dynamic Model

Utilizing the developed dynamic model, a cushion design optimization process was implemented to find cushion design designs that will best meet the desired velocity response profiles specified by the end user. Tests were run on dynamic model to compare them with the expected results of cushion design generated through an **analytical analysis based on Berninger's** method. Additional tests are run to evaluate the effectiveness of the optimizing to compare the performance of various common cushion shapes used in industry. A dynamic model developed in Mat lab and analysis was done to find a cushion spear geometry resulting in constant deceleration. In dynamic model development the two factors that influence the performance of the cushion are considered to be the orifice created by the cushion spear entering the cylinder cushion cavity and the other factor is the impact of the viscous resistance with in the annual passage created by the cushioning spear as it enters the cushioning cavity.

4. Methodology

With the completion of the dynamic model and optimization procedure, numerous tests were run to evaluate the simulated results. The dynamic cushion model was used to simulate the relationship of cushion orifice area to spear depth for constant deceleration. During the development of this

relationship, two assumptions were made: the fluid pressure in both ends of the cylinder was constant and viscous effects were neglected. Therefore, to effectively compare the results of the dynamic model to the expected results of the analytically designed cushioning spear, adjustments were made to the system being represented in the dynamic model. To maintain constant fluid pressure, the metering orifices were opened to 0.5 in. To remove the viscous effects, the fluid viscosity was set to zero.

The initial velocity of the piston assembly and the required rate of deceleration were specified. Based on the dimensions of the cylinder, the steady state velocity was found to be 34.44 fpm. Therefore, with a final velocity of 0 fpm and a deceleration time of 1.5 seconds, the cushioning deceleration was calculated to be 0.12m/s² or 22.96 feet/min². The shape of the spear design generated by the analytical equation cannot be described by any of the spear types common to industry. Thus, tests were run to see whether the constant deceleration response could be replicated with the tapered or parabolic spear types. To calculate the tapered and parabolic spear profiles that would best match the results of the analytical equation, linear and quadratic regression curves were fit to the orifice area-spear depth function. Additionally, to investigate the effect of the assumptions made during the development of the analytical equation, the dimensions of the analytically developed cushioning spear were simulated with viscous effects included.

To investigate how well the commonly-used spear types could achieve a constant deceleration velocity profile, the cushion design optimization was run for each of the four spear shapes using the same system parameters (Table 4.1). The difference between the desired velocity profile and the response produced by the optimized result for each spear type was quantified by calculating the root mean square error (RMSE). The calculated RMSE value serves as a performance metric for the common spear types.

Lastly, the optimization process works by repeatedly running the model while varying spear dimensions (shown in Figure 3.2) such as cushion spear diameter and length. Due to the nature of this process, the optimizer produced different designs each time the process was run. Therefore, the cushion design optimization procedure was run ten times for each of the four cushion spear design types to capture the range of results that the optimizer produced using the system parameters shown in Table 3..

Table 4.1: System parameters entered into the optimization program.

Bore Diameter (in)	5	Final Speed (fpm)	0
Rod Diameter (in)	2	Deceleration Time (s)	1.5

Cushion Cavity Diameter (in)	1	Fluid Density (Kg/m^3)	861
Max Spear Length (in)	5	Dynamic Viscosity (Pa-s)	0
Metering Orifice Diameter (in)	0.5	Viscous damping Coefficient [N/(m/s)]	100

5. Results and Discussion

By executing the parameters mentioned above the orifice required for constant deceleration was found along the length of the spear with the diameter of the sphere. In the below profile the observations means the ideal shape is a mixture of the tapered and parabolic shapes used.

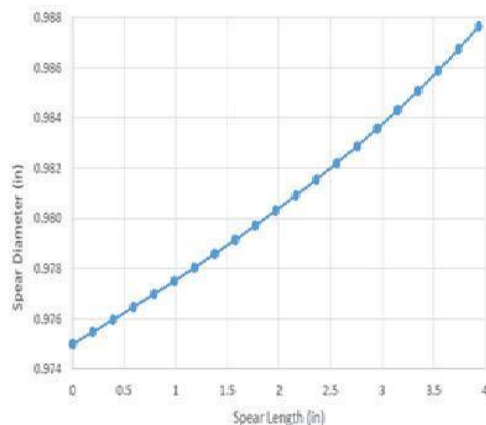


Fig.3.8: Constant deceleration spear design showing spear diameter as a function of length.

When this shape was entered into the dynamic model and simulated, the resulting velocity profile matched the desired response very closely (Figure 3.9). The rapid oscillations at the beginning of the cushioning phase were due to the change in the dynamics as the system switches from not being cushioned to additional cushioning resistances being added to the system in a step-like manner. The oscillations represent the interaction between the fluid capacitance and the rod-piston-load mass. The RMSE being the simulated response and the expected response was $1.47 \times 10^{-3} \text{ m/s}$ (0.29 fpm) which is quite low indicating a good match between the simulation and the design velocity profile

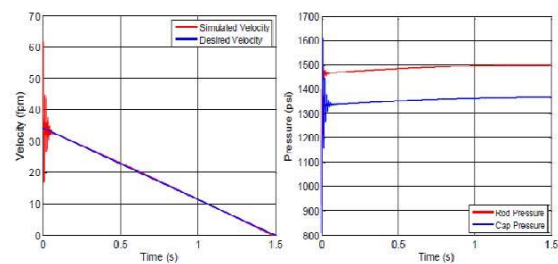


Fig.3.9: Velocity (a) and pressure (b) results of entering the analytically calculated spear profile into the dynamic model.

To represent the tapered spear type, the analytical data was fit with two linear regressions, one from a length of 0 to 65 mm (0 to 2.56 in.) and the other from 65 to 102 mm (2.56 in. to 4 in.). The two resulting lines were used because of the curved nature of the data and because many tapered cushioning spears do have multiple sections with different taper angles along their length. These regression curves fit the ideal relationship with coefficient of determination, R^2 , value of 0.998 for both lines (Figure 3.10). The second order polynomial regression resulted in a parabolic spear shape and had an R^2 value of 0.9997 (Figure 3.11).

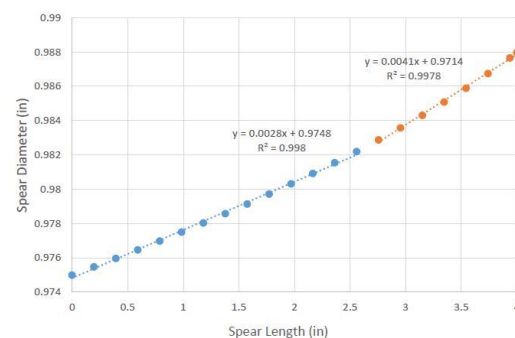


Fig. 3.10: Analytical data fit with two linear regression curves.

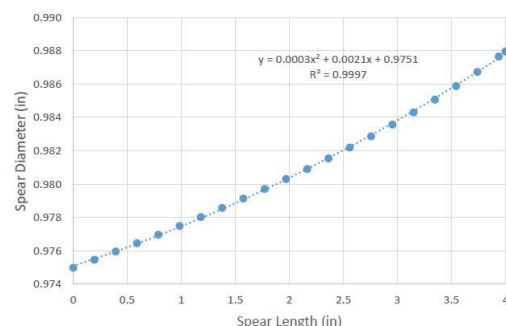


Fig.3.11: Analytical data fit with a quadratic regression curves.

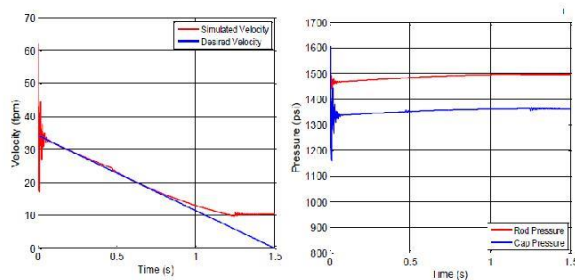


Fig.3.12: Velocity (a) and pressure (b) results of the tapered regression curve fit to analytical data.

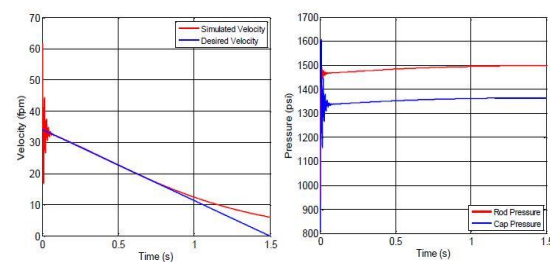


Fig.3.13: Velocity (a) and pressure (b) results of the parabolic regression curve fit to analytical data

The dynamic cushion model was simulated with the tapered and parabolic spear shapes arising from the regression curves, the resulting velocity profiles matched the constant deceleration profiles, but with some departure from that observed in the simulations with the ideal relationship. Specifically, in the case of the tapered spear, the simulated velocity profile started to depart from the desire at the end of the first taper segment (as observed at about 0.4 seconds; Figures 3.12) and then near the end of the second segment (as observed at about 0.75 seconds). The start of the flat velocity at about 1.25 seconds signals the end of the cushioning spear. For the parabolic spear, the simulated velocity profile closely matched the desired profile until about 0.75 seconds (Figure 3.13). This type of response in which the deceleration is reduced near the end of the spear is due to the relationship between spear area and flow rate not resulting in sufficient cushion pressure to continue to decelerate piston-rod assembly as desired. The error in the velocity profiles of the tapered and parabolic spears matched the error in the diameter of the spears (Figure 3.14). A positive error means the diameter of the tapered and parabolic spears was larger than the analytically developed spear and a negative error means that the diameter was smaller.

The dynamic cushion model was simulated with the tapered and parabolic spear shapes arising from the regression curves, the resulting velocity profiles matched the constant deceleration profiles, but with some departure from that observed in the simulations

with the ideal relationship. Specifically, in the case of the tapered spear, the simulated velocity profile started to depart from the desire at the end of the first taper segment (as observed at about 0.4 seconds; Figures 3.12) and then near the end of the second segment (as observed at about 0.75 seconds). The start of the flat velocity at about 1.25 seconds signals the end of the cushioning spear. For the parabolic spear, the simulated velocity profile closely matched the desired profile until about 0.75 seconds (Figure 3.13). This type of response in which the deceleration is reduced near the end of the spear is due to the relationship between spear area and flow rate not resulting in sufficient cushion pressure to continue to decelerate piston-rod assembly as desired. The error in the velocity profiles of the tapered and parabolic spears matched the error in the diameter of the spears (Figure 3.14). A positive error means the diameter of the tapered and parabolic spears was larger than the analytically developed spear and a negative error means that the diameter was smaller.

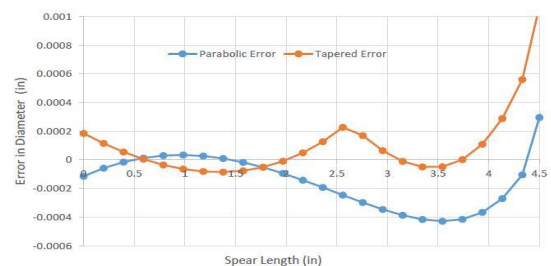


Fig.3.14: Dimensional error between the two spear types developed from the regression fits and the spear type developed analytically

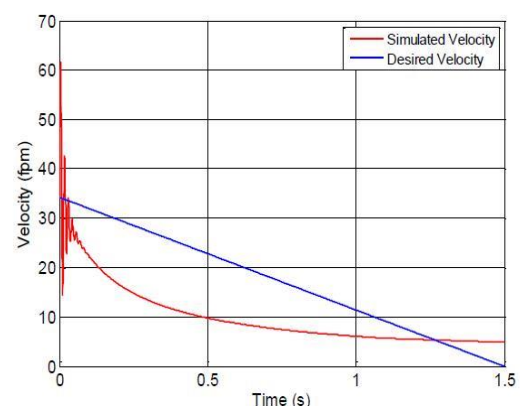


Fig. 3.15: Velocity response of the analytically designed cushioning spear with viscous effects Included.

Cushion Design Optimization

To analyze and compare the simulated results for multiple spears designs with varied dimensions, the

cushion design optimization procedure utilized the RMSE value calculated by measuring the difference between the simulated velocity profile and the desired velocity profile. The applications of the design optimization procedure to the parabolic spear shape produced RMSE values ranging from 21.4×10^{-3} - 30.8×10^{-3} m/s (4.22-6.06 fpm) with an average error of 25.2×10^{-3} m/s (4.96 fpm) and a standard deviation of 3.2×10^{-3} m/s (0.63 fpm). The solutions tended to fall within a 25.4×10^{-3} m/s (5 fpm) band for most of the cushioning phase (Figure 3.16).

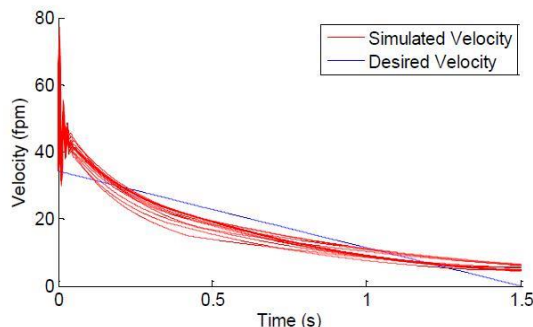


Fig. 3.16: Optimized velocity results for a parabolic cushioning spear

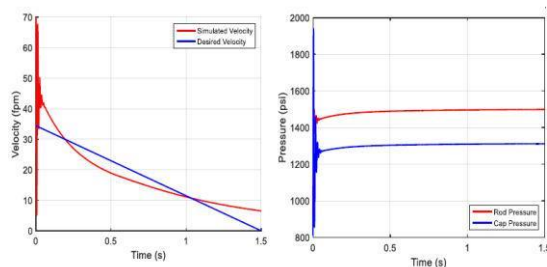


Fig 3.17: The velocity (a) and pressure (b) response of the optimized parabolic profile.

A similar process was conducted for the stepped profile cushion spear type. The RMSE of the resulting velocity profiles ranged from 22×10^{-3} – 28×10^{-3} m/s (4.35-5.52 fpm) with an average error of 25×10^{-3} m/s (4.93 fpm) and a standard deviation of 1.9×10^{-3} m/s (0.38 fpm). The location of the sudden drops in velocity caused by the stepped spear shape shifts as the cushion design optimization procedure finds designs with steps of varying length (Figure 3.18).

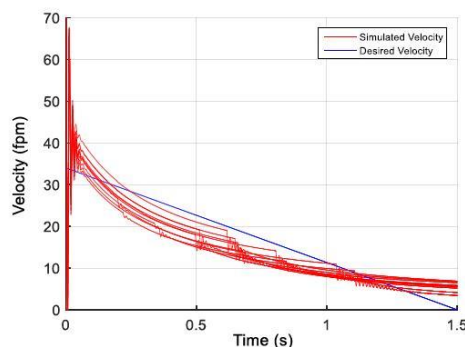


Fig 3.18: Optimized velocity results for a stepped cushioning spear.

Sudden changes in the diameter of the stepped spear shape lead to points along the velocity response where the piston speed drops abruptly, Figure 3.19. The velocity reduction upon the start of cushioning is more pronounced because the design optimizer selected spear dimensions with larger starting diameters when compared to the parabolic and tapered spear types.

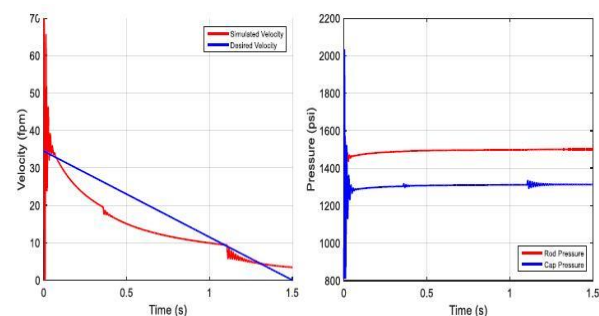


Fig.3.19: The velocity (a) and pressure (b) response of the optimized stepped profile.

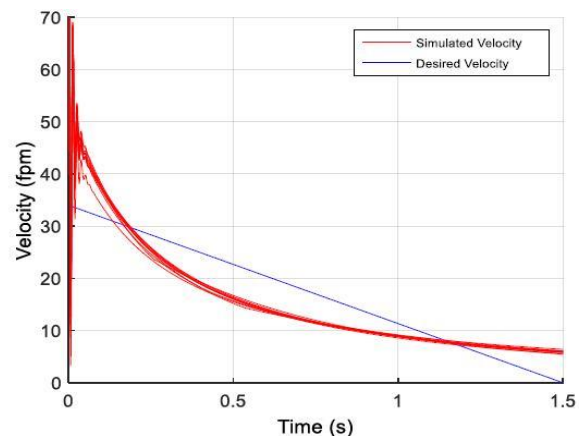


Fig.3.20: Optimized velocity results for a tapered cushioning spear.

When optimization was performed with the tapered cushion, the resulting velocity Profiles were more consistent than those observed with the other cushion types (Figure 3.20). The resulting velocity profiles had RMSE ranging from 22.9×10^{-3} – 26.9×10^{-3} m/s (4.51-5.31 fpm) with the average error being 24.4×10^{-3} m/s (4.81 fpm) and a standard deviation of 1×10^{-3} m/s (0.20 fpm).

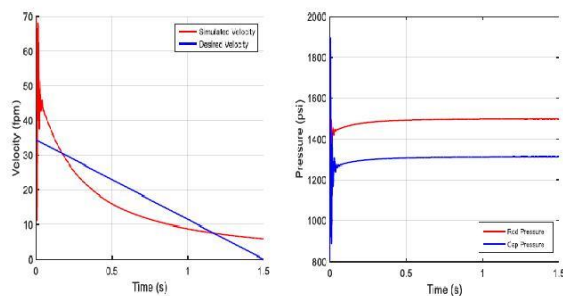


Fig. 3.21: The velocity (a) and pressure (b) response of the optimized tapered profile.

Lastly, the piccolo style spear produced results similar to the stepped spear (Figure 3.22), but with substantially more error and variation in error. The RMSE values ranged from 22.4×10^{-3} - 33.6×10^{-3} m/s (4.41-6.61 fpm) with an average error of 25.8×10^{-3} m/s (5.07 fpm) and a standard deviation of 3.7×10^{-3} m/s (0.73 fpm).

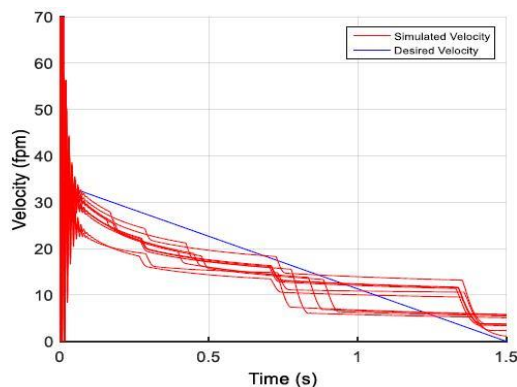


Fig 3.22: Optimized velocity results for a piccolo shaped cushioning spear.

The velocity and pressure results of the piccolo profile were similar to those associated with the stepped spear shape, Figure 3.23. The sudden drop in velocity occurred as each of the piccolo holes were cut off.

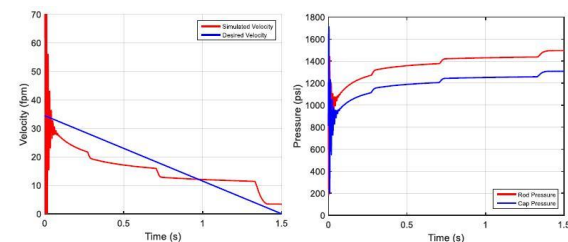


Fig 3.23: The velocity (a) and pressure (b) response of the optimized piccolo profile.

The calculated RMSE values for the four optimized spear types, the analytically produced spear geometry and the two regression curves are compared in Table 4.2. The optimized spear types include viscous effects while the analytical spear along with the parabolic and tapered approximations does not include viscous effects. The results indicate that the effects of including a viscous fluid of

cushioning were represented in the size of the error between the simulated velocity profile and the desired velocity profile.

Table 4.2: RMSE values for the various spear types tested

Spear Type	RMSE (fpm)	Standard Deviation(fpm)
Stepped	4.93	0.38
Tapered	4.81	0.20
Parabolic	4.96	0.63
Piccolo	5.12	0.75
Analytically Developed Cushion	0.29	
Tapered Fit to Analytical Curve	4.28	
Parabolic fit to Analytical Curve	2.94	

6. Conclusion

Based on the results generated from analysis

1. Spear profile produced by the analytical model to achieve constant deceleration results in simulated cushion velocity results representing nearly constant deceleration based the dynamic model of the cushion system. The correspondence between the two approaches lends credibility to the fidelity of the dynamic cushion model.
2. By neglecting the viscous effects during the development of the analytical equation, the system being modeled does not fully capture the effects of cushioning.
3. The profile produced by the analytical analysis was a mixture of two common spear types with the first part representative of a tapered spear while the second portion was more similar to a parabolic spear. When the results of the analytical analysis were fit with more common tapered or parabolic curves, the resulting velocity responses deviated from constant deceleration responses. Therefore, the velocity response of the cushioning spears is highly sensitive to changes in the spear profile.
4. Under conditions where the pressures in each end of the cylinder were held constant, the four common spear types performed very similarly. The main difference indicated by the results was that the parabolic and tapered spear types produce smoother velocity profiles.
5. The results of the optimization tests demonstrated that the optimization procedure was effective in selecting spear shapes that most closely follow the desired velocity profile. The results of this project have potential to impact manufacturers of cylinders with cushions. Where previous cushion designs were based on a more time consuming iterative process done by the designer, this dynamic modelling

approach and cushion design optimization procedure can enhance the design process by providing more information to the designer and their customers. Also, with the sophistication of modern manufacturing equipment, it is possible to manufacture the new cushion designs developed using the approach.

7. References

- [1] Anon. "Constant deceleration cylinder has special built-in shock absorber", *Product Engineering*, 1973.
- [2] Daines, James R. *Fluid Power: Hydraulics and Pneumatics*. Tinley Park, IL: Good heart-Wilcox, 2009.
- [3] Esposito, A. *Fluid Power with Applications* (6th ed.). Upper Saddle River, N.J.: Prentice Hall. 2003.
- [4] Hall. 2003.
- [5] Merritt, H. *Hydraulic Control Systems*. New York: Wiley, 1967.
- [6] Norvelle, F. *Fluid Power Technology*. Minneapolis/St. Paul: West Pub, 1995.
- [7] Stelson, Kim. "Engineering research centre for compact and efficient fluid power
- [8] Strategic research plan", *Centre for Compact and Efficient Fluid Power*, 2015.
- [9] <http://www.technavio.com/report/global-hydraulic-equipment-market-2015-2019>
- [10] Kratz, A., H. Macintire, and R. Gould. **"Flow of liquids in pipes of circular and annular cross-sections."** *University of Illinois Engineering Experiment Station* (1931).
- [11] Schwartz, C., V. J. De Negri, and J. V. Climaco. "Modeling and analysis of an autoadjustable stroke end cushioning device for hydraulic cylinders." *J. Braz. Soc. Mech. Sci. Eng.* 27.4 (2005): 415-25.
- [12] Shampine, L. F. and M. W. Reichelt, "The MATLAB ODE suite." *SIAM Journal on Scientific Computing*, Vol. 18, 1997, pp. 1–22.
- [13] Thorner, Frank. *Investigation of Hydraulic Cylinder Cushioning*. Sheffield Hallam University, (1998).

Cryogenic Tool Treatment

Mr. K Prudhvi & Mrs. Venkata Vara Lakshmi

M.Tech 2nd year, Department of Mechanical Engineering, MREC, Hyderabad, India.
Associate Professor, Department of Mechanical Engineering, MREC, Hyderabad, India.

Abstract: The high speed steel is used as a cutting tool, since it has good quality and reliability at cheaper rate when compared to other cutting tools. So it is very important to increase the ability of the tool further for its reliability. So the best way is to increase the hardness. We have brainstormed to find out alternate tool materials. One novel method namely dipping the ordinary tool bit in a CRYOGENIC SOLUTION, which improves the wear properties of the cutting tool consequently machining time is also reduced.

Cryogenic treatment of high speed steel is one of the developments in manufacturing field. It offers much better wear resistance and hardness for the high speed steel. The conventional cryogenic treatment process involves cooling down the samples to 93k (-180°C) soaking for 15-20 minutes and then slowly heating back to room temperature in 6 hrs. In this project we have explained our approach and methodology to arrive at an optimum solution having two sample pieces of round of EN8 & EN19.

A method called deep cryogenic process, subjects steel components placed in a specially constructed tank to temperature around 77k (196°C) for half an hour using liquid nitrogen as the refrigerant. The results are encouraging that, there is 34.17 seconds reduction in machining time and there is no tool wear when machining EN8 and when machining EN 19 there is 22.04 seconds reduction in machining time and 0.03g increase in tool wear resistance.

Key Words: CRYOGENIC SOLUTION, Cryogenic treatment, tool wear.

1. INTRODUCTION

NASA engineers were the first to notice the effects of cold temperatures on materials. They noticed that many of the metal parts in the aircraft that had returned from the cold vacuum of space came back stronger than they were before flight. Since then sub-zero treatment (-80°C) has been used for many years, but with inconsistent results. Many of the inconsistencies were reduced by longer soaking periods and with deep cryogenic treatment (-190°C). Tool steels are high quality steels made to close compositional and physical tolerances. These are used to make tools for cutting, forming or shaping a material into a part or component adapted for a specific use. In service most tool steels are

subjected to extremely high loads that are applied rapidly. The material must withstand these loads a great number of times without breaking and without undergoing excessive wear or deformation. The performance of a tool in service depends on

- Proper tool design,
- Accuracy with which the tool is made,
- Selection of proper tool steel, and
- Application of proper heat treatment.

In the heat treatment of tool steels the problem of retained austenite after heat treatment has prevailed since the development of tool steels. The retained austenite is soft and unstable at lower temperatures that it is likely to transform into martensite. Freshly formed martensite is brittle and only tempered martensite is acceptable. The transformation of austenite into martensite yields 4% volume expansion causing distortion, which cannot be ignored. Therefore, the retained austenite should be transformed to the maximum possible extent before any component or tool is put into service. Treating the material after heat treatment at sub-zero or cryogenic temperatures transforms the retained austenite into martensite. Greater wear resistance can be obtained with longer soaking periods because of the formation of η -carbides which improves the wear resistance to the maximum possible extent.

2. METHODOLOGY

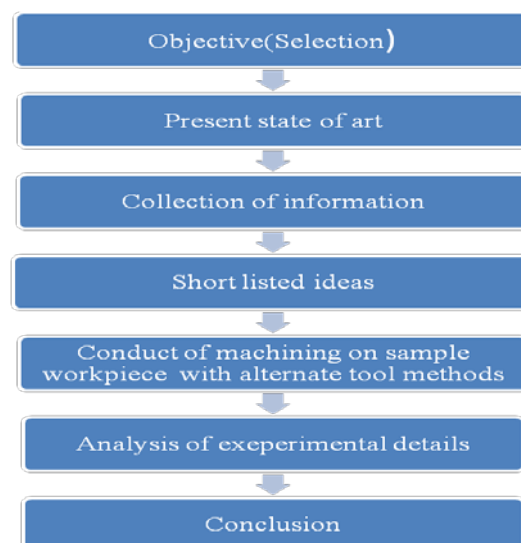


Fig: 1

3. CUTTING TOOL

3.1 Tool Life

Tool life improvement is essential to reduce the cost of production as much as possible. Cutting tools have a limited life due to inevitable wear and consequent failures and avenues must be found to increase tool life.

3.2 Tool Failure

The failure of cutting tools may be a result of :

- Wear and the flank of the tool
- Wear at the tool chip interface
- A combination of flank wear and cratering
- The sagging and crumbling of the cutting edge

3.3 Factors Affecting Tool Life

The life of a tool is affected by many factors such as cutting speed, feed depth of cut, chip thickness tool geometry, material of the cutting fluid and rigidity of the machine. The physical and chemical properties of work materials influence tool life by affecting from stability and rate of wear of tools. The nose radius also tends to affect the tool life.

3.3.1 Cutting Speed:

Cutting tool has the greatest influence on the tool life. As the cutting speed increases temperature increases. The heat is more concentrated on the tool than on the work and the hardness of the tool matrix changes so the relative increase in the hardness of the work accelerates the abrasive action. The criterion of wear may be wear for flank or crater if cutting speed is increased. It has been found that the cutting speeds greater than 100 m/min in carbide turning of steel, crater wear may become predominant. The relation of the cutting speed to the tool life expressed by the formula:

$$VT^n = C$$

V = cutting speed in m/min

T = tool life in min

N = exponent which depends on the tool and the work piece. The value of the exponent n is about 0.1 for high speed tools, 0.20 to 0.25 for carbide tools and 0.4 to 0.55 for ceramic tools. C = constant which is numerically equal to cutting speed that gives a tool life of one minute. The relation indicates that as cutting tools speed increases, tool life decreases.

3.3.2 Feed and Depth of cut:

The tool life is influenced by the feed rate also. With a fine feed area of chip passing over the

tool face is greater than that of coarse feed of a given volume of swarf removal, but to offset this chip will be greater. The effect of feed and depth of cut on tool life is given below:

$$V = \frac{257}{T^{0.19} \times S^{0.36} \times T}$$

S = feed in mm/min
T = depth of cut in mm

TYPICAL ANALYSIS

C.	Si.	Mn.	Cr.	Mo.
0.40%	0.25%	0.70%	1.20%	0.30%

Table: 1

Another relation between cutting speed for a given tool life, depth of cut and feed is given by,

$$V_t = \frac{CV}{T^x \times S^y}$$

V_t = cutting speed m/min

CV = a coefficient depending upon machine and work piece variables

X, Y = exponents which depend on mechanical properties of the material being machined.

The above relation shows that for a constant tool life cutting speed decreases with the increase of feed and depth of cut.

3.4 Properties of Machining Steels (Cutting Tool)

3.4.1 EN8

TYPICAL ANALYSIS

C.	Si.	Mn.	S.	P.
0.40%	0.25%	0.80%	0.015%	0.015%

Table: 2

Hardening:

Heat uniformly to 830/860C until heated through. Quench in oil or water. Can also be induction or flame hardened.

Tempering:

Heat uniformly and thoroughly at the selected tempering temperatures, between 550C to 660C and hold at heat for one hour per inch of total thickness.

Normalising:

Normalise at 830-860C, and cool in air.

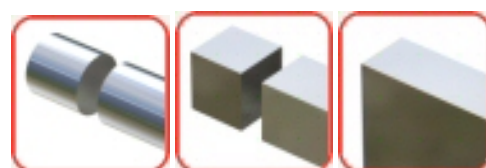


Fig: 2 Available sections of EN8

3.4.2 EN19

Hardening:

Heat uniformly to 820/840°C until heated through
Quench in oil.

Tempering:

Heat uniformly and thoroughly at the selected tempering temperature, and hold at heat for one hour per inch of total thickness.

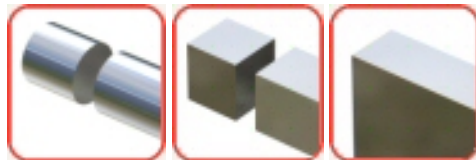


Fig: 3 Available sections of EN19

3.5 DEFINITION OF CRYOGENIC

In physics, cryogenics is the study of the production of very low temperature (below -150°C , -238°F or 123 K) and the behavior of materials at those temperatures. Rather than the familiar temperature scales of Fahrenheit and Celsius, cryogenicists use the Kelvin (and formerly Rankine) scales. A person who studies elements under extremely cold temperature is called a cryogenicist.

3.6 CRYOGENIC SOLUTION

The different types of cryogenic solutions used for the treatment of high speed steels. They are,

- Liquid Nitrogen (-196°C)
- Liquid Helium (-297°C)

3.6.1 Liquid Nitrogen

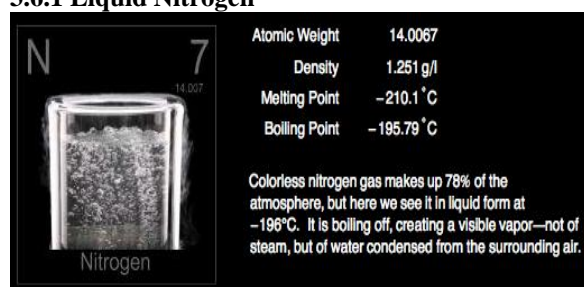


Fig: 4

Liquid nitrogen is a cryogenic liquid. At atmospheric pressure, it boils at -195.8°C . When insulated in proper containers such as Dewar flasks, it can be transported without much evaporative loss.

Like dry ice, the main use of liquid nitrogen is as a refrigerant. Among other things, it is used in the cryopreservation of blood, reproductive cells (sperm and egg), and other biological samples and materials. It is used in cold traps for certain laboratory equipment and to cool x-ray detectors. It has also been used to cool central processing units

and other devices in computers which are over clocked, and which produce more heat than during normal operation.

3.6.1.1 Properties of Liquid Nitrogen

Density	1.251 g/L
Melting point	63.153K (210°C)
Boiling point	77.36K (-195.79°C)
Critical point	126.19K
Heat of vapourization	5.56KJ/mol

In these two types of cryogenic solutions, we are selected to do our project in Liquid Nitrogen. Since it can be get from Veterinary hospital and easily available than liquid helium. The liquid nitrogen is used as a preservative to preserve the semen distributing injection in it.

4. EXPERIMENTAL WORK

4.1 Sample Material

There are different types of materials are used for machining purposes due to the requirements. We have selected the hardened steels for machining. They are EN8 and EN19.

For these two sample work pieces the hardness test is performed at various sections using Rockwell Hardness testing machine. Therefore the test readings are tabulated and it is shown

TESTS	EN8	EN19
T-1	34	19
T-2	37	21
T-3	34	23
T-4	38	24
T-5	37	19

Table: 3

Rockwell Hardness:

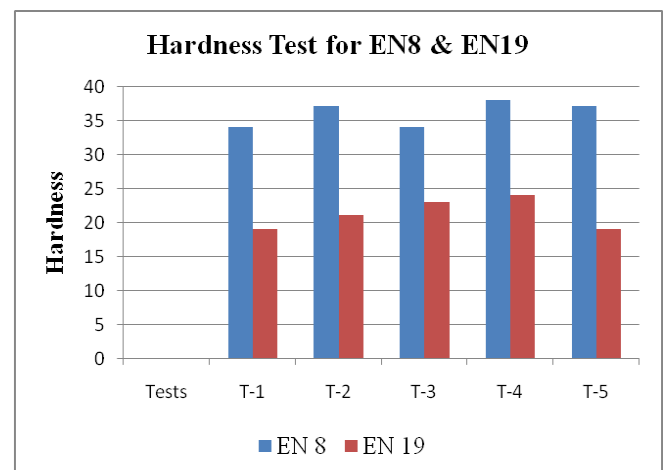


Fig: 5

4.2 Preparation of Tool

Although we have selected the normal high speed steel tool for machining, it is not possible to machine the hardened materials. Due to this drawback we prepared to dip the tool in the cryogenic solution for certain minutes. The hardness is tested for the tool before dipping and after dipping it in the solution.

4.3 Salt Spray Test

4.3.1 HSS tool without Cryogenic Treated

4.3.1.1 Test Parameters:

Chamber temperature : 34.5 – 35.5 °c
pH Value : 6.65-6.85
Volume of Salt Solution Collected : 1.0 – 1.5ml/hr
Concentration of Solution : 4.80 – 5.90% of Nacl
Air pressure : 14-18 Psi

4.3.1.2 Observation: Red Rust formation noticed at 12 Hours

4.3.1.3 Micro Photographs:



Fig: 6 Mag: 100x

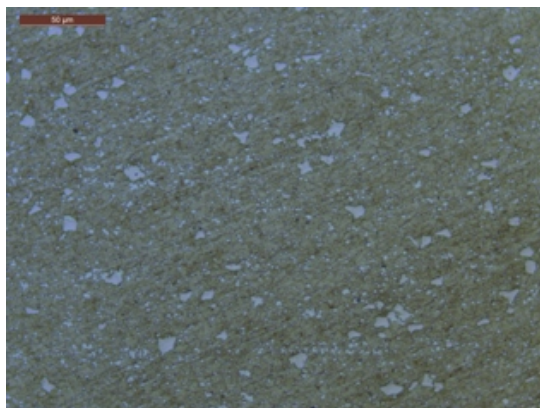


Fig: 7 Mag : 500x

4.3.2 HSS tool with Cryogenic Treated

4.3.2.1 Test Parameters:

Chamber temperature : 34.5 – 35.5 °c
pH Value : 6.65-6.85

Volume of Salt Solution Collected : 1.0 – 1.5ml/hr
Concentration of Solution : 4.80 – 5.90% of Nacl
Air pressure : 14-18 Psi

4.3.2.2 Observation: No Red Rust formation noticed at 12 Hours

4.3.2.3 Micro Photographs:

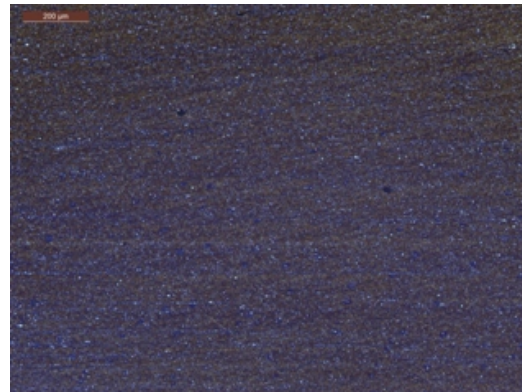


Fig: 8 Mag: 100x

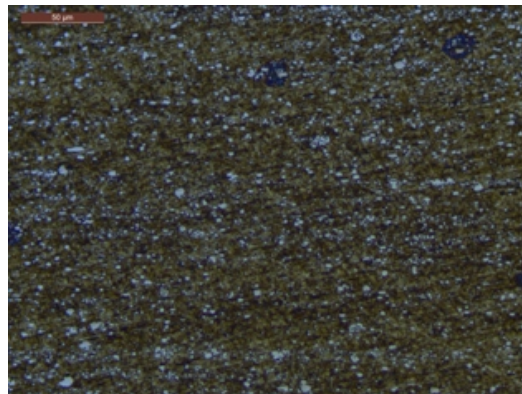


Fig: 9 Mag : 500x

4.4 Rockwell Hardness Test for Treated and Untreated Tool

TESTS	Untreated tool	HSS	Treated tool	HSS
T-1	64.8		65.4	
T-2	63.3		66.3	
T-3	64.1		65.8	

Table: 4

The hardness tests are done for a untreated single point cutting tool at various sections the average is **64.06 HRC**.

The hardness tests are done for a treated single point cutting tool at various sections the average is **65.83 HRC**.

Therefore the hardness is increased by **1.73 HRC** than the untreated tool.

5. PROCESS

5.1 Tool Process

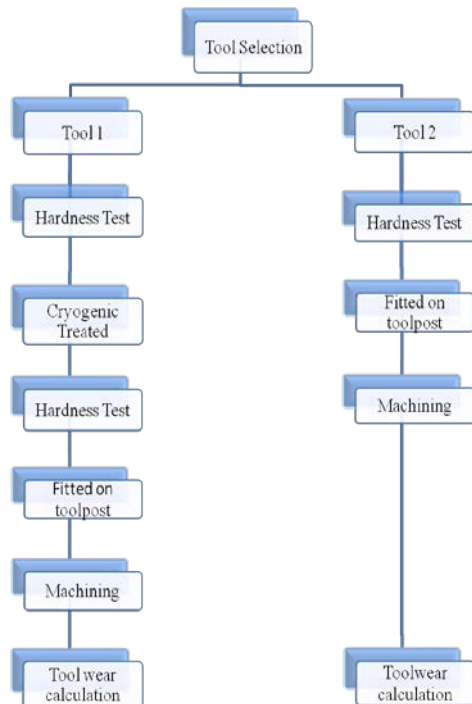


Fig: 10

5.2 Job Process

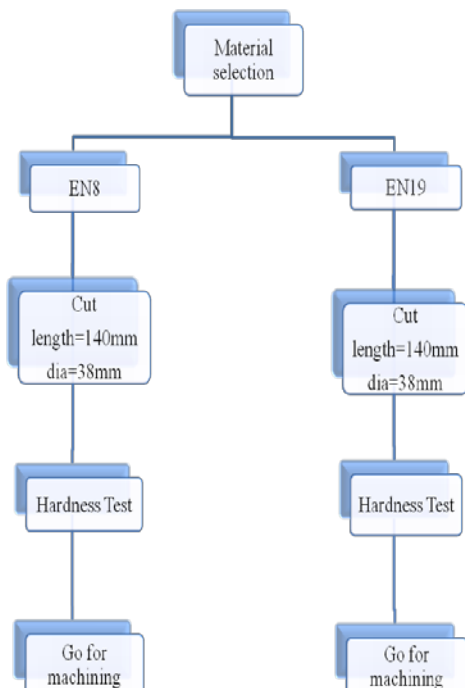


Fig: 11

6. OPERATIONS

6.1 DRAWING

JOB MACHINING DIAGRAM

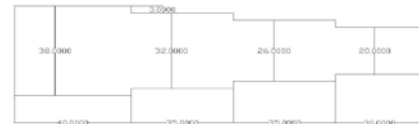


Fig: 12

6.2 Operation 1:

In this first operation we selected the machining material as En8 and performed the machining by reducing the material for various diameters of the desired length. The material is removed by turning operation performed in the lathe for a constant speed and feed. The depth of cut is given as 3mm for the metal removal for various diameters. In this shaft of 100mm length, the first 40mm is used for holding the shaft in the lathe.

Dia. Of Shaft (mm)	Tool Travel length (mm)	Tool Wt.		M.R.R (g)	M/C time (sec)
		Initial	Final		
38-32	35	49.26	49.25	98.2	143.23
32-26	35	49.25	49.23	87.47	130.07
26-20	30	49.23	49.21	46.48	61.91

Table: 5 EN8 Machined with Untreated HSS tool

Dia. Of Shaft (mm)	Tool Travel length (mm)	Tool Wt.		M.R.R (g)	M/C time (sec)
		Initial	Final		
38-32	35	55.27	55.27	156.1	89
32-26	35	55.27	55.27	106.12	84.01
26-20	30	55.27	55.27	83.31	59.71

Table: 6 EN8 Machined with Treated HSS tool

6.3 Operation 2:

In this second operation we selected the machining material as En19 and performed the machining by reducing the material for various diameters of the desired length. The material is removed by turning operation performed in the lathe for a constant speed and feed. The depth of cut is given as 3mm for the metal removal for various diameters. In this shaft of 140mm length, the first 40mm is used for holding the shaft in the lathe.

Dia. Of Shaft (mm)	Tool Travel length (mm)	Tool Wt.		M.R.R (g)	M/C time (sec)
		Initial	Final		
26-20	30	50.40	50.38	59.50	60.46
32-26	35	50.38	50.36	65.92	139.6
38-32	35	50.36	50.35	73.48	146.77

Table: 7 EN19 Machined with Untreated HSS tool

Dia. Of Shaft (mm)	Tool Travel length (mm)	Tool Wt.		M.R.R (g)	M/C time (sec)
		Initial	Final		
26-20	30	55.31	55.31	62.16	56.75
32-26	35	55.31	55.30	69.43	120.98
38-32	35	55.30	55.29	75.88	102.99

Table: 8 EN19 Machined with Treated HSS tool

It may be concluded from these tests that treatment at -196°C improves wear resistance and reduces the machining time much more.

6.3 Cryogenic Treatment Enhances Performance of Metals

Cryogenic treatment, which is sometimes called cryogenic processing, utilizes ultra-cold temperatures to modify the micro-structure of metals and other materials. Cryogenic treatment has been widely adopted as a cost reduction and performance enhancing technology. Cryo treatment is also used as an enabling technology, when its stress relieving benefits are utilized to permit the fabrication (or machining) of critical tolerance parts.

The Cryo treatment process uses sub-zero temperatures down to -300°F to modify the micro-structure of the material. Cryogenic treatment promotes additional transformations in metals. It ultimately improves the performance of the metal.

Cryo treatment is an extension of the heat-treating process that further enhances metals in the following ways:

- Relieves residual stresses
- Promotes a more uniform micro-structure
- Precipitates eta-carbides in steels for increased resistance to wear.
- Cryo treated metals enjoy the following benefits:
- Longer life due to reduced wear
- Less failures due to cracking that result from the propagation of stress lines
- Improved thermal properties
- Better electrical properties with reduced electrical resistance
- Reduced coefficient of friction on polished metals
- Less creep & walk, and improved flatness for critical tolerance parts
- Easier machining, polishing and grinding for better edges and finishes.

Cryogenic treatment can make a major contribution to solving these problems:

- High abrasive wear in cutting tools, molds, dies, brake rotors, gears, engine components, etc.
- High corrosive wear in chemical, food, and oil equipment applications.
- High erosive wear from, water, slurries and other abrasive grit carriers.
- Distortions induced by design, forming, machining or environment.
- Stress relief in complex tools, components, and welds.
- Stress relief cracking of weld zones.
- Surface finishing in any application where long life is needed.
- Stabilization in parts and components as a result of stresses.
- Machinability in aluminum and copper parts.
- Electrode life in copper resistance welding electrodes.

7. Advantages:

- Increases abrasive wear resistance.
- Requires only one permanent treatment.

- Creates a denser molecular structure. The result is a larger contact surface area that reduces friction, heat and wear.
- Eliminates thermal shock through a dry, computer controlled process.
- Transforms almost all soft retained austenite to hard martensite.
- Forms micro fine carbide fillers to enhance large carbide structures.
- Increases durability or wear life.
- Decreases residual stresses in tool steels.
- Decreases brittleness.
- Increases tensile strength, toughness and stability coupled with the release of internal stresses.

8. CONCLUSION

8.1 Difference in Tool wear

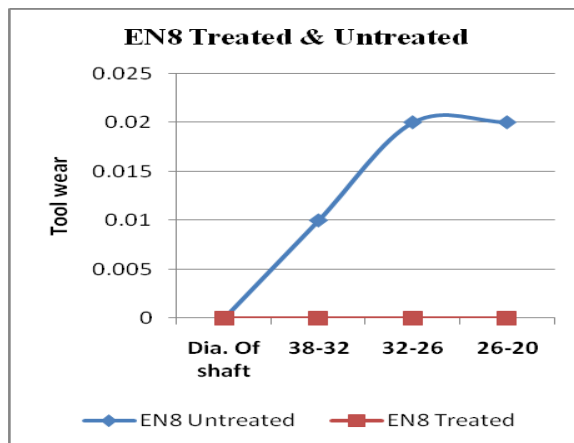


Fig 13

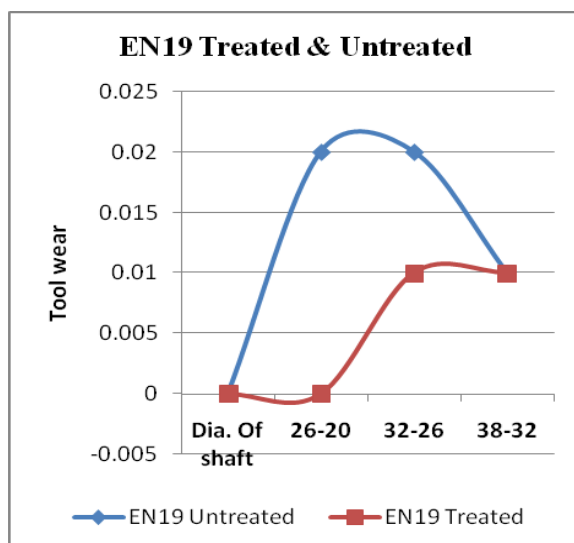


Fig 14

8.2 Difference in Machining Time

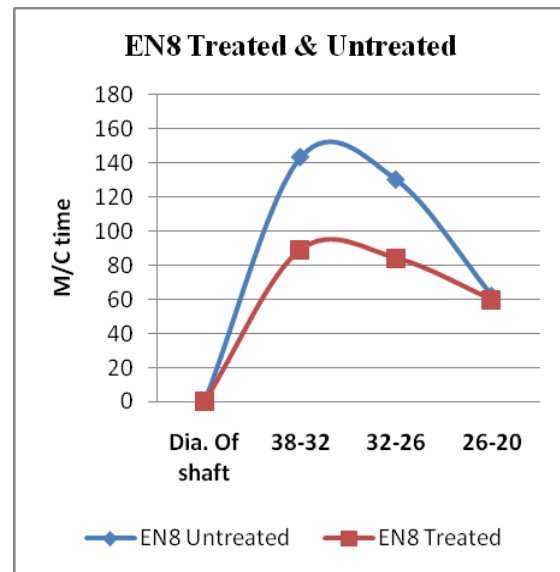


Fig: 15

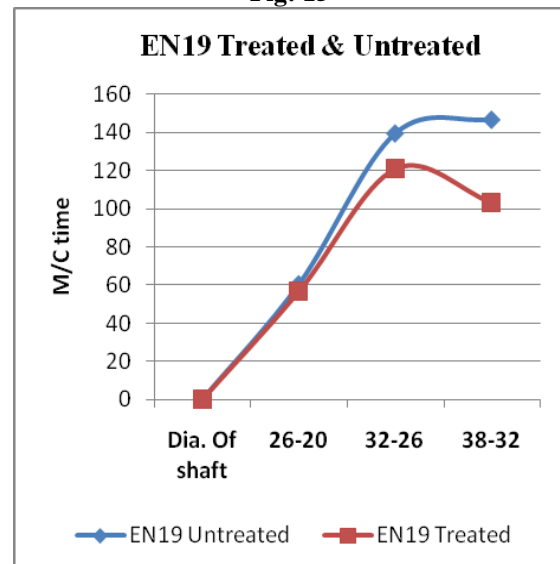


Fig: 16

It will be evident experimental details there is 34.17 seconds decreases in machining time and there is no tool wear when machining EN8 and when machining EN 19 there is 22.04 seconds decrease in machining time and 0.03g increase in tool wear resistance.

Deep cryogenic treatment has shown to result in significant increase in the wear resistance and correspondingly reduces machining time of steels such as EN8 and EN19. The basic mechanisms at work during the cryogenic process helps to control wear by producing a tough surface, which helps to prevent particles from tearing out of the material and resist penetration of the surface by other particles.

This concept can be extended to machine various work pieces of different material.

9. REFERENCES

- [1] Astakhov, Viktor P. and J. Paulo Davim, 2008. *Machining Fundamentals and Recent Advances*, Springer, Portugal, 2008, p.48-52
- [2] Blackley W.S., Scattergood R.O., 1991. Ductile Regime Model for Diamond Turning of Brittle Material. *Precision Engineering* 13(2). pp. 95-102
- [3] Bouzid Sa'I, 2005. An Investigation of Tool Wear in High-Speed Turning of AISI 4340 Steel, *International Journal Advance of Manufacturing Technology* 26. Pp. 330–334
- [4] Fang F.Z., Venkatesh V.C., 1998. Diamond cutting of Silicon with Nanometric Finish. *Annual CIRP* 47(1) pp. 45-49
- [5] Feng, C., 2001. An Experimental Study of the Impact of Turning Parameters on Surface Roughness. *Proceedings of the 2001 Industrial Engineering Research Conference*. Institute of Industrial Engineers.
- [6] Ghani A. K., Choudhury, Husni., 2001. Study of Tool Life, Surface Roughness and Vibration in Machining Nodular Cast Iron with Ceramic Tool, *Journal of Materials Processing Technology* 127 (2002) pp. 17-22
- [7] Gunay M., 2003. Experimental investigation of the influence cutting tool rake angle on forces during metal cutting, M.Sc. Thesis, Gazi University Institute of Science and Technology, Ankara, Turkey, pp. 69-93.
- [8] Gunay, M., Aslan E., Korkut, I., Seker, U., 2004. Investigation of the effect of rake angle on main cutting force. *International Journal of Machine Tools and Manufacture*, 44, 953-959.
- [9] Gunay M., Korkut I., Aslan E., Seker U., 2005. Experimental Investigation of the effect of cutting rake angle on main cutting force, *Journal of Materials Processing Technology*, pp. 44- 49
- [10] Gunay, M, 2008. Investigation of the interaction between the surface quality and rake angle in machining of AISI 1040 steel, *Journal of Engineering and Natural Sciences*, Vol. 26.
- [11] Jaspers P.F.C., Serge, 1999. *Metal Cutting Mechanics and Material Behaviour*. Ph.D Thesis, Technischueniversiteit Eindhoven.
- [12] Khan A.A., Hajjaj S.S., 2006. Capabilities of Cermets Tools For High Speed Machining of Austenitic Stainless Steel, *Journal of Applied Sciences* 6 (4): pp. 779-784.
- [13] Khan, A.A., A.N.R. Zuraida, and Y. Izayusmati, 2002. High Speed Milling of Cast Iron and Medium Carbon Steel using Cermet and Carbide Tools. *Proceeding of the BSME-ASME International Conference on Thermal Engineering*, 31 Desember 2001, 2 January 2002, Dhaka, Bangladesh, pp. 711-717.
- [14] Kılıçkap E., Cakir O., Aksoy M., Inan A., 2005. Study of tool wear and surface roughness in machining of homogenised SiC-p reinforced aluminium metal matrix composite, *Journal of Materials Processing Technology*, Vol 164-165, 15 May 2005, pp. 862-867
- [15] Komanduri R., Chandrasekaran N., Raff L.M., 1998, Effect of Tool Geometry in Nanometric Cutting: A Molecular Dynamics Simulation Approach. *Wear* 219, pp. 84-97.
- [16] Lin, H.M., Liao, Y.S., Wei, C.C., 2008. Wear Behavior in turning hardness alloy steel by CBN tool, *Wear* 264, pp. 679-684
- [17] Ozses, B., 2002. Different cutting conditions effect on surface roughness in computer numerical controlled machine tools, MSc Thesis, Gazi University Institute of Science and Technology, Ankara.
- [18] Rao, B.C., Gao R.X., Friederich C.R., 1995. Integrated Force Measurement for On-line Cutting Geometry Inspection. *IEEE Trans. Instruments. Measurement*. 44pp. 977-980.
- [19] Senthilkumar A., Rajadurai A., and Sornakumar A., 2003. Machinability of hardened steel using alumina based ceramic cutting tools, *International Journal of Refractory Metals and Hard Materials*, 21 pp. 109-117.
- [20] Shaw, M.C., *Metal Cutting Principles*, 1984. Oxford University Press, London.
- [21] Thamizhmanii S., Hassan S., 2006. Analyses of roughness, forces and wear in turning gray cast iron, of Achievements in Materials and Manufacturing Engineering, VOLUME 17, ISSUE 1-2 July-August.
- [22] Thamizhmanii S., Kamarudin K., Rahim E.A., Saparudin A., Hassan S., 2007. Tool Wear and Surface Roughness in Turning AISI 8620 using Coated Ceramic Tool, *Proceedings of The World Congress on Engineering Vol. II WCE 2007*, London, UK.
- [23] Thomas, M., Beauchamp Y., 2003. Statistical investigation of modal parameters of cutting tools in dry turning. *International Journal of Machine Tools and Manufacture*, 43, 1093-1106.
- [24] Trent, E.M. and Wright, P.K., 2000. *Metal Cutting*, 4th ed., Butterworth-Heinemann, Boston, MA.

Design and Analysis of a Heat Sink for a High Power LED System

J. Padmaja ^{a*} A. Ravindra ^b

Department of Mechanical Engineering
Mallareddy College of Engineering
Sec-bad-500100,India.

Abstract - Recently, the high-brightness LEDs have begun to be designed for illumination application. The enhanced electrical currents accustomed drive LEDs result in thermal problems. Thermal management for crystal rectifier module could be a key style parameter as high operation temperature directly affects their most light-weight output, quality, dependability and life time. during this study a conductor is intended to dissipate heat created by the contact of a high power crystal rectifier light-weight. the look involves a series of crystal rectifier lights in a very industrial setting that required to be cooled. the warmth sinks area unit designed to use water (60psi) because the fluid to cool down the LED's properly. every conductor could be a compact device with semi-circular fins to function buffer plates to reinforce heat transfer. The mass flow rates of the fluid varied because the parameter for explicit fin styles. 3 mass flow rates and 4 fin geometries were investigated parametrically. the ultimate results of the study proposes Associate in Nursing optimum style with minimum pressure drop across every conductor whereas maintain the crystal rectifier junction temperature underneath check.

Key words: LED, p-n junction, heat sink, heat exchanger, fin etc.

Nomenclature

Φ	Dissipation function due to viscous forces	T	Time scale
S_h	Energy Source	$\frac{T}{v'^2}$	Velocity scale
G	Generation	k	Turbulence kinetic energy
RNG k- ϵ		CFD	Computational Fluid Dynamics
K	Thermal conductivity	LED	Light Emitting Diode
ϵ		COB	Chips On Board
G_k	Generation of turbulence kinetic energy due to the mean velocity gradients	Re	Reynolds Number
G_b	Generation of turbulence kinetic energy due to buoyancy	ΔP	Pressure Difference
$C_{1\epsilon}, C_{2\epsilon}, C_{3\epsilon}$	Constants	SM_x, SM_y and SM_z	The source terms
ρ	Density	T	Temperature
u, v and w	velocity components	α	Thermal Expansion
p, P	Pressure	C_μ	Turbulence model constant
S	Source terms	C_L	Co-efficient of lift
T	viscous stress	L'	Variable length
μ_t	Eddy-viscosity		

1. INTRODUCTION

In recent years High power LED's are becoming more popular because of their low power usage. About twenty percent of power input to LED is converted into the light energy and the rest into heat, if the heat could not be dissipated immediately, it will concentrate on the tiny LED chip and cause the junction temperature of the chip to rise to a harmful level. LED is particularly suitable for illumination due to the advantages of lower power consumption, little infrared emission, no UV, and relatively long life. Even though LEDs may have a very long life, poorly designed LED lamps can experience a short life and a poor lighting quality. The lifetime and lighting quality of LED lamps largely depend on junction temperature. LED lamps may experience wavelength shifts, epoxy degradation and low quantum efficiency, under high junction temperature.

Narendran N et al [1] have experimentally verified that the LED life diminish with rise in junction temperature in an exponential manner. Therefore, low junction temperature is essential for LED performance, which is a characteristic feature of LED lamp versus conventional lighting. Since the market requires that LEDs have high power and packaging density, it poses a contradiction between the power density and the operation temperature, especially when LEDs are operated at a normal or higher driver current to obtain the desired lumen output. So heat dissipation becomes a key issue in the application of high-power LED.

Maw-Tyan Sheen et al [2] were stated that micro-tube water-cooling systems rendered an improvement in thermal management that effectively decreases the thermal resistance and provides very good thermal dissipation.

Simulation and experimental results show that the LED module with a water-cooling tube exhibits better thermal performances than the others. Dae-Whan Kim et al [3] demonstrated that the two-phase thermo fluid characteristics of a dielectric liquid data obtained for single-phase water yielded excellent agreement with predictions for the convective heat transfer coefficients, dielectric fluids and therefore the back surface of a full of life electronic part, supply a most promising approach for cooling high-powered LEDs.

T.Cheng et al[4] were demonstrated Increasing pump rate of flow can build a pointy increase of the flow resistance. the fabric of device shell with high thermal physical phenomenon will ameliorate the cooling performance, however the perform is restricted. in line with preliminary tests and numerical optimization, An optimized small jet cooling system is unreal and applied in thermal management of a light-emitting diode lamp. The temperature check demonstrates the cooling system works well.

Ming-Tzer Lin et al [5] were explained water-cooling container in the high power LED array gave more efficient convection and the heat created by the LEDs was easily removed in the experiments. It was shown that micro-tube water-cooling systems rendered an improvement in thermal management that effectively decreases the thermal resistance and provides very good thermal dissipation.

2. HEAT GENERATION AND TRANSFER IN LED

LEDs produce light and heat by means of different mechanisms as compared to the incandescent bulb. By supplying electrical energy, the electron energy will be partly transformed into light and fairly into heat. Apparently the research into LED technology is paying attention on optimizing the light emitting efficiency.

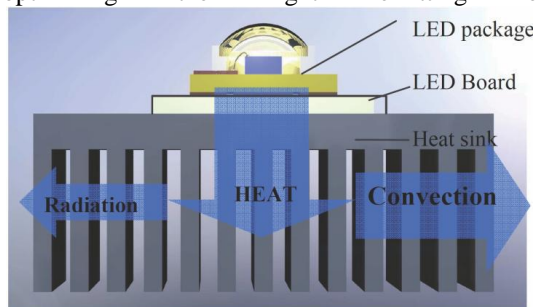


Figure 1. shows various means of heat dissipation from LED

Although each module has a unique structure, generally the LED package consists of a LED chip enclosed in a package of a polymer lens and a plastic carrier holder. Heat is generated by the LED chip inside the package. Although some amount of heat can be dissipated to surroundings by radiation and natural convection along the package surfaces, most of the heat will be conducted to the heat sink. The major part of the heat is transferred to the surroundings by convection from an optimized designed heat sink. On the other hand, radiation on the surface of the heat sink occurs

naturally and it cannot be ignored as the average critical temperature of the LED module is high.

2.1 ADHESIVE

Adhesive is commonly used as bonding material between LED and board, and board and heat sinks. Using a thermal conductive adhesive can optimize the thermal performance. Epoxy is costlier than tape, however provides a larger mechanical bond between the heat sink and element, in addition as improved thermal conduction. Most epoxies are two-part liquid formulations that has got to be totally mixed before being applied to the heat sink, and before the heat sink is placed on the element.

The epoxy is then cured for a nominative time, which might vary from a pair of hours to forty eight hours. quicker cure time are often achieved at higher temperatures. The surfaces to that the epoxy is applied should be clean and freed from any residue [6].

2.2 HEAT SINK

Heat flows from the LED source to outside through the Heat sinks. Heat sinks can dissipate heat in three ways: conduction (heat transfer from one solid to another), convection (heat transfer from a solid to a moving fluid), or radiation.

2.2.1 Material – The thermal conductivity of the material plays an important role in conduction of heat from the heat sink. Normally this is aluminum (Al), even though copper may be used with an advantage for flat-sheet heat sinks. More advanced materials like thermoplastics that are used when heat dissipation requirements are lower than normal or complex shape would be advantaged by injection molding, and natural graphite solutions which offer better thermal transfer than copper with a lower weight than aluminum plus the ability to be formed into complex 2D shapes. Graphite is considered an interesting cooling solution and does come at a higher production cost. Heat pipes may also be further added to aluminum or copper heat sinks to ease spreading resistance.

2.2.2 Shape - Heat transfer takes place at the surface of the heat sink. Therefore, heat sinks should be considered to have a large surface area. This goal can be reached by using a large number of fine fins or by increasing the size of the heat sink itself.

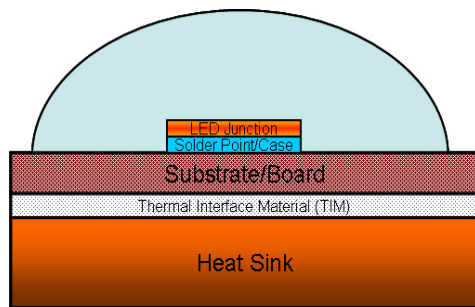


Figure 2 Construction of LED with a Heat Sink

2.2.3 Surface Finish - Thermal radiation of heat sinks could be a operate of surface finish, particularly at higher temperatures. A painted surface can have a greater emissivity than a bright, unpainted one. The impact is most outstanding with flat-plate heat sinks, wherever concerning tierce of the heat is dissipated by radiation. Moreover, a perfectly flat contact space permits the employment of a agent layer of thermal compound, which is able to cut back the thermal resistance between the heat sink and LED supply. On the opposite hand, anodizing or etching also will decrease the thermal resistance. Heat-sink mountings with screws or springs are better higher than regular clips, thermal conductive glue or sticky tape.

2.3 PCB (Printed Circuit Board)

MCPCB - MCPCB (Metal Core PCB) are those boards which incorporate a base metal material as heat spreader as an integral part of the circuit board. The metal core usually consists of aluminum alloy. Furthermore MCPCB can take advantage of incorporating a dielectric polymer layer with high thermal conductivity for lower thermal resistance.

Separation - Separating the LED drive circuitry from the LED board prevents the heat generated by the driver from raising the LED junction temperature.

2.4 PACKAGE TYPE

Flip chip - The concept is similar to flip-chip in package configuration widely used in the silicon integrated circuit industry. Briefly speaking, the LED die is assembled face down on the sub-mount, which is usually silicon or ceramic, acting as the heat spreader and supporting substrate. The flip-chip joint can be eutectic, high-lead, lead-free solder or gold stub. The primary source of light comes from the back side of the LED chip, and there is usually a built-in reflective layer between the light emitter and the solder joints to reflect the light emitted downwards up. Several companies have adopted flip-chip packages for their high-power LED, achieving about 60% reduction in the thermal resistance of the LED while keeping its thermal reliability.

3. DESIGN AND CFD SIMULATION

The main objective of this project is analyze the performance of a heat sink which uses tap water to maintain and reduce the junction temperature while providing warm water for heating purpose.

3.1. PARAMETERS

The parameters that affect the study are volume, temperature, time and height of the heat exchanger. How much volume of water is sent into the heat exchanger, water with ambient temperature is sent into the exchanger.

- Heat Input 56 W (20% illumination power of 70W LED)
- Dimensions are according to the drawing.
- Variation of Thickness in the inner cylinder
- Flow rate 0.15kg/s, 0.25kg/s and 0.44kg/s

3.2. DESIGN METHODOLOGY

The commercial LED which we started working on is WHITELION LED product High bay Bridge lux LED 70W, 5400Lm. It is an chip on Board LED suitable for outdoor applications especially for the warehouses and factories. The specifications are as follows

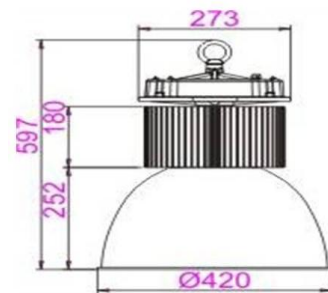


Figure 3 dimensions (mm) of the 70W COB White lion LED light.

- LED High Bay Light 70W as high efficiency replament for 640W Sodium/Metal Halide
- 70W LED High Bay Lights reduces energy savings up to 80%
- LED 70W High Bay reaches full brightness instantly.
- Operating temperature range between -45° and 60°C
- Rated life of 50,000 hours
- 70W COB LED High Bay IP65 is suited to install on the 9-12M height, ideal for warehouse, factory and industry spaces
- Input Voltage: AC85-265V, 50/60Hz



Figure 4 3D view of White lion LED Light

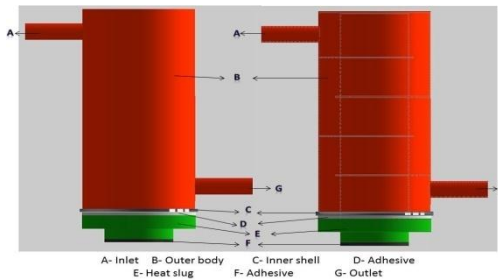


Figure 5 The model and parts

Figure 5 is the diagram for the newly designed heat sink in this project. In the design, inner shell (C) and heat slug (E) are made of Aluminum. The Adhesives (D and F) are CoolPoly® E8103 Thermally Conductive Thermoplastic Elastomer (TPE). The properties of these materials are listed below.

Table 1 Material properties of solid materials

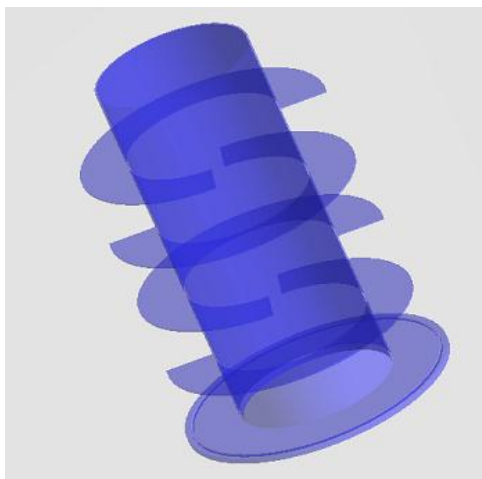


Figure 6 The inner shell, made of Aluminium with fin partitions

Above figure shows the inner shell made of Aluminum with partitions to guide the flow. Each circular fin is designed to be segmental to cover 270° to allow flow to go in a cross flow pattern to take advantage of high heat transfer in the cross flows. There are total 4 fins. The inner shell passes the water with guiding towards outlet. This inner shell is made up of Aluminium material.

3.3. Governing Equations

Numerical simulations are performed to predict the flow and heat transfer characteristics of the designed heat sink. This chapter gives descriptions of the mathematics model used.

3.4. Governing Equations of Fluid Flow

The general form of fluid flow and heat transfer equations of incompressible for a Newtonian fluid in steady state flow is given as follows:

$$\text{mass:} \quad \nabla \cdot (\rho \vec{V}) = 0$$

Momentum equation:

$$\frac{\partial}{\partial x_j} (\rho u_i u_j) = -\frac{\partial P}{\partial x_i} + \frac{\partial}{\partial x_j} \left(\mu \left(\frac{\partial u_j}{\partial x_i} + \frac{\partial u_i}{\partial x_j} \right) - \rho \overline{u'_i u'_j} \right)$$

energy:

$$\frac{\partial}{\partial x_i} (\rho u_i c_p T) = \frac{\partial}{\partial x_i} \left(\frac{\mu}{\sigma} \frac{\partial T}{\partial x_i} - \rho c_p \overline{u'_i \theta} \right)$$

3.5. RNG k-ε model equations:

RNG turbulence model (Yakhot and Orzag, 1986) differs from the standard k-ε model in few aspects. The RNG model solves an additional term in the ε equation compared to the standard k-ε model and it solves an analytical formula

Material	Thermal conductivity (W/m-K)	Specific heat (J/kg-K)	Density kg/m ³
Adhesive	5	1940	1130
Aluminum	202.4	871	2719

for turbulent Prandtl numbers, while the standard k-ε model uses user-specified, constant values. The RNG model also provides for an option to treat the effective viscosity using the analytically derived formula that accounts for low-Reynolds-number effect (Yakhot and Orzag, 1986). The kinetic energy of the turbulence, k and its dissipation rate, ε are governed by separate transport equations. The RNG-based k-ε turbulence model contains very few empirically adjustable parameters.

$$\frac{\partial}{\partial x_i} (\rho k u_i) = P - \rho \epsilon + \frac{\partial}{\partial x_j} \left[\left(\mu + \frac{\mu_t}{\sigma_k} \right) \frac{\partial k}{\partial x_j} \right] + S_k$$

$$\frac{\partial}{\partial x_i} (\rho \epsilon u_i) = \frac{C_{\epsilon 1} P - C_{\epsilon 2} \rho \epsilon}{T} + \frac{\partial}{\partial x_j} \left[\left(\mu + \frac{\mu_t}{\sigma_\epsilon} \right) \frac{\partial \epsilon}{\partial x_j} \right] + S_\epsilon$$

$$\frac{\partial}{\partial x_i} (\rho \overline{v'^2} u_i) = \rho k f - 6 \rho \overline{v'^2} \frac{\epsilon}{k} + \frac{\partial}{\partial x_j} \left[\left(\mu + \frac{\mu_t}{\sigma_k} \right) \frac{\partial \overline{v'^2}}{\partial x_j} \right] + S_k$$

$$f - L^2 \frac{\partial^2 f}{\partial x_j^2} = (C_1 - 1) \frac{3}{T} \frac{\overline{v'^2}}{k} + C_2 \frac{P}{\rho k} + \frac{5 \overline{v'^2}}{T} + Sk \quad 3.3.7$$

where

$$P = 2\mu_t S^2 \quad (i)$$

$$T = \min \left[T', \frac{\alpha}{\sqrt{3}} \frac{k^{3/2}}{v^2 C_\mu \sqrt{2S^2}} \right] \quad (ii)$$

$$L = C_L \max \left[L', C_\eta \left(\frac{v^3}{\varepsilon} \right)^{1/4} \right] \quad (iii)$$

$$T' = \max \left[\frac{k}{\varepsilon}, 6 \sqrt{\frac{v}{\varepsilon}} \right] \quad (iv)$$

$$L' = \min \left[\frac{k^{3/2}}{\varepsilon}, \frac{1}{\sqrt{3}} \frac{k^{3/2}}{v^2 C_\mu \sqrt{2S^2}} \right] \quad (v)$$

The eddy-viscosity (μ_t) is modeled using one time scale (T) and one velocity scale ($\overline{v'^2}$) instead of the turbulence kinetic energy (k) used in the k - ε model. The velocity variance scale ($\overline{v'^2}$) can be thought of as the velocity fluctuations normal to the streamlines. This distinguishing feature of $\overline{v'^2}$ - f model seems to provide a proper scaling in representing the damping of turbulent transport close to the wall, a feature that k does not provide in other eddy-viscosity model.

3.6. PRE-PROCESSING AND MESH

In CFD calculations, there are three main steps.

- 1) Pre-Processing
- 2) Solver Execution
- 3) Post-Processing

Pre-Processing is the step where the modeling goals are determined and computational grid is created. In the second step numerical models and boundary conditions are set to start up the solver. Solver runs until the convergence is reached. When solver is terminated, the results are examined which is the post processing part.

In this study, the aim is to investigate the cooling characteristics of different heat sinks designed to cool the Light Emitting Diode (LED). So, an adequate numerical model is to be created. There are two important points here. The first one is the size of the domain, and the second one is the quality. Model size is the computational domain where the solution is done. It is important to build it as small as possible to prevent the model to be computationally expensive. On the other hand it should be large enough to resolve all the fluid and energy flow affecting the heat transfer around the LED. Inside the LED, Adhesive, and Heat slug are modeled. Since there were no CAD data for the chosen problem geometry, all the devices inside the case are created using ANSYS FLUENT Design Modeler creation tools. A high quality unstructured tetrahedral mesh is generated before the solution of the governing equations.

A top quality unstructured tetrahedral mesh is generated before the solution of the governing equations. A wall is formed between the water and thus lid surface so on have a interface between the two mediums to transfer heat between them. Linear tetrahedral parts are either constant stress parts with four nodes or linear stress parts with ten nodes. These parts area unit developed in 3-dimensional house with three degrees of freedom per node; these area unit the translational degrees of freedom within the X, Y and Z directions, severally. The ten-node part is Associate in Nursing isoparametric part and stresses area unit calculated at the nodes. the subsequent element-based loadings could also be applied:

Uniform or hydrostatic pressure on the element faces. Thermal gradients defined by temperatures at the nodes. Uniform inertial load in three directions.

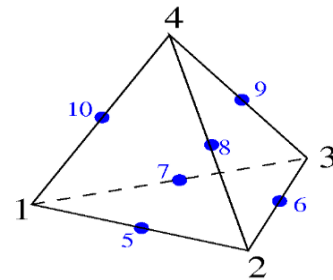


Figure 7 10-Noded Tetrahedral Element

Table 2 Meshing information of each part

Domain	Nodes	Elements
Adhesive	5957	11943
Big Adhesive	8199	16692
Heat slug	67561	193833
Inner shell	187740	406418
Outer body	347414	972142
All parts	616871	1601028

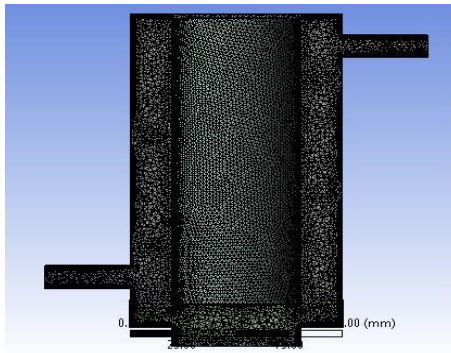


Figure 8 the half section of the mesh

3.7. SOLVER SETTINGS

Settings are applied by ANSYS FLUENT to solve for Temperature variations. The model is having with Pressure based condition, energy condition is enabled for temperature variations, and then atmospheric pressure is taken as 60 psi to solve this analysis. Desired boundary conditions are applied by selecting boundary conditions tab. The wall created for the interface between the Fluid and Solid medium is set as 'Interface' and is coupled. Inlet has different mass flow rates for each case. Pressure velocity coupling method is SIMPLE (Semi Implicit Pressure Linked Equation). For solution methods Solution methods Pressure body force weighted, momentum, turbulent kinetic energy, turbulent viscosity, energy are first order upwind. Solution controls under relaxation factors values are taken as Pressure 0.3, density 1, body forces 1, momentum 0.3, turbulent kinetic energy 0.8, turbulent viscosity 1, energy 0.8. For all cases, since the Reynolds number being greater than transition limit value, a RNG Turbulence model was sufficient. In this analysis flow model is k- ϵ turbulence with RNG model. The residual monitor is checked to print and plot the integration. The iterations are run at least 2000 in each case to ensure convergence of solutions.

4. RESULTS AND DISCUSSION

4.1. Effect of Heat Sink Thickness

With the increase in the thickness of the inner cylinder of the heat sink the amount of aluminum increases and volume of water passing through decreases. So an optimum solution is considered by minimum thickness of the material and maximum heat transfer to the water. Several thickness 0.1-0.25 inches with an interval of 0.5 inches are tested and the results are shown below with a constant mass flow rate of 0.15kg/s and varying thickness. All other are maintained as follows

Inlet Temperature	293K
Inlet Pressure	60 psi
Heat	56Watts

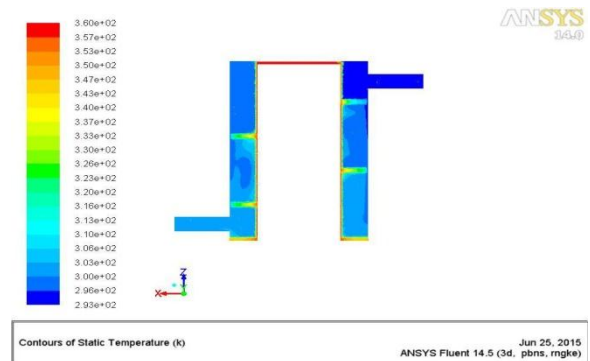


Figure 9 the temperature contour for 0.1inch thickness inner cylinder with 0.15kg/s mass flow rate

Fig.9 shows the temperature contour variation for 0.1 inch thickness inner cylinder with 0.15kg/s mass flow rate. Temperature variation at the outlet is 299.35 K.

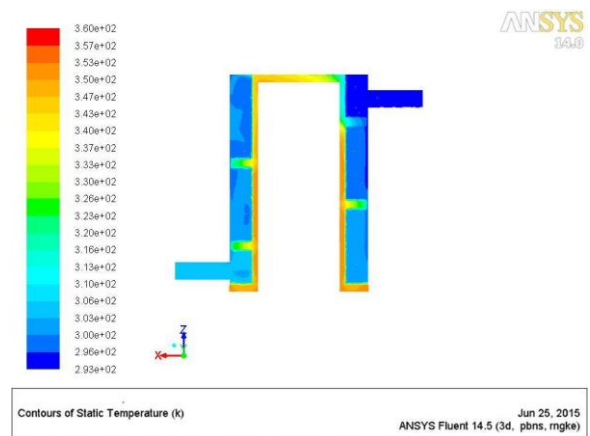


Figure 10 the temperature contour for 0.2 inch thickness inner cylinder with 0.15kg/s mass flow rate

Figure 10 shows the temperature contour variation for 0.2 inch thickness inner cylinder with 0.15kg/s mass flow rate. Temperature variation at the outlet is 302.35 K.

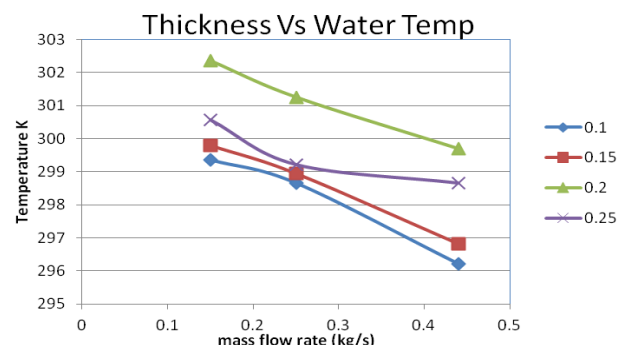


Figure 11 Variation of Water Temperature with mass flow rate and thickness of Inner Cylinder

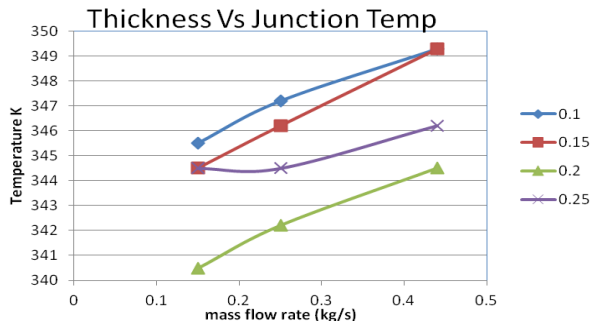


Figure 12 Variation of Junction Temperature with mass flow rate and thickness of Inner Cylinder

The above graph shows at different thickness to temperature variation graph at different mass flow rate. Here mass flow rate and thickness varies, then the temperature variation is increasing and then decreasing at different thickness. For 0.15kg/s case with 0.1 inch thickness temperature (299.35 K) variation is minimum, at 0.2 inch thickness temperature is maximum (302.35 K), and then it is decreasing to up to minimum (300.56 K). With increase in the thickness the volume of material increase and there is a decrease in the volume of water, in turn resulting less contact with heated surface.

4.2. Effect of Reynolds number

With the increase in the Reynolds number (flow rate) for the fixed thickness inner cylinder the temperature of the outlet water decreased. This is because of more velocity and less time of contact between the water and inner cylinder.

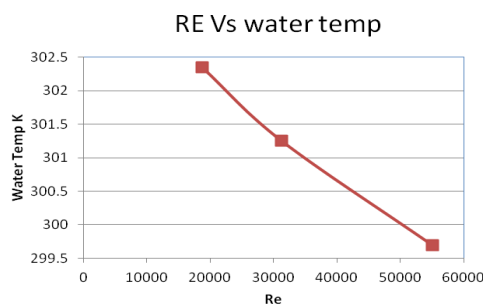


Figure 13 Temperature variation at 0.2 inch thicknesses.

The above graph shows at different Reynolds number to temperature variation graph at 0.2 inch thickness. Here thickness is constant mass flow rate is varying, and then the temperature variation is increasing and then decreasing at different mass flow rate. At $Re = 18768$ (0.15 kg/sec) the temperature variation is maximum (302.35 K), at $Re = 55052$ (0.44 kg/sec) mass flow rate the temperature is minimum (299.69 K). With decrease in the mass flow rate the temperature will further increase, but the water moving needs to maintain pressure in order to get the flow all along the pipes. So the further reduction of mass flow rate is not considered.

With increase in the mass flow rate for the constant pressure 60psi, the pressure drop is calculated and the graph below shows the variation of Reynolds number with the pressure drop.

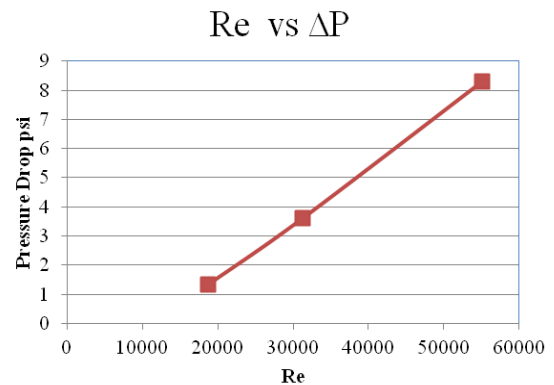


Figure 14 Variation of pressure drop with Reynolds number for a 0.2 inch thick inner cylinder

Fluent results for the cases, with all the input parameters and the desired output values are documented in the table below. Final Junction temperature shows the junction temperature of the LED light after the Heat Sink addition.

Table 3 the output values of all the cases

Mass-flow inlet (kg/s)	Thickness (inches)	Water Temp (K)	Final Junction temp (K)
0.44	0.1	296.2	349.38
0.25		298.65	347.26
0.15		299.35	345.5
0.44	0.15	296.82	349.31
0.25		298.95	346.25
0.15		299.8	344.51
0.44	0.2	299.69	344.56
0.25		301.25	342.21
0.15		302.35	340.59
0.44	0.25	298.65	346.2
0.25		299.21	344.54
0.15		300.56	344.55

5. CONCLUSIONS

With this study a new heat sink is proposed for a 70W COB (chip on board) to improve the thermal management of LED light. Additionally heat slug and adhesives are designed. The performance is numerically simulated with 4 different flow rates from 0.44 – 0.15kg/s and thickness of the heat sink

from 0.1 - 0.25 inch while keeping the pressure 60psi constant. The conclusions are drawn:

The chip junction temperature decreases as a function of thickness. Pressure drop across each heat sink increase with Reynolds number.

The results indicate that 0.15kg/s mass flow rate and 0.2 inch thickness is found to be optimal to give the lowest junction temperature.

The temperature rise for the water at 293K initially is 9.65K. With the introduction of heat sink the junction temperature is kept at 340K which is below the junction temperature of 360K without a heat sink.

The simulation results shows that the introduction of Heat sink could lead to significant reduction the LED junction temperature .

REFERENCES

1. Narendran N, Gu Y M. Life of LED-Based white light sources. IEEE Journal of display technology, Vol.1, No.1,(2005), pp. 167-171
2. Maw-Tyan Sheen and Ming-Der Jean, Design and Simulation of Micro-Tube Device in Thermal Performance for High Power LED Cooling System, Department of Electronic Engineering, Yung-Ta Institute of Technology and Commerce
3. Dae-Whan Kim, Emil Rahim, Avram Bar-Cohen, Direct Submount Cooling of High-Power LEDs Fellow, IEEE, and Bongtae Han, IEEE transactions on components and packaging technologies, vol. 33, no. 4,
4. T. Cheng, X. Luo, S. Huang, S. Liu. Thermal analysis and optimization of multiple LED packaging based on a general analytical solution. International Journal of Thermal Sciences 49 (2010) 196-201.
5. Ming-Tzer Lin ,Chao-Chi Changl, Ray-Hua Homg, De-Shau Huang, Chi-Ming Lai, Heat Dissipation Performance for the Application of Light Emitting Diode, Institute of Precision Engineering, National Chung Hsing University, Taichung 402, TaiwanZukauskas A, Shur MS, Gaska R. Introduction to solid-state lighting. New York: John Wiley & Sons, Inc.,(2002), pp .21-29
6. Xiaobing Luo; Sheng Liu, "A Closed Micro Jet Cooling System for High Power LEDs," *Electronic Packaging Technology*, 2006. ICEPT '06. 7th International Conference on , vol., no., pp.1,7, 26-29 Aug. 2006 doi: 10.1109/ICEPT.2006.359873

PERFORMANCE ANALYSIS OF I.C ENGINE USING DIESEL AND ETHANOL BLENDS

PASULA RAJU¹ K. BHARADWAJA²

DEPARTMENT OF MECHANICAL ENGINEERING

MALLA REDDY ENGINEERING COLLEGE (AUTONOMOUS)

(An Autonomous Institution approved by UGC and affiliated to JNTUH, Approved by AICTE, Accredited by NAAC with 'A' Grade and NBA & Recipient of World Bank Assistance under TEQIP Phase- II S.C.1.1) Maisammaguda, Dhulapally (Post. Via.Kompally), Secunderabad – 500 100.

ABSTRACT: Ethanol is a bio-based renewable and oxygenated fuel, thereby providing potential to reduce the particulate matter emission in diesel engine and to provide reduction in life cycle of carbon dioxide. So that reduces ozone layer depletion. There are several studies which reports improvement in the engine performance and emission by using ethanol blend fuels. Many researches going on in the area of ethanol as alternate fuel, the commercialization of this fuel is not achieved in the Indian automobile scenario. It is mainly because of installation of refilling stations and the problems encountered in the engine while ethanol is used as a fuel. The problem such as starting trouble, cold starting problem, Aldehyde emission coming out from the engine and the stringent norms followed by the government for the use of ethanol. The main objective of this project is to study the performance of the diesel engine using blended fuel. The present work has been carried out using single cylinder, four-stroke, water-cooled diesel engine. In this phase, experiment investigations are conducted using four sets of blended fuels i.e. 5%, 10%, 15%, 20% Ethanol – Diesel blend have been prepared. The performance evaluation of the I.C engine is done and compared with the base fuel. The performance parameters like brake thermal efficiency and volumetric efficiency are evaluated and compared with the base fuel.

Introduction

Biodiesel is the name of a clean burning alternative fuel, produced from domestic, renewable resources. Biodiesel contains no petroleum, but it can be blended at any level with petroleum diesel to create a biodiesel blend. It can be used in compression-ignition (diesel) engines with little or no modifications. Biodiesel is simple to use,

biodegradable, nontoxic, and essentially free of sulfur and aromatics.

Biodiesel is made through a chemical process called transesterification whereby the glycerin is separated from the fat or vegetable oil. The process leaves behind two products-methyl esters (the chemical name for biodiesel) and glycerin (a valuable byproduct usually sold to be used in soaps and other products.

Biodiesel is better for the environment because it is made from renewable resources and has lower emission compared to petroleum diesel.

The transesterification is achieved with monohydric alcohols like methanol and ethanol in the presence of an alkali catalyst. Biodiesel and its blends with petroleum-based diesel fuel can be used in diesel engines without any significant modifications to the engines. The advantages of biodiesel are that it displaces petroleum thereby reducing global warming gas emissions, tail pipe particulate matter, hydrocarbons, carbon monoxide, and other air toxics. Biodiesel improves lubricity and reduces premature wearing of fuel pumps.

Project objectives

The main objective is to calculate the performance analysis of a 4-S Diesel Engine using various blends of bio-diesel and diesel to predict the outcome of the best possible blend that can be used in day-to-day life.



4-s Diesel engine

Literature review

Ethanol has been successfully used to blend with gasoline fuel as part of the alternative to reduce the consumption of conventional gasoline. However, it has not been commercially used to replace part of diesel fuel to diesel engines, because the barriers for application have not been overcome yet, due to the difference in chemical and physical properties between ethanol and diesel fuel. At present, significant investigations of the potential application of ethanol - diesel (ED) fuel blends on diesel engine have been carried out. Hansen et al investigated the Cummins engine performance with 15 % ED fuel blends and found that the engine power decreases by about of 7 to 10 % and the brake thermal efficiency increases by about of 2 – 3 % at rated speed. Kass et al tested the torque output from the same model engine with two blends containing 10 % and 15 % ethanol and reported an approximate 8 % engine power reduction for both fuel blends. Huang et al investigated the engine performance and exhaust emissions of diesel engine when using 10%, 20%, 25% and 30% ethanol-blended diesel fuels. In that study, the results showed that the brake thermal efficiencies decreased with increasing amount of ethanol in the blended fuels. Rakopoulos et al studied the effects of ethanol blends with diesel fuel, with 5% and 10% (v/v) on the performance and emissions of a turbocharged direct injection diesel engine. The results showed that increasing the ethanol amount in the fuel blend increased the brake specific fuel consumption and decreased the brake thermal efficiency.

INTRODUCTION TO I.C ENGINES

Heat Engine:

Heat engine is a device which transforms the chemical energy of a fuel into thermal energy and

utilizes this thermal energy to perform useful work. Thus, thermal energy is converted to mechanical energy in a heat engine.



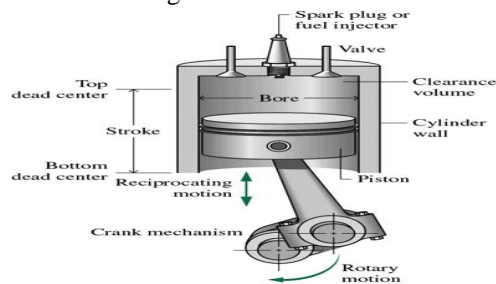
Test ring setup

Heat Engines can be broadly classified into two categories.

- Internal Combustion Engines (I.C. Engines)
- External Combustion Engines (E.C. Engines)

3.2 Internal Combustion Engines:

Here, combustion of fuel with oxygen of the air occurs within the cylinder of the engine. The internal combustion engines group includes engines employing mixtures of combustible gases and air, known as gas engines, those using lighter liquid fuel or spirit known as petrol engines and those using heavier liquid fuels, known as oil, compression ignition or diesel engines.



ETHANOL

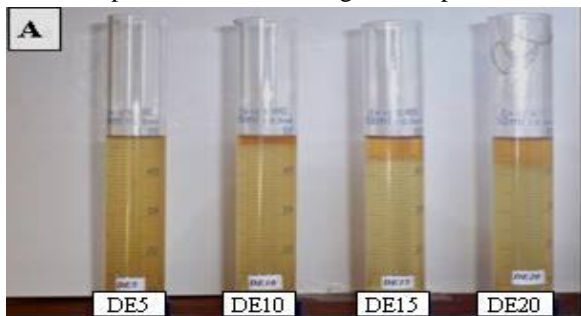
Ethanol is also called as ethyl alcohol, pure alcohol, grain alcohol, or drinking alcohol, is a volatile, flammable, colorless liquid with the structural formula $\text{CH}_3\text{CH}_2\text{OH}$, often abbreviated as $\text{C}_2\text{H}_5\text{OH}$ or $\text{C}_2\text{H}_6\text{O}$. Ethanol is a psychoactive drug and is one of the oldest recreational drugs still used

by humans. Ethanol can cause alcohol intoxication when consumed. Best known as the type of alcohol found in alcoholic beverages, it is also used in thermometers, as a solvent, and as a fuel. In common usage, it is often referred to simply as alcohol or spirits.

Blends

Ethanol can be blended at any level with petroleum diesel to create a ethanol blend. It can be used in compression-ignition (diesel) engines with little or no modifications. Several studies show ethanol can run in a conventional diesel engine for an extended time. Researchers have run diesel engines in pickups, city buses, large trucks and tractors on various mixes of ethanol/diesel fuel.

We can use the ethanol blends from 5% (v/v) and mix ethanol in any proportion. This project includes four blends. They are E5 (5% of ethanol), E10 (10% of ethanol), E15 (15% of ethanol) and E20 (20% of ethanol). Ethanol blends of up to 20% reduce the emissions of HC, CO, SO₂, and particulates, as well as improve the engine performance.



Diesel and Ethanol blends



KirloskarEngine setup

The following table shows the properties of Diesel fuel and Ethanol:

Fuel Properties	Diesel Fuel	Ethanol
Density kg/m ³	837	788
Cetane number	50	5-8
Stoichiometric A/F	15.0	9.0
Viscosity Pa s	2.6	1.2
Boiling point °C	180-360	78
Pour point °C	-1to3	-117.3
Flash point °C	65-88	13-14
Oxygen% weight	0	34.8
Heat content MJ/kg	42.5	26.8

Calculations:

- Mass of fuel consumed,

$$m_{fc} = \frac{X_{cc} * \text{specific gravity of fuel} * 3600}{1000 * t}$$

Where,

Specific gravity of diesel=0.827

X=volume of fuel consumed=10cc

t=time taken (sec)

- Heat input, HI

HI= (m_f x calorific value of fuel) in kW

Where,

Calorific value of diesel=44631.96 in kJ/kg

- Output or Brake Power, BP

$$BP = \frac{2 \pi NT}{60000} \text{ kW}$$

Where,

N=speed (rpm)

T=torque on the load indicator (N-m)

- Specific fuel consumption, SFC

$$SFC = \frac{m_{fc}}{BP} \text{ Kg/kWhr}$$

- Brake Thermal Efficiency,

$$\eta_{bth} \% = \frac{3600 * 100}{SFC * BP}$$

- Mechanical Efficiency,

$$\eta_{mech} \% = \frac{BP}{IP} * 100$$

IP can be determined, using WILLAN'S LINE method and the procedure is below:

- Draw the graph of fuel consumption Vs brake power
- Extend the line obtained till it cuts the Brake power axis
- The point where it cuts the brake power axis till the zero point will give the Power losses (Friction Power loss)
- With this the IP can be found using the relation: IP=BP+FP

- Volumetric Efficiency, η_{vol}

$$\eta_{vol} \% = \frac{Q_a}{Q_{th}} * 100$$

Where,

C_d = Coefficient of discharge of orifice = 0.62

a = area at the orifice = $(\pi/4)*d^2$

H_a = head in air column, m of air, $H_a = \frac{h_w * \rho_{water}}{\rho_{air}}$

ρ_{air}

Where,

$\rho_{water} = 1000 \text{ kg/m}^3$

$\rho_{air} = 1.2 \text{ kg/m}^3$

$$Q_{th} = \frac{(\pi/4)*D*D*L*N}{60*2}$$

Where,

D = Bore diameter of the engine = 0.08 m

L = Length of the Stroke = 0.110 m

N is speed of the engine in RPM

5.7 Sample Calculation of E20 Blend

- Mass of fuel consumed,

$$m_{fc} = \frac{X_{cc} * \text{specific gravity of fuel} * 3600}{1000 * t}$$

Where,

Specific gravity of E20=0.8289

X =volume of fuel consumed=10cc

t =time taken (sec)

$$m_{fc} = \frac{10 * 0.8289 * 3600}{1000 * 69.69}$$

$$m_{fc} = 1.189 * 10^{-4}$$

- Heat input, HI

HI= (m_f x calorific value of fuel) in kW

Where,

Calorific value of E20=41874.5 in kJ/kg

$$HI = 1.189 * 10^{-4} * 41.874.5$$

$$HI = 4.968 \text{ kW}$$

- Output or Brake Power, BP

$$BP = \frac{2 \pi NT}{60000} \text{ kW}$$

Where,

N =speed (rpm)

T =torque on the load indicator (N-m)

$$BP = \frac{2 \pi * 1512 * 2}{60000} \text{ kW}$$

$$BP = 0.3166 \text{ kW}$$

- Specific fuel consumption, SFC

$$SFC = \frac{m_{fc}}{BP} \text{ Kg/kWhr}$$

$$SFC = \frac{1.189 * 10^{-4}}{0.3166}$$

$$SFC = 1.3519 \text{ kg/kWhr}$$

- Brake Thermal Efficiency,

$$\eta_{bth} \% = \frac{3600 * 100}{SFC * BP}$$

$$\eta_{bth} = \frac{3600 * 100}{1.3519 * 0.3166}$$

$$\eta_{bth} = 6.359 \%$$

- Mechanical Efficiency,

$$\eta_{mech} \% = \frac{BP}{IP} * 100$$

IP can be determined, using WILLAN'S LINE method and the procedure is below:

- Draw the graph of fuel consumption Vs brake power
- Extend the line obtained till it cuts the Brake

S. No	Speed	Load	BP	SFC	T5	η_{bth}	η_{mech}	η_{vol}
1	1514	2	0.317	1.42	150	5.68	22.3	71.35
2	1506	4	0.630	0.814	180	9.90	36.2	71.73
3	1502	6	0.943	0.618	215	13	46	71.92
4	1495	8	1.254	0.539	240	14.96	53.2	72.06

power axis

- The point where it cuts the brake power axis till the zero point will give the Power losses (Friction Power loss)

- With this the IP can be found using the relation:

$$IP = BP + FP$$

$$IP = .3166 + 1.2$$

$$IP = 1.5166 \text{ kW}$$

$$\eta_{mech} = (0.3166/1.5166)*100$$

$$\eta_{mech} = 20.87 \%$$

- Volumetric Efficiency, η_{vol}

S. No	Speed	LOAD	BP	SFC	T5	η_{bth}	η_{mech}	η_{vol}
1	1580	2	0.330	1.472	202	5.66	30.61	68.38
2	1539	4	0.644	0.844	229	9.877	46.19	70.20
3	1504	6	0.944	0.629	254	13.25	55.72	71.83
4	1498	8	1.254	0.551	286	15.12	62.74	72.12

$$\eta_{vol} \% = \frac{Q_a}{Q_{th}} * 100$$

$$Q_a = C_d * a * \sqrt{2gH_a}$$

Where,

C_d = Coefficient of discharge of orifice = 0.62

a = area at the orifice = $(\pi/4)*d^2$

$$a = (\pi/4)*0.02^2$$

$$a = 3.14*10^{-4}$$

H_a = head in air column, m of air, $H_a = \frac{h_w * \rho_{water}}{\rho_{air}}$

ρ_{air}

Where,

$$\rho_{water} = 1000 \text{ kg/m}^3$$

$$\rho_{air} = 1.2 \text{ kg/m}^3$$

$$H_a = 4*10^{-2}*(1000/1.2)$$

$$H_a = 33.333 \text{ m}$$

$$Q_a = C_d * a * \sqrt{2gH_a}$$

$$Q_a = 0.62*3.14*10^{-4}*\sqrt{2*9.81*33.333}$$

$$Q_a = 4.978*10^{-3} \text{ m}^3/\text{s}$$

$$Q_{th} = \frac{(\pi/4)*D*D*L*N}{60*2}$$

Where,

D = Bore diameter of the engine =

0.08 m

L = Length of the Stroke = 0.110 m

N is speed of the engine in RPM

$$Q_{th} = \frac{(\pi/4)*0.08*0.08*0.110*1512}{60*2}$$

$$Q_{th} = 6.966*10^{-3} \text{ m}^3/\text{s}$$

$$\eta_{vol} = (4.978/6.966)*100$$

$$\eta_{vol} = 71.45 \%$$

Diesel

Compression Ratio=18.0

E5950 ml Diesel and 50ml Ethanol

Compression Ratio=18

S. No	SPEED	LOAD	BP	SFC	T5	η_{bth}	η_{mech}	η_{vol}
1	1511	2	0.316	1.332	171	6.19	20.84	71.50
2	1506	4	0.630	0.788	197	10.47	34.42	71.73
3	1501	6	0.943	0.603	228	13.68	44.00	71.97
4	1497	8	1.254	0.522	260	15.80	51.10	72.16

E10 900 ml Diesel and 100ml Ethanol

Compression Ratio=18

E15 850 ml Diesel and 150ml Ethanol

Compression Ratio=18

S. No	Speed	Load	BP	SFC	T5	η_{bth}	η_{mech}	η_{vol}
1	1509	2	0.316	1.330	157	6.332	24.012	71.59
2	1508	4	0.631	0.775	188	10.850	38.681	71.64
3	1499	6	0.941	0.665	218	12.661	48.501	72.07
4	1497	8	1.254	0.525	247	16.041	55.634	72.16

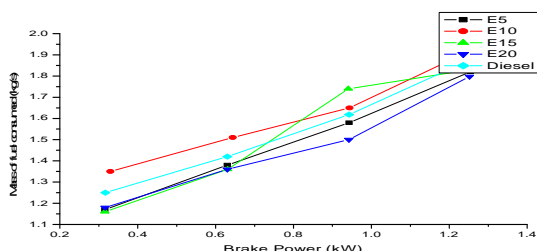
800 ml Diesel and 200ml Ethanol

Compression Ratio=18

S. No	Speed	Load	BP	SFC	T5	η_{bth}	η_{mech}	η_{vol}
1	1512	2	0.3166	1.3519	179	6.359	20.87	71.45
2	1504	4	0.6299	0.7782	201	11.052	34.42	71.98
3	1500	6	0.9425	0.5939	223	14.475	43.99	72.02
4	1495	8	1.2521	0.5161	246	16.663	51.06	72.26

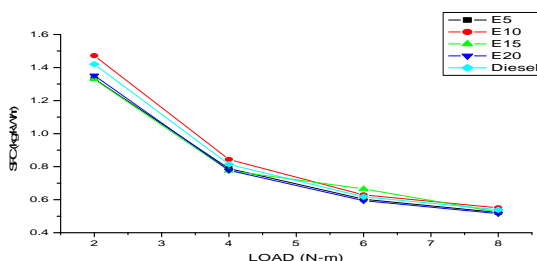
Graphs

Brake Power Vs Mass of fuel consumed



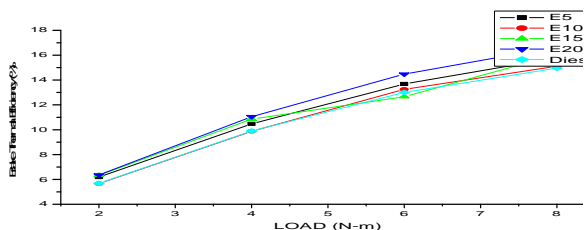
comparison of Brake power Vs Mass of fuel consumed for ethanol blends

LOAD Vs SFC



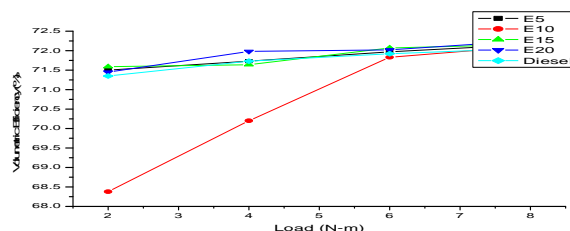
comparison of Load Vs SFC for different blends

LOAD Vs Brake Thermal Efficiency



comparison of Load Vs Brake Thermal Efficiency for different blends

LOAD Vs Volumetric Efficiency



Comparison of Load Vs Volumetric Efficiency for different blends.

Conclusion

From the results, we can observe that the performance of C.I Engine has increased by using diesel and ethanol blends in comparison with pure diesel. From this project we have observed that ethanol can be used as an alternate fuel for the C.I engine without any engine modifications when blended with diesel.

It is inferred, from the results that the Brake Thermal Efficiency and Mechanical Efficiency are higher for the blend E20. Further, it also has lower Specific Fuel Consumption. Hence E20 blend of Ethanol is preferable from the Performance Characteristics of 4-Stroke Single cylinder Diesel Engine

References

- [1] D. Li, H. Zhen, X. Lu, W. Zhang, and J. Yang, "Physiochemical properties of ethanol-diesel blend fuel and its effect on performance and emissions of diesel engines," Renewable Energy, Vol. 30, no. 6, pp. 967-976, (2005).
- [2] Kass, M.D., Thomas, J.F., Storey, J.M., Domingo, N., Wade, J., Kenreck, G., 2001. Emissions from a 5.9 liter diesel engine fueled with ethanol diesel blends. SAE Technical Paper 2001-01-1632 (SP- 1632).
- [3] Corkwell, K.C., Jackson, M.M. and Daly, D.T., "Review of Exhaust Emissions of Compression Ignition Engines Operating on E Diesel Fuel Blends", SAE Paper No. 2003-01- 3283, 2003

[4] B.Q. He, S.J. Shuai, J.X. Wang, and H. He, "The effect of ethanol blended diesel fuels on emissions from a diesel engine,"

[5] C. Sayin and M. Canakci, "Effects of injection timing on the engine performance and exhaust emissions of a dual-fuel diesel engine," *Energy Conversion and Management*, Vol. 50, no. 1, pp. 203-213, 2009.

[6] N. Noguchi, H. Terao, and C. Sakata, "Performance improvement by control of flow rates and diesel injection timing on dual-fuel engine with ethanol," *Bioresource Technology*, Vol. 56, no. 1, pp. 35-39, (1996).

[7] C.D. Rakopoulos, K. Antonopoulos, D. C. Rakopoulos, and D.T. Hountalas, "Multi-zone modeling of combustion and emissions formation in DI diesel engine operating on ethanol diesel fuel blends," *Energy Conversion and Management*, Vol. 49, no. 4, pp. 625-643, 2008.

[8] H. Chen, J. Wang, S. Shuai, and W. Chen, "Study of oxygenated biomass fuel blends on a diesel engine," *Fuel*, vol. 87, no. 15- 16, pp. 3462-3468, 2008.

[9] M. Lapuerta, O. Armas, and J.M. Herreros, "Emissions from a diesel-bioethanol blend in an automotive diesel engine," *Fuel*, Vol. 87, no. 1, pp. 25-31, (2008).

[10] Xing-Cai, L., Jian-Guang, Y., Wu-Gao, Z., Zhen, H. *Fuel*, pp. Vol. no. 83, pp. : 2013-2020, (2004).

[11] *Internal Combustion Engines* by Fernando Salazar Department of Aerospace and Mechanical Engineering University of Notre Dame Notre Dame, IN 46556

[12] *Internal Combustion Engines* by Dr. Mohammedali Abdulhadi & Dr. A. M. Hassan

[13] *Internal Combustion Engines* by V. Ganesan

1. PASULA RAJU



Studying M.Tech in stream of Thermal Engineering from MALLAREDDY ENGINEERING COLLEGE. Completed B.Tech in Mechanical Engineering in 2014 CMR COLLEGE OF ENGINEERING & TECH ,Ranga Reddy.

E-mail id: rajuar123@gmail.com

K. BHARADWAJA



Completed A.M.I.E (INDIA) Mechanical in 2001 from Institute of Mechanical Engineers, and M.Tech in Thermal Engineering in 2012 from JNTU College of Engineering(A),JNTUH (Campus),and completed M.Tech in (Cad/Cam) in VITS Affiliated to JNTUH,Hyderabad,and completed Master of Business Administration in 2010 from University of Madras.

Working as Assistant Professor at MALLAREDDY ENGINEERING COLLEGE(A) Maismmaguda,SECUNDERABAD. Telangana,India. Area of Intrest:ThermalEngineering,IC Engines

E-mail id:bharadwajak@mrec.ac.in

CFD Analysis of Emission Characteristics of 4-Stroke Single Cylinder SI Engine by Using Eucalyptus Oil and Gasoline Blend



Udutha Raghupathi

PG Student (M.Tech Thermal Engineering),
Department of Mechanical Engineering,
Malla Reddy Engineering College,
Hyderabad, Telangana, India.



C. Chandra Sekhara

Assistant Professor,
Department of Mechanical Engineering,
Malla Reddy Engineering College,
Hyderabad, Telangana India.

ABSTRACT:

Majority of the automobiles run with internal combustion engines such as spark ignition (SI) and compression ignition (CI) engines which use conventional fuels such as Petrol, Diesel etc. The use of automobiles increasing day by day in the human life. As the use of the automobiles increases, the consumption of the fuels like petrol, diesel also increases and due to the increased consumption of the fuels depletion of fuel resources occur. Along with the depletion the emissions from the automobile engines increases and there by affect human health, and environment. The main emissions like hydrocarbons(HC), carbon monoxide (CO), nitrogen oxides(NOx) and oxides of sulphur (SOx) emitted from automobile engines affect human lungs and also affects the environment which causes global warming and acid rains. From the above reasons in order to reduce the emissions various researches going on petrol and diesel engines. The petrol engines are very popular from the time of their invention; most of the automobiles are run by these engines mainly because of its simplicity and ease of operations, they are the choice for number of researches. As crude oil reserves are decreasing and increasing price of petrol alternative fuels are coming in to picture.

Now a day's most of the alternative fuels like ethanol, methanol, orange oil, eucalyptus oil are biomass

derived and easily available. Alternative fuels which are eco friendly, reduce the dependency on fossil fuels and they help to preserve the atmosphere by reducing the emission levels. Alternate fuels can be in the form of solid, liquid, and gaseous form. The solid fuels are not used in ic engines due to their physical properties, the liquid fuels are alcohols (ethanol, methanol) and vegetable oils (edible and non edible), and the gaseous fuels are LPG, CNG, H₂ and producer gas. Liquid fuels are easy to handle and calorific value of these types of fuels is more...

Many alternative fuels blends has been introduced in past and they gave satisfying results. Therefore, in this project the eucalyptus oil which is high octane biomass derived fuel is blended with petrol 15% by volume that is Eu15 and used as fuel in four stroke single cylinder petrol engine and pollution characteristics were studied and analyzed using ANSYS-FLUENT software.

KEY WORDS: CFD Analysis, Gasoline, Eucalyptus oil, Petrol engine.

1 INTRODUCTION:

The first chapter of the thesis devotes to the general view of a Petrol engine, in relation to the combustion and emissions. The chapter presents the operation of the Petrol engine with alternate fuels, especially bio fuels which are to be blended with petrol and also

discusses intake system of air fuel mixture into the engine. At the end of the chapter, the types of fuels are presented.

1.1 Background of the petrol engines:

A petrol engine (known as a gasoline engine) is an internal combustion spark ignition engine, designed to run on petrol (gasoline) and similar volatile fuels.

The first practical petrol engines was built in Germany by Nikolas August Otto, although there had been earlier attempts by Etienne Lenoir, Siegfried Marcus, Julius hock and George brayton.

The first petrol combustion engine (one cylinder 121.6 cm³ displacement) was prototyped in 1882 in Italy by Enrico bernardi.

In most petrol engines, the fuel and air are usually premixed before compression (although some modern petrol engines now use cylinder – direct petrol engine) the pre-mixing was formally done in a carburettor. But now it is done by electronically controlled fuel injection except in small engines where the cost/ complication of electronics do not justify the added engine efficiency.

The process different from a diesel engine in the method of mixing the fuel and air, and in spark plugs to initiate the combustion process. In diesel engine only air is compressed (and therefore heated) and the fuel is injected into hot air at the end of the compression stroke and self ignites.

1.2 Alternate fuels for the petrol engine:

As the time passes it is believed that the petroleum products and crude oil will not be enough and will be costly. various researches are going on for the improvement of fuel economy of engines. However as the demand and availability for petrol and diesel is somewhat un balanced and there is a need to balance since that is mainly happened due to enormous increase in number of vehicles, if the same situation continuous then the scenario will be more disastrous and petrol and diesel will be more costly and limited. with increase use and the depletion of fossil fuels today more emphasis is given on the alternate fuels.

There is an essential need of alternate fuels in a way or other. Today intensive search for the alternative fuels for both spark ignition (SI) and compression ignition (CI) engines and it has been found out that the biomass derived fuels are suited for the alternate fuels. in spark ignition engines fuels like eucalyptus oil and orange oil are the suitable substituents for the petrol. They can be blended with petrol over a wide range of percentage according to the requirement. Another reason for the need of alternate fuel for ic engines is the emission problems. Combine with other air polluting factors, the large no of automobiles is a major contributor to the air. The main problems with the altenate fuels cannot be run directly in the engines. therefore these are blended with gasoline at various percentages. One of the main reason for neglecting these fuels is the similarity in the properties of these with gasoline and they are miscible with gasoline without any phase separation. The engines used for these blending with alternate fuels are modified engines which were originally designed for gasoline fuelling. the eucalyptus oil can be used in spark –ignition engines with very little engine modification has a blend with gasoline. since the octane number of eucalyptus oil is more than gasoline, so it enhances the octane value of the fuel when it is blended with low octane gasoline. at the same time the compression ratio (CR) which is dependent on knock can be increased when these fuels are blended with gasoline.

1.3 Types of alternative fuels:

Basically there are three types of fuels liquid, gaseous and solid fuel.

SOLID FUELS have very less practical applications mainly because of handling problems and disposing off the left over components. But they played a vital role during the initial stage of engine development. solid fuels such as the pulverized coal, slurry and charcoal which are not used in IC engines due to their physical properties.

LIQUID FUELS are the derivatives of liquid petroleum and they are used in most of the modern internal combustion engines. The three principal

commercial types of fuels are benzyl, alcohol and petroleum products. Today the petroleum products form the main fuels for internal combustion engines. the liquid fuels are alcohols (ethanol, methanol) and vegetable oil (edible and non edible)

GASEOUS FUELS are considered ideal fuel and display very few problem when they are used in internal combustion engines because they mix with the air very easily and give a significantly homogeneous mixture. They also suffer with the problem of handling and storage .their principle application can be seen in stationery power plants. Some of the gaseous fuels can be liquefied under pressure resulting in less storage volume but this type of arrangement is very expensive as well as risky. The gaseous fuels are LPG, CNG, H₂ and producer gas.

2 EUCALYPTUS OIL:

Eucalyptus oil is the generic name for the distilled oil from the leaf of Eucalyptus, a genus of the Plant family myrtaceae, native to Australia and cultivated worldwide. the leaves of selected Eucalyptus species are steam distilled to extract eucalyptus oil. the main chemical component of eucalyptus is 1,8 –cineole.

Eucalyptus is a tall ever green tree .it attains the height more than 100 meter. The adult leaves are 15 to 30 cm long and 2 to 5 cm broad .Eucalyptus oil has a history of wide application , as a pharmaceutical ,antiseptic, repellent, flouring, fragrance and industrial uses. The cineole (eucalyptol) based oils can also be used as an insect repellent and bio pesticide .Eucalyptus oil has been used as an effective way of killing dust mites.



Fig. 1 eucalyptus oil

2.1PHYSICAL AND CHEMICAL PROPERTIES OF EUCALYPTUS OIL(HIGH OCTANE FUEL):

Eucalyptus oil is mainly from the leaves of the eucalyptus tree. a very eucalyptus species like mallees species produces the leaf oil . this is composed of mixture of volatile organic compounds hydro carbons, alchols, aldehydes, key tones, acids , ether,esters.1-8 cineole is the active components of eucalyptus oil. cineole is cyclic ether with empherical formula C₁₀H₁₈O. and its systematic name is 1,3,3trimethyl1-2-oxabicyclooctane.

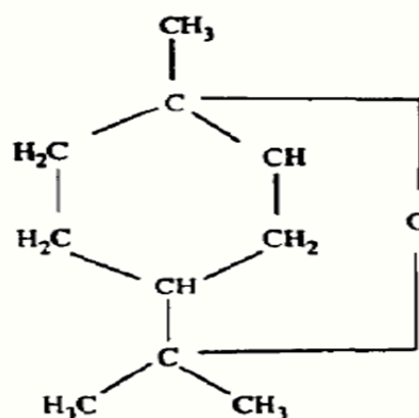


Fig 2.Chemical structure of the 1-8 cineole

2.2PROPERTIES OF THE EUCALYPTUS OIL AND GASOLINE BLEND

Table -1 properties of the eucalyptus oil and gasoline blend

S. No	PROPERTIES	EUCALYPTUS OIL(Eu15)	GASOLINE	BLEND
1	%Mass	15	85	
2	Density at 40 ⁰ Centigrade	913	780	797
3	Viscosity at 40 ⁰ centigrade	2.0	0.40	0.47
4	Specific heat(kj/kgk)	3.2	1.8	2.1

3 OVERVIEW OF FLUENT PACKAGE

FLUENT is a state-of-the-art computer program for modeling fluid flow and heat transfer in complex geometries. FLUENT provides complete mesh flexibility, solving your flow problems with unstructured meshes that can be generated about complex geometries with relative ease. Supported mesh types include 2D triangular/quadrilateral, 3D FLUENT also allows user to refine or coarsen Mesh based on the flow solution.

FLUENT is written in the C computer language and makes full use of the flexibility and power offered by the language. Consequently, true dynamic memory allocation, efficient data structures, and flexible solver control are all made possible. In addition, FLUENT uses a client/server architecture, which allows it to run as separate simultaneous processes on client desktop workstations and powerful computer servers, for efficient execution, interactive control, and complete flexibility of machine or operating system type.

All functions required to compute a solution and display the results are accessible in FLUENT through an interactive, menu-driven interface. The user interface is written in a language called Scheme, a dialect of LISP. The advanced user can customize and enhance the interface by writing menu macros and functions.

3.1 MODELING THE GEOMETRY:

Engine specifications for modeling geometry

Fuel type: Eucalyptus oil and gasoline

Engine type :V6

Displacement :2721cm³

Induction system : Twin-turbo(VGT)

Valves/cylinder:1

Bore x Stroke : 81 mm X 88mm

Connecting rod length :160mm

Compression ratio(CR) : 17.3

Intake valve max lift:8.00mm

Exhaust valve max lift :8.1mm

Intake valve diameter : 25.9mm

Exhaust valve diameter :23mm

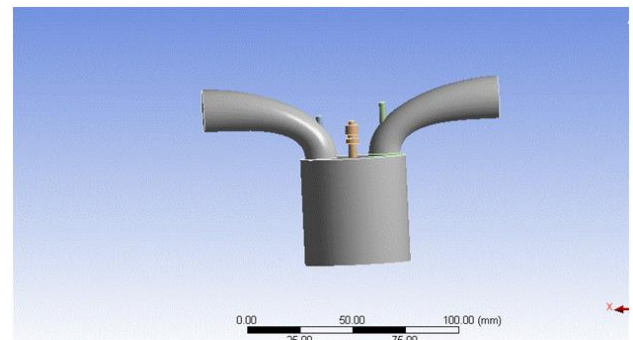
Intake duration : 252CAD

Exhaust duration:291 CAD

ANSYS WORKBENCH:

Importing the geometry

Ansyes mainly supports the cad interactive interface with any software or the most common file formats like STEP IGES and Para solid. STEP file is a CAD file format, usually used to share 3D models between users with different CAD systems. CAD file interchangeability is a huge, huge headache in the field, so it has to be make uniform. Standard ISO 10303 is trying to solve this problem. Initial Graphics Exchange Specification (IGES) is a neutral file format designed to transfer 2D and 3D drawing data between dissimilar CAD systems. The IGES standard defines two file formats: fixed-length ASCII, which stores information in 80-character records, and compressed ASCII.



The above Fig 3 represents the volume imported to do the fluent analysis in ansys (step)

BOUNDARY CONDITIONS

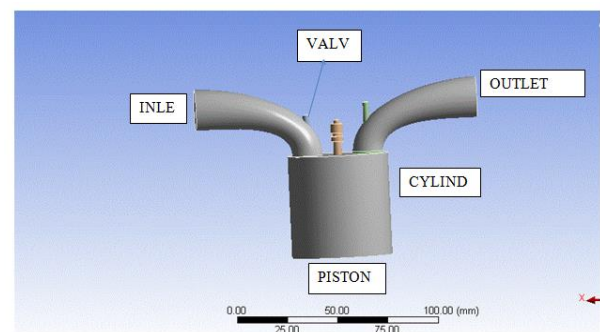


Fig 4 shows the Boundary conditions for imported 3D volume

4 -IMPLEMENTATION METHODOLOGY

ANSYS Fluent Solver set up:

Set up:
 -models

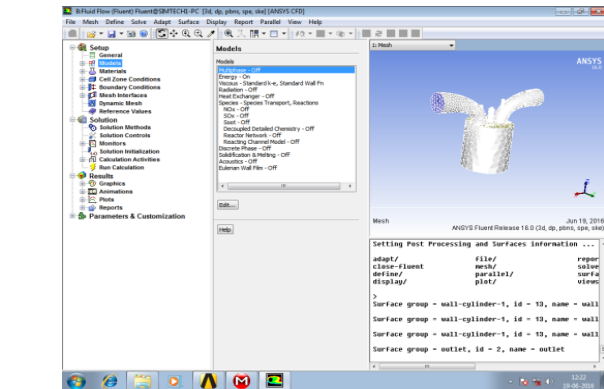


Fig:5 cfd models –multiphase off

Materials:

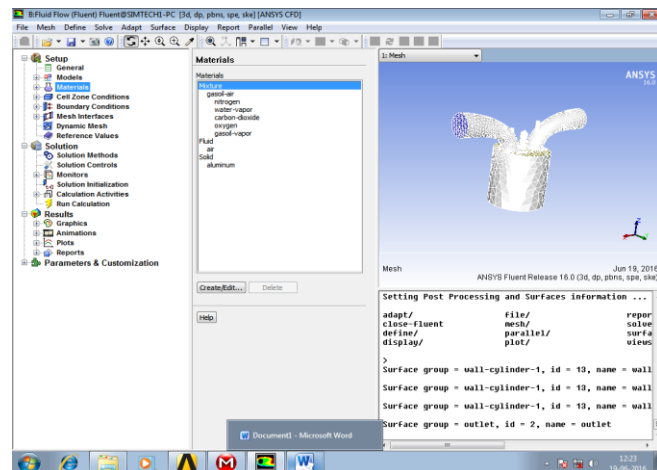


Fig 6 shows about the materials mixture of the gasoline and eucalyptus blends

Cell Zone conditions:

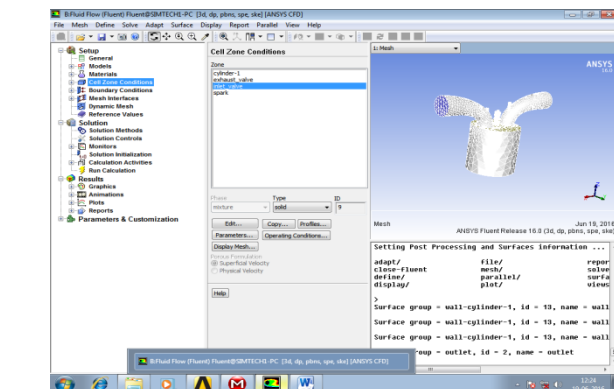


Figure 7 about the Cell zone conditions to inlet valve

Boundary Conditions:

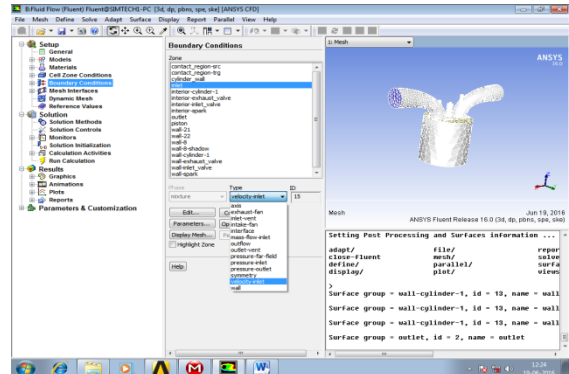


Figure 8 shows the Boundary conditions - inlet – velocity inlet

Solution:

Solution Methods:

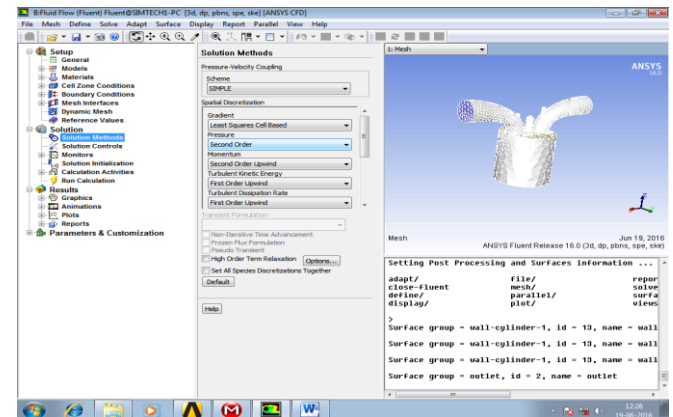


Fig 9 shows the solution methods – second order.

Solution Control:

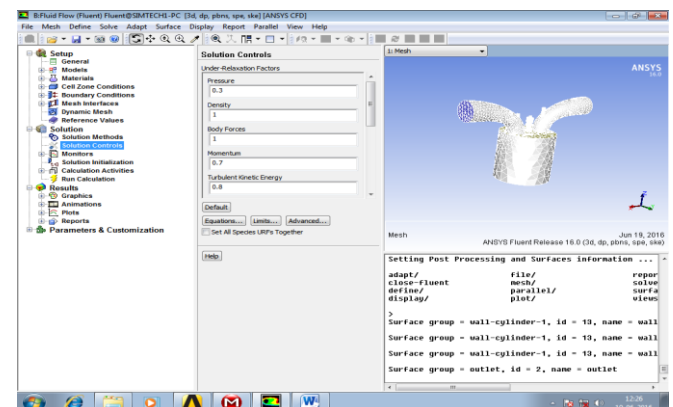


Figure 10 shows the Solution Controls
 Pressure= 0.3pa
 Density= 1kg/m³
 Momentum =0.7m/s
 Turbulent kinetic energy= 0.8m²/s²

Solution Initialization:

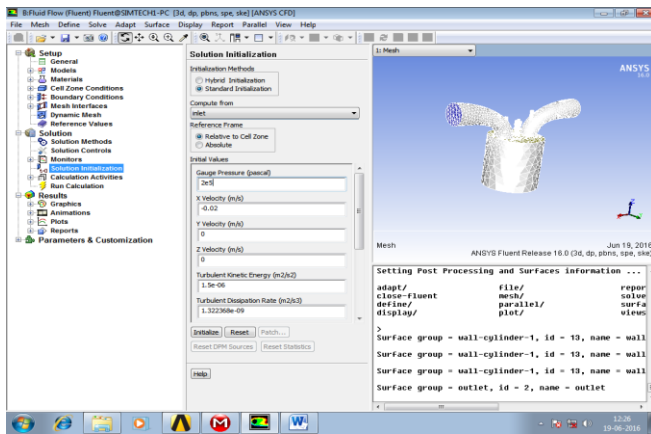


Figure 11 shows the Solution Initialization

Run Calculation:

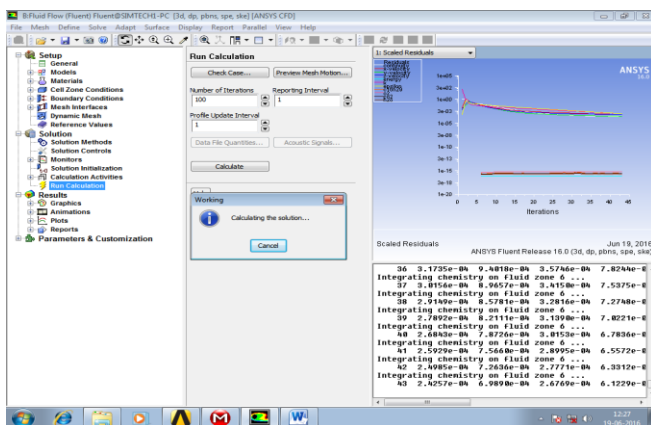


Fig 12 shows the Running the Calculations

RESULTS:

Graphics

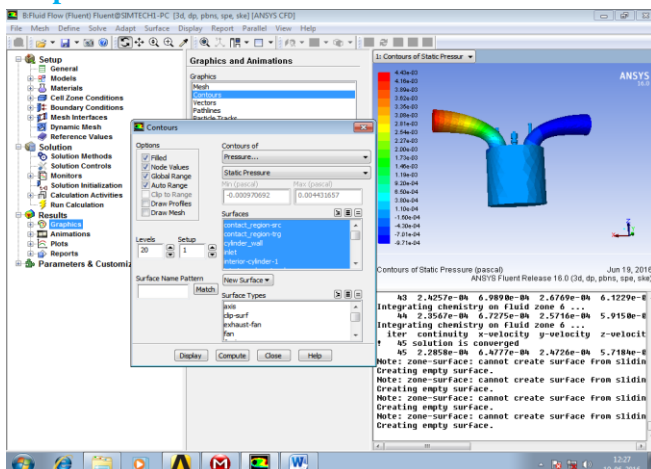


Fig 13 shows the Graphics of the contours of pressure

5 RESULTS AND DISCUSSIONS

The results show the contour plots of the different pollutants of the IC engine like as HC, NH₃, and NO etc.

THE CONTOUR PLOT OF THE HYDROCARBONS:

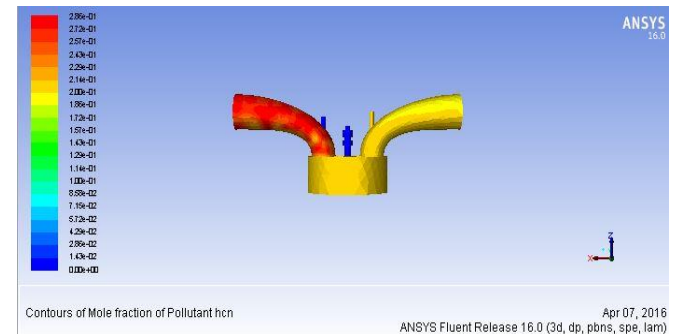


Figure 14 shows the contours of Mole fraction of HC.

CONTOURS OF MOLE FRACTION OF NITROGEN MONOXIDE

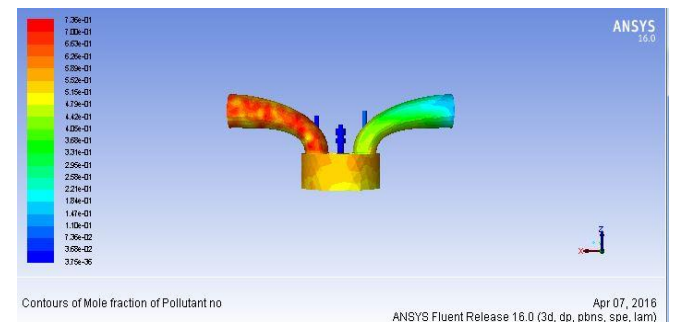


Fig 15 shows the mole fraction of pollutant NO

CONTOURS OF THE MOLE FRACTION OF POLLUTANT NH3:

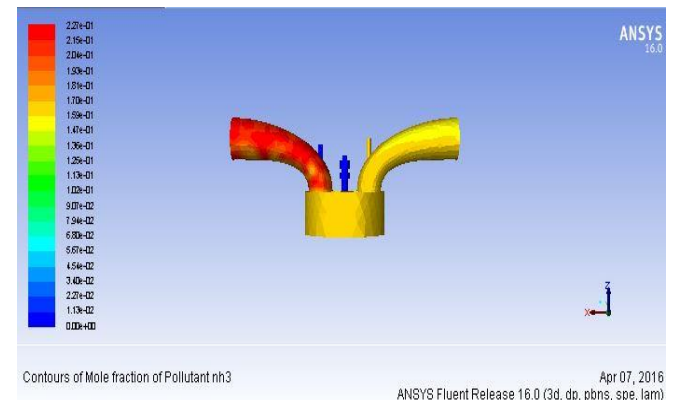


Fig 16 shows the mole fraction of pollutant NH3

5.1 EMISSION ANALYSIS:

The emissions coming out from the internal combustion engine undesirable. These emissions are exhausted into the surroundings, pollute the atmosphere and causes the various problems like global warming, acid rain, smog, odours and hazard to the respiratory system.

The engine running with the petrol as the fuel emission parameters are not specifically ideal that results in more emission of unburnt hydrocarbons (HC), carbon monoxide (CO) and oxides of nitrogen (NO_x)

Engine emissions are classified into two types

- 1 Exhaust emissions
- 2 Non exhaust emissions

Exhaust emissions:

The exhaust emissions as the mentioned above are

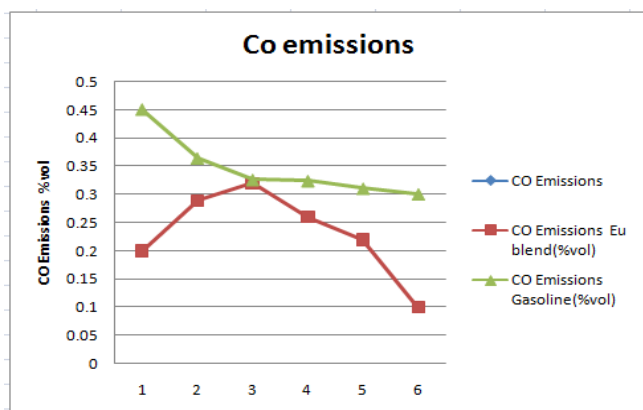
- Unburnt hydro carbon (HC)
- Oxides of carbon
 1. Carbon monoxide (CO)
 2. Carbon dioxide (CO₂)
- Oxides of nitrogen (NO_x)

These emissions common to both SI and CI engines

Non exhaust emissions:

Non exhaust emissions are the un burnt hydrocarbons from the fuel tank and crank case emissions

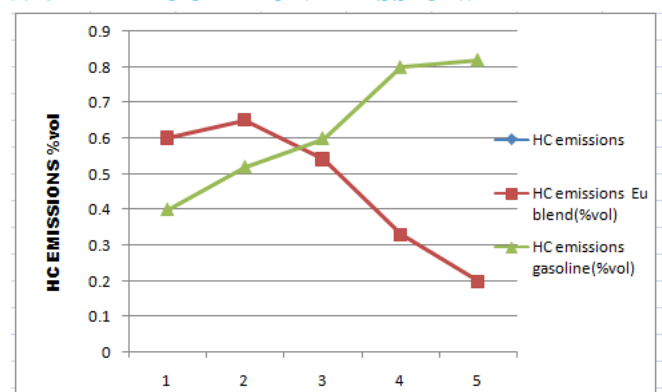
5.1.1 CARBON MONOXIDE EMISSION:



Graph 1 shows the variation of CO emission with average iterations

The graph-1 shows at initial iteration CO emissions are significantly reduced but higher as the iterations increases CO emissions decreases due to the reason for the low CO emission is due to the enrichment of O₂ in the eucalyptus oil principle component of cineole which increases the production of oxygen and promotes for the oxidation of CO during the engine exhaust process.

5.1.2 HYDROCARBON EMISSION:



Graph 2 shows the variation of HC emission with the average iterations

SI engine exhaust gases leaving the combustion chamber consists of 600ppm of HC components about 1-1.5% of fuel. HC emission different for gasoline blends and different engine geometry and operating conditions.

One of the main reason for the HC emission is absence of Oxygen to react with all the carbon present in a rich fuel mixture resulting in high level of HC and CO in the exhaust products.

This mainly occurs during the starting conditions where air fuel mixture is very rich and if the air fuel mixture is kept lean then there will be poor combustion again resulting in HC emission.

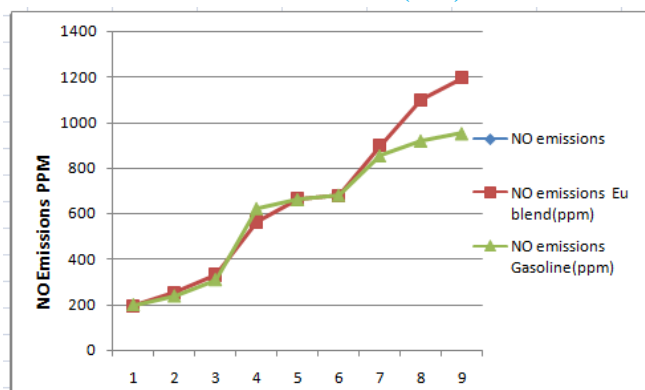
CAUSES OF HC EMISSION:

- In complete combustion due to improper mixing and flame quenching
- Leakage of exhaust valve

- Flow of fuel between the piston, piston rings, and cylinder walls
- Deposition of fuel on walls
- Oil on combustion walls

The graph- 2 shows the HC emissions with iterations. HC emissions low as compared to normal gasoline. the HC emission decreases when the gasoline blends with eucalyptus oil and operated entire conditions due to the reason for the less HC emission is equivalent ratio and easily decomposition of eucalyptus oil which gives more intermediate compounds and presence of oxygen in cineole which is main component of eucalyptus oil results in availability of more oxygen for carbon to react causing less HC emission.

5.1.3 OXIDES OF NITROGEN (NO) EMISSION:



Graph 3 shows the variation of NOx emissions with average iterations

The graph- 3 shows the NOx emission with variation of iterations. NOx emissions increases with continuously increasing with iterations increases because of the oxygen present in the eucalyptus oil and oxygenated fuel blends causes an increase in NOx emission and also complete combustion of fuel high combustion temp is achieved which results in formation of NOx

Another major reason for raise in NOx emission is due to longer ignition delay caused by eucalyptus oil and releases more heat during premixed phase of combustion

6 CONCLUSIONS:

After detailed cfd analysis of the 4-stroke single cylinder SI engine HC emissions are low as compared normal gasoline engine. The reason due to equivalent mixture ratio and easily decomposition of eucalyptus oil gives more intermediate compounds and presence of oxygen in cineole which is the main component of eucalyptus oil results in availability of more oxygen for carbon to react causing less HC emission

CO emissions are low due to the reason that the enrichment of O₂ in eucalyptus oil principal component of cineole which increases the production of oxygen and promotes for the oxidation of CO during the engine exhaust process.

NOx emission increases with continuously increasing the iterations because the presence of the oxygen in eucalyptus oil and oxygenated fuel blends causes an increase in NOx emission

7 FUTURE SCOPES:

More experiments can be performed

- By using different kinds of eucalyptus oil and gasoline blends.
- By changing the engine parameters like compression ratio, design of combustion chamber etc.
- By using different types of alternate fuels and fuel blends.

REFERENCES:

1. Irwin Osmond toppo (1), 'Cfd analysis of Jatropha in CI engine.
2. Ramesh B. Poola, Nagalingam B and Gopalakrishnan K.V (1994), 'Performance studies with bio mass –derived high octane fuel additives on a 2-stroke SI engine.
3. Tamivendhan .D , Ilangoan.V , 'Performance emission and combustion characteristics of a methyl ester sunflower oil-eucalyptus oil on a single cylinder air cooled and DI diesel engine'. ISSN:0975-5462, VOL-3, MARCH 2011

4.M.Senthil Kumar M, Ramesh A, Nagalingam B (2001) , ‘Complete vegetable oil fuelled dual fuel compression ignition engine’ SAE International ,28-0067,p.441-448.

5.Devan P.K and Mahalaksmi N.V (2010) , ‘Combustion Emission and performance characteristics of Diesel engine using poon oil –based fuels’ fuel processing technology90513-519 .

6.K.Purushotham and G.Nagarajan (2009) , ‘Study of Perfomance, emission and combustion characteristics of a CI engine operating with neat Orange oil renewable energy. Vol 34

7.Anandavelu ,N.Alagurmurthi, C.G.Saravannan. ‘ Conducted experimental investigation on performance ,combustion and exhaust emission on 4 –stroke single cylinder kirloskar tv-1 engine with eucalyptus oil and gasoline blends in five types of blends’

8.Misra .R.D . ‘ Carried out experiment on a non edible oil straight vegetable oil blended with diesel in various proportions to evaluate the performance , and emission characteristics of asingle cylinder DI constant speed diesel engine.

9.N.S.Senthur, T.S Ravikumar ,Cijil .B.John eucalyptus bio diesel an environmental fuel for CI Engines. E-ISSN:2320-0847, p-ISSN:2320-0936. Vol - 03, issue -03,pp-144-149

10.Devan P.K and Mahalakhmi N.V.2010. Combustion ,Emission and Perfomance characteristics of Diesel engine fuels with eucalyptus oil with an ignition enhancer. International journal of green energy and environment.1(1):40-49.

11.J.Zubik ,S.C .Sorenson and C.E.Goering (1948) , ‘Diesel engine combustion of sunflower oil fuels’ Trans ASAE 27(5),pp.1252-1256.

12.Karthikeyan and Mahalakshmi N.V (2005), ‘Perfomance and emission characteristics of Four

stroke Diesel engine fuelled with Turpentine diesel blends’ proceedings of ICEF 2005-1229,ASME Internal combustion Engine Division , September 11-14,ottowa, Canada, pp.1-6.

13.Ramesh B.P., Nagalngam.B and Gopal Krishnan K.V .(1994a). ‘The Influence of High –Octane fuel blends on the performance of Two-Stroke Spark Ignition Engine with knock limited- Compression ratio’ , Conference on Alternate fuel ,pp1-10.

14.Scholl K.W and Sorenson S.C.(1993), ‘Combustion of Soyabean Oil Methyl Ester in a Direct Injection Diesel Engine ‘ SAE paper no ,1450-1462.

15.Shaik Magbul Hussain ,Dr .K.Vijaya Kumar Reddy ,Dr.B. Sudheer Prem Kumar et al ,CFD analysis of combustion and emission to study the effect of compression ratio and biogas substitution in a Diesel engine with experimental verification , IJEST.ISSN:095-5462 vol.4No.02February 2012

16.P.S Rao,K.V.Gopalkrishnan .’Vegetable Oils and their methyl esters as fuels for Diesel engines. Indian Journal of Technology vol 29 june 1991.pp292-297.

17.Ram prakash ,S.P .Pandey , ‘Emission analysis of Compression Ignition engines using rice bran oil and their esters ‘ JERS/Vol 2/issue2011,173-178.

18.Ganesan. V., internal combustion engines . New Delhi, Tata McGraw-Hill,2013

Author Details

Udutha Raghupathi

PG Student (M.Tech Thermal Engineering),
Department of Mechanical Engineering,
Malla Reddy Engineering College,
Hyderabad, Telangana, India.

C.Chandra Sekhara

Assistant Professor,
Department of Mechanical Engineering,
Malla Reddy Engineering College,
Hyderabad, Telangana India.

Design and Analysis of Composite Disk Brake

K. SHIVA KUMAR¹, A. RAMESH², S. S. CH. MOULI³

¹PG Scholar, Dept of Mech, Malla Reddy Engineering College (Autonomous), Maisammaguda, Secunderabad, TS, India.

²Asst Prof, Dept of Mech, Malla Reddy Engineering College (Autonomous), Maisammaguda, Secunderabad, TS, India.

³Asst Prof, Dept of Mech, Malla Reddy Engineering College (Autonomous), Maisammaguda, Secunderabad, TS, India.

Abstract: A disc brake is a wheel brake that slows rotation of the wheel by the friction caused by pushing brake pads against a brake disc with a set of calipers. Disk brake offer higher performance, light weight, simpler design, better resistance to water interface than drum brakes. The brake disc is usually made of cast iron, but may in some cases be made of composites such as reinforced carbon-carbon or ceramic matrix composites. This is connected to the wheel and/or the axle. To stop the wheel, friction material in the form of brake pads, mounted on a device called a brake caliper, is forced mechanically, hydraulically, pneumatically, or electromagnetically against both sides of the disc. Friction causes the disc and attached wheel to slow or stop. Brakes convert motion to heat, and if the brakes get too hot, they become less effective, a phenomenon known as brake fade. In this project we design the model of disk brake its components by using solid works premium 2016 and structural and transient analysis is carried out by using ansys workbench to find efficient heat flux and static structural analysis is carried out in solid works simulation tool at different rpms.

Keywords: Ansys, RPMS, Heat.

I. INTRODUCTION

A brake is a device which is used to bring to rest or slow down a moving body. Safe operation of vehicle demands dependable brakes is required to absorb the kinetic energy of the moving parts or the potential energy of the object being lowered by host when the rate of descent is controlled. The energy absorbed by brakes is dissipated in the form of heat. This heat is dissipated in the surrounding atmosphere to stop the vehicle, so the brake system should have following requirements:

- The brakes must be strong enough to stop the vehicle within a minimum distance in an emergency.
- The driver must have proper control over the vehicle during braking and vehicle must not skid.
- The brakes must have well anti fade characteristics i.e. their effectiveness should not decrease with its constant prolonged application.
- The brakes should have well anti wear properties.

The important requirements of the brake drum are following:

- It should provide a surface having well anti wear qualities.
- It should allow the optimum rate of heat transfer.
- Heat is generated during each brake application and it must be dissipated to the atmosphere immediately, because the next brake application would again produce more heat. Any excess heating of brakes would cause the drum to expand resulting in loss of effective pedal travel and fading of brake lining.
- It should have sufficient strength but minimum weight.

- It should be able to be accommodated within the wheel space available.



Fig.1. disc brake.

Types of Brakes:

- Drum brakes
- Disc brakes
- Parking brakes
- Anti lock braking system
- Vacuum brakes
- Hydraulic brakes

Disk Brakes: The disc brake is a wheel brake which slows rotation of the wheel by the friction caused by pushing brake pads against a brake disc with a set of calipers. The brake disc (or rotor in American English) is usually made of cast iron, but may in some cases be made of composites such as reinforced carbon-carbon or ceramic matrix composites. This

is connected to the wheel and/or the axle as shown in Fig.1. To stop the wheel, friction material in the form of brake pads, mounted on a device called a brake caliper, is forced mechanically, hydraulically, pneumatically or electro - magnetically against both sides of the disc. Friction causes the disc and attached wheel to slow or stop. Brakes convert motion to heat, and if the brakes get too hot, they become less effective, a phenomenon known as brake fade.

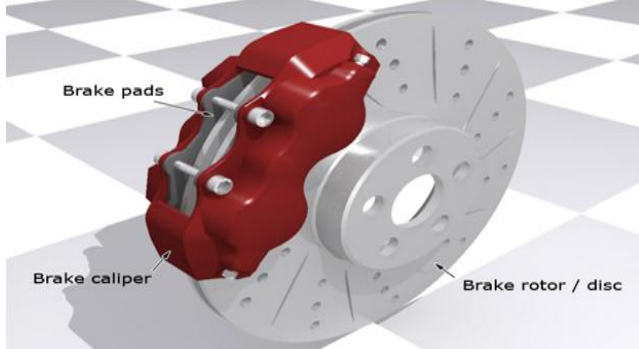


Fig.2. Disc Brake.

The machining process is performed in a brake lathe, which removes a very thin layer off the disc surface to clean off minor damage and restore uniform thickness. Machining the disc as necessary will maximize the mileage out of the current discs on the vehicle as shown in Fig.2. Braking systems rely on friction to bring the vehicle to a halt – hydraulic pressure pushes brake pads against a cast iron disc or brake shoes against the inside of a cast iron drum. When a vehicle is decelerated, load is transferred to the front wheels –this means that the front brakes do most of the work in stopping the vehicle.

Components of Disk Brakes: The brake disc is the component of a disc brake against which the brake pads are applied. The material is typically grey iron, a form of cast iron as shown in Fig.3. The design of the disc varies somewhat. Some are simply solid, but others are hollowed out with fins or vanes joining together the disc's two contact surfaces (usually included as part of a casting process).

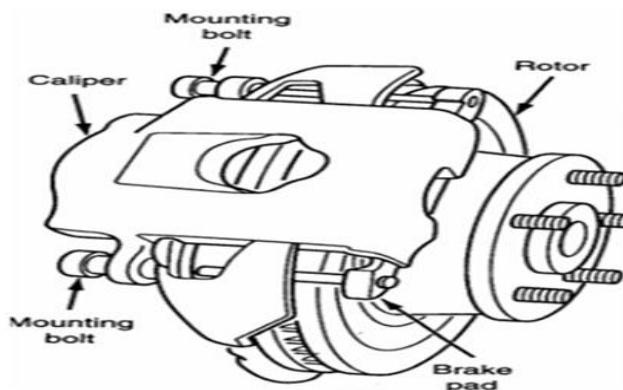


Fig.3. Disc Brake Components.

Advantage of Disc Brakes:

- Main advantage of disc brakes is their resistance to wear as the discs remain cool even after repeated brake applications.

- Brake pads are easily replaceable.
- The condition of brake pads can be checked without much dismantling of brake system.

Disadvantage of Disc Brakes:

- More force is needed be applied as the brakes are not self emerging.
- Pad wear is more.
- Hand brakes are not effective if disc brakes are used in rear wheels also.(Hand brakes are better with mechanical brakes).

II. SOLID WORKS

Solid Works is mechanical design automation software that takes advantage of the familiar Microsoft Windows graphical user interface. It is an easy-to-learn tool which makes it possible for mechanical designers to quickly sketch ideas, experiment with features and dimensions, and produce models and detailed drawings.

A. Introduction to Solid Works

Solidworks mechanical design automation software is a feature-based, parametric solid modeling design tool which advantage of the easy to learn windowsTM graphical user interface. We can create fully associate 3-D solid models with or without while utilizing automatic or user defined relations to capture design intent. Parameters refer to constraints whose values determine the shape or geometry of the model or assembly. Parameters can be either numeric parameters, such as line lengths or circle diameters, or geometric parameters, such as tangent, parallel, concentric, horizontal or vertical, etc. Numeric parameters can be associated with each other through the use of relations, which allow them to capture design intent as shown in Fig.4.

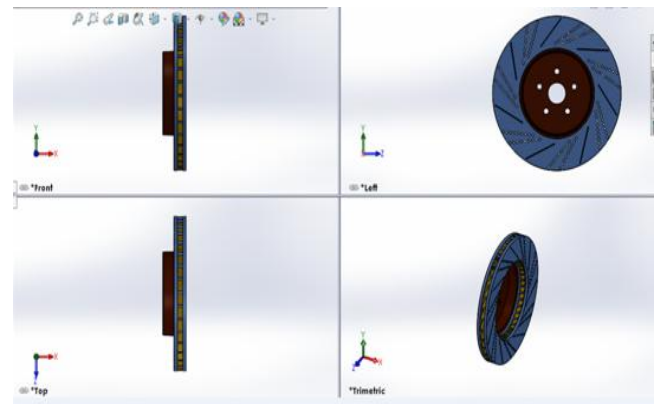


Fig.4. Design of Disk Brake.

III. FINITE ELEMENT ANALYSIS

Finite Element Analysis (FEA) is a computer-based numerical technique for calculating the strength and behaviour of engineering structures as shown in Figs.7 to 39. It can be used to calculate deflection, stress, vibration, buckling behaviour and many other phenomena. It also can be used to analyze either small or largescale deflection under loading or applied displacement. It uses a numerical technique called the finite element method (FEM).

Design and Analysis of Composite Disk Brake

A. Basic Concepts of Analysis

Meshing: The software uses the Finite Element Method (FEM). FEM is a numerical technique for analyzing engineering designs. FEM is accepted as the standard analysis method due to its generality and suitability for computer implementation as shown in Fig.5. FEM divides the model into many small pieces of simple shapes called elements effectively replacing a complex problem by many simple problems that need to be solved simultaneously.

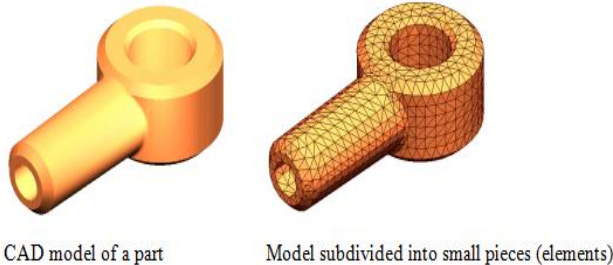


Fig.5. Meshing.

Material Data:

Beryllium copper:

TABLE I: Beryllium Copper> Constants

Density	8.26e-009 tonne mm ⁻³
---------	----------------------------------

TABLE II: Beryllium Copper> Isotropic Elasticity

Temperature C	Young's Modulus MPa	Poisson's Ratio	Bulk Modulus MPa	Shear Modulus MPa
221		0.3	184.17	85

TABLE III: Beryllium Copper> Tensile Yield Strength

Tensile Yield Strength MPa
483

TABLE IV: Grey cast Iron

Density	7.2e-009 tonne mm ⁻³
Coefficient of Thermal Expansion	1.1e-005 C ⁻¹
Specific Heat	4.47e+008 mJ tonne ⁻¹ C ⁻¹
Thermal Conductivity	5.2e-002 W mm ⁻¹ C ⁻¹
Resistivity	9.6e-005 ohm mm

IV. ANALYSIS ON DISC BRAKE (CIRCULAR HOLES)

Structural Analysis:

Fixed Support:

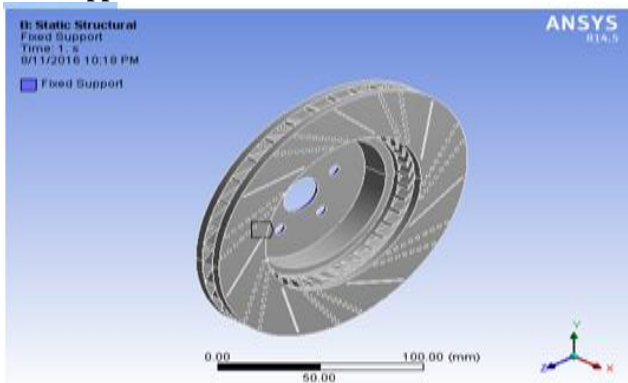


Fig.6.

Load applied:

Pressure applied on a face 1.2mpa:

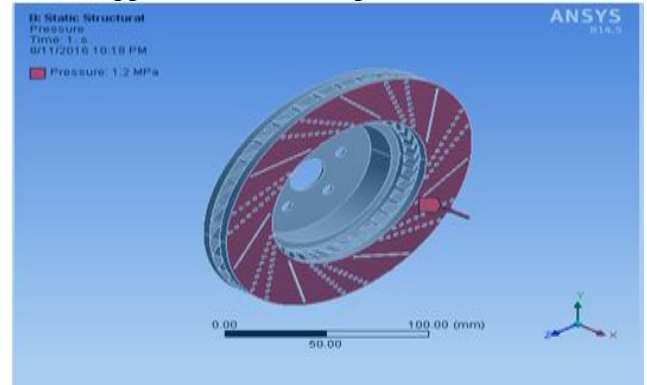


Fig.7.

Meshing:

TABLE V:

Model (B4) > Mesh	
Object Name	Mesh
State	Solved
Defaults	
Physics Preference	Mechanical
Relevance	0
Sizing	
Use Advanced Size Function	Off
Relevance Center	Fine
Element Size	Default
Initial Size Seed	Active Assembly
Smoother	Medium
Transition	Fast

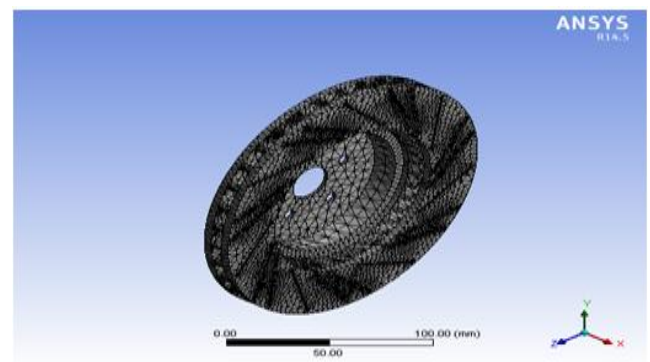


Fig.8.

V. RESULTS

A. Beryllium Copper

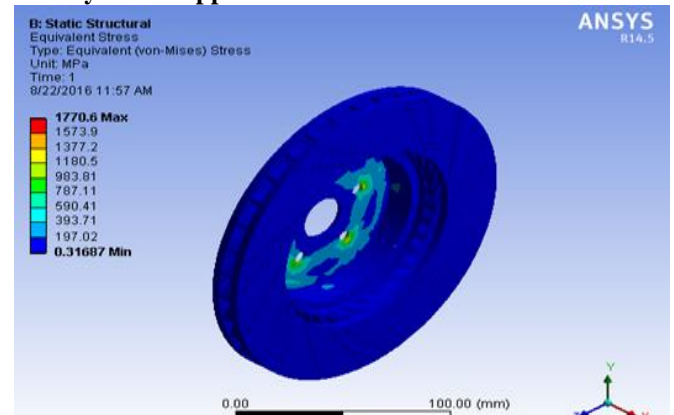


Fig.9. Maximum stress.

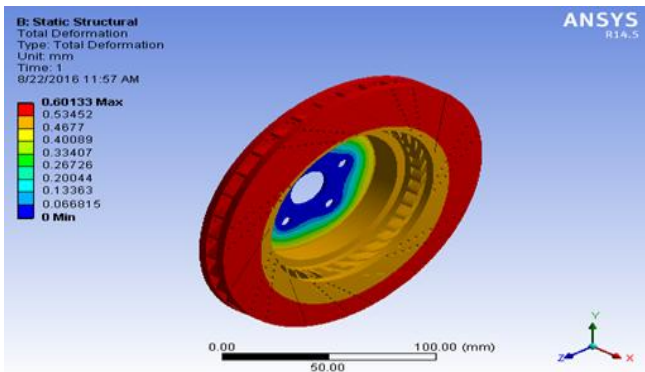


Fig.10.Total deformation.

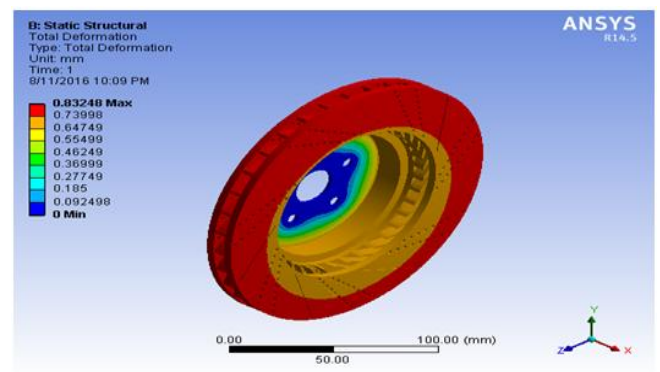


Fig.14.Total deformation.

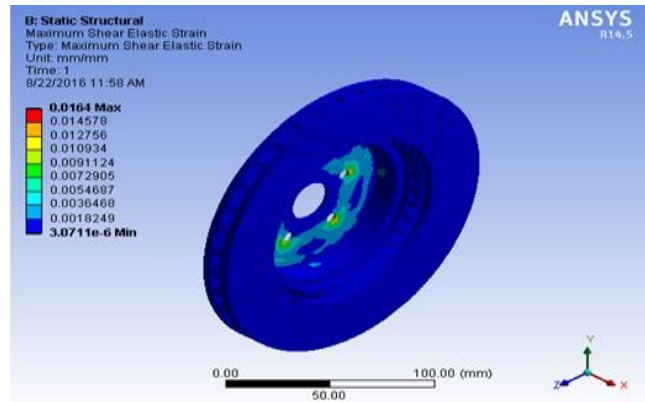


Fig.11.Maximum strain.

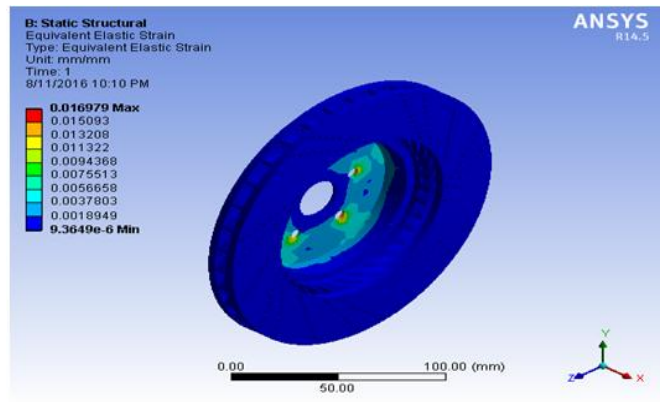


Fig.15.Maximum strain.

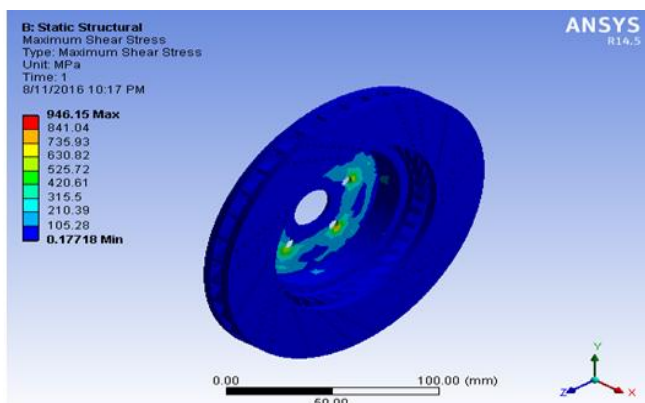


Fig.12.Maximum shear stress.

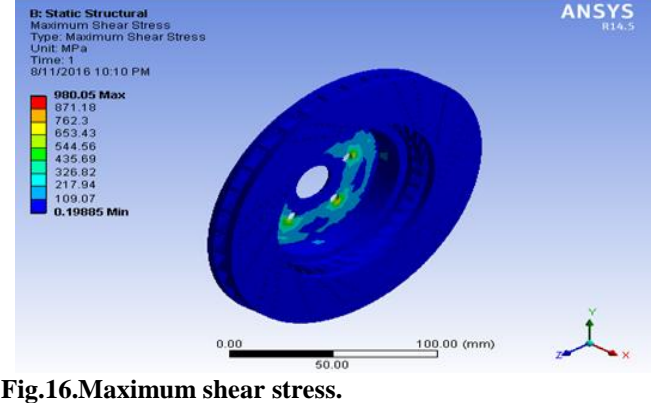


Fig.16.Maximum shear stress.

B. Grey Cast Iron

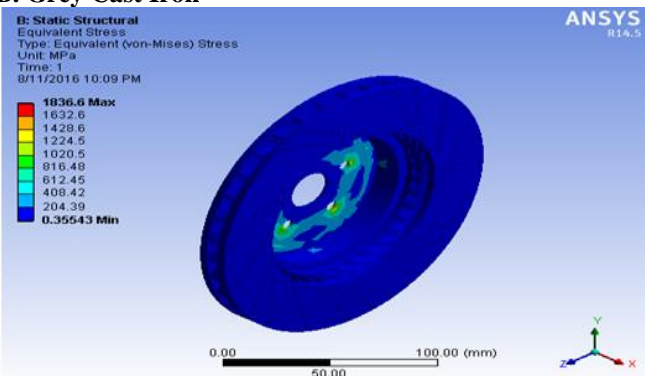


Fig.13.Maximum stress.

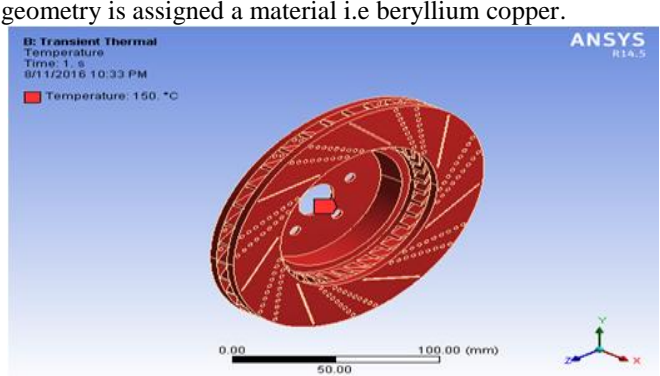


Fig.17. Temperature load 150deg.

Design and Analysis of Composite Disk Brake

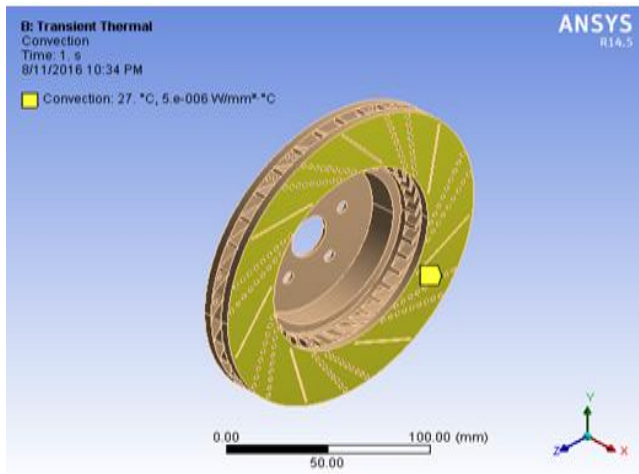


Fig.18.Convection 27deg.

VI. RESULTS

A. Beryllium Copper At 1 sec:

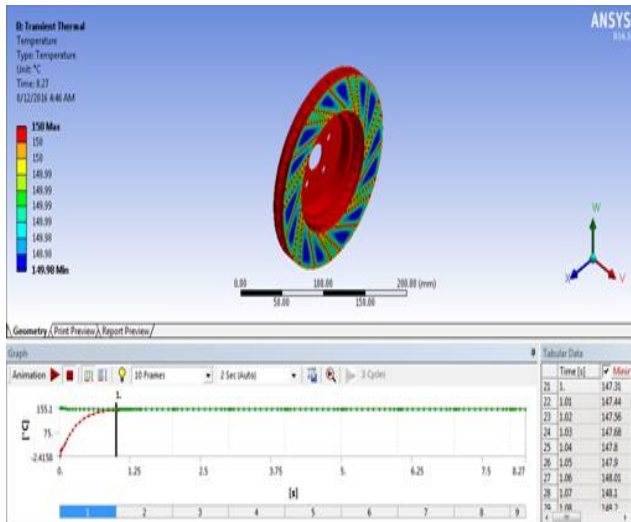


Fig.19.Temperature distribution.

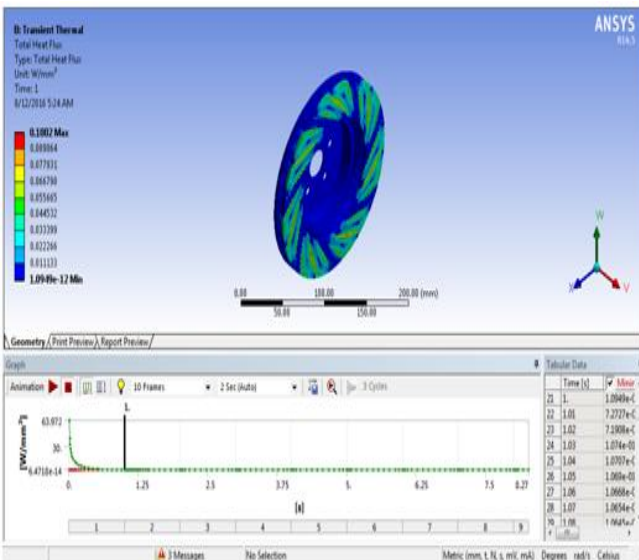


Fig.20.Heat flux.

At 2sec:

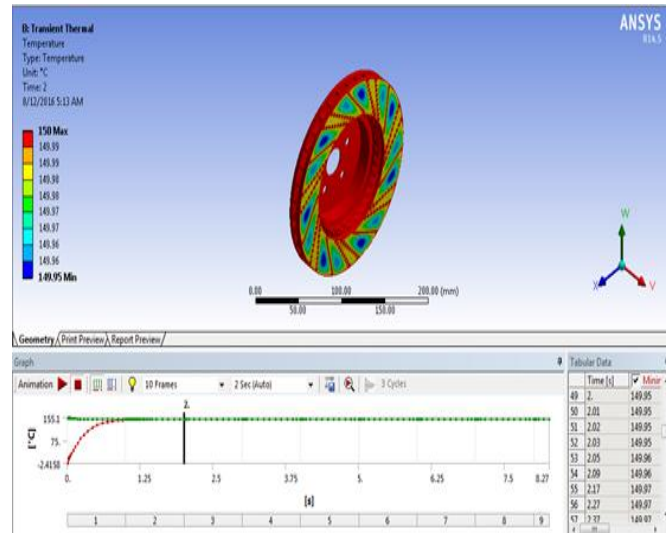


Fig.21.Temperature distribution.

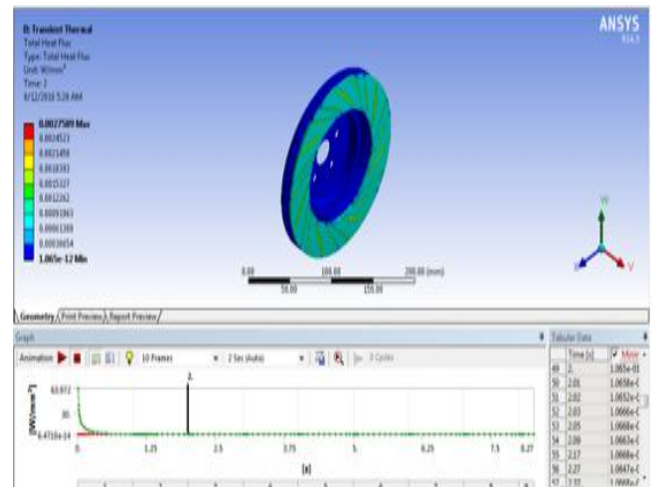


Fig.22.Heat flux.

B. Grey Cast Iron At 1 sec:

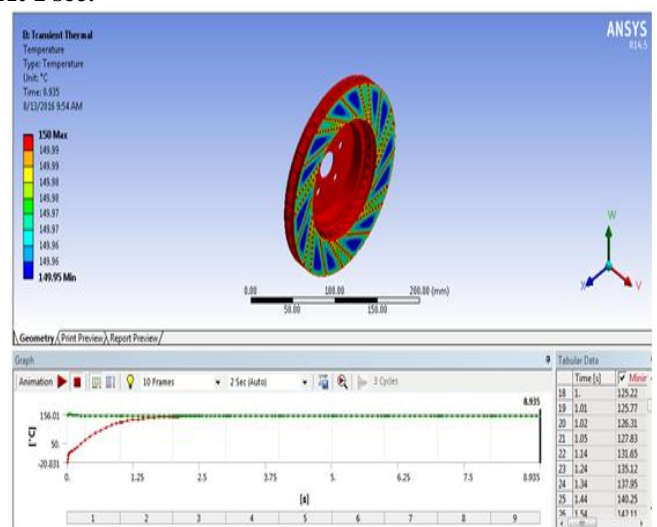


Fig.23.Temperature distribution.

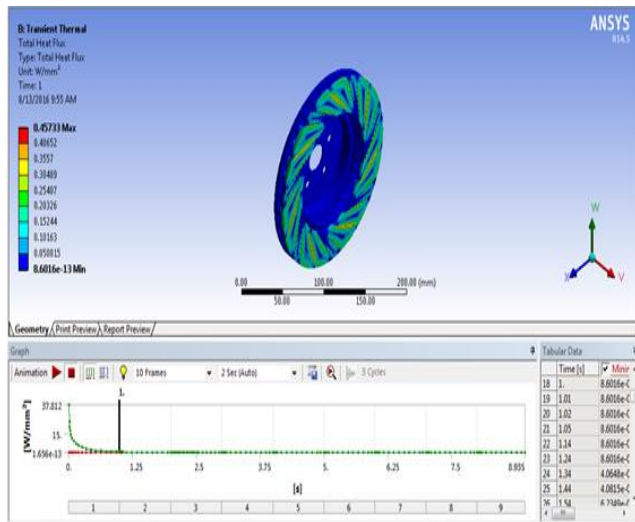


Fig.24.Heat flux.

At 2 sec:

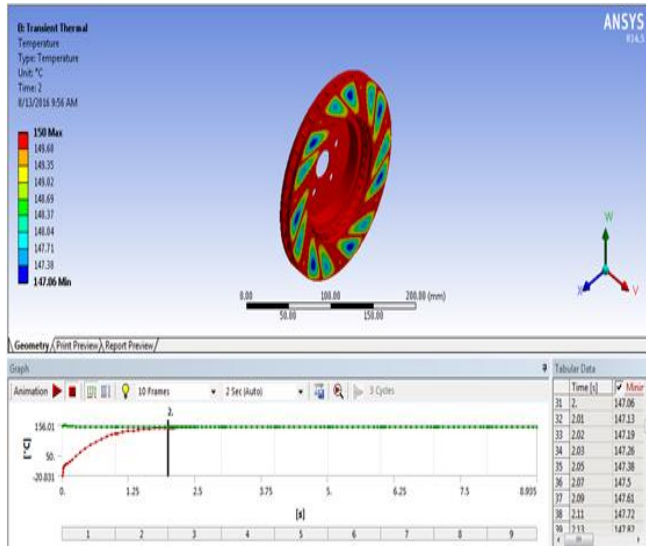


Fig.25.Temperature distribution.

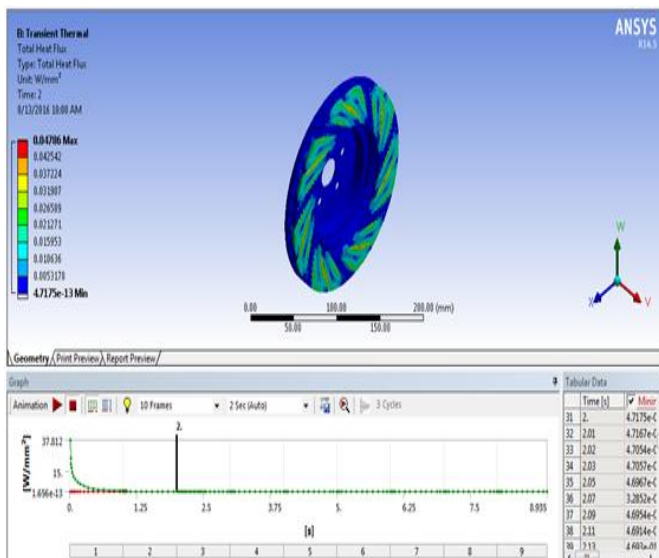



Fig.26.Heat flux.

C. Static Structural (Solid Works)

Fixture name	Fixture Image	Fixture Details		
Fixed-1		Entities: 5 face(s) Type: Fixed Geometry		
Resultant Forces				
Components	X	Y	Z	Resultant
Reaction force(N)	12794.9	-46272.9	-65.8368	48009.3
Reaction Moment(N.m)	0	0	0	0



Load name	Load Image	Load Details
Pressure-1		Entities: 1 face(s) Type: Normal to selected face Value: 1.2 Units: N/mm^2 (MPa) Phase Angle: 0 Units: deg
Centrifugal-1		Centrifugal, Ref: Face<1> Angular Velocity: 9000 rpm Angular Acceleration: 0 rpm^2

Fig.27.loads and fixtures.

At 9000 rpm:
Beryllium Copper:

Name	Type	Min	Max
Stress1	VON: von Mises Stress	0.374718 N/mm^2 (MPa) Node: 6317	7507.16 N/mm^2 (MPa) Node: 13812



Fig.27.Maximum stress.

Name	Type	Min	Max
Displacement1	URES: Resultant Displacement	0 mm Node: 5194	7.03539 mm Node: 6608

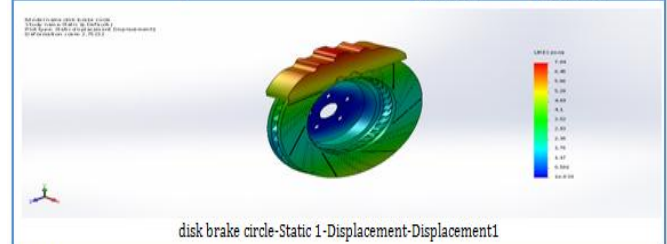
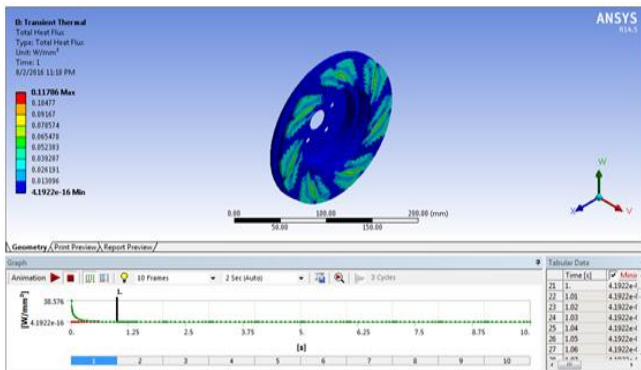


Fig.28.Total deformation.

Name	Type	Min	Max
Strain1	ESTRN: Equivalent Strain	1.62467e-006 Element: 78297	0.0399386 Element: 62972



Fig.29.Maximum strain.



Grey Cast Iron
At 1 sec:

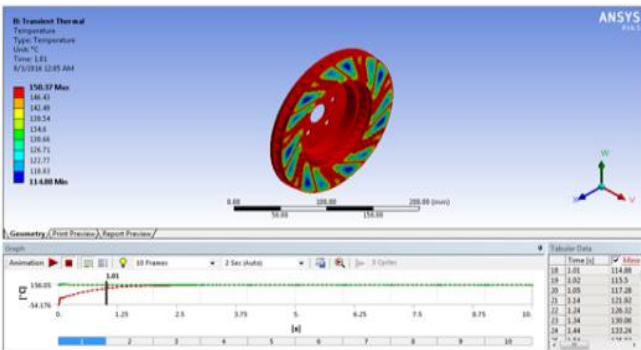


Fig.39. Temperature distribution.

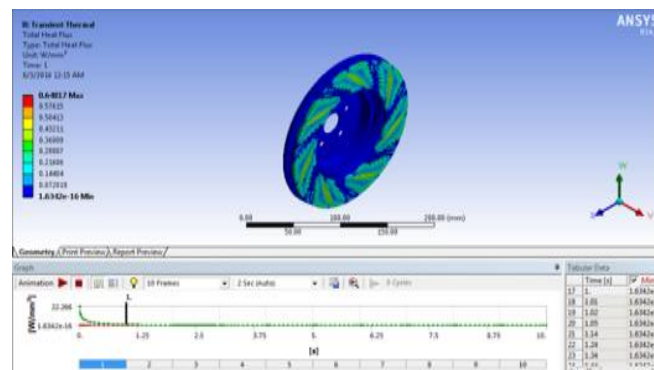


Fig.40. Heat flux.

F. Static Structural(Solid Works)
at 9000rpm:
Beryllium copper:



Fig.41. Maximum stress.

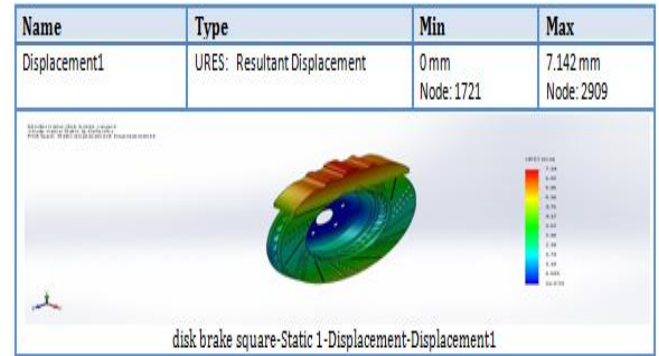


Fig.42. Total deformation.

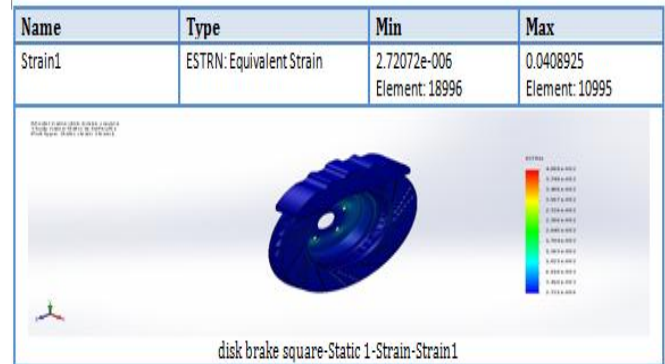


Fig.43. Maximum strain.

Grey Cast Iron:

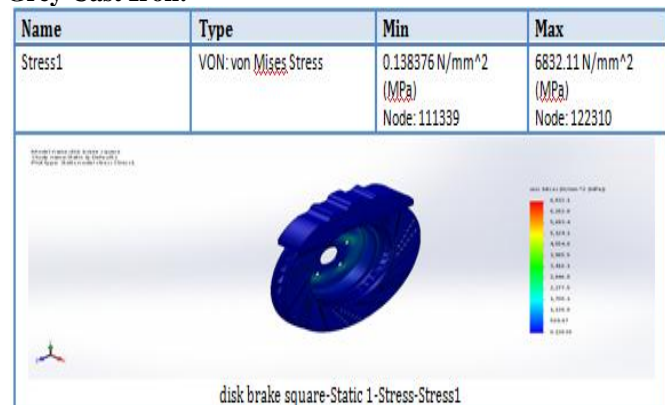


Fig.44. Maximum stress.

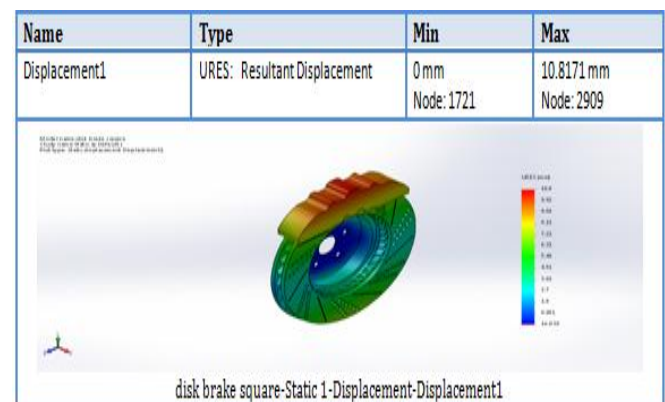


Fig.45. Total deformation.

Design and Analysis of Composite Disk Brake

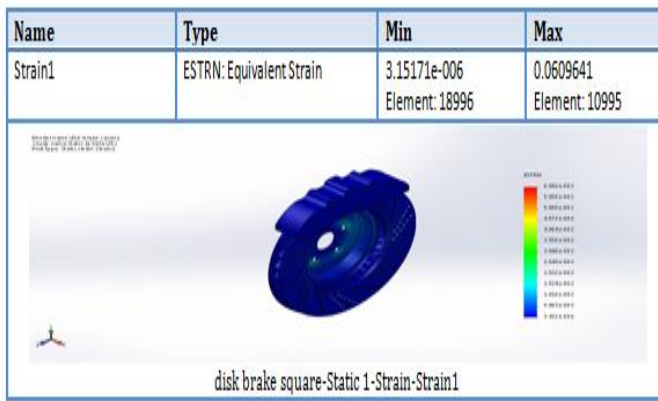


Fig.46. Maximum strain.

VII. RESULTS

A. Disc Brake Circular

TABLE VI: Structural Analysis Results

	Max stress	Total deformation	Max strain	Max stress	shear
Beryllium copper	1770.6	0.60133	0.0164	946.15	
Grey cast iron	1836	0.83248	0.016979	980.05	

TABLE VII: Transient Thermal Results

	1sec	2sec	5sec	7sec
Beryllium copper	0.1002	0.0027589	0.0019447	0.0019447
Grey cast iron	0.45733	0.04786	0.0019688	0.0019445

TABLE VII: Static Structural Results

At 9000rpm:

	Max stress	Total deformation	Max strain
Beryllium copper	7507.16	7.03539	0.0399386
Grey cast iron	6768.41	10.6355	0.0592825

At 12000rpm:

	Max stress	Total deformation	Max strain
Beryllium copper	13224.1	13.2108	0.0704311
Grey cast iron	11908.2	20.1516	0.104442

14.2 disc brake (square):

TABLE VIII: Structural Analysis Results

	Max stress	Total deformation	Max strain	Max stress	shear
Beryllium copper	0.01652	0.3285	0.075647	880.9	
Grey cast iron	0.021505	0.80556	0.021505	924.03	

TABLE IX: Transient Thermal Results

	1sec	2sec	5sec	7sec
Beryllium copper	0.11786	0.0018969	0.0012425	0.0012425
Grey cast iron	0.6484	0.11089	0.0012453	0.0012422

TABLE X: Static Structural Results

At 9000rpm:

	Max stress	Total deformation	Max strain
Beryllium copper	749.12	7.142	0.0408925
Grey cast iron	6832.11	10.8171	0.0609041

At 12000rpm:

	Max stress	Total deformation	Max strain
Beryllium copper	13169.3	13.3568	0.0718747
Grey cast iron	11991.2	20.3975	0.106975

VIII. CONCLUSION

- The design and analysis of disc brake is performed in solidworks
- Brief information about disc brake is introduced in this project
- Modeling of disc brake is done by using different commands in solid works
- Then structural and thermal analysis is carried out in ansys by using different materials such as beryllium copper, grey cast iron.
- Thus temperature distribution, heat flux are found out in transient thermal and stress, displacement, strain are obtained in structural analysis
- Static analysis at different rpms is carried out in solidworks simulation tool
- Thus stress, displacement and strain values are found out for each material
- Minimum and maximum values of stress, strain and displacement of three different materials are tabulated.
- Heat flux values are also tabulated at different timings.

IX. REFERENCES

- [1]Dr. Ramesha, Santhosh Kumar And Bharath Shekar, "design and analysis of brake drum using solidworks", 'International Journal Of Emerging Trends In Engineering And Development', 2 Vol. 3, Issn 2249-6149, Pp 281-292,2012.
- [2]"Tribological Investigation Of Titanium-Based Materials For Brakes" Peter J. Blau *, Brian C. Jolly, Jun Qu, William H. Peter, Craig A. Blue,2007.
- [3]V. M. Thilak, R. Krishnara Deepan & R.Palani, "Transient Thermal And Structural Analysis Of The Rotor Disc Of Disc Brake", International Journal Of Scientific & Engineering Research Volume 2, Issue 8, August-2011 Issn 2229-551.
- [4]"Finite Element Analysis Of Disc Brake Rotor", 2014 .
- [5]M.A.Maleque, S.Dyuti. Mirza Grebovic, "Investigation of the Effects on Braking Performance of Different Brake Rotor Designs".2013
- [6]Limpert, Rudolf "Brake Design and Safety", Society of Automotive Engineers., Inc, PA, USA, 2012
- [7]Warren Chan, "Analysis of Heat Dissipation in Mechanical Braking Systems". 2012
- [8] David A. Johnson, Bryan A. Sperandei, et.al., "Analysis of the Flow Through a Vented Automotive Brake Rotor,2011
- [9] David Antanaitis and Anthony Rifici, "The Effect of Rotor Crossdrilling on Brake Performance". SAE 2006-01-0691
- [10] Brake Design and Safety, 2nd Ed., Rudolf Limpert, 2010.
- [11]Dr. N.K. Giri, Automobile Mechanics, Khanna publishers,2010.
- [12]James D. Halderman, Automotive Braking S ystem, 2007. 9

Author's Profile:



Katkuri Shivakumar Department of mechanical engineering Mallareddy Engineering College (Autonomous) Maisammaguda, Dhulapally (Post. Via.Kompally), Secunderabad – 500 100. E-mail Katkurishivakumar327@gmail.com.



A.Ramesh, Assistant Professor Department of mechanical engineering Mallareddy Engineering College(Autonomous) Maisammaguda, Dhulapally (Post. Via.Kompally), Secunderabad – 500 100. E-mail: ramesh340mech@gmail.com.

D S Ch Mouli, Assistant Professor Department of Mechanical Engineering Mallareddy Engineering College (Autonomous) Maisammaguda, Dhulapally (Post. Via.Kompally), Secunderabad – 500 100. E-mail: dcmouli309@gmail.com

Design and Analysis of Composite Alloy Wheel

M. SWAMY¹, D. SURESH REDDY²

¹PG Scholar, Dept of Mech, Malla Reddy Engineering College (Autonomous), Maisammaguda, Secunderabad, TS, India.

²Assistant Professor, Dept of Mech, Malla Reddy Engineering College (Autonomous), Maisammaguda, Secunderabad, TS, India.

Abstract: This project deals with the design of alloy wheel for automobile application which is carried out for optimization of the mass of alloy wheel. Alloy wheels are wheels that are made from an alloy of aluminum or magnesium. They are typically lighter for the same strength and provide better heat conduction. Lighter wheels can improve handling by reducing unsprung masses, allowing suspension to follow more closely to improve grip. Reduction in overall vehicle mass can also help to reduce fuel consumption and alloy wheels are non corrosive and can resist the vibrations. However not all alloy wheels are lighter than their steel equivalents. In this project is to generate the alloy wheel of light weight alloy materials like magnesium alloy, crpf material and aluminium alloys and perform the structural analysis by applying varying loads by using solid works premium 2014.

Keywords: Alloy Wheel, Lighter Wheels Structural Analysis.

I. INTRODUCTION

Alloy wheels are wheels that are made from an alloy of aluminum or magnesium. Alloys are mixtures of metal and other elements. They generally provide greater strength over pure metals, which are usually much softer and more ductile. Alloys of aluminum or magnesium are typically lighter for the same strength, provide better heat conduction and often produce improved cosmetic appearance over steel wheels. Although steel is also an alloy, consisting of iron and carbon, it is the most common material used in wheel production. The term "alloy wheel" is usually reserved for wheels made from nonferrous alloys.

A. Characteristics of Alloy Wheel

Lighter wheels can improve handling by reducing unsprung masses, allowing suspension to follow the terrain more closely and thus improve grip, however not all alloy wheels are lighter than their steel equivalents. Reduction in overall vehicle mass can also help to reduce fuel consumption. Better heat conduction can help dissipate heat from the brakes, which improves braking performance in more demanding driving conditions and reduces the chance of reduced brake performance or even failure due to overheating. An aluminum alloy wheel designed to recall the crossed spokes of a wire wheel. Alloy wheels are also purchased for cosmetic purposes although the alloys used are not corrosion-resistant. Alloys allow the use of attractive bare-metal finishes, but these require to be sealed with paint or wheel covers. Even if so protected the wheels in use will eventually start to corrode after 3 to 5 years but refurbishment is now widely available at a cost. The manufacturing processes also allow intricate, bold designs as shown in Fig.1. In contrast, steel wheels are usually pressed

from sheet metal, and then welded together (often leaving unsightly bumps) and must be painted to avoid corrosion and/or hidden with wheel covers / hub caps.



Fig.1. aluminum alloy wheel design.

1. The Design Phase of An Alloy Wheel, The Following Characteristics Must Be Considered:

Stiffness: The structural stiffness is the basic engineering parameter to be examined when designing an aluminum wheel which offers at least the same vehicle performance as an equivalent steel wheel. The structural stiffness is determined by the final shape of the wheel; the material stiffness (Young's modulus) is more or less given and little depending on alloy and temper.

Static Performance (Strength): In order to avoid any deformation under maximal axial (accelerations and braking) and radial stresses (turning), the yield strength of the material must be considered. Misuse cases have to be evaluated in relation to the tensile strength. Yield tests under pressure are also conducted to check this behavior. An additional, important factor is the temperature resistance, i.e. the wheel must be able to tolerate Temporarily 200°C due to the

proximity of the brakes and temperatures around 100°C over longer periods.

II. TYPES OF WHEEL AND MATERIAL

A. Wire Spoke Wheel

Wire spoke wheel is an essential where the exterior edge part of the wheel (rim) and the axle mounting part are linked by numerous wires called spokes. Today's automobiles with their high horsepower have made this type of wheel manufacture obsolete. This type of wheel is still used on classic vehicles. Light alloy wheels have developing in recent years, a design to give emphasis to this spoke effect to fulfill users fashion requirements.

B. Steel Disc Wheel

This is a rim which practices the steel-made rim and the wheel into one by joining (welding), and it is used mainly for passenger vehicles especially original equipment tires.

C. Light Alloy Wheel

These wheels are based on the use of light metals, such as aluminum and magnesium has come to be popular in the market. This wheel rapidly become standard for the original equipment vehicle in Europe in 1960's and for the replacement tire in United States in 1970's. The advantages of each light alloy wheel are explained as below.

Types of Alloy Wheels:

- Aluminum alloy wheels
- Magnesium alloy wheels
- Titanium alloy wheels
- Composite material wheels

Production Methods for Alloy Wheels:

- Forging process
- High pressure die casting
- Low pressure die casting
- Gravity casting

Different aluminum casting technologies are suitable for wheel production. High productivity casting methods are primarily applied for the production of aluminum wheels to be used for factory production cars (supply to the OEM market). On the other hand, the aftermarket is looking for more versatile designs, but relatively small series, i.e. specialty casting processes are more useful. The main casting processes used for the production of aluminum wheels are:

- low-pressure die casting (mainly)
- gravity permanent mould casting (less used)
- squeeze-casting process (marginally used)

In addition, a few other casting processes have been or are used:

- counter pressure die casting
- casting-forging (Cob press)
- Thixocasting.

III. SOLID WORKS

Solid Works is mechanical design automation software that takes advantage of the familiar Microsoft Windows graphical user interface. It is an easy-to-learn tool which

makes it possible for mechanical designers to quickly sketch ideas, experiment with features and dimensions, and produce models and detailed drawings.

A. Introduction to Solid Works

Solid works mechanical design automation software is a feature-based, parametric solid modeling design tool which advantage of the easy to learn windowsTM graphical user interface. We can create fully associate 3-D solid models with or without while utilizing automatic or user defined relations to capture design intent. Parameters refer to constraints whose values determine the shape or geometry of the model or assembly. Parameters can be either numeric parameters, such as line lengths or circle diameters, or geometric parameters, such as tangent, parallel, concentric, horizontal or vertical, etc. Numeric parameters can be associated with each other through the use of relations, which allow them to capture design intent.

B. Design Procedure of Alloy Wheel

For designing the alloy wheel the following procedure has to be follow Figs.2 to 5.

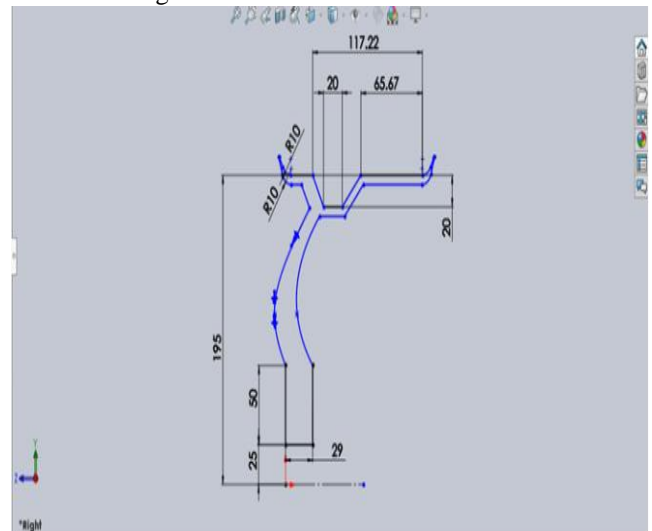


Fig.2.

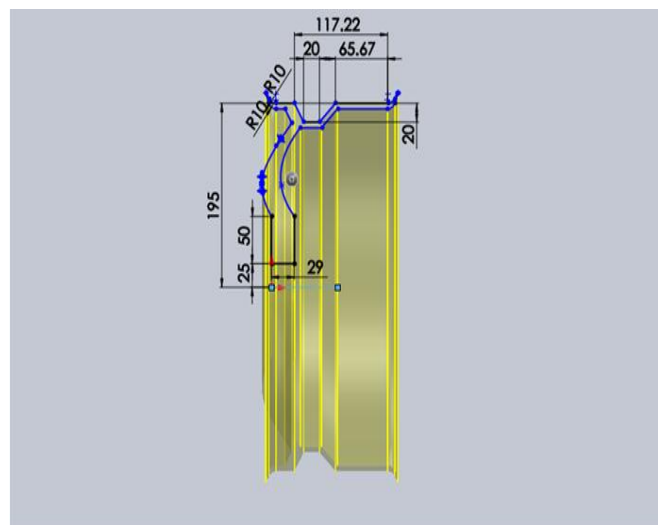


Fig.3.

Design and Analysis of Composite Alloy Wheel

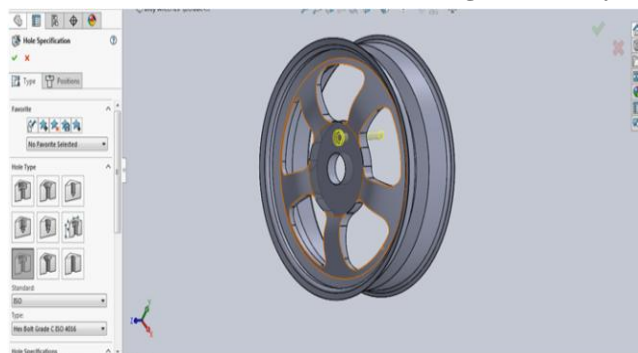


Fig.4.

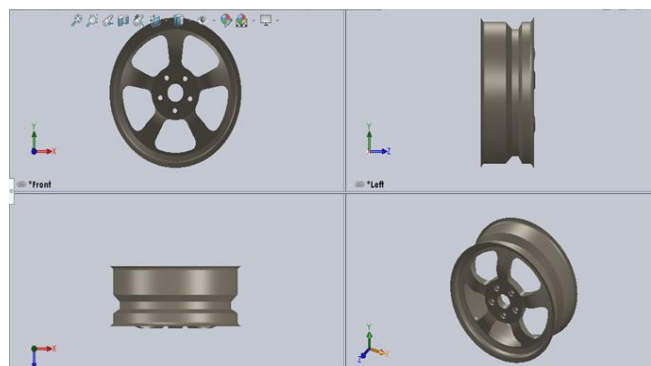


Fig.5.

IV. FINITE ELEMENT ANALYSIS

Finite Element Analysis (FEA) is a computer-based numerical technique for calculating the strength and behaviour of engineering structures as shown in Figs.7 to 39. It can be used to calculate deflection, stress, vibration, buckling behaviour and many other phenomena. It also can be used to analyze either small or largescale deflection under loading or applied displacement. It uses a numerical technique called the finite element method (FEM).

A. Basic Concepts of Analysis

Meshing: The software uses the Finite Element Method (FEM). FEM is a numerical technique for analyzing engineering designs. FEM is accepted as the standard analysis method due to its generality and suitability for computer implementation as shown in Fig.6. FEM divides the model into many small pieces of simple shapes called elements effectively replacing a complex problem by many simple problems that need to be solved simultaneously.

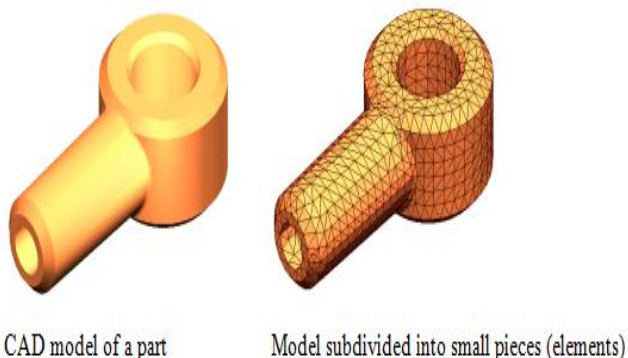


Fig.6. Meshing.

Material Data:

TABLE I: Aluminium Alloy

Density	2.77e-009 tonne mm ⁻³
Coefficient of Thermal Expansion	2.3e-005 C ⁻¹
Specific Heat	8.75e+008 mJ tonne ⁻¹ C ⁻¹

TABLE II: Magnesium Alloy

Density	1.8e-009 tonne mm ⁻³
Coefficient of Thermal Expansion	2.6e-005 C ⁻¹
Specific Heat	1.024e+009 mJ tonne ⁻¹ C ⁻¹
Thermal Conductivity	0.156 W mm ⁻¹ C ⁻¹
Resistivity	7.7e-004 ohm mm

TABLE III: Peek Material

peek material > Constants
Density 1.32e-009 tonne mm⁻³

TABLE IV: Peek Material > Isotropic Elasticity

Temperature C	Young's Modulus MPa	Poisson's Ratio	Bulk Modulus MPa	Shear Modulus MPa
3600		0.39	5454.5	1295

TABLE V: Material: Peek (20% Carbon Fibre)

Temperature C	Young's Modulus MPa	Poisson's Ratio	Bulk Modulus MPa	Shear Modulus MPa
22000		0.4556	82583	7557

Structural Analysis on Alloy Wheel:

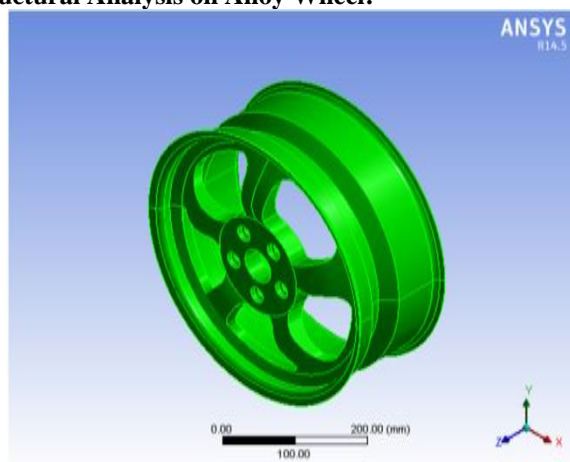


Fig.7.Meshing.

Size: Fine:

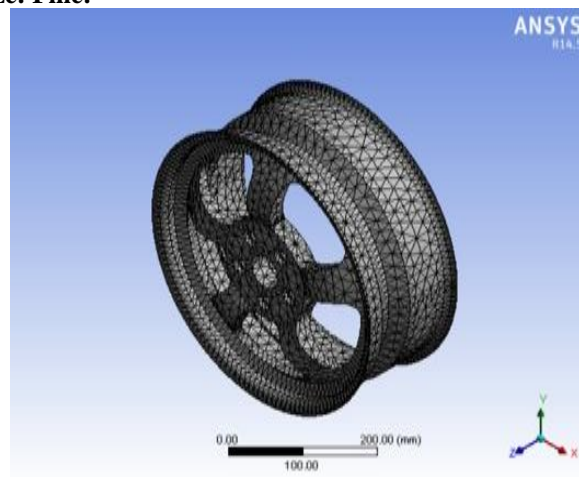


Fig.8. At 0.8 mpa of pressure.

B. Material: Aluminium Alloy

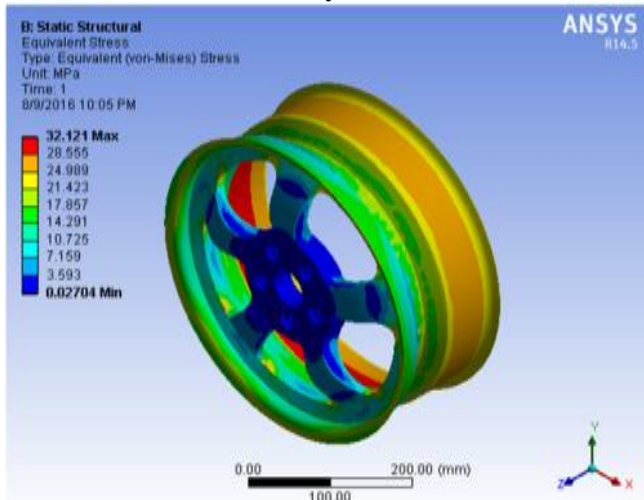


Fig.9. Maximum stress.

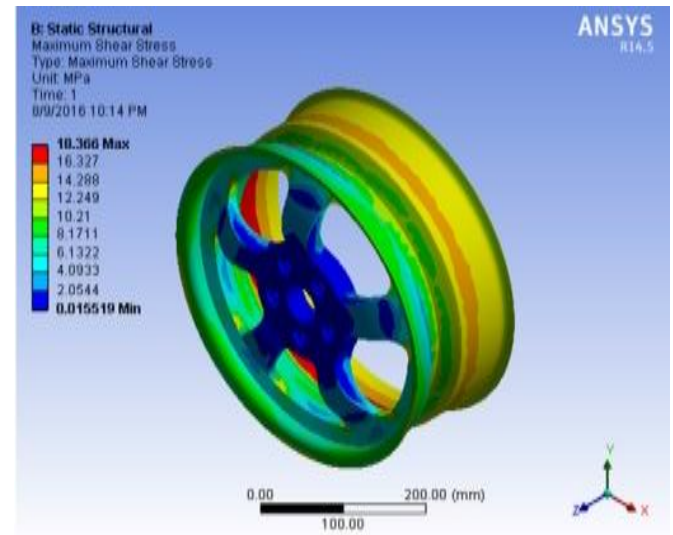


Fig.12. Maximum shear stress.

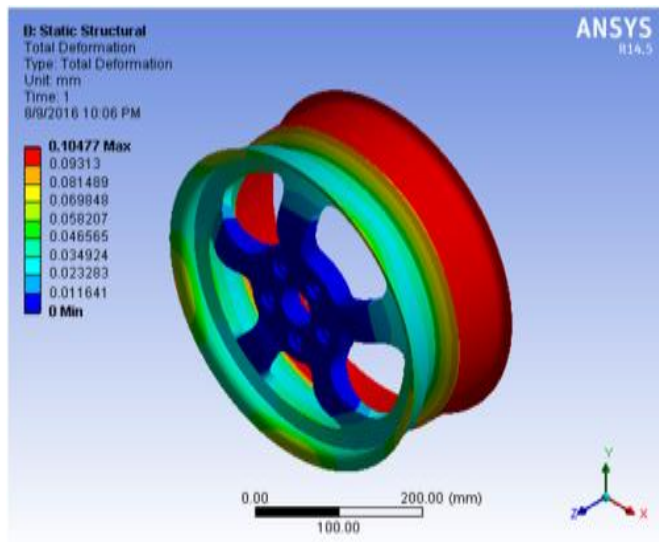


Fig.10. Total deformation.

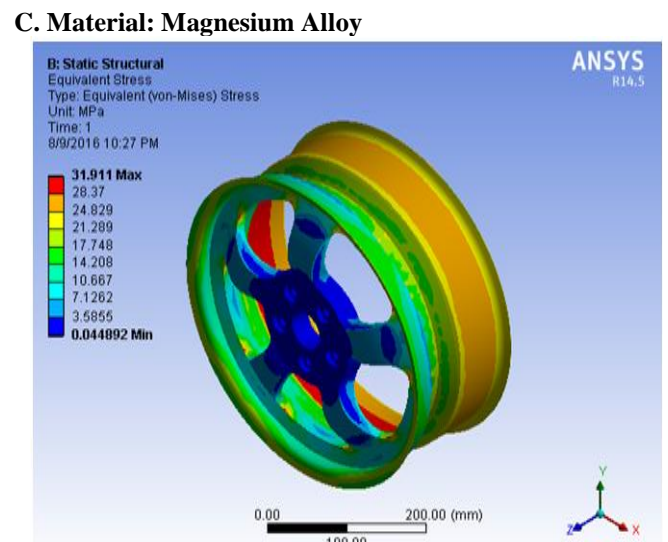


Fig.13. Maximum stress.

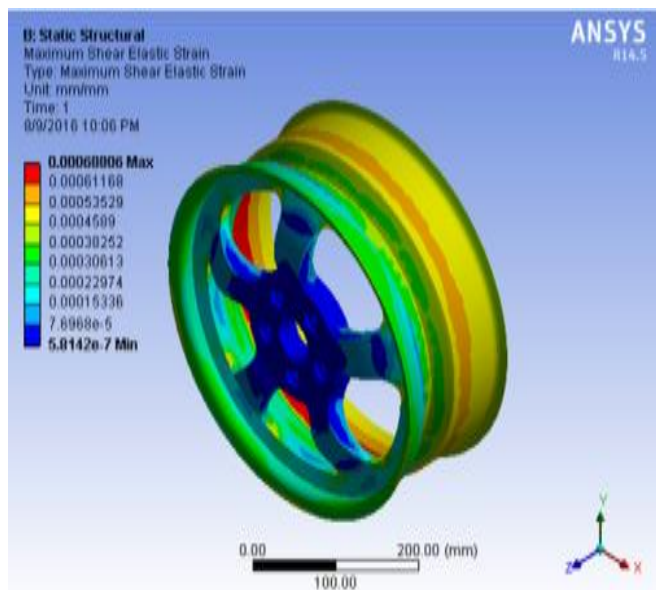


Fig.11. Maximum strain.

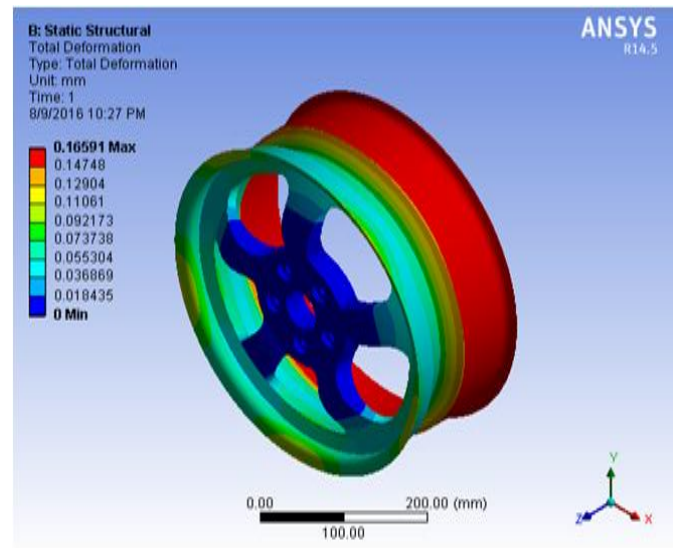


Fig.14. Total deformation.

Design and Analysis of Composite Alloy Wheel

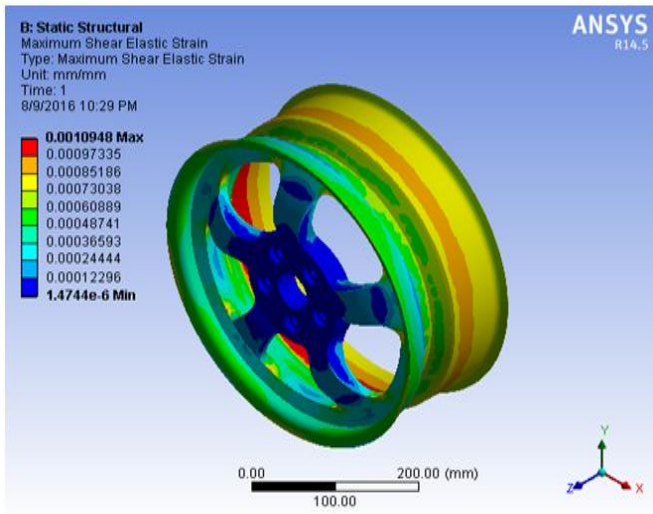


Fig.15. Maximum strain.

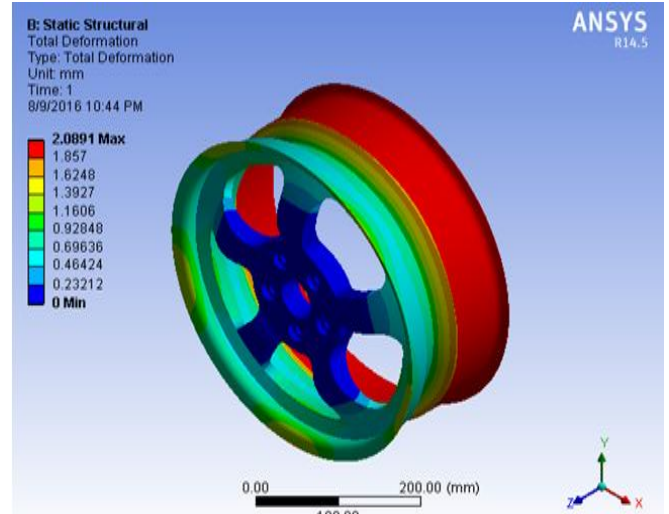


Fig.18. Total deformation.

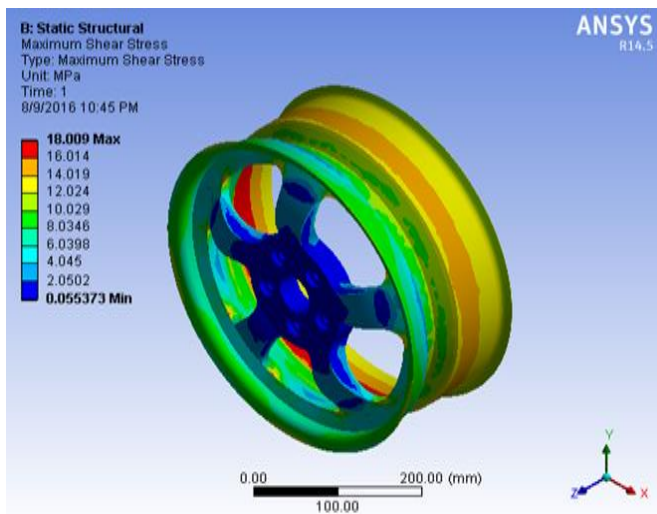


Fig.16. Maximum shear stress.

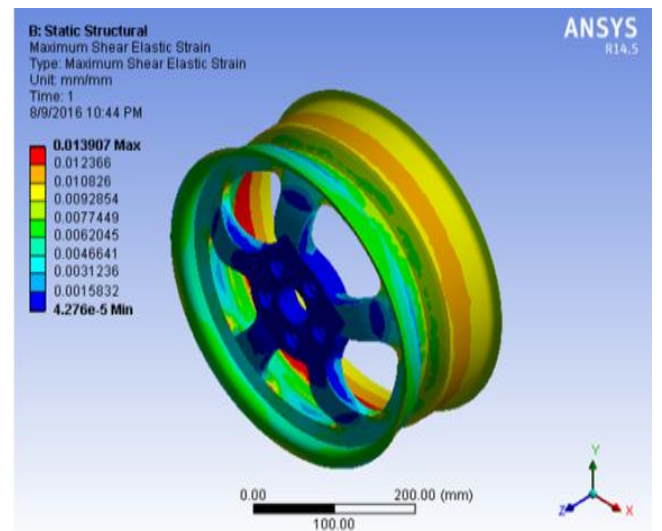


Fig.19. Maximum strain.

D. Material: Peek Material

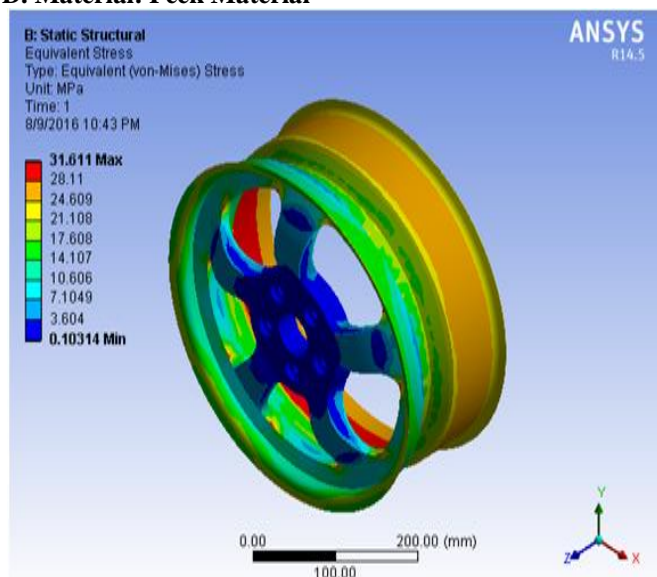


Fig.17. Maximum stress.

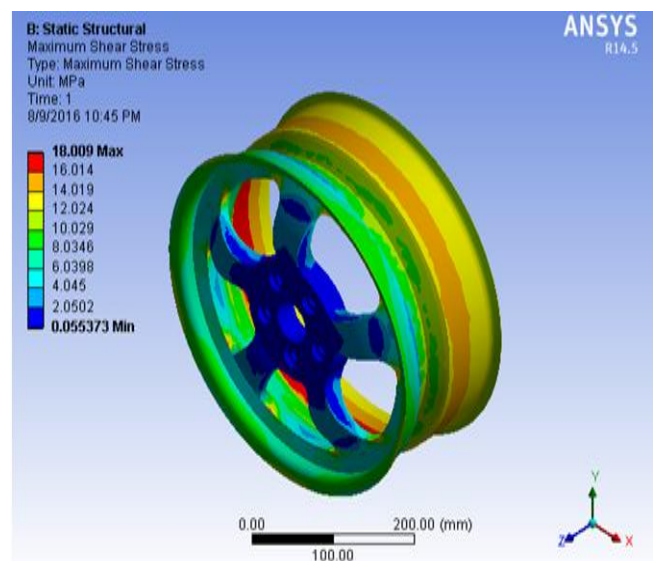


Fig.20. Maximum shear stress.

E. Material: Peek (20% Carbon Fibre)

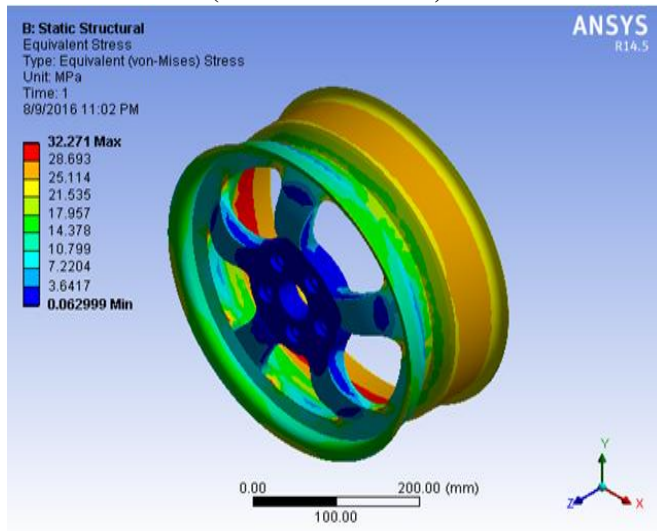


Fig.21. Maximum stress.

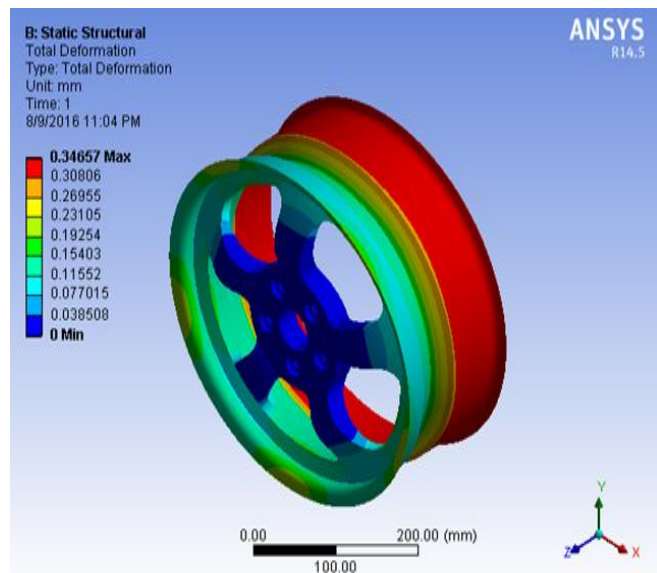


Fig.22. Total deformation.

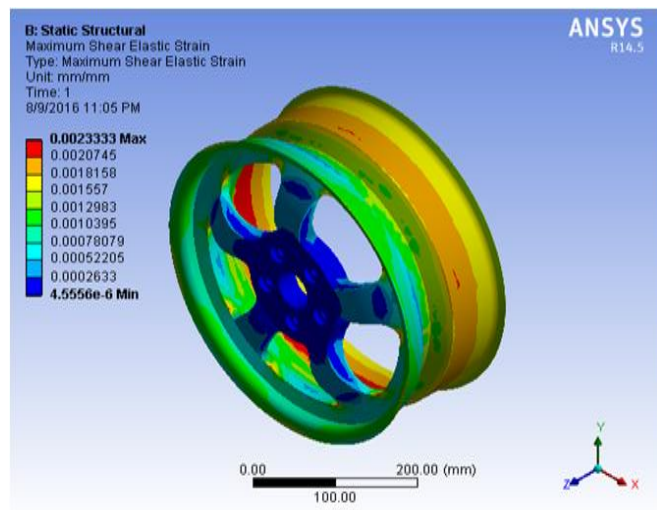


Fig.23. Maximum strain.

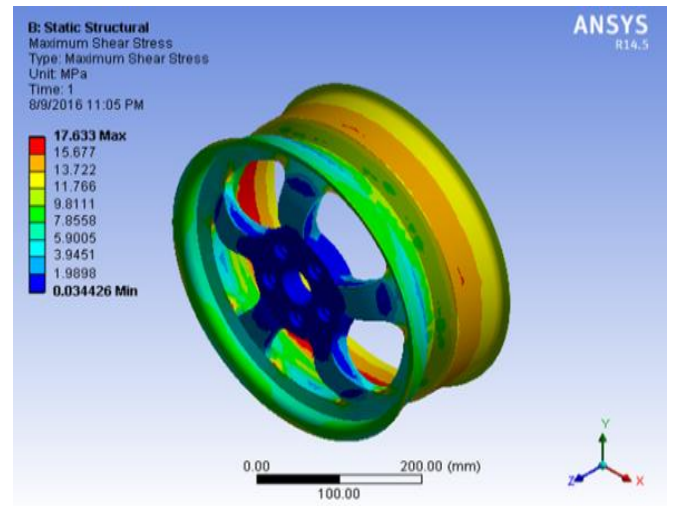


Fig.24. Maximum shear stress.

At Pressure 1.2MPa

F. Material: Aluminum Alloy

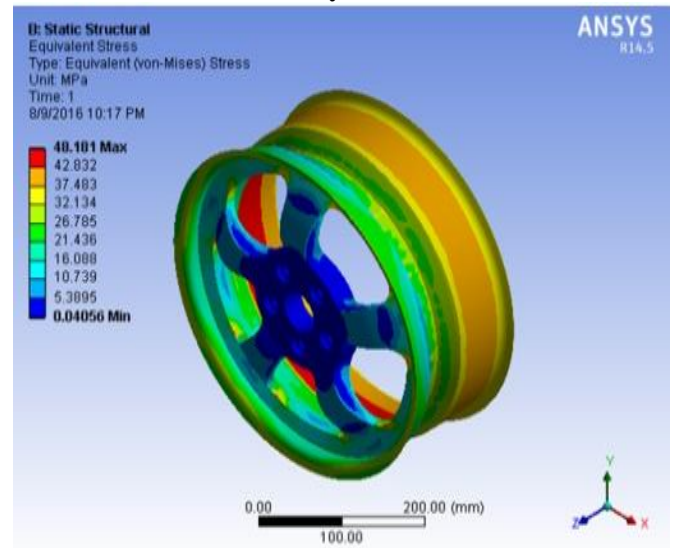


Fig.25. Maximum Stress.

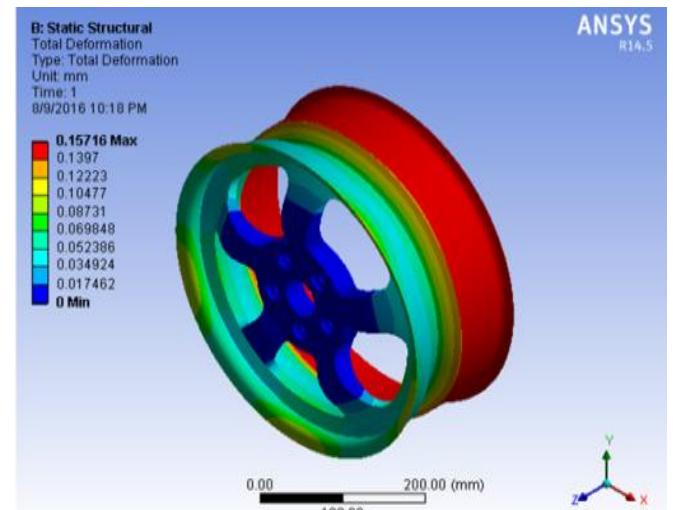


Fig.26. Total deformation.

Design and Analysis of Composite Alloy Wheel

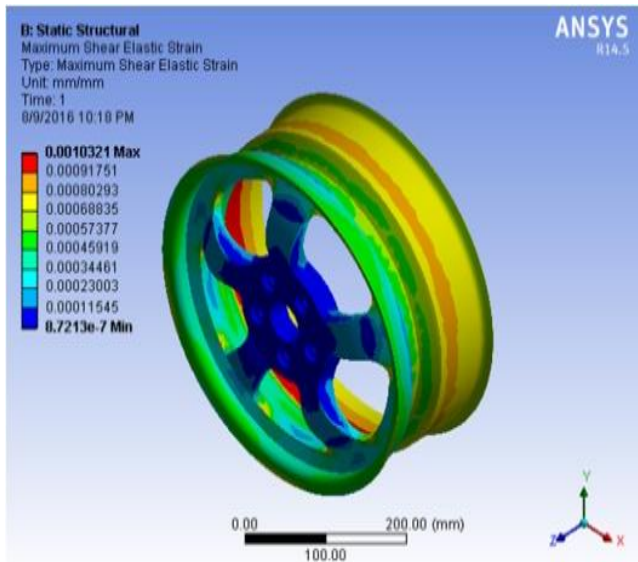


Fig.27. Maximum strain.

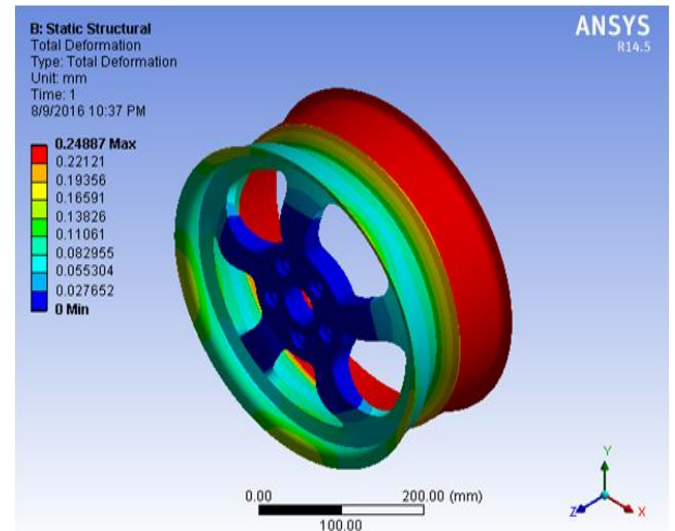


Fig.30. Total deformation.

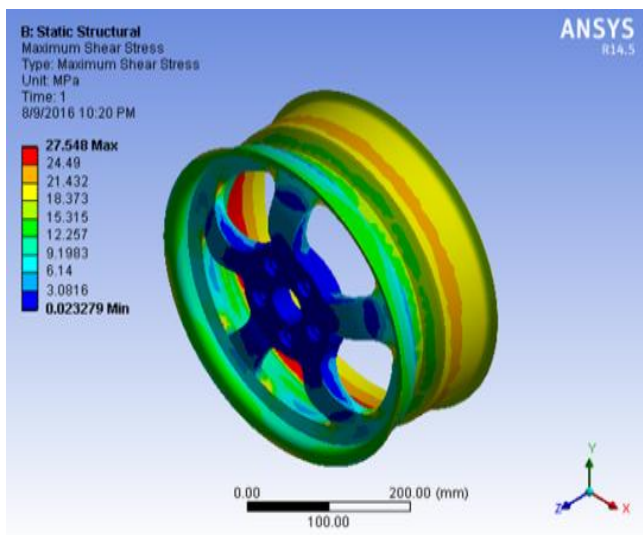


Fig.28. Maximum shear stress.

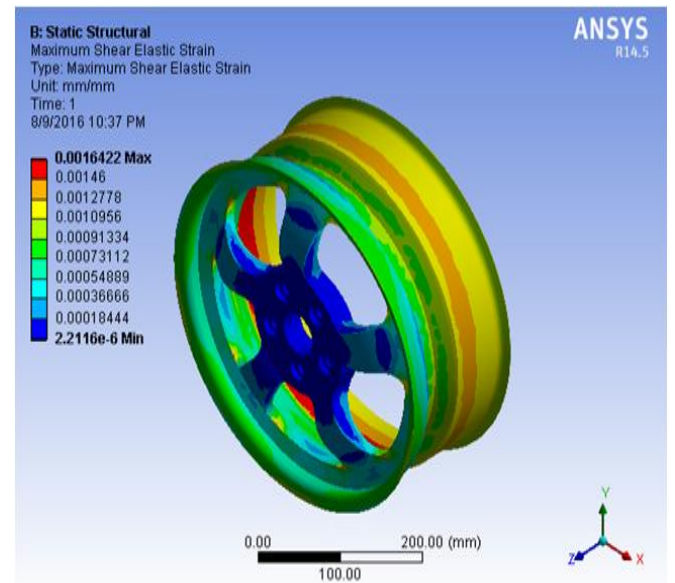


Fig.31. Maximum strain.

G. Material: Magnesium Alloy

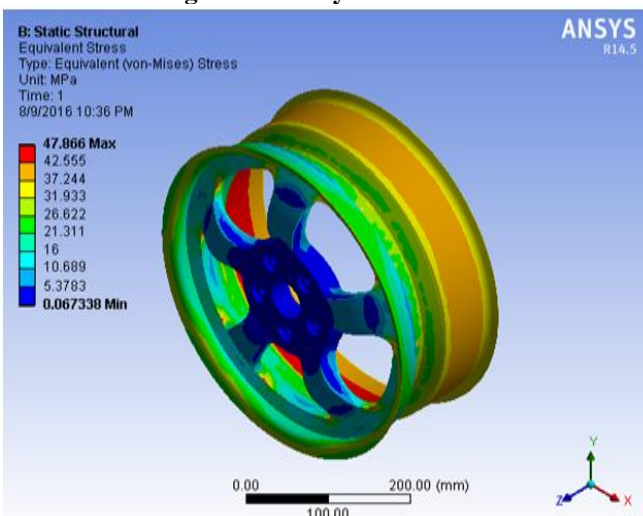


Fig.29. Maximum stress.

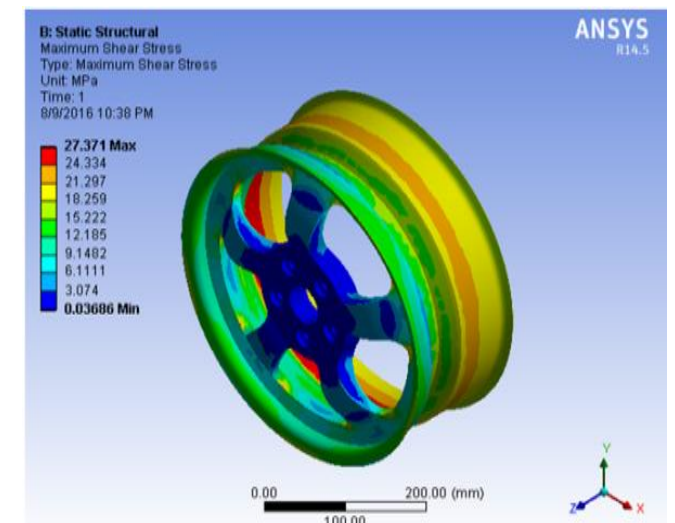


Fig.32. Maximum shear stress.

H. Material: Peek Material

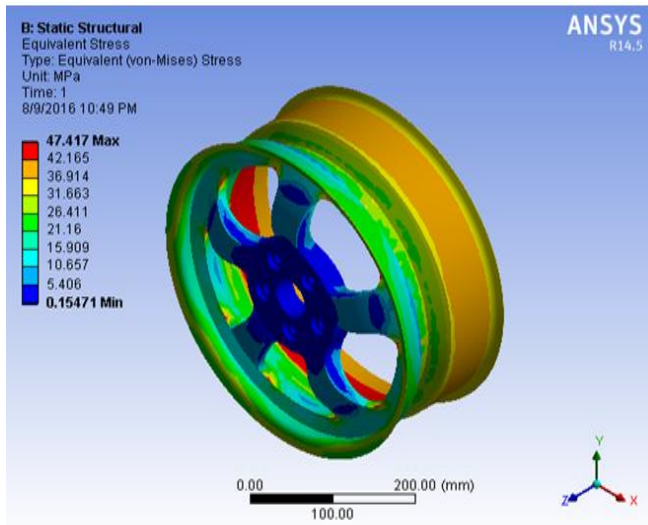


Fig.33. Maximum stress.

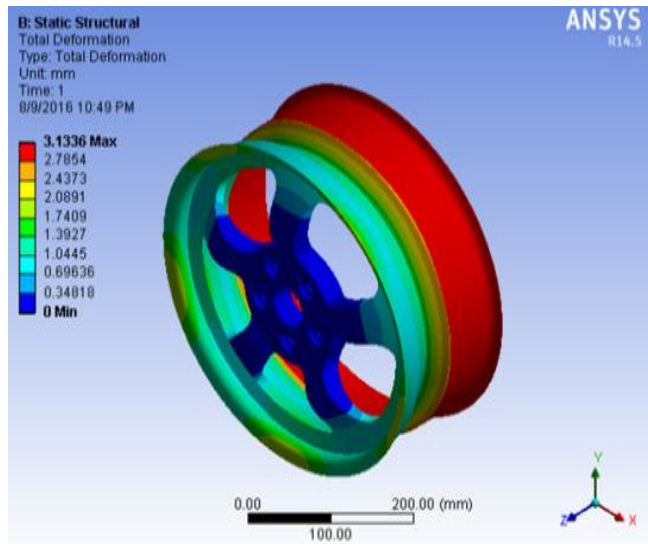


Fig.33. Total deformation.

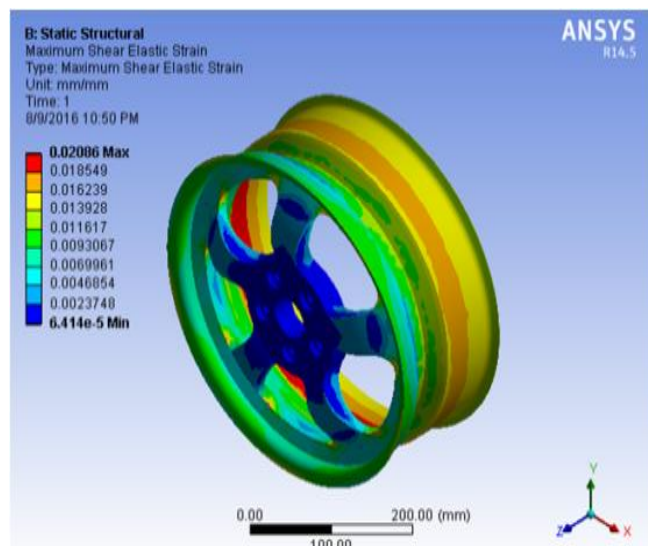


Fig.34. Maximum strain.

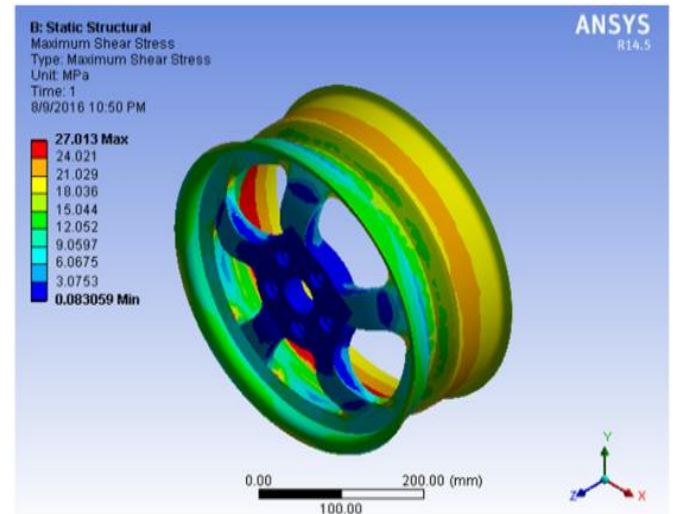


Fig.35. Maximum shear stress.

I. Material: Peek (20% Carbon Fibre)

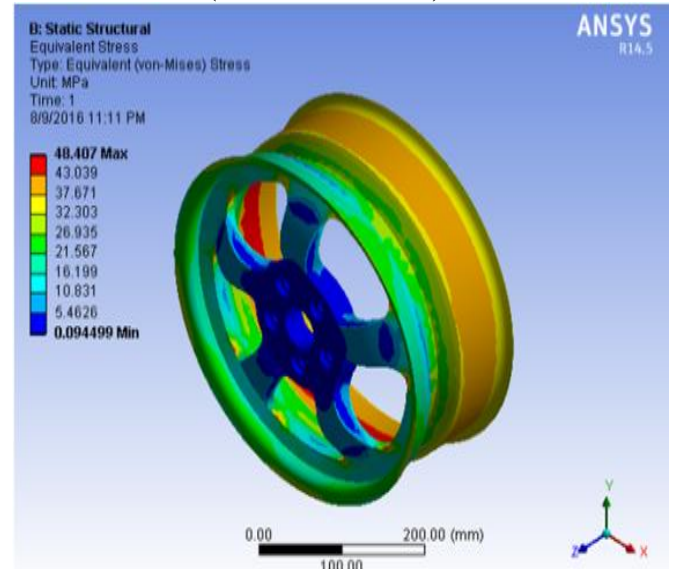


Fig.36. Maximum stress.

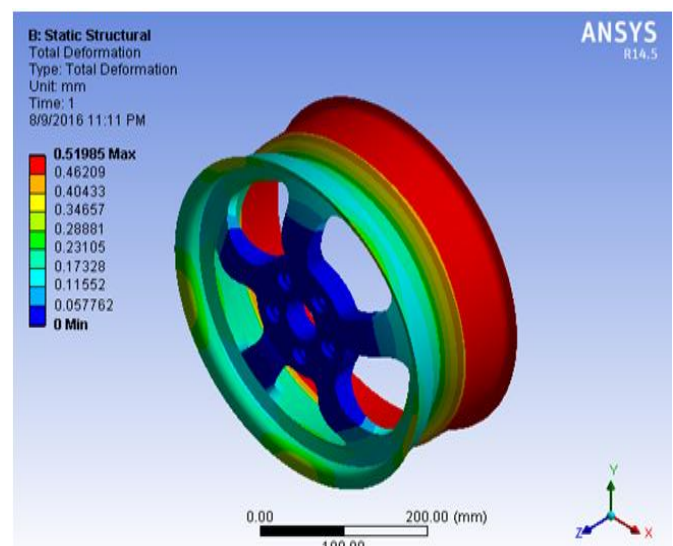


Fig.37. Total deformation.

Design and Analysis of Composite Alloy Wheel

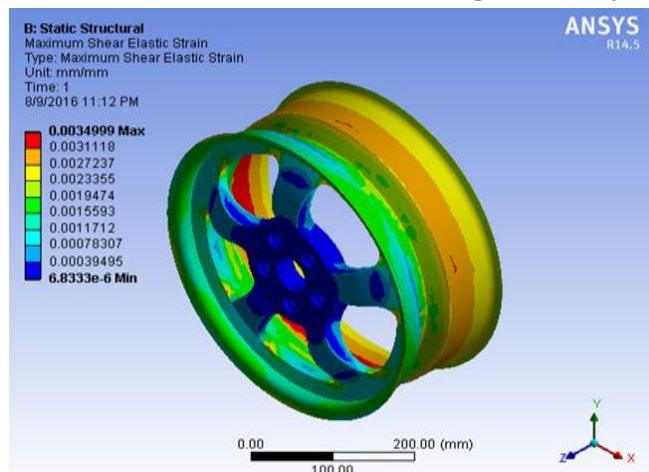


Fig.38. Maximum strain.

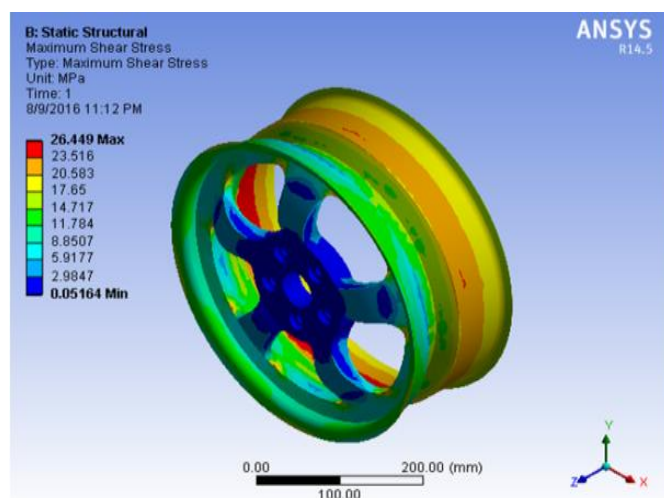


Fig.39. Maximum shear stress.

V. RESULTS

TABLE VI: At Pressure 0.8 MPa

Material	Max stress	Total deformation	Max strain	Max shear stress
Aluminum alloy	32.121	0.10477	0.000688	18.366
Magnesium alloy	31.911	0.16591	0.001094	18.009
Peek material	31.611	2.0891	0.013902	18.009
Peek(20%carbon fibre)	32.271	0.34657	0.002333	17.633

TABLE VII: At Pressure 1.2 Mpa

Material	Max stress	Total deformation	Max strain	Max shear stress
Aluminum alloy	48.181	0.15716	0.0010321	27.548
Magnesium alloy	47.866	0.24887	0.0016422	27.371
Peek material	47.417	3.1336	0.02086	27.013
Peek(20%carbon fibre)	48.407	0.51985	0.0034999	26.449

VI. CONCLUSION

- Design and analysis of alloy wheel is done.
- Modeling of alloy wheel is done in solid works design software by using various commands.
- Static structural analysis is carried out in ansys workbench at two different pressures with four different

materials such as aluminum alloy, mg alloy, peek material, peek (20% carbon fibre) material.

- Stress, deformation, strain, max shear stress of these four materials at two different pressures(i.e; 0.8MPa & 1.2 MPa) are noted and tabulated.
- Generally aluminum alloy and magnesium alloy are commonly used materials whereas peek material and peek (20%carbon fibre) materials are rarely used.
- From the analysis we notified that that stress values of peek material and peek(20% carbon fibre) material are also equivalent to al alloy and mg alloy.
- Hence these materials are also preferable.

VII. REFERENCES

- [1] Fatigue Analysis of Aluminium Alloy Wheel Under Radial Load, International Journal of Mechanical and Industrial Engineering (IJMIE), ISSN No. 2231 –6477, Vol-2, Issue-1, 2012.
- [2] “An analysis of stress and displacement distribution in a rotating rim subjected to pressure and radial loads” by P.C.Lam and T.S.Srivastam.
- [3] THE TIRE AND RIM ASSOCIATION, INC (1996), “50 Drop Centre Rim Contours”, J (ISO) Contour for 14,15,16,18 and 20 diameter Designation, pp7.05.
- [4] Stress Analysis Of Wheel Rim International Journal of Mechanical Engineering and Research Volume 1 Issue 1 (Page, 34-37), ISSN: 2277-8128.
- [5] AdelbertPhilloMills, (1922), Materials of Construction: Their Manufacture and Properties, John Wiley & sons, inc, originally published by the University of Wisconsin, Madison.
- [6] Hogan,(1969), “Density of States of an Insulating Ferro magnetic Alloy”.
- [7] Zhang, X.; Suhl, H.(1985)," Spin- wave-related period doublings and chaos under transverse pumping " Michael Bauccio (2005).
- [8] ASM metals reference book, ASM International Jon L. Dossett, HowardE.Boyer(2006) Practical heat treating.
- [9] T. A. Rickard (1941), "The Use of Meteoric Iron ". The Journal of the Royal Anthropological Institute of Great Britain and Ireland.

Author's Profile:



Mekala Swamy, Department of Mechanical Engineering, Mallareddy Engineering College (Autonomous) Maisammaguda, Dhulapally (Post. Via.Kompally), Secunderabad, Email: Swamy858@gmail.com.



Dumpa Suresh Reddy (Assistant Professor) Department of Mechanical Engineering, Malla Reddy Engineering College (Autonomous) Maisammaguda, Dhulapally(Post. Kompally), Secunderabad.

Preparation and Testing of a Composite Plate Using Shrimp Shell Filler



K.Aravind Babu
 PG Student, Machine Design,
 Dept of Mechanical Engineering,
 Malla Reddy Engineering College.



K.Srinivasa Rao
 Associate professor,
 Dept of Mechanical Engineering,
 Malla Reddy Engineering College.

ABSTRACT:

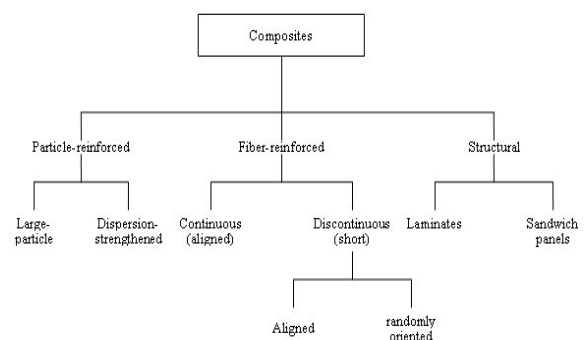
Composite materials[6] have interesting properties such as high strength to weight ratio, ease of fabrication, good electrical and thermal properties compared to metals. A composite material consists of several layers of a composite mixture consisting of matrix and fibers. Each layer may have similar or dissimilar material properties with different fiber orientations under varying stacking sequence. The major composite which is used in this project are SHRIMP SHELLS filler. This shrimp shells are converted as filler by the chemical process and added as an ingredient to the composite material in order to increase the strength of the composite material and to obtain the more accurate results. In this the composites are prepared and tensile testing is done on it

1. INTRODUCTION :

Today Composites [1] are receiving much attention not only because they are on the cutting edge of active material research field but also because there is a great deal of promise for their potential applications in various industries ranging from aerospace to construction due to their various outstanding properties. Realities of the modern world demand that engineering materials simultaneously possess high stiffness, strength and impact toughness, which is not a trivial task. Typically, stiff and strong materials such as ceramics are brittle, whereas tough materials, for example rubber, are soft and weak. On an Ashby plot this translates into an inverse correlation between strength and toughness. Such problematic behavior, however, is much less pronounced in natural composites like nacre, bone, turtle shell or sponge spicule, where a number of complex reinforcing mechanisms including crack bridging, crack deflection and geometric/structural intricacy provide resistance to fracture propagation and impact toughness.

2. LITERATURE REVIEW:

A composite material (also called a composition material or shortened to composite) is a material[2] made from two or more constituent materials with significantly different physical or chemical properties, that when combined, produce a material with characteristics different from the individual components. The new material may be preferred for many reasons: common examples include materials which are stronger, lighter, or less expensive when compared to traditional materials. Composite materials are generally used for buildings, bridges, and structures such as boat hulls, swimming pool panels, race car bodies, shower stalls, bath tubs, storage tanks, imitation granite and cultured marble sinks and countertop. Woody plants, both true wood from trees and plants such as palms and bamboo, yield natural composites that were used prehistorically by mankind and are still used widely in construction and scaffolding. One of the most common and familiar composite is fiber-glass, in which small glass fiber are embedded within a polymeric material (normally an epoxy or polyester). The glass fiber is relatively strong and stiff (but also brittle), whereas the polymer is ductile (but also weak and flexible). Thus the resulting fiberglass is relatively stiff, strong, flexible, and has ductile strength especially at higher temperatures. It has improved thermal shock resistance and corrosion resistance. Increase in Young's modulus and reduction of thermal elongation.



Composites are made up of individual materials referred to as constituent materials. There are two main categories of constituent materials: matrix and reinforcement. At least one portion of each type is required. The matrix material surrounds and supports the reinforcement materials by maintaining their relative positions. The reinforcements impart their special mechanical and physical properties to enhance the matrix properties. A synergism produces material properties unavailable from the individual constituent materials, while the wide variety of matrix and strengthening materials allows the designer of the product or structure to choose an optimum combination. Engineered composite materials must be formed to shape. The matrix material can be introduced to the reinforcement before or after the reinforcement material is placed into the mould cavity or onto the mould surface. The matrix material experiences a melting event, after which the part shape is essentially set. Depending upon the nature of the matrix material, this melting event can occur in various ways such as chemical polymerization or solidification. One of the most common and familiar composite is fiberglass, in which small glass fiber are embedded within a polymeric material (normally an epoxy or polyester). The glass fiber is relatively strong and stiff (but also brittle).

3. PURPOSE OF RESEARCH :

The main purpose of this research is to find the strength of the composite material with filler ingredient and without filler ingredients. As we all know that composite materials are strong enough with their properties and nature, but by adding other ingredients to this composite we can increase more strength and accuracy. So, in order to increase the stiffness to that material composite, in my research I am using the filler to the composite material. The filler which I am using to this composite is the shrimp shells filler, this filler is converted to powder and this mixture is added to the composite while preparation of the composite. By adding this filler to composite the quantity of the composite can be reduced because the filler is being added. Due to this the strength of the material will increase and the thickness can be reduced and material quantity can be reduced easily. So, in this the composite and filler are mixed and different testing has been done. By this research I can prove that strength and efficiency can be better when compared to the composite material without any ingredients. The reinforcement of metals can have many different objectives.

Tensile tests are performed on two different materials and the load Vs displacement graph is obtained in each case. The ultimate load, elongation and area of cross section according to standards is considered to calculate the ultimate tensile strength and young's modulus of the specimens.

4. PREPARATION METHOD :

4.1 GLASS FIBER:

It is a material made of extremely fine fibers of Glass [5] material. It is used as a reinforcement in the polymer. It is a light weight material used to form the reinforced polymer. The fiber pieces are taken according to dimension of 300mmX10mmX7mm.

4.2 FABRICATION OF COMPOSITE MATERIAL:

The preparation of COMPOSITE MATERIAL involves the following major activities. A brief illustration of the activities is given below.



Fig 1: COMPOSITE MATERIAL

The above figure shows the preparation of Composite by the combination of GLASS fiber, Shrimp shell powder 100 gms and resin by manual layup method.

4.3 Material Deposition:

In this releasing agent is applied on the mould and it is set to dry for 2 minutes. Then the resin mixture is applied on the surface of the mould and the GLASS fiber piece is placed on it. Again resin is applied and fiber is placed till we get 4 layers. Now the metal sheet is placed and again 4 layers of resin and fiber are placed on the metal sheet in the form of a laminate. The major composite which is used in this project are SHRIMP SHELLS filler upon arrival at the Laboratory,

the visible fat was mechanically removed, while the shrimp shell was washed with warm water and slight ethanol before stored in the freezer until it was used for the experiments. Prior to be used, the shrimp shell was allowed to reach room temperature, and dried under the heat of the sun, crushed and sieved

4.4 Material Deposition:

Hydrochloric acid (HCl), sulfuric acid (H₂SO₄), nitric acid (HNO₃), oxalic acid (H₂C₂O₄), Na borax and NaOH. The shrimp shell powder was soaked in a HCl solution for 24 hours at room temperature with ratio of shrimp shell powder [7] and HCl solution was 1:6 (m/v).

4.6 Cyclic process for converting shrimp shells to paste:

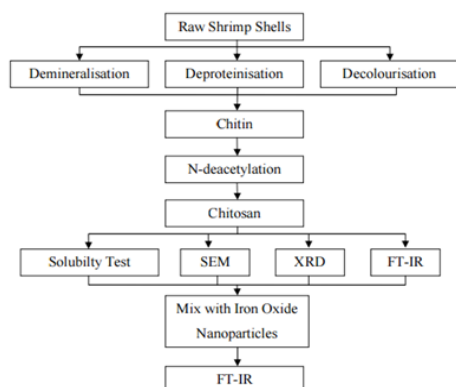


Fig 2. Composite as per dimensions according to ASTM standards

5. RESULTS AND DISUCSSIONS:

Tensile tests are performed on two different material and the load Vs displacement graph is obtained in each case. The ultimate load, elongation and area of cross section according to standards is considered to calculate the ultimate tensile strength and young's modulus of the specimens. By the two graphs we can see the differences in the strength of the materials. By this the strength of the composite material with filler is more than without filler.

From the tensile test the ultimate load for particular elongation is found. The ultimate tensile strength and Young's modulus are calculated as follows:

- Ultimate tensile strength = Ultimate load/Area of cross section.
- Young's Modulus E = Ultimate tensile strength / Strain.
- Strain = change in length / Original length.

4.5 TESTING:

The composite is machined as per dimensions shown in the below figure and the area of cross section 12.785mm X 6.96. 6mm is maintained for all specimens. In order to perform tensile test on a laminate it is made to required dimensions as per ASTM[3] standards

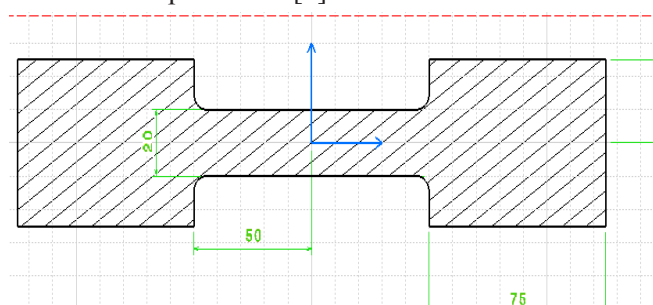
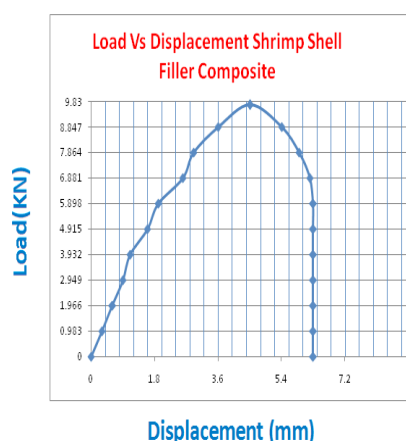
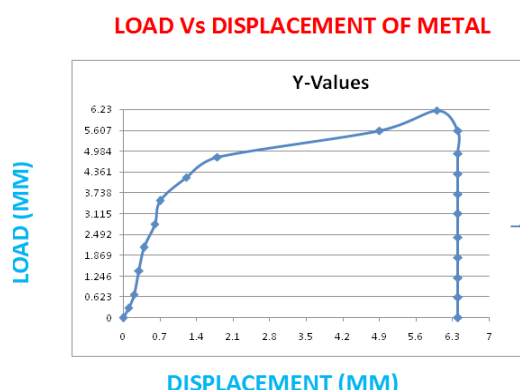


Fig 3. Metal piece placed in Universal Testing Machine





Standard Fiber Properties

	US Units	SI Units
Tensile Strength	600 Ksi	4137 MPa
Tensile Modulus	35 Msi	242 GPa
Elongation	1.5%	
Density	0.065 lb/in ³	1.81 g/cc
Fiber Diameter	0.283 mils	7.2 microns
Carbon Content	95%	
Yield	400 ft/lb	270 m/kg

Fig: Properties[4]

Glass Fiber Mechanical Properties

	E-glass	R-glass	HS2,HS4	T-glass	S-1	S-2
Tensile Strength GPa	1.9-2.5	3.1-3.4	3.1-4.0	4.0-4.2	3.8-4.1	4.3-4.6
Tensile Modulus GPa	69-80	86-89	82-90	84	85-87	88-91

6.CONCLUSION:

Both materials have equal properties but overall the superior material fiber glass. So by adding the shrimp shell powder as an ingredient to fiber glass the strength of fiberglass would be considered the stronger material due to its nature to flex to avoid breaking. Also the price of fiberglass makes it superior to carbon fiber in certain aspects. In much of the commercial consumer market carbon fiber has been favored; this has resulted to extreme raises in the prices in products that involve carbon fiber. Fiber glass has proven itself to be superior in the industrial industry.

MATERIAL	FIBER GLASS WITH SHRIMP SHELL POWDER	CARBON FIBER WITH OUT SHRIMP SHELL
ULTIMATE TENSILE STRENGTH	73.23	62.23

ACKNOWLEDGEMENT:

I express my sincere and heart full gratitude towards my guide Associate professor K.Srinivasa Rao for accepting me as his student and giving me opportunity to work on this project. I am thankful to sir for his support, guidance and encouragement throughout the M-Tech course.

REFERENCES:

- 1.Hull D, 1981, An Introduction to Composite Materials, (Cambridge University Press)
- 2.IISc Bangalore: Fibre reinforced metal matrix composite-a review,Jan-Feb 1996, 76,pp 1-14.
3. ASTM Journal: Standard test methods for tension testing of metallic materials.
4. <https://infogr.am/carbon-fiber-vs-fiberglass>
5. Dong CS, Duong J and Davies IJ. Flexural properties of S-2 glass and TR30S carbon fiber-reinforced epoxy hybrid composites. Polym Compos 2012; 33: 773-781
6. https://en.wikipedia.org/wiki/Composite_material
7. https://www.google.co.in/search?q=shrimp+shell+powder&biw=1360&bih=643&source=lnms&tbm=isch&sa=X&ved=0ahUKEwjprLuH_8zNAhVLqY8KHRIcB3sQ_AUIBigB#imgrc=_3HPBHeW52qhiM%3A

DESIGN AND ANALYSIS OF COMPOSITE DRIVE SHAFT

KETHAVATH RAJESH, Mr A. RAMESH M.Tech (P.hD) Asst. Professor

Abstract

Drive shaft is the most important component to any power transmission application; automotive drive Shaft is one of this. A drive shaft, also known as a propeller shaft or Cardan shaft, it is a mechanical part that transmits the torque generated by a vehicle's engine into usable motive force to propel the vehicle. Substituting composite structures for conventional metallic structures has many advantages because of higher specific stiffness and strength of composite materials. This work deals with the replacement of conventional two-piece steel drive shafts with a single-piece aluminum silicon carbide composite drive shaft for an automotive application. The design parameters were optimized with the

Objective of minimizing the weight of composite drive shaft. The CAD model is Designed in SOLID WORKS PREMIUM 2014 SOFTWARE. To obtain the stress and deformation values solid works simulation software was used. By comparing the results proper material for drive shaft can be selected.

Introduction to drive shaft:

A drive shaft, driveshaft, driving shaft, propeller shaft (prop shaft), or Cardan shaft is a mechanical component for transmitting torque and rotation, usually used to connect other components of a drive train that cannot be connected directly because of distance or the need to allow for relative movement between them.

As torque carriers, drive shafts are subject to torsion and shear stress, equivalent to the difference between the input torque and the load. They must therefore be strong enough to bear the stress, whilst avoiding too much additional weight as that would in turn increase their inertia.

To allow for variations in the alignment and distance between the driving and driven components, drive shafts frequently incorporate one or more universal joints, jaw couplings, or rag joints, and sometimes a splined joint or prismatic.

Drive Shaft description:

As mentioned above, recent developments in the applications of composite materials have shown that a composite material structural member used in power transmission can be of a great assistance in overcoming a few of the problems faced with conventional drive shafts. The assessment of the extent of this fact is the essence of this work. Therefore a good understanding of the drive shaft would be a prerequisite and is discussed in the following section.

A drive shaft, propeller shaft (prop shaft), or Cardan shaft is a mechanical component for transmitting torque and rotation, usually used to connect other

components of a drive train that cannot be connected directly because of distance or the need to allow for relative movement between them. Drive shafts are carriers of torque. They are subject to torsion and shear stress, equivalent to the difference between the input torque and the load. They must therefore be strong enough to bear the stress, whilst avoiding too much additional weight as that would in turn increase their inertia. Therefore a drive shaft is expected to function, as follows.

It must transmit torque from the transmission to the differential gear box.

The drive shaft must also be capable of rotating at very high speeds as required by the vehicle.

The drive shaft must also operate through constantly changing angles between the transmission, the differential and the axels.

The length of the drive shaft must also be capable of changing while transmitting torque.

- Thus the design of a drive shaft presents itself as a case of torsion problem. Further, with regard to the conventional drive shafts

following shortcomings were observed some of which could be addressed better with a composite shaft.

- They have less specific modulus and strength
- Increased weight
- Conventional steel drive shafts are usually manufactured in two pieces to increase the fundamental bending natural frequency because the bending natural frequency of a shaft is inversely proportional to the square of beam length and proportional to the square root of specific modulus.

Therefore the steel drive shaft is made in two sections connected by a support structure, bearings and U-joints and hence overall weight of assembly will be more.

- Its corrosion resistance is less as compared with composite materials.
- Steel drive shafts have less damping capacity.

Since a drive shaft is a case of torsion problem an understanding of the

methodology of solving such a problem in structural mechanics is necessary.

Drive Shaft

The drive shaft, or cardan shaft as it is sometimes called, is a cylindrical piece of metal, which plays a crucial role in the operation of a motor vehicle. Main drive shafts are tubular and are usually constructed from steel. They will generally be of a large diameter and hollow because weight plays a large part in the efficiency of their performance. It is for this very reason that some have aluminum incorporated in their makeup. There are also short drive shafts, which are used to connect the main drive shaft to the wheels themselves. In these cases, and in front-wheel drive vehicles where the engine and wheels are in close proximity, these short drive shafts are not hollow but solid pieces of metal.

Drive shaft working

While the importance of an engine to the running of an automobile is well known, it can be argued that the drive shaft plays an equally vital role. The drive shaft acts as a medium for transferring the power generated by the engine to the wheels, enabling them to turn. This in turn puts the vehicle in motion.

The force that is transmitted by the drive shaft is referred to as torque. Torque is basically the technical term to describe the force associated with a twisting or spinning motion. Because drive shafts have to endure conditions that could cause them to bend or break they are made to be “flexible”. Flexible in this sense does not mean the ability to bend. What it speaks to is an allowance for some small degree of movement at the points where the drive shafts are connected.

This is accomplished via what are known as universal joints, or u-joints. It is necessary for drive shafts to be straight and balanced. If this is not so vibrating will result. This can lead to damage to the components that are connected to the drive shaft. One example is the engine, which is turning at high speed.

The importance of the drive shaft is best appreciated in circumstances where it bridges the gap between inconveniently located components. This inconvenience can arise because of the component's long distance apart, or their awkward positioning/alignment.

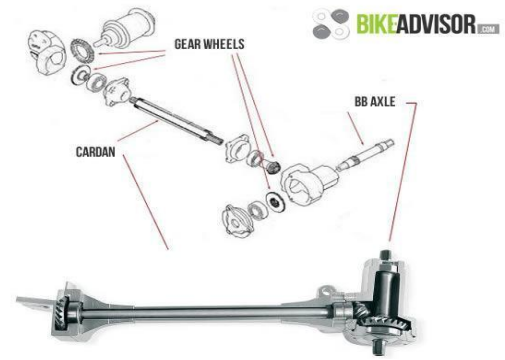


Fig: drive shaft

Purpose of the Drive Shaft (or Propeller Shaft):

The torque that is produced from the engine and transmission must be transferred to the rear wheels to push the vehicle forward and reverse. The drive shaft must provide a smooth, uninterrupted flow of power to the axles. The drive shaft and differential are used to transfer this torque.

Functions of the Drive Shaft:

First, it must transmit torque from the transmission to the differential gear box.

During the operation, it is necessary to transmit maximum low-gear torque developed by the engine.

The drive shafts must also be capable of rotating at the very fast speeds required by the vehicle.

The drive shaft must also operate through constantly changing angles between the transmission, the differential and the axles. As the rear wheels roll over bumps in the road, the differential and axles move up and down. This movement changes the angle between the transmission and the differential.

The length of the drive shaft must also be capable of changing while transmitting torque. Length changes are caused by axle movement due to torque reaction, road deflections, braking loads and so on. A slip joint is used to compensate for this motion. The slip joint is usually made of an internal and external spline. It is located on the front end of the drive shaft and is connected to the transmission.

Literature Survey:

Composites have high specific modulus, strength and less weight. The fundamental natural frequency of carbon fiber drive shaft can be twice as that of the steel or aluminum, because the carbon fiber

Composite material has more than 4 times the specific stiffness, which makes it possible to manufacture the drive shaft of passenger cars in one piece. A one piece composite shaft can be manufactured so as to satisfy the vibration requirements. This eliminates all the assembly, connecting the two piece steel shaft and thus minimizes the overall weight, vibrations and cost. Due to weight reduction fuel consumption will be reduced. They have high damping capacity and hence they produce less vibrations and noise. They have good corrosion resistance, greater torque capacity, longer fatigue life than steel and aluminium.

Mechanical characterization of Al-SiC composite done in previous work by Behera et al. [2013], Wang et al [2008], Pathak et al. [2006] The hardness, impact strength, and material toughness were evaluated. The improved value of coefficient of thermal expansion for Aluminum composites is one of the reasons they are widely used in electronics industry as studied by Martin et al. [2011], Dunia Abdul Saheb[2011], Occhionero et al.[2010], Wang et al.[2006] .

Composite drive shafts

Introduction:

Composite materials have been widely used to improve the performance of various types of structures. Compared to conventional materials, the main advantages of composites are their superior stiffness to mass ratio as well as high strength to weight ratio. Because of these advantages, composites have been increasingly incorporated in structural components in various industrial fields. Some examples are helicopter rotor blades, aircraft wings in aerospace engineering, and bridge structures in civil engineering applications. Some of the basic concepts of composite materials are discussed in the following section to better acquaint ourselves with the behaviour of composites.

Basic Concepts of Composite Materials:

Composite materials are basically hybrid materials formed of multiple materials in order to utilize their individual structural advantages in a single structural material. The constituents are combined at a macroscopic level and are not soluble in each other. The key is the macroscopic examination of a material where in the components can be identified by the naked eye. Different materials can be combined on a microscopic scale, such as in alloying of metals, but the resulting material is, for all

practical purposes, macroscopically homogeneous, i.e. the components cannot be distinguished by the naked eye and essentially acts together. The advantage of composite materials is that, if well designed, they usually exhibit the best qualities of their components or constituents and often some qualities that neither constituent possesses. Some of the properties that can be improved by forming a composite material are strength, fatigue life, stiffness, temperature-dependent behaviour, corrosion resistance, thermal insulation, wear resistance, thermal conductivity, attractiveness, acoustical insulation and weight. Naturally, not all of these properties are improved at the same time nor is there usually any requirement to do so. In fact, some of the properties are in conflict with one another, e.g., thermal insulation versus thermal conductivity. The objective is merely to create a material that has only the characteristics needed to perform the designed task. There are two building blocks that constitute the structure of composite materials. One constituent is called the reinforcing phase and the one in which it is embedded is called the matrix. The reinforcing phase material may be in the form of fibers, particulates, flakes. The matrix phase materials are generally

continuous. Examples of composite systems include concrete reinforced with steel, epoxy reinforced with graphite fibers, etc.

Classification of Composites:

Composite Material:

A material composed of 2 or more constituents is called composite material.

Composites consist of two or more materials or material phases that are combined to produce a material that has superior properties to those of its individual constituents. The constituents are combined at a macroscopic level and or not soluble in each other. The main difference between composite and an alloy are constituent materials which are insoluble in each other and the individual constituents retain those properties in the case of composites, whereas in alloys, constituent materials are soluble in each other and forms a new material which has different properties from their constituents.

Material properties of aluminum silicon carbide:

	Baseline AlSiC	AlSiC- 20% vol %	AlSiC- 30% vol %	AlSiC- 40% vol %	AlSiC- 50% vol %
Property Comparison	AlSiC (70)	AlSiC-20% vol % (70)	AlSiC-30% vol % (70)	AlSiC-40% vol % (70)	AlSiC-50% vol % (70)
Density (g/cc)	2.7	2.5	2.5	2.5	2.5
Tensile Modulus (GPa)	12	100	100	115	115
Failure (%)	1	4	4	4	4
Tensile Strength (MPa)	100	100	100	100	100
Tensile Strength (MPa)	100	100	100	100	100

Introductions to Solid Works:

Solid works mechanical design automation software is a feature-based, parametric solid modeling design tool which advantage of the easy to learn windows TM graphical user interface. We can create fully associate 3-D solid models with or without while utilizing automatic or user defined relations to capture design intent. Parameters refer to constraints whose values determine the shape or geometry of the model or assembly. Parameters can be either numeric parameters, such as line lengths or circle diameters, or geometric parameters, such as tangent, parallel, concentric, horizontal or vertical, etc. Numeric parameters can be associated with each other through the use of relations, which allow them to capture design intent.

Basic Concepts of Analysis:

The software uses the Finite Element Method (FEM). FEM is a numerical technique for analyzing engineering designs. FEM is accepted as the standard analysis method due to its generality and suitability for computer implementation. FEM divides the model into many small pieces of simple shapes called elements effectively replacing

a complex problem by many simple problems that need to be solved simultaneously.

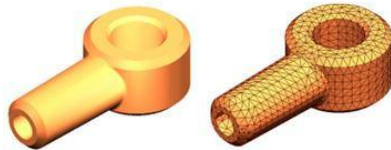


Fig: 11.2 CAD model of a part Fig:11.2(1)Model subdivided into small pieces (elements)

Elements share common points called nodes. The process of dividing the model into small pieces is called meshing.

Von mises failure criteria

The von Mises yield criterion suggests that the yielding of materials begins when the second deviatoric stress

Invariant reaches a critical value. It is part of a plasticity theory that applies best to ductile materials, such as metals. Prior to yield, material response is assumed to be elastic.

In materials science and engineering the von Mises yield criterion can be also formulated in terms of the von Mises stress or equivalent tensile stress, a scalar stress value that can be computed from the Cauchy stress tensor. In this case, a material is said to start yielding when its von Mises stress reaches a critical value known as the yield strength. The von Mises stress is used to predict yielding of materials under any loading condition from results of simple uniaxial tensile tests. The von Mises stress satisfies the property that two stress states with equal distortion energy have equal von Mises stress.

IJPRES

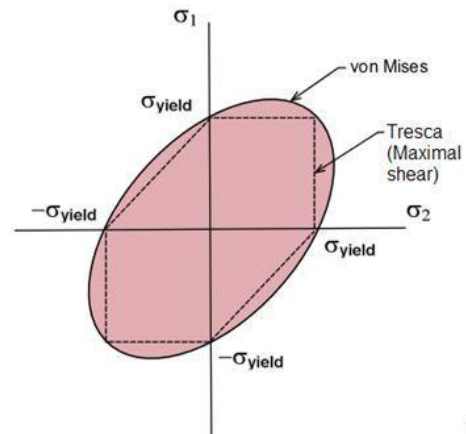


Fig: von misses

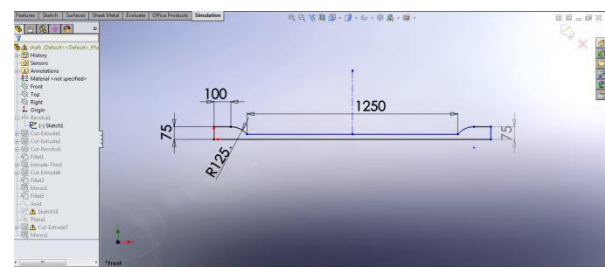
von misses

$$\sigma_{\text{von Mises}} = \sqrt{\frac{1}{2}(\sigma_1 - \sigma_2)^2 + (\sigma_2 - \sigma_3)^2 + (\sigma_3 - \sigma_1)^2}$$

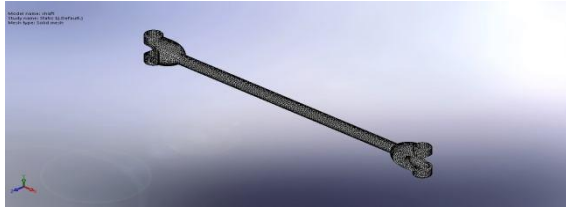
Modeling of Drive Shaft:

Drive shaft is modeled with proper dimensions in solid works. The design of composite drive shaft is as follows

Draw the sketch with dimensions as shown below



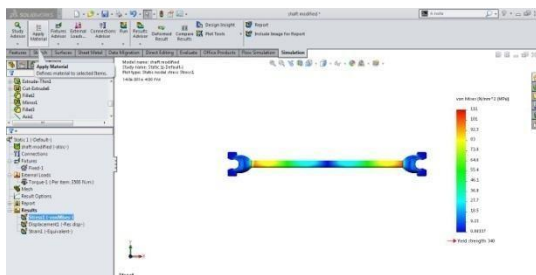
Revolve the sketch with base axis:



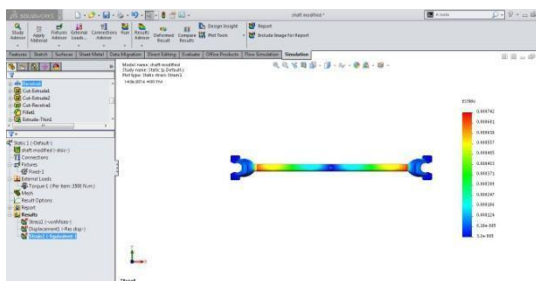
Analysis results

Material: aluminum silicon carbide.

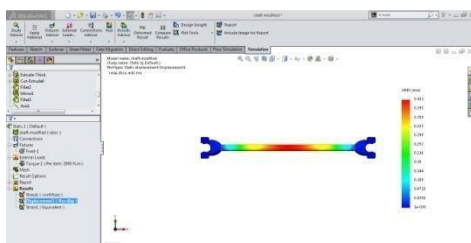
Maximum von misses stress



Maximum strain



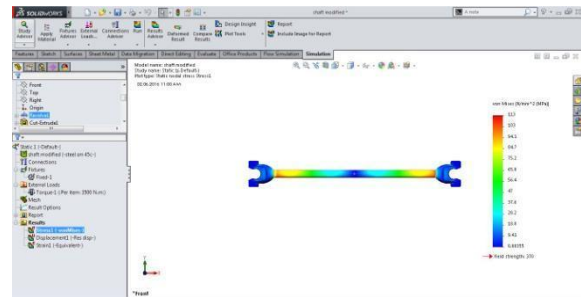
Total Deformation



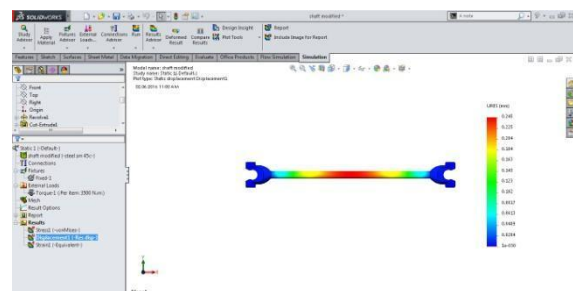
Material: steel

IJPRES

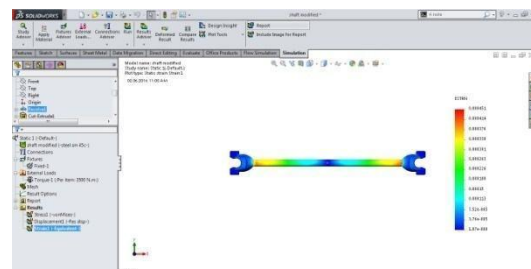
Maximum von-mises stress



Total deformation



Maximum strain



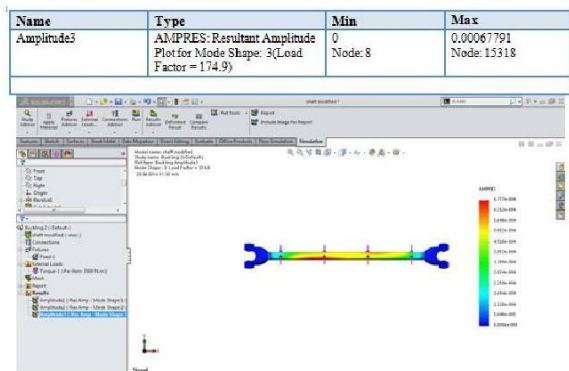
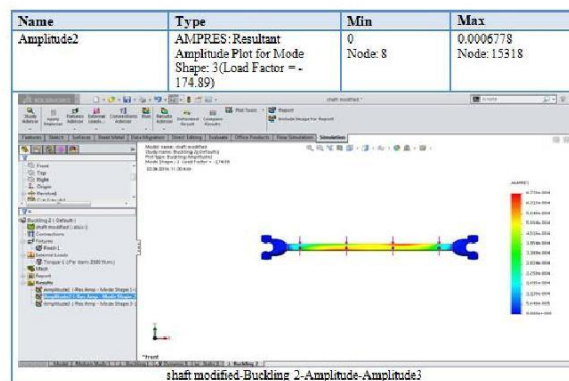
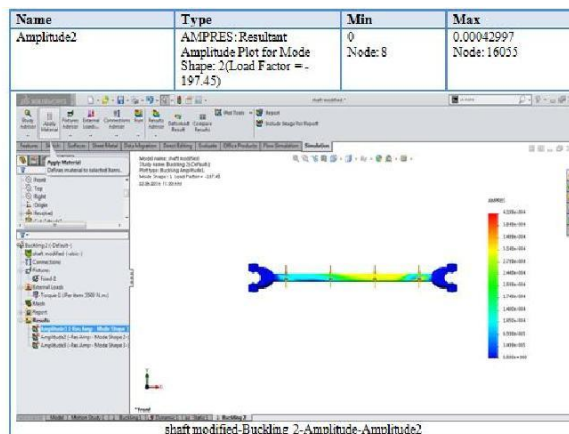
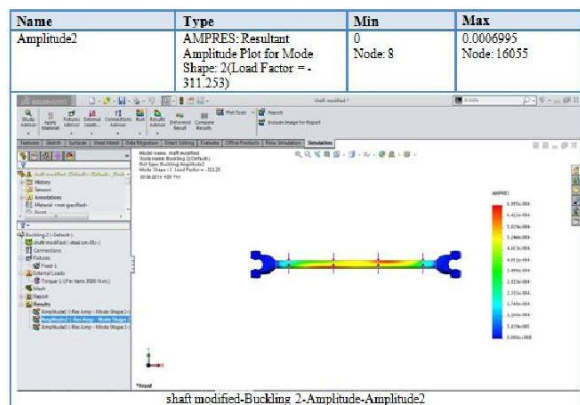
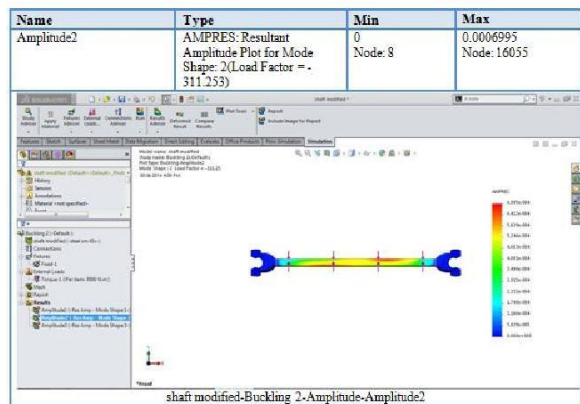
Buckling analysis

Material: steel

Buckling analysis results at different modes

Material: composite aluminum silicon
carbide

Name	Type	Min	Max
Amplitude1	AMPRES: Resultant Amplitude Plot for Mode Shape: 1(Load Factor = - 363.221)	0 Node: 8	0.0026748 Node: 8608



Load factor at different modes

Mode Number	Load Factor
1	-363.22
2	-311.25
3	311.33

Table5: Buckling factor at different modes

Mode Number	Load Factor
1	-197.45
2	-174.89
3	174.33

Table6: results:

s.no	Material	Torque(N-m)	Max. stress(Mpa)	Deformation (mm)
1	Steel sm 45c	3500	112.808	0.245
2	Aluminum silicon carbide	3500	110.797	0.432

Table7: Buckling analysis results:

Steel	Minimum	Maximum
Amplitude 1	0 Node-8	0.000267431 Node-6754
Amplitude 2	0 Node-8	0.000699511 Node-14066
Amplitude 3	0 Node-8	0.000699204 Node-14725
Aluminum Silicon Carbide		
Amplitude 1	0 Node-8	0.000429975 Node-6754
Amplitude 2	0 Node-8	0.000677104 Node-14066
Amplitude 3	0 Node-8	0.000677755 Node-14725

Conclusion:

Composite drive shaft is modeled and analyzed by using solid works 2014

Material properties and uses of composite materials are studied
Composite drive shaft is modeled in solid works by using required commands

Then analysis is done on drive shaft by using different materials such as steel and aluminum silicon carbide

Stress, strain and deformations are found out for two materials (i.e; steel and aluminum silicon carbide)

Results of stress, strain and deformations are tabulated

Aluminum silicon carbide has shown less weight when compared with steel shaft

References

1. Jones,R.M., 1990, *Mechanics of Composite Materials*, 2e, McGrawHill Book Company, New York.
2. AurtarK.Kaw, 1997, *Mechanics of Composite Materials*, CRC Press, New York..Belingardi.G, Calderale.P.M. and Rosetto.M.,1990, "Design Of Composite Material Drive Shafts For Vehicular Applications", *Int.J.ofVehicle Design*, Vol.11,No.6,pp. 553-563.
3. Jin Kook Kim.DaiGilLee, and Durk Hyun Cho, 2001, "Investigation of Adhesively Bonded Joints for Composite Propeller shafts", *Journalof CompositeMaterials*, Vol.35, No.11, pp.999-1021.
4. Dai Gil Lee, et.al, 2004, "Design and Manufacture of an Automotive Hybrid Aluminum/Composite Drive Shaft, *Journal of CompositeStructures*, Vol.63, pp87-89.
5. Agarwal B. D. and Broutman L. J., 1990, "*Analysis and performanceof*

KETHAVATH RAJESH



M.Tech, Machine Design
Dept. of Mechanical Engineering
Malla Reddy Engineering College.
E-mail id:
rajeshkethavath332@gmail.com

A.RAMESH



Assistant professor,
Dept. of Mechanical Engineering,
Malla Reddy Engineering College.
E-mail id:
ramesh340mech@gmail.com

Preparation and Testing of Metal and Fiber Reinforced Polymer Laminates



P.Sandeep

M.Tech, Machine Design,
Dept of Mechanical Engineering,
Malla Reddy Engineering College.



K.Srinivasa Rao

Associate professor,
Dept of Mechanical Engineering,
Malla Reddy Engineering College.

ABSTRACT:

In recent years there has been an increasing demand from the core industries for the materials possessing high strength to weight ratio. The process of improving the properties of conventional materials has lead to the technique of reinforcing polymers, ceramics and metals with particles, fibres[1] and whiskers. Thus leading to the production of composites. In this project MFRP laminates are prepared and tensile testing is done on it. The results are compared with the metals and FRP laminates. The comparison is made to find out the strength and weight of different materials.

1.INTRODUCTION :

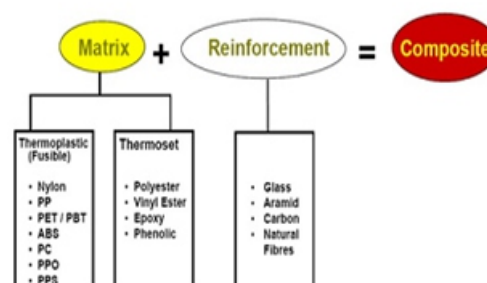
Materials play an important role in designing and manufacturing of any component. This factor has lead to the innovation and development of new materials. As we know the materials are divided into metals, non-metals and composites. The metals and non-metals are used extensively in past and in recent years. But now it is replaced by composites due to their good properties and life compared to them. In the composite materials also there are many different materials which are obtained by changing the composition of the constituents. These composites are brittle and light weight compared to metals. Here we are going to introduce a new material which has both the properties of metals and composites i.e., ductility and brittleness . So, the material is named as MFRP (Metal and Fiber Reinforced Polymer). It is a composite in which metals and fiber are reinforced into a polymer matrix. The applications of the material includes for buildings, bridges and structures such as boat hulls, swimming pool panels, race car bodies, bath tubs and storage tanks.

2. LITERATURE REVIEW:

A composite material[4] is a material made from two or more constituent materials with significantly different physical or chemical composition, that when combined, produces a material with characteristics different from the individual components. The individual components remain separate and distinct within the finished structure. The new material may be preferred for many reasons: common examples include materials which are stronger, lighter, or less expensive when compared to traditional materials.

Typical engineered composite materials include:

- Reinforced plastics, such as fiber-reinforced polymer
- Metal composites
- Ceramic composites
- Laminates



Composite materials are generally used for buildings, bridges, and structures such as boat hulls, swimming pool panels, race car bodies, shower stalls, bathtubs, storage tanks, imitation granite and cultured marble sinks and countertop. Woody plants, both true wood from trees and plants such as palms and bamboo, yield natural composites that were used prehistorically by mankind and are still used widely in construction and scaffolding.

Composites are made up of individual materials referred to as constituent materials. There are two main categories of constituent materials: matrix and reinforcement. At least one portion of each type is required. The matrix material surrounds and supports the reinforcement materials by maintaining their relative positions. The reinforcements impart their special mechanical and physical properties to enhance the matrix properties. A synergism produces material properties unavailable from the individual constituent materials, while the wide variety of matrix and strengthening materials allows the designer of the product or structure to choose an optimum combination.

Engineered composite materials must be formed to shape. The matrix material can be introduced to the reinforcement before or after the reinforcement material is placed into the mould cavity or onto the mould surface. The matrix material experiences a melting event, after which the part shape is essentially set. Depending upon the nature of the matrix material, this melting event can occur in various ways such as chemical polymerization or solidification from the melted state. Plywood 3400 BC by the Ancient Mesopotamians gluing wood at different angles gives better properties than natural wood. The first artificial fiber reinforced plastic was bakelite[4], has been used for hundreds of years which was invented in the year 1905 by Dr. Leo Baekeland had originally set out to find a replacement for shellac. He announced his invention

3.PURPOSE OF RESEARCH :

The reinforcement of metals can have many different objectives. The reinforcement of light metals opens up the possibility of application of these materials in areas where weight reduction has first priority. The precondition here is the improvement of the component properties. The development objectives for light metal composite materials are: Increase in yield strength and tensile strength at room temperature and above while maintaining the minimum ductility or rather toughness. Increase in creep resistance at higher temperatures compared to that of conventional alloys. Increase in fatigue Many commercially produced composites use a polymer matrix material often called a resin solution. There are different type of polymers which are available depending upon the starting raw ingredients. There are several broad categories, each with numerous variations. The most common are polyester[2], vinylester, epoxy, phenolic, polyimide, polyamide, polypropylene. at a meeting of the American Chemical Society on February 5, 1909.

One of the most common and familiar composite is fiberglass, in which small glass fiber are embedded within a polymeric material (normally an epoxy or polyester). The glass fiber is relatively strong and stiff (but also brittle), whereas the polymer is ductile (but also weak and flexible). Thus the resulting fiberglass is relatively stiff, strong, flexible, and has ductile strength especially at higher temperatures. It has improved thermal shock resistance and corrosion resistance. Increase in Young's modulus and reduction of thermal elongation.

4. PREPARATION METHOD :

4.1.1 GLASS FIBER :

It is a material made of extremely fine fibers of glass material. It is used as a reinforcement in the polymer. It is a light weight material used to form the reinforced polymer. The fiber pieces are taken according to dimension of 250mmX30mmX0.3mm.

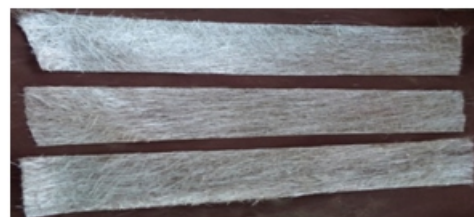


Fig 1. Glass fiber pieces as per dimensions.

4.1.2 METAL:

It is a solid material which is typically hard, shiny, malleable and ductile with good electrical and thermal resistance. A M.S plate of 250mmX30mmX2mm is used for reinforcing into the polymer matrix.

4.1.3 RESIN:

In material science or polymer chemistry resin[2] is a solid or highly viscous substance which are typically convertible into polymers. Such viscous substances may be derived from plant or synthetic origin. They are mixtures of organic compounds. In the preparation of MFRP general purpose resin is used as a matrix and as a bonding agent.

4.2 FABRICATION OF MFRP LAMINATES:

The preparation of MFRP laminates involves the following major activities. A brief illustration of the activities is given below.

Now the metal sheet and glass fiber is prepared according to the required dimensions. 100gms of general purpose resin is taken, 2ml of catalyst cobalt octate and 2ml of accelerator is added. Then the mixture is stirred till the light pink colour is observed.



Fig 2. Metal piece as per dimensions.

4.2.1 Raw material preparation:

During this the mild steel sheet surface is made rough by using emery paper in order to improve the adhesive bonding between metal layer and fiber reinforced laminate.

4.2.2 Material Deposition:

In this releasing agent is applied on the mould and it is set to dry for 2 minutes. Then the resin mixture is applied on the surface of the mould and the fiber piece is placed on it. Again resin is applied and fiber is placed till we get 4 layers. Now the metal sheet is placed and again 4 layers of resin and fiber are placed on the metal sheet in the form of a laminate.

4.2.3 Curing of laminates:

The laminates along with the mould is left to dry for 6-8 hrs at room temperature. Finally the laminates are removed from the mould.



Fig3. Fiber and metals pieces taken according to dimensions.

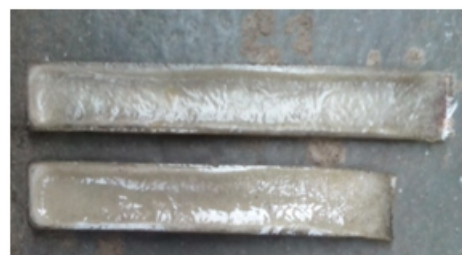


Fig 4. MFRP laminates after curing

The above figures shows the preparation of laminates by the combination of fiber, metal and resin by manual layup method.

4.3. TESTING:

The testing includes measuring of weights of FRP, MFRP and Metal laminates of same dimensions and tensile testing[3] is done for finding the strength of the laminates.

4.3.1 WEIGHT COMPARISON:

The weight of FRP, MFRP and metal laminates of dimensions 9mm x 30mm x 250mm are given below

FRP	MFRP	METAL
110 gms	230 gms	405 gms

4.3.2 TENSILE TESTING:

In order to perform tensile test on a laminate it is made to required dimensions as per ASTM standards. The FRP laminates are tested according to ASTM D638 and metals are tested as per ASTM AE8M[7] as shown in the figure. The laminate is machined as per dimensions shown in the below figure and the area of cross section 12.85mm X 5.6mm is maintained for all specimens.

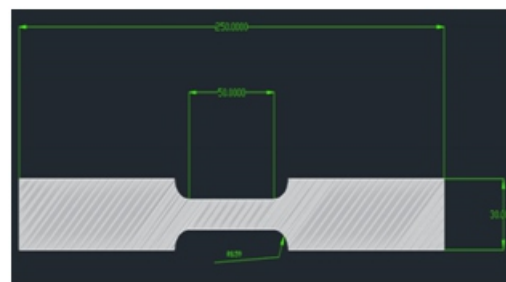




Fig 5. Laminate as per dimensions according to ASTM standards.



Fig 6. Laminate and metal piece placed in Universal Testing Machine.

5. RESULTS AND DISUCSSIONS:

The a tensile tests are performed on three different material laminates and the load Vs displacement graph is obtained in each case .The ultimate load, elongation and area of cross section according to standards is considered to calculate the ultimate tensile strength and young's modulus of the specimens .

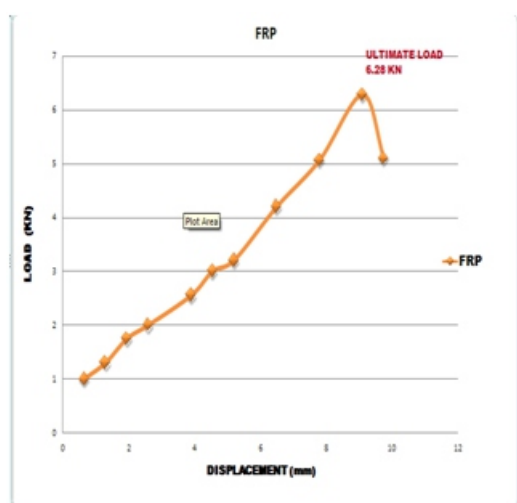


Fig 7. Load Vs Displacement graph of FRP laminate.

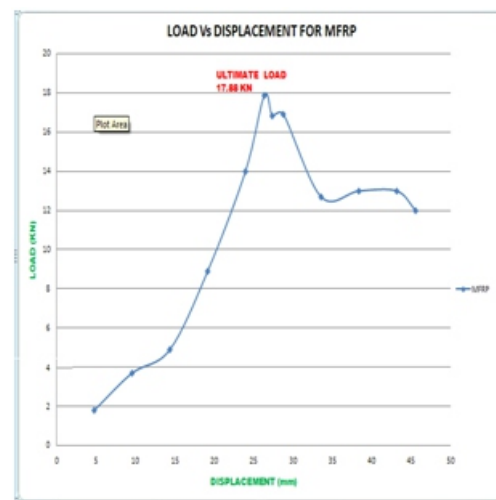


Fig 8. Load Vs Displacement graph of laminate. MFRP

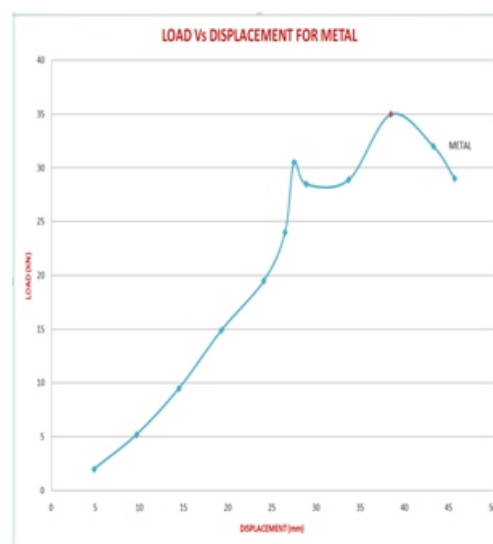


Fig 9. Load Vs Displacement graph of metal laminate.

From the tensile test the ultimate load for particular elongation is found. The ultimate tensile strength and Young's modulus are calculated as follows:

- Ultimate tensile strength = Ultimate load/Area of cross section.
- Young's Modulus E = Ultimate tensile strength / Strain.
- Strain = change in length / Original length.

MATERIAL / PROPERTI ES	FRP	MFRP	METAL
YOUNG'S MODULUS, E (GPa)	8.47	19	24.319
ULTIMATE LOAD(KN)	6.28	17.88	35
ULTIMATE STRENGTH (MPa)	86.3	139.62	486.65

6.CONCLUSION :

From the below table the ultimate tensile strength of MFRP lies in between the metal and FRP for same cross-section .It specifies that MFRP possesses the combined properties of FRP and metal.

MATERIAL	FRP	MFRP	MET AL
ULTIMATE TENSILE STRENGTH (MPa)	486.65	139.62	86.3

ACKNOWLEDGEMENT:

I express my sincere and heartfelt gratitude towards my guide Associate professor K.Srinivas Rao for accepting me as his student and giving me opportunity to work on this project. I am thankful to sir for his support, guidance and encouragement throughout the M-Tech course.

REFERENCES:

- [1].IOSR journal: Analysis of lpg cylinder using composite materials, Mechanical Engineering department K.S.R.M College of Engineering , Kadapa, A.P. Volume 9, Issue 2(sep-oct.2013),pp 33-42.
- [2]. IOSR journal: Modelling and Testing of hybrid composite laminate, Mechanical Engineering department S.R. Engineering College, Warangal, T.S.
- [3]. APRN journal of Engineering and Applied Sciences: Strength behaviour of FRP strengthened beam, Vol.04, No. 09, Nov-2009.
- [4]. IISc Bangalore: Fibre reinforced metal matrix composite-a review, Jan-Feb 1996, 76, pp 1-14.
- [5]. IJETT: Mechanical characterization and analysis of perforated fibre metal laminates, Vol.13, No.01, July 2014.
- [6].Schwartz ,M.M.,” composite materials hand book” , Mc Graw Hill,1988.

- [7]. ASTM Journal: Standard test methods for tension testing of metallic materials.

WEB REFERENCES:

- [1].https://en.wikipedia.org/wiki/Glass_fiber.
- [2].https://en.wikipedia.org/wiki/Polyester_resin.
- [3].https://en.wikipedia.org/wiki/Tensile_testing .
- [4].https://en.wikipedia.org/wiki/Composite_material.

Development and Experimental Characterization of Flexible Joint for Air Borne Propulsion System



P.Chandrasekhara Reddy
 M.Tech, Machine Design,
 Dept of Mechanical Engineering,
 Malla Reddy Engineering College.



K.Srinivasa Rao
 Associate professor,
 Dept of Mechanical Engineering,
 Malla Reddy Engineering College.

Abstract:

Solid rocket motors are propulsion devices for both satellite launchers and air borne vehicles, which require guidance or steering to fly along a commanded trajectory and to compensate for flight disturbances. Direction is controlled by controlling the thrust vector. To achieve this, the nozzle usually incorporates a flexible joint that allows the nozzle to vector (or rotate) in any direction. The movable nozzle with a flexible joint consists of four main sub-systems: the movable nozzle section, the attachment to the rocket motor, the actuation system, and the flexible joint.

The flexible joint is a non-rigid pressure – tight connection between the rocket motor and a movable nozzle that allows the nozzle to be deflected in a specified direction. The deflection of the nozzle deflects the motor thrust vector and generates a moment about the vehicle center of gravity, thereby altering the course of the vehicle. This paper brings out the development of flexible joint for air borne propulsion system followed by experimental characterization.

Keywords:

Optimization, GUI, MATLAB, thickness, etc .

1. INTRODUCTION:

Propulsion system is the basic driving aid for any air borne vehicle. It is required to control the direction of thrust developed by the propulsion system so as to control vehicles' pitch, yaw and roll motions. Propulsion system of a typical air borne vehicle is shown in Fig. 1.

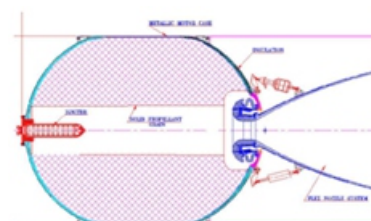


Fig. 1. Propulsion system of a typical air borne vehicle

The thrust control is obtained by steering the nozzle of the propulsion system using actuator-driven ball and socket system also called elastic bearing. The flexible joint may be depicted as a stack of spherical-shaped shims and rubber pads. The rubber sheets are chemically bonded to the rigid inserts, using adhesive agents laid on the inserts, which react during the moulding and vulcanization processes. Typical flexible joint is shown in Fig. 2.

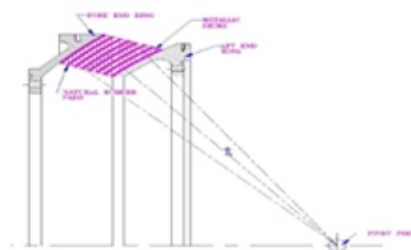


Fig. 2. Typical flexible joint

The flexible joint is the most widely used device in modern nozzles for ballistic or space applications. The flex nozzle system offers advantages of efficiency, low reduction of thrust and specific impulse. The moulded, multi-layer bearing acts as a seal, load transfer bearing and a visco-elastic flexure. It uses the deformation of stacked set of curved elastomeric (rubbery) layers between spherical metal or composite sheets to carry the loads and permits angular deflections of the nozzle axis.

The flexible joint is a non-rigid pressure-tight connection between the rocket motor and a movable nozzle that allows the nozzle to be deflected in a specified direction. The deflection of the nozzle deflects the motor thrust vector and generates a moment about the vehicle center of gravity, thereby altering the course of the vehicle. For many years, the development and qualification of new flexible joints for several generations of solid rocket motors have been relying on an experimental approach based on numerous tests and full scale manufacturing components. A short implementation using subscale hardware and the corresponding model had been previously developed before the availability of the design and 2D model. This preliminary activity allowed one to identify the relevant design modeling, parameters, and values to address.

Relying on this predictive approach, laboratory tests have started early in the development schedule, with the advantage of reducing the most important risks at a preliminary step where no costly hardware was committed on. Design of complex nozzle systems for solid rocket motors of satellite launchers and air borne vehicles and its validation through finite element modeling and testing are challenging tasks for designers in aerospace industries. Empirical relations for the design of nozzle systems developed by researchers based on extensive tests have limitations. Wood Berry [1] developed empirical relations from the experiments and confirmed by Walker for designing an elastomeric seal for Omni axial movable nozzle. Gajbir Singh and Rao [2] proposed

empirical relations for reinforcement stresses for both pressure loads and vectoring loads for joint diameters between 19.3 cm to 56 cm. Their FEA results are compared with the empirical relations only for pressure loads. However, these relations are applicable for conical shims only. Preliminary theoretical flex seal design sensitivity studies of James Donat [3] indicate that any modifications to reduce stress may cause increase of torque and weight. Regarding the overall configuration aspects of the nozzle systems. Jeffrey Foote [4] presented the details of TITAN IV solid rocket motor upgrade program. There was a need for increased lift capability and improved booster reliability. The increased lift is obtained by three ways. The diameter of the rocket motor has been increased. The propellant density and specific impulse were increased.

The inert weight of the rocket motor was reduced. Kirby and Van Vooren [5] discussed selection of thrust vector control systems for solid rocket motor and liquid engines. The usability and suitability of various thrust vector methods are discussed. Sivaramakrishnan and Bhagwan [6] characterized the natural rubber and determined the material constants of the Mooney-Rivlin model. Press [7] expressed the strain energy as a function of extension ratio, which is used to obtain material constants from the stress-strain data of hyper elastic material like elastomers. Taine et al. [8] presented four most commonly used hyper elastic models of Mooney-Rivlin, Ogden, neo-Hookean and Yeoh to use in the design/analysis of tyres for manufacturing. As can be seen, development of flexible joint for air borne propulsion system is not dealt more in fabrication perspective. Furthermore almost no literature is available which speaks about experimental characterization of flexible joint. Based on these limitations development and experimental characterization of flexible joint for air borne propulsion system is taken up in the current research work.

2. DEVELOPMENT OF FLEXIBLE JOINT:

The properties required for flexible joint are low shear modulus, high shear strength and high bulk modulus. These properties are required to design a flexible joint with low spring torque, high shear stress capability and less axial compression. In addition, compatibility with shims for bonding or vulcanizing and good ageing properties are also required. As latex rubber cannot meet these requirements, natural Rubber has been chosen as material for flexible joint. It has been processed to increase the mechanical properties and the properties achieved after processing are given in Table 1.

Table 1 Properties of rubber for flexible joint

Sl. No.	Property	Value
1.	Type of Polymer	Natural Rubber
2.	Shear Modulus	1.8 ± 1.2 Ksc
3.	Ultimate Shear Strength	25 ± 5 Ksc
4.	Ultimate Shear Strain	$800 \pm 100\%$
5.	Ultimate Tensile Strength, (min.)	100 Ksc
6.	Hardness, Shore 'A' (max.)	40
7.	Ageing coefficient	0.8 mm
8.	Compression set	20 %

Chemlok has been used as an adhesive between rubber and metal. To begin with silicon Oil has been applied to all the mould components. All the mould components were assembled as per tool drawing. Rubber Slab has been cut as per requirement to place between shim. Quantity 8 number slab was placed between shim. Spacer has been provided between shim to achieve exact thickness of Rubber sleeves. Fore End Ring, Shims -7 nos & Aft End Ring have been placed in the mould cavity as per drawing. Rubber slabs were placed between the shims with the help of spacers. Finally top plate of mould was closed and hydraulic press was loaded. In the later stage the stack of shims and rubber pads were obtained by means of a compression molding process. In both cases, the shims were maintained in the heating mold by combs.

These combs determine the final thickness of the rubber pads. Bonding agents were applied on both faces of the shims, and then a layer of elastomer is applied above by means of an air-slip process. The mold was equipped with several resistive heating zones. The heating cycles usually involve several stages. The first ones aim to heat the remaining elastomer and to decrease its viscosity so that it may be easily transferred from the transfer pot to the injection channels. The second ones are effective curing stages. Natural Rubber compound has been cured in hydraulic press. The following curing cycle and loading has been followed

- $140 \pm 5^\circ\text{C}$ for 13 minutes
- Hydraulic load of 30 – 40 tones was applied on mould

Flexible joint thus developed has been shown in Fig. 3.



Fig. 3. Flexible joint after Extraction

3.EXPERIMENTAL CHARACTERIZATION:

The following are the test objectives of the various tests that were performed on the flexible joint.

- To test pressure sealing capability of flexible joint.
- To evaluate the axial compression and strains due to pressure.
- To evaluate the pivot point shift at null positions at maximum ejection load simulated pressure.
- To test pressure sealing capability of flexible joint during vectoring.
- To evaluate the strains due to pressure and vectoring (up to $\pm 5^\circ$).
- To evaluate rotational stiffness of the flexible joint.
- To test the structural integrity of flexible joint.

The following tests were carried out to meet above mentioned objectives.

- Pull Test
- Proof Pressure Test
- Null Position Test
- Vectoring Test

3.1 Pull test:

This test was done to access the bonding between shims and elastomers immediately after seal moulding and after acceptance tests as shown in Fig. 4.

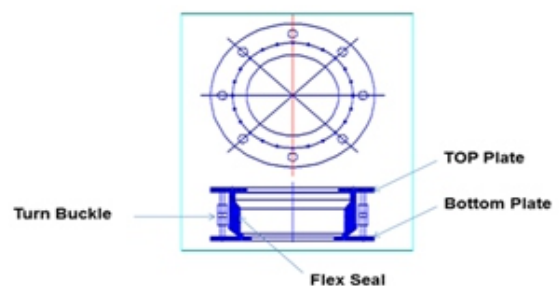


Fig. 4. Pull test setup

The flexible joint was subjected to a maximum pull of 2 mm in steps of 0.5 mm by using four turn buckles at 90° apart operated simultaneously. The pull was measured by 4 dial indicators. Typical acceptable value of minimum bond area between shims and elastomer is 95% with 2 mm axial pull. The flexible joint sub assembly after moulding and spacer removal was assembled in pull test fixture and an axial pull of 2mm has been applied. Minor debonds, if any, were recorded with reference to R2T and noted the depth of debond using feeler gauges.

3.2.Proof Pressure Test:

This test is done to simulate motor maximum expected operating pressure up to proof pressure levels and check the pressure sealing capability.

The chamber will be pressurized to the proof pressure in steps of 1.0 MPa with a hold time of 3 minutes at proof pressure and return back to zero pressure in same steps. At each pressure step, strains on shims, seal compression and pressure will be recorded in the data acquisition system. The flexible joint along with throat housing is tested up to proof pressure level of 63 Ksc. Test setup is shown in Fig. 5.

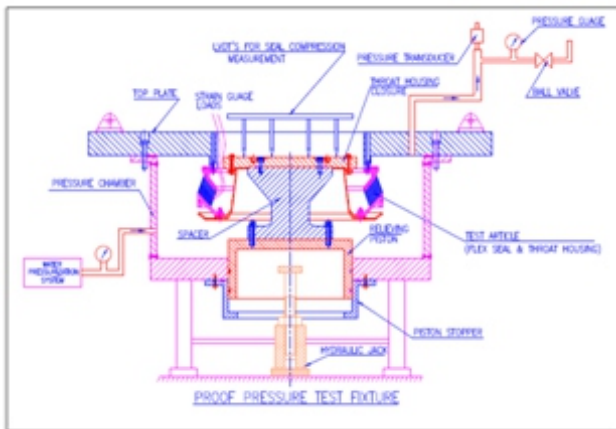


Fig. 5. Proof pressure test setup

The test set up comprises the B2 seal test fixture fabricated with interfaces to assemble the test article. It consists of a pressure chamber and closure plate and a relieving piston supported on a jack. The pressurization system is capable of maintaining the chamber pressure for the entire test duration and is independent of the actuator / control system. The relieving piston is provided to prevent overloading of the seal during the proof pressure test. The relieving piston with jack is kept engaged to the closure plate during the proof pressure test and will be disengaged for the actuation tests. The test set up has got provisions for mounting the actuators and, LVDTs for measurement of the displacement/deflection.

The first phase of testing comprises leak testing, cyclic testing and proof pressure testing. For these tests the piston is jacked up and engaged to the top plate. No data is recorded during the leak and cyclic tests and chamber pressure alone is monitored. The seal shall be pressurized up to 94.5 KSC in steps of 10, 20, 30, 40, 50, 60, 70, 80, 90, 94.5 KSC and depressurized to zero in the same steps. The axial deflection and strain gauge readings were monitored at the different steps both during pressurization as well as depressurization.

3.3.Null Position Test :

This test has been done to simulate ejection load and measure the behavior of flexible joint due to asymmetry in geometry. In this test, the pressure is increased from zero to a pressure, which creates equivalent ejection load in steps of 1.0 MPa with a hold time of 3 minutes at maximum pressure. Apart from this, the readings at 0.5 MPa and motor average pressure will also be recorded. Seal compression, the force required to correct the deflection due to asymmetry, pressure and strains on the shims are measured during each load step. The pivot point shift is measured by placing four LVDTs radially on the simulated divergent nearest to the pivot point. At every pressure step the shift is recorded after null correction and the maximum is reported. Test setup is shown in Fig. 6.

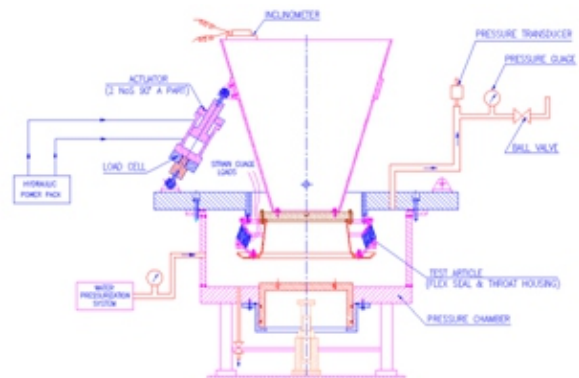


Fig. 6. Null position test setup

The flexible joint and throat housing assembly is tested up to a pressure of 48 Ksc, simulating proof ejection load of 23.1 tons corresponding to 63 Ksc. The actuators are in assembled condition at R2T and R1L locations during the null test. For assuring null position, 2 inclinometers are used. In the second phase of testing involves characterization of the seal. The actuators are connected at R2B and R1L locations and the relieving piston is disengaged during this phase of testing. Tensile loading of the seal is avoided by pressurizing the chamber to 0.5 KSC prior to mounting the actuator frame. The actuators, load cells and LVDTs are kept in position and connected. The position of the seal prior to pressurization is taken as null position for the actuator. The assembly shall be pressurized in steps of 5, 10, 20, 30, 40, 50, 60, 69 and then depressurized in the same steps. The null position of the seal will be maintained by monitoring the LVDT readings and giving commands to one of the actuators.

The axial deflection, strain, LVDT and load cell readings will be monitored and recorded at each pressure level. The test is repeated keeping the second actuator in the null position and commanding the first actuator alone for retaining the seal in null position.

3.4. Vectoring Test:

The thrust vectoring requires the nozzle to be vectored in perpendicular planes resulting in shear loads in the elastomer of the flexible joint. The seal stiffness in shear has to be minimum to reduce the actuator load and its associated design. The requirement of actuator force is inversely proportional to the pressure. Test setup is shown in Fig. 6 is also applicable for this test. These tests are done to simulate angular deflection of flexible joint with ejection load to characterize seal torque / Actuator force requirement and Actuator stroke requirements. The flexible joint is vectored from 0° – maximum angle – 0° – negative maximum angle – 0° in steps in one degree. Separate tests are done in individual pitch, yaw and in simultaneous planes. Vectoring tests are done at three pressures for configuration-D namely 0.5 MPa, 4.02 and 5.3 MPa to map the characteristics at lower, average and upper bound of rocket motor operations. Similar test have been done for other configurations with vectoring angles given in Table 6-1. The actuator force, stroke, deflection angle, pressure and strains on shims are measured at every load step. The seal throat housing assembly is tested at 5 Ksc, 38 and 48 Ksc under actuation conditions of ± 4.5 degrees in two planes individually and also in simultaneous actuation condition.

4. RESULTS AND DISCUSSION:

Results obtained in all the tests are discussed below.

4.1 Pull test:

The flexible joint sub assembly, after moulding and spacers removal, an axial pull of 2mm has been applied. No de-bonds were observed.

4.2. Proof pressure and null position test:

Seal compression noticed during proof pressure test is shown in Fig. 7.

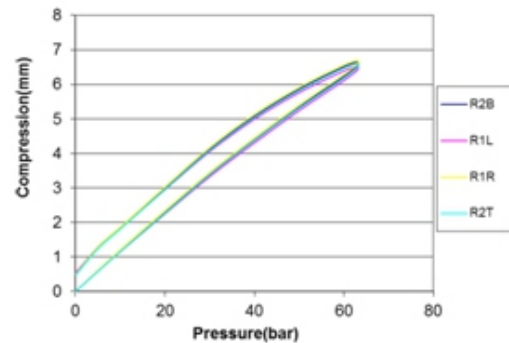


Fig. 7. Seal Compression during Proof Pressure Test
 Seal compression noticed during null position test is shown in Fig. 8.

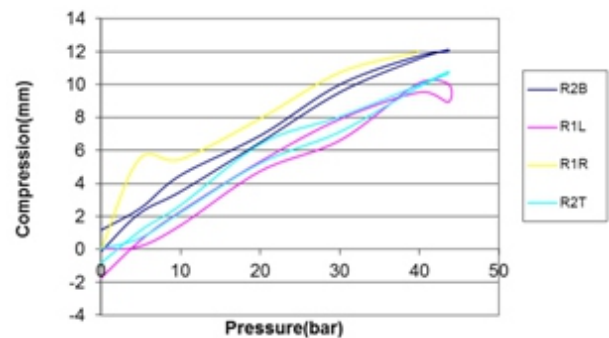


Fig. 8. Seal Compression during null position Test

- Seal compression was measured with 4 LVDTs mounted 90° apart and average is reported which match very well with the predictions for seal tested for each configuration.
- Average seal compression measurements show a maximum variation of 0.22 mm from FEA predictions
- This is attributed to the variation in rubber properties. Pivot point shift and null correction force vary from seal to seal depending on asymmetry and is mapped for every seal tested.
- Simulation of ejection load is as per requirement during PPT and NPT with a pressure controller of ± 0.01 MPa accuracy used to control the load.

4.3. Vectoring test:

Actuators loads on seal for Pitch actuation test is shown in Fig. 9.

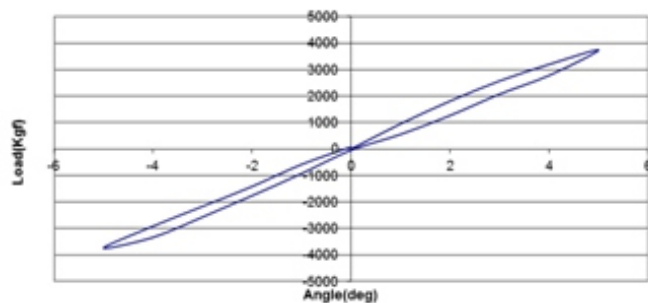


Fig. 9. Actuators loads on seal for Pitch actuation test

- During testing, the nozzle is vectored from 0° to -5° to 0° to 5° in steps of one degree in individual planes of pitch and yaw and repeated in both planes simultaneously. The test is repeated at three pressures.
- The actuator force / seal torque is maximum at minimum pressure.
- The stresses on the shims are maximum during maximum chamber pressure and vectoring angle.
- Plot of stress versus angle during simultaneous actuation shows that increase/decrease in stress only in the resultant plane of actuation whereas in planes 90° to resultant plane of actuation the stress remains almost unchanged.
- This is as per predicted behavior of seal. the hoop stress in mid shim with vectoring angle shows a good match with FEA prediction. The vectoring pattern from -5° to $+5^\circ$ is examined in detail for the middle shim. The actuator force is directly proportional to the vectoring angle.

5. CONCLUSIONS:

Development of flexible joint has been taken up with new methodology to avoid time and cost-consuming experimental iterative steps. Acceptance and qualification tests have been done as per the test procedure of flexible joints.

6. ACKNOWLEDGEMENT:

This research is supported by Department of mechanical Engineering, Malla Reddy Engineering College (Autonomous), Hyderabad.

7. REFERENCES:

1. Woodberry, "Flexible joints for thrust vector controls", AIAA-75-1221, October, 1975.

2. Gajbir Singh and G. V. Rao. "New design formulas for a flex-bearing joint", Journal of Spacecraft and Rockets, Vol. 30, No. 6 (1993), pp. 779-780.

3. Donat James, "Solid Rocket Motor Nozzle Flexible joint Design" AIAA-1993-1122, AHS and ASEE, Aerospace Design Conference, Irvine, CA; United States; 16-19 Feb. 1993.

4. Jeffrey Foote and Jeffrey Foote. "Titan IV Solid Rocket Motor Upgrade Program at Alliant Techsystems Inc", 33rd Joint Propulsion Conference and Exhibit, Joint Propulsion Conferences.

5. Kirby, D. C, "Solid rocket motor thrust vector control system selection", AIAA-1964-230, American Institute of Aeronautics and Astronautics, Annual Meeting, 1st, Washington, D.C., Jun 29- Jul 2, 1964.

6. Sivaramakrishnan. R and Bhagawan.S.S., "Characterisation of Natural Rubber Based Flex Nozzle Material for Solid Rocket Motors", IRMRA 15th Rubber Conference, pp 221 - 230

7. Press, W.H., S.A. Teukolsky, W.T. Vetterling, and B. P. Flannery. 1992. Numerical recipes in F77. 2nd ed. Cambridge University Press.

8. Taine, J., and J.P. Petit. 1989. Transferts thermiques: Mécanique des guides anisothermes. Dunod: Dunod Université.

Mold Flow Analysis on Fan Part using Plastic advisor

B. Pavani¹, M.V.Varalakshmi²

¹M.Tech Scholar, Department of Mechanical Engineering, Mallareddy Engineering College (Autonomous), Secunderabad, India

Email: pavani.gova@gmail.com

²Associate Professor, Department of Mechanical Engineering, Mallareddy Engineering College (Autonomous), Secunderabad, India

Email: varalakshmi@gmail.com

Abstract— Injection molding is the most widely used method for the production of intricate shape plastic parts with good dimensional accuracy. For plastic components manufacturing process used is Injection molding. While doing this manufacturing process we have to face some problems in filling process, clamping, cooling, and amount of material to inject into the cavity area. Due to the above problems there is wastage of material, time, poor component quality. Optimization of cycle time in injection molding plays a vital role in manufacturing of plastic parts to improve the productivity of the process. At the same time it should not affect the quality of the final product. The process parameters like cooling time, filling time are optimized in which it contributes more in the cycle time by changing the mold temperature, melt temperature and injection pressure. We can optimize Injection molding manufacturing process.

Keywords— Mold Flow, Injection Molding, Melt Temperature, Mold Temperature, Injection Pressure

I. INTRODUCTION

Thermoplastic injection molding is a well known process for manufacturing effortless and complex shaped products in short time and at low cost. Nowadays there is a need for optimizing the processing parameters to increase productivity. In the cycle time the cooling time can represent more than 70% of the injection cycle. Cutting down the cycle time for each part is a major concern in injection molding machine.

Problems found after tooling development are always expensive and frustrating. For plastic part design and manufacture, there is a better way. By simulating the plastic-filling process for injection-molded parts, Pro/ENGINEER Plastic Advisor enables engineers to design for manufacturability, uncover problems, and propose remedies, reducing development time and expensive. Pro/ENGINEER Plastic Advisor simulates mold filling for injection molded plastic parts. Advanced features provide valuable manufacturability insight - insight that can significantly reduce late-cycle design changes and mold reengineering costs.

By changing the mold temperature, melt temperature and injection pressure. We can optimize Injection molding manufacturing process.

II. EXPERIMENTAL PROCEDURE

In this project i have selected the fan part and then designed using the pro-e software as shown in the fig.1.

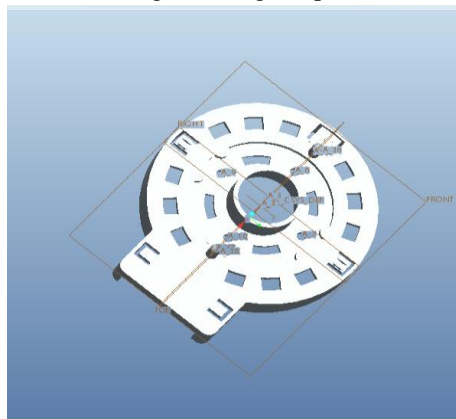


FIGURE 1. FAN PART

Once the part is designed in pro-e then that part is opened in the plastic advisor software for the mold flow analysis as shown in the fig. 2

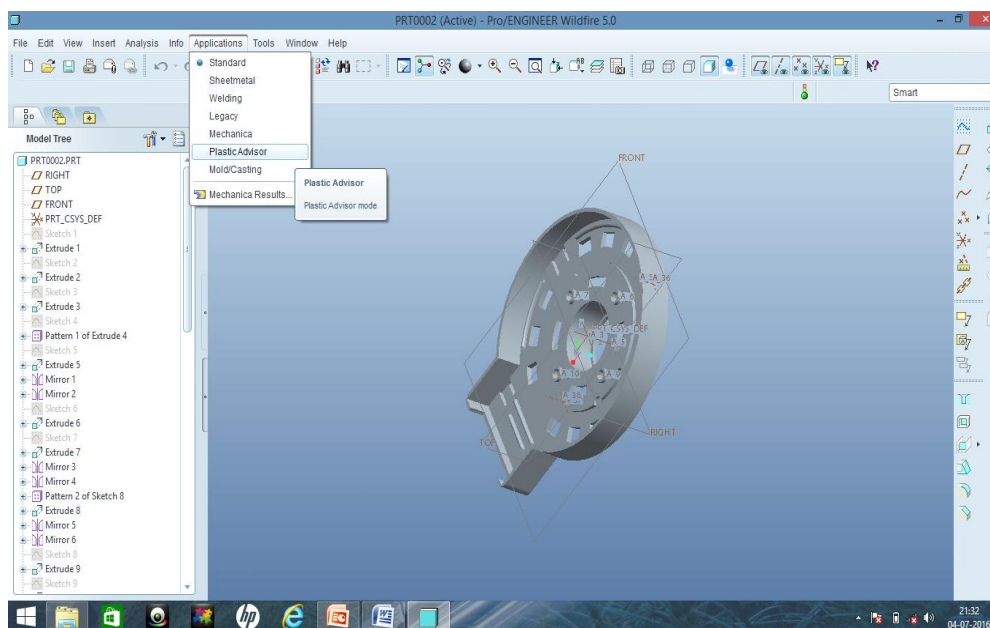


FIGURE 2. PART OPENED IN PLASTIC ADVISOR

Now the selection of the material that is generic pp is selected in this project for analysis. Then by changing the mold temperature, melt temperature and injection pressure we can optimize the cycle time.

I have considered six cases to optimize the cycle time.

From the Table3, we can observe that the case four has got lest cycle time when compared to the other cases. And in this case the confidence is high, quality is good and cooling quality is also better when compared with other cases.

Case 4

TABLE 1
INITIAL VALUES TAKEN IN CASE 4

Material used	Generic pp
Melt Density	0.82021g/cm ³
Solid Density	0.96221g/cm ³
Young's modulus	1340Mpa
Poisson ratio	0.3918
Mould Surface temperature	40 deg. C
Melt Temperature	240.00 deg.C
Maximum machine injection pressure	160 Mpa
Automatic Injection time	3sec
Machine clamp/open time	3sec

Case 4 Summary report for Generic PP

TABLE 2
FINAL RESULT IN CASE 4

Part Name	Fan part
Material Supplier	Kumho Chemicals Inc
Material Grade	Pp
Max Injection Pressure	160 Mpa
Mold Temperature	40 degC
Melt Temperature	240.00 degC
Model Suitability	Part model was highly suitable for analysis.
Filling Analysis	Fan part
Moldability	Your part has completed filling
Confidence	high
Fill Time	0.85 sec
Injection Pressure	17.18 Mpa
Weld Lines	Yes
Air Traps	Yes
Shot Volume	44.07 cu.cm
Filling Clamp Force	14.48 tonne
Surface Temperature Variance Range	-1.03 deg C to 8.72 deg C
Freeze TimeVarianceRange	-5.09 sec to 20.35 sec
Cycle Time	12.68 sec
Cooling quality	Low
Quality predication	medium
Warnings	Cooling quality is un acceptable.

TABLE 3
MOLD FLOW ANALYSIS OPTIMUM PARAMETERS FOR MAXIMUM PRODUCTION

	Cases					
	1	2	3	4	5	6
Mould Surface Temperature(Deg.C)	40.00	40.00	40.00	40.00	40.00	40.00
Melt Temperature(Deg.C)	210.0	220.00	230.0	240.0	250.0	255.0
Maximum Machine Injection Pressure(Mpa)	160.0	180.00	160.0	160.0	180.0	180.0
Fill Time(Sec)	0.51	0.47	0.13	0.11	0.22	0.19
Cycle Time(Sec)	1.36	1.36	1.09	0.85	0.97	0.97

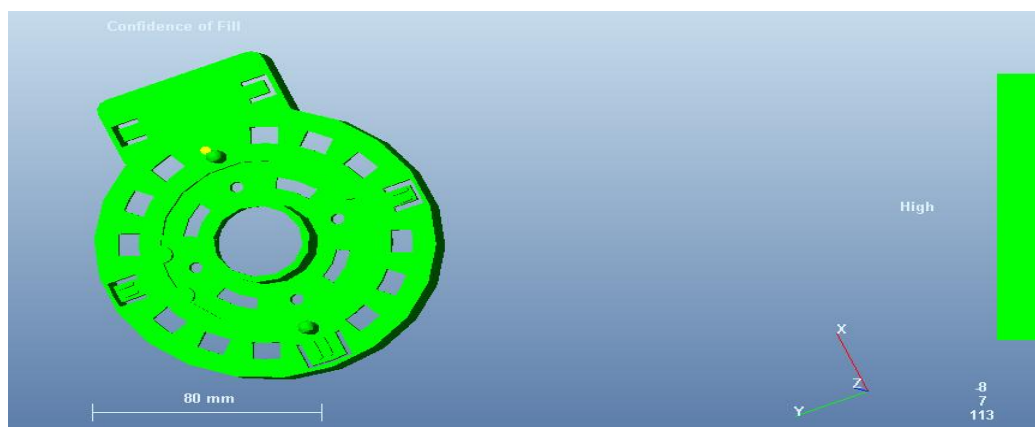


FIGURE 3. CONFIDENCE OF FILL

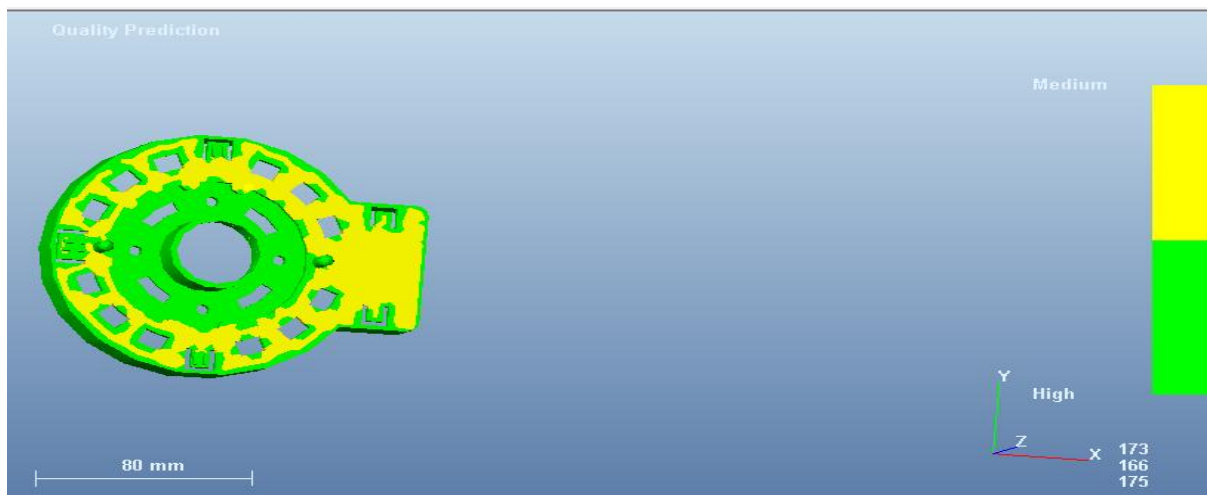


FIGURE 4. QUALITY PREDICTION

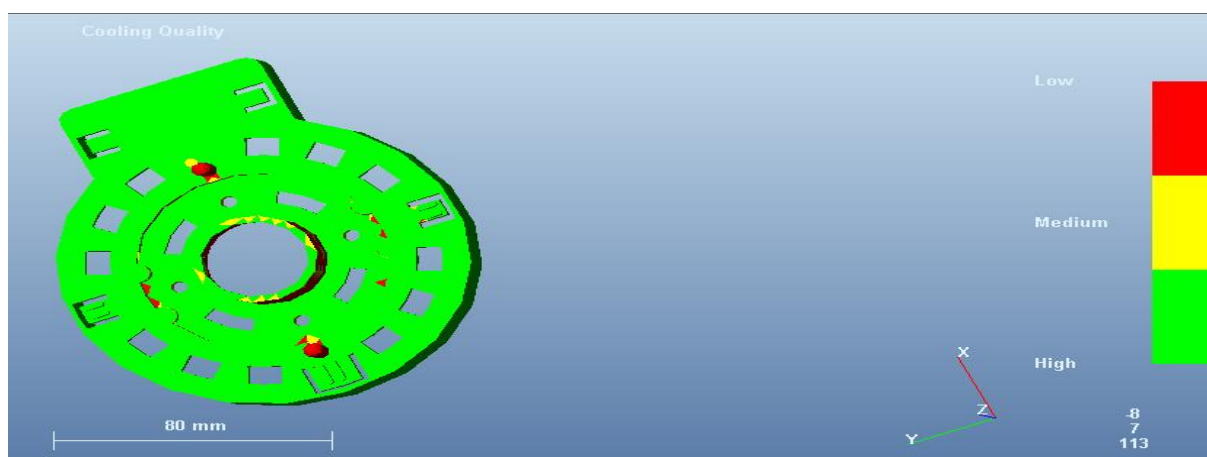


FIGURE 5. COOLING QUALITY

III. RESULTS AND DISCUSSION

In this study, the simulation have performed by changing injection molding process parameters in the application software Plastic Advisor. According to the experiment and simulation analysis, the melt temperature, mold temperature and injection time are considered as the main factors to optimize cycle time. The experimental result explains the minimum time required to fill the mold cavity.

In **case 1** the mold temperature initially set to 40°C, Melt temperature set to 210 °C, injection pressure 160mpa, for generic PP material. The estimated cycle time is less i.e. 12.24 and the filling time are more i.e. 1.36 in this case when compared to case 4. if the filling time is more than the material gets solidified fastly without the total fill of cavity. So that the fill time should be minimized.

In **case 2** the mold temperature set to 40 °C, Melt temperature set to 220 °C, injection pressure 180mpa, for generic pp materials. In this case the estimated cycle time is less i.e. 11.88sec and the filling time is same 1.36 sec .when compared with case 4 and the air traps and weld lines are found.

In **case 3** the mold temperature set to 40 , Melt temperature set to 230 deg.c,injection pressure 160mpa, for generic pp materials. In this case the estimated cycle time less i.e. 12.28sec and the filling time is more i.e. 1.09 sec when compared with case 4 and the cooling quality is poor.

In **case 4** the mold temperature set to 40 °C, Melt temperature set to 240 °C, injection pressure 160mpa, for generic pp materials. The cycle time is more than the previous cases i.e. 12.68sec but the filling time is less than the other cases i.e. 0.85sec if the fill time is less than the weld lines and air traps not present and the confidence of fill is high in this case 4. And the part quality is good than other cases.

In **case 5** the mold temperature set to 40 °C, Melt temperature set to 250 °C, injection pressure 180mpa, for generic pp materials. In this case the estimated cycle time is more i.e. 13.18 sec and the filling time is more i.e. 0.97 sec when compared with case 4 and the air traps and weld lines are found with poor quality.

In **case 6** the mold temperature set to 40 °C, Melt temperature set to 255 °C, injection pressure 180mpa, for generic pp materials. In this case the estimated cycle time is more i.e. 13.07sec and the filling time is more i.e. 0.97sec when compared with case 4 and the air traps and weld lines are found and quality is affected.

- 1) In the above test cases Fourth Test case Machining Parameters are satisfying the part quality.
- 2) The given machining parameters can used in component production.
- 3) Mould Surface temperature = 40 °C
- 4) Melt Temperature = 240 °C
- 5) Maximum machine injection pressure = 160Mpa
- 6) Automatic Injection time = 3sec
- 7) Machine clamp/open time = 3 Sec
- 8) From above mould flow analysis we are getting following output results
 - a) These results can feed to the Injection moulding machine
 - b) Injection Pressure = 17.18MPa
 - c) Shot Volume = 44.07 Cm³
 - d) Filling Clamp Force = 11.88 Ton
 - e) Fill time = 0.85 sec
- 9) By using cycle time We can estimate Number of components can produce in some period of time
 - a) Cycle Time = 12.68Sec
 - b) In one hour we can produce 284 components.

IV. CONCLUSION

After the introduction and knowledge of all the details and concepts with mold flow simulation we can finally conclude that mold flow simulation is a very popular and important technology in the field of molding process.

1. In the production of components in injection moulding process by changing processing parameters by trail and error method, the company is incurring loss in material, time and power.
2. In this thesis, the above problem is rectified by taking software support of plastic advisor which is a module in Pro/Engineer. In this software, the component can be checked for filling by given processing parameters before going to manufacturing.
3. In this project fan part is analyzed for mould flow using material Generic PP. By changing processing parameters for six times, the production of the component is good. In the trial and error method nearly 20 components are wasted but by using this mould flow analysis only 5 components are wasted.
4. And also by using this analysis, the exact processing parameters for production can be determined. Number of components for one hour can be estimated by using cycle time. The numbers of components produced are 284.
5. In this project I have optimized the cycle time by changing the processing parameters like mold temperature, melt temperature and injection pressure.

REFERENCES

- [1] Vishnuvarthanan , M., Rajesh Panda, Ilangovan, S. and Nayak, S. K. "Optimization Of Injection Molding Cycle Time Using Mold Flow Analysis", International Journal of Current Research Vol. 4, Issue, 01, pp.259-261, January, 2012
- [2] Dr.J.Fazlur Rahman*,Mohammed Yunus "Optimizing the Die Design Parameters for FRP Components Produced in Injection Molding using Mold Flow Analysis" ,(IJERA) Vol. 2, Issue4, July-August 2012

- [3] J.A.Brydson, Plastic materials, British Cataloging sixth edition, 1995, Butterworth Heinemann Ltd.
- [4] Bown,J, Injection Moulding of Plastic Components, McGraw-Hill, 1979.
- [5] Shia-Chung Chen^{1,2}, Pham Son Minh^{1,2},I-Sheng Hsieh³, Yan-Chen Chiou³”Improve Cooling Effect Of Injection Molding By Pulsed-Cooling Method”, 3CoreTech System (Moldex3D) Co., Ltd., ChuPeiCity,Hsinchu, Taiwan, R.O.C..
- [6] P.K.Bharti “Recent Methods For Optimization Of Plastic Injection Molding Process “,International Journal of Engineering Science and Technology Vol. 2(9), 2010, 4540-4554
- [7] Arvind Kumar Singh¹and D.K. Singh ² “Modelling and Analysis of Mold Filling Parameters for PP and ABS Materials Using Software Simulation”, International Journal of Engineering Research & Technology (IJERT) ISSN: 2278-0181 Vol. 1 Issue 7, September - 2012
- [8] K. Banik’ Effect of mold temperature on short and long-term mechanical properties of PBT”, Received 11 September 2007; accepted in revised form 29 December 2007
- [9] E. Boci'ga, T. Jaruga, “Experimental investigation of polymer flow in injection mould” International Scientific Journal ,Volume 28 Issue 3 March 2007
- [10] J. Nabialek*, J. Koszkul’ “Model optimisation for mould filling analysis with application CAE package C-Mold”, of Achievements in Materials and Manufacturing Engineering AMME journal of Achievements in Materials and Manufacturing Engineering VOLUME 19 ISSUE 1 November 2006
- [11] B. A. McCalla, P. S. Allan and P. R. Hornsby, “Polymer processing engineering”, 03, 52. (2003)
- [12] Shia-Chung Chen, Ying chang, Tsung-Hai Chang, Rean-Der Chen, Inter. Commun Heat & Mass Trans., 35, 130. (2008)
- [13] Shia-Chung Chen, Shih-Hsien Tarng, Yan-Chen Chiou, T. P. Tsai, Wen-Hsien Yang, , SPE Antec Tech. Paper, 52, 385. (2008)
- [14] Technical paper by Johanna Lamminmäki, Totti Lindgren, JukkaSilén and Heli Vesanto, “Influence of injection molding process parameters on mechanical properties of polypropylene-specimen”.
- [15] Villalon, ADA VENUS, Electron Beam,”Fabrication of Injection Mold Tooling with Conformal Cooling Channels”.
- [16] Glanvill& Denton “Injection mould design fundamentals” 1st Edition 1965, The Machinery Publishing Co. Ltd.
- [17] Jin Zhang and Suraj M. Alexander, Fault Diagnosis in Injection Molding via Cavity Pressure Signals, Department of Industrial Engineering ,University of Louisville.

Computational Investigation of the Effects of Leading-Edge Bluntness on Drag at Supersonic Speeds

M. Abhinav, V. Narasimha Reddy
Department of Mechanical Engineering,
Malla Reddy Engineering College,
Secunderabad-500100, India

Abstract-The present paper discusses the computational investigation of the effects of leading edge bluntness on drag at supersonic speeds by using CFD software FLUENT at different supersonic Mach numbers. The main design factors that affect projectile configuration is the lift and drag force, with lowest drag as possible. In this study three widely known nose shapes with different geometries are considered.

The present paper would deal with the computation of the drag or various configurations considered with respect to the Mach number and bluntness or fineness ratios ($n = 0.5$, $n = 0.667$, $n = 0.8$). As fineness ratio and Mach number increases the overall drag decreases. The drag is compared based on the 3 main drag components; skin friction drag, wave drag and base drag. For this paper only the conical nose shape with different fineness ratios are presented. The results from the flow analysis for various configurations have been analysed and presented in the report.

Keywords- Mach number; Fineness ratio; Drag force; Nose cone configurations; Flow velocity.

I. INTRODUCTION

A. Blunt Nose Cones

Supersonic vehicles are commonly designed and manufactured with blunt nose. Supersonic cruise vehicles need low drag to efficiently maintain velocity. Understanding, analyzing and predicting high speed flow around blunt bodies thus poses a practical and important engineering problem.

Gas flow around the fore body of blunt-nose vehicles is typically clean, and subjected to few upstream disturbances. The effect of nose cone geometry on penetration performance has been studied for decades. A variety of analytical methods have been performed to attempt to optimize the nose shape for a penetrator. The new shape design was created by diving the nose shape into line segments and searching through numerical space for the combination of line segment slopes that produced the nose geometry with the lowest nose shape factor. This nose shape factor is derived using penetration mechanics theory. The new design should provide an updated perspective on nose shape design [1].

B. Blunt Body Flows

The figure.1 shows the diagram of air flow around a cylinder at Mach 4, the initially uniform free-stream flow is processed by a detached bow shock (S), and subsequently enters the shock layer.

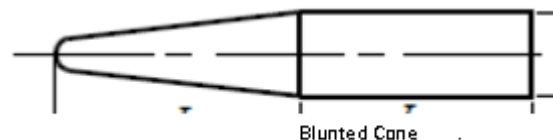


Fig. 1. Nose cones

The hypersonic free stream is undisturbed by the down-stream obstacle, since the speed of information propagation in that region is slower than the flow speed. The shock wave is strongest at the point where it is normal to the free stream inflow (N). Away from this location, the bow shock becomes oblique to the inflow and weakens, due to relief afforded by the body curvature.

Inside the shock layer, the sonic surface (L) demarks the transonic interface between subsonic and supersonic flow. For lower speed supersonic inflow, the interface would occur further downstream than pictured. Within the subsonic region bounded by the sonic surface, shock, and body, flow information is everywhere propagated in all directions via pressure waves. The stagnation point (T), is located within the subsonic region, and is defined as the location where flow impinges on the body in the surface-normal direction. In the case of an ideal, calorific ally perfect gas, and an adiabatic body surface, flow pressure and temperature are highest at the stagnation point. The viscous boundary layer (B) is initiated at the stagnation point, and grows along the body surface in the downstream direction. In the presence of adverse pressure gradients, particularly in the shadow region behind the body, the boundary layer may at some stage separate from the surface [2].

As gas advents out of the subsonic region, it expands (E) and accelerates into the in-creased volume between shock and body. The decreasing shock angle, combined with the effects of flow expansion, usually results in a decrease of both pressure and temperature. At points downstream of the subsonic region, the increased flow speed means that pressure waves cannot travel back upstream. Hence, the state of the downstream flow field does not affect the subsonic region, except possibly via electromagnetic field or the boundary layer. Hence, the simulation of a complete supersonic vehicle is not necessarily required to accurately reproduce the flow around its nose. Figure.2 shows a blunt body in a supersonic stream.

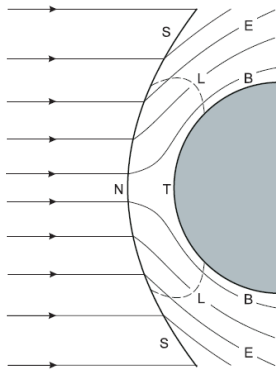


Fig. 2. A blunt body in a supersonic stream

C. Nose Cone Shapes And Equations

i. General Dimensions

In all the following nose cone shape equations, L is the overall length of the nose cone and R is the radius of the base of the nosecone. y is the radius at the point x , as x varies from 0, at the tip of the nosecone, to L . The equation define the 2-dimensional profile of the nose shape. The full body of revolution of the nosecone is formed by rotating the profile of the nosecone around the centerline (C/L).

The figure.3 shows the nose cone dimensions used in equations.

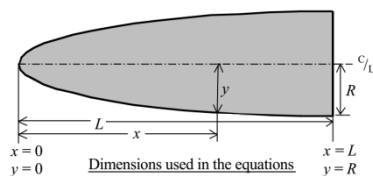


Fig. 3. General Nosecone Dimensions

ii. Fineness Ratio

Fineness ratio is a term used in naval architecture and aerospace engineering to describe the overall shape of a streamlined body. Specifically, it is the ratio of the length of a body to its maximum width; shapes that are “short and fat” have low fineness ratio, those that are “long and skinny” have high fineness ratios. Aircraft that spend time at supersonic speeds generally have high fineness ratios, a canonical example being Concorde.

At speeds below critical mach, one of the primary forms of drag is skin friction. As the name implies, this is drag caused by the interaction of the airflow with the aircrafts skin. To minimize this drag, the aircraft should be designed to minimize the exposed skin area, or “wetted area”, which generally implies the fuselage should be somewhat “egg shaped”, with a fineness ratio about 4.5. A good example of such a design is the Questair Venture.

Most aircraft have fineness ratios significantly greater than this, however. This is often due to the competing need to place the tail control surfaces at the end of a longer moment arm to increase their effectiveness. Reducing the length of the fuselage would require larger controls, which would offset the drag savings from using the ideal fineness ratio. An example with of a high-performance design with an imperfect fineness ratio is the Lancir.

D. Aerodynamics

Aerodynamics is the branch of science that deals with the motion of air and the forces on bodies moving through the air. There are four forces that act on a rocket: weight, lift, drag, and thrust. Weight is a force that is always directed toward the centre of the Earth. To overcome the weight force, aircraft generate an opposing force called lift. Lift is generated by the motion of the aircraft through the air. Most of the lift is generated by the wings. In most rocket designs, fins are more engaged to steer or direct the airflow for flight stability, instead of providing lift. Drag is a force that opposes the upward movement of the rocket. It is generated by every part of the rocket. Drag is a sort of aerodynamic friction between the surface of the rocket and the air. To overcome drag, aircraft and rockets use a propulsion system to generate a force called thrust. In the present study we are dealing with the variation of the drag force over blunted nose cone profiles. So let us discuss about aerodynamic drag force in detail.

II. COMPUTATIONAL REPRESENTATION

The first objective of this study is to obtain the steady-flow field (inviscid flow) results for blunt-nosed profiles of various fineness ratios at Mach 2. The second objective is to obtain the simulations of viscous flow over blunt nosecone profiles of fineness ratios $L/D = 0.5, 0.667, 0.8$ configuration at Mach 2, Mach 3 and Mach 4. This chapter describes the problem and the computational arrangements made to achieve these two objectives.

A. Problem Description

Blunt nose profile configurations. (Axisymmetric profiles)

- i. Fineness ratio $L/D = 0.5$
Horizontal length $x = 27.9$ mm
Vertical length $y = 9.844$ mm
Diameter $d = 20$ mm
Area $A = 0.000183093$ m²

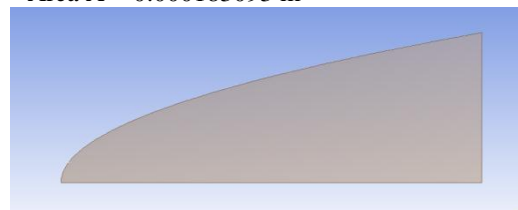


Fig. 4. Blunt-nosed profile of fineness ratio $n=0.5$

Figure.4 shows a blunt-nosed profile of horizontal length 27.9 mm and vertical length of 9.844 mm and diameter of this profile is 20 mm area is 0.000183093 m². Since this profile is studied in this computational study for the variation of coefficient of drag over it in supersonic flows under inviscid case at mach 2 and viscous case at mach 2, 3 & 4. Since it is axisymmetric profile only half of the profile is used for this study.

- ii. Fineness ratio $L/D = 0.667$
Horizontal length $x = 37.2$ mm
Vertical length $y = 9.844$ mm
Diameter $d = 20$ mm
Area $A = 0.000219678$ m²

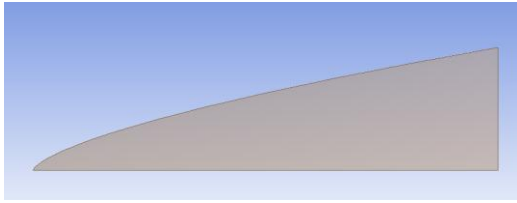


Fig. 5. Blunt-nosed profile of fineness ratio $n = 0.667$

Figure.5 shows a blunt-nosed profile of horizontal length 37.2 mm and vertical length of 9.844 mm and diameter of this profile is 20 mm and area is 0.000219678 m². Since this profile is studied in this computational study for the variation of coefficient of drag over it in supersonic flows under inviscid case at mach 2 and viscous case at mach 2, 3 & 4. Since it is axisymmetric profile only half of the profile is used for this study.

- iii. Fineness ratio $n = 0.8$
Horizontal length $x = 44.6$ mm
Vertical length $y = 9.844$ mm
Diameter $d = 20$ mm
Area $A = 0.000243659$ m²

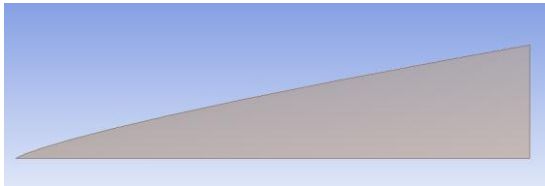


Fig. 6. Blunt-nosed profile of fineness ratio $n = 0.8$

Figure.6 shows a blunt-nosed profile of horizontal length 44.6 mm and vertical length of 9.844 mm and diameter of this profile is 20 mm and area is 0.000243659 m². Since this profile is studied in this computational study for the variation of coefficient of drag over it in supersonic flows under inviscid case at mach 2 and viscous case at mach 2, 3 & 4. Since it is axisymmetric profile only half of the profile is used for this study.

In this study we are performing the flow analysis over these profiles to know the variation of drag on them in supersonic flows at different mach numbers under different conditions.

III. NUMERICAL ASSUMPTIONS

Several simplifying assumptions are made in the simulations. The models used in this investigation are assumed to be on a flat base. In view of the small scale of the flow field (i.e., the nose region), laminar flow is assumed. The free stream Reynolds number is roughly $5.0 \times 10^7/m$. The actual Reynolds number (per meter) is much smaller along the body surface inside the cavity and outside the cavity near the lip, because of the low-speed flow. The wall temperature is assumed isothermal ($T_{wall} = 300$ K) and the flow is assumed calorically perfect considering the previous numerical studies. The models are axisymmetric. Figure.7 shows the flow domain assumed in the present investigation.

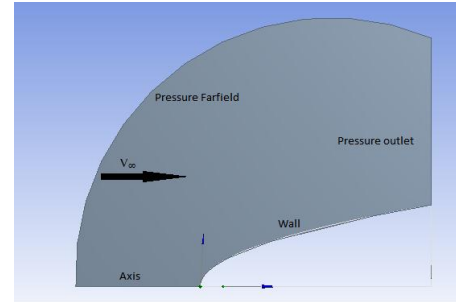


Fig. 7. Figure showing the flow domain

Boundary conditions for the assumed blunt nosed profiles are defined as follows

TABLE I. BOUNDARY CONDITIONS FOR ASSUMED BLUNT NOSE PROFILES

		$n = 0.5$	$n = 0.667$	$n = 0.8$
Pressure	farfield	101325	101325	101325
(Pascal)				
Temperature (kelvin)		300	300	300
Mach no	Inviscid	2	2	2
	Viscous	2, 3, 4	2, 3, 4	2, 3, 4

These conditions are specified for every profile assumed to be in this investigation and the flow simulation is performed on these profiles.

IV. FLOW ANALYSIS OVER BLUNT BODIES

Rapid technological advancements have increased computer power tremendously. With the boost of processor speed and graphic software, computers are widely used in aerodynamic prediction modelling. This led to a new field of study named computational fluid dynamics (CFD). CFD uses fundamental conservation laws, like Navier-Stokes equations, to numerically solve fluid flow over a region of interest with specific boundary conditions. It provides an excellent cost-effective tool to study fluid flows and complements empirical methods and wind tunnel testing.

In this study, the computer program ANSYS CFX was used to compute the axisymmetric flow over various conical blunt bodies which are defined. ANSYS CFX uses the full Navier-Stokes equations to solve. ANSYS CFX is an advanced CFD solver that has the facilitating technologies of geometry handling and meshing pre- and post-processing all housed within and integrated into the ANSYS Workbench. ANSYS Workbench has a platform's project page that can launch and track the geometry module, mesh module, setup pre-processor, solution module and results post-processor. These modules form the process of creating a CFD analysis on various conical blunt nose profiles.

A. Assessment Of Conical Blunt Nose Profiles

i. Creating Geometries

Ansys workbench was used to sketch and design a conical blunt nose with generated co-ordinates in the excel sheet with necessary calculations. Dimensions of the generated axisymmetric conical blunt nose profiles are as follows

TABLE II. GEOMETRIC CONDITIONS OF BLUNT NOSE PROFILES

Bluntness ratio	Boundary Horizontal length	Boundary Vertical length	Profile length (horizontal)	Profile length (vertical)
0.5	42.9	30	27.9	9.844
0.667	52.2	30	37.2	9.844
0.8	59.6	30	44.6	9.844

ii. Meshing Geometries

After creating the geometries in the Ansys workbench design modeller, that geometry files are opened in the mesh for meshing purpose. The meshing data for each profile is shown in the following table. Figure. 8 meshing of conical blunt nose profile.

TABLE III. MESHING OF BLUNT NOSE PROFILES

Bluntness ratio	Horizontal mesh	Vertical mesh	Profile mesh	bias
0.5	200	200	500	200
0.667	200	200	600	200
0.8	200	200	700	200

By following the above mentioned data conical blunt nose profiles are meshed. Final generated mesh files are shown as follows.

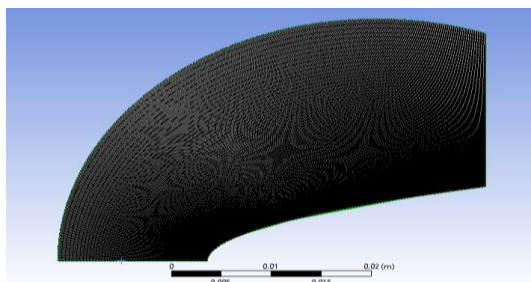


Fig. 8. mesh of 0.5 conical blunt nose profile

After meshing these files are saved and opened in fluent for the solving purpose.

TABLE IV. INPUT DATA (VISCOUS FLOW)

Solver type	Density based, Axisymmetric
Models	Energy (on), Spalart-Allmarms
Materials	Ideal gas, viscosity=Sutherland
Cell zone conditions	Operating pressure = 0
Boundary conditions (Farfield)	Pressure farfield, P=101325, M=2, T=300 Specification-intensity and hydraulic diameter (5, 20)
Boundary conditions (outlet)	Pressure outlet, P=0.1, T=300 Specification=from neighbouring cell
Reference values	Farfield, Area=0.000183093, L=27.9
Solution methods	Flow=first order
Solution controls	Courant number=0.01
Monitors	Edit, criteria change to 1e-6
Monitors	Create, drag
Monitors	Surface monitors, mass flow rate
Solution initialization	Standard, farfield, initialize
Calculation activities	Auto save=500
Run calculation	Iterations=1000, calculate

V.RESULTS AND DISCUSSION

Two main computational studies were performed during the course of this study; inviscid flow and the viscous flow over blunt nose profiles of various fineness ratio configurations at different mach numbers. In this chapter, the results from these computational studies will be discussed. The figure.9 and 10 shows static pressure contours of blunt nose profile for mach number 2.

A. Inviscid flow results

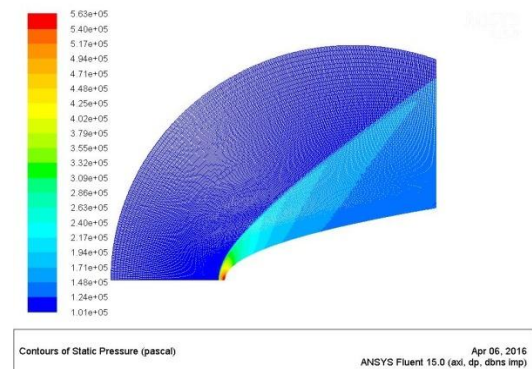


Fig. 9. Static pressure contours of blunt nose profile n = 0.5 for M = 2

B. Viscous flow results

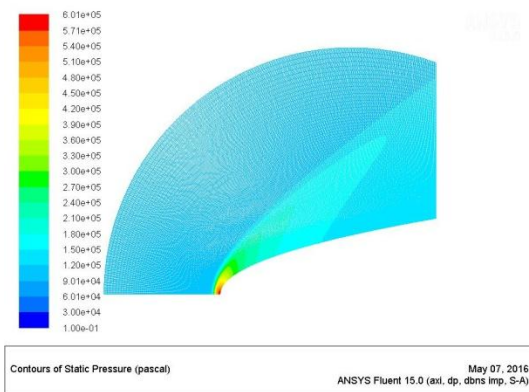
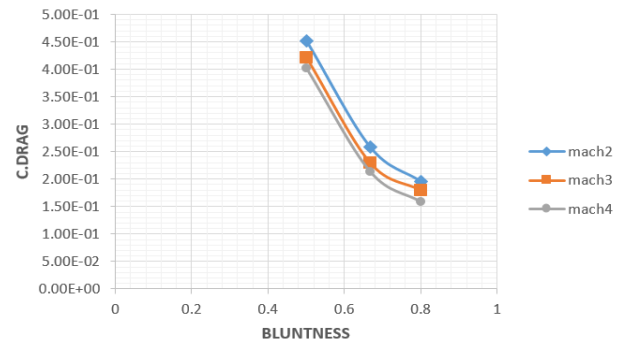


Fig. 10. Static pressure contours of blunt nose profile $n = 0.5$ for $M = 2$

TABLE VI. C_D VALUES FOR VARIOUS FINENESS RATIOS AND MACH NUMBERS

Mach-2 Inviscid flow	
Fineness ratio	Coefficient of drag
0.5	0.392
0.667	0.215
0.8	0.153
Mach-2 Viscous flow	
Fineness ratio	Coefficient of drag
0.5	0.452
0.667	0.258
0.8	0.19
Mach-3 Viscous flow	
Fineness ratio	Coefficient of drag
0.5	0.421
0.667	0.229
0.8	0.179
Mach-4 Viscous flow	
Fineness ratio	Coefficient of drag
0.5	0.401
0.667	0.213
0.8	0.159

This investigation showed the above mentioned results. Over all drag coefficient variation over these profiles at different mach numbers is shown in the following plot.1



Plot. 1. Graph showing the drag coefficient variation vs. blunt nose profiles at different mach numbers

VI. CONCLUSION

By increasing the fineness ratio of the nose, it is possible to reduce the overall drag of the projectile. However, increasing the fineness ratio without proper study could possibly result in a higher drag coefficient. Increasing the fineness ratio in fact increases the skin friction drag, while it doesn't contribute much as seen with its small C_D values compared to the total C_D but if the fineness ratio is increased beyond the values of the graph it may become more significant as the graph clearly shows an increasing trend.

Also it can be noted that the wave drag is the largest contributor especially at low Mach number and low fineness ratio due to more energy losses. While the base drag is only affected by the Mach number, however as it enters the supersonic speed range the base drag decreases as such it is less of a concern. From this study, a projectile designer aiming to reduce drag should focus more on the wave drag component as it is the largest contributor and care should be taken not to increase the fineness ratio without proper consideration as he may end up increasing drag instead.

From the present investigation we performed on the blunt nosed profiles of fineness ratios $n = 0.5$, $n = 0.667$, $n = 0.8$, at various mach numbers, we found that as fineness ratio increases the drag force effect decreases simultaneously. So from this we conclude that as blunt nose with fineness ratio increases from $n = 0.5$ to $n = 0.8$ the drag force effect decreases so $n = 0.8$ turned out to be the best profile at supersonic speeds with minimum effect on drag force due to its bluntness from this investigation.

For further study, it is recommended that Computational Fluid Dynamics (CFD) be used as an additional verification tool due to its current advancement and ease of use in providing and displaying graphics to help understand the airflow around the nose. CFD also allows multiple configurations to be tested initially without resorting to expensive wind tunnel testing.

REFERENCES

- [1] "The Descriptive Geometry of Nose Cones". The Descriptive Geometry Of Nose Cones- Word document by Gary A. Crowell Sr.
- [2] "Nose cones equations". Nose Cones excel sheet by Kemal Payza. <http://www.info-central.org/?article=125>. Retrieved October 23, 2009.
- [3] Mason, W. H. and Lee, J., "On Optimal Supersonic/Hypersonic Bodies," AIAA Paper 90-3072, 1990.
- [4] Mahdi, A. and Al-Atabi, M. (2008) Effect of Body Shape on the Aerodynamics of Projectiles at Supersonic Speeds. Journal of Engineering Science and Technology (JESTEC), 3 (3), 278-292.
- [5] McCoy, R. (1981). "MC DRAG"- A Computer Program for Estimating the Drag Coefficients of Projectiles. [report]
- [6] Maryland: US Army Armament Research and Development Command.

COMPARATIVE DESIGN AND ANALYSIS OF TRI-NOZZLE WITH CONVERGENT-DIVERGENT NOZZLE

¹K NAGARJUNA REDDY, ²N SRINIVASA RAJNEESH

DEPARTMENT OF MECHANICAL ENGINEERING

MALLA REDDY ENGINEERING COLLEGE (AUTONOMOUS)

(An Autonomous Institution approved by UGC and affiliated to JNTUH, Approved by AICTE, Accredited by NAAC with 'A' Grade and NBA & Recipient of World Bank Assistance under TEQIP Phase- II S.C.1.1)

Maisammaguda, Dhulapally (Post. Via.Kompally), Secunderabad – 500 100.

Abstract:

Nozzle is a device designed to control the rate of flow, speed, direction, mass, shape, and/or the pressure of the Fluid that exhaust from them. Convergent-divergent nozzle is the most commonly used nozzle since in using it the propellant can be heated in combustion chamber. In this project we designed a new Tri-nozzle to increase the velocity of fluids flowing through it. It is designed based on basic convergent-Divergent nozzle to have same throat area, length, convergent angle and divergent angle as single nozzle. But the design of Tri-nozzle is optimized to have high expansion co-efficient than single nozzle without altering the divergent angle. In the present paper, flow through the Tri-nozzle and convergent divergent nozzle

study is carried out by using SOLID WORKS PREMIUM 2014. The nozzle geometry modeling and mesh generation has been done using SOLID WORKS CFD Software. Computational results are in good acceptance with the experimental results taken from the literature.

Introduction To Nozzle

Swedish engineer of French descent who, in trying to develop a more efficient steam engine, designed a turbine that was turned by jets of steam. The critical component – the one in which heat energy of the hot high-pressure steam from the boiler was converted into kinetic energy – was the nozzle from which the jet blew onto the wheel. De Laval found that the most efficient conversion occurred when the

nozzle first narrowed, increasing the speed of the jet to the speed of sound, and then expanded again.^{[1][5]} Above the speed of sound (but not below it) this expansion caused a further increase in the speed of the jet and led to a very efficient conversion of heat energy to motion. The theory of air resistance^[1] was first proposed by Sir Isaac Newton in 1726. According to him, an aerodynamic force depends on the density and velocity of the fluid, and the shape and the size of the displacing object. Newton's theory was soon followed by other theoretical solution of fluid motion problems. All these were restricted to flow under idealized conditions, i.e. air was assumed to possess constant density and to move in response to pressure and inertia.

A nozzle is a device designed to control the direction or characteristics of a fluid flow (especially to increase velocity) as it exits (or enters) an enclosed chamber. A nozzle is often a pipe or tube of varying cross sectional area.

Literature Review

Convergent-Divergent nozzle is designed for attaining speeds that are greater than speed of sound. The design of this

nozzle came from the area-velocity relation $(dA/dV) = -(A/V) (1-M^2)$ M is the Mach number (which means ratio of local speed of flow to the local speed of sound) A is area and V is velocity the following information can be derived from the area-velocity relation.^[5]

1. For incompressible flow limit, $AV = \text{constant}$. This is the famous volume conservation equation or continuity equation for incompressible flow.^[5]
2. For $M < 1$, a decrease in area results in increase of velocity and vice versa. Therefore, the velocity increases in a convergent duct and decreases in a Divergent duct.^[5]
3. For $M > 1$, an increase in area results in increases of velocity and vice versa, i.e. the velocity increases in a divergent duct and decreases in a convergent duct. This is directly opposite to the behavior of subsonic flow in divergent and convergent ducts.^[5]
4. For $M = 1$, $dA/A = 0$, which implies that the location where the Mach number is unity, the area of the passage is either minimum or maximum. We can easily show that the minimum in area is the only physically realistic solution.

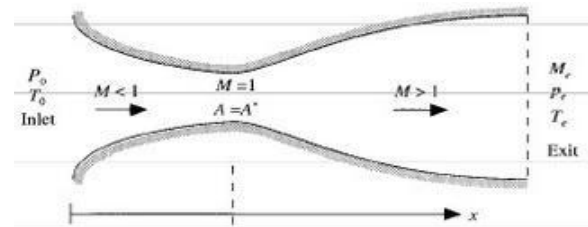
Functions Of Nozzle

The purpose of the exhaust nozzle is to increase the velocity of the exhaust gas before discharge from the nozzle and to collect and straighten the gas flow. For large values of thrust, the kinetic energy of the exhaust gas must be high, which implies a high exhaust velocity. The pressure ratio across the nozzle controls the expansion process and the maximum uninstalled thrust for a given engine is obtained when the exit pressure (P_e) equals the ambient pressure (P_0). The functions of the nozzle may be summarized by the following list:^[2]

1. Accelerate the flow to a high velocity with minimum total pressure loss.
2. Match exit and atmospheric pressure as closely as desired.
3. Mix core and bypass streams of turbofan if necessary.
4. Allow for thrust reversing if desired.
5. Suppress jet noise, radar reflection, and infrared radiation (IR) if desired.
6. Do all of the above with minimal cost, weight, and boat tail drag

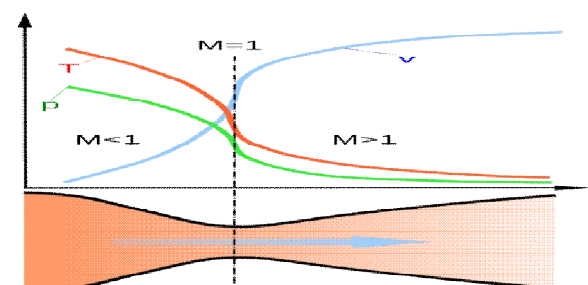
while meeting life and reliability goals.

Introduction To Convergent And Divergent Nozzle



A de Laval nozzle (or convergent-divergent nozzle, CD nozzle or con-di nozzle) is a tube that is pinched in the middle, making a carefully balanced, asymmetric hourglass shape. It is used to accelerate a hot, pressurized gas passing through it to a higher speed in the axial (thrust) direction, by converting the heat energy of the flow into kinetic energy.^{[3][5]} Because of this, the nozzle is widely used in some types of steam turbines and rocket engine nozzles. It also sees use in supersonic jet engines.

Conditions for operation



Its operation relies on the different properties of gases flowing at subsonic and supersonic speeds. The speed of a subsonic flow of gas will increase if the pipe carrying it narrows because the mass flow rate is constant.^[3] The gas flow through a de Laval nozzle is isentropic (gas entropy is nearly constant). In a subsonic flow the gas is compressible, and sound will propagate through it. At the "throat", where the cross-sectional area is at its minimum, the gas velocity locally becomes sonic (Mach number = 1.0), a condition called choked flow. As the nozzle cross-sectional area increases, the gas begins to expand, and the gas flow increases to supersonic velocities^[3]

THEORETICAL BACK GROUND

Flowthrough Nozzles:

The steam flow through the nozzles may be assumed as adiabatic flow. Since during the expansion of steam in nozzle neither heat is supplied or rejected work^[5]. As steam passes through the nozzle it loses its pressure as well as heat.

When the steam flows through a nozzle the final velocity of steam for a given pressure drop is reduced due to following reasons^[5]

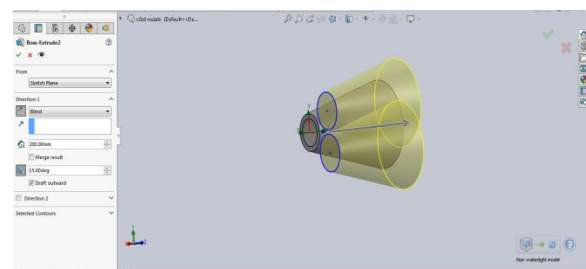
- I. The friction between the nozzle surface and steam
- II. Internal friction of steam itself and
- III. The shock losses

Most of these frictional losses occur between the throat and exit in convergent divergent nozzle.

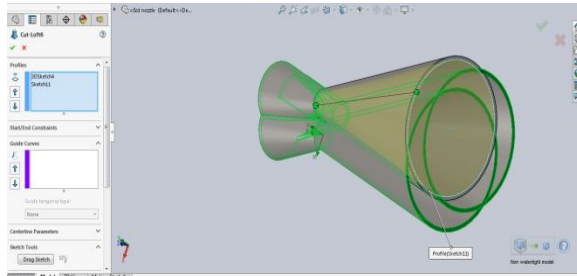
Steam Enters nozzle with high pressure and very low velocity (velocity is generally neglected). Leaves nozzle with high velocity & low pressure. All this is due to the reason that heat energy at steam is converted into K.E as it passes through nozzle^[5].

Modeling of Tri-Nozzle:

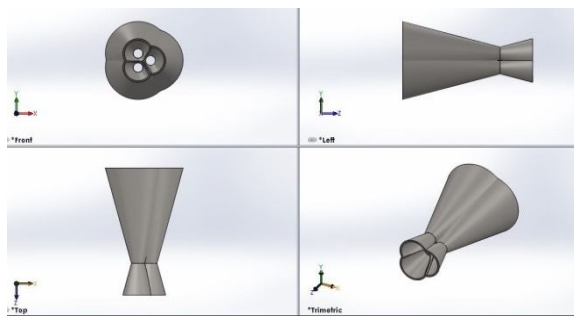
First of all convergent section of Tri-Nozzle was designed for our convenience to view and modify the cross-section of Throat. Leaving thickness of nozzle Loft cut is performed three times.



Similarly after construction of convergent section we work on divergent section.



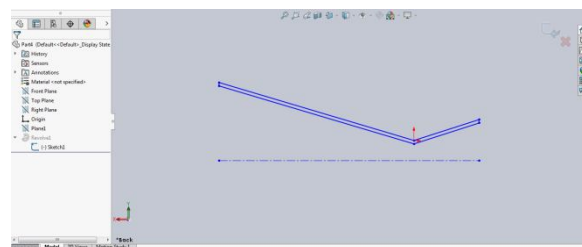
It was designed to have three different entrances in throat and one in entrance of Nozzle.



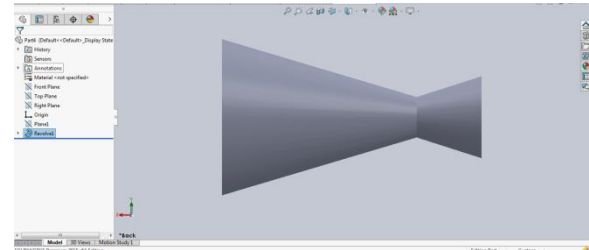
Modeling of single nozzle:

First select a new file and front plane

Draw sketch as follows



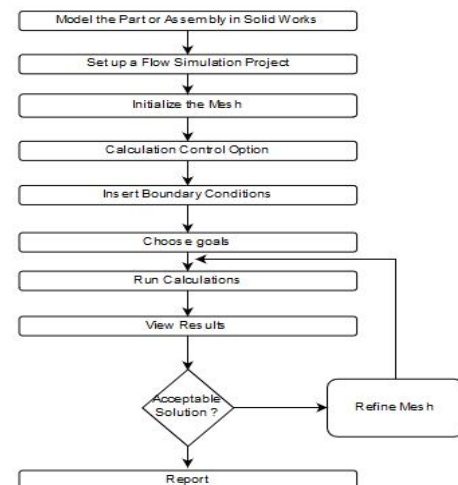
With the help of revolve option in solidworks taking the axis line as reference revolve the sketch around axis forms the single nozzle.



Solidworks Flow Simulation

Introduction:

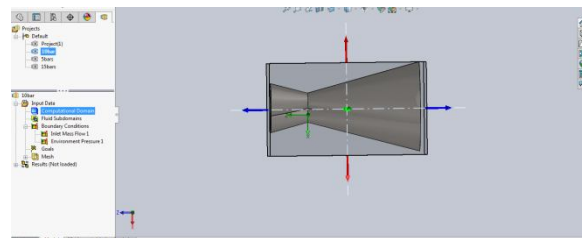
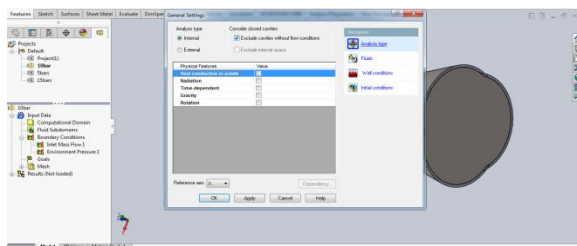
Solid Works Flow Simulation 2010 is a fluid flow analysis add-in package that is available for SolidWorks in order to obtain solutions to the full Navier-Stokes equations that govern the motion of fluids. Flow Simulation involves a number of basic steps that are shown in the following flowchart in figure.



Flowchart for fluid flow analysis using Solidworks Flow simulation setting up aSolid works

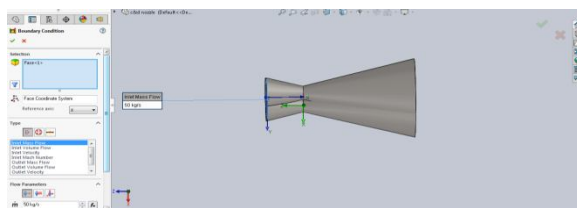
Flow simulation of tri nozzle:

Simulation of Tri-Nozzle is done step by step with the help of simulation wizard of Solid Works flow simulation software, those involves selection of inlet, outlet from Nozzle geometry and type of fluid flowing inside the nozzle also to be selected and boundaries has to be assigned.

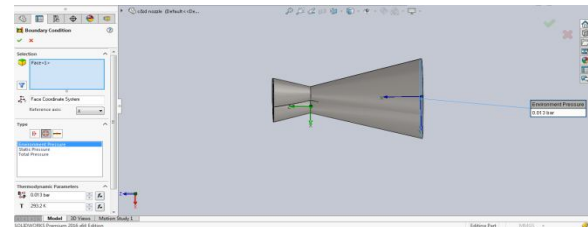


After selection of boundaries and fluids we have to assign the boundary conditions like inlet mass flow rate, pressure, and exit conditions.

Here Inlet mass flow rate is taken as 50kg/s with 5 bar and 10 bar pressure separately

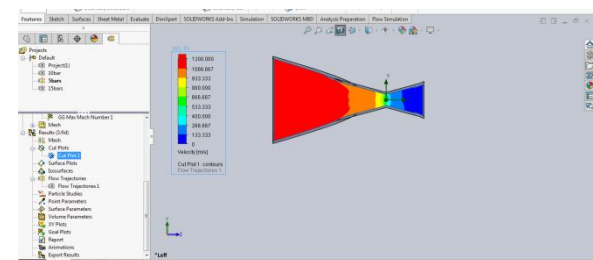


And exit conditions of nozzles are selected as vacuum.

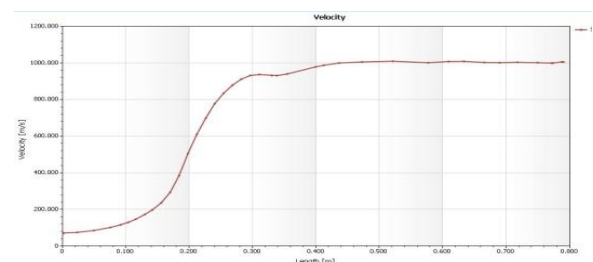


Results:

At given input conditions and 5 bar pressure the exit velocity of fluid from nozzle reached to 1040 m/s. images showing velocity distribution along the length of nozzle and respective graph are shown below

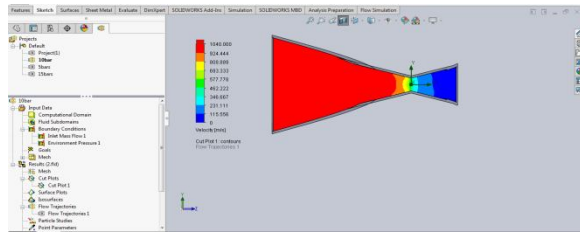


Graph showing velocity curve

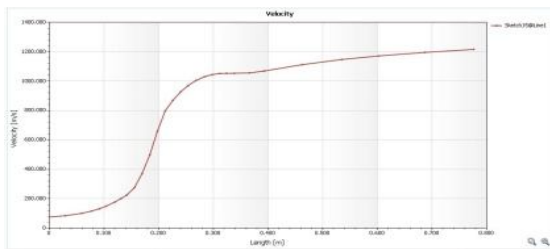


At given input conditions and 5 bar pressure the exit velocity of fluid from

nozzle reached to 1200 m/s. images showing velocity distribution along the length of nozzle and respective graph are shown below



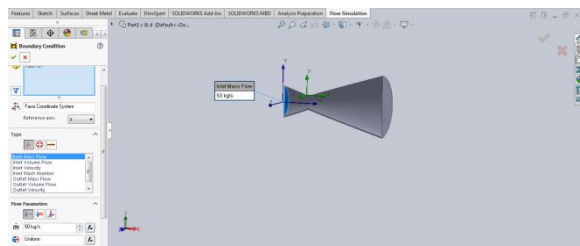
Graph showing velocity curve



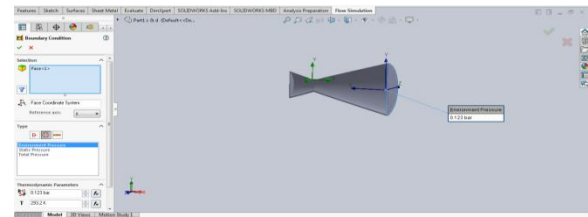
For single nozzle

Simulation of Single Nozzle is done similarly as Tri-Nozzle. All the boundary conditions are also same given to Tri-Nozzle.

Here also Inlet mass flow rate is taken as 50kg/s with 5 bar and 10 bar pressure separately

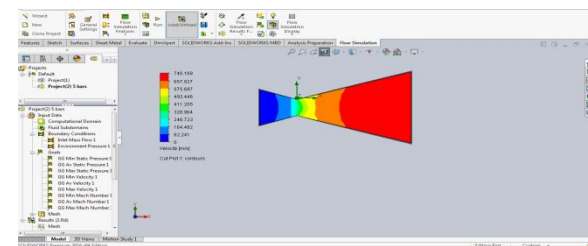


Vacuum pressure outlet

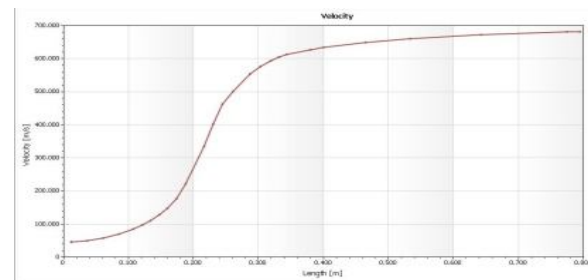


Results:

At given input conditions and 5 bar pressure the exit velocity of fluid from nozzle reached to 661.6 m/s. images showing velocity distribution along the length of nozzle and respective graph are shown below

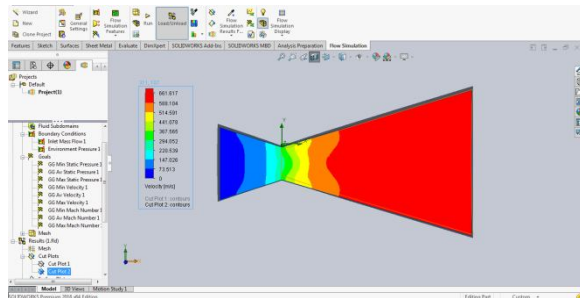


Graph showing velocity curve

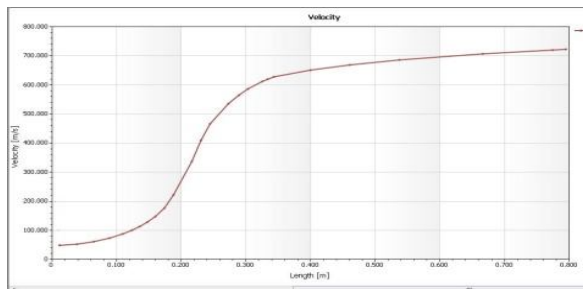


At given input conditions and 10 bar pressure the exit velocity of fluid from nozzle reached to 740 m/s. images showing velocity distribution along the length of

nozzle and respective graph are shown below



Graph showing velocity curve



Conclusion and Results:

- Modeling and analysis of Convergent and divergent nozzle is done in Solid works 2016
- Tri-nozzle is first modeled and analyzed in Solid works then an individual single nozzle is designed with same throat area and done analysis at 5bars and 10bars respectively.
- Analysis is done on Tri-nozzle at 5bars and 10 bars and values are noted.

- Analysis is done on single nozzle at 5 bars and 10 bars and values are noted.
- Velocity of both nozzles at 5 bar and 10barpressure are tabulated in results table.
- Thus variations in velocities at certain given pressures of convergent and divergent nozzle are analyzed in this project.

Pressure	Velocity(m/s)	
	Single Nozzle	Tri-Nozzle
5 bar	661.6	1040
10 bar	740	1200

From our experiment we can say that Tri-nozzle is giving more exit velocity of fluid than single nozzle at same input conditions and vacuum exit conditions.

Both the nozzles are designed to have same throat area, length, same convergent angle and divergent angles.

References:

- [1] Pardhasaradhi Natta, V.Ranjith Kumar, Dr.Y.V.Hanumantha Rao"Flow Analysis of Rocket Nozzle Using Computational Fluid

- Dynamics (Cfd)” Vol. 2, Issue 5, September- October 2012
- [2] Jack D. Mattingly, David T. Pratt(University of Washington), William H. Heiser, U.S. Air Force Academy.
- [3] C.J. Clarke and B. Carswell (2007). Principles of Astrophysical Fluid Dynamics (1st ed.). Cambridge University Press. p. 226
- [4] A.A.Khan and T.R.Shembharkar, “Viscous flow analysis in a Convergent-Divergent nozzle”. Proceedings of the international conference on Aero Space Science and Technology, Bangalore, India, June 26-28, 2008.
- [5] Gutti Rajeswara Rao, U.S. Ramakanth, A Lakshman “Flow analysis in a Convergent-Divergent Nozzle using CFD”“Volume-1,Issue-2,October-December, 2013.
- [6] H.K.Versteeg and W.MalalaSekhara, “An introduction to Computational fluid Dynamics”, British Library cataloguing pub, 4th edition, 1996.
- [7] M.M.Atha vale and H.Q. Yang, “Coupled field thermal structural simulations in Micro Valves and Micro channels” CFD Research Corporation.
- [8] Kazuhiro Nakahashi, “Navier-Stokes Computations of two and three dimensional cascade flow fields”, Vol.5, No.3, May-June 1989.
- [9] Romine, G. L., “Nozzle Flow separation,” AIAA Journal, Vol. 36, No.9, Sep. 1998. Pp 1618- 1625.
- [10] Dutton, J.C., “Swirling Supersonic Nozzle Flow,” Journal of Propulsion and Power, vol.3, July 1987, pp. 342-349.
- [11] Elements of Propulsion: Gas Turbines and Rockets ---- Jack D. Mattingly
- [12] Introduction To Cfd---- H K Versteeg &W Malalasekera
- [13] Rocket and Spacecraft Propulsion Principles, Practice and New Developments (2nd ed., Springer, 2005) ---- Turner M.

1. K NAGARJUNA REDDY



Studying M.Tech in stream of Thermal Engineering from MALLAREDDY ENGINEERING COLLEGE. Completed B.Tech in Mechanical Engineering in 2013 from QIS COLLEGE OF ENGINEERING AND TECHNOLOGY, Ongole.

E-mail id: **nani.arjun555@gmail.com**

2. N SRINIVASA RAJNEESH



Completed B.Tech. in Mechanical engineering in 2001 from V.N.R.VJIET Engineering College, Hyderabad Affiliated to JNTUH, and M.Tech in Energy Technology in 2005 from Pondicherry Engineering college Affiliated to Pondicherry University, Pondicherry. Working as Associate Professor at MALLA REDDY ENGINEERING COLLEGE(AUTONOMOUS) , Dulapally Rd, Maisammaguda, Hyderabad, Telangana, India.

Area of interest includes: I.C Engine, Biofuel, Energy.

E-mail id: **rajneeshsrinivasa@gmail.com**

IMPROVING PRODUCTIVITY AND QUALITY BY CHANGING FEEDING SYSTEM IN AN INJECTION MOULDING PROCESS

¹K Abhilash Korvi, ² A. Raveendra

¹M.Tech, Advanced Manufacturing Systems, Malla Reddy Engineering College (Autonomous), JNTU - Hyderabad, Telangana, India.

² HOD, Department of Mechanical Engineering, Malla Reddy Engineering College (Autonomous), JNTU - Hyderabad, Telangana, India

Abstract: In this thesis, the feeding system is optimized for a plastic product to improve the productivity as well as the quality. One gate and four gates are designed and modeled in 3D modeling software Pro/Engineer. A repeated number of analyses are carried out by plastic flow advisor software to reduce fill time, scrap and automatic degating. The process parameters used are maximum injection pressure, melt temperature and mould temperature to analyze fill time, shrinkage, weld lines, pressure drop, and air traps in successive trials. The materials considered are GE plastics, grade Cyclic 28818E and grade Cyclic 29254E.

I. INTRODUCTION

Literature Survey

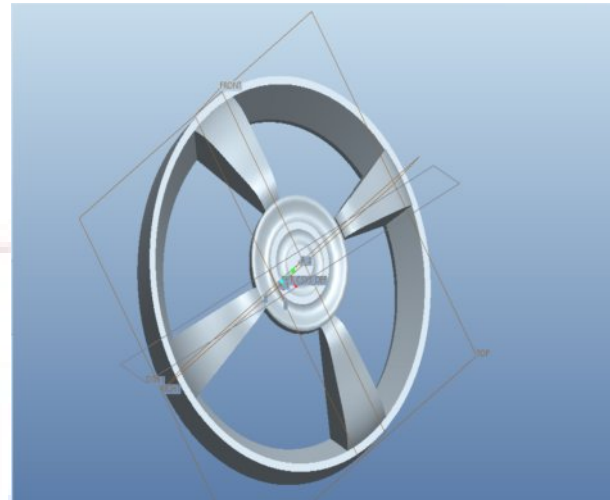
The following are some of the papers done by different authors:

Vikas B J, Chandra Kumar R[1], describes the influence of gate location and size through a repeated number of analyses which is carried out by plastic flow advisor software to reduce fill time, scrap and automatic degating. The process parameters like fill time, shrinkage, weld lines, pressure drop, and air traps are analysed by simulation in successive trials. Experimental verification has been done with new optimized gate location with designed mould in injection moulding machine. The results showed an improvement in fill time from 1.64 sec to 1.2 sec with increase in injection pressure by 15 MPa. Shrinkage and air traps were reduced minimizing trouble shooting defeats.

Lam, Y.C., Jin, S.[2], an automated routine is developed to handle design constraints in automated gating synthesis, taking advantages of functionality of both CAD and CAE systems. Standard deviation of filling time is used as the objective function and hill-climbing search algorithm is employed during the gate optimization process. Design constraints considered so far are no-gate constraints for three-plate molded part and edge-gate constraints for two-plate molded part. These constraints are defined in an Integrated CAD/CAE design environment for plastic injection

molding using the functionality of CAD system, and then translated into CAE features.

II. MODELING OF PLASTIC WHEEL



Mould Flow Analysis Using Plastic Advisor Input Parameters

	CASE 1	CASE 2	CASE 3
Injection Pressure (Mpa)	180	140	240
Mold Temperature (°c)	50	55	60
Melt Temperature (°c)	230	220	300

MATERIAL – Cyclic 28818E

Gate Location -1

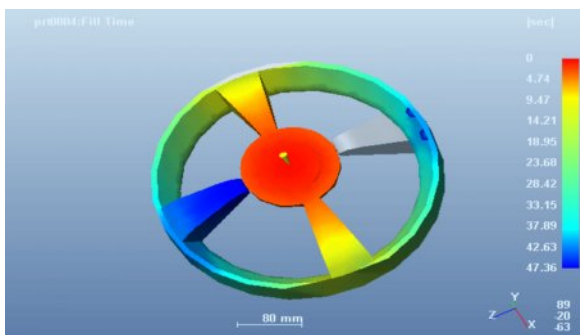
- Max Injection Pressure:
- 140MPa,
- Mold Temperature: 55 deg C,
- Melt Temperature: 220 deg C

Summary:

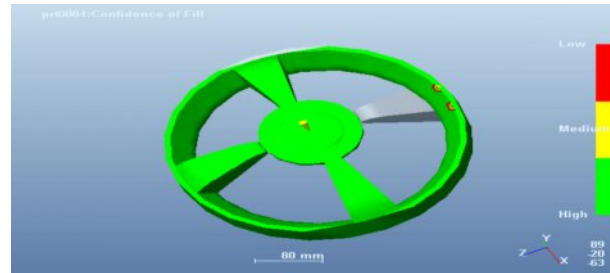
Release Level:	7.0
prt0004	
Part Name	prt0004
Part Revision	1
Material Supplier	GE Plastics (USA)
Material Grade	Cyclac 28818E
Max Injection Pressure	140.00 MPa
Mold Temperature	55.00 deg.C
Melt Temperature	220.00 deg.C
Model Suitability	Part model was generally suitable for analysis.

Filling Analysis	prt0004
Mold ability:	Your part has not completed filling and is a short shot. Part quality will be unacceptable. View the Confidence of Fill plot and use the Dynamic Adviser to get help on how to improve the filling of the part.
Confidence:	Low
Injection Time:	47.36 sec
Injection Pressure:	2.04 MPa
Weld Lines:	Yes
Air Traps:	Yes
Shot Volume :	1896.85 cu.cm

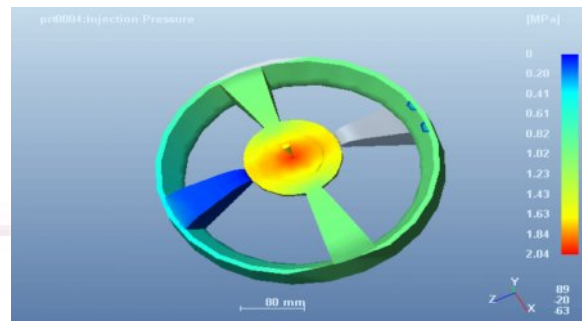
Fill Time



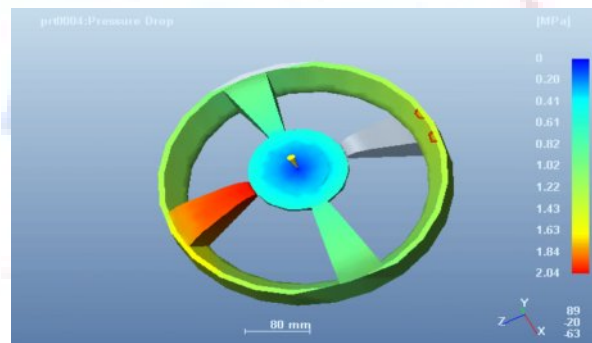
Confidence of Fill



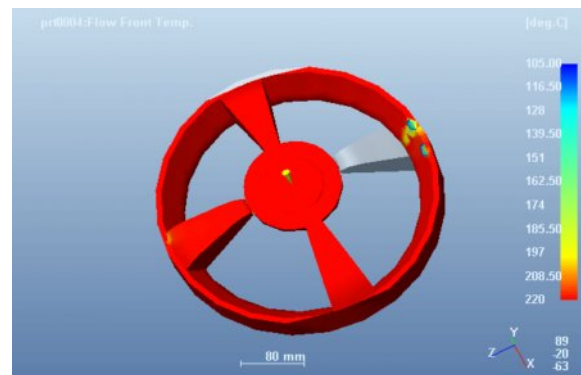
Injection Pressure



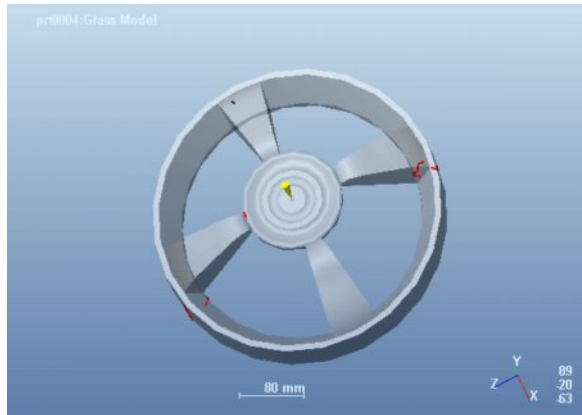
Pressure Drop



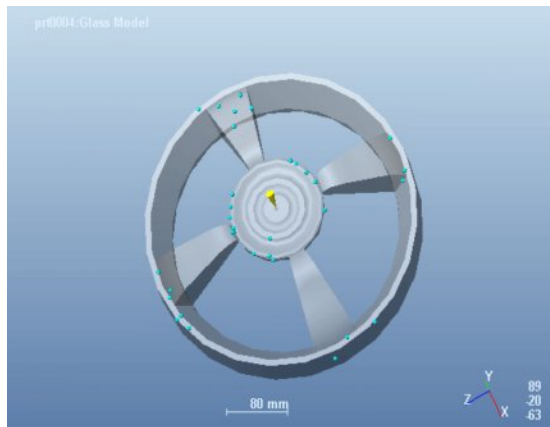
Flow Front Temp.



Weld Lines



Air Traps



Skin Orientation



III. RESULTS TABLE

Material - Cyclic 28818e

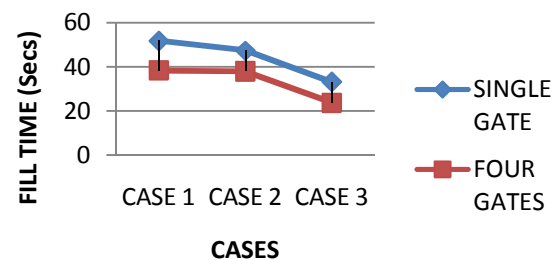
Single Gate

	Case 1	Case 2	Case 3
Confidence	Low	High	Medium
Fill Time (Secs)	51.8	47.36	33.15
Injection Pressure (Mpa)	2.34	2.04	0.21
Weld Lines	No	Yes	Yes
Air Traps	No	Yes	Yes

Four Gates

	Case 1	Case 2	Case 3
Confidence	High	High	High
Fill Time (Secs)	38.38	37.98	23.78
Injection Pressure (Mpa)	8.70	10.21	2.72
Weld Lines	Yes	Yes	Yes
Air Traps	Yes	Yes	Yes

Fill Time Comparison For Single Gate And Four Gates

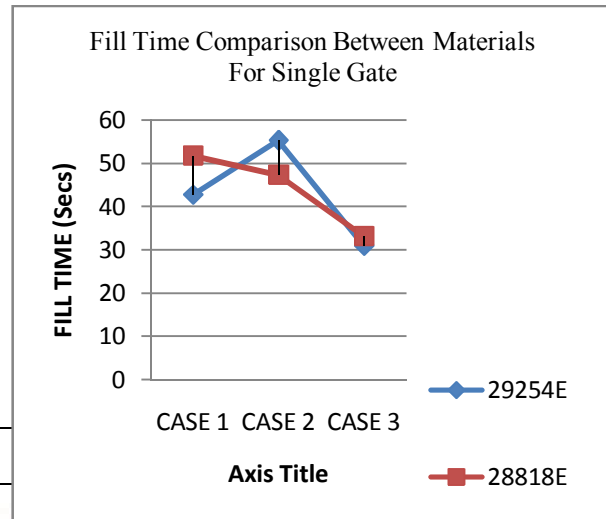


By observing the results for fill time, for case 1, the fill time is reduced almost by 26% when four gates are used than single gate. For case 2, the fill time is reduced almost by 19.8% when four gates are used than single gate. For case 3, the fill time is reduced almost by 28% when four gates are used than single gate.

Material- Cycolac 29254e
Single Gate

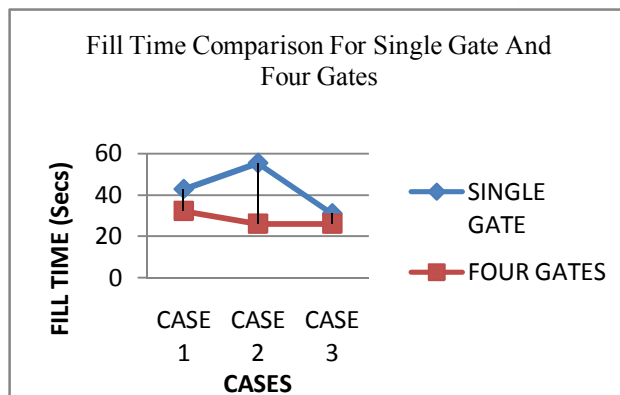
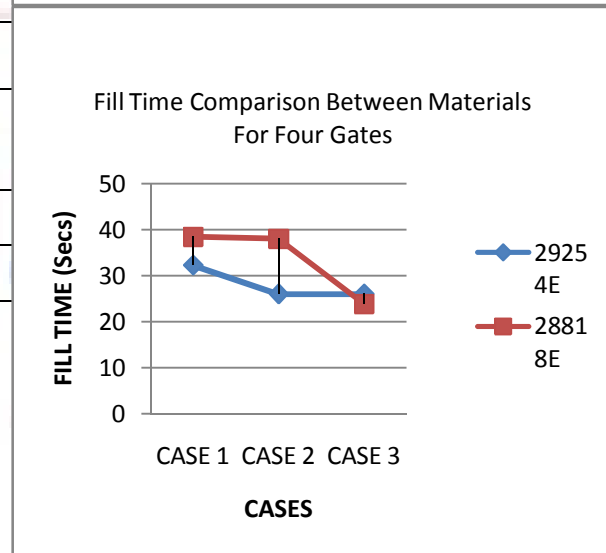
	Case 1	Case 2	Case 3
Confidence	High	High	High
Fill Time (Secs)	42.71	55.28	30.94
Injection Pressure (Mpa)	0.29	0.50	0.03
Weld Lines	Yes	Yes	Yes
Air Traps	Yes	Yes	Yes

gate. For case 3, the fill time is reduced almost by 16% when four gates are used than single gate.



Four Gates

	Case 1	Case 2	Case 3
Confidence	High	High	High
Fill Time (Secs)	32.18	25.97	25.99
Injection Pressure (Mpa)	1.97	1.59	1.56
Weld Lines	Yes	Yes	Yes
Air Traps	Yes	Yes	Yes



By observing the results for fill time, for case 1, the fill time is reduced almost by 24.6% when four gates are used than single gate. For case 2, the fill time is reduced almost by 53% when four gates are used than single

gate. By comparing the fill time between materials, the fill time is less for material 29254E.

IV. CONCLUSION

By observing the analysis results, by using four gates the fill time is increased thereby increasing the production time. The fill time is less for the parameters, Max Injection Pressure: 140MPa, Mold Temperature: 55 deg C, Melt Temperature: 220 deg C and the confidence of fill is also high. The better material is Cycolac 29254E.

REFERENCES

- [1] Vikas B J, Chandra Kumar R, *Influence of feeding system in injection moulding for lower washer of a bearing*, Volume: 02, Issue: 08, Aug-2013, *International Journal of Research in Engineering and Technology*
- [2] Lam, Y.C., Jin, S., *Optimization of the gate location for plastic injection moulding*, *Journal of Injection Moulding Technology*, 2001.
- [3] Sahputra, I.H., *Comparison of two flow analysis software for injection moulding tool design*. *Proceedings of the International Conference on Industrial Engineering and Engineering Management*, 2-4 Dec. 2007, Singapore..
- [4] Saman, A.M., Abdullah, A.H., Nor, M.A.M., *Computer simulation opportunity in plastic injection mould development for automotive part*. *International Conference on Computer Technology and Development*, 13-15 Nov. 2009, Kota Kinabalu, Malaysia..
- [5] Mr. Yat.hish Kumar K.R, Prof. Nagaraja.R, *Significance of Mold Filling Analysis for Finding Optimal Gate Location in Injection Molding Process for Bobbin*, *International Journal of Scientific and Research Publications*, Volume 4, Issue 4, April 2014 1 ISSN 2250-3153.
- [6] P. Hussain Babu, T. Vishnu Vardan[6], *Computer Simulation for Finding Optimum Gate Location in Plastic Injection Moulding Process*, *Int. Journal of Engineering Research and Applications*, ISSN : 2248-9622, Vol. 3, Issue 6, Nov-Dec 2013, pp.947-950.
- [7] David O. Kazmer and Russell G. Speight, *Polymer Injection Molding Technology for the Next Millennium*, *Journal of Injection Molding Technology*.
- [8] Wei Guo, Lin Hua, Huajie Mao, Zhenghua Meng, *Prediction of warpage in plastic injection molding based on design of experiments*, *Journal of Mechanical Science and Technology*, April 2012, Volume 26, Issue 4, pp 1133–1139.
- [9] Nik Mizamzul Mehat, Shahrul Kamaruddin, and Abdul Rahim Othman, *Modeling and Analysis of Injection Moulding Process Parameters for Plastic Gear Industry Application*, *ISRN Industrial Engineering*, Volume 2013 (2013), Article ID 869736, 10 pages.
- [10] L.M. Galantucci, R. Spina, *Evaluation of filling conditions of injection moulding by integrating numerical simulations and experimental tests*, *Journal of Materials Processing Technology* 141(2):266-275 · October 2003.

AUTHORS

Student: Abhilash Korvi, completed his B.Tech degree in Mechanical Engineering from Malla Reddy College of Engineering (Formerly known as: C M Engineering College), JNTU - Hyderabad, Telangana, India, in the year 2013, presently pursuing his M.Tech in Advanced Manufacturing Systems from Malla Reddy Engineering College (Autonomous), JNTU - Hyderabad, Telangana, India.

Guide: Mr. A. Raveendra, HOD, Department of Mechanical Engineering, Malla Reddy Engineering College (Autonomous), JNTU - Hyderabad, Telangana, India.

Comparing and Optimizing the Process Parameters of two types of Al-MMC's in Turning

Shaik Noor Ahamed¹, PG Scholar, Department of Mechanical Engineering, MREC, Hyderabad, India.

K.Rajesh², Assistant Professor, Department of Mechanical Engineering, MREC, Hyderabad, India.

Abstract - Aluminium Metal Matrix Composites (Al MMC's) are the nearby elements which can replace conventional materials which are in use. Al MMC's, now gained the space in applications such as aerospace, structural members, automotive, ship buildings etc because of their properties like high strength to weight ratio, hardness, stiffness and corrosion resistance. This paper presents an investigation on machining (Turning) of Al (6061)-SiC and Al (6063)-SiC MMC's. SiC particles are reinforced in Al matrix with 0%, 10%, and 20% by weight. Taguchi's L27 orthogonal array experimentation was used to optimize the parameters of Al-SiC MMC's. The effect of parameters such as Speed, Feed, Depth of cut and Percentage of contribution on Metal Removal Rate and Cutting Force in turning was calculated. Signal to Noise ratio and ANOVA was used for finding significant parameter. Required comparisons are done between two Al MMC's. The experiments are conducted using HSS tool under dry condition. A Taguchi analysis is carried out. The effect of parameters is studied and presented.

Key Words: Signal to Noise ratio, ANOVA, metal removal rate, cutting Force.

1. INTRODUCTION

Frequent use of modern materials for the required applications in the present scenario, made clear that a quality product at the end is necessary, after performing the machining operations on the work piece. Therefore quality is an important part of production. Machining operations are performed in the process to achieve the required output, so now product's quality depends on the operations performed on the product. Turning is the operation performed for metal removal in most applications, as it can give a good surface finish. Volume of metal removed from a cylindrical work piece per unit time is called as metal removal rate and highest metal removal rate is expected from turning operation, so that it leads to reduced cost and highest production. The cutting tool feeds into the rotating work piece and cuts away material in the form of small chips to create the desire shape.

Problems associated with machining of MMC's should be minimised if these materials need to be used extensively. Here in this paper study of effects of process parameters such as speed, feed, depth of cut and percentage of composition on metal removal rate and cutting force in

turning of Al MMCs is calculated. Taguchi methods are statistical methods developed by Genichi Taguchi to improve the quality of manufactured goods and more recently also applied to engineering.

Design of experiments or Taguchi's technique is used to complete the objective and generate the optimised value. Here L27 orthogonal array was used for conducting the experiments and ANOVA was employed to analyze the percentage contribution and influence of process parameters. Taguchi's technique was found using Minitab 17 software.

2. METHODOLOGY

In this paper, the machining parameters are determined by using Taguchi's design method. Orthogonal arrays of Taguchi, the signal-to-noise (S/N) ratio, the analysis of variance (ANOVA), and regression analysis are used to get the optimal levels and to analyze the effect of the machining parameters on material removal rate & cutting force.

2.1 TAGUCHI METHOD

Taguchi has developed a methodology for the application of factorial design experiments that has taken the design of experiments from the exclusive world of the statistician and brought it more fully into the world of manufacturing [1]. Thus the marriage of design of experiments with optimization of control parameters to obtain best results is achieved in Taguchi method. Orthogonal arrays provide a set of well balanced experiments & desired output. [2]

Conventional procedures need more number of experiments to be performed, when more number of parameters increased, this issue is resolved by Taguchi method, it uses special design to study the parameters with small number of experiments. Saving time, cost and finding significant factors at more ease. Taguchi uses the S/N ratio to measure the quality characteristic deviating from the desired value. There are several S/N ratios available, depending on the type of characteristic; lower the better, nominal the best or higher the better.

The S/N ratio for the higher-the-better criterion is given by Taguchi as:

$$\frac{S}{N} = -10 \log_{10} \left[\frac{1}{n} \sum \frac{1}{y^2} \right] \quad (1)$$

The S/N ratio for the lower-the-better criterion is given by Taguchi as:

$$\frac{S}{N} = -10 \log_{10} \left[\frac{\sum y^2}{n} \right] \quad (2)$$

Where 'y' is the observed data and 'n' is the number of observations.

Regardless of the category of the performance characteristics, a greater S/N value corresponds to a better performance. Therefore, the optimal level of the machining parameters is the level with the great S/N ratio value [10].

2.2 ANALYSIS OF VARIANCE (ANOVA)

ANOVA is a statistical process in which the existence of differences among several population means determined. While the aim of ANOVA is the detect differences among several populations means, the technique requires the analysis of different forms of variance associated with the random samples under study-hence the name analysis of variance. The relative influence of the parameters is measured by total sum of square value (SST) and is given by:

$$SS_T = \sum_{i=1}^n [n_i - n_m]^2 \quad (3)$$

Where n is the number of experiments in the orthogonal array, n_i is the mean S/N ratio for the i_{th} experiment and n_m is the total mean S/N ratio of all experiments.

2.3 REGRESSION ANALYSIS

A statistical tool that allows you to examine how multiple independent variables are related to a dependent variable. Once you have identified how these multiple variables relate to your dependent variable, you can take information about all of the independent variables and use it to make much more powerful and accurate predictions about why things are the way they are. It is also used to understand which among the independent variables are related to the dependent variable and to explore the forms of these relationships. The general form of a multiple regression model is as follows:

$$\text{Independent variable} = b_0 + b_1 (\text{Independent variable 1}) + b_2 (\text{Independent variable 2}) + \dots + \epsilon \quad (4)$$

Where $b_1, b_2 \dots$ are estimates of the independent variables 1, 2 ... and ϵ is the error.

3. EXPERIMENTAL WORK

Samples of 30mm dia and 30cm length of Al (6061)-SiC and Al (6063)-SiC composites with 0%, 10% and 20% weight of SiC are fabricated by stir casting method [12].

Experiments are conducted on lathe based on Taguchi's design of experiments. Speed, feed and depth of cut values are controllable and are maintained nominal, thus preventing harm to the machine. Machining criteria also depends on the work piece density, with increasing the percentage of reinforcement in composites the density too varies. Therefore to study the effect of percentage of reinforcement on machining criteria, SiC is varied from 0%-20% by weight in Al-SiC composites. The factors to be studied and their levels are given in Table 1. Tool used for machining is High speed steel. The observations (MMR and Cutting force) are made by changing speed, feed, depth of cut and percentage of reinforcement. Figure 1 & 2 shows the prepared work pieces of Al (6061)-SiC and Al (6063)-SiC respectively. Table 2 & Table 3 lists Taguchi's L27 orthogonal array, the measured values of responses and the S/N ratios of both Al MMC's.

Metal Removal Rate, $MMR = \pi * D_{avg} * d * f * N \quad (5)$

Where

$$D_{avg} = (D_i + D_f) / 2$$

D_i =Initial dia of rod

D_f =Final dia of rod

d = depth of cut

f = feed

N = spindle speed

Cutting force,

$$CF = (\text{Torque}) / D_{avg} \quad (6)$$

Where

$$\text{Torque} = (\text{Power consumed}) / \omega$$

$$\omega = 2\pi N$$

Table 1. Factors and their levels

Symbol	Factors	Level 1	Level 2	Level 3
A	Speed (rpm)	315	500	775
B	Feed (mm/rev)	0.71	1.42	2.85
C	Depth of cut (mm)	0.4	0.8	1.2
D	% of reinforcement	0	10	20

Table 2. L27 orthogonal array for Al 6061-SiC

S. no	Factors				Responses		S/N ratio	
	A	B	C	D	MMR mm ³ /min	CF N	MMR	CF
1	1	1	1	1	8660	0.0370	78.962	28.622
2	1	1	2	2	16420	0.040	83.311	27.931
3	1	1	3	3	18219	0.0579	86.021	24.733
4	1	2	1	1	16870	0.037	84.393	28.470
5	1	2	2	2	31040	0.041	88.742	27.592
6	1	2	3	3	32390	0.066	91.452	23.571
7	1	3	1	1	32955	0.041	89.799	27.564
8	1	3	2	2	58687	0.042	94.148	27.384
9	1	3	3	3	56881	0.079	96.858	22.007

10	2	1	1	2	11068	0.034	82.472	29.272
11	2	1	2	3	23921	0.029	87.472	30.690
12	2	1	3	1	36952	0.0297	90.039	30.532
13	2	2	1	2	21422	0.0326	87.903	29.732
14	2	2	2	3	44986	0.0328	92.903	29.675
15	2	2	3	1	67478	0.0320	95.47	29.877
16	2	3	1	2	41561	0.0334	93.309	29.508
17	2	3	2	3	84555	0.0366	98.308	28.713
18	2	3	3	1	122534	0.0357	100.87	28.940
19	3	1	1	3	20476	0.0219	85.487	33.185
20	3	1	2	1	28777	0.0256	90.344	31.814
21	3	1	3	2	44825	0.0311	92.404	30.124
22	3	2	1	3	39844	0.0196	90.918	34.122
23	3	2	2	1	53126	0.0241	95.775	32.336
24	3	2	3	2	79689	0.0359	97.835	28.892
25	3	3	1	3	77748	0.0175	96.324	35.092
26	3	3	2	1	97740	0.0291	101.18	30.704
27	3	3	3	2	139946	0.0449	103.24	26.942



Figure 1. Al 6061-SiC



Figure 2. Al 6063-SiC

Table 3. L27 orthogonal array for Al 6063-SiC

S. no	Factors				Responses		S/N ratio	
	A	B	C	D	MMR mm ³ /min	CF N	MMR	CF
1	1	1	1	1	8885	0.03324	79.203	29.671
2	1	1	2	2	16420	0.03874	83.309	27.342
3	1	1	3	3	18219	0.05611	85.991	26.122
4	1	2	1	1	17319	0.03607	84.64	28.814
5	1	2	2	2	31040	0.04208	88.746	26.486
6	1	2	3	3	32390	0.06207	91.428	25.265
7	1	3	1	1	33858	0.03771	90.053	28.217
8	1	3	2	2	58687	0.04195	94.159	25.888
9	1	3	3	3	56881	0.06974	96.841	24.668
10	2	1	1	2	11068	0.03079	82.442	31.687
11	2	1	2	3	23921	0.02944	87.484	30.597
12	2	1	3	1	38024	0.02957	90.31	29.194
13	2	2	1	2	21422	0.03287	87.88	30.831
14	2	2	2	3	44986	0.03232	92.921	29.740
15	2	2	3	1	69621	0.03279	95.747	28.337
16	2	3	1	2	41561	0.03511	93.293	30.233
17	2	3	2	3	84555	0.03451	98.335	29.143
18	2	3	3	1	126833	0.03721	101.16	27.739
19	3	1	1	3	20476	0.01692	85.485	34.322
20	3	1	2	1	29883	0.02547	90.671	33.049
21	3	1	3	2	44825	0.02813	92.417	30.590
22	3	2	1	3	39844	0.01767	90.922	33.465
23	3	2	2	1	55339	0.02873	96.108	32.192
24	3	2	3	2	79689	0.03421	97.854	29.733
25	3	3	1	3	77748	0.02052	96.336	32.868
26	3	3	2	1	102183	0.03034	101.52	31.594
27	3	3	3	2	139970	0.03421	103.26	29.136

4. ANALYSIS OF EXPERIMENTAL RESULTS

After conducting 27 experiments each on Al 6061-SiC and Al 6063-SiC composites, performance evaluation and the effects of process parameters on metal removal rate and cutting force is studied.

4.1 ANALYSIS OF SIGNAL TO NOISE RATIO

Metal removal rate and cutting force values are obtained by equation (5) & (6) respectively and there signal to noise ratio values are calculated by equation (1) & (2) respectively.

4.1.1 Metal removal rate

The metal removal rate response table for each level of machining parameters (speed, feed, D.O.C & % of SiC) is obtained and results are presented in Table 4 for Al 6061-SiC and in Table 6 for Al 6063-SiC. Optimal levels at which optimal values can be obtained are darkened in the tables. Chart 2 and 4 shows the effect of process parameters on metal removal rates.

Table 4. Response Table for SN Ratios for Al 6061-SiC

Level	Speed	Feed	D.O.C	% of reinforcement
1	88.19	86.28	87.73	91.87
2	92.08	91.71	92.46	91.49
3	94.83	97.12	94.91	91.75
Delta	6.65	10.84	7.18	0.39
Rank	3	1	2	4

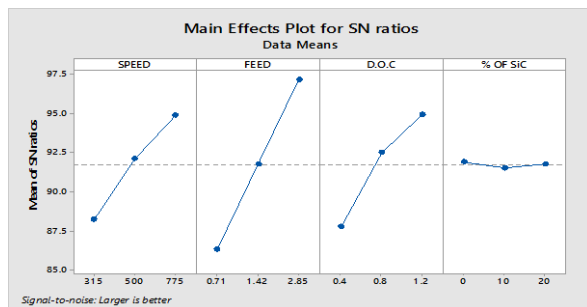


Chart-1: Main effects plot for SN ratios for Al 6061-SiC

Table 5. Response table for means for Al 6061-SiC

Level	Speed	Feed	D.O.C	% of reinforcement
1	30236	23257	30067	51677
2	50497	42983	48806	49406
3	64686	79179	66546	44336
Delta	34450	55921	36479	7341
Rank	3	1	2	4

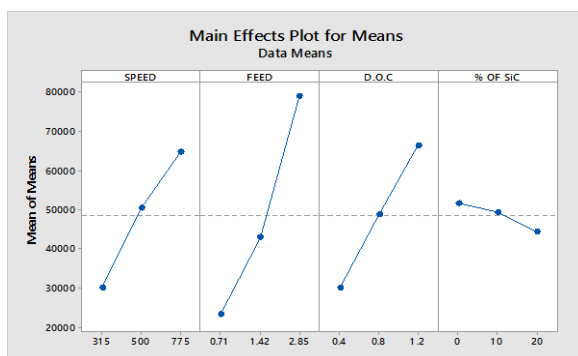


Chart-2: Main effects plot for means for Al 6061-SiC

Table 6. Response Table for SN Ratios for Al 6063-SiC

Level	Speed	Feed	D.O.C	% of reinforcement
1	88.26	86.37	87.81	92.16
2	92.17	91.81	92.58	91.49
3	94.95	97.22	95	91.75
Delta	6.69	10.85	7.20	0.67
Rank	3	1	2	4

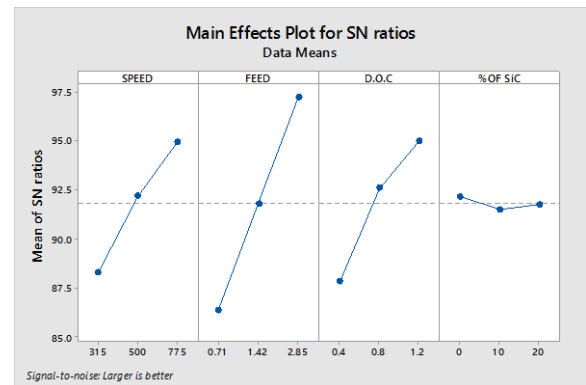


Chart-3: Main effects plot for SN ratios for Al 6063-SiC

Table 7. Response table for means for Al 6063-SiC

Level	Speed	Feed	D.O.C	% of reinforcement
1	30236	23257	30067	51677
2	50497	42983	48806	49406
3	64686	79179	66546	44336
Delta	34450	55921	36479	7341
Rank	3	1	2	4

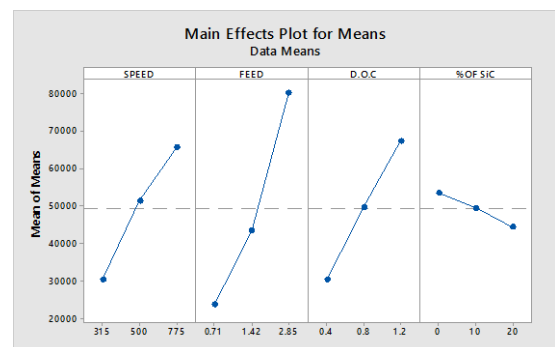


Chart-4: Main effects plot for means for Al 6063-SiC

4.1.2 CUTTING FORCE

The cutting force response table for each level of machining parameters (speed, feed, D.O.C & % of SiC) is obtained and results are presented in Table 8 for Al 6061-SiC and in Table 10 for Al 6063-SiC. Optimal levels at which optimal values can be obtained are darkened in the tables. Chart 6 and 8 shows the effect of process parameters on cutting force in Al MMC's. Previous researchers stated that the factors affecting the cutting force are the feed rate and spindle speed [9].

Table 8. Response Table for SN Ratios for Al 6061-SiC

Level	Speed	Feed	D.O.C	% of reinforcement
1	26.43	29.66	30.62	29.87
2	29.66	29.36	29.65	28.60
3	31.47	28.54	27.29	29.09
Delta	5.04	1.12	3.33	1.28
Rank	1	4	2	3

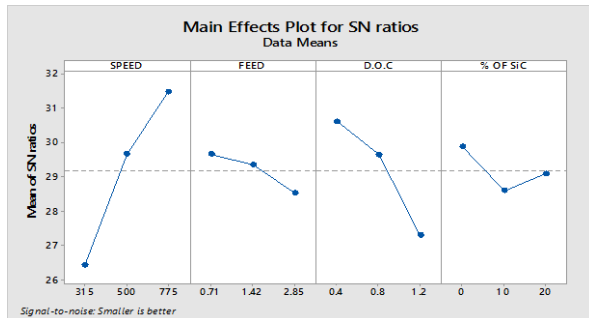


Chart-5: Main effects plot for SN ratios for Al 6061-SiC

Table 9. Response table for means for Al 6061-SiC

Level	Speed	Feed	D.O.C	% of reinforcement
1	0.04943	0.03414	0.03070	0.03257
2	0.03297	0.03589	0.03359	0.03746
3	0.02780	0.04017	0.04592	0.04017
Delta	0.02162	0.00603	0.01522	0.00760
Rank	1	4	2	3

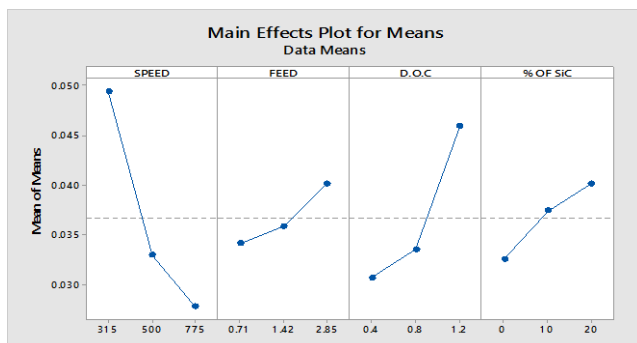


Chart-6: Main effects plot for means for Al 6061-SiC

Table 10. Response Table for SN Ratios for Al 6063-SiC

Level	Speed	Feed	D.O.C	% of reinforcement
1	26.94	30.29	31.12	29.87
2	29.72	29.43	29.56	29.10
3	31.88	28.83	27.87	29.58
Delta	4.94	1.45	3.26	0.76
Rank	1	3	2	4

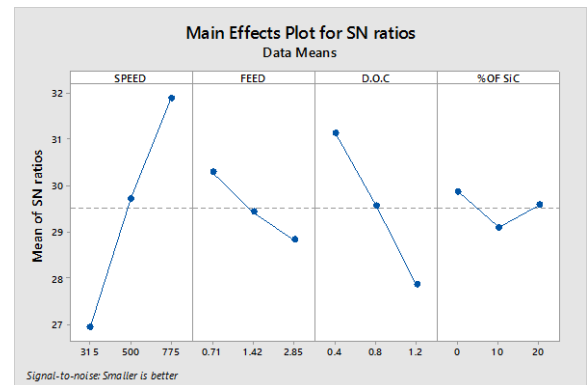


Chart-7: Main effects plot for SN ratios for Al 6063-SiC

Table 11. Response table for means for Al 6063-SiC

Level	Speed	Feed	D.O.C	% of reinforcement
1	0.04642	0.03205	0.02899	0.03235
2	0.03274	0.03543	0.03374	0.03535
3	0.02625	0.03793	0.04268	0.03771
Delta	0.02017	0.00588	0.01368	0.00535
Rank	1	3	2	4

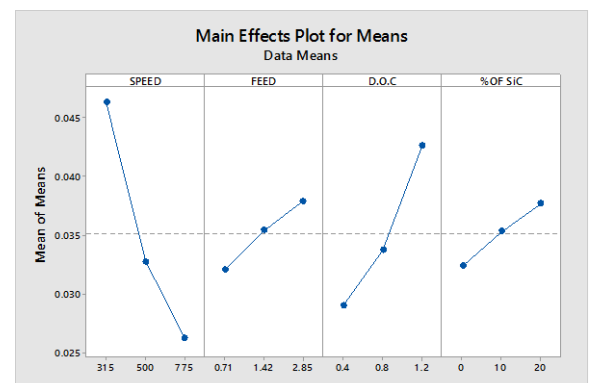


Chart-8: Main effects plot for means for Al 6063-SiC

4.2 ANALYSIS OF VARIANCE (ANOVA)

4.2.1 METAL REMOVAL RATE

Table 12 and 13 shows the ANOVA results for MMR values. During machining of composites, each factor has its own significance on the MMR. Darkened values in tables show their respective effects in percentage wise. Results shows feed is parameter which effects in both composites.

Table 12. ANOVA for MMR for Al 6061-SiC

Source	DF	SS	MS	F-value	Pr (%)
Speed	2	5395912165	2697956082	14.42	18.29
Feed	2	14479305580	7239652790	38.70	49.10
D.O.C	2	5989751197	2994875598	16.01	20.31
% of SiC	2	254288630	127144315	0.68	0.86
Error	18	3367574028	187087446		
Total	26	29486831599			

Table 13. ANOVA for MMR for Al 6063-SiC

Source	DF	SS	MS	F-value	Pr (%)
Speed	2	5623232649	2811616324	14.70	18.39
Feed	2	14900703415	7450351708	38.95	48.75
D.O.C	2	6211121075	3105560538	16.24	20.32
% of SiC	2	383322285	191661142	1.00	1.25
Error	18	3443067870	191281548		
Total	26	30561447294			

4.2.2 CUTTING FORCE

Table 14 and 15 shows the ANOVA results for CF values. During machining of composites, each factor has its own significance on the CF. Darkened values in tables show their respective effects in percentage wise. Results shows speed is the effective parameter which effects in both composites.

Table 14. ANOVA for CF for Al 6061-SiC

Source	DF	SS	MS	F-value	Pr (%)
Speed	2	0.002296	0.001148	25.15	48.51
Feed	2	0.000173	0.000087	1.90	3.65
D.O.C	2	0.001176	0.000588	12.88	24.84

% of SiC	2	0.000267	0.000133	2.92	5.64
Error	18	0.000821	0.000046		
Total	26	0.004733			

Table 15. ANOVA for CF for Al 6063-SiC

Source	DF	SS	MS	F-value	Pr (%)
Speed	2	0.001908	0.000954	29.45	52.33
Feed	2	0.000157	0.000078	2.42	4.30
D.O.C	2	0.000869	0.000434	13.41	23.83
% of SiC	2	0.000130	0.000065	2.00	3.56
Error	18	0.000583	0.000032		
Total	26	0.003646			

4.3 REGRESSION ANALYSIS

A correlation between machining process parameters and machining criteria for machining of Al MMC's are obtained by multiple linear regressions. MINITAB software package is used to develop these relations or models.

4.3.1 REGRESSION ANALYSIS FOR MMR

Equation below is for Al 6061-SiC

$$\text{MMR} = -66259 + 73.1 (\text{SPEED}) + 26013 (\text{FEED}) + 45599 (\text{D.O.C}) - 367 (\% \text{ OF SiC}) \quad (7)$$

Equation below is for Al 6063-SiC

$$\text{MMR} = -66717 + 74.5 (\text{SPEED}) + 26389 (\text{FEED}) + 46423 (\text{D.O.C}) - 461 (\% \text{ OF SiC}) \quad (8)$$

4.3.2 REGRESSION ANALYSIS FOR CF

Equation below is for Al 6061-SiC

$$CF = 0.03676 - 0.00045 (\text{SPEED}) + 0.00284 (\text{FEED}) + 0.01902 (\text{D.O.C}) + 0.000380 (\% \text{ OF SiC}) \quad (9)$$

Equation below is for Al 6063-SiC

$$CF = 0.03687 - 0.000042 (\text{SPEED}) + 0.00260 (\text{FEED}) + 0.01710 (\text{D.O.C}) + 0.000268 (\% \text{ OF SiC}) \quad (10)$$

Table 16. Optimum sequence for MMR in Al 6061-SiC

Speed	Feed	D.O.C	% of SiC	MMR
775	2.85	1.2	10	139946

Table 17. Optimum sequence for MMR in Al 6063-SiC

Speed	Feed	D.O.C	% of SiC	MMR
775	2.85	1.2	10	139970

Table 18. Optimum sequence for CF in Al 6061-SiC

Speed	Feed	D.O.C	% of SiC	CF
775	2.85	0.4	20	0.0175

Table 19. Optimum sequence for CF in Al 6063-SiC

Speed	Feed	D.O.C	% of SiC	CF
775	0.71	0.4	20	0.01692

5. COMPARING AL 6061 SiC AND AL 6063

Table 20. Compositions of elements in Al 6061 & Al 6063

Composite	6061	6063
Fe	0.70	0.35
Mn	0.15	0.10
Zn	0.25	0.10
Ti	0.15	0.10
Si	0.70	0.50
Cu	0.40	0.10
Mg	0.80	0.50
Cr	0.15	0.15
Al	remainder	remainder

- Elements present in Al 6061-SiC and Al 6063-SiC is as described above.
- Comparison between Al MMC's is done according to the results obtained in analysis of experiments in this study.

- In analysis of SN ratios for MMR, Tables 4 & 6 shows the ranks allotted to the parameters according to their significant effect. A much alike similarity is observed in between them.
- Chart 2 & 4 shows the behavior of MMR with respect to process parameters selected and it confirms that major similarity occurs between them.
- In analysis of SN ratio for CF, Tables 8 & 10 shows the ranks of parameters. It shows some what difference in the ranks comparing between them, but speed remaining the major factor to affect the CF.
- Chart 6 & 8 shows the behavior of CF with respect to process parameters, a slight difference occurs between them.
- In analysis of variance for MMR, from Tables 12 & 13 same parameters from both MMC's have same impact with some negotiable difference. Here feed is the major parameter which has most impact on MMR.
- In analysis of variance for CF, from Tables 14 & 15 same parameter from each side shows same impact, with some negotiable difference. Here speed is the major parameter which has most impact on CF.

6. SCOPE OF FUTURE WORK

- Same analysis can be done for other materials like steel, brass, copper etc.
- We can use other process parameters for MMR and CF.
- Study can be performed on milling, drilling, grinding and other metal removal processes.
- Cutting fluids and other lubricants are not used in this process, so these can be employed for improvements.

7. CONCLUSION

This study shows the usage of parameter design in optimization of metal removal rate and cutting force of Al MMC's in Turning and its application led to opt optimal values. To obtain accurate study, L27 orthogonal array is used in Taguchi method and ANOVA. ANOVA is used to know the accurate contribution of each factor and their percentage in operation. Study shows Taguchi method and ANOVA has same result in Al MMC's machining with minor difference. Spindle speed is the parameter with 48.51% and 52.31% in Al 6061-SiC and Al 6063-SiC respectively which affects the CF and stood first in rank in Taguchi method. Feed is the parameter with 49.10% and 48.75% in Al 6061-SiC and Al 6063-SiC respectively which affects the MMR and stood first in rank in Taguchi method. Optimal sequence in selected design for MMR and CF is found. Experiments shows that comparison of both Al MMC's based on MMR and CF has mere difference and it proved that they can be used at common machining parameters. Taguchi can be used for analyzing similar problems as of this study. Parameter design obtained is simple and it proved that it is an efficient methodology for optimizing process parameters.

NOMENCLATURE

s= Spindle speed, rpm
f= Feed, mm
d= Depth of cut, mm
 D_{avg} = Average diameter, mm
 D_i = Initial diameter, mm
 D_f = Final diameter, mm
MMR= Metal removal rate, mm/min
CF= Cutting force, N
S/N or SN ratio= Signal to Noise ratio

ACKNOWLEDGMENT

We express our sincere gratitude to Dr. A. Raveendra, Professor and Head of the Department of Mechanical Engineering, MREC, for his helpfulness and motivation.

We are also thankful to all the staff and my friends who made our work to be done with more ease.

REFERENCES

- [1] Das, S.R., Nayak R.P., & Dhupa, D. (December 2012). *International Journal of Lean Thinking*, 3(2).
- [2] Mahendra K., & Neeraj A. (October 2012). Optimization of different machining parameters of En 24 alloy steel in CNC turning by use of Taguchi method. *International Journal of Engineering Research and Application*, 2(5), 160-164.
- [3] Yang, W. H. and Tarng, Y. S. 1998. Design optimization of cutting parameters for turning operations based on the Taguchi method. *Journal of Materials Processing Technology*, 84: 122-129.
- [4] J. Sateesh et al. 2003 Optimal Machining Conditions For Turning Of Al SiC Metal Matrix Composites Using ANOVA.
- [5] Md. Maksudul Islam et al. 2012 Optimization of Metal Removal Rate for ASTM A48 Grey Cast Iron using Taguchi Method.
- [6] S. R. Rao and G. Padmanabha. 2014 Optimization of Machining Parameters in ECM of Al/B4C Composites Using Taguchi Method.
- [7] Senthilkumar, et al. 2009. Study of electrochemical machining characteristics of Al/SiCp composites. *International Journal of Advanced Manufacturing Technology*.
- [8] Fortana, M. G. 1986. "Corrosion Engineering". McGraw-Hill, New York
- [9] M. Ramulu, P. N. Rao, H. Kao, Drilling of Al2O3 p/6061 metal matrix composites, *Journal of Materials Processing Technology*, 124(2002)
- [10] Ravinder Kumar, Ramakant Rana, Surabhi Lata, Rahul kumar Sonkar, Abhinav Kumar, Shekhar Pawar, Roop Lal. 2015.

Optimization of process parameters on Over-Cut in drilling of Al-B4C MMC.

[11] Patnaik, S.S.M.A., & Prabina K. P., (2006). Parametric analysis and optimization of cutting parameters for turning operations based on Taguchi method. *Proceedings of the International Conference on Global Manufacturing and Innovation*, (pp. 1-8).

[12] M.M. Schwartz. 1997. *Composite Materials: Processing, Fabrication, and Applications*. Prentice-Hall, Englewood Cliffs, NJ.

EXPERIMENTAL INVESTIGATION TO DETERMINE INFLUENCE OF PROCESS PARAMETERS ON SURFACE QUALITY AND MRR IN WIRE CUT EDM

¹UNGARALA SOMASEKHAR, ²M V VARALAKSHMI

¹M.Tech Department of Mechanical, Mallareddy Engineering College Maisammaguda ,Hyderabad, T.S, India.

²Associate Professor, Department of Mechanical, Mallareddy Engineering College Maisammaguda, Hyderabad, T.S, India.

Abstract - The objective of the present work is to investigate the effects of the various Wirecut EDM process parameters on the surface quality, maximum material removal rates and obtain the optimal sets of process parameters so that the quality and MRR of machined parts can be optimized. Experiments will be conducted on the pieces by parameters. The material used for machining is Aluminum alloy and the process parameters varied are Pulse Time on 110µsec, 109µsec, 108 µsec, Pulse Time off 60µsec, 61µsec, 61µsec and Peak Current 180Amps, 170Amps, 160Amps. Wire Feed, ServoVoltage and Wire Tension are kept constant. The optimization is done by using Taguchi technique by considering L9 orthogonal array. Optimization is done using Minitab software.

I. INTRODUCTION TO WIRE-CUT EDM

The wire-cut type of machine arose in the 1960s for the purpose of making tools (dies) from hardened steel. The tool electrode in wire EDM is simply a wire. To avoid the erosion of material from the wire causing it to break, the wire is wound between two spools so that the active part of the wire is constantly changing. Electrical discharge machining is a machining method primarily used for hard metals or those that would be very difficult to machine with traditional techniques. EDM typically works with materials that are electrically conductive, although methods for machining insulating ceramics with EDM have also been proposed. EDM can cut intricate contours or cavities in pre-hardened steel without the need for heat treatment to soften and re-harden them. This method can be used with any other metal or metal alloy such as titanium, hastelloy, kovar, and inconel. Also, applications of this process to shape polycrystalline diamond tools have been reported.

II. LITERATURE SURVEY

In the paper by S V Subrahmanyam, et al^[1], the optimization of Wire Electrical Discharge Machining process parameters for the machining of H13 HOT DIE STEEL, with multiple responses Material Removal Rate (MRR), surface roughness (Ra) based on the Grey-Taguchi Method. Taguchi'S127(21x38) Orthogonal Array was used to conduct experiments, which correspond to randomly chosen different combinations of process parameter setting, with eight process parameters: TON, TOFF, IP, SV WF, WT, SF, WP each to be varied in three different levels. Data related to the each response viz. material removal rate (MRR), surface roughness (Ra) have been measured for each experimental run; With Grey Relational Analysis Optimal levels of process parameters were identified. In the paper by Atul

Kumar, et al^[2], variation of cutting performance with pulse on time, pulse off time, open voltage, feed rate override, wire feed, servo voltage, wire tension and flushing pressure were experimentally investigated in wire electric discharge machining (WEDM) process. Brass wire with 0.25mm diameter and Skd 61 alloy steel with 10mm thickness were used as tool and work materials in the experiments. The cutting performance outputs considered in this study were material removal rate (MRR) and surface roughness. Experimentation has been completed by using Taguchi L18 (21 different conditions of parameters).

III. EXPERIMENTAL SETUP AND PROCEDURE

Experiments have been performed in order to investigate the effects of one or more factors of the process parameters on the surface finish of the wire cut machined surface of Aluminum material. The main aim of the project is to determine the influence of time on, time off, wire feed and input power. The investigation is based on surface roughness during machining of Aluminum material.

EXPERIMENTAL PROCEDURE

The selected work piece materials for this research work are Aluminum alloy material. Experiments have been conducted on wire cut edm. The machine details are:



Fig 1: Wire cut CNC

An electrolytic brass (Zinc coated) wire with a diameter of 2mm has been used as a tool electrode (positive polarity) and work piece materials used are Aluminum alloy and Copper materials rectangular plates of dimensions 80×30 mm and of thickness 6 mm.

IV. PROCESS PARAMETERS AND DESIGN

Input process parameters such as Pulse Ontime (TON), Pulse Offtime (TOFF), Peak Current (Amp), used in this thesis are shown in Table. Each factor is investigated at three levels to determine the optimum settings for the WEDM process. All other parameters such as Wire Tension is 4Kgf, Servo Feed is 20V, Servo Feed 2100 are kept constant. The selection of parameters for experimentation is done as per Taguchi design. An orthogonal array for three controllable parameters is used to construct the matrix of three levels of controllable factors. The L9 orthogonal array contains 9 experimental runs at various combinations of three input variables.

The L9 orthogonal array for input parameters Pulse on time, pulse off time and peak current is shown in table below:

Table 1: L9 parameters

TRAIL	A	B	C
1	108	60	160
2	108	61	170
3	108	62	180
4	109	60	170
5	109	61	180
6	109	62	160
7	110	60	180
8	110	61	170
9	110	62	160

V. OBSERVATION

The following are the surface roughness observations made by testing using Surface Roughness Measurement Tester, Model No: SJ-210, Mitutoyo. Surface Roughness Values with no. of trials

Table 2: L9 parameters and Surface Roughness Results

Trail	Pulse Time On (μsec)	Pulse Time Off (μsec)	Peak Current (Amps)	Surface Finish Values R_a μm
1	108	60	160	2.214
2	108	61	170	3.359
3	108	62	180	3.987
4	109	60	170	3.881
5	109	61	180	2.632
6	109	62	160	3.218
7	110	60	180	3.98
8	110	61	170	3.89
9	110	62	160	3.775

a) Material Removal Rates Results

Material Removal Rate Calculations

$$MRR = \frac{W_1 - W_2}{\rho * t}$$

W_1 = Weight before machining (gms)

W_2 = Weight after machining (gms)

ρ = Density (gm/mm³)

t = Time in min

Table 2: L9 parameters and MRR Results

Trail	Pulse Time On (μsec)	Pulse Time Off (μsec)	Peak Current (Amps)	MRR (mm ³ /sec)
1	108	60	160	0.5515
2	108	61	170	1.8347
3	108	62	180	1.8614
4	109	60	170	2.1414
5	109	61	180	0.6818
6	109	62	160	3.3333
7	110	60	180	3.7515
8	110	61	170	4.5586
9	110	62	160	0.6303

MRR Results Table

b) Selection of Optimal Parameter Combination For Better Surface Quality In Wire Cut EDM Using Taguchi Technique

RESULTS

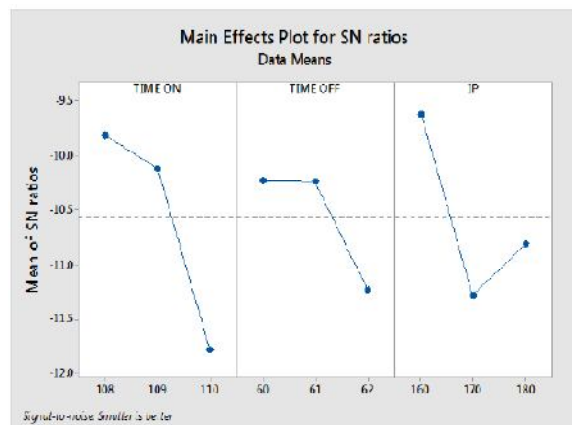


Fig.2. Effect of parameters surface roughness for S/N ratio

Taguchi method stresses the importance of studying the response variation using the signal-to-noise (S/N) ratio, resulting in minimization of quality characteristic variation due to uncontrollable parameter. The surface roughness is considered as the quality characteristic with the concept of "the smaller-the-better". The S/N ratio for the smaller-the-better is:

$$S/N = -10 * \log(\Sigma(Y^2)/n)$$

Where n is the number of measurements in a trial/row, in this case, n=1 and y is the measured

value in a run/row. The S/N ratio values are calculated by taking into consideration above Eqn. with the help of software Minitab 17.

The surface roughness measured from the experiments and their corresponding S/N ratio values are listed in Table

Table3. S/N Ratio Results

Worksheet 1 ***					
↓	C1	C2	C3	C4	C5
	TIME ON	TIME OFF	IP	SURFACE ROUGHNESS	SNRA1
1	108	60	160	2.214	-6.9036
2	108	61	170	3.359	-10.5242
3	108	62	180	3.987	-12.0129
4	109	60	170	3.881	-11.7789
5	109	61	180	2.632	-8.4057
6	109	62	160	3.218	-10.1517
7	110	60	180	3.980	-11.9977
8	110	61	160	3.890	-11.7990
9	110	62	170	3.775	-11.5383

Pulse Time On:-The effect of parameter “pulse time on” on surface roughness values is shown above figure for S/N ratio. The optimum pulse time on is 108µsec.

Pulse Time Off:-The effect of parameter “pulse time off” on surface roughness values is shown above figure for S/N ratio. The optimum pulse time off is 60µsec.

Peak Current:-The effect of parameter “Peak Current” on surface roughness values is shown above figure for S/N ratio. The optimum Peak Current is 160Amps.

c) Selection Of Optimal Parameter Combination For Better MRR In Wire Cut EDM Using Taguchi Technique

RESULTS

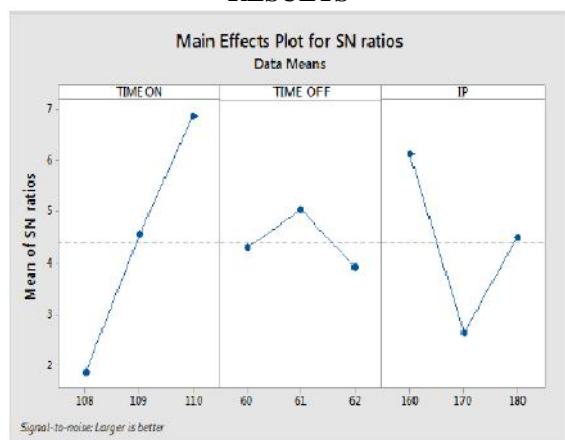


Fig.3. Effect of parameters on MRR for S/N ratio

The MRR measured from the experiments and their corresponding S/N ratio values are listed in Table

Table4. S/N Ratio Results

Worksheet 1 ***					
↓	C1	C2	C3	C4	C5
	TIME ON	TIME OFF	IP	MRR	SNRA2
1	108	60	160	0.5515	-5.1691
2	108	61	170	1.8347	5.2713
3	108	62	180	1.8614	5.3968
4	109	60	170	2.1414	6.6140
5	109	61	180	0.6818	-3.3269
6	109	62	160	3.3333	10.4575
7	110	60	180	3.7515	11.4841
8	110	61	160	4.5586	13.1766
9	110	62	170	0.6303	-4.0091

Pulse Time On - The effect of parameter “pulse time on” on MRR is shown above figure for S/N ratio. The optimum pulse time on is 110µsec.

Pulse Time Off- The effect of parameter “pulse time off” on MRR is shown above figure for S/N ratio. The optimum pulse time off is 61µsec.

Peak Current - The effect of parameter “Peak Current” on MRR is shown above figure for S/N ratio. The optimum Peak Current is 160Amps.

CONCLUSION

By observing the experimental results and by optimizing the parameters using Taguchi Method, the following conclusions can be made:

- To get better surface finish the optimized parameters are pulse time on - 108µsec, pulse time off is 60µsec and Peak current is 160Amps.
- To get high MRR the optimized parameters are pulse time on - 110µsec, pulse time off is 61µsec and Peak current is 160Amps.

REFERENCES

- [1] Evaluation of Optimal Parameters for machining with Wire cut EDM Using Grey-Taguchi Method by S V Subrahmanyam, M. M. M. Sarcar
- [2] Performance Analysis of Wire Electric Discharge Machining (W-EDM) by Atul Kumar, DR.D.K.Singh
- [3] Analysis of Process Parameters in Wire EDM with Stainless Steel Using Single Objective Taguchi Method and Multi Objective Grey Relational Grade by M. Durairaja, D. Sudharsunb, N. Swamynathan
- [4] Optimization of process parameters of micro wire EDM by Ricky Agarwal
- [5] A Study to Achieve a Fine Surface Finish in Wire-EDM by J.T. Huang, Y.S. Liao and Y.H. Chen
- [6] Rajurkar K.P., Scott D, Boyina S., “Analysis and Optimization of Parameter Combination in Wire Electrical Discharge Machining”, International Journal of Production Research, Vol. 29, No. 11, 1991, PP 2189- 2207.
- [7] Y. S. Tarng., Ma S.C., Chung L.K., “Determination of Optimal Cutting Parameters in Wire Electrical Discharge Machining”, International Journal of Machine Tools and Manufacture, Vol. 35, No. 12, 1995, PP. 1693-1701.
- [8] J.Prohaszka, A.G. Mamalis and N.M.Vaxevanidis, “The effect of electrode material on machinability in wire electro-discharge machining”, Journal of Materials Processing technology, 69, 1997, PP 233-237.
- [9] (A) Y.S. Liao, Y.Y. Chu and M.T. Yan, Study of wire breaking process and monitoring of WEDM, International Journal of Machine Tools & Manufacture, 37 (1997) pp. 555-567. (B) Y.S. Liao , J.T.Huang, A study on the machining parameter optimization of WEDM, Journal of Material Processing Technology,71(1997) pp. 487-493
- [10] Jose Marafona, Catherine Wykes., “A new method of optimizing MRR using EDM with Copper-tungsten electrodes”. International journal of Machine tools and manufacturing. Vol. 40, 22 June 1999, PP 153-164.



DESIGN AND OPTIMIZATION OF FIXTURES TO MINIMIZING MANUFACTURING FAILURES OF TURBINE BLADE: A FINITE ELEMENT APPROACH

VENNA SWATHI

Mtech (Machine Design)
Mallareddy Engineering College
(Autonomous)
Email: vennaswathi360@gmail.com

M.V. VARALAXMI

Associate Professor
Mallareddy Engineering College
(Autonomous)
Email: varalu_sree@yahoo.co.in

ABSTRACT:

Many of the parts require sophisticated fixture in order to be machined. A variety of CNC machine brands all of which have differently designed tables. They needed a way of sharing the clamping systems with all of the machines. After reviewing the fixtures and machines, we designed, and tested a clamping system to minimise the manufacturing defects obtained in turbine blade machining. Gas turbine rotor blade of stage 3 taken in to consideration for machining mistakes to develop an alternative fixture. The fixture design based on the practical considerations taken from the manufacturing industry to show the solution of minimising optimal values of the blade formation as per the requirement. The design carried out by using Uni-Graphics NX8.0 software. The assembly of the fixture taken to finite element approach to get the comparison of present using fixture to modified fixture. Ansys 15.0 workbench used to simulate fixture load conditions and the material boundary conditions taken from the practical loads applied.

Keyword: M/c design applicability on fixtures, turbine blades, fixture design, manufacturing techniques, FE approach.

INTRODUCTION

Fixtures: Being used in machine shop, are strong and rigid mechanical devices which enable easy, quick and consistently accurate locating, supporting and clamping, blanks against cutting tool(s) and result faster and accurate machining

with consistent quality, functional ability and interchange ability.

Jig: is a fixture with an additional feature of tool guidance.

Purpose of Using Fixtures and Jigs: The fixture is a special tool for holding a work piece in proper position during manufacturing operation. For supporting and clamping the work piece, device is provided. Frequent checking, positioning, individual marking and non-uniform quality in manufacturing process is eliminated by fixture. This increase productivity and reduce operation time. Fixture is widely used in the Industry practical production because of feature and advantages.

Problem statement for present project:

To initiate the fixture-design process, clearly state the problem to be solved or needs to be met. State these requirements as broadly as possible, but specifically enough to define the scope of the design project.

Important considerations while designing fixtures: Designing of jigs and fixtures depends upon so many factors. These factors are analyzed to get design inputs for jigs and fixtures. The list of such factors is mentioned below:

- a. Study of work piece and finished component size and geometry.



- b. Type and capacity of the machine, its extent of automation.
- c. Provision of locating devices in the machine.
- d. Available clamping arrangements in the machine.
- e. Available indexing devices, their accuracy.
- f. Evaluation of variability in the performance results of the machine.
- g. Rigidity and of the machine tool under consideration.
- h. Study of ejecting devices, safety devices, etc.
- i. Required level of the accuracy in the work and quality to be produced.

Introduction to design of fixtures: While designing for clamping the following factors essentially need to be considered:

- 1. Clamping need to be strong and rigid enough to hold the blank firmly during machining.
- 2. Clamping should be easy, quick and consistently adequate
- 3. Clamping should be such that it is not affected by vibration, chatter or heavy pressure
- 4. The way of clamping and unclamping should not hinder loading and unloading the blank in the jig or fixture.
- 5. The clamp and clamping force must not damage or deform the work piece.
- 6. Clamping operation should be very simple and quick acting when the jig or fixture is to be used more frequently and for large volume of work.
- 7. Clamps, which move by slide or slip or tend to do so during

applying clamping forces, should be avoided.

- 8. Clamping system should comprise of less number of parts for ease of design, operation and maintenance.
- 9. The wearing parts should be hard or hardened and also be easily replaceable.
- 10. Clamping force should act on heavy part(s) and against supporting and locating surfaces.
- 11. Clamping force should be away from the machining thrust forces.
- 12. Clamping method should be fool proof and safe.
- 13. Clamping must be reliable but also inexpensive.

OBJECTIVES:

- (1) Turbine blades manufacturing defects.
- (2) Clamping system for Fourth axis Rotary.
- (3) Blade fixing system.
- (4) Fourth axis clamping system.
- (5) Special purpose fixture for blade machining operations.
- (6) Study of market requirements for the present application.
- (7) Comparative study on both clamping system with motion analysis

Specifications for present project:

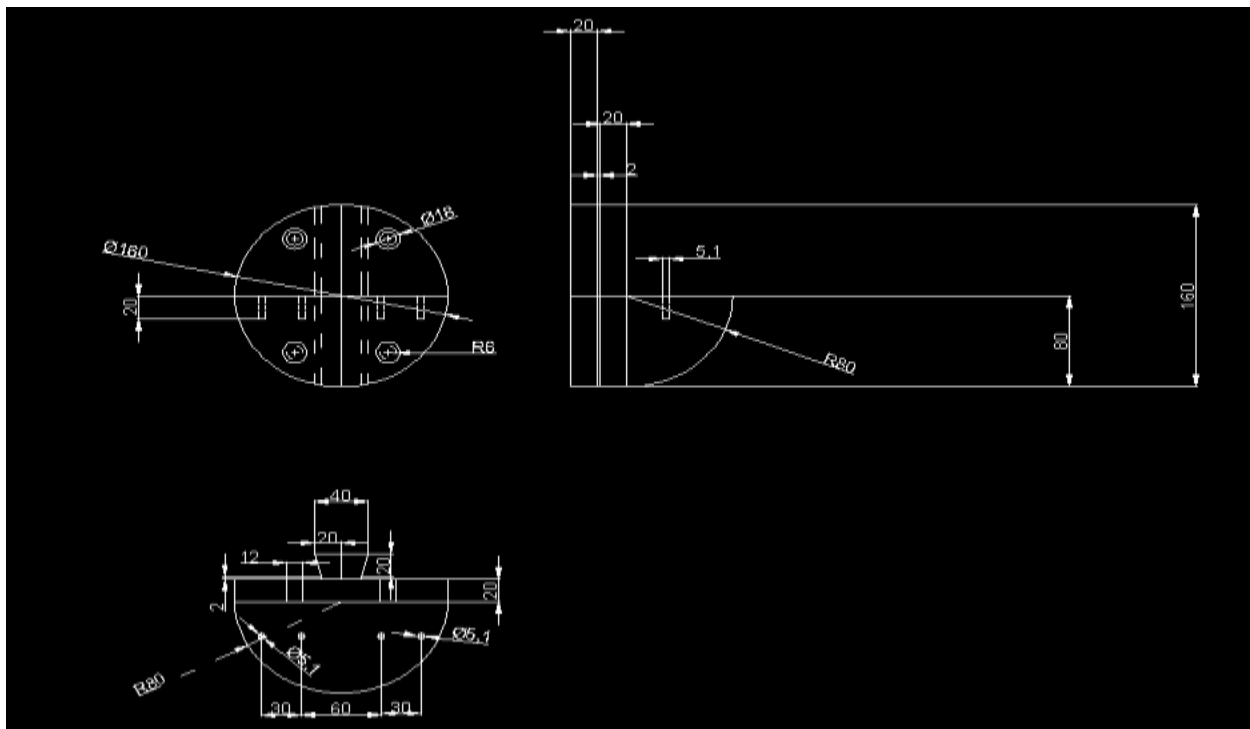
- (1) The indexing chuck to chuck distance =450mm
- (2) Bed length in CNC VMC bmv45 =600 -850mm
- (3) Indexing chuck Diameter (ID - 150mm)
- (4) In case of flat Fixture the Side plates dimensions =80x80

- (5) No of Tap holes 16 no's of M12
Tap –on both plates
- (6) These side plates size is less than
the job so that it can clamp rigidly.
- (7) side plates Thickness = 30mm
- (8) Overall chuck dia in O.D=350mm

Failure considerations in manufacturing of blade

1. Machining paths adjustment in cam programming
2. Tool safety considerations while machining.
3. Tool marks and blade finishing.
4. Quality check of blade profiles at different sections.
5. Blade accuracy levels after machining.

DESIGN ANALYSIS

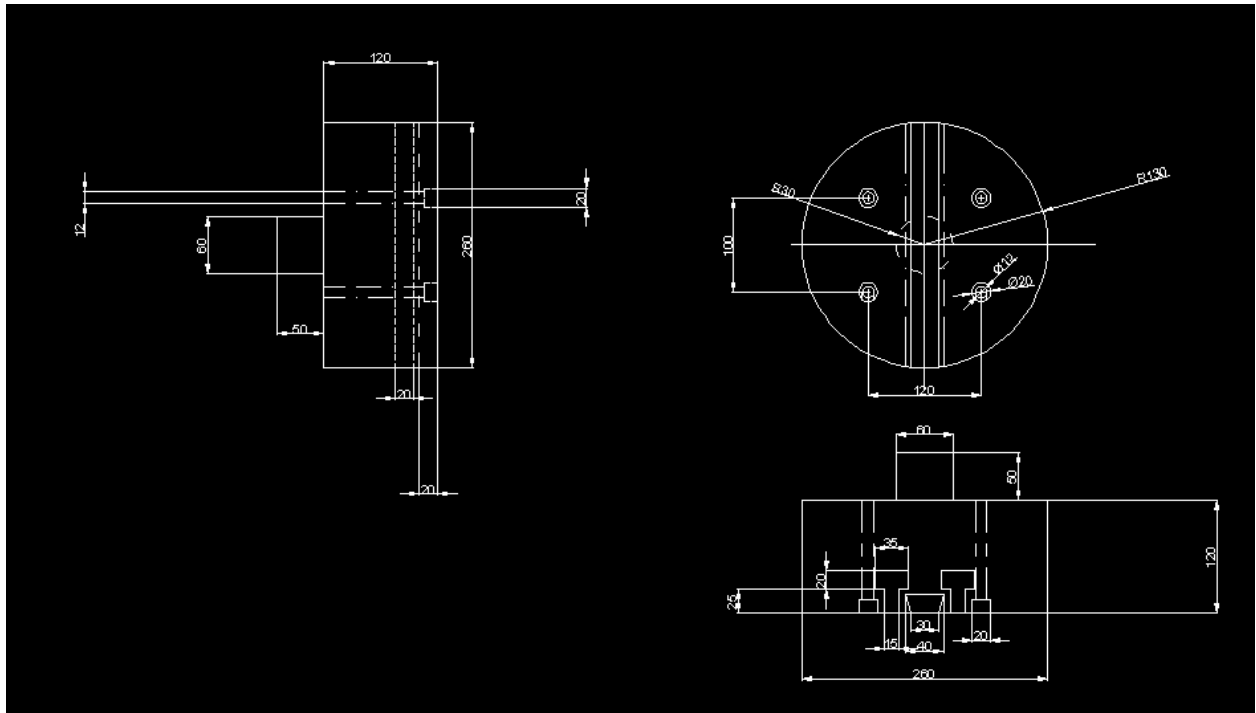


Insert preparation in AutoCAD for 2nd side modified fixture

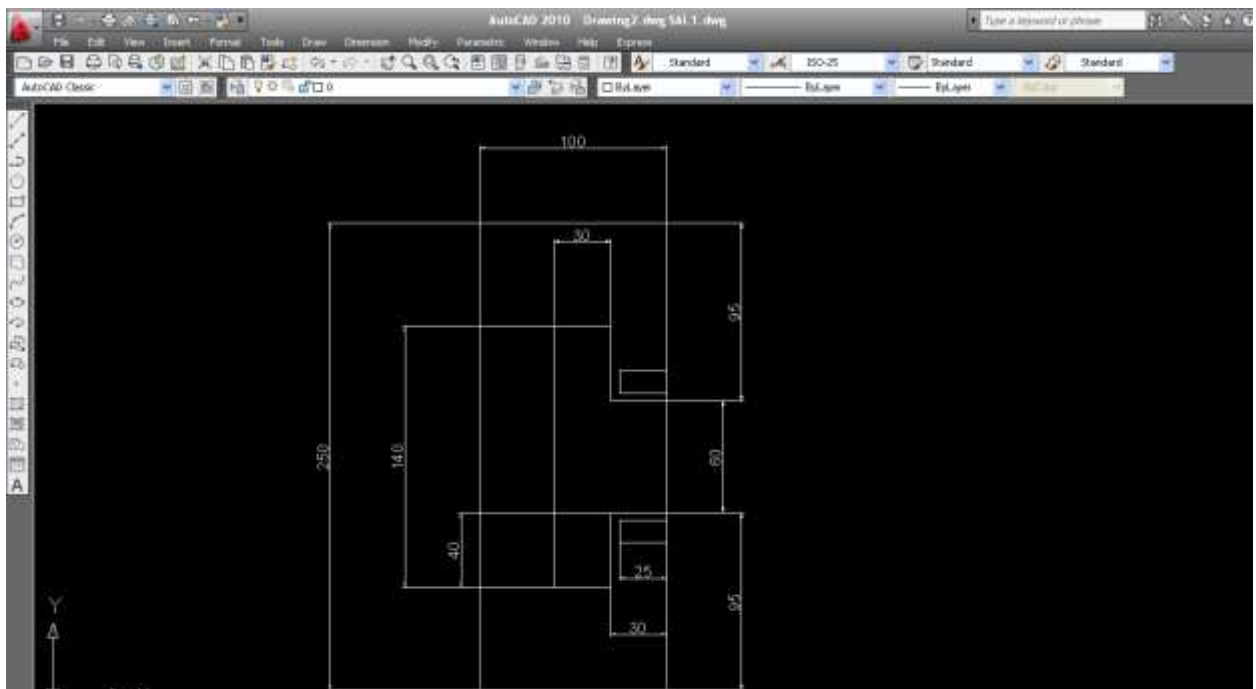
Introduction to CAD

Computer-aided design (CAD) is the use of computer systems to assist in the creation, modification, analysis, or optimization of a design. CAD software is used to increase the productivity of the designer, improve the quality of design, improve communications through documentation, and to create a database for manufacturing. CAD output is often in the form of electronic files for print, machining, or other manufacturing operations.

Auto CAD design Layouts



Fixing insert f second side modified



Fixture base on second side modified

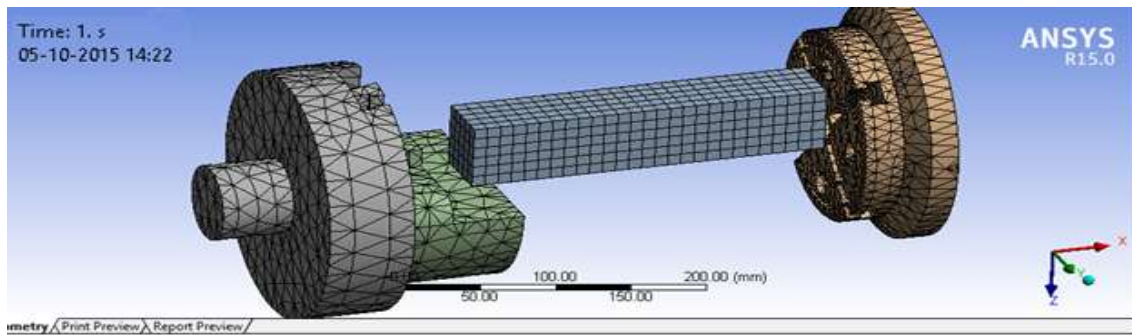
FINITE ELEMENT ANALYSIS

In finite element analysis of fixture stiffness, the main task is to describe the fixture unit stiffness by using a numerical method. In this chapter, a finite element model of fixture unit stiffness is developed. A contact element is utilized to solve the contact problems encountered in the study of fixture unit stiffness analysis. Due to the contact conditions, the status of contact elements may change, and contact stiffness is not constant in the analysis of

process. In the FEA model, the contact and friction conditions will be represented mathematically and discussed in detail. The finite element model and the analysis procedure are validated by case study.

FEA Formulation Consider a general fixture unit with two components I and J. For multi-component fixture units, the model can be expanded. The fixture unit is discretized into finite element models using a standard procedure, except for the contact surfaces, where each nodes on the finite element mesh for the contact surface is modeled by a pair of nodes at the same location belonging to components I and J, respectively, which are connected by a set of contact elements. The basic assumptions include that material is homogenous and linearly elastic, displacements and strains are small in both components I and J, and the frictional force acting on the contact surface follows the Coulomb law of friction.

MESHING OF PRESENT PROJECT:

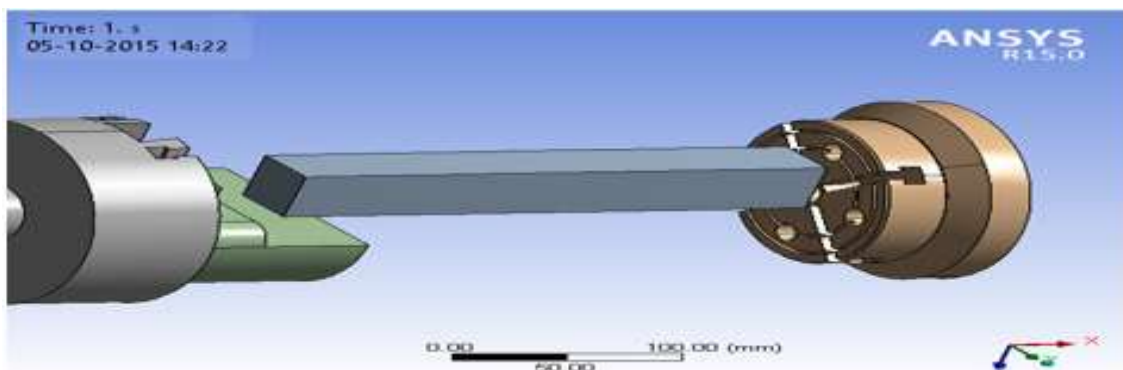


Material Data - Structural Steel

Density	7.85e-006 kg mm ⁻³
Coefficient of Thermal Expansion	1.2e-005 C ⁻¹
Specific Heat	4.34e+005 mJ kg ⁻¹ C ⁻¹
Thermal Conductivity	6.05e-002 W mm ⁻¹ C ⁻¹
Resistivity	1.7e-004 ohm mm

RESULTS & DISCUSSIONS

Static Structural



Frictionless Support2

TABLE: Structural Steel > Constants



Density	7.85e-006 kg mm ⁻³
Coefficient of Thermal Expansion	1.2e-005 C ⁻¹
Specific Heat	4.34e+005 mJ kg ⁻¹ C ⁻¹
Thermal Conductivity	6.05e-002 W mm ⁻¹ C ⁻¹
Resistivity	1.7e-004 ohm mm

TABLE : Structural Steel > Compressive Ultimate Strength

Compressive Ultimate Strength MPa
0

TABLE: Structural Steel > Compressive Yield Strength

Compressive Yield Strength MPa
250

TABLE: Structural Steel > Tensile Yield Strength

Tensile Yield Strength MPa
250

TABLE : Structural Steel > Tensile Ultimate Strength

Tensile Ultimate Strength MPa
460

TABLE : Structural Steel > Isotropic Secant Coefficient of Thermal Expansion

Reference Temperature C
22

TABLE : Structural Steel > Alternating Stress Mean Stress

Alternating Stress MPa	Cycles	Mean Stress MPa
3999	10	0
2827	20	0
1896	50	0
1413	100	0
1069	200	0
441	2000	0
262	10000	0
214	20000	0
138	1.e+005	0
114	2.e+005	0
86.2	1.e+006	0

TABLE : Structural Steel > Strain-Life Parameters

Strength Coefficient MPa	Strength Exponent	Ductility Coefficient	Ductility Exponent	Cyclic Strength Coefficient MPa	Cyclic Strain Hardening Exponent
920	-0.106	0.213	-0.47	1000	0.2

TABLE : Structural Steel > Isotropic Elasticity

Temperature C	Young's Modulus MPa	Poisson's Ratio	Bulk Modulus MPa	Shear Modulus MPa
	2.e+005	0.3	1.6667e+005	76923

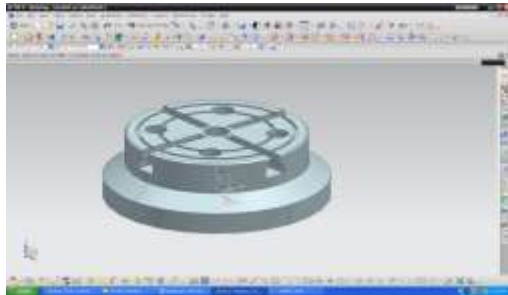
TABLE : Structural Steel > Isotropic Relative Permeability

Relative Permeability
10000

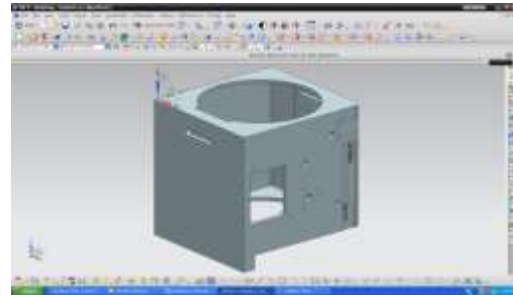
DESIGN CONSIDERATIONS OF BEARING HOUSING:

Housing fixing bore-100mm, bearing size-60mm dia (I.D), supported wall thickness-12mm, Bottom wall thickness-10mm

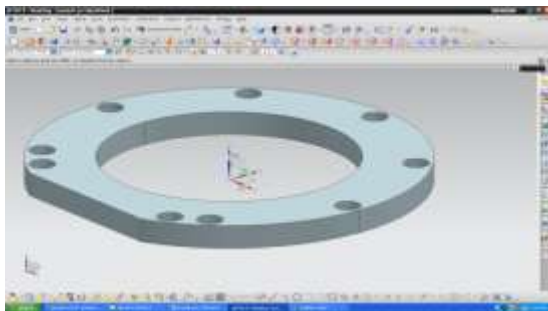
DRAWING OF PROPOSED PROJECT



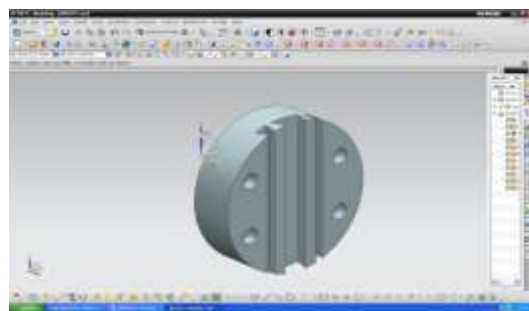
Chuck



Housing



Chuck support ring



fixture plate

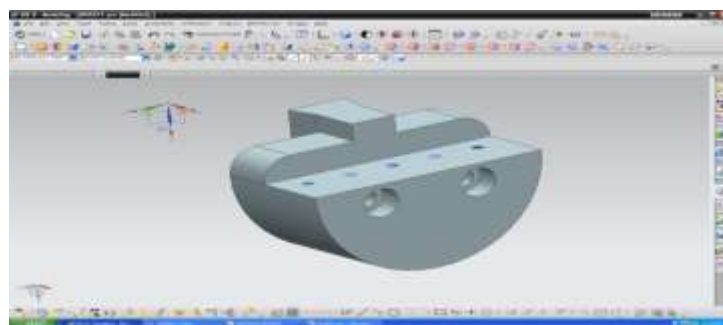
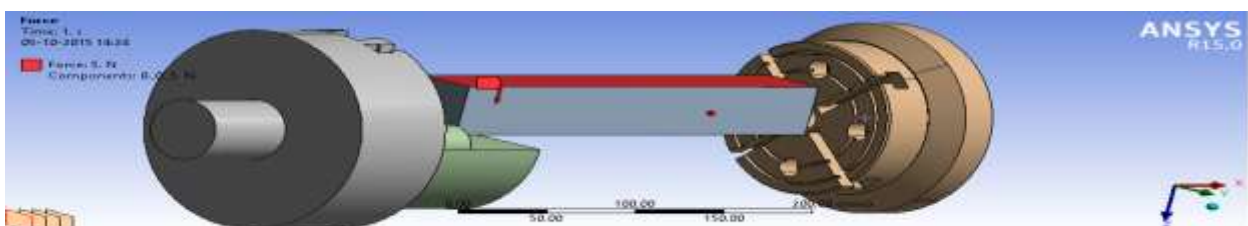
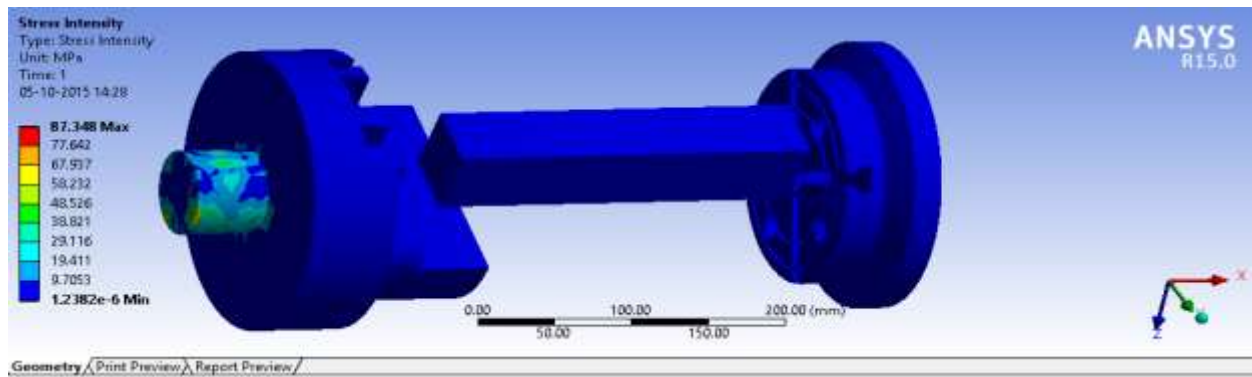


Plate section view

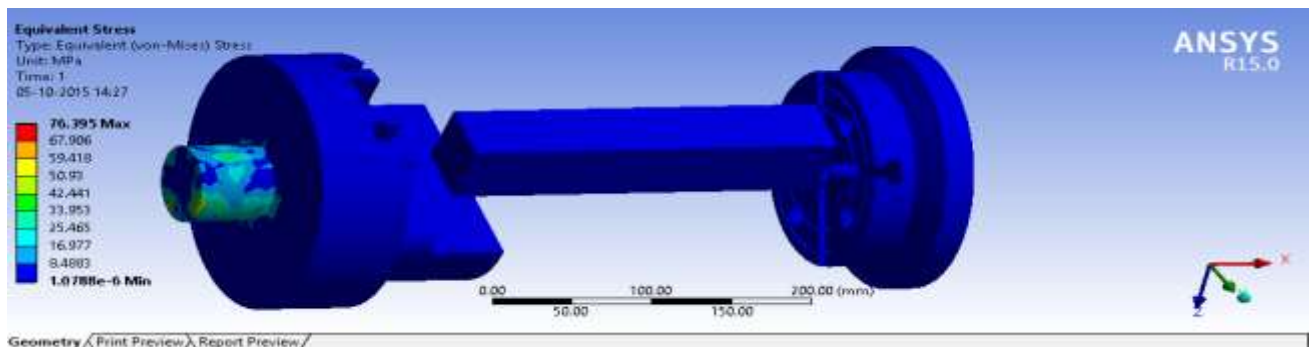
RESULTS & DISCUSSIONS



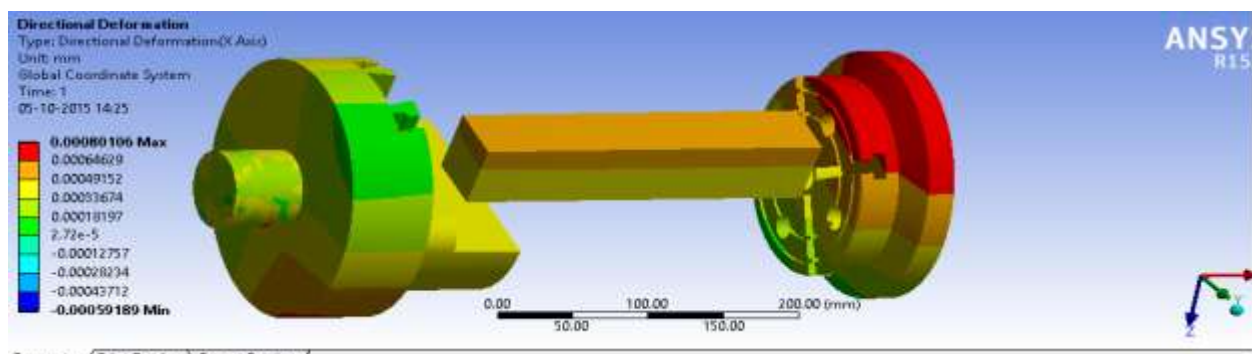
Force



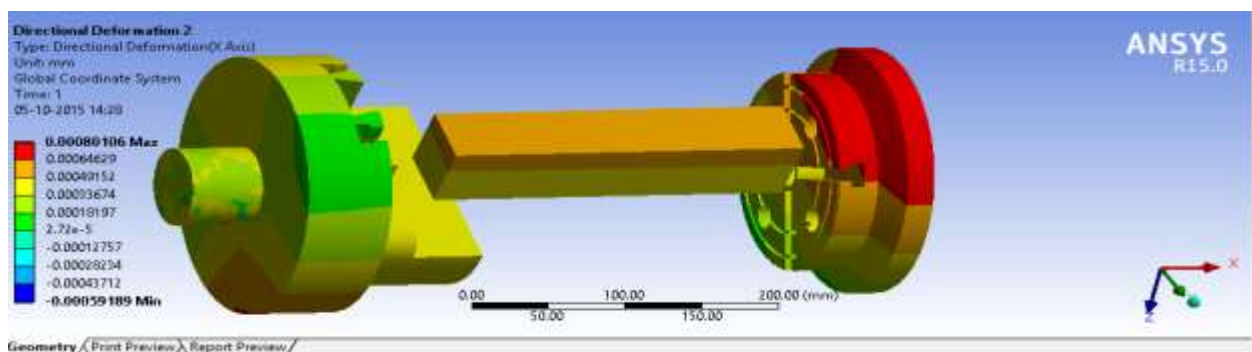
Equivalent Stress



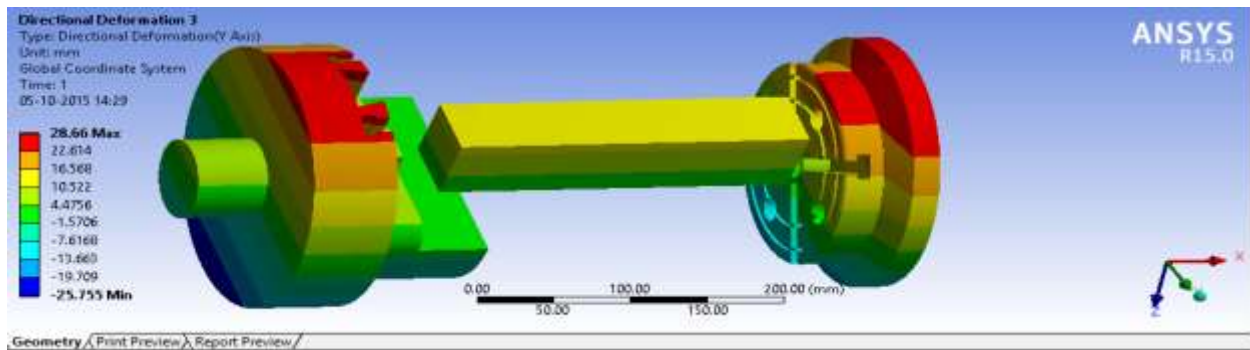
Stress Intensity



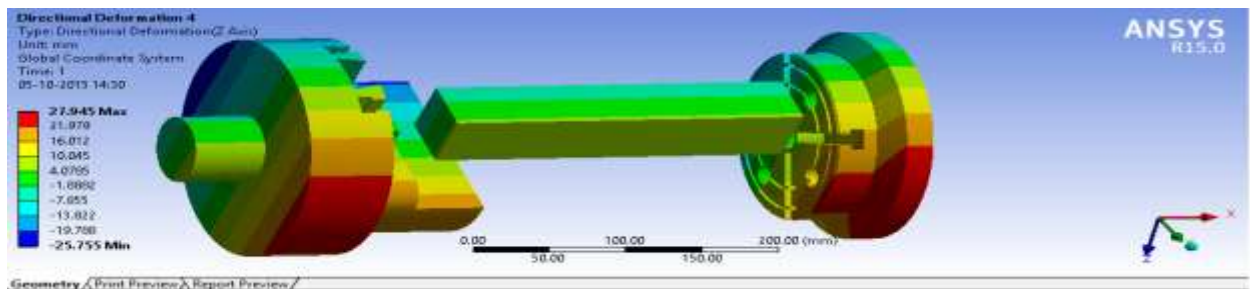
Directional Deformation



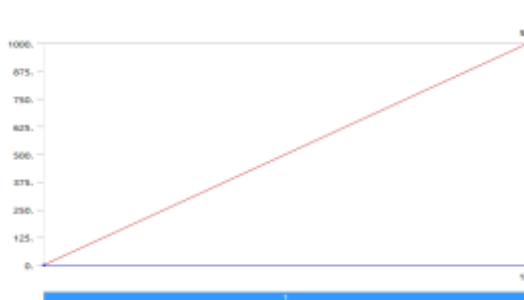
Directional Deformation2



Directional Deformation 3



Directional Deformation 4



Static Structural > Moment



Static Structural (A5) > Force

Static Structural (A5) > Moment 2



CONCLUSIONS:

The efficiency and reliability of the fixture design has enhanced by the system and the result of the fixture design has made more

reasonable. To reduce cycle time required for loading and unloading of part, this approach is useful. If modern CAE, CAD are used in designing the systems then



significant improvement can be assured. To fulfil the multifunctional and high performance fixturing requirements optimum design approach can be used to provide comprehensive analyses and determine an overall optimal design. Fixture layout and dynamic clamping forces optimization method based on optimal fixture layout could minimize the deformation and uniform the deformation most effectively. The proposed fixture will fulfilled researcher production target and enhanced the efficiency, Hydraulic fixture reduces operation time and increases productivity, high quality of operation, reduce accidents. From the study of simulations on fixture there is not so much deflection occurring on the fixture when compared to single stated inserted fixture. The multipurpose use of the present fixture not showing any rotational deflection but with load and forces taken into account it shows a slight deflection comparably negligible as considered for practical approach. This project shows an edge of multipurpose job work can be done without changing number of inserts for each job.

Limitations & Future scope

1. Theoretical simulations only observed in the present project with material and work piece and loads are taken from practical values of work place.
2. Rotational forces can be studied by applying practical rpm of components can be studied.
3. Practical study may given a direct solution to the extension of this work.

4. Limitation of present study can be extended to a materialized practical work and comparison in industry.

REFERENCES:

1. Guohua Qin, Weihong, Zhang Min Wan —Analysis and Optimal Design of Fixture Clamping Sequence ASME for publication in the JOURNAL OF MANUFACTURING SCIENCE AND ENGINEERING, 2006.
2. Michael Stampfer —Automated setup and fixture planning system for box-shaped Parts|| International Journal of Advance Manufacturing Technology 45:540–552 DOI 10.1007/s00170-009-1983-1, 2008.
3. Djordje Vukelic, Uros Zuperl & Janko Hodolic —Complex system for fixture selection, modification, and design|| Int J Adv Manuf Technol 45:731–748 DOI 10.1007/s00170-009-2014-y, 2009
4. Weifang Chen, Lijun Ni & Jianbin Xue —Deformation control through fixture layout design and clamping force optimization|| Int J Adv Manuf Technol 38:860–867 DOI 10.1007/s00170-007-1153-2, 2008
5. J. Cecil —A Clamping Design Approach for Automated Fixture Design|| Int J Adv Manuf Technol 18:784–789, 2008
6. Nicholas Amaral · Joseph J. Rencis · Yiming (Kevin) Rong —Development of a finite element analysis tool for fixture design integrity verification and optimization|| Int J Adv Manuf Technol 25: 409–419, 2005
7. Y. Wang, X. Chen. N, Gindy —Surface error decomposition for fixture development|| Int J Adv Manuf Technol DOI 10.1007/s00170-005-0270-z, 2007

DESIGN AND ANALYSIS OF A PJ15 PULSE JET ENGINE

¹K VISHNU TEJA, ²N SRINIVASA RAJNEESH

DEPARTMENT OF MECHANICAL ENGINEERING

MALLA REDDY ENGINEERING COLLEGE (AUTONOMOUS)

(An Autonomous Institution approved by UGC and affiliated to JNTUH, Approved by AICTE, Accredited by NAAC with 'A' Grade and NBA & Recipient of World Bank Assistance under TEQIP Phase- II S.C.1.1)

Maisammaguda, Dhulapally (Post. Via.Kompally), Secunderabad – 500 100.

ABSTRACT: Pulse jet engines or Pulsejets are family of internal combustion engine that have few or no moving parts. The project design and analysis of pulsejet engine is based on thrust produce in form of pulses. This is a powerful jet unit and one which can be made by anyone with access to lathe and welding facilities with few or no moving parts. The main purpose to design pulse jet engine is to produce high amount of thrust by performing analysis on jet engine. These engines are an efficient and simple way to convert fuel into heat. Pulsejets are used today in target drone aircraft, home heating equipment, fog generation purpose and many more. The reason they are called pulse jets, is due to how they produce intermittent pulses of thrust. The Main Purpose of this project is to design PJ15 pulse Jet Engine and analysis it on different Mass Flow rate at different Pressures. Pulsejets can be fitted with specially shaped ducts called Thrust Augmenters, which increase thrust output by harnessing aerodynamic forces, exhaust gas heat, and providing a reactive surface for

high velocity pulses of exhaust to pull in additional air and transfer momentum to it. The pulse jet body will be designed and analysis will be done using the SOLID WORKS 2014.

INTRODUCTION:

A pulsejet engine (or pulse jet) is a type of jet engine in which combustion occurs in pulses. A

pulsejet engine can be made with fewer no parts and is capable of running statically (i.e. it does not need to have air forced into its inlet typically by forward motion). Pulsejet engines are a lightweight form of jet propulsion, but usually have a poor compression ratio, and hence give a low specific impulse. One notable line of research of pulsejet engines includes the pulse detonation engine which involves repeated detonations in the engine, and which can potentially give high compression and good efficiency.

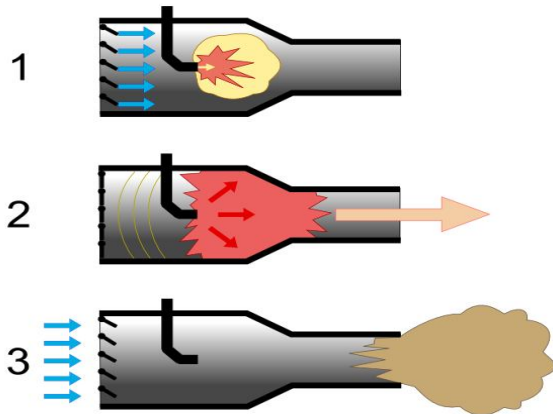


Fig 1.1 PROCESS OF COMBUSTION

1. LITERATURE REVIEW:

Current research status Although in pilot tests and technical reports of pulse combustion dryers, short drying time, high energy efficiency and product quality are generally reported, there are few theoretical studies of the pulse combustion drying process. Liu et al (2001) demonstrated experimentally that the pressure amplitude and the oscillating frequency Literature Review 38 of the unsteady flow, generated by Helmholtz pulse combustor, enhanced the convective heat transfer coefficient. Smucrowicz (1999) carried out research on in-situ analysis of the mechanism of the pulse combustion spray drying process. Smucrowicz (1999) and Wu et al (2002) have conducted CFD modeling of the pulse combustion spray drying process. Experimental and simulation results showed the complex nature of the pulsating flow in

the drying chamber and the very rapid decrease of material moisture content in the intensive drying. Wu et al (2002) have also conducted experiments in which the pulsating gas jet from pulse combustor was used to directly atomize and dry the slurry (a solution of 10 % NaCl).

Impinging jets are encountered in many practical applications because of their high heat and mass transfer rates (Zumbrunmen, et al, 1993; Azevedo, et al, 1994). Flow pulsation can considerably affect the jet expansion, mixing and entrainment. Thus, pulsating jets should have high potential to enhance the heat transfer performance of such flows compared to their steady counterparts. Liewkongsataporn et al (2006b) investigated numerically the effects of jet pulsation amplitude and impingement zone geometry on net heat flux enhancement factors. They found that for pulsating jet impingement, an enhancement on heat transfer can be achieved only in the case, wherein the amplitude ratio of jet velocity oscillation must be great enough so that heat transfer during positive cycle would be able to compensate for lower heat transfer during negative cycle. This is a preliminary result and needs further investigation. Also, in Liewkongsataporn et al' experiments (2006a), the drying rate is evaluated

averagely based on the whole paper sheet; the local drying rate in paper sheet is unknown. Information about the local drying rate contributes to the design of impinging jet dryer where an array of pulse jets is used.

Pulse combustion spouted bed drying of particles is a new concept proposed here. This concept is motivated by the fact that the pressure drop of spout bed is generally about several thousand Pascals, which is in the range of pressure oscillation in pulse combustion flow. Thus, pulse combustion can, in principle, be used in spouted bed drying. There are numerous experimental works on “conventional” spouting bed drying of different materials, such as for grains (Madhiyanon, et al, 2002), dispersed materials (Devahastin, et al, 1998; Berghel, 2005; Wachiraphansakul, 2005), paste-like materials on inert bodies (Kutsakova, 2004), slurries and solutions (Tia, et al, 1995), etc. However, the knowledge of flow characteristics in such contactors is still limited. There are several experimental studies which investigated the particle flow pattern in spouted beds. Yokogawa (1970) measured particle velocities in a half-cylindrical vessel using a high speed video camera. However, the effect of the smooth flat wall on the motion of particles is now known to be non-negligible. Benkrid and

Caram (1989) used a fiber optic technique to measure particle velocities in the annulus of a full column and concluded that there is a plug flow zone in the upper part of the annulus. He et al (1992) observed dead zone boundaries in a 0.91 m diameter column. He et al (1994a and b) used a fiber optic probe system to obtain the profiles for vertical particle velocities in spout, annulus and fountain regions of a full column spouted bed. Roy et al (1994) measured the particle velocities in a spouted bed using a γ -ray emitting particle tracking technique. These experimental results have improved our understanding of the mechanism of spouting^[1].

2. THEORETICAL BACKGROUND:

2.1 Pulse combustion:

Historical development Pulse combustion is not a new concept. Heat-excited acoustic oscillations were first reported by Higgins in 1777, who observed the so-called hydrogen “singing” flames in tubes (Tyndall, 1897). Later, in 1859, Rijke discovered that strong acoustic oscillations appeared when a heated metallic grid was positioned in the lower half of a vertical tube opened at both ends (Lord Rayleigh, 1945). The pulse combustor with mechanical valves was first built by Esnault-Pelterie in

France in 1906 and it was used as a drive for a gas turbine. In 1909, Marconnet constructed the first pulse combustor with an aerodynamic valve for propulsion. Although his basic patent was for a mechanically-valved unit, his design (Figure 2.1) is similar to many aero-valved current units. It consisted of two diffusers: inlet and outlet. The recirculation of fuel and air flows in this configuration resulted in the specific combustion chamber where the combustible mixture was ignited by spark plug^[2].

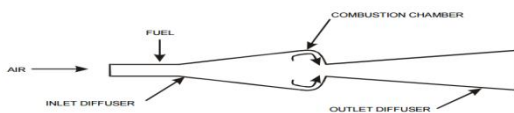


Fig 2.1 Marconnet pulse combustor

In 1931, Paul Schmidt obtained a German patent on the pulse combustor shown in Figure 2.2. A new feature of this combustor is the injection of the fuel downstream of the mechanical valve rather than upstream of it (Putnam et al., 1986). This design of essentially uniform cross section through the combustion chamber and resonance tube became known as the Schmidt design. The pulse combustion technology developed by Schmidt was utilized to produce thrust for propulsion of the German V-1 “buzz” flying bomb during the Second World War (or the

Cruise missile in more modern terms) (Wojcicki, 1962).

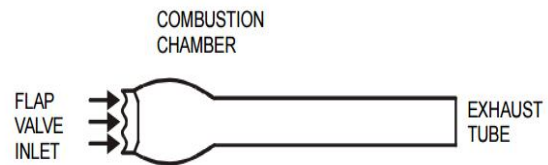


Fig 2.2 Schmidt pulse combustor

In the following years, the interest in pulse combustion declined due to relatively poor specific fuel consumption, and low specific thrust produced by pulse combustors compared with the more modern thrust producers such as the turbojets or turbofans. A major development in the field of pulse combustor was made in the 1950's when the mechanical valves were replaced by an inertial gas valve. Since the 1970's, the pulse combustion technology has been re-examined for use in different applications, e.g. boilers, heat exchangers, dryers, etc, where high combustion efficiency and low toxic components of the combustion gases is necessary^[3].

2.4 Merits and limitations:

Compared with steady combustion, pulse combustion offers the potential for higher efficiency of the combustion process and heat transfer rate with lower pollutant

emission (Dec et al., 1992). Some of the key features are presented in Tables 2.1 (Sonodyne Industries Inc, 1984).

Comparison of steady -state and pulse combustion:

Process parameters	Steady - state	Pulse
Combustion intensity (kW/m ³)	100-1000	10000-50000
Efficiency of combustion	80-96	90-99
Losses due to chemical underburning (%)	0-3	0-1
Losses due to mechanical underburning (%)	0-15	0-5
Temperature level (K)	2000-2500	1500-2000
CO concentration in exhaust (%)	0-2	0-1
NO _x concentration in exhaust (mg/m ³)	100-7000	20-70

Noise produced (dB)	85-100	110-130
Convective heat transfer coefficient (W/m ² K)	50-100	100-500
Time of reaction (s)	1-10	0.01-0.5
Excess air coefficient	1.01-1.2	1.00-1.01

3.1 DESIGNING OF PULSE JET ENGINE:

PJ15 pulsejet engines have been designed and constructed in order to provide Power and reliability, Light weight, Ease of assembly and maintenance, a choice of fuel systems, extended reed valve life, throttle able (injected version only). These engines are the result of a comprehensive development program that has produced a number of innovative new designs. These simple, effective, light-weight engines can be put to many different uses including Powering model airplanes, boats, cars, etc. Basically an enhanced Schmidt tube design, these engines have an enlarged combustion zone, straight tailpipe and divergent tail cone. The valving system uses a mix of traditional petal-valves and two unique features perfected after almost two years of research and development.

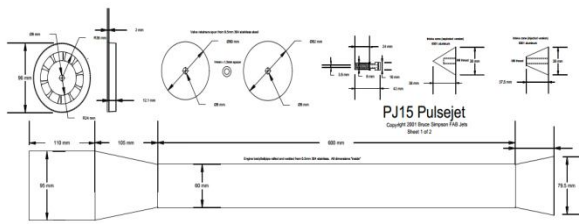


Fig3.1 drawing of a pulse jet engine^[9]

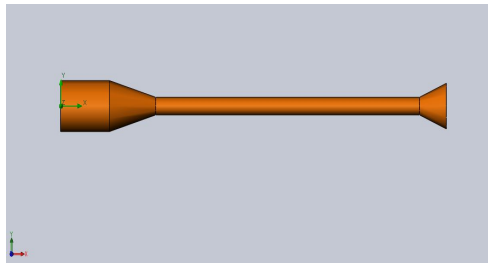


Fig3.2 modeling of a pulse jet engine

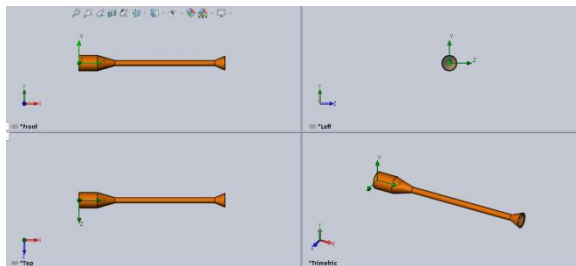


Fig3.3 Different views of a pulse jet engine

4.CFD ANALYSIS ON PULSE JET ENGINE: CFD Analysis has to be done for the given design of Pulse Jet Engine Pj15 based on different Mass Flow Rate conditions at different pressures. Based on analysis, construct a table with results obtained at different conditions^[7].

4.2 At a Mass flow rate of 10kg/s:

4.2.1 5 bars of pressure:

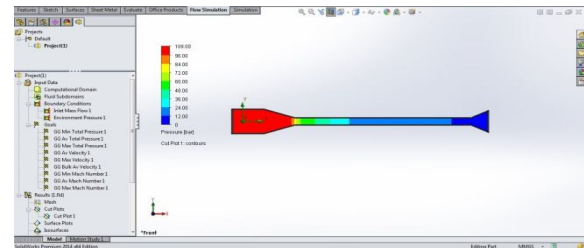


Fig 4.1 Pressure Contour at 5 bar Pressure

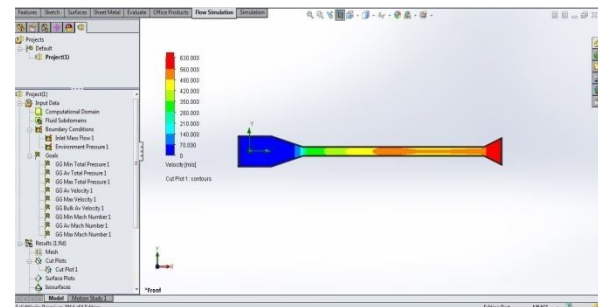
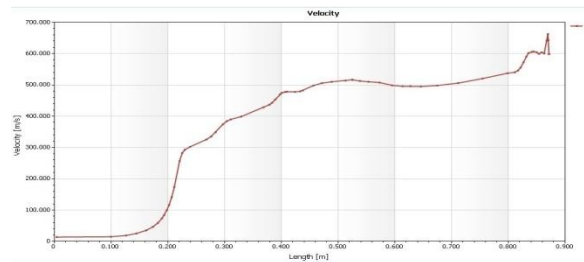


Fig 4.2 Velocity Contour at 5 bar Pressure



Velocity graph at 5 bar pressure at Mass flow rate of 10kg/s

By applying the input conditions the velocity and pressure contour can be seen at massflow rate of 10kgs/s of 5 bar of pressure.

4.2.210 bars of pressure: Inlet boundary conditions:

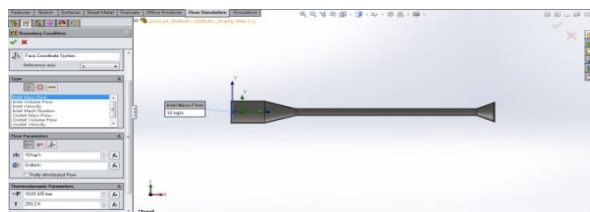


Fig 4.3 Pressure Contour at 10 bar Pressure

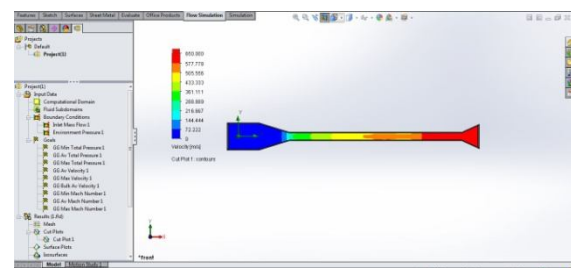
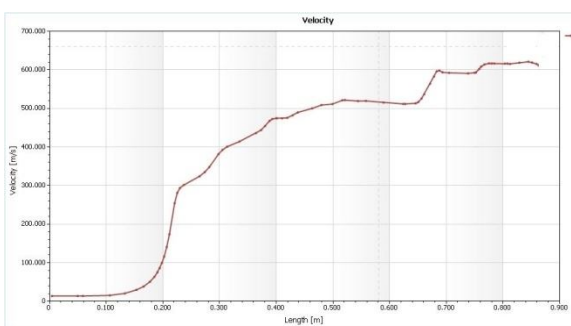


Fig 4.4 Velocity Contour at 10 bar Pressure



Velocity graph at 10 bar pressure at Mass
flow rate of 10kg/s

By applying the input conditions the
velocity and pressure contour can be seen at

mass flow rate of 10kgs/s of 10 bar of
pressure.

In the similar way analysis of PJ Engine has
been done on different mass flow rates at
different pressures and detailed values have
been noted in the below table.

5. RESULTS:

For 10kgs (mass flow rate)

Massflow rate[10kgs]	Maximum pressure	Maximum velocity
5bar	108	630
10bar	120	650

For 15kgs (mass flow rate)

Massflow rate[20kgs]	Maximum pressure	Maximum velocity
5bar	110	630
10bar	125	635

For 20kgs (mass flow rate)

Massflow rate[20kgs]	Maximum pressure	Maximum velocity
5bar	113	630
10bar	128	682

6. CONCLUSION:

- Designing and analysis of pulse jet engine is done in solid works software
- CFD analysis is done on pulse jet engine at three different mass flow rates with two different pressures i.e.; 10kgs, 15kgs and 20kgs with 5 bar and 10bar pressures.
- By performing the analysis on the PJ15 Pulse Jet Engine, we can conclude that by increasing mass flow rate the velocity can be increased.
- The Mach number of the Jet engine can be increased with different pressure and mass flow rate which is mainly important using target drone aircraft, flying control line model aircraft
- The Pulse Jet Engine is a new technology, though they are functioning from 19th century. The pulse jet engines have many advantages over the other engines for propulsive purposes and can be more reliable.

- Pulse jet engine is the best option due to its pulsating firing nature. This inherent characteristic of intermittent pulses create good amount of thrust and same utilized for fumigation purpose to get better coverage.
- There is a scope of conducting further research on Pulse Jet Engines to increase the Mach number by brining modifications to design and analyzing the design to required needs.

7.REFERENCE:

- [1] Experimental investigations into the operational parameters of a 50 centimeter class pulsejet engine – Ordon, Robert Lewis., 2006.
- [2] AshishWadhawan, Neeraj Mehta, “Development in the performance of the Valveless Pulse Jet Engine”, Vol. 1, issue 3, April 2012, ISSN: 2251-8843
- [3] Experimental investigations in 15 centimeter class pulsejet engines – Schoen, Michael Alexander., 2005.
- [4] Brady J. Bartosh, Thesis, “Thrust measurement of a split-path,

Valveless Pulse Detonation Engine”,
Naval Postgraduate School,2007.

- [5] Frequencies on heat transfer”, Vol. 4,
No. 1, 2007,pp. 86-94. [8] Paul J.
Litke and Frederick R. Schauer,
“Assessment of the Performance of a
Pulsejet and Comparison with a
Pulsed-Detonation Engine”, 43rd
AIAA Aerospace Sciences Meeting
and Exhibit January 10-13, 2005,
AIAA 2005-0228.

- [6] Computational fluid dynamics for
pulsejets and pulsejet related
technologies - SayresJr, John Scott.,
2011.

- [7] Computational investigations of high
speed pulsejets – Zheng, Fei., 2009.
[vi].

- [8] The synchronous injection ignition
valveless pulsejet – Dudley,
Edington Smith., 1987.

1.K.VISHNU TEJA



Studying M.Tech in stream of Thermal
Engineering from MALLAREDDY
ENGINEERING COLLEGE. Completed
B.Tech in Mechanical Engineering in 2013
Sreedattha college of Engineering,,Ranga
Reddy.

E-mail id: vishnuteja141745@gmail.com

2.N. SRINIVASA RAJNEESH



Completed B.Tech.in Mechanical
engineering in 2001 from V.N.R.VJIET
Engineering College,Hyderabad Affiliated
to JNTUH, and M.Tech in Energy
Technology in 2005 from Pondicherry
Engineering college Affiliated to
Pondicherry University, Pondicherry.
Working as Associate Professor at MALLA
REDDY ENGINEERING
COLLEGE(AUTONOMOUS) ,Dulapally
Rd, Maisammaguda,Hyderabad, Telangana,
India.

Area of interest includes: I.C
Engine,Biofuel,Energy.

E-mail id: rajneeshsrinivasa@gmail.com

CFD Simulation of Dual Fuel Natural Gas Based IC Engine Using Ansys ICE Package

P. Venu Gopal

PG student (M.Tech Thermal Engineering),
Department of Mechanical Engineering,,
Malla Reddy Engineering College,
Hyderabad, Telangana, India.

Shaik Hussain

Associate Professor,
Department of Mechanical Engineering,,
Malla Reddy Engineering College,
Hyderabad, Telangana, India.

ABSTRACT:

A Dual Fuel IC Engine is designed on the concept of the injection of a liquid fuel to start the combustion of the working mixture of a gaseous fuel and air in the engine cylinder. Due to stricter air pollution controls and the rise in the cost of fuels in general and relatively reduced availability of liquid fuels of right quality, the demand for gas-fuelled engine applications began increasing, mainly in the stationary electric power generation and commercial vehicle sectors. However the design and development of such engine needs a lot of time and costs for the conventional prototyping and experimental setup of any IC Engine. These time and cost constraints can be overcome by doing CFD simulation using Ansys Fluent and Ansys IC Engine packages. These simulation packages help to design and development of efficient IC Engines by predicting the heat transfer rate along with temperature, pressure and pollutants.

Also by understanding the in-cylinder combustion process of dual fuel combustion engine helps us to develop low emission engines. A multidimensional 2D model of Dual Fuel IC Engine was developed using solid works based on which the flow, heat and pollutant analysis was done using Ansys IC Engine package. The meshing was done by tetrahedral element using copper tool. The results were analyzed to get the values of heat transfer rate, temperature, dynamic & average pressures, the torque generated and emissions of combustion process. To validate the Ansys ICE simulation the results were compared with the experimental values and also with Ansys Fluent simulation and found that the predicted values are in conformance with the experimental results

Keywords:

CFD simulation, Ansys IC Engine, Natural-gas based, Dual Fuel IC Engine, Rate of Heat transfer, Combustion modeling, Diesel combustion.

I.INTRODUCTION TO CFD SIMULATION

With the increased computational power of modern computers, the CFD has become useful to many applications using diesel engine research, design and development. Hence it reduces the time and costs involved in conventional prototyping and testing the engine prototype to design and develop fuel efficient and low emission engines. Usually CFD analysis is done by using Ansys Software's Fluent or CFX Modules. However it needs lot of expertise and takes more time to do the setup and complete the simulation. Ansys's IEngine module is gaining momentum as it takes very less time compared to other simulation techniques and also we can perform port flow simulation, combustion simulation, cold flow simulation with ease. In addition the Ansys IC Engine is user friendly and has intuitive interface. It also has the capability to predict the gas flow pattern, Fuel spray patterns and other features similar to Fluent. It helps in understanding the Heat Transfer in IC Engine which causes thermally induced stresses impacting the life of engine parts and thereby it helps in designing and developing better engines for more durability and efficiency.

II ANSYS IC ENGINE SETUP, GEOMETRY AND MESHING

The first step for simulation is creating the geometry of the Engine cylinder & valves. This geometry was created using Solidworks in 3D and the geometry was saved as .STEP file. The simulation was started by dragging the ICE Module from the left side of the Ansys panel into the right panel. The properties of IEngine are set suitably as below:

Simulation type: Combustion simulation

Connecting rod length: 122 mm

Crank radius: 20.5 mm

Piston offset wrench: 75 mm

Engine speed: 1800 RPM

Minimum lift: 2 mm

Inlet Valve Closing: 542 degrees

Exhaust Valve Opening: 460 degrees

Fuel Type: Mixture of natural gas + air + other minor constituents

Next, the Valve Lift profile was uploaded.

Next, the Geometry menu of the ICE instance was double clicked to open the Design Modeler (DM) window. Here the previously created Geometry STEP file was imported into the Modeler and the Generate button was clicked to get the Geometry appeared in the DM window. Then a spark point is created with appropriate co ordinates like x, y, z. Then the Input Manager was added to the Design view. In the InputManager the configuration was done to select the two of cylinder faces, Inlet valve and Exhaust Valve. In the Inlet Valve button the Valve body and two faces are selected and necessary parameters such as spray height, spray radius, pilot ignition pipe angle etc were applied. Similarly, the Exhaust valve is also added and corresponding valve body and two faces were selected. The Geometry was updated and then it is decomposed by clicking on Decompose button. Next in the 'Mesh' section of the ICE the meshing parameters such as mesh type = Medium, Element length=10 mm etc with Tetrahedral meshing option were set and chosen Animate option to 'yes'. The Generate option will create the generation of Mesh on the selected surfaces. The Final step, is setting up the solver and running Calculation



Figure: 1 Running calculations in Ansys IC Engine CFD simulation

III SOLVER SETUP

The solver setup menu is available next to the generate mesh menu. Below are various settings and parameters in each setting that were used to run the solution to solve the equations. Basic settings: Autosave type: Crank Angle and ICE Swirl Number: 1.3

Physics settings: Species Model: Laminar Flow rate,

Material Input: Ansys ICE Fluent

Mixture Material: Natural gas-air

Boundary Conditions: ice-outlet-exvalve, ice-outlet-invalve

Monitor settings: vol-mon, vol-avg-temp-mon, vol-avg-pressure-mon, max-vel-mon,max-temp-mon, max-pressure-mon,mass-mon, mass-avg-tke-mon

Initialization parameters such as: x,y,z co ordinates, Temperature=300 K, Turbulent K.E, Turbulent Dissipation Rate, c7h16 and below other parameters are setup Location of spray: Height: 22 mm from the top of the cylinder,

Spray radius: 15 mm,

Inlet valve angle: 14 degrees,

Pilot injection pipe angle: 90 degrees,

Pilot injection time: 1.5 sec

Engine specifications used:

Bore: 84 mm

Stroke length 82 mm

Connecting rod length: 122 mm

Crank radius: 20.5 mm

Displacement: 1817cc

Engine speed=1800 RPM

Compression Ratio: 16:1. For this study the main fuel used is the mixture of natural gas with air. The Diesel was used for pilot ignition purpose with an ignition time of 1.5 seconds.

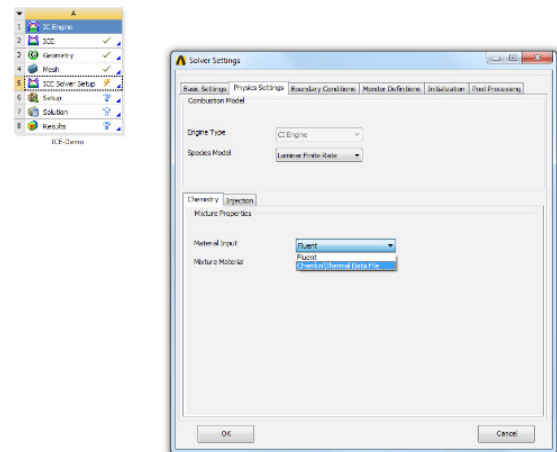


Fig: 2 Setting up of solver

IV FLUID FLOW SIMULATION & RATE OF HEAT RELEASE

The distribution of temperature and other thermal quantities under a transient thermal analysis is conducted to obtain the values of Heat transfer rate at various mass flow rates of the natural gas + air fuel mixture.

The rate of heat transfer, pressures, temperature contours and torque are obtained for various mass flow rates. These observations were in turn used to calculate the Efficiency and Brake power.

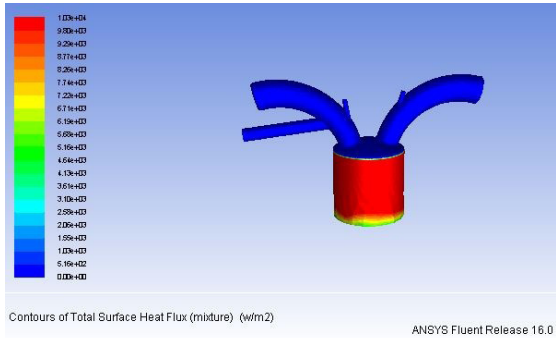


Figure 3: Total Heat Release rate

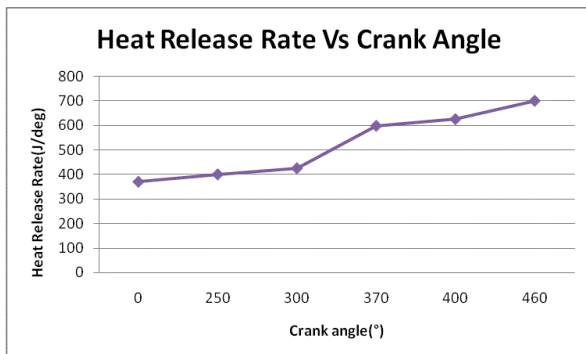


Figure 4.1: Total Heat Release rate Vs Crank Angle

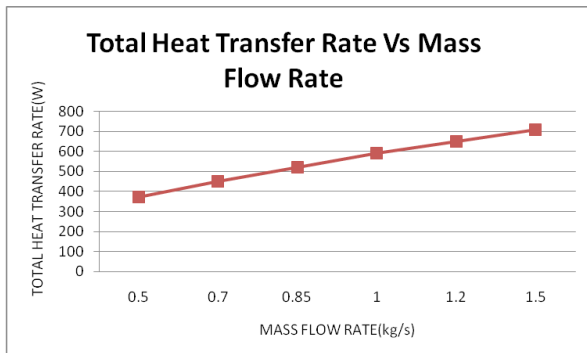


Figure 4.2: Total Heat Release rate Vs Crank Angle

COMPOSITION OF BIOGAS

The composition of biogas depends on a number of factors such as the process design and the nature of the substrate that is digested. A special feature of gas produced at landfills is that it includes nitrogen. The table below lists the typical properties of biogas from landfills, digesters and a comparison with average values for Danish natural gas for 2005.

		Landfill gas	Biogas from AD	Natural gas
Calorific value, lower	MJ/Nm ³	16	23	40
	kWh/Nm ³	4.4	6.5	11
	MJ/kg	12.3	20.2	48

Figure 4.3: Composition of Biogas

WHAT IS THE ENERGY CONTENT OF BIOGAS?

A typical normal cubic metre of methane has a calorific value of ca. 10 kWh, while carbon dioxide has none at all. The energy content of biogas is therefore directly related to the methane content. Thus, if biogas comprises 60 % methane, the energy content is ca. 6.0 kWh per cubic metre.

The energy content of different fuels:

1 Nm ³ biogas (97 % methane)	= 9.67 kWh
1 Nm ³ natural gas	= 11.0 kWh

Figure 4.4: Energy Content of Biogas

V. COMBUSTION SIMULATION

In the simulation of Dual Fuel Engines, the combustion modeling mainly deals with three processes, the first two being of the pilot ignition of Diesel Fuel [3] and third process is of the main combustion of the mixture of natural gas and air. The intermediate species produced by auto ignition in the first process trigger high temperature reactions subsequently in the second process which releases some heat energy. In case of Dual Fuel Engines, the heat released from the above second process ignites the main fuel consisting of natural gas + air mixture. which triggers high temperature reactions and causes the main heat release as well as further release of complete and incomplete combustion products. By choosing time scale combustion model, we can ensure the significance of effect of turbulence on the combustion process.

This combustion of dual fuel i.e. Diesel + Mixture of natural gas and air was simulated using Ansys IC Engine package. A single cylinder, single zone, multidimensional Combustion model was applied. The natural gas composition, Diesel and air properties were copied from various web resources, for combustion analysis. This combustion model includes both laminar and turbulent time scales to calculate the equilibrium concentration of each species. The major species like Methane, Ethane, Propane, Butane and other minor species like Pentane, Hexanes, Nitrogen, Carbon Dioxide, Oxygen etc were used for combustion species [2] and corresponding contours of pollutants such as HCN, NH₃, NO_x, CO₂ etc were obtained.

VI. RESULTS AND DISCUSSIONS

1. HEAT TRANSFER RATE AT VARIOUS MASS FLOW RATES AND CRANK ANGLES

The Heat Transfer data obtained from the modeled cylinder is shown in fig.3. From the graph the heat transfer co-efficient is in the order of 1.08×10^2 W/m²K and the maximum heat transfer of 700 watts at a mass flow rate of 1.5 kg/sec.

The total heat transfer rate at various mass flow rates and the total heat release rate at various crank angles were obtained. These heat values [Fig 4.1 & 4.2] were found to be comparable with the extrapolated experimental results of natural-gas based dual fuel engine [1]. The results of natural gas + air combustion are also in agreement with the energy content of bio gas⁷ [Fig 4.3 & 4.4]. Also the maximum cycle temperature is observed to be 2160 K.

2. TORQUE VS EFFICIENCY:

After running the calculations in the post processing->Function Calculator, the torque values are obtained and observed results are plotted in a graphical format as shown below in Fig 5. Here the efficiency of the engine is calculated theoretically. Based on maximum torque of about 29 to 30 N-m.

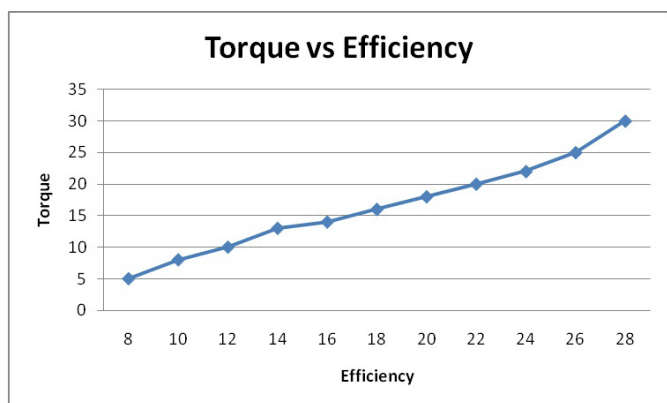


Figure 5: Torque Vs Efficiency

3. IN CYLINDER PRESSURE AND MASS FRACTION

The maximum pressure observed to be about 10.5 bars approximately as shown in the Fig. 6. The average dynamic pressure is observed to be about 50 bars as shown in the Fig. 7. A graph is drawn between mass flow rate and dynamic pressure which is shown in the Fig. 8. The contours of mass fraction are shown as in Figure 9

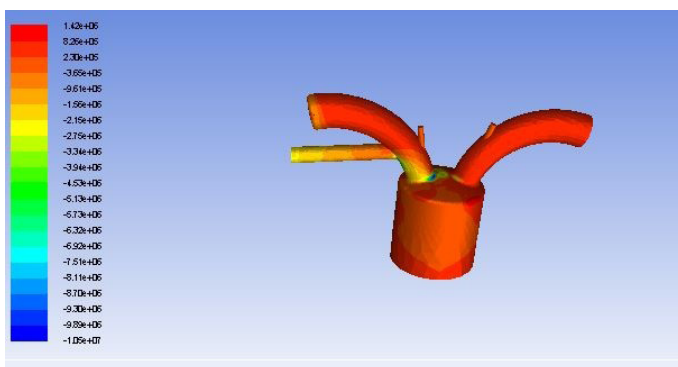


Figure 6: In cylinder pressure and Mass fraction

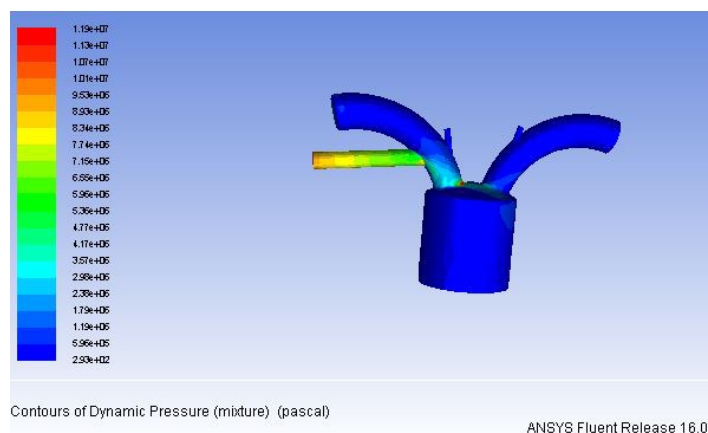


Figure 7: Average Dynamic pressure

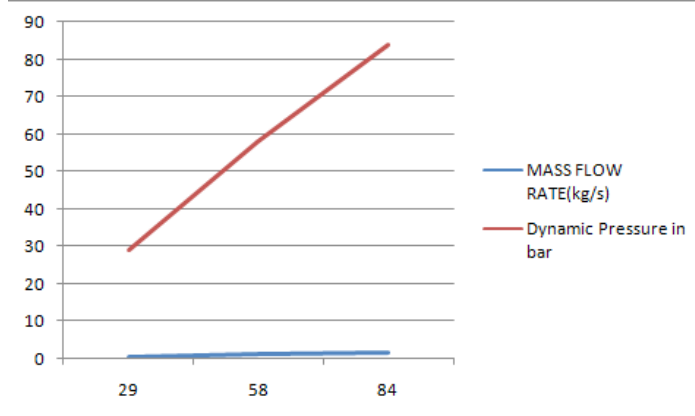


Figure 8: Average Dynamic pressure

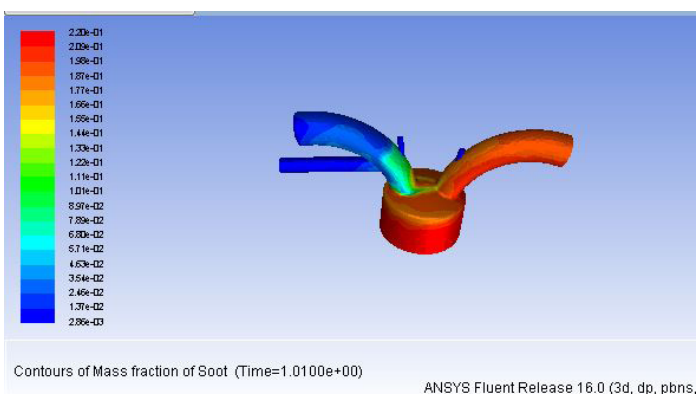


Figure 9: Contours of Mass fraction of soot

4 TEMPERATURE PROFILES

The temperatures contours are derived from the premixed combustion inside the cylinder as shown in Figure 10. Also the maximum cycle temperature is observed to be 2160 K.

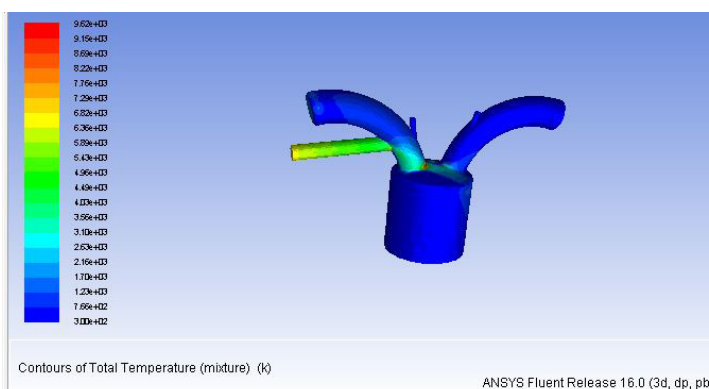


Figure 10: Contours of Total Temperature

5 COMPARISON OF BRAKE POWER OF CFD SIMULATION WITH EXPERIMENTAL SETUP

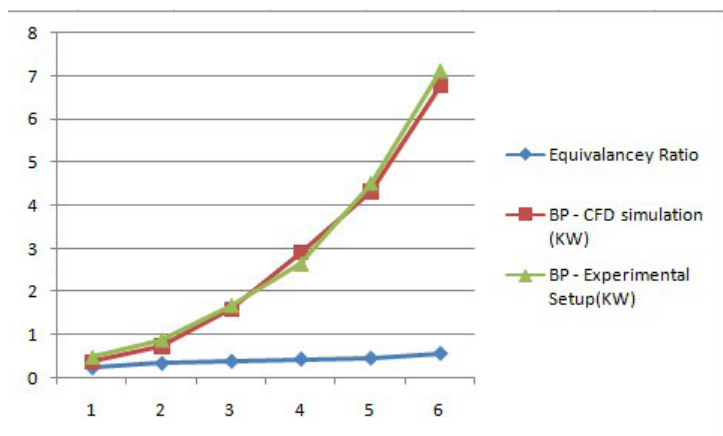


Figure 10: Comparison of Brake power of CFD Simulation with Experimental setup

6. THE MASS FRACTION OF POLLUTANTS

HCN, NH₃, NO_x Pollutants are observed to be as per the below figure 11, 12 & 13.

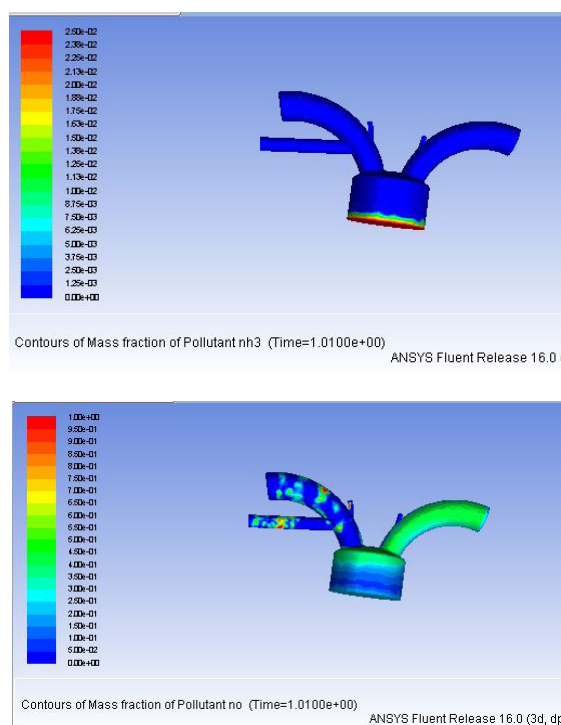
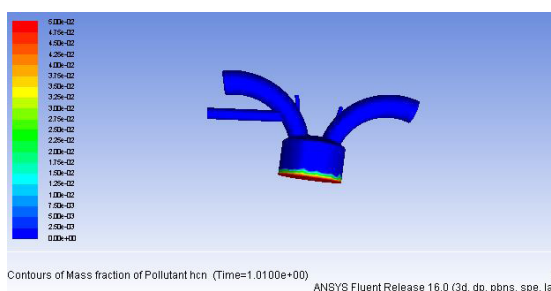


Figure 11, 12, 13: Mass fraction of Pollutants (HCN, NH₃, NO_x)

VII. CONCLUSIONS:

1. The model was created using Solid works, and the Heat transfer rate and combustion phenomenon was analyzed using Ansys 16 ICE. The results shows values of Heat Release, Pressure and Temperature are comparable with the Experimental Setup of dual fuel engine working on Natural Gas[1] for the same given equivalence ratio and output power. Hence the developed model is suitable for predicting the Heat transfer analysis and combustion characteristics of a Dual Fuel IC engine.

2. In the Dual Fuel IC Engine with combustion of Natural gas and air mixture, for the given compression ratio of 16:1, the heat transfer rate is observed to be about 700 Joules at about 460 degrees of crank Angle. At about 350 degrees of crank angle, the heat release rate is about 580 Joules [1], which is much higher than the heat release rate of 370 Joules as per the experimental setup of Bio-gas air mixture used for comparison[2]. The same can be verified from the fact that the Calorific Value of natural gas is about 48 MJ/Kg, which is much higher when compared to that of Biogas which is about 20.2 MJ/kg [7] as shown in figures 4.3. Similarly the energy content of natural gas is about 11 KWh for 1 Nm³ when compared with 9.67 KWh for 1Nm³ of biogas as shown in Fig 4.4.

The results data from CFD simulation is nearly close with both the experimental and statistical information. Hence CFD simulation is a good alternative for designing and developing Dual Fuel IC engine when compared to prototyping and experimental setup which is expensive and time consuming process.

3. From the results of simulation it can be observed that the average dynamic pressure is about 50 bars at 1800 RPM in this study of natural gas-diesel dual fuel engine. The combustion pressure of LPG-Diesel dual fuel engine is about 57 bars at 1300 RPM itself [3] which support the fact that the LPG engines are poor knock resistance. Also, LNG engines have higher thermal efficiencies compared to LPG Engines [8]. Hence the Natural gas-Diesel based dual fuel engines are much preferable for the commercial vehicles & heavy engine applications.

4. The results of CFD simulation of natural-gas-diesel engine shows that the CO₂ emissions are almost negligible when compared to 0.0048 as in case of Diesel only engine. Hence it is proved that the dual fuel engines are less polluting and recommended for better environment. Also the Natural gas engines produce less emissions particularly NO_x and other particulates. Hence the Natural-gas-Diesel can be considered as a choice for dual fuel engine compared to Diesel only engines.

5. The results of CFD simulation using Ansys 16 ICAEngine package are comparable with Ansys 15 Fluent package. Hence the Ansys ICE can be used as an alternative to the Ansys Fluent to leverage the benefits already explained at the beginning of this paper.

6. The simulation results of this study with natural-gas diesel engine such as average pressure and mean temperatures are observed to be much higher when compared with a naturally aspirated gasoline direct engine [9]. Hence sufficient care is to be taken in the aspects of engine vibrations, cooling system for the engine, lubrication of engine components etc for natural-gas diesel dual fuel Engine.

7. It is possible to export the results like the heat transfer co-efficient, temperatures etc to Ansys Finite Element Solver to find the thermally induced stresses to come up with better materials to manufacture robust engines to with stand high pressures and temperatures

REFERENCES:

- [1] Miqdam Tariq Chaichan et. al, Combustion of Dual Fuel Type Natural Gas/Liquid Diesel Fuel in Compression Ignition Engine e-ISSN: 2278-1684, p-ISSN: 2320-334X, Volume 11, Issue 6 Ver. IV (Nov- Dec. 2014), PP 48-58 page | 51
- [2] Shaik Magbul Hussain^{1*}, Dr.B. Sudheer Prem Kumar², Dr.K. Vijaya Kumar Reddy³ et. al, CFD analysis of combustion and emissions to study the effect of compression ratio and biogas substitution in a diesel engine with experimental verification, IJEST, ISSN: 0975-5462 Vol. 4 No.02 February 2012, pp2, 489, fig 25&26.
- [3] B. Ashok, S. Denis Ashok, C. Ramesh ,et. al, LPG diesel dual fuel engine – A critical review Alexandria Engineering Journal (2015) 54, 105–126 | Page 105
- [4] S Gavudhama Karunanidhi, Melvinraj C R, Sarath Das K P, G Subba Rao et.al CFD Studies of Combustion in Diesel Engine International Journal of Engineering Research and Applications (IJERA) ISSN: 2248-9622 www.ijera.com Vol. 3, Issue 4, Jul-Aug 2013, pp.827-830 , 828
- [5] Weaver, C. and Turner, S. et. al Dual Fuel Natural Gas/Diesel Engines: Technology, Performance, and Emissions, SAE Technical Paper 940548, 1994, doi:10.4271/940548.
- [6] Pawlak, G. et. al The Concept of a Dual Fuel Highly Efficient Internal Combustion Engine, SAE Int. J. Fuels Lubr. 3(2):135-141, 2010, doi:10.4271/2010-01-1480.
- [7] Swedish Gas Technology Center, Basic Data on Bio Gas. <http://www.sgc.se/ckfinder/userfiles/files/BasicDataonBiogas2012.pdf>
- [8] P. M. Darade, R. S. Dalu et al Investigation of Performance and Emissions of CNG Fuelled VCR Engine ISSN 2250-2459, ISO 9001:2008 Certified Journal, Volume 3, Issue 1, January 2013
- [9] T. Morauszki, P. Mandli, Z. Horvath, M.R Dreyer Simulation of Fluid Flow, Combustion and Heat transfer process In Internal Combustion Engines et.al Hungarian journal of Industrial chemistry Vol 39(1) pp 27-30 (2011)
- [10] John J. Kargul, Director of Technology Transfer, National Center for Advanced Technology Efficient, Use of Natural Gas Based Fuels in Heavy-Duty Engines
- [11] Ansys Inc, Internal Combustion Engine workbench technical guide et al https://www.academia.edu/12969241/ANSYS_Internal_Combustion_Engines_Tutorial_Guide.pdf

Comparisional Simulational Analysis of Sheet Hydro Forming of a Mechanical Component (Automobile Door)

Prakash kumar mandal¹ & M V Varalakshmi²

¹M.Tech 2nd year, Department of Mechanical Engineering, MREC, Hyderabad, India.

²Associate Professor, Department of Mechanical Engineering, MREC, Hyderabad, India.

Abstract: *The increasing application of numerical simulation in metal forming field has helped engineers to solve problems one after another to manufacture a qualified formed product reducing the required time. The present project aims at the simulation of hydro forming process, whose aim is to model and analyzing of Al-sheet at different stages in process of sheet metal hydro forming by using ANSYS taking into account the geometries of a car's luggage compartment door.*

1. Introduction

There are many metal forming processes which are well established, among them the established, sheet hydro forming is one of the best unconventional metal forming process which is widely used in order to form complex shapes. Hydro forming is a deformation process that shapes metal sheets or tube into a predefined geometry by using a fluid under high pressure. Hydro forming is similar to the conventional method in that a fluid is used instead of a die to forming into final shape. This deformation process requires application of fluid load up to 4000 bars depending on the size of the component.

Hydro forming is a relatively new process, which uses water pressure to form complex shapes from sheet or tube material. Design studies suggests that automobiles can be made much lighter by using hydro formed components made of steel. Structural strength and stiffness can be improved and the tooling costs reduced because several components can be consolidated into one hydro formed part.

As the automobile industry strives to make car, lighter, stronger and more fuel efficient, it will continue to drive hydro forming applications. Some automobile parts such as structural chassis, instrument panel beam, engine cradles and radiator closures are becoming standard hydro formed parts.

Recently hydro forming has also been used for manufacturing of clad pipe used in oil and chemical industry. The capability of hydro forming can be more fully used to create complicated parts.

Using a single hydro formed item to replace several individual parts eliminate welding, holes, punching etc. Hydro forming simplifies assembly and reduce inventory.

The process involves forming a straight or a pre-bent sheet into a die cavity using internal hydraulic pressure, which may be coupled with controlled axial feeding of the sheet. Structural strength and stiffness can be improved and the tooling costs reduced because several components can be consolidated into one hydro formed part.

2. Methodology

In this paper, the parameters of bending of sheets are to be decided on the basis of loads applied on the cantilever beam. Hydro forming uses fluid pressure in place of the punch in a conventional tool set to form the part into the desired shape of the die. In this method, the initial work piece is placed into a die cavity, which corresponds to the final shape of the component, the dies are closed under the force.

2.1. Sheet Hydro forming

Sheet hydro forming involves forming of sheet with application of fluid pressure. During the sheet hydro forming process, the hydraulic pressure varies in the range equal to or less than 100Mpa. A sheet metal blank is formed by hydraulic counter pressure generated by punch drawing sheet into pressurized water chambers. The water pressure effectively punches the sheet firmly against punch to form required shape.

The major advantage of fluid forming is increased drawing ratio. The process take place in two stages performed during one press stroke. The sheet is performed by applying low fluid pressure while it is clamped firmly by a blank holder pressure.

achieves Pre forming on evenly distributed strengthening in the component centre. In next step fluid pressure increased gradually and blank holder pressure is controlled relative to sheet reformation.

2.2. Tube Hydro Forming

Tube Hydro forming is a kind of soft-tool forming technology and developed rapidly in part decades. For taking tubes as processing blanks and liquid as flexible punch, it is more suitable for manufacturing special tubular components, such as different kinds of hollow shafts, discharge pipe of automobile & aero planes, sectional pipes etc.

Tubes are placed in the die and sealed on the end. Then under the co-action of compressive axial force and internal pressure, it is forced to deform from elastic stage to plastic stage. With the increased force correspondingly, finally, under the extremely high pressure, the tube assumed the internal canter of the die precisely, in tube hydro forming, a cylinder is pressurized internally with 80 to 450 Mpa pressure by a fluid like water.

Compared with traditional processing technology, tube hydro forming always manufactures components at one step. So it can enhance part quality, such as tighter tolerance and increase rigidity, and lower production costs and reduction in production cycle. In this method the tube is placed in die and as press clamps the die valves low pressure fluid introduced into tube to pre forms it. One the maximum clamping pressure is achieved, the fluid pressure inside the tube is increased so that tube bulges to take internal shape of the die. Simultaneously additional cylinders axially compress the tube to prevent thinning and brushing swing expansion. It is possible that some parts of the component thin excessively during hydro forming. This can sometimes be feed material into the bulges, thereby reducing bulging.

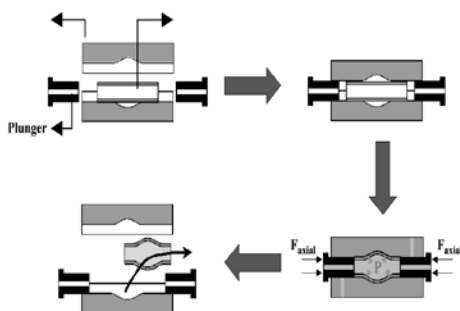


Figure1. Tube Hydro Forming

3. Experimental Work

Plastic bending of a cantilever ANALYSIS:

The analysis is carried out for the case of a cantilever beam for purpose of establishing the solution method for use later

3.1. Geometry Properties

Length	=	120 mm
Height	=	25 mm
Thickness	=	5 mm

3.2. Material Properties

Material	=	alloy steel.
Young's Modulus	=	25 N/mm ²
Poisons Ratio	=	0.3
Yield stress	=	200 N/mm ²
Tangent Modulus	=	2000 N/mm ²

Loading is varied for the problem in order to determine the on-set of plasticity and plastic strain beyond.

Point loads with 1000N, 2000N.....

3.3. GUI for Analysis by ANSYS

The graphical user interface (GUI) commands are given below.

k Choose menu path main menu
>preferences>structural>ok.

3.4. Define Element Type

- Choose menu path main menu > pre processor> element type > Add/Edit/Delete.
- Click Add.
- In left scroll box, click on "shell".
- In right scroll box, Plastic Node 43 then click ok.

3.5. Define Element Thickness

- Choose menu path Main menu > Pre processor > Sections>
- Click on Shell > Ok.
- Click on Thickness 5 mm, click Ok.

3.6. Define material properties

- Choose menu path Main menu > Pre-processor > Material properties > material models.
- Click on Structural > Non Linear > Inelastic > Rate independent > Isotropic hardening plasticity > Misses plasticity > Linear.
E* (young's modulus) = 2e5

PR*Y (poisson's ratio) = 0.3
Yield stress = 200 and
TANH (Tangent modulus) = 2000

3.7. Define Modeling

Choose menu path Main menu > Modeling > Create> area > rectangle > by 2 corners.

Then enter the width as 160 mm and height as 25 mm, Ok

3.8. Define meshing

Choose menu path Main menu > Pre-processor > Meshing > Mesh > Free, Ok.

3.9. Define loads

Choose menu path Main menu > Pre-processor > Loads > Apply > Structural > Displacement > on Nodes.

- Click on Nodes.
- Option dialog box appears. Select the Nodes and Click Ok.
- Dialog box will appear.
- Select ALL DOF for constrained in all directions and click Ok.
- Choose menu path Main menu > Pre-processor > Loads > Apply > Structural > Force/ (momentum) > on Nodes.
- Dialog box appears.
- Click on Nodes, Ok.
- Dialog box appears, (-Ve) direction for Load and load (1000, 2000) Ok.

Note:

Before applying the new load. Must delete the previous load on nodes.

Solve

- Choose menu Main menu > Solutions > Solve.
- Dialog box appears, click yes.

4. Review the results

- Choose menu path Main menu > General > List results > Last set.

- Choose menu path Main menu > General > Plot results > Deformation > Displacement. Click on it.
- Click on Stress > Vonmises stress.
- Click on elastic strain > Vonmises elastic strain.
- Click on plastic strain > Vonmises plastic strain.
- Click on plastic strain > elastic strain intensity.
- Click on plastic strain > plastic strain intensity.
- Click on plastic strain > energy plastic work / volume.

4.1. Exit ANSYS

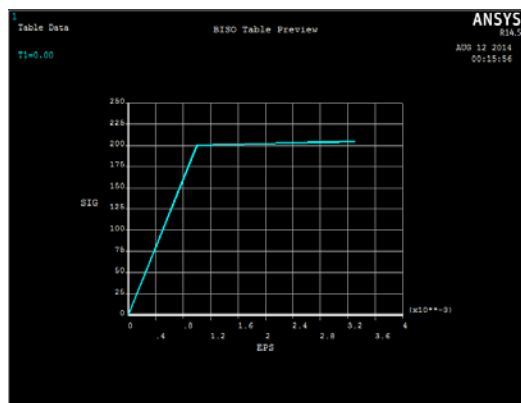
- Choose quit from the ANSYS tool bar.
- Click on the save options you want, and click on Ok.

5. Results analysis

$E = 2 \times 10^5$, $\mu = 0.3$ $E_T = 2000$, $\sigma_y = 200$ MPa

Table 1. Deflection, Stress and Strains for Different Thickness

Thickness	Case	Load applied	DMX (mm)	Stress Max (N/m ²)	Strain Plastic Max	Strain Elastic Max	Max Equivalent Plastic Strain
5mm Thickness	1	500	12.423	73.569	0.0265	0.368E-03	0.0265
	2	1000	32.166	146.787	0.0629	0.736E-03	0.0629
	3	2000	57.683	383.74	0.909	0.001919	0.9095
10mm Thickness	1	500	3.0659	36.797	0.0837	0.184E-03	0.0083
	2	1000	12.366	73.321	0.0264	0.367E-03	0.0264
	3	2000	32.036	146.21	0.062	0.733E-03	0.0626



Graph 1. Stress – Strain graph for the idealized material.

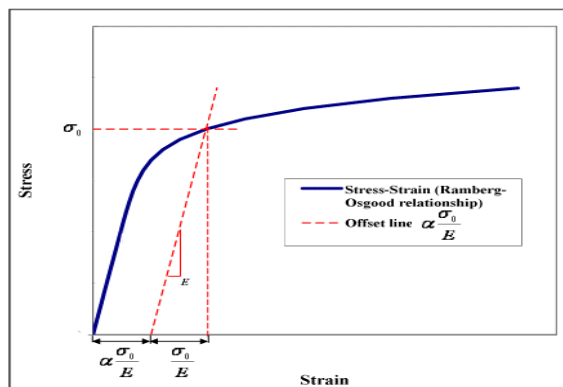


Figure: 5.2 Stress – Strain curve

$$\sigma_0 = 200 \text{ yield point,} \quad \frac{\sigma_0}{E} = 0.092$$

Elastic strain = $\frac{\sigma}{E}$ at max fiber

$$= \left(\frac{MY}{E} \right) \frac{1}{E} = \left(\frac{PLY}{I} \right) \frac{1}{E} = \frac{2000 \cdot 120 \cdot 12.5}{\frac{1}{12} \cdot 5 \cdot 25^3 \cdot 2 \cdot 10^5} = \frac{3000000}{(0.092 \cdot 5 \cdot 25^3) \cdot 2 \cdot 10^5} = 0.2313e-3 \text{ (by FEM } 0.19e-3 \text{)}$$

Plastic strain by FE = 0.09 (the total strain obtained being 0.092).

It can be seen from above that as against the theoretical value of 0.0023 for elastic strain, the FE value is 0.00192 (fig 4.5) which matches closely. The difference is because the beam theory is one dimensional whereas FE considered this case as two dimensional.

6. Scope of future work

1. The present methodology can be extended by Test rig with hydraulic clamping in the initial stages of ram movement, together with pressure gauge readings.
2. Rubber sheets of different composition like vinyl rubber, neoprene rubber, which are expensive, can be tried.
3. Better sealing to prevent leakages by using better gaskets
4. Methodology of analysis can be the same with no modifications.

7. Conclusion

In the present case of forming model components, the increased stiffness of the component due to small dimension requires very high pressures. The major conclusions are:

- i. Finite element simulation through plastic analysis is established.
- ii. A simple test rig is fabricated and its use demonstrated.
- iii. Results between theory and experiment match fairly well.

Such test rigs will be useful in initial stage of development of the first few cars (numbering ten numbers) for showing in exhibition without the need for manufacture of costly dies.

8. Acknowledgment

We express our sincere gratitude to Mrs MV Varalakshmi and Head of Department of Mechanical Engineering, MREC, for his helpfulness and motivation.

We are also thankful to all staff and my friends who made our work to be done with more ease.

9. References

- [1].Yudieski Bernal, Aguilar, José Roberto Marty, Delgado, Celestine Okoye- Nwoye, Edel Hernandez Santana, Ediel Hernández Santana, Control of critical parameters for square cup deep drawing of AISI 304 DDQ using genetic algorithm, Ingeniería Mecánica, Ingeniería Mecánica. Vol. 16, p. 144-151.
- [2].H.Arfa & R.Bahloul & H.BelHadjSalah, Finite element modeling and experimental investigation of single point incremental forming process of aluminum sheets: influence of process parameters on punch force monitoring and on mechanical and geometrical quality of parts, Int Je of Mater Form, DOI 10.1007/s12289-012-1101-z.
- [3].G. L. Damoulis, E. Gomes, G. F. Batalha, New trends in sheet metal forming analysis and

optimization through the use of optical measurement technology to control spring back, Springer/ESAFORM 2009, Int J Mater Form (2010) 3:29–39.

[4]. R. Aerens, P. Eyckens, A. Van Bael, J. R. Duflou, Force prediction for single point incremental forming deduced from experimental and FEM observations Springer-Verlag London Limited 2009, Int J Adv Manuf Technol,....

[5]. Shiwen Wang, Weimin Zhuang, Jian Cao, Jianguo Lin, An investigation of spring back scatter in forming ultra-thin metal-sheet channel parts using crystal plasticity FE analysis, Springer-Verlag London Limited 2009, Int J Adv Manuf Technol (2010) 47:845–852.

[6]. J.F. Carvalho, P.S. Cruz, R.A.F. Valente, A. Andrade-Campos, An Integrated Methodology For Parameter Identification And Shape Optimization In Metal Forming And Structural Applications, EngOpt 2008 - International Conference on Engineering Optimization Rio de Janeiro, Brazil, 01 - 05 June 2008.

[7]. C.T Kwan C.Y.Lin Y.S. Luo Die shape design for t-shape tube hydro forming Journal advance manufacturing technology (2004) 23:169_175. 74

[8].Nw numeric, hydro forming example 150 Nickerson street, suite 102 Seattle WA98109, Company brochure.

[9]. Nico Langerak, Dinesh Kumar Rout, Rahul Verma, G.Manikandan, Arunansu Halder, Tube Hydro forming in Automotive Applications, Tata Steel Research Development & Technology, IJmuiden, The Netherlands Tata Steel, Tubes Division, Jamshedpur, India

[10]. Braf F. Kuvim (2000) metal forming, www.metalforming.com.

[11].Finite element modeling by Ibrahim zahid.

[12] Harinder singh, fundamental of hydro forming.

[13]. H.K.D.H.Bhadeshia, hydro forming University of Cambridge.

[14].Zhang Yong a; Luen Chow Chan b; Wang Chunguang a; Wu Pei optimization for loading paths of tube hydro forming using a hybrid method. MatOerial and manufacturing process.

**Department of
Electronics and
Communication Engineering**

New VLSI Architecture for FM0/Manchester Encoding using SOLS Technique using Wireless Sensor Network

Ingilela Suahsini¹, K. Rajendra Prasad²

¹Scholar, Dept of ECE, Malla Reddy Engineering College (Autonomous), Telangana, India

²Assistant Professor, Dept of ECE, Malla Reddy Engineering College (Autonomous), Telangana, India

Abstract: In this paper we studied the implementation of Manchester coding is being described. Manchester coding technique is a digital coding technique in which all the bits of the binary data are arranged in a particular sequence. The Intersil HD-15530 is a high performance CMOS device intended to service the requirements of MIL-STD-1553 and similar Manchester II encoded, time division multiplexed serial data protocols. This LSI chip is divided into two sections, an Encoder and a Decoder. These sections operate completely independent of each other, except for the Master Reset functions. This circuit meets many of the requirements of MIL-STD-1553. The Encoder produces the sync pulse and the parity bit as well as the encoding of the data bits. The Decoder recognizes the sync pulse and identifies it as well as decoding the data bits and checking parity. This integrated circuit is fully guaranteed to support the 1MHz data rate of MIL-STD-1553 over both temperature and voltage. It interfaces with CMOS, TTL or N channel support circuitry. The HD-15530 can also be used in many party line digital data communications applications, such as an environmental control system driven from a single twisted pair cable of fiber optic cable throughout the building. The functions of the encoder section of the MED include a microprocessor interface, parallel to serial conversion, frame generation, and NRZ to Manchester encoding. This circuitry can run very fast since it does not require a high-frequency clock. The frame format used is similar to that of a UART. The Manchester decoder limits the maximum frequency of operation of the MED, since it uses a high-frequency clock. The receiver circuitry is more complex, since clock recovery and center sampling is done. Additional receiver functions are frame detection, decoding of Manchester to NRZ, serial to parallel conversion, and a microprocessor interface.

Keywords: Manchester coding, Encoder, Decoder, NRZ, Moore's law, UART, clock frequency

I. INTRODUCTION

Manchester coding technique is a digital coding technique in which all the bits of the binary data are arranged in a particular sequence. Here a bit '1' is represented by transmitting a high voltage for half duration of the input signal and for the next halftime period an inverted signal will be send. When transmitting '0' in Manchester format, for the first half cycle a low voltage will send, and for the next half cycle a high voltage is send. The advantage of Manchester coding is that, when sending a data having continuous high signals or continuous low signal (e.g.: 11110000), it is difficult to calculate the number of 1 S and 0s in the data. Because there is no transition from low to high or high to low for a particular time period (Here it is $4 \times T$, T is the time duration for a single pulse). The detection is possible only by calculating the time duration of the signal. But when we code this signal in Manchester format there will always be a transition from high to low or low to high for each bit. Thus for a receiver it is easier to detect the data in Manchester format and also the probability for occurrence of an error is very low in Manchester format and it is a universally accepted digital encoding technique.

The dedicated short range communication is a protocol for one or two way medium range communication. The DSRC can be briefly classified into two categories: automobile-to-automobile and automobile-to-roadside. In automobile-to-automobile, the DSRC enables the message sending and broadcasting among automobile. The automobile-to-roadside focuses on the intelligent transportation service, such as electronic toll collection (ETC). The DSRC architecture having the transceiver. The transceiver having the baseband processing, RF front end and microprocessor. The microprocessor is used to transfer the instruction to the baseband processing and RF front end. The RF front end is used to transmit and receive the wireless signals using the antenna. The baseband processing is responsible for modulation, error correction, encoding and synchronization. The

transmitted signal consists of the arbitrary binary sequence, it is very difficult to obtain the dc-balance. The FM0 and Manchester codes are used to provide the transmitted signal and then the dc-balance. The (SOLS) similarity oriented logic simplification having the two methods: area compact retiming and balance logic operation sharing. The area compact retiming is used to reduce the transistor counts. The balance logic operation sharing is used to combine the FM0 and Manchester encoding.

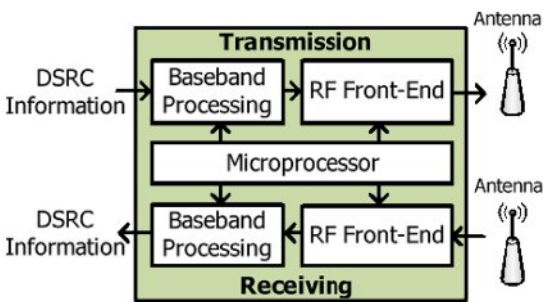


Figure 1: System architecture of DSRC transceiver.

The system architecture of DSRC transceiver is shown in Fig. 1. The upper and bottom parts are dedicated for transmission and receiving, respectively. This transceiver is classified into three basic modules: microprocessor, baseband processing, and RF front-end. The microprocessor interprets instructions from media access control to schedule the tasks of baseband processing and RF front-end. The baseband processing is responsible for modulation, error correction, clock synchronization, and encoding. The RF front-end transmits and receives the wireless signal through the antenna.

The DSRC standards have been established by several organizations in different countries. These DSRC standards of America, Europe, and Japan are shown in Table I. The data rate individually targets at 500 kb/s, 4 Mb/s, and 27 Mb/s with carrier frequency of 5.8 and 5.9 GHz. The modulation methods incorporate amplitude shift keying, phase shift keying, and orthogonal frequency division multiplexing. Generally, the waveform of transmitted signal is expected to have zero mean for robustness issue, and this is also referred to as dc-balance.

II. LITERATURE SURVEY

The transmitted signal consists of arbitrary binary sequence, which is difficult to obtain dc-balance. The purposes of FM0 and Manchester codes can provide the

transmitted signal with dc-balance. Both FM0 and Manchester codes are widely adopted in encoding for downlink. The VLSI architectures of FM0 and Manchester encoders are reviewed as follows

A. Review of VLSI Architectures for FM0 Encoder and Manchester Encoder

The literature [4] proposes a VLSI architecture of Manchester encoder for optical communications. This design adopts the CMOS inverter and the gated inverter as the switch to construct Manchester encoder. It is implemented by 0.35- μ m CMOS technology and its operation frequency is 1 GHz. The literature [5] further replaces the architecture of switch in [4] by the nMOS device. It is realized in 90-nm CMOS technology, and the maximum operation frequency is as high as 5 GHz. The literature [6] develops a high-speed VLSI architecture almost fully reused with Manchester and Miller encodings for radio frequency identification (RFID) applications. This design is realized in 0.35- μ m CMOS technology and the maximum operation frequency is 200 MHz. The literature [7] also proposes a Manchester encoding architecture for ultrahigh frequency (UHF) RFID tag emulator. This hardware architecture is conducted from the finite state machine (FSM) of Manchester code, and is realized into field-programmable gate array (FPGA) prototyping system. The maximum operation frequency of this design is about 256 MHz. The similar design methodology is further applied to individually construct FM0 and Miller encoders also for UHF RFID Tag emulator [8]. Its maximum operation frequency is about 192 MHz. Furthermore, [9] combines frequency shift keying (FSK) modulation and demodulation with Manchester codec in hardware realization.

III. CODING PRINCIPLES OF FM0 CODE AND MANCHESTER CODE

In the following discussion, the clock signal and the input data are abbreviated as CLK, and X, respectively. With the above parameters, the coding principles of FM0 and Manchester codes are discussed as follows.

A. FM0 Encoding As shown in Fig. 2, for each X, the FM0 code consists of two parts: one for former-half cycle of CLK, A, and the other one for later-half cycle of CLK, B. The coding principle of FM0 is listed as the following three rules.

- 1) If X is the logic-0, the FM0 code must exhibit a transition between A and B.
- 2) If X is the logic-1, no transition is allowed between A and B.

3) The transition is allocated among each FM0 code no matter what the X is.

A FM0 coding example is shown in Fig. 3. At cycle 1, the X is logic-0; therefore, a transition occurs on its FM0 code, according to rule 1. For simplicity, this transition is initially set from logic-0 to -1. According to rule 3, a transition is allocated among each FM0 code, and thereby the logic-1 is changed to logic-0 in the beginning of cycle 2. Then, according to rule 2, this logic-level is hold without any transition in entire cycle 2 for the X of logic-1. Thus, the FM0 code of each cycle can be derived with these three rules mentioned earlier.

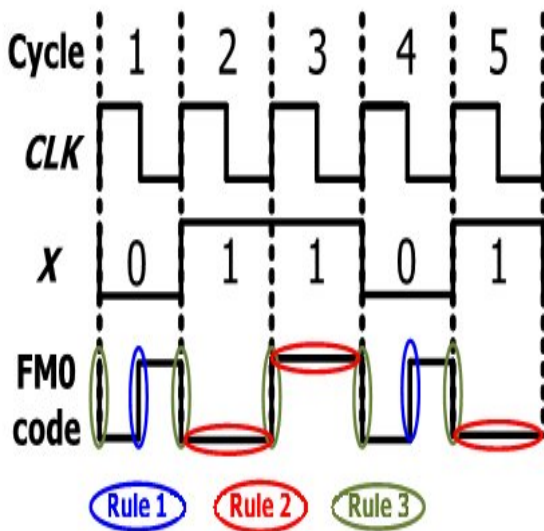


Figure 2: Illustration of FM0 coding example.

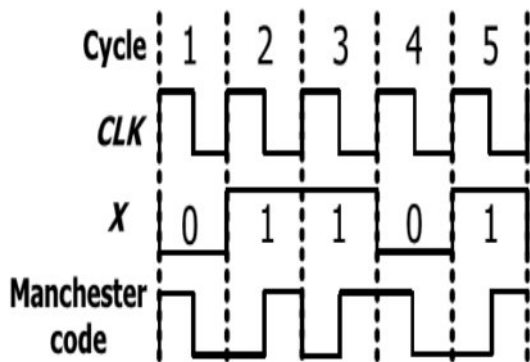


Figure 3: Illustration of Manchester coding example.

Hardware Architecture of Fm0/Manchester Code:

This is the hardware architecture of the fm0/Manchester code. the top part is denoted the fm0 code and then the bottom part is denoted as the Manchester code. in fm0 code the DFFA and DFFB are used to store the state code of the fm0 code and also mux_1 and not gate is used in the fm0 code. When the mode=0 is for the fm0 code. The Manchester code is developed only using the XOR gate and when the mode=1 is for the Manchester code. The hardware utilization rate is defined as the following

$$HUR = \frac{\text{Active components}}{\text{total components}} \times 100 \quad (1)$$

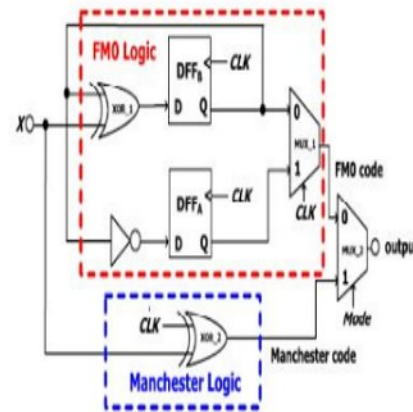


Figure 4: Hardware architecture

The active components means the components are work in the both fm0 and Manchester code. The total components means the number of the components are present in the hole circuit. The HUR rate is given below the following section

Table I : HUR rate Analysis

Coding	Active components(transistor count)/ total components (transistor count)	HUR
FM0	6(86)/7(98)	85.71%
MANCHESTER	2(26)/7(98)	28.57%
AVERAGE	4(56)/7(98)	57.14%

For both the encoding methods the total components is 7.for the fm0 code the total component is 7 and then the active component is 6.in Manchester code the total

component is 7 the active component is 2.in both coding having 98 transistors are used without SOLS. The fm0 having 86 transistor, and then the Manchester having the 26 transistor. The average for both coding is 56 transistors .In proposed work reduce the total components from 7 to 6 and reduce the transistor counts. In this paper two multiplexer is used in proposed work reduce two multiplexer from one multiplexer, when reduce the multiplexer the total components are reduced the area and then the power consumption also reduced.

IV. FMO and Manchester Encoder Using Sols Technique

The SOLS technique is classified into two parts area compact retiming and balance logic operation sharing

A. Area compact retiming

For fm0 the state code of the each state is stored into DFFA and DFFB .the transition of the state code is only depends on the previous state of B(t-1) instead of the both A(t-1) and B(t-1)

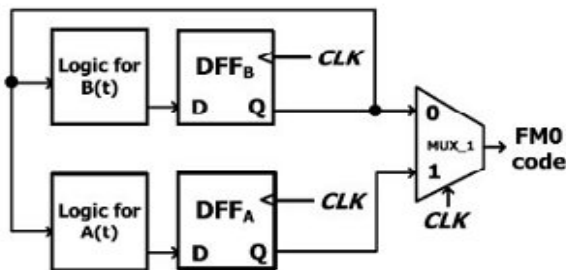


Figure 5: Area compact retiming

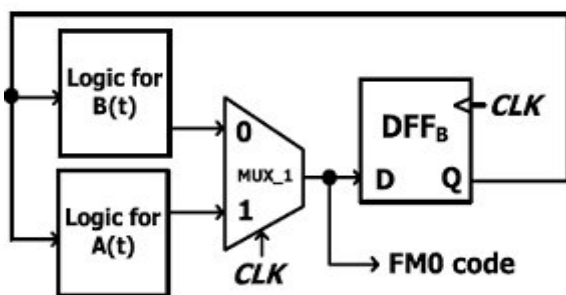


Figure 6:FM0 encoding without area compact retiming

The previous state is denoted as the A(t-1) and then the B(t-1).and then the current state is denoted as the A(t) and then the B(t).

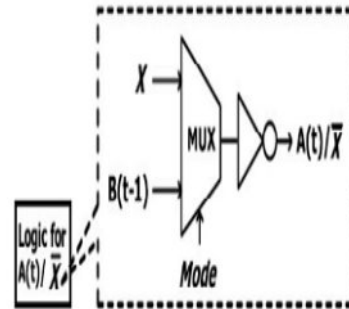


Figure 7: FM0 encoding with area compact retiming.

Thus, the FM0 encoding just requires a single 1-bitflip-flop to store the previous value B(t-1).If the DFFA is directly removed, a non synchronization between A(t) and B(t)causes the logic fault of FM0 code. To avoid this logic-fault, the DFFB is relocated right after the MUX-1, where the DFFB is assumed be positive-edge triggered flip flop. At each cycle, the FM0 code, comprising A and B, is derived from the logic of A(t) and the logic of B(t), respectively. The FM0 code is alternatively switched between A(t) and B(t) through the MUX-1 by the control signal of the CLK. In the Q of DFFB is directly updated from the logic of B(t)with 1-cycle latency. when the CLK is logic-0, the B(t) is passed through MUX-1 to the D of DFFB. Then, the upcoming positive-edge of CLK updates it to the Q of DFFB. the timing diagram for the Q of DFFB is consistent whether the DFFB is relocated or not. the B(t) is passed through MUX-1 to the D of DFFB. Then, the upcoming positive-edge of CLK updates it to the Q of DFFB. the timing diagram for the Q of DFFB is consistent whether the DFFB is relocated or not. The transistor count of the FM0 encoding architecture without area-compact retiming is 72,and that with area-compact retiming is 50. The area-compact retiming technique reduces 22 transistors.

B. Balance logic operation sharing

The Manchester encoding is derived using the XOR operation. the equation of the XOR gate is given below.
 $X \oplus CLK = X CLK + \sim X CLK$

the concept of balance logic-operation sharing is to integrate the X into A(t) and X into B(t).the fm0 and Manchester logics have a common point of the multiplexer like logic with the selection of the CLK. the diagram for the balance logic operation sharing given the following.

The A(t) can be derived from an inverter of B(t - 1), and X is obtained by an inverter of X. The logic for

A(t)/X can share the same inverter, and then a multiplexer is placed before the inverter to switch the operands of $B(t-1)$ and X. The Mode indicates either FM0 or Manchester encoding is adopted. The similar concept can be also applied to the logic for B(t)/X.

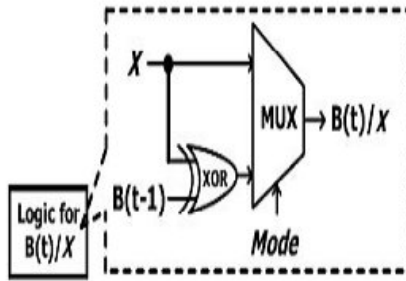
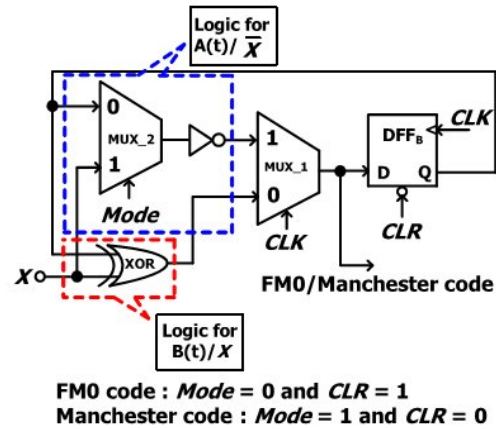
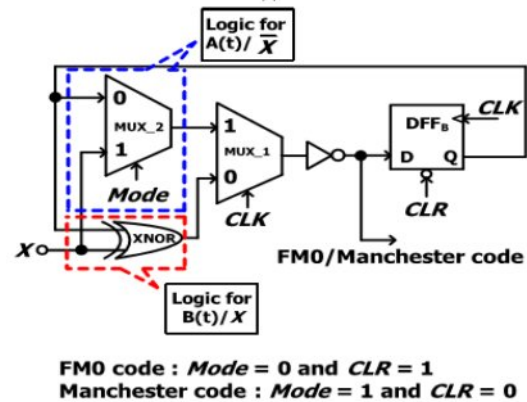


Figure 8: Balance logic operation sharing

Nevertheless, this architecture exhibits a drawback that the XOR is only dedicated for FM0 encoding, and is not shared with Manchester encoding. Therefore, the HUR of this architecture is certainly limited. The X can be also interpreted as the X₀, and thereby the XOR operation can be shared with Manchester and FM0 encodings, where the multiplexer irresponsible to switch the operands of B(t-1) and logic-0. This architecture shares the XOR for both B(t) and X, and there by increases the HUR. When the FM0 code is adopted, the CLR is disabled, and the B(t-1) can be derived from DFFB. Hence, the multiplexer can be totally saved, and its function can be completely integrated into the relocated DFF. The logic for A(t)/X includes the MUX-2 and an inverter. Instead, the logic for B(t)/X just incorporates a XOR gate. In the logic for A(t)/X, the computation time of MUX-2 is almost identical to that of XOR in the logic for B(t)/X. However, the logic for A(t)/X further incorporates an inverter in the series of MUX-2. This unbalance computation time between A(t)/X and B(t)/X results in the glitch to MUX-1, possibly causing the logic fault on coding. To alleviate this unbalance computation time, the architecture of the balance computation time between A(t)/X and B(t)/X. The XOR in the logic for B(t)/X is translated into the XNOR with an inverter, and then this inverter is shared with that of the logic for A(t)/X. This shared inverter is relocated backward to the output of MUX-1. Thus, the logic computation time between A(t)/X and B(t)/X is more balance to each other.



(a)



(b)

Figure 9: VLSI architecture of FM0 and Manchester encodings using SOLS technique. (a) Unbalance computation time between $A(t)/X$ and $B(t)/X$. (b) Balance computation time between $A(t)/X$ and $B(t)/X$.

The adoption of FM0 or Manchester code depends on Mode and CLR. In addition, the CLR further has another individual function of a hardware initialization. If the CLR is simply derived by inverting Mode without assigning an individual CLR control signal, this leads to a conflict between the coding mode selection and the hardware initialization. To avoid this conflict, both Mode and CLR are assumed to be separately allocated to this design from a system controller. Whether FM0 or Manchester code is adopted, no logic component of the proposed VLSI architecture is wasted. Every component is active in both FM0 and Manchester encodings. Therefore, the HUR of the proposed VLSI architecture is greatly improved.

V. SIMULATION RESULTS

FM0 Module:

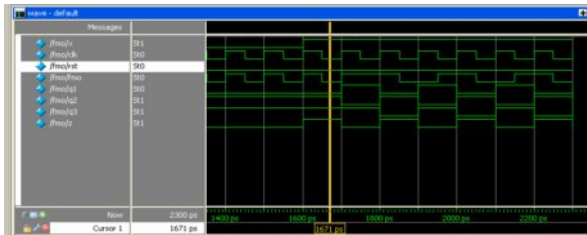


Figure 10: FM0 Code

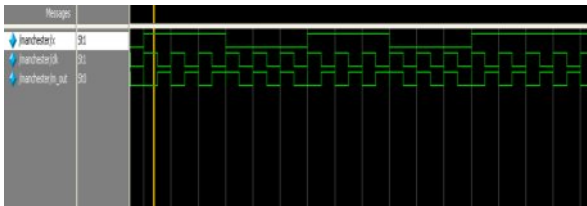


Figure 11: Manchester Coding

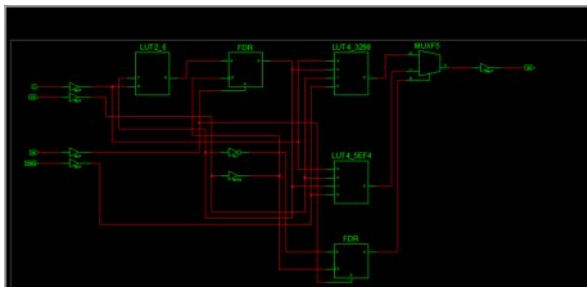


Figure 12: RTL Schematic

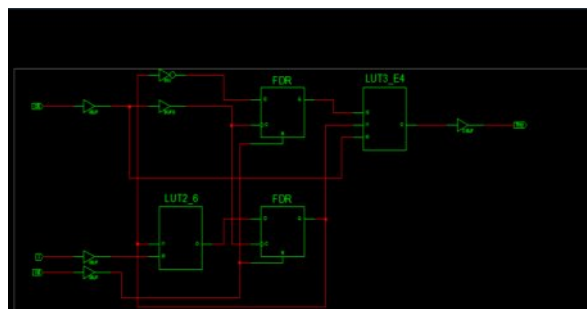


Figure 13: Technology Schematic

VI. CONCLUSION

The coding-diversity between FM0 and Manchester encodings causes the limitation on hardware utilization of VLSI architecture design. A limitation analysis on hardware utilization of FM0 and Manchester encodings is discussed in detail. In this paper, the fully reused VLSI architecture using SOLS technique for both FM0 and Manchester encodings is proposed. The SOLS technique eliminates the limitation on hardware utilization by two core techniques: area compact retiming and balance logic-operation sharing. The area-compact retiming relocates the hardware resource to reduce the transistors. The balance logic-operation sharing efficiently combines FM0 and Manchester encodings with the identical logic components. This paper is realized in 180nm technology with outstanding device efficiency. The power consumption is 29392.843nW for Manchester encoding and FM0 encoding.

REFERENCES

- [1] F. Ahmed-Zaid, F. Bai, S. Bai, C. Basnayake, B. Bellur, S. Brovold, et al., "Vehicle safety communications—Applications (VSC-A) final report," U.S. Dept. Trans., Nat. Highway Traffic Safety Admin., Washington, DC, USA, Rep.DOT HS 810 591, Sep. 2011.
- [2] J. B. Kenney, "Dedicated short-range communications (DSRC) standards in the United States," *Proc. IEEE*, vol. 99, no. 7, pp. 1162–1182, Jul. 2011.
- [3] J. Daniel, V. Taliwal, A. Meier, W. Holfelder, and R. Herrtwich, "Design of 5.9 GHz DSRC-based vehicular safety communication," *IEEE Wireless Commun. Mag.*, vol. 13, no. 5, pp. 36–43, Oct. 2006.
- [4] P. Benabes, A. Gauthier, and J. Oksman, "A Manchester code generator running at 1 GHz," in *Proc. IEEE, Int. Conf. Electron., Circuits Syst.*, vol. 3, Dec. 2003, pp. 1156–1159.
- [5] A. Karagounis, A. Polyzos, B. Kotsos, and N. Assimakis, "A 90nm Manchester code generator with CMOS switches running at 2.4 GHz and 5 GHz," in *Proc. 16th Int. Conf. Syst., Signals Image Process.*, Jun. 2009, pp. 1–4.

- [6] Y.-C. Hung, M.-M. Kuo, C.-K. Tung, and S.-H. Shieh, "High-speedCMOS chip design for Manchester and Miller encoder," in *Proc. Intell. Inf. Hiding Multimedia Signal Process.*, Sep. 2009, pp. 538–541.
- [7] M. A. Khan, M. Sharma, and P. R. Brahmanandha, "FSM based Manchester encoder for UHF RFID tag emulator," in *Proc. Int. Conf.Comput., Commun. Netw.*, Dec. 2008, pp. 1–6.
- [8] M. A. Khan, M. Sharma, and P. R. Brahmanandha, "FSM based FM0 and Miller encoder for UHF RFID tag emulator," in *Proc. IEEE Adv. Comput. Conf.*, Mar. 2009, pp. 1317–1322.
- [9] J.-H. Deng, F.-C. Hsiao, and Y.-H. Lin, "Top down design of joint MODEM and CODEC detection schemes for DSRC codedFSK systems over high mobility fading channels," in *Proc. Adv. Commun. Technol.* Jan. 2013, pp. 98–103.
- [10] I.-M. Liu, T.-H. Liu, H. Zhou, and A. Aziz, "Simultaneous PTL buffer insertion and sizing for minimizing Elmore delay," in *Proc. Int. Workshop Logic Synth.*, May 1998, pp. 162–168.

VLSI DESIGN OF ERROR DETECTION AND CORRECTION USING ORTHOGONAL LATIN SQUARE CODES

Banoth Venkata Sai Kumar¹, G Prasanna Kumar²

¹PG Scholar in DSCE, ²M.Tech, Asst. Professor, ECE Department
Malla Reddy Engineering College, Hyderabad, Telangana

Abstract: Reliability is a major concern in advanced electronic circuits. Errors caused for example by radiation become more common as technology scales. To ensure that those errors do not affect the circuit functionality a number of mitigation techniques can be used. Among them, Error Correction Codes (ECC) are commonly used to protect memories and registers in electronic circuits. When ECCs are used, it is of interest that in addition to correcting a given number of errors, the code can also detect errors exceeding that number.

This ensures that uncorrectable errors are detected and therefore silent data corruption does not occur. Among the ECCs used to protect circuits, one option is Orthogonal Latin Squares (OLS) codes for which decoding can be efficiently implemented. In this paper, an enhancement of the decoding for Double Error Correction (DEC) OLS codes is proposed. The proposed scheme tries to reduce the probability of silent data corruption by implementing mechanisms to detect errors that affect more than two bits.

Keywords: Concurrent error detection, error correction codes (ECC), Latin squares, majority logic decoding (MLD), parity, memory.

I. INTRODUCTION

The general idea for achieving error detection and correction is to add some redundancy which means to add some extra data to a message, which receiver can use to check uniformity of the delivered message, and to pick up data determined to be corrupt. Error-detection and correction scheme may be systematic or it may be non-systematic. In the system of the module non-systematic code, an encoded is achieved by transformation of the message which has least possibility of number of bits present in the message which is being converted.

Another classification is the type of systematic module unique data is sent by the transmitter which is attached by a fixed number of parity data like check bits that obtained from the data bits. The receiver applies the same algorithm when only detection of the error is required to the received data bits which is then compared with its output with the receive check bits if the values does not match, there we conclude that an error has crept at some point in the process of transmission. Error correcting codes are regularly used in lower-layer communication, as well as for reliable storage in media such as CDs, DVDs, hard disks and RAM.

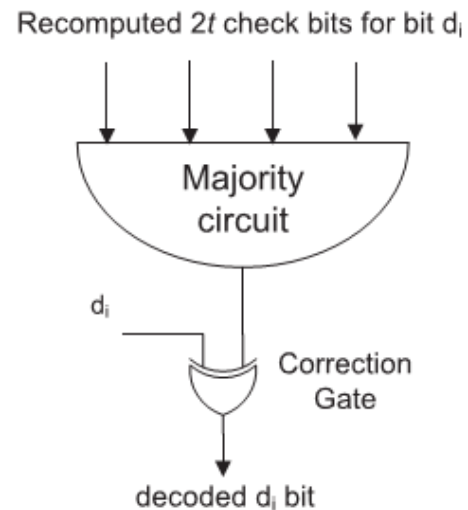


Fig.1. Illustration of OS-MLD decoding for OLS codes

Provision against soft errors that appear they as the bit-flips in memory is the main motto of error detection and correction. Several techniques are used present to midi gate upsets in memories. For example, the Bose – Chaudhuri– Hocquenghem codes, Reed–Solomon codes, punctured difference set codes, and matrix codes has been used to contact with MCUs in memories. But the above codes mentioned requires more area, power, and delay overheads since the encoding and decoding circuits are more complex in these complicated codes. Reed-Muller code is another protection code that is able to detect and correct additional error besides a Hamming code. But the major drawback of this protection code is the more area it requires and the power penalties. Reliability is a major issue for advanced electronic circuits. As technology scales, circuits become more vulnerable to error sources such as noise and radiation and also to manufacturing defects and process variations. A number of error mitigation techniques can be used to ensure that errors do not compromise the circuit functionality. Among those, Error Correction Codes (ECCs) are commonly used to protect memories or registers. Traditionally, Single Error Correction (SEC) codes that can correct one bit error in a word are used as they are simple to implement and require few additional bits. A SEC code requires a minimum Hamming distance between code-words of three. This means that if a double error occurs, the erroneous word can be at distance of one from another valid word. In that case, the decoder will miss-correct the word creating an undetected error. To avoid this issue, Single

Error Correction Double Error Detection (SEC-DED) codes can be used. Those codes have a minimum Hamming distance of four. Therefore, a double error can in the worst case cause the word to be at a distance of two of any other valid word so that miss-correction is not possible. More generally, for a code that can correct t errors, it is of interest to also detect $t+1$ errors. This reduces the probability of undetected errors that can cause Silent Data Corruption (SDC). SDC is especially dangerous as the system continues its operation unaware of the error and this can lead to further data corruption or to an erroneous behavior long after the original error occurred.

II. LITERATURE SURVEY

Most prior work in memory ECC has focused on low failure rates present at normal operating voltages, and has not focused on the problem of persistent failures in caches operating at ultra low voltage where defect rates are very high. For high defect rates, memory repair schemes based on spare rows and columns are not effective. Much higher levels of redundancy are required that can tolerate multi-bit errors in each cache line. In addition to the techniques in [Wilkerson 08] mentioned earlier, other prior work includes the two dimensional ECC proposed by [Kim 07] which tolerates multiple bit errors due to non-persistent faults, but is slow and complicated to decode. Similarly the approach in [Kim 98] can tolerate as many faults as can be repaired by spare columns, which would be insufficient in the present context with high bit-error rate. In some cases, check bits are used along with spare rows and columns to get combined fault-tolerance. In [Stapper 92], interleaved words with redundant word lines and bit lines are used in addition to the check bits on each word. [Su 05] proposes an approach where the hard errors are mitigated by mapping to redundant elements and ECC is used for the soft errors. Such approaches will not be able to provide requisite fault tolerance under high bit error rates when there are not enough redundant elements to map all the hard errors. The application of OLS codes for handling the high defect rates in low power caches as described in [Christi 09] provides a more attractive solution. While OLS codes require more redundancy than conventional ECC, the one-step majority encoding and decoding process is very fast and can be scaled up for handling large numbers of errors as opposed to BCH codes, which while providing the desired level of reliability requires multi-cycles for decoding [Lin 83]. The post-manufacturing customization approach proposed in this paper can be used to reduce the number of check bits and hence the amount of redundancy required in the memory while still providing the desired level of reliability. Note that the proposed approach does not reduce the hardware requirements for the OLS ECC as the whole code needs to be implemented on-chip since the location of the defects is not known until post-manufacturing test is performed.

III. ORTHOGONAL LATIN SQUARES CODES

The concept of Latin squares and their applications are well known [12]. A Latin square of size m is an $m * m$ matrix

that has permutations of the digits $0, 1, \dots, m-1$ in both its rows and columns. For each value of m there can be more than one Latin square. When that is the case, two Latin squares are said to be orthogonal if when they are superimposed every ordered pair of elements appears only once. Orthogonal Latin Squares (OLS) codes are derived from Orthogonal Latin squares [9]. These codes have $k=m^2$ data bits and $2tm$ check bits where t is the number of errors that the code can correct. For a Double Error Correction (DEC) code $t=2$ and therefore $4m$ check bits are used. One advantage of OLS codes is that their construction is modular. This means that to obtain a code that can correct $t+1$ errors, simply $2m$ check bits are added to the code that can correct t errors. The modular property enables the selection of the error correction capability for a given word size. As mentioned in the introduction, OLS codes can be decoded using One Step Majority Logic Decoding (OS-MLD) as each data bit participates in exactly $2t$ check bits and each other bit participates in at most one of those check bits. This enables a simple correction when the number of bits in error is t or less. The $2t$ check bits are recomputed and a majority vote is taken, if a value of one is obtained, the bit is in error and must be corrected. Otherwise the bit is correct. As long as the number of errors is t or less this ensures the error correction as the remaining $t-1$ errors can, in the worst case affect $t-1$ check bits so that still a majority of $t+1$ triggers the correction of an erroneous bit. For an OLS code that can correct t errors using OS-MLD, $t+1$ errors can cause miss-corrections. This occurs for example if the errors affect $t+1$ parity bits in which bit d_i participates as this bit will be miss-corrected. The same occurs when the number of errors is larger than $t+1$. Each of the $2t$ check bits in which a data bit participates is taken from a group of m parity bits. Those groups are bits 1 to m , $m+1$ to $2m$, $2m+1$ to $3m$ and $3m+1$ to $4m$.

1	1	1	1	0	0	0	0	0	0	0	0	0	0	0	0
0	0	0	0	1	1	1	1	0	0	0	0	0	0	0	0
0	0	0	0	0	0	0	0	1	1	1	1	0	0	0	0
0	0	0	0	0	0	0	0	0	0	0	0	1	1	1	1
1	0	0	0	1	0	0	0	1	0	0	0	1	0	0	0
0	1	0	0	0	1	0	0	0	1	0	0	0	1	0	0
0	0	1	0	0	0	1	0	0	0	1	0	0	0	1	0
0	0	0	1	0	0	0	1	0	0	0	1	0	0	0	1
0	0	0	0	0	0	0	0	0	0	0	0	0	0	0	0
1	0	0	0	0	0	0	0	0	0	0	0	0	0	0	0
0	1	0	0	0	0	0	0	0	0	0	0	0	0	0	0
0	0	1	0	0	0	0	0	0	0	0	0	0	0	0	0
0	0	0	1	0	0	0	0	0	0	0	0	0	0	0	0
0	0	0	0	1	0	0	0	0	0	0	0	0	0	0	0
0	0	0	0	0	1	0	0	0	0	0	0	0	0	0	0
0	0	0	0	0	0	1	0	0	0	0	0	0	0	0	0
0	0	0	0	0	0	0	1	0	0	0	0	0	0	0	0

Fig 2: Parity check matrix for OLS code having k and t as 16&1

The „H“ matrix for OLS codes is build from their properties. The matrix is capable of correcting single type error. By the fact that in direction of the modular structure it might be able to correct many errors. They have check bits of number „ $2tm$ “ in which, „ t “ stands for numeral of errors such that code corrects. If we wanted to correct a double bit then we have „2“ as the value of t and thereby the check bits required are $4m$. the H matrix, of Single Error Code „OLS“ code is construct as :

$$H = \begin{bmatrix} M_1 & I_{2m} \\ M_2 & I_{2m} \end{bmatrix} \quad (1)$$

One particular case for which a simple solution can be found is when $m=2t \times l$. In this case, an OLS code with a smaller data block size (12) can be used in each group. One example for $t=2$ is when $m=16$ ($k=256$) for which the OLS code with block size $k=4^2$ can be used in each group as explained before. Similarly, for $t=2$, when $k=1024$ ($m=32$) the OLS code of size $k=8^2$ can be used in each group.

V. CONCLUSION

In this brief, a CED technique for OLS codes encoders and syndrome computation was proposed. The proposed technique took advantage of the properties of OLS codes to design a parity prediction scheme that could be efficiently implemented and detects all errors that affect a single circuit node. The technique was evaluated for different word sizes, which showed that for large words the overhead is small. This is interesting as large word sizes are used, for example, in caches for which OLS codes have been recently proposed. The proposed error checking scheme required a significant delay; however, its impact on access time could be minimized. This was achieved by performing the checking in parallel with the writing of the data in the case of the encoder and in parallel with the majority voting and error correction in the case of the decoder. In a general case, the proposed scheme required a much larger overhead as most ECCs did not have the properties of OLS codes. This limited the applicability of the proposed CED scheme to OLS codes. The availability of low overhead error detection techniques for the encoder and syndrome computation is an additional reason to consider the use of OLS codes in high-speed memories and caches.

REFERENCES

- [1] C. L. Chen and M. Y. Hsiao, "Error-correcting codes for semiconductor memory applications: A state-of-the-art review," *IBM J. Res. Develop.*, vol. 28, no. 2, pp. 124–134, Mar. 1984.
- [2] E. Fujiwara, *Code Design for Dependable Systems: Theory and Practical Application*. New York: Wiley, 2006.
- [3] A. Dutta and N. A. Touba, "Multiple bit upset tolerant memory using a selective cycle avoidance based SEC-DED-DAEC code," in *Proc. IEEE VLSI Test Symp.*, May 2007, pp. 349–354.
- [4] R. Naseer and J. Draper, "DEC ECC design to improve memory reliability in sub -100nm technologies," in *Proc. IEEE Int. Conf. Electron., Circuits, Syst.*, Sep. 2008, pp. 586–589.
- [5] G. C. Cardarilli, M. Ottavi, S. Pontarelli, M. Re, and A. Salsano, "Fault tolerant solid state mass memory for space applications," *IEEE Trans. Aerosp. Electron. Syst.*, vol. 41, no. 4, pp. 1353–1372, Oct. 2005.
- [6] S. Lin and D. J. Costello, *Error Control Coding*, 2nd ed. Englewood Cliffs, NJ: Prentice-Hall, 2004.
- [7] S. Ghosh and P. D. Lincoln, "Dynamic low-density parity check codes for fault-tolerant nano-scale memory," in *Proc. Found. Nanosci.*, 2007, pp. 1–5.
- [8] H. Naeimi and A. DeHon, "Fault secure encoder and decoder for nanoMemory applications," *IEEE Trans. Very Large Scale Integr. (VLSI) Syst.*, vol. 17, no. 4, pp. 473–486, Apr. 2009.

Implementation of Crypto System Based on TEA Cryptography Application

MADDERLA RAHUL¹, B. SAGAR²

¹PG Scholar, Dept of ECE, Malla Reddy Engineering College, Hyderabad, TS, India, E-mail: rahulmadderla@gmail.com.

²Asst Prof, Dept of ECE, Malla Reddy Engineering College, Hyderabad, TS, India, E-mail: sagarboyanapalli@mrec.ac.in.

Abstract: We design a short program which will run on most machines and encipher safely. It uses a large number of iterations rather than a complicated program. It is hoped that it can easily be translated into most languages in a compatible way. It uses little set up time and does a weak non linear iteration enough rounds to make it secure. There are no preset tables or long set up times. It assumes 32 bit words.

Keywords: LPC2148 Microcontroller, Zigbee Module, LCD Display, EEPROM, Public Key Cryptography.

I. INTRODUCTION

The communication system which requires data transfer uses secured cryptographic algorithms to convert the data into an unrecognizable format. This algorithm is classified into symmetric and asymmetric, which employs private and public keys respectively. The symmetric cipher is further classified into stream and block ciphers. This proposed paper focuses on the block cipher which allows feasibility for the key generation and those generated keys are used for cryptographic applications which reduces the hardware complexity. With the proposed system implements the above statement using the light-weighted, secure and efficient block cipher TEA with different modes of communication.

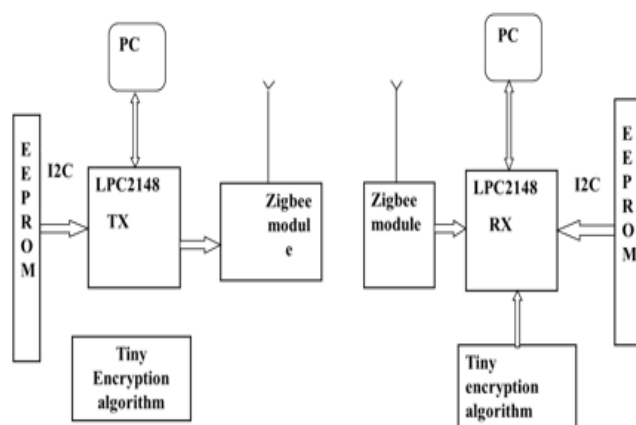


Fig.1. Block Diagram.

The two modes of communication include serial (UART) and wireless communication (using Zigbee transmission) and this proposed system uses KGU to increase the key security further. The work also extends with the random test for the generated key using the principle component analysis

method. This research work uses ARM7 LPC2148 microcontroller and the performances are analyzed by implementing with TEA which offers moderate security and simplicity in implementation processes and the wireless communication as shown in Fig.1.

II. MAIN CONCEPT

Tiny Encryption Algorithm (TEA) is a cryptographic algorithm designed for minimize the memory footprint and maximize the speed. TEA seems to be highly resistant to differential cryptanalysis, and achieves complete diffusion (where a one bit difference in the plaintext will cause approximately 32 bit differences in the cipher text) after only six rounds. Time performance on a modern desktop computer or workstation is very impressive. The TEA is a Feistel type cipher (Feistel, 1973) that uses operations from orthogonal algebraic groups. A dual shift causes all bits of the data and key to be mixed repeatedly. The key schedule algorithm is simple; the 128-bit key K is split into four 32-bit blocks $K = (K[0], K[1], K[2], K[3])$.

III. ZIGBEE TECHNOLOGY

The ZigBee offers full wireless mesh networking capable of supporting more than 64,000 devices on a single network. It is designed to connect the widest range of devices, in any industry, into a single control network. The ZigBee specification has two implementation options or Feature Sets: ZigBee and ZigBee PRO. The ZigBee specification enhances the IEEE 802.15.4 standard by adding network and security layers and an application framework. From this foundation, Alliance developed standards, technically referred to as public application profiles, can be used to create a multi-vendor interoperable solutions. For custom application where interoperability is not required, manufacturers can create their own manufacturer specific profiles ZigBee protocols are intended for use in embedded applications requiring low data rates and low power consumption. ZigBee's current focus is to define a general-purpose, inexpensive, self-organizing mesh network that can be used for industrial control, embedded sensing, medical data collection, smoke and intruder warning, building automation, home automation, etc. The resulting network will use very small amounts of power so individual devices might run for a year or two using the originally installed battery.

IV. OBSERVATION AND RESULT

Encryption of cipher texts with more than six rounds produced a very good mixture of intermediate values and showed high resistance to cryptanalytic attacks. With this few exceptions, the research concludes TEA as a best fit cryptographic algorithm for small devices where memory and power are primary.

Advantages: The Tiny encryption algorithm is mainly compromise for safety, ease of implementation, lack of specialized tables, and reasonable performance. It has many advantages over the DES encryption algorithm. The TEA is used to encrypt the plain text with the mix of key at the transmitter and its corresponding decryption algorithm is used at the receiver to obtain the plain text from the ciphered text.

V. CONCLUSION

This research presented a comprehensive in-depth perceptive of TEA with Cryptanalysis. This research implemented the TEA with auto key generation system and analyzed the published attacks, weakness of TEA.

Future Scope: We feel that cryptanalysis of TEA like feistel ciphers is far from complete task. This section presents several directions for future research.

- Finding more equivalent keys (if exists) for TEA.
- Extending the results in this thesis to study other feistel ciphers.
- Investigation of key space for other fiestel ciphers.

VI. REFERENCES

- [1] Biham, E., & Shamir, A. (1992). Differential cryptanalysis of the data encryption Standard. New York: Springer-Verlag.
- [2] Feistel, H. (1973, May). "Cryptography and computer privacy." Scientific American, 228.
- [3] Kelsey, J., Schneier, B., & Wagner, D. (1997). Related key cryptanalysis of 3-WAY, Biham-DES, CAST, DES-X, NewDES, RC2, and TEA. In Information and Communications Security—Proceedings of ICICS, 1334.

Obstacle Detection in Textured Environment by using Color Coherence

V. DATTA KIRAN¹, DR. M. J. C. PRASAD²

¹PG Scholar, Dept of ECE, Malla Reddy Engineering College, JNTUH, Hyderabad, TS, India,
E-mail: dattakiran2010@gmail.com.

²Associate Professor, Dept of ECE, Malla Reddy Engineering College, JNTUH, Hyderabad, TS, India,
E-mail: jagdissh@mrec.ac.in.

Abstract: Obstacle detection algorithm that makes use of color information and color coherence vectors for robust obstacle detection. The algorithm makes use of color cue to classify a pixel in an image as an obstacle or a path. Color is one of the prominent image features. Color information is readily available as input from a color camera. Our algorithm makes use of coherence vectors for representation and matching instead of histograms. A color histogram provides no spatial information. It merely describes the color information present in an image. Color coherence vectors represent pixels as either coherent or incoherent. Color coherence vectors prevent coherent pixels from getting matched with incoherent pixels. The color histogram cannot make such fine distinction. This paper a novel algorithm for obstacle detection is proposed that makes use of color cue and color coherence vectors for robust obstacle detection. The algorithm detects obstacles based on the appearance of individual pixels. Whether an individual pixel belongs to an obstacle or a navigable path is determined by a color classifier. The coherence vectors are better than histograms as they incorporate spatial information. Moreover, our approach does not have any learning requirement prior to the use of classifier.

Keywords: Obstacle Detection Algorithm, Color Histogram, Color Coherence Vectors.

I. INTRODUCTION

To get the perception of the environment around them, humans depends upon five senses – vision, hearing, smell, touch and taste. Out of these, vision is undoubtedly the one that people depend upon the most for the performance of their everyday activities. Most people cannot even imagine what life would be if they lose it- unable to read, requiring assistance for daily activities and difficulty in recognizing near and dear ones. This is however, a hardcore reality for nearly 45 million people worldwide, who are blind. A further 135 million people have severely impaired vision in both the eyes and additional 100 million people suffer from monocular vision loss. These visually impaired people experience serious difficulties in leading an independent life due to the reduced perception of the environment. Most of them confront serious difficulties in mobility and navigation

when they find themselves in new environment. Obstacle detection is one of the major problems to be solved to ensure safe navigation for visually impaired users. The visually impaired people experience serious difficulties in leading an independent life due to the reduced perception of the environment.

Most of them confront serious difficulties in mobility and navigation when they find themselves in new environment. Obstacle detection is one of the major problems to be solved to ensure safe navigation for visually impaired users. To avoid this problem we proposed this novel algorithm. In this paper, a novel algorithm for obstacle detection is proposed that makes use of color cue and color coherence vectors for robust obstacle detection. The algorithm detects obstacles based on the appearance of individual pixels. Whether an individual pixel belongs to an obstacle or a navigable path is determined by a color classifier. The color classifier makes use of color information which is readily available as input in a color image. Color is one of the prominent image features and easy to process. Our approach makes use of coherence vectors instead of histogram for color representation and matching. The coherence vectors are better than histograms as they incorporate spatial information. Moreover, our approach does not have any learning requirement prior to the use of classifier. Whatever is left of this paper is organized as follows. Segment II presents the literature survey. Segment III locations the proposed system taking into account and HVS color coherence analysis, results and discussion are given in Section IV. At last, conclusions are made in Section VI.

II. LITERATURE SURVEY

In this chapter, we will discuss about the information found by study and research that is critical and have an important value in the contribution of the whole paper. It also gives some basic knowledge or theoretical base and is used as a foundation to successfully achieve the main objectives. Most of the literatures are from the related articles, journals, books and previous works of the same fields. These literatures are then compiled and use as a guidance to the work of this paper. In the implementation of certain human vision properties in the real time image

processing for vision substitution by acoustic transform of visual information. An experimental prototype has been developed with vision sensor fixed in a headgear and stereo earphone and a laptop computer interconnected. Captured image from vision sensor is processed and transformed into a stereo sound through the earphone. The image processing is critically designed as a model of human vision. It involves edge detection, background suppression, normalization and stepped weightage. The scheme is tested with a blind volunteer and his suggestions in formatting the sound pattern are considered. The software module suits most of the commercially available vision sensors.

In [2], Color histograms are used to compare images in many applications. Their advantages are efficiency, and insensitivity to small changes in camera viewpoint. However, color histograms lack spatial information, so images with very different appearances can have similar histograms. For example, a picture of fall foliage might contain a large number of scattered red pixels; this could have a similar color histogram to a picture with a single large red object. We describe a histogram-based method for comparing images that incorporates spatial information. We classify each pixel in a given color bucket as either coherent or incoherent, based on whether or not it is part of a large similarly-colored region. A color coherence vector (CCV) stores the number of coherent versus incoherent pixels with each color. By separating coherent pixels from incoherent pixels, CCV's provide distinctions than color histograms. CCV's can be computed at over 5 images per second on a standard workstation. A database with 15,000 images can be queried for the images with the most similar CCV's in less than 2 seconds. We show that CCV's can give superior results to color histograms for image retrieval.

A. Color Coherence Vector

Color Coherence Vector (CCV) is a more complex method than Color Histogram. It classifies each pixel as either coherent or incoherent. Coherent pixel means that it's part of a big of connected component (CC) while incoherent pixel is part of a small connected component. Of course first we define the criteria which we use to measure whether a connected component is big or not.

Feature Extraction Algorithm

- Blur the image (by replacing each pixel's value with the average value of the 8 adjacent pixels surrounding that pixel).
- Discretize the color-space (images' colors) into n distinct color.
- Classify each pixel either as coherent or incoherent. This is computed by
 - Find connected components for each discretized color.
 - Determine tau's value (Tau is a user-specified value (Normally it's about 1% of image's size)).
 - Any Connected Component has number of pixels more than or equal to tau then its pixels are considered coherent and the others are incoherent.

- For each color compute two values (C and N).
 - C is the number of coherent pixels.
 - N is the number of incoherent pixels.

It's clear that the summation of all color's C and N = number of pixels.

B. Matching Function

To compare 2 images a, b.

C_i : number of coherent pixels in color i.

N_i : number of incoherent pixels in color i.

$$D(a, b) = \sum_{i=0}^n (|a_{C_i} - b_{C_i}|) + (|a_{N_i} - b_{N_i}|) \quad (1)$$

Let's take this example to make algorithm's steps clear. Assuming that the image has 30 colors instead of 16777216 colors (256*256*256).

13	15	11	17	15
27	10	12	25	22
23	4	25	11	9
29	3	21	23	8
1	9	24	2	7

Now we'll discredited the colors to only three colors (0:9, 10:19, 20, 29).

1	1	1	1	1
2	1	1	2	2
2	0	2	1	0
2	0	2	2	0
0	0	2	0	0

Assuming that our tau is 4

For color 0 we have 2 CC (8 coherent pixels)

For color 1 we have 1 CC (8 coherent pixels)

For color 2 we have 2 CC (6 coherent pixels and 3 incoherent pixels)

So finally our feature vector is

Color	0	1	2
C	8	8	6
N	0	0	3

C. Drawbacks of Color Coherence Vector

Now we see that Color Coherence Vector method considers information about color spatial distribution between pixels in its coherence component. But this method has some drawbacks. The remaining part of this post will discuss two main drawbacks of it. Coherent pixels in CCV represent the

Obstacle Detection in Textured Environment by using Color Coherence

pixels which are inside remarkable components in image. But what we combined these entire components into one component as shown in Fig.1. We will have only one component the number of its pixels will be obviously equal to the number of pixels in the remarkable components. To make it clear look at these pictures assuming tau equals to 8.

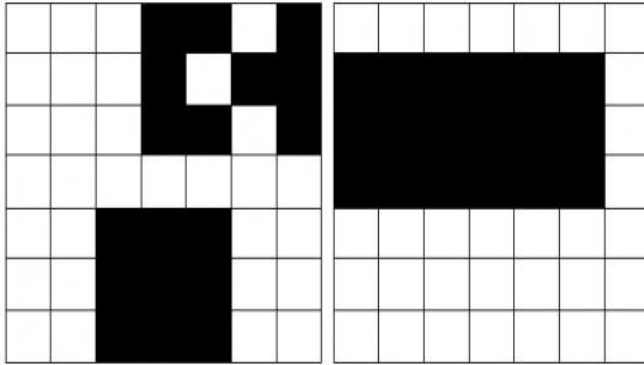


Fig.1. Combining entire components into one component.

Although they are different pictures but they have the same CCV. Another problem we may encounter is the positions of these remarkable connected components relative to each other. These pictures have the same CCV with different appearance as shown in Fig.2.

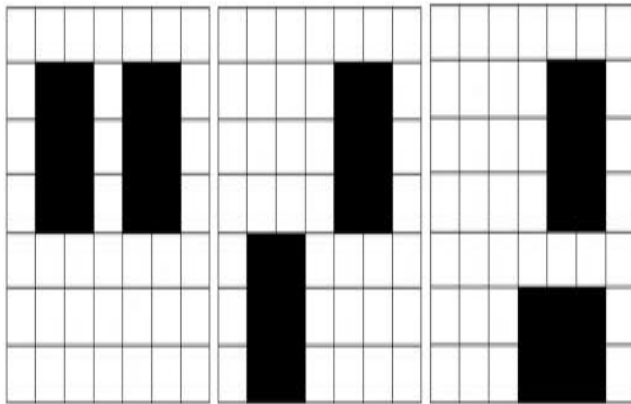


Fig.2. The above pixels having same CCV with different appearance.

There are many solutions to these problems. Most of them add another dimension in feature vector which is components' position relative to each other. So this dimension is used in the comparison in order to differentiate between pictures that have the same CCV. The color coherency vector (Color Coherence Vector, CCV) is histogram - method was based for the determination of the similarity between two pictures. The disadvantage of the pure color histograms is the absence of spatial information. Differently appearing pictures can possess very similar color histograms, then for example a picture with a chessboard sample possesses the same histogram as one in that half of the picture is black and the other one knows. Color coherency vectors do not know the exact positions of the objects in the display space, but they can differentiate

whether a certain color with respect to few large or with respect to many small ranges occur. Thus this method makes a finer distinction possible between pictures contrary to pure color histograms.

III. PROPOSED METHODOLOGY

The system consists of two parts- storing ground representation in form of color coherence vectors and a classifier. The classifier compares a patch of pixels in the acquired images with the stored ground representation to decide if a patch is a path or an obstacle. The system makes the following assumptions that are reasonable for a variety of indoor environments:

- Ground plane is flat.
- Obstacles differ in appearance from the ground, protrude out from the ground plane and there are no overhanging obstacles.
- Initially, a small area ahead of the user is free from obstacles.

The work assumes that the ground plane is flat and is free from steps, stairs and ramps. Steps, stairs and ramps can be better detected by making use of range based stereo vision instead of appearance based monocular vision. The second assumption allows us to distinguish obstacles from the ground and estimate the distance of obstacles from the user. If the first two assumptions are satisfied then, the distance is monotonically increasing function of the pixel height in the image.

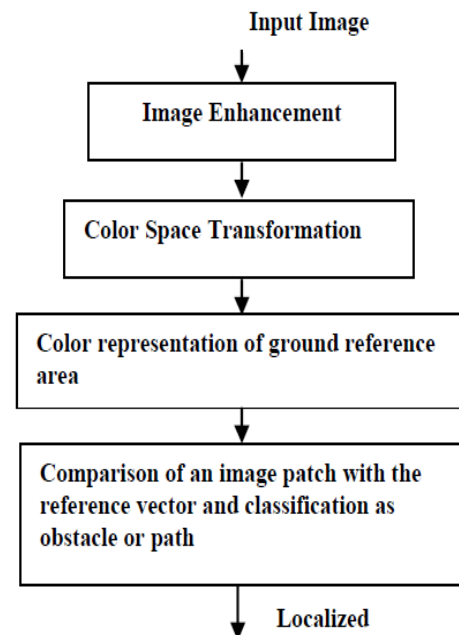


Fig.3. CCV Algorithm Steps.

The algorithm consists of steps listed below and shown in Fig.3.

- Image enhancement.
- Transformation to color space.
- Color representation of reference area in form of coherence vectors.

- Comparison of an image patch with reference vectors for obstacle detection.

A. RGB Color Model

The RGB (Red, Green, Blue) color model is an especially important one in digital image processing because it is used by most digital imaging devices (e.g., monitors and color cameras). In the RGB model, a color is expressed in terms that define the amounts of Red, Green and Blue light it contains. In a 24-bit, color image, pure red would be represented as 255/000/000, where 255 represents the highest level of red light possible, untainted by any green (000) or blue (000) light. Various combinations of the Red, Green and Blue values allow us to define 224 (over 16 million) colors. (See also RGB image class.)

B. HIS Color Model

The HSI (Hue, Saturation, Intensity) color model describes a color in terms of how it is perceived by the human eye. "Hue" is what an artist refers to as "pigment"; it is what we think of as "color" -- yellow, orange, cyan and magenta are examples of different hues. An artist usually starts with a highly saturated (i.e., pure), and intense (i.e., bright) pigment, and then adds some white to reduce its saturation and some black to reduce its intensity. Red and Pink are two different "saturation" of the same hue, Red. The HSI model is useful when processing images to compare two colors, or for changing a color from one to another. For example, changing a value from Cyan to Magenta is more easily accomplished in an HSI model; only the H value needs to be changed (from 180 to 300). Making the same change in an RGB view is less intuitive; since you must know the correct amounts of Red, Green and Blue needed to create Magenta. The HSI model is also a more useful model for evaluating or measuring an object's color characteristics, such as the "redness" of a berry or the "yellowness" of an autumn leaf.

C. HSV Color Model

Hue, Saturation, Value or HSV is a color model that describes colors (hue or tint) in terms of their shade (saturation or amount of gray) and their brightness (value or luminance). The HSV color wheel may be depicted as a cone or cylinder. Instead of Value, the color model may use Brightness, making it HSB (Photoshop uses HSB).

- Hue is expressed as a number from 0 to 360 degrees representing hues of red (starts at 0), yellow (starts at 60), green (starts at 120), cyan (starts at 180), blue (starts at 240), and magenta (starts at 300).
- Saturation is the amount of gray (0% to 100%) in the color.
- Value (or Brightness) works in conjunction with saturation and describes the brightness or intensity of the color from 0% to 100%.
- The hue (H) of a color refers to which pure color it resembles. All tints, tones and shades of red have the same hue.

Hues are described by a number that specifies the position of the corresponding pure color on the color wheel, as a fraction between 0 and 1. Value 0 refers to red; 1/6 is yellow; 1/3 is green; and so forth around the color wheel.

- The saturation (S) of a color describes how white the color is. A pure red is fully saturated, with a saturation of 1; tints of red have saturations less than 1; and white has a saturation of 0.
- The value (V) of a color, also called its lightness, describes how dark the color is. A value of 0 is black, with increasing lightness moving away from black.

This diagram, called the single-hexcone model of color space, can help you visualize the meaning of the H, S, and V parameters as shown in Fig.4.

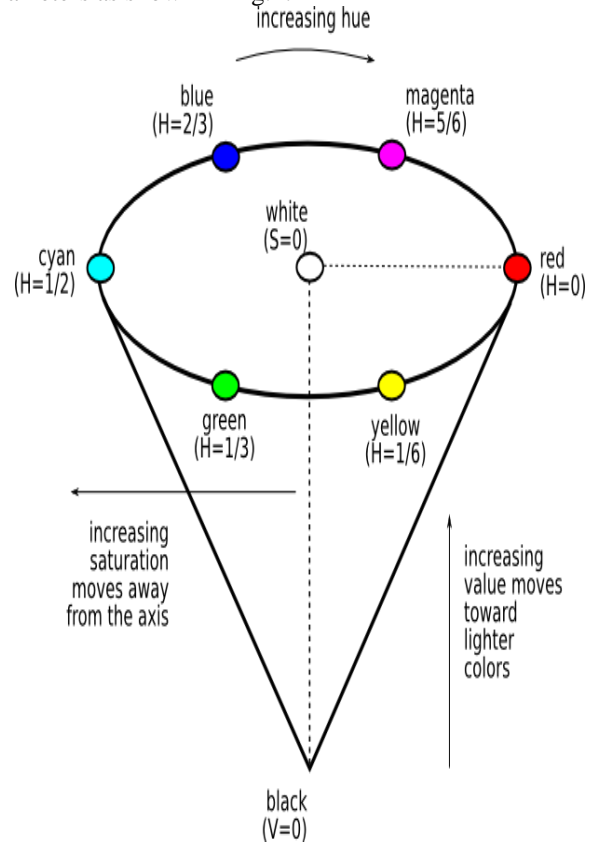


Fig.4. Single hexcone model of color space.

- The outer edge of the top of the cone is the color wheel, with all the pure colors. The H parameter describes the angle around the wheel.
- The S (saturation) is zero for any color on the axis of the cone; the center of the top circle is white. An increase in the value of S corresponds to a movement away from the axis.
- The V (value or lightness) is zero for black. An increase in the value of V corresponds to a movement away from black and toward the top of the cone.

IV. SIMULATION RESULTS

In this chapter all the simulation results which are done using Xilinx ise 9.1 are shown in below Figs.5 to 10.

Obstacle Detection in Textured Environment by using Color Coherence

A. Simulation Results

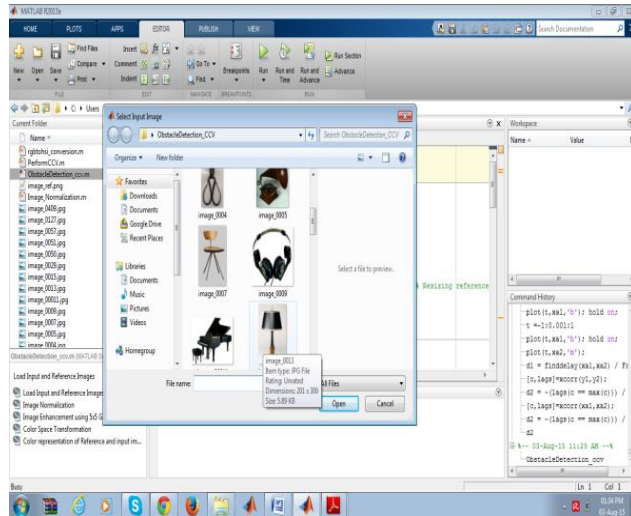


Fig.5. Input selection form.

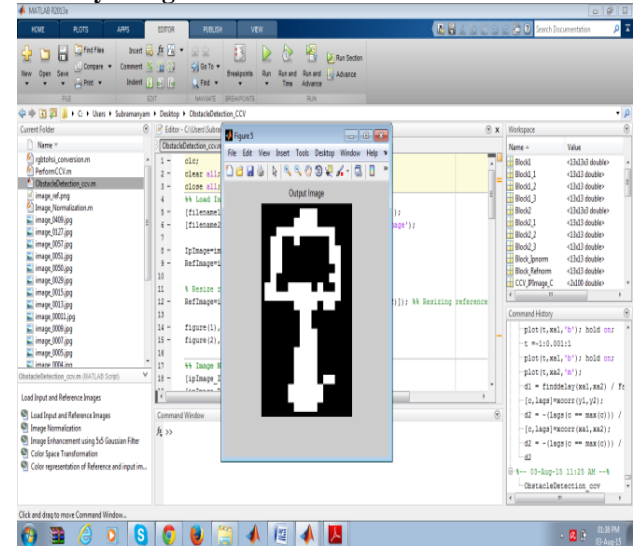


Fig.8. Obstacle detected image using CCV.

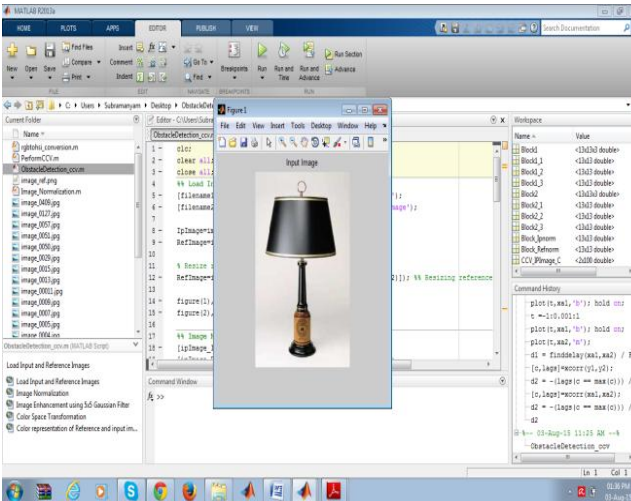


Fig.6. Input selected image.

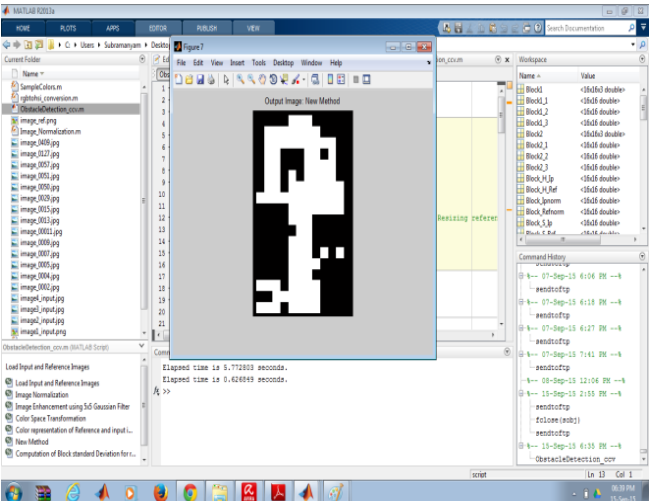


Fig.9. Obstacle detection using HSV

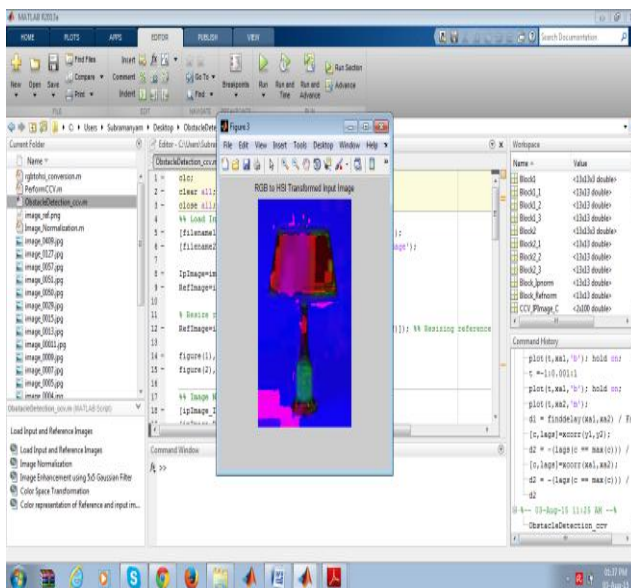


Fig.7. RGB to HIS transformed original image.

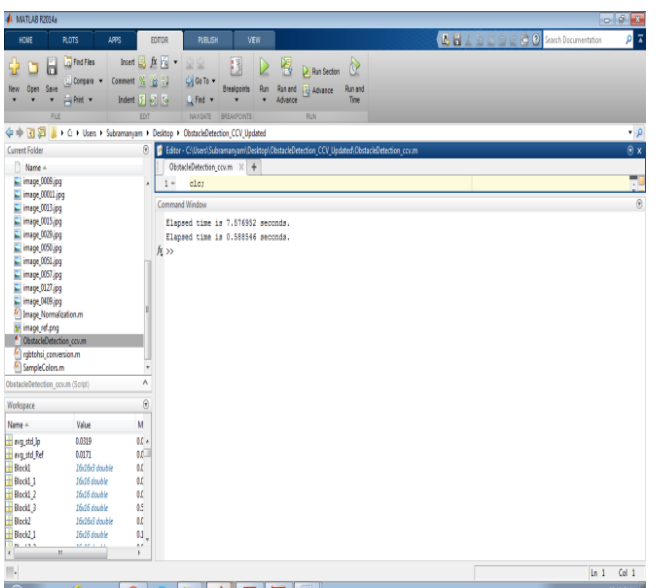


Fig.10. Time difference between HSI and HSV.

V. CONCLUSION

An efficient algorithm for obstacle detection that is using the reference of color cue and color coherence vector is presented. The algorithm is used in guidance system for visually impaired and helps them in navigating both indoor and outdoor environments. The algorithm makes use of color coherence vectors which can be computed in linear time. The color coherence vector matching is computationally inexpensive and hence the algorithm has good efficiency. Moreover, the algorithm does not have any learning requirements. We are using color cue and coherence as our main area of concern rather than the color histogram, which gives no spatial information. HIS color model is used in this project for convert the original image into HSI image and we also proposed HSV color model for same obstacle detection.

VI. REFERENCES

- [1] E. T. Cunningham and J. Blindness, "A global priority for the twenty-first century," presented at Special theme report on blindness, Bulletin of the World Health Organization, 2001.
- [2] J. P. Whitcher and C. Blindness: "A global perspective," presented at Special theme report on blindness, Bulletin of the World Health Organization, 2001.
- [3] G. Pass, R. Zabih, and J. Miller, "Comparing Color images using Color Coherence Vectors," in Proc. 4th ACM International conference on Multimedia, 1997.
- [4] G. Sainarayanan, "Incorporating certain human vision properties in vision substitution by stereo acoustic transform," Int. symp. on Signal processing and its applications, pp. 13-16, Aug. 2001.
- [5] W. Miled, "Robust Obstacle detection based on Dense disparity maps," Int. conf. on computer aided systems theory- EUROCAST, 2007.
- [6] F. Ferrari et al., "A stereo-vision system for real time obstacle avoidance in unknown environment," Int. workshop on Intelligent Robots and Systems, 1990.
- [7] David Aldavert, "Obstacle Detection and alignment using an stereo camera pair," Technical report, Artificial Intelligence research institute, Spain, 2008.
- [8] T. Hong, "Obstacle detection using a TOF Range Camera for Indoor AGV Navigation," Int. Conf. on advanced robotics, 2005.
- [9] N. Chumerin, "Ground plane estimation based on dense stereo disparity," Int. Conf. on neural networks and artificial intelligence, 2008.
- [10] I. Ulrich, "Appearance based obstacle detection with Monocular color vision," AAAI National Conference on Artificial Intelligence, July-August 2000.
- [11] C. N. Viet, "An efficient obstacle detection algorithm using color and texture," World Academy of Science and Technology, 2009.

VLSI DESIGN OF DATA ENCODING SCHEMES FOR LOW POWER

Badugu Chaitanya¹, V.Srinivas²

¹P.G Scholar, VLSI, Malla Reddy Engineering College

²Assistant Professor, Dept. of ECE, Malla Reddy Engineering College

Abstract: As technology improves, the power dissipated by the links of a network-on-chip (NoC) starts to compete with the power dissipated by the other elements of the communication subsystem, namely, the routers and the network interfaces (NIs). Here, we present a set of data encoding schemes to reduce the power dissipated by the links of an NoC. In this paper, the encoder in LDPC is replaced with our data encoding schemes in order to reduce the power consumption in Low Density Parity Check Techniques. Experiments carried out on both synthetic and real traffic scenarios show the effectiveness of the proposed schemes.

Index Terms: Data encoding, interconnection on chip, low density parity check, majority logic decoding, power analysis.

I. DATA ENCODING TECHNIQUES

The data encoding techniques are developed to reduce the power consumption caused by the transitions in the interconnect on the chip. The data encoding techniques are based on reducing the number of transitions by considering the types of transitions in the interconnects and by considering them as discussed in the table below and also consider the transitions as different types of inversions available for us. The different types of inversions available for us are odd inversion, full inversion and even inversions. By reducing these inversions we can control the number of transitions in the interconnects which reduces the power consumption caused by these transitions in the links.

Time	Normal			Odd Inverted		
	Type I			Types II, III, and IV		
$t-1$	00, 11	00, 11, 01, 10	01, 10	00, 11	00, 11, 01, 10	01, 10
t	10, 01	01, 10, 00, 11	11, 00	11, 00	00, 11, 01, 10	10, 01
	T1*	T1**	T1***	Type III	Type IV	Type II
$t-1$	Type II			Type I		
t	01, 10			01, 10		
	10, 01			11, 00		
$t-1$	Type III			Type I		
t	00, 11			00, 11		
	11, 00			10, 01		
$t-1$	Type IV			Type I		
t	00, 11, 01, 10			00, 11, 01, 10		
	00, 11, 01, 10			01, 10, 00, 11		

By assuming these we have designed three schemes which are as follows:

A. Scheme I

In scheme I, we focus on reducing the numbers of Type I transitions (by converting them to Types III and IV transitions) and Type II transitions (by converting them to Type I transition). The scheme compares the current data

with the previous one to decide whether odd inversion or no inversion of the current data can lead to the link power reduction.

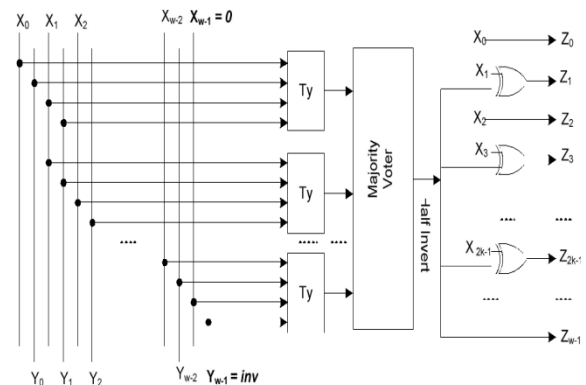
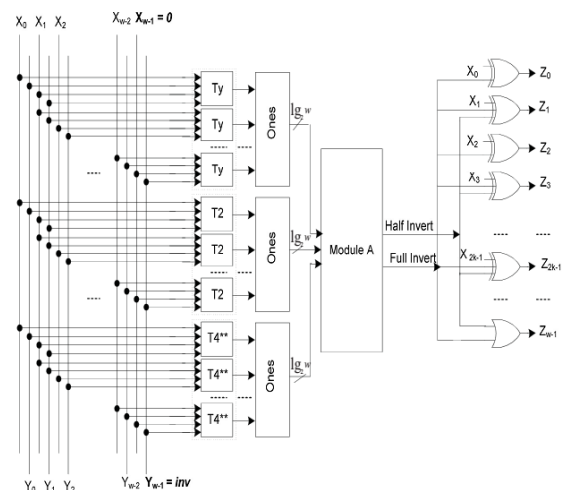


Fig. 1. Encoder architecture scheme I. (a) Circuit diagram [27]. (b) Internal view of the encoder block

B. Scheme II

In the proposed encoding scheme II, we make use of both odd (as discussed previously) and full inversion. The full inversion operation converts Type II transitions to Type IV transitions. The scheme compares the current data with the previous one to decide whether the odd, full, or no inversion of the current data can give rise to the link power reduction.



C. Scheme III

In the proposed encoding Scheme III, we add even inversion to Scheme II. The reason is that odd inversion converts some of Type I (T1***) transitions to Type II transitions. As can be observed from Table II, if the flit is even inverted, the transitions indicated as T** 1 / T1*** in the table are converted to Type IV/Type III transitions. Therefore, the

even inversion may reduce the link power dissipation as well. The scheme compares the current data with the previous one to decide whether odd, even, full, or no inversion of the current data can give rise to the link power reduction.

Low Density Parity Check Code:

The LDPC code is based on a set of one or more fundamental LDPC codes. Each of the fundamental codes is a systematic linear block code. The fundamental codes can accommodate various code rates and packet sizes.

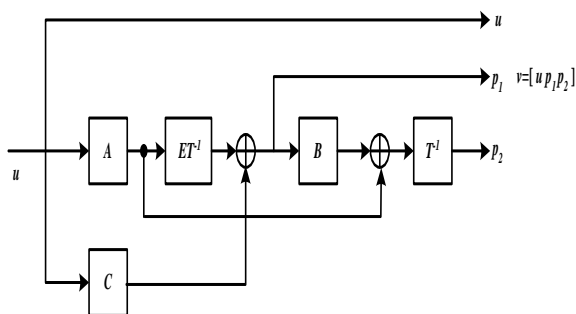
Each LDPC code in the set of LDPC codes is defined by a matrix H of size m -by- n , where n is the length of the code and m is the number of parity check bits in the code. The number of systematic bits is $k=n-m$.

The matrix H is defined as

$$H = \begin{bmatrix} P_{0,0} & P_{0,1} & P_{0,2} & \cdots & P_{0,n_b-2} & P_{0,n_b-1} \\ P_{1,0} & P_{1,1} & P_{1,2} & \cdots & P_{1,n_b-2} & P_{1,n_b-1} \\ P_{2,0} & P_{2,1} & P_{2,2} & \cdots & P_{2,n_b-2} & P_{2,n_b-1} \\ \vdots & \vdots & \vdots & \cdots & \vdots & \vdots \\ P_{m_b-1,0} & P_{m_b-1,1} & P_{m_b-1,2} & \cdots & P_{m_b-1,n_b-2} & P_{m_b-1,n_b-1} \end{bmatrix} = P^{H_b}$$

where $P_{i,j}$ is one of a set of z -by- z permutation matrices or a z -by- z zero matrix.

The encoding of a packet at the transmitter generates parity-check bits $p=(p_0, \dots, p_{m-1})$ based on an information block $s=(s_0, \dots, s_{k-1})$, and transmits the parity-check bits along with the information block. Because the current symbol set to be encoded and transmitted is contained in the transmitted codeword, the information block is also known as systematic bits. The encoder receives the information block $s=(s_0, \dots, s_{k-1})$ and uses the matrix H_{bm} to determine the parity-check bits. The expanded matrix H is determined from the model matrix H_{bm} . Since the expanded matrix H is a binary matrix, encoding of a packet can be performed with vector or matrix operations conducted over GF.



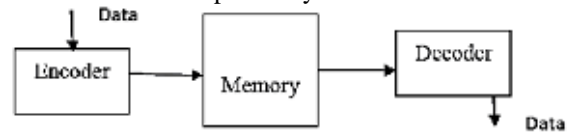
Block diagram of the encoder architecture for the block LDPC code

Using two decoding techniques majority logic decoding and majority logic decoder/detector in LDPC to reduce the delay occurring in these techniques.

Majority Logic Decoding:

Majority-logic decoding is a simple and effective scheme for

decoding certain classes of block codes, especially for decoding certain classes of cyclic codes. Majority logic decoding is a method to decode repetition codes, based on the assumption that the largest number of occurrences of a symbol was the transmitted symbol. It will increase the power consumption. Syndrome vector is oldest technology, which is used to detect the error in the code word. Hamming code is one of the examples of syndrome decoder.



Simple memory system schematic

Majority Logic detector/decoder:

The ML detector/decoder (MLDD) has been implemented using the Euclidean Geometry LDPC. G-LDPC codes there is an subclass of codes that is one step majority logic decodable (MLD) This method is very practical to generate and check all possible error combinations for codes with small words and affected by a small number of bit flips. When the size of code and the number of bit flip increases, it is difficult to exhaustively test all possible combinations. Therefore the simulations are done in two ways, the error combinations are exhaustively checked when it is feasible and in the rest of the cases the combinations are checked randomly. Since it is convenient to first describe the chosen design and also for simplicity.

II. DATA ENCODING TECHNIQUES USING LDPC

These data encoding schemes which are discussed in the above sections are replaced by these encoding schemes instead of the encoder in the LDPC block:

- Scheme1 encoding technique in LDPC.
- Scheme2 encoding technique in LDPC.
- Scheme3 encoding technique in LDPC.

Scheme1 encoding technique in LDPC:

The proposed encoding architecture, which is based on the odd invert condition defined is shown in Fig. 1. We consider a link width of w bits. If no encoding is used, the body flits are grouped in w bits by the NI and are transmitted via the link. In our approach, one bit of the link is used for the inversion bit, which indicates if the flit traversing the link has been inverted or not.

This encoding technique which is scheme 1 of our encoding techniques in used in low density parity check of majority logic decoding are replaced with our encoding scheme1 technique.

Scheme2 encoding technique in LDPC:

The principles of this encoder are similar to those of the encoder implementing Scheme I. The proposed encoding architecture, which is based on the odd invert condition and the full invert condition, is shown in Fig. 2. Here again, the w th bit of the previously and the full invert operating

condition is shown in Fig. 2. Here again, the with bit of the previously encoded body flit is indicated with inv which defines if it was odd or full inverted (inv = 1) or left as it was (inv = 0). In this encoder, in addition to the Ty block in the Scheme I encoder, we have the T2 and T4** blocks which determine if the inversion based on the transition types T2 and T4** should be taken place for the link power reduction. The second stage is formed by a set of 1s blocks which count the number of 1s in their inputs. The output of these blocks has the width of log2 w. The output of the top 1s block determines the number of transitions that odd inverting of pair bits leads to the link power reduction. The middle 1s block identifies the number of transitions whose full inverting of pair bits leads to the link power reduction. Finally, the bottom 1s block specifies the number of transitions whose full inverting of pair bits leads to the increased link power.

The encoding technique discussed above which is scheme2 which is based on the logic of full inversion which is the proposed method of the odd inversion which is scheme1. The technique which is mentioned above is ldpc using shem1 now is replaced with scheme2 in the ldpc and thereby reducing some amount of power compared from scheme1.

Scheme3 encoding technique in LDPC:

The operating principles of this encoder are similar to those of the encoders implementing Schemes I and II. The proposed encoding architecture, which is based on the even invert condition of (28), the full invert condition of (29), and the odd invert condition of (30), is shown in Fig. 4.

The (inv = 0). The first stage of the encoder determines the transition types while the second stage is formed by a set of 1s blocks which count the number of ones in their inputs. In the first stage, we have added the Te blocks which determine if any of the transition types of T2, T1**, and T1*** is detected for each pair bits of their inputs. For these transition types, the even invert action yields link power reduction. Again, we have four Ones blocks to determine the number of detected transitions for each Ty, Te, T2, T4** blocks. The output of the Ones blocks are inputs for Module C. This module determines if odd, even, full, or no invert action corresponding to the outputs "10," "01," "11," or "00," respectively, should be performed.

The encoding technique discussed above which is scheme3 which is based on the logic of even inversion which is the proposed method of the full inversion which is scheme2. The technique which is mentioned above is ldpc using shem1 now is replaced with scheme2 in the ldpc and thereby reducing some amount of power compared from scheme2. Hence, we analyzed that scheme3 is the one which is used in LDPC technique.

III. RESULTS

Power report for scheme1:

Name	Power (w)	Used	Total Available	Utilization (%)
Clocks	0.001	1	—	—
Logic	0.000	96	3312	1.0
Signals	0.000	149	—	—
I/Os	0.011	102	232	44.0
Total Quiescent Power	0.001			
Total Dynamic Power	0.012			
Total Power	0.013			

Area report for scheme1:

```
Total REAL time to Xst completion: 7.00 secs
Total CPU time to Xst completion: 6.99 secs

-->

Total memory usage is 161352 kilobytes

Number of errors : 0 ( 0 filtered)
Number of warnings : 0 ( 0 filtered)
Number of info : 0 ( 0 filtered)
```

Power report for scheme2:

Name	Power (w)	Used	Total Available	Utilization (%)
Clocks	0.001	1	—	—
Logic	0.000	96	3312	1.0
Signals	0.000	149	—	—
I/Os	0.002	102	232	44.0
Total Quiescent Power	0.001			
Total Dynamic Power	0.003			
Total Power	0.004			

Area report for scheme2:

```
Total REAL time to Xst completion: 7.00 secs
Total CPU time to Xst completion: 6.39 secs

-->

Total memory usage is 161352 kilobytes

Number of errors : 0 ( 0 filtered)
Number of warnings : 0 ( 0 filtered)
Number of info : 0 ( 0 filtered)
```

Power report for scheme3:

Name	Power (w)	Used	Total Available	Utilization (%)
Clocks	0.001	1	—	—
Logic	0.000	96	3312	1.0
Signals	0.000	149	—	—
I/Os	0.002	102	232	44.0
Total Quiescent Power	0.001			
Total Dynamic Power	0.003			
Total Power	0.004			

Area report for scheme3:

```
Total REAL time to Xet completion: 6.00 secs
Total CPU time to Xet completion: 6.01 secs

-->

Total memory usage is 161352 kilobytes

Number of errors   :    0 (    0 filtered)
Number of warnings :    0 (    0 filtered)
Number of infos    :    0 (    0 filtered)
```

IV. CONCLUSION

In this paper, we have presented data encoding techniques which are used in the place of encoders in LDPC which reduces the power consumption by eliminating the transitions as discussed before. Here, we analyzed the power consumption for these three schemes and compared their power and area performances.

REFERENCES

- [1] International Technology Roadmap for Semiconductors. (2011) .
- [2] M. S. Rahaman and M. H. Chowdhury, "Crosstalk avoidance and error correction coding for coupled RLC interconnects," in Proc. IEEE Int. Symp. Circuits Syst., May 2009, pp. 141–144.
- [3] W. Wolf, A. A. Jerraya, and G. Martin, "Multiprocessor system-on-chip MPSoC technology," IEEE Trans. Comput.-Aided Design Integr. Circuits Syst., vol. 27, no. 10, pp. 1701–1713, Oct. 2008.
- [4] Pedro Reviriego, Juan A. Maestro, and Mark F. Flanagan, "Error Detection in Majority Logic Decoding of Euclidean Geometry Low Density Parity Check (EG-LDPC) Codes," IEEE Trans. Very Large Scale Integra. (VLSI) syst., vol. 21, no. 1, pp.156-159, Jan. 2013.
- [5] Youn Sung Park, Yaoyu Tao, Zhengya Zhang, "A 1.15Gb/s Fully Parallel Nonbinary LDPC Decoder with Fine-Grained Dynamic Clock Gating," 2013 IEEE International Solid-State Circuits Conference.

Implementation of an Efficient Image Denoising Algorithm on FPGA

VARKOLU KIRAN VARMA¹, A. R. S. BALAJI²

¹PG Scholar, Dept of VLSI, Malla Reddy Engineering College, Hyderabad, TS, India.

²Assistant Professor, Dept of VLSI, Malla Reddy Engineering College, Hyderabad, TS, India.

Abstract: A novel plan of victimisation median deviation parameter in estimating the noise within the pictures is proposed and with success applied to each grey level also as color pictures. The median filter that is incredibly popular in removing the salt and pepper noise from the pictures has undergone several changes in recent past. to the present changed median filter the thought of median deviation is side and employed in estimating and removing the noise. The projected methodology is enforced by implemented victimisation the Spartan 3EDK Filed Programmable Device. The results area unit found to be higher than earlier methods and additionally strong in terms of protective the distinction and fine details of the image even at high noise densities.

Keywords: Image Improvement Issue (IEF), Peak Signal/Noise Ratio (PSNR), Adaptive Median Filter (AMF).

I. INTRODUCTION

Impulse noise in pictures is gift owing to bit errors in transmission or introduced throughout the signal acquisition stage. There square measure 2 kinds of impulse noise, they're salt and pepper noise and random valued noise. Salt and pepper noise will corrupt the photographs wherever the corrupted picture element takes either maximum or minimum grey level. Many nonlinear filters have been projected for restoration of pictures contaminated by salt and pepper noise. Among these normal median filter has been established as reliable technique to get rid of the salt and pepper noise while not damaging the sting details. However, the major disadvantage of ordinary Median Filter (MF) is that the filter is effective solely at low noise densities. When the noise level is over five hundredth the sting details of the first image will not be preserved by normal median filter. Adaptive Median Filter (AMF) performs well at low noise densities. however at high noise densities the window size needs to be increased which can cause blurring the image. In shift median filter the choice is predicated on a pre-defined threshold price. The most important disadvantage of this technique is that defining a sturdy call is troublesome. Additionally these filters cannot take under consideration the native options as a results of that details and edges might not be recovered satisfactorily, especially once the amplitude is high. To overcome the on top of disadvantage, call based mostly algorithmic rule (DBA) is projected.

In this, image is denoised by employing a three 3 window. If the process picture element price is zero or 255 it's processed as an alternative it's left unchanged. At high noise density the median value are zero or 255 that is screaming. In such case, neighboring picture element is employed for replacement. This perennial replacement of neighboring picture element produces streaking result. In order to avoid

this disadvantage, call based mostly asymmetrical Trimmed Median Filter (DBUTMF) is projected. At high noise densities, if the chosen window contains all 0's or 255's or each then, cut average cannot be obtained. So this algorithmic rule doesn't provide higher results at terribly high noise density that's at eightieth to ninetieth. The projected changed Decision based mostly asymmetrical cut Median Filter (MDBUTMF) algorithmic rule removes this disadvantage at high noise density and offers higher Peak signal/noise ratio (PSNR) and Image improvement issue (IEF) values than the present algorithm.

II. MEDIAN FILTERS

Typically, out and away the bulk of the process effort and time is spent on hard the median of each window. as a result of the filter should method each entry within the image. the most downside of the median filter is that the same price is employed for each shrie and the fine info values and therefore the improved image contains unwanted noise in some regions and loss of data in some regions. It will filter the image in five hundredth of shrie level. This won't works above five hundredth amplitude. To overcome these drawbacks the accommodative Median Filter is introduced.

III. ADAPTIVE MEDIAN FILTER

As a sophisticated technique compared with customary median filtering, the adaptive Median Filter performs abstraction process to preserve detail and smooth non-impulsive noise. The window is replaced by the mean or the average. This filter switches' in between Mean and Median. A prime benefit to the current adaptive approach to median filtering is that recurrent applications of this adaptive Median Filter don't erode away edges or alternative small structure within the image. This filter additionally unable to work at the high noise densities. To overcome this drawback the

choice primarily based algorithm is proposed. call primarily based algorithmic program during this algorithmic program, image is denoised by employing a3X3 window. If the process constituent price is zero or255 it's processed alternatively it's left unchanged. This method will reconstructs the image at low noise densities. it produces the streaming impact, to overcome this the DBUTMF algorithmic program was introduced.

IV. UNSYMMETRICAL TRIMMED MEDIAN FILTER

This filter is termed cut median filter as a result of the element values 0's and 255's square measure far from the selected window. This procedure removes noise in better method than the ATMF. Alpha cut Mean Filtering (ATMF) could be a symmetrical filter wherever the trimming is bilateral at either finish. In this procedure, even the uncorrupted pixels are trimmed. This ends up in loss of image details and blurring of the image. So as to beat this drawback, AN asymmetric cut Median Filter (UTMF) is planned. During this UTMF, the chosen three X3 window components square measure organized in either increasing or decreasing order. Then the element values 0's and 255's within the image (i.e., the pixel values liable for the salt and pepper noise) square measure removed from the image. Then the average of the remaining pixels is taken. This average is used to replace the noisy element as shown in Fig.1.

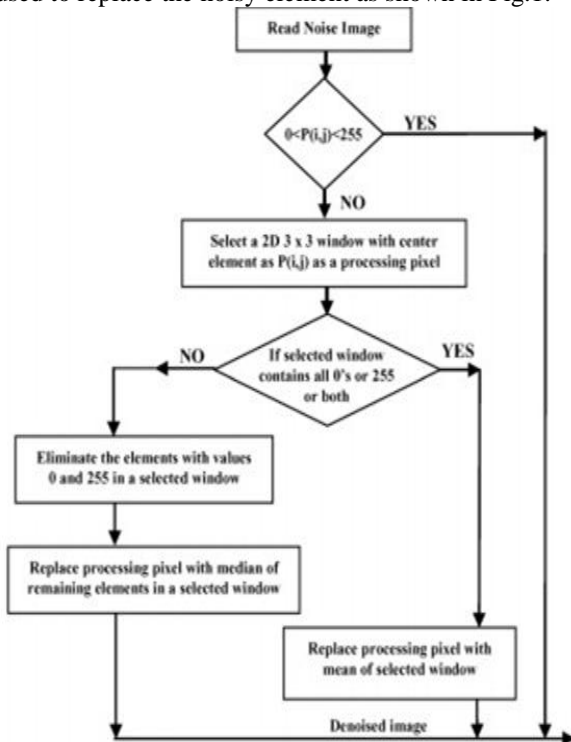


Fig.1.Flow-chart of Proposed MDBUT Filter.

Step 1: Select 2-D window of size 3X3. Assume that the pixel being processed is P_{ij} .

Step 2: If $0 < P_{ij}$ then P_{ij} is an uncorrupted pixel and its value is left unchanged.

Step 3: If $P_{ij} = 0$ or $P_{ij} = 255$ then P_{ij} is a corrupted pixel then two cases are possible as bellow.

- **Case i:** If the selected window contains all the elements as 0's and 255's. Then replace P_{ij} with the mean of the element of window.
- **Case ii:** If the selected window contains not all elements as 0's and 255's. Then eliminate 255's and 0's and find the median value of the remaining elements. Replace P_{ij} with the median value.

Step 4: Repeat steps 1 to 3 until all the pixels in the entire image are processed. Each and every pixel of the image is checked for the presence of salt and pepper noise Each and every pixel of the image is checked for the presence of salt and pepper noise. Different cases are illustrated in this. If the processing pixel is noisy and all other pixel values are either 0's or 255's is illustrated in Case i). If the processing pixel is noisy pixel that is 0 or 255 is illustrated in Case ii). If the processing pixel is not noisy pixel and its value lies between 0 and 255 is it left to unchanged and processed to output.

V. SIMULATION RESULTS

Experiments are performed on gray level images to verify the proposed method. These images are represented by 8bits/pixel and size is 128 x 128. Image used for experiments are shown in below figs.2 to 4.

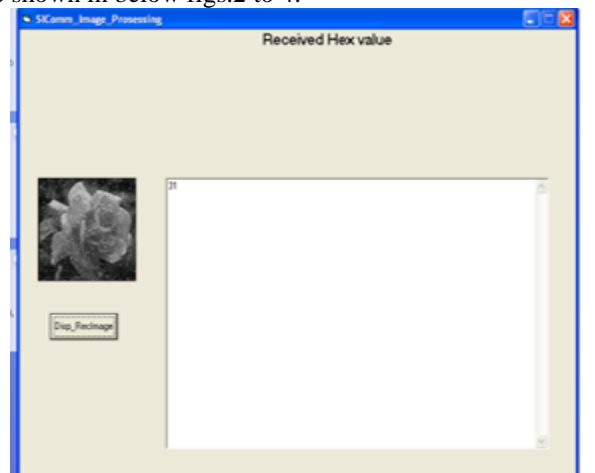


Fig.2. input image.

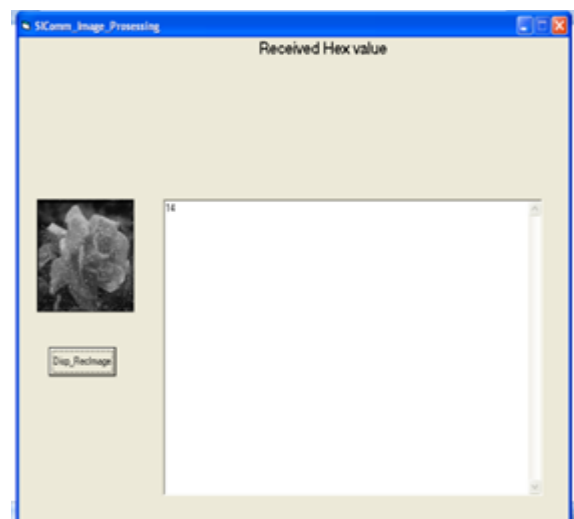


Fig.3. output image.

Implementation of an Efficient Image Denoising Algorithm on FPGA

And the synthesis report is below

Selected Device : 3s500efg320-4				
Number of Slices:	2649	out of	4656	56%
Number of Slice Flip Flops:	3343	out of	9312	35%
Number of 4 input LUTs:	3794	out of	9312	40%
Number used as logic:	3118			
Number used as Shift registers:	356			
Number used as RAMs:	320			
Number of IOs:	83			
Number of bonded IOBs:	40	out of	232	17%
IOB Flip Flops:	55			
Number of BRAMs:	7	out of	20	35%
Number of MULT18X18SIOs:	3	out of	20	15%
Number of GCLKs:	7	out of	24	29%
Number of DCMs:	2	out of	4	50%
Timing Summary:				

Speed Grade: -4				
Minimum period: 12.384ns (Maximum Frequency: 80.749MHz)				
Minimum input arrival time before clock: 41.553ns				
Maximum output required time after clock: 13.840ns				
Maximum combinational path delay: 3.344ns				

Fig. 4. Synthesis report.

VI. CONCLUSION

In this paper, a We have presented an alternative implementation of median filtering. The architecture is immune to changes in window size, the area being determined solely by the bit width. This allows for a flexible window-size that can change from one calculation to another and we finally presented the results which are implemented on the Spartan-3edk evolution board.

VII. CONCLUSION

In this letter, a replacement formula (MDBUTMF) is planned which gives higher performance as compared with radio frequency, AMF and different existing noise removal algorithms in terms of PSNR and IEF. The performance of the formula has been tested at low, medium and high noise densities on each gray-scale and color pictures. Even at high noise density levels the MDBUTMF offers higher ends up in comparison with different existing algorithms. each visual and quantitative results area unit demonstrated. The planned formula is effective for salt and pepper noise removal in pictures at high noise densities.

VIII. REFERENCES

- [1] J.Astola and P.Kusmanen, "Fundamentals of non linear digital filtering", CRC press, 1997.
- [2] R.C.Gonzalez and R.E.Woods, "Digital Image Processing", Addison Wesley Longman Inc., 2000.
- [3] M.C. Motwani, M.C. Gadiya, R.C. Motwani. "Survey of Image De-noising Techniques", Proceedings of GSPx, Santa Clara, CA, 2004.
- [4] T.K.Thivakaran and Dr.RM.Chandrasekaran, "Nonlinear Filter Based Image Denoising Using AMF Approach",

International Journal of Computer Science and Information Security, Vol. 7, No. 2, 2010.

[5] PawanPatidar, Manoj Gupta, SumitSrivastava, Ashok Kumar, "Image De-noising by Various Filters for Different Noise", International Journal of Computer Applications (0975 – 8887) Volume 9– No.4, November 2010.

[6] DoddaShekar, RanguSrikanth, "Removal of High Density Salt & Pepper Noise in Noisy Images Using Decision Based Un-Symmetric Trimmed Median Filter", International Journal of Computer Trends and Technology-ISSN: 2231-2803, volume2Issue1- 2011.

[7] K.Vasanth, V.JawaharSenthilkumar, "A Decision Based Unsymmetrical Trimmed Midpoint Algorithm for the Removal of High Density Salt and Pepper Noise", Journal of Theoretical and Applied Information Technology, 31 August 2012. Vol. 42 No.2.

Design and Power Analysis of 8T SRAM Cell Using Charge Sharing Technique

Lingam Rajesh

M.TECH Mallareaddy Eng College (VLSISD) Hyderabad
ls.rajeshce@gmail.com

Santosh J

Assistant Professor in ECE at MREC, Hyderabad

Abstract: *The aim of the paper is to design and analyze 8T SRAM Cell using Charge Sharing Technique where a standard 8T SRAM cell performance degrades with low power supplies. In the design the SRAM cell uses a charge sharing technique between the transistors to make SRAM more rigid against noises that occur due to low power supplies. Apart from noise reduction the read discharge power is reused. The comparison between standard 6T, 8T and 8T with charge sharing is made. It shows that less power is consumed by 8T with charge sharing than others.*

Keywords: 6T SRAM, 8T SRAM, CMOS, dynamic power budge, SNM

1. INTRODUCTION

Due to growing demand of portable battery operated embedded systems made a necessity for energy efficient design. As predicted 90 % of systems will be made up of memory and the memory management is need of the time. The SRAM is popular choice for embedded systems for its high speed, robustness and ability easy to manufacture. The larger SRAM cell the larger the power consumed.

A basic low power SRAM cell is designed by using cross-coupled CMOS inverters with 6 transistors giving basic 6T SRAM cell. However with technology scaling below nanometer the power dissipation of 6T SRAM becomes significant with low power supplies as due to this the gate delay is increased which reduces the frequency of operations.

An 8T SRAM cell with charge sharing technique which used at architecture level is implemented at the cell level of design.

2. EXISTING WORKS

2.1. Basic SRAM

A number of SRAM cell topologies are reportable within the past years. Among these many design architectures, resistive load four-transistor (4T) SRAM bit cell, that load less 4T cell and 6 transistor(6T) SRAM cell have received attention in use, attributable to their symmetry in storing logic 'one' and logic 'zero'. The information storage within the 4T SRAM cells is ensured by the leakage current of the access NMOS transistors. Hence, they're not correct candidates for low-power applications. On the opposite hand, the information stability during a 6T SRAM cell is free lance of the outflow current. Moreover, 6T configuration exhibits a significantly higher tolerance against noise that is a very important benefit particularly within the scaled technologies wherever the noise margins area unit lowering. That's the most reason for the recognition of the 6T SRAM cell in low-power SRAM units rather than the 4T configurations in usage.

The Six Transistor SRAM cell is most generally utilized in embedded memory attributable to its quick time interval and relatively little space. 6T cell style involves complex tradeoffs between varied factors specifically abrupt scaling done on area, most sensible soft error immunity ability, high cell on current, low leakage current through off transistors, has good stability with minimum voltage &

minimum word line voltage pulse. The total CMOS 6T SRAM bit cell configuration is shown in Fig.1. Full CMOS SRAM configuration provides greater noise margin, low static or leakage power dissipation, high change speeds suitability for high density SRAM arrays. Every 6T cell contains a capability of storing one little bit of information.

The 6T SRAM cell consists of two inverters connected back to back. M5, M6 are access transistors that are controlled by the word line (WL) pulse. The cell preserves one in all its 2 possible states denoted as 0 and 1 as long as power is obtainable to the 6T bit cell.

There are 3 operations in SRAM memory cell particularly write, browse and storage operations. Read and write operations are initiated by enabling the word-line (WL). To do write operation the value to be written is applied to the bit lines and for browse operation each BL and BLB is recharged to VDD. Whenever the browse operation the zero storing node is flustered & this might flip the keep data, but the palm write operation desires that information ought to be flipped terribly simply. Historically device size has been adopted to balance the browse versus write style needs.

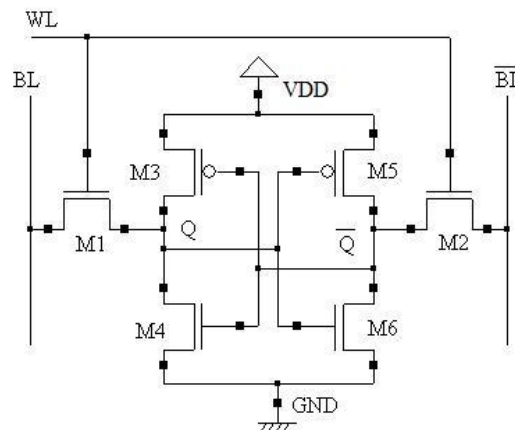


Fig1. Conventional 6T SRAM

The 6T SRAM cell design consists of two access transistors and two cross coupled CMOS inverters. Bit lines are the input/output ports of the cell with high capacitive loading. The operations READ and WRITE are conducted by these bit lines only; we will see how these are carried out. Write style needs.

A 6T SRAM cell consists of 2 cross-coupled CMOS inverters and 2 NMOS access transistors. The output (input) of the inverters construct the internal nodes of the cell A and B. Once active, the access transistors facilitate the communication of the cell internal nodes with the input/output ports of the cell. The input/output ports of the cell unit of measurement called bit lines (BL and BL.) Bit lines unit of measurement a shared data communications medium among the cells on an {analogous the same} column in an array of cells. Consequently, they need high physical phenomenon loading. The browse and write operations unit of measurement conducted through the bit lines as we tend to are reaching to see inside the long run sections.

2.2. Read Operation

Figure 1 illustrates the operation of the cell throughout a browse access. During this design, node node a carries a logic 'zero' and node B carries a logic 'one' before the cell is accessed. Thus, the transistors, M3 and M6, measure 'off' whereas M4 and M5 live 'on' and catch up on the escape current of power supply and M6. In In customary vogue, the bit lines are precharged to VDD before the browse operation begins. An SRAM cell during read operation

Enabling of the word lines (WL), i.e., the gate of the access transistors starts the read operation. Because the word lines go high, power provide goes to saturation region whereas M4 operates in thermionic vacuum tube region. Attributable to the short-channel impact, this associated with power provide encompasses a linear relationship with the voltage of the node 'A'. Hence, these transistors behave sort of a resistance throughout this operation. Therefore, power provide and M4 A resistance and elevate node 'A' voltage by ΔV .

This voltage drives the input of the convertor M5-M3. to confirm CMOS SRAM: a outline sixteen a non-destructive browse operation ΔV is chosen such it does not trigger the M5-M3 electrical

converter and node B remains at VDD over the whole cell interval. Having a seamless voltage of VDD at the gate of M4 warrants the constant resistance assumption for M4 over the interval.

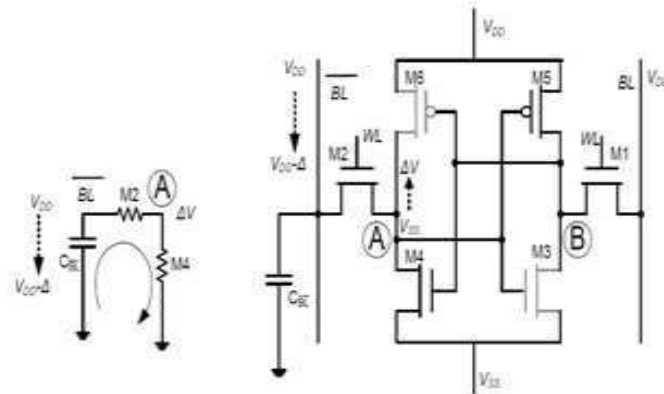


Fig2. An SRAM Cell during Read operation

Figure 2 shows the linear model of the bit line discharge path. Throughout this model the bit line capacitance of CBL is pre-charged to VDD. Upon the activation of power offer, CBL discharges through power offer and M4 and causes a free fall of ϕ on BL. Since the gate supply voltage of M1 remains at zero volts (i.e., $V_{gs1} = 0V$), CBL cannot discharge and remains at VDD. The regardful voltage between BL and BL, ϕ , is amplified using a way electronic equipment to supply the regular logic levels.

Clearly, a faster bit line discharge is achieved by reducing the resistance at intervals the discharge path. However, such enhancements return at the price of larger cell semiconductor device sizes that may not urged for prime density SRAMs.

DC analysis of the operation of the cell transistors is conventionally adopted to substantiate the soundness of the cell throughout the browse operation. as a result of it had been mentioned before, an occasional enough ΔV ensures that the output of inverters M5-M3 remains constant at node B. to make sure a non-de structive browse operation, the voltage level ΔV is controlled by the resistive magnitude relation of power provide and M4.

2.3. Write Operation

Figure 3.3 illustrates the operation of the cell inside the write operation. Throughout this figure the initial conditions of nodes A and B unit VSS and VDD, severally. Re-writing the recent data to the cell is trivial thus we have a tendency to tend to focus on propellant the knowledge of the cell.

In different words, the write operation is complete providing the voltage level on node A and B becomes VDD and VSS, severally. The activation of the word line cannot cause a spare voltage increase on node A to trigger the CMOS inverter M5-M3 if every bit lines unit of measurement pre-charged to VDD.

Therefore, the write operation is conducted by reducing the bit line associated with node B, BL, to a sufficiently low voltage (e.g., VSS.) This operation forms a possible divider comprising of M5 and power offer at the beginning of the operation.

To assess the voltage that appears at node B upon activation of the word lines in write operation, ΔV . A sufficiently low ΔV triggers the convertor M6-M4 that lands up in charging up node A to VDD. Since node a drives the convertor M5-M3, node B is force all the approach right down to VSS through power offer and M5 turns off. Hence, the logic state of the cell is changed. The word line becomes inactive once the completion of the operation. A in write operation ar usually bonded by choosing an accurate PR. A lower PR lands up during a lower ΔV , and a lower ΔV is expounded to higher drive at the input of convertor M6-M4.

3. 8T SRAM CELL

It is noteworthy that for associate SRAM cell, the specified form of operation is commonly set with the correct choice of the bit line voltage. However, this involves additional edge circuits like bit line precharge circuits and writes drivers to create positive correct bit line voltage setting before any

operation. At low provide voltages due the soundness limitations of 6T SRAM cell we tend to use 8T SRAM cell for quick transmission applications. it's like 6T SRAM cell with a scan decoupled path that consists of M5 and M6 transistors. Allow us to see the operating of 8T SRAM style.

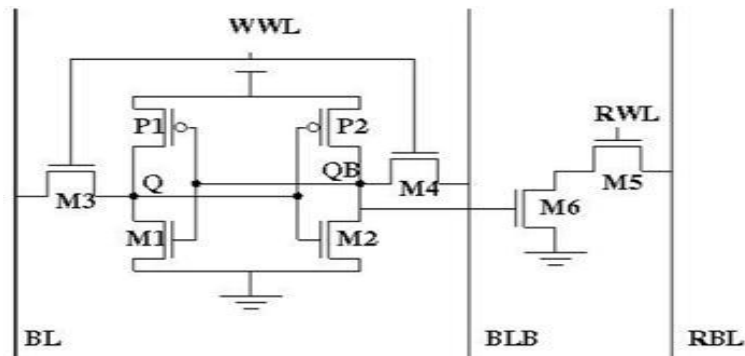


Fig3. 8T SRAM Cell

3.1. Write Operation

The write operation of 8T SRAM cell is same as to the conventional 6T SRAM. The write operation in 8T SRAM is carried out as shown and discussed below

3.2. Write '0' Operation

For writing '0', the bit line has to give zero volts and VDD to the bit line (BLbar). And write word line is asserted which makes both the transistors M3 and M4 ON. Hence the value in the bit line is stored at Q. Hence '0' is stored at Q.

3.3. Write '1' Operation

Likewise writing '1' is also carried in the likely same. The bit line has to give a value VDD and bit line bar is given a value 0 volts. As WWL is enabled for write operation, the values in bit lines are store at respective nodes that is at Q will have value logical '1' and logical '0' at Qbar. There is no change in the write operation when compared with the basic SRAM operation.

3.4. Read Operation

The read operation is initiated by pre-charging the read bit line to VDD which is required in the conventional one.

3.5. Read '0' Operation

Read word line (RWL) drives the access transistor M5 ON. If the value stored at Q is '0' then transistor M6 will be ON and RBL is connected to ground directly through M5&M6 transistors discharges. This implies that the value stored at Q in the SRAM is zero.

3.6. Read '1' Operation

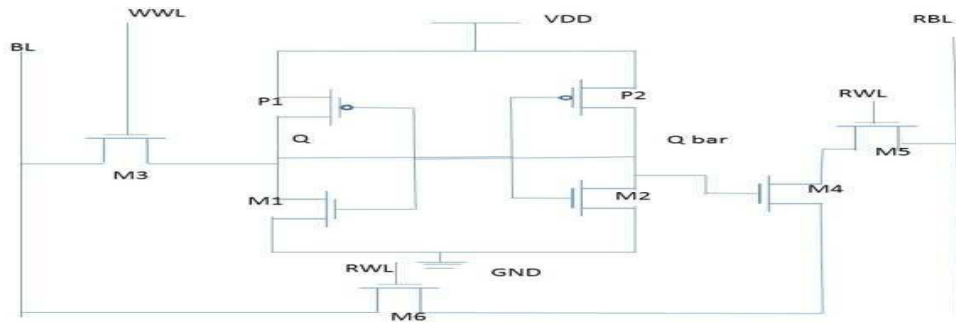
If the value stored at Q is '1', due to M6 transistor will be OFF and there is no discharge path for RBL, and the value in RBL is VDD which shows that value stored at Q is '1'. The circuit diagram of 8T SRAM shown in the figure 4.

The disadvantages in 6T SRAM are minimized in 8T SRAM, even though the transistor count increased the power consumption. The circuit diagram and operations of conventional and 8T SRAM are discussed in this chapter. The SRAM with charge sharing concept is discussed next.

4. PROPOSED SRAM DESIGN

Here the proposed SRAM design is using the concept of charge sharing of 10T SRAM design. But the difference is that the design is done with less number of transistors when compared to the above 10T SRAM which also decreases the area of the design and in the proposed design we also reduced the power consumption when compared with the previous design.

The proposed SRAM consists of a single ended 7T bit cell which has one bit line (BL) for write operation and one Read Bit cell for read operation.



During the write operation WWL was enabled and RWL was disabled (i.e $RWL=0$) so M4 M5 M6 are in the off state. The cell acts like single ended 5T SRAM Cell and writes the Bit line data into the cross coupled inverter pair P1 M3 and P2 M2.

During the read operation the bit line disconnected from inverter pair because of $WWL=0$ during read phase and RWL was enabled so M6 M5 will be in the ON state. For read operation here we are using separate bit line called RBL instead of using same BL. SO during read operation RBL was pre-recharged.

Read '0': In reading '0' M4 was ON state, so RBL has a discharging path from M4 M5 and M6, the M6 will acts like a charge sharing network, instead of discharging the charge to the ground M6 will charge the bit line (BL) so there will no loss of power to the ground.

Read '1': In reading '1' M4 was OFF state so there will be no discharging path for RBL to discharge maintains the charge and reads the '1'

5. SIMULATION AND RESULTS

These SRAM designs are designed and simulated using S-edit and T-Spice using TSMC018 technology in Tanner Tools 13.0. The Conventional 8T SRAM, and Proposed SRAM are simulated there power dissipations are compared and shown in below:

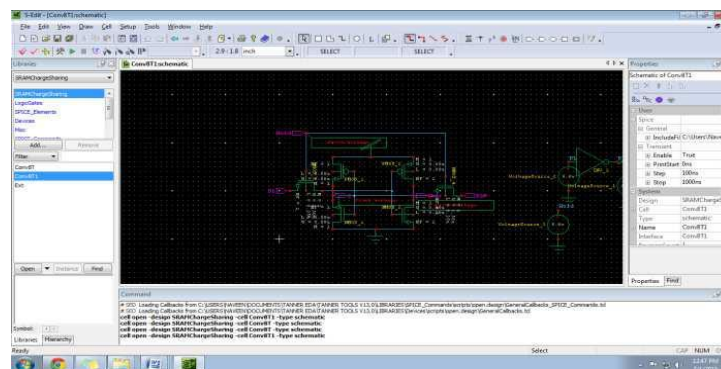


Fig5. S-edit Design of 6T SRAM Cell

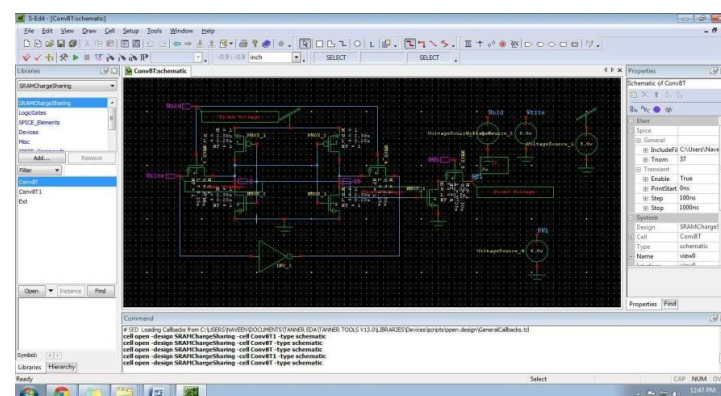


Fig6. S-edit Design of 8T SRAM Cell

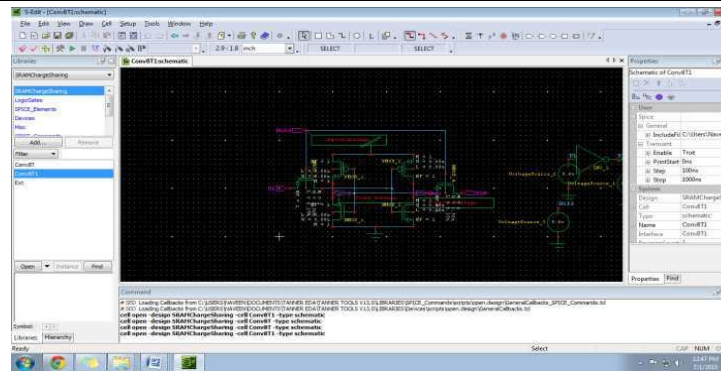


Fig7. S-edit Design of Proposed SRAM Cell

Circuit	Power Consumption
Conventional 6T SRAM	5.517330e-004 watts
8T SRAM Cell	9.461892e-010 watts
Proposed SRAM Cell	5.806951e-010 watts

6. CONCLUSION

Here we have used the designs of SRAM of charge sharing and analyzed the design for minimum area and power as well. The design technique will reduce power and maintain at good stability levels.

7. FUTURE SCOPE

In future we can extend this multi bit SRAM Cells and overall bit line discharge losses can be reduced by using adiabatic logics.

REFERENCES

- [1] Kevin Z. Embedded Memories for Nano-Scale VLSIs. Springer Publishing Company, Incorporated. 2009; 400.
- [2] Brown AR, Roy G, Asenov A. Poly-Si-Gate- Related Variability in Decananometer MOSFETs with Conventional Architecture. Electron Devices. IEEE Transactions on 2007; 54(11): 3056-3063.
- [3] Bo Z et al. A Sub-200mV 6T SRAM in 0.13um CMOS.inSolid-State Circuits Conference. ISSCC 2007. Digest of Technical Papers. IEEE International. 2007.
- [4] Cheng B, Roy S, Roy G, Brown A, Asenov A. Impact of Random Dopant Fluctuation on Bulk CMOS 6-T SRAM Scaling. inSolid-State Device Research Conference. ESSDERC 2006.Proceeding of the 36th European. 2006.
- [5] Singh J, Simon Hollis DKR, Mohanty SP. A single ended 6T SRAM cell design for ultra-low-voltage applications. IEICE Electronics Express 2008; 5(18): 750-755.
- [6] Mizuno H, Nagano T. Driving source-line cell architecture for sub-1-V high-speed low-power applications. Solid-State Circuits. IEEE Journal of 1996; 31(4): 552-557.
- [7] Takeda K. et al. A read-static-noise-margin-free SRAM cell for low-VDD and high-speed applications. Solid-State Circuits, IEEE Journal of 2006; 41(1): 113-121.
- [8] Chang L. et al. An 8T-SRAM for Variability Tolerance and Low-Voltage Operation in High-Performance Caches. Solid-State Circuits, IEEE Journal of 2008; 43(4): 956-963.
- [9] Tae-Hyoung K. et al. A High-Density Subthreshold SRAM with Data-Independent Bitline Leakage and Virtual Ground Replica Scheme.inSolid-State Circuits Conference. ISSCC 2007. Digest of Technical Papers. IEEE International. 2007.
- [10] Wang X, Roy S, Asenov A. Impact of Strain on the Performance of high-k/metal replacement gate MOSFETs. Proc. 10th Ultimate Integration on Silicon (ULIS 2009), 2009.

AUTHOR'S BIOGRAPHY



Lingam Rajesh, Completed B.TECH in SREE Rama Eng College (ECE) (JNTU-A), M.TECH Mallareaddy Eng College (VLSISD) Hyderabad, Area of Interest: VLSI System Design.



Santosh J, Assistant Professor in ECE At MREC, Completed B.TECH: CVR College Of Eng. JNTU-H, M.TECH: VLSI System Design, SDES, JNTU-H Area of Interest VLSI System design Reconfigurable Architecture & Design of Fault Tolerant Systems.

Time Interleaved Parallel ADC with Efficient Decoder and Improved Sampling Switch

Balaji Bantupalli

M. Tech, ECE department,
Malla Reddy Engineering College (Autonomous), Hyderabad, India.
balaji.bantupalli@gmail.com

Abstract: Buffered multiplexer based decoder are proposed in the literature for high speed parallel ADCs with low power and less hardware requirements. The parallel ADC designed by using voltage controlled amplifier (VCA), bootstrap switch, a comparator array consists of 63 comparators, D flip-flop's and buffered mux based decoder. A buffered mux based decoder compares with the folded decoder with respect hardware, power consumption and critical path. Bootstrapped switches is used to migrate the problem with varying on-resistance and poor conduction. The buffered mux based decoder is used to convert 63-bit thermometer code into 6-bit binary code. The parallel ADC integrated on chip micro controller calibration, it is used for watchdog and it compensate the nominal non linearity of the fine VCA. The parallel ADC with 0.9 supply, 400mv of full scale voltage at 2.5-GSamples/second consumes 15-28mW of power approximately in 130nm cmos technology.

Keywords: 10G Ethernet, bootstrap switch, folded decoder, A/D convertors, buffered mux based decoder, Meta stability errors, and critical path.

1. INTRODUCTION

The most of signals in the real world are analog (continuous in amplitude and time). In order to produce the digital signal, the analog signals are converted into the digital form by using a circuit called analog-to-digital converter. The usage of 10G Ethernet is extremely increased to amuse the demand for higher bandwidth. This paper implements a 6 bit parallel A/D Converters with 2.5-GS/s which can be used in the way of 4 times interleaved parallel architecture for 10GE functionalities. This parallel ADC design facilitates lower predicted meta stability errors, flexibility, low hardware design than remaining high speed low to medium resolution ADC's. The basic diagram of time interleaved parallel adc is shown in the figure.1. It is implemented in 130nm CMOS technology. The ADC characterized in this document is used for the 4way interleaved runs at 10GSample/s for DSP based receiver that could be used the NRZ 10GE standards. This paper targets on the design of bootstrap switch and implementation of buffered decoder for the ADC and on comparative analysis of folded decoder and buffered multiplexer decoder implementations. In addition, owing to the nature of successive bit decoding, momentous time interleaving may be unavoidable to ensure better metastability error rate, which is one of major requirement in such applications.

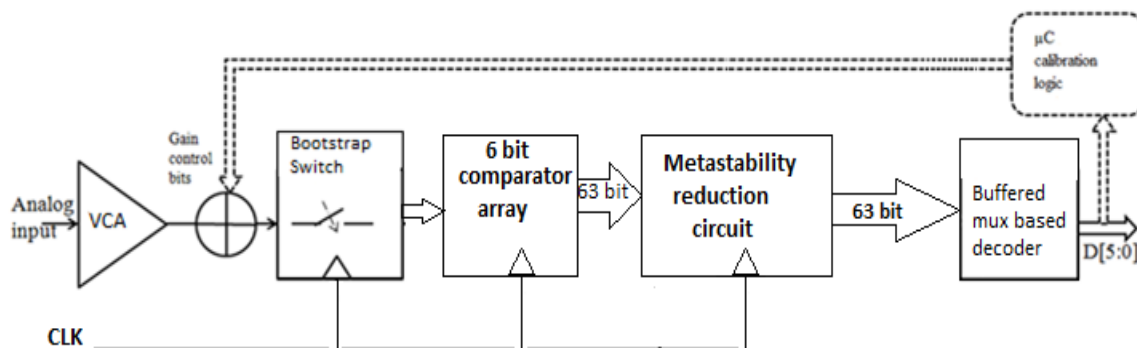


Figure1. Top level of parallel ADC

2. CIRCUIT IMPLEMENTATION

2.1. Voltage-Controlled Amplifier (VCA)

The VCA adjust the input signal to provide a swing approximately 400 mV differential peak-to-peak to the bootstrap switch. Fig. 2 shows the circuit of the source degenerated differential amplifier equipped with VCA. The purpose of source degeneration is to improve the linearity of the amplification. The source degeneration utilizes a linear resistor at the source terminal as shown in figure 2. This resistor reduces the swing at the gate to source, making the input/output characteristics more linear. Over all transconductance of the source degenerative amplifier is

$$G_m = g_m / (1 + g_m \cdot R_s).$$

Where R_s is equivalent source resistance of resistor network.

The M3 and M4 is used to extending bandwidth during normal operation also detach the input signal from the load during calibration. Charge feedback through the gate-to-drain overlap capacitance of M1 and M2 can disturb circuit functionality. A Cross-coupled device M3 and M4 implements the first-order cancellation of this effect.

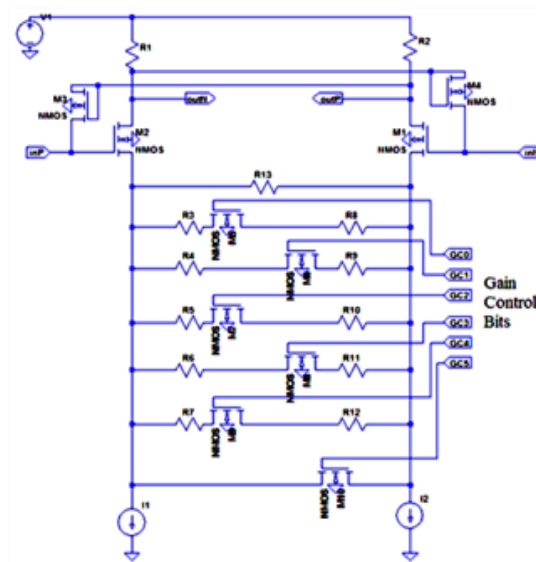


Figure2. Source-degenerated variable controlled amplifier (G)

2.2. Bootstrap Switch

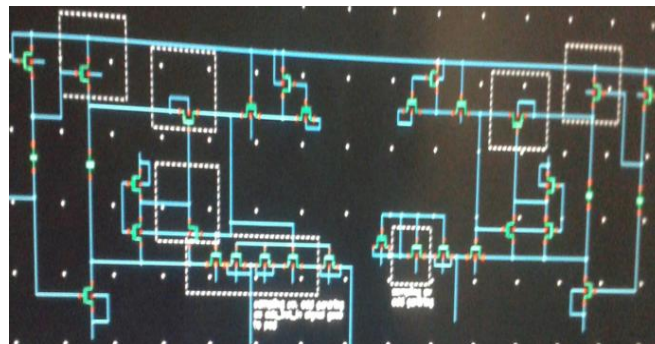


Figure3. Bootstrap switch

A bootstrapped switch is a design technique to migrate the problem with varying on-resistance and poor conduction. These switches are realized with a one pass transistor and supplementary devices for generation of gate-source voltages for the pass transistor. When the off-state the gate is aligned to ground and the transistor is in cut-off region. The main difference between the regular analog switches and bootstrapped switch is present in the on-state, where the gate to channel voltage is kept constant.

It is done by connecting a constant offset voltage between the source and gate terminals of the main switch. This voltage could be obtained by the using of a capacitor pre-charged in the off-state. Depending upon the information signal, this offset will reach voltages equal to V_{dd} . Considering the complete voltage at the gate terminal exceeds the supply voltage, mentioned switches have to be designed correctly to prevent they don't violate all reliability constraints.

2.3. Dynamic Comparator

Dynamic comparator uses dual input and single output differential amplifier as latch stage suitable for high speed ADC with low power dissipation, high speed and high immune to noise. The comparator array consists of resistor ladder and 63 active comparators. The ladder range is 400 mV_{dpp}, resulting in a nominal LSB value of 6.25 mV. In order to achieve a power efficient design, the dynamic comparator in this ADC doesn't contain any pre-amplifiers. In clock tree, local clock buffer is provided for each comparator and that can be deactivated during individual comparator power down to save the power.

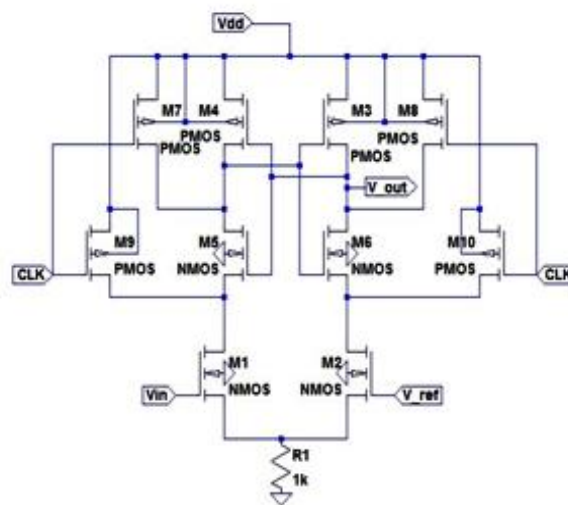


Figure3. Dynamic comparator

Fig. 4 shows the design of the dynamic comparator, which is based on a dynamic-sense amplifier latch incorporating several modifications. The comparator compares the output of bootstrap switch sampled input signal with the reference generated by the resistor ladder. A voltage of 400 mV_{dpp} is provided to the resistor ladder as full-scale voltage of parallel ADC. Comparison is performed by differential amplifier pair M1–M2. The output of a dynamic comparator is HIGH whenever sampled input voltage is larger than the reference voltage generated by ladder at the another input of the comparator, otherwise the output is inverted clock since the comparator is working in dual input and single output mode the inverted clock region will be cancelled and considered as LOW. The output of comparator array is 63 bit thermometer code. To prevent Metastability-related error propagation, the thermometer code goes through a sequence of flip-flops before arriving at the decoder inputs.

2.4. Decoders

2.3.1. Folded Wallace Tree Decoder

In the parallel ADC, the purpose is to reduce the amount of hardware by using the same comparator for different reference voltages. The dimensions of the Wallace tree and the delay is depending on the number of bits that will be added, i.e. the width of the base of the tree. An idea is to split the output of the comparators into 2^k different intervals. They were multiplexed to a single Wallace tree decoder, which can be reduced in size compared with the full one in. A full adder might be constructed from three 2:1 multiplexers with two multiplexers in the critical path. so, according to the number of 2:1 multiplexers needed (Y_N) and the critical path (C_N) for the folded decoder is

$$y_N = 3 \cdot \left(\sum_{i=1}^{N-k} (i-1) \cdot 2^{(N-k-i)} \right) + 2^N - 2^{N-k} \quad (1)$$

$$c_N = 4N - 3k - 6, \quad (2)$$

respectively. Each C_N is equal to the propagation delay of a 2-input ex-or gate (t_{xor}) which can similar to the propagation delay of a 2:1 multiplexer (t_{mux}).

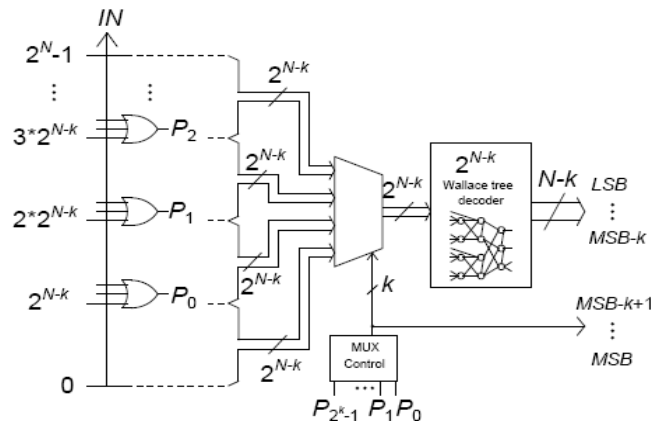


Figure4. Folded Wallace tree decoder

2.3.2. Buffered Multiplexed Based Decoder

The 2x1 inverted multiplexer is shown in the figure5. The output of pass transistor is connected to odd number of inverters in order to provide stronger signal. This segment will first illuminate the idea behind the presented buffered multiplexer based decoder and second describe how it will be generalized. For an N-bit parallel ADC the most significant bit (MSB) of the binary output is high if more than half of the outputs in the thermometer scale are logic one. So most significant bit (MSB) is the same as the thermometer output at 2^{N-1} level. To find the value of the second most significant bit (MSB-1) the original thermometer scale is prorated into partial thermometer scales, separated by the output at 2^{N-1} level as depicted as the flow diagram in Figure 7.

The partial thermometer scale to decode is chosen by a set of inverted 2:1 multiplexers, where the preceding decoded binary output is connected as the control input of the inverted multiplexers. MSB-1 is then determined from the selected partial thermometer scale in the likewise as MSB initiated from the full thermometer scale. The preferred scale is thereby the scale that consists of the information about MSB-1, i.e. the lower partial thermometer scale if the output at level is logic zero or else the upper partial thermometer scale is used.

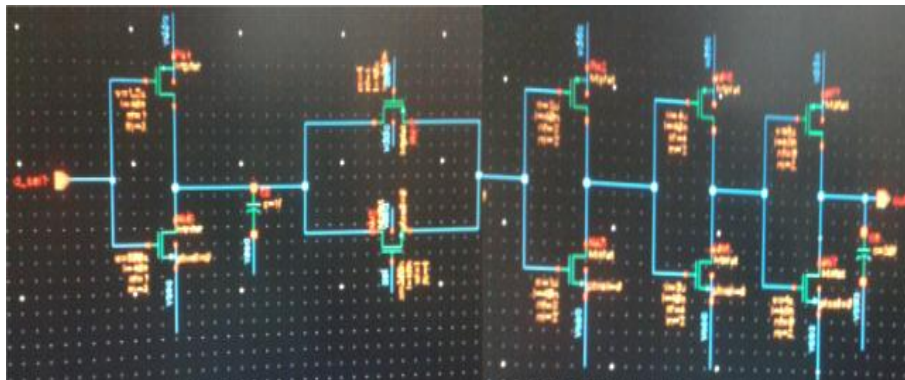


Figure5. Inverted 2x1 mux

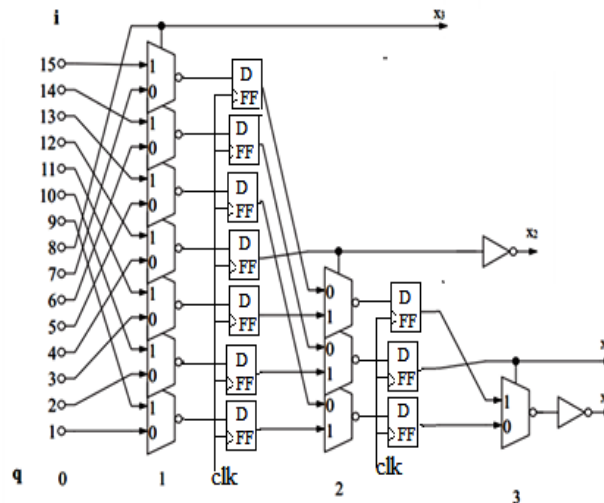


Figure6. Buffered mux based decoder for 4 bit decoder

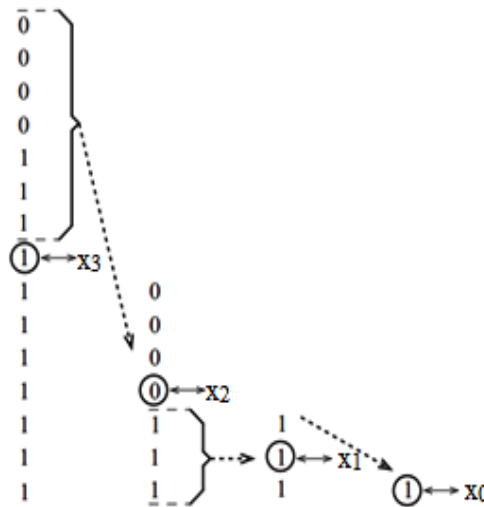


Figure7. Flow of buffered multiplexer based decoding

The buffered based decoder for 4 bit decoder is shown in figure6. It is continued recursively until only one 2:1 multiplexer remains. Its output is the LSB of the binary output. Due to the regular design of this decoder it can easily be widened to function in a system of higher resolution than 4 bits, which is explained further below. The regular design should also help in the physical layout. The outputs x_q of the decoder is the equivalent binary value of the thermometer code, where $q=0, 1, 2, 3, \dots, N-1$. The column $q=1$ is the first multiplexer column. Hence the output $i_q = 2^{N-q-1}$ is fed to the control inputs of the multiplexers in $q+1$ column. This is also the output of the x_{N-q-1} decoder, where x_{N-1} is the MSB of the binary output. The output of the multiplexer in column $q=N-1$ is the LSB of the binary output, i.e. x_0 .

In general, for an N -bit parallel ADC the thermometer output has $2^N - 1$ levels ($i_{q=0}$). The thermometer output $i_{q=0}$ or multiplexer output $i_{q>0}$ is fed to the '0' ($i_q < 2^{N-q-1}$) or '1' ($i_q \geq 2^{N-q-1}$) input of the multiplexer of level $i_q \text{ modulo } 2^{N-q-1}$ and column $q+1$, where $i_q = 1, 2, 3, 4, \dots, 2^N - 1$. So the presented decoder required number of 2:1 multiplexers Y_N and the critical path C_N in units of t_{MUX} can be formulated as:

$$Y_N = \sum_{i=1}^{N-1} [2^{(N-i)} - 1] \quad (3)$$

$$C_N = N - 1 \quad (4)$$

3. COMPARISON OF THE DECODERS

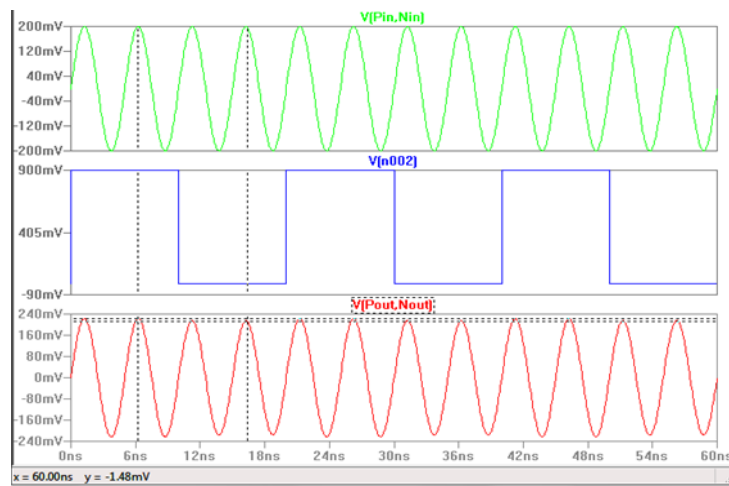
The buffered multiplexer based decoders have capable and promising properties in terms of amount of hardware and critical path. If instead an ones-counter is used as the decoder it concedes speed versus power trade-off not only by directly trading power for speed, but also in terms of selecting appropriate ones counter/adder topology. A comparison of the performance between the folded decoder and the buffered Mux based decoder is given in Table 1. The performance is considered in terms of amount of hardware and length of the critical path.

Table1. Performance comparison of 6 bit parallel ADC

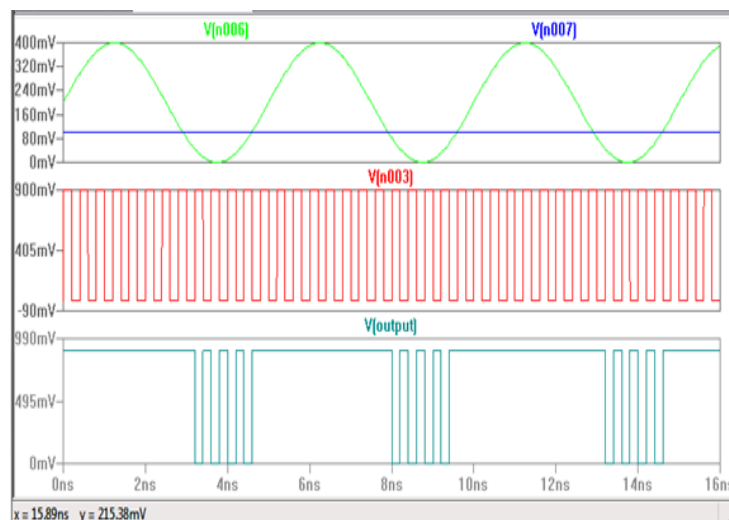
Type of Decoder	N.of MUX's	Critical path
Folded Decoder	81	12 t_{MUX}
Buffered MUX based Decoder	57	5 t_{MUX}

As seen in Table 1, the hardware is extremely reduced when using the buffered MUX based decoder. For the buffered MUX based decoder, the number of multiplexers is reduced by more than 30% compared to the folded decoder. This is likely to translate to a power saving. Table 1 also indicates that the suggested solution has the potential of being faster than the folded decoder, since its critical path is shorter. The metastability will be reduced by placing flip-flop between the muxes.

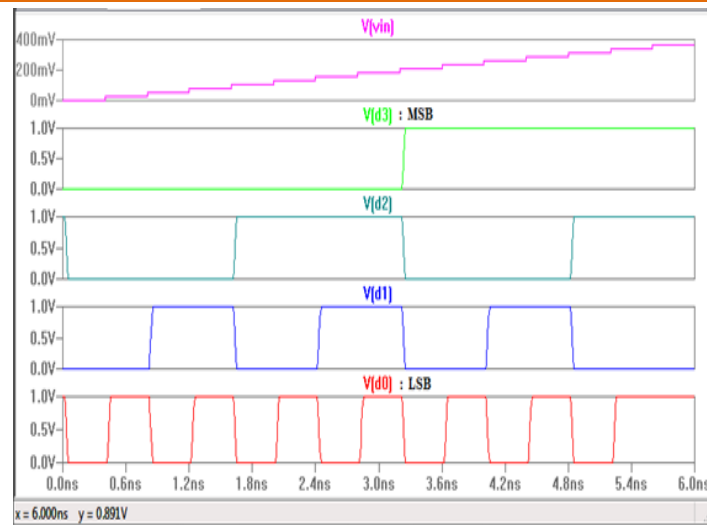
4. SIMULATION RESULTS



Figuer8. Simulation of VCA



Figuer9. Simulation of dynamic comparator



Figurer10. Simulation of time interleaved parallel ADC

5. CONCLUSION

We have presented a 2.5-GS/s, 0.9V supply, 6-bit, 15- 28 mW, parallel ADC for a universal 10GE DSP-based receiver. Our study demonstrates that the bootstrap switch is for to minimize the on-resistance during track mode and also minimize sample-to-hold step size during hold mode. Buffered multiplexer based decoder is a pleasant approach for designing thermometer-to-binary decoder. The hardware used and area consumption is lesser than compared to the other exiting decoders and the critical path is briefer and it is useful for lower power applications. In addition, it is more traditional design than the other decoders, which can be added advantage when doing the layout.

REFERENCES

- [1] Aida Varzaghani, "A 10.3-GS/s, 6-Bit Flash ADC for 10G Ethernet Applications"IEEE JOURNAL OF SOLID-STATE CIRCUITS, VOL. 48, NO. 12, pp. 3038-3048, December 2013.
- [2] Erik Sail, and mark Vesterbacka, "A MUL- TIPLEXER BASED DECODER FOR FLASH ANALOG-TODIGITAL CONVERTERS" IEEE, August, 2004.
- [3] B. Hochet, and F. Kaess, "New Encoding Scheme For High-speed Flash ADC's", 1997 IEEE International Symposium on Circuits and Systems, pp. 5-8, June 9-12,1997, Hong Kong .
- [4] K. Uyttenchove, A. Marque, "A 6-bit 1 GHz Acquisition Speed CMOS Flash ADC with Digital Error Correction", IEEE, pp. 249-252, CUSTOM INTEGRATEDCIRCUITS CONFERENCE, 2000.
- [5] J. Terada, Y. Matsuya, and F. Morisawa, "8- mW, 1-V, 100-MSPS, 6-BIT A/D CONVERTER USING A TRANSCONDUCTANCE LATCHED COMPARATOR", pp.53-56, IEEE.
- [6] M. F. Flynn et al, "Digital calibration incorporating redundancy of flash ADCs" ,IEEE Trans. Circuits Syst.II, vol. 50, no. 5, pp. 205–213,May 2003.
- [7] Sunghyun Park, "A 4-GS/s 4-bit Flash ADC in 0.18- μ m CMOS", In IEEE Journal of Solid-State Circuits,VOL.42, NO.9, pp. 1865-1872, September 2007.
- [8] Hamid Reza Mafi, and Hossein Shamsi, "A 10-Bit 50-MS/s Charge Injection Pipelined ADC Using a Digital Calibration", IEEE, 9th International Multi-Conference on systems, signals and Devices, 2012.
- [9] Vladimir Stojanovic, Chih-Kong Ken Yang, "A Serial-Link Transceiver Based on 8-GSamples/s A/D and D/A Converters in 0.25- μ m CMOS"IEEE Journal of Solid-State circuits, vol. 36, NO. 11, November 2001.

DESIGN AND IMPLEMENTATION OF AREA EFFICIENT FM0/MANCHESTER ENCODING ARCHITECTURES

Amancha Varun Raj¹, V.Srinivas²

¹P.G Scholar, ²Assistant Professor

^{1,2}VLSI System Design, Malla Reddy Engineering College, Hyderabad

ABSTRACT: An implementation of Manchester coding is being described in this paper. Manchester coding technique is a digital coding technique in which all the bits of the binary data are arranged in a particular sequence. The Intersil HD-15530 is a high performance CMOS device intended to service the requirements of MIL-STD-1553 and similar Manchester II encoded, time division multiplexed serial data protocols. This LSI chip is divided into two sections, an Encoder and a Decoder. These sections operate completely independent of each other, except for the Master Reset functions. This circuit meets many of the requirements of MIL-STD-1553. The Encoder produces the sync pulse and the parity bit as well as the encoding of the data bits. The Decoder recognizes the sync pulse and identifies it as well as decoding the data bits and checking parity. This integrated circuit is fully guaranteed to support the 1MHz data rate of MIL-STD-1553 over both temperature and voltage. It interfaces with CMOS, TTL or N channel support circuitry. The HD-15530 can also be used in many party line digital data communications applications, such as an environmental control system driven from a single twisted pair cable of fiber optic cable throughout the building. The functions of the encoder section of the MED include a micro processor interface, parallel to serial conversion, frame generation, and NRZ to Manchester encoding. This circuitry can run very fast since it does not require a high-frequency clock. The frame format used is similar to that of a UART. The Manchester decoder limits the maximum frequency of operation of the MED, since it uses a high-frequency clock. The receiver circuitry is more complex, since clock recovery and center sampling is done. Additional receiver functions are frame detection, decoding of Manchester to NRZ, serial to parallel conversion, and a microprocessor interface.

Keywords: Manchester coding, Encoder, Decoder, NRZ, Moore's law, UART, clock frequency

I. INTRODUCTION

Manchester coding technique is a digital coding technique in which all the bits of the binary data are arranged in a particular sequence. Here a bit '1' is represented by transmitting a high voltage for half duration of the input signal and for the next halftime period an inverted signal will be send. When transmitting '0' in Manchester format, for the first half cycle a low voltage will send, and for the next half cycle a high

voltage is send. The advantage of Manchester coding is that, when sending a data having continuous high signals or continuous low signal (e.g.: 11110000), it is difficult to calculate the number of 1 S and 0s in the data. Because there is no transition from low to high or high to low for a particular time period (Here it is $4 \times T$, T is the time duration for a single pulse). The detection is possible only by calculating the time duration of the signal. But when we code this signal in Manchester format there will always be a transition from high to low or low to high for each bit. Thus for a receiver it is easier to detect the data in Manchester format and also the probability for occurrence of an error is very low in Manchester format and it is a universally accepted digital encoding technique. The dedicated short range communication is a protocol for one or two way medium range communication. The DSRC can be briefly classified into two categories: automobile-to-automobile and automobile-to-roadside. In automobile-to-automobile, the DSRC enables the message sending and broadcasting among automobile. The automobile-to-roadside focuses on the intelligent transportation service, such as electronic toll collection (ETC). The DSRC architecture having the transceiver. The transceiver having the baseband processing, RF front end and microprocessor. The microprocessor is used to transfer the instruction to the baseband processing and RF front end. the RF front end is used to transmit and receive the wireless signals using the antenna. The baseband processing is responsible for modulation, error correction, encoding and synchronization. The transmitted signal consists of the arbitrary binary sequence, it is very difficult to obtain the dc-balance. the fm0 and Manchester are provide the transmitted signal and then the dc-balance. The (SOLS) similarity oriented logic simplification having the two methods: area compact retiming and balance logic operation sharing. The area compact retiming used to reduce the transistor counts. the balance logic operation sharing is used to combine the fm0 and Manchester encoding.

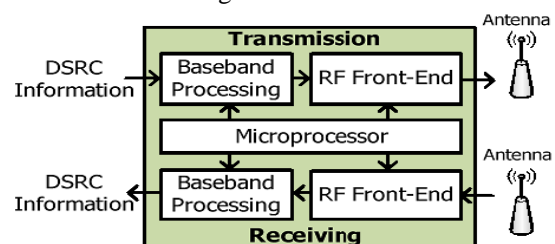


Fig. 1. System architecture of DSRC transceiver.

The system architecture of DSRC transceiver is shown in Fig. 1. The upper and bottom parts are dedicated for transmission and receiving, respectively. This transceiver is classified into three basic modules: microprocessor, baseband processing, and RF front-end. The microprocessor interprets instructions from media access control to schedule the tasks of baseband processing and RF front-end. The baseband processing is responsible for modulation, error correction, clock synchronization, and encoding. The RF frontend transmits and receives the wireless signal through the antenna. The DSRC standards have been established by several organizations in different countries. These DSRC standards of America, Europe, and Japan are shown in Table I. The data rate individually targets at 500 kb/s, 4 Mb/s, and 27 Mb/s with carrier frequency of 5.8 and 5.9 GHz. The modulation methods incorporate amplitude shift keying, phase shift keying, and orthogonal frequency division multiplexing. Generally, the waveform of transmitted signal is expected to have zero mean for robustness issue, and this is also referred to as dc-balance.

II. LITERATURE SURVEY

The transmitted signal consists of arbitrary binary sequence, which is difficult to obtain dc-balance. The purposes of FM0 and Manchester codes can provide the transmitted signal with dc-balance. Both FM0 and Manchester codes are widely adopted in encoding for downlink. The VLSI architectures of FM0 and Manchester encoders are reviewed as follows

A. Review of VLSI Architectures for FM0 Encoder and Manchester Encoder

The literature [4] proposes VLSI architecture of Manchester encoder for optical communications. This design adopts the CMOS inverter and the gated inverter as the switch to construct Manchester encoder. It is implemented by 0.35- μ m CMOS technology and its operation frequency is 1 GHz. The literature [5] further replaces the architecture of switch in [4] by the nMOS device. It is realized in 90-nm CMOS technology, and the maximum operation frequency is as high as 5 GHz. The literature [6] develops a high-speed VLSI architecture almost fully reused with Manchester and Miller encodings for radio frequency identification (RFID) applications. This design is realized in 0.35- μ m CMOS technology and the maximum operation frequency is 200 MHz. The literature [7] also proposes a Manchester encoding architecture for ultrahigh frequency (UHF) RFID tag emulator. This hardware architecture is conducted from the finite state machine (FSM) of Manchester code, and is realized into field-programmable gate array (FPGA) prototyping system. The maximum operation frequency of this design is about 256 MHz. The similar design methodology is further applied to individually construct FM0 and Miller encoders also for UHF RFID Tag emulator [8]. Its maximum operation frequency is about 192 MHz. Furthermore, [9] combines frequency shift keying (FSK) modulation and demodulation with Manchester codec in hardware realization.

III. CODING PRINCIPLES OF FM0 CODE AND MANCHESTER CODE

In the following discussion, the clock signal and the input data are abbreviated as CLK, and X, respectively. With the above parameters, the coding principles of FM0 and Manchester codes are discussed as follows.

A. FM0 Encoding As shown in Fig. 2, for each X, the FM0 code consists of two parts: one for former-half cycle of CLK, A, and the other one for later-half cycle of CLK, B. The coding principle of FM0 is listed as the following three rules.

- 1) If X is the logic-0, the FM0 code must exhibit a transition between A and B.
- 2) If X is the logic-1, no transition is allowed between A and B.
- 3) The transition is allocated among each FM0 code no matter what the X is.

A FM0 coding example is shown in Fig. 3. At cycle 1, the X is logic-0; therefore, a transition occurs on its FM0 code, according to rule 1. For simplicity, this transition is initially set from logic-0 to -1. According to rule 3, a transition is allocated among each FM0 code, and thereby the logic-1 is changed to logic-0 in the beginning of cycle 2. Then, according to rule 2, this logic-level is hold without any transition in entire cycle 2 for the X of logic-1. Thus, the FM0 code of each cycle can be derived with these three rules mentioned earlier.

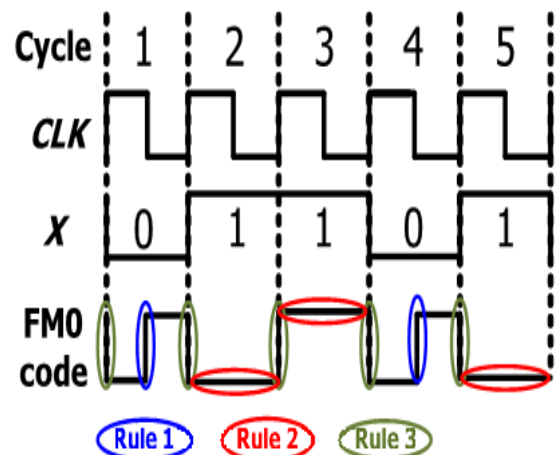


Illustration of FM0 coding example.

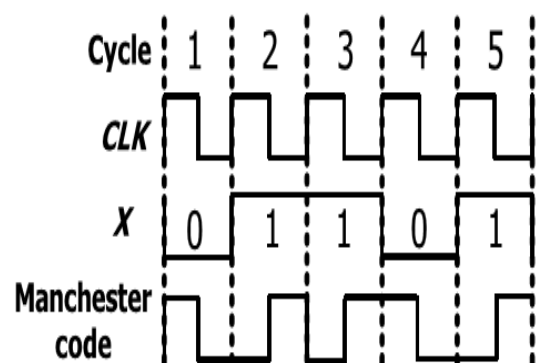
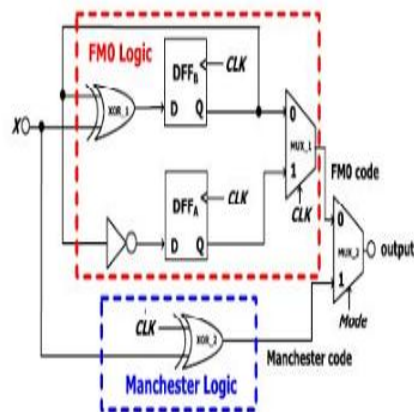


Illustration of Manchester coding example.

Hardware Architecture Of Fm0/Manchester Code:

This is the hardware architecture of the fm0/Manchester code. the top part is denoted the fm0 code and then the bottom part is denoted as the Manchester code. in fm0 code the DFFA and DFFB are used to store the state code of the fm0 code and also mux_1 and not gate is used in the fm0 code. When the mode=0 is for the fm0 code. The Manchester code is developed only using the XOR gate and when the mode=1 is for the Manchester code. the hardware utilization rate is defined as the following

$$HUR = \frac{\text{Active components}}{\text{total components}} \times 100$$



Hardware architecture

The active components means the components are work in the both fm0 and Manchester code. The total components means the number of the components are present in the hole circuit. the HUR rate is given below the following section

TABLE-II

Coding	Active components(transistor count)/ total components (transistor count)	HUR
FM0	6(86)/7(98)	85.71%
MANCHESTER	2(26)/7(98)	28.57%
AVERAGE	4(56)/7(98)	57.14%

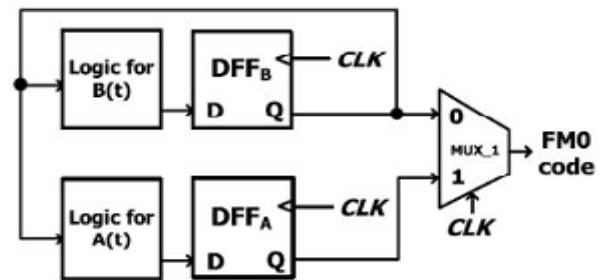
For both the encoding methods the total components is 7. for the fm0 code the total component is 7 and then the active component is 6. in Manchester code the total component is 7 the active component is 2. in both coding having 98 transistors are used without SOLS. The fm0 having 86 transistor, and then the Manchester having the 26 transistor. the average for both coding is 56 transistors. In proposed work reduce the total components from 7 to 6 and reduce the transistor counts. In this paper two multiplexer is used in proposed work reduce two multiplexer from one multiplexer, when reduce the multiplexer the total components are reduced the area and then the power consumption also reduced.

IV. FMO AND MANCHESTER ENCODER USING SOLS TECHNIQUE

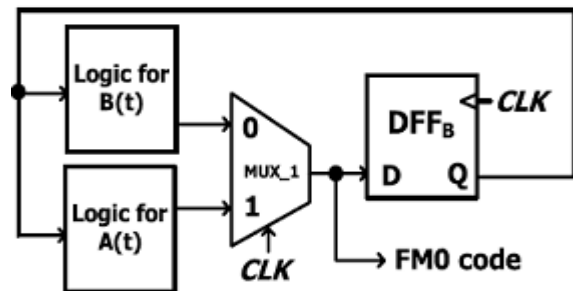
The SOLS technique is classified into two parts area compact retiming and balance logic operation sharing

A. area compact retiming

For fm0 the state code of the each state is stored into DFFA and DFFB .the transition of the state code is only depends on the previous state of B(t-1) instead of the both A(t-1) and B(t-1)

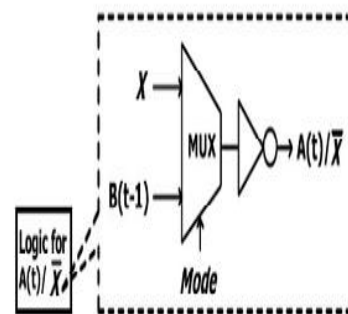


Area compact retiming



FMO encoding without area compact retiming

The previous state is denoted as the A(t-1) and then the B(t-1). and then the current state is denoted as the A(t) and then the B(t).



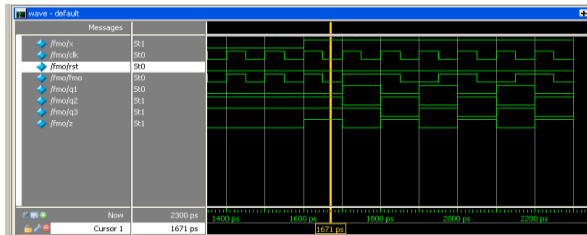
FMO encoding with area compact retiming.

Thus, the FM0 encoding just requires a single 1-bit flip-flop to store the previous value B(t-1). If the DFFA is directly removed, a non synchronization between A(t) and B(t) causes the logic fault of FM0 code. To avoid this logic-fault, the DFFB is relocated right after the MUX-1, where the DFFB is assumed be positive-edge triggered flip flop. At each cycle, the FM0 code, comprising A and B, is derived from the logic of A(t) and the logic of B(t), respectively. The FM0 code is alternatively switched between A(t) and B(t) through the MUX-1 by the control signal of the CLK. In the Q of DFFB is directly updated from the logic of B(t) with 1-cycle

1313

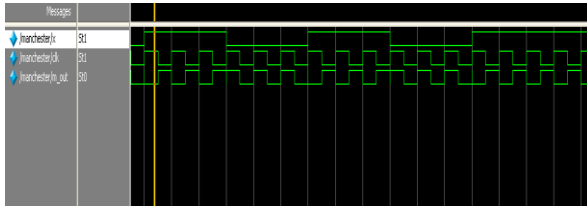
V. SIMULATION RESULTS

FM0 Module:



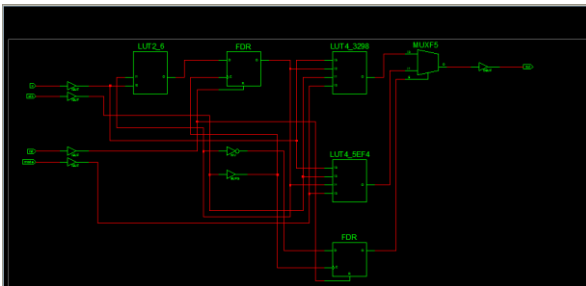
FM0 Code

Manchester:

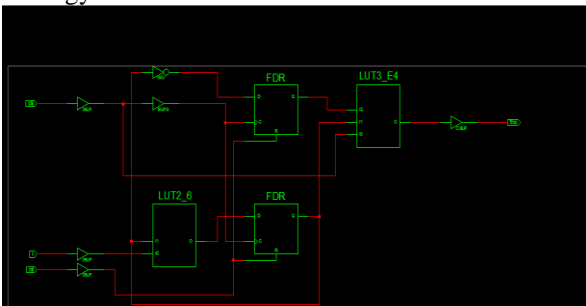


Manchester Coding

RTL Schematic



Technology Schematic



VI. CONCLUSION

The coding-diversity between FM0 and Manchester encodings causes the limitation on hardware utilization of VLSI architecture design. A limitation analysis on hardware utilization of FM0 and Manchester encodings is discussed in detail. In this paper, the fully reused VLSI architecture using SOLS technique for both FM0 and Manchester encodings is proposed. The SOLS technique eliminates the limitation on hardware utilization by two core techniques: area compact retiming and balance logic-operation sharing. The area-compact retiming relocates the hardware resource to reduce the transistors. The balance logic-operation sharing efficiently combines FM0 and Manchester encodings with the identical logic components. This paper is realized in 180nm technology with an outstanding device efficiency. The power consumption is 29392.843nW for Manchester encoding and FM0 encoding.

REFERENCE

- [1] F. Ahmed-Zaid, F. Bai, S. Bai, C. Basnayake, B. Bellur, S. Brovold, et al., "Vehicle safety communications—Applications (VSC-A) final report," U.S. Dept. Trans., Nat. Highway Traffic Safety Admin., Washington,DC, USA, Rep.DOT HS 810 591, Sep. 2011.
- [2] J. B. Kenney, "Dedicated short-range communications (DSRC) standards in the United States," Proc. IEEE, vol. 99, no. 7, pp. 1162–1182, Jul. 2011.
- [3] J. Daniel, V. Taliwal, A. Meier, W. Holfelder, and R. Herrtwich, "Design of 5.9 GHz DSRC-based vehicular safety communication," IEEE Wireless Commun. Mag., vol. 13, no. 5, pp. 36–43, Oct. 2006.
- [4] P. Benabes, A. Gauthier, and J. Oksman, "A Manchester code generator running at 1 GHz," in Proc. IEEE, Int. Conf. Electron., Circuits Syst., vol. 3, Dec. 2003, pp. 1156–1159.
- [5] A. Karagounis, A. Polyzos, B. Kotsos, and N. Assimakis, "A 90nm Manchester code generator with CMOS switches running at 2.4 GHz and 5 GHz," in Proc. 16th Int. Conf. Syst., Signals Image Process., Jun. 2009, pp. 1–4.
- [6] Y.-C. Hung, M.-M. Kuo, C.-K. Tung, and S.-H. Shieh, "High-speed CMOS chip design for Manchester and Miller encoder," in Proc. Intell. Inf. Hiding Multimedia Signal Process., Sep. 2009, pp. 538–541.
- [7] M. A. Khan, M. Sharma, and P. R. Brahmanandha, "FSM based Manchester encoder for UHF RFID tag emulator," in Proc. Int. Conf. Comput., Commun. Netw., Dec. 2008, pp. 1–6.
- [8] M. A. Khan, M. Sharma, and P. R. Brahmanandha, "FSM based FM0 and Miller encoder for UHF RFID tag emulator," in Proc. IEEE Adv. Comput. Conf., Mar. 2009, pp. 1317–1322.
- [9] J.-H. Deng, F.-C. Hsiao, and Y.-H. Lin, "Top down design of joint MODEM and CODEC detection schemes for DSRC codedFSK systems over high mobility fading channels," in Proc. Adv. Commun. Technol. Jan. 2013, pp. 98–103.
- [10] I.-M. Liu, T.-H. Liu, H. Zhou, and A. Aziz, "Simultaneous PTL buffer insertion and sizing for minimizing Elmore delay," in Proc. Int. Workshop Logic Synth., May 1998, pp. 162–168.

VLSI DESIGN OF A NOVEL PRESTO WITH PROGRAMMABLE PRPG

P.Vinod Kumar¹, K.S.Indrani²

¹M.Tech Scholar, VLSI System Design, ²Associate Professor, ECE Dept,
Malla Reddy Engineering College

Abstract: This paper describes a low-power (LP) programmable generator capable of reducing pseudorandom take a look at patterns with desired toggling levels and increased fault coverage gradient compared with the best-to-date intrinsic self-test (BIST)- primarily based pseudorandom take a look at pattern generators. It's comprised of a linear finite state machine (a linear feedback register or a hoop generator) driving associate degree applicable section shifter, and it comes with variety of options permitting this device to supply binary sequences with preselected toggling (PRESTO) activity. We tend to introduce a technique to mechanically choose many controls of the generator providing straightforward and precise calibration. Identical technique is afterwards used to deterministically guide the generator toward take a look at sequences with improved fault-coverage-to pattern-count ratios. Moreover, this paper proposes associate degree disc take a look at compression technique that permits shaping the take a look at power envelope during a absolutely certain, accurate, and versatile fashion by adapting the PRESTO-based logic BIST (LBIST) infrastructure. The projected hybrid theme expeditiously combines take a look at compression with LBIST, wherever each technique will work synergistically to deliver top quality tests. Experimental results obtained for industrial styles illustrate the practicableness of the projected take a look at schemes and are rumored herein.

I. INTRODUCTION

Although over successive years, the first objective of producing take a look at can stay essentially an equivalent to confirm reliable and prime quality semiconductor merchandise conditions and consequently additionally take a look at solutions could endure a major evolution. The semiconductor technology, style characteristics, and also the style method area unit among the key factors that may impact this evolution. With new sorts of defects that one can have to be compelled to concede to give the specified take a look at quality for successive technology nodes like 3D, it's applicable to create the question of what matching design-for-test (DFT) ways can ought to be deployed. Take a look at compression, introduced a decade ago, has quickly become the most stream DFT methodology. However, it's unclear whether or not take a look at compression are going to be capable of managing the fast rate of technological changes over successive decade. Curiously, logic integral self-test (LBIST), originally developed for board, system, and in-field take a look at, is currently gaining acceptance for production

take a look at because it provides terribly strong DFT and is employed more and more usually with take a look at compression. This hybrid approach looks to be successive logical biological process step in DFT. it's potential for improved take a look at quality; it should augment the talents to run at-speed power aware tests, and it will scale back the price of producing take a look at whereas protective all LBIST and scan compression benefits. Tries to beat the bottleneck of take a look at knowledge information measure between the take a look at after and also the chip have created the conception of mixing LBIST and test knowledge compression an important analysis and development space. particularly, many hybrid BIST schemes store settled indefinite quantity patterns (used to sight random pattern resistant faults) on the tester in an exceedingly compressed type, then use the prevailing BIST hardware to decompress these take a look at patterns. Some solutions enter settled stimuli by victimisation compressed weights or by heavy pseudorandom vectors in numerous fashions varied schemes for power reduction throughout scan testing are devised. Among them, there are unit solutions specifically planned for BIST to stay the common and peak power below a given threshold. As an example, the take a look at power will be reduced by preventing transitions at memory parts from propagating to combinable logic throughout scan shift. This is often achieved by inserting gating logic between scan cell outputs and logic they drive during this paper, we tend to propose a PRPG for record BIST applications. The generator primarily aims at reducing the switch activity throughout scan loading attributable to its preselected toggling (PRESTO) levels. This paper culminates in showing that the fast generator may also with success act as a take a look at knowledge decompressor, therefore permitting one to implement a hybrid take a look at methodology that mixes LBIST and ATPG-based embedded take a look at compression.

II. BASIC ARCHITECTURE

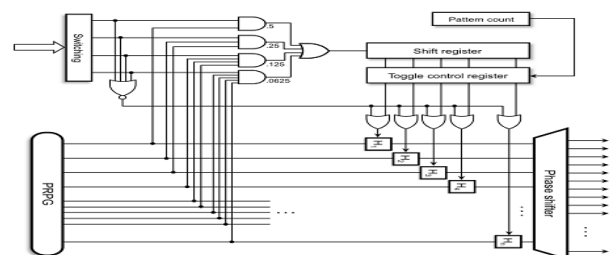


Fig.1. Basic architecture of a PRESTO generator

Fig. one shows the fundamental structure of a fast generator. Associate n-bit PRPG connected with a part shifter feeding scan chains forms a kernel of the generator manufacturing the particular pseudorandom check patterns. A linear feedback register or a hoop generator will implement a PRPG. A lot of significantly, however, n hold latches area unit placed between the PRPG and also the part shifter. Every hold latch is {individually|separately|singly|severally|one by one|on associate individual basis} management led via a corresponding stage of an n-bit toggle control register. As long as its alter input is declared, the given latch is clear for information going from the PRPG to the part shifter, and it's aforementioned to be within the toggle mode. Once the latch is disabled, it captures and saves, for variety of clock cycles, the corresponding little bit of PRPG, therefore feeding the part shifter (and probably some scan chains) with a relentless price. It's currently within the hold mode. It's price noting that every part shifter output is obtained by XOR-ing outputs of 3 completely different hold latches. Therefore, each scan chain remains in a very low-power mode provided solely disabled hold latches drive the corresponding part shifter output. As mentioned antecedently, the toggle management register supervises the hold latches. Its content contains 0s and 1s, wherever 1s indicate latches within the toggle mode, so clear for knowledge returning from the PRPG. Their fraction determines a scan shift activity. The management register is reloaded once per pattern with the content of an extra register. The change signals injected into the register area unit made in an exceedingly probabilistic fashion by mistreatment the first PRPG with a programmable set of weights. The weights area unit determined by four AND gates manufacturing 1s with the chance of zero.5, 0.25, 0.125, and 0.0625, severally. The OR circuit permits selecting possibilities on the far side straightforward powers of two. A 4-bit register shift is used to activate AND gates, and permits choosing a user-defined level of shift activity. It will correspond to a precise level of toggling within the scan chains. With solely fifteen totally different shift codes, however, the offered toggling coarseness might render this answer too coarse to be invariably acceptable. Section III presents further options that build the fast generator absolutely operational in an exceedingly big selection of desired shift rates.

III. FULLY OPERATIONAL GENERATOR

Much higher flexibility in forming low-toggling take a look at patterns is achieved by deploying a theme given in Fig. 2. Basically, whereas conserving the operational principles of the fundamental resolution, this approach splits up a shifting amount of each take a look at pattern into a sequence of alternating hold and toggle intervals. To maneuver the generator back and forth between these 2 states, we have a tendency to use a T-type flip-flop that switches whenever there's a one on its knowledge input. If it's set to zero, the generator enters the hold amount with all latches quickly disabled no matter the management register content. This is often

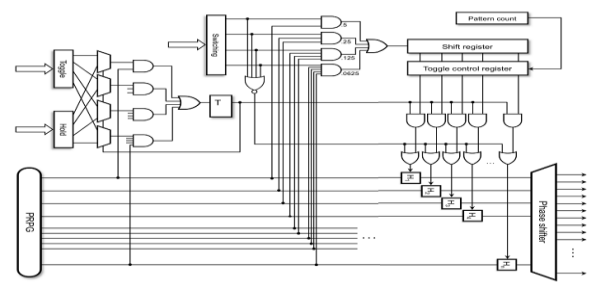


Fig. 2. Fully operational version of PRESTO accomplished by inserting AND gates on the management register outputs to permit freeze of all part shifter inputs. This property is crucial in SoC styles wherever solely one scan chain crosses a given core, and its abnormal toggling could cause regionally unacceptable cooling which will solely be reduced owing to temporary hold periods. If the T flip-flop is about to one (the toggle period), then the latches enabled through the management register will pass take a look at knowledge moving from the PRPG to the scan chains.

Two further parameters unbroken in 4-bit Hold and Toggle registers confirm however long the whole generator remains either within the hold mode or within the toggle mode, severally. To terminate either mode, a one should occur on the T flip-flop input. This weighted pseudorandom signal is created in a very manner just like that of weighted logic accustomed feed the register. The T flip-flop controls additionally four 2-input multiplexers routing knowledge from the Toggle and Hold registers. It permits choosing a supply of management knowledge which will be utilized in subsequent cycle to probably modification the operational mode of the generator. as an example, once within the toggle mode, the input multiplexers observe the Toggle register. Once the weighted logic outputs one, the flip-flop toggles, and as a result all hold latches freeze within the last recorded state. They're going to stay during this state till another one happens on the weighted logic output. The random incidence of this event is currently associated with the content of the Hold register that determines once to terminate the hold mode.

A scan change profile once deploying the fast generator in a very hypothetic atmosphere with fifteen scan chains is shown in Fig. three for 2 take a look at patterns. Blue (0s) and red (1s) stripes frame the low power-toggling pattern, whereas grey areas correspond to periods of toggling. All-blue and all-red scan chains area unit fed by the constant values solely. Note that their quantity doesn't amendment between patterns though they're not precisely the same in every case. As are often seen, check patterns area unit divided into hold and toggle intervals of random length, whereas LP scan chains stay still for the whole period of one check pattern. When exploitation the fast generator with associate existing DFT flow, all LP registers area unit either loaded once per check or each check pattern. The registers loaded just one occasion act as check information registers or area unit components of associate IJTAG network, and area unit initialized by the check setup procedure. The area unit triggered employing a slow scan shift clock and operates at a

really low speed thereby imposing no temporal order constraints. Though the remaining registers area unit loaded once per check pattern (also at the scan shift speed), temporal order isn't compromised as a result of shallow logic generating bits to be loaded serially into the registers. With the assistance of shadow registers, values stay unchanged throughout capture

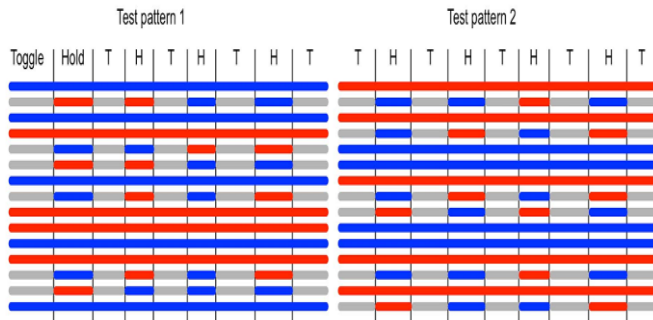


Fig.3. Switching activity in scan chain

IV. LP DECOMPRESSOR

In order to facilitate take a look at information decompression whereas protective its original practicality, the electronic equipment of Fig. two should be rearchitected. This is often shown in Fig. 8. The core principle of the decompressor is to disable each weighted logic blocks (V and H) and to deploy settled management information instead. Particularly, the content of the toggle management register will currently be elect in an exceedingly settled manner attributable to an electronic device placed before of the register. What is more, the Toggle and Hold registers area unit utilized to alternately predetermine a 4-bit binary down counter, and so to work out durations of the hold and toggle phases. Once this circuit reaches the worth of zero, it causes a passionate signal to travel high so as to toggle the T flip-flop. Constant signal permits the counter to own the input file unbroken within the Toggle or Hold register entered because the next state.

Both the down counter and also the T flip-flop have to be compelled to be initialized each take a look at pattern. The initial worth of the T flipflop decides whether or not the decompressor can begin to work either within the toggle or within the hold mode, whereas the initial worth of the counter, any stated as associate degree offset, determines that mode's period. As will be seen, practicality of the T flip-flops remains constant as that of the disc PRPG (see Section III) however 2 cases. 1st of all, the cryptography procedure might utterly disable the hold part (when all hold latches area unit blocked) by loading the Hold register with associate degree applicable code, as an example, 0000. If detected (No Hold signal within the figure), it overrides the output of the T flip-flop by exploitation an extra logic gate, as shown in Fig. 8. As a result, the whole take a look at pattern goes to be encoded among the toggle mode solely. Additionally, all hold latches got to be properly initialized. Hence, an impression signal 1st cycle made at the tip of the ring generator data format part reloads all latches with the present content of this a part of the decompressor. Finally, external Ate channels

(feeding the initial PRPG) permit one to implement a continual flow take a look at information decompression paradigm like the dynamic LFSR reseeding. Given the scale of PRPG, the amount of scan chains and also the corresponding part shifter, the shift code, the offset, furthermore because the values unbroken within the Toggle and Hold registers, the whole decompressor can manufacture settled (decompressed) take a look at patterns having a desired level of toggling provided the scan chains area unit balanced.

V. SIMULATION RESULTS

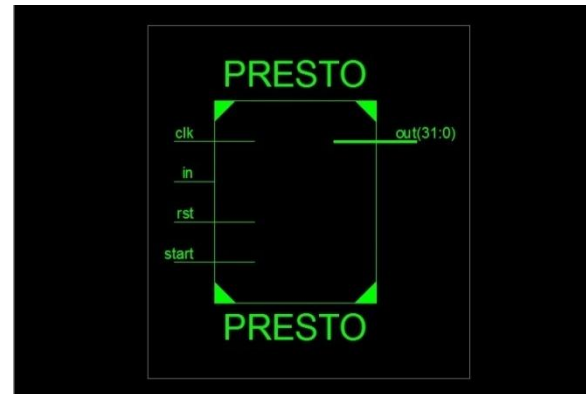


Fig. 4 Presto RTL block

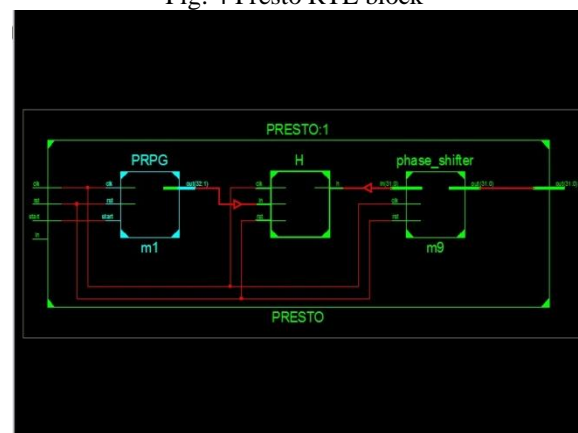


Fig.5 Presto Schematic



Fig.6 Simulation Result

VI. CONCLUSION

As shown within the paper, PRESTO—the phonograph

record generator—can manufacture pseudorandom check patterns with scan shift-in shift activity exactly elite through machine-driven programming. Identical options are often wont to management the generator, in order that the resultant check vectors will either yield desired fault coverage quicker than the standard pseudorandom patterns whereas still reducing toggling rates all the way down to desired levels, or they'll supply visibly higher coverage numbers if run comparable check times. This phonograph record PRPG is additionally capable of acting as a totally useful check knowledge decompressor with the flexibility to regulate scan shift-in shift activity through the method of encryption. The planned hybrid answer permits one to with efficiency mix check compression with logic BIST, wherever each technique will work synergistically to deliver top quality check. it's so a really enticing phonograph record check theme that permits for trading-off check coverage, pattern counts, and toggling rates in an exceedingly} very versatile manner.

REFERENCES

- [1] A. S. Abu-Issa and S. F. Quigley, "Bit-swapping LFSR for low-power BIST," *Electron. Lett.*, vol. 44, no. 6, pp. 401–402, Mar. 2008.
- [2] C. Barnhart et al., "Extending OPMISR beyond 10x scan test efficiency," *IEEE Design Test*, vol. 19, no. 5, pp. 65–73, Sep./Oct. 2002.
- [3] S. Bhunia, H. Mahmoodi, D. Ghosh, S. Mukhopadhyay, and K. Roy, "Low-power scan design using first-level supply gating," *IEEE Trans. Very Large Scale Integr. (VLSI) Syst.*, vol. 13, no. 3, pp. 384–395, Mar. 2005.
- [4] M. Chatterjee and D. K. Pradham, "A novel pattern generator for near perfect fault- overage," in *Proc. 13th IEEE Very Large Scale Integr. (VTSI) Test Symp.*
- [5] F. Corno, M. Rebaudengo, M. S. Reorda, G. Squillero, and M. Violante, "Low power BIST via non-linear hybrid cellular automata" in *Proc. 18th IEEE Very Large Scale Integr. (VTSI) Test Symp.*, May 2000,
- [6] D. Das and N. A. Touba, "Reducing test data volume using external/LBIST hybrid test patterns," in *Proc. Int. Test Conf. (ITC)*,
- [7] R. Dorsch and H. Wunderlich, "Tailoring ATPG for embedded testing," in *Proc. Int. Test Conf. (ITC)*, 2001, pp. 530–537.
- [8] M. Filipek et al., "Low power decompressor and PRPG with constant value broadcast," in *Proc. 20th Asian Test Symp. (ATS)*, Nov. 2011, pp. 84–89.

ITERATIVE CANCELLATION OF NON-LINEAR DISTORTION NOISE IN DIGITAL COMMUNICATION SYSTEMS

Amtul Shakera ¹

A.Rama Satya Balaji ²

1) Amtul Shakera [M.Tech], Mallareddy College of Engineering, Hyderabad, Telangana, India.

2) A.Rama Satya Balaji, Assistant Professor, Mallareddy College of Engineering, Hyderabad, Telangana, India.

Abstract—In this paper, an iterative receiver that performs nonlinear distortion noise cancellation is presented. The performance is assessed for time division multiple access (TDMA), orthogonal frequency division multiple access (OFDMA) and single-carrier frequency division multiple access (SC-FDMA) waveforms. Even though a return link setup is considered, the receiver is equally applicable in the forward link, taking into account the differences in the data multiplexing and the channel. Analytical modeling of the received electrical signal-to-noise ratio (SNR) is carried out for OFDMA with one iteration of non-linear distortion noise cancellation. The performance is assessed in terms of power efficiency and spectral efficiency, where the total degradation (TD) of the received SNR in a non-linear channel is minimized. The modulation formats of the DVB-RCS2 satellite return link standard and a respective non-linear channel have been used. OFDMA shows the highest power efficiency gain of 1.1–2.5 dB with 2 iterations of non-linear noise cancellation across the different modulation orders. In SC-FDMA, the gain is in the range of 0.3–1.1 dB, while gains of 0.1–0.8 dB and 0.2–1.9 dB are presented in TDMA with 20% roll-off and 5% roll-off, respectively.

Index Terms—Non-linear distortion, OFDMA, SC-FDMA, TDMA, power efficiency

I. INTRODUCTION

Nowadays, broadband access is considered a commodity. To provide coverage to all households on the territory of the European Union and Turkey, the project on Broadband Access via Integrated Terrestrial and Satellite Systems (BATS) [1] develops

an integrated network solution, merging the benefits of terrestrial mobile networks, digital subscriber line (DSL) networks and satellite communication systems. In particular, intelligent network and user gateways are designed which can classify the traffic of different types of applications and route it via low-latency terrestrial networks or high-bandwidth satellite links to maximize the quality of experience. Due to the ongoing shift towards more bandwidth demanding applications and services, next generation networks need to offer higher system throughput and user data rates, flexibility to adapt to traffic demand across the coverage area, and at the same time decrease the cost per transmitted bit. For this purpose, a higher spectral efficiency without a significant increase in the computational complexity of the air interface is imperative.

The utilization of larger pieces of bandwidth in the higher frequency bands, such as Ka, Q and V radio frequency (RF) bands, imposes significant hardware implementation challenges, and imperfections cause signal distortion. Therefore, suitable signal processing techniques at the transmitter or receiver side that maximize the information rate of the link are still an open issue. For example, communication over the satellite channel suffers from linear and non-linear distortion. The linear distortion is attributed to mismatch of the signal spectrum and the spectral response of the filters along the chain, while the non-linear distortion originates from the non-linear transfer characteristic of the high-power amplifiers (HPAs) onboard the satellite and at the user terminal. These adverse effects reduce the power and spectral efficiencies of the transmission waveform. Time division multiplexing (TDM) is the waveform of choice in the latest DVB-S2X standard for the

satellite forward link, while TDMA is employed in the return satellite link according to the DVB-RCS2 standard. Waveforms such as OFDMA and SC-FDMA are at the heart of terrestrial mobile long-term evolution (LTE) networks due to their high spectral efficiency and flexible traffic allocation. These waveforms have also been recently considered for application over satellite for the sake of vertical network hand-over. The performance of TDM for the forward satellite link has been studied. In addition, SC-FDMA and OFDMA have been compared for the return satellite link for amplifier characteristics in the K and S bands. In this study, a novel receiver is developed that performs iterative cancellation of the inter modulation interference (IMI) from the non-linear distortion, and it is tested for practical amplifier characteristics in Ka band with TDMA, OFDMA and SC-FDMA waveforms.

The aim of state-of-the-art communication systems to achieve higher data rates and throughput, and at the same time to use low cost consumer devices, results in the increase of the interference levels in the physical layer. The application of wideband signals in channels with insufficient coherence bandwidth due to frequency selectivity or dispersion results in inter-symbol interference (ISI). Similar effects are introduced also by imperfections in the frequency responses of the filters employed along the transmission chain. In addition, non-linear distortion effects, such as IMI, are introduced by the non-linear transfer characteristics of HPAs. In state-of-the-art systems, a common approach to handle the ISI is equalization, where the knowledge of the channel, obtained for instance by channel estimation, is used to counter the ISI. The IMI is handled by means of power control, such as input and output back-off (OBO). This approach is known to penalize the power efficiency of the system when high OBO is applied. In state-of the-art systems, signal detection is performed in the presence of the interfering component and the additive white Gaussian noise (AWGN). A major shortcoming is that no measure is taken to extract the information carried in the interfering component, since the interference is

treated as an additional component to the noise. However, the transfer characteristics of the non-linear devices in the system are generally well known and easily obtainable through measurements. Therefore, the knowledge of the mechanisms causing the IMI can be used for interference cancellation. Cancellation of the IMI has been first proposed for OFDMA systems with an extension for coded OFDMA signals. The approach has been adopted for SC-FDMA. The interfering component is estimated by means of a model for the received constellation centroids based on the Bussgang decomposition, where the attenuation of the transmitted symbols in the channel is exploited. In the estimation of the interfering component, a single attenuation factor is used for all the symbols in the constellation. This approach is applicable in systems, where the non-linear distortion noise is uncorrelated with the symbols, such as in OFDMA. However, when the IMI is correlated with the signal, such as in SCFDMA and TDMA, individual scaling factors for each constellation point need to be computed.

In this paper, an improved receiver design is proposed. The received constellation centroids are individually estimated and used for maximum likelihood (ML) signal detection. In addition, individual scaling factors are applied to the detected symbols, to improve the estimation procedure for the interfering component in systems such as SC-FDMA and TDMA. The improved estimate is iteratively re-estimated and subtracted from the signal for the sake of an improved bit error rate (BER). In general, only a few iterations are sufficient to significantly improve the performance of the receiver, resulting in an increased power and spectral efficiency. The performance of this receiver is compared with static data pre-distortion at the transmitter which is used in state-of-the art systems as a nonlinearity compensation technique. In addition, an analytical model for the received SNR and TD is developed and validated for OFDMA with one iteration of IMI cancellation. In a model is presented for an optical system with a soft limiter amplifier with ideal clipping for a 16-quadrature amplitude-modulation-(QAM) constellation.

In this paper, a general model is developed which is applicable to any nonlinear transfer characteristic and any constellation of a digital modulation scheme in an RF OFDMA system. The improved receiver enables operation with optimum TD at a much lower OBO, providing significant gains in the power efficiency. In the considered modulation setup, gains of up to 2.5 dB are expected for OFDMA, 1.1 dB for SC-FDMA, 0.8 dB for TDMA with 20% roll-off and 1.9 dB for TDMA with 5% roll-off. The gains of IMI cancellation are shown to increase for higher order modulations due to their higher sensitivity to non-linear distortion.

II. DIGITAL TRANSMISSION SCHEMES

Commercial digital communication systems include mobile wireless communications, DSL and cable communications, satellite communications and optical wireless communications such as infrared and visible light communications (VLC). In a digital transmission scheme, streams of bits are mapped to information symbols from a given constellation at the modulator. To provide protection from the impairments in the channel, the bits can be encoded by a forward error correction (FEC) code. Common modulation formats include pulse amplitude modulation (PAM), pulse position modulation (PPM), QAM, phase shift keying (PSK), amplitude and phase shift keying (APSK), etc. It is assumed that the receiver knows the modulation order on the received symbols for every user through information in the frame preamble or control channel information. The modulated symbols are multiplexed in accordance with the underlying transmission format. TDMA is the common transmission format in satellite and ethernet communications, while frequency division multiple access (FDMA), such as OFDMA and SC-FDMA are used in the fourth generation (4G) LTE mobile wireless communications. In addition, SC-FDMA has been proposed as an option in the DVB-RCS2 satellite return link standard, due to its moderate peak-to-average-power ratio (PAPR) and high spectral efficiency.

In TDMA, the sequence of symbols dedicated to different users in the system is time multiplexed. In OFDMA, the signal bandwidth is split in orthogonal subcarriers, resulting in a high spectral efficiency. The inverse fast Fourier transforms (IFFT) and the FFT are employed as multiplexing and demultiplexing techniques at the transmitter and the receiver, respectively. Due to the commonly applied cyclic prefix (CP), multi-path fading effects in the form of ISI, as well as multiple access interference (MAI), are mitigated, reducing the equalization effort to a single-tap equalizer. The multiple access is realized by assigning a number of subcarriers to a user. The assignment can follow a localized allocation in the form of sub bands or an interleaved allocation. In SC-FDMA, the frequency domain symbols are pre-coded by means of a n -point FFT. After subcarrier mapping, a N -point IFFT ($N > n$) is used for multiplexing, and a CP is inserted. The multiple access realizations of SC-FDMA are commonly known as localized FDMA (LFDMA) and interleaved FDMA (IFDMA). Since the analog IFDMA and LFDMA signals exhibit similar PAPR, the focus in this study falls on LFDMA, due to its better applicability with synchronization techniques.

After symbol multiplexing according to the transmission format, the information symbols are pulse shaped by means of a square root raised cosine filter (SRRCF) to ensure signal and spectrum integrity for RF transmission. In optical communication systems with intensity modulation and direct detection (IM/DD), this digital pulse shaping block is generally omitted due to the unipolar signal constraint. Next, the signal is passed through a digital-to-analog converter (DAC) and possibly through a transmit filter, e.g. during up-conversion to the carrier frequency. The transmitter device can introduce nonlinear distortion, due to the non-linear transfer function of the HPA in RF systems or the light emitting diode (LED) or laser diode (LD) in optical systems. This distortion is particularly prominent with amplitude modulated signals. Here, the distortion is described through a generalized non-linear transfer function, $F(\cdot)$. The signal is then passed through the channel. The channel can be RF

wired, RF wireless, optical fiber or optical wireless, and it is characterized by its impulse and frequency responses. Multi-path effects in terrestrial communication channels introduce a linear distortion such as ISI. Similar effects are also introduced by the imperfect frequency responses of the filters along the transmission chain. In this study, it is assumed that the channel effect can be compensated by means of sufficiently frequent channel estimation and equalization at the receiver. In general, the channel can be a cascade of linear and non-linear devices as in relay systems with amplify and forward operation, such as in satellite communications. Without loss of generality, the signal at the receiver can be expressed as $h * F(x)$, where h is the cumulative impulse response, $F(x)$ is the cumulative non-linear transfer function, and $*$ is the linear convolution operator. At the receiver, the signal is distorted by AWGN, w . As a result, the received signal, y , can be expressed as follows[1]:

$$y = h * F(x) + w \quad (1)$$

The receiver can include a receive filter, e.g., during down- conversion back to baseband. The signal is then passed through an analog-to-digital converter (ADC) and a matched SRRCF is applied. In optical systems, the digital matched filter is generally omitted, if no pulse shaping filter is applied at the transmitter. The transmitter and receiver are assumed to be fine synchronized. This assumption is shown to be valid even in demanding applications such as synchronization over satellite. Suitable synchronization acquisition and tracking algorithms have been proposed in to maintain the fine synchronization of the transmitted and received signals. Next, an equalizer is applied to counter the channel effect and the linear distortion. Here, zero forcing (ZF) or minimum mean squared error (MMSE) criteria are generally applied. The symbols are then demultiplexed, demodulated and decoded, to obtain the received bits.

III. ITERATIVE CANCELLATION OF NON-LINEAR DISTORTION

In this section, the non-linear distortion in the channel is elaborated; a suitable iterative receiver is

presented that performs iterative IMI cancellation for the sake of the maximization of the received SNR, followed by analytical modeling of the performance.

A. Non-Linear Distortion Effects

The non-linear distortion in a digital communication system introduces constellation warping and symbol clustering at the input of the demodulator at the receiver. The IMI is dependent on the signal waveform, and therefore it contains useful information of the transmitted signal. In digital transmission schemes, where a low number of analog carriers are modulated, such as TDMA, the interfering component is generally correlated with the transmitted symbols. Therefore, each constellation point at the receiver can be individually warped, scaled and rotated with respect to the original transmit symbol constellation at the modulator. In OFDMA systems, where the analog carrier is digitally subdivided in a large number of subcarriers, as well as in multi-carrier systems with a large number of analog carriers, the large degree of symbol multiplexing results in a signal with a close to Gaussian distribution. According to the Bussgang theorem, the interfering component is in this case uncorrelated with the signal component. Therefore, multicarrier systems are robust to the constellation warping effects. In state-of-the-art systems, common approaches to compensate the non-linear distortion include pre-distortion at the transmitter and equalization at the receiver. Signal pre-distortion can be used to linearize the amplifier characteristic. It generally involves additional analog electronics which implement the inverse of the amplifier characteristic. Signal pre-distortion is known to introduce unwanted out-of-band radiation. Data predistortion, on the other hand, is a purely digital technique which preserves the signal spectrum. Here, the transmit constellation is modified such that the received centroids coincide with the original transmit constellation. At the receiver, the knowledge of the non-linear transfer function can be used in the design of an equalizer. In addition, it also performs automatic gain control (AGC), where the received constellation symbols are

collectively scaled, to minimize the error with respect to the original transmit constellation according to ZF or MMSE criteria. Next, the demodulator and the decoder perform maximum likelihood (ML) detection with respect to the original transmit constellation. In state-of-the-art systems, the receiver does not attempt to extract the useful information from the IMI, and the interfering component is treated as noise. In this paper, the following decomposition of the signal and the interfering component is employed, where the output of the non-linear device is given as[1]:

$$F(x) = k_x + d \quad (2)$$

Here, the output signal, $F(x)$, is an attenuated and possibly rotated replica of the information-carrying signal, x , plus nonlinear distortion noise, d . The scaling factor K can be complex valued or real-valued based on the non-linear distortion function. It is obtained as the covariance of the transmitted and received symbols normalized by the average transmit symbol power. There is no general assumption on the distribution of the non-linear distortion noise, and it can be correlated or not with the signal. Memory effects can be modeled by the introduction of an additional dimension in this model to account for preceding and following symbols. In this study, a practical model of a non-linear Ka-band solid state power amplifier (SSPA) of a user terminal in a satellite return link is considered. The input amplitude/output amplitude (AM/AM) and input amplitude/output phase (AM/PM) characteristics are presented in Fig. 1.

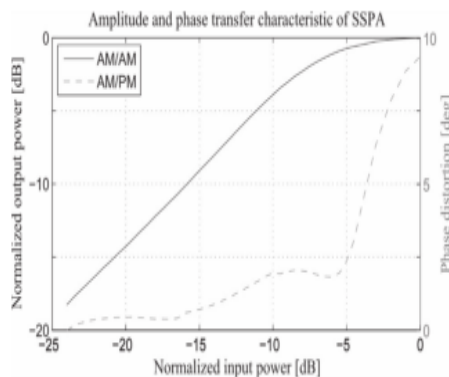


Fig. 1. AM/AM and AM/PM transfer characteristics of an SSPA.

The effects of the nonlinear distortion on the received 16-QAM symbols are presented in Figs. 2 and 3 for TDMA, SC-FDMA and OFDMA according to (2). In TDMA, roll-off factors of 5% and 20% are assumed. In addition, a block of 2048 symbols is assigned to 32 users with 64 localized symbols per user. A similar setup of the subcarrier frame, number of users and subcarriers per user is considered in SC-FDMA and OFDMA. As a result, a large degree of symbol multiplexing is achieved in the latter two schemes, to obtain a stable signal distribution.

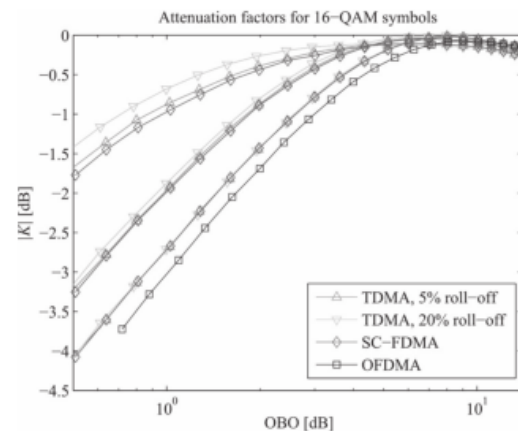


Fig. 2. Attenuation factor of the non-linear distortion for 16-QAM with an SSPA in return link.

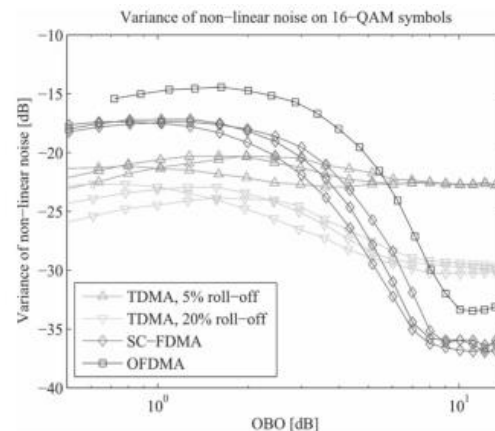


Fig. 3. Variance of non-linear distortion noise for 16-QAM with an SSPA in return link.

In Figs. 2 and 3, the amplitude of the attenuation factors and the variance of the non-linear distortion noise are presented as a function of the OBO. TDMA and SC-FDMA experience an almost identical warping of the amplitude of the received centroids. The three distinct symbol amplitudes in the 16-QAM constellation have three distinct

attenuation factors and noise variances. The degree of attenuation and the noise variance correspond to the PAPR of the schemes. TDMA with 20% roll off experiences the least distortion, followed by TDMA with 5% roll-off, SC-FDMA and OFDMA. It can be noticed that received symbols in OFDMA are expectedly scaled by a single attenuation factor and have the largest noise variance. It should be noted that the truncation of the SRRCF impulse response (16 periods considered with an oversampling factor of 8) to reduce the processing complexity and latency in TDMA contributes additional non-linear distortion noise which is evident in the high OBO region, and it is more prominent in TDMA with 5% roll-off.

B. Iterative Receiver for Cancellation of Non-Linear Distortion Noise

The receiver can extract the useful signal information in the IMI by means of interference cancellation. It has been first proposed for systems with OFDMA. A set of received symbols, e.g. a received frame, is buffered. In the first iteration, the symbols are demodulated. Based on the knowledge of the distortion function along the transmission chain, the demodulated symbols are used to obtain an estimate of the received symbols, which is subtracted from the scaled demodulated symbols to obtain an estimate of the interfering component. It is then subtracted from the buffered symbols to obtain a new set of received symbols as an output of the first iteration of IMI cancellation. In the original approach, one factor is used to scale all the constellation symbols. In the second iteration, the newly obtained received symbols are demodulated and used to better estimate the interfering component which is again subtracted from the originally buffered received symbols.

The output of this process are the newly obtained received symbols after a number of iterations. Finally, the buffer is released and a new set of received symbols is processed. The IMI cancellation approach has been studied for coded OFDMA signals and adopted for systems with SC-FDMA. However, the same estimator for the

interfering component based on a single scaling factor for all symbols from (2) is applied. This approach is suboptimum for SC-FDMA and TDMA, where individual scaling factors for each constellation point need to be computed as shown in Fig. 2.

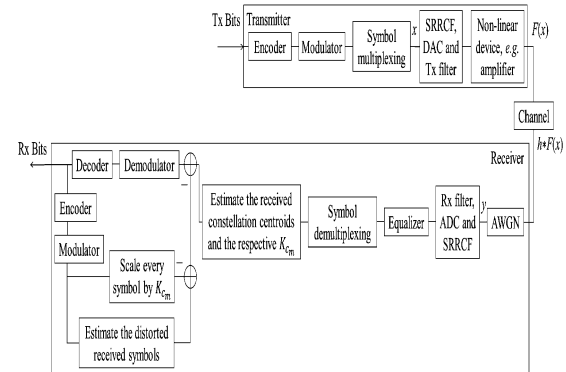


Fig. 4. Block diagram of a digital transmission scheme with an iterative receiver, performing cancellation of the non-linear distortion noise.

The block diagram of the proposed modified receiver is presented in Fig. 4. This block diagram can be considered as representative for all types of commercial digital communication systems. In addition, it describes the forward as well as the return links, where the major differences are related to the data framing and signal multiplexing, as well as the resulting channel and distortion functions. Due to the added processing complexity, the receiver is more suitable for application in the return link, where the complexity is confined at the server side. However, when user equipment for professional applications is considered, a higher computational load can be afforded at the user side, and the system can benefit from the application of the proposed receiver in the forward link. After the symbol demultiplexing stage, the received symbols are buffered for further processing. At this point, estimates of the received constellation centroids and the respective scaling factors, K_{cm} , are calculated for every constellation point, c_m , $m = 1, \dots, M$, where M is the modulation order. This can be performed in several ways. First, training frames can be used at the beginning of the transmission, involving a number of symbols for every constellation point.

This method can be used in a time invariant channel. In slow fading or mobile channels, pilot symbols in the frame can be employed, e.g. in the preamble, given the pilot overhead is tolerable. In the case when the transmitter is the main contributor to the non-linear distortion and if the channel state information is available, the transmitter can estimate the dislocation of the constellation centroids in an offline setup and signal it to the receiver. Finally, if the dynamics in the system prohibit the application of the above methods, the received centroids can be estimated directly from the received data using mode estimation techniques for the M modes of the received probability distribution function. The scaling factors, K_{cm} , can be obtained as the ratio of received centroid and transmitted constellation point.

The received centroids and the associated scaling factors are stored in a look-up table for every user, so they can be used in the subsequent processing blocks. In satellite communications, where TDM(A) is used, the demodulation is performed over long symbols frames, e.g., 1616 symbols per burst (of which 140 symbols are in header) in DVB-RCS2 return link and 16984 symbols per physical layer frame (of which 784 symbols are pilots and header) in DVB-S2X forward link. In such a setup, stable statistics of the constellation warping can be obtained, which implies stable scaling factors over time. In addition, a single modulation format is employed on the frame to be demodulated, and the channel is static. Therefore, the scaling factors can be estimated in an offline setup and stored in look-up tables for the different modulation orders.

The received constellation centroids are used as a reference for the ML demodulator or in the calculation of the log-likelihood ratios (LLRs) in the case of a subsequently applied decoder. The detected symbols (obtained by encoding and modulation of the decoded bits in the case of coded transmission) are used to obtain an estimate of the interfering component and cancel it from the signal in an iterative fashion. The vector of detected symbols used in the i -th iteration can be expressed as follows[3]:

$$\hat{x}(i-1) = \text{Det} \left[\text{Demux} \left[\text{Eq} \left[\text{ADC} [y] \right] \right] \right] \quad (3)$$

where the ADC block accounts for the receive filter, the ADC and the SRRCF. The order of the equalizer and the demultiplexer may vary in the different systems. For example, time domain equalization in TDMA is performed before demultiplexing of the symbols, frequency domain equalization in SCFDMA comes between the FFT and the IFFT operations, while the equalizer in OFDMA is applied after the FFT block. Using the model from (2), an estimate of the non-linear distortion noise can be obtained by subtracting the suitably scaled detected symbols from an estimate of the received symbols:

$$d^{(i)} = \text{Demux} \left[\text{Eq} \left[\text{ADC} \left[* F \left(\text{DAC} \left[\text{Mux} \left[\hat{x}(i-1) \right] \right) \right] \right] \right] \right] - \hat{x}(i-1) \quad (4)$$

This is essential to account for the constellation warping effects in systems, where the non-linear distortion noise is correlated with the signal, such as TDMA and SC-FDMA. From the detected symbols, an estimate of the received symbols can be obtained using the knowledge of the distortion sources and the processing blocks along the chain. First, the detected symbols are passed through the known multiplexing block according to the employed transmission scheme. Next, the known SRRCF and the transmitter filter function are applied, followed by the function of the non-linear device. The signal is then passed through the known channel function obtained by means of channel estimation at the receiver, e.g., by means of dedicated pilots in the frame. In the receiver chain, the known receiver filter function and the SRRCF are applied, followed by the known equalizer function to counter the linear distortion in the system and the symbol demultiplexing stage. Knowledge of the linear and non-linear distortion mechanisms is a common assumption in state-of-the-art communication system. The measured frequency response of the filters along the chain and the estimated channel taps are used in the design of the equalizers, e.g., the linear equalizer in DVB-S2X, or the pre-coding

techniques, e.g., bit-and-power loading techniques in OFDMA for 4G LTE. The transfer characteristics of SSPAs can be considered relatively stable over time and are commonly used in the linearization electronics that implement signal predistortion techniques.

The estimate of the interfering component is subtracted from the buffered received symbols, and the demodulation and possibly decoding stages are repeated. The improved received vector of symbols after the i -th iteration can be expressed as follows:

$$x^{(i)} = \text{Demux} \left[\text{Eq}[\text{ADC}[y]] \right] - d^{(i)} \quad (5)$$

The iterations continue until no further change is observed at the output of the demodulator and decoder.

C. Analytical Modeling

The performance of the IMI cancelling receiver is analyzed in the non-linear channel with AWGN. In OFDMA, the signal follows a close-to-Gaussian distribution for a large number of subcarriers which does not depend on the underlying digital modulation format and modulation order. In addition, the nonlinear distortion noise component is uncorrelated from the signal. These two facts allow for the derivation of a semi analytical model. In this paper, the effective electrical SNR at the detector and the TD metrics are derived for a standard receiver without IMI cancellation and for 1 iteration of IMI cancellation. Iteration is sufficient to achieve the majority of power efficiency improvement. In SCFDMA and TDMA, due to the modulation dependent signal distribution [and the fact that the non-linear distortion noise component is correlated with the signal resulting in individual scaling factors for the received constellation centroids illustrated in Fig. 2, the analysis is performed only in a Monte Carlo simulation. To quantify the power efficiency penalty induced by the IMI, the TD metric [3] is defined as follows:

$$TD[\text{db}] = OBO + SNR_{\text{required in non-lin.chan.}} - SNR_{\text{required in lin.chan.}} \quad (6)$$

In addition to the OBO penalty, the TD incorporates the penalty on the SNR requirement to achieve a target BER in the nonlinear channel with respect to the SNR requirement in the linear channel with AWGN. Using the effective received SNR expression, the SNR requirement to achieve a target BER in the non-linear channel can be expressed by means of the inverse function $G^{-1}(\cdot)$ as $G^{-1}(\gamma)$. Therefore, the TD can be derived in the linear domain as a function of the required SNR for a target BER in the linear channel, γ , as follows:

$$TD = OBO \frac{\xi^{-1}(\gamma)}{\gamma} = \frac{B}{R_s} \frac{OBO}{|H|^2} \left((|K|^2) - \gamma \frac{\sigma_D^2}{\sigma_x^2} \right)^{-1} \quad (7)$$

In the case of the soft limiter amplifier, the OBO is derived as follows:

$$OBO_{\text{clip}} = P_{\text{max}}^{\text{out}} \left((G\sigma_x^2) \left(1 - \exp \left(-\frac{p_{\text{max}}^{\text{out}}}{\sigma_x^2} \right) \right) \right)^{-1} \quad (8)$$

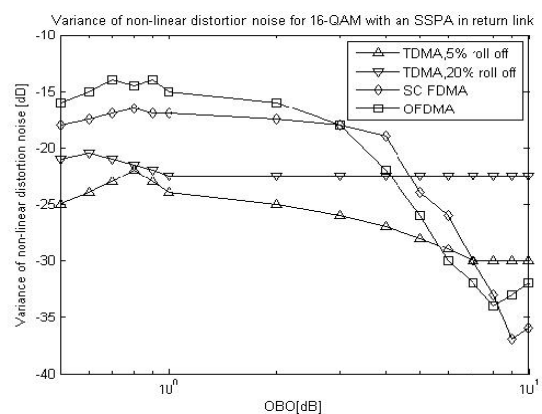
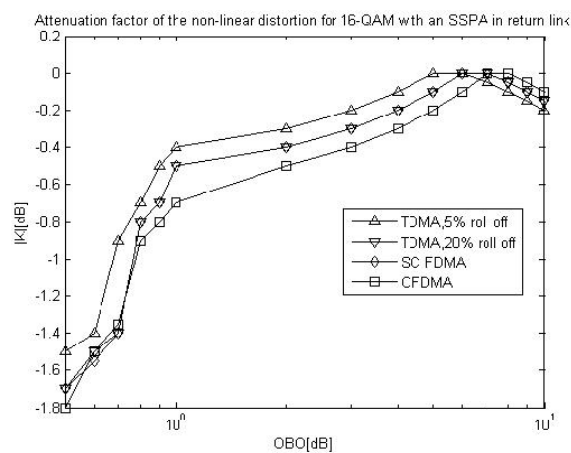
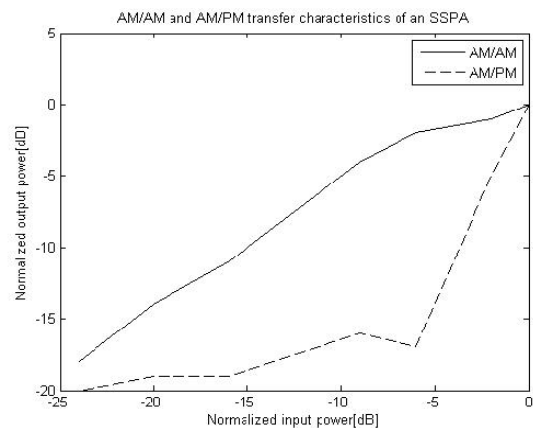
The derived SNR after the first iteration, can be used to derive the TD as follows [4]:

$$TD^{(1)} = \frac{B}{R_s} \frac{OBO}{|H|^2} \beta \left(\alpha |K|^2 - \gamma \frac{\sigma_D^{(1)}}{\sigma_x^2} \right)^{-1} \quad (9)$$

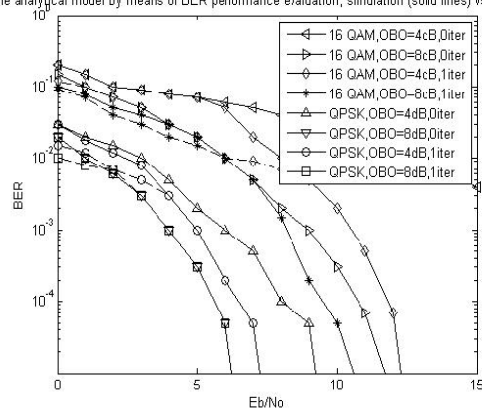
The analytical model is verified against a Monte Carlo BER simulation. For this purpose, the amplifier characteristics from Fig. 1 are assumed, and 2048 OFDMA subcarriers are shared among 32 users in a return link setup with 64 subcarriers per user. The subcarriers are modulated by means of M-QAM symbols. The derived expressions for the effective received electrical SNR are inserted in the analytical model for the BER in M-QAM [5]

$$BER = \frac{4(\sqrt{M}-1)}{\log_2(M)\sqrt{M}} Q \left(\sqrt{\frac{3 \log_2(M)}{M-1}} \Gamma \right) \quad (10)$$

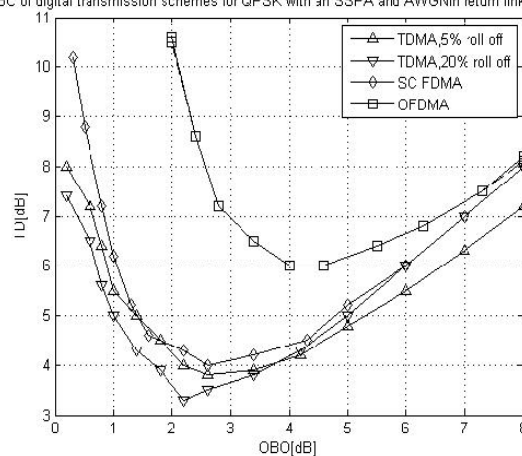
IV.RESULTS



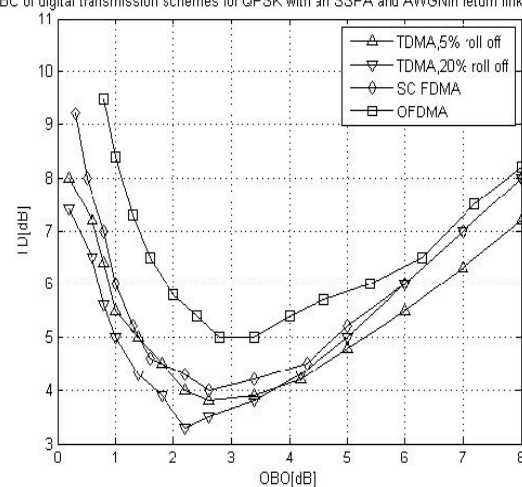
the analytical model by means of BER performance evaluation, simulation (solid lines) vs. theory



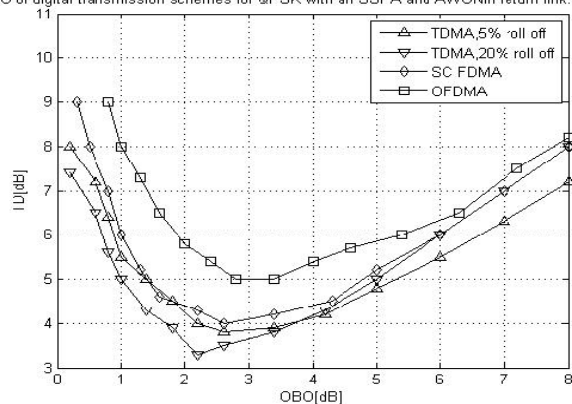
OBC of digital transmission schemes for QPSK with an SSPA and AWGN in return link.



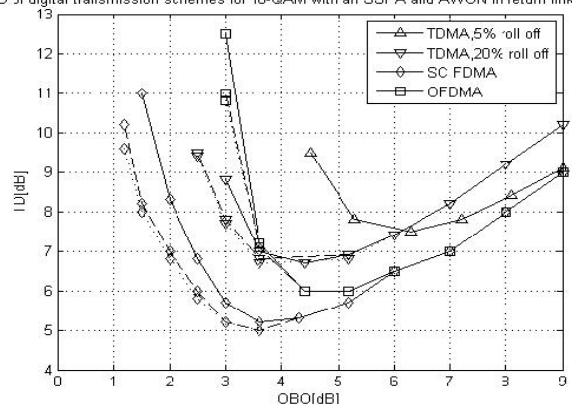
OBC of digital transmission schemes for QPSK with an SSPA and AWGN in return link.



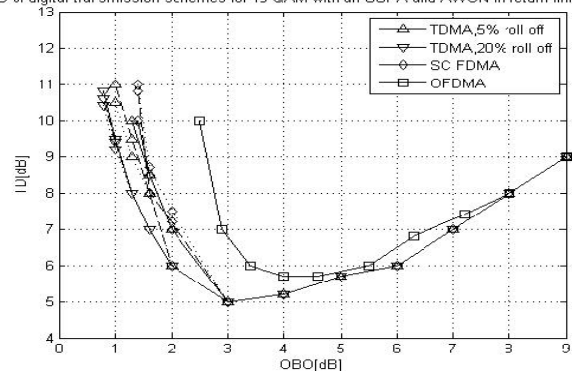
OBO of digital transmission schemes for QPSK with an SSPA and AWGN in return link.



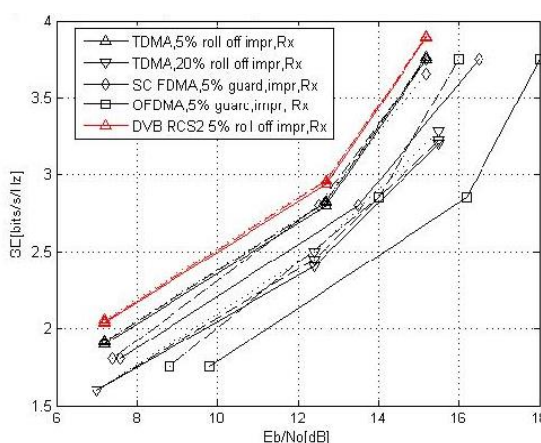
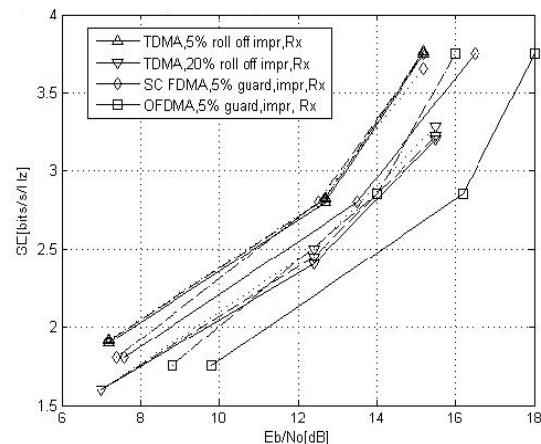
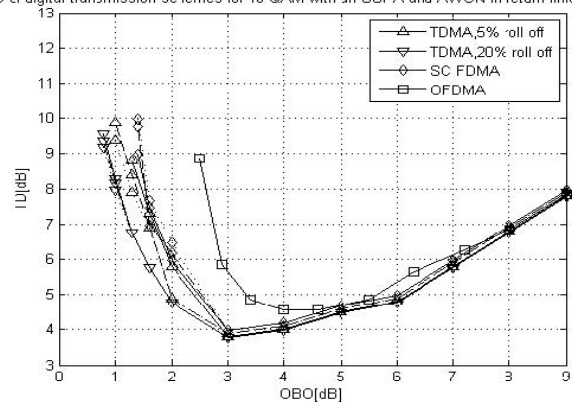
OBO of digital transmission schemes for 16-QAM with an SSPA and AWGN in return link.



OBO of digital transmission schemes for 15-QAM with an SSPA and AWGN in return link.



OBO of digital transmission schemes for 16-QAM with an SSPA and AWGN in return link.



V.CONCLUSION

In this paper, an iterative receiver has been presented which performs cancellation of the IMI that originates from the nonlinear distortion in the channel. The performance of single carrier transmission schemes such as TDMA and SC-FDMA is maximized by the joint application of ML detection with respect to the received constellation centroids and non-linear noise cancellation using individual scaling factors for the detected symbols. The proposed receiver can be applied in all types of commercial digital communication systems. These include terrestrial mobile wireless communications, DSL and cable communications, satellite communications and optical wireless communications such as infrared communications and VLC. In addition, it can be applied in both the forward and the return links. The receiver has been tested with TDMA, SCFDMA and OFDMA transmission formats, and it has demonstrated significant gains in the power efficiency.

An analytical model has been developed for 1 iteration of IMI cancellation in OFDMA. It has been shown that even 1 iteration is sufficient to present the majority of the gain of IMI cancellation in the tested transmission schemes. In the considered modulation setup, gains of up to 2.5 dB are expected for OFDMA, 1.1 dB for SC-FDMA, 0.8 dB for TDMA with 20% roll-off and 1.9 dB for TDMA with 5% roll-off. The receiver is particularly suitable for application with higher order modulation formats which are more vulnerable to non-linear distortion, and as a result higher gains are expected. Consequently, higher spectral efficiency can be achieved which can be translated into higher throughput and lower cost per transmitted bit.

REFERENCES

- [1] Broadband Access via Integrated Terrestrial and Satellite Systems (BATS), "ICT-2011.1.1 BATS D4.1: Satellite network mission requirements," European Project, Avanti PLC, London, U.K., Tech. Rep., 2012.
- [2] *Second Generation Framing Structure, Channel Coding and Modulation Systems for Broadcasting, Interactive Services, News Gathering and Other Broadband Satellite Applications; Part II: S2-Extensions (DVBS2X)–(Optional), Digital Video Broadcasting (DVB) Standard*, ETSI EN 302307-2, Mar. 2014.
- [3] *Second Generation DVB Interactive Satellite System (DVB-RCS2); Part 2: Lower Layers for Satellite Standard, Digital Video Broadcasting (DVB) Standard*, ETSI EN 301 545-2, Jan. 2012.
- [4] E. Casini, R. De Gaudenzi, and A. Ginesi, "DVB-S2 modem algorithms design and performance over typical satellite channels," *Int. J. Satell. Commun. Netw.*, vol. 22, no. 3, pp. 281–318, Jun. 2004.
- [5] V. Dalakas, P. Mathiopoulos, F. Do Cecca, and G. Gallinaro, "A comparative study between SC-FDMA and OFDMA schemes for satellite uplinks," *IEEE Trans. Broadcast.*, vol. 58, no. 3, pp. 370–378, Sep. 2012.
- [6] G. Karam and H. Sari, "Analysis of predistortion, equalization, and ISI cancellation techniques in digital radio systems with nonlinear transmit

amplifiers," *IEEE Trans. Commun.*, vol. 37, no. 12, pp. 1245–1253, Dec. 1989.

- [7] H. Chen and A. M. Haimovich, "Iterative estimation and cancellation of clipping noise for OFDM signals," *IEEE Commun. Lett.*, vol. 7, no. 7, pp. 305–307, Jul. 2003.
- [8] R. Djardin, M. Colas, and G. Gelle, "Comparison of iterative receivers mitigating the clipping noise of OFDM based system," in *Proc. Eur. Wireless Conf.2007*, Paris, France, Apr. 2007, pp. 1–7.

MULTI-STREAM TRANSMISSION FOR HIGHLY FREQUENCY SELECTIVE CHANNELS IN MIMO-FBMC/OQAM SYSTEMS

Althaf Pasha Mohammed¹

N. Pandu Ranga Reddy²

1) Althaf Pasha Mohammed, M.Tech (ES), Malla Reddy Engineering College (Autonomous), Hyderabad, India

2) N. Pandu Ranga Reddy, Associate Professor, Malla Reddy Engineering College (Autonomous), Hyderabad, India

Abstract—This paper addresses the joint design of MIMO precoding and decoding matrices for filter bank multicarrier (FBMC) systems based on OQAM, known as FBMC/OQAM. Existing solutions that support multi-stream transmission only give satisfactory performance in scenarios with high coherence bandwidth channels. To make progress towards the application of FBMC/OQAM to MIMO channels, we study the design of novel solutions that provide robustness against the channel frequency selectivity and support multi-stream transmission. To this end, two techniques have been devised under the criterion of minimizing the sum mean square error. The non-circular nature of the OQAM symbols has not been ignored, making evident the convenience of performing a widely linear processing. The first technique keeps the complexity at a reasonable level but in exchange the original problem is relaxed yielding a suboptimal solution. With the objective of performing closer to the optimum solution, the second option iteratively computes precoders and equalizers by resorting to an alternating optimization method, which is much more complex. We have demonstrated via

simulations that the first technique nearly achieves the same results as the iterative design. Simulation results show that the proposed low-complexity solution outperforms existing MIMO-FBMC/OQAM schemes in terms of bit error rate. As for the comparison with OFDM, the numerical results highlight that FBMC/OQAM remains competitive, with and without perfect channel state information, while it provides spectral efficiency gains. Under highly frequency selective channels the proposed technique significantly outperforms OFDM.

Index Terms—FBMC based on OQAM., MIMO precoder/decoder design, multi-stream transmission, OFDM.

I. INTRODUCTION

In this work we study the joint design of transmit and receive beam formers for frequency selective multiple-input-multiple-output (MIMO) channels. With respect to the figure of merit that governs the design, we consider the minimization of the sum mean square error (MSE) subject to a power constraint. Since this topic has been widely studied

over the recent years we review right after the different approaches that have been proposed to tackle the problem. In this sense, we first introduce a narrowband point-to-point MIMO communication system, where the transmitter and the receiver are equipped with N_t and N_r antennas, respectively. At the channel access the system equation is $\mathbf{d}[n] = \mathbf{A}^H \mathbf{H} \mathbf{B} \mathbf{N}[n] + \mathbf{A}^H \mathbf{w}[n]$. According to the system model, the optimization problem that is proposed reduces to

$$\begin{aligned} \arg \min_{\mathbf{A}, \mathbf{B}} \mathbb{E} \left\{ \|\tilde{\mathbf{d}}[n] - \mathbf{d}[n]\|_2^2 \right\} \\ \text{s.t.} \quad \mathbb{E} \left\{ \|\mathbf{B} \mathbf{d}[n]\|_2^2 \right\} \leq P_T. \end{aligned}$$

The restriction imposed on the average transmitted power ensures that the problem is well-posed. In this sense, the maximum allowable transmit power is given by P_T . The solution of (1) can be computed when the channel state information (CSI) is known at both ends of the link, see e.g. [1], [2]. When the channel has memory it is mandatory to carry out a different processing than [1], [2].

One alternative is to operate on a block-by-block fashion, [3]. To avoid inter-block interference (IBI) a guard interval (GI) is inserted before the transmission of the next block. If the receiver stacks the snapshots obtained when the transmitter is not idle, then the optimization problem is the one in (1) with a channel matrix that is block Toeplitz. In order not to sacrifice rate, the precoder and the equalizer have to diagonalize the MIMO channel transfer function. To do so, it is required to perform a broadband singular value decomposition (BSVD) of

the polynomial channel matrix, [4]. Since the resulting independent subchannels are frequency selective it is deemed necessary to further process the signals to eliminate the residual inter-symbol interference (ISI).

Another alternative to deal with the frequency selectivity of the channel consists in partitioning the band into narrower subchannels. In this respect, the most prominent multicarrier modulation is the so-called orthogonal frequency division multiplexing (OFDM). The beauty of this technique stems from the fact that the end-to-end system can be modeled as a set of parallel flat fading channels thanks to the transmission of a cyclic prefix (CP). This enables us to pre- and post-process the symbols on a per-subcarrier basis as follows:

$$\tilde{\mathbf{d}}_q[k] = \mathbf{A}_q^H \mathbf{H}_q \mathbf{B}_q \mathbf{d}_q[k] + \mathbf{A}_q^H \mathbf{w}_q[k], \quad q = 0, \dots, M-1,$$

Where M is the number of sub bands. Now \mathbf{H}_q accounts for the MIMO channel transfer function evaluated on the radial frequency. Unlike the single carrier case the optimization problem in the multicarrier context boils down to solve

$$\begin{aligned} \arg \min_{\{\mathbf{A}_q, \mathbf{B}_q\}} \sum_{q=0}^{M-1} \mathbb{E} \left\{ \|\tilde{\mathbf{d}}_q[k] - \mathbf{d}_q[k]\|_2^2 \right\} \\ \text{s.t.} \quad \sum_{q=0}^{M-1} \mathbb{E} \left\{ \|\mathbf{B}_q \mathbf{d}_q[k]\|_2^2 \right\} \leq P_T. \end{aligned}$$

The authors in [5] have developed a framework that enables us to solve (3). At the expense of increasing the computational complexity, the performance can be improved by jointly processing all the sub bands as [3], [5] detail. To overcome the signal to noise ratio loss, which is due to the CP transmission, the

authors in [6] have proposed the utilization of the filtered multitone (FMT) modulation, [7]. The main difference with respect to OFDM is that the subcarrier signals decay faster in the frequency domain than the sinc-shaped filter. However, both OFDM and FMT systems suffer a bandwidth loss. In the OFDM case, the loss has to do with the CP transmission. In the FMT modulation, although no redundancy is transmitted a guard band between subcarriers is inserted to ensure that there is no overlapping, which results in a spectral efficiency loss. If maximum bandwidth efficiency is desired, then the filter bank multicarrier modulation based on the offset quadrature amplitude modulation (FBMC/OQAM) is the best alternative [8]. This scheme was first introduced by Saltzberg in [9]. The efficient implementation of FBMC/OQAM as well as the perfect reconstruction property is derived in [10].

With the aim of exploiting the spatial diversity without sacrificing the rate, we propose combining MIMO precoding and decoding techniques with FBMC/OQAM. To the best of authors' knowledge the work derived in [11] is one of the few publications that have studied the design of MIMO precoding and decoding techniques in the FBMC/OQAM context. The results in [11] confirm that the solution gives a satisfactory performance in scenarios where the channel coherence bandwidth exceeds the subcarrier spacing. However, when the channel frequency Selectivity becomes stronger the bit error rate (BER) plots exhibit an error floor [11].

To remedy it, the authors in [12] propose a joint transmitter and receiver beam forming design that is ISI and inter-carrier interference (ICI) aware, which makes the system more robust to the channel frequency selectivity than [11]. Nevertheless, the scheme is only able to accommodate a single stream per-subband for a fixed power allocation. It must be mentioned that most of the existing solutions that combine multi-stream techniques with the FBMC/OQAM modulation solely resort to the CSI at the receiver, see e.g. [13]–[23].

As a summary the contributions of this paper are as follows:

- We design MIMO precoding and decoding matrices with the objective of transmitting several streams on a per-subcarrier basis in the FBMC/OQAM context. In this sense, two different designs have been described. The first one aims at keeping the complexity low. To this end, the original problem is relaxed and, therefore, the solution is suboptimal. In the second case, we are able to find a local optimal solution. However, the complexity is drastically increased because the solution is based on the alternating optimization method. In both cases, we make no assumptions about the flatness of the channel and we exploit the non-circular nature exhibited by the OQAM symbols by performing a widely linear (WL) processing.
- We have carried out an analysis of the quality of the links after pre- and post-processing the symbols when the non-iterative technique is applied. The

analysis reveals in which multi-antenna configurations the FBMC/OQAM modulation scheme may remain competitive with OFDM.

II. MIMO-FBMC/OQAM SYSTEM MODEL

In this work we focus on the FBMC/OQAM modulation, [10]. We consider a multi-antenna configuration that consists of deploying N_T antennas at transmission and N_R antennas at reception. The resulting superimposed signal at the i^{th} ($1 \leq i \leq N_T$) transmit antenna output is given by

$$s_i[n] = \sum_{k=-\infty}^{\infty} \sum_{m=0}^{M-1} v_{im}[k] f_m \left[n - k \frac{M}{2} \right]$$

$$f_m[n] = p[n] e^{j \frac{2\pi}{M} m \left(n - \frac{L-1}{2} \right)}$$

The received signal at the input of the j^{th} receive antenna is contaminated by additive noise and degraded by multipath fading. As a result, the signal received by the j^{th} antenna is

$$r_j[n] = \sum_{i=1}^{N_T} s_i[n] * h_{ij}[n] + w_j[n], \quad j = 1, \dots, N_R,$$

Where $w[n]$ denotes the noise samples of the j^{th} receive antenna and the term $h_{ij}[n]$ refers to the channel impulse response associated to the transmitter and the receiver. To demultiplex the low-rate signals, the received signal is passed through a bank of matched filters, whose outcomes are down sampled by the factor $M/2$, yielding

$$y_q^j[k] = \left(r_j[n] * f_q^*[-n] \right) \downarrow_{\frac{M}{2}},$$

For $1 \leq j \leq N_R$ and $0 \leq q \leq M-1$. As for the mathematical notation, the expression $(.)_{\downarrow x}$ performs a decimation by a factor of x . Unlike the processing carried out at the transmit side, now the matched filters $\{f_q^*[-n]\}$

$n\}$ are used to build the analysis filter bank (AFB). Bearing in mind (4), the AFB outputs can be compactly formulated as

$$y_q^j[k] = \sum_{m=q-1}^{q+1} \sum_{i=1}^{N_T} v_{im}[k] * g_{qm}^{ij}[k] + w_q^j[k]$$

$$g_{qm}^{ij}[k] = \left(f_m[n] * h_{ij}[n] * f_q^*[-n] \right) \downarrow_{\frac{M}{2}}$$

$$w_q^j[k] = \left(w_j[n] * f_q^*[-n] \right) \downarrow_{\frac{M}{2}}.$$

Note that ICI exclusively comes from the most immediate neighbors thanks to the good confinement of the pulses in the frequency plane, see e.g. [10], [24], [25]. In the same line, we assume that only the first and the second order neighbours bring about ISI. In order to enhance the quality of the estimates, the demodulated data is further processed on a per-subcarrier basis by means of a broadband MIMO equalizer. This means that on the subcarrier the multi-tap equalizers, which are different from zero for, are responsible for performing the receive processing that is aimed at recovering the stream. Then, it follows that the PAM symbols are estimated by compensating the phase term and extracting the real part of the equalized signals, which boils down to operate as follows:

$$\tilde{d}_q^l[k] = \Re \left(u_q^l[k] \right), \quad l = 1, \dots, S, \quad q = 0, \dots, M-1,$$

$$u_q^l[k] = \theta_q^* [k] \left(\sum_{j=1}^{N_R} (a_{jq}^l[k])^* * y_q^j[k] \right).$$

$$u_q^l[k] = \theta_q^* [k] \left(\sum_{j=1}^{N_R} (a_{jq}^l[k])^* * w_q^j[k] \right. \\ \left. + \sum_{m=q-1}^{q+1} \sum_{j=1}^{N_R} \sum_{i=1}^{N_T} (a_{jq}^l[k])^* * v_{im}[k] * g_{qm}^{ij}[k] \right)$$

A. Compact Formulation

The problem of devising transmit and receive matrices directly difficult. To get a more tractable expression we use this equality

$$\mathbf{G}_{qm}^j[t] = \begin{bmatrix} g_{qm}^{1j}[t + L_a] & \cdots & g_{qm}^{N_T j}[t + L_a] \\ \vdots & & \vdots \\ g_{qm}^{1j}[t - L_a] & \cdots & g_{qm}^{N_T j}[t - L_a] \end{bmatrix}$$

$$\mathbf{B}_m = \begin{bmatrix} b_{1m}^1 & \cdots & b_{1m}^S \\ \vdots & & \vdots \\ b_{N_T m}^1 & \cdots & b_{N_T m}^S \end{bmatrix}$$

With the aim of all eviating the complexity, the precoder has been restricted to be real-valued and to have a single-tap. The reason why we have discarded the alternative configuration where both MIMO precoding and decoding matrices are complex-valued is further justified at the end of this section. Now, plugging (15) into (14) leads to

$$u_q^l[k] = \theta_q^*[k] \left(\sum_{m=q-1}^{q+1} \sum_{t=-L_a-2}^{L_a+2} \theta_m[k-t] (\mathbf{a}_q^l)^H \right. \\ \left. \times \mathbf{G}_{qm}[t] \mathbf{B}_m \mathbf{d}_m[k-t] \right) + (\mathbf{a}_q^l)^H \mathbf{w}_q[k]$$

As the subcarrier model that is depicted in Fig. 1 highlights, the symbol detection is sensitive to be affected by ISI and ICI and thus the precoders and the equalizers have to be interference aware, which complicates the design.

$$u_q^l[k] = \sum_{m=q-1}^{q+1} \sum_{t=-L_a-2}^{L_a+2} (\mathbf{a}_q^l)^H \mathbf{E}_{qm}^k[t] \mathbf{B}_m \mathbf{d}_m[k-t] \\ + (\mathbf{a}_q^l)^H \mathbf{w}_q[k]$$

Let \mathbf{a} be either a matrix or a vector, we can define the extended notation by stacking column-wise the real and imaginary components, This enables us to formulate the estimated real PAM symbols as follows:

$$d_q^j[k] = \sum_{m=q-1}^{q+1} \sum_{t=-L_a-2}^{L_a+2} (\mathbf{a}_{q,e}^l)^T \mathbf{E}_{qm,e}^k[t] \mathbf{B}_m \mathbf{d}_m[k-t] \\ + (\mathbf{a}_{q,e}^l)^T \mathbf{w}_{q,e}[k].$$

At this point it is reasonable to question why precoders are restricted to be real-valued. By examining (20) and (21) we can assert that if precoders are complex-valued, then there are more degrees of freedom at the transmit side whereas the number of interference terms in (21) increases. Thus, at first glance it is not obvious to foresee if complex-valued precoders are advantageous.

In order to exploit the non-circular nature exhibited by the OQAM symbols we have adopted a real-valued representation. By examining (21) it becomes noticeable that real and imaginary parts are independently processed giving rise to WL filtering [26]. In other words, (21) depends linearly on the real and the imaginary parts of the equalizer inputs. Note that the structure of the proposed receiver hinges on the use of real valued equalizers the length of which is two-fold with respect to the complex-valued linear counterpart. As a result, there is no penalty in terms of complexity for treating real and imaginary parts separately. Therefore, WL filters are as attractive as linear filters to devise low-complexity solutions.

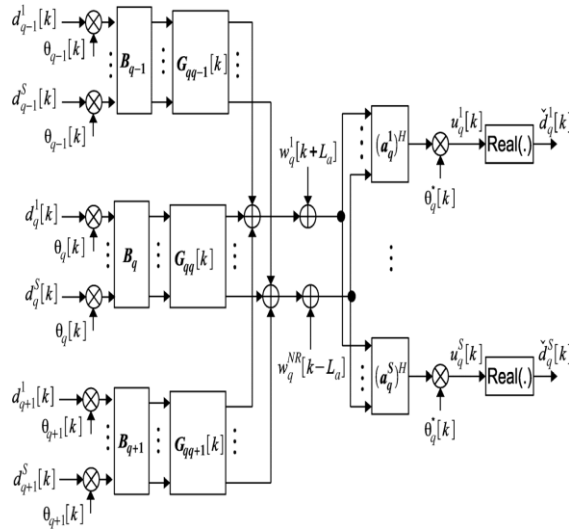


Fig. 1. Subcarrier model of the MIMO-FBMC/OQAM scheme.

III. JOINT TRANSMITTER AND RECEIVER DESIGN

In this section we devise a new subband processing that supports multi-stream transmission in MIMO-FBMC/OQAM systems. Since the required complexity to solve the original problem may render the solution impractical, we have relaxed the problem. This strategy poses a simpler problem to be solved but the solution is suboptimal. For this reason we have carried out an analysis of the quality of the links to determine in which multi-antenna configurations FBMC/OQAM and OFDM may give similar performance.

A. Suboptimal Subband Processing

In this subsection we study how to jointly design transmit and receive processing when perfect CSI is available. Regarding the optimization criterion, we

opt for the minimization of the sum MSE. the problem to be solved is

$$\begin{aligned} \arg \min_{\{\mathbf{s}_{q,e}^t, \mathbf{B}_q\}} & \sum_{q=0}^{M-1} \sum_{t=1}^S MSE_q^t \\ s.t. & \sum_{\alpha=\Omega}^{M-1} \mathbb{E} \left\{ \|\mathbf{B}_q \mathbf{d}_q[k]\|_2^2 \right\} = \sum_{\alpha=\Omega}^{M-1} \|\mathbf{B}_q\|_F^2 \leq P_T, \end{aligned}$$

Note that we have assumed that symbols are independent and have unit-energy. Then, the MSE can be formulated as

$$\begin{aligned} MSE_q^t = 1 + & \sum_{m=q-1}^{q+1} \sum_{t=-L_a-2}^{L_a+2} \left\| (\mathbf{a}_{q,e}^t)^T \mathbf{E}_{qm,e}^k[t] \mathbf{B}_m \right\|_2^2 \\ & + (\mathbf{a}_{q,e}^t)^T \mathbf{R}_q \mathbf{a}_{q,e}^t - 2 (\mathbf{a}_{q,e}^t)^T \mathbf{E}_{qq,e}^k[0] \mathbf{B}_q \mathbf{e}_1. \end{aligned}$$

In notation terms the unitary vector is zero-valued except in the position. The noise correlation matrix is given by. The analytical expression can be found in [12]. It can be readily checked that the MSE is independent of and, therefore, the same metric is used for odd and even. Due to the ICI we cannot decouple the problem into disjoint problems. This highlights that some relaxation has to be applied if we want to alleviate the complexity of the optimization procedure. In this sense, we propose to substitute the objective function by the upper bound.

$$\begin{aligned} MSE_q^t & \leq MSE_{tq}^{UB} \\ & = 1 + \sum_{m=q-1}^{q+1} \sum_{t=-L_a-2}^{L_a+2} \lambda_1 (\mathbf{B}_m \mathbf{B}_m^T) \left\| (\mathbf{a}_{q,e}^t)^T \mathbf{E}_{qm,e}^k[t] \right\|_2^2 \\ & \quad + \sum_{\substack{t=-L_a-2 \\ t \neq 0}}^{L_a+2} \lambda_1 (\mathbf{B}_q \mathbf{B}_q^T) \left\| (\mathbf{a}_{q,e}^t)^T \mathbf{E}_{qq,e}^k[t] \right\|_2^2 \\ & \quad + \left\| (\mathbf{a}_{q,e}^t)^T \mathbf{E}_{qq,e}^k[0] \mathbf{B}_q \right\|_2^2 + (\mathbf{a}_{q,e}^t)^T \mathbf{R}_q \mathbf{a}_{q,e}^t \\ & \quad - 2 (\mathbf{a}_{q,e}^t)^T \mathbf{E}_{qq,e}^k[0] \mathbf{B}_q \mathbf{e}_1. \end{aligned}$$

where A and B are two positive semi definite Hermitian matrices. Then, the new minimization problem becomes

$$\begin{aligned} \arg \min_{\{\mathbf{a}_{q,e}^l, \mathbf{B}_q\}} & \sum_{q=0}^{M-1} \sum_{l=1}^S U B_q^l \\ \text{s.t.} & \sum_{q=0}^{M-1} \|\mathbf{B}_q\|_F^2 \leq P_T \\ & \lambda_1(\mathbf{B}_q \mathbf{B}_q^T) \leq b_q, \quad 0 \leq q \leq M-1 \end{aligned}$$

As a consequence, (27) minimizes an upper bound of the sum MSE. As we will show in the following, the expressions that come into play when solving (27) offer a good analytical tractability, which is of paramount importance to formulate a solution in a closed-form expression. Towards this end, we propose to apply the two-step algorithm described in [5] to obtain the precoding matrices and the receive vectors. The first problem to be solved is given by

$$\arg \min_{\{\mathbf{a}_{q,e}^l\}} \sum_{q=0}^{M-1} \sum_{l=1}^S U B_q^l.$$

For a fixed transmit processing the problem (28) is convex, thus the optimal equalizers are written in this form

$$\mathbf{a}_{q,e}^l = \left(\mathbf{C}_q + \mathbf{E}_{qq,e}^k[0] \mathbf{B}_q (\mathbf{E}_{qq,e}^k[0] \mathbf{B}_q)^T \right)^{-1} \mathbf{E}_{qq,e}^k[0] \mathbf{B}_q \mathbf{e}_l$$

$$\begin{aligned} \mathbf{C}_q = & \sum_{\substack{m=q-1 \\ m \neq q}}^{q+1} \sum_{t=-L_q-2}^{L_q+2} b_m \mathbf{E}_{qm,e}^k[t] (\mathbf{E}_{qm,e}^k[t])^T \\ & + \sum_{\substack{t=-L_q-2 \\ t \neq 0}}^{L_q+2} b_q \mathbf{E}_{qq,e}^k[t] (\mathbf{E}_{qq,e}^k[t])^T + \mathbf{R}_q. \end{aligned}$$

In the second step of the algorithm, the receive vectors are particularized) and the transmit matrices

are optimized so that the upper bound on the sum MSE is minimized. Thus, the problem reduces to

$$\begin{aligned} \arg \min_{\{\mathbf{B}_q\}} & \sum_{q=0}^{M-1} \sum_{l=1}^S U B_q^l \\ \text{s.t.} & \sum_{q=0}^{M-1} \|\mathbf{B}_q\|_F^2 \leq P_T \\ & \lambda_1(\mathbf{B}_q \mathbf{B}_q^T) \leq b_q, \quad 0 \leq q \leq M-1 \end{aligned}$$

where the objective function can be written as

$$\begin{aligned} \sum_{l=1}^S U B_q^l &= \text{tr} \left(\mathbf{I}_S - (\mathbf{E}_{qq,e}^k[0] \mathbf{B}_q)^T \right. \\ & \quad \times \left(\mathbf{C}_q + \mathbf{E}_{qq,e}^k[0] \mathbf{B}_q (\mathbf{E}_{qq,e}^k[0] \mathbf{B}_q)^T \right)^{-1} \\ & \quad \left. \times \mathbf{E}_{qq,e}^k[0] \mathbf{B}_q \right) \\ &= \text{tr} \left(\left(\mathbf{I}_S + (\mathbf{E}_{qq,e}^k[0] \mathbf{B}_q)^T \mathbf{C}_q^{-1} \mathbf{E}_{qq,e}^k[0] \mathbf{B}_q \right)^{-1} \right) \end{aligned}$$

In order to find a low-complexity solution we have forced per-stream powers to be lower than ,i.e. .If the coefficients that delimit the allowed values are too high the exact MSE will lie far below with respect to (26). Conversely, if the parameters take small values, the streams transmitted on the worst subchannels may not receive enough power to overcome the spectral nulls. In this regard, we have empirically observed that when the values of are around , we achieve a good trade-off. The problem of finding a tight upper bound for that relies on analytical expressions is not fully explored in this paper and, therefore, it remains open.

B. Refinement of the Subband Processing

To perform closer to the optimum, we propose to update the receive matrices so that the exact sum MSE is minimized having fixed the transmit processing. In other words, having computed the

precoders with (31), the receivers are recalculated to solve. Therefore it results in

$$\begin{aligned}\mathbf{A}_{q,e} &= [\mathbf{a}_{q,e}^1 \dots \mathbf{a}_{q,e}^S] \\ &= \left(\mathbf{R}_q + \sum_{m=q-1}^{q+1} \sum_{t=-L_a-2}^{L_a+2} \mathbf{E}_{qm,e}^k[t] \mathbf{B}_m \right. \\ &\quad \left. \times (\mathbf{E}_{qm,e}^k[t] \mathbf{B}_m)^T \right)^{-1} \mathbf{E}_{qq,e}^k[0] \mathbf{B}_q.\end{aligned}$$

Note that matrix inversion is allowed since it is assumed that the noise autocorrelation matrix is full rank. The MIMO decoding matrix can be expressed as

$$\begin{aligned}\mathbf{A}_{q,e} &= \bar{\mathbf{C}}_q^{-1} \mathbf{E}_{qq,e}^k[0] \mathbf{B}_q \\ &\quad \times \left(\mathbf{I}_S + (\mathbf{E}_{qq,e}^k[0] \mathbf{B}_q)^T \bar{\mathbf{C}}_q^{-1} \mathbf{E}_{qq,e}^k[0] \mathbf{B}_q \right)^{-1} \\ \bar{\mathbf{C}}_q &= \mathbf{R}_q + \sum_{m=q-1}^{q+1} \sum_{t=-L_a-2}^{L_a+2} \mathbf{E}_{qm,e}^k[t] \mathbf{B}_m \times (\mathbf{E}_{qm,e}^k[t] \mathbf{B}_m)^T \\ &\quad - \mathbf{E}_{qq,e}^k[0] \mathbf{B}_q (\mathbf{E}_{qq,e}^k[0] \mathbf{B}_q)^T\end{aligned}$$

C. Widely Linear vs. Linear Processing

In this section we compare a MIMO-FBMC/OQAM system that is based on the proposed WL processing with a MIMO OFDM system that relies on the linear processing described in [5]. The expressions presented in the following are built on optimistic assumptions for the ease of the tractability when FBMC/OQAM is considered. Thus, the comparison might be unfair. The analysis derived in this section does not allow us to conclude which is the best technique but it allows us to find out in which multi-antenna configurations FBMC/OQAM may remain competitive with OFDM. Then, the signal to interference plus noise ratio (SINR) is given by

$$\text{SINR}_q^l = \frac{1}{\text{MSE}_q^l} - 1 = \frac{p_q^l \bar{\lambda}_q^l}{0.5 N_0}.$$

At this point, it would be interesting to know how the upper bound in (38) compares with the solution based on the linear processing [5]. To this end, we formulate the SINR in the OFDM case, which is given by

$$\text{SINR}_q^l = \frac{2 p_q^l \beta_q^l}{N_0}.$$

The variance of the noise is not halved because the technique is designed over the complex field. The factor 2 in the numerator highlights that the real PAM symbols are obtained from in-phase and quadrature components of the QAM symbols, which are transmitted in OFDM systems.

IV. ITERATIVE DESIGN

The processing developed in Section III gives rise to a suboptimal design. Examining (22) from a different perspective, that is forgetting about the complexity, we can find a local solution that is computed via the alternating optimization method. The idea is to independently optimize receive and transmit matrices in an iterative fashion. The resulting design will be used as a benchmark for the results of Section III. Without making any relaxation the sum MSE is given by

$$\begin{aligned}\text{MSE}(\{\mathbf{A}_{q,e}, \mathbf{B}_q\}) &= \sum_{q=0}^{M-1} \mathbb{E} \left\{ \|\mathbf{d}_q[k] - \bar{\mathbf{d}}_q[k]\|_2^2 \right\} \\ &= M \times S + \sum_{q=0}^{M-1} \sum_{m=q-1}^{q+1} \sum_{t=-L_a-2}^{L_a+2} \|\mathbf{A}_{q,e}^T \mathbf{E}_{qm,e}^k[t] \mathbf{B}_m\|_F^2 \\ &\quad + \sum_{q=0}^{M-1} \text{tr} \left(\mathbf{A}_{q,e}^T \mathbf{R}_q \mathbf{A}_{q,e} - 2 \mathbf{A}_{q,e}^T \mathbf{E}_{qq,e}^k[0] \mathbf{B}_q \right).\end{aligned}$$

A. Receiver Design

The receiver design hinges on minimizing for fixed MIMO precoding matrices. Then, the optimal equalizers are

$$\mathbf{A}_{q,e} = \left(\mathbf{R}_q + \sum_{m=q-1}^{q+1} \sum_{t=-L_a-2}^{L_a+2} \mathbf{E}_{mq,e}^k[t] \mathbf{B}_m \times (\mathbf{E}_{mq,e}^k[t] \mathbf{B}_m)^T \right)^{-1} \mathbf{E}_{qq,e}^k[0] \mathbf{B}_q$$

B. Transmitter Design

The transmitter design is challenging because of the total power constraint. Given the equalizers, the problem becomes

$$\begin{aligned} & \arg \min_{\{\mathbf{B}_q\}} MSE(\{\mathbf{A}_{q,e}, \mathbf{B}_q\}) \\ & s.t. \quad \sum_{q=0}^{M-1} \|\mathbf{B}_q\|_F^2 \leq P_T. \end{aligned}$$

The MIMO precoding matrix that solves given by

$$\mathbf{B}_q^*(\lambda) = \left(\sum_{m=q-1}^{q+1} \sum_{t=-L_a-2}^{L_a+2} (\mathbf{E}_{mq,e}^k[t])^T \mathbf{A}_{m,e} \times \mathbf{A}_{m,e}^T \mathbf{E}_{mq,e}^k[t] + \lambda \mathbf{I}_{N_T} \right)^{-1} (\mathbf{E}_{qq,e}^k[0])^T \mathbf{A}_{q,e}.$$

Plugging into (48) yields the optimal precoder. In this sense, we propose to compute the optimal Lagrange multiplier by performing a bisection search assuming that the criterion to bisect the plane is based on evaluating the supra gradient of the dual function since it might not be differentiable. The authors have demonstrated that the dual function can be upper bounded as follows:

$$g(\bar{\lambda}) \leq g(\lambda) + (\bar{\lambda} - \lambda) \left(\sum_{q=0}^{M-1} \|\mathbf{B}_q^*(\lambda)\|_F^2 - P_T \right)$$

Bearing the complementary slackness in mind along with the trace inequality

$$\begin{aligned} P_T &= \sum_{q=0}^{M-1} \|\mathbf{B}_q^*(\lambda_{opt})\|_F^2 \\ &\leq \sum_{q=0}^{M-1} \sum_{i=1}^{N_T} \frac{\alpha_q^i}{(\lambda_{opt} + \gamma_q^{N_T+1-i})^2} \\ &\leq \sum_{q=0}^{M-1} \sum_{i=1}^{N_T} \frac{\alpha_q^i}{\lambda_{opt}^2}, \end{aligned}$$

For $\lambda_{opt} > 0$ Therefore

$$0 \leq \lambda_{opt} \leq \sqrt{\frac{1}{P_T} \sum_{q=0}^{M-1} \|\mathbf{A}_{q,e}^T \mathbf{E}_{qq,e}^k[0]\|_F^2} = \lambda_{max}.$$

Taking this result into account, the Algorithm 1 enables us to perform as close to the optimal value as desired.

Algorithm 1: Precoder design

```

1: If  $\partial g(0) < 0$  then  $\lambda = 0$ 
2: else
3: Set  $l = 0, u = \lambda_{max}$ 
4: repeat
5:  $\lambda = 0.5(l + u)$ 
6: If  $\partial g(\lambda) < 0$  then  $u = \lambda$  else  $l = \lambda$ 
7: until  $\sum_{q=0}^{M-1} \|\mathbf{B}_q^*(\lambda)\|_F^2 \in [\delta P_T, P_T], 0 < \delta < 1$ 
8: end if
9:  $\mathbf{B}_q = \mathbf{B}_q^*(\lambda), 0 \leq q \leq M-1$ 

```

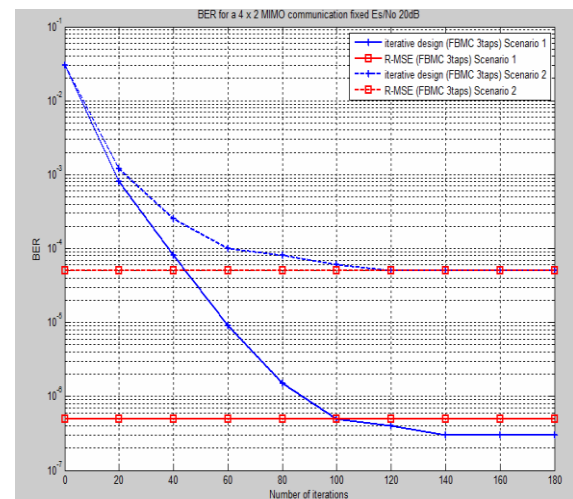
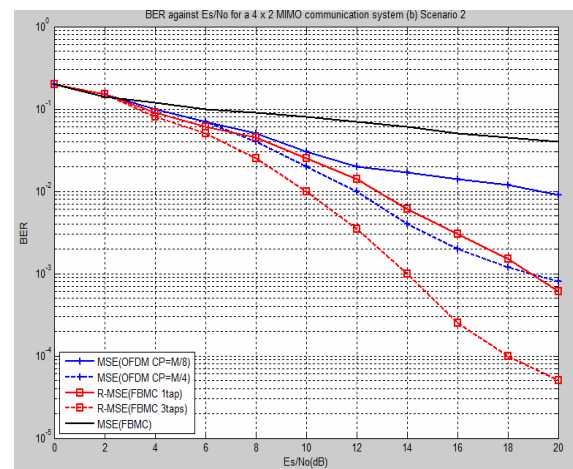
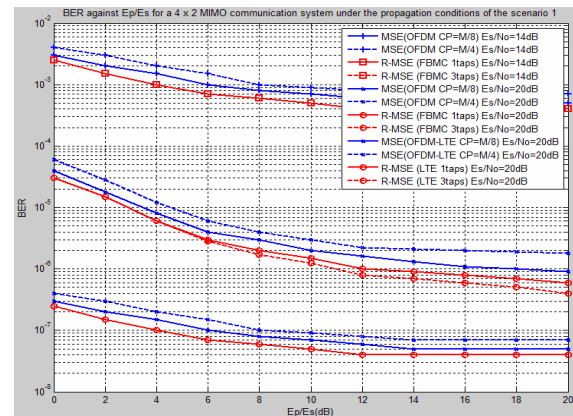
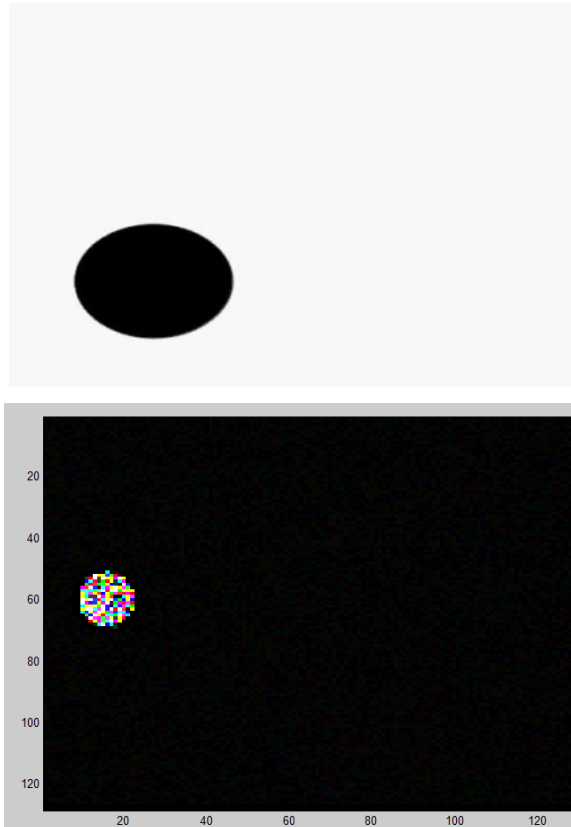
The algorithm stops when the desired precision is reached. In this paper we fix . It is important to remark that through a different reasoning we have arrived at the same result as [33]. The overall algorithm operates as the Algorithm 2 describes. At each iteration the sum MSE decreases because the

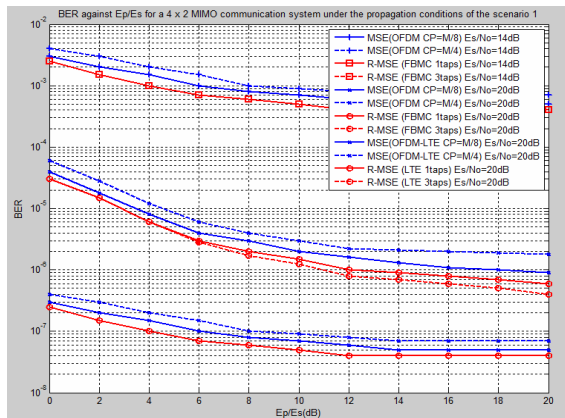
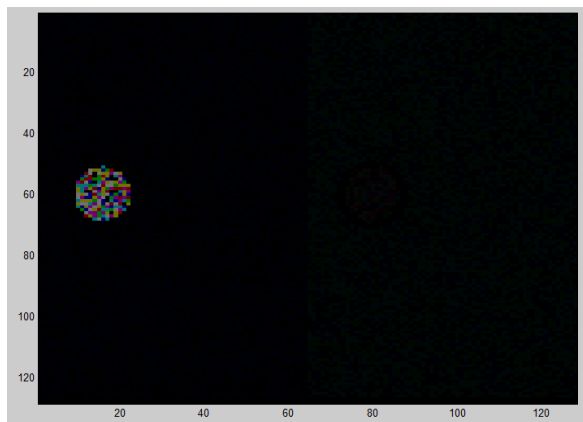
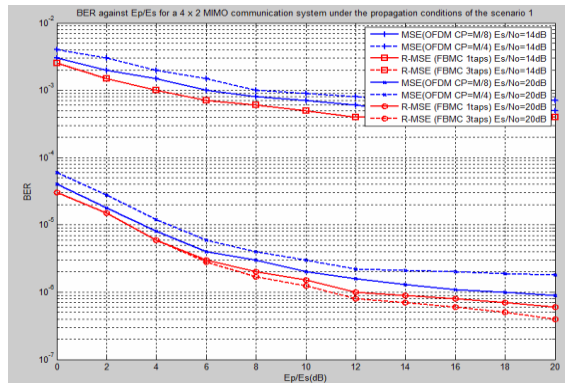
design of precoders and equalizers is governed by the same objective function. Hence, the Algorithm 2 converges to a minimum point since the sum MSE is lower bounded by zero [33]. However, we cannot state that the solution is a global optimum point

Algorithm 2: Alternating optimization method

- 1: Initialize $A_{q,e}, B_q, 0 \leq q \leq M-1$
 - 2: **for** $i = 1, \dots, N$
 - 3: Compute $A_{q,e}$ using (43)
 - 4: Compute B_q executing the Algorithm 1
 - 5: **end for**
-

V.SIMULATION RESULTS





VI. CONCLUSIONS

In this paper we have tackled the joint design of MIMO precoding and decoding matrices for

FBMC/OQAM systems under highly frequency selective channels. It is worth mentioning that the non-circular nature exhibited by the OQAM symbols has not been ignored. This has revealed the convenience of performing Awl filtering. Regarding the objective function, we have opted for the minimization of the sum MSE for a given global power budget. Due to the difficulty of solving the original problem, we have replaced the objective function by an upper bound, which poses a problem easier to solve. Simulation-based results show that the proposed solution clearly outperforms existing MIMO-FBMC/OQAM schemes in terms of BER. This work also demonstrates that FBMC/OQAM compares favourably to OFDM as long as the number of streams transmitted over each subband and the number of antennas deployed at each side satisfy this relation:, which has been theoretically justified. Although the comparison in terms of BER is interesting, the decision that tips the balance towards OFDM or FBMC/OQAM may be determined by other aspects such as the synchronization requirements. Having said that, it must be mentioned that the numerical results highlight that FBMC/OQAM can compete with OFDM even in presence of imperfect CSI. By contrast, in those scenarios where the CP is not long enough to avoid IBI, the FBMC/OQAM modulation scheme shows superior performance than OFDM since the devised subband processing can cope with the loss of orthogonality. Finally, we have demonstrated via simulations that the proposed joint trans mit and

receive design, which is suboptimal, performs close to a local optimal point that can be reached by means of an alternating optimization method.

REFERENCES

- [1] J. Yang and S. Roy, "On joint transmitter and receiver optimization for multiple-input-multiple-output (MIMO) transmission systems," *IEEE Trans. Commun.*, vol. 42, no. 12, pp. 3221–3231, Dec. 1994.
- [2] H. Sampath and A. Paulraj, "Joint transmit and receive optimization for high data rate wireless communication using multiple antennas," in *Proc. Conf. Rec. 33rd Asilomar Conf. Signals, Syst., Comput.*, Oct. 1999, vol. 1, pp. 215–219.
- [3] H. Sampath, P. Stoica, and A. Paulraj, "Generalized linear precoder and decoder design for MIMO channels using the weighted MMSE criterion," *IEEE Trans. Commun.*, vol. 49, no. 12, pp. 2198–2206, Dec. 2001.
- [4] C. H. Ta and S. Weiss, "A design of precoding and equalisation for broadband MIMO systems," in *Proc. 15th Int. Conf. Digit. Signal Process.*, Jul. 2007, pp. 571–574.
- [5] D. Palomar, J. Cioffi, and M. Lagunas, "Joint Tx-Rx beamforming design for multicarrier MIMO channels: A unified framework for convex optimization," *IEEE Trans. Signal Process.*, vol. 51, no. 9, pp. 2381–2401, Sep. 2003.
- [6] N. Moret, A. Tonello, and S. Weiss, "MIMO precoding for filter bank modulation systems based on PSVD," in *Proc. IEEE 73rd Veh. Technol. Conf. (VTC Spring)*, May 2011, pp. 1–5.
- [7] G. Cherubini, E. Eleftheriou, and S. Olcer, "Filtered multitone modulation for very high-speed digital subscriber lines," *IEEE J. Sel. Areas Commun.*, vol. 20, no. 5, pp. 1016–1028, Jun. 2002.
- [8] B. Farhang-Boroujeny, "OFDM versus filter bank multicarrier," *IEEE Signal Process. Mag.*, vol. 28, no. 3, pp. 92–112, May 2011.
- [9] B. Saltzberg, "Performance of an efficient parallel data transmission system," *IEEE Trans. Commun. Technol.*, vol. 15, no. 6, pp. 805–811, Dec. 1967.
- [10] P. Siohan, C. Siclet, and N. Lacaille, "Analysis and design of OFDM/OQAM systems based on filterbank theory," *IEEE Trans. Signal Process.*, vol. 50, no. 5, pp. 1170–1183, May 2002.

REGION BASED SEGMENTATION IN PRESENCE OF INTENSITY INHOMOGENEITY USING LEGENDRE POLYNOMIALS

G.V.Siva Tejasvi¹

Murali Krishna²

1) G.V.Siva Tejasvi, M.Tech, Malla Reddy Engineering College, Hyderabad, India

2) Murali Krishna, Associate Professor, Malla Reddy Engineering College, Hyderabad, India

Abstract—We propose a novel region based segmentation method capable of segmenting objects in presence of significant intensity variation. Current solutions use some form of local processing to tackle intra-region inhomogeneity, which makes such methods susceptible to local minima. In this letter, we present a framework which generalizes the traditional Chan-Vese algorithm. In contrast to existing local techniques, we represent the illumination of the regions of interest in a lower dimensional subspace using a set of pre-specified basis functions. This representation enables us to accommodate heterogeneous objects, even in presence of noise. We compare our results with three state of the art techniques on a dataset focusing on biological/biomedical images with tubular or filamentous structures. Quantitatively, we achieve a 44% increase in performance, which demonstrates efficacy of the method.

Index Terms—Active contour, level set, segmentation.

I.INTRODUCTION

ACTIVE contours have gained popularity for image segmentation due to their ability to elastically

deform and delineate object boundaries with sub-pixel accuracy. Furthermore, the energy minimization framework, which serves as the basic platform for most active contour based techniques, can be manipulated easily to introduce additional constraints based on shape, appearance etc. to assist segmentation. Geometric active contours are favored when the application requires the propagating curves to be able to adapt to the varying topology of the underlying object by automated splitting or merging. Broadly, the geometric active contours may be divided in two subgroups. Edge based techniques perform curve evolution geometrically, with the stopping criteria governed by edge dependent features extracted from the image. However, in many applications where the edge information is unreliable, region based techniques have gained popularity. Chan and Vese proposed a level set formulation to minimize the Mumford Shah functional for segmentation. The Chan-Vese framework models the image as a set of constant illumination regions and performs two-class segmentation by computing the optimal partition which satisfies the constant illumination constraint. The authors also propose a multi-phase variant of their approach to perform multi-class grouping.

The constant illumination assumption is challenged in applications where the signal intensity is inhomogeneous. This is encountered frequently in many medical and biological imaging applications like magnetic resonance (MR) imaging, ultrasound, X-ray, confocal and electron microscopy, etc. While edge based techniques are better suited for heterogeneous images, they are unable to tackle fragmented object boundaries or blurred edges, which occur frequently in medical applications. In this letter we propose an edge independent segmentation approach *Legendre Level Set* (L2S) which is robust to variations in intensity levels. State of the art techniques that tackle inhomogeneity typically require some form of local processing. However, while a global method like Chan-Vese's is insufficient in handling large scale intensity variations, a strictly local approach may lead to undesired segmentation artifacts, especially in presence of noise. Such artifacts are shown in .We aim to eradicate these issues by proposing a generalized solution for region based segmentation in presence of significant intensity variation and additive noise.

II.BACKGROUND AND MOTIVATION

The piecewise constant model of Chan-Vese models the object foreground and background by the scalars. where is the image defined over the domain. The level set function is defined to be positive inside the zero level set and negative outside it Zero level sets of represents the object boundary denotes the regularized version of the

Heaviside function. That minimizes creates segments in a manner such that the foreground and background are best approximated by the intensity levels and. As mentioned previously, this model is incapable of handling spatially varying illumination. A solution was proposed in, where the authors replaced the scalars in with smooth functions, the smoothness enforced by minimizing the total variation. While the solution is attractive, this piecewise smooth model is computationally expensive, since it requires simultaneous solution of two PDEs at each stage of the level set evolution. Recently, Li *et al.* Introduced a region scalable model to localize the energy functional. The region localization is controlled by the scale of a Gaussian kernel, which is manually tuned for optimal performance. Efforts have been made to incorporate the region statistics for segmentation. These methods are robust to initialization and relatively less sensitive to noise. However, Lankton *et al.* demonstrated that global statistics may not be the best resort for segmenting inhomogeneous objects. Instead, the authors generalize the local region based methods, by proposing a generic energy functional capable of performing segmentation using different region based criteria.

However, one downside of their approach is that it requires additional local computation, thus increasing the risk of being stuck within local minima. Feng *et al.* proposed a method for tomographic reconstruction by using a low order parametric model to represent object texture. However, the algorithm is tailored for tomographic reconstruction and is difficult to generalize. Recently

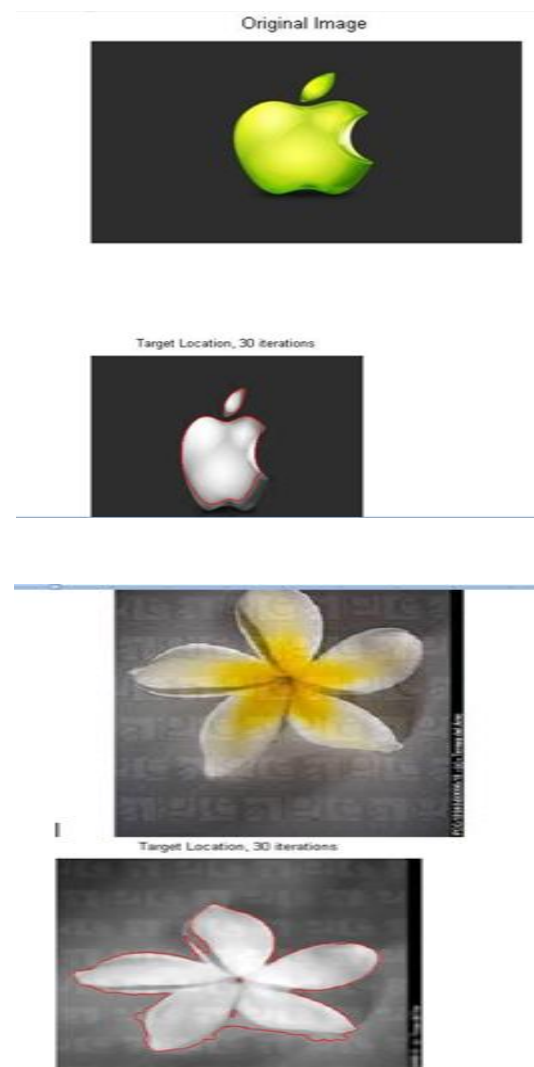
a method was proposed to model the foreground and background by a linear function . This approach is an improvement over the model of Chan-Vese, but does not accommodate nonlinear illumination change. From the above discussion we observe that a majority of these approaches rely on local information only. While localizing the segmentation energy is essential in dealing with in homogeneity, a generic global framework is also necessary to avoid the local minima problem. We propose to model the foreground and background illumination by a set of Legendre basis functions. This model allows the region intensities to be represented in a lower dimensional subspace, thereby permitting smooth approximation. Low dimensional signal representation has been used in a slightly different context in the literature, primarily to accomodate shape priors for segmentation . However, although shape based information assists segmentation, such techniques require an atlas of pre-registered objects, which may be unavailable for general purpose segmentation. We further show that our model (called L2S) is computationally simple, since we achieve a stable, closed form solution at each iteration, which allows faster processing.

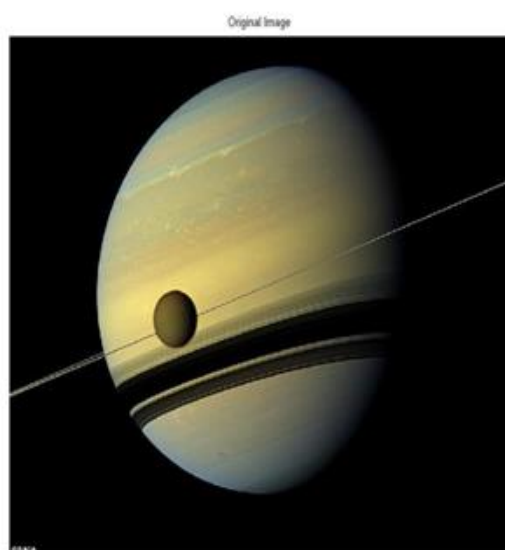
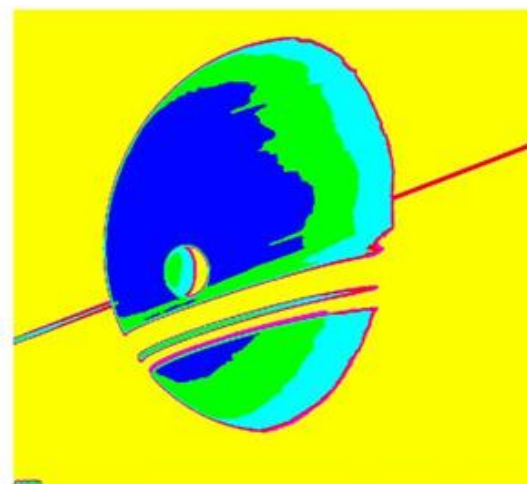
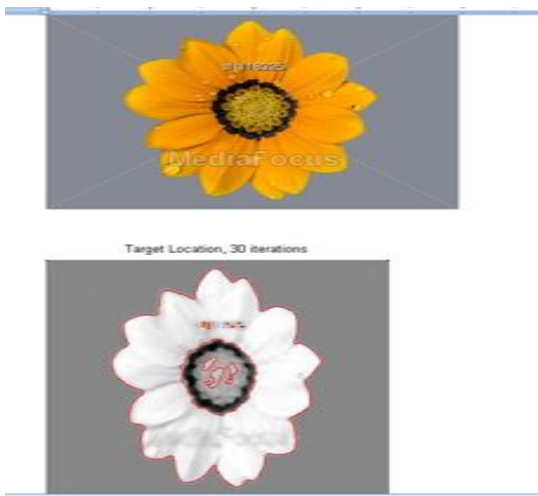
III. METHODOLOGY

The traditional Chan-Vese functional can be reformulated and generalized by replacing the scalars and by two smooth functions and . These functions are used to model the intensity in the two regions separated by the zero level set curves of . The essence of our approach is embedded in computing these functions. To preserve the

smoothness and flexibility of the functions, we represent them as a linear combination of a few Legendre basis functions. Mathematically, we can write and Here is a multidimensional Legendre polynomial, which can be written as the outer product of the one dimensional counterparts.

IV. EXPERIMENTAL RESULTS





V. CONCLUSION

A novel framework for segmentation in presence of significant intra-region illumination variation is presented. Qualitative and quantitative results and comparison with the state of the art techniques suggest robustness of our approach. Here we have focused on bi-level segmentation, although extension to a multi-level framework appears straightforward. Also, our formulation allows easy incorporation of *a priori* shape information, which

may enhance performance in select cases. However, like most level set methods, L2S is somewhat biased towards contour initialization. Recently, there have been efforts to make such algorithms robust against initial curve placement. Incorporating L2S to such a framework would be an interesting future research topic. Using Legendre polynomials for region intensity approximation provides an elegant solution. However, without further analysis it is difficult to comment on the optimality of this choice of basis. Effectiveness of other polynomials such as splines or wavelets needs further investigation. In select cases, it may also be possible to learn a compact set of bases for representation. We wish to investigate the effectiveness of these approaches in the future.

REFERENCES

- [1] M. Kass, A. Witkin, and D. Terzopoulos, "Snakes: Active contour models," *Int. J. Comput. Vis.*, vol. 1, no. 4, pp. 321–331, 1988.
- [2] S. Osher and J. A. Sethian, "Fronts propagating with curvature-dependent speed: Algorithms based on hamilton-jacobi formulations," *J. Comput. Phys.*, vol. 79, no. 1, pp. 12–49, 1988.
- [3] T. F. Chan and L. A. Vese, "Active contours without edges," *IEEE Trans. Image Process.*, vol. 10, no. 2, pp. 266–277, 2001.
- [4] C. Xu and J. L. Prince, "Snakes, shapes, and gradient vector flow," *IEEE Trans. Image Process.*, vol. 7, no. 3, pp. 359–369, 1998.
- [5] R. Malladi, J. A. Sethian, and B. C. Vemuri, "Shape modeling with front propagation: A level set approach," *IEEE Trans. Patt. Anal. Machin Intell.*, vol. 17, no. 2, pp. 158–175, 1995.
- [6] V. Caselles, R. Kimmel, and G. Sapiro, "Geodesic active contours," *Int. J. Comput. Vis.*, vol. 22, no. 1, pp. 61–79, 1997.
- [7] D. Mumford and J. Shah, "Optimal approximations by piecewise smooth functions and associated variational problems," *Commun. Pure Appl. Math.*, vol. 42, no. 5, pp. 577–685, 1989.
- [8] L. A. Vese and T. F. Chan, "A multiphase level set framework for image segmentation using the mumford and shah model," *Int. J. Comput. Vis.*, vol. 50, no. 3, pp. 271–293, 2002.
- [9] C. Li, C.-Y. Kao, J. C. Gore, and Z. Ding, "Minimization of regionscalable fitting energy for image segmentation," *IEEE Trans. Image Process.*, vol. 17, no. 10, pp. 1940–1949, 2008.
- [10] J. Kim, J. W. Fisher, A. Yezzi, M. Çetin, and A. S. Willsky, "A nonparametric statistical method for image segmentation using information theory and curve evolution," *IEEE Trans. Image Process.*, vol. 14, no. 10, pp. 1486–1502, 2005.

PEAK-TO-AVERAGE POWER RATIO REDUCTION FOR OFDM/OQAM SIGNALS VIA ALTERNATIVE-SIGNAL METHOD

Sangepu Rajesh Kumar¹

Dr.S.Madhu Babu²

1) Sangepu Rajesh Kumar, M.Tech, Malla Reddy Engineering College (Autonomous), Hyderabad, India.

2) Dr.S.Madhu Babu, Assistant Professor, Malla Reddy Engineering College (Autonomous), Hyderabad, India.

Abstract— In this paper, we consider the peak-to-average power ratio (PAPR) reduction problem for orthogonal frequency-division multiplexing with offset quadrature amplitude modulation (OFDM/OQAM). In particular, the OFDM/OQAM signal is generated by summing over M time-shifted OFDM/OQAM symbols, where successive symbols are interdependent with each other. The alternative-signal (AS) method, which directly leads to the independent AS (AS-I) and joint AS (AS-J) algorithms, is employed to reduce the PAPR of the OFDM/OQAM signal. The AS-I algorithm reduces the PAPR symbol by symbol with low complexity, whereas the AS-J algorithm applies optimal joint PAPR reduction among M OFDM/OQAM symbols with much higher complexity. To balance the performance and the computation complexity, we propose a sequential optimization procedure, which is denoted AS-S, which achieves a desired compromise between performance and complexity.

Index Terms—Alternative signals (ASs), orthogonal frequency-division multiplexing with offset quadrature amplitude modulation (OFDM/ OQAM), peak-to-average power ratio (PAPR).

I. INTRODUCTION

As a promising candidate multicarrier modulation technique for Long-Term Evolution Advanced (LTE-A) and other future wireless standards, orthogonal frequency-division multiplexing with offset quadrature amplitude modulation (OFDM/OQAM) has drawn more and more attention due to its high spectrum efficiency [1]–[3]. In OFDM/OQAM systems, the OFDM/OQAM signal is obtained by summing over M time-shifted OFDM/OQAM symbols, each of which is obtained by letting N QAM symbols pass through a prototype filter [4]–[6] and be modulated with N orthogonal subcarriers. Compared with traditional OFDM systems, the OFDM/OQAM systems own some noticeable advantages: 1) The cyclic prefix is no longer required [4], [5]; and 2) the sidelobe of its power spectrum density is very low [4], [5]. The main disadvantages of OFDM/OQAM are the heavier computation cost due to the extra filtering operations and the more complex channel equalization. For the multicarrier modulation systems (including both the OFDM and OFDM/OQAM), one of the critical issues for implementations is their relatively high peak-to-

average power ratio (PAPR) [7]. For OFDM systems, various schemes (including companding [8], clipping [9], partial transmit sequence (PTS) [10], and selective mapping (SLM) [11]) have been proposed in the literatures for PAPR reduction. For example, the companding scheme [8] compressed the large samples and expanded the small samples. The clipping method [9] limited the OFDM signal at a given amplitude threshold to reduce the PAPR. The PTS [10] and the SLM [11] methods generated several candidate OFDM symbols by multiplying the original symbol with different phase rotation vectors, and chose the one with the lowest PAPR for transmission. For OFDM/OQAM systems, the clipping scheme [12]–[14], the SLM method [15], and the precoding scheme [16] have been employed for PAPR reduction.

In [12], the clipping scheme was introduced to the OFDM/OQAM systems, and it increased the bit error rate (BER) and enlarged the sidelobe. To avoid the BER increasing, an iterative noise cancelation technique called Busgang noise cancelation was applied at the receiver [13], but it may increase the decoding complexity at the receiver. In [14], the clipping-based schemes (including the tone reservation and active constellation extension) were employed to reduce the PAPR of OFDM/OQAM signals. However, these schemes may sacrifice the throughput. In [15], the SLM method was applied. It divided each OFDM/OQAM symbol into two parts (real and imaginary), randomly adopted the phase rotation vectors for the first 2° parts, with K being the parameter associated with the length of the prototype filter, and then optimized the $(2K + 1)$ th

part to reduce the PAPR. Due to the random choice of the phase rotation vectors, the PAPR reduction performance was poor when the length of the prototype filter was long. In [16], the single-carrier OFDM/OQAM system was considered, in which a precoding matrix was inserted between the multiplexer and the OFDM/OQAM modulator to reduce the PAPR.

In this paper, we employ the alternative-signal (AS) method to reduce the PAPR of OFDM/OQAM signals. We first apply the traditional SLM scheme to the OFDM/OQAM systems to obtain the independent AS (AS-I) and joint AS (AS-J) algorithms. Specifically, AS-I reduces the PAPR of each OFDM/OQAM symbol independently, and AS-J applies joint PAPR reduction among M OFDM/OQAM symbols. AS-J intuitively should yield a better performance than AS-I. However, the computation complexity of AS-J exponentially increases with M , which is impractical. To balance the performance and the computation complexity, we propose a sequential AS (AS-S) algorithm, which adopts a sequential optimization procedure over time with the computation complexity linearly increasing with M . Simulation results will be provided to compare the performance among the three algorithms.

II. ORTHOGONAL FREQUENCYDIVISION MULTIPLEXING WITH OFFSETQUADRATURE AMPLITUDE MODULATION SYSTEM MODEL

The OFDM/OQAM transmitter structure is shown in Fig. 1, which consists of N subcarriers. After the QAM modulation, the input QAM symbols are first

serial-to-parallel converted to data matrix X , which is defined as

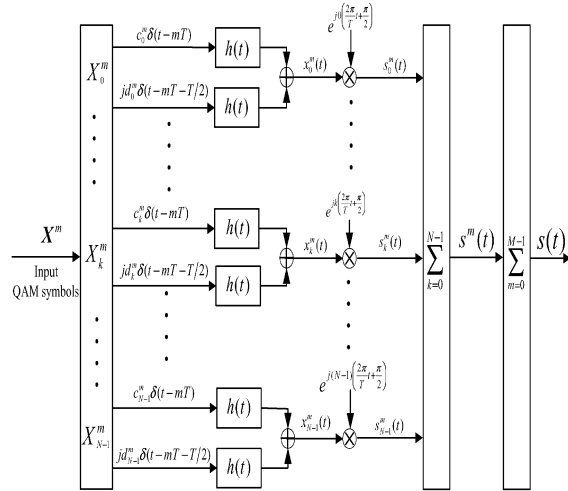


Fig. 1. Typical OFDM/OQAM transmitter

$$X = [X^0, X^1, X^2, \dots, X^{M-1}]$$

where M is the number of data blocks, and X_m is the m th data block, which is defined as

$$X^m = [X_0^m, X_1^m, X_2^m, \dots, X_{N-1}^m]^T$$

with denoting the transpose and X_k^m denoting the m th QAM symbol on the k th subcarrier, which is defined as

$$X_k^m = c_k^m + j d_k^m$$

where c_k^m and d_k^m denote the real and imaginary parts of X_k^m , respectively.

The real and imaginary parts of X_k^m are staggered by $T/2$ and passed through the prototype filter to obtain

$$x_k^m(t) = c_k^m h(t - mT) + j d_k^m h\left(t - \frac{T}{2} - mT\right)$$

where T denotes the symbol period [4], and $h(t)$ is the response on the prototype filter satisfying the perfect reconstruction condition [5]. It is worth noting that the length of $h(t)$ is KT , with K being an

even integer [4], [5]. In this paper, we adopt $K = 4$, similar to [4] and [5].

Finally, the desired OFDM/OQAM signal $s(t)$ is obtained by summing over the M OFDM/OQAM symbols, i.e.,

$$s(t) = \sum_{m=0}^{M-1} s^m(t), \quad 0 \leq t \leq \left(M + K - \frac{1}{2}\right)T.$$

Thus, we show the structure of OFDM/OQAM signal in Fig. 2. It is shown that the symbol rate is $1/T$, and the length of each OFDM/OQAM symbol is equal to $(K + 1/2)T$. Compared with $s(t)$ is right-shifted with mT . Obviously, $s(t)$ overlaps with the next K OFDM/OQAM symbols. The OFDM/OQAM signal $s(t)$ is obtained by summing over the M OFDM/OQAM symbols, and the length of $s(t)$ is $(K + M - 1/2)T$.

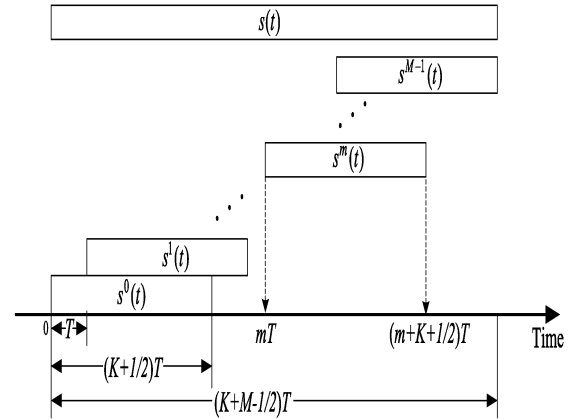


Fig. 2. Structure of the OFDM/OQAM signal.

In the conventional OFDM systems, the OFDM symbol is obtained by taking the inverse fast Fourier transform operation over the N QAM symbols, and the length of each OFDM symbol is T . Since the OFDM symbol rate is $1/T$, there is no overlap between any adjacent OFDM symbols, and the PAPR of each OFDM symbol is defined as the ratio of the peak power to the average power [8]. Due to the special signal structure, the PAPR definition for the

proposed OFDM/OQAM systems needs to be modified. OFDM/OQAM signal $s(t)$ is first divided into $M + K$ intervals, each of which is with length T (except the last one, with length $T/2$). Then, the PAPR for $s(t)$ in the p th interval is defined as

$$\xi^p = 10 \log_{10} \frac{\max_{pT \leq t \leq (p+1/2)T} |s(t)|^2}{P_{\text{ave}}}, \quad p = M + K - 1$$

where P_{ave} is the average power of $s(t)$.

We now summarize the notations that we have defined so far.

- X is the input data matrix.
- X^m is the m th data block.
- X^m is the m th QAM symbol on the k th subcarrier.
- $s^m(t)$ is the m th OFDM/OQAM symbol.
- $s(t)$ is the OFDM/OQAM signal.

III. ALTERNATIVE-SIGNAL METHOD

A. AS-I Algorithm

Inspired by the SLM method, the AS-I algorithm reduces the PAPR by optimally choosing one phase rotation vector from a given set for each OFDM/OQAM symbol. Over different OFDM/OQAM symbols, the phase rotation vectors might be different. Denote the set of candidate phase rotation vectors as

$$\mathcal{B} = \{b^0, b^1, \dots, b^{U-1}\}$$

Then, the new OFDM/OQAM symbol $s^m(t)$ is expressed as

$$\bar{s}^m(t) = \sum_{k=0}^{N-1} s_k^m(t) b_k^{m,u}.$$

Thus, the PAPR reduction problem with the AS-I algorithm for the m th OFDM/OQAM symbol $s(t)$, $m = 0, 1, \dots, M - 1$, can be formulated as

$$(P1): \quad \min_{b^{m,u}} \max_{mT \leq t \leq (m+K+\frac{1}{2})T} \left| \sum_{k=0}^{N-1} s_k^m(t) b_k^{m,u} \right|^2$$

subject to: $b^{m,u} \in \mathcal{B}$.

Note that we adopt the peak power as the design metric throughout this paper. This is because the PAPR reduction should come from the peak power reduction rather than the average power increasing [11]. Given the finite dimensionality of \mathcal{B} , exhaustive search is adopted here to search the optimal $b^{m,u}$. For each $s^m(t)$, the complexity of searching the optimal $b^{m,u}$ is on the order of $O(U)$, i.e., for each $s^m(t)$, $m = 0, 1, \dots, M - 1$, is on the order of $O(UM)$. U searches. Thus, the complexity for all $s^m(t)$, $m=0, 1, \dots, M-1$, is on the order of $O(UM)$.

Remark 1: After obtaining the PAPR-reduced OFDM/OQAM signal $\hat{s}(t)$, the transmitter should send side information to the receiver about which phase rotation vector is selected for $s(t)$, $m = 0, 1, \dots, M - 1$. Obviously, $\log_2 m(U)$ bits are needed for such side information transmission [11] of each OFDM/OQAM symbol and, thus, $M \log(U)$ bits for all the M symbols in total. At the receiver, if the side information is correctly received, the original data matrix X can be thus successfully recovered.

We will illustrate the PAPR reduction performance achieved by the AS-I algorithm. As we will discussed later, the AS-I algorithm does not perform well enough since it ignores the structure of the OFDM/OQAM signals, i.e., the correlation among adjacent OFDM/OQAM symbols, whereas reducing the PAPR of $s^m(t)$ independently is strictly suboptimal. To improve the PAPR reduction performance, the AS-J algorithm is proposed in the

following to fully explore the inter symbol correlations.

B. AS-J Algorithm

For each OFDM/OQAM symbol $s(t)$, the AS-J algorithm first chooses one phase rotation vector from the given B ; then, it applies a joint PAPR reduction scheme among all the M OFDM/OQAM symbols. Similarly, after $\tilde{s}_k^m(t)$ is generated, as we did in the AS-I algorithm, the PAPR reduction problem could be formulated as

$$(P2): \min_{b^{0,u}, \dots, b^{M-1,u}} \max_{0 \leq t \leq (M+K-\frac{1}{2})T} \left| \sum_{m=0}^{M-1} \sum_{k=0}^{N-1} s_k^m(t) b_k^{m,u} \right|^2$$

subject to: $b^{m,u} \in B, \quad m = 0, 1, \dots, M-1.$

It is easy to check that the complexity of exhaustive searching to solve Problem (P2) are on the order of $O(U)$, which makes the exhaustive search method impractical. Similarly, the number of bits for the side information is equal to $M \log 2M(U)$. It is earlier shown that the AS-I algorithm is simple but performs badly, whereas the AS-J algorithm performs well but bears high complexity. To balance the PAPR reduction performance and the complexity, the AS-S algorithm is proposed in the following.

C. AS-S Algorithm

The main idea of the AS-S algorithm is shown in Fig. 3, which shows that the AS-S algorithm adopts a sequential optimization procedure.

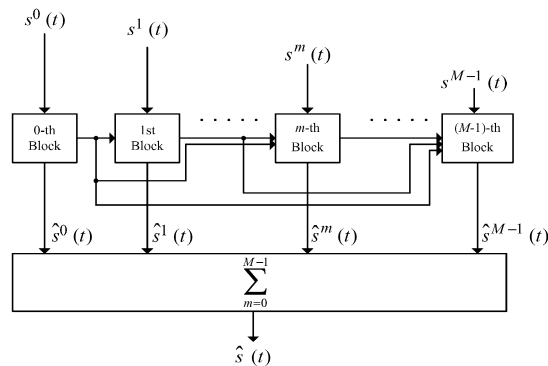


Fig. 3. Structure of the AS-S algorithm.

In the m th block, by taking into account the previous OFDM/OQAM symbols, we reduce the peak power of $s^0(t)$. A detailed illustration of the proposed algorithm is described as follows. In the zeroth block, we multiply $s^0(t)$ by different phase rotation vectors and choose the one with the minimum peak power, which is denoted as $\hat{s}^0(t)$. Then, $\hat{s}^0(t)$ is sent to the first block to solve the following problem:

$$\min_{b^{1,u}} \max_{2T \leq t \leq 4T} \left| \hat{s}^0(t) + \sum_{k=0}^{N-1} s_k^1(t) b_k^{1,u} \right|^2$$

subject to: $b^{1,u} \in B.$

Thus, AS-S is a sequential optimization procedure. Specifically, in the m th block, $m = 1, 2, \dots, M-1$, the optimization problem could be cast as follows:

$$(P3): \min_{b^{m,u}} \max_{(m+1)T \leq t \leq (m+\Gamma)T} \left| \sum_{l=0}^{m-1} \hat{s}^l(t) + \sum_{k=0}^{N-1} s_k^m(t) b_k^{m,u} \right|^2$$

subject to: $b^{m,u} \in B.$

Note that Γ is a key parameter that significantly affects the PAPR reduction performance and will be discussed in Remark 2. In Problem (P3), the search complexity for each symbol $s(t)$ is on the order of $O(U)$, and the complexity for all the M symbols is on the order of $O(UM)$. Similarly, the number of bits to transmit the side information is also equal to $M \log m(U)$.

Remark 2: We plot the amplitudes of $h(t - mT)$ and $s(t)$ in Fig. 4, where the parameters of the prototype filter are the same as those in [2], [4], and [5]. It can be seen that the large-amplitude samples of $h(t - mT)$ are located within $\{(m + K/2 - 1/2)T \leq t \leq (m + K/2 + 1/2)T\}$. For $(t - mT - T/2)$, its large-amplitude samples are located within $\{(m + K/2)T \leq t \leq (m + K/2 + 1)T\}$. According to (5) and (6), we could obtain that

the large-amplitude samples of $s(t)$ are located within $\{(m + K/2 - 1/2)T \leq t \leq (m + K/2 + 1)T\}$. Intuitively, to obtain a good PAPR reduction performance, the large-amplitude samples of $s^m(t)$ should be included in the optimization duration $\{(m + 1)T \leq t \leq (m + G)T\}$ in Problem(P3), i.e., G should satisfy $G = K/2 + 1$. Furthermore, since $s^m(t)$ only spans over $\{mT \leq t \leq (m + K + 1/2)T\}$, it follows that $G = (K + 1/2)$. Thus, we conclude that $K/2 + 1 = G = (K + 1/2)$ is a good choice.

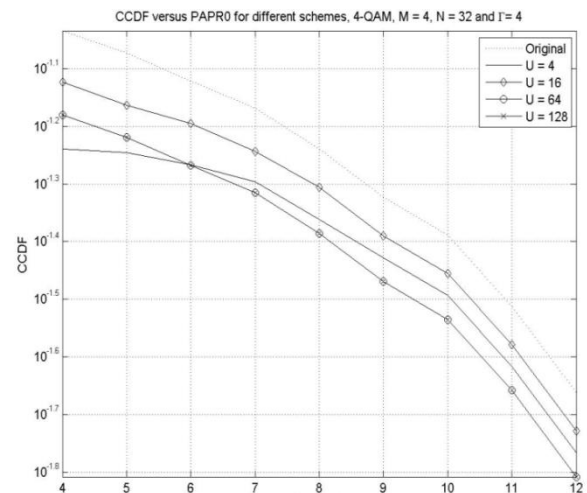
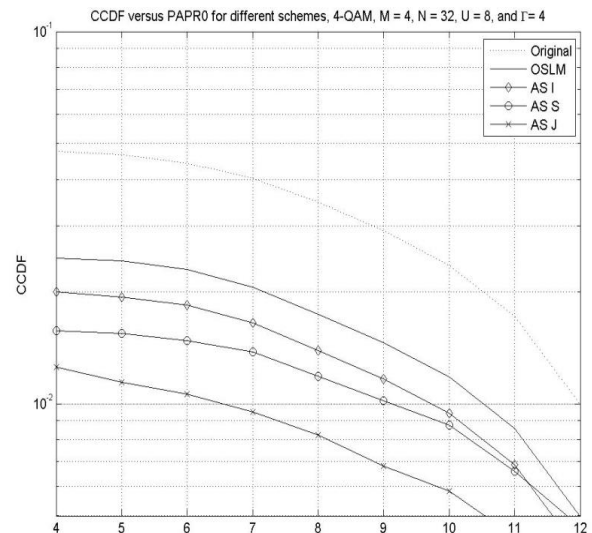
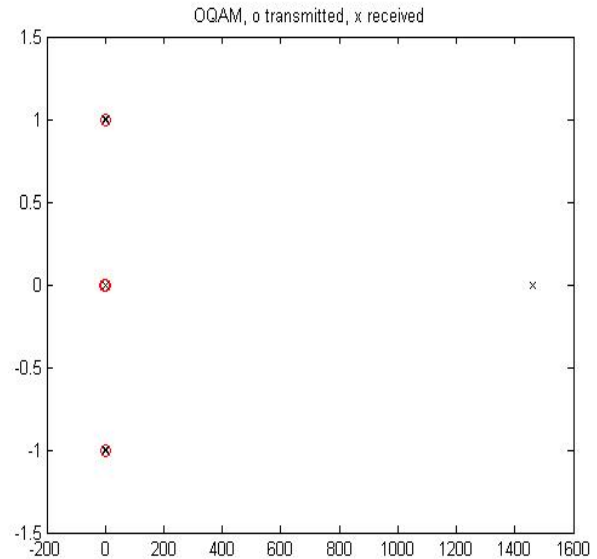
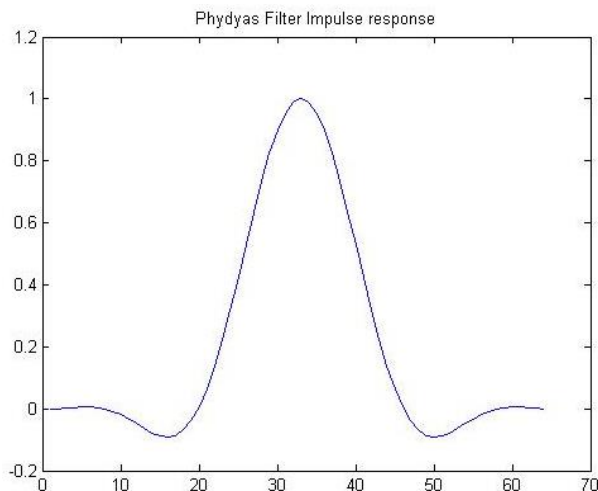
Thus, the AS-S algorithm is summarized as follows.

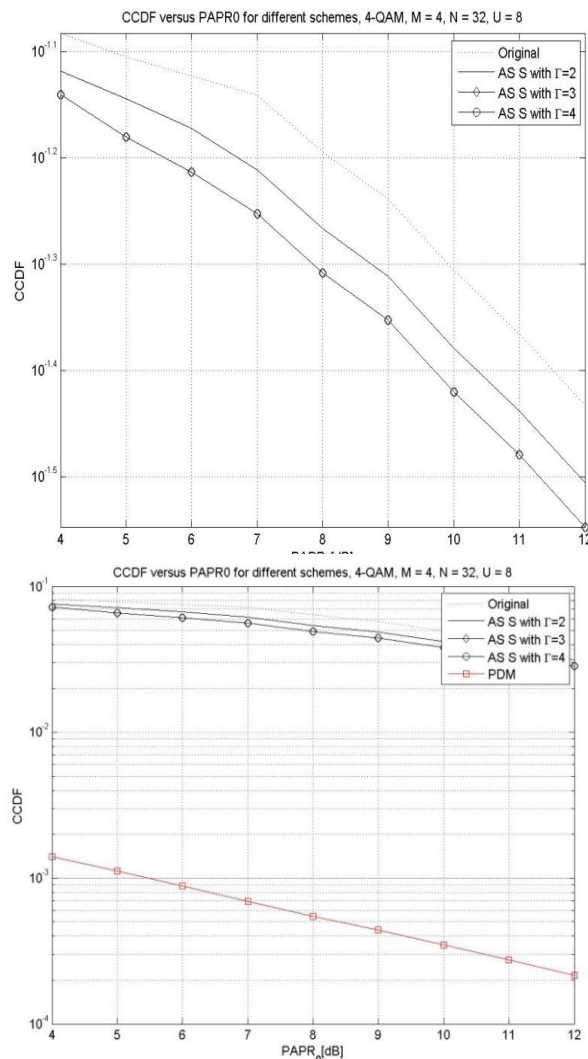
Step 1: Initialization: $m = 1$. Multiply $s_0(t)$ by different phase rotation vectors and denote the one with the minimum peak power as $\hat{s}_0(t)$. Then, $\hat{s}(t)$ is sent to the first block.

Step 2: In the m th block, solve Problem (P3), and the new symbol is denoted $\hat{s}^m(t)$. Send $\hat{s}^m(t)$, $\hat{s}^m(t), \dots, \hat{s}^m(t)$ to the next block.

Step 3: Set $m = m + 1$, if $m \leq M - 1$, go to 2); otherwise, calculate $\hat{s}(t) = \sum_{m=0}^{M-1} \hat{s}^m(t)$ and output the value.

IV.SIMULATION RESULTS





V. CONCLUSION

In this paper, we have employed the AS method, leading to the AS-I, AS-J, and AS-S algorithms, for the PAPR reduction of the OFDM/OQAM signals. The three algorithms required the same amount of side information. The computation complexities of AS-I and AS-S are on the order of $O(U)$ with U being the number of the phase rotation vectors and M being the number of the OFDM/OQAM symbols, which was much lower than that of AS-J, i.e., on the order of $O(UMM)$. Simulation results depicted that the AS-S algorithm is a good choice since it can provide a much better PAPR reduction performance than the

AS-I algorithm and incur much lower computational complexity than the AS-J algorithm.

REFERENCES

- [1] Physical Layer for Dynamic Spectrum Access and Cognitive Radio, An European Project, i.e., phydyas project, D5.1 and D8.1. [Online]. Available: <http://www.ict-phydyas.org/>
- [2] S. Mirabbasi and K. Martin, "Overlapped complex-modulated transmultiplexer filters with simplified design and superior stopbands," *IEEE Trans. Circuits Syst., Analog Digit. Signal Process.*, vol. 50, no. 8, pp. 456–469, Aug. 2003.
- [3] B. Farhang-Boroujeny, "OFDM versus filter bank multicarrier," *IEEE Signal Process. Mag.*, vol. 28, no. 3, pp. 92–112, May 2011.
- [4] D. Chen, D. Qu, and T. Jiang, "Prototype filter optimization to minimize stopband energy with NPR constraint for filter bank multicarrier modulation systems," *IEEE Trans. Signal Process.*, vol. 61, no. 1, pp. 159–169, Jan. 2013.
- [5] P. Siohan, C. Siclet, and N. Lacaille, "Analysis and design of OFDM/OQAM systems based on filterbank theory," *IEEE Trans. Signal Process.*, vol. 50, no. 5, pp. 1170–1183, May 2002.
- [6] A. Viholainen, T. Ihalainen, T. H. Stitz, M. Renfors, and M. Bellanger, "Prototype filter design for filter bank based multicarrier transmission," in *Proc. Eusipco*, Glasgow, Scotland, Aug. 2009, pp. 1459–1363.
- [7] J. Tellado, "Peak-to-average power reduction for multicarrier modulation," Ph.D. dissertation, Stanford Univ., Stanford, CA, USA, Sep. 1999.
- [8] T. Jiang, W. Xiang, P. C. Richardson, D. Qu, and G. Zhu, "On the nonlinear companding transform for reduction in PAPR of MCM signals," *IEEE Trans.*

Wireless Commun., vol. 6, no. 6, pp. 2017–2021, Jun. 2007.

[9] J. Armstrong, "Peak-to-average power reduction for OFDM by repeated clipping and frequency domain filtering," *Electron. Lett.*, vol. 38, no. 5, pp. 246–247, Feb. 2002.

[10] S. H. Muller and J. B. Huber, "OFDM with reduced peak-to-average power ratio by optimum combination of partial transmit sequences," *Electron. Lett.*, vol. 33, no. 5, pp. 368–369, Feb. 1997.

ARM Based Smart Cart and Automatic Billing System with Theft Detection

Dr.M.J.C.Prasad^{#1}, N.Haritha^{*2}

[#]Professor in ECE Department,

Malla Reddy Engineering College (Autonomous), Jawaharlal Nehru Technological University, Hyderabad, India,
jagadishmatta@gmail.com

^{*}PG Scholar

Malla Reddy Engineering College (Autonomous), Jawaharlal Nehru Technological University, Hyderabad, India,
nelluri.haritha@gmail.com

Abstract— As shopping at the malls has become a daily activity in metro cities and due to the heavy rush the whole shopping experience is ruined by long billing queues and checkout lines. The main aim of this paper is to provide an automatic billing system to avoid queues in malls and super markets. This can be done by replacing the item bar code with RFID tags, and the cart is equipped with a microcontroller, LCD, an RFID reader, EEPROM, keypad, Load-cell and ZigBee module. The item placed in the cart will be read through a RFID reader on shopping cart and the item information will be stored in EEPROM .once the shopping is done the information will be sent to the central billing system where it calculates the total billing of the specific cart. Along with this ability, the system design also ensures detection of theft performed by dishonest customers, which makes the smart system fair and attractive to both the buyers and sellers.

Keywords: - RFID, Microcontroller, ZigBee Modules, DC Motors and Loadcell

I. INTRODUCTION

In this modern world, technology changes our culture, society as well as our lifestyle. One such upcoming technology is Wireless Sensor Networks (WSN), which is maturing at a very fast rate because of its suitability in a wide range of application areas. It consists of a large number of small, low-power, cost-effective, autonomous devices termed as sensor nodes. When interfaced with sensors and actuators, they play the combined role of environment sensing, special-computing and wirelessly communicating devices. In this new era, WSN finds its use in consumer application areas such as Smart Home, Smart Grid, etc.

In this paper we take the particular application of Supermarket/Shopping malls. While doing survey on shopping malls we found that most of the people prefer to leave the shopping mall instead of waiting in long queues to buy a few products. People find it difficult to locate the product they wanted to buy, after selecting product they need to stand in a long queue for billing and payment. To try to solve the problems previously identified, recent years have seen the appearance of several technological solutions for hypermarket assistance. All such solutions share the same objectives of save consumer's time and money, help the retailers to win loyal clients.

A number of attempts have been made to design a Smart Shopping Cart with various different functionalities.

Awati and Awati [2], describe a Smart Trolley design that concentrates on how to get the customers rid of dragging heavy trolleys and to automate billing, but it assumes all the customers to be honest and hence does not tackle cases of deception, if there are any.

Further, Chihhsiong Shih, et al., [3] proposed an automatic embedded software generated framework that can create and evolve ZigBee applications. The framework consists of two major modules, pattern extraction and code generation. Pattern extraction and development are designed to provide ZigBee application with model reuse and modification. (System Modelling Language)SysML serves as a medium between pattern development and code generation A smart shopping cart application has been implemented using this pattern based software framework.

In this paper, the system is designed in such a way that each cart is identified by their unique identification number. The cart is equipped with a microcontroller, LCD, an RFID reader, keypad, EEPROM, Load-cell and ZigBee module. The item placed in the cart will be read through a RFID reader on shopping cart and the item information will be stored in EEPROM .once the shopping is done the information will be sent to the central billing system where it calculates the total billing of the specific cart. Along with this ability, the system design also ensures detection of theft performed by dishonest customers.

II. METHODOLOGY

This system uses the RFID and ZigBee wireless communication technologies

Radio frequency identification (RFID) is the wireless use of electromagnetic fields to transfer data, for the purposes of automatically identifying and tracking tags attached to objects. The tags contain electronically stored information. Some tags are powered by electromagnetic induction from magnetic fields produced near the reader. Some types collect energy from the interrogating radio waves and act as a passive transponder. Other types have a local power

source such as a battery and may operate at hundreds of meters from the reader. Unlike a barcode, the tag does not necessarily need to be within line of sight of the reader, and may be embedded in the tracked object. Radio frequency identification (RFID) is one method for Automatic Identification and Data Capture (AIDC).

There are multiple reasons why one would want to use RFID:

- It is used when you want to wirelessly identify something without line of sight
- It is used when a simple wireless means to store a small amount of information on things, and even better: change the information dynamically:
- It is used when we need a computing device but not humans to see the ID
- It is used when a computing device to see an object from far away

ZigBee modules are designed with low to medium transmit power and for high reliability wireless networks. The modules require minimal power and provide reliable delivery of data between devices. The interfaces provided with the module help to directly fit into many industrial applications. The modules operate within the ISM 2.4-2.4835 GHz frequency band with IEEE 802.15.4 baseband.

ZigBee protocol has many benefits:

- The ZigBee network is very scalable and it consumes little energy.
- The consumer has complete authority to add or remove devices as he/she sees fit.
- ZigBee compliant products only use one lithium battery that lasts the lifetime of the device.
- It supports many network topologies.
- ZigBee design is used in many areas of operation such as scalability of large networks, security, network resilience and ease of commissioning.

III. BLOCK DIAGRAM OF THE SYSTEM

The project consists of two sectional units

- Trolley or Smart Cart Section
- Automated Billing System Section

The main board is resided at the Trolley/Smart Cart Section as shown in Figure 1, so as to, program according to the requirements of cart section. In the automated billing system section there is a server computer which is maintained with the front end application and database according to the requirements of the project. The Communication between Cart Section and automated billing Section can be done wirelessly using ZigBee Modules. Each cart in the Retail Store is equipped with an RFID Reader, motor, keypad and load-cell as shown in block diagram figure1. Initially the cart is sealed. Once the start button is pressed the cart will be opened with the help of the motor. Every item that is dropped into the cart is identified by the

RFID tag which is attached to the item. The main board monitors if the customer is adding the item or removing the item from the cart using the keypad and load-cell. The controller even detects the malfunction of the process using the load-cell. Once the shopping is done the cart will be closed and the items information will be sent to the billing section through the ZigBee modules.

As shown in the Figure 2 at the Automated billing system section the total operation of displaying the items of the selected cart number, calculating the total amount of items and theft detection are handled by the visual basics and the database applications. RFID in the Retail store speeds up shopping processes and thus reduced the manual delays to provide the services and also enhances more user-service tasks. But the performance varies with respect to the vendors of RFID readers and tags. The efficient utilization of the technology also depends upon the information to be written in tag. Experimental results with respect to effectiveness of RFID reader, ZigBee Modules are presented in the paper. The work is in progress to utilize more enhancements using RFID technology. Developments in RFID technology continue to yield larger memory capacities, wider reading ranges, and faster processing.

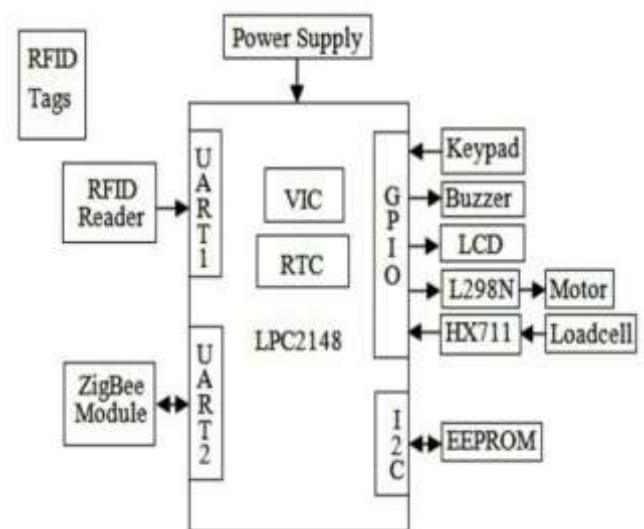


Fig.1. Block Diagram of Smart Cart Section



Fig.2. Block Diagram of Automatic Billing Section

IV. OPERATION OF THE SMART SHOPPING SYSTEM

As the customer enters the Smart Shopping Centre, he/she first picks a Smart Shopping cart. Each cart is given a unique ID and every customer is associated with the ID of the shopping cart chosen. The functioning of the system is listed below:

- Initially the cart is sealed using a motor. Once the start button is pressed the cart is opened and the cart is ready for shopping
- By default the smart shopping cart will be in add mode.
- When the customer picks the product then he/she drops the item into the cart that is identified through the RFID tag which is attached to the item and the information related to the product will be stored on to the EEPROM. At the same time the loadcell identifies the item added to the cart.
- If the customer wishes to remove the items from the cart. He/she needs to press the remove button and remove the item from the cart so that RFID reader reads the tag details, by which the particular item will be removed from the EEPROM too.
- If the customer wishes to remove the item from the cart and doesn't press the remove button and removes the item. Then loadcell identifies the decreasing of weight indicating item is removed and RFID identifies which item is removed and removes that particular item from the EEPROM.
- If the customer wishes to remove the item and press the remove button, but instead of removing, if he/she adds the item to the cart. The loadcell identifies the increase of weight indicating item is added in remove mode, which activates the theft flag and alerts that seller of theft. At the same time RFID reader identifies which item is added in remove mode.
- Once the shopping is done and when he/she presses the "shopping done" button the cart gets sealed with the help of motor and all the information from the EEPROM with the Cart identification number and theft flag status will be sent to the central billing system through the ZigBee module.
- At central billing system, with the help of database all the products information like item name, quantity and price will displayed and calculates the total bill. Once final bill is ready the total bill amount will be sent to the cart and displays on the cart for the customer notification that the bill is ready and his/her's total bill amount.
- If the central billing system identifies the theft flag, it also displays the theft information on the bill.
- Once the shopping is done and got the bill customer just pays the amount and leaves the mall.

V. HARDWARE IMPEMETATION

The various components that are used in the implementation along with the important considerations are explained in details.

A. RFID Reader and Cards

A radio frequency identification reader (RFID reader) EM-18 is a device used to gather information from an RFID tag, which is used to track individual objects. Radio waves are used to transfer data from the tag to a reader.

The EM-18 RFID Reader module operating at 125 kHz, The Reader module comes with an on-chip antenna and can be powered up with a 5V power supply.



Fig.3. EM-18 RFID Reader and Passive Card

B. Loadcell and HX711 Amplifier

A load-cell is configured as a weight sensor. This straight bar load cell (sometimes called a strain gauge) can translate up to 10kg of pressure (force) into an electrical signal. The HX711 load cell amplifier is used to get measurable data out from a load cell and strain gauge in digital form.



Fig.4. Loadcell and HX711 Arrangement

C. ZigBee Transceiver

The Tarang F20 ZigBee modules require minimal power and provide reliable delivery of data between smart cart device and billing device. The interfaces provided with the module help to directly fit into many industrial applications. The modules operate within the ISM 2.4-2.4835 GHz frequency band with IEEE 802.15.4 baseband.



Fig.5. ZigBee Module

D. LCD Display

LCD has the ability to display numbers, characters & graphics. The display is interfaced to I/O port of microcontroller. The display is in multiplexed mode i.e. only one display remains on at a time.



Fig.6. LCD Display

E. DC Motor and L298N Driver

As the controller can't handle the 5v output motors, we use this H bridge motor driver board to switch the 5v motor to forward/ reverse directions. The L298 is an integrated monolithic circuit in a 15- lead Multiwatt and PowerSO20 packages. It is a high voltage, high current dual full-bridge driver designed to accept standard TTL logic levels and drive inductive loads such as relays, solenoids, DC and stepping motors.

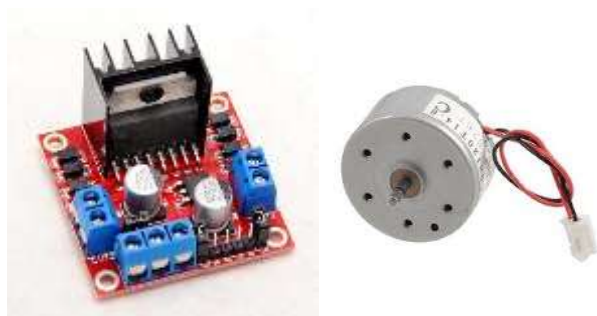


Fig.7. DC Motor and L298N Driver

VI. RESULTS

The experimental set-up is tested for various test cases, with various products tested for all the possible cases. As the RFID card reader read the product, details were displayed on the display unit. The product details of the shopped items were temporarily stored in the EEPROM. Once the "Shopping done" button was pressed, the memory contents were read and billing was done. The same product information data was sent to the server to update the inventory.

The following test case scenarios were used in the integrated system testing to prove the working of the developed system.

- Identifying items based on RFID tags and storing the information.
- Identifying whether the items are getting added or removed from the cart based on switch and load-cell data.
- Displaying the complete process step by step on LCD
- Automatic billing update when the products are dropped in the cart or removed from the cart.
- Identifying the theft in add and remove modes.
- Detecting the cart seal is open when start button pressed and seal is closed when shopping is done.
- Shopping cart and server system communication using ZigBee modules.
- Display of the individual item and total billing on the server system.
- Finally displaying the total billing on the cart display.

All test cases were successfully tested. The system developed is user friendly and no special training is required to use the cart.



Fig.8. Prototype Model of Smart Cart Section



Fig.9. Prototype Model of Automatic Billing Section



Fig.10. Generated Theft Free Bill



Fig.11. Generated Theft Detected Bill

VII. CONCLUSION

The project successfully demonstrates the possibility of using WSN for developing a Smart Shopping System which automates the entire billing procedure. RFID in the Retail store speeds up shopping processes and thus reduced the manual delays to provide the services and also enhances more user-service tasks. The system developed is highly reliable, fair and cost-effective. It is reliable and fair because of the effectiveness of WSN combined with a highly reliable RFID Technology. The system is also energy constraint as it uses a passive sensor and it reduces the communication

requirement. The decision making process is done locally within the cart, thereby eliminating an overhead to the communication between the nodes. In the bigger picture, it reduces the man-power requirements, easy to use, low-cost and does not need any special training.

REFERENCES

- [1] D.V.S Chandra Babu, “wireless intelligent billing trolley for supermarket”, International Journal of Advanced Research in Technology, vol.3, issue 1, Aug. 2012.
- [2] J. Awati and S. Awati, “Smart Trolley in Mega Mall,” vol. 2, Mar 2012.
- [3] Chihhsiong Shih, Bwo-cheng Liang and Cheng-zu Lin, “An Automatic Smart Shopping Cart Deployment Framework based on Pattern Design”, IEEE 15th International Symposium on Consumer Electronics, 2011.
- [4] Ergen, S. C., “ZigBee/IEEE 802.15.4 Summary,” EECS Berkely, September 2004.
- [5] T. Dimitriou. A lightweight RFID protocol to protect against traceability and cloning attacks. In Conference on Security and Privacy for Emerging Areas in Communication Networks – SecureComm, Athens, Greece, September 2005. IEEE.
- [6] Ankit Anil Aggarwal, “RFID Based Automatic Shopping Cart”, The International Institute for Science, Technology and Education journal on Control Theory and Informatics ,vol.1, no.1, 2011.
- [7] H. Karl and A. Willig, “Protocols and Architectures for Wireless Sensor Networks,” Chichester, England, 2005.
- [8] www.nxp.com/documents/user_manual/LPC2148.pdf
- [9] <http://en.wikipedia.org/wiki/zigbee>

Travolution-An embedded system in passenger car for road safety

Ch. Bhanu Prakash^{#1}, T. Ashwini^{*2}

[#]Associate professor in ECE Department,

Malla Reddy Engineering College (Autonomous), Jawaharlal Nehru Technological University, Hyderabad, India,

chandragiri.bhanuprakash@gmail.com

^{*}PG Scholar

Malla Reddy Engineering College (Autonomous), Jawaharlal Nehru Technological University, Hyderabad, India,

ashkutty.t@gmail.com

Abstract- Driver inattentiveness, to fatigue, callousness, to drunk driving, is responsible. Simple sensors can be fitted inside vehicles embedded with various features like, automatic collision notification, vehicle security, speed control which can give impetus to an efficient road safety system. The features that are proposed in this work are: Automatic collision notification that gives notification to the victim's relative, Speed control alters speed in different zones, Alcohol detection detects drunk driving, and Vehicle security is used to prevent theft. An Alarm indication if the driver does not wear Seatbelt.

Keywords: ARM CORTEX M3, GSM module, GPS module, MEMS, Alcohol detection, Seat belt detection, Zone alerts, RF TX& RX.

I. INTRODUCTION

Road traffic crashes are one of the world's largest public health and injury prevention problems. According to WHO, more than a million people are killed in road accidents, each year, all over the world. A report published by the WHO in 2009 revealed that more people die on roads in India than anywhere else in the world. The statistics for India are chilling. At least 13 people die every hour in road accidents in the country; the latest report of the National Crime Records Bureau reveals. In 2007, 1.14 lakh people in India lost their lives in road mishaps. Poor road infrastructure, failure to comply with speed limits, growing drinking and driving habits are among the main factors contributing to deaths from road crashes, WHO said in its report on 'Decade of Action for Road Safety 2011-2010'.

Travolution is an attempt to make an embedded system which is to bring a positive difference in the field of road safety and road discipline. The project tackles some major causes of road accidents such as drunken driving. It also has a major objective of exercising road discipline such as speed control in different areas and horn control in horn prohibited zones.

II. DESIGN OF PROPOSED HARDWARE SYSTEM

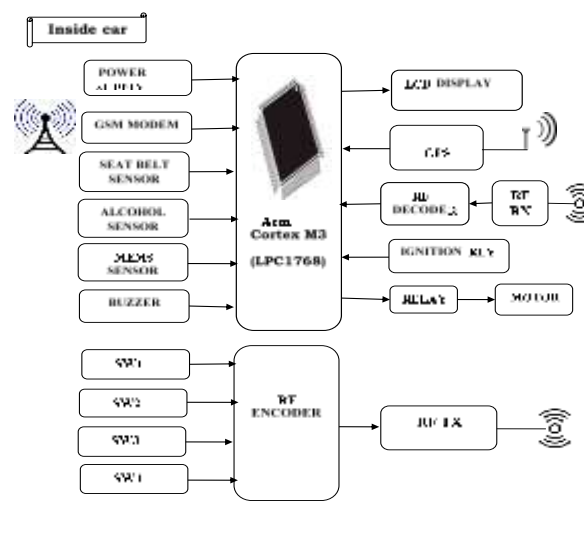


Fig.1.Block Diagram

In this project the vehicle is monitored to provide a more accurate detection. The features added in this work are

(i)**Vehicle Speed Control in Variable Zones**-in this feature, speed of the vehicle is controlled in different areas such as flyovers, bridges, highways, schools, cities and internal areas.

(ii)**Automatic Collision Notification**- In this feature when vehicle meet with an accident, the system of this project sends messages (SMS) to control room and the owner of the vehicle via GSM modem .

(iii)**Vehicle security**- In this feature, if the vehicle is stolen or someone tries to break in, if we give a miss call to the registered number automatically GPS tracks the vehicle and message is sent to control room and the owner of the vehicle via GSM modem.

(iv)**Alcohol Control**- The alcohol sensor prevents the ignition key from working if the driver breathes into it and a significant quantity of alcohol is detected and the message is sent to control room and the owner of the vehicle via GSM modem.

(v)**Seatbelt alert**- Alarm indication which means Buzzer rings if the driver does not wear seat belt.

III. THE HARDWARE SYSTEM DETAILS

The various components that are used in the implementation along with the important considerations are explained in detail.

A. ARM CORTEX-M3 (LPC1768)

The ARM Cortex-M3 is a next generation core that offers system enhancements such as enhanced debug features and a higher level of support block integration. The LPC1768 is an ARM Cortex-M3 based microcontrollers for embedded applications featuring a high level of integration and low power consumption. The LPC1768 operates at CPU frequencies of up to 100 MHz. Cortex-M3 is a 32-bit microprocessor. The ARM Cortex-M3 CPU incorporates a 3-stage pipeline and uses Harvard architecture with separate local instruction and data buses as well as a third bus for peripherals. The ARM Cortex-M3 CPU also includes an internal pre-fetch unit that supports speculative branching. The LPC1768 is pin-compatible to the 100-pin LPC236x ARM7-based microcontroller series. It has a 32-bit data path, a 32-bit register bank, and 32-bit memory interfaces. For complex applications that require more memory system features, the Cortex-M3 processor has an optional Memory Protection Unit (MPU), and it is possible to use an external cache if it's required. The Cortex-M3 processor includes a number of fixed internal debugging components. These components provide debugging operation supports and features, such as breakpoints and watch points.



Fig.2.LPC1768 IC

B. ALCOHOL SENSOR

Sensitive material of MQ-3 gas sensor is SnO_2 , which with lower conductivity in clean air. When the target alcohol gas exists, the sensor's conductivity is more high along with the gas concentration rising. MQ-3 gas sensor is highly sensitive to Alcohol, and has good resistance to disturb of gasoline, smoke and vapor. The sensor could be used to detect alcohol with different concentration, it is with low cost and suitable for different applications.



Fig.3.Alcohol sensor

C. SEATBELT SENSOR (LM 358)

LM 358 consist of two independent, high gain, internally frequency compensated operational amplifiers which were designed specifically to operate from a single power supply over a wide range of voltage. Operation from split power supplies is also possible and the low power supply current drain is independent of the magnitude of the power supply voltage. Application areas include transducer amplifier, DC gain blocks and all the conventional OP-AMP circuits which now can be easily implemented in single power supply systems.



Fig.4.LM 358 IC

D. MEMS SENSOR

The Free Scale Accelerometer consists of a MEMS capacitive sensing g-cell and a signal conditioning ASIC contained in a single package. The sensing element is sealed hermetically at the wafer level using a bulk micro machined cap wafer. The MMA7660FC is a $\pm 1.5 \text{ g}$ 3-Axis Accelerometer with Digital Output (I2C). It is a very low power, low profile capacitive MEMS sensor featuring a low pass filter, compensation for 0g offset and gain errors, and conversion to 6-bit digital values at a user configurable samples per second. The device can be used for sensing data changes, product orientation, and gesture detection through an interrupt pin (INT). This device is sensitive to electrostatic discharge. Although the Free scale accelerometer contains internal 2000 V ESD protection circuitry, extra precaution must be taken by the user to protect the chip from ESD. A charge of over 2000 V can accumulate on the human body or associated test equipment. A charge of this magnitude can alter the performance or cause failure of the chip. When handling the accelerometer, proper ESD precautions should be followed.

E. MAX 232

MAX232 is a 16 pin IC. It converts signals from an RS232 serial port to signals suitable for use in TTL compatible digital logic circuits. The MAX232 is a dual driver/receiver and typically converts the RX, TX, CTS and RTS signals.

F. LIMIT SWITCH

Limit Switches are used for control of a machine, as safety interlocks, or to count objects passing a point. A limit switch is an electromechanical device that consists of an actuator which is mechanically linked to a set of contacts. When an object comes into contact with the actuator, the device operates the contacts to make or break the electrical contact. Thus, this device proves to be very useful for safety purposes.

G. BUMPER SWITCH

Bumper switch is a very effective sensor for collision detection. Bumper switch works as a pushbutton i.e. it gets activated when pressed and the microcontroller then performs the necessary action for this condition. This sensor is a very simple way to test collision detection function in any locomotive.

H. RELAY CONTACTOR

Relays are used where it is necessary to control a circuit by a low-power signal (with complete electrical isolation between control and controlled circuits), or where several circuits must be controlled by one signal. A type of relay that can handle the high power required to directly control an electric motor is called a contactor

I. BUZZER

A piezoelectric element may be driven by an oscillating electronic circuit or other audio signal source. Sounds commonly used to indicate that a button has been pressed are a click, a ring or a beep. Electronic buzzers find many applications in modern days.



Fig.5.Buzzer

J. LIQUID CRYSTAL DISPLAY (LCD)

LCD is a flat panel display, electronic visual display that uses the light modulation properties of liquid crystals. Liquid crystals do not emit light directly. LCD's are available to display arbitrary images or fixed images which can be displayed or hidden, such as preset words, digits, and 7-segment displays as in a digital clock. They use the same basic technology, except that arbitrary images are made up of a large number of small pixels, while other displays have larger elements.



Fig.6.LCD Display

K. GPS

The Global Positioning System (GPS) is a U.S. space-based radio navigation system that provides reliable positioning, navigation, and timing services to civilian users on a continuous worldwide basis freely available to all. For anyone with a GPS receiver, the system will provide location and time. GPS provides accurate location and time information for an unlimited

number of people in all weather, day and night, anywhere in the world. GPS technology became a reality through the efforts of the American military, which established a satellite-based navigation system consisting of a network of 24 satellites orbiting the earth. GPS is also known as the NAVSTAR (Navigation System for Timing and Ranging). GPS works all across the world and in all weather conditions, thus helping users track locations, objects, and even individuals, GPS technology can be used by any person if they have a GPS receiver.

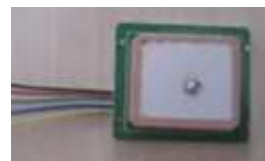


Fig.7.GPS Module

L. GSM

GSM (Global System for Mobile communications) is an open, digital cellular technology used for transmitting mobile voice and data services.



Fig.8.GSM Modem

GSM supports voice calls and data transfer speeds of up to 9.6 kbps together with the transmission of SMS. By having harmonized spectrum across most of the globe, GSM's international roaming capability allows users to access the same services when travelling abroad as at home.

IV. DESIGN DETAILS

There are 2 modules - Transmitter and Receiver Section. Receiver module will be placed on the car and the Transmitter module can be fitted on a sign board. Following are the circuit diagrams: To transmit the information, RX TX module is needed. In this circuit, 433 Mega Hertz frequency transmitter is being used. Parameters: ASK modulation and transmission range is 100-300 square feet (10-15 feet). There are 4 pins: 1. Antenna- there is a built in helical antenna 2. Data Pin-To receive Data for transmission 3. Ground pin-connected to ground 4. VCC - 3Volts Power Supply.

A. RF TRANSMITTER SECTION

In this section, HT 12 E Encoder is used. There are 4 data lines D0, D1, D2 and D3. On Data Lines, 4 switches are connected. This will generate the data for the project and will be decoded on vehicle side. On receiver side, each switch closure

will have a particular meaning. There is a TE pin which is active low, when this pin goes low, transmitter is enabled. The data out pin is connected to data pin of TX. Here pulse stream is generated and given to TX. This pulse stream will consist of 8 bit address and 4 bit data.

The STT-433 is ideal for remote control applications where low cost and longer range is required. The transmitter operates from a 1.5-12V supply, making it ideal for battery-powered applications. The transmitter employs a SAW-stabilized oscillator, ensuring accurate frequency control for best range performance. Output power and harmonic emissions are easy to control, making FCC and ETSI compliance easy. The manufacturing-friendly SIP style package and low-cost make the STT-433 suitable for high volume applications.

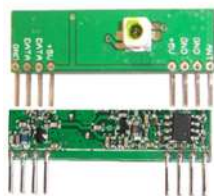


Fig.9.RF TRANSMITTER

B. RF RECEIVER SECTION

To receive the data from the road side transmitter, RF Receiver is needed. RX will have 4 pins same as that of Transmitter. HT 12 D decoder IC is used. D0, D1, D2 and D3 are the data lines, so whatever information is received from the transmitter is fed to these data lines. The output of RF RX is fed to the Data in pin of the Decoder. VCC is connected to 5 Volts. Valid Tone Pin goes high on receiving data. To indicate reception of data, LED is connected to Valid Tone pin. Alcohol sensor MQ3 has 2 heater plates and a sensor plate. Sensing plate is connected through a variable resistor to the controller which controls the sensitivity. Gas ions will fall on the sensing plate and will generate the electron current flow that will be given as voltage and this voltage will be sensed by the controller. So whenever alcohol is sensed, it will give a high logic output which will stop the car and send SMS to RTO along with the location of the car i.e. its latitude and longitude. The bumper switch is used for collision detection. When collision is detected, SMS is sent to the Emergency room along with the GPS location of the car. To detect car theft, limit switch is connected to the doors. When someone attempts to break in the vehicle, the lever of the limit switch is pressed thus making contact. This gives a logic high signal to the microcontroller hence indicating car theft. To show the driver the exact condition by which the vehicle is being controlled, the LCD display is connected on port 0. LCD display is 16 characters by 2 rows. To control the vehicle, on port 1, two relay contacts are connected to control the motor of the vehicle. Relays have two sets of contacts- normally open and normally closed. The first relay is connected such that when it is normally closed, motor operates at 12 V and in normally open it operates in 0 V. This relay halts the vehicle in case of collision

detection and when alcohol is sensed by the MQ3 Sensor. The second relay is connected such that when it is normally closed, motor operates at 6 V and in normally open it operates in 0 V. It is used when speed limit condition is received by the receiver circuit. The car will move at half the voltage.

The STR-433 is ideal for short-range remote control applications where cost is a primary concern. The receiver module requires no external RF components except for the antenna. It generates virtually no emissions, making FCC and ETSI approvals easy. The super-regenerative design exhibits exceptional sensitivity at a very low cost. The manufacturing-friendly SIP style package and low-cost make the STR-433 suitable for high volume applications.

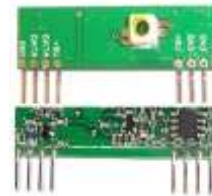


Fig.10.RF RECEIVER

V. RESULTS

The system is implemented in a toy car and tested. This method causes less mental or physical loads to drivers and is advantageous for long-term driver monitoring purpose.

- For collision detection, Bumper switch is used. Bumper switch has “ON” and “OFF” condition. The tension which triggers the bumper switch is approx. 144gms. On being triggered i.e. on the event of a collision, it sends a Binary 1 signal to the microcontroller thereby which the car is halted and “Collision Detected” is displayed on the screen. SMS is sent to the number that is pre fed. In real life SMS would be sent to the nearest relative of the person and the control room along with the GPS location of the vehicle.
- For the Alcohol Detection, MQ3 alcohol sensor is being exposed to a liquid solution that has 30% or more alcohol content in it. If detected, the buzzer rings, the car comes to a halt and “SMS to R.T.O” is displayed on the LCD screen. The SMS is sent to the number pre fed for this feature via GSM. “Alcohol Sensed” message is also displayed on the LCD.
- When the vehicle enters the zonal areas such as school, military, flyovers, the speed of the vehicle is controlled by using relays so that the motor speed reduces automatically in the vehicle. In Normally closed state, Car is driven by the complete 12V of the motor. In normally open state the car is halted because motor is brought to 0 V. Motor will operate at 6V if speed limit condition is transmitted. The transmitter sends the signal alerting that this area’s speed limit is 40 Kmph as example

- Before entering into the particular zone the driver is notified by an SMS through GSM and the location is predicted before entering into the zone by using GPS wireless communication system.

➤



Fig.11.Design of Proposed Hardware System

VI. CONCLUSION

The project “**Travolution- an embedded system in passenger car for road safety**” has been successfully designed and tested. Integrating features of all the hardware components used have developed it. Presence of every module has been reasoned out and placed carefully thus contributing to the best working of the unit. Secondly, using highly advanced IC’s and with the help of growing technology the project has been successfully implemented.

VII. REFERENCES

- [1]http://www.who.int/violence_injury_prevention/publications/road_traffic/world_report/en/[Date of Access: June 26, 2013].
- [2]http://articles.timesofindia.indiatimes.com/2009-0817/india/28181973_1_road-accidents-road-fatalities-global-road-safety
- [3]<http://www.sproboticworks.com/products/gsm-gps/sim-300module.html>
- [4] <https://www.sparkfun.com/products/8880>
- [5]http://www.allaboutcircuits.com/vol_4/chpt_5/2.html
- [6]<http://www.engineersgarage.com/tutorials/89s51-89s52-programmerbasics?Page=1>
- [7]http://www.rhydolabz.com/documents/gps_gsm/GPS1269_UserManual.pdf
- [8] <http://en.wikipedia.org/wiki/MAX232>
- [9]Mikael J. Pont, “Programming Embedded Systems using C”, 2002
- [10]<http://electronicdesign.com/embedded/programmer-flash-based-csupport-ics> [Date of Access: March 3, 2013].
- [11]http://www.vexrobotics.com/wiki/Bumper_Switch [Date of Access: March 22, 2013].
- [12] Y. Cui and S. S. Gee, “Autonomous vehicle positioning with GPS in urban canyon environments; IEEE Transactions on Robotics and Automation”, vol. 19, pp. 110, 1 February2003.



www.ijatir.org

International Journal of Advanced Technology and Innovative Research

ISSN 2348-2370
Vol.08, Issue.14,
October-2016,
Pages:2764-2767

A Raspberry Pi eHealth Smart Monitoring System

BIJO ABRAHAM MATHEW¹, SRINIVAS VUTKURI²

¹PG Scholar, Dept of ECE, Malla Reddy Engineering College (Autonomous), Dhulapally, Secunderabad, TS, India,
E-mail: abrahbijo@gmail.com.

²Assistant Professor, Dept of ECE, Malla Reddy Engineering College (Autonomous), Dhulapally, Secunderabad, TS, India,

Abstract: This system is aimed to prevent delays in the influx of patients' medical information to the hospices, particularly in casualties and exigency situations, to ease off hand-operated data recording, and to optimize bed sufficiency in hospices, preeminently during social events where numbers of people throng at a place. This system is based on medical sensors which measure patient's physical parameters by using WSNs. These sensors transfer data from the subjects' bodies over the wireless network to the cloud environment. Therefore, patients will have a great distinction in services because the e-health smart system reinforces medical staff by providing real-time data accumulation, dismissing hand-operated data recording.

Keywords: Data Monitoring; Sensors; Raspberry Pi; LPC2103; Web Service.

I. INTRODUCTION

Wireless Sensor Networks (WSNs) have aided the way for advancement of varied prospects of sensing. WSNs have been enforced in diverse applications such as military operations, climate supervising applications, underwater networks operations, and structural health check applications. WSN are facing many confrontations such as constrained computing power, memory size and data transmission proficiency. Henceforth, using Data monitoring would be an appropriate solution to improve sensors efficiency. Data will be stored in a Raspberry pi. It is a generic assertion for any technological benefit provided through the Internet [1]. Raspberry pi provides compatible and on-demand network access for profuse computing resources such as networks, systems, applications, and services. Moreover, Data monitoring are using modern and flexible methods to contribute, administer, and remunerate for information technology services with minimal management effort and cost. Data monitoring technology has several favorable edges such as adaptability, highly auto-mated, low priced, rapid service yielding, and a huge storage capacity. The monitoring features enable customers to construct, evaluate, and deploy their operations on virtual servers using diverse framework and manifold operating systems. Monitoring service providers offer three different types of facilities in order to achieve their clients more adaptability, which are Software as a Service (SaaS), Platform as a Service (PaaS), and Infrastructure as a Service (IaaS).

SaaS provides remotely access to software applications and their operations as a Web-based service. (PaaS) offers application schemes and operating systems, procures to diminish the progression attempts, and facilitates varied functions in the monitoring for users without installing any framework or software on their machines. (IaaS) offers a pool of Data monitoring resources including hardware, servers, networking components, and a massive storage space [2]. In this paper, we target on the objective of assimilation between wireless sensor network and Raspberry pi. After health sensors that are connected to patients' bodies record and transmit data to the LPC2103, services which are available in this LPC2103 are responsible for receiving and distributing this data. We presume that this result offers a relevant scenario to provide a comprehensive telemedicine service which automates the proceedings from compiling patients' data to delivering congruent medical findings based on patients' prevailing conditions and their factual medical data. The significant additions of this paper are: A prototype implementation using e-health sensors and the Raspberry Pi. Applying Raspberry pi technology to extract an appropriate decision based on patient's condition and factual data. To this borderline, the rest of the paper is organized as follows. The system motivation is mentioned in Section II. Section III highlights the related works. The proposed solution is taken into consideration in Section IV. We have discussed the future works in the concluding section.

II. MOTIVATION

WSNs have been applied in different applications such as military applications, climate monitoring applications, underwater networks operations, and basic health monitoring applications. WSN are facing many challenges such as limited computing power, memory and data transmission. This type of application provides compatible and on-demand network access for numerous computing assets such as networks, operations, systems, and services. Moreover, as this type of modern and flexible methods to contribute, administer, and remunerate for information technology services with less management constraints, price and also gives relevant and on-demand network access for a number of computing resources such as networks, systems, applications, and services.

III. RELATED WORK

Lounis et al. [5] offer a peculiar pattern for collection and retrieving a large amount of data produced by WSNs. The prime intention of their architecture is to overcome the challenges of dealing with a huge amount of data and makes partaking of info accessible for healthcare specialists. The paper focuses on data management in WSNs, particularly sensors' data accumulated that have been produced from medical sensors which introduce many challenges for the existing architectures. Rolim et al. [6] targeted on improving patients' data accumulation technique. This paper presents an initial framework to resolve the issues of recording notes manually which is a slow process. Besides, they cause lateness for analyzing real-time data and that inhibits the capability of clinical monitoring and diagnostics. Thus, authors proposed a framework to automate patients' information processing using wireless sensor networks which are connected to medical machinery, and then uploading this data to the healthcare provider centers in the cloud to cache, process, and analyze patients' data. Nonetheless, this paper does not take protection liability in consideration, practically in the architecture of suggested explication. Fortino et al. [7] attributes that the assimilation of cloud computing and wireless sensor networks can facilitate commendable powerful data storage, and advancement of processing framework and scrutiny of body sensor data.

This paper presents the administering and monitoring of sensor framework. In inclusion, this study also acknowledges some components in the framework of cloud computing such as data management and making use of APIs for communication among sensor data streams and the cloud. The authors actualize their work by means of an application of the Google App Engine (GAE) which is one of the cloud computing providers for hosting and evolve web applications in the cloud. Hwang et al. [8] attributes a compelling business model for cloud computing based on the concept of performing the encryption and decryption procedure, along with a cloud contributor must make certain that the information has been saved in encrypted format. Furthermore, after the computation operations are accomplished, all data must be destroyed. This study discusses many points associated to encrypting data in the cloud. On the other hand, this paper did not mention the security part during uploading and downloading operations in terms of safe guarding the channel between the client and cloud provider.

IV. PROPOSED SOLUTION

The architecture of the proposed solution is based on the integration between medical sensors which are liable for collecting patients' physical substantial parameters and the cloud environment to cater a smart health system.

A. Hardware Prerequisites for Accomplishment of the Function Module

Raspberry-Pi (ARM CORTEX/A7), ARM7(LPC2103), W/L Modules(optional), WI-FI Module (optional), Heartbeat Module, Temperature, B.P Sensor, MEMS, Power Supply Unit, Miscellaneous Components.

B. Software Prerequisites for Accomplishment of the Function Module for Raspberry Pi:

>Python Language for Programming.

C. Block Diagram

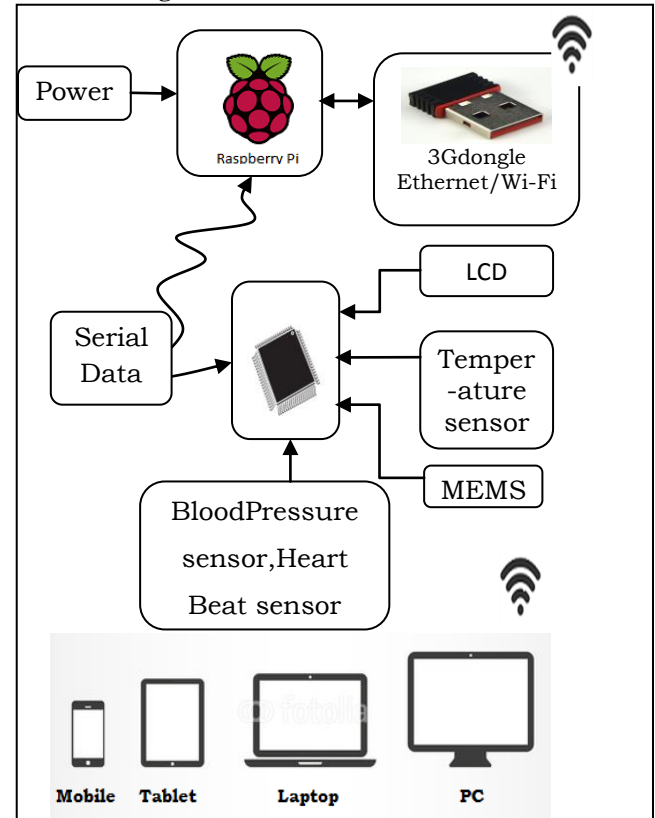


Fig.1. Proposed System Architecture

1. For Arm7

The KEIL MDK-ARM is complete software development environment for ARM7. Flash the device using FLASH MAGIC, a free software utility sponsored by NXP.

2. Language

All editions provide a complete Embedded C/ C++/Python development environment includes extensive middleware libraries. For Web development Projects we use HTML and PHP. Raspbian (Linux Oriented Recommended) As shown in Figure 1, the wireless health sensors are connected to a LPC2103 controller. This LPC2103 is responsible for collecting data from sensors and transmitting this data through Serial communication channels to platform services hosted on the Raspberry pi. This platform has many services: (1) Storage service, which is responsible for storing sensors' data; (2) Data monitoring service, which is responsible for providing a medical decisions based on patients factual medical data; and (3) Running service for updating, reviewing and testing patients' data which is required by medical staff. Medical staff and patients can utilize the application from different mobile and stationary gadgets linked to the Internet. Security and privacy are the significant factors related to the Raspberry pi environment. The data monitoring environment provides numerous

A Raspberry Pi eHealth Smart Monitoring System

computing resources that are shared. Therefore, sharing hardware resources and storage data areas in the Raspberry pi is at risk from insider and/or outsider attacks. In order to attain data security and privacy in our system, we employ two techniques, which are: Serial communication which is a popular technique for establishing an encrypted channel between a web server and the Raspberry Pi is used to transmit patients' data to the server through secure channels. According block diagram all sensor data stored in LPC 2103 micro controller .that sensors are temperature and MEMS, heart beat 'blood pressure, these are connected to LPC2103 .this controller is keep on continuous monitoring patient data and these data is transfer through serially to Raspberry pi. These data is collected through serially that data stored in Raspberry pi. That stored data upload in web. The web shows the all monitoring data.

D. Raspberry Pi

The Raspberry Pi 2 Model B is an upgraded ARMv7 multi-core processor, and a 1GB RAM, this pocket computer has advanced from being just a 'play computer' to match a desktop PC. The Raspberry Pi 2 delivers 6 times the processing capacity of earlier models. This 2nd generation Raspberry Pi has an upgraded Broadcom BCM2836 processor, which is a powerful ARM Cortex-A7 based quad-core processor that performs at 900MHz. The board also features an increase in memory capacity to 1Gbyte. Best of all, the Pi 2 keeps the same shape, connectors and mounting holes as the Raspberry Pi B+. Those resources - all of your HATs and other plug-in boards will run efficiently. 99% of cases and accessories will be fully compatible with both versions.



Fig.2. Raspberry Pi

1. MEMS

The MMA7660FC is a 3-Axis $\pm 1.5g$ Accelerometer with Digital Output (I2C). It is characterized with very less power consumption, low profile capacitive MEMS sensor headlining a low pass filter, compensation for 0g offset and gain errors, and conversion to 6-bit digital values at client configurable samples per second. The device can be used for sensor data changes, product orientation, and gesture detection via an interrupt pin (INT). The device is housed in a small 3mm x 3mm x 0.9mm DFN package.



Fig.3. MEMS

2. Temperature Sensor (LM35)

The LM35 series are precision integrated-circuit LM35 temperature sensors, whose output voltage is linearly proportional to the Celsius (Centigrade) temperature. The LM35 sensor thus has an advantage over linear temperature sensors calibrated in ° Kelvin, as the user is not required to subtract a large constant voltage from its output to obtain convenient Centigrade scaling.



Fig.4. Temperature Sensor

3. Blood Pressure Sensor

Blood Pressure & Pulse reading are shown on display with serial out for external projects of embedded circuit processing and display shows Systolic, Diastolic and Pulse Readings. Compact design fits over your wrist like a watch. Easy to use wrist style eliminates pumping.



Fig.5. BP Sensor.

TABLE I. Classification of Blood Pressure for Adults (18 Years and Older)

	Systolic (mm Hg)	Diastolic (mm Hg)
Hypotension	< 90	< 60
Desired	90–119	60–79
Pre-hypertension	120–139	80–89
Stage 1 Hypertension	140–159	90–99
Stage 2 Hypertension	160–179	100–109
Hypertensive Crisis	≥ 180	≥ 110

V. PROTOTYPE

We have used commercial wireless health sensors that are connected with e-Health Sensor Shield [10] that allows Raspberry Pi developers to perform biometric and medical applications to measure patient's physical parameters. In out implementation, we used two types of sensors which are pulse and oxygen in blood sensor, and body temperature sensor. The Raspberry Pi is a Linux-based microcomputer that connects with a computer monitor or TV, and uses a keyboard and mouse. It includes 2 USB ports, HDMI and Ethernet port, SD card slot, memory, video/audio outputs, and power source [11]. We used C++ to implement the application (on the raspberry pi) for reading the data from the LPC2103 and stored it. We utilized serial channel to establish a connection between the Pi and the application in the web. The server program was written in python.

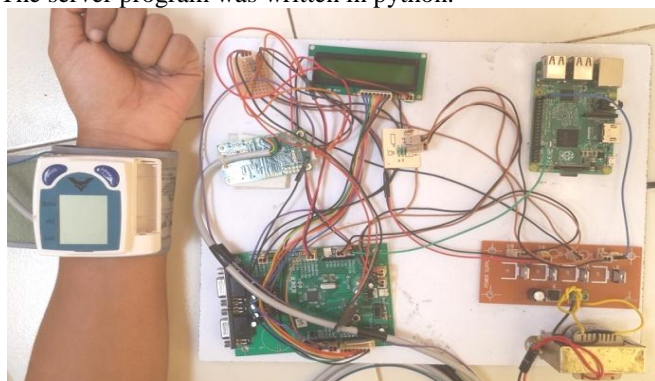


Fig.6. eHealth Sensor – Raspberry Pi Prototype

VI. CONCLUSIONS AND FUTURE WORKS

The integration between wireless sensor networks and Data monitoring will create a new generation of technology in many aspects such as patient monitoring with minimal cost, reducing the number of occupied beds in hospitals, and improving medical staff performance. In addition, applying various data mining techniques help to extract and analyze patients' data. The system introduced in this paper provides decisions based on patients' historical data, real-time data gathering, and thus eliminating manual data collection. For future work, we are planning to enhance the functionality of the system by adding more sensors and using it to collect data from a larger sample size of patient.

VII. REFERENCES

- [1]Srinivasa, R. V., Nageswara, R., & Kumari, E. K. (2009). Cloud computing: An overview. *Journal of Theoretical and Applied Information Technology*, 9(1), 71-76.
- [2]Buyya, R., Broberg, J., & Goscinski, A. M. (Eds.). (2010). *Cloud computing: Principles and paradigms* (Vol. 87). John Wiley & Sons.
- [3]Mell, P., & Grance, T. (2011). The nist definition of cloud computing, recommendations of the national institute of standards and technology. *National Institute of Standards and Technology*, 800-145.
- [4]AWS | Amazon Elastic Compute Cloud (EC2) - Scalable Cloud Hosting. (n.d.). Amazon Web Services, Inc. Retrieved June 22, 2014, from <http://aws.amazon.com/ec2/>
- [5]Lounis, A., Hadjidj, A., Bouabdallah, A., & Challal, Y. (2012, July). Secure and scalable cloud-based architecture for e-health wireless sensor networks. In *Computer communications and networks (ICCCN), 2012 21st international conference on* (pp. 1-7). IEEE.
- [6]Rolim, C. O., Koch, F. L., Westphall, C. B., Werner, J., Fractalossi, A., & Salvador, G. S. (2010, February). A cloud computing solution for patient's data collection in health care institutions. In *eHealth, Telemedicine, and Social Medicine, 2010. ETELEMED'10. Second International Conference on* (pp. 95-99). IEEE.
- [7]Fortino, G.; Pathan, M.; Di Fatta, G., "BodyCloud: Integration of Cloud Computing and body sensor networks," *Cloud Computing Technology and Science (CloudCom), 2012 IEEE 4th International Conference on*, vol., no., pp.851, 856, 3-6 Dec. 2012 doi: 10.1109/CloudCom.2012.6427537.
- [8]Hwang, J. J., Chuang, H. K., Hsu, Y. C., & Wu, C. H. (2011, April). A business model for cloud computing based on a separate encryption and decryption service. In *Information Science and Applications (ICISA), 2011 International*.
- [9]Lab Manual for UCSF Clinical Laboratories. (n.d.). Retrieved February 23, 2015, from <http://labmed.ucsf.edu/sfghlab/test/ReferenceRanges.html>
- [10]E-Health Sensor Platform Complete Kit V2.0 for Arduino, Raspberry Pi. (2014, July 3). Retrieved from <http://www.cooking-hacks.com/ehealth-sensors-complete-kit-biometric-medical-arduino-raspberry-pi>
- [11]Raspberry Pi: www.raspberrypi.org. Last accessed, July 27, 2014.

Author's Profile:



Bijo Abraham Mathew presently pursuing M.Tech Electronics&Communication Engineering in MallaReddyEngineering College (Autonomous), Dhulapally, Secunderabad - 500100, Ts, India.



Srinivas Vutkuri is presently working as assistant professor Of ECE department in Malla Reddy Engineering College (Autonomous), Dhulapally, Secunderabad - 500100, India. TS, India.

Implementation of Deep Representations for Iris, Face and Fingerprint Spoofing Detection Using Open Source Platform

B.Vani

PG Scholar,

Department of ECE,

Malla Reddy Engineering College, Hyderabad.

P.Ashok Babu

Associate Professor,

Department of ECE,

Malla Reddy Engineering College, Hyderabad.

Abstract:

In this Paper, the actual presence of a real legitimate trait in contrast to a fake self-manufactured synthetic or reconstructed sample is a significant problem in biometric authentication, which requires the development of new and efficient protection measures. In this paper, we present a novel software-based fake detection method that can be used in multiple biometric systems to detect different types of fraudulent access attempts. The objective of the proposed system is to enhance the security of biometric recognition frameworks, by adding livens assessment in a fast, user-friendly, and non-intrusive manner, through the use of image quality assessment.

The proposed approach presents a very low degree of complexity, which makes it suitable for real-time applications, using 25 general image quality features extracted from one image (i.e., the same acquired for authentication purposes) to distinguish between legitimate and impostor samples. The experimental results, obtained on publicly available data sets of fingerprint, iris, and 2D face, show that the proposed method is highly competitive compared with other state-of-the-art approaches and that the analysis of the general image quality of real biometric samples reveals highly valuable information that may be very efficiently used to discriminate them from fake traits.

Index Terms:

Image quality assessment, biometrics, security, attacks, and countermeasures.

INTRODUCTION:

A novel software-based multi-biometric and multi-attack protection method which targets to overcome part of these limitations through the use of image quality assessment (IQA). It is not only capable of operating with a very good performance under different biometric systems (multi-biometric) and for diverse spoofing scenarios, but it also provides a very good level of protection against certain non-spoofing attacks (multi-attack).[14] Moreover, being software-based, it presents the usual advantages of this type of approaches: fast, as it only needs one image (i.e., the same sample acquired for bio-metric recognition) to detect whether it is real or fake; non-intrusive; user-friendly (transparent to the user); cheap and easy to embed in already functional systems (as no new piece of hardware is required).

An added advantage of the proposed technique is its speed and very low complexity, which makes it very well suited to operate on real scenarios (one of the desired characteristics of this type of methods). As it does not deploy any trait-specific property (e.g., minutiae points, iris position or face detection), the computation load needed for image processing purposes is very reduced, using only general image quality measures fast to compute, combined with very simple classifiers. It has been tested on publicly available attack databases of iris, fingerprint and 2D face, where it has reached results fully comparable to those obtained on the same databases and following the same experimental protocols by more complex trait-specific top-ranked approaches from the state-of-the-art. [13]

II.SYSTEM ARCHITECTURE:

The system makes use embedded board which makes use of less power consumptive and advanced micro controller like Raspberry Pi. Our ARM11 board comes with integrated peripherals like USB, ADC and Serial etc. On this board we are installing Linux operating system with necessary drivers for all peripheral devices .Mainly this system consists of peripherals like UVC driver camera and Fingerprint module. After connecting all the devices, power uPs the device. When the device starts booting from flash, it first loads the Linux to the device and initializes all the drivers and the core kernel. After initialization of the kernel it first checks weather all the devices are working properly or not. After that it loads the file system and starts the start up scripts for running necessary processes and daemons. Finally it starts the main application.

This system captures image by means of web camera connected to ARM micro-controller through USB and the image is processed by using image processing technique. Image processing is any form of signal processing for which the input is an image, such as a photograph or video frame; the output of image processing may be either an image or a set of characteristics or parameters related to the image. Using algorithms child movement is monitored continuously like child position, child crying etc. And all these captured images are displayed on Display unit connected to ARM micro-controller.

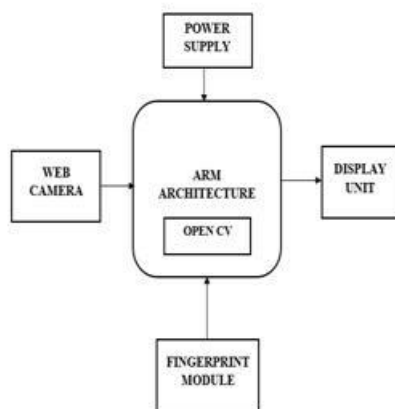


Fig1: Block Diagram for Proposed Method

When our application starts running it first check all the devices and resources which it needs are available or not. After that it checks the connection with the devices and gives control to the user. The controller will recognize the face and iris of the particular person from the image. The finger print module will take the finger print from the person and send to controller. The controller will recognize the finger print of particular person from the data base. If they are matched then it will display the data on display unit.

A.Haar Cascade:

Haar-like features are digital image features used in object recognition. They owe their name to their intuitive similarity with Haar wavelets and were used in the first real-time face detector. Here we will work with face detection. Initially, the algorithm needs a lot of positive images (images of faces) and negative images (images without faces) to train the classifier. Then we need to extract features from it. For this, haar features shown in below image are used. They are just like our convolutional kernel. Each feature is a single value obtained by subtracting sum of pixels under white rectangle from sum of pixels under black rectangle.

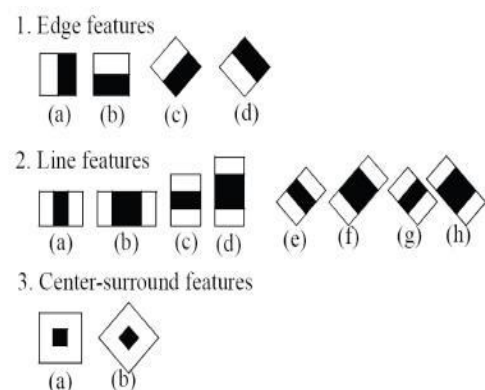


Fig.2: Haar Features

Now all possible sizes and locations of each kernel is used to calculate plenty of features. For each feature calculation, we need to find sum of pixels under white and black rectangles. To solve this, they introduced the integral images.

It simplifies calculation of sum of pixels, how large may be the number of pixels, to an operation involving just four pixels.[1]

B. PCA Algorithm:

PCA method (i.e., Eigen face method) is M. Turk and A. Pent land proposed in the literature, the basic idea is: the image vector by KL transformation from high-dimensional vector is converted to low-dimensional vector, and the formation of low-dimensional linear vector space, that is, subspace, and then face the projector to the low dimensional space, with the resulting projection coefficients as the recognition feature vectors. Recognize faces, just the projection coefficient of samples to be identified in the target database sample set of projection coefficients were compared to determine what types of recently. PCA algorithm is divided into two steps: the core face database generation phase, the training phase and identification phase.

III.HARDWARE IMPLEMENTATION

A.Raspberry Pi Board:



Fig.3: Raspberry Pi Board

The Raspberry Pi is a credit-card-sized single-board computer developed in the UK by the Raspberry Pi Foundation with the intention of promoting the teaching of basic computer science in schools. The Raspberry Pi is manufactured in two board configurations through licensed manufacturing deals with Newark element14 (Premier Farnell), RS Components and Egoman. These companies sell the Raspberry Pi online.

Egoman produces a version for distribution solely in China and Taiwan, which can be distinguished from other Pis by their red coloring and lack of FCC/CE marks. The hardware is the same across all manufacturers. The Raspberry Pi has a Broadcom BCM2835 system on a chip (SoC), which includes an ARM1176JZF-S 700 MHz processor, Video Core IV GPU, and was originally shipped with 256 megabytes of RAM, later upgraded to 512 MB. It does not include a built-in hard disk or solid-state drive, but uses an SD card for booting and persistent storage.[15]

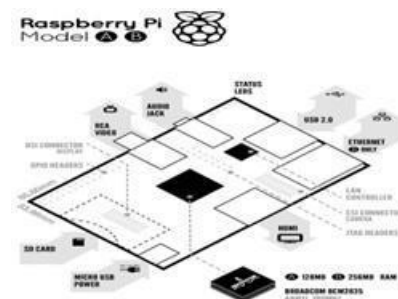


Fig.4: Board features

The Foundation provides Debian and Arch Linux ARM distributions for download. Tools are available for Python as the main programming language, with support for BBC BASIC (via the RISC OS image or the Brandy Basic clone for Linux), C, Java and Perl.

B.TFT display unit:

TFT stands for Thin Film Transistor, and is a type of technology used to improve the image quality of an LCD. Each pixel on a TFT-LCD has its own transistor on the glass itself, which offers more control over the images and colors that it renders. While TFT-LCDs can deliver sharp images, they also tend to offer relatively poor viewing angles, meaning they look best when viewed head-on. If you view a TFT-LCD from the side, it can be difficult to see. TFT-LCDs also consume more power than other types of cell phone displays.

C.Camera:

We utilize usb camcorder. It catches the pictures continuously to processor through usb link.

The web camera has the determination 500k pixels. Webcam comprises a focal point, a picture sensor, bolster gadgets. Picture sensors can be CMOS or CCD, the previous being predominant for minimal effort cameras, yet CCD cameras don't as a matter of course outperform CMOS-based cameras in the ease value range.[9]



Fig.5: USB video camera

D. Fingerprint Module:

A fingerprint is an impression of the friction ridges on all parts of the finger. A friction ridge is a raised portion of the epidermis on the palmar (palm) or digits (fingers and toes) or plantar (sole) skin, consisting of one or more connected ridge units of friction ridge skin. These are sometimes known as “epidermal ridges” which are caused by the underlying interface between the dermal papillae of the dermis and the interpapillary (rete) pegs of the epidermis. These epidermal ridges serve to amplify vibrations triggered when fingertips brush across an uneven surface, better transmitting the signals to sensory nerves involved in fine texture perception. The ridges assist in gripping rough surfaces, as well as smooth wet surfaces.



Fig.6: Fingerprint Module

Fingerprints may be deposited in natural secretions from the eccrine glands present in friction ridge skin (secretions consisting primarily of water) or they may be made by ink or other contaminants transferred from

the peaks of friction skin ridges to a relatively smooth surface such as a fingerprint card. The term fingerprint normally refers to impressions transferred from the pad on the last joint of fingers and thumbs, though fingerprint cards also typically record portions of lower joint areas of the fingers (Which are also used to make identifications). [10][12]

IV.SOFTWARE REQUIREMENTS

A.Linux Operating System:

Linux or GNU/Linux is a free and open source software operating system for computers. The operating system is a collection of the basic instructions that tell the electronic parts of the computer what to do and how to work. Free and open source software (FOSS) means that everyone has the freedom to use it, see how it works, and changes it. There is a lot of software for Linux, and since Linux is free software it means that none of the software will put any license restrictions on users. This is one of the reasons why many people like to use Linux.[6] Projects that interface with the kernel provide much of the system's higher-level functionality. The GNU user land is an important part of most Linux-based systems, providing the most common implementation of the C library, a popular shell, and many of the common UNIX tools which carry out many basic operating system tasks. The graphical user interface (or GUI) used by most Linux systems is built on top of an implementation of the X Window System

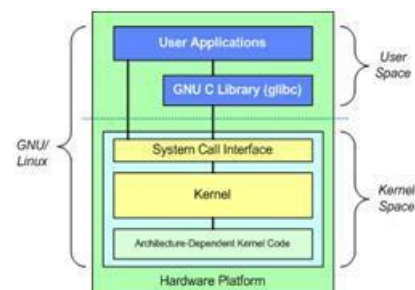


Fig.7: Architecture of Linux Operating System

B. Integrated Development Environment (QT):

Qt is a cross-platform application framework that is widely used for developing application software with a

graphical user interface (GUI) (in which cases Qt is classified as a widget toolkit), and also used for developing non-GUI programs such as command line tools and consoles for servers.[7] Qt uses standard C++ but makes extensive use of a special code generator (called the Meta Object Compiler, or moc) together with several macros to enrich the language. Qt can also be used in several other programming Languages via language bindings. It runs on the major desktop platforms and some of the mobile platforms. Non-GUI features include SQL database access, XML parsing, thread management, network support, and a unified cross-platform application programming interface for file handling. It has extensive internationalization support.

C. Open CV Library:

Computer vision is a rapidly growing field, partly as a result of both cheaper and more capable cameras, partly because of affordable processing power, and partly because vision algorithms are starting to mature. Open CV itself has played a role in the growth of computer vision by enabling thousands of people to do more productive work in vision. With its focus on real-time vision, Open CV helps students and professionals efficiently implement projects and jump-start research by providing them with a computer vision and machine learning infrastructure that was previously available only in a few mature research labs.[2]

V.RESULTS AND DISCUSSION

In this section, we are giving the complete description on the proposed system architecture. Here we are using Raspberry Pi board as our platform. It has an ARM-11 SOC with integrated peripherals like USB, and serial, etc. finger print module and camera externally connected to Raspberry pi board. On this board we are installing Linux operating system with necessary drivers for all peripheral devices and user level software stack which includes a light weight GUI based on X Server, V4L2 API for interacting with video devices like cameras, TCP/IP stack to communicate with network devices and some standard system libraries for system level general IO operations

After connecting all the devices power up the device. When the device starts booting from flash, it first loads the Linux to the device and initializes all the drivers and the core kernel. After initialization of the kernel it first checks whether all the devices are working properly or not. After that it loads the file system and starts the startup scripts for running necessary processes and daemons. Finally it starts the main application. When our application starts running it first checks all the devices and resources which it needs are available or not. After that it checks the connection with the devices and gives control to the user. Then we can enter the program path we can get the LXTerminal window.



Fig.8: Raspberry pi connections

This system captures image by means of web camera connected to ARM controller through USB and the image is processed by using image processing technique. The input is an image, such as a photograph or video frame; the output of image processing may be either an image or a set of characteristics or parameters related to the image.

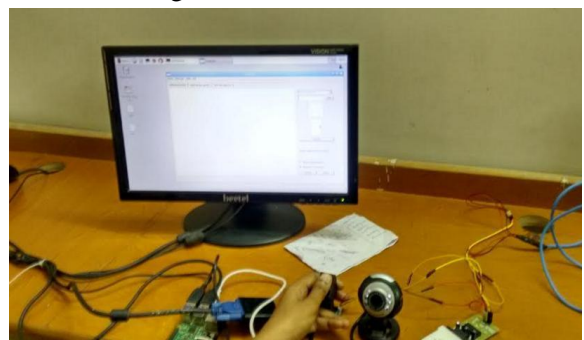


Fig.9: Overall view of the System

Using algorithms person movement is monitored continuously like person position, person crying etc. And all these captured images are displayed on Display unit connected to ARM controller. The controller will recognize the face and iris of the particular person from the image. The finger print module will take the finger print from the person and send to controller. The controller will recognize the finger print of particular person from the data base. If they are matched then it will display the data on display unit.

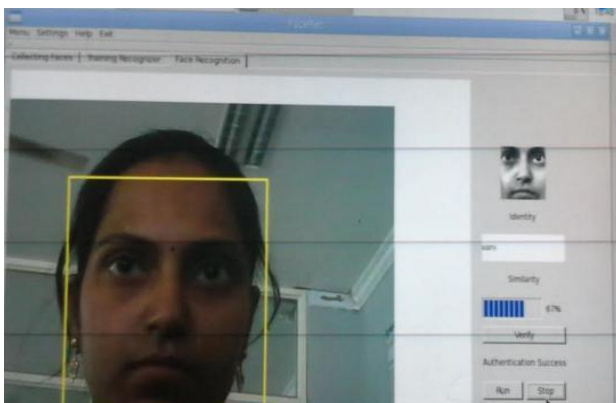


Fig.10: Identification of Person

VI.CONCLUSION

The project “Implementation of Deep Representations for Iris, Face and Fingerprint Spoofing Detection using Open Source Platform” has been successfully designed and tested. It has been developed by integrating features of all the hardware components and software used. Presence of every module has been reasoned out and placed carefully thus contributing to the best working of the unit. Secondly, using highly advanced ARM11 board and with the help of growing technology the project has been successfully implemented.

REFERENCES

[1] Dmitry Pertsau, Andrey Uvarov “Face Detection Algorithm Using Haar-Like Feature for GPU Architecture” The 7th IEEE International conference on Intelligent Data Acquisition and Advanced

Computing Systems: Technology and Applications 12-14 september 2013.

[2] Paul Viola and Michael Jones in their paper “Rapid Object Detection using a Boosted Cascade of simple Features” The IEEE International conference on computer vision and pattern recognition.

[3] Dr. Sunil Kumar Singlain his paper “A Review of Image Based Fingerprint Authentication Algorithms”. The International Journal of Advanced Research in Computer science and Software Engineering: Volume 3, issue 6, june 2013.

[4] J. Galbally, J. Ortiz-Lopez, J. Fierrez, and J. Ortega-Garcia, “Iris liveness detection based on quality related features”, in Proc. 5th IAPR ICB, Mar./Apr. 2012, pp. 271–276.

[5] J. Galbally, F. Alonso-Fernandez, J. Fierrez, and J. Ortega-Garcia, “A high performance fingerprint liveness detection method based on quality related features”, Future Generat. Comput. Syst., vol. 28, no. 1, pp. 311–321, 2012.

[6] “Linux for Embedded and Real time Application”, by Doug Abbott.

[7] <http://download.qt.io/learning/developer/guides/qtquickappdevintro/QtQuickApp>

[8] R. Cappelli, D. Maio, A. Lumini, and D. Maltoni, “Fingerprint image reconstruction from standard templates,” IEEE Trans. Pattern Anal. Mach. Intell., vol. 29, no. 9, pp. 1489–1503, Sep. 2007.

[9] Liu Chun-cheng. USB Webcam Driver Development Based on Embedded Linux [J]. Computer Engineering and Design, 2007, 28(8):1885-1888.

[10] J. Galbally, F. Alonso-Fernandez, J. Fierrez, and J. Ortega-Garcia, “A high performance fingerprint liveness detection method based on quality related

features”, *Future Generat. Comput. Syst.*, vol. 28, no. 1, pp.311–321, 2012.

[11]J. Galbally, J. Fierrez, F. Alonso-Fernandez, and M. Martinez-Diaz, “Evaluation of direct attacks to fingerprint verification systems”, *J. Telecommun. Syst.*, vol. 47, nos. 3–4, pp. 243–254, 2011.

[12]D. Maltoni, D. Maio, A. Jain, and S. Prabhakar, *Handbook of Fingerprint Recognition*. New York, NY, USA: Springer-Verlag, 2009.

[13]A. Liu, W. Lin, and M. Narwaria, “Image quality assessment based on gradient similarity”, *IEEE Trans. Image Process.*, vol. 21, no. 4, pp.1500–1511, Apr. 2012.

[14]I. Chingovska, A. Anjos, and S. Marcel, “On the effectiveness of local binary patterns in face anti-spoofing”, in *Proc. IEEE Int.Conf. Biometr. Special Interest Group*, Sep. 2012, pp. 1–7.

[15] Steve Furber, *Arm System-On-Chip Architecture*, Second Edition Person Education Limited, 2000.

DESIGN AND IMPLEMENTATION OF AGRICULTURAL AUTOMATION THROUGH WIRELESS NETWORK AND GPRS

B. SHYLAJA ¹, B. SRINIVAS ²

¹ B. Shylaja, M.Tech student, Dept Of Ece, Malla Reddy Engineering College, Maisammaguda, Dhulapally, Hyderabad, Ranga reddy Dist, Telangana, India.

² Guide Details, B. Srinivas, M.E., Associate professor, Dept Of Ece, Malla Reddy Engineering College, Maisammaguda, Dhulapally, Hyderabad, Ranga reddy Dist, Telangana, India.

Abstract: An automated irrigation system was developed to optimize water use for agricultural crops. The system has a distributed wireless network of soil-moisture and temperature sensors placed in the root zone of the plants. In addition, a gateway unit handles sensor information, triggers actuators, and transmits data to a web application. An algorithm was developed with threshold values of temperature and soil moisture that was programmed into a microcontroller-based gateway to control water quantity. The system was powered by photovoltaic panels and had a duplex communication link based on a cellular-Internet interface that allowed for data inspection and irrigation scheduling to be programmed through a web page. The automated system was tested in a sage crop field for 136 days and water savings of up to 90% compared with traditional irrigation practices of the agricultural zone were achieved. Three replicas of the automated system have been used successfully in other places for 18 months. Because of its energy \autonomy and low cost, the system has the potential to be useful in water limited geographically isolated areas.

Keywords: Microcontroller, GSM/GPRS Modem, LCD display, Temperature Sensor, Humidity Sensor, Water Level Sensor, Soil Sensor, Voltage Sensor, ZIGBEE module

I. Introduction

Agriculture uses 85% of available freshwater resources worldwide, and this percentage will continue to be dominant in water consumption because of population growth and increased food demand. There is an urgent need to create strategies based on science and technology for sustainable use of water, including technical, agronomic, managerial, and institutional improvements. There are many systems to achieve water savings in various crops, from basic ones to more technologically advanced ones. For instance, in one system plant water status was monitored and irrigation scheduled based on canopy temperature distribution of the plant, which was acquired with thermal imaging. In addition, other systems have been developed to schedule irrigation of crops and optimize water use by means of a crop water stress index (CWSI) [3]. The empirical CWSI was first defined over 30 years ago [4]. This index was later calculated

II. The Hardware System

Micro controller:

This section forms the control unit of the whole project. This section basically consists of a Microcontroller with its associated circuitry like Crystal with capacitors, Reset circuitry, Pull up resistors (if needed) and so on. The Microcontroller

forms the heart of the project because it controls the devices being interfaced and communicates with the devices according to the program being written.

ARM7TDMI:

ARM is the abbreviation of Advanced RISC Machines, it is the name of a class of processors, and is the name of a kind technology too. The RISC instruction set, and related decode mechanism are much simpler than those of Complex Instruction Set Computer (CISC) designs.

Liquid-crystal display (LCD):

LCD is a flat panel display, electronic visual display that uses the light modulation properties of liquid crystals. Liquid crystals do not emit light directly. LCDs are available to display arbitrary images or fixed images which can be displayed or hidden, such as preset words, digits, and 7-segment displays as in a digital clock. They use the same basic technology, except that arbitrary images are made up of a large number of small pixels, while other displays have larger elements.

III. Design of Proposed Hardware System

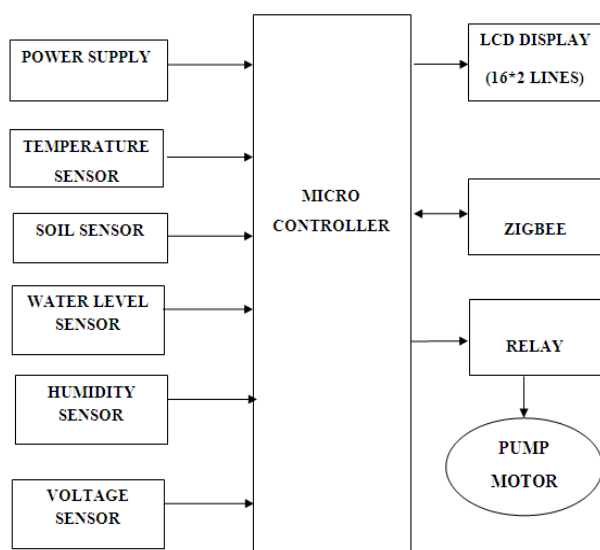


Fig.1.block diagram

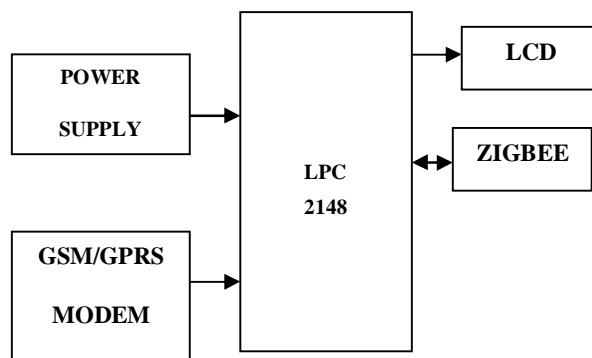


Fig.2.block diagram

In this paper, the development of the automated irrigation system based on microcontrollers and wireless communication at experimental scale within rural areas is presented. The aim of the implementation was to demonstrate that the automatic irrigation can be used to reduce water use. A microcontroller for data acquisition, and transceiver; the sensor measurements are transmitted to a microcontroller based receiver. This gateway permits the automated activation of irrigation when the threshold values of soil moisture and temperature is reached. Communication between the sensor nodes and the data receiver is via the Zigbee. This receiver unit also has a duplex communication link based on a cellular Internet interface, using General Packet Radio Service (GPRS) protocol, which is a packet oriented mobile data service cellular global system for mobile communications (GSM).

IV. Board Hardware Resources Features

Temperature Sensor:

Thermistors are thermally sensitive resistors whose prime function is to exhibit a large, predictable and precise change in electrical resistance when subjected to a corresponding change in body temperature. Negative Temperature Coefficient (NTC) thermistors exhibit a decrease in electrical resistance when subjected to an increase in body temperature and

Positive Temperature Coefficient (PTC) thermistors exhibit an increase in electrical resistance when subjected to an increase in body temperature. U.S. Sensor produces thermistors capable of operating over the temperature range of -100° to over $+600^{\circ}$ Fahrenheit. Because of their very predictable characteristics and their excellent long term stability, thermistors are generally accepted to be the most advantageous sensor for many applications including temperature measurement and control.

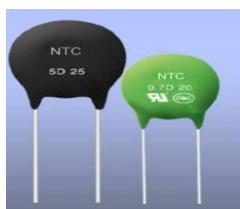


Fig.3.Temperature Sensor

Soil sensor:

The circuit designed uses a 5V supply, fixed resistance of 100Ω , variable resistance of $10K\Omega$, two copper leads as the sensor probes, 2N222N transistor. It gives a voltage output corresponding to the conductivity of the soil. The conductivity of soil depends upon the amount of moisture present in it. It increases with increase in the water content of the soil. The voltage output is taken at the transmitter which is connected to a variable resistance. This variable resistance is used to adjust the sensitivity of the sensor



Fig.4.Soil Sensor

Humidity Sensor:

Humidity is the presence of water in air. The amount of water vapor in air can affect human comfort as well as many manufacturing processes in industries. The presence of water vapor also influences various physical, chemical and biological processes.

In agriculture, measurement of humidity is important for plantation protection (dew prevention), soil moisture monitoring, etc. For domestic applications, humidity control is required for living environment in buildings, cooking control for microwave ovens, etc. In all such applications and many others, **humidity sensors** are employed to provide an indication of the moisture levels in the environment.

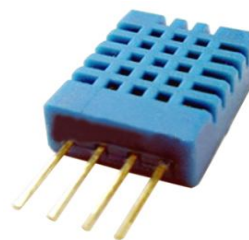


Fig.5.Humidity Sensor

Water level Sensor:

The purpose for this Sensor is to allow the user to evaluate a pressure sensor for not only water level sensing and to replace a mechanical switch, but also for water flow measurement, leak detection, and other solutions for smart appliances. This system continuously monitors water level and water flow

ZIGBEE:

ZIGBEE is a specification for a suite of high level communication protocols using small, low-power digital radios based on the IEEE 802.15.4-2003 standard for Low-Rate Wireless Personal Area Networks (LR-WPANs), such as wireless light switches with lamps, electrical meters with in-home-

displays, consumer electronics equipment via short-range radio needing low rates of data transfer. The technology defined by the ZIGBEE specification is intended to be simpler and less expensive than other WPANs, such as Bluetooth. ZIGBEE is targeted at radio-frequency (RF) applications that require a low data rate, long battery life, and secure networking.

ZIGBEE is a low-cost, low-power, wireless mesh networking standard. First, the low cost allows the technology to be widely deployed in wireless control and monitoring applications. Second, the low power-usage allows longer life with smaller batteries. Third, the mesh networking provides high reliability and more extensive range.



Fig.6.ZIGBEE Module

Relays:

A relay is an electrically controllable switch widely used in industrial controls, automobiles and appliances. Relays are used where it is necessary to control a circuit by a low-power signal (with complete electrical isolation between control and controlled circuits), or where several circuits must be controlled by one signal.

The relay allows the isolation of two separate sections of a system with two different voltage sources i.e., a small amount of voltage/current on one side can handle a large amount of voltage/current on

the other side but there is no chance that these two voltages mix up.

GPRS:

GPRS technology enabled much higher data rates to be conveyed over a cellular network when compared to GSM. GPRS technology offering data services with data rates up to a maximum of 172 kbps, facilities such as web browsing and other services requiring data transfer became possible. GPRS and GSM are able to operate alongside one another on the same network, and using the same base stations. However upgrades are needed. The network upgrades reflect many of those needed for 3G, and in this way the investment in converting a network for GPRS prepares the core infrastructure for later evolution to a 3G W-CDMA / UMTS.



Fig.7.GSM Module

V. CONCLUSION

The automated irrigation system implemented was found to be feasible and cost effective for optimizing water resource for agricultural production. This irrigation system allows cultivation in places with water scarcity thereby improving sustainability. The automated irrigation system developed proves that the use of water can be diminished for a given amount of fresh biomass production. The use of solar power in this irrigation system is pertinent and

significantly important for organic crops and other agricultural products that are geographically insolated, where the investment in electric power supply would be expensive. The irrigation system can be adjusted to a variety of specific crop needs and requires minimum maintenance. The modular configuration of the automated irrigation system allows it to be scaled up for larger greenhouses or open fields. In addition, other applications such as temperature monitoring in compost production can be easily implemented. The Internet controlled duplex communication system provides a powerful decision making device concept for adaptation to several cultivation scenarios. Furthermore, the Internet link allows the supervision through mobile telecommunication devices, such as a smart phone. Besides the monetary savings in water use, the importance of the preservation of this natural resource justify the use of this kind of irrigation systems.

VI. REFERENCES

- [1] W. A. Jury and H. J. Vaux, "The emerging global water crisis: Managing scarcity and conflict between water users," *Adv. Agronomy*, vol. 95, pp. 1–76, Sep. 2007.
- [2] X. Wang, W. Yang, A. Wheaton, N. Cooley, and B. Moran, "Efficient registration of optical and IR images for automatic plant water stress assessment," *Comput. Electron. Agric.*, vol. 74, no. 2, pp. 230–237, Nov. 2010.
- [3] G. Yuan, Y. Luo, X. Sun, and D. Tang, "Evaluation of a crop water stress index for detecting water stress in winter wheat in the North China Plain," *Agricult. Water Manag.*, vol. 64, no. 1, pp. 29–40, Jan. 2004.
- [4] S. B. Idso, R. D. Jackson, P. J. Pinter, Jr., R. J. Reginato, and J. L. Hatfield, "Normalizing the stress degree day parameter for environmental variability," *Agricult. Meteorol.*, vol. 24, pp. 45–55, Jan. 1981.
- [5] Y. Erdem, L. Arin, T. Erdem, S. Polat, M. Deveci, H. Okursoy, and H. T. Gültas, "Crop water stress index for assessing irrigation scheduling of drip irrigated broccoli (*Brassica oleracea* L. var. *italica*)," *Agricult. Water Manag.*, vol. 98, no. 1, pp. 148–156, Dec. 2010.
- [6] K. S. Nemali and M. W. Van Iersel, "An automated system for controlling drought stress and irrigation in potted plants," *Sci. Hortic.*, vol. 110, no. 3, pp. 292–297, Nov. 2006.
- [7] S. A. O'Shaughnessy and S. R. Evett, "Canopy temperature based system effectively schedules and controls center pivot irrigation of cotton," *Agricult. Water Manag.*, vol. 97, no. 9, pp. 1310–1316, Apr. 2010.
- [8] R. G. Allen, L. S. Pereira, D. Raes, and M. Smith, *Crop Evapotranspiration-Guidelines for Computing Crop Water Requirements—FAO Irrigation and Drainage Paper 56*. Rome, Italy: FAO, 1998.
- [9] S. L. Davis and M. D. Dukes, "Irrigation scheduling performance," *Agricult. Water Manag.*, vol. 98, no. 1, pp. 19–28, Dec. 2010.
- [10] K. W. Migliaccio, B. Schaffer, J. H. Crane, and F. S. Davies, "Plant response to evapotranspiration and soil water sensor irrigation scheduling methods for papaya production in south Florida," *Agricult. Water Manag.*, vol. 97, no. 10, pp. 1452–1460, Oct. 2010.
- [11] J. M. Blonquist, Jr., S. B. Jones, and D. A. Robinson, "Precise irrigation scheduling for turfgrass using a subsurface electromagnetic soil moisture

- sensor,” *Agricult. Water Manag.*, vol. 84, nos. 1–2, pp. 153–165, Jul. 2006.
- [12] O. M. Grant, M. J. Davies, H. Longbottom, and C. J. Atkinson, “Irrigation scheduling and irrigation systems: Optimising irrigation efficiency for container ornamental shrubs,” *Irrigation Sci.*, vol. 27, no. 2, pp. 139–153, Jan. 2009.
- [13] Y. Kim, R. G. Evans, and W. M. Iversen, “Remote sensing and control of nan irrigation system using a distributed wireless sensor network,” *IEEE Trans. Instrum. Meas.*, vol. 57, no. 7, pp. 1379–1387, Jul. 2008.
- [14] Y. Kim and R. G. Evans, “Software design for wireless sensor-based site-specific irrigation,” *Comput. Electron. Agricult.*, vol. 66, no. 2, pp. 159–165, May 2009.
- [15] D. K. Fisher and H. A. Kebede, “A low-cost microcontroller-based system to monitor crop temperature and water status,” *Comput. Electron. Agricult.*, vol. 74, no. 1, pp. 168–173, Oct. 2010.
- [16] Y. Kim, J. D. Jabro, and R. G. Evans, “Wireless lysimeters for realtime online soil water monitoring,” *Irrigation Sci.*, vol. 29, no. 5, pp. 423–430, Sep. 2011.
- [17] O. Mirabella and M. Brischetto, “A hybrid wired/wireless networking infrastructure for greenhouse management,” *IEEE Trans. Instrum. Meas.*, vol. 60, no. 2, pp. 398–407, Feb. 2011.
- [18] I. F. Akyildiz, W. Su, Y. Sankarasubramaniam, and E. Cayirci, “A survey on sensor networks,” *IEEE Commun. Mag.*, vol. 40, no. 8, pp. 104–112, Aug. 2002.
- [19] J. Yick, B. Mukherjee, and D. Ghosal, “Wireless sensor network survey,” *Comput. Netw.*, vol. 52, no. 12, pp. 2292–2330, Aug. 2008.
- [20] M. Winkler, K.-D. Tuchs, K. Hughes, and G. Barclay, “Theoretical and practical aspects of military wireless sensor networks,” *J. Telecommun. Inf. Technol.*, vol. 2, pp. 37–45, Apr./Jun. 2008.
- [21] M. P. Durisic, Z. Tafa, G. Dimic, and V. Milutinovic, “A survey of military applications of wireless sensor networks,” in *Proc. MECO*, Jun. 2012, pp. 196–199.
- [22] M. C. Rodríguez-Sánchez, S. Borromeo, and J. A. Hernández-Tamames, “Wireless sensor networks for conservation and monitoring cultural assets,” *IEEE Sensors J.*, vol. 11, no. 6, pp. 1382–1389, Jun. 2011.
- [23] G. López, V. Custodio, and J. I. Moreno, “LOBIN: E-textile and wireless-sensor-network-based platform for healthcare monitoring in future hospital environments,” *IEEE Trans. Inf. Technol. Biomed.*, vol. 14, no. 6, pp. 1446–1458, Nov. 2010.
- [24] J. M. Corchado, J. Bajo, D. I. Tapia, and A. Abraham, “Using heterogeneous wireless sensor networks in a telemonitoring system for healthcare,” *IEEE Trans. Inf. Technol. Biomed.*, vol. 14, no. 2, pp. 234–240, Mar. 2010.
- [25] G. X. Lee, K. S. Low, and T. Taher, “Unrestrained measurement of arm motion based on a wearable wireless sensor network,” *IEEE Trans. Instrum. Meas.*, vol. 59, no. 5, pp. 1309–1317, May 2010.

A Remote Test Platform for Mobile Application

Dr. M.J.C.Prasad¹, Chakradhar Chegu²

¹Professor & Head, Department of ECE, Malla Reddy Engineering College, Hyderabad, Telangana, India

²Student, Malla Reddy Engineering College, Hyderabad, Telangana, India

¹jagdissh@mrec.ac.in

³WhitePaperRemote@gmail.com

Abstract—In this paper, a system is proposed to provide a remote test platform for mobile application. The launch of devices and up gradation of the operating system, sustaining and enhancing mobile applications have become time-consuming and expensive for enterprises. It is difficult to estimate a mobile application to work as expected on so many mobile phones in the market. Due to the limited budget, most of the development teams may not have enough testing phones. But under market pressure, the applications have to be launched on time. To overcome this, a unique cloud-based remote testing platform introduced to facilitate testing on any mobile application on multiple platforms and devices. This project provides platform for mobile OS including IOS, Windows Phone and Android. This platform helps clients streamline their testing processes, reduce capital expenditure and ensure compatibility with various device types and platforms. The operation process contains automated test scripts that will be executed on different mobile phones to improve testing efficiency. By using this proposed system, we can provide a remote test platform which reduces the cost of buying many mobile phones and improve mobile application testing efficiency, quality and reliability.

Keywords—A remote test platform, mobile application, remote testing, cloud testing.

I. INTRODUCTION

There are approximately seven billion mobile subscriptions worldwide, as estimated by the International Telecommunication Union, investing in and developing mobile applications has become essential for organizations [2]. The adoption of the mobile application is increasing at an enormous rate due to their advanced functionality and features. However, it is challenging for these organizations to manage and maintain an inventory of devices required for testing these mobile applications [1].

To address this problem, this project offers a cloud-based remote testing platform for testing mobile applications across various physical device types, platforms (iOS, Android, and Windows Phone). In this project, clients can enjoy the flexibility of remotely connecting to this platform anytime. It also allows configuring and controlling devices remotely to test scenarios that may require hard keys, soft keys or screen interaction on the device.

The platform can be used to run both manual and automated test scenarios. There are many features that are provided by this proposed system, like mirroring android devices, monitoring CPU, checking memory logs, device control, app control etc. It is intuitive, easy to use and can help clients reduce capital expenditure.

II. LITERATURE SURVEY

This chapter includes the study and research of the document related to the project. Theoretical base is needed to implement the project in a successful way reaching all objectives. This literature is taken from related articles, journals, newspapers, internet and books.

It is a great revolution in the global world that remote testing of the application on a variety of devices (i.e. Smartphone) with different platforms is possible. There are many cloud testing services which provide software testing [5] [6] and mobile applications. Most of these services provide remote access to smartphones in order to accomplish their testing (Keynote Device Anywhere, 2013) [7] [8]. But the quality of testing fails like the remote app does not work on some machines. Among them, we provide optimum features for remote test platform for mobile application.

Interest in critical mobile applications that require high-level reliability and stability is growing rapidly. Smartphones are used for many purposes, but few applications require high security, stability and need prompt reply like online banking (State Bank of India), notifications on hurricanes [3], voice detection, monitoring cardiac patients and traffic monitoring. To ensure the mobile applications' reliability and security, sufficient testing is required on a variety of phones as well as on different platforms [4].

Adequately testing on all these platforms is too expensive for small resource-constrained mobile development companies. The idea is to create a unique cloud-based remote testing platform to facilitate mobile application to test on multiple platforms and devices. The proposed framework is based on a system that connects operational

computers, mobile devices, and databases with applications. This framework is presented as a combination of hardware (smartphones) and software (applications) that allows for different testing methods. For example, it is possible to test a new smartphone for its compatibility with mobile applications and also to test a new application on different smartphones.

III. HARDWARE IMPLEMENTATION

This chapter provides a brief explanation of system architecture, working procedure and various hardware components used in the project.

A. System Architecture

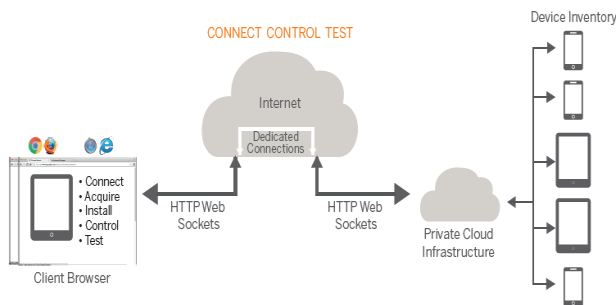


Figure 1 Block Diagram

This proposed system provides cloud server, governor node server, main node server, a PC on the client side and a device inventory.

On the client side, this system provides flexibility for the client to access the device from any location. No need to procure device hardware or maintain inventory. We can install the application and test on various devices remotely. On the server side, it provides high-end severer, huge inventory of devices, dedicated connection with high speed and private cloud infrastructure with redundant backup power supply. The Private cloud infrastructure used for security and data encapsulation, so that devices using the application are not corrupted.

B. Device inventory

The platform has vast device inventory that is updated as and when new devices are introduced to the market. Both android device inventory and iOS device inventory are maintained. These smartphones are connected to the server via USB cables. Android phones with version 4.3 or above are supported. iOS device inventory includes iPhones,

iPads, etc... This proposed system provides centralized device inventory database.

C. Main Node Server

Main node Server is primary application server which is connected to Database server. The system maintains a backup server for redundancy. It requires a PC with configuration as following:

1. OS: Windows 7
2. RAM: 4 GB minimum
3. Memory: 30 GB minimum
4. Processor: i5 or above

D. Governor Node Server

Governor Node is close to device inventory, as the devices are directly connected to the server. These devices are connected to the server via SB cable using ADB framework. It requires a PC with the following configuration:

1. OS: Windows 7
2. RAM: 8GB minimum
3. Memory: 30GB minimum
4. Processor: i5 or above

E. Topology

The system topology includes all the network setup from remote client location to the device inventory.

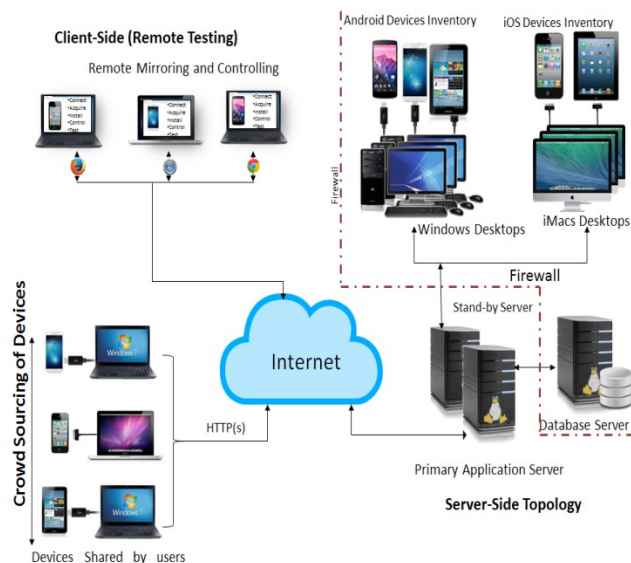


Figure 2 Network Topology

Remote mirroring and controlling of the real devices is done on the client side. Crowd sourcing of devices is additional feature provided by the proposed system. A device inventory is maintained with Governor Node connected directly via USB cables. In the above figure a primary application server is maintained, which is connected to internet. A database server is connected to the primary server. Stand-by server is provided for redundancy. This primary server is connected to real devices via Governor Node. Governor Node requires high configuration systems to process the data and forward to main node.

F. Crowd Sourcing of devices

Crowd sourcing of devices is the additional feature of the proposed system. In this scenario Clients have the flexibility to connect their own devices to the network (on client side), so as to test application on it. This feature makes the user to have two kinds of facilities. First instance device selection. Next step is to test the performance of brand new device (product yet to release in market) on various applications. This feature extends the device inventory on client location.

G. Working Procedure

System implementation includes all the devices used in the project, combining and establishing communication between them. Initially, launch the remote test platform portal from PC then sign-up as the user. Later sign-in with username and password. A screen appears with Dashboard mentioned with “select a device”.

Search the device by typing the device name at the top left of the screen and select the device. After selection of the device, a pop-up window appears. Select the group name and allocation time. Once the device is allocated, you can see two options “release” and “stop”. “Release button” will help you to release the device in between. “Stop button” will stop your allocation time and will allow other users to use the device.

There are various android device controls of the phone visible on the screen like volume, zoom, lock, reboot, menu, etc... Complete phone mirroring is done. You can avail full device features like call, SMS, video etc... Performance overview of the app installed on your device can be checked by clicking on the monitor option. Performance overview includes logs, CPU, and memory utilization. This system provides two kinds of testing. Automation testing uses scripts and manual testing is done by the user. After you complete an “Automated” test, you can replay, view, download your test results in the same way you do for the manual test.

System generated logs/graphs are compared with the expected outputs given by users, using Galen layout comparison test. After that application developer will analyze the reports and release the application in the market.

IV. FIRMWARE IMPLEMENTATION

Firmware implementation deals with developing, debugging and configuring of source code. To control the operation of hardware, software implementation is required. There are many software tools used in this project. They are:

1. MySQL
2. JDK
3. Android SDK
4. Wildfly
5. Node.js
6. .Net Framework

MySQL is used for installing database on Main Node server with version 5.6. JDK is used for configuring Java. Android SDK is used for android device support in remote test platform like ADB tool. Wildfly is used for setting-up Main Node and Governor Node Server. Node.js and .Net Framework is used for automation setup & Database.

V. RESULTS

The implementation of “Remote test platform for mobile application” is done successfully. A cloud-based remote testing platform is introduced to facilitate testing any mobile application on multiple platforms and devices remotely. The setup was successfully done and the Software tools like MySQL, JDK, Android SDK and .Net Framework were used in the project. The Server nodes were maintained with continuous power supply and backup nodes. The remote access of the real devices from client side is shown in the figure 3. System generated logs/graphs are compared with the expected outputs given by users, using Galen layout comparison test.

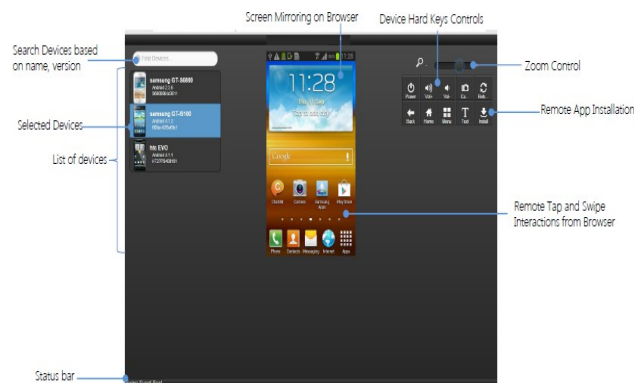


Figure 3 Remote monitoring and controlling of devices on browser

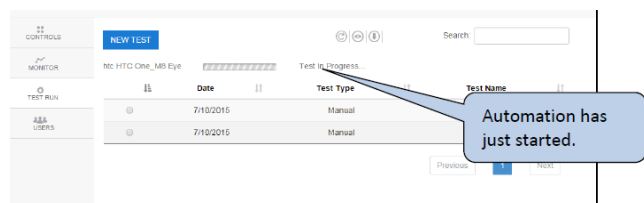


Figure 4. Test run application on the real devices

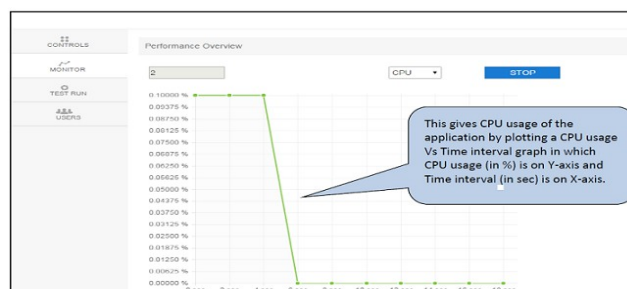


Figure5. CPU utilization by application

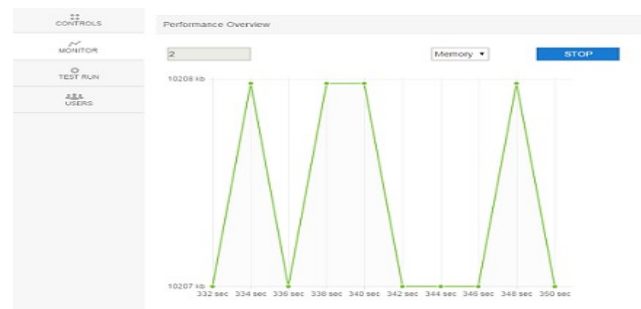


Figure6. Memory utilization of application

VI. CONCLUSION AND FUTURE SCOPE

A. Conclusion.

The remote test platform for mobile application on various real devices has been successfully tested and implemented. The proposed system gains many advantages over traditional systems of remote testing. This system provides an inventory of devices required for testing the mobile applications. The platform supports testing of applications across iOS, Android, and Windows Phone OS. This also supports tests related to the audio application. It provides low cost, low latency, high availability of servers, dedicated devices, good reliability and the perfect choice for the application developers to test their product.

B. Future Scope

The Remote testing platform for mobile application can be made more reliable by increasing the level of security at the dedicated servers and improve the testing of applications by adding additional features.

C. Advantages.

The advantages are:

1. Reduced capital expenditure for application development companies.
2. High availability of server 24/7.
3. Helps the application developers to launch the product faster in the market.
4. Low latency.
5. Dedicated connection near servers.
6. Dedicated device inventory.

D. Applications.

This project has a wide range of applications. Among them few are:

1. This project is a boon for application development companies. As it reduces the burden of cost, time and manpower.
2. This idea helps the mobile manufacturers to test the performance of new product before releasing. As the device is tested with various applications. Helps to increase the quality, stability and reliability of the product.

References

- [1] Jun-Fei Huang , Yun-Zhan Gong, Remote mobile test system: a mobile phone cloud for application testing, Cloud Computing Technology and Science (Cloud Com), 2012 IEEE 4th International Conference, Taipei, 3rd December, 2012, E-ISBN - 978-1-4673-4509-5.-5.
- [2] ICT Data and Statistics Division, Telecommunication Development Bureau, International Telecommunication Union, Place des Nations1211 Geneva 20 – Switzerland, indicators@itu.int , www.itu.int/ict .
- [3] Carr, D. F. 2012. Hurricane Sandy: Mobile, Social Tools Help Emergency Management, Brain yard news(Oct.2012). Available at:http://www.informationweek.com/thebrainyard/news/social_media_monitoring/240012463/hurricane-sandy-mobile-social-tools-helpemergency-management.
- [4] Oleksii Starov, Sergiy Vilkomir and Vyacheslav Kharchenk, Cloud Testing for Mobile Software Systems-concepts and prototyping, ICSOFT2013-8th International Joint Conference on Software Technologies.
- [5] Vilkomir, S., 2012. Cloud Testing: A State-of-the-Art Review, Information & Security: An International Journal. Volume 28, Issue 2, Number 17, 2012, 213- 222.
- [6] Tilley, S., Parveen, T., 2012. Software Testing in the Cloud: Perspectives on an Emerging Discipline, Information Science Reference, Nov. 2012.
- [7] Perfecto Mobile, 2013. The MobileCloud Company.Available at: <http://www.perfectomobile.com/>
- [8] Keynote DeviceAnywhere, 2013. The Mobile Testing Platform. Available at: <http://www.keynotedevicewhere.com>
- [9] Online:
https://en.wikipedia.org/wiki/Cloud_computing
<https://appkitbox.com>
<https://java.com>
<http://www.apple.com>

Mobile Environment for Industrial Automation

M.Murali krishna^{#1}, CH.Durga Bhavani^{*2}

[#]Assistant Professor in ECE Department,

Malla Reddy Engineering College (Autonomous), Jawaharlal Nehru Technological University, Hyderabad, India,

muralimuthe@mrec.ac.in

^{*}PG Scholar

Malla Reddy Engineering College (Autonomous), Jawaharlal Nehru Technological University, Hyderabad, India,

durgabhavanichitturi@gmail.com

Abstract— from the last two decades many automated machines are introduced which will not only reduce manpower, also it produces high quantity. Even though automation takes place, the user presence becomes mandatory to monitor the environment in control room. To evade this situation we have designed a project with a fine combination of android and embedded system. The main objective of industrial automation is security and is to reduce the user efforts to save money, energy and time. It is also used to help handicapped and old aged people who will enable them to control machine parameters automatically and alert them in critical situations. This paper put forward the design of industrial automation and security system using cortex m3 board and General Packet Radio Service (GPRS) module with android mobile. Here everything will be done by automatic. Also user can monitor machine parameters anywhere at any time in his mobile through GPRS. If he/she notices any changes he can make a call to control machine parameters manually.

Keywords: - CORTEX M3 Board, GPRS, Android Mobile.

I. INTRODUCTION

Now a day's so many technologies are coming out to make our life style more comfortable, luxurious and secure. Today we are living in 21st century where automation is playing an important role in human life. In our project we are mainly concentrates on user comfort and security. Here the controller is used to collect the process control parameters with the help of sensors and these results will be sent to mobile phone through GPRS module. When user opens webpage he can monitor the live updates of entire process of whole plant. So user presence is not necessary at all times nearby monitoring process control stations. Previously many technologies have been used in industrial automation like RF, ZIGBEE, and Bluetooth.etc with limited parameters. The limitations of all these technologies are, the user can only monitor the machine parameters within the short range. With advanced technology we have used GPRS module so that the user can monitor the process from anywhere. Hence an effective system has to be developed for avoidance of difficulties to user in monitoring the process.

The proposed system is implemented on powerful microcontroller CORTEX M3-android platform which is more useful to extend for future applications. The main objective of industrial automation is to control all the

machine parameters automatically, also to monitor the machine parameters in user mobile phone at anywhere at any time to check whether everything will be in normal condition or not. If user notices any abnormal changes he can take immediate actions by conveying his message to the person who is in industrial plant. This process will make the user to prevent the risks in large industrial plants.

II. METHODOLOGY

In this project we have used two main technologies.

- GPRS
- MEMS Accelerometer

A. General Packet Radio Service (GPRS)

GPRS is mainly used for wireless communication in industrial automation with the help of GPRS we can monitor the parameters from long distances. GPRS is a packet based wireless communication service that promises data rates from 56kbps to 114 kbps and continuous connection to the internet for mobile phone. It is an upgrade over the basic feature of GSM. It is the most widely used technology in the world for mobile communication. GPRS providing a move from circuit switched technology to packet switched technology. The GPRS network architecture added new elements including the Gateway GPRS Supporting Node (GGSN) and Serving GPRS Supporting Node (SGSN) to existing GSM network to be able to accommodate this.

The main reasons for choosing GPRS is

- It is more effective for long data packet transmission than short ones.
- Multi-slots operation in GPRS leads to efficient channel utilization.
- Available resources shared by active users
- Standard data network based on IP applications
- High capacity internet access
- Quick access to internet
- Low cost via volume based billing.

Hence to monitor the machine parameters GPRS is the best technology for communication

B. MEMS Accelerometer

In this project we have used accelerometer under Micro Electro Mechanical System (MEMS) technology. In industrial automation accelerometers are mainly used for machinery health monitoring. MEMS or micro electro

mechanical system is a technique of combining electrical and mechanical components together on a chip to produce a system of miniature dimensions. It is the integration of a number of micro components on a single chip which allows the micro-system to both sense and control the environment. To report the vibration in machines and also its changes in time shafts at the bearing of rotating equipment such as turbines, pumps, fans, rollers and bearing faults, which if not attended promptly can lead to costly repair. This accelerometer vibration data allows the user to monitor machines and detect these faults before rotating equipment fails completely. Hence MEMS promises to be an effective technique of producing sensors with high quality at low cost.

III. BLOCK DIAGRAM OF THE SYSTEM

The project here is divided into two sectional units.

- Data storage section
- Mobile for monitoring and controlling

In the industrial automation there is an android mobile which is maintained with front end application also as database as per project requirement. The communication between the controller and android mobile can be done using GPRS module which is wireless. All the sensor information is displayed on web page which we can open with URL address. Here we created a webpage for monitoring and to control all the parameters from anywhere at any time through GPRS. If the sensor parameters like temperature, humidity, fire and water level values exceeds particular value then user can take action by operating the required device. With all these accelerometer has been used which is based on Micro Electro Mechanical System (MEMS) technology. In industrial automation it is very helpful to detect machinery faults. So the user can prevent total damages of machines by checking with minor changes.

The main board of automation section as shown in figure 1. As shown in figure 1 all the sensor values will be displayed on the mobile through GPRS from the controller through web page in data acquisition unit. Here everything will be done by automatic mode. All the parameters are controlled by automatic. For every parameter we are fixing particular value according to environment. When the value exceeds particular value then it takes action by selecting the device on to control the parameter. All these can be done by sending and receiving commands through GPRS from the controller to mobile and vice versa.

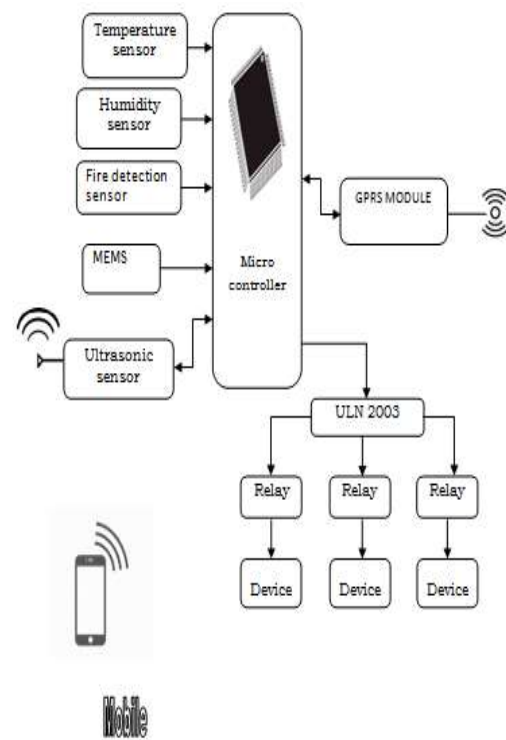


Figure 1. Block diagram of hardware

IV. HARDWARE IMPLEMENTATION

The controller LPC1768 has special and unique features which are used for industrial automation. The main features of arm cortex M3 processor are:

- It is Harvard bus architecture and it is a three stage pipeline with branch speculation.
- Configured nested vectored interrupt controller (NVIC).
- Wake up interrupt controller. It enables ultra low power stand by operation.
- Optional components for specific market requirements.
- Support for fault robust implementation via configured observation interface.
- Physical IP support.
- Greater performance efficiency with enhanced determinism.
- Wide choice of development tools with low cost solutions

A. SENSORS

In our project different sensors are used to monitor different parameters. LM35 series are precision integrated circuit temperature devices with an output voltage linearly proportional to centigrade and calibrated in Kelvin. It does not require any external calibration or trimming to provide typical accuracies with stability and reliability. This sensor has resistive type humidity measurement component.

Hence it is preferably used in most laboratories and industrial process to measure both temperature and humidity.

To measure liquid levels we have used HC-SR04 ultrasonic sensor which provides 2cm-400cm non contact measurement functions. The ultrasonic works on a principle which is similar to radar or sonar which evaluate attributes of a target by interpreting the echoes from radio or sound waves respectively.

MQ5 gas/smoke sensor can be used to detect combustible, flammable and toxic gasses. It makes an alert when it detects leakage of dangerous gasses in industries.

B. GPRS MODULE



Figure 2. GPRS MODULE

General Packet Radio Service (GPRS) modem is built with dual band sim900A works on frequencies 900/1800 MHz, the modem is coming with RS232 interface, which allows us to connect pc as well as microcontroller. The baud rate is configurable from 9600-115200 through AT commands and it has internal TCP/IP stack to enable you to connect with internet via GPRS. It is most suitable for data transfer application in Mobile to mobile interface. Hence GPRS is used to monitor the parameters in industrial automation.

V. RESULTS

Figure 3 shows entire hardware of the system which includes microcontroller, sensors, GPRS module and required devices. There are two sections in the system: One is at industrial monitoring board and the second section is mobile. All the parameter values are displayed on the monitoring board and these Values are updated in the webpage. By selecting automatic mode everything will be done by automatic. The parameters temperature, humidity, fire all these sensor values exceeds particular limit immediately the controller takes action by selecting particular device on .ultrasonic sensor is used to control water level depends on tank status the controller makes motor on/off. Accelerometer is another parameter which is used to detect machinery faults. The following figure

shows data acquisition unit in mobile phone. Hence the user can monitor all the parameters from anywhere in his mobile phone.



Figure 3. Complete Hardware of the Project



Figure 4. Data Acquisition Unit in Mobile Phone

VI. CONCLUSION

The industrial automation system has been experimentally proven to work satisfactorily by connecting sample appliances to it and the appliances were successfully controlled automatically. By the GPRS the user can successfully monitor the environment of total industrial plant from long distances. Thus proving portability and

wide compatibility, this proposed system will not only provide convenience to the common man but will be a boon for the elderly and disabled.

REFERENCES

- [1] A. H. Shajahan and A. Anand, “ Data acquisition and control using arduino – android platform: Smart plug ,” International Conference on Energy Efficient Technologies for Sustainability (ICEETS), pp. 241-244, April 2013.
- [2] E.T. Coelho et al, “A Bluetooth-based Wireless Distributed Data Acquisition and Control System,” IEEE International Conference on Robotics and Biomimetics, ROBIO '06., pp.543 – 548, Dec-2006.
- [3] N.Suresh; E. Balaji; K.Jeffry Anto ; J. Jenith4., “ Raspberry Pi Based Liquid Flow Monitoring And Control” International Journal of Research in Engineering and Technology, Vol.03, Issue no.07, Jul-2014.
- [4] Ana Priscila Alves, Hugo Silva, Andre Lourenco and Ana Fred, “BITalino: A Biosignal Acquisition System based on the Arduino,” BIODVICES 2013.
- [5] Cortex M3[Online], <https://www.exploreembedded.com>
- [6] http://www.webopedia.com/TERM/D/data_logging.html

Advanced Anti-Theft ATM Security using Raspberry Pi

G. Jakeer Hussain¹, T. Srinivas Reddy²

¹PG Scholar (Embedded Systems), Department of ECE, MREC (A), Hyderabad, Telangana, India

²Associate Professor, Department of ECE, MREC (A), Hyderabad, Telangana, India

Abstract - Automated Teller Machines ATMs are used for different ways, mostly cash withdrawals. ATM users utilize many services on ATM and they will do some billions of transactions. Meanwhile robberies occurring in the ATMs are also high with the lack of security. The main objective of our study is to minimize the robberies occurring in the ATM's. For that we have to implement a low cost standalone Embedded Web Server based on ARM11 processor and Linux operating system using Raspberry Pi. This setup is proposed for ATM security, comprising of the modules namely Door lock, web access Wi-Fi, GSM Modem, sensors and camera. Whenever robbery occurs, Vibration sensor, Fire sensor is used here which senses vibration and heat produced from ATM machine and takes necessary action. This system uses ARM7 controller based embedded system to process real time data collected using the vibration sensor. Once the vibration is sensed, information is passed to ARM11 based master device. Then the DC Motor is used to close the door of ATM, a relay will be triggered to leak the gas inside the ATM to bring the thief into unconscious stage, Camera is always in processing and it sends the images to web server and also it will be saved in computer, GSM Modem sends messages to nearby police station and corresponding bank authorities and finally an alarm sound will occurs from buzzer. This will prevent the robberies, and the person involving in the robbery can be easily carried out.

Key Words: Raspberry Pi 2, MEMs accelerometer, GSM, USB Camera, WI-FI router, IR sensor, DC motor, Buzzer

1. INTRODUCTION

Automated Teller Machine (ATM) is also known as Cash Machine is an electronic telecommunication device that allows the customers to perform financial transactions, mostly cash withdrawal. As per ATM Industry Association (ATMIA) progress there are 3 million cash machines are installed in worldwide. On ATMs, the customer is identified by inserting a plastic ATM card or smart card with a magnetic stripe that contains a unique card number and some security information such as CVVC (CVV). Authentication is provided by customer entering a Personal Identification Number (PIN). Meanwhile ATM Thefts are also occurring more in the society. The cause of ATM robberies are occurs due to the lack of security present at the ATM installed machines. Though security guards are present at ATMs, robbers are keep doing the robberies by using some

technological methods. With the result of this, GOVT had losses some lakhs and crores of money.

2. STUDY OBJECTIVE

The main objective of our study is to minimize the robberies occurring in the ATM's. Here we are implementing a low cost standalone Embedded Web Server (EWS) based on ARM11 processor and Linux operating system using Raspberry Pi. This is a real time application project where we can overcome the disadvantages of present situations that are occurs in the ATMs.

3. DESIGN OF PROPOSED HARDWARE SYSTEM

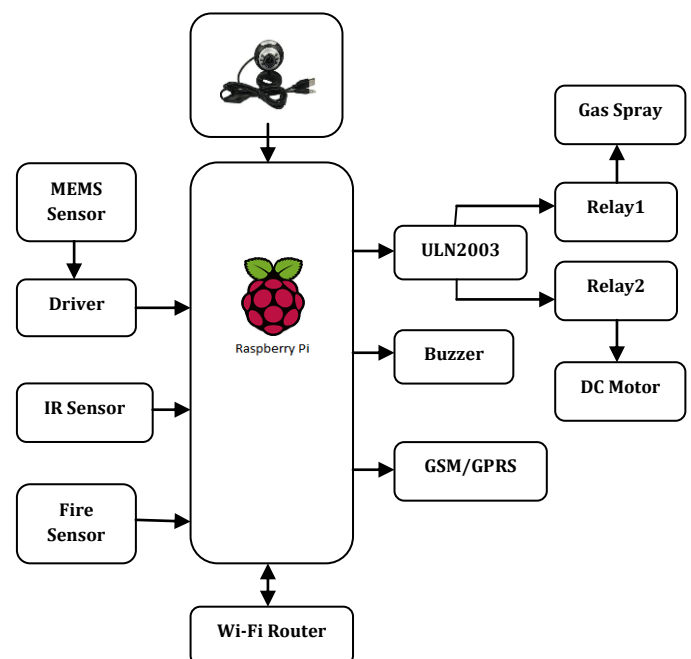


Fig -1: Block Diagram

3. DESCRIPTION OF HARDWARE COMPONENTS

3.1 Raspberry Pi

The Raspberry Pi 2 delivers 6 times the processing capacity of previous models. This second generation Raspberry Pi has an upgraded Broadcom BCM2836 processor, which is a powerful ARM Cortex-A7 based quad-core processor that runs at 900MHz. The board also features an increase in memory capacity to 1Gbyte. The total specifications of raspberry is mention below

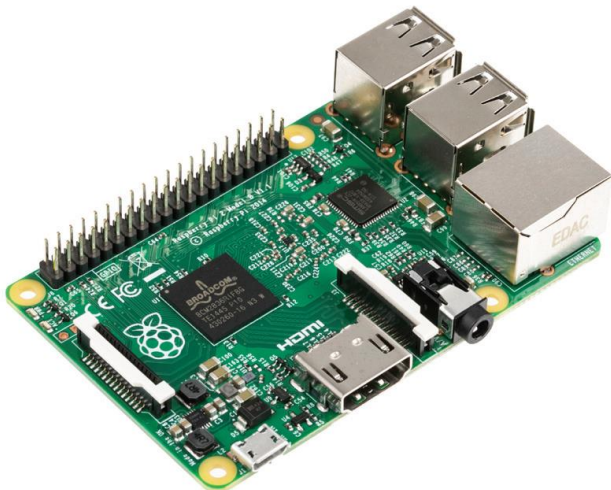


Fig -2: Raspberry Pi board

Raspberry Pi has Broadcom BCM2836 System on Chip. The core architecture of Raspberry pi is a Quad-core ARM Cortex-A7. Linux operating system is used in Raspberry Pi that boots from Micro SD card. It has 10/100 Base Ethernet socket connector. It supports a HDMI video output and 3.5mm jack audio output and 4*USB 2.0 connectors and 40 GPIO pins.

3.2 MEMS Sensor

Micro Electro Mechanical System (MEMS) sensor is a type of accelerometer is mainly used for monitoring the system value changes. MEMS sensor is a technique of combining electrical and mechanical components together on a chip to produce a system of miniature dimensions. It is the integration of a number of micro components on a single chip which allows the micro-system to both sense and control the environment. The MMA7660FC is a ± 1.5 g 3-Axis Accelerometer with Digital Output (I2C). It is a very low power, low profile capacitive MEMS sensor featuring a low pass filter, compensation for 0g offset and gain errors, and conversion to 6-bit digital values of samples per second. The device can be used for sensor data changes, product orientation, and gesture detection through an interrupt pin (INT). The device is housed in a small 3mm x 3mm x 0.9mm DFN package. This device senses the data in XYZ coordinates.

Initially it has the some predefined values. If the user try to operate on this device it will disturbs on predefined values and process the signal corresponding to raspberry system.

3.3 IR Sensor

Here Infrared sensor is used to open the door. Whenever any obstacle passes between two IR sensors then the door will be automatically opened. IR LEDs are fabricated from narrow band hetero structures with energy gap from 0.25 to 0.4 eV. Typical forward bias is $V \sim 0.1 - 1$ V only.

3.4 Fire Sensor

Here we are using MQ5 smoke detecting sensor to detect the smoke/fire/gas accidents that occurs in the ATMs. It operates on a circuit voltage of 5v.

3.5 ULN2003

ULN is mainly used for interfacing between low-level circuits and multiple peripheral power loads. The ULN20XX series has high voltage, high current darling ton arrays. The driving circuitry decodes the coding and conveys the necessary data to the stepper motor. The driver makes use of the ULN2003 driver IC, which contains an array of 7 power Darlington arrays, each capable of driving 500mA of current. At an approximate duty cycle, depending on ambient temperature and number of drivers turned on, simultaneously typical power loads totaling over 230v can be controlled. Here in this proposed system we are using two DC motors ant it requires 12v. So we are using interfacing connector as ULN2003 between power load and DC motors.

3.6 USB Camera

Here we are using a USB camera to take pictures and video on the Raspberry Pi. USB cam uses 1280*720 resolutions. Whenever theft occurs in the ATM it takes the snaps and stores in the Embedded Web Server (EWS).

3.7 GSM/GPRS

GSM/GPRS modem is built with dual band sim900A works on frequencies 900/1800 MHz. The modem is coming with RS232 interface, which allows us to connect pc as well as microcontroller. The baud rate is configurable from 9600-115200 through AT commands and it has internal TCP/IP stack to enable you to connect with internet via GPRS. It is most suitable for data transfer application in Mobile to mobile interface. Some important features of GSM are listed below

- Quad-Band 850/900/1800/1900 MHz
- GPRS multi-slot class 10/8
- GPRS mobile station class B
- Control via AT commands (GSM 07.07, 07.05 and SIMCON enhanced AT commands)
- Supply voltage range is 3.4 to 4.5 V

3.8 Wi-Fi Router

Wi-Fi router is used for accessing any kind of data through wireless mode. In this system we are using a Digisol Wi-Fi router for communication. In order to communicate between Wi-Fi router and any android device/pc, first we have to know the IP address of that router. For that we have to assign IP address to the router and later we can use. It supports the wireless speed of 150Mbps, And it also supports the LAN ports and the wired Ethernet ports, Here in this proposed system we create a small embedded web server, which we can access our required data by using the communication device as Wi-Fi router.

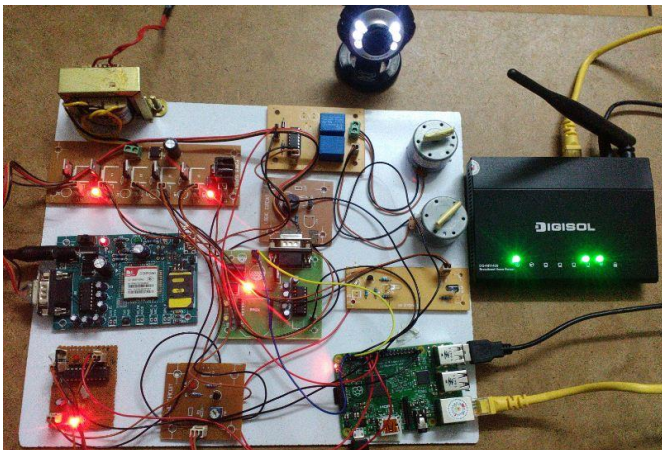
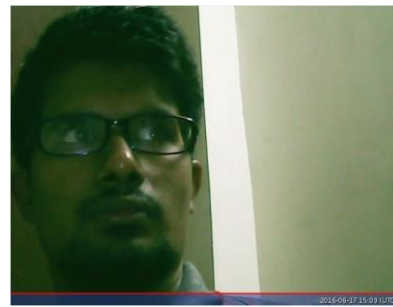
4. WORKING PROCESS

- Initially the entrance door is closed at the ATMS.
- IR sensor is used here to opens the door. Whenever the person is passing in between IR sensors the door opens. Here we are using a DC motor to open and close the door. If a person passes in between IR sensors, it detects and sends the information to Raspberry Pi through GPIO pins. A python code is written for IR detection. If IR detects, Raspberry Pi sends the signal to DC motor via relay and the dc motor turns ON for some seconds. At the same time camera is in processing state, 4-5 snaps will be taken while the person enters and stores in the embedded web server.
- After enters in to ATM room a person need to withdrawal money or he can use some ATM services.
- A MEMs sensor is placed at the money locker area in the ATM. If a person tries to robbery he must break or cut the money locker area. Then MEMs sensor will be there to detect the vibrations and sends the signal to the Raspberry Pi.
- Then the Raspberry pi will automatically close the door and releases the unconscious spray to become thief in unconscious condition.
- Same time a message will be send to the nearest police station and corresponding bank authorities through the GSM.
- And buzzer will be there to alarm the sound to give indication to the public that the theft had occurred.

- And the camera is in always processing state and it takes the pictures at the time of MEMs detection and it stores in the embedded web server.
- A fire/smoke/gas sensor is placed in the ATMs and it sends message and sounds alarm and takes pictures whenever any fire accidents will occur.
- Images that are captured will be stored in embedded web server. For that we have to create a web server.
- The web server runs on an embedded system having limited resources to serve embedded web page to a web browser. Different software can be used to implement the embedded web server, and these are mentioned below:
 - Linux-operating system.
 - Apache – web server (http) software.
 - Mysql – database server.
 - PHP or Perl – programming languages
- Html is used for web designing which is nothing but a client web browser.
- All server side web components are dynamic web components generating dynamic web pages like php, asp.net etc.
- All client side web components are static web components generating static pages like html, java script etc.
- First we have to go in browser and then we have to enter in to the web server to see the captured images. Separate python code will be written for system application and for browser application and for web server. Here we are using Apache 2 server for web access.

5. RESULTS

1. First the overall project kit is shown in figure 3.
2. Whenever MEMs disturbed, raspberry Pi closes the door and releases the unconscious gas spray to become thief in unconscious state, and similarly GSM sends the messages to the nearby police station and to the banks, and buzzer will make sound for theft indication and camera will captures images and sends to the web server. Above all operation images are shown in below figures.
3. Similarly when the fire sensor detects, alarm will come and messages will send to the police station or bank authorities.
4. Captured images are stored in database and we can see the images through embedded web server by using web access.


Fig -3: Overall Project Kit

Fig -7: Images captured by USB Camera

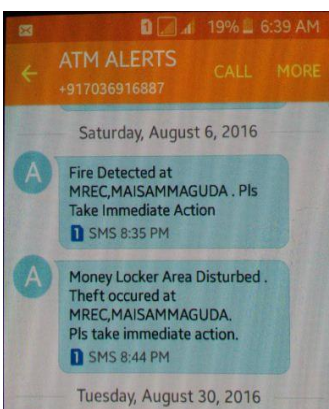
6. CONCLUSION

The project "ADVANCED ANTI-THEFT ATM SECURITY USING RASPBERRY PI" has been successfully designed and tested. It has been developed by integrating features of all the hardware components and software used and tested. Presence of every module has been reasoned out and placed carefully thus contributing to the best working of the unit.

REFERENCES

- [1] Fang, Xiang et al: An extensible embedded terminal platform for wireless telemonitoring, Information and Automation (ICIA), 2012 International Conference on Digital Object Identifier: 10.1109/ICInfA.2012.6246761 Publication Year: 2012 , Page(s): 668 - 673.
- [2] Kannan, P, and Ms P. Meenakshi Vidya. "Design and Implementation of Security Based ATM theft Monitoring system."
- [3] Dujak, Mico, et al. "Machine-to-machine communication as key enabler in smart metering systems." Information & Communication Technology Electronics & Microelectronics (MIPRO), 2013 36th International Convention on. IEEE, 2013.
- [4] Liu, Yakun, and Xiaodong Cheng. "Design and implementation of embedded Web server based on arm and Linux." Industrial Mechatronics and Automation (ICIMA), 2010 2nd International Conference on. Vol. 2. IEEE, 2010.
- [5] Matt Richardson and Shawn Wallace, *Getting Started with Raspberry Pi*. United States of America: O'Reilly Media, 2013.
- [6] SIM900_AT Command Manual_V1.03, Shanghai SIMCom Wireless Solutions Ltd.2010.
- [7] Eben Upton and Gareth Halfacree, Raspberry Pi User Guide. A John Wiley and Sons Ltd., 2012.
- [8] Python Software Foundation[US], <https://pypi.python.org/pypi>
- [9] Raspberry Pi Foundation, <http://www.raspberrypi.org>


Fig -4: Html Web Browser page

Fig -5: List of Images stored in Database

Fig -6: Message alerts through GSM

WEB SERVER BASED EFFICIENT WATER MANAGEMENT

Emmanuel Raju Gummadi^{*1}, C.H. Bhanu Prakash^{*2}

M. Tech (ES), Department ECE from MREC(A), Hyderabad, Telangana, India.^{#1}

Associate Professor, Department ECE from MREC(A), Hyderabad, Telangana, India.^{#2}

Abstract— Water is one of the important factors of life. In industrial areas, co-operative society, office and likewise system require water supply every day. Such system management of water supply using dynamic IP based Embedded Web server (EWS) is presented in this paper. In current era of networking, to maintain EWS with static Internet Protocol (IP) is costly and difficult to manage. Novel approach of assign dynamic IP to board is developed and tested for different dynamic IPs. Dynamic IP is obtained for embedded board by enabling General Packet Radio Service (GPRS) of USB data card through point to point protocol daemon (PPPoE). The embedded system consists of Advanced RISC Machine (ARM) processor running on Linux operating system, USB data card and a Very secure file transfer protocol (vsftp). Embedded board (EB) having dynamic IP contains in file transfer to vsftp dummy server through Bourne again shell (Bash) scripts and C language. EWS pages are designed in hyper text meta language (html) and JavaScript. The embedded system has tested for water management of different wings of society for dynamic IPs provided by USB data card and results are shown.

I. INTRODUCTION

Water supply, a routine daily service. Managing such supply makes efficient usage of natural resource of water and avoids wastage of it as well. Management system merges communication, network, internet and integrated technology together to bring development in field of supply-demand of available resource. Emerging updating in technology opens the world of novel ideas. It allows access of information via internet over network quickly and accurately at any time. Exchange of information can be analyzed and decisions are taken accordingly. Reliable water management by data acquisition is always needed of consumers. To understand the requirement of consumers and suppliers, data acquisition provide them better services, economic benefits, security, safety and convenience of accessing these services.

II. STUDY OBJECTIVE

The main objective of our study is to analyze the water utilization and identify the water consumption. This study will enable us to develop efficient water utilization to reduce the water consumption.

III. PROPOSED METHOD

In the proposed method we overcome the drawback present in existing system by monitoring the status of water. Our approach is based on the development of low cost sensor nodes for real time. The main sensor node consists of level sensor is the biological indicator of water sophistication. And with the help of these parameters we can monitor the water consumption. From the sensor node we are sending monitored values to raspberry-pi board. The controller transmits the data to remote PC through internet by using FTP. FTP is a protocol through which users can upload files from their systems to server. Once data is placed at server we can view the data at remote PC (with internet) on web page with unique IP address. We can view continuously the sensor's data. With the help of sensor node, we can monitor the detecting the level of water with the help of water level sensor. If the level sensor values decreases beyond the range then motor will automatically start and if level sensor values increases beyond the range then motor will automatically become OFF. In some cases if we want to start the motor manually then also it is possible.

IV. DESIGN OF PROJECT

The design is about the efficient utilization of water for minimizing the water consumption in major areas like resorts, industrial areas and etc., by automating the whole design. We use level sensors for water level detection and through Wi-Fi we can view the water status. The time of water usage is stored in database (in quantity of litres) continuously. We use a dynamic IP for request processing through browser and we can view the current status as well as consumption of water (in quantity of litres). We use python code.

V. RESULTS

5.1 Working process and design flow:

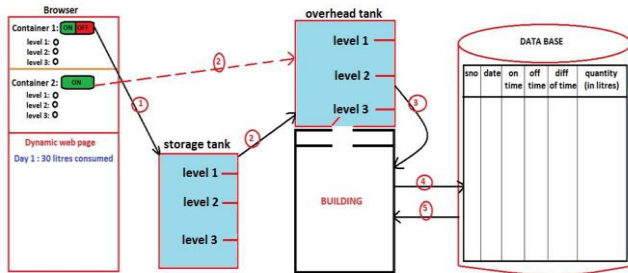


Fig 5.1: Working process

1. Above design represents the working of whole project in which we send request through browser to storage and overhead tanks.
2. Storage tank fills water into overhead tank and overhead tank supplies water to respective building.
3. The water usage throughout the building is been calculated and stored into permanent/temporary database (quantity in litres).
4. The status of water will be displayed on browser.
5. If overhead tank is emptied then the motor will turn on automatically and the water is filled into that tank through storage tank and if storage tank is emptied then automatically that tank is filled through underground water.

5.2 Client Side and Server Side:

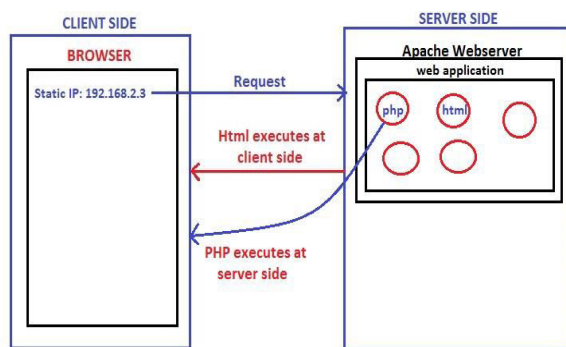


Fig 5.1: Client side and server side

1. Html is a client side web component that comes to browser(client) from webserver for execution when requested.
2. Decide whether webcomp is client side based on place where it executes; don't decide based on place where it resides.
3. Generally all server side web components are dynamic web components generating dynamic webpages like php component,jsp component or asp.net etc.,
4. Generally all client side web components are static web components generating static webpages like html files,java script files etc.,

5.3 Storing into Database:

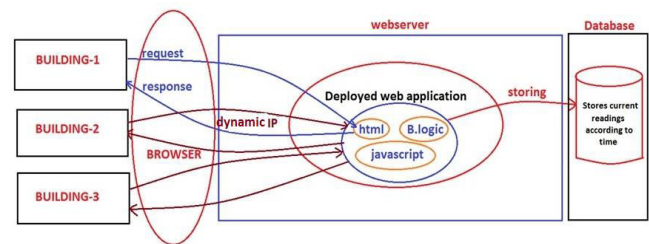


Fig 5.3: Storing into Database

1. Request comes from browser and goes to webserver.
2. In webserver we have deployed web application in which html, B.logic and php scripting resides.
3. Depending on the request mainly request webserver and this server will send request to html component which will be executed at client side.
4. We can view the display screen of water management on browser.
5. And at background python code is been executed and the status of water will be stored into database (permanent/temporary).
6. Finally we can retrieve the consumed water onto the browser (quantity in liters).

5.4 Project Architecture:

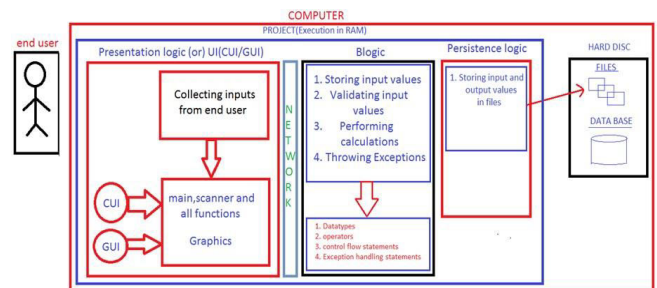


Fig 5.4: Architecture

1. In this design we can observe the whole project working process section by section.
2. Mainly the end user will open the client browser and gives the request to deployed application.
3. We are collecting the inputs which is called presentation logic/UI(user interface). In CUI main, scanner and all functions are developed and in GUI we develop graphics related data.
4. In Business logic we are storing input values validating input values, performing calculations and throwing exceptions.
5. Also data types, operators, control flow statements are also developed.
6. In Presentation logic we are storing input and output values in database software (permanent/temporary).

VI. CONCLUSION

The project "WEB SERVER BASED WATER MANAGEMENT" has been successfully designed and tested. Integrating features of all the hardware components used have developed it. Presence of every module has been reasoned out and placed carefully thus contributing to the best working of the unit. Secondly, using highly advanced IC's and with the help of growing technology the project has been successfully implemented.

VII. REFERENCES

- [1] Srinivasa, R. V., Nageswara, R., & Kumari, E. K. (2009). Cloud computing: An overview. Journal of Theoretical and Applied Information Technology, 9(1), 71-76.
- [2] Buyya, R., Broberg, J., & Goscinski, A. M. (Eds.). (2010). Cloud computing: Principles and paradigms (Vol. 87). John Wiley & Sons.
- [3] Mell, P., & Grance, T. (2011). The nist definition of cloud computing, recommendations of the national institute of standards and technology. National Institute of Standards and Technology, 800-145.
- [4] AWS | Amazon Elastic Compute Cloud (EC2) - Scalable Cloud Hosting. (n.d.). Amazon Web Services, Inc. Retrieved June 22, 2014, from <http://aws.amazon.com/ec2/>
- [5] Lounis, A., Hadjidj, A., Bouabdallah, A., & Challal, Y. (2012, July). Secure and scalable cloud-based architecture for e-health wireless sensor networks. In Computer communications and networks (ICCCN), 2012 21st international conference on (pp. 1-7). IEEE.
- [6] Rolim, C. O., Koch, F. L., Westphall, C. B., Werner, J., Fracalossi, A., & Salvador, G. S. (2010, February). A cloud computing solution for patient's data collection in health care institutions. In eHealth, Telemedicine, and Social Medicine, 2010. ETELEMED'10. Second International Conference on (pp. 95-99). IEEE.
- [7] Fortino, G.; Pathan, M.; Di Fatta, G., "BodyCloud: Integration of Cloud Computing and body sensor networks," Cloud Computing Technology and Science (CloudCom), 2012 IEEE 4th International Conference on, vol., no., pp.851,856, 3-6 Dec. 2012 doi: 10.1109/CloudCom.2012.6427537.
- [8] Hwang, J. J., Chuang, H. K., Hsu, Y. C., & Wu, C. H. (2011, April). A business model for cloud computing based on a separate encryption and decryption service. In Information Science and Applications (ICISA),

2011 International.

[9] Lab Manual for UCSF Clinical Laboratories. (n.d.). Retrieved February

23, 2015, from

<http://labmed.ucsf.edu/sfghlab/test/ReferenceRanges.html>

[10] E-Health Sensor Platform Complete Kit V2.0 for Arduino, Raspberry Pi.

(2014, July 3). Retrieved from

[http://www.cooking-hacks.com/ehealthsensors-](http://www.cooking-hacks.com/ehealthsensors-Complete-kit-biometric-medical-arduino-raspberry-pi)

[Complete-kit-biometric-medical-arduino-raspberry-pi](http://www.cooking-hacks.com/ehealthsensors-Complete-kit-biometric-medical-arduino-raspberry-pi)



Emmanuel Raju Gummadi

M.Tech (Embedded Systems), from Mallareddy Engineering College (A) Hyderabad, Telangana, India. Areas of interest are Embedded Systems, Microcontrollers



Chandragiri Bhanu Prakash

Associate Professor (Electronics and communication), from Mallareddy Engineering College(A) Hyderabad, Telangana, India. Areas of interest area is Analog and digital communication, signal processing and signal estimation

ARM Based Smart Cart and Automatic Billing System with Theft Detection

Dr.M.J.C.Prasad^{#1}, N.Haritha^{*2}

[#]Professor in ECE Department,

Malla Reddy Engineering College (Autonomous), Jawaharlal Nehru Technological University, Hyderabad, India,
jagadishmatta@gmail.com

^{*}PG Scholar

Malla Reddy Engineering College (Autonomous), Jawaharlal Nehru Technological University, Hyderabad, India,
nelluri.haritha@gmail.com

Abstract— As shopping at the malls has become a daily activity in metro cities and due to the heavy rush the whole shopping experience is ruined by long billing queues and checkout lines. The main aim of this paper is to provide an automatic billing system to avoid queues in malls and super markets. This can be done by replacing the item bar code with RFID tags, and the cart is equipped with a microcontroller, LCD, an RFID reader, EEPROM, keypad, Load-cell and ZigBee module. The item placed in the cart will be read through a RFID reader on shopping cart and the item information will be stored in EEPROM .once the shopping is done the information will be sent to the central billing system where it calculates the total billing of the specific cart. Along with this ability, the system design also ensures detection of theft performed by dishonest customers, which makes the smart system fair and attractive to both the buyers and sellers.

Keywords: - RFID, Microcontroller, ZigBee Modules, DC Motors and Loadcell

I. INTRODUCTION

In this modern world, technology changes our culture, society as well as our lifestyle. One such upcoming technology is Wireless Sensor Networks (WSN), which is maturing at a very fast rate because of its suitability in a wide range of application areas. It consists of a large number of small, low-power, cost-effective, autonomous devices termed as sensor nodes. When interfaced with sensors and actuators, they play the combined role of environment sensing, special-computing and wirelessly communicating devices. In this new era, WSN finds its use in consumer application areas such as Smart Home, Smart Grid, etc.

In this paper we take the particular application of Supermarket/Shopping malls. While doing survey on shopping malls we found that most of the people prefer to leave the shopping mall instead of waiting in long queues to buy a few products. People find it difficult to locate the product they wanted to buy, after selecting product they need to stand in a long queue for billing and payment. To try to solve the problems previously identified, recent years have seen the appearance of several technological solutions for hypermarket assistance. All such solutions share the same objectives of save consumer's time and money, help the retailers to win loyal clients.

A number of attempts have been made to design a Smart Shopping Cart with various different functionalities.

Awati and Awati [2], describe a Smart Trolley design that concentrates on how to get the customers rid of dragging heavy trolleys and to automate billing, but it assumes all the customers to be honest and hence does not tackle cases of deception, if there are any.

Further, Chihhsiong Shih, et al., [3] proposed an automatic embedded software generated framework that can create and evolve ZigBee applications. The framework consists of two major modules, pattern extraction and code generation. Pattern extraction and development are designed to provide ZigBee application with model reuse and modification. (System Modelling Language)SysML serves as a medium between pattern development and code generation A smart shopping cart application has been implemented using this pattern based software framework.

In this paper, the system is designed in such a way that each cart is identified by their unique identification number. The cart is equipped with a microcontroller, LCD, an RFID reader, keypad, EEPROM, Load-cell and ZigBee module. The item placed in the cart will be read through a RFID reader on shopping cart and the item information will be stored in EEPROM .once the shopping is done the information will be sent to the central billing system where it calculates the total billing of the specific cart. Along with this ability, the system design also ensures detection of theft performed by dishonest customers.

II. METHODOLOGY

This system uses the RFID and ZigBee wireless communication technologies

Radio frequency identification (RFID) is the wireless use of electromagnetic fields to transfer data, for the purposes of automatically identifying and tracking tags attached to objects. The tags contain electronically stored information. Some tags are powered by electromagnetic induction from magnetic fields produced near the reader. Some types collect energy from the interrogating radio waves and act as a passive transponder. Other types have a local power

source such as a battery and may operate at hundreds of meters from the reader. Unlike a barcode, the tag does not necessarily need to be within line of sight of the reader, and may be embedded in the tracked object. Radio frequency identification (RFID) is one method for Automatic Identification and Data Capture (AIDC).

There are multiple reasons why one would want to use RFID:

- It is used when you want to wirelessly identify something without line of sight
- It is used when a simple wireless means to store a small amount of information on things, and even better: change the information dynamically:
- It is used when we need a computing device but not humans to see the ID
- It is used when a computing device to see an object from far away

ZigBee modules are designed with low to medium transmit power and for high reliability wireless networks. The modules require minimal power and provide reliable delivery of data between devices. The interfaces provided with the module help to directly fit into many industrial applications. The modules operate within the ISM 2.4-2.4835 GHz frequency band with IEEE 802.15.4 baseband.

ZigBee protocol has many benefits:

- The ZigBee network is very scalable and it consumes little energy.
- The consumer has complete authority to add or remove devices as he/she sees fit.
- ZigBee compliant products only use one lithium battery that lasts the lifetime of the device.
- It supports many network topologies.
- ZigBee design is used in many areas of operation such as scalability of large networks, security, network resilience and ease of commissioning.

III. BLOCK DIAGRAM OF THE SYSTEM

The project consists of two sectional units

- Trolley or Smart Cart Section
- Automated Billing System Section

The main board is resided at the Trolley/Smart Cart Section as shown in Figure 1, so as to, program according to the requirements of cart section. In the automated billing system section there is a server computer which is maintained with the front end application and database according to the requirements of the project. The Communication between Cart Section and automated billing Section can be done wirelessly using ZigBee Modules. Each cart in the Retail Store is equipped with an RFID Reader, motor, keypad and load-cell as shown in block diagram figure1. Initially the cart is sealed. Once the start button is pressed the cart will be opened with the help of the motor. Every item that is dropped into the cart is identified by the

RFID tag which is attached to the item. The main board monitors if the customer is adding the item or removing the item from the cart using the keypad and load-cell. The controller even detects the malfunction of the process using the load-cell. Once the shopping is done the cart will be closed and the items information will be sent to the billing section through the ZigBee modules.

As shown in the Figure 2 at the Automated billing system section the total operation of displaying the items of the selected cart number, calculating the total amount of items and theft detection are handled by the visual basics and the database applications. RFID in the Retail store speeds up shopping processes and thus reduced the manual delays to provide the services and also enhances more user-service tasks. But the performance varies with respect to the vendors of RFID readers and tags. The efficient utilization of the technology also depends upon the information to be written in tag. Experimental results with respect to effectiveness of RFID reader, ZigBee Modules are presented in the paper. The work is in progress to utilize more enhancements using RFID technology. Developments in RFID technology continue to yield larger memory capacities, wider reading ranges, and faster processing.

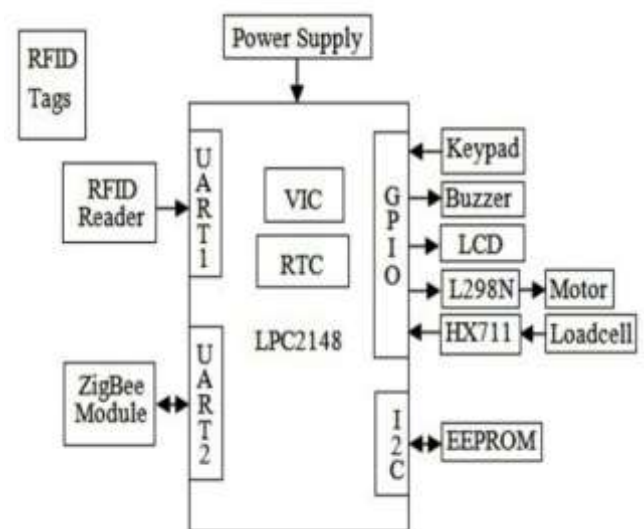


Fig.1. Block Diagram of Smart Cart Section



Fig.2. Block Diagram of Automatic Billing Section

IV. OPERATION OF THE SMART SHOPPING SYSTEM

As the customer enters the Smart Shopping Centre, he/she first picks a Smart Shopping cart. Each cart is given a unique ID and every customer is associated with the ID of the shopping cart chosen. The functioning of the system is listed below:

- Initially the cart is sealed using a motor. Once the start button is pressed the cart is opened and the cart is ready for shopping
- By default the smart shopping cart will be in add mode.
- When the customer picks the product then he/she drops the item into the cart that is identified through the RFID tag which is attached to the item and the information related to the product will be stored on to the EEPROM. At the same time the loadcell identifies the item added to the cart.
- If the customer wishes to remove the items from the cart. He/she needs to press the remove button and remove the item from the cart so that RFID reader reads the tag details, by which the particular item will be removed from the EEPROM too.
- If the customer wishes to remove the item from the cart and doesn't press the remove button and removes the item. Then loadcell identifies the decreasing of weight indicating item is removed and RFID identifies which item is removed and removes that particular item from the EEPROM.
- If the customer wishes to remove the item and press the remove button, but instead of removing, if he/she adds the item to the cart. The loadcell identifies the increase of weight indicating item is added in remove mode, which activates the theft flag and alerts that seller of theft. At the same time RFID reader identifies which item is added in remove mode.
- Once the shopping is done and when he/she presses the "shopping done" button the cart gets sealed with the help of motor and all the information from the EEPROM with the Cart identification number and theft flag status will be sent to the central billing system through the ZigBee module.
- At central billing system, with the help of database all the products information like item name, quantity and price will displayed and calculates the total bill. Once final bill is ready the total bill amount will be sent to the cart and displays on the cart for the customer notification that the bill is ready and his/her's total bill amount.
- If the central billing system identifies the theft flag, it also displays the theft information on the bill.
- Once the shopping is done and got the bill customer just pays the amount and leaves the mall.

V. HARDWARE IMPEMETATION

The various components that are used in the implementation along with the important considerations are explained in details.

A. RFID Reader and Cards

A radio frequency identification reader (RFID reader) EM-18 is a device used to gather information from an RFID tag, which is used to track individual objects. Radio waves are used to transfer data from the tag to a reader.

The EM-18 RFID Reader module operating at 125 kHz, The Reader module comes with an on-chip antenna and can be powered up with a 5V power supply.



Fig.3. EM-18 RFID Reader and Passive Card

B. Loadcell and HX711 Amplifier

A load-cell is configured as a weight sensor. This straight bar load cell (sometimes called a strain gauge) can translate up to 10kg of pressure (force) into an electrical signal. The HX711 load cell amplifier is used to get measurable data out from a load cell and strain gauge in digital form.



Fig.4. Loadcell and HX711 Arrangement

C. ZigBee Transceiver

The Tarang F20 ZigBee modules require minimal power and provide reliable delivery of data between smart cart device and billing device. The interfaces provided with the module help to directly fit into many industrial applications. The modules operate within the ISM 2.4-2.4835 GHz frequency band with IEEE 802.15.4 baseband.



Fig.5. ZigBee Module

D. LCD Display

LCD has the ability to display numbers, characters & graphics. The display is interfaced to I/O port of microcontroller. The display is in multiplexed mode i.e. only one display remains on at a time.



Fig.6. LCD Display

E. DC Motor and L298N Driver

As the controller can't handle the 5v output motors, we use this H bridge motor driver board to switch the 5v motor to forward/ reverse directions. The L298 is an integrated monolithic circuit in a 15- lead Multiwatt and PowerSO20 packages. It is a high voltage, high current dual full-bridge driver designed to accept standard TTL logic levels and drive inductive loads such as relays, solenoids, DC and stepping motors.



Fig.7. DC Motor and L298N Driver

VI. RESULTS

The experimental set-up is tested for various test cases, with various products tested for all the possible cases. As the RFID card reader read the product, details were displayed on the display unit. The product details of the shopped items were temporarily stored in the EEPROM. Once the "Shopping done" button was pressed, the memory contents were read and billing was done. The same product information data was sent to the server to update the inventory.

The following test case scenarios were used in the integrated system testing to prove the working of the developed system.

- Identifying items based on RFID tags and storing the information.
- Identifying whether the items are getting added or removed from the cart based on switch and load-cell data.
- Displaying the complete process step by step on LCD
- Automatic billing update when the products are dropped in the cart or removed from the cart.
- Identifying the theft in add and remove modes.
- Detecting the cart seal is open when start button pressed and seal is closed when shopping is done.
- Shopping cart and server system communication using ZigBee modules.
- Display of the individual item and total billing on the server system.
- Finally displaying the total billing on the cart display.

All test cases were successfully tested. The system developed is user friendly and no special training is required to use the cart.



Fig.8. Prototype Model of Smart Cart Section



Fig.9. Prototype Model of Automatic Billing Section



Fig.10. Generated Theft Free Bill



Fig.11. Generated Theft Detected Bill

VII. CONCLUSION

The project successfully demonstrates the possibility of using WSN for developing a Smart Shopping System which automates the entire billing procedure. RFID in the Retail store speeds up shopping processes and thus reduced the manual delays to provide the services and also enhances more user-service tasks. The system developed is highly reliable, fair and cost-effective. It is reliable and fair because of the effectiveness of WSN combined with a highly reliable RFID Technology. The system is also energy constraint as it uses a passive sensor and it reduces the communication

requirement. The decision making process is done locally within the cart, thereby eliminating an overhead to the communication between the nodes. In the bigger picture, it reduces the man-power requirements, easy to use, low-cost and does not need any special training.

REFERENCES

- [1] D.V.S Chandra Babu, "wireless intelligent billing trolley for supermarket", International Journal of Advanced Research in Technology, vol.3, issue 1, Aug. 2012.
- [2] J. Awati and S. Awati, "Smart Trolley in Mega Mall," vol. 2, Mar 2012.
- [3] Chihhsiong Shih, Bwo-cheng Liang and Cheng-zu Lin, "An Automatic Smart Shopping Cart Deployment Framework based on Pattern Design", IEEE 15th International Symposium on Consumer Electronics, 2011.
- [4] Ergen, S. C., "ZigBee/IEEE 802.15.4 Summary," EECS Berkely, September 2004.
- [5] T. Dimitriou. A lightweight RFID protocol to protect against traceability and cloning attacks. In Conference on Security and Privacy for Emerging Areas in Communication Networks – SecureComm, Athens, Greece, September 2005. IEEE.
- [6] Ankit Anil Aggarwal, "RFID Based Automatic Shopping Cart", The International Institute for Science, Technology and Education journal on Control Theory and Informatics ,vol.1, no.1, 2011.
- [7] H. Karl and A. Willig, "Protocols and Architectures for Wireless Sensor Networks," Chichester, England, 2005.
- [8] www.nxp.com/documents/user_manual/LPC2148.pdf
- [9] <http://en.wikipedia.org/wiki/zigbee>

RFID- GSM- GPS Imparted School Bus Transportation Management System

K.Swapna Priya

M. Tech, ECE department, Malla Reddy Engineering College (Autonomous), Hyderabad, India
kswapnapriya93@gmail.com

N.Raju

Assistant Professor, ECE department, Malla Reddy Engineering College (Autonomous), Hyderabad
India
razucontact@gmail.com

Abstract: *Children Safety is the topmost concern and priority of parents these days regarding their children. In present time parents worry about their children due to increase in number of kidnapping and road accident cases. The safety mechanism for the children travelling from home to the school and back to home during the daily bus transportation is a crucial part to the parents and to the school management. This proposed system mainly ensures the overall safety of school children and to monitor pick-up/drop-off of school children during the daily bus transportation from and to school. The bus unit is used to detect when a child boards/ leaves the bus and this information is sent to controller and an alert message is issued accordingly.*

Keywords: *RFID, GSM modem, GPS module, MEMS Accelerometer.*

1. INTRODUCTION

Children Safety is the topmost concern and priority of parents these days. Children are our most important resource, but they lack skills to protect themselves. So it is the responsibility of parents/teachers and as a person, to safeguard and to teach them the skills to be safe. Now a day's most of the parents are working due to which they are not to pick up/drop off their children daily to/from the school. Today, most of students are travelling to school by school buses or school vans. Parents think that their children are safe if they travel by school bus. There are many common problems such as school bus getting delayed in traffic, school bus accident. To improve transportation safety, some schools employ bus supervisor's to take care of the children inside the bus. This paper presents a system to enhance the overall safety of children during daily bus transportation to/from school by monitoring the daily bus pick-up/drop-off of children to/from school. This system provides the best solution in reducing the parent work load and shows the current location of the bus. The system mainly aims at automatically detecting a child when he/she boards or leaves the bus and issues an alert message accordingly.

2. RELATED WORKS

There are many works done using Radio Frequency identification (RFID), it transmits the identity of an object using radio waves. One of the work done by K.Vidyasagar and G.Balaji [1] proposed a system which uses RFID Technology and GSM Technology and ARM 7 microcontroller .This system provides the status of the student and is made available to the school principal and with the parent time to time. The information of the children is secured by providing the message to the parent along with the obstacle detection in daily bus transportation. Another work done by Ali-al Maharuqi and Dr. Jayavrinada Vrindavanam [2] proposed a system which uses RFID Technology and GSM Technology and PIC microcontroller .This system provides the entry and exit of the school children in transportation. Another work done by Anwaar Al-Lawati presented an RFID-based system that aims at enhancing the safety of children in the daily bus trip to and from the school. RFID-based system includes a detection unit which is located inside the bus detects the RFID tags worn by the children's. The system sends data to the system database server, via a GSM modem. The system detects if a child did not board the bus and issues an alert message. In addition; the system also checks the children attendance and updates the database. The parents can log on into system website and monitor the details of their children.

3. PROPOSED METHODOLOGY

The system proposed mainly aims at monitoring the school children during the daily transportation to/from the school. For implementing this system we have used Radio Frequency Identification (RFID), Global System for Mobile Communication (GSM), Global Positioning System (GPS), and Micro Electro Mechanical System (MEMS) based Accelerometer and ARM CORTEX M-3 Microcontroller. RFID technology locates the child position GSM will pass information about the child to his or her parents. The system mainly consists of bus unit. The bus unit is used to detect when a child enters the bus. Child's information at entry/exit level is recorded automatically when they pass nearby the reader. At the same time parents will automatically receive the SMS from the system that inform their child boards/leaves to/from bus. In case if an accident is occurred, an SMS is sent to the school administration. The system will send SMS to the parents informing the location and the time at which the child has boarded the school bus. This system will be beneficial to the parents, school children's and school administrator. This system proposed will be promising to enhance the overall safety of the children during daily bus transportation.

3.1. Block Diagram

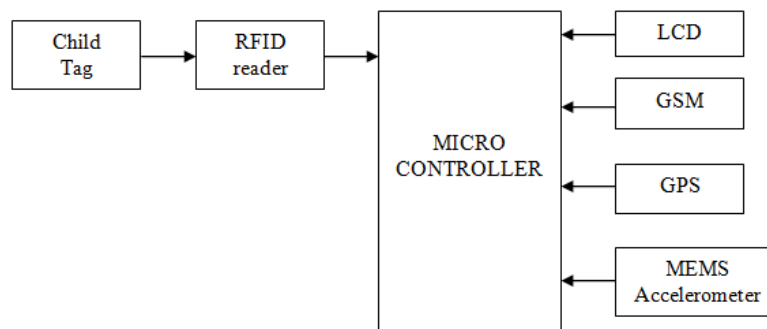


Figure1. Block Diagram

3.1.1. ARM Controller

The microcontroller does all the operations; it sends data to GSM module and LCD display. It handles both input and outputs. The Cortex-M3 is a 32-bit microprocessor with 32-bit data path, a 32-bit register bank, and 32-bit memory interfaces. The LPC1768 is a ARM Cortex-M3 based microcontroller for embedded applications featuring a high level of integration and low power consumption. The main features of the LPC1768 controller are:

- 512 kB of flash memory , 64 kB of data memory
- Single 3.3 V power supply (2.4 V to 3.6 V) , Non-maskable Interrupt (NMI) input
- Built-in Nested Vectored Interrupt Controller (NVIC)
- Brown-out detection with separate threshold for interrupt

3.1.2. Power supply

Regulated power supply is an electronic circuit that is designed to provide a constant DC voltage of predetermined value across load terminals irrespective of AC mains fluctuations or load variations.

The two main parts of a regulated power supply are a simple power supply and a voltage regulating device. The power supply output is given as input to the voltage regulating device that provides the final output. The voltage output of the power supply remains constant irrespective of large variations in the input AC voltage or output load current.

3.1.3. RFID Module

Radio Frequency Identification Technology is the fastest growing automatic data collection (ADC) technologies and is a wireless communication that uses radio waves to identify objects or people. It comprises of one or more reader and RF tags/transponders through which data transfer is achieved using electromagnetic waves. The EM-18 RFID Reader has an inbuilt antenna coil .When power is applied; the reader generates electromagnetic field which is induced by the antenna present inside the tag.

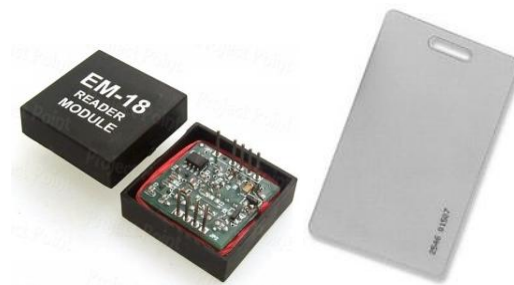


Figure2. RFID Module

3.1.4. GSM Modem

GSM module sends data via SMS to users (Parents/School Authorities). Global System for Mobile Communication (GSM) can be used to send and receive SMS or make/receive voice calls. GSM Modem is built with Dual Band GSM/GPRS engine. SIM900A, works on frequencies 900/ 1800 MHz. The baud rate can be configurable from 9600-115200 through Attention (AT) command. The GSM/GPRS Modem is having an internal TCP/IP stack which enables to connect it to the internet via GPRS. GSM module sends data via SMS to users. It establishes serial communication with the microcontroller. The Transmitter and Receiver pins of GSM modem are connected to the UART of the microcontroller.

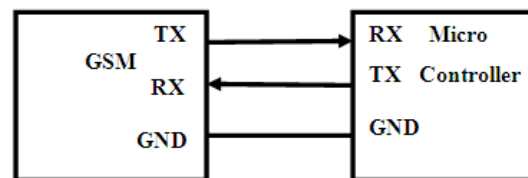


Figure3. Serial Communication between GSM modem and Microcontroller

3.1.5. GPS

Global Positioning System finds the location co-ordinates of the children where he/she boarded the bus and sends the data to the microcontroller. The GPS-634R is a smart GPS module integrated with a ceramic GPS patch antenna connected via an LNA (Low Noise Amplifier). The module consists of 51 channel acquisition engine and 14 channel track engine, which are capable of receiving signals from 65 GPS satellites. The precise information is transferred and can be read through UART port or RS232 serial port. It is provided with an interface connector for both the LVTTTL-level and RS232 signal interface with supply voltage is 3.6 - 6v DC. It supports the National Marine Electronics Association's (NMEA) 0183 protocol, as do many GPS modules. GPS module continuously sends the data to the microcontroller. The transmitter of GPS-634r is connected to the receiver of microcontroller. It establishes serial communication with the microcontroller.

3.1.6. MEMS Accelerometer

An accelerometer is an electro-mechanical device used for measuring the acceleration of a moving or vibrating body. The MMA7660FC is a 3-Axis digital output accelerometer and can be used for sensor data changes product orientation and gesture detection through and interrupt (INT). This accelerometer features programmable functions such as orientation, tap, and shake detection that provides embedded intelligence. It is a low profile capacitive MEMS sensor featuring a low pass filter with reduced power consumption, and it provides conversion to digital values at user configurable samples per second.

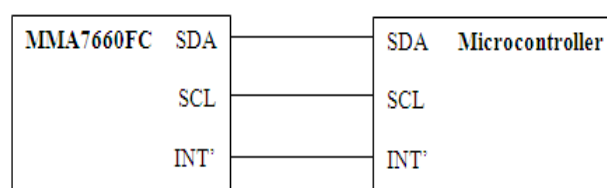


Figure4. I2C Communication between MEMS Accelerometer and Microcontroller

MEMS Accelerometer will detect and send information to the controller, if an accident occurs. It establishes I2C Communication to the controller i.e. the data line and clock line is connected to the microcontroller

4. RESULT

Figure 5 given below shows the entire setup of the system that includes microcontroller, RFID module, GSM modem, GPS module and MEMS Accelerometer



Figure5.Overall Setup of the System

The following figure 6 show the messages received by the parents and the school from the GSM of the bus unit. Messages include student boarding the bus, latitude and longitude of the bus current position and the time at which the child boarded the bus.

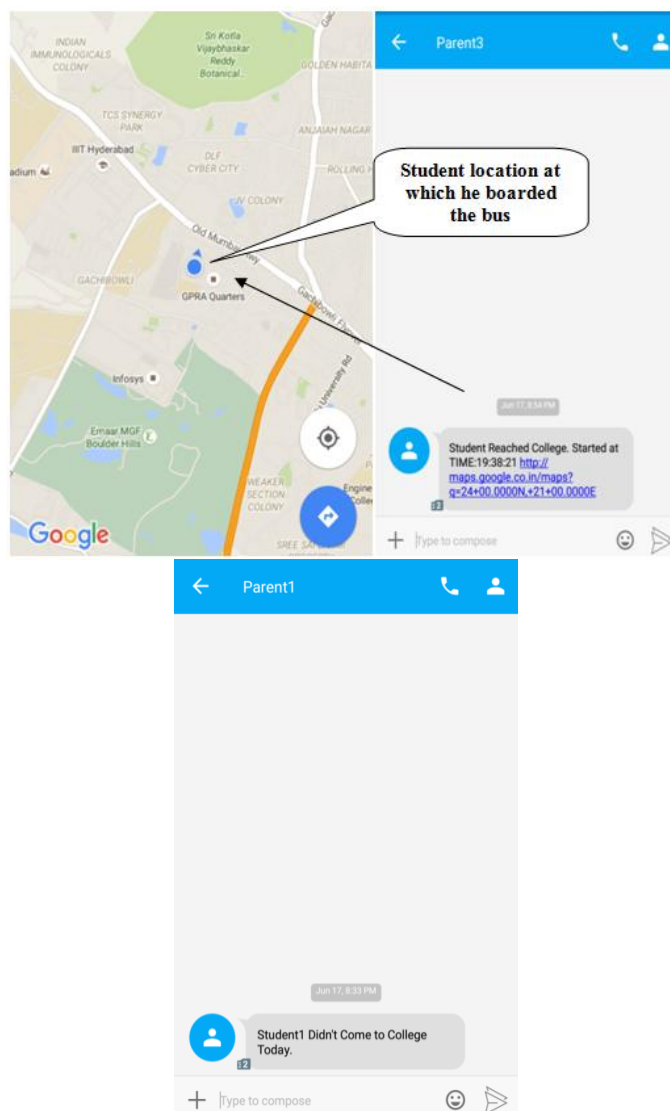


Figure6. Messages received by Parents

Figure 7 shows if an accident is occurred, a message will be sent to School authority along with the location at which the accident occurred.

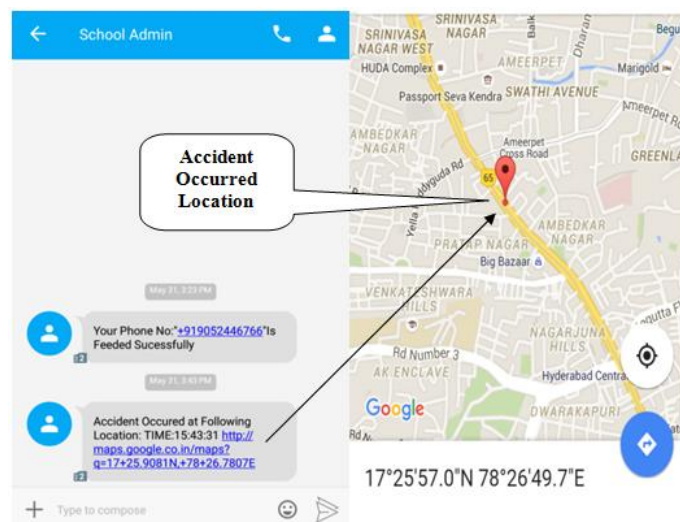


Figure7. Location of Accident Occurred

5. CONCLUSION

The system implemented to mainly ensures the safety of the children during daily transportation to/from the school. The system intimate parents and school authorities regarding the children i.e. the time and also the location of the student which is provided by the GPS Module, at which he/she boarded, via a GSM modem. The system detects which child did not board or leave the bus and issues an alert message accordingly. In addition, the system also detects if an accident occurs and a message is being issued. It is very important to ensure the safety of the children during the bus transportation and the system proposed to provide safety and secured information.

REFERENCES

- [1] K. Vidyasagar, G. balaji "RFID-GSM imparted school children security system" vol-2, number-2, June, 2015.
- [2] Ali-al Maharuqi, Dr. Jayavrinda vrindavanam "Bus safety for school children using RFID-and sim 900 GSM modem" vol- 5, 2015.
- [3] Anwar Ali-Lawati, Shaikha Al-Jahdhami, Asma Al-Belushi, Dalal Al-Adawi, Medhat Awadalla and Dawood Al-Abri, Department of Electrical and Computer Engineering, Sultan Qaboos University, "RFID BASED SYSTEM FOR SCHOOL CHILDREN TRANSPORTATION SAFETY ENHANCEMENT" proceedings of the 8th IEEE GCC Conference and Exhibition, Muscat, Oman. 1- 4 February, 2015
- [4] <https://alselectro.wordpress.com/2013/03/14/gps-receiver-modulepart-2/>
- [5] <http://www.alldatasheet.com/datasheet-pdf/pdf/432945/NXP/LPC1768.html>

AUTHORS' BIOGRAPHY



Kankelli Swapna Priya, Pursuing final Semester M.Tech in Embedded Systems at Malla Reddy Engineering College (Autonomous), Dhulapally, Secunderabad -500100, India

B.Tech: Electronics and Communication engineering from G.Narayanamma Institute of Technology and Science, shaikpet, Hyderabad.



N.Raju, Presently Working as Assistant Professor, Department of Electronics and Communication Engineering at Malla Reddy Engineering College (Autonomous)

M.E: Embedded Systems from CVR College of Engineering

B.E: Electronics and Communication Engineering from Mona College of Engineering and technology.

Low Cost Real Time Monitoring Using Raspberri

Mr.Kumaraswamy^{#1},Mamidi Dishalini^{*2}

[#]Assistant Professor in ECE Department,

Malla Reddy Engineering College (Autonomous), Jawaharlal Nehru Technological University, Hyderabad, India,

Kumaraswamy@mrec.ac.in

^{*}PG Scholar

Malla Reddy Engineering College (Autonomous), Jawaharlal Nehru Technological University, Hyderabad, India,

mamidi.dishalini@gmail.com

Abstract— Raspberry Pi which follows Motion Detection Sensor Program written in Python as a default. In addition, the system uses the PIR sensor to detect motion which significantly decrease storage and save investment. The motion detection is being implemented on Raspberry Pi. The streaming can be viewed from any web browser, even from mobile in real-time. By using PIR sensor we can reduce the memory storage, this allows the system to analyze incoming images from cameras, and recognize when movement occurs. Then automatically sends alert to our mobile through GSM. And then, the video system can collect the data using IP address and store the most importance items for the administrators review. Mainly it can be used for security purposes.

KEYWORDS: - Raspberri, PIR sensor, GSM (Global System for Mobile communications)

I. INTRODUCTION

Now a days we are facing many security issues .This system can overcome the security issue as well as storage issue. Raspberry Pi which follows Motion Detection Sensor Program written in Python as a default. In addition, the system uses the PIR sensor to detect motion which significantly decrease storage and save investment. The motion detection is being implemented on Raspberry Pi. It has been widely used in many fields like security, banking, and home. Regular video surveillance can generally achieve certain distance monitoring by using the PC as a monitor. But the Low Cost Real Time Monitoring system is introduced to overcome the week points of the Traditional video surveillance systems, such as expensive cost and Memory usage.

The proposed system is implemented using the tiny super computer called Raspberry Pi. Here we are using PIR sensor for Motion Detection which is used to save the memory as well. Instead of using the regular wireless CCTV surveillance cameras, customers can now go for inexpensive security systems with the Raspberry Pi.IP cameras can serve better as they can send and receive data via network and internet based on internet protocol. Also resolution clarity of IP cameras is better when compared with CCTV cameras.

II. METHODOLOGY

In this project we have used two main technologies.

- PIR Module
- GSM Module

A. PIR Module

A passive infrared sensor (PIR sensor)is an electronic sensor that measures infrared (IR) light radiating from objects in its field of view. PIR sensors used to detect the motion, almost always used to detect whether a human has moved in or out of the sensors range. PIRs are basically made of a pyroelectric sensor which can detect levels of infrared radiation. Everything emits some low level radiation, and the hotter something is, the more radiation is emitted. The sensor in a motion detector is actually split in two halves. The reason for that is that we are looking to detect motion not average IR levels. The two halves are wired up so that they cancel each other out. If one half sees more or less IR radiation than the other, the output will swing high or low.

The main reasons for choosing PIR Sensor is

- Can detect any motion object.
- They Consumes low power.
- Low Of Cost.
- Pretty Rugged.
- They have a wide lens range.
- They are easy to interface with.

B. GSM Module

In this project we have used GSM Module.GSM module sends data via SMS. Global System for Mobile Communication (GSM) can be used to send and receive SMS or make/receive voice calls. GSM Modem is built with Dual Band GSM/GPRS engine. The baud rate can be configurable from 9600-115200 through Attention (AT) command. The GSM/GPRS Modem is having an internal TCP/IP stack which enables to connect it to the internet via GPRS. GSM module sends data via SMS to users. It establishes serial communication with the microcontroller. The Transmitter and Receiver pins of GSM modem are connected to the UART of the microcontroller.

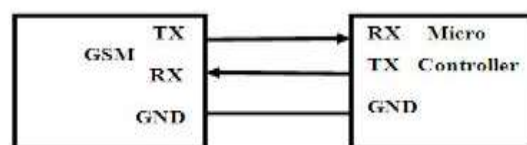


Figure1. Serial Communication between GSM modem and Microcontroller

III. BLOCK DIAGRAM OF THE SYSTEM

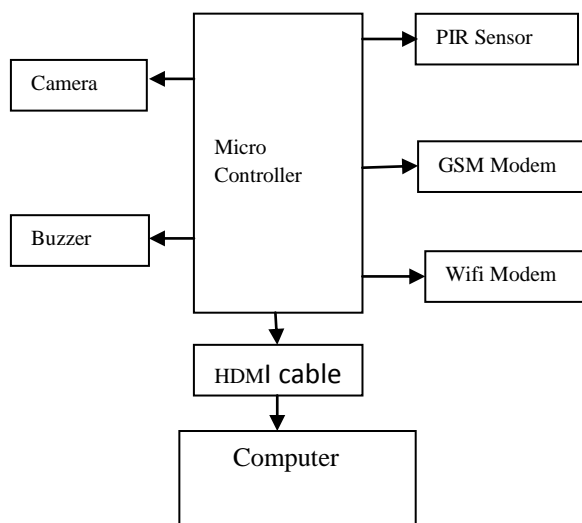


Figure 2. Block diagram of hardware

- **Raspberry Pi:** Raspberry pi is a tiny super computer capable of performing various functionalities.
- **GSM Modem:** GSM module sends data via SMS to user. GSM module sends sms alert through GSM network to anywhere in the world.
- **PIR SENSOR:** PIRs are basically made of a pyroelectric sensor which can detect levels of infrared radiation. Everything emits some low level radiation, and the hotter something is, the more radiation is emitted.
- **USB Camera:** USB Camera captures the image and sends it to the USB Port of the Raspberry Pi board.
- **BUZZER:** A Buzzer or beeper is an audio signaling device, which may be mechanic or electromechanical. Typical uses of buzzers and beepers include alarms and timers

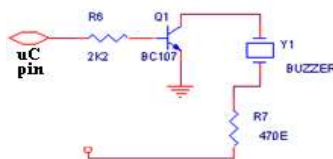


FIGURE3.Buzzer Schematic Diagram

IV. HARDWARE IMPLEMENTATION

- Power supply
- Keypad
- PIR Module

Power Supply: Power supply is an electronic circuit which is designed to allow a constant DC voltage.

Keypad: In this switch pad we have four switches which perform the negative logic i.e. as the switch is pressed the supply which is given will be grounded. And as the switch is open the supply passes through the resistor of 10k then it passes to the J2 microcontroller. The controller takes the i/p and performs the operation as per the program written in the controller.

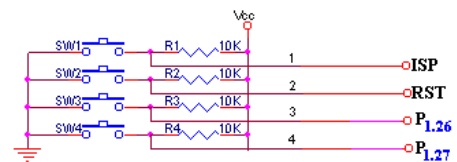


FIGURE4.Keypad schematic diagram

PIR SENSOR: A passive infrared sensor (PIR sensor) is an electronic sensor that measures infrared (IR) light radiating from objects in its field of view.

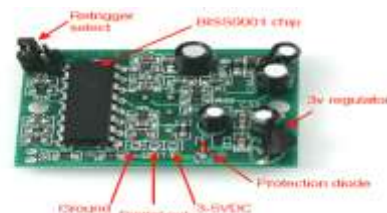


FIGURE5.PIR MODULE

V. RESULTS

Figure 3 shows entire hardware of the system which includes microcontroller, sensor, GSM module and required devices. In this system, Whenever the PIR sensor detects a motion, and then it will automatically capture the video and images. After that an alert will be sent to our mobile through GSM. By using certain IP address we can access the data from any device from anywhere.



Figure6.Overall setup of the system



Figure7.Result in the system

VI. CONCLUSION

In this paper, Motion Detection algorithm to decrease storage usage based on Raspberry Pi single board computer was proposed in this paper.

From this paper, I want to conclude that Low cost real time monitoring system is a secure system and will be used for security purposes. Due to the use of PIR sensor, the streaming will be done if it detects any object otherwise it will be in sleep mode which leads to the reduce of memory. We can get this at low of cost when compared to the other surveillance systems. Due to the use of buzzer and sms alert, we can be alert at anytime. It is mainly used to avoid the fitting and for security purposes at low of cost.

REFERENCES

- [1] Yong-ik Yoon, Jee-ae Chun, *Tracking System for mobile user Based on CCTV*. Information Networking (ICOIN), 2014 International Conferenceon, Phuket, 10-12 Feb. 2014, pp. 374-378.
- [2] Viren Pereira, Vandyk Amsdem Fernandes, Junieta Sequeira, *Low Cost Object Sorting Robotic Arm using Raspberry Pi*. Global Humanitarian Technology Conference - South Asia Satellite (GHTC-SAS), 2014 IEEE, Trivandrum, 26-27 Sept. 2014, pp. 1-6.
- [3] Yimamuaishan. Abudoulikemu, Yuanming Huang, Changqing, *A Scalable Intelligent Service Model for Video Surveillance System Based on RTCP*. Signal Processing Systems (ICSPS), 2010 2nd International Conference on (Volume:3), Dalian, 5-7 July 2010, V3-346 - V3-349.
- [4] C. Bahlmann, Y. Zhu, Y. Ramesh, M. Pellkofer, T. Koehle, *A system for traffic sign detection, tracking, and recognition using color, shape, and motion information*. IEEE Intelligent Vehicles Symposium, Proceedings, 2005, pp. 255-260.
- [5] Adrienne Heinrich, Dmitry Znamenskiy, Jelte Peter Vink, *Robust and Sensitive Video Motion Detection for Sleep Analysis*. Biomedical and Health Informatics, IEEE Journal of (Volume:18 , Issue: 3), 2168-2194, 20 September 2013, pp. 790-798.
- [6] www.google.com

DESIGN AND DEVELOPMENT OF ENERGY MONITORING AND AUTOMATED CONTROL SYSTEM USING LABVIEW FOR ENERGY CONSERVATION

V. MOUNIKA¹, T. RAVI THEJA²

¹V, Mounika, M.Tech Student, Malla Reddy Engineering College, Maisammaguda, Dhulapally, Hyderabad, Ranga Reddy Dist.,Telangana, India.

² Thota Ravi Theja, Asst.Professor, Malla Reddy Engineering College, Maisammaguda, Dhulapally, Hyderabad, Ranga Reddy Dist.,Telangana, India.

Abstract- The excess usage of energy in a building is identified and it is controlled and conserved using Laboratory Virtual Instrumentation Engineering Workbench. The unnecessary usage of energy for appliances in human absence is detected and the appliance is switched off, using ARM controller, embedded LPC2148, by continuous monitoring of appliance status. ACS712 is the power meter module capable of reading the power information as voltage.. The fan and light are automatically controlled by monitoring the human emplacement in the environment using the web cam. The human intervention information are traced,. The system modeled provides the efficient energy conservation strategy.

I. Introduction

Many home automation systems are considered mission-critical, in the sense that the malfunctioning can bring about catastrophic consequences in terms of loss of human life or property. Therefore extraordinary care must be exercised during their design to make them flawless. In spite of that, elaborate mechanisms are often deployed to ensure that any unforeseen circumstances can also be handled in a predictable manner. The motivation is mainly to facilitate the users to automate their Industrials having universal access. The system is based on wireless technology using GSM. This system provides ideal solution to the problems faced

by Industrialist in day to day life. GSM module is a bridge responsible for enabling/ disabling of SMS capability. The system is capable enough to send feedback to user about the condition of the home appliance according to the user's needs and requirements. The home appliances monitoring and control system with an affordable cost was thought to be built that should be mobile providing remote access to the appliances. The ease of deployment is due to wireless mode of communication. GSM technology provides the benefit that the system is accessible in remote areas as well. A prototype of the controller is implemented, and the experiment results show that the FPGA can easily and flexibly control the Industrial appliances. A processing unit that was microcontroller and a communication module that used GSM module or cell, phone. The ease of deployment is due to wireless mode of communication. GSM technology provides the benefit that the system is accessible in remote areas as well. The low cost remote monitoring system can be implemented using programmable logic devices (PLDs). PLDs allow fast development of prototypes and the design of complex hardware system using FPGA. The system contains low cost components easily available which cuts down the overall system cost. The technology and processes associated with manufacturing have undergone a major change during the last few decades for being able to compete

in today's economy, the time-to-market has to be reduced while at the same time, mass production with high quality standards is required. While these aspects are true for products in almost any domain, the notable ones are automotive and aerospace, having a high rate of production involving operations like cutting, shaping, molding, welding, polishing and assembly operations and in the large processing industries such as chemical industries, where time- or process critical and hazardous operations are involved. Thus, the demand for high production rate coupled with strict-quality norms can be achieved with less and less direct human interaction and an increasing degree of automation. A GSM, Internet and Speech Controlled Wireless Interactive Industrial Automation System [1] shows the design and realization of a Industrial automation system where communication technologies GSM (Global System for Mobile Communication), Internet, and speech recognition, Bluetooth have been used. All these techniques are successfully compound in a single wireless home automation system.

II. Hardware system

Micro controller: This section forms the control unit of the whole project. This section basically consists of a Microcontroller with its associated circuitry like Crystal with capacitors, Reset circuitry, Pull up resistors (if needed) and so on. The Microcontroller forms the heart of the project because it controls the devices being interfaced and communicates with the devices according to the program being written.

ARM7TDMI: ARM is the abbreviation of Advanced RISC Machines, it is the name of a class of processors, and is the name of a kind technology too. The RISC instruction set, and related decode

mechanism are much simpler than those of Complex Instruction Set Computer (CISC) designs.

Liquid-crystal display (LCD) is a flat panel display, electronic visual display that uses the light modulation properties of liquid crystals. Liquid crystals do not emit light directly. LCDs are available to display arbitrary images or fixed images which can be displayed or hidden, such as preset words, digits, and 7-segment displays as in a digital clock.

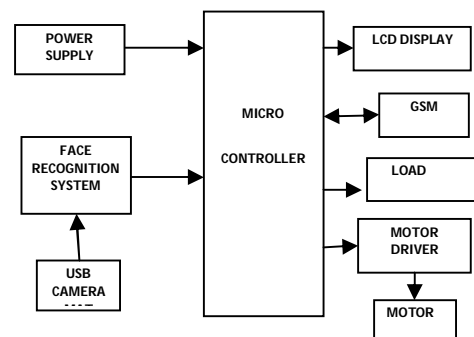


Fig 1: Block diagram

We can overcome above disadvantage by using our proposed system. It is having face recognition of person by using camera interface. We can overcome above disadvantage by using our proposed system. An efficient and accurate embedded access control system based on face recognition is very important for wide range of commercial and security application. The proposed system is a wireless access control system designed and developed for smart home environment. The system identifies the visitor's presence capture and transfers the identified name through an alert SMS via GSM network automatically to home owner to recognize the visitors. It has a variety of features such as energy efficient, intelligence, low cost, portability and high performance.

III. Board Hardware Features

GSM:

Global System for Mobile Communication (GSM) is a set of ETSI standards specifying the infrastructure for a digital cellular service.

The network is structured into a number of discrete sections:

- Base Station Subsystem – the base stations and their controllers explained
- Network and Switching Subsystem – the part of the network most similar to a fixed network, sometimes just called the "core network"
- GPRS Core Network – the optional part which allows packet-based Internet connections
- Operations support system (OSS) – network maintenance

SM was intended to be a secure wireless system. It has considered the user authentication using a pre-shared key and challenge-response, and over-the-air encryption. However, GSM is vulnerable to different class of attacks, each of them aiming a different part of the network.

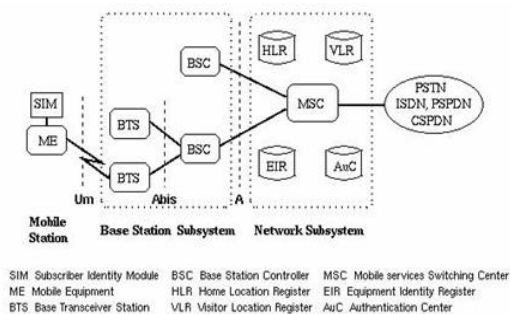


Fig 2: GSM architecture

DC Motor:

A DC motor relies on the fact that like magnet poles repels and unlike magnetic poles attracts each other. A coil of wire with a current running through it generates an electromagnetic field aligned with the center of the coil. By switching the current on or off in a coil its magnetic field can be switched on or off or by switching the direction of the current in the coil the direction of the generated magnetic field can be switched 180°.



Fig 3: DC Motor

Motor driver:

DC motors are typically controlled by using a transistor configuration called an "H-bridge". This consists of a minimum of four mechanical or solid-state switches, such as two NPN and two PNP transistors. One NPN and one PNP transistor are activated at a time. Both NPN and PNP transistors can be activated to cause a short across the motor terminals, which can be useful for slowing down the motor from the back EMF it creates. H-bridge. Sometimes called a "full bridge" the H-bridge is so named because it has four switching elements at the "corners" of the H and the motor forms the cross bar. The switches are turned on in pairs, either high left and lower right, or lower left and high right, but never both switches on the same "side" of the bridge. If both switches on one side of a bridge are turned on it creates a short circuit between the battery plus and battery minus terminals. If the bridge is sufficiently

powerful it will absorb that load and your batteries will simply drain quickly. Usually however the switches in question melt.

High Side Left	High Side Right	Low Side Left	Low Side Right	Quadrant Description
On	Off	Off	On	Forward Running
Off	On	On	Off	Backward Running
On	On	Off	Off	Braking
Off	Off	On	On	Braking

Table: operation of H-Bridge

WEBCAM

"Webcam" refers to the technology generally; the first part of the term ("web-") is often replaced with a word describing what can be viewed with the camera, such as a net cam or street cam. Webcams are video capturing devices connected to computers or computer networks, often using USB or, if they connect to networks, Ethernet or Wi-Fi. They are well-known for low manufacturing costs and flexible applications. **Video capture** is the process of converting an analog video signal—such as that produced by a video camera or DVD player—to digital form. The resulting digital data are referred to as a digital video stream, or more often, simply video stream. This is in contrast with screen casting, in which previously digitized video is captured while displayed on a digital monitor

Webcams typically include a lens, an image sensor, and some support electronics. Various lenses are available, the most common being a plastic lens that can be screwed in and out to set the camera's focus. Fixed focus lenses, which have no provision for adjustment, are also available. Image sensors can be CMOS or CCD, the former being dominant for low-cost cameras, but CCD cameras do not necessarily outperform CMOS-based cameras in the low cost price range. Consumer webcams are usually VGA resolution with a frame rate of 30 frames per second. Higher resolutions, in mega pixels, are available and higher frame rates are starting to appear.



Fig 4: Webcam

The video capture process involves several processing steps. First the analog video signal is digitized by an analog-to-digital converter to produce a raw, digital data stream. In the case of composite video, the luminance and chrominance are then separated. Next, the chrominance is demodulated to produce color difference video data. At this point, the data may be modified so as to adjust brightness, contrast, saturation and hue. Finally, the data is transformed by a color space converter to generate data in conformance with any of several color space standards, such as RGB and YCbCr. Together, these steps constituted video decoding, because they "decode" an analog video format such as NTSC or PAL.

Support electronics are present to read the image from the sensor and transmit it to the host computer. The camera pictured to the right, for example, uses a Sonix SN9C101 to transmit its image over USB. Some cameras - such as mobile phone cameras - use a CMOS sensor with supporting electronics.

FEATURES:

- Smallest wireless video & audio camera
- Wireless transmission and reception
- High sensitivity
- Easy installation & operation
- Easy to conceal
- Light weight
- Low power consumption
- Small size

SPECIFICATIONS:

- Output frequency: 900MHZ 1200MHZ
- Output power: 50mW 200mW
- Power supply: DC +6~12v
- Distance covered: 10m

IV. CONCLUSION

Energy Efficient Automation through central FPGA controller introduces design for home Automation using different task scheduling. In this paper, we propose home automation system which consists of face detection, GSM module and a controller module. Experiment results prove that this proposed system works well, and can be use for future application. There are many advantages of FPGA compared to microcontroller in terms of maximum no of input and output port which is present in FPGA. Using on board LCD display, it minimize wiring and power consumption And reduces use of driver circuit. The system is suitable for real time monitoring and controlling of various appliances.

V. REFERENCES

- [1] A.J. Dinusha Rathnayaka, Vidyasagar M. Potdar Samitha J. Kuruppu "Evaluation of Wireless Home Automation Technologies". 5th IEEE International Conference on Digital Ecosystems and Technologies (IEEE DEST 2011), Daejeon, Korea June 2011.
- [2] Bojan Mrazovac, Milan Z. Bjelica, D ragan Kukolj Branislav M. Todorovic "A Human Detection Method f or Residential Smart Energy Systems Based on Zigbee RSSI Changes", 2012.
- [3] Michael Angelo A. Pedrasa, Ted D. Spooner, Iain F. MacGill "Coordinated Scheduling of Residential Distributed Energy Resources to Optimize Smart Home Energy Services", IEEE TRANSACTIONS ON SMART GRID, VOL. 1, NO. 2, SEPTEMBER 2010.
- [4] Blerim Qela, Hussein T. Mouftah "Observe, Learn, and Adapt (OLA)—An Algorithm for Energy Management in Smart Homes Using Wireless Sensors and Artificial Intelligence", IEEE TRANSACTIONS ON SMART GRID, VOL. 3, NO. 4, DECEMBER 2012.
- [5] Zhanbo Xu, Qing-Shan Jia, Xiaohong Guan, Jiang Wu, Dai Wang, Siyun Chen "Optimal Scheduling of Storage Devices for Building Energy Saving", 10th World Congress on Intelligent Control and Automation, Beijing, China July 6-8, 2012.
- [6] Kim Baraka, Marc Ghobril, Sami Malek, Rouwaida Kanj, Ayman Kayssi, "Low cost Arduino/Android-based Energy-Efficient Home Automation System with Smart Task Scheduling", Fifth International Conference on Computational Intelligence, Communication Systems and Networks, 2013.

- [7] Jaime Caffarel, Guillermo Del Campo-Jimenez, Jorge M. Perandones, César Gomez-Otero, Rocio Martínez and Asunción Santamaría, “Open Multi-Technology Building Energy Management System” 2012.
- [8] Mao-Yung Weng, Chao-Lin Wu, Ching-Hu Lu, Hui-Wen Yeh, and Li-Chen Fu “Context-aware Home Energy Saving based on Energy-Prone Context”, 2012 IEEE/RSJ International Conference on Intelligent Robots and Systems Vilamoura, October 7-12, 2012.
- [9] Mansour Saber, Wiest Nicolas, Lefevre Olivier, Mazac Sebastien Ubiant, “Hemis: Hybrid Multi-agent architecture for energy management and home automation” 2012.
- [10] Dhiren Tejani, Ali Mohammed A. H. Al-Kuwari, Vidyasagar Potdar, “Energy Conservation in a Smart Home” Daejeon, Korea 31 May -3 June 2011.

PIBOT: Surveillance & Live Streaming System using Raspberry Pi

R.KARAN KUMAR¹, RAJU.N²

M. Tech (ES), Department ECE from MREC (A), Hyderabad, Telangana, India¹

Assistant Professor, Department ECE from MREC (A), Hyderabad, Telangana, India²

Abstract— In the present world, everyone is worried about their safety due to increase in crime rate. This has led to an increase in the importance of a surveillance system. A system is designed for continuous monitoring and also the system provides live streaming. The system can be deployed at the anyplace i.e. office, house and some remote place where people cannot monitor the particular place. The system acts like a Robot within a local area network through Wi-Fi technology using Raspberry pi 2 model B. The live streaming is accomplished by using a webcam interfaced with raspberry Pi, it data provided is processed by MJPEG (Motion Joint Photographic Experts Group) streamer and the robot is controlled through webpage's created. The system is programmed using python programming language.

Keywords— Surveillance, Pibot, Raspberry-pi, mjpeg streamer

I. INTRODUCTION

As the growth rate of crime has been increased in past years, as a result, everyone is concerned about their safety and security. Due to this reason, people started to consider the significance of surveillance systems. The majority of the people are doing Internet Protocol (IP) based installations rather than analog because of IP-based installations are from anywhere. In order to make the IP-based systems affordable for the people having a low budget, we need to develop a system which is cost effective and portable. This paper describes the system which acts as a robot. This robot uses raspberry pi model 'B' for making this real-time surveillance possible by providing the installing and processing high resource software's which makes it possible to live streaming & controlling the robot.

II. EXISTING SYSTEMS

Smart Security Camera using Raspberry pi and OpenCV is a system constructed for surveillance and it is designed to be used inside a warehouse facility. This system is devised using a low-cost security camera with night vision capability using a raspberry pi. This system is having the ability of human detection and smoke detection that can be used to avoid potential crimes and potential fire. The researchers evolved a light-footed surveillance camera that has the potential of identifying the condition of the scene that is being monitored and also gives notification or alarm as the event occurs This system also provides security during night time as it is having the potential to provide night vision. Night vision capability is attained by simply taking off infra-red (IR) filter from an ordinary webcam and thus can be used for night vision sensing with the help of IR Light Emitting Diode illuminator.

The system can also detect motion of an object using background subtraction algorithm. Once moving entity is diagnosed, the system can classify it as human or smoke. If smoke is detected, the system notify in the form of alarm and email to indicate fire or unauthorized person [2].

Multi-environment robot for surveillance and live streaming is developed to assemble real-time surveillance system possible within a local network. The live streaming is accomplished using mjpeg streamer and the server-client model is build using java. As IP-based installation provide access from anywhere and hence are preferred over the analogue system. IP-based systems offer superior picture quality and they are also favorable when it comes to scalability and flexibility. But IP-based system needs some knowledge about networking and these systems are too expensive than the analog ones. This raspberry pi controlled robot is incorporated by a server-client model. This client-server model is constructed on java and thus can work on any systems such as windows, Mac or Linux. This entire model is connected to a local network and anyone available in that particular local network can control it from anywhere. The live streaming is done by MJPG streamer [3].

III. PROPOSED SYSTEM

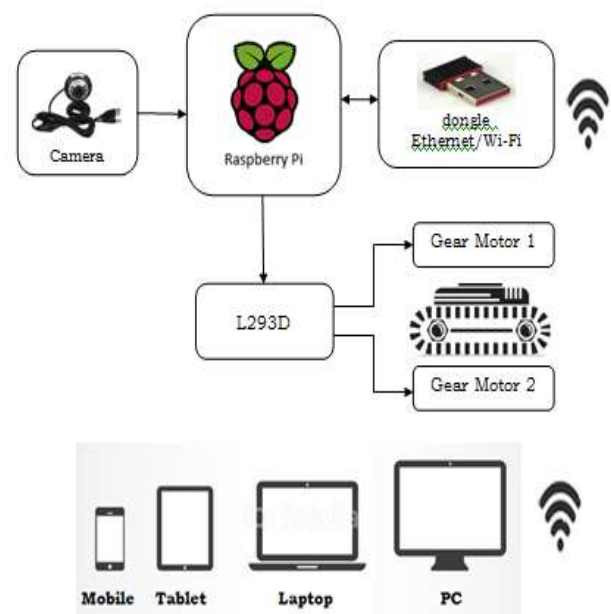


Fig 3.1 Block Diagram of Proposed System

We proposed a system to build a real-time live streaming and monitoring system using Raspberry pi with installed wifi connectivity. In monitoring phase, the pi will record the video of the location in real-time. Capturing video is done through commands given through the computer to the raspberry pi. This command will be communicated to the pi using Wi-Fi. The pi camera is being used which will give a very good quality of the picture in the video.

The connection of Raspberry pi with the motor driver is done using the General Purpose Input Output (GPIO) pins of Raspberry Pi. The GPIO pins are connected to the input pins of the motor shield. The output pins of the motor shield are connected to the motors. A portable charger of 2 amp current is connected to the motor shield and raspberry pi. Once the connections are done properly the raspberry pi is ready to boot up. A Python program is written for controlling the motors wherein the GPIO pins will give out the output from the raspberry pi to the motor shield. The robot movement is controlled through the directions mentioned on the web page created using HyperText Markup Language (HTML) code and webpage Universal Resource Locator (URL) address. This process is communicated through Wi-Fi to the Raspberry Pi model B. The camera module is installed into its port and it is enabled in raspberry pi settings. For the Live Streaming of videos, MJPEG streamer is installed and configured. After the configuration steps are done just view the live streaming in the app as well as the website. The website has been developed to allow a large number of people to experience the live streaming irrespective of their location. Here admin rights are given to authenticate the visibility of critical information by only authentic users.

Raspberry Pi: Raspberry Pi 2 model B is the main control board, which will do the majority of the operations. The camera module sends the images to it. A Wi-Fi router is used for communication between data transmission and receiving. The DC motors are attached to the wheels and are controlled through the General Purpose Input Output (GPIOs) Pins of Raspberry Pi via the Wi-Fi network. The Pi will send out signals to the microcontroller for control of the motors required for the robot. The Raspberry Pi 2 packs a 900MHz Broadcom BCM2836 ARMv7 quad-core processor, 1GB of RAM, support for up to four USB devices, HDMI support and micro SD port. The board also features an increase in memory capacity to 1Gbyte. The 40-pin GPIO enables multiple sensors, connectors, and expansion boards to be added, with the first 26 pins identical to the Model A and B boards, for full backward compatibility.



Fig 3.2 Raspberry Pi 2 Model 2 Board

DC Motor Driver

L293D is a dual H-bridge motor driver integrated circuit (IC). Motor drivers act as current amplifiers as they take a low-current control signal and provide a high current signal.

This high current signal is used to drive the motors. L293D contains two inbuilt H-bridge driver circuits used to drive the motors. The DC motors can be driven simultaneously i.e. Both Forward or backward direction in its common mode of operation. The motors are controlled by input logics 2 & 7 and 10 & 15 pins. Enable pins must be high for motors to start operating. When enable input is high, the associated driver gets enabled.



Fig 3.3 L293D H-Bridge motor Driver IC

Motors

Motors are required for its motion and mobility of the robot. The motors are interfaced to raspberry pi through drivers because the output ports of the microcontroller cannot source the required amount of current. The Motors are complete motive force systems consisting of an electric motor and a reduction gear train integrated into one easy-to-mount and easy to configure. This greatly reduces the complexity and cost of designing and constructing power tools, machines and appliances calling for high torque at relatively low shaft speed or Rotations Per Minute (RPM).



Fig 3.4 Motor to drive the robot

USB CAMERA

The camera board is a small PCB that connects to the CSI-2 camera port on the Raspberry Pi using a short ribbon cable. It provides connectivity for a camera capable of capturing still images or video recordings. The camera connects to the Image System Pipeline (ISP) in the Raspberry Pi's System On Chip (SoC), where the incoming camera data is processed and eventually converted to an image or video on the SD CARD.



Fig 3.5 Camera for Capturing Pictures/Live streaming

SD Card

The Raspberry Pi 2 Model B (second generation) require the smallest one, the MicroSD. SD cards come in a range of storage sizes. Generally, micro SD card we require is more than 2GB.

Wi-Fi Router

A Wi-Fi adapter will probably need more power than the Raspberry Pi USB port can provide, especially if there is a large distance from the Wi-Fi adapter to the Wi-Fi Access Point, or it is transferring large amounts of data. Therefore, you may need to plug the Wi-Fi adapter into a powered USB hub.

Key Features

- 802.11b/g/Draft-N compatible
- High-efficiency antenna that expands the scope of your wireless network
- Supports major encryption methods like WEP, WPA, and WPA2 encryption
- USB 2.0 interface for easy installation.
- Wireless access control - prevent unauthorized network access to your network and computer

The system designed has advantages and disadvantages and these are as follows:

PROS:

- The System is useful for the organization where they can't afford the costly surveillance systems
- Can occupy the wide area for surveillance i.e.; whole auditorium or big hall
- It has all utilities and software's required for live streaming and surveillance so that the user can use it without any hesitation or fear that they might not be able to control it

CONS:

- Separate Wi-Fi adapter has to be connected
- Only one location would be under surveillance at a time
- For configuring the robot user has to go to the system every time
- Not compatible with Windows operating system

IV. RESULTS

The system has been implemented and the following results have been observed.

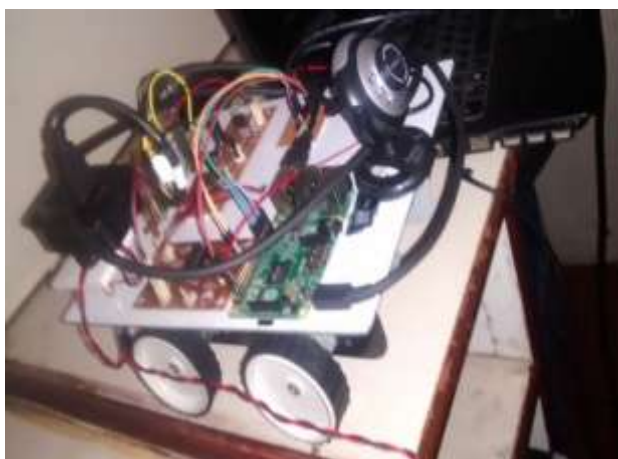


Fig 5.1 Overview of PIBOT

The pibot is controlled and monitored using the webpage's designed. The HTML page created provides the user for controlling the robot and also the live streaming.



Fig 5.2. HTML page for Robot Controlling

If the user selects for the robot controlling, the page is directed to another page which provides controlling of the robot.



Fig 5.3. Controlling of Robot through HTML Page

For live streaming the user should select the live streaming option, the live streaming is monitored through the HTML page designed.



Fig 5.4. Live Streaming

V. CONCLUSION AND FUTURE SCOPE

The system designed mainly aims at monitoring and surveillance at sensitive areas or unreachable areas. It will be helpful for the user who need surveillance of any place and this system provides the best results with low cost of deployment. This paper can be extended further by making the robot accessible via the internet. If user wants to use the location, they can use mapping algorithms to make it map the complete environment and then move autonomously after a certain periodic intervals to check everything. Also by giving it the ability to detect and recognize faces it can be made to alert us about any unknown person and take a snap of it and email us the same.

REFERENCES

- [1]. Charles Severance, "Eben Upton: Raspberry Pi", Published by IEEE computer society, October 2013
- [2]. Ikhankar, R.; Kuthe, V.; Ulabhaje, S.; Balpande, S.; Dhadwe, M., "Pibot: The raspberry pi controlled multi-environment robot for surveillance & live streaming," in *Industrial Instrumentation and Control (ICIC)*, 2015 International Conference on, vol. no., pp.1402-1405, 28-30 May 2015
- [3]. Michael Potmesil., "Generating octree models of 3D objects from their silhouettes in a sequence of images", in *Science direct Computer vision, graphics and image processing*, vol., no., pp.1-29 October 1987
- [4]. S Mukherjee and K. Das "A Novel Equation based Classifier for Detecting Human in Images", *International Journal of Computer Applications* (0975-8887), vol 72, no. 6, 2013
- [5]. https://en.wikipedia.org/wiki/Raspberry_Pi#Model_B
- [6]. <http://www.gizmojunkee.com/product/raspberry-pi-2-model-b-quadcore-1gb-ram-2/>

Authors Details



R. Karan Kumar, Pursuing final Semester M.Tech in Embedded Systems at Malla Reddy Engineering College (Autonomous), Dhulapally, Secunderabad -500100, India



N. Raju, Presently Working as Assistant Professor, Department of Electronics and Communication Engineering at Malla Reddy Engineering College (Autonomous).

Portable Camera-Based Assistive Text and Product Label Reading from Hand-Held Objects for Blind Persons

SHAIK MANSOOR BASHA¹, T. RAVI TEJA², S. RAJESH³

¹PG Scholar, Malla Reddy Engineering College, Maisammaguda, Dhulapally, Hyderabad, TS, India.

²Assistant Professor, Malla Reddy Engineering College, Maisammaguda, Dhulapally, Hyderabad, TS, India.

Abstract: We advise a camcorder-based assistive text studying framework to help blind persons read text labels and presentation from hands-held objects inside their lives. To isolate the item from cluttered backgrounds or other surrounding objects within the camera view, we first propose an efficient and effective motion based approach to define a place of curiosity (Roi) inside the video by asking the customer to shake the product. This method extracts moving object region having mixture-of-Gaussians-based background subtraction method. Inside the removed Roi, text localization and recognition are transported to get text information. To instantly localize the writing regions within the object Roi, we advise a manuscript text localization formula by learning gradient top features of stroke orientations and distributions of edge pixels inside an Adaboost model. Text figures inside the localized text regions is going to be binarized and recognized by off-the-shelf optical character recognition software. The recognized text codes are output to blind clients in speech. Performance in the recommended text localization formula is quantitatively evaluated on ICDAR-2003 and ICDAR-2011 Robust Studying Datasets. The proof-of-concept prototype can also be evaluated around the dataset collected using ten blind persons to judge the success in the system's hardware.

Keywords: Assistive Products, Blindness, Distribution of Edge Pixels, Hands-Held Objects.

I. INTRODUCTION

The dots per inch are keeps growing rapidly as the baby boomer generation ages. Recent developments in computer vision, camera models, and laptop systems ensure it is achievable to help these folks by developing camera-based items that combine computer vision technology as well as other existing commercial products such optical character recognition (OCR) systems. You'll find handful of items that may provide use of common hands-held objects for instance product packages, and objects printed with text for instance prescription medicine bottles. Ale individuals who're blind and also have significant visual impairments to determine printed labels and product packages will enhance independent living and promote social and economic self-sufficiency. Today, finances a couple of systems that have some promise for portable use, nonetheless they cannot

handle product labeling. Some studying-assistive systems for instance pen scanning devices might operate in these and other situations. Such systems integrate OCR software to own reason for checking and recognition of text along with a couple of have integrated voice output. However, scalping methods are often produced for and work most effectively with document images with simple backgrounds, standard fonts, just a little choice of font dimensions, and well-organized figures instead of commercial product boxes with multiple decorative designs. Numerous portable studying assistants are actually designed particularly for your visually impaired.

KReader Mobile works on the cell phone and enables the customer to determine mail, receipts, booklets, and a lot of other documents. Additionally, KReader Mobile precisely reads black print around the white-colored-colored background, but has problems recognizing colored text or text around the colored background. It cannot read text with complex backgrounds, text printed on cylinders with warped or incomplete images. Additionally, scalping strategies need a blind user to manually localize parts of interest and text regions round the objects. To assist blind persons to determine text from these kinds of hands-held objects, we've produced from the camera-based assistive text studying framework to trace the product of curiosity within the camera view and extract print text information within the object. Our suggested formula can effectively handle complex background multiple designs, and extract text information from both of your hands-held objects and nearby signs, objects and nearby signs. We approach the problem gradually. To make sure both your hands-held object appears inside the camera view, we utilize a camera with sufficiently wide position to support customers with simply approximate goal. This may frequently result in other text objects turning up inside the camera's view.

To extract both your hands-held object from you image, we produce a motion-based approach to acquire a region of curiosity (Roi) in the object. Then, we perform text recognition only in this particular Roi. It is a challenging problem to right away localize objects and text ROIs from taken images with complex backgrounds, fonts, and colors. For that text orientations, this paper assumes that text strings

in scene images keep roughly horizontal alignment. Many calculations happen to be created for localization of text regions in scene images. We divide them into two groups: rule-based and learning-based. Rule-based computations apply pixel-level image processing to extract text information from predefined text designs for example character size, aspect ratio, edge density, character structure, color uniformity of text string, etc. Whereas learning-based text classifier training, which define novel feature maps based on stroke orientations and edge distributions. These, consequently, generate representative and discriminative text features to distinguish text figures from background outliers.

II. FRAMEWORK AND ALGORITHM OVERVIEW

This paper presents a prototype system of assistive text studying. The device framework includes three functional components: scene capture, human resources, and audio output. The scene capture component collects moments that contains objects of curiosity by way of images or video. Inside our prototype, it matches a camcorder installed on a set of shades. The human resources component can be used as implementing our recommended computations, The audio output component is always to inform the blind user of recognized text codes. A Bluetooth earpiece with minimicro phone is helpful for speech output. Our primary contributions embodied in this particular prototype system are : 1) a manuscript motion-based formula to solve the striving problem for blind clients by their simply shaking the product of great interest for a while 2) a manuscript formula of automatic text localization to extract text regions from complex background multiple text designs and three) a conveyable camera-based assistive framework to help blind persons studying text from hands-held objects.

III. AUTOMATIC TEXT EXTRACTION

We design a learning-based formula for automatic localization of text regions in image as shown in Fig.1. To have the ability to handle complex backgrounds, we advise two novel feature maps to extracts text features based on stroke orientations and edge distributions, correspondingly. Here, stroke is determined just like a uniform region with bounded width and significant textent. These feature maps are combined to create an Adaboost based text classifier.

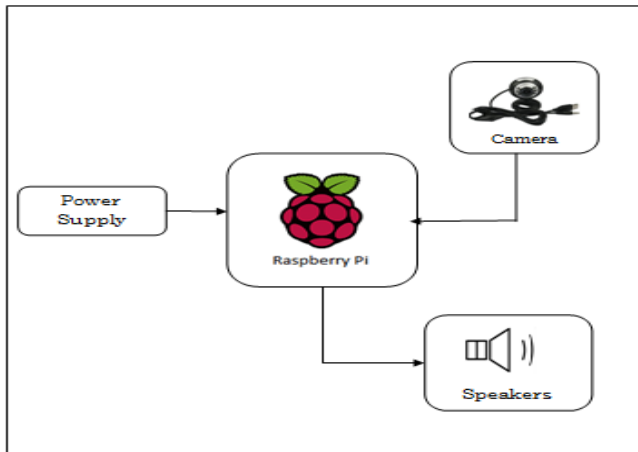


Fig.1. Proposed system Architecture.

IV. CONCLUSION

Within this paper, we've described a prototype system to see printed text on hands-held objects for aiding blind persons. To be able to solve the most popular striving problem for blind customers, we've suggested a motion-based approach to identify the object of interest, as the blind user simply shakes the item for a couple of seconds. To extract text regions from complex backgrounds, we've suggested a manuscript text localization formula based on models of stroke orientation and edge distributions.



Fig.2.HDMA and camera interface.

This process can effectively distinguish the object of great interest from background or any other objects within the camera view as shown in Fig.2. The corresponding feature maps estimate the worldwide structural feature of text at each pixel. Block designs project the suggested feature maps of the image patch right into a feature vector. Off-the-shelf OCR can be used to do word recognition around the localized text regions and transform into audio output for blind customers. Adjacent character grouping is carried out to calculate candidates of text patches prepared for text classification. An Adaboost learning model is employed to localize text in camera-based images.

V. REFERENCES

- [1] X. Chen and A. L. Yuille, "Detecting and reading text in natural scenes," in Proc. Comput. Vision Pattern Recognit., 2004, vol. 2, pp. II-366–II-373.
- [2] X. Yang, Y. Tian, C. Yi, and A. Arditi, "Context-based indoor object detection as an aid to blind persons accessing unfamiliar environments," in Proc. ACM Multimedia, 2010, pp. 1087–1090.
- [3] K. Kim, K. Jung, and J. Kim, "Texture-based approach for text detection in images using support vector machines and continuously adaptive mean shift algorithm," IEEE Trans. Pattern Anal. Mach. Intell., vol. 25, no. 12, pp. 1631–1639, Dec. 2003.
- [4] International Workshop on Camera-Based Document Analysis and Recognition (CBDAR 2005, 2007, 2009, 2011). [Online]. Available: <http://www.m.cs.osakafuu.ac.jp/cbdar2011/>

Portable Camera-Based Assistive Text and Product Label Reading from Hand-Held Objects for Blind Persons

[5] World Health Organization. (2009). 10 facts about blindness and visual impairment [Online]. Available: www.who.int/features/-/factfiles/blindness/blindness_facts/en/index.html.

Author's Profile:



Shaik Mansoor Basha, Pursuing final Semester M.Tech in Embedded Systems at Malla Reddy Engineering College (Autonomous), Dhulapally, Secunderabad -500100, India.



Thota Ravi Theja, Presently working as Assistant Professor, Department of Electronics & Communication Engineering at Malla Reddy Engineering College(Autonomous). Dhulapally, Secunderabad -500100, India.

Camera Based Eye Pupil Controlled Wheelchair System using Raspberry Pi

A. SRINIVAS¹, B. SRINIVAS²

¹PG Scholar, Dept of ECE, MREC(A), Hyderabad, TS, India, E-mail: anupuram.srinivas@gmail.com.

²Associate Professor, Dept of ECE, MREC(A), Hyderabad, TS, India, E-mail: srinivas499@gmail.com.

Abstract: The purpose of eye movement based control electric wheelchair system is to eliminate the requirements of the assistance required for the disabled person. The implemented system will be allowing the disabled persons to control the wheelchair movement without the assistance from other persons. In this system control of wheelchair carried out based on Eye pupil movements. The camera is mounted in front of the user, to capture the image of any one of the Eye pupil (either left or right) and tracks the position of eye pupil with the use of Image processing techniques. According to the position of the eye, wheelchair motor will be directed to move left, right and forward. In addition to this, for the safety purpose ultrasonic sensor is mounted in front of wheelchair to detect the obstacles and automatically stop the wheelchair movement.

Keywords: Image Processing, Open Computer Vision Library, Python, Raspberry Pi, Wheelchair.

I. INTRODUCTION

The Motorized wheel chair depends upon system utilized by seniors and physical disable persons. Here presenting the design implementation types of totally independent Eye control electric motorized wheel chair. According to dependence on the disabilities deferent type of automatic systems can be found in market. Sometime for totally paralysis person might be have tough to use that type of systems. Here the attention control system provides the independence to create their existence simple and easy, easier [1]. For that advance degree of Image Processing open computer vision (Open CV) library can be used for Face and Eye recognition [2]. And many application and calculations are utilized to find out accurate pupil location recognition and monitoring of this. One of them is Haar cascade like features recognition formula used to detects single or multiple face and recognition of both eye [3]. To discovering the precise Eye pupil and look for its centerpiece is ultimate objective of this technique. For instantly discover Eye pupil and monitoring eye pupil many computer vision library of Image processing are utilized like object recognition, motion detection, Image color conversion, edge recognition, pattern matching etc. One of these ECG, EEG and EOG sensor based eye pupil recognition strategy is available, where voltage variation based output assumed to determine the place of pupil.

However for different user, different output current will be generates, resulting faulty location from the eye pupil. The mind movement based system has limitation, when user can unable to connect to the system physically. Furthermore, voice triggered power motorized wheel chair which works properly, when user speak the command system works according into it like left, right, forward, back, stop. However a noisy environment throws the machine and system cannot respond properly. Along with other infrared reflection based eye pupil detection system supplying accurate recognition from the eye pupil center location, in addition to system can track the attention movement. However the infrared radiations affected the attention and user may loss the eye visibility. Therefore, a highly effective camera captured image based eye pupil recognition and monitoring system is introduced. This really is efficient in addition to economical system. Here real time video image recording according to Face, Eye and Eye Pupil detection with minimum delay of your time can be used [2]. The system includes multistage that's mainly track the attention pupil center. The manuscript Eye monitoring technique, which capture the image and detects the presence of human face. After discovering the face, it detects part of the eye location evidently detected image, and performs several operation of fundamental image processing like colour image to gray conversion, filtering, threshold, pattern matching, noise reduction and circle recognition onto it.

The Raspberry pi board can be used to do the charge of the complete system operation. Digital Image processing based output signal delivered to the Raspberry pi board. The Raspberry pi acquired the information and analyses it. Raspberry pi send the control signal to motor driving circuit in line with the location of eye pupil. This can choose to perform operation on motor like run the motor in clock voice direction, anti-clock voice direction and steer clear of the motor. Inside a Motorized wheel chair two individual motors are embedded on every wheel. The Ultrasound sensor is also mounted around the motorized wheel chair for recognition associated with a static or mobile obstacle. If sensor will get the obstacle not far from the wheel chair, it'll indicate towards the raspberry pi and raspberry sends the signal to motor driving circuit to prevent the motor.

II. SYSTEM DESIGN MODEL

This technique is completely autonomous system, and all sorts of the module works independent one another. For that basic requirement from the any electronic product is Power.

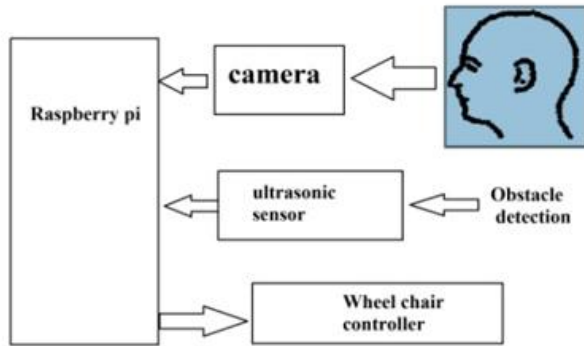


Fig.1. Complete System Framework

In this system there's mandatory to offers the proper power supply to individual components, as well as the standard power supply needs to be useful for Raspberry pi, camera, sensor, and motors. An authentic time data acquisition and analyzing the signal Raspberry pi B model board is very efficiently process the multiple image frames by frame. For recording the image normal web camera may be used inside our system. In addition, High resolution HD web camera can be utilized. The Raspberry gives the commands for the motor driver circuit, that's enable the GPIO pin to complete operation. For instance forward, left, right and stop operation transported out based on eye actions. Sensors may also be placed on your brain of mobility device for detecting the obstacles and adjusting the mobility device. Ultrasound examination sensor can be used as finding the obstacle or any moving object before mobility device. The sensor is directly connected for the Raspberry pi board, it acquired the data and measuring the area between mobility device and obstacle. A completely new image processing technique useful for eye pupil center detection and monitoring, which inserts based on open computer vision (Open CV) library. For hooking up the raspberry pi board to desktop Putty software packages are used. Python language may be used for coding, that's simple to use and helpful to resolve the error efficiently. Open CV 3. library with python may be used in this system.

III. METHODOLOGY

The key of the product is eye pupil recognition and eye tracking according to computer vision technology. A new algorithm introduced for discovering the attention pupil location by Image processing. Within this technique several stages accustomed to find out the movement of eye, for example Face recognition and Eye detection, color conversion, Edge recognition, Hough Transformed, motion recognition and object monitoring. First camera module will begin to capture the pictures. For the face recognition Haar cascade formula can be used. After detection of a good face, it'll attempting to identify the attention inside the face region of great interest. And again Haar cascade algorithm is used like as face recognition to identify eye. It'll draw the

rectangular box within the Eye. Now, the primary target is to detects the attention pupil and define its center points. There is several image processing operation carried out in system, such as blur Image, color conversion, thresholding, filtering, edge detection and Hough transform can be used. For circle detection Hough transform technique is used. Using the USB webcam allowed to capture the pictures on raspberry. And Image Processing based all Open CV library are set up in raspberry pi memory. There it'll process and dealing without any processing delay. The machine will crop the attention region of great interest initially will detects all possible circle presented with that particular area. Of computer will effectively detect the attention ball. After that corner recognition method we requested eyes region of great interest, and discover the corners. Where average of both two pointed fined its Centerpiece.

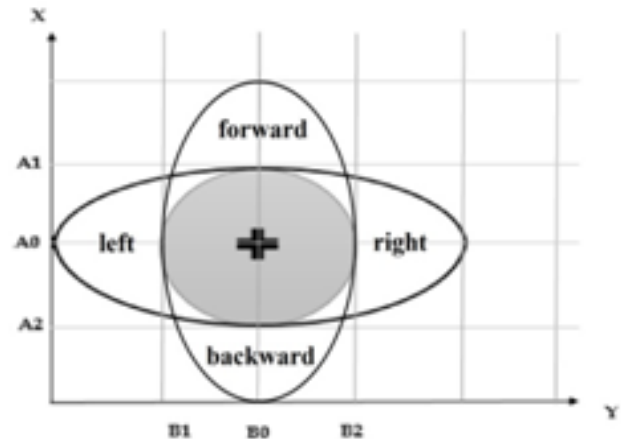


Fig.2. Eye Pupil Movements.



Fig.3. Wheel Chair System.

Now we measure distance between he Centerpiece and eye circle Centerpiece using coordinates system logic. Based on the eye pupil actions, distance will be vary. The absolute minimum distance signifies the attention pupil presented in left, and maximum values signifies the eye moved on right. And when there are no actions from the eye, than it concludes eye is incorporated in the middle position. Than the commands requested all operation, when eye movement is left, a motorized wheel chair left

Camera Based Eye Pupil Controlled Wheelchair System using Raspberry Pi

side motor will run. So when the eye moved is appropriate the best side motor ought to be moved. If eye will maintain Center both motor moved, and motorized wheel chair relocating forward direction. For stop and start operation of wheel chair actions for eye blinking logic applied. If eye closed for several sec. a method completely stops and when again it will close the attention for several sec, system reactivated. A method began with recording images continuously by camera. And taken images processed in Raspbian system.USB camera can be used to capture the look at high pixel rates. In idle condition the attention is going to be considering open. Once the power provided is on, the machine will begin working, and according towards the command values system will labored.

IV. CONCLUSION

The aim of applying an autonomous eye controlled wheel chair is to focus on the characteristics of digital Image processing. The idea of the attention controlled motorized wheel chair isn't only represents the choice sources but more essential to help physically disabled persons to create their existence independent. There are some real-time design constants measured just like a system takes a while (4second) to complete the machine for processing the video instantly Atmosphere. And so the system performs the Motorized wheel chair movement operation with a few delay time. It's very difficult to track the attention pupil in dark light places, therefore the system works perfect on ecological light as well as in a room light with fluorescent mercury vapor lights, which is low in infrared.

V. REFERENCES

- [1]Automation of wheelchair using ultrasonic and body kinematics,PreethikaBritto, Indumathi. J, SudeshSivasasu, Lazar Mathew,CSIO Chandigarh, INDIA, 19-20 March 2010.
- [2]Sarangi, P., Grassi, V., Kumar, V., Okamoto, J.:”IntegratingHuman Input with autonomous behaviours on an IntelligentWheelchair Platform”, *Journal of IEEE Intelligent System*, 22,2, 33-41, [2007].
- [3]Eye Controlled Wheel Chair Using EOG, Alex Dev, Horizon CChacko and Roshan Varghese, *International Conference onComputing and Control Engineering (ICCCCE 2012)*, 12 & 13April, 2012.
- [4]Eyeball and Blink Controlled Robot with Fuzzy Logic BasedObstacle Avoidance System for Disabled K.S.Sabarish,A.M.Suman, (*ICEEE'2012*) June 16-17, 2012, Bangkok.

Author's Profile:



A Srinivas, Pursuing final semester M.Tech in Embedded systems at Mallareddy Engineering College (Autonomous), Dhulapally, Secunderabad-500100,India.



B Srinivas, Presently working as Associate professor, Department of ECE at Mallareddy Engineering College (Autonomous), Dhulapally, Secunderabad-500100, India.

Tweeting PI an Household Computerization

SAI KUMAR PYDI¹, SRINIVAS BOLLINENI²

¹PG Scholar, Dept of ECE, MREC(A), Hyderabad, TS, India, E-mail: saikumarpydi1676@gmail.com.

²Associate Professor, Dept of ECE, MREC(A), Hyderabad, TS, India, E-mail: srinivas499@gmail.com.

Abstract: In the recent times, of advanced technology, everything that is used is automatic. There are efficient household devices as well as technologies that are being developed thus automation as well as technology together, if resourceful, can be a huge contribution. We focus on key of power which is a method for controlling of automated devices which are functional to resourceful process that magnifies the efficiency. We suggest usage of Raspberry pi for receiving of messages from user twitter account across Internet for controlling of household appliances. Home automation that is implemented by means of Raspberry pi is consistent as well as strong. The algorithm that is implemented within the pi listens to request as well as sends acknowledgement towards user instinctively based on content of message that are received. For exhibition light-emitting diode were used, that shows circuitry is realistic as well as consistent.

Keywords: Automated Devices, Light-Emitting Diode, Internet, Twitter Account, Household Appliances, Raspberry Pi.

I. INTRODUCTION

Our daily lives are becoming so fast that requirement for automatic voice control within cars has turn into a requirement. Regardless of how automated machines are, some type of control is required in support of decision of when they need to be switched on or else switched off. While machines are relatively resourceful, man holds key towards powerhouse and, in reality it's extremely flattering to consider in this way [1]. Our work focus on key of power which is a method for controlling of automated devices. Automation which is applied to resourceful process magnifies the efficiency. There are well-organized household devices and the technologies which are being developed in the entire world. Hence automation as well as technology together, if resourceful, can be a huge contribution. Because, it would denote more freedom, more occasions in hands that are used for useful task and simultaneously automation is done the means that is simple and by means of a method which is preferred by everybody. In our work an additional feature was added in Social Media that is twitter as shown in Fig.1. The usage of Twitter later adds to simplicity of control and increases security and the important benefit in this case, is simplicity within usage and increases user responsiveness [2]. This paper deals with the system of household computerization that is installed by means of Raspberry Pi. The system is developed with twitter, which is an online

social network that is used for sending of direct-messages towards raspberry pi which performs a task accordingly by examining the messages.

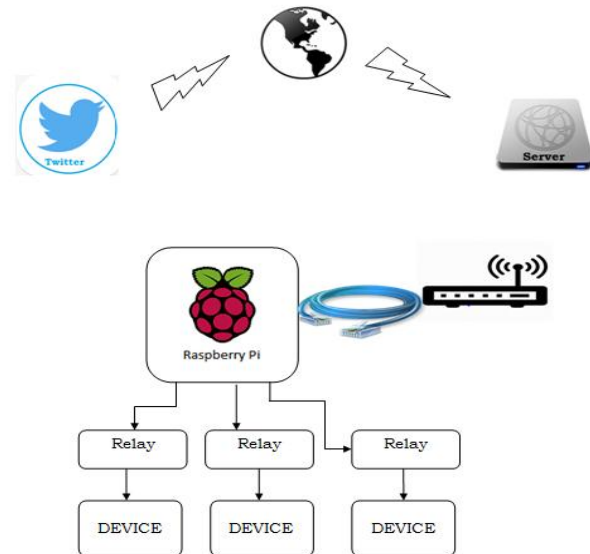


Fig.1. Proposed system configuration.

II. METHODOLOGY

Raspberry pi model B+ is a variant which has better specs like improved General-purpose input/output pins, additional Universal Serial Bus slots as well as micro Secure Digital and this representation is more flexible by means of decreased power expenditure. Our work suggests usage of Raspberry pi for receiving of messages from user twitter account across Internet for controlling of household appliances. RaspberryPi is credit card sized microcomputer which contains unimaginable applications and it can be exploited based on the needs of an individual. The algorithm that is implemented within the pi listens to request as well as sends acknowledgement towards user instinctively based on content of message that are received. For exhibition light-emitting diode were used, that shows circuitry is realistic as well as consistent. Our work adds an additional feature in Social Media that is twitter. In the times of social media as well as gadgets, automating devices by means of a social network is going viral. The extraordinary opportunities to improve relatedness of gadgets inward native for reason of household automation above Internet are thus far be studied. The system configuration includes gadgets that are associated across relay driver towards

Raspberry pi [3]. The relay is employed to turn on as well as off devices by means of a low voltage circuit and pi functions as an interface among devices as well as Internet. The component of Modulator Demodulator (MODEM) assists to obtain requests from user as well as reply accordingly by means of python algorithm implemented within pi. The layout of the projected configuration of system was ripened however this methodology is primitive. Sriskanthan et al. has popularized the system of home automation which makes usage of Bluetooth, understanding single elementary controller as well as multitude of Bluetooth sub-controllers. AI-Ali et al has refined the system of home automation by means of Java that provides an indestructible solution.

III. AN OVERVIEW OF PROPOSED SYSTEM

The system of home automation is developed. Initially a twitter account for 1308 Raspberry pi is formed and an application of twitter is created to use it for system. The algorithm is developed within python along by Twython which is package in support of usage of twitter facilities such as the status of updating, reading tweets, sending with receiving direct messages as shown in Fig.2. The program initially obtains permission to make use of twitter by means of submission of customer key, access token, customer secret as well as access token secret in support of twitter application [5]. The direct messages are employed rather than tweets in support of security then direct message from particular sender or else approved sender is perused and message which is received is analogized with predefined situations that are used to work gadgets associated to General-purpose input/output pins. These pins are used as an input pin or else an output pin hence General-purpose input/output pins are employed to turn on different gadgets. We spotlight on key of power which is a method for controlling of automated devices. Automation which is applied to resourceful process magnifies the efficiency. Our work uses Raspberry pi for receiving of messages from user twitter account across Internet for controlling of household appliances.

The algorithm within pi listens to request as well as sends acknowledgement towards user instinctively based on content of message that are received. For showing light-emitting diode, that shows circuitry is realistic as well as consistent. In the Raspberry PI General-purpose input/output pin layout, two pins are utilized to manage two gadgets. Light-emitting diodes are used as gadgets to determine practicability. The system configuration comprises of gadgets that are associated across relay driver towards Raspberry pi. The relay is employed to turn on as well as off devices by means of a low voltage circuit and pi functions as an interface among devices as well as Internet. The pins that are used are pin 12 as well as pin 38. The task of analogizing is replicated by means of time lapse of 1 second. The control structure of algorithm projected is programmed within python here, direct message that are received is stored up within an array message, and control arrangement is defined whence. When the direct message is engage gadget one, then raspberry sends direct message towards sender as gadget one is engaged and simultaneously gadget at pin38 is activated, following this it

loops back yet again checking for novel messages by means of a gap of one second.

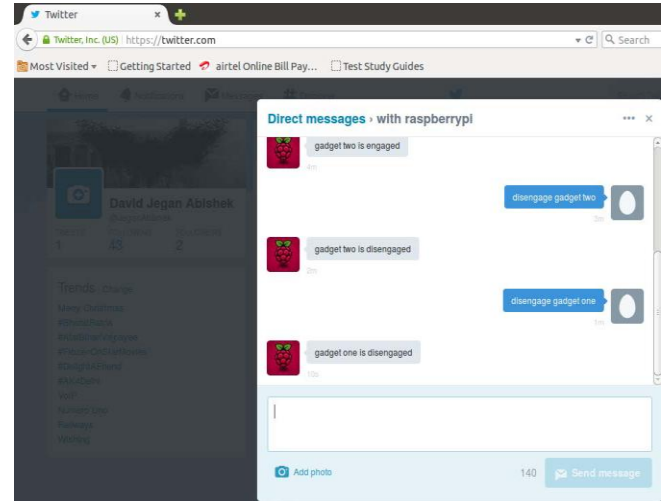


Fig.2. Screenshot of interaction among user as well as raspberry pi twitter account.

IV. CONCLUSION

In the times of social media as well as gadgets, automating devices by means of a social network is going viral. However the recent as well as remarkable opportunities to enhance the relatedness of gadgets inward native for reason of household automation above Internet are thus far be researched. We focus on key of power which is a method for controlling of automated devices. Automation which is applied to resourceful process magnifies the efficiency. Our work put forward usage of Raspberry pi for receiving of messages from user twitter account across Internet for controlling of household appliances. Raspberry pi is a safe bet in this age of technological development. The usage of Twitter later adds to simplicity of control and increases security. The important benefit in this case, is simplicity within usage and increases user responsiveness. The field is so far to be studied and has huge possibilities for additional investigation. The algorithm that is implemented within the pi listens to request as well as sends acknowledgement towards user instinctively based on content of message that are received. For showing light-emitting diode were used, that shows circuitry is realistic as well as consistent.

V. REFERENCES

- [1] Ardam H. and Coskun I., "A remote controller for home and office appliances by telephone", IEEE Transactions on Consumer Electronics, vol. 44, no. 4, pp. 1291-1297, 1998.
- [2] Baudel T. and Beaudouin-Lafon M., "Charade: remote control of objects using free-hand gestures", Communications of the ACM, vol. 36, no. 7, pp. 28-35, 1993.
- [3] Saito T., Tomoda I., Takabatake Y., Ami J. And Teramoto K., "Home Gateway Architecture And Its Implementation", IEEE International Conference on Consumer Electronics, pp. 194-195, 2000.
- [4] Sriskanthan N. Tan F. and Karande A. , "Bluetooth based home automation system", Microprocessors and

Tweeting PI an Household Computerization

Microsystems, Vol.26, no.6, pp.281-28, 2002, www.raspberrypi.org/jarchives/tag/raspberry-pi/user-guide

[5] Yoon D., Bae D., Ko H. and Kim H., "Implementation of Home Gateway and GUI for Control the Home Appliance", The 9th International Conference on Advanced Communication Technology, pp. 1583- 1586, 2007.

Author's Profile:



P Sai Kumar, Pursuing final semester M.Tech in Embedded systems at Mallareddy Engineering College (Autonomous), Dhulapally, Secunderabad-500100, India.



B Srinivas, Presently working as Associate Professor, Department of ECE at Mallareddy Engineering College (Autonomous), Dhulapally, Secunderabad-500100, India.

A Method of Detecting Abnormal Program Behavior on Embedded Devices

K. Ramya¹**P.Sowjanya²**¹ M.Tech (ES), Malla Reddy Engineering College (Autonomous), Hyderabad, India.² Associate Professor, Malla Reddy Engineering College (Autonomous), Hyderabad, India.

Abstract

A potential threat to embedded systems is the execution of unknown or malicious software capable of triggering harmful system behavior, aimed at theft of sensitive data or causing damage to the system. Commercial off-the-shelf embedded devices, such as embedded medical equipment, are more vulnerable as these types of products cannot be amended conventionally or have limited resources to implement protection mechanisms. In this paper, we present a self-organizing map (SOM)-based approach to enhance embedded system security by detecting abnormal program behavior. The proposed method extracts features derived from processor's program counter and cycles per instruction, and then utilizes the features to identify abnormal behavior using the SOM. Results achieved in our experiment show that the proposed method can identify unknown program behaviors not included in the training set with over 98.4% accuracy.

Index Terms— *Embedded system security, abnormal behavior detection, intrusion detection, self-organizing map.*

I.INTRODUCTION

The widespread use of embedded systems today has significantly changed the way we create, destroy, share, process and manage information. For instance, an embedded medical device often processes sensitive information or performs critical functions for multiple patients. Consequently, security of embedded systems is emerging as an important concern in embedded system design [1], [2]. Although security has been extensively explored in the context of general purpose

computing and communications systems, for example via cryptographic algorithms and security protocols [3], such security solutions usually are often incompatible with particular embedded architectures. The reason for this is, that embedded architectures use custom firmware or operating systems, and are normally specific to a certain function with limited cost and resource [4], which makes e.g. conventional antivirus (AV) programs difficult to implement. Generally, the protection of embedded systems can be developed either at hardware or/and at software level.

II.EXISTING SYSTEM

In existing system nodes sending information to target device will be common factor in industries but we don't know whether nodes sending correct information or garbage values or previous values immediately to rectify the situation. To overcome this problem we are implementing the proposed method.

III.PROPOSED SYSTEM

In this proposed method, we are using an advanced open source ARM32 bit microprocessor [6] which is having advanced features support to complete our task. In order to overcome the disadvantage in existing method we are implementing the concept to get the proper information about the status of the modules (Memory Unit and Nodes unit) whether active or inactive stages in runtime to take an immediate action. In general run time modules information up-gradation can be accessible in control panel. In case of runtime devices disconnection we will get an recently updated information or garbage information for the control

unit, where they need more response time to identify the updated info will proper or not. In order to reduce troubleshooting time on run time module issues this concept will provide a solution. Nodes unit data will be store on memory unit for any accuracy comparison between time period and the total data will be updated lively on web server through IP (Internet Protocol) Address. In this paper Temperature, Gas and LDR sensors are connected to Nodes unit of the Raspberry pi board. These sensors data will be store on memory unit for any accuracy comparison between time period and the total data will be updated lively on web server through IP (Internet Protocol) Address. If any sensor disconnected we will get recently updated information or garbage information for the control unit, at that time busier will be on.

Block Diagram:

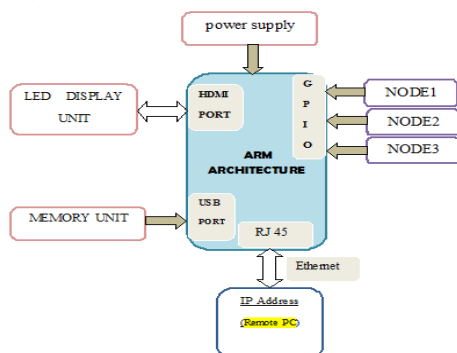


Fig: 1. A Method of Detecting Abnormal Program Behavior on Embedded Devices Block Diagram

IV.HARDWARE IMPLEMENTATION

Raspberry Pi Board:



Fig: 2. Raspberry Pi Board

The Raspberry Pi [7] is a credit-card-sized single-board computer developed in the UK by the Raspberry Pi Foundation with the intention of promoting the teaching of basic computer science in schools. The Raspberry Pi is manufactured in two board configurations through licensed manufacturing deals with Newark element14 (Premier Farnell), RS Components and Egoman. These companies sell the Raspberry Pi online. Egoman produces a version for distribution solely in China and Taiwan, which can be distinguished from other Pis by their red coloring and lack of FCC/CE marks. The hardware is the same across all manufacturers. The Raspberry Pi has a Broadcom BCM2835 system on a chip (SoC), which includes an ARM1176JZF-S 700 MHz processor, Video Core IV GPU, and was originally shipped with 256 megabytes of RAM, later upgraded to 512 MB. It does not include a built-in hard disk or solid-state drive, but uses an SD card for booting and persistent storage.

Raspberry Pi Board features

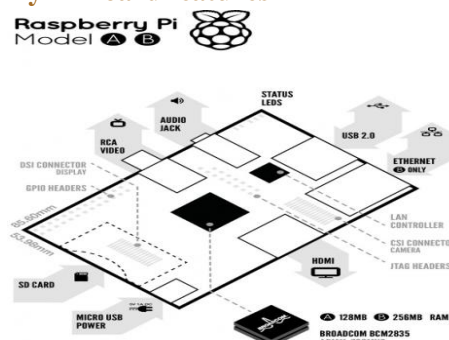


Fig: 3. Raspberry Pi Board features

The Foundation provides Debian and Arch Linux [6] ARM distributions for download. Tools are available for Python as the main programming language, with support for BBC BASIC (via the RISC OS image or the Brandy Basic clone for Linux), C, Java and Perl.

TFT display unit:

TFT stands for Thin Film Transistor, and is a type of technology used to improve the image quality of an LCD. Each pixel on a TFT-LCD has its own transistor

on the glass itself, which offers more control over the images and colors that it renders.

While TFT-LCDs can deliver sharp images, they also tend to offer relatively poor viewing angles, meaning they look best when viewed head-on. If you view a TFT-LCD from the side, it can be difficult to see. TFT-LCDs also consume more power than other types of cell phone displays.

Temperature Sensor:



Fig: 4. Temperature Sensor

Temperature sensor is a device which is designed specifically to measure the hotness or coldness of an object. LM35 is a precision IC temperature sensor with its output proportional to the temperature (in °C). With LM35, the temperature can be measured more accurately than with a thermistor. It also possesses low self heating and does not cause more than 0.1 °C temperature rise in still air. The operating temperature range is from -55°C to 150°C. The LM35's low output impedance, linear output, and precise inherent calibration make interfacing to readout or control circuitry especially easy.

Light Dependent Resistors:

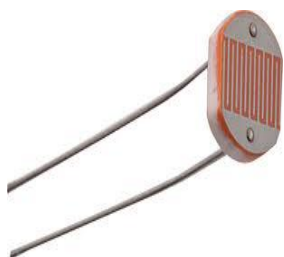


Fig: 5. LDR

Light dependent resistors are used to re-charge a light during different changes in the light, or they are made to turn a light on during certain changes in lights. One of the most common uses for light dependent resistors is in traffic lights. The light dependent resistor controls a built in heater inside the traffic light, and causes it to recharge over night so that the light never dies. Other common places to find light dependent resistors are in: infrared detectors, clocks and security alarms.

LPG Gas Sensor



Fig: 6. LPG gas sensor

LPG Gas Sensor Module is designed to detect the presence of a dangerous LPG leak in your Home, car or in a service station, storage tank environment by interfacing with Microcontroller without ADC Channels and programming. In this version of LPG Gas sensor module two pots are included, one for trigger level setting and the other for setting sensitivity of the sensor. It allows to determining when a preset LPG gas level has been reached or exceeded.

There are two potentiometers used in Gas Sensor Module. They are as follows:

POT P1:

The on-board POT P1 is used to set tolerance voltage for detecting the LPG presence. When LPG is detected, the OUT pin will be high. This will occur when the output voltage is greater than the tolerance level set, using the POT P1.

POT P2:

The on-board POT P2 is used to set the sensitivity of the Gas sensor. We recommend you to calibrate the detector for 1000ppm of LPG concentration in air and use value of POT P2 about 20KΩ.

There are two leads in Gas Sensor Module. They are:

D1: PWR Led. This Green Led indicates the Power input.

D2: STS Led. The red status Led (STS) indicates the various status of LPG Sensor module

Ethernet:

Ethernet LAN Features:

- Bus topology, Wired LAN in IEEE 802.3 physical layer standard
- 10 Mbps, 100 Mbps (Unshielded and Shielded wires) and 4 Gbps (in twisted pair wiring mode)
- Broadcast medium-Passive, Wired connections based.
- Frame format like the IEEE 802.2
- SNMP (Simple Network Management Protocol) Open system (therefore allows equipment of different specifications)
- Each one connected to a common communication channel in the network listens and if the channel is idle then transmits. If not idle, waits and tries again.
- Multi access is like in a Packet switched network

V.SOFTWARE REQUIREMENTS

A. Linux Operating System:

Linux [6] or GNU/Linux is software operating for computers. The operating system is a collection of the basic instructions that tell the electronic parts of the computer what to do and how to work. Free and open source software (FOSS) means that everyone has the freedom to use it, see how it works, and changes it. There is a lot of software for Linux, and since Linux is free software it means that none of the software will put any license restrictions on users. This is one of the reasons why many people like to use Linux.

A Linux-based system is a modular Unix-like operating system. It derives much of its basic design from principles established in UNIX during the 1970s and 1980s. Such a system uses a monolithic kernel, the

Linux kernel, which handles process control, networking, and peripheral and file system access. Device drivers are either integrated directly with the kernel or added as modules loaded while the system is running.

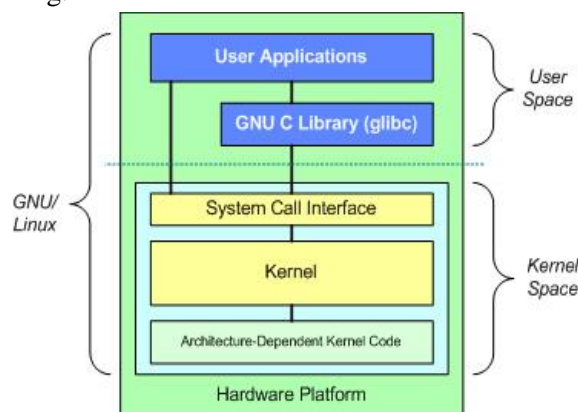


Fig. 7. Architecture of Linux Operating System

B. Qt for Embedded Linux:

Qt [5] is a cross-platform application framework that is widely used for developing application software with a graphical user interface (GUI) (in which cases Qt is classified as a widget toolkit), and also used for developing non-GUI programs such as command-line tools and consoles for servers.

Qt uses standard C++ but makes extensive use of a special code generator (called the Meta Object Compiler, or moc) together with several macros to enrich the language.

Qt can also be used in several other programming languages via language bindings. It runs on the major desktop platforms and some of the mobile platforms. Non-GUI features include SQL database access, XML parsing; thread management, network support, and a unified cross-platform application programming interface for file handling. It has extensive internationalization support.

VI.RESULTS

In this section, we are giving the complete description on the proposed system architecture. Here we are using Raspberry Pi board as our platform. It has an ARM-11

SOC with integrated peripherals like USB, Ethernet and serial etc. On this board we are installing Linux operating system with necessary drivers for all peripheral devices and user level software stack which includes a light weight GUI based on XServer, V4L2 API for interacting with video devices like cameras, TCP/IP stack to communicate with network devices and some standard system libraries for system level general IO operations.

The Raspberry Pi board equipped with the above software stack is connected to the outside network and a camera is connected to the Raspberry Pi through USB bus. On the other side we have to host a web server with cloud facility, Temperature, Gas and LDR sensors are connected to Nodes unit of the Raspberry pi board. After connecting all the devices power up the device. When the device starts booting from flash, it first loads the Linux to the device and initializes all the drivers and the core kernel.

After initialization of the kernel it first checks weather all the devices are working properly or not. After that it loads the file system and starts the startup scripts for running necessary processes and daemons. Finally it starts the main application.

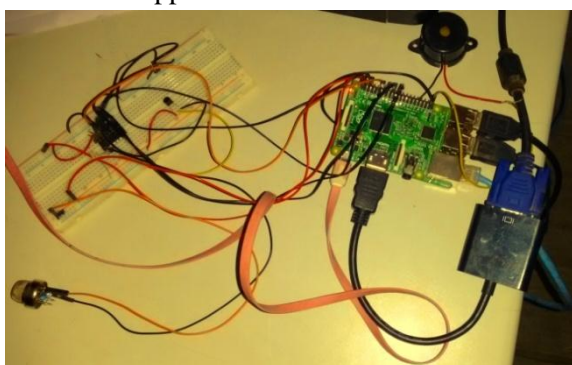


Fig: 8.Raspberry Pi Board Connections

Once the application starts running it first check all the devices and resources which It needs are available or not. After that it checks the connection with the devices and gives control to the user. Then we can enter the program path we can get the sensors output on the LXTerminal window.

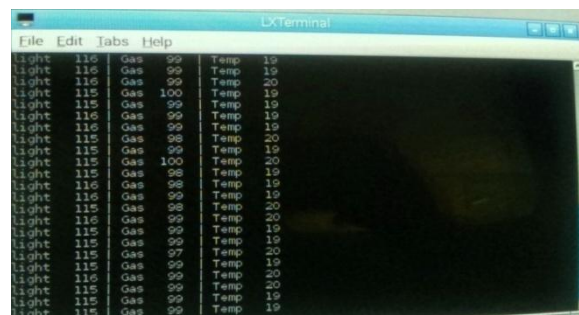


Fig: 9.Sensors Values on LX Terminal Window

IF any sensor is disconnected from the circuit we can get the alert on LXTerminal window. At the same time busier will be on.

Example: If sensor 1 is disconnected we can get Check Sensor 1 alert on the LXTerminal window and sensor 1 get the garbage values.

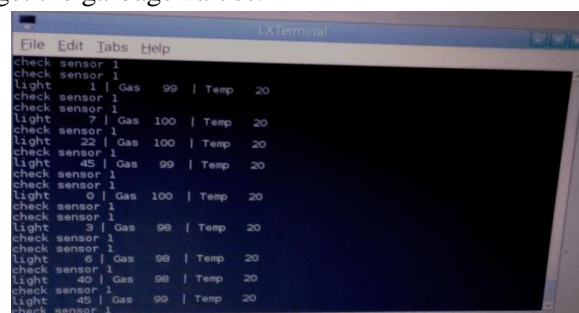


Fig: 10.Identification of Sensor1 (LDR) Disconnection

Enter the ifconfig command on the LXTerminal window we can get internet address. Enter this internet address in another system web browser. At that time we can see the sensors information on that system.

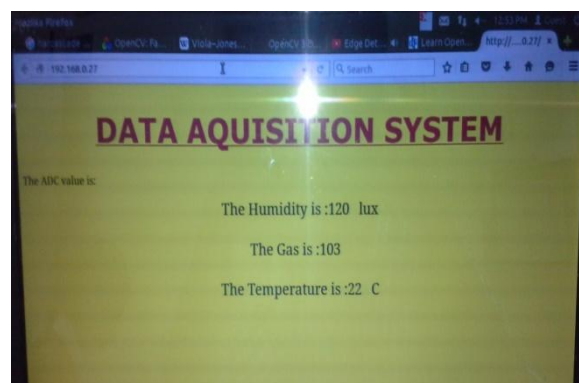


Fig: 10 Data Acquisition System

VII.CONCLUSION

The project “A Method of Detecting Abnormal Program Behavior on Embedded Devices” has been successfully designed and tested. It has been developed by integrating features of all the hardware components and software used. Presence of every module has been reasoned out and placed carefully thus contributing to the best working of the unit. Secondly, using highly advanced ARM11 board and with the help of growing technology the project has been successfully implemented.

REFERENCES

- [1] D. Arora, S. Ravi, A. Raghunathan, and N. K. Jha, “Secure embedded processing through hardware-assisted run-time monitoring,” in Proc. Design, Autom., Test Eur., 2005, pp. 178–183.
- [2] D. Arora, S. Ravi, A. Raghunathan, and N. K. Jha, “Hardware-assisted run-time monitoring for secure program execution on embedded processors,” IEEE Trans. Very Large Scale Integr. (VLSI) Syst., vol. 14, no. 12, pp. 1295–1308, Dec. 2006.
- [3] P. Dongara and T. N. Vijaykumar, “Accelerating private-key cryptography via multithreading on symmetric multiprocessors,” in Proc. IEEE Int. Symp. Perform. Anal. Syst. Softw., Mar. 2003, pp. 58–69.
- [4] G. E. Suh and S. Devadas, “Physical unclonable functions for device authentication and secret key generation,” in Proc. 44th ACM/IEEE Design Autom. Conf., Jun. 2007, pp. 9–14.
- [5] Wiki.qt.io.
- [6] elinux.org/Processors
- [7] www.raspberrypi.org

Design of a JPEG Compressor with an Efficient and Reconfigurable DCT Algorithm

Nekkanti Lakshmi Indira Rani ¹, G.Barathi subhashini ²

P.G Student, Department of Electronics and Communication Engineering, Mallareddy Engineering College

Hyderabad, Telangana, India

Associate Professor, Department of Electronics and Communication Engineering, Mallareddy Engineering College

Hyderabad, Telangana, India

ABSTRACT: Approximation of discrete cosine transform (DCT) is useful for reducing its computational complexity without significant impact on its coding performance. Most of the existing algorithms for approximation of the DCT target only the DCT of small transform lengths, and some of them are non-orthogonal. This paper presents a generalized recursive algorithm to obtain orthogonal approximation of DCT where an approximate DCT of length could be derived from a pair of DCTs of length at the cost of additions for input pre processing. We perform recursive sparse matrix decomposition and make use of the symmetries of DCT basis vectors for deriving the proposed approximation algorithm. Proposed algorithm is highly scalable for hardware as well as software implementation of DCT of higher lengths, and it can make use of the existing approximation of 8-point DCT to obtain approximate DCT of any power of two length. It is shown that proposed algorithm involves lower arithmetic complexity compared with the other existing approximation algorithms. We have presented a fully scalable reconfigurable parallel architecture for the computation of approximate DCT based on the proposed algorithm. One uniquely interesting feature of the proposed design is that it could be configured for the computation of a 32-point DCT or for parallel computation of two 16-point DCTs or four 8-point DCTs with a marginal control overhead. The proposed architecture is found to offer many advantages in terms of hardware complexity, regularity and modularity. We implement the JPEG compressions scheme with the DCT proposed above.

KEYWORDS: Algorithm-architecture code sign, DCT approximation, discrete cosine transform (DCT), high efficiency video coding (HEVC).

I. INTRODUCTION

The discrete cosine transform (DCT) is popularly used in image and video compression. Since the DCT is computationally intensive, several algorithms have been proposed in the literature to compute it efficiently [1]–[3]. Recently, significant work has been done to derive approximate of 8-point DCT for reducing the computational complexity [4]–[9]. The main objective of the approximation algorithms is to get rid of multiplications which consume most of the power and computation- time, and to obtain meaningful estimation of DCT as well. Haweel [8] has proposed the signed DCT (SDCT) for 8 8 blocks where the basis vector elements are replaced by their sign, i.e., 1. Bouguezel-Ahmad-Swamy (BAS) have proposed a series of methods. They have provided a good estimation of the DCT by replacing the basis vector elements by 0, 1/2, 1 [7]. In the same vein, Bayer and Cintra [5], [6] have proposed two transforms derived from 0 and 1 as elements of transform kernel, and have shown that their methods perform better than the method in [7], particularly for low- and high-compression ratio scenarios.

II. RELATED WORK

The need of approximation is more important for higher-size DCT since the computational complexity of the DCT grows nonlinearly. On the other hand, modern video coding standards such as high efficiency video coding (HEVC) [10] uses DCT of larger block sizes (up to 32 32) in order to achieve higher compression ratio. But, the extension of the design strategy used in H264 AVC for larger transform sizes, such as 16-point and 32-point is not possible [11]. Besides, several image processing applications such as tracking [12] and simultaneous compression and

International Journal of Innovative Research in Science, Engineering and Technology

(An ISO 3297: 2007 Certified Organization)

Vol. 5, Issue 9, September 2016

encryption [13] require higher DCT sizes. In this context, Cintra has introduced a new class of integer transforms applicable to several block-lengths [14]. Cintra *et al.* have proposed a new 16 16 matrix also for approximation of 16-point DCT, and have validated it experimentally [15]. Recently, two new transforms have been proposed for 8-point DCT approximation: Cintra *et al.* have proposed a low-complexity 8-point approximate DCT based on integer functions [16] and Potluri *et al.* have proposed a novel 8-point DCT approximation that requires only 14 addition [17]. On the other hand, Bouguezel *et al.* have proposed two methods for multiplication-free approximate form of DCT. The first method is for length , 16 and 32; and is based on the appropriate extension of integer DCT[18]. Also, a systematic method for developing a binary version of high-size DCT (BDCT) by using the sequency-ordered Walsh-Hadamard transform (SO-WHT) is proposed in [4].

III. PROPOSED DCT APPROXIMATION

The elements of -point DCT matrix are given by:

$$c(i, j) = c_i \sqrt{\frac{2}{N}} \cos \frac{(2j+1)i\pi}{2N} \quad (1)$$

For any even value of N we can find that

$$c(2k, j) = c_{2k} \sqrt{\frac{2}{N}} \cos \frac{(2j+1)2k\pi}{2N} \quad (2)$$

Dct matrix CN can be calculated as

$$\mathbf{C}_N = \frac{1}{\sqrt{2}} \mathbf{M}_N^{per} \mathbf{T}_N \mathbf{M}_N^{add} \quad (3)$$

Where Tn can be block spare matrix expressed by

$$\mathbf{T}_N = \begin{bmatrix} \mathbf{C}_{\frac{N}{2}} & \mathbf{0}_{\frac{N}{2}} \\ \mathbf{0}_{\frac{N}{2}} & \mathbf{S}_{\frac{N}{2}} \end{bmatrix} \quad (4)$$

Permutation matrix is expressed by

$$\mathbf{M}_N^{per} = \begin{bmatrix} \mathbf{P}_{N-1, \frac{N}{2}} & \mathbf{0}_{1, \frac{N}{2}} \\ \mathbf{0}_{1, \frac{N}{2}} & \mathbf{P}_{N-1, \frac{N}{2}} \end{bmatrix} \quad (5)$$

$$\mathbf{P}_{N-1, \frac{N}{2}}^{(i)} = \begin{cases} \mathbf{0}_{1, \frac{N}{2}} & \text{if } i = 1, 3, 5, \dots, N-1 \\ \mathbf{I}_{\frac{N}{2}} \left(\frac{i}{2} \right) & \text{if } i = 0, 2, 4, \dots, N-2 \end{cases}$$

Finally matrix addition is defined by

$$\mathbf{M}_N^{add} = \begin{bmatrix} \mathbf{I}_{\frac{N}{2}} & \mathbf{J}_{\frac{N}{2}} \\ \mathbf{I}_{\frac{N}{2}} & -\mathbf{J}_{\frac{N}{2}} \end{bmatrix}, \quad (6)$$

When we closely look at (3) and (4), we note that C8 operates on sums of pixel pairs while S8 operates on differences of the same pixel pairs. Therefore, if we replace S8 with C8 by , we shall have two main advantages. Firstly, we shall have good compression performance due to the efficiency of C8 and secondly the implementation will be much simpler, scalable and reconfigurable. For approximation of S8 we have investigated two other low-complexity alternatives, and in the following we discuss here three possible options of approximation of S8.

International Journal of Innovative Research in Science, Engineering and Technology

(An ISO 3297: 2007 Certified Organization)

Vol. 5, Issue 9, September 2016

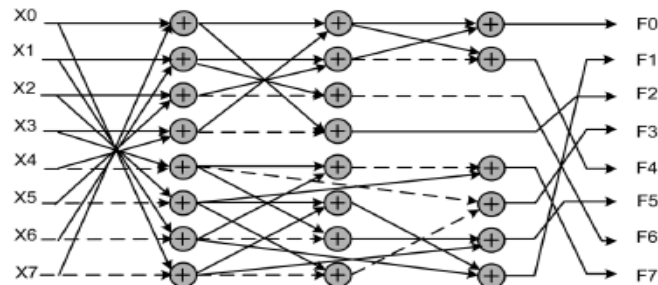


fig. 1. Signal flow graph (SFG) of (). Dashed arrows represent multiplications by 1.

We have not done exhaustive search of all possible solutions. So there could be other possible low-complexity implementation of S8. But other solutions are not expected to have the potential for reconfigurability what we achieve by replacement of S8 by C8. Based on this third possible approximation of S8, we have obtained the proposed approximation as:

$$\hat{C}_N = \frac{1}{\sqrt{2}} M_N^{per} \begin{bmatrix} \hat{C}_{\frac{N}{2}} & 0_{\frac{N}{2}} \\ 0_{\frac{N}{2}} & \hat{C}_{\frac{N}{2}} \end{bmatrix} M_N^{add}. \quad - (7)$$

As stated before, matrix is orthogonalizable. Indeed, for each we can calculate given by:

$$D_N = \sqrt{\left(\hat{C}_N \times (\hat{C}_N)^t \right)^{-1}}, \quad - (8)$$

Where $(.)^t$ denotes matrix transposition. For data compression, we can use $C_N^{orth} = D_N \times C_N$ instead of C_N since $(C_N^{orth})^{-1} = (C_N^{orth})^t$. since D_N is a diagonal matrix, it can be integrated into the scaling in the quantization process (without additional computational complexity). Therefore, as adopted in [4]–[8], the computational cost of C_N^{orth} is equal to that of C_N . Moreover, the term of $1/\sqrt{2}$ in (9) can be integrated in the quantization step in order to have multiplier less architecture. The procedure for the generation of the proposed orthogonal approximated DCT is stated in algorithm 1.

Algorithm 1 Generation of proposed DCT matrix

```

function PROPOSED DCT(N)      ▷ N power of 2, N ≥ 8
    N0 ← log2(N/8) ▷ N0 is the number of 8-sample blocks
    CN/2N0 ← [2C8]
    while N0 > 0 do
        Ñ ← (N/2N0-1)
        Calculate MÑper, MÑadd
        Calculate ĈÑ
        N0 ← N0 - 1
    end while
    Calculate DN
    return ĈN, DN
end function
    
```

III SCALABLE AND RECONFIGURABLE ARCHITECTURE FOR DCT COMPUTATION

The basic computational block of algorithm for the proposed DCT approximation C_8 , is given in [6]. The block diagram of the computation of DCT based C_8 on is shown in Fig. 1. For a given input sequence the approximate DCT coefficients are obtained by $F = C^N \cdot X^t$. An example of the block diagram of C^{16} is illustrated in Fig. 2, where two units for the computation of are used along with an input adder unit and output permutation unit. The functions of these two blocks are shown respectively in (8) and (6). Note that structures of 16-point DCT of Fig. 2 could be extended to obtain

International Journal of Innovative Research in Science, Engineering and Technology

(An ISO 3297: 2007 Certified Organization)

Vol. 5, Issue 9, September 2016

the DCT of higher sizes. For example, the structure for the computation of 32-point DCT could be obtained by combining a pair of 16-point DCTs with an input adder block and output permutation block.

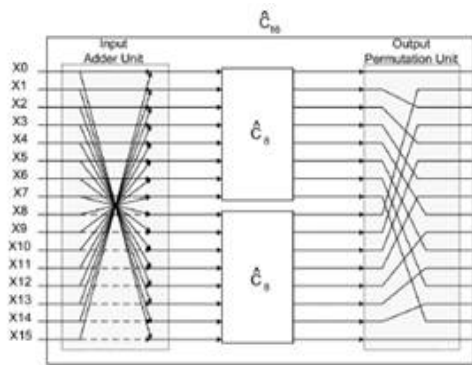


Fig. 2. Block diagram of the proposed DCT for $N = 16$ (\hat{C}_{16}).

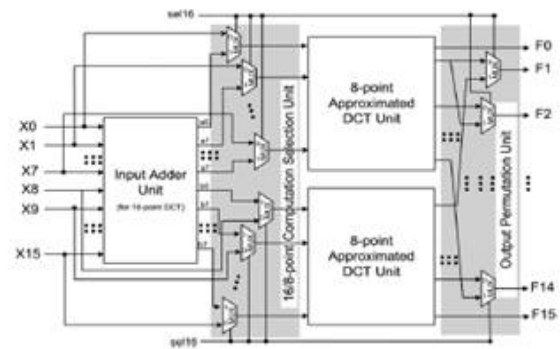


Fig. 3. Proposed reconfigurable architecture for approximate DCT of lengths $N = 8$ and 16 .

to assess the computational complexity of proposed N -point approximate DCT, we need to determine the computational cost of matrices quoted in (9). As shown in Fig. 1 the approximate 8-point DCT involves 22 additions. Since M_N^{per} has no computational cost and M_N^{add} require N additions for N -point DCT, the overall arithmetic complexity of 16-point, 32-point, and 64-point DCT approximations are 60, 152, and 368 additions, respectively. More generally, the arithmetic complexity of N -point DCT is equal to $N(\log_2 N - 1/4)$ additions. Moreover, since the structures for the computation of DCT of different lengths are regular and scalable, the computational time for N DCT coefficients can be found to be $\log_2(N)T_A$ where T_A is the addition-time. The number of arithmetic operations involved in proposed DCT approximation of different lengths and those of the existing competing approximations are shown in Table I. It can be found that the proposed method requires the lowest number of additions, and does not require any shift operations. Note that shift operation does not involve any combinational components, and requires only rewiring during hardware implementation. But it has indirect contribution to the hardware complexity since shift-add operations lead to increase in bit-width which leads to higher hardware complexity of arithmetic units which follow the shift-add operation. Also, we note that all considered approximation methods involve significantly less computational complexity over that of the exact DCT algorithms. According to the Loeffler algorithm [2], the exact DCT computation requires 29, 81, 209, and 513 additions along with 11, 31, 79, and 191 multiplications, respectively for 8, 16, 32, and 64-point DCTs.

Pipelined and non-pipelined designs of different methods are developed, synthesized and validated using an integrated logic analyzer. The validation is carried out by using the Diligent EB of Spartan6-LX45. We have used 8-bit inputs, and we have allowed the increase of output size (without any truncations). For the 8-point transform of Fig. 1, we have 11-bit and 10-bit outputs. The pipelined design are obtained by insertion of registers in the input and output stages along with registers after each adder stage, while the no pipeline registers are used within the non-pipelined designs.

PROPOSED RECONFIGURABLE SCHEME

As specified in the recently adopted HEVC [10], DCT of different lengths such as , 16, 32 are required to be used in video coding applications. Therefore, a given DCT architecture should be potentially reused for the DCT of different lengths instead of using separate structures for different lengths. We propose here such reconfigurable DCT structures which could be reused for the computation of DCT of different lengths. The reconfigurable architecture for the implementation of approximated 16-point DCT is shown in Fig. 3. It consists of three computing units, namely two 8-point approximated DCT units and a 16-point input adder unit that generates $a(i)$ and $b(i)$, $i \in [1 : 7]$. The input to the first 8-point DCT approximation unit is fed through 8 MUXes that select either $[a(0), a(1), \dots, a(7)]$ or $[X(1), X(1), \dots, X(7)]$, depending on whether it is used for 16-point DCT calculation or 8-point DCT calculation. Similarly, the input to the second 8-point DCT unit (Fig. 3) is fed through 8 MUXes that select either $[b(0), b(1), \dots, b(7)]$ or $[X(8), X(9), \dots, X(15)]$, depending on whether it is used for 16-point DCT calculation or 8-point DCT calculation. On the other hand, the output permutation unit uses 14 MUXes to select and re-order the output depending on the size of the selected DCT. Sel16 is used as control input of the MUXes to select inputs and to perform permutation according to the size of the DCT to be computed. Specifically, enables the computation of 16-point DCT and enables the computation of a pair of

International Journal of Innovative Research in Science, Engineering and Technology

(An ISO 3297: 2007 Certified Organization)

Vol. 5, Issue 9, September 2016

8-point DCTs in parallel. Consequently, the architecture of Fig. 3 allows the calculation of a 16-point DCT or two 8-point DCTs in parallel.

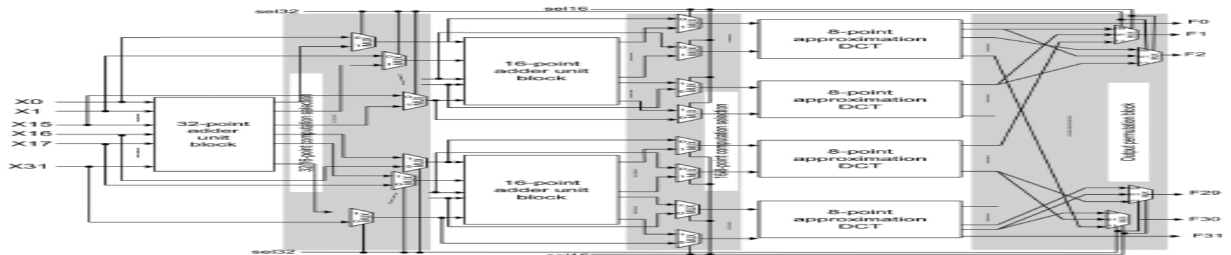


Fig.4 proposed reconfigurable architecture.

A reconfigurable design for the computation of 32-, 16-, and 8-point DCTs is presented in Fig. 4. It performs the calculation of a 32-point DCT or two 16-point DCTs in parallel or four 8-point DCTs in parallel. The architecture is composed of 32-point input adder unit, two 16-point input adder units, and four 8-point DCT units. The reconfigurability is achieved by three control blocks composed of 64 2:1 MUXes along with 30 3:1 MUXes. The first control block decides whether the DCT size is of 32 or lower. If, the selection of input data is done for the 32-point DCT, otherwise, for the DCTs of lower lengths. The second control block decides whether the DCT size is higher than 8. If the length of the DCT to be computed is higher than 8 (DCT length of 16 or 32), otherwise, the length is 8. The third control block is used for the output permutation unit which re-orders the output depending on the size of the selected DCT. and are used as control signals to the 3:1 MUXes. Specifically, for equal to {00}, {01} or {11} the 32 outputs correspond to four 8-point parallel DCTs, two parallel 16-point DCTs, or 32-point DCT, respectively. Note that the throughput is of 32 DCT coefficients per cycle irrespective of the desired transform size.

IV. DCT AND IDCT IN JPEG

The type of data for information in the form of images, one of the most popular compression methods is JPEG. JPEG stands for Joint Photographic Expert Group. According to widely used in JPEG image included on the internet web pages. Use JPEG create a web page with a picture can be accessed faster than a web page with an image without compression.

Color image JPEG compression consists of five steps. This is shown in figure 5. The steps are: color space conversion, down sampling, 2-D DCT, quantization and entropy coding. Grayscale image compression uses only last three steps.

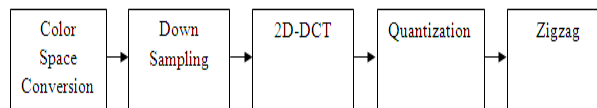


Fig.5 JPEG compression steps of colour images.

JPEG stands for Joint Photographic Expert Group. According to widely used in JPEG image included on the internet web pages. Use JPEG create a web page with a picture can be accessed faster than a web page with an image without compression Color image JPEG compression consists.

Block diagram of entire system to be implemented in FPGA is shown in figure. Input data is inserted into the system every 8 bit sequentially. Actually, many DCT designs insert the input to the DCT in parallel. For example is 8 x 8 bit. This is ideal for DCT computing because it only consumes a clock cycle to insert data to 1D-DCT unit. With sequential manner, it takes 8 clock cycles to insert a set of data (8 points) to the DCT unit.

International Journal of Innovative Research in Science, Engineering and Technology

(An ISO 3297: 2007 Certified Organization)

Vol. 5, Issue 9, September 2016

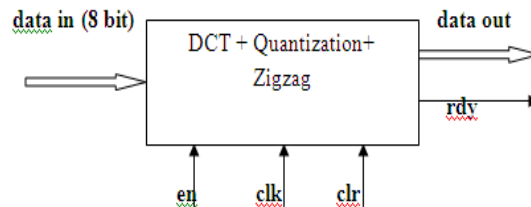


Fig.6 Block representation of entire system.

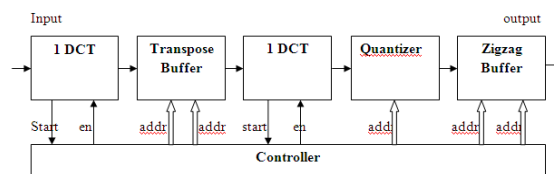


Fig.7 system architecture.

The 2D-DCT architecture, combined with zigzag and quantization used in this paper is shown in Fig. The 2DDCT module construction is modified from that also put the data sequentially into the module. Thus, the architecture of 2D-DCT was divided into two 1D DCT modules and one transpose buffer.

V. IMPLEMENTATION RESULTS

To get the matrix form of equation(1) we will use the following equation

$$T_{ij} = \begin{cases} \frac{1}{\sqrt{N}} & \text{if } i = 0 \\ \sqrt{\frac{2}{N}} \cos \left[\frac{(2j+1)i\pi}{2N} \right] & \text{if } i > 0 \end{cases}$$

Doing dct on an 8X8 block

Before we begin, it should be noted that the pixel values of a black and white image range from 0 to 255 in step 1, where pure black is represented by 0 and pure white is represented by 1 thus how a photo, illustration etc can be accurately represented by these 256 shades of grey. since the image comprises hundreds or even thousands of 8X8 block pixels, the following description of what happens to one 8X8 block is a microcosm of the JPEG process.

Now let's start with a block of image pixel values. This particular block was choose from the very upper left hand corner of an image

$$Original = \begin{bmatrix} 154 & 123 & 123 & 123 & 123 & 123 & 123 & 136 \\ 192 & 180 & 136 & 154 & 154 & 154 & 136 & 110 \\ 254 & 198 & 154 & 154 & 180 & 154 & 123 & 123 \\ 239 & 180 & 136 & 180 & 180 & 166 & 123 & 123 \\ 180 & 154 & 136 & 167 & 166 & 149 & 136 & 136 \\ 128 & 136 & 123 & 136 & 154 & 180 & 198 & 154 \\ 123 & 105 & 110 & 149 & 136 & 136 & 180 & 166 \\ 110 & 136 & 123 & 123 & 123 & 136 & 154 & 136 \end{bmatrix}$$

because the DCT is designed to work on pixel values range from -128 to +127, the original block is "leveled off" by subtracting 128 from each entity this result in the following matrix

$$M = \begin{bmatrix} 26 & -5 & -5 & -5 & -5 & -5 & -5 & 8 \\ 64 & 52 & 8 & 26 & 26 & 26 & 8 & -18 \\ 126 & 70 & 26 & 26 & 52 & 26 & -5 & -5 \\ 111 & 52 & 8 & 52 & 52 & 38 & -5 & -5 \\ 52 & 26 & 8 & 39 & 38 & 21 & 8 & 8 \\ 0 & 8 & -5 & 8 & 26 & 52 & 70 & 26 \\ -5 & -23 & -18 & 21 & 8 & 8 & 52 & 38 \\ -18 & 8 & -5 & -5 & -5 & 8 & 26 & 8 \end{bmatrix}$$

We are now ready to perform the discrete cosine transform. which is accomplished by matrix multiplication

International Journal of Innovative Research in Science, Engineering and Technology

(An ISO 3297: 2007 Certified Organization)

Vol. 5, Issue 9, September 2016

$$D = TMT'$$

In previous equation matrix M is first multiplied on the left by the DCT matrix T from the previous section, this transforms the rows. the columns are then transformed by multiplying on the right by the transpose of the dct matrix. this yields the following matrix.

1298	229	-482	-247	-250	-21	228	-83
178	678	-231	-370	128	-83	97	5
62	85	59	-26	-4	73	37	42
483	269	-197	-167	-69	-9	136	-112
242	209	-204	-89	114	183	-30	143
227	31	-76	-18	-35	65	-35	-13
-146	62	-25	9	72	22	21	1
-166	-175	124	122	-62	38	38	81

This block matrix now consists of 64DCT coefficients, c_{ij} , where I and j range from 0 to 7 the top left coefficients c_{00} , correlates to the low frequencies of the original image block.

As we move away from c_{00} in all directions, the DCT coefficients correlates too higher and higher frequencies of the image block, where c_{77} corresponds to the higher frequencies it is important to note that the human eye is most sensitive to low frequencies and result from the quantization step will reflect this fact.

If however, another level of quality and compression is desired, scalar multiples of the JPEG standard quantization matrix may be used. for a quality level grater than 50. the standard quantization matrix is multiplied by (100 quality level by 50).

Quantization is achieved by dividing each element in the transformed image matrix D by the corresponding elements in the quantization matrix, and then rounding to the nearest integer value. for the following step, quantization matrix is

$$C_{i,j} = \text{round}\left(\frac{D_{i,j}}{Q_{i,j}}\right)$$

16	4	-10	-3	-2	0	1	0
3	11	-3	-4	1	0	0	0
1	1	1	0	0	0	0	0
7	3	-1	-1	0	0	1	0
3	2	-1	-1	0	1	0	1
2	0	0	0	0	0	0	0
-1	0	0	0	0	0	0	0
-1	-1	0	0	0	0	0	0

The quantized matrix c is now ready for the final step of compression. Before storage, all coefficients of c are converted by an encoder to a stream of binary data .in depth coverage of the coding process is beyond the scope of the article. However we can point out one key aspect that the reader is sure to appreciate. After quantization it is quite common for most of the coefficients equal to zero. the advantage lies in the consolidation of relatively large runs of zeros, which compress very well.

The reason to use zigzag scanning is that it's reasonable to expect pixels in a block have more in common than pixels going across in a straight line. Having more in common means they can be compressed more.. the zig zag output is 16 4 3 1 11 -10 -3 -3 1 7 3 3 1 -4 -2 0 1 0 -1 2 2 -1 0 -1 -1 0 0 1 0 0 0 0 0 0 -1 -1 0 0 0 0 0 0 1 1 0 0 0 0 0 0 0 1 0 0 0 0 0 0 0 0 0 0.

Run-length encoding (RLE) is a very simple form of lossless data compression in which *runs* of data (that is, sequences in which the same data value occurs in many consecutive data elements) are stored as a single data value and count, rather than as the original run.. the run length encoding output is 16 4 3 1 11 -10 -3 -3 1 7 3 3 1 -4 -2 0 1 0 -1 2 2 -1 0 -1 -1 0 0 1 0 127 7 -1 -1 0 127 7 1 1 0 127 8 1 0 127 9.

International Journal of Innovative Research in Science, Engineering and Technology

(An ISO 3297: 2007 Certified Organization)

Vol. 5, Issue 9, September 2016

VI. CONCLUSION

In this paper, we have proposed a recursive algorithm to obtain orthogonal approximation of DCT where approximate DCT of length N could be derived from a pair of DCTs of length $(N/2)$ at the cost of N additions for input preprocessing. The proposed approximated DCT has several advantages, such as of regularity, structural simplicity, lower-computational complexity, and scalability. Comparison with recently proposed competing methods shows the effectiveness of the proposed approximation in terms of error energy, hardware resources consumption, and compressed image quality. We have also proposed a fully scalable reconfigurable architecture for approximate DCT computation where the computation of 32-point DCT could be configured for parallel computation of two 16-point DCTs or four 8-point DCTs. The DCT algorithm mentioned above is used in the implementation of a JPEG compression scheme whose results are presented in the previous section.

REFERENCES

- [1] A. M. Shams, A. Chidanandan, W. Pan, and M. A. Bayoumi, "NEDA: A low-power high-performance DCT architecture," *IEEE Trans. Signal Process.*, vol. 54, no. 3, pp. 955–964, 2006.
- [2] C. Loeffler, A. Lightenberg, and G. S. Moschytz, "Practical fast 1-D DCT algorithm with 11 multiplications," in *Proc. Int. Conf. Acoust., Speech, Signal Process. (ICASSP)*, May 1989, pp. 988–991.
- [3] M. Jridi, P. K. Meher, and A. Alfalou, "Zero-quantised discrete cosine transform coefficients prediction technique for intra-frame video encoding," *IET Image Process.*, vol. 7, no. 2, pp. 165–173, Mar. 2013.
- [4] S. Bouguezel, M. O. Ahmad, and M. N. S. Swamy, "Binary discrete cosine and Hartley transforms," *IEEE Trans. Circuits Syst. I, Reg. Papers*, vol. 60, no. 4, pp. 989–1002, Apr. 2013.
- [5] F. M. Bayer and R. J. Cintra, "DCT-like transform for image compression requires 14 additions only," *Electron. Lett.*, vol. 48, no. 15, pp. 919–921, Jul. 2012.
- [6] R. J. Cintra and F. M. Bayer, "A DCT approximation for image compression," *IEEE Signal Process. Lett.*, vol. 18, no. 10, pp. 579–582, Oct. 2011.
- [7] S. Bouguezel, M. Ahmad, and M. N. S. Swamy, "Low-complexity 8 8 transform for image compression," *Electron. Lett.*, vol. 44, no. 21, pp. 1249–1250, Oct. 2008.
- [8] T. I. Haweel, "A new square wave transform based on the DCT," *Signal Process.*, vol. 81, no. 11, pp. 2309–2319, Nov. 2001.
- [9] V. Britanak, P. Y. Yip, and K. R. Rao, *Discrete Cosine and Sine Transforms: General Properties, Fast Algorithms and Integer Approximations*. London, U.K.: Academic, 2007.
- [10] G. J. Sullivan, J.-R. Ohm, W.-J. Han, and T. Wiegand, "Overview of the high efficiency video coding (HEVC) standard," *IEEE Trans. Circuits Syst. Video Technol.*, vol. 22, no. 12, pp. 1649–1668, Dec. 2012.

BIOGRAPHY



N L Indhira rani pursuing her Masters in the domain VLSI design in mallareddy engineering college (hyd). she completed her graduate from the college of GIET college of engineering (east Godavari) in the stream of E.C.E in the year 2013.

Area and Power Efficient Booth's Multipliers Based on Non Redundant Radix-4 Signed- Digit Encoding

S.Reshma ¹, K.Rjendra Prasad ²

P.G Student, Department of Electronics and Communication Engineering, Mallareddy Engineering College
Hyderabad, Telangana, India

Assistant Professor, Department of Electronics and Communication Engineering, Mallareddy Engineering College
Hyderabad, Telangana, India

ABSTRACT: In this paper, we introduce an architecture of pre-encoded multipliers for Digital Signal Processing applications based on off-line encoding of coefficients. To this extend, the Non-Redundant radix-4 Signed-Digit (NR4SD) encoding technique, which uses the digit values $\{-1, 0, +1, +2\}$ or $\{-2, -1, 0, +1\}$, is proposed leading to a multiplier design with less complex partial products implementation. Extensive experimental analysis verifies that the proposed pre-encoded NR4SD multipliers, including the coefficients memory, are more area and power efficient than the conventional Modified Booth scheme.

KEYWORDS: Multiplying circuits, Modified Booth encoding, Pre-Encoded multipliers, VLSI implementation.

I. INTRODUCTION

MULTIMEDIA and Digital Signal Processing (DSP) applications (e.g., Fast Fourier Transform (FFT), audio/video CoDecs) carry out a large number of multiplications with coefficients that do not change during the execution of the application. Since the multiplier is a basic component for implementing computationally intensive applications, its architecture seriously affects their performance.

Constant coefficients can be encoded to contain the least non-zero digits using the Canonic Signed Digit (CSD) representation [1]. CSD multipliers comprise the fewest non-zero partial products, which in turn decreases their switching activity. However, the CSD encoding involves serious limitations. Folding technique [2], which reduces silicon area by time multiplexing many operations into single functional

units, e.g., adders, multipliers, is not feasible as the CSD-based multipliers are hard-wired to specific coefficients. In [3], a CSD-based programmable multiplier design was proposed for groups of pre-determined coefficients that share certain features. The size of ROM used to store the groups of coefficients is significantly reduced as well as the area and power consumption of the circuit. However, this multiplier design lacks flexibility since the partial products generation unit is designed specifically for a group of coefficients and cannot be reused for another group. Also, this method cannot be easily extended to large groups of pre-determined coefficients attaining at the same time high efficiency.

Modified Booth (MB) encoding tackles the aforementioned limitations and reduces to half the number of partial products resulting to reduced area, critical delay and power consumption. However, a dedicated encoding circuit is required and the partial products generation is more complex. Kim et al. proposed a technique similar to [3], for designing efficient MB multipliers for groups of pre-determined coefficients with the same limitations described in the previous paragraph.

II. MODIFIED BOOTH ALGORITHM

The proposed NR4SD encoding scheme uses one of the following sets of digit values: $\{-1, 0, +1, +2\}$ or $\{-2, -1, 0, +1\}$. In order to cover the dynamic range of the 2's complement form, all digits of the proposed representation are encoded according to NR4SD except the most significant one that is MB encoded. Using the proposed encoding formula, we pre-encode the standard coefficients and store them into a ROM in a condensed form (i.e., 2 bits per digit). Compared

International Journal of Innovative Research in Science, Engineering and Technology

(An ISO 3297: 2007 Certified Organization)

Vol. 5, Issue 9, September 2016

to the pre-encoded MB multiplier in which the encoded coefficients need 3 bits per digit, the proposed NR4SD scheme reduces the memory size. Also, compared to the MB form, which uses five digit values{-2,-1,0,+1,+2}, proposed NR4SD encoding uses four digit values. Thus, the NR4SD-based pre-encoded multipliers include a less complex partial products generation circuit. We explore the efficiency of the aforementioned pre-encoded multipliers taking into account the size of the coefficients' ROM.

Modified Booth (MB) is a redundant radix-4 encoding technique [6], [7]. Considering the multiplication of the 2's complement numbers A, B, each one consisting of n=2k bits, B can be represented in MB form as

$$\begin{aligned} B &= \langle b_{n-1} \dots b_0 \rangle_{2's} = -b_{2k-1}2^{2k-1} + \sum_{i=0}^{2k-2} b_i 2^i \\ &= \langle \mathbf{b}_{k-1}^{MB} \dots \mathbf{b}_0^{MB} \rangle_{MB} = \sum_{j=0}^{k-1} \mathbf{b}_j^{MB} 2^{2j}. \end{aligned} \quad (1)$$

$$\mathbf{b}_j^{MB} = -2b_{2j+1} + b_{2j} + b_{2j-1}, \quad (2)$$

where $b_{-1} = 0$. Each MB digit is represented by the bits s, one and two (Table 1). The bit s shows if the digit is negative (s=1) or positive (s=0). One shows if the absolute value of a digit equals 1 (one=1) or not (one=0). Two shows if the absolute value of a digit equals 2 (two=1) or not (two=0). Using these bits, we calculate the MB digits MB \mathbf{b}_j as follows:

$$\mathbf{b}_j^{MB} = (-1)^{s_j} \cdot (one_j + 2two_j). \quad (3)$$

Equation (4) from the mb encoding signals

$$\begin{aligned} s_j &= b_{2j+1}, \quad one_j = b_{2j-1} \oplus b_{2j}, \\ two_j &= (b_{2j+1} \oplus b_{2j}) \wedge \overline{one_j}. \end{aligned} \quad (4)$$

b_{2j+1}	b_{2j}	b_{2j-1}	\mathbf{b}_j^{MB}	s_j	one_j	two_j
0	0	0	0	0	0	0
0	0	1	+1	0	1	0
0	1	0	+1	0	1	0
0	1	1	+2	0	0	1
1	0	0	-2	1	0	1
1	0	1	-1	1	1	0
1	1	0	-1	1	1	0
1	1	1	0	1	0	0

Table 1.modified booth encoding table

III. NON REDUNDANT SIGNED DIGIT ENCODING

In this section, we present the Non-Redundant radix-4 Signed Digit (NR4SD) encoding technique. As in MB form, the number of partial products is reduced to half. When encoding the 2's complement number B, digits b_{NR-} take one of four values: {-2,-1,0,+1} at the NR4SD- and b_{NR+} take one of four values {-1,0,+1,+2} at the NR4SD+. algorithm, respectively. Only four different values are used and not five as in MB algorithm, which leads to $0 < j < k - 2$. As we need to cover the dynamic range of the 2's complement form, the most significant digit is MB encoded (i.e., $b_{MB}\{-2,-1,0,+1,+2\}$). The NR4SD- and NR4SD+ encoding algorithms are illustrated in detail in Fig. 1 and 2, respectively.

International Journal of Innovative Research in Science, Engineering and Technology

(An ISO 3297: 2007 Certified Organization)

Vol. 5, Issue 9, September 2016

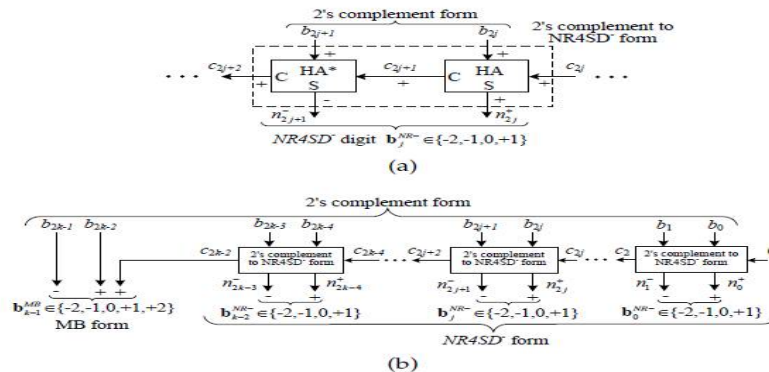


Fig.1 Block Diagram of the NR4SD- Encoding Scheme at the (a) Digit and (b) Word Level.

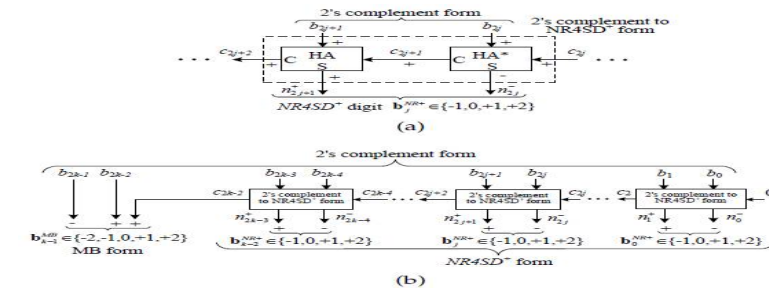


Fig.2 Block Diagram of the NR4SD+ Encoding Scheme at the (a) Digit and (b) Word Level.

NRS4D- algorithm

Step 1: Consider the initial values $j = 0$ and $c_0 = 0$.

Step 2: Calculate the carry c_{2j+1} and the sum n_{2j} of a Half Adder (HA) with inputs b_{2j} and c_{2j} (Fig. 1a).

$$c_{2j+1} = b_{2j} \wedge c_{2j}, \quad n_{2j}^+ = b_{2j} \oplus c_{2j}.$$

Step 3: Calculate the positively signed carry c_{2j+2} (+) and the negatively signed sum n_{2j+1} (-) of a Half Adder* (HA*) with inputs b_{2j+1} (+) and c_{2j+1} (+). The outputs c_{2j+2} and n_{2j+1} of the HA* relate to its inputs as follows

$$2c_{2j+2} - n_{2j+1}^+ = b_{2j+1} + c_{2j+1}.$$

Step 4: Calculate the value of the b_j^{NR-} digit.

$$b_j^{NR-} = -2n_{2j+1}^+ + n_{2j}^+. \quad (5)$$

Equation (5) results from the fact that n_{2j+1} is negatively signed and n_{2j} is positively signed.

Step 5: $j := j + 1$.

Step 6: If $(j < k \div 1)$, go to Step 2. If $(j = k \div 1)$, encode the most significant digit based on the MB algorithm and considering the three consecutive bits to be b_{2k-1} , b_{2k-2} and c_{2k-2} (Fig. 1b). If $(j = k)$, stop.

Table 2 shows how the NR4SD- digits are formed. Equations (6) show how the NR4SD- encoding signals.

2's complement			NR4SD- form			Digit	NR4SD- Encoding		
b_{2j+1}	b_{2j}	c_{2j}	c_{2j+2}	n_{2j+1}^+	n_{2j}^+	b_j^{NR-}	one_j^+	one_j^-	two_j^-
0	0	0	0	0	0	0	0	0	0
0	0	1	0	0	1	+1	1	0	0
0	1	0	0	0	1	+1	1	0	0
0	1	1	1	1	0	-2	0	0	1
1	0	0	1	1	0	-2	0	0	1
1	0	1	1	1	1	-1	0	1	0
1	1	0	1	1	1	-1	0	1	0
1	1	1	1	0	0	0	0	0	0

table.2 NRS4D- encoding.

International Journal of Innovative Research in Science, Engineering and Technology

(An ISO 3297: 2007 Certified Organization)

Vol. 5, Issue 9, September 2016

$$\begin{aligned} one_j^+ &= \overline{n_{2j+1}^-} \wedge n_{2j}^+, \\ one_j^- &= n_{2j+1}^- \wedge n_{2j}^+, \\ two_j^- &= n_{2j+1}^- \wedge \overline{n_{2j}^+}. \end{aligned} \quad -(6)$$

We observe that the NR4SD⁺ form has larger dynamic range than the 2's complement form.

NRS4D⁺ encoding

Step 1: Consider the initial values $j = 0$ and $c_0 = 0$.

Step 2: Calculate the carry c_{2j+1} and the sum n_{2j+1} of a Half Adder (HA) with inputs b_{2j} and c_{2j} (Fig. 2a).

$$2c_{2j+1} - n_{2j+1}^- = b_{2j} + c_{2j}.$$

Step 3: Calculate the positively signed carry c_{2j+2} (+) and the negatively signed sum n_{2j+1} (-) of a Half Adder* (HA*) with inputs b_{2j+1} (+) and c_{2j+1} (+)

The outputs c_{2j+2} and n_{2j+1} of the HA* relate to its inputs as follows

$$c_{2j+2} = b_{2j+1} \vee c_{2j+1}, \quad n_{2j+1}^- = b_{2j+1} \oplus c_{2j+1}.$$

Step 4: Calculate the value of the bNR_j digit.

$$b_j^{NR+} = 2n_{2j+1}^+ - n_{2j}^- \quad -(7)$$

Equation (7) results from the fact that n_{2j+1} is negatively signed and n_{2j} is positively signed.

Step 5: $j := j + 1$.

Step 6: If ($j < k-1$), go to Step 2. If ($j = k-1$), encode the most significant digit based on the MB algorithm and considering the three consecutive bits to be b_{2k-1} , b_{2k-2} and c_{2k-2} (Fig. 1b). If ($j = k$), stop.

Table 3 shows how the NR4SD⁺ digits are formed. Equations (8) show how the NR4SD⁺ encoding signals.

2's complement			NR4SD ⁺ form			Digit	NR4SD ⁺ Encoding		
b_{2j+1}	b_{2j}	c_{2j}	c_{2j+2}	n_{2j+1}^+	n_{2j}^-	b_j^{NR+}	one_j^+	one_j^-	two_j^+
0	0	0	0	0	0	0	0	0	0
0	0	1	0	1	1	+1	1	0	0
0	1	0	0	1	1	+1	1	0	0
0	1	1	0	1	0	+2	0	0	1
1	0	0	0	1	0	+2	0	0	1
1	0	1	1	0	1	-1	0	1	0
1	1	0	1	0	1	-1	0	1	0
1	1	1	1	0	0	0	0	0	0

Table.3 NR4SD⁺ encoding

As observed in the NR4SD⁻ encoding technique, the NR4SD⁺ form has larger dynamic range than the 2's complement form.

Considering the 8-bit 2's complement number N, Table 4 exposes the limit values and two typical values of N, and presents the MB, NR4SD⁻ and NR4SD⁺ digits that result when applying the corresponding encoding techniques to each value of N we considered. We added a bar above the negatively signed digits in order to distinguish them from the positively signed ones.

2's Complement	10000000	10011010	01011001	01111111
Integer	-128	-102	+89	+127
Modified Booth	$\bar{2} 0 0 0$	$\bar{2} 2 \bar{1} \bar{2}$	$1 2 \bar{2} 1$	$2 0 0 \bar{1}$
NR4SD ⁻	$\bar{2} 0 0 0$	$\bar{1} \bar{2} \bar{1} \bar{2}$	$2 \bar{2} \bar{2} 1$	$2 0 0 \bar{1}$
NR4SD ⁺	$\bar{2} 0 0 0$	$\bar{2} 1 2 2$	$1 1 2 1$	$2 0 0 \bar{1}$

Table.4 numerical examples of encoding techniques.

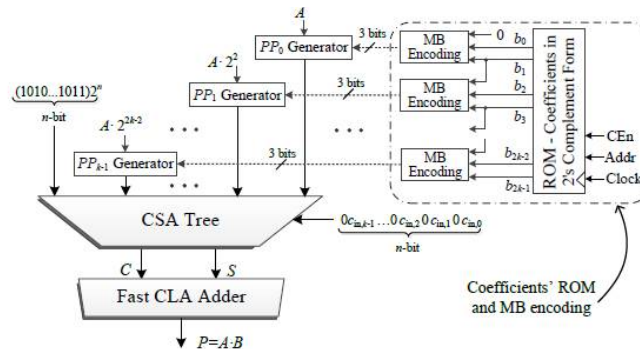


Fig3.system architecture of mb multiplier.

IV. PRE-ENCODED MB MULTIPLIER DESIGN

In this section, we explore the implementation of pre-encoded multipliers. One of the two inputs of these multipliers is pre-encoded either in MB or in NR4SD \square / NR4SD+ representation. We consider that this input comes from a set of fixed coefficients (e.g. the coefficients for a number of filters in which this multiplier will be used in a dedicated system or the sine table required in an FFT implementation). The coefficients are encoded off-line based on MB or NR4SD algorithms and the resulting bits of encoding are stored in a ROM. Since our purpose is to estimate the efficiency of the proposed multipliers, we first present a review of the conventional MB multiplier in order to compare it with the pre-encoded schemes.

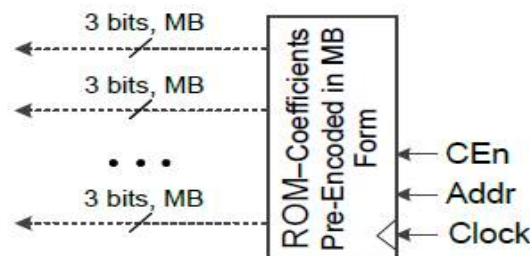


Fig.4the ROM of Pre-Encoded multipliers with standard coefficients in MB form.

In the pre-encoded MB multiplier scheme, the coefficient B is encoded off-line according to the conventional MB form (Table 1). The resulting encoding signals of B are stored in a ROM. The circled part of Fig. 3, which contains the ROM with coefficients in 2's complement form and the MB encoding circuit, is now totally replaced by the ROM of Fig. 4. The MB encoding blocks of Fig. 3 are omitted. The new ROM of Fig. 5 is used to store the encoding signals of B and feed them into the partial product generators (PPj Generators - PPG) on each clock cycle. Targeting to decrease switching activity, the value '1' of sj in the last entry of Table 1 is replaced by '0'. The sign sj is now given by the relation

$$sj = b_{2j+1} _ (b_{2j+1} \wedge b_{2j} \square 1):$$

As a result, the PPG of Fig. 4a is replaced by the one of Fig. 4b. Compared to (4), (12) leads to a more complex design. However, due to the pre-encoding technique, there is no area / delay overhead at the circuit. The partial products, properly weighted, and the correction term (COR) of (11) are fed into a CSA tree. The input carry cin;j of (11) is computed as cin;j = sj based on (12) and Table 1. The CS output of the tree is finally merged by a fast CLA adder. However, the ROM width is increased. Each digit requests three encoding bits (i.e., s, two and one (Table 1)) to be stored in the ROM. Since the n-bit coefficient B needs three bits per digit when encoded in MB form, the ROM width requirement is 3n/2 bits per coefficient. Thus, the width and the overall size of the ROM are increased by 50% compared to the ROM of the conventional scheme (Fig. 3).

International Journal of Innovative Research in Science, Engineering and Technology

(An ISO 3297: 2007 Certified Organization)

Vol. 5, Issue 9, September 2016

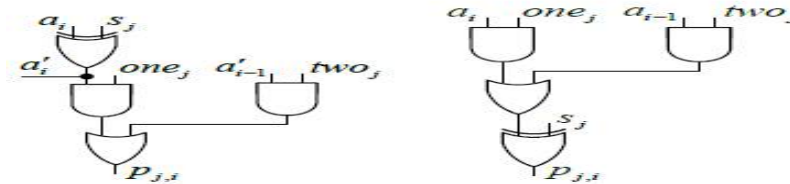


Fig.5 generation of ppj for conventional and pre-encoded mb multiplier.

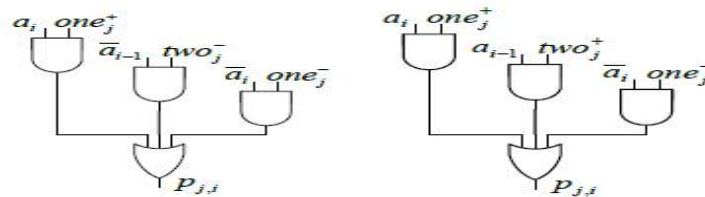


Fig.6 generation of ppj for NR4SD- and NR4SD+ multiplier.

Pre-Encoded NR4SD Multipliers Design

The system architecture for the pre-encoded NR4SD multipliers is presented in Fig. 6. Two bits are now stored in ROM: n_{2j+1} , n_{2j} (Table 2) for the NR4SD or n_{2j+1} , n_{2j} (Table 3) for the NR4SD+ form. In this way, we reduce the memory requirement to $n+1$ bits per coefficient while the corresponding memory required for the pre-encoded MB scheme is $3n/2$ bits per coefficient. Thus, the amount of stored bits is equal to that of the conventional MB design, except for the most significant digit that needs an extra bit as it is MB encoded. Compared to the pre-encoded MB multiplier, where the MB encoding blocks are omitted, the pre-encoded NR4SD multipliers need extra hardware to generate the signals of (6) and (8) for the NR4SD- and NR4SD+ form, respectively. The NR4SD encoding blocks of Fig. 6 implement the circuitry of Fig. 7. Each partial product of the pre-encoded NR4SD- and NR4SD+ multipliers is implemented based on Fig. 4c and 4d, respectively, except for the PP_{k1} that corresponds to the most significant digit. As this digit is in MB form, we use the PPG of Fig. 4b applying the change mentioned in Section 4.2 for the s_j bit. The partial products, properly weighted, and the correction term (COR) of (11) are fed into a CSA tree. The input carry cin_j of (11) is calculated as $cin_j = two_j \cdot one_j$ and $cin_j = one_j$ for the NR4SD- and NR4SD+ pre-encoded multipliers, respectively, based on Tables 2 and 3. The carry-save output of the CSA tree is finally summed using a fast CLA added.

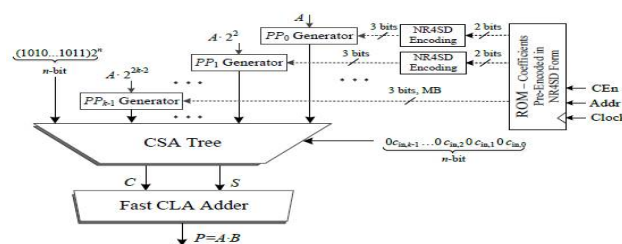


Fig.7 system architecture of NR4SD encoding.

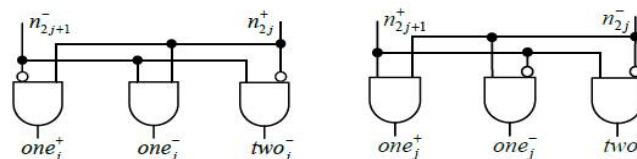


Fig.8 Extra Circuit Needed in the NR4SD Multipliers to Complete the (a) NR4SD- and (b) NR4SD+ Encoding.

V. IMPLEMENTATION RESULTS

We implemented in Verilog the multiplier designs of Table 4. The PPGs for the NR4SD-, NR4SD+ multipliers (Fig. 5) contain a large number of inverters since all the A bits are complemented in case of a negative digit. We used Xilinx's

International Journal of Innovative Research in Science, Engineering and Technology

(An ISO 3297: 2007 Certified Organization)

Vol. 5, Issue 9, September 2016

ise to synthesize the evaluated designs, considering the highest optimization degree and keeping the hierarchy of the designs.

Design		Input A	Input B Encoding		ROM width
			Type	Technique	
Conventional MB		2's complement n -bit	MB	MB encoding	n -bit
Pre-Encoded	MB		MB	Fully Pre-Encoded	$3n/2$ -bit
	NR4SD ⁻		NR4SD ⁻	Partially Pre-Encoded	$(n+1)$ -bit
	NR4SD ⁺		NR4SD ⁺		$(n+1)$ -bit

Table 4.multiplier design

The below table 5 and table 6 are the synthesis results for the modified booth and non-redundant sign digit encoding minus and non redundant sign digit encoding plus for 16 and 32 bits respectively.

	Mb encoding	NR4SD-	NR4SD +
NUMBER OF SLICES	207	129	134
NUMBER OF FLIPFLOPS	11	6	6
4INPUT LUTS	364	222	230
NUMBER OF IOBS	54	54	54

Table 5.synthesis result comparison for 16 bit.

	Mb encoding	NR4SD-	NR4SD +
NUMBER OF SLICES	783	431	393
NUMBER OF FLIPFLOPS	13	8	9
4INPUT LUTS	1402	754	689
NUMBER OF IOBS	102	102	102

Table 6 syntasis result and comparison for 32 bit.

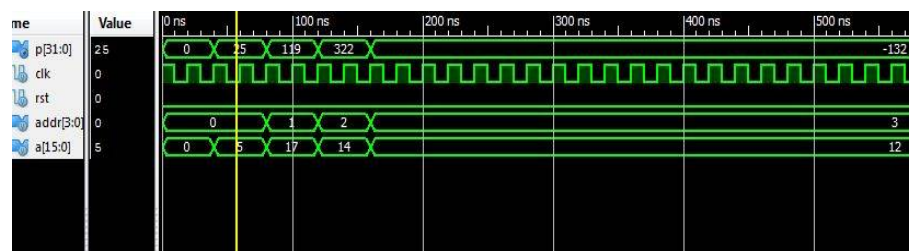


Fig.9 simulation result for modified booth encoding.

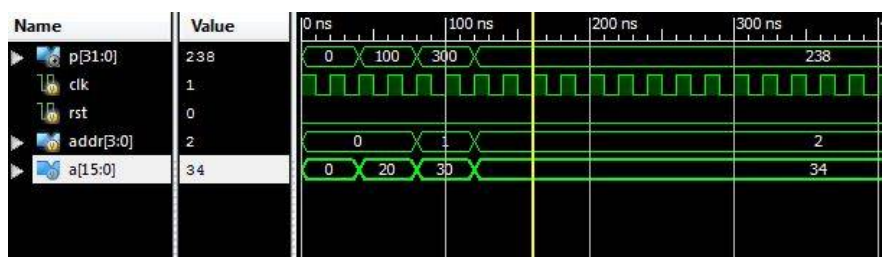


Fig 10 simulation result for NRS4D-encoding

International Journal of Innovative Research in Science, Engineering and Technology

(An ISO 3297: 2007 Certified Organization)

Vol. 5, Issue 9, September 2016

Fig9,fig10,fig11 shows the simulation result for multiplier based on modified booth encoding and non redundant signed digit encoding minus and non redundant signed digit encoding plus respectively.

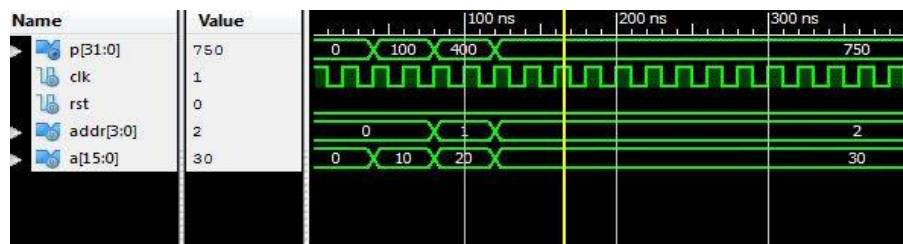


Fig.11 simulation result for NRS4D+encoding.

VI. CONCLUSION

In this paper, new designs of pre-encoded multipliers are explored by off-line encoding the standard coefficients and storing them in system memory. We propose encoding these coefficients in the Non-Redundant radix-4 Signed-Digit (NR4SD) form. The proposed pre-encoded NR4SD multiplier designs are more area and power efficient compared to the conventional and pre-encoded MB designs. Extensive experimental analysis verifies the gains of the proposed pre-encoded NR4SD multipliers in terms of area complexity and power consumption compared to the conventional MB multiplier.

REFERENCES

- [1] G. W. Reitwiesner, "Binary arithmetic," *Advances in Computers*, vol. 1, pp. 231–308, 1960.
- [2] K. K. Parhi, *VLSI Digital Signal Processing Systems: Design and Implementation*. John Wiley & Sons, 2007.
- [3] K. Yong-Eun, C. Kyung-Ju, J.-G. Chung, and X. Huang, "Csdbased programmable multiplier design for predetermined coefficient groups," *IEICE Trans. Fundam. Electron. Commun. Comput. Sci.*, vol. 93, no. 1, pp. 324–326, 2010.
- [4] O. Macsorley, "High-speed arithmetic in binary computers," *Proc. IRE*, vol. 49, no. 1, pp. 67–91, Jan. 1961.
- [5] W.-C. Yeh and C.-W. Jen, "High-speed booth encoded parallel multiplier design," *IEEE Trans. Comput.*, vol. 49, no. 7, pp. 692–701, Jul. 2000.
- [6] Z. Huang, "High-level optimization techniques for low-power multiplier design," Ph.D. dissertation, Department of Computer Science, University of California, Los Angeles, CA, 2003.
- [7] Z. Huang and M. Ercegovic, "High-performance low-power left-to-right array multiplier design," *IEEE Trans. Comput.*, vol. 54, no. 3, pp. 272–283, Mar. 2005.
- [8] Y.-E. Kim, K.-J. Cho, and J.-G. Chung, "Low power small area modified booth multiplier design for predetermined coefficients," *IEICE Trans. Fundam. Electron. Commun. Comput. Sci.*, vol. E90-A, no. 3, pp. 694–697, Mar. 2007.

**Department of
Computer Science and
Engineering**

An Effective Routing for Managing of Critical Issues in Resource Constrained System

Dr. K.Rama Krishna Reddy¹ & Dr. G.Charles Babu²

*¹ Associate Professor, Dept of CSE, Malla Reddy Engineering College (A),
Hyderabad, Telangana.*

² Professor, Dept of CSE, Malla Reddy Engineering College (A), Hyderabad.

Abstract

The most important rationale of multipath routing approach is to accomplish data reliability, security as well as load balancing. Due to nature of multipath routing that employs redundant paths, multipath routing can mostly deal with security, reliability as well as load balancing issues thus, multipath routing plays a significant responsibility in wireless sensor networks. A variety of techniques have been projected in designing proficient multipath routing protocols. Routing concerning single path is easy and scalable, however does not resourcefully convince the requests of resource controlled wireless systems. Multipath routing is a different routing method, which chooses several paths for distribution of data from source towards destination. In our work we put forward the protocols of multipath routing and the advantages in terms of security, reliability as well as load balancing issues. Multipath routing can prevail over important drawbacks concerning single path routing method since it can make available consistent data transmission, constant distribution of network traffic, as well as data security. Multipath routing approach is employed to make progress from failures and helps load balance to keep away from network congestion, which gets better data reliability.

Keywords: Multipath routing, Wireless sensor networks, Security, Redundant paths.

1. INTRODUCTION

A wireless sensor system includes outsized number of light-weight sensor nodes containing restricted battery duration, storage as well as bandwidth. This emerging

knowledge has been accepted by numerous fields as a hopeful solution in the direction of several challenges [1]. In major wireless sensor networks, the nodes are positioned distant from sink and consequently employ the intermediate nodes to direct the data packet in the direction of the sink. Routing in sensor networks is considered as important and it is differentiated from several networks as two types of routing methods, such as single path routing as well as multiple path routing. Routing concerning single path is easy and scalable, however does not resourcefully convince the requests of resource controlled wireless systems. Multipath routing is a different routing method, which chooses several paths for distribution of data from source towards destination. Single path routing is effortless for the reason that the route among source as well as destination node can be recognized in a particular period of time. It is scalable because, even though network changes from ten nodes to ten thousand nodes, difficulty as well as the procedure to determine path remains the similar. In single path routing, existence of a malicious node on path can control and damage the data devoid of catching the consideration of the sink node [2]. Due to nature of multipath routing that employs redundant paths, multipath routing can mostly deal with security, reliability as well as load balancing issues thus, multipath routing plays a significant responsibility in wireless sensor networks. Many procedures of multipath routing were put forward in the literary of wireless systems. In our work we put forward the protocols of multipath routing and the advantages in terms of security, reliability as well as load balancing issues.

2. AN OVERVIEW TOWARDS ADVANTAGES OF MULTIPATH ROUTING

By means of multipath routing we can utilize the obtainable resources at every node more resourcefully. Multipath routing can prevail over important drawbacks concerning single path routing method since it can make available consistent data transmission, constant distribution of network traffic, as well as data security. We specify most important advantages concerning multipath routing procedures over single path routing such as Data Reliability: which is defined as ratio of amount of data which is received by destination node to quantity of data that is sent by source node. Multipath routing enhances data reliability by means of sending the data all along numerous redundant paths. Even if several paths fail, data will contain an extremely high possibility to be received by destination node. Multipath routing approach is employed to make progress from failures and helps load balance to keep away from network congestion, which gets better data reliability. Data Security: Multipath routing can get better security for the reason that of nature of multiple paths. By means of multipath routing, malicious attacks are counter measured by means of increasing confidentiality as well as robustness of the data that is conveyed. By incorporating the coding method with multipath routing, data is transmitted in an encoded structure and merely decoded at the destination node, which put off eavesdrop on sensing data throughout transmission. This approach is proficient and is a perfect mechanism in a resource constrained background since it requires very less energy in encoding as well as decoding than in communications [3]. Energy-Efficient: Wireless sensor nodes contain restricted energy supply; consequently

capable usage of energy is essential to exploit the network duration. Load distribution by means of multipath routing helps to get better network duration by delaying appearance of network partition, even though more data could be conveyed than that by means of single path routing as a result, load can be circulated to multiple paths and every path transmits very less data when compared with a finest single path. In multipath routing, to attain similar level of reliability, with assistance of network coding as well as multiple paths, acknowledgment and re-transmission are avoided, lessening message overhead in addition to providing a longer network duration [4].

3. AN OVERVIEW OF PROTOCOLS CONCERNING MULTIPATH ROUTING

The most important rationale of multipath routing approach is to accomplish data reliability, security as well as load balancing. Multipath routing is a different routing method, which chooses several paths for distribution of data from source towards destination. A variety of techniques have been projected in designing proficient multipath routing protocols. Fig1 shows existing multipath routing procedures into three categories such as: Infrastructure based multipath routing procedures which find out and keep up multiple paths from source towards destination earlier than data transmission, and the entire data are transmitted by means of those which are discovered multiple paths. The most significant features of infrastructure based multipath routing method is safeguarding of several paths from the source in the direction of destination and provides reliable and speedy data transmission since every intermediate node of data routing contain its subsequent hop set up beforehand. It moreover provides the procedure dropping failure recovery time by means of assigning the optional route, which is moreover discovered in advance. Non-infrastructure based multi- path routing procedures do not attempt to set up and maintain multiple paths; instead, they transmit data to numerous next hops based on basis of the local heuristic information [5]. Protocols which do not build any infrastructure to convey the data are measured as non-infrastructure multipath routing protocols and in these the path is revealed as data packet moves forward. One of the most important concerns of non-infrastructure multipath routing is forwarding data packet towards sink which protects the packet from looping in network which not only causes important delay in packet delivery, but moreover wastes lots of energy. Coding Based Multipath Routing procedures consists of multipath routing protocols that employ coding techniques in transmission of data [6]. Most important concern of protocols by means of coding technique is to determine number of sufficient paths, since number of fragments sending all the way through several different exposed paths affects decoding procedure directly at the node of destination.

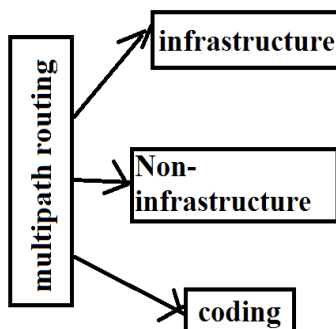


Figure 1: Existing multipath routing procedures.

4. CONCLUSION

Multipath routing is a different routing method, which chooses several paths for distribution of data from source towards destination. Due to nature of multipath routing that employs redundant paths, multipath routing can mostly deal with security, reliability as well as load balancing issues thus, multipath routing plays a significant responsibility in wireless sensor networks. By means of multipath routing we can utilize the obtainable resources at every node more resourcefully. Multipath routing can prevail over important drawbacks concerning single path routing method since it can make available consistent data transmission, constant distribution of network traffic, as well as data security. Many procedures of multipath routing were put forward in the literary of wireless systems. In our work we put forward the protocols of multipath routing and the advantages in terms of security, reliability as well as load balancing issues. Multipath routing approach is employed to make progress from failures and helps load balance to keep away from network congestion, which gets better data reliability. By means of multipath routing, malicious attacks are counter measured by means of increasing confidentiality as well as robustness of the data that is conveyed.

REFERENCES

- [1] P. Kamat, Y. Zhang, W. Trappe, and C. Ozturk, "Enhancing Source-Location Privacy in Sensor Network Routing," Proc. IEEE 25th Int'l Conf. Distributed Computing Systems (ICDCS '05), pp. 599- 608, 2005.
- [2] C. Ozturk, Y. Zhang, and W. Trappe, "Source-Location Privacy in Energy-Constrained Sensor Network Routing," Proc. Second ACM Workshop Security of Ad Hoc and Sensor Networks (SASN '04), pp. 88- 93, 2004.
- [3] Y. Ouyang, Z. Le, G. Chen, J. Ford, F. Makedon, and U. Lowell, "Entrapping Adversaries for Source Protection in Sensor Networks," Proc. IEEE Seventh Int'l Symp. World of Wireless, Mobile and Multimedia Networks (WOWMOM '06), pp. 32-41, 2006.

- [4] X. Wang, X. Li, Z. Wan, and M. Gu, "CLEAR: A Confidential and Lifetime-Aware Routing Protocol for Wireless Sensor Network," Proc. IEEE 20th Ann. Int'l Symp. Personal, Indoor and Mobile Radio Comm. (PIMRC '09), pp. 2265-2269, 2009.
- [5] Y. Li and J. Ren, "Source-Location Privacy through Dynamic Routing in Wireless Sensor Networks," Proc. IEEE INFOCOM, pp. 1-9, 2010.
- [6] Y. Xi, L. Schwiebert, and W. Shi, "Preserving Source Location Privacy in Monitoring-Based Wireless Sensor Networks," Proc. IEEE 20th Int'l Parallel & Distributed Processing Symp. (IPDPS '06), pp. 1-8, 2006.

**IMPROVISATION OF PERFORMANCE IN CLUSTER NETWORKS****Dr. G. Charles Babu*, Mr. K. Rajeshwar Rao**

* Dr. G. Charles Babu, Professor, CSE Dept, MREC (A), Secunderabad

Mr.K. Rajeshwar Rao, Asst. Professor, CSE Dept, MREC (A), Secunderabad

DOI: 10.5281/zenodo.61145**KEYWORDS:** Identity-based digital signature, Wireless sensor network, Cluster, Data transmission, Identity-based cryptography.**ABSTRACT**

Recently identity-based digital signature has been made available as a key management in wireless sensor networks for security. We study effective data transmission meant for cluster-basis sensor system, in our work in which clusters are created dynamically and intermittently. We aim to study the proposals regarding two Secure and Efficient data Transmission procedures for cluster-based wireless sensor networks known as secure and effective data transmission-Identity-based on digital signature and secure and effective data transmission-based on online/offline digital signature. Data transmission protocol based on Identity based online/offline digital signature is projected to further decrease computational overhead for security by means of secure and effective data transmission-based on online/offline digital signature in which security depends on hardness of discrete logarithmic complexity. Identity-based protocol of digital signature on basis of complexity of factoring integers from cryptography of identity-basis is to obtain an entity's public key from its identity information. The important notion of proposed data transmission protocols is to authenticate encrypted sensed data, by means of application of digital signatures which are efficient in communication. Both of these schemes totally work out orphan-node problem from using symmetric key management for cluster-based wireless sensor system.

INTRODUCTION

Data transmissions based on cluster in wireless sensor networks were examined by researchers to attain management and scalability of network, which make the most of node duration and decrease bandwidth consumption by means of local collaboration between sensor nodes [1]. In cluster based wireless sensor networks sensor nodes are set into clusters, in which each cluster include a cluster head sensor node, which is selected independently. In a cluster-based wireless sensor networks every cluster enclose a leader sensor node, known as cluster head which aggregates data that is collected by leaf nodes in its cluster, and forward aggregation to base station. In cluster-based wireless sensor networks data sensing, processing, as well as transmission consume energy concerning sensor nodes. The expenditure of data transmission is extremely pricey than data processing hence system that the intermediate node aggregate data and send it to base station is preferred than technique that each sensor node openly sends data towards base station. We put forward two Secure and Efficient data Transmission procedures for cluster-based wireless sensor networks known as secure and effective data transmission-Identity-based on digital signature (SET-IBS) and secure and effective data transmission- based on online/offline digital signature (SET-IBOOS) [2][3]. These procedures make available protected data transmission meant for cluster-basis sensor system with concrete identity-based settings, which use identity information. The scheme of identity-based digital signature on basis of complexity of factoring integers from cryptography of identity-basis is to obtain an entity's public key from its identity information. In the modern times, identity-based digital signature has been build up as key managing in wireless bandwidth consumption by means of local collaboration between sensor nodes [1]. In cluster based wireless sensor networks sensor nodes are set into clusters, in which each cluster include a cluster head sensor node, which is selected independently. Sensor networks for security. Identity-based online/offline digital signature scheme has been projected to decrease computation as well as storage costs of signature processing.



AN OVERVIEW OF PROPOSED SECURE DATA TRANSMISSION PROTOCOLS MATERIALS AND METHODS

In literature, researchers have been extensively studied cluster-based wireless sensor networks in the past few years in literature. Operation of cluster-based architecture in real world is relatively complicated. The objective of projected secure data transmission meant for cluster-basis sensor system is to assurance and efficient data transmissions among leaf nodes and cluster heads, as well as transmission involving cluster heads and base station. For the most of traditional protocols of secure transmission for cluster-based wireless sensor networks in literature on the other hand, apply symmetric key management intended for security, which undergo from orphan node difficulty we solve orphan node setback by means of Identity based cryptosystem that assurance security requirements, and recommend secure and effective data transmission-Identity-based digital signature. Secure and efficient data transmission-Identity based on online/offline digital signature is projected to further decrease computational overhead for security by means of secure and effective data transmission-based on online/offline digital signature in which security depends on hardness of discrete logarithmic difficulty. In our work we learn secure data transmission meant for cluster-basis sensor system where clusters are created dynamically and intermittently. Secure and effective data transmission- identity based on online/offline digital signature necessitates less energy for computation and storage and is more appropriate for node-to-node communications within cluster basis sensor networks [4]. The key proposal of secure and effective data transmission-Identity-based on digital signature and secure and effective data transmission- based on online/offline digital signature is to authenticate encrypted sensed data, by means of application of digital signatures which are efficient in communication. In these proposed procedures, secret keys as well as pairing parameters are distributed and preloaded in the entire sensor nodes by base station initially, which overcome key escrow difficulty described in ID-based cryptosystems. Secure communication in secure and effective data transmission-Identity-based on digital signature relies on identity basis cryptography, in which, user public keys are their identity information consequently, and users can get hold of corresponding private keys devoid of auxiliary data. Both secure and effective data transmission-Identity-based on digital signature and secure and effective data transmission-identity based on online/offline digital signature solve orphan node difficulty in protected data transmission through symmetric key management.

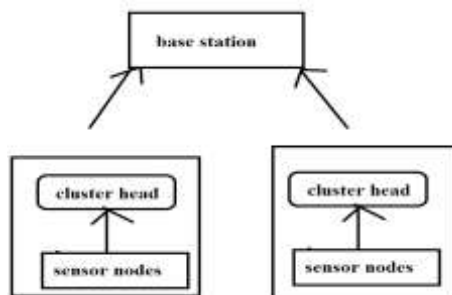


Figure 1: An overview of Cluster system.

CHARACTERISTICS OF PROPOSED PROTOCOL

Both the proposed SET-IBS and SET-IBOOS procedures make available protected data transmission meant for cluster-basis sensor system with concrete identity-based settings, which use identity information as well as digital signature for authentication. Consequently, both of these schemes completely work out orphan-node problem from using symmetric key management for cluster-based wireless sensor networks. When compared with SET-IBS, the procedure of SET-IBOOS necessitates less energy for computation and storage and is more appropriate for node-to-node communications within cluster basis sensor networks as computation is lighter to be performed [5]. In secure and effective data transmission- identity based on online/offline digital signature offline signature is executed by cluster head sensor nodes; consequently, sensor nodes do not have to implement offline algorithm before it wants to mark on a new message. Both secure and effective data transmission-Identity-based on digital signature and secure and identity based on online/offline digital signature solve orphan node difficulty in secure data transmission by means of symmetric key management. The projected SET-IBS include a protocol initialization earlier to the network consumption and operates in rounds throughout communication, which



Global Journal of Engineering Science and Research Management

consists of a setup phase as well as a steady-state phase in each round [6]. By means of this scheme allows well-organized aggregation of encrypted data at the cluster heads and the base station, which moreover guarantees data privacy.

CONCLUSION

We introduce Secure and Efficient data Transmission procedures for cluster-based wireless sensor networks known as secure and effective data transmission-Identity-based on digital signature and secure and effective data transmission- based on online/offline digital signature. The objective of projected data transmission protocol in support of cluster-based wireless sensor networks is to assurance and efficient data transmissions among leaf nodes and cluster heads, as well as transmission involving cluster heads and base station. For conventional protocols of secure transmission for cluster-based wireless sensor networks in literature on the other hand, apply symmetric key management intended for security, which undergo from orphan node difficulty. We solve orphan node problem by means of IDbased cryptosystem that assurance security requirements, and recommend secure and effective data transmission-Identity-based digital signature. The protocol based on online/offline digital signature system has been projected to decrease computation as well as storage costs of signature processing. Both secure data transmission protocols solve orphan node difficulty in protected data transmission through symmetric key management.

REFERENCES

1. K. Pradeepa, W.R. Anne, and S. Duraisamy, "Design and Implementation Issues of Clustering in Wireless Sensor Networks," Int'l J. Computer Applications, vol. 47, no. 11, pp. 23-28, 2012.
2. L.B. Oliveira et al., "SecLEACH-On the Security of Clustered Sensor Networks," Signal Processing, vol. 87, pp. 2882-2895, 2007.
3. P. Banerjee, D. Jacobson, and S. Lahiri, "Security and Performance Analysis of a Secure Clustering Protocol for Sensor Networks," Proc. IEEE Sixth Int'l Symp. Network Computing and Applications (NCA), pp. 145-152, 2007.
4. K. Pradeepa, W.R. Anne, and S. Duraisamy, "Design and Implementation Issues of Clustering in Wireless Sensor Networks," Int'l J. Computer Applications, vol. 47, no. 11, pp. 23-28, 2012.
5. L.B. Oliveira et al., "SecLEACH-On the Security of Clustered Sensor Networks," Signal Processing, vol. 87, pp. 2882-2895, 2007.
6. P. Banerjee, D. Jacobson, and S. Lahiri, "Security and Performance Analysis of a Secure Clustering Protocol for Sensor Networks," Proc. IEEE Sixth Int'l Symp. Network Computing and Applications (NCA), pp. 145-152, 2007.

Decision Tree Clustering and Classification Based One-To-Many Data Linkage

K.Rajeshwar Rao¹, Dr.G.Charles Babu²

Asst. Professor, Dept. of CSE, MREC (A), Secunderabad, India

Professor, Dept. of CSE, MREC (A), Secunderabad, India .

ABSTRACT: Data has its own place and its own value to a valued customer and makes to for strategic decision making. Technology makes us enabling to go next level decision management system in the perspective of the mining the information which is the great boom to the Industry of Automation In the real scenario , Implementation is not that much easy to compete with various vendors who come with various unique features to attract the client. In this paper , we generically giving emphasis on the techno world concept of the mining the data in terms of domain link either in the perspective map reduced one to meant techno mechanism in implementing the algorithmic approach which may in turn make us to give the robust, effective and performance oriented solution . In this Paper we have used the map reduce program to reduce time and effectiveness of the solution to the link various domain keyword on the umbrella of one domain. Hence, we have given the architectural solution to batch based process based on the user requirement to which extend to go forward for the shortest period with strategic decision making process.

KEYWORDS: clustering, classification, data matching, and decision tree induction

I. INTRODUCTION

Generalization is the most prevalent method for table anonymity, and it can also be valuable when inducing k-anonymous decision trees. In generalization, an attribute value is replaced with a less specific but semantically consistent value. In most works, attributes are generalized using a pre-determined hierarchy of values. For example, for a Zip Code attribute, the lowest level of the hierarchy could be a 5-digit zip code. This value could be generalized by omitting the rightmost digit to obtain a 4-digit zip code. Similarly, additional digits could be omitted up to a 1-digit zip code consisting only of the left-most digit. When this digit is omitted as well, the highest level of the generalization hierarchy is reached, with a single value (usually denoted *). Practically, replacing a value with * means suppression of the value. When the market grows, usually no one cares about the churn because the churn rate is low and the customer acquisition is very large.

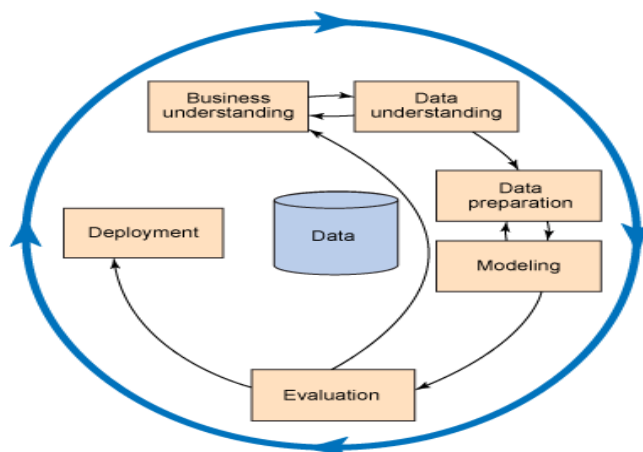


Fig.1.1. Illustration of the Cycle of the Cluster

International Journal of Innovative Research in Computer and Communication Engineering

(An ISO 3297: 2007 Certified Organization)

Vol. 4, Issue 4, April 2016

The profile of each cluster is determined only by attributes which are different from population means; two clusters may have different attributes in their definitions. This method needs to have the data very well prepared.

II. RELATED WORK

It is often used in companies with very large data analysis activities to improve the common set of data analyses. The accepting or rejecting hypotheses task usually starts with some hypothesis (based on manager's intuition) and tries to find a suitable data which can say whether the hypothesis is correct or not. This task has various applications in most of major business activities in a organization. Classification and prediction tasks usually estimate some value for each record. The decision tree is a classifier with a very high capacity. Data mining methods require the data in a specified form, called a table based hash mechanism. Some algorithms for the data mining have particular requirements on data. The data preparation includes all tasks which ensure that the data will be available in a table. Typical tasks solved by data analysis vary from organization to organization, from industry to industry and from country to country. The level of data analysis in a particular industry in a particular country usually depends on the level of data analysis of organization's competitors. But there are some common applications of the data analysis. The first typical application is customer retention. The churn is usually the big problem. The next clustering method is called the EM clustering, or the model based clustering. This method is based on the probability and it can handle more attributes. A minor improvement in the customer acquisition is usually much better than a churn analysis. But one day we can found that the market became exhausted and divided to conquer.

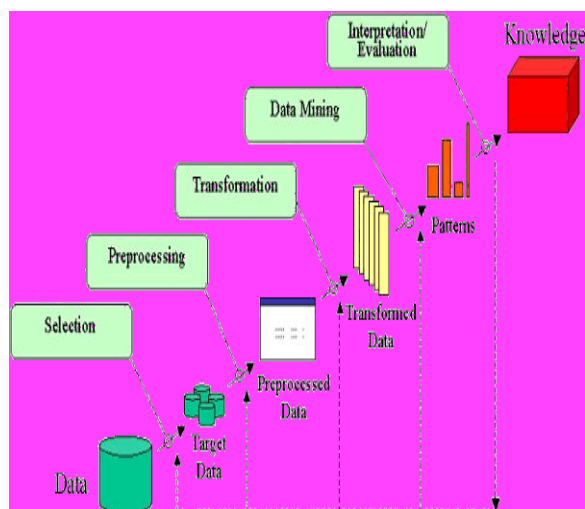


Fig.2.1. Index Based Data Mining in the Ranking Model

When we have an individual person which offers services to his customers, he usually knows his customers, he is able to estimate the profit from each individual customer, and he knows their preferences and so on. So he can estimate who is likely to churn, to whom offer a new product and other business tasks.

III. METHODOLOGY

These models try to estimate which customers are willing to buy some product. Application of propensity to buy models is in selecting the target group for direct marketing campaigns. The typical situation is that the organization has models for all key products. So it can say for each key product to who is good to offer this product. The more advanced application is that the organization estimates the best product for the customer and this is the one which the organization offers him in a direct marketing campaign. To apply the similar task in a organization which has several millions of customers is a very hard issue. The customer segmentation is dividing customers into groups, within these groups customers have similar properties like behavior, the value and preferences and between group customers have different properties. The strategy can be established for every individual segment. The effect of missing values on

International Journal of Innovative Research in Computer and Communication Engineering

(An ISO 3297: 2007 Certified Organization)

Vol. 4, Issue 4, April 2016

model privacy depends on the way they have been treated during the model's induction. If, as is customary in many anonymity preserving algorithms, tuples with missing values are deleted from the database before the algorithm is executed, then the missing values will have no effect on privacy.

Algorithm 3.1 Node Mapping Cluster from One to Many Algorithms

```
1: Input:  $T$  - private dataset,  $A$  - public attributes,  $B$  - private attributes,  $C$ 
   attribute,  $k$  - anonymity parameter
2: procedure MAIN()
3:   Create root node in Tree
4:   Create in root one bin  $b_c$  for each value  $c \in C$ , divide  $T$  among the bins
5:   if  $C \in A$  then
6:     Create one span  $S_c$  for every value  $c \in C$ .  $S_c.Bins \leftarrow \{b_c\}$ ,
        $S_c.Population \leftarrow b_c.Population$ ,  $S_c.Nodes \leftarrow \{root\}$ 
7:     set root.Spans to the list of all spans
8:   else
9:     Create a single span  $s$ . Set  $s.Bins$  to the list of all bins,
        $s.Population \leftarrow T$ ,  $s.Nodes \leftarrow \{root\}$ ,  $root.Spans \leftarrow \{s\}$ 
10:    if  $0 < |s.Population| < k$  then
11:      return nil
12:    end if
13:  end if
14:  for  $att \in A \cup B \setminus \{C\}$  do
15:    add (root, att, gain(root, att)) to Queue
16:  end for
17:  while Queue has elements with positive gain do
18:    Let  $(n, a, gain) = \arg \max_{gain} \{Queue\}$ 
19:    if  $n.sons \neq \emptyset$  then
20:      continue
21:    end if
22:    if Breach( $n, a, k$ ) then
23:      if  $a$  has generalization  $a'$  then
24:        insert  $(n, a', gain(n, a'))$  to Queue
25:      end if
26:    else
27:      Split( $n, a$ )
28:    end if
29:  end while
30:  Set the Class variable in each leaf to the value with the largest bin.
31:  return Tree
32: end procedure
```

The suppression of tuples with missing values can be formalized by modeling it as splitting the root node on a binary public attribute that marks the existence of missing values. All tuples with missing values are routed to a distinct leaf in which no private information is provided. Since no private values are provided in this leaf, it comprises a span with a

International Journal of Innovative Research in Computer and Communication Engineering

(An ISO 3297: 2007 Certified Organization)

Vol. 4, Issue 4, April 2016

single equivalence class, thereby maintaining anonymity regardless of the number of suppressed tuples. Suppression of tuples with missing values, however, might strongly bias the input and might also produce a poorer outcome as a result, especially when missing values are abundant. Another possible approach would be to treat a missing value as a value in its own right, and then analyze the privacy of the model using the methods described earlier for regular values.

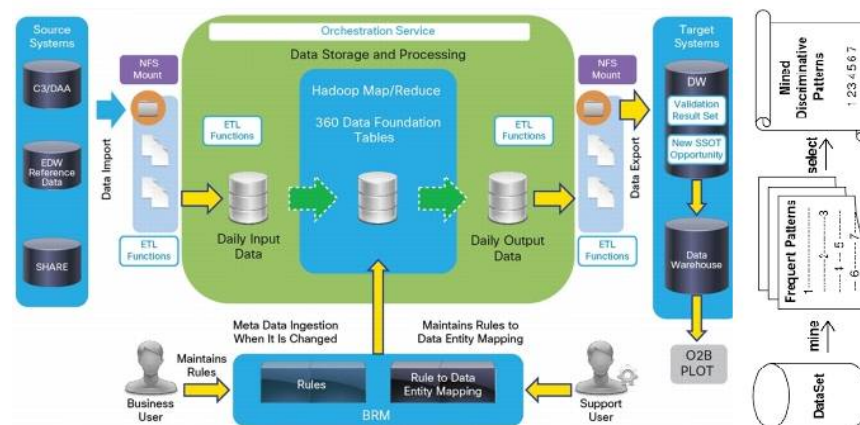


Fig.3.1. Architectural Model View of the Map Reduce Design

We should better focus on high value segments; ask how to convert customers from low value segments into high value segments, to develop products for segments and so on. Many of these results become to be regular reports. The data description task has various applications, including a costs analysis and a customer behaviour analysis. The Data Exploration task is a task where the only goal is to find something that will help to solve some (usually given) business problem. The data exploration is a very interesting task, but it is not so typical, because there is no guarantee that investments into this data analysis will bring any results/benefits. The analysis of the best product for the customer is a very advanced analysis. It usually requires all propensities to buy models for individual products, profit analyses for products and the other information which also comes from the strategy of the organization. Ensuring that results of modeling are usable for the business application is a very crucial thing. We should focus on data sources available. In this phase, we should explore, which data sources are available, to obtain the data, to profile the data, attributes and their values, to identify problems with the data (quality, availability, checking whether the data are up-to-date, periodicity of data refreshment) and to exactly formulate the problem in the language of the data (to extend the problem definition with specific attribute names and values). In the Data Description task, the goal is usually to organize and visualize the data, maybe in a form in which the data were not displayed and this can bring a new knowledge to the organization. The data description task is a typical task of the data analysis. The K-means clustering is a widely used method in a situation, where we have only a few attributes (less than 10) and all attributes are important in all cluster profiles. Applications of the K-means clustering include a demographical segmentation and supplementary segmentations for prediction models.

3.1 Evaluation and Analysis

It has been chosen as the first method intentionally decision trees are what this work is about. Here we provide only a brief description. Decision trees will be described in a more detail later. The decision tree induction is a method based on two principles. The first principle is called divide and conquer. This means, that in every step, the dataset is split into two or more parts and the algorithm continues recursively on individual parts. The second principle is a greedy principle. That means that the splitting is based only on little information. Decision trees are used mainly for predictions, classifications and descriptions.

International Journal of Innovative Research in Computer and Communication Engineering

(An ISO 3297: 2007 Certified Organization)

Vol. 4, Issue 4, April 2016

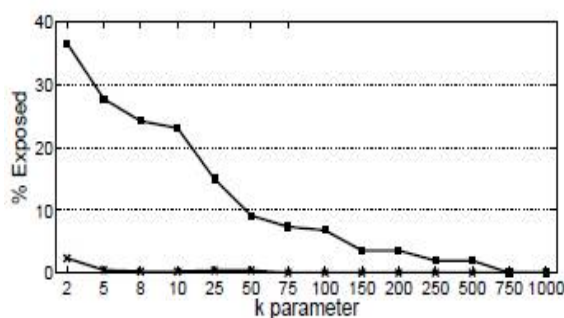


Fig.3.1.1. Comparison of the Nodes

The evaluation phase also deals with consequences of data quality problems. This phase should find any mistakes we could have made during all previous phases.

IV .CONCLUSION AND FUTURE WORK

Technology has its own limitation to extend which needs future research. A data owner who wishes to publish a decision tree while maintaining customer anonymity can use this technique to induce decision trees which are more accurate than those acquired by anonymizing the data first and inducing the decision tree later. This way, anonymity is done in a manner that interferes as little as possible with the tree induction process. To the best of our knowledge, this problem was not studied before in the context of anonymization and privacy. According to our experiments, the utility of handling missing values may change in accordance with the specific data set at hand and the anonymity parameter. Nevertheless, the inability to handle missing values might render data sets with abundant missing values unusable.

REFERENCES

- [1] I.P. Fellegi and A.B. Sunter, "A Theory for Record Linkage," J. Am. Statistical Soc., vol. 64, no. 328, pp. 1183-1210, Dec. 1969.
- [2] M. Yakout, A.K. Elmagarmid, H. Elmeleegy, M. Quzzani, and A.Qi, "Behavior Based Record Linkage," Proc. VLDB Endowment, vol. 3, nos. 1/2, pp. 439-448, 2010.
- [3] J. Domingo-Ferrer and V. Torra, "Disclosure Risk Assessment in Statistical Microdata Protection via Advanced Record Linkage," Statistics and Computing, vol. 13, no. 4, pp. 343-354, 2003.
- [4] F. De Comite, F. Denis, R. Gilleron, and F. Letouzey, "Positive and Unlabeled Examples Help Learning," Proc. 10th Int'l Conf. Algorithmic Learning Theory, pp. 219-230, 1999.
- [5] M.D. Larsen and D.B. Rubin, "Iterative Automated Record Linkage Using Mixture Models," J. Am. Statistical Assoc., vol. 96, no. 453, pp. 32-41, Mar. 2001.
- [6] S. Ivie, G. Henry, H. Gatrell, and C. Giraud-Carrier, "A Metric-Based Machine Learning Approach to Genealogical Record Linkage," Proc. Seventh Ann. Workshop Technology for Family History and Genealogical Research, 2007.
- [7] A.J. Storkey, C.K.I. Williams, E. Taylor, and R.G. Mann, "An Expectation Maximisation Algorithm for One-to-Many Record Linkage," Univ. of Edinburgh Informatics Research Report, 2005.
- [8] P. Christen and K. Goiser, "Quality and Complexity Measures for Data Linkage and Deduplication," Quality Measures in Data Mining, vol. 43, pp. 127-151, 2007.
- [9] P. Langley, Elements of Machine Learning. Morgan Kaufmann, 1996.
- [10] H. Blockeel, L.D. Raedt, and J. Ramon, "Top-Down Induction of Clustering Trees," ArXiv Computer Science e-prints, pp. 55-63, 1998.
- [11] D.J. Rohde, M.R. Gallagher, M.J. Drinkwater, and K.A. Pimblett, "Matching of Catalogues by Probabilistic Pattern Classification," Monthly Notices of the Royal Astronomical Soc., vol. 369, no. 1, pp. 2-14, May 2006.
- [12] L. Gu and R. Baxter, "Decision Models for Record Linkage," Data Mining, vol. 3755, pp. 146-160, 2006.
- [13] P. Christen and K. Goiser, "Towards Automated Data Linkage and Deduplication," technical report, Australian Nat'l Univ., 2005.
- [14] E. Frank, M.A. Hall, G. Holmes, R. Kirkby, and B. Pfahringer, "WEKA - A Machine Learning Workbench for Data Mining," The Data Mining and Knowledge Discovery Handbook, pp. 1305-1314, Springer, 2005.
- [15] J.R. Quinlan, C4.5: Programs for Machine Learning. Morgan Kaufmann, 1993.
- [16] O. Benjelloun, H. Garcia, D. Menestrina, Q. Su, S. Whang, and J. Widom, "Swoosh: A Generic Approach to Entity Resolution," The VLDB J., vol. 18, no. 1, pp. 255-276, 2009.
- [17] S.E. Whang and H. Garcia-Molina, "Joint Entity Resolution," technical report, Stanford Univ., 2009.



ISSN(Online): 2320-9801
ISSN (Print): 2320-9798

International Journal of Innovative Research in Computer and Communication Engineering

(An ISO 3297: 2007 Certified Organization)

Vol. 4, Issue 4, April 2016

BIOGRAPHY



¹**Mr. K. RAJESHWAR RAO** (ISTE, CSI Life Member), working as Asst. Professor in Department of Computer Science and Engineering, Malla Reddy Engineering College, MREC (A), Secunderabad, Telangana State. He has rich teaching experience and his research domains are Data mining, cloud computing, Computer Networks, software engineering.



²**Dr. G. Charles Babu** completed B.Tech from KLCE in 1997 and M.Tech from JNTU in 1999. He Completed his Ph.D in ANU, Guntur in 2015. He has 17 Years of Teaching Experience and Presently Working as a Professor in MREC(Autonomous), Hyderabad. His Research areas are Data Mining, Cloud Computing, Networks and Image Processing.

A Survey on Security Challenges in Cloud Computing

Dr.K.Ratna Babu ¹, Dr.G.Charles Babu ²

Lecturer, Department of Computer Engineering, Government Polytechnic, Addanki, Prakasam Dt, A.P.India¹

Professor, Department of C S E, Malla Reddy Engineering College(Autonomous), Hyderabad, Telangana, India²

ABSTRACT: The importance of the cloud is increasing exponentially and people start realising the reliability, scalability, and efficiency of the cloud computing. In recent generation since around 2008 the hype increasing like anything. Dramatically the cloud size increasing, and the problems also in the same fashion. Despite the potential advantages of cloud the organizers are slow down accepting the cloud services provided by service providers. In cloud the organizations store their data by handover it to service providers or third party who own the infrastructure. In this way the data is most vulnerable in cloud network it is obvious that there is lots of security issues need to be concern both for the normal client and business oriented client. Although the service providers guarantee the security in terms of technical aspects, but it is very difficult to achieve clients trust. In the present paper a review on security issues, how to challenge them and cloud manageability is presented.

KEYWORDS: Cloud, security issues, cloud networks, cloud services, cloud computing.

1. INTRODUCTION

Cloud services become more popular for even for a normal person because people can access social networking sites, photo sharing sites, email and chatting. The Cloud computing refers internet services which allow the clients to save their data at remote locations instead of using home hard disk or any other home devices. In cloud the client uses some others resources to store their data and applications. Here the clients store their personal data or business data or both in the remote systems. The clients need not to purchase any infrastructure or need not to upgrade their infrastructure at home or their organizations. That means client utilises some others infrastructure which are placed domestic or foreign whereabouts. The cloud not only provides data storage facility it provides lot of shard base pool of sources. Like grid computing the clients can share all the resources of the cloud. Heterogeneous systems and platforms can share all the resources. The cloud provides different resources like networks, softwares, and operating systems. The client need not to spent money on purchasing all these resources to process all their current and future requirements. The cloud user can use third party infrastructure to store all the data or to process the data. The cloud can take the data as input from the client and implement some operations on the data as per the client requirement and updates the results back to client, which are obtained from the operations done in cloud. These operations are done with the help of softwares available on cloud. So the clients need not to install the softwares on systems. So, the client can avoid unnecessary software installations time, and upgrading new software configurations. Indirectly the user is hiring required software and hard ware from service provider.

In this way the cloud extends the services for an organization or individual to increase their capabilities. They need not to spent heavy expenditures to renew their software licence, investing in up gradation of hardware, save time in training to run softwares. The statistics are saying that cloud computing has grown enormously than any other segment in IT. Day by day the number of organizations and individual clients is drastically increasing in cloud segment. Although the companies and users are more enthusiastic in amalgamation to cloud, still users are more concern about their privacy and security. Despite of their interest towards cloud services they are more anxiety about data security and privacy.

International Journal of Innovative Research in Science, Engineering and Technology

(An ISO 3297: 2007 Certified Organization)

Vol. 5, Issue 5, May 2016

Still Cloud services are popular because of their reliability, efficiency, and scalability. The cloud provides unlimited storage capacity, more reliable to access the day from anywhere in the universe, and more efficient because it allows the companies to run their applications successfully more accurately even in the absence of their products. Despite of their fear clients are excited to used cloud services because it drastically reduces infrastructure maintenance cost and complex in networks. Clouds can also provide extra services in which providers are expertise to some small companies, such as email systems, along with data maintenance.

The cloud computing has been defined by the U.S. National Institute of Standards and Technology (NIST) as, “the cloud computing is a model for enabling convenient, on-demand network access to a shared pool of configurable computing resources (e.g., networks, servers, storage, applications, and services) that can be rapidly provisioned and released with minimal management effort or service provider interaction”. [1][2].

Cloud has potential benefit of providing high security to clients by storing all the data in highly secured control rooms. Cloud has less prone of loss of data from their data management systems. The data will be stored in highly technical infrastructure located in one domicile or domestic they can be retrieved even in case of natural calamities. The multinational companies can serve their clients throughout the world by sharing their data into different cloud servers located at different nations. Social networking sites, multinational organizations run their operations successfully with the help of cloud providers. But the locating and sharing of data between servers may raise the scale of exposure to possible breaches both accidental and deliberately [3]. Some cloud providers sharing their customer personal information to business organization or some other adverting agency for their benefit without providing full information to the customer. The client them self must be vigilant while sharing their data to cloud to whom it is shared and on what network and on what type of condition. Only the client need to be assured by them to which provider they are sending and in this context there must be transparency between a client and cloud provider.

Hence, the clients are more stimulating to reduce capital cost and divert that amount for the future expansion and research. But, finally the standards are immature and insufficient to handle current technologies [4]. A user has to consider many factors while moving into cloud. They have to check the availability of good internet connections to avoid data latency. In natural calamities, network failures, clients need to confirm how cloud service providers are able to secure clients data and how the cloud providers giving privacy to their cluster of data.

II. ARCHITECTURE OF CLOUD COMPUTING

As per NIST the cloud is composed of five essential characteristics, three service models, and four deployment models [1][4]. Typical cloud architecture looks as shown in figure 1. It contains clients accessing cloud resources through terminals and various cloud service providers [7].

2.1 Essential Characteristics

2.1.1 Resource Pooling: It describes about the clients selects a service or multiple services from pooled resources available at the service provider or third party who own the infrastructure. The pool of resources contains storage, software, and network infrastructure resources. Broad network access allows sharing services to different organizations via internet or private networks. These resources are pooled as part of service delivery. This type of pooling system services are provided as tenant to serve their services through various resources.

International Journal of Innovative Research in Science, Engineering and Technology

(An ISO 3297: 2007 Certified Organization)

Vol. 5, Issue 5, May 2016

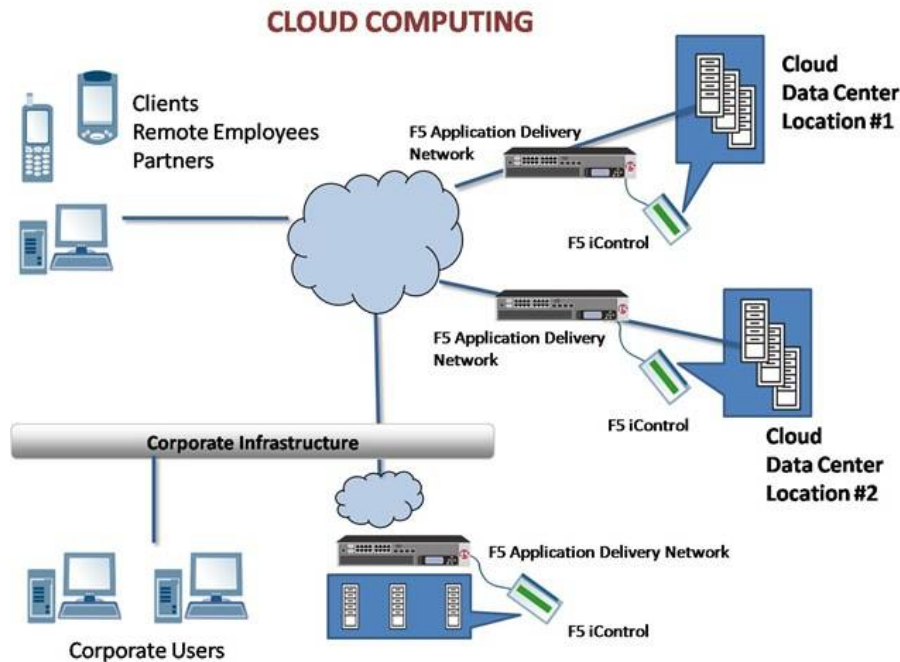


Figure 1: Basic Cloud Architecture [7]

- 2.1.2 **Resource Egalitarianism:** This labels that any user on the cloud can access all types of cloud services. All the pooled resources made available by the service provider, and grant authentication to all clients on the network to access the resources by standard methods.
- 2.1.3 **Service oriented Architecture:** As the abstraction of infrastructure from cloud application yields that cloud resources are allowed to access but not management of infrastructure by cloud democratic clients. On-demand self-service means usually organizations can request and manage their own computing resources.
- 2.1.4 **Rapid Elasticity:** This indicates the size of the cloud service. The client can select the number of services and the scale of the cloud. According the scale of the cloud the client pay bill to the provider. For instance, the domain owner will pay the maintenance bill to the service provider according to the size of the resources in terms of the storage, software, and server services allocated to the client that to for a stipulated time period. The client at any time can increase his requirement level capacity. Dynamically the service provider must be able to provide all the extra resources demanded by the client. Since all resources are pooled at the cloud the client can achieve maximum services that they demanded.
- 2.1.5 **Utility model of consumption and allocation:** The rapid elastic nature of cloud tightly automated. The automated cloud has a provision of self service provider. It allocates services dynamically depends upon the utilization scale of the customer. The utilization scale is representing the client previous usage and demanded for resources. These measurements help the customer a lot to predict the current usage level. Hence the client will pay only for the required level of services. For instance the mobile network utilizer can select appropriate plan based on the reviews and predictions produced by automated software provided by network provider.

International Journal of Innovative Research in Science, Engineering and Technology

(An ISO 3297: 2007 Certified Organization)

Vol. 5, Issue 5, May 2016

2.2 Service Models

The service of the cloud is deployed to client in three model forms. Service providers may also include systems integrators that build and support data center hosting private clouds and they offer different services. The cloud user has no idea and worry about the internal arrangement of the cloud service provider network [4][5][6][8]. Service models allow the clients to develop complete Software Development Life Cycle. The cloud computing service models used to deploy client services are Software as a Service (SaaS), Platform as a Service (PaaS) and Infrastructure as a Service (IaaS). IaaS is the base layer for all service levels, and SaaS building upon PaaS as shown in figure 2.

2.2.1 Software as a Service (SaaS): In this model a complete pre- defined application along with any required software is provided to the client. On the user side the users no need to invest for software up gradation and purchase new software. Only a single application needs to be installed and managed by the customer. The customer has no rights to control network, operating system, servers, and infrastructures. SaaS is accessed via web browsers over internet. So Web browser security is important. Startups and business people can run their ideas on SaaS with collaboration of service providers.

2.2.2 Platform as a Service (PaaS): In this model system software is provided as service to create a development environment. The customer has a freedom to design their own application which runs under cloud infrastructure. The Virtual machines provide the PaaS layer in cloud computing. Virtual Machines must be protected by malicious software by accurate authentication throughout the network.

2.2.3 Infrastructure as a Service (IaaS): This model providing all storage services and computation capabilities to the client. Some cloud providers are providing this service with free of cost up to certain storage limit which is more help full for researchers, startups, and other small scale clients. IaaS allows startups and other business clients to consume the infrastructure without worrying to spend expenditures on core infrastructure developments. The Cloud is compelled to spend more expenditure on IaaS but now many of the providers came out from this problem as the IaaS tenants number is growing. The History of cloud computing is shown in figure 3 [7].

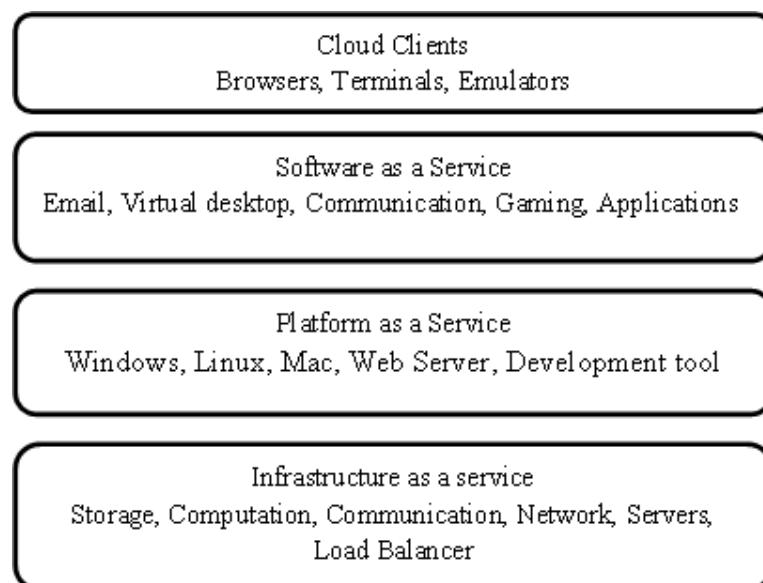


Figure 2: Levels of Cloud service Delivery models

International Journal of Innovative Research in Science, Engineering and Technology

(An ISO 3297: 2007 Certified Organization)

Vol. 5, Issue 5, May 2016

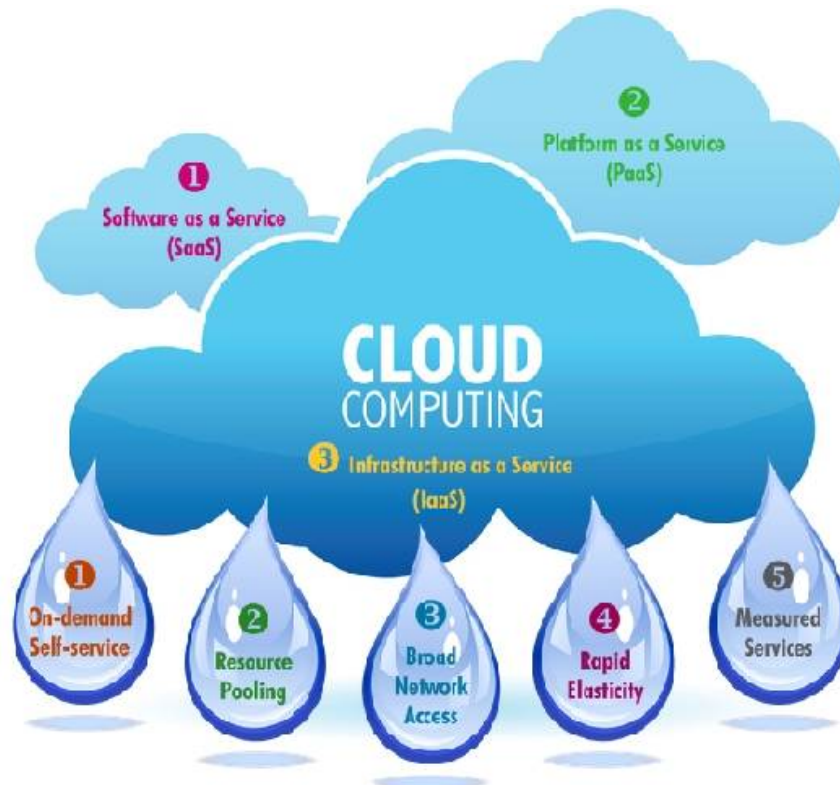


Figure 3: History of Cloud Computing

2.3 Deployment models

There are four ways of how a cloud provider deploys the services to the client. They are Public, Private, Community, and Hybrid cloud [4][8].

2.3.1 Public Cloud: Public cloud is designated by cloud provider and services are offered by internet. Public clouds are operated with multi-tenant and offers benefits of elasticity and the accountability/utility model of cloud [4]. Public clouds are less secure and less privacy when compared with other clouds, because the documents in the cloud are accessible and manageable by different clients.

2.3.2 Private Cloud: The private cloud is designated for an organization or few organizations. The data is setup for that organization only. It provides high security and privacy, but costs more to deploy separate architecture for an organization. That means it allows only those organizations can access pool of resources in the cloud. There is possibility of security threat for private cloud because of possibility of malicious software attacks and hackers from outside competitors.

2.3.3 Community Cloud: This cloud is created between know people. In recent days people are complaining about their data security and privacy. They are managed by cloud providers. As the community cloud network increasing enormous problems are facing by clients and as well as by the cloud provider. There is problem of losing sensitive data in community cloud. There is chance of hack the client data base for misuse or steal the information of an person or organization. They have a large benefit of elasticity and the accountability/utility model of cloud.

2.3.4 Hybrid Cloud: It is the combination of both public and private cloud. Hybrid cloud is a private cloud linked to one or more external cloud services, centrally managed, provisioned as a single unit, and circumscribed by a secure network [9]. It provides virtual IT solutions through a mix of both public and private clouds [8]. It allows different clients to access the cloud services through different gadgets and networks. In hybrid cloud, a service

International Journal of Innovative Research in Science, Engineering and Technology

(An ISO 3297: 2007 Certified Organization)

Vol. 5, Issue 5, May 2016

provider utilizes third party services to increase flexibility of computing. Here the clients need to ensure the authentication of the third party service provider. The cloud provider must be transparent in providing the details of third party.

III. SECURITY AND PRIVACY ISSUES IN CLOUD

The cloud includes various technologies like database, network, operating system, softwares, virtualisation, and storage management. So, security issues of these systems are applicable to cloud. Also virtualization leads many security concerns. Data security is highly essential while copying data from virtual machines to physical machines. Data base systems must effectively work in detecting malware software systems and intruders [4][10][11][12]. Mainly there are four types of issues need to be considered while discussing security issues. They are Data issues, Privacy issues, infected applications, and Security issues.

III.1 Data Issues

In the cloud from anywhere and anyone can fetch the data in the cloud. It is very embarrassing if somebody sees or acquires one's sensitive data. It is a very big challenge in cloud to provide security from intruders and avoiding accessing one's account by some other or un known person. In some cases the cloud providers does not store the data directly in their systems. The cloud providers store the data at third party vendors to save their infrastructure or to reduce expenses or to provide high security. This may lead data steal in the cloud. In this case it is very important for a client to know third party location. During data transition there may be a chance of data loss. The data loss may occur due to network failure on the cloud infrastructure, power failures, natural calamities, or due to legal problem. Some cases the cloud provider receives the data and computation on the data is done at some third party agencies. After the computation the results again store at cloud provider to allow the client to access the results. During the data transition there is a chance o misuse the sensitive data by intruders.

III.11 Privacy Issues

It mainly deals with customer personal and sensitive information. The community cloud there is a chance of external people interference in their account. Although there is proper and secure authentication other will intrude into the cloud because of client mistakes or innocence.

III.III Infected Applications

This is mainly deals with malicious software. This type of problem may severely damage the client system but also cloud service models. The providers and client must be aware of the softwares they are using and downloading. This method can prevent downloading unknown and malicious software.

III.IV Security Issues

The cloud computing service provider makes sure that there service is secured and less threatened. Although the service providers provide security the clients need to be ensuring that there is no loss in the data or steal. A service provider is said be successful only if they able to provide a secure data and creates trust in client minds.

IV. TECHNIQUES TO FACE SECURITY ISSUES IN CLOUD

The data issues can be managed by providing proper authentication while logging into cloud. While using third party vendors it is very important to see that they are providing their services under government rules and regulations. There must be a regular government committee to see all cloud activities and third party activities at regular intervals of time. The privacy of a customer can be maintained by regular monitoring of the server provider and be sure who is maintaining server. Proper anti-virus softwares must be installed both in client and at cloud provider side. Cloud provider must ensure these softwares must be regularly upgraded. Typically the virtual machines provide high security with the help of virtual network separator.

International Journal of Innovative Research in Science, Engineering and Technology

(An ISO 3297: 2007 Certified Organization)

Vol. 5, Issue 5, May 2016

V. CONCLUSIONS

The cloud is creating wonders and revolutions in the internet world. Although it has many advantages it is also highly essential to think about challenges in the cloud computing securities. The scale of cloud services are radically increasing but still it need have improvement in the scale when compared with size of network. The cloud service providers need to be very cautious who is uploading and what content on the cloud. It is highly essential for the service providers to scan their data base with high and efficient softwares. For accessing sensitive data client authentication is highly essential to login and accessing the data. Service providers also need to check their virtual machines locations and who is operating those machines. The service providers need to check their cloud network throughout their network regularly, for identifying intruder, malwares, port disconnections, power loss, wavering of hardware, and local disasters. Finally for cloud providers, it is very important to offer their services within the national legal issues and obligations to gain the client trust. Before all, the client prime responsibility is use cloud by knowing the service providers details. It is highly secure to use standard cloud service providers, genuine and who are registered organizations. Still many governments are framing rules for cloud to face security issues and other obligations in critical situations.

REFERENCES

- [1] NIST cloud definition, version 15 <http://csrc.nist.gov/groups/SNS/cloud-computing/>
- [2] Badger, L., Grance, T., Patt-Corner, R., & Voas, J. (2011). Draft Cloud Computing Synopsis and Recommendations. National Institute of Standards and Technology (NIST) Special Publication 800-146. US Department of Commerce. May 2011. Available online at: <http://csrc.nist.gov/publications/drafts/800-146/Draft-NIST-SP800-146.pdf>.
- [3] Casola, V., Cuomo, A., Rak, M. and Villano, U. (2013). The CloudGrid approach: Security analysis and performance evaluation. Future Generation Computer Systems, 29, 387–401. doi:10.1016/j.future. 2011.08.008.
- [4] Jaydip Sen, "Security and Privacy Issues in Cloud Computing", Technical Report, Innovation Labs, Tata Consultancy Services Ltd., Kolkata, India.
- [5] Rabi Prasad Pet al., "Cloud Computing: Security Issues and Research Challenges", IJCSITS, Vol. 1, No. 2, December 2011.
- [6] Monjur Ahmed et al., "Cloud computing and security issues in the cloud", IJNSA, Vol.6, No.1, January 2014, pp25-36.
- [7] Technical report by http://america.pink/cloud-computing_1024784.html
- [8] Kuyoro S. O, "Cloud Computing Security Issues and Challenges", (IJCN), Volume (3) : Issue (5) : 2011, pp247-255.
- [9] Global Netoptex Incorporated. "Demystifying the cloud. Important opportunities, crucial choices." pp4-14. Available: <http://www.gni.com> [Dec. 13, 2009].
- [10] Sen, J. & Sengupta, I. (2005). Autonomous Agent-Based Distributed Fault-Tolerant Intrusion Detection System. In Proceedings of the 2nd International Conference on Distributed Computing and Internet Technology (ICDCIT'05), pp. 125-131, December, 2005, Bhubaneswar, India. Springer LNCS Vol 3186.
- [11] Sen, J., Sengupta, I., & Chowdhury, P.R. (2006b). Architecture of a Distributed Intrusion Detection System Using Cooperating Agents. In Proceedings of the International Conference on Computing and Informatics (ICOCI'06), pp. 1-6, June, 2006, Kuala Lumpur, Malaysia.
- [12] Sen, J., Ukil, A., Bera, D., & Pal, A. (2008). A Distributed Intrusion Detection System for Wireless Ad Hoc Networks. In Proceedings of the 16th IEEE International Conference on Networking (ICON'08), pp.1-5, December 2005, New Delhi, India.
- [13] Irena Bojanova et al., "Cloud Computing", IT Pro, IEEE Computer Society, doi: 1520-9202/13, March/April 2013.
- [14] Ting Wang, "Rethinking the Data Center Networking: Architecture, Network Protocols, and Resource Sharing", Journal for Rapid open acces, IEEE Access, Vol 2 2014, pp1481-1496.

Cloud Environment Using Many Phrasal Words Concealment Preserving To Perform Safe Search

N.GRACE NAOMI

M.Tech Student, Dept of CSE
Malla Reddy Engineering College
Hyderabad, T.S, India

Dr. G. CHARLES BABU

Professor, Dept of CSE
Malla Reddy Engineering College
Hyderabad, T.S, India

Dr. CH. RAMESH BABU

Dept of CSE
Malla Reddy Engineering College
Hyderabad, T.S, India

Abstract: Using the development of cloud computing, it's increasingly popular for data entrepreneurs to delegate their data to public cloud servers while enabling data clients to retrieve this data. For privacy concerns, secure searches over encoded cloud data have motivated several research works beneath the single owner model. However, most cloud servers used don't merely serve one owner rather, they support multiple entrepreneurs to speak about the benefits created by cloud computing. In this particular paper, we advise schemes to deal with Privacy safeguarding Ranked Multi-keyword Search in the Multi-owner model (PRMSM). To allow cloud servers to complete secure search lacking the knowledge of the specific data of both keywords and phrases and trapdoors, we methodically create a manuscript secure search protocol. To put searching results and preserve the privacy of relevance scores between key phrases and files, we advise a manuscript Additive Order and Privacy Safeguarding Function family. To prevent the attackers from eaves shedding secret keys and pretending to get legal data clients posting searches, we advise a manuscript dynamic secret key generation protocol plus a new data user authentication protocol. Additionally, PRMSM supports efficient data user revocation. Extensive experiments on real-world datasets browse the effectiveness and efficiency of PRMSM.

Keywords: Cloud Computing; Ranked Keyword Search; Multiple Owners; Privacy Preserving; Dynamic Secret Key.

I. INTRODUCTION

Cloud computing can be a subversive technology that is modifying the way hardware and software are designed and acquired [1]. As new of computing, cloud computing provides abundant benefits including fast access, decreased costs, quick deployment and versatile resource management, etc. Companies of dimensions can leverage the cloud to increase innovation and collaboration. Whatever the abundant benefits of cloud computing, for privacy concerns, people and enterprise users are reluctant to delegate their sensitive data, including emails, personal health records and government confidential files, for the cloud. Cloud providers (CSPs) would promise to make certain owners' data security using mechanisms like virtualization and firewalls. However, these mechanisms don't safeguard owners' data privacy from the CSP itself, since the CSP offers full control of cloud hardware, software, and owners' data. Encryption on sensitive data before outsourcing can preserve data privacy against CSP. Just like a matter of fact, most cloud servers used don't just serve one data owner rather, they often times support multiple data entrepreneurs to speak about the benefits created by cloud computing. In contrast while using single-owner plan, developing a full-fledged multi-owner plan will have many new challenging problems. First, inside the single owner scheme, the data owner must stay online to generate trapdoors for

data users. Second, since nobody could be ready to share our secret keys with others, different data entrepreneurs would prefer to use their particular secret strategies of secure their secret data. Third, when multiple data entrepreneurs are taking part, we have to ensure efficient user enrollment and revocation systems, to make sure that our physiques likes excellent security and scalability. In this particular paper, we advise PRMSM, a privacy preserving ranked multi-keyword search protocol in a multi-owner cloud model. To permit cloud servers to perform secure search lacking the knowledge of the actual value of both keywords and phrases and trapdoors, we systematically construct a manuscript secure search protocol. As a result, different data entrepreneurs use different keys to encrypt their files and keywords and phrases. Authenticated data users can issue an issue lacking the knowledge of secret keys of these different data entrepreneurs [1]. To put the search results and preserve the privacy of relevance scores between keywords and phrases and files, we advise a completely new additive order and privacy safeguarding function family, which supports the cloud server return most likely probably the most relevant search results in data clients without revealing any sensitive information. To prevent the attackers from eaves dropping secret keys and pretending to get legal data clients posting searches, we advise a novel dynamic secret key generation protocol plus a new data user

authentication protocol. Consequently, attackers who steal the important thing key and perform illegal searches would be easily detected. Additionally, once we want to revoke an info user, PRMSM ensures efficient data user revocation. Extensive experiments on real-world datasets browse the effectiveness and efficiency of our proposed schemes. The main contributions from the paper are listed as follows:

- We define a multi-owner model for privacy preserving keyword search over encoded cloud data.
- We advise a reliable data user authentication protocol, which not only prevents attackers from eaves dropping secret keys and pretending to be illegal data clients transporting out searches, but also enables data user authentication and revocation.
- We methodically produce a novel secure search protocol, which not only enables the cloud server to perform secure ranked keyword search without knowing the specific data of both keywords and trapdoors, but furthermore allows data entrepreneurs to encrypt keywords and phrases with self-selected keys and allows authenticated data clients to question without knowing these keys.
- We advise an Additive Order and Privacy Preserving Function family (AOPPF) which allows data entrepreneurs to guard the privacy of relevance scores using different functions according to their preference, while still enabling the cloud server to rank the data files precisely.
- We conduct extensive experiments on real-world data sets to ensure the success and efficiency of our recommended schemes. The comfort from the paper is organized the next.

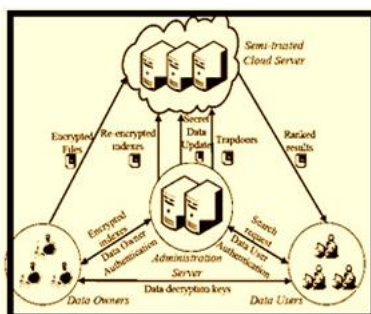


Fig. 1: Architecture of privacy preserving keyword search in a multi-owner & Multi-user cloud

II. PROBLEM FORMULATION

Within this section, we present a proper description for the target condition in this paper. We first define a system model along with a corresponding threat model. Then we elucidate the look goals in

our solution plan and a listing of notations utilized in later discussions.

1. **System Model:-** Within our multi-owner and multi-user cloud computing model, four organizations are participating, they're data proprietors, the cloud server, administration server, and knowledge customers. Data owners have an accumulation of files F . To allow efficient search operations on these files which is encoded, data proprietors first develop a secure searchable index I around the keyword set W removed from F , then they submit I towards the administration server [3]. Finally, data owners secure their files F and delegate the corresponding ncrrypted files C towards the cloud server. Upon receiving I , the administration server re-encrypts I for that authenticated data proprietors and out sources the re-encoded index towards the cloud server.

2. **Threat Model:-** Within our threat model, we assume the administration server is reliable. The executive server can be any reliable 3rd party, Information proprietors and knowledge customers who passed the authentication from the administration server are also trusted.

3. **Design Goals and Security Definitions:-** To allow privacy protecting rated multi-key word search within the multi-owner and multi-user cloud at morpheme, our bodies design should simultaneously satisfy security and grati faction goals.

• **Rated Multi-keyword Search over Multiowner:** The suggested plan should allow multi-keyword search over encoded files which would be encoded with various keys for different data proprietors. It must also permit the cloud server to position looking results among different data proprietors and return the very best-k results.

• **Data owner scalability:** The suggested schemes should allow new data proprietors to go in this system without affecting other data proprietors or data users, i.e., the plan should support data owner scalability inside a plug-and-play model.

• **Data user revocation:** The suggested scheme should make sure that only authenticated data users can perform correct searches. Furthermore, once ad ata user is revoked, he can't perform correct searches within the encoded cloud data [5].

• **Security Goals:** The suggested plan should achieve the next security goals: 1) Keyword Semantic Security (Definition 1). We'll prove that PRMSM accomplishes semantic security against the selected keyword attack. 2) Keyword secrecy (Definition 2). Because the foe A can know whether an encoded keyword matches a trapdoor, we make use of the less strong security goal (i.e., secrecy), that's, we ought to be sure that the probability or the foe A to infer the particular value

of the keyword is negligibly greater than randomly guessing. 3) Relevance score secrecy. We should ensure the cloud server cannot infer the actual worth of the encoded relevance scores [6].

III. CONCLUSIONS

We explore the issue of secure b multi-keyword look for multiple data proprietors and b multiple data customers within the cloud computing atmosphere. Not the same as prior works, our schemes enable authenticated data customers to attain secure, convenient, and efficient searches over multiple data owners' data. To efficiently authenticate data users and identify attackers who steal the key and perform illegal searches, we advise a manuscript dynamic secret key generation protocol along with a new data user authentication protocol. To allow the cloud server to perform secure search among multiple owners' with various secret keys, we systematically construct a manuscript secure search protocol. To position the search results and preserve the privacy of relevance scores between key phrases and files, we advise an Additive Order and Privacy Protecting Function family. Furthermore, we reveal that our approach is computationally efficient, for large data and keyword sets. As our future work, on a single hand, we will think about the problem of secure fuzzy key word search inside a multi-owner paradigm. However, we intend to implement our plan around the commercial clouds.

IV. REFERENCES

- [1] C. Wang, N. Cao, J. Li, K. Ren, and W. Lou, "Secure ranked keyword search over encrypted cloud data," in *Proc. IEEE Distributed Computing Systems (ICDCS'10)*, Genoa, Italy, Jun. 2010, pp. 253–262.
- [2] Z. Xu, W. Kang, R. Li, K. Yow, and C. Xu, "Efficient multikeyword ranked query on encrypted data in the cloud," in *Proc. IEEE Parallel and Distributed Systems (ICPADS'12)*, Singapore, Dec. 2012, pp. 244–251.
- [3] R. Curtmola, J. Garay, S. Kamara, and R. Ostrovsky, "Searchable symmetric encryption: improved definitions and efficient constructions," in *Proc. ACM CCS'06*, VA, USA, Oct. 2006, pp. 79–88.
- [4] I. H. Witten, A. Moffat, and T. C. Bell, *Managing gigabytes: Compressing and indexing documents and images*. San Francisco, USA: Morgan Kaufmann, 1999.
- [5] D. Boneh and M. Franklin, "Identity-based encryption from the weil pairing," *SIAM Journal on Computing*, vol. 32, no. 3, pp. 586–615, 2003.



A HEALTHY TECHNIQUE FOR REMOVING REDUNDANT COPIES OF DATA

Kesireddy Radhika¹, G.Charles Babu²

¹M.Tech Student, Dept of CSE, Malla Reddy Engineering College, Hyderabad, T.S, India

²Professor, Dept of CSE, Malla Reddy Engineering College, Hyderabad, T.S, India

ABSTRACT:

Previous systems cannot support differential authorization duplicate check, in several programs. Inside the recent occasions, structural design was offered that made up of dual clouds for effective outsourcing of understanding in addition to arbitrary computations towards an untrustworthy commodity cloud. With the introduction of cloud computing, efficient secure data deduplication has attracted much concentration in recent occasions from research community. Data deduplication might be a committed data compression technique that's generally introduced for eliminating duplicate copies of repeating storage data. Different to established systems, private cloud is supplied like a proxy towards enabling data owner to securely execute duplicate check by differential legal rights and thus this architecture is useful and includes attracted much consideration from researchers. Inside our work we solve impracticality of deduplication by differential legal rights within cloud computing, we create a hybrid cloud structural design made up of everybody cloud and cloud.

Keywords: *Cloud computing, Public cloud, Outsourcing, twin clouds, Data storage.*

1. INTRODUCTION:

The process is needed for improving of storage utilization and could furthermore be functional to network data transfers for reduction in quantity of bytes that needs to

be sent. Rather than safeguarding of multiple data copies with identical content, deduplication method removes redundant data by means of safeguarding of just one physical copy and mentioning of other

redundant data towards that copy [1]. Conventional file encryption, while provision of understanding confidentiality, is unsuited with data deduplication. Particularly, conventional file encryption necessitates various clients to secure their information by their own keys consequently, matching data copies of numerous clients will direct to distinctive cipher-texts, making deduplication difficult. While file encryption process is deterministic and comes from data content, matching data copies will produce similar convergent key which describes why exactly the same ciphertext. To create efficient data management in cloud computing, deduplication was considered like famous strategies by which has acquired elevated attention in recent occasions. Convergent file encryption remains forecasted to utilize data privacy while making deduplication practicable. Earlier deduplication systems cannot maintain differential authorization duplicate check, that's significant in lots of programs. Even though data deduplication provides various benefits, security in addition to privacy concerns happen since users' sensitive data are more inclined to insider in addition to outsider attacks. . Inside our work we goal at resourcefully fixing impracticality of

deduplication by differential legal rights within cloud computing, we create a hybrid cloud design made up of everybody cloud and cloud. No differential legal rights were considered in deduplication according to convergent file encryption method. In approved deduplication system, each user is provided some legal rights through system initialization.

2. METHODOLOGY:

Inside the recent occasions, providers of cloud service recommend highly accessible storage in addition to very parallel computing sources at comparatively low expenses. Data deduplication might be a devoted data compression method by that's mainly introduced for eliminating duplicate copies of repeating storage data. It's helpful for elimination of duplicate copies of repeatative information, and it also was extensively contained in cloud storage to reduce quantity of safe-keeping in addition in order to save bandwidth. Deduplication system can happen at block level, which removes duplicate blocks of understanding available in non-identical files. Conventional systems of deduplication according to convergent file encryption, even though offering confidentiality to some

extent, don't maintain duplicate check by differential legal rights [2]. No differential legal rights were considered in deduplication according to convergent file encryption method. Typically, conventional file encryption necessitates various clients to secure their information by their own keys consequently, matching data copies of numerous clients will direct to distinctive cipher-texts, making deduplication difficult. Inside the recent occasions, architecture was offered that made up of dual clouds for effective outsourcing of understanding in addition to arbitrary computations towards an untrusted commodity cloud. Cloud computing comprises a provision of limitless virtualized sources towards clients as services across Internet, while hiding platform in addition to implementation particulars. To greater defend data security, our work goal at resourcefully fixing impracticality of deduplication by differential legal rights within cloud computing, by imagining a hybrid cloud design made up of everybody cloud and cloud [3]. Modified from conventional deduplication systems, differential legal rights of clients are furthermore considered in duplicate check besides data itself. A manuscript deduplication structure

supporting differential duplicate check is forecasted in hybrid cloud structural design where Storage-cloud company resides in public areas cloud. The customer is simply approved to possess duplicate look for files that are marked with equivalent legal rights. Unlike the current systems of understanding deduplication, private cloud is anxious like a proxy enabling data owner to securely execute duplicate check by differential legal rights and thus this architecture is useful and includes attracted much concern from researchers. The data entrepreneurs just delegate their information storage by means of utilizing public cloud whereas data procedure is handled within private cloud.

3. AN OVERVIEW OF ROPOSED SYSTEM FOR SOLVING OF DEDUPLICATION DIFFICULTY:

Deduplication plan removes redundant data by way of safeguarding of merely one physical copy and mentioning of other redundant data towards that copy to some extent than safeguarding of multiple data copies sticking with the same content. Data deduplication may be the significant data compression approach to removal of duplicate copies of repeatative information, plus it was extensively present in cloud

storage to lessen amount of safe-keeping furthermore to save bandwidth. Within our work, we are feeling to deal with approved deduplication difficulty above data in public places cloud hence we goal at resourcefully fixing impracticality of deduplication by differential legal rights within cloud computing, we produce a hybrid cloud design comprised of everyone cloud and cloud. Since cloud computing technologies are prevalent, an growing quantity of particulars are now being stored and shared by clients in cloud with specific legal rights. One key challenge regarding cloud storage services is charge of growing data volume [4]. Unlike conventional deduplication systems, differential legal rights of customers are additionally considered in duplicate check besides data itself. A person transmits duplicate-check tokens toward public cloud for approved duplicate check. Within the storage system that supports deduplication, user only uploads exceptional data however doesn't upload any duplicate data to help keep upload bandwidth, which can be possessed by similar user otherwise different clients. Private could be a recent entity introduced for aiding user's protected usage of cloud service.

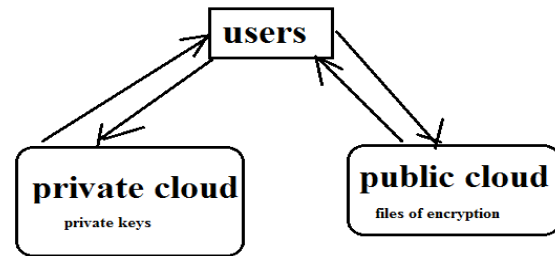


Fig1: provision of design for approved Deduplication.

The standard file encryption system requires various clients to secure their information by their particular keys consequently, matching data copies of several clients will direct to distinctive cipher-texts [5]. To guard privacy of sensitive data though supporting deduplication, convergent file encryption method remains forecasted to secure data earlier than outsourcing. A manuscript structure supporting differential duplicate check is forecasted in hybrid cloud structural design where Storage-cloud Company resides in public areas cloud [6]. You'll find three organizations that are described inside our system, for instance clients, private cloud and storage cloud providers within public cloud as revealed in fig1.

4. CONCLUSION:

A design in recent occasions was offered that made up of dual clouds for effective outsourcing of understanding in addition to

arbitrary computations towards an difficult to depend on commodity cloud. We exercise impracticality of deduplication by differential legal rights within cloud computing, we create a hybrid cloud structural design made up of everybody cloud and cloud. Different to established systems, private cloud is supplied like a proxy towards enabling permit data owner to securely execute duplicate check by differential legal rights and thus this architecture is useful and includes attracted much consideration from researchers. In recent occasions, providers of cloud service advise greatly accessible storage in addition to very parallel computing sources at comparatively low expenses. Even if data deduplication provides a number of advantages, security in addition to privacy concerns happen since users' sensitive data are more inclined to insider in addition to outsider attacks. Totally different from the standard systems of deduplication, differential legal rights of clients are furthermore considered in duplicate check besides data itself.

REFERENCES

[1] M. Bellare and A. Palacio. Gq and schnorr identification schemes: Proofs of

security against impersonation under active and concurrent attacks. In CRYPTO, pages 162–177, 2002.

[2] S. Bugiel, S. Nurnberger, A. Sadeghi, and T. Schneider. Twin clouds: An architecture for secure cloud computing. In Workshop on Cryptography and Security in Clouds (WCSC 2011), 2011.

[3] J. R. Douceur, A. Adya, W. J. Bolosky, D. Simon, and M. Theimer. Reclaiming space from duplicate files in a serverless distributed file system. In ICDCS, pages 617–624, 2002.

[4] W. K. Ng, Y. Wen, and H. Zhu. Private data deduplication protocols in cloud storage. In S. Ossowski and P. Lecca, editors, Proceedings of the 27th Annual ACM Symposium on Applied Computing, pages 441–446. ACM, 2012.

[5] R. D. Pietro and A. Sorniotti. Boosting efficiency and security in proof of ownership for deduplication. In H. Y. Youm and Y. Won, editors, ACM Symposium on Information, Computer and Communications Security, pages 81–82. ACM, 2012.

[6] S. Quinlan and S. Dorward. Venti: a new approach to archival storage. In Proc. USENIX FAST, Jan 2002.

Applications Domains of Internet of Things: A Survey

¹**Dr. R. P. Ram Kumar**
Professor

²**Hima Sampathrao**
Assistant Professor

³**Vijay Kumar Burugari**
Associate Professor

⁴**Sanjeeva Polepaka**
Associate Professor

^{1,2,3,4} Malla Reddy Engineering College (Autonomous), Secunderabad, Telangana State, India.

ABSTRACT

The objective of this article is to address the features of Internet of Things. The promising paradigm of this approach is the integration of technology with wired and wireless sensor networks, communication protocols and bright smart objects. Apart from focusing the Internet of Things vision and its emerging applications in this paper, however, major issues faced by the research community on Internet of Things are discussed in detail.

Keywords

Applications of Internet of Things, RFID Scanner, RFID Reader, Machine-to-Machine, Wireless Sensor Network.

INTRODUCTION

Internet of Things (IoT) is defined as the scenario of devices connected to the network for communication with less human interaction and intervention. IoT uses different communication models, like Cloud-to-Device, Device-to-Device, Device-to-Gateway and Sharing-Database. In 1999, the term “Internet of Things” was first devised by technologist Kevin Ashton. Figure 1 shows the example of interconnected networks in IoT depicted from [1]. The interconnected system includes vehicle, asset, person, pet, agriculture automation, energy consumption, security and surveillance, building management, telemedicine and health care, smart homes and cities, everyday things, machine-to-machine communication, wireless sensor network and embedded mobile.

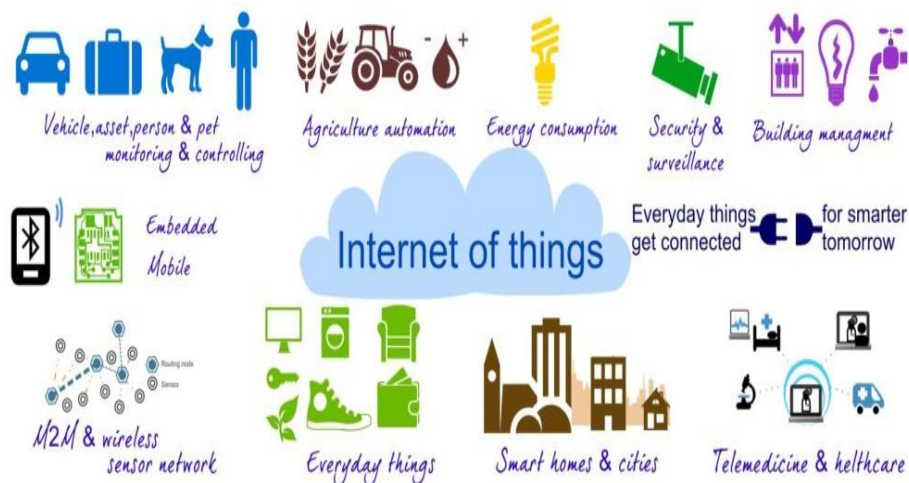


Fig 1: Interconnected networks in IoT

The term “things” in Internet of Things refers to a physical object or entity with a unique identifier and an embedded system with the capability of transferring the data over the network [2]. Intel’s prediction on IoT is summarized from [3]. It includes intelligent devices, authenticated sharing of data and to deliver the end-to-end customer value. Figure 2 shows the Intel’s vision on IoT.

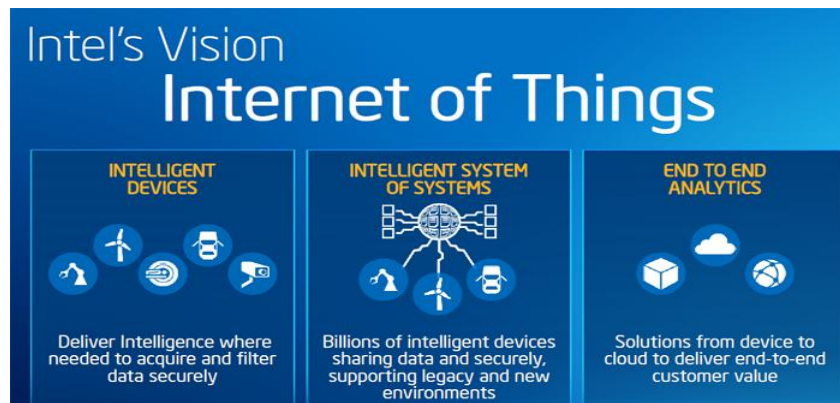


Fig 2: Intel's vision on IoT

McKinsey Global Institute listed the “settings” range for IoT applications [4]. Table 1 shows the “settings” for IoT applications. Due to the advent of connected devices over the Internet, there is a significant raise in the Internet traffic too. According to the Cisco's forecasting, there will be an increase in Machine-to-Machine connections from 24% to 43% in the years 2014 and 2019, respectively.

Table 1. Settings for IoT Applications summarized from [4]

Settings	Description
Human	Monitor the health issues
Home	Security systems
Retail Environments	Provides self-checkout and inventory optimization
Offices	Deals with energy management and security
Factories	Optimizes equipment usage, operating efficiency and inventory
Worksites	Predicts safety and maintenance
Vehicles	Usage-based design and maintenance
Cities	Monitor environment, Smart traffic control and resource management.
Outside	Tracks airways and roadways with real-time routing

Rest of the paper is organized as three sections, namely, the study of IoT-based domains, conclusion and future scope.

APPLICATION DOMAINS OF IOT

This section deals with the exploration of IoT-based applications in the real world scenario.

Srinivas and Vanithamani [5] proposed an automated library management system using RFID and GSM module. The automation process includes borrowing, renewal, return, stock maintenance and mishandling of library holdings. Passive 125KHZ RFID tags were used to identify the books and articles in the library. For quick and efficient processing, the RFID readers were equipped with

circulation counters, library and classroom entrances and reference section. Users will get updated notification in their mobile phones about their transaction with the help of GSM module. The major advantage of this system is the automation of library processes with low cost.

Brain, Arockiam and Malar Selvi [6] proposed an IOT based Library Management System using Near Field Communication (NFC) tags and Local Positioning System (LPS). Apart from automating the library activities, this method imposed authentication through fingerprint recognition. Even though LPS based approach helped the user in locating the book rack, lacks in identifying the exact location of the required book or article.

Viswanath et al [7] proposed an IoT based model to monitor the soil moisture and temperature parameters in a Green House System. Soil moisture was sensed at regular intervals and reported to concern application. The moisture content in the ground, for example, dry, semi-dry and wet cases, were discussed by the sensed data and necessary action was planned accordingly.

Sreekanth and Nitha [8] proposed an IoT-based health care system to monitor the patient's healthiness. Under energy scenarios, the wearable devices connected to the patient convey the compelling message to the concerned doctor and family members. Henceforth, the immediate action saves the patient's life. Some of the IoT-based smart healthcare sensors includes ECG sensor, body sensor, blood pressure sensor, heart rate sensor, an activity sensor, light sensor, room temperature sensor, and environment sensor.

Takpor and Atayero [9] proposed an eHealth solutions based on IoT to monitor the student's health care. During the enrollment process at Universities, Electronic Medical Records (EMR) were created with the necessary details (such as their bio-data, medical history, diagnostic records with results, blood pressure and vital signs) and linked with concern RFID tags. During the emergency cases, the healthcare information stored in the RFID tags assists the doctors to explore more about the patient's history and corresponding medical assistance can be sought. Most importantly, integrated IoT-based eHealthcare systems lead to quick diagnosis and fast recovery process.

Karthikeyan et al [10] proposed an attendance based intrusion detection system. This approach dealt with developing an attendance monitoring system for educational institutions and organizations to detect intrusions in the restricted areas. A Passive Infrared (PIR) sensor was used to detect the human or motion in the particular range. The RFID sensor (Mifare RC522) was used to identify the Unique Identification (UID) of any RFID tag. Raspberry Pi B+ governs the communication between the peripherals. The camera would be activated if no cards were placed within two seconds and termed as "intruders."

Sahoo and Sharma [11] proposed RFID-based Central Library Management (CLM) system. The various services in the CLM include OPAC, Self Check-in / Check-out, Self-Renewal of Books, Electronic Book Drop and access to publications through I-Portal. In this method, users can borrow and return the books if they are having a smart library card and a PIN. Various modules in this approach were tagging station; users self check-out station; book drop box, and antitheft security gates. RFID tags placed in the library materials were used to read the barcode and allow automatic check-in and check-out processes. Most promptly, the RFID Security gates installed at entrance(s) checks all the items before leaving the library to provide authentication and security issues.

Praveen Kumar and Mani Kumar [12] proposed attendance monitoring system using cloud spreadsheets. Control became comfortable with RFID tag for identifying each student and their profiles too. Every user has to swipe the RFID cards in the RFID readers placed at library entrance.

Once accessed by the RFID reader, Short Message Service (SMS) alert will be sent to the mobiles using GSM module. MFRC522 supports contactless communication, and WIFI connectivity was backed by CC3200 launch pad, which makes safer and less overhead of taking attendance by calling each person names.

Sree Lakshmi and Sree Gowri [13] implemented RFID technology-based library management system. In this system, each student was provided with login and password to access the library's web portal. During each and every transaction, user's id-card and book tags were scanned and penalty (if applicable) might be raised. By showing the RFID-based id-card to RFID reader, the student can lend/return books. During the return/renewal of books, the user just needs to pass the RFID reader, so that, the database was updated automatically. Hence, managing and automation were made easy, but the details in the database should be updated accurately.

Ankit Kumar and Rama Krishna [14] proposed intelligent book conveyor using RFID technology. RFID reader connected with the computer was used to update the transactions. While issuing the book to the users, it was added to the database and whenever the book was returned, it was updated in the library database. However, the efficiency of the method was determined by the quality of the RFID tags used to identify the book materials.

Basavaraju [15] proposed an IoT-based automatic and smart vehicle parking system. The components of this approach include centralized server, camera, navigation system, display devices and user interface. Once the surrounding area was captured, the administrator marks the available and allotted parking slots in the server and concern clients were serviced with appropriate results, while surfing the parking area. System administrators were provided with sufficient rights to add, update and remove the availability of parking area. Integrating the IoT with smart parking system greatly influenced in finding the free slots for parking with less fuel consumption and carbon footprints.

Joseph [16] proposed a wireless based RFID technology for automatic identification of library books. RFID system is used to store and update the information about books transactions. RFID reads information from tags through radio waves. RFID software makes the interaction between library management system and RFID components. The user could use the self-check-in/self-check-out stations for various book transactions such as lend, renewal and return process. Even though the RFID-based library operations resulted in favorable and quick processing, maintenance of such RFID technology becomes vulnerable.

Mamdapur and Rajgoli [17] implemented library management system based on RFID technology. RFID tag is programmed to store the book information. This method was equipped with various modules, like self-check-in/self check-out station, book drop reader, exit sensors and so on. The efficiency of this approach lies in scanning the books in the shelves without removing or searching for a particular book. Book drop-in and drop-out station make the automatic lend and return process thereby decreasing the manual power. Moreover, advantages of RFID-based library management includes rapid information management, assistance in searching, utilizing statistics for serials, automated material handling, sorting, guiding and personal service. Surprisingly, RFID-based applications suffer from the serious issues like sensor maintenance, high-cost RFID, privacy invasion and tag collisions.

Jay Kumar and Blessy [18] addressed on securing the communication during the online transactions. This method adopted "access password" and "kill password" approach to provide additional security,

confidentiality and authentication. Each product is equipped with Electronic Product Code (EPC) with 96 bits of data, like manufacturer details, product name, product details and retailer outlets. As a result, RFID and IoT-based transaction yield secure and smart communications.

Mathew et al [19] proposed an IoT-based surveillance method for quick recovery from diseases. While examining the patient's health issues, their medical history was updated in the central server. Collecting and storing such data was used to analyze and identify the symptoms and signs of chronic diseases. Authors concluded that integrating RFID and IoT with healthcare would result in timely accurate decisions, maintaining sufficient stocks of medicines and a therapeutic approach for an additional rise in death toll rate due to under-reporting cases.

CONCLUSION AND FUTURE SCOPE

There is no doubt that IoT has added a new dimension to the living being by communicating among smart objects. Thus making the communication among any media and anything at anywhere and anytime was plausible. Moreover, the paper emphasized on the applications of IoT and focused on the future research domains of IoT. Most importantly, the major fields of IoT yet to explore include privacy, security, interoperability standards, legal rights and emerging development. Indeed, we believe that, in the forthcoming years, these issues will be sorted out by the research groups from academia and industries.

REFERENCES

- [1] <http://saphanatutorial.com/introduction-to-internet-of-things-part-1/>
- [2] <http://internetofthingsagenda.techtarget.com/definition/thing-in-the-Internet-of-Things>
- [3] <https://www.linkedin.com/pulse/intel-pushing-aggressively-internet-things-robert-n-castellano>
- [4] Manyika, J., Michael, C., Peter, B., Jonathan, W., Richard, D., Jacques, B., and Dan, A. The Internet of Things: Mapping the Value beyond the Hype. McKinsey Global Institute, (June 2015), 1-24.
- [5] An Internet of Things Approach to Library Management and Monitoring. International Journal of Research in Engineering & Advanced Technology. 1(2), (April-May, 2013), 1-4.
- [6] Brian, A., Arockiam, L. and Malarchelvi, P. D. 2014. An IoT based Secured Smart Library System with NFC based Book Tracking. International Journal of Emerging Technology in Computer Science & Electronics. 11(5), (Nov 2014), 18-21.
- [7] Viswanath Naik. S., Pushpa Bai, S., Rajesh. P and Mallikarjuna Naik. B. 2015. IoT based Green House Monitoring System. International Journal of Electronics and Communication Engineering & Technology. 6(6), (June – 2015), 45-47.
- [8] Sreekanth, K. U. and Nitha, K. P. 2016. A Study on Health Care in Internet of Things. International Journal on Recent and Innovation Trends in Computing and Communication. 4(2), (Feb 2016), 44-47.
- [9] Temitope O. Takpor and Aderemi A. Atayero. 2015 Integrating Internet of Things and EHealth Solutions for Students' Healthcare. In Proceedings of the World Congress on Engineering.
- [10] Karthikeyan, B, Astha Puri, Rohan Mathur and Anurag Mishra. 2016. Internet of Things (IOT) based Attendance and Intrusion Detection System. International Journal of Innovative Research in Computer and Communication Engineering. 4(3) (Mar. 2016), 3246-3252.
- [11] Dipti Ranjan Sahoo and Dhara Sharma. 2015. RFID Technology at Central Library, IIT Madras, An Overview. International Journal of Scientific Engineering and Applied Science. 1(5) (Aug. 2015), 156-172.
- [12] Praveen Kumar, M and Mani Kumar, B. 2015. RFID based Attendance monitoring system Using IOT with TI CC3200 Launchpad. 2(7) (July 2015), 1465-1467.
- [13] Sree Lakshmi, A and Sree Gowri, A. 2014. Library Management System Using RFID Technology. International Journal of Computer Science and Information Technologies. 5(6), 6932-6935.
- [14] Ankit Kumar, J, A and Rama Krishna, T. 2014. Dynamic Book Search Using RFID Technology. International Journal of Engineering Research and General Science. 2(6) (Oct. - Nov. 2014), 138-142.

-
- [15] Basavaraju S R. 2015. Automatic Smart Parking System using Internet of Things (IOT). International Journal of Scientific and Research Publications. 5(12), (Dec. 2015), 629-632.
- [16] Joseph M. K. 2014. Use of RFID technology in Libraries: A perspective from the Catholic University of Eastern Africa, Nairobi. Proceedings and report of the 7th Ubuntu Net Alliance Annual Conference. 133-142.
- [17] Mamdapur, G. M. N., and Rajgoli, I. U. 2011. Implementing radio frequency identification technology in libraries: Advantages and disadvantages. International Journal of Library and Information Science. 3(3) 46-57.
- [18] Jebah Jaykumar and Abishlin Blessy. 2014. Secure Smart Environment Using IOT based on RFID. International Journal of Computer Science and Information Technologies. 5(2), 2493-2496.
- [19] Ashly Mathew, Farha Amreen S.A, Pooja H.N and Aakriti Verma. 2015. Smart Disease Surveillance Based on Internet of Things (IoT). International Journal of Advanced Research in Computer and Communication Engineering. 4(5) May 2015.

QoS Web Service Security Dynamic Intruder Detection System for HTTP SSL services

M.Swami Das¹, A.Govardhan², D.Vijaya lakshmi³

Assoc. Professor, CSE, MREC¹, Professor, SIT,JNTU Hyderabad², Professor, Dept. of CSE, MGIT
Hyderabad, India³

Abstract: Web services are expected to play significant role for message communications over internet applications. Most of the future work is web security. Online shopping and web services are increasing at rapid rate. In this paper we presented the fundamental concepts related to Network security, web security threats. QoS web service security intrusion detection is important concern in network communications and firewalls security; we discussed various issues and challenges related to web security. The fundamental concepts network security XML firewall, XML networks. We proposed a novel Dynamic Intruder Detection System (DIDA) is safe guard against SSL secured transactions over message communications in intermediate routers that enable services to sender and receiver use Secured Session Layer protocol messages. This can be into three stages 1) Sensor 2) Analyzer and 3)User Interface..

Keywords: Web Security, QoS web service, HTTP, Intruder detection, Secure Socket Layer, Network Security

1.Introduction

Intrusion detection system is a device or software application that monitors malicious attacks or network traffic if any policy violations [1]. Web services applications communicate and coordinate message passing between client and server. A web service provides functionality and services to the web users. The users to communicate in network channels, the hacker or Intruder tries to operate various attacks such as, DDOS attack, side channel attack, authentication attack, man in the middle attack, cloud computing attacks and steal sensitive information. Hacker execute arbitrary or malicious code in the system due to vulnerability, weak security and no Intruder Detection and Monitoring system.[2]. In Intrusion detection system is a device or software application that monitors malicious attacks or network traffic if any policy violations [1]. A web service provides functionality and services to the web users. The users to communicate in network channels, the hacker or Intruder tries to operate various attacks such as, DDOS attack, side channel attack, authentication attack, man in the middle attack, cloud computing attacks and steal sensitive information. Hacker execute arbitrary or malicious code in the system due to vulnerability, weak security and no Intruder Detection and

Monitoring system.[2]. In recently ISRO website homepage hacked by hackers, other examples related to Government and other web sites discussed[3,4]. It is essential to provide Intruder Detection and monitoring system for Government Institutions, Diplomatic offices, Energy, oil and gas companies, Research Institutions, private equity firms, and activist. Frequently to monitor and control the valid and authorized data operations over the network.

Web security has three important concepts confidentiality, integrity and availability. Confidentiality means Information not available to unauthorized users. Integrity defined by the property that data has not been modified by unauthorized users, and availability means web services are accessible to authorized users with access restrictions.[5] Intrusion: attempting to attack into or misuse the system from outside network or legitimate users of the network, intrusion can be a physical, system or remote intrusion. Automatic Intrusion detection system sensor, Analyzer and user interface. Intrusion Detection systems can be classified as i)Anomaly detection ii) signature based misuse iii) host based iv) network based v) stack based The rest of this paper is organized as follows Section 2: Related work, Section: 3 Issues and challenges, Section 4: Web security and Network

security, Section: 5 Discussions and Interpretations and Section 6. Conclusion.

2. Related Work

Zhiwen Bai etl, Proposed DTAD, a dynamic taint analysis detector aiming to protect malicious attacks and vulnerabilities. Attacker process is detected and precision intrusion, signature of collection of virtual systems and comparing network data and log files used to identify the attacks.[6]

Jiang Du etl, studied man in the middle attacker use ARP deception for both sides communication. Man in the middle will generate own public, private and self digital certificate, and this is interactive process validated by Service provider.[7]

Taro Ishitaki,etl proposed intrusion detection system using Neural network, Fuzzy logic, Probabilistic reasoning, Genetic algorithms capable for finding pattern behavior to detect normal and attack conditions[8].

The SOAP messages to ensure integrity and authentication during the data transmission. Web services require partial signing of SOAP request which is achieved using XML signature by WSDL documents and operations as suggested by Padmanabhuni and Adarkar etl[9,10]. Web service security is critical task for message invocations by web servers. SOAP uses XML encryption, XML digital signature, SSL/TLS methods. XML message security is achieved by service oriented security functionality.

Web service standards SOAP level security authentication, authorization management. Web security is defined as attach signature and encryption header to SOAP messages. It describes security tokens. Web security policy is defined as set of specifications that describe rules, constraints and other business policies on intermediaries and end points. (Example. Encryption algorithms).Web security trust describes a frame work to design a model that enables web services to securely inter-operate request, issues, and exchange security operations.

2.1 XML Firewall

Web services environment, malicious attacks and DoS attacks are new challenges. Firewall allows to the Service providers residing in a network to be invoked from outside the network, and keeping a high security[9]. HTTP protocol is

not suitable for creating public key infrastructure. The prototype is used by application behind a firewall.[11]

2.2 XML networks

web service management vendors develop network based solution for web service applications to provide better QoS web services with security to various networks endpoints service consumers and service providers.[11].

Fang Qi .etl, .proposed Automatic Detecting Security Indicator (ADSI) for preventing Web spoofing on a confidential computer which is a harmless environment. It creates a random indicator to identify and detect bogus pages with URL screening data.[13]

Jaing Du,.etl analyzed as a case study secured socket layer man in the middle attack based on SSL certification interaction. Attacker place computer gives a vital role two communication processes. [14]

Lin-Shung Huang., etc introduced a new method for detecting SSL man -in- the middle attacks against website users, over of SSL connections at the top web sites by checking certificates as number of CA certificates. Trace any malware in SSL connections for identify and provide better protection. [15]

3 Issues and challenges

The following are the list of issues /challenges in Web security/network security. Digital certificates are designed to establish credentials of the people use Router configurations with weak vulnerabilities and security policies described in Table.1. Web security developers provide secured operations and safety steps necessary to identify trusted systems. [16]

Table.1. Router or firewall configurations with weak or vulnerabilities

Web services Solutions or threats	Problem in domain or Safety precautions
Web service has arbitrary disclosure policy	Provide strong policies to web services
Passwords stored in browser	Do not save passwords in browser history
Institutions, organizations malicious code attacks, virus	Web security , Frequently monitor network operations. Use SSL security

Malware, Denial of service attacks to modems / routers against other systems by unknown users by stealing personal information and credentials to access certain web sites.

Hackers used stolen laptops/equipment to hack web data where there is vulnerability like private wireless network or wireless network is unsecured with no password is immediately accessible to hackers. Hacker used wireless antenna and software nearby buildings and capture/ steal information like passwords, email-messages, and any data transmitted over the network when a network is not secured. [5].Hacker will use some tools described in table.2. Brute-force attack is the password cracking method, trying all the solutions seeking one fits[11].Stealing the login password controlling the devices by malicious scripts and malicious DNS servers attacked on DSL modems.

3.1 Man-in-the-Middle (MIM) attacks

This attack where the attacker secretly relays and possibly alters the communication between two parties who believe they are openly communicating with each other. Attacker intercept all relevant messages by passing between victims and adding extra information. Attackers trying to access the services using fake address, fake certifications. Examples of MIM attacks One provides free Wi-Fi service with malicious software.

3.1.1 ARP Cache Poisoning

Sender and receiver over message communication, PC sends IP packets broad cast to all systems in subnet. ARP(address resolution protocol is not secured protocol).

3.1.2 DNS Spoofing

DNS cache poisoning is a computer hacking attack, where by data is communicated into a Domain Name System (DNS) resolver's cache, causing the name server to return an incorrect IP address, diverting traffic to the attacker's computer (or any other computer).Attackers creating a fake web site by redirecting data to shadow servers.

3.1.3 Session Hijacking: Client to server when session established, the hacker capture cookies information and diverting the session communications to un-trusted systems

3.1.4 Session hijacking attack

Communication over TCP connections. Session normally consists of string of variables used in URL stealing and predicting valid session token to gain unauthorized access to the

web server [17]

Table.2.Tools and software's used to steal the data

Web services Solutions or threats	Problem in domain or Safety precautions
Suspicious downloads or plugins	Use firewall in secure network
Terminals with chip card vulnerabilities	Alert any where service by authentication and secret key.

4.Web Security Network security

Web Service Security: Three types of digital certificates are domain validated certificate, organizational validation certificate and Extended validation certification. Domain validated Certificate: trusted domain name of owner. Organizational Validation Certificate: validation of organization by DNS names. Extended validation certification: Certificate Agent must meet minimum validation criteria. Organizations, application vendors, Browser makers issue extended validation certificate.[4] Web services standards worked at w3C, OASIS, IETF and other bodies to enable faster inventions of web services and security. A web service provides a flexible set of mechanism to design a range of security protocols. It is essential to design non-vulnerable protocols for web services security. Web services specifications goals to provide multiple security token formats, multiple trust domains, multiple signature formats, multiple encryption methodologies, and end to end message content security.[12]

4.1 Intruder Identification and Detection System

4.1.1 Various Attacks

Unauthorized system used to attack on router or servers using various attacks (DDOS attack, side channel attack, Man in the middle attack , Authentication attack and cloud computing attacks) methods practiced due to various reasons like, not secured web site, malicious code, denying encrypt , weak secret keys, vulnerabilities in content security, and policy constraints. In Figure.1. shows the intruder attacks on router.

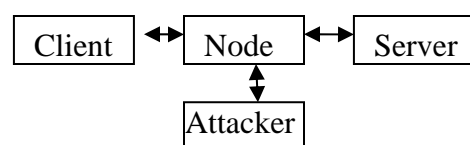


Figure.1. Intruder attacks on services

4.1.1.1 Denial of Service attacks

DDOS attack were launched from distributed attacking hosts. This is launched two phases. First an attacker builds a network which is distributed and consists of thousand of compromised computers are called(Zombies, attacking hosts). The attacker hosts flood of tremendous volume of traffic towards victims either under command or automatically [32].

4.1.1.2 Attack to change DNS settings

Attackers directly targeting DNS server two ways Cybersquatting aim is to steal the Victims identity and or divert traffic from victims website. Name jacking or theft : by appropriate the domain name (updating the holders field or taking control) by technical means to divert the traffic such as modifying the name of hosting the site.[18]

4.1.1.3 Authentication attack

This type of attack targets and attempt to take advantage of following Brute force : allow attacker to guess persons username, other credentials by using Automated trail and error Insufficient Authentication: Allows an attached to access a web site sensible information without having to properly authenticate in web site. Sending phishing mail to user to steal sensitive information[19]

4.2 Intruder Detection System

Intruder Detection System has two type namely Network Intrusion Detection System and Host based Intrusion Detection System

4.2.1 Network based Intrusion Detection System

It deals with traffic accounting and network flow information. This system is implementing in Routers and switches Input and Output HTTP / TCP data, and testing various functions like port scanning , Reassembling, decoding, detecting virus, protocol violations.

4.2.2 Host based Intrusion Detection System

It deals with Analyzing logging facility for almost all failed or success services. The system is implementing in Routers or Firewall to access authorized client. It calculates the cryptographic checks of files, including owner ,group changes, and also checks system integrity.[20]

Web services accessed by sending SOAP messages to endpoints. This is handed by transport layer security protocol such as HTTP,

SSL, and TLS others. This ensures secured peer to peer messages. Web based security standards mapping to XML message security. All protocols use to carry security data as part of XML document. The XML document is critical part of security requirement of web services. [9]

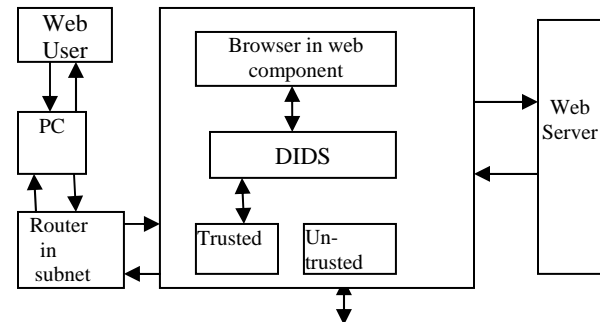


Figure.2. Dynamic Intrusion Detection System

4.3 Secure Socket Layer and Transport Layer

Security HTTP Secured Socket Layer Protocol: HTTP over Secured Socket Layer combination to secure communication between browser and web server systems. SSL Secured Socket Layer Protocol is transient, peer to peer communication, SSL protocol stack link associated with SSL session Record Protocol operation. These SSL sessions in association

between client & server by handshake protocol, with defined set of cryptographic parameters that may be shared by multiple SSL connections. [3, 12, 13]. HTTP protocol stack provides transfer information for web services interaction can operate on top of SSL. Three layers are defined as part of SSL such as Hand shake protocol, The change of cipher spec protocol and the Alert protocol. These protocols are used in management of SSL exchange.

4.4 Proposed Model: Dynamic Intruder Detection system

The Automated Intruder Detection System shown in Figure. 2. It will detect the unauthorized or hacker requests by invoking a procedure Intrusion Detection System in four subpaths, that are user requests to subnet router point to point in Transport layer, browser in the Intrusion detection system detection system invokes a procedure to check, Certification, digital signature of trusted client. If trusted request as a result then it inserts the process for further processing into Deque. The deque holds a batch of trusted services routed to next hop via point to

point protocol. In subpath3 browser contents security not known to attacker by padlock security. The forth sub-path content in the web server connecting a session request for web services. The algorithm:1,2 and 3 depicted table. Intrusion Detection System Message Format alert:(messageid; create time;nt pstamp;date;time; source;node;address;message; flag)

4.4.1 Components of DIDS

Dynamic Intrusion Detection System has three components are sensor, Analyzer and User interface. Overall network security maintains a security state. when threat occurs by executing an event, the system will check the context of the event and data by following

4.4.1.1 Sensor

Sensors are responsible for collecting data. Example network packet, log files, and system call traces, sensors collect and forward to the analyzer

4.4.1.2 Analyzer

Analyzer receives input from one or more sensors from the system. Control the behavior of the system.

4.4.1.3 User Interface

The user interface to DIDS that enables a user to view output from the system or control the behavior of the system. System component as manager or console component.[20]

Algorithm: 1 Initialization of Request Procedure: DYNAMIC INTRUDER DETECTON SYSTEM

Input : Sensor/ node send a service request

Output: Trusted service or Un-trusted service
begin

1. Establish connection between sender and receiver
2. User system to web server consists of four sub paths
3. subpath1: user request to router in subnet(trusted system)
4. Subpath2:Web browser in router checks the procedure using Dynamic Intruder detection system.
5. Identify the request process trusted request pushed onto Deque and un-trusted requests rejected and access restricted.
6. Subpath3: Web browser content and security sign which are not known to the attacker. Ex icon with Padlock security sign unknown to the attacker.
7. Subpath4:Web content to Web server: Connecting via subnet routers with trusted

systems the request connection established between sender to receiver
using SSL handshake protocol
end

Algorithm.2: Connection Establishment.

Procedure PROCESS DETECTING TRUSTED REQUEST

Input : Web service request

Output : Secured HTTP Session layer

Begin

1. Read DIDS
2. Client sends a request to Web server by invoking HandShake protocol using cryptographic parameters (clientid, clientMAC, ClientSecretKey, serverid)
3. During handshaking protocol session is created successfully by resuming the new state if already the state is running. With Session identified by its state, prior to encryption algorithms.
4. Each connection creates a secure session layer and sets the flag. Here flag indicated the connection.
5. The request process is checking by Certificate Agent, and Digital certificate.
6. Detecting trusted service or un-trusted service. if request is trusted service then insert the process in Deque for further processing communication to next hop if connection request is un-trusted requests are denied/ rejected
end

Algorithm.3 Closing the Connection

Procedure WS SECURED CONNCTION

Input: web service request message

Output: Secure access control by encryption

Begin

1. Read PROCESS DETECTING TRUSTED REQUEST
2. User data is verified with the data with existing data of concerned web server.
3. If(HTTPPrequest is successful) then Connection is established, under service access policy else Connection is closed with notification
4. if connection is established enable decryption of data at the web server
5. Message communication is accomplished by SSL encryption method.
6. close the connection
7. Connection closure if connection is closed in HTTP record
8. TLS level exchange close notify alert then close TCP connection
9. handle TCP close before alert exchange send or completed

End

5 Discussions and Interpretations

Secure Socket Layer provides security services between TCP and applications that use TCP. Internet standards TLS, SSL/TLS provide confidentiality using symmetric encryption and message integrity and Authentication code. This DIDS (Dynamic Intruder Detection System) protecting the man-in-the-middle attacks and deny services. And allows trusted services forwarded to next hop to reach peer entity web server and Web service applications. The discussions and interpretations for web securities, precautions and remedies are described in table.2 provides the information related to web security/network security problems and proposed solutions/precautions to meet network securities QoS parameters such as confidentiality, integrity, data authentication, and availability of information to trusted users from web service systems to detect various attacks. The genuine merchants by Digital certificates and required policy constraints to validate authentication process in DIDS system architecture.

6 Conclusions

Web services are expected to play increasing important role for message communications over internet applications. Most of future work is web security. Online shopping and web services are increasing in the world. In this paper we described the fundamental concepts related to web security threats, web server architectures, web server protocols. QoS web service security is important concern in network communications. Firewalls security, various issues and challenges of web security. Discussed fundamental concepts, network security encryption and decryption process, and Network security hierarchies.

We proposed a novel Dynamic Intruder Detection System(AIDA) is safe guard against SSL secured transactions over message communications to intermediate routers that enable services to sender and receiver use Secured Session Layer protocol messages. This can be into three stages 1) Weak security assumption 2) Intruder attacks on browser 3)Trusted system detect service and safe guard information. As a case study we proposed the architecture of system in Figure .2.In future we can extend this paper to E-Commerce, Online Financial transactions, and this security concepts

used for designing and developing Firewalls which will protect web services applications.

References

- [1] <https://en.wikipedia.org/>
- [2] www.livehacking.com
- [3] <http://www.thehindu.com/news/national>
- [4] <http://www.ndtv.com/topic/websites-hacked>
- [5] M.Swami Das, A.Govardhan, and D.Vijya lakshmi: QoS web service Security Access Control case study using HTTP Secured Socket Layer Approach ICEMIS 15, September 24-26, 2015, Istanbul, Turkey 2015 ACM. ISBN 978-1-4503-3418-1/15/09
- [6] Zhiwen Bai,Liming Wang, Jinglin Chen,Jain Liu,Xiyang Liu on " DTAD A Dynamic Taint Analysis Detector for Information Security",IEEE, Web age Information system 2008, pp,591-597
- [7] Jaing Du,Xing Li and Hua Huang :A study of man in the middle attack based on SSL certificate interaction",IEEE,ICIMCCC 2011, pp 445-448
- [8] Taro Ishitaki, Donald , Yi Liu, Tetsuya Oda, Leonard Barolli, and Kazunori Uchida : Application of Neural Networks for Intrusion Detection in Tor Networks.IEEE, ICAINAW 2015, pp 67-72
- [9] https://events.ccc.de/congress/2005/fahrplan/638-22c3_ids.pdf
- [10] www.cs.ucsb.edu
- [11]Service-oriented Software System Engineering: Challenges and Practices by Z Stojanovi, Ajantha D
- [12]Service-oriented Software System Engineering: Challenges and Practices by Z Stojanovi, Ajantha D
- [13] Fang Qi, Zhe Tang, Guojun Wang on" Attacks vs. Countermeasures of SSL Protected Trust Model", IEEE confernece 2008, pp1886-1991
- [14] Jin-Ha Kim, Gyu Sang Choi and Chita R. Das :A Load Balancing Scheme for Cluster-based Secure Network Servers,IEEE
- [15] Lin-Shung Huang, Alex Ricey, Erling Ellingseny,Collin Jackson :Analyzing Forged SSL Certificates in the Wild,2014 IEEE Symposium on Security and Privacy,pp.83-97
- [16] Neal Leavitt :Internet Security under Attack: The Undermining of Digital Certificates",Technology news in IEEE 2011,pp17-20
- [17] <https://en.wikipedia.org>
- [18] <https://www.afnic.fr/> DNS Types of attack and security techniques
- [19][http://www1.ibm.com/support/knowledgecenter/SB2MG.6.0/com.ibm.ips.doc/concepts/wap authenticaton.htm](http://www1.ibm.com/support/knowledgecenter/SB2MG.6.0/com.ibm.ips.doc/concepts/wap_authenticaton.htm)
- [20] <https://s2.ist.psu.edu/paper/ddos-chap-gu-june-07.pdf>

Multi-Annotator Approach to Automatically build the Annotation Wrapper

Ms. Bhagyashri¹, M. Swami Das²

¹M.Tech Student, Malla Reddy Engineering College(A), Telangana State, India

²Associate Professor, Department of CSE, Malla Reddy Engineering College(A), Telangana State, India

Abstract— *Web search engines are designed to find data from the web database & return active websites. Data unit returns from the databases as well as information technology are available via HTML form-based interfaces and web technology. Websites are retrieved once a query is assigned to the search interface. Every online page contains many Search Result Records (SRRs) associated with user query. Each SRR includes multiple information units each one of which describes one facet of a real-world entity. The SRR get extracted and allotted significant labels. To Decrease human efforts a multi-annotator approach is planned to automatically extract data units and assign labels. When the successful extraction aligns the data units into different teams, data within constant cluster have constant semantic (meaning). The annotation wrapper will be generated automatically and want to annotate new result records from a constant web database.*

Keywords— *Annotator, HTML, Web search Engine*

I. INTRODUCTION

The use of web and E- Commerce has been multiplied wide over an amount of time. The online Databases are managing the massive quantity of knowledge. There are varied technologies and researches are concentrated on the extraction of relevant info from massive web data storage. However still there's demand of accessibility of automatic annotation of this extracted info into a scientific means to be processed later for varied functions. Web data extraction and annotation has been active analysis space in net mining. The user enter the search input query within the computer program, which return the dynamically search output records on application program. The online databases are accessed through markup language based computer program. The result returned from net info is of the type of Search Result Record (SRR). SRR includes text nodes and data units. There's a high claim data of interest from multiple web Databases. For instance, a book contrast looking system gathers several result records from various book sites; it must verify whether or not any 2 SRRs present with a similar book. The system must list the costs offered by every web site. Thus, the system must grasp the linguistics of every knowledge unit. Every SRRs represents one book with many data and text units. It consists of text node outside the <HTML>, Tag node enclosed by HTML Tags and title, author, price, publication and therefore the values related to it as knowledge units. An information unit may be some text that represents one conception of an entity. It corresponds to the significance of record underneath an attribute. It is different from the text node, which refers to the sequence of text enclosed by a combine of markup language tag. The link between the data unit and text node is incredibly necessary for the aim of annotation as the text node don't appear to be similar to data nodes. The WDBs has multiple sites to store in it. For this task, labeling to needed information and storing the collected SRR into an information base is vital. Looking and changing any info on web databases is tough task. It will increase by Alignment and annotation of information. Data alignment is positioning the data or arrangement the information in such the simplest way that data within a similar cluster have a similar meaning. Data annotation is the method for adding info to a document. Data annotation permits quick retrieval of data within the deep net.

In present, databases become net accessible, these databases having data units are encrypted into the result pages for human browsing. A data unit may be a part of text that semantically represented planet entity ideas. To split data allocates significant labels. To allocate labels there is associate habitual annotation that initially arranges all data into totally different teams i.e. within a similar cluster have same linguistics. Then every cluster is annotated in several

aspects and aggregative to predict a final label. There are 6 essential annotators, for each essential commentator we have to manufacture label for the information unit among their cluster. A chance model is chosen to see the foremost applicable label for every cluster. Finally, wrapper is generated that offers annotation wrappers for the search web site to mechanically created & annotate the new result pages from similar WDBs. This annotation wrapper generates an annotation rule, which explains a way to extract the data from end result page. Already the annotation wrapper annotate the data there's spare to execute the alignment and annotation phases once more. The wrapper may be a software package conception that wraps the contents of an internet page utilizing its ASCII text file through hypertext transfer protocol however it doesn't modify the first query mechanism of that online page.

II. RELATED WORK

W. Liu, X. Meng, and W. Meng et al. developed one paper for extracting structured knowledge from deep websites have a difficult drawback due to fundamental complex Structures of such pages. An oversized variety of techniques are proposed to handle this drawback, however all of them have inherent limitations as a result of their Webpage-programming-language-dependency. This approach mainly utilizes the visual options on the deep websites to implement deep web data extraction, together with knowledge record extraction & knowledge item mining. It's additionally proposed as new analysis live review to confine the number of human effort required supplying excellent extraction.

J. Madhavan, D. Ko, L. Lot, V. Ganapathy et al developed a paper for content hidden behind HTML forms, has long been acknowledged as a big gap in search engine coverage. The paper describes a system for egress. Deep - website, i.e., pre-computing submissions for every HTML type and adding the resulting HTML pages into a research engine index. The consequences of our egress are integrated into the Google search engine & nowadays drive more than 1000 queries per second to Deep-Web content.

S. Mukherjee, I.V. Ramakrishnan, and A. Singh et al developed a paper for distinctive and annotation the linguistics ideas inherent such documents makes them openly willing for semantic web process. This work describes an extremely machine-driven technique for annotating HTML documents, particularly template-based content-rich documents, which includes several various semantic ideas per document. Beginning by a (small) seed of hand-labeled instances of semantic ideas in an exceedingly in a very set of HTML documents we tend to bootstrap an annotation method that automatically identifies unlabelled construct instances in alternative documents. The bootstrapping technique exploits the observation that linguistically connected things in content-rich documents exhibit consistency in presentation style and abstraction neighbourhood to find out an applied math model for totally different semantic ideas in HTML documents drawn from a variety of web sources.

Y. Zhai and B. Liu et al developed a paper for the problem of extracting knowledge from an internet page that includes many structured data records. The primary category of ways is predicated on machine learning, which requires human classification of the several instances from every web site that one is curious about mining data from. The method is time consuming thanks to the big variety of web sites and pages on the web. The 2nd category of rules is predicated on automatic pattern discovery. These ways are either incorrect or build several assumptions.

III. FRAME WORK

A. Structural Design of Deep Annotation

The Deep Annotation has 3 major building blocks corresponding to 3 different roles those are, database owner, annotator, and querying party.

Database and web site provider

At the web site, we assume that there's a fundamental database and a server-side scripting surroundings, like JSP or ASP, used to produce active sites. Moreover, the web site may give an online service API to third parties who wish to query the database openly.

Annotator

An observer victimizes an extensive version of the OntoMat-Annotizer so as to physically produce relative information, that communicate to a given user ontology, for a few web pages. The extensive OntoMat-Annotizer

considers as an account issues which will arise from generic annotations needed by deep annotation. With the help of OntoMat-Annotizer, we tend to produce mapping rules from such annotations that are later exploited by an inference engine.

Querying Party

The querying party uses a corresponding instrument to examine the client ontology, to compile a question from the client ontology and to research the mapping. In this case, we victimize OntoEdit for those 3 functions, investigation, debugging and alter of given mapping rules. To it extend, OntoEdit integrates and exploits the Ontobroker inference engine.

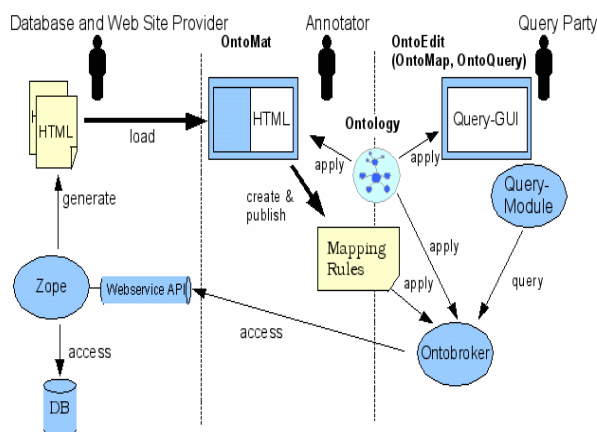


Fig. 1 System Architecture

B. Analysis of Search Result Records (SRRs)

1) One-to-One Relationship:

In this relationship, every text node grasp accurately one data unit that's the text of this node encloses the worth of a distinct attribute. Every text node is enveloped by the combination of tags that refers to the label attribute. This could be stated as varieties of text nodes referred to as atomic text nodes that are up to the data units.

2) One-to-Many Relationship:

During this type of relationship, complex knowledge units are caught in one text node. This text node contains 4 linguistics data units specifically Date, ISBN, Publisher relevancy Score and Publication. The text of these styles of nodes is a masterpiece of the texts of many data units, and referred as composite text node. Generally, this assessment is appropriate for the reason that SRRs are constructed by template programs. Finally every advanced text node is divided to induce real data units and annotate them.

3) Many-to-One Relationship:

During this type of relationship, multiple nodes of text collectively form an information unit. Author attribute worth consists with multiple nodes of text with every embedded contained by a definite combine of HTML tags. Generally the webpage designers use explicit HTML tags to brighten definite data. This sort of tags is termed as ornamental tags since they're utilized primarily for different looks of a part of the text nodes.

4) One-to-Nothing Relationship:

During this type of relationship, the text nodes supported to the current cluster aren't enclosed of any knowledge unit within SRRs. Additionally, its examinations means that these text nodes are exhibited in an exceedingly definite pattern across each SRRs. Hence, this is often referred to as guide text nodes. This identifies guide text nodes by utilizing frequency-based annotator.

C. Data Alignment Algorithm

Our data alignment algorithm follows the concept that although the SRR contains different attributes, the order of the attributes in all SRRs is same on same result page since the SRRs from same WDB are generated by same program. So the result page SRRs can be considered as table where rows are represented by single SRR and column depicting the data unit. Each column is considered as alignment group and if this group contains all data units of single concept, it is known as well aligned group. Our data alignment method consists of the following four steps.

Step 1: Merge text nodes. In this step, tags are removed from each SRR to allow the text nodes corresponding to the same attribute to be merged into a single text node.

Step 2: Align text nodes. The text nodes of the same concept (for atomic nodes) or same set of concepts (for composite nodes) are grouped together in this step.

Step 3: Split (composite) text nodes. In this step the values in composite nodes are split into individual data units.

Step 4: Align data units. In this step the data units of same concept are separated from composite group so as to form multiple aligned groups.

D. Ontology Creation

The aim of this ontology construction is to construct ontology for a domain victimizing the query interfaces as well as query result pages from websites in the domain. The ontology construction consists of four modules. They are:

- 1) Query Result Pages
- 2) Query Interfaces
- 3) Primary Labeling
- 4) Matching

Pseudo code for ontology construction:

Step 1: Analyze the query interface

Step 2: Analyze the query result page

Step 3: Data wrapping method

Step 4: Primary labeling depends on step 1 and step 2

Step 5: Matching

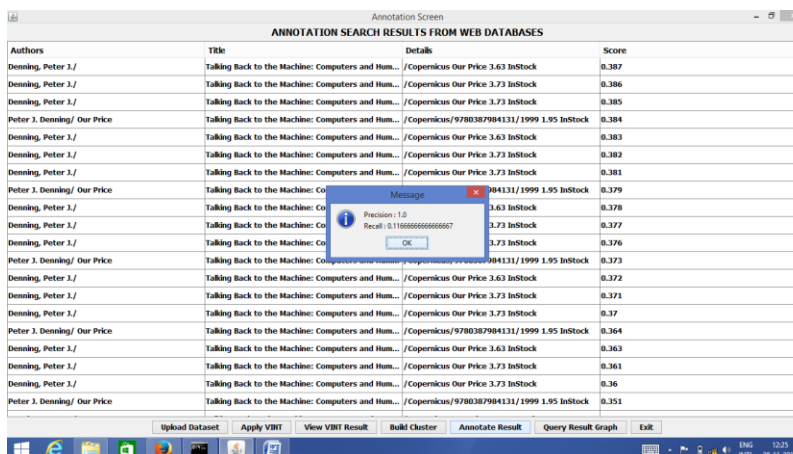
Step 6: Construct domain ontology

E. Automatically getting tag-matching weight

A kind of linear regression technique is utilized to induce the load of varied tag matching. The block components are components that generally, contain alternative components. They ordinarily act as containers of some kind. The inline components price the linguistics that means of one thing. The higher-level nodes should have higher weight as they act as larger structure block. Completely different weight should be appointed to different kind of tag matching. Initially we found assortment of comparable sites belong to a similar "class". It's possible to induce this sort of sites assortment mechanically. Then we will use this collection for obtaining the weight schema that is perfect.

IV. EXPERIMENTAL RESULTS

In our experiments, to extract SRRs from end result pages we have to apply the ViNTs. Figure 2 shows the annotation results on the searching queries. The corresponding graph is shown in figure 3.



Authors	Title	Details	Score
Denning, Peter J./	Talking Back to the Machine: Computers and Hum...	/Copernicus Our Price 3.63 InStock	0.387
Denning, Peter J./	Talking Back to the Machine: Computers and Hum...	/Copernicus Our Price 3.73 InStock	0.386
Denning, Peter J./	Talking Back to the Machine: Computers and Hum...	/Copernicus Our Price 3.73 InStock	0.385
Peter J. Denning/ Our Price	Talking Back to the Machine: Computers and Hum...	/Copernicus/9780387984131/1999 1.95 InStock	0.384
Denning, Peter J./	Talking Back to the Machine: Computers and Hum...	/Copernicus Our Price 3.63 InStock	0.383
Denning, Peter J./	Talking Back to the Machine: Computers and Hum...	/Copernicus Our Price 3.73 InStock	0.382
Denning, Peter J./	Talking Back to the Machine: Computers and Hum...	/Copernicus Our Price 3.73 InStock	0.381
Peter J. Denning/ Our Price	Talking Back to the Machine: Co...	/944131/1999 1.95 InStock	0.379
Denning, Peter J./	Talking Back to the Machine: Co...	3.63 InStock	0.378
Denning, Peter J./	Talking Back to the Machine: Co...	3.73 InStock	0.377
Denning, Peter J./	Talking Back to the Machine: Co...	3.73 InStock	0.376
Peter J. Denning/ Our Price	Talking Back to the Machine: Co...	/Copernicus/9780387984131/1999 1.95 InStock	0.373
Denning, Peter J./	Talking Back to the Machine: Computers and Hum...	/Copernicus Our Price 3.63 InStock	0.372
Denning, Peter J./	Talking Back to the Machine: Computers and Hum...	/Copernicus Our Price 3.73 InStock	0.371
Denning, Peter J./	Talking Back to the Machine: Computers and Hum...	/Copernicus Our Price 3.73 InStock	0.37
Peter J. Denning/ Our Price	Talking Back to the Machine: Computers and Hum...	/Copernicus/9780387984131/1999 1.95 InStock	0.364
Denning, Peter J./	Talking Back to the Machine: Computers and Hum...	/Copernicus Our Price 3.63 InStock	0.363
Denning, Peter J./	Talking Back to the Machine: Computers and Hum...	/Copernicus Our Price 3.73 InStock	0.361
Denning, Peter J./	Talking Back to the Machine: Computers and Hum...	/Copernicus Our Price 3.73 InStock	0.36
Peter J. Denning/ Our Price	Talking Back to the Machine: Computers and Hum...	/Copernicus/9780387984131/1999 1.95 InStock	0.351

Fig. 2 Annotation results

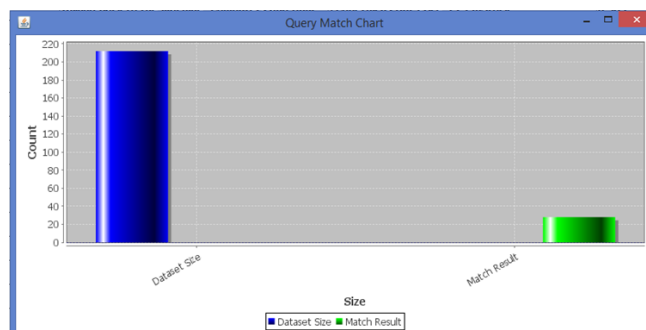


Fig. 3 Chart for Annotation results

These experiments show that our proposed annotation technique performance is incredibly effective.

V. CONCLUSION

In this paper, we introduced an automatic annotation approach that first aligns the data units on an end result page into various groups specified the data within the same cluster have constant semantics. Then, for every cluster we have a tendency to annotate it from completely different aspects and combine the various annotations to predict a final annotation label for it. An annotation wrapper for the search website is involuntarily build and can be utilized to annotate new result pages from the similar web database.

REFERENCES

- [1] Y. Lu, H. He, H. Zhao, W. Meng, C. Yu, "Annotating Search Results from Web databases" In IEEE Transaction on Knowledge and Data Engineering, Vol. 25, No.3, 2013.
- [2] J. Wang and F.H. Lochovsky, "Data Extraction and Label Assignment for Web Databases," Proc. 12th Int'l Conf. World Wide Web (WWW), 2003.
- [3] W. Liu, X. Meng, and W. Meng, "ViDE: A Vision-Based Approach for Deep Web Data Extraction," IEEE Trans. Knowledge and Data Eng., vol. 22, no. 3, pp. 447-460, Mar. 2010
- [4] W. Su, J. Wang, and F.H. Lochovsky, "ODE: OntologyAssisted Data Extraction," ACM Trans. Database Systems, vol. 34, no. 2, article 12, June 2009.
- [5] J. Zhu, Z. Nie, J. Wen, B. Zhang and W.-Y. Ma, "Simultaneous Record Detection and Attribute Labeling in Web Data Extraction, Proc. ACM SIGKDD Int'l Conf. Knowledge Discovery and Data Mining, 2006.
- [6] Y. Zhai and B. Liu, "Web Data Extraction Based on Partial Tree Alignment," Proc. 14th Int'l Conf. World Wide Web (WWW '05), 2005.
- [7] S. Mukherjee, I.V. Rama krishnan, and A. Singh, "Bootstrapping Semantic Annotation for Content-Rich HTML Documents," Proc. IEEE Int'l Conf. Data Eng. (ICDE), 2005.

Improving Performance in Parallel and Independent Access to Encrypted Cloud Databases

¹B. DIVYA KEERTHI, ² SANJEEVA POLEPAKA

¹M.Tech Student, Department of CSE, Mallareddy Engineering College, Maisammaguda Village, Medchal Mandal,
Ranga Reddy District, Telangana, India.

²Associate Professor, Department of CSE, Mallareddy Engineering College, Maisammaguda Village, Medchal
Mandal, Ranga Reddy District, Telangana, India.

ABSTRACT— *A cloud storage system consists of a bunch of storage servers over the online. The foremost aim is to provide secure storage services terribly very cloud storage system. There are several entirely totally different techniques were exist for storage services, whereas providing an data confidentiality solutions for the data as a service models are still in operative and is not completed still. We tend to tend to propose a novel style that integrates cloud data services with data confidentiality and thus the chance of punishment synchronic operations on encrypted data. Writing schemes are used to offer data confidentiality, data robustness and utility. We tend to tend to use associate writing data and Key verification for implementing for data secure storage. The planned style has the extra advantage of eliminating intermediate proxies that limit the property, accessibility, and quality properties that are intrinsic in cloud-based solutions. We tend to tend to propose associate style for higher security and confidentiality of a data hold on among the cloud databases. The effectuality of the planned style is evaluated through theoretical analyses and intensive experimental results supported a model implementation subject to the TPC-C customary benchmark for varied numbers of shoppers among the network. Writing schemes are used to offer data confidentiality, data robustness and utility. We tend to tend to use associate writing data and Key verification for implementing for data secure storage.*

1. INTRODUCTION

Cloud primarily based services are getting standard as they focus on high availableness and measurability at low value. While providing high availableness and measurability, placing essential knowledge to cloud poses several security issues. For avoiding these security problems the info square

measure stored within the cloud info in Associate in Nursing encrypted format.

The encrypted cloud info permits the execution of SQL operations by choosing the encoding schemes that support SQL operators. Encrypted cloud info permits differing types of accesses like distributed, concurrent, and freelance. one in all the design that supports these three sorts of access is SecureDBaaS, that was projected by Luca Ferretti. The SecureDBaaS design supports multiple and freelance shoppers to execute concurrent SQL operations on encrypted knowledge. Data consistency ought to be maintained by investing concurrency management mechanisms employed in package engines.

This survey explains the assorted concurrency management protocols that may be employed in the encrypted cloud database. The applications would like 1SR if knowledge is replicated. Hence, to ensure the deserves of cloud, it is essential to produce high measurability, availableness, low value and knowledge with sturdy consistency, which is able to dynamically adapt to system conditions. Selfoptimizing one copy serializability (SO-1SR) is that the concurrency management protocol that dynamically optimizes all stages of group action execution on replicated knowledge within the cloud info. Current DBMSs supported by cloud suppliers permits relaxed consistency guarantees that successively increase the design complexness of applications.

The second concurrency management protocol is that the snapshot isolation (SI) that provides increased concurrency in cloud setting in comparison to 1SR. Transactions square measure scan from the photo, reads square measure ne'er blocked thanks to write locks that in turn will increase

concurrency. SI doesn't permit several of the inconsistencies, however permits write skew anomalies. SI permits group action inversions. To avoid transaction inversions sturdy consistency guarantee is required, i.e. sturdy SI (SSI).

The third concurrency management protocol is that the session consistency (SC). Session consistency may be a different kind of ultimate consistency. The system provides scan your writes consistency within every session. Session consistency is at an occasional value whereas considering reaction time and group action value.

The cost primarily based concurrency management within the cloud is that the C3 i.e. cost-based adaptive concurrency management in cloud. C3 dynamically switch between sturdy consistency level and weak consistency level of transactions in an exceedingly cloud info in step with the value at runtime. it's engineered on the highest of ISR and SSI.

2. RELATED WORK

With a huge growth in user knowledge in cloud, user needs ever-changing knowledge storage whereas their roaming, privacy and security for his or her personal knowledge, better transferring knowledge, better broadband facilities, etc... And cloud computing junction rectifier to the emergence of cloud databases. For this issue this survey shows some existing techniques for resolution their user problem during this review section. Ryan K L KO et.al studied the issues and challenges of the trusty cloud, where the unauthorized user will access the whole knowledge while not distressing the particular user. An unauthorized user could do the 2 things that is accessing the knowledge and putt duplicate data as a result of cloud storage provides a geographical information. it's not a trusty one to store the info of the users. For this problem Ryan K L KO et.al projected a TrustCloud framework, to attain a trusty cloud to the user, to provide a service by creating use of detective controls in cloud setting. detection method has the responsibility access with the cloud. Here user may be a accountable person for his or her knowledge, thus user should tell the responsibility with the technical and policy primarily based services. By providing the responsibility through user it's going to solve the matter from the untrusted one. thus this approach provides privacy,

security, responsibility and auditability. Muhammad Rizwan Asghar et.al discusses the issues of imposing security policies in cloud setting. With the high growth of knowledge in cloud they wherever downside arises thanks to untrusted person access of the info. To make sure the safety is immature, they didn't guarantee for the safe knowledge in cloud environments. Security drawback may be a nice issue; here we tend to enforce the safety for the owner's knowledge. Providing high security they will high costly for the users. For the higher than mentioned downside Muhammad Rizwan Asghar et.al planned associate degree ESPOON policy that is Encrypted Security Policies for Outsourced eNvironments. This policy is in use to deal with the higher than downside and provides higher confidentiality to the users. It provides a more robust security by separating the safety policy and also the social control mechanism. Here M R Asghar uses an encrypted theme to safeguard the user's knowledge. This can be accustomed shield confidentiality policies supported user's policy. This method has 2 main theme, that is policy preparation and policy analysis theme. Policy preparation is employed to use the user's pointers and also the policy analysis is employed to estimate the user pointers. By mistreatment this technique user will safe their knowledge. L Ferretti et al considered the matter of information leak of the legitimate user in cloud setting by the cloud provider; they didn't provide higher security to the user for his or her personal knowledge or internal data. Main drawback arise attributable to no encrypted knowledge were found, and conjointly it offer the protection for the frond-end information solely and not controlled the backend information, therefore the malicious attackers could gain the information access to the outsourced data. L Ferretti et al studied the matter and planned a multiple key primarily based theme to permit the information administrator to get a scientific discipline key for top access management policies. By providing this key theme it supported multi user mechanism thus each time a key are going to be generated to the particular user for the info access. By mistreatment the key, user could decipher it and use the info over cloud. It provides the service used for public cloud DaaS. It enforces the access management mechanism. By this social control

user will guaranteeing in their knowledge. It minimizes the info leak downside. A.J. Feldman et al realize the issues of unseaworthy knowledge in server aspect and study the chance of privacy problem. thanks to centralization of knowledge attackers could simply hack the info through cloud computing. Access management underneath this cloud provider isn't a strong one; user knowledge could loss at any time as a result of all a user isn't continuously within the on-line to examine the standing of the info. thus it's simple to hack the information in anytime by the attackers and conjointly they will modify their data at any time thus it's risky one.

3. FRAME WORK

Below figure describes, the proposed system contain Owner, User, Cloud. Whenever owner store the information in encrypted format discrimination keys. TPA is a controller of owner, user and Cloud. The users are use this system by receiving the message as well as getting information from Cloud. Cloud information Base is freelance Access between owner and user.

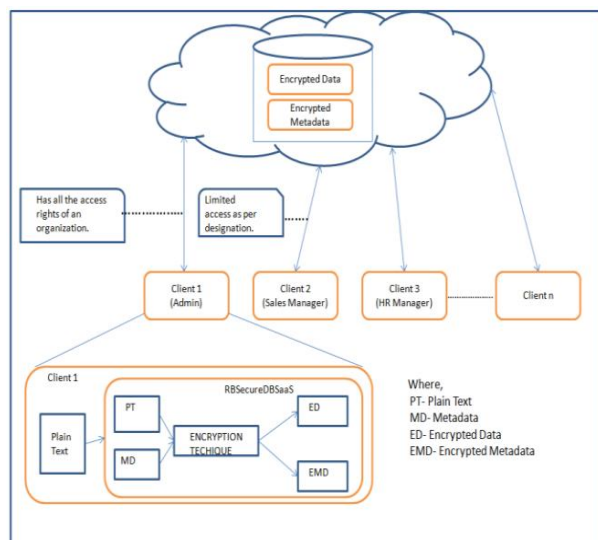


Fig .1. Architecture Diagram

1. User request to access a file from Cloud.
3. User authenticates CSP by his password
5. User decrypts the file by applying decryption algorithm
6. If User modify the file he will send file to CSP and TTP with a message like Md as $(F', \$, M)$ and F' here M denotes for modification F' for encrypted file, Md for message digest file and $\$$ for signature.
11. If file is same as previous one, drop this packet and move to step 1 or step 13.
12. Else ask CSP to follow step 11 again.
13. Exit 'F'

User side Process

2. Cloud ask User for authentication just like login page.
4. Verify password if correct send a file that he wants to access. Else move to step 2.
7. Cloud check the signature for authenticity and compute the message digest to find encrypted file which is compare with encrypted file of another message.
8. If correct it will change previous file with this one and move to step 12.
9. Else ask the client to follow the step 8.
10. CSP sends a same message to client after addition of his signature.

CSP Side Process

A. Message Authentication Code (MAC)

Authenticity, integrity

Electronic Signature (= asymmetric signature)

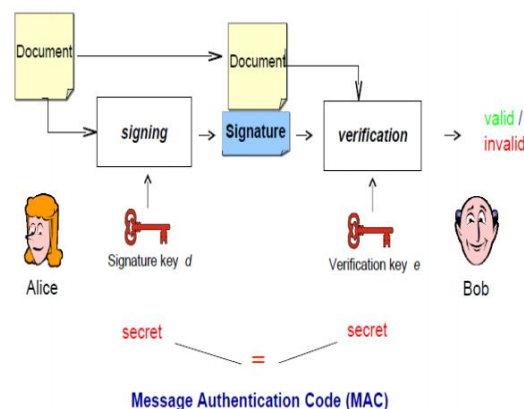
Authenticity, integrity, non-repudiation

Encryption:

Confidentiality

Encryption: $c \equiv me \pmod n$ (m is the plaintext)

Decryption: $m \equiv cd \pmod n$ (c is the cipher text)



Recently Novell proclaimed guide for the CloudMe service of their Dynamic record offerings Suite. Novosoft available Backup version seven.3 additionally proclaimed aid for CloudMe. There rectangular degree numerous third celebration cell apps and software out there for CloudMe, several usage the WebDAV help of CloudMe. The users will beautify the employment of CloudMe via having iPhone or robotic cellphone. as soon as CCloudMe is put in on the device, one will without a doubt get entry to the data anywhere the network. If the person makes adjustments within the cloud, then all the required changes are going to be created to distinct facts similarly. For example, if a photograph is loopy CloudMe iPhone application and stored within the CloudMe folder, then it's going to also be accessible on the computer force further. CloudMe can also be put in on multiple computer systems at regular time, for instance, on domestic and work computer so that you could have all the documents accessible on each the computer systems. There isn't a need to own a USB-reminiscence stick with you. in addition, CloudMe lets in the consumer synchronize a couple of folders at the identical time. presently you'll be capable of keep your photos, music, motion pictures and documents all prepared inside the equal folder as you commonly wanted to possess but presently with an additional CloudMe alternatives.

B. Concurrent SQL Operations

Maintain to the execution of SQL statements issued by multiple freelance (and presumptively geographically distributed) customers is one in each of the foremost necessary edges of SecureDBaaS with relevancy progressive solutions. Our style ought to guarantee consistency among encrypted tenant information and encrypted data as results of corrupted or absolute information would stop purchasers from cryptography encrypted tenant information resulting in permanent information losses. An intensive analysis of the potential issues and solutions related to synchronic SQL operations on encrypted tenant information and information is contained, out there inside the on-line supplemental material. Here, we've got an inclination to comment the importance of characteristic 2 classes of statements that square measure supported by SecureDBaaS: SQL operations not inflicting modifications to the knowledge structure, like

browse, write, and update; operations involving alterations of the knowledge structure through creation, removal and modification of data tables. Here, we have got an inclination to remark the importance of distinctive 2 categories of statements that unit supported by SecureDBaaS: SQL operations not inflicting modifications to the info structure, like scan, write, and update; operations involving alterations of the info structure through creation, deletion, and alteration of data tables (data definition layer operators). In eventualities defined by a static data structure, SecureDBaaS permits purchasers to issue synchronize SQL commands to the encrypted cloud data whereas not introducing any new consistency issues with relevancy unencrypted databases. Once data retrieval, a noticeable text SQL command is translated into one SQL command operative on encrypted tenant information. As data doesn't would like alteration, a consumer will browse them once and cache them for added uses successively thus rising performance. SecureDBaaS is that the primary style that allow to synchronize and consistent accesses even once there are operations that will modify the knowledge structure. In such cases, we have got to make sure the consistency of data through isolation levels that we have a tendency to tend to demonstrate can work for several victimization eventualities.

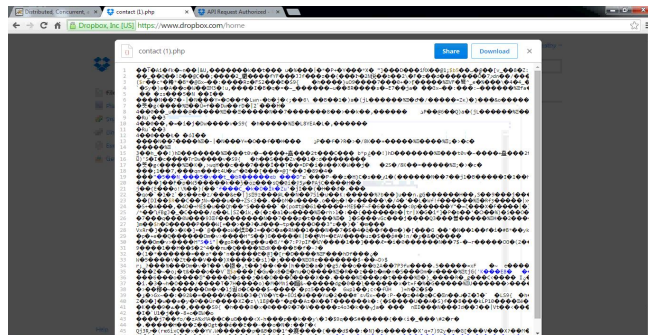
4. EXPERIMENTAL RESULTS

In our experiments, user must be registered in the system. But, when the administrator activates the user until then user cannot get the files means ha cannot activate to perform the action in the system.



When the user upload a file it will store in the form of encryption. To encrypt user's file he must get one secrete key. Without secrete key user cannot encrypt his file. Above screen shows that the secrete key entering to encrypt the files.

The below screen shows that after encryption of file is,



If user wants to download a file from cloud he will done by using decryption keys.

5. CONCLUSION

In this project we proposed architecture to provide the confidentiality to the data in cloud. The SecureDBaaS architecture assures the data confidentiality for data stored into cloud databases. A data which is stored on the cloud database are encrypted through cartographic algorithms as well as allows the execution of SQL queries on encrypted database. This architecture is also giving multiple independent clients access to data at cloud database. It does not trust on a trusted intermediate proxy that represents and also avoids the single point of failure and a system bottleneck, which in turn increases the availability and scalability of cloud database services.

REFERENCES

- [1] W. Jansen and T. Grance, "Guidelines on Security and Privacy in Public Cloud Computing" Technical Report Special Publication800-144, NIST, 2011.
- [2] P. Mahajan, S. Setty, S. Lee, A. Clement, L. Alvisi, M. Dahlin, and M. Walfish, "Depot: Cloud Storage with Minimal Trust" ACMTrans. Computer Systems, vol. 29, no. 4, article 12, 2011.
- [3] M. Armbrust et al., "A View of Cloud Computing" Comm. Of theACM, vol. 53, No.4, pp. 50-58, 2010.
- [4] A.J. Feldman, W.P. Zeller, M.J. Freedman, and E.W. Felten, "SPORC: Group Collaboration Using Untrusted Cloud Resources" Proc. Ninth USENIX Conf. Operating Systems Design and Implementation, Oct. 2010.
- [5] E. Mykletun and G. Tsudik, "Aggregation Queries in the Database-as-a-Service Model" Proc. 20th Ann. IFIP WG 11.3Working Conf. Data and Applications Security, July/Aug. 2006.
- [6] J. Li and E. Omiecinski, "Efficiency and Security Trade-Off in Supporting Range Queries on Encrypted Databases" Proc. 19th Ann. IFIP WG 11.3 Working Conf. Data and Applications Security,Aug. 2005.
- [7] J. Li, M. Krohn, D. Mazie`res, and D. Shasha, "Secure Untrusted Data Repository (SUNDR)" Proc. Sixth USENIX Conf. Opearting Systems Design and Implementation, Oct. 2004.
- [8] Hacigumus, B. Iyer, and S. Mehrotra, "Providing Database as a Service" Proc. 18th IEEE Int'l Conf. Data Eng., Feb. 2002.
- [9] Amazon elastic compute cloud (Amazon EC2), <http://aws.amazon.com/ec2/>.
- [10] Handling Confidential Data on the Untrusted Cloud: An Agent-based Approach Ernesto Damiani, Francesco Pagano Cloud Computing 2010: International Conference on Cloud Computing, GRIDs, and Virtualization.

HMAC-SHA-1 & Proof of Ownership Protocol on Cloud Data Storage

T. MADHUKAR REDDY¹ & P. SANJEEVA²

¹M-Tech Dept. of CSE, Malla Reddy Engineering College (A), Secunderabad

Mail Id: - madhu50538@gmail.com

²Associate Professor, Dept. of CSE, Malla Reddy Engineering College(A), Secunderabad

Mail Id: - psanjesus@gmail.com

Abstract

A Hybrid cloud is a coalescence of public and private clouds bound together by either standardized or proprietary technology that alters information plus application movability. Proposed system aiming to expeditiously resolving yequandary from deduplication on derivative favors in remote location computing. An hybrid remote locationstructure lying of a populace remote locationplus a individual remote locationplus ye information owners simply source their information storage by utilizing public cloud while the information operation is managed in private cloud. To build information management scalability in cloud computing, deduplication has been a very well-kenned technique recently is use. Deduplication reduces your bandwidth requisites, expedites the data transfers, and it keeps your cloud storage needs to a minimum. Proposed system demonstrate respective incipient deduplication expressions fortifying sanctioned duplicate assure inside hybrid remote locationstructure. To hold the secrecy of informationye convergent encoding proficiency holds made up used to encrypt ye information afore source. Sanctioned deduplication system support differential sanction duplicate check. As a proof of concept, a prototype is implemented in sanctioned duplicate check scheme and conduct test bed experiments utilizing prototype, sanctioned duplicate check scheme incurs minimal overhead compared to mundane operations.

Keywords: Deduplication, Proof of Ownership, Convergent Encryption, Key Management.

1. Introduction

To make information management scalable in cloud computing, deduplication has been a well-kenned technique plus has magnetized more plus more care recently. Information deduplication is a specialized information compression method for rejecting duplicate replicas of reiterating information in memory. The method is used to ameliorate memory

utilization plus can withal be used to network information transfers to reduce ye number of bytes that must be sent. In lieu of keeping numerous information copies with yesimilar content, deduplication excretes superfluous information by holding only solitary physical copy plus referring further redundant information to redundant imitate. Deduplication can carry lay at yedata records

level or yechunk level. For data records level deduplication, infotech rejects repeat facsimiles from yelike data records. Deduplication can adscitiouslychoose home astatine yechunk level, which excretes double chunksfrom information that occur in non-identical data records.

Albeit information deduplication brings an plethora of profits, protection plussecrecy pertains stand up while utilizer's sensitive information are sensitive to some insider plus foreigner approaches .Traditional encoding, while supplying information confidentiality, is uncongenial with information deduplication. Concretely, naturalencoding desires different utilizer's to encipher their information with their possess keys. Thus, very information replicas of different utilizers will lead to different ciphertexts, building deduplication infeasible. Convergent encryption has been suggested to enforce information confidentiality while building deduplication feasible. Infotech cipher text/normal text a information copy with a confluent key, which is incurred throughcalculating the cryptanalytic hash measure from yemessage fromyeinformationimitate.Afterward key propagation plusinformationencoding, utilizer'shold yekey valuesplussend outyeciphertext to yeremote location. Afterwards ye encryption procedure is

deterministic plus is derived from the information content, identical l information copies will engender the same convergent key plus hence the same ciphertext. To avert wildcat access, a insure proof of ownership protocol is withal needed to supply the proof that the utilizer indeed owns yeLapp data filewhenever a double is detected. Afterward yeproofread, subsequent utilizer'son yeLapp data file volition be supplied anarrow of yewaiter less wanting to transfer yelike data file. A utilizer can download yecipher textrecords with yearrow of yehost, which can alone be decoded by yerepresenting information owners with their focused keys. Hence, convergent encryption sanctions yeremote location to perform deduplication on yeciphertextsplus ye proof of ownership obviates ye unauthorized utilizer to get at yedata files.

2. Related Work

Hybrid cloud can be built utilizing any technology it changes granting to unlike vendors. Key constituents In many of the situations, implementation of the hybrid cloud has a comptroller that will hold track of all placements of private and public clouds, IP address, servers and other resources that can run systems efficiently.

2.1 Existing System:

Data deduplication be solitary of consequential information compression techniques for rejecting duplicate replicas of reiterating information, and has been widely used in cloud memory to reduce the sum of memory space plus preserve bandwidth. To forfendye confidentiality of sensitive information while fortifying deduplication, Cloud computing provide ostensibly illimitable “virtualized” resources to users as accommodations across the whole Internet, while obnubilating platform and implementation details. Today’s cloud accommodation providers offer both highly useable storage plus massively parallel calculating resources at relatively low costs. As remote location computing turns prevailing, a incrementing number from information makes up restored in yeremote location and shared by utilizer’s with designated favors, which determine the approach corrects of yememoryinformation.

Disadvantages of Existing System:

- One critical challenge of cloud memory accommodations is the management of ye ever-incrementing volume of information.

2.2 Proposed System:

Hybrid Cloud can be built utilizing any technology it changes granting to unlike vendors. Key components In many of the

situations, implementation of the hybrid cloud has a comptroller that will hold track of all positions of private and public clouds, IP address, servers plusearlyresources that can run systems efficiently.

Some of the key components include

- Orchestration manager plus cloud purveying for storage, populace cloud resources which includes virtual machines and networks, the private and public clouds, which are not compulsorily compatible or identical.
- Synchronization element and Data transfer expeditiously replace information among private plus public clouds.
- Changing configurations of storage, network and some early resources are constituting crossed by configuration monitor.[1]

In the Fig 1, the simplest view of hybrid cloud is allowed for, a single off-premises public cloud plus on-premises private cloud is within the Enterprise Datacenter is shown plus public cloud demonstrates the safe association to store information on to the cloud is denoted by the arrow:

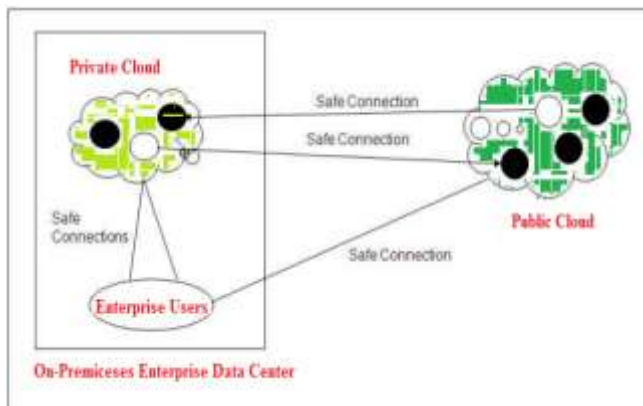


Fig 1: Hybrid Cloud Environment.

The ebony circles shows active virtual server images and white circles shows virtual server images which have been migrated by utilizing safe connections. The arrows designate that the direction of migration. Utilizing safe connections initiative utilizers are linked to ye clouds, which can be secure HTTP browsers or virtual private networks (VPNs) .A hybrid cloud could additionally can consist of multiple public or/and private clouds. [3]

Data de-duplication has many patterns. Generally, there is no one best way to enforce information de-duplication across an entire an organization. Instead, to maximize the gains, systems may spread more than one de-duplication strategy. It is very essential to understand the backup and backup challenges, when culling de-duplication as a solution.

We have introduced a hybrid cloud architecture in our aimed deduplicationscheme. The private keys for exclusive right will not be supplied to utilizer's directly, which will be held plush

plus led by ye private cloud server rather. In this manner, the utilizer's cannot contribution these private keys of favors in this suggested structure, which betokens that it can avoid ye privilege key distributingamongst utilizers in the over straight structure. To get a data filekeys, ye utilizer inevitably to ship a call for to yeindividual remote locationwaiter. Ye suspicion fromsuch building can be reported as follows. To perform the duplicate check for some data file, the utilizer wants to get yedata file keysonyeindividualremote locationwaiter. The Individualremote locationwaiter will additionally assure yeutilizer'sindividuality afore publishing ye representing data file keys to ye utilizer. The sanctioned double assure as such information data file bum be did throughye utilizer on yepopulateremote location afore transferring this data records. Predicated on yeanswers of double assure, ye utilizer either uploads this data file or runs PoW.

3. Implementation

Afore affording our construction of yededuplicationscheme, we determine an binary cognation $R = f((p, p')g$ because comes. Given 2 privileges p plus p' , we verbally show that p corresponds p' if plus only if $R(p, p') = 1$.

3.1 System Setup:

An identification protocol $\pi = (\text{Proof}, \text{Verify})$ is additionally determined, where Proof plus swear constitute the proof plus check algorithm severally. Moreover, for a piece one utilizer U exists surmised to have a mystery key sk_U to execute the identification with waiters. Postulate that utilizer U features the favor adjust PU . It additionally formats a PoW set of rules POW for the data records ownership proof. The private cloud server will control a table which shops each utilizer's public information pk plus its representing privilege set PU .

3.2 File Uploading:

Suppose that a information proprietor requires to transfer plus apportion an data records F on user's whose privilege belongs to the set $PF = \{p_j\}$. The information owner demands act with the secret remote location afore doing duplicate assure with the S-CSP. Information owner does an recognition to try out if the teches individuality on secret tokens sk_U . If it is communicated, the secret remote location waiter testament get the representing favors PU of the utilizer of its memory table list. The utilizer calculates plus sends the information data records tag $\phi F = \text{TagGen}(F)$ to the secret remote location waiter, who will return $\{ \phi F; p_+ = \text{TagGen}(\phi F, kp_+) \}$ back to the utilizer for total p_+ gratifying $R(p, p_+) = 1$

plus $p_+ \geq PU$. Then, the utilizer will act plus ship the file token $\{ \phi F; p_+ \}$ to the S-CSP.

- If and double data is detected by the S-CSP, the utilizer continues proof of ownership of this data file with the S-CSP. If the cogent evidence is passed, the utilizer will be assigned a pointer, which approves him to access the file.
- Otherwise, if no duplicate is found, the utilizer computes the encrypted file $CF = \text{EncCE}(k_F, F)$ with the convergent key $k_F = \text{KeyGenCE}(F)$ plus uploads $(CF, \{ \phi F; p_+ \})$ to the cloud server. The convergent key k_F is stored by the utilizer locally.

3.3 File Retrieving:

Guess a utilizer requires to getting a data records F . It beginning sends out an call for the data records name to the S-CSP. Upon getting the request plus data file designation, the S-CSP will assure whether the utilizer is worthy to download F . If failed, the S-CSP sends back an terminate signal to the utilizer to denote the data getting from network loser. Differently, the S-CSP affords the representing ciphertext CF . On experiencing the ciphered information from the S-CSP, the utilizer utilizes the key k_F memory topically to recuperate the pristine file F .

4. Experimental Work



Fig:-2 New Account Opening



Fig:-3 Secure Login

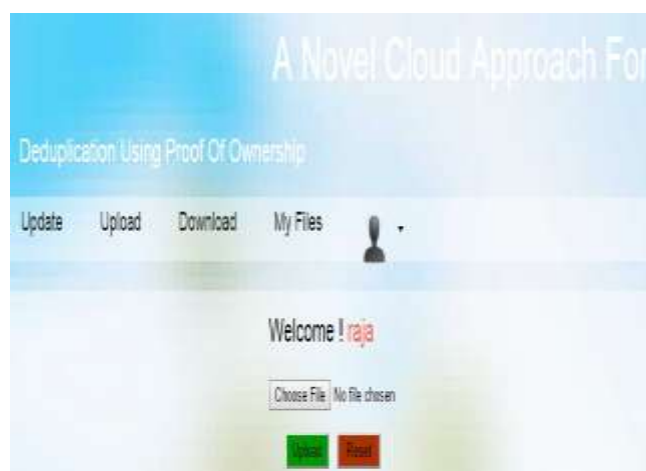


Fig:-4 Data upload

A Novel Cloud Approach For

Deduplication Using Proof Of Ownership

Uploads Downloads Updates Logout

UPLOADS

FILE NAME	OWNER NAME	UPLOAD TIME	SIZE
aa.jpg	radaragally	2014/11/04 11:28:36	110bytes
no_access_java.txt	radara	2014/11/04 13:28:19	110bytes
test.txt	radara	2015/02/28 19:58:33	110bytes
schwaftacker.java	radar	2015/03/16 11:14:45	4810bytes
shwaft.txt	shwaft	2015/09/19 11:48:30	852bytes
shwaft.txt	shwaft	2015/09/19 11:54:12	852bytes
upg.docx	upg	2015/09/23 19:21:40	1440bytes

Fig:-5 Data

A Novel Cloud Approach For

Deduplication Using Proof Of Ownership

Update Upload Download My Files

Welcome ! innadraja

View or Modify Permissions on raj.txt

Username	Update Permission	Download Permission
radara	Current Status: No Change	Current Status: No Change
radaragally	Current Status: No Change	Current Status: No Change
rad	Current Status: No Change	Current Status: Yes Change
upg	Current Status: No Change	Current Status: No Change

Fig:-5 Access Permissions

A Novel Cloud Approach For

Deduplication Using Proof Of Ownership

Update Upload Download My Files

Welcome ! raja

FILES

FILE NAME	OWNER NAME	UPLOAD TIME	SIZE	DOWNLOAD	File Integrity Status	Check File Integrity
aa.jpg	radaragally	2014/11/04 11:28:36	110bytes	Download	Respected	Respect TPA
no_access_java.txt	radara	2014/11/04 13:28:19	110bytes	Download	Respected	Respect TPA
test.txt	radara	2015/02/28 19:58:33	110bytes	Download	File Updated	Respect TPA

Fig:-5 Editing File Permissions

5. Conclusion

The celebration of sanctioned information deduplicationbesuggested to ascertain the information security through counting

disparity gains of clients in yeduplicate replica check. The presentation of aelite incipient deduplicationgrowths fortifying sanctioned duplicate re-create in hybrid cloud architecture, in that ye duplicate assure tokens of documents are caused via ye private remote locationwaiterholding secrete keys. Security check presents that ye methods are assure regarding insider plus outsider assaults detailed in the suggested security model. As an issue verification of conception, the developed model of the proposed sanctioned duplicate copy check method and tested the model. That showed the sanctioned duplicate copy check method experience minimum overhead comparing convergent encryption and data transfer.

6. References

- [1] Bugiel, Sven, et al. "Twin clouds: Secure cloud computing with low latency." Communications and Multimedia Security.Springer Berlin Heidelberg, 2011.
- [2] Anderson, Paul, and Le Zhang. "Fast and Secure Laptop Backups with Encrypted Deduplication." LISA. 2010.
- [3] Bellare, Mihir, SriramKeelveedhi, and Thomas Ristenpart. "DupLESS: server-aided encryption for deduplicated storage." Proceedings of the 22nd USENIX conference on Security.USENIX Association, 2013.
- [4] Bellare, Mihir, SriramKeelveedhi, and Thomas Ristenpart. "Message-locked encryption and secure deduplication."Advances in Cryptology–EUROCRYPT 2013.Springer Berlin Heidelberg, 2013.296-312.
- [5] Bellare, Mihir, ChanathipNamprempre, and Gregory Neven. "Security proofs for identity-based identification and signature schemes." Journal of Cryptology 22.1 (2009): 1-61.
- [6] M. Bellare, S. Keelveedhi, and T. Ristenpart.Dupless: Serveraided encryption for deduplicated storage. In *USENIX Security Symposium*, 2013.
- [7] K. Zhang, X. Zhou, Y. Chen, X.Wang, and Y. Ruan.Sedic: privacyaware data intensive computing on hybrid clouds. In *Proceedings of the 18th ACM conference on Computer and communications security*, CCS'11, pages 515–526, New York, NY, USA, 2011. ACM.
- [8] S. Halevi, D. Harnik, B. Pinkas, and A. Shulman-Peleg.Proofs of ownership in remote storage systems. In Y. Chen, G. Danezis, and V. Shmatikov, editors, *ACM Conference on Computer and Communications Security*, pages 491–500. ACM, 2011.

Unreliable Portrait Information Screening with Contrast Enhancement

SATRAJUPALLI NAGA LAKSHMI¹, SANJEEVA POLEPAKA²

Student of M.Tech(CSE)¹, Associate. Professor, CSE Dept²

Mallareddy Engineering College (Autonomous),

Maisammaguda, Hyderabad, Telangana, India

satrasupalli@gmail.com¹, sanjeeva.p@mrec.ac.in²

ABSTRACT

Steganography is that the art of activity info in ways in which avert the revealing of activity messages. Video files are usually a set of pictures. Thus most of the conferred techniques on pictures and audio will be applied to video files too. The good benefits of video are the massive quantity of knowledge that may be hidden within and also the incontrovertible fact that it's a moving stream of image. During this paper, we have a tendency to project a replacement technique mistreatment the motion vector, to cover the info within the moving objects. Moreover, to boost the protection of the info, the info is encrypted by mistreatment the DES formula then hided. The info is hided within the horizontal and also the vertical elements of the moving objects

KEYWORDS: Data hiding, encrypted domain, code word substituting.

INTRODUCTION:

The rise of the web one among the foremost necessary factors of data technology and communication has been the safety of data. Cryptography was created as a way for securing the secrecy of communication and plenty of completely different strategies are developed to inscribe and decode information so as to stay the message secret. Sadly it's generally not enough to stay the contents of a message secret, it should even be necessary to stay the existence of the message secret. The technique wont to implement this, is named steganography. it's differs from cryptography within the sense that wherever cryptography focuses on keeping the contents of a message secret, steganography focuses on keeping the existence of a message secret. Steganography and cryptography square measure each ways in which to safeguard data from unwanted parties. Once the presence of hidden data is discovered or maybe suspected, the aim steganography is part defeated. The strength of steganography will therefore be amplified by combining it with cryptography.

EXISTING SYSTEM:

- In special domain, the activity method like least vital bit (LSB) replacement, is finished in special domain, whereas remodel domain methods; hide knowledge in another domain like ripple domain.
- Least vital bit (LSB) is that the simplest variety of Steganography. LSB relies on inserting knowledge within the least vital little bit of pixels that cause a small modification on the quilt image that's not noticeable to human eye. Since this technique are often simply cracked, it's a lot of susceptible to attacks.
- LSB technique has intense effects on the applied math info of image like bar graph. Attackers may well be awake to a hidden communication by simply checking the bar graph of a picture. an honest answer to eliminate this defect was LSB matching. LSB-Matching was an excellent success in Steganography strategies and lots of others get ideas from it

DISADVANTAGES:

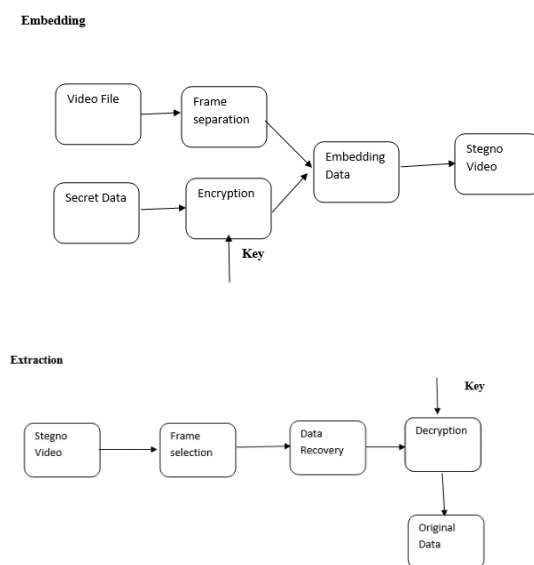
- The secret key used for cryptography of compressed image and also the information concealing is same. So, the user World Health Organization is aware of the key used for cryptography will access {the information the info the information} embedded and also the original data.
- The original video will be retrieved from the compressed video when extracting or removing the information hidden within the image.

PROPOSED SYSTEM:

Data concealing in video sequences is performed in 2 major ways: bit stream-level and data-level. During this paper, we have a tendency to propose a brand new block-based selective embedding sort information concealing Framework. By suggests that of easy rules applied to the frame markers, we have a tendency to introduce bound level of strength against frame drop, repeat and insert attacks.

ADVANTAGES:

- It isn't simply cracked.
- To increase the protection.
- To increase the dimensions of hold on information.
- We will hide quite one bit.

ARCHITECTURE DIAGRAM:**LITERATURE SURVEY:****Watermarking Security: Theory and Practice**

This paper proposes a theory of watermarking security supported a cryptography purpose of read. The most plan is that info concerning the key leaks from the observations, for example, watermarked items of content, obtainable to the opponent. Tools from scientific theory (Shannon's mutual info and Fisher's info matrix) will live this discharge of data. The protection level is then outlined because the range of observations the assailant has to with success estimate the key. This theory is applied to 2 common watermarking methods: the substitutive theme and therefore the unfold spectrum-based techniques. Their security levels square measure calculated against 3 styles of attack. The experimental work illustrates however Blind supply Separation (especially freelance element Analysis) algorithms facilitate the opponent exploiting this info discharge to disclose the key carriers within the unfold spectrum case. Simulations assess the protection levels derived within the theoretical a part of the paper.

Secure Spread Spectrum:

This paper presents a secure (tamper-resistant) rule for watermarking pictures, and a technique for digital watermarking that will be generalized to audio, video, and transmission knowledge. we tend to advocate that a watermark ought to be created as AN freelance and identically distributed (i.e.) Gaussian random vector that's unnoticeably inserted in an exceedingly spread-spectrum-like fashion into the perceptually most vital spectral parts of the info. we tend to argue that insertion of a watermark below this regime makes the watermark strong to signal process operations (such as lossy compression, filtering, digital-analog and analog-digital conversion, quantization, etc.), and customary geometric transformations (such as cropping, scaling, translation, and rotation) as long as the first image is out there which it is with success registered against the reworked watermarked image. In these cases, the watermark detector unambiguously identifies the owner. Further, the employment of Gaussian noise, ensures robust resilience to multiple-document, or

collisional, attacks. Experimental results are provided to support these claims, beside AN exposition of unfinished open issues.

The Zero-Rate Spread - Spectrum Watermarking Game

This paper develops a game-theoretic methodology to style and implant messages in signals and pictures within the presence of an opponent. Here, is assumed to be sub exponential within the signal's sample size (zero-rate transmission), and also the embedding is finished victimization spread-spectrum watermarking. The detector performs applied mathematics hypothesis testing. The system is meant to attenuate likelihood of error underneath the worst-case attack in a much prescribed category of attacks. The variables during this game are likelihood distributions for the water marker and aggressor. Analytical solutions are derived underneath the idea of mathematician host vectors, watermarks and attacks, and squared-error distortion constraints for the water marker and also the aggressor. The Karhunen-Loève remodel (KLT) plays a central role during this study. The best distributions for the water marker and also the aggressor are mathematician take a look at channels applied to the KLT coefficients; the sport is then reduced to a maxim power-allocation drawback between the channels. As a byproduct of this analysis, we are able to verify the best exchange between victimization the foremost economical (in terms of detection performance) signal elements for transmission and spreading the transmission across several elements (to fool the attacker's tries to eliminate the watermark). We tend to conjointly conclude that during this framework, additive watermarks ar suboptimal; they're, however, nearly best in a very small-distortion regime. The speculation is applied to watermarking of autoregressive processes and to wavelet-based image watermarking. The best watermark style outperforms typical styles supported heuristic power allocations and/or easy correlation detectors

Kirchhoff's-Based Embedding Security

It has recently been discovered that victimization pseudorandom sequences as carriers in spread-spectrum techniques for data-hiding isn't in the slightest degree a sufficient condition for

guaranteeing data-hiding security. Victimization correct and realistic apriority hypothesis on the messages distribution, it's attainable to accurately estimate the key carriers by casting this estimation downside into a blind supply separation downside. once reviewing relevant works on spread-spectrum security for watermarking, we have a tendency to additional develop this subject to introduce the construct of security categories that broaden previous notions in watermarking security and fill the gap with steganography security as outlined by Caching. We have a tendency to outline four security categories, namely, by order of creasing security: insecurity, key security, mathematical space security, and stegosecurity. Let's say these views, we have a tendency to gift 2 new modulations for really secure watermarking within the watermark-only-attack (WOA) framework. The primary one is named natural watermarking and may be created either stegosecurity or mathematical space secure. The second is named circular watermarking and is vital secure. we have a tendency to show that circular watermarking has hardness love that of the insecure classical unfold spectrum. we have a tendency to shall conjointly propose info escape measures to focus on the protection level of our new spread-spectrum modulations.

Modules

Video Compression

Video compression uses fashionable writing techniques to cut back redundancy in video knowledge. Video compression usually operates on square-shaped teams of neighboring pixels, usually referred to as macro blocks. These picture element teams or blocks of pixels area unit compared from one frame to consecutive and also the video compression code sends solely the variations inside those blocks. In areas of video with additional motion, the compression should inscribe additional knowledge to stay up with the larger variety of pixels that area unit dynamical.

Encryption

Encryption is that the conversion of knowledge into a type, referred to as a cipher text that can't be simply understood by unauthorized individuals. Original message is being hidden inside a carrier specified the

changes thus occurred within the carrier don't seem to be noticeable. data the knowledge the data} regarding the user outlined information, the decoding non-public key wont to cipher the text and also the average time of the frame format is given. The encoding of the text is finished by victimizations the DES customary algorithmic rule since the key size is larger for the DES.

Extraction of original data

Decoding is that the method of changing encrypted knowledge back to its original type, thus it will be understood. Once the user inputs the right key that's used at the decoding method, this can extract the first message that's encrypted and embedded.

CONCLUSION

In this paper, we have a tendency to propose and investigate the information concealing methodology exploitation the motion vector technique for the moving objects. Within the existing works the information is hided at intervals the still photos wherever because it can resulted in the image distortion? By embedding the information within the moving objects the standard of the video is raised. During this paper, the compressed video is employed for the information transmission since it will hold giant volume of the information. The adjective based mostly compression technique is evaluated specified the information is embedding within the vertical and horizontal part pixels. The PSNR price is calculated to point out that the frame is transmitted with none loss or distortion. As a result, the motion vector technique is found because the higher resolution since it hides the information within the moving objects instead of within the still photos. The cryptography enhances the protection of the information being transmitted.

REFERENCE

[1] W. J. Lu, A. Varna, and M. Wu, "Secure video processing: Problems and challenges," in Proc. IEEE Int. Conf. Acoust., Speech, Signal Processing, Prague, Czech Republic, May 2011, pp. 5856–5859.

[2] B. Zhao, W. D. Kou, and H. Li, "Effective watermarking scheme in the encrypted domain for

buyer-seller watermarking protocol," *Inf. Sci.*, vol. 180, no. 23, pp. 4672–4684, 2010.

[3] P. J. Zheng and J. W. Huang, "Walsh-Hadamard transform in the homo- morphic encrypted domain and its application in image watermarking," in Proc. 14th Inf. Hiding Conf., Berkeley, CA, USA, 2012, pp. 1–15.

[4] W. Puech, M. Chaumont, and O. Strauss, "A reversible data hiding method for encrypted images," *Proc. SPIE*, vol. 6819, pp. 68191E-1–68191E-9, Jan. 2008.

[5] X. P. Zhang, "Reversible data hiding in encrypted image," *IEEE Signal Process. Lett.*, vol. 18, no. 4, pp. 255–258, Apr. 2011.

[6] W. Hong, T. S. Chen, and H. Y. Wu, "An improved reversible data hiding in encrypted images using side match," *IEEE Signal Process. Lett.*, vol. 19, no. 4, pp. 199–202, Apr. 2012.

[7] X. P. Zhang, "Separable reversible data hiding in encrypted image," *IEEE Trans. Inf. Forensics Security*, vol. 7, no. 2, pp. 826–832, Apr. 2012.

[8] K. D. Ma, W. M. Zhang, X. F. Zhao, N. Yu, and F. Li, "Reversible data hiding in encrypted images by reserving room before encryption," *IEEE Trans. Inf. Forensics Security*, vol. 8, no. 3, pp. 553–562, Mar. 2013.

[9] A. V. Subramanyam, S. Emmanuel, and M. S. Kankanhalli, "Robust watermarking of compressed and encrypted JPEG2000 images," *IEEE Trans. Multimedia*, vol. 14, no. 3, pp. 703–716, Jun. 2012.

[10] S. G. Lian, Z. X. Liu, and Z. Ren, "Commutative encryption and watermarking in video compression," *IEEE Trans. Circuits Syst. Video Technol.*, vol. 17, no. 6, pp. 774–778, Jun. 2007.

[11] S. W. Park and S. U. Shin, "Combined scheme of encryption and watermarking in H.264/scalable video coding (SVC)," *New Directions Intell. Interact. Multimedia*, vol. 142, no. 1, pp. 351–361, 2008.

[12] T. Wiegand, G. J. Sullivan, G. Bjontegaard, and A. Luthra, "Overview of the H.264/AVC video coding standard," *IEEE Trans. Circuits Syst. Video Technol.*, vol. 13, no. 7, pp. 560–576, Jul. 2003.

- [13] S. G. Lian, Z. X. Liu, Z. Ren, and H. L. Wang, "Secure advanced video coding based on selective encryption algorithms," *IEEE Trans. Consumer Electron.*, vol. 52, no. 2, pp. 621–629, May 2006.
- [14] Z. Shahid, M. Chaumont, and W. Puech, "Fast protection of H.264/AVC by selective encryption of CAVLC and CABAC for I and P frames," *IEEE Trans. Circuits Syst. Video Technol.*, vol. 21, no. 5, pp. 565–576, May 2011.
- [15] M. N. Asghar and M. Ghanbari, "An efficient security system for CABAC bin-strings of H.264/SVC," *IEEE Trans. Circuits Syst. Video Technol.*, vol. 23, no. 3, pp. 425–437, Mar. 2013.
- [16] T. Stutz and A. Uhl, "A survey of H.264 AVC/SVC encryption," *IEEE Trans. Circuits Syst. Video Technol.*, vol. 22, no. 3, pp. 325–339, Mar. 2012.
- [17] Advanced Video Coding for Generic Audiovisual Services, ITU, Geneva, Switzerland, Mar. 2005.
- [18] J. G. Jiang, Y. Liu, Z. P. Su, G. Zhang, and S. Xing, "An improved selective encryption for H.264 video based on intra prediction mode scrambling," *J. Multimedia*, vol. 5, no. 5, pp. 464–472, 2010.
- [19] I. E. G. Richardson, *H.264 and MPEG-4 Video Compression: Video Coding for Next Generation Multimedia*. Hoboken, NJ, USA: Wiley, 2003.
- [20] D. K. Zou and J. A. Bloom, "H.264 stream replacement watermarking with CABAC encoding," in *Proc. IEEE ICME*, Singapore, Jul. 2010, pp. 117–121.
- [21] D. W. Xu and R. D. Wang, "Watermarking in H.264/AVC compressed domain using Exp-Golomb code words mapping," *Opt. Eng.*, vol. 50, no. 9, p. 097402, 2011.
- [22] D. W. Xu, R. D. Wang, and J. C. Wang, "Prediction mode modulated data-hiding algorithm for H.264/AVC," *J. Real-Time Image Process.*, vol. 7, no. 4, pp. 205–214, 2012.
- [23] T. Shanableh, "Data hiding in MPEG video files using multivariate regression and flexible macroblock ordering," *IEEE Trans. Inf. Forensics Security*, vol. 7, no. 2, pp. 455–464, Apr. 2012.

Content Caching And Scheduling In Wireless Networks With Elastic And Inelastic Traffic

Mr. DEVERNENI SAGAR RAO
M.Tech Student, Dept of CSE Malla Reddy
Engineering College
Hyderabad, T.S, India

Mr.B.VIJAY KUMAR
Associate Professor, Dept of CSE
Malla Reddy Engineering College
Hyderabad, T.S, India.

Abstract: There is a huge growth in the wireless networks in current days. With this growth, accessing the content through wireless networks needs placing the content at the base stations and scheduling them. Users who are in the network are divided into groups based on the channel conditions, their requests are placed in the front end of the logical queue. All these requests are elastic and inelastic. These requests are placed in the queues which are known as requests queues and the deficit queues contains the deficits which are had in the in elastic services. The data which are stored in the cache are of limited size and they will be getting refreshed frequently to constant time intervals. This paper considering the two different models which will be concentrating on inelastic requests for streaming stored content and real-time streaming of events. In this paper some of the suggestions are made which are used to design the optimal policies which are used to stabilize the request queues and to reduce the deficit to zero

I. INTRODUCTION

From the last 2 to 3 decades there is a huge growth in usage of hand held devices. These devices may be electrical or electronics and some are called as smart devices. In the current generation usage of smart devices has been grown vastly. These devices are using different resource in achieving their functionality. While working all these devices will work under the constraints which includes hard and soft constraints. For example if we take streaming applications in which chunks of the file must be received under hard delay constraints, as well as file downloads such as software updates that do not have such hard constraints. Since the core of the Internet is far less bandwidth constrained than access wireless networks, a natural location to implement a content distribution network (CDN) would be at the wireless gateway, which could be a cellular base-station through which users obtain network access. Broadcasting the information to the multiple clients simultaneously is one of the natures further, it is natural to try to take advantage of the inherent broadcast nature of the wireless medium to satisfy multiple clients simultaneously.

Every network will be having the base station where the data will be storing in the cache of each station. These caches are periodically refreshed by accessing the media vault. All the nodes are divided into the clusters which are geographically nearer to each other. The front end will be run on any of the device and the requests which are posed will be under tracking by the system.

This paper mainly concentrating on the issues like joint content placement and the problems of scheduling the traffic for both elastic and inelastic wireless networks.

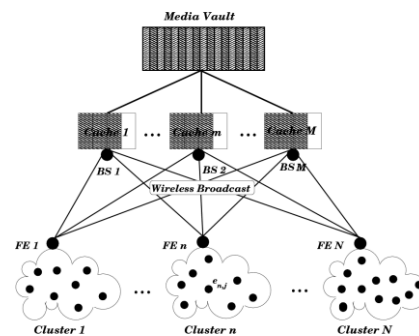


Figure 1: Wireless Broadcast Distribution Network.

II. LITERATURE SURVEY

Jeffrey E. Wieselthier et al develop the Broadcast Incremental Power Algorithm, and adapt it to multicast operation as well. This algorithm exploits the broadcast nature of the wireless communication environment, and addresses the need for energy-efficient operation. we have identified some of the fundamental issues associated with energy-efficient broadcasting and multicasting in infrastructure less wireless networks, and we have presented preliminary algorithms for the solution of this problem. Our studies show that improved performance can be obtained when exploiting the properties of the wireless medium; i.e., networking schemes should reflect the node based nature of wireless communications, rather than simply adapt link-based schemes originally developed for wired networks. In particular, the Broadcast Incremental Power (BIP) Algorithm, which exploits the wireless multicast advantage, provides better performance than the other algorithms we have studied over a wide range of network examples. [1]

Meghana M Amble et al objective is to design policies for request routing, content placement and content eviction with the goal of small user delays. Stable policies ensure the finiteness of the request queues, while good polices also lead to short queue

lengths. We first design a throughput-optimal algorithm that solves the routing-placement-eviction problem. The design yields insight into the impact of different cache refresh policies on queue length, and we construct throughput optimal algorithms that engender short queue lengths. We illustrate the potential of our approach through simulations on different CDN topologies.. Future work includes streaming traffic with requests that have hard delay constraints, and which are dropped if such a constraint cannot be met. [2]

Bo Zhou et al formulate this stochastic optimization problem as an infinite horizon average cost Markov decision process (MDP). It is well known to be a difficult problem and there generally only exist numerical solutions. By using relative value iteration algorithm and the special structures of the request queue dynamics,. we consider the optimal dynamic multicast scheduling to jointly minimize the average delay, power and fetching costs for cache-enabled content-centric wireless networks. We formulate this stochastic optimization problem as an infinite horizon average cost MDP. We show that the optimal policy has a switch structure in the uniform case and a partial switch structure in the non-uniform case. Moreover, in the uniform case with two contents, we show that the switch curve is monotonically non-decreasing. The optimality properties obtained in this paper can provide design insights for multicast scheduling in practical cache-enabled content centric wireless networks [4].

III. SYSTEM IMPLEMENTATION

Based on the published content, I have started implementing algorithms for content distribution with elastic and inelastic requests. Here in the implementation of the application used a request queue to implicitly determine the popularity of elastic content. Similarly, the deficit queue determines the necessary service for inelastic requests. It is said that Content may be refreshed periodically at caches. Two different cost models are studied in implementation, each of which is appropriate for a different content distribution scenario. The first is the case of file distribution (elastic) along with streaming of stored content (inelastic), where we model cost in terms of the frequency with which caches are refreshed. The second is the case of streaming of content that is generated in real-time, where content expires after a certain time, and the cost of placement of each packet in the cache is considered.

The following are the main functionalities which we are concentrating in implementation of this application are

- a. Creating System Model
- b. Content Caching System Module

- c. Elastic Traffic Module
- d. Inelastic Traffic Module

IV. CONCLUSION

To implement the above system, I have studied different papers and analyzed the whole concept. Mainly, I have concentrated on the algorithms for content placement and scheduling in wireless broadcast networks. While there has been significant work on content caching algorithms, there is much less on the interaction of caching and networks. Converting the caching and load balancing problem into one of queuing and scheduling is hence interesting. A system is considered in which both inelastic and elastic requests coexist. Our objective was to stabilize the system in terms of finite queue lengths for elastic traffic and zero average deficit value for the inelastic traffic. In designing these schemes, showed that knowledge of the arrival process is of limited value to taking content placement decisions. Incorporated the cost of loading caches is in proposed problem with considering two different models. In the first model, cost corresponds to refreshing the caches with unit periodicity. In the second model relating to inelastic caching with expiry, directly assumed a unit cost for replacing each content after expiration. A max-weight-type policy was suggested for this model, which can stabilize the deficit queues and achieves an average cost that is arbitrarily close to the minimum cost.

V. REFERENCES

- [1]. On the Construction of Energy-Efficient Broadcast and Multicast Trees in Wireless Networks by Jeffrey E. Wieselthier ,Gam D. Nguyen , Anthony Ephremides.
- [2]. Content-Aware Caching and Traffic Management in Content Distribution Networks by Meghana M Amble,, ParimalParag, SrinivasShakkottai , and Lei Ying.
- [3]. Relay-Based Identification of a Class of NonminimumPhase SISO Processes by SomanathMajhiOptimal Dynamic Multicast Scheduling for Cache-Enabled Content-Centric Wireless Networks by Bo Zhou, Ying Cui and Meixia Tao.
- [4]. Kaleidoscope: Cloud Micro-Elasticity via VM State Coloring by Roy Bryant, Alexey Tumanov ,Olga IrzakAdinScannell, Kaustubh Joshi , MattiHiltunen, H. Andr esLagar-Cavilla, Eyal de Lara.
- [5] N. Abedini and S. Shakkottai, "Content caching and scheduling in wireless broadcast networks with elastic and inelastic

- traffic,” in *Proc.IEEEWiOpt*, 2011, pp. 125–132.
- [6] I. Hou, V. Borkar, and P. Kumar, “A theory of QoS for wireless,” in *Proc. IEEE INFOCOM*, Rio de Janeiro, Brazil, Apr. 2009, pp.486–494.
 - [7] R. M. P. Raghavan, *Randomized Algorithms*. New York, NY, USA: Cambridge Univ. Press, 1995.
 - [8] P. Cao and S. Irani, “Cost-aware WWW proxy caching algorithms,” in *Proc. USENIX Symp. Internet Technol. Syst.*, Berkeley, CA, Dec. 1997, p. 18.
 - [9] K. Psounis and B. Prabhakar, “Efficient randomized Web-cache replacement schemes using samples from past eviction times,” *IEEE/ACM Trans. Netw.*, vol. 10, no. 4, pp. 441–455, Aug. 2002.
 - [10] N. Laoutaris, O.T. Orestis, V. Zissimopoulos, and I. Stavrakakis, “Distributed selfish replication,” *IEEE Trans. Parallel Distrib. Syst.*, vol. 17, no. 12, pp. 1401–1413, Dec. 2006.
 - [11] S. Borst, V. Gupta, and A. Walid, “Distributed caching algorithms for content distribution networks,” in *Proc. IEEE INFOCOM*, San Diego, CA, USA, Mar. 2010, pp. 1–9.
 - [12] L. Tassiulas and A. Ephremides, “Stability properties of constrained queueing systems and scheduling policies for maximum throughput in multihop radio networks,” *IEEE Trans. Autom. Control*, vol. 37, no. 12, pp. 1936–1948, Dec. 1992.
 - [13] X. Lin and N. Shroff, “Joint rate control and scheduling in multihop wireless networks,” in *Proc. 43rd IEEE CDC*, Paradise Islands, Bahamas, Dec. 2004, vol. 2, pp. 1484–1489.
 - [14] A. Stolyar, “Maximizing queueing network utility subject to stability: Greedy primal-dual algorithm,” *Queueing Syst. Theory Appl.*, vol. 50, no. 4, pp. 401–457, 2005.

Guarantee End-User Routine While Contents Are Gathered From Numerous Facts Hub

TUNIKAPATI KIRAN KUMAR

M.Tech Student, Department of CSE
Malla Reddy Engineering College(Autonomous).
Dulapally Rd, Maisammaguda, Dhulapally,
Kompally, Medchal,Hyderabad, Telangana

B.VIJAY KUMAR

Associate Professor, Department of CSE
Malla Reddy Engineering College(Autonomous).
Dulapally Rd, Maisammaguda, Dhulapally,
Kompally, Medchal,Hyderabad, Telangana

Abstract: As electricity prices vary across data centers and usage price varies across CAS, scheduling data centers and CAS includes a tremendous consequence for optimizing content service cost. The facility costs for data centers and also the usage costs for CAS are major contributors towards the contents service cost. Content service is a kind of Internet cloud service that gives finish-users plentiful contents. To make sure high end for content delivering, content service relies on a technology referred to as content multi homing: contents are produced by multiple geographically distributed data centers and delivered by multiple distributed content allotment system (CAS). Using real-existence electricity prices and CAS traces, the experiments show Suggested effectively cuts down on the content service cost by greater than 20 %. Within this paper, we advise a singular framework named Cost Optimization for Internet Content Multi homing. Suggested dynamically balances finish-users' loads among data centers and CAS in order to minimize the information service cost.

Keywords: Content Allotment System (CAS); Multihoming; Cost; Optimization;

I. INTRODUCTION

A content allotment system (CAS) accounts for efficient delivery of contents: it replicates contents originated in an information center, and uses the in your area stored contents for everyone finish-users' demands. To make sure high end for content delivering, content service relies on a technology referred to as content multi homing for content generation and distribution [1]. First, contents could be produced by several data centers distributed in various regions. Second, contents may also be delivered by several CAS distributed on the internet. A content company chooses a CAS according to performance, cost along with other reasons. As data centers develop quickly to satisfy the soaring cloud-computing demands, the consumption and price of one's by data centers are skyrocketing. There's growing curiosity about how to pick CAS for content delivery and reduce the CAS usage costs as the performance requirement is content. A couple of recent reports required a restricted optimization method of the usage cost minimization for CAS. Couple of research has investigated the information service cost minimization problem and required both discovered another means for data centers and usage costs for CAS into account. Within this paper, we study how to pick data centers for content generation and CAS for content delivery in order to minimize the information service cost inside a content-multi homing atmosphere [2]. The minimization of content service price is formulated from service provider's perspective also it can considerably lessen the operation cost in order to increase the profits. To the best understanding, our jobs are the very first that can take an all natural

approach by since the content service cost in the content generation towards the content delivery.

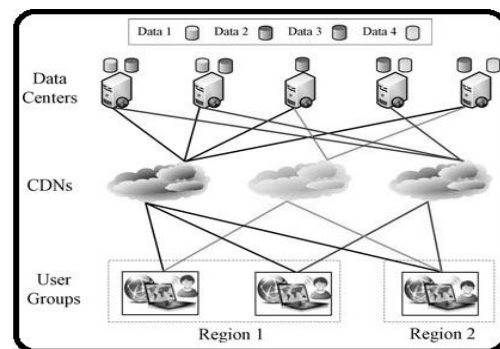


Fig.1.Proposed system

II. PROPOSED SYSTEM

Our suggested framework to optimize the sum of the discovered another means for data centers and usage costs for CAS through content multi homing. The entities within the Suggested framework mainly include four parts: user group, data, and CAS and knowledge center. A person group may be the group of users who're symbolized through the one and same identity within the Suggested framework [3]. Data would be the assortment of content objects the users request online. CAS is really a large distributed system of servers, which replicates contents originated in data centers, and offers the in your area stored contents to finish users through network. An information center is an accumulation of servers inside a certain place to serve the information demands from users. A CAS can be used to provide both static and dynamic content more than a vast network infrastructure with excellent links. When a finish-user demands a

content service, the request is going to be redirected in the originating site's server to some server in a single of CAS. Whenever a request makes an advantage server inside a selected CAS, the static submissions are offered from it. However, the dynamic submissions are away from the cache, and then your edge server within the CAS constitutes a request for an origin server in a single of information centers. Within this paper, we advise the Suggested framework which runs an expense-aware optimization formula to select which data center for content generation and which CAS for content delivery [4]. To describe our designing method, we'll provide a whole process about how exactly a request of dynamic content information is processed one of the four entities with parameters given. To formulate the price optimization problem, then we have to calculate the price for that request distribution process. The price for content providers mainly originates from a double edged sword: the usage price of CAS and also the electricity price of data centers. First, the prices purpose of a CAS is connected using its charging region that the user group is found in and how big traffic the consumer transmits towards the CAS. Second, we simply concentrate on the electricity cost in data centers also it depends upon the amount of assigned demands and also the electricity cost for processing per request. The price minimization could be modeled like a request distribution problem, where the primary objective would be to minimize the sum electricity price of data centers and also the usage price of CAS. The issue is NP-complete along with a standard integer straight line programming, that is a special situation within the mixed integer straight line programming (MILP) by which all the variables is fixed to become integers. To resolve this NP-hard problem, many approximating or heuristics algorithms are suggested, for example Branch and Bound, Cutting Plane and Practicality Pump. Although this paper mainly concentrates on the framework of cost optimization for Internet content multi homing and also the impregnation can pick certainly one of approximating or heuristics algorithms to facilitate the answer. Within this example, three user groups situated in two regions request four kinds of data through five data centers and three CAS. The variables of fuc we must handle for that request distribution process from user groups to CAS are as much as thrice $4 = 36$, and also the request distribution process from CAS to data centers has variables of fad as much as thrice $5 \times 4 = 60$. In addition, CAS c1 is associated with data center n1 n2 n3 n5 and CAS c2 is associated with data center n3 n5, therefore the demands from user group u1 for each one of the four data can be treated through the distribution of CAS c1. In addition, data center n1 could only handle the request of information d1 and d2;

therefore the demands from each one of the three CAS for data d3 or d4 in data center n1 are zero. Observe that we are able to make use of a MILP solver inside a free MATLAB toolbox namely YALMIP to resolve the conventional integer straight line programming problem. However, MILP solver prevents a web-based practical implementation because of its high complexities. We assess the performance from the Suggested framework. First, we describe the experimental setup for performance evaluation, particularly the actual-existence workload traces, CAS usage costs, and electricity prices [5]. Only then do we assess the decrease in discovered another means for data centers and usage costs for CAS within the Suggested framework. To judge the suggested cost minimization framework Suggested, we make use of the configuration and generate a simulation atmosphere in which a content company operates five data centers situated in five different regions: Indiana, Michigan, Illinois, Wisconsin, and Minnesota. The workload is symbolized through the average quantity of demands per second. Within the experiments, we make use of the workload data with an Environmental protection agency server. Within the real existence, different CAS might have different charging region coverage different CAS might have different usage fee structures inside a charging region along with a CAS might have different usage fee structures in the different charging regions. The facility system in America can run at real-time prices mechanism, which provides consumers prices information for that actual price of electricity anytime. Real-time prices gives consumers and chance to regulate their electricity usage accordingly to lower their cost to evaluate the suggested within this paper, we conduct an evaluation simulation having a traditional method, which adopts two request distribution concepts.

III. PREVIOUS STUDY

In line with the general trend of related research works, we are able to broadly classify them into two groups: optimizing electricity cost for data centers, and optimizing cost for CAS. The very first number of works targets minimizing total power cost. Yao et al. propose an engaged control plan of electricity cost with power demand smoothing and peak shaving for distributed Internet data centers. Xu and Li propose an optimization framework to guarantee the fairness of performance on directing user' demands from disadvantageous locations to some appropriate data center. The 2nd number of work targets optimizing the price for CAS. Even though this subject has attracted many researchers' attentions, the study on it's still in the initial phase. Goldenberg et al. design a number of novel smart routing algorithms to optimize cost and gratification for multihued users

[6]. Liu et al. present relationships between user groups and CAS, along with the charging purpose of the CAS.

IV. CONCLUSION

This paper studies the minimization of content service cost. Internet content service involves content generation from data centers and content delivery by CAS. Discovered another means for data centers and usage costs for CAS are a couple of major contributors to content service cost. Our extensive experiments show suggested work efficiently cuts down on the content service cost by greater than 20 %. We advise a singular framework and create a centralized optimization formula to dynamically balance finish-users' loads among data centers and CAS in order to minimize the information service cost within the content multihoming atmosphere. We use real-existence electricity prices and CAS prices to judge the potency of Suggested System.

V. REFERENCES

- [1] Y. Feng, B. Li, and B. Li, "Jetway: Minimizing costs on inter-datacenter video traffic," in Proc. 20th ACM Int. Conf. Multimedia, New York, NY, USA, 2012 pp. 259–268.
- [2] D. Meisner, B. T. Gold, and T. F. Wenisch, "Powernap: Eliminating server idle power," in Proc. 14th Int. Conf. Archit. Support Program. Lang. Oper. Syst., New York, NY, USA, 2009, pp. 205–216.
- [3] J. Yao, X. Liu, W. He, and A. Rahman, "Dynamic control of electricity cost with power demand smoothing and peak shaving for distributed internet data centers," in Proc. IEEE 32nd Int. Conf. Distrib. Comput. Syst., 2012, pp. 416–424.
- [4] J. Luo, L. Rao, and X. Liu, "Temporal load balancing with service delay guarantees for data center energy cost optimization," IEEE Trans. Parallel Distrib. Syst., vol. 25, no. 3, pp. 775–784, Mar. 2014.
- [5] M. Adler, R. K. Sitaraman, and H. Venkataramani, "Algorithms for optimizing the bandwidth cost of content delivery," Comput. Netw., vol. 55, no. 18, pp. 4007–4020, Dec. 2011.
- [6] Z. Liu, M. Lin, A. Wierman, S. Low, and L. Andrew, "Greening geographical load balancing," in Proc. Int. Conf. Meas. Model. Comput. Syst., San Jose, CA, USA, Jun. 2011, pp. 7–11.

SURVEY ON ATTACKS AND SECURITY ISSUES IN MOBILE Ad Hoc NETWORKS

¹ **S.Sandhya Rani**

B.Tech, M.Tech, (P.hd)
Assistant Pfofessor
Department of CSE
MREC(A)-Hyderabad

² **Dr.G.Apparao Naidu**

B.Tech, M.Tech,P.hd
Professor
Department of CSE
JBLET- Hyderabad

³ **Dr. V. UshaShree**

B.Tech, M.Tech,P.hd
Professor
Department of ECE
VJIT-Hyderabad

Abstract :- Mobile ad hoc network (MANET) is a continuously self-configuring, infrastructure-less network of mobile devices connected wirelessly. Each device in a MANET is free to move independently in any direction, and will therefore change its links to other devices frequently. Each must forward traffic unrelated to its own use, and therefore be a router. In this paper, the security issues and their current solutions in the mobile ad hoc network have been discussed. Owe to the vulnerable nature of the mobile ad hoc network, there are numerous security threats that disturb the development of it. We first analyze the main vulnerabilities in the mobile ad hoc networks, which have made it much easier to suffer from attacks than the traditional wired network. Then we discuss the security criteria of the mobile ad hoc network and present the main attack types that exist in it. Finally we

survey the current security solutions for the mobile ad hoc network.

Key Words: *Mobile Ad Hoc Network, Security, Intrusion Detection, Secure Routing*

1. Introduction

An autonomous system of mobile hosts connected by wireless links, often called *Mobile Ad hoc Networks'* (MANETs). Recent computer networks have introduced a new technology for future wireless communication, a mobile ad hoc network (MANET). Ad hoc networks do not rely on any fixed infrastructure. Instead, hosts rely on each other to keep the network connected. Nodes in ad hoc network are mobile and they can communicate with each other within radio range through direct wireless links or multichip routing. Mobile ad hoc networks (MANETs) represent complex distributed systems that comprise wireless mobile nodes

that can freely and dynamically self-organize into arbitrary and temporary, “ad-hoc” network topologies, allowing people and devices to seamlessly internetwork in areas with no pre-existing communication infrastructure “

Characteristics of MANET

- 1.No fixed infrastructure
 - 2.Dynamic changing topology Mobile devices join/leave the network unexpectedly they can also move freely
 - 3.Energy-constrained
 - 4.Limited bandwidth
 - 5.Each node also serves as router Help to relay packets received from neighbors
- Interoperation with the Internet

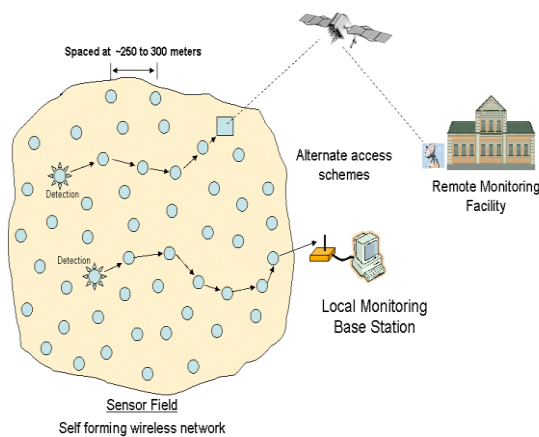


Fig 1:- Example MANET

2. Security issues in Mobile Ad Hoc Network

Availability: ensures the survivability of network services despite denial of service attacks.

Authentication: enables a node to ensure the identity of the peer node it is communicating with.

Non-repudiation: ensures that the origin of a message cannot deny having sent the message.

Confidentiality: Ensures that secret information or data is never disclosed to unauthorized devices.

Integrity: Ensures that a message received is not corrupted.

Layer	Security issues
Application layer	Detecting and preventing viruses, worms, malicious codes, and application abuses
Transport layer	Authenticating and securing end-to-end communications through data encryption
Network layer	Protecting the ad hoc routing and forwarding protocols
Link layer	Protecting the wireless MAC protocol and providing link-layer security support
Physical layer	Preventing signal jamming denial-of-service attacks

**Table: 1 Security Issues in Mobile Ad Hoc
Network
Threats**

- Attacks
- External attacks
- Internal attacks
- Passive attacks
- Active attacks
- Misbehavior

3. Threats from Compromised nodes Inside the Network

In this section we discussed about the link attacks the link attacks place their emphasis on the links between the nodes, and try to perform some malicious behaviors to make destruction to the links. However, there are some other attacks that aim to gain the control over the nodes themselves by some unrighteous means and then use the compromised nodes to execute further malicious actions. This vulnerability can be viewed as the threats that come from the compromised nodes inside the network.

Since mobile nodes are autonomous units that can join or leave the network with freedom, it is hard for the nodes themselves to work out some effective policies to prevent the possible malicious behaviors from all the

nodes it communicate with because of the behavioral diversity of different nodes. Furthermore, because of the mobility of the ad hoc network, a compromised node can frequently change its attack target and perform malicious behavior to different node in the network, thus it is very difficult to track the malicious behavior performed by a compromised node especially in a large scale ad hoc network. Therefore, threats from compromised nodes inside the network are far more dangerous than the attacks from outside the network, and these attacks are much harder to detect because they come from the compromised nodes, which behave well before they are compromised.

3.1 Vulnerabilities of the Mobile Ad Hoc Networks

As per previous discussion we can conclude that the mobile ad hoc network is insecure by its nature: there is no such a clear line of defense because of the freedom for the nodes to join, leave and move inside the network; some of the nodes may be compromised by the adversary and thus perform some malicious behaviors that are hard to detect; lack of centralized machinery may cause some problems when there is a need to have such a centralized coordinator; restricted

power supply can cause some selfish problems; and continuously changing scale of the network has set higher requirement to the scalability of the protocols and services in the mobile ad hoc network. As a result, compared with the wired network, the mobile ad hoc network will need more robust security scheme to ensure the security of it. In the next section, we will survey several security solutions that can provide some helps to improve the security environment in the ad hoc network.

Security Challenges of MANETS

1. **Channel vulnerability** – broadcast wireless channels allow message eavesdropping and injection easily.
2. **Node vulnerability** – nodes do not reside in physically protected places, thus easily fall under attack.
3. **Absence of infrastructure** – certification/ authentication authorities are absent.
4. **Dynamically changing network topology** puts security of routing protocols under threat.
5. **Power and computational**

Types of Attacks

There are two types of security attacks:

- passive
- Active

□ In a **passive attack**, a malicious node either ignores operations supposed to be accomplished by it (examples: silent discard, partial routing information hiding), or listens to the channel, attempting to retrieve valuable information (example: eavesdropping).

□ In a **active attack**, information is inserted to the network and thus the network operation or some nodes may be harmed. Examples are impersonation/spoofing, modification, fabrication and disclosure attack.

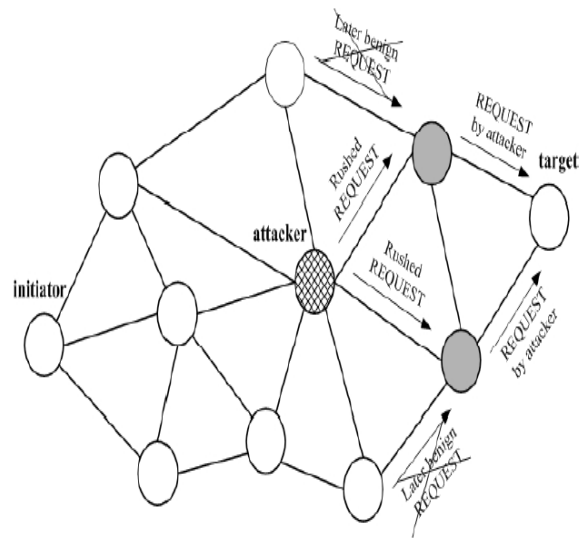


Fig :- 2 Rush Attacks in example mobile Ad Hoc Networks

4. Security criteria

Availability

The term *Availability* means that a node should maintain its ability to provide all the designed services regardless of the security state of it. This security criterion is challenged mainly during the denial-of-service attacks, in which all the nodes in the network can be the attack target and thus some selfish nodes make some of the network services unavailable, such as the routing protocol or the key management service

Integrity

Integrity guarantees the identity of the messages when they are transmitted. Integrity can be compromised mainly in two ways

- Malicious altering
- Accidental altering

A message can be removed, replayed or revised by an adversary with malicious goal, which is regarded as malicious altering; on the contrary, if the message is lost or its content is changed due to some benign failures, which may be transmission errors in communication or hardware errors such as hard disk failure, then it is categorized as accidental altering.

Authenticity

Authenticity is essentially assurance that participants in communication are genuine and not impersonators. It is necessary for the communication participants to prove their identities as what they have claimed using some techniques so as to ensure the authenticity. If there is not such an authentication mechanism, the adversary could impersonate a benign node and thus get access to confidential resources, or even propagate some fake messages to disturb the normal network operations.

Authorization

Authorization is a process in which an entity is issued a credential, which specifies the privileges and permissions it has and cannot be falsified, by the certificate authority. Authorization is generally used to assign different access rights to different level of users. For instance, we need to ensure that network management function is only accessible by the network administrator. Therefore there should be an authorization process before the network administrator accesses the network management functions.

Anonymity

Anonymity means that all the information that can be used to identify the owner or the current user of the node should default be

kept private and not be distributed by the node itself or the system software. This criterion is closely related to privacy preserving, in which we should try to protect the privacy of the nodes from arbitrary disclosure to any other entities.

Security Criteria: Summary

We have discussed several main requirements that need to be achieved to ensure the security of the mobile ad hoc network. Moreover, there are some other security criteria that are more specialized and application-oriented, which include location privacy, self-stabilization and Byzantine Robustness, all of which are related to the routing protocol in the mobile ad hoc network. Having dealt with the main security criteria, we then move to the discussion on the main threats that violate the security criteria, which are generally called as attacks.

5. Security Solutions to the Mobile Ad Hoc Networks

We have discussed several vulnerabilities that potentially make the mobile ad hoc networks insecure in the previous section. However, it is far from our ultimate goal to secure the mobile ad hoc network if we merely know the existing vulnerabilities in it. As a result, we need to find some security

solutions to the mobile ad hoc network. In this section, we survey some security schemes that can be useful to protect the mobile ad hoc network from malicious behaviors.

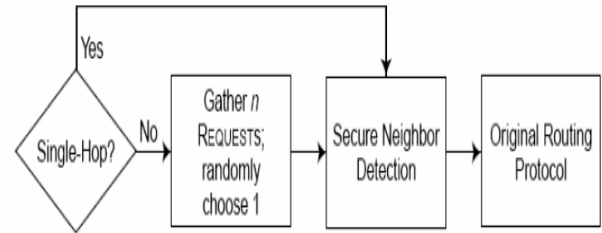


Fig 3: - Combined mechanism to secure MANET

Denial of Service attack

In a denial-of-service (DoS) attack, an attacker attempts to prevent legitimate users from accessing information or services. A denial of service (DoS) attack is an attack that clogs up so much memory on the target system that it cannot serve its users, or it causes the target system to crash, reboot, or otherwise deny services to legitimate users. These days, DoS attacks are very common; indeed, just about every server is bound to experience such an attack at some time or another. Denial of Service can easily be launched and flood the network with spurious routing messages through a malicious node

that gives incorrect updating information by pretending to be a legitimate change of routing information. By targeting your computer and its network connection, or the computers and network of the sites you are trying to use, an attacker may be able to prevent you from accessing email, websites, online accounts (banking, etc.), or other services that rely on the affected computer.

6. Conclusion

Finally we conclude one can see that attacks against the ad hoc networks may vary depend on (1) which environment the attacks are launched, (2) what communication layer the attacks are targeting, and (3) what level of ad hoc network mechanisms are targeted and we try to inspect the security issues in the mobile ad hoc networks, which may be a main disturbance to the operation of it. Due to the mobility and open media nature, the mobile ad hoc networks are much more prone to all kind of security risks, such as information disclosure, intrusion, or even denial of service. As a result, the security needs in the mobile ad hoc networks are much higher than those in the traditional wired networks. First we briefly introduce the basic characteristics of the mobile ad hoc network. Because of the emergence of the concept pervasive

computing, there is an increasing need for the network users to get connection with the world anytime at anywhere, which inspires the emergence of the mobile ad hoc network.

7. References

1. T. Karygiannis and L. Owens, "Wireless Network Security, 802.11, Bluetooth and Handheld Devices," NIST Publication, p. 800(48), November 2002.
2. S. A. Razak, S. M. Furnell, P. J. Brooke, Attacks against Mobile Ad Hoc Networks Routing Protocols"
3. Abhay Kumar Rai, Rajiv Ranjan Tewari & Saurabh Kant Upadhyay, "Different Types of Attacks on Integrated MANET-Internet Communication," International Journal of Computer Science and Security (IJCSS) Volume: 4 Issue:
4. H. Deng, W. Li, Agrawal, D.P., "Routing security in wireless ad hoc networks", Cincinnati Univ., OH, USA; IEEE Communications Magazine, Oct. 2002, Volume: 40, page(s): 70- 75, ISSN: 0163-6804
5. H.Deng, H.Li, and D.P.Ararwal, "Routing security in wireless Ad hoc networks", *IEEE Communication magazine*. Vol. 40, No.10. Oct.2002.

6. Marco Conti, Body, Personal and Local Ad Hoc Wireless Networks, in Book *The Handbook of Ad Hoc Wireless Networks (Chapter 1)*, CRC Press LLC, 2003
7. M. Weiser, The Computer for the Twenty-First Century, *Scientific American*, September 1991.

Investigating of Social Server Scalability Organizing in Mobile Presence Service Applications

A. Karthik¹, Vijay Krupa Vatsal²

¹M.Tech Student, CSE, Malla Reddy Engineering College (Autonomous), TS, India

²Assistant Professor, CSE, Malla Reddy Engineering College (Autonomous), TS, India

¹karthikathmakoori@gmail.com, ²vijaykrupa@mrec.ac.in

ABSTRACT: Vicinity is characterized as the administration gave by distributed computing to discover the web availability status of the gadget. Presently A-days the utilization of web was becoming colossally. The innovation of advanced cells, plain mobiles results in quick development in the use of web. The advanced mobile phones give different long range interpersonal communication applications, for example, Face book Messenger, Yahoo Messenger, GTalk and so forth. These applications when utilized as a part of the advanced cells they naturally hunt down the companion's rundown of the client through the client contacts. As the person to person communication contains a few a great many clients it requires extensive preparing. This procedure requires parcel of messages to be sent from one server to other server which might bring about clog in the middle. To evade this kind of blockages we proposed Cloud Services for versatile joining with Social Networking Applications. The vicinity cloud will diminish the pursuit expense and inactivity brought about between the servers. The vicinity servers mechanize the procedure of seeking the companions and informing them at whatever point another portable client joins the system. Vicinity cloud deals with every one of the servers to shape a circulated building design. We consider two elements in vicinity cloud. One is the aggregate number of messages created when another client joined in the system and second is the time taken by the servers under the vicinity cloud for getting the companion's rundown of new client.

Keywords: Distributed architecture, Presence Services, Cloud Computing, Presence cloud

I. INTRODUCTION

Cell phones and distributed computing situations can give vicinity empowered applications, i.e., informal community applications/administrations, around the world. Facebook [1], Twitter [2], Foursquare [3], Google Latitude [4], pal cloud [5] and Mobile Instant Messaging (MIM) [6], as a

result of universality of Internet. These vicinity empowered applications are become quickly in the most recent decade.

Portable system serves misuse the data about the status of members including their appearances and exercises to communicate with their companions. Presently a day's a result of the wide accessibility of versatile, informal community administrations empower members to share live encounters in a flash crosswise over incredible separations. Vicinity is an administration that permits a client to be educated about the predetermined condition of another client. The predefined state, for example, online/logged off status, mien (out to lunch, far from the PC), movement status (occupied, unmoving), temperament (upbeat, miserable) and area of client, mirrors the client's openness, accessibility and will to convey. Vicinity has turned into a key empowering agent for cutting edge administrations, for example, push-to-talk (PTT), texting(IM) and web2.0, which have encouraged interchanges among groups of interest, for example, gatherings of companions, partners taking a shot at the same ventures and families [1,2]. There are four key elements in a vicinity administration [3, 5]: an essential, an exhibited, a watcher and a vicinity server, which might exist freely or as a major aspect of utilization servers (e.g., PTT, IM and Web2.0). A key alludes to a client who utilizes vicinity benefit and is the proprietor of presentations or watchers; a presentation is an element that is equipped for giving state data to vicinity server; a watcher is an element that subscribes to or demands the state data around a presentation; and a vicinity server is a system substance which has three fundamental obligations: dealing with the membership connections in the middle of watcher and presentity; keeping the most recent presentity state; and advising relating watchers when the presentity state is upgraded. A versatile vicinity administration is a vital segment of interpersonal organization administrations in distributed computing situations. The key capacity of a versatile vicinity administration is to keep up an up and

coming rundown of vicinity data of every single portable client.

The administration should likewise tie the client's ID to his/her present vicinity data, and additionally recover and subscribe to changes in the vicinity data of the client's companions. In interpersonal organization benefits, every portable client has a companion list, ordinarily called a pal rundown, which contains the contact data of different clients that he/she needs to speak with. The versatile client's status is show naturally to every individual on the mate list at whatever point he/she travels from one status to the next. For instance, when a portable client sign into an interpersonal organization application, for example, an IM framework, through his/her cell phone, the versatile vicinity administration hunt down and informs everybody on the client's mate list. To amplify a portable vicinity administration's pursuit speed and minimize the warning time, most vicinity administrations use server bunch innovation [7]. Currently, more than 500 million individuals use interpersonal organization administrations on the Internet [1]. Given the development of informal organization applications and portable system limit, it is normal that the quantity of versatile In the most recent decade, numerous Internet administrations have been conveyed in dispersed standards and additionally distributed computing applications. For instance, the administrations created by Google and Facebook are spread among whatever number appropriated servers as could be expected under the circumstances to bolster the colossal number of clients around the world. Subsequently, we investigate the relationship between disseminated vicinity servers and server system topologies on the Internet, and propose an effective and adaptable server-to-server overlay construction modeling called Presence Cloud to enhance the proficiency of portable vicinity administrations for extensive scale interpersonal organization administrations.

Billion shared things consistently and Twitter gets more than 55 million tweets every day. Later on, cell phones will turn out to be all the more capable, detecting, and media catch gadgets. Subsequently, we trust it is inescapable that informal community administrations will be the up and coming era of portable Internet applications. A versatile vicinity administration is a key part of interpersonal organization administrations in distributed computing situations. The key capacity of a portable vicinity administration is to keep up state-of-the-art rundown of

vicinity data of every single versatile client. The vicinity data incorporates insights around a versatile client's area, accessibility, movement, gadget ability, and inclinations. The administration should likewise tie the client's ID to his/her present vicinity data, and in addition recover and subscribe to changes in the vicinity data of the client's companions. In interpersonal organization benefits, every portable client has a companion list, normally called a mate rundown, which contains the contact data of different clients that he/she needs to correspond with.

The rest of this paper is composed as takes after. The following area contains an outline of IMS Presence Server. The outline of Presence Cloud server is displayed in area 3. Area 4 contains some closing comments.

II. ANALYSIS AN ARCHITECTURE FOR MOBILE PRESENCE SERVICE

In a gullible building design of versatile vicinity administrations unsurprising rate of messages created to hunt down amigos of recently arrived client. Every portable client can connect and vanish the vicinity benefit haphazardly, and every PS hub just knows those versatile clients specifically appended to it. We likewise expect the prospect for a portable client to join to a PS hub to be uniform. How about we signify the normal internal rate of portable clients in a versatile vicinity administration. Here we need to tell about construction modeling of versatile vicinity administrations and the issue of outlining vicinity servers. Every PS hub has endless administration limit. Consequently, is the normal rate of portable clients appending hub, the n is recognized the quantity of PS hubs in a versatile vicinity examination. Where h indicate the possibility of having all clients in the pal rundown of u_i to be connecting to the same PS hub as u_i .

$$h = \prod_{|B_i|} \frac{1}{n} = n^{-|B_i|}.$$

The anticipated number of hunt messages generated by PS node in unit time then

$$(n - 1) \times (1 - h) \times \mu.$$

Reasonable size of set B_i an consider the expected number Q of messages generated by the n PS nodes per piece time, we have

$$\begin{aligned} Q &= n \times (n-1) \times (1-h) \times \mu \\ &= n \times (n-1) \times (1-h) \times \frac{\lambda}{n} \\ &\simeq (n-1) \times \lambda. \end{aligned}$$

The quantity of PS hubs increment, both the aggregate correspondence and aggregate CPU preparing overhead additionally increment. Increments significantly, a noteworthy back end on the framework straightforwardness. Be that as it may, a versatile vicinity framework ought to have the capacity to bolster more than 20, 000 portable client logins every second. In the accompanying Figure we plot insights for every single expected querie transmitted in a portable vicinity administration to demonstrate the expansion in number of mate hunt messages as lambda increments. The figure indicates 1,000 PS hubs, then the normal entry rate of portable client's increments from 2, 000 to 21,000. From the aftereffects of study, the amount of buddy seeking messages increments with expanding normal entry rate of portable clients. This plot most vital for to outline versatile server construction modeling.

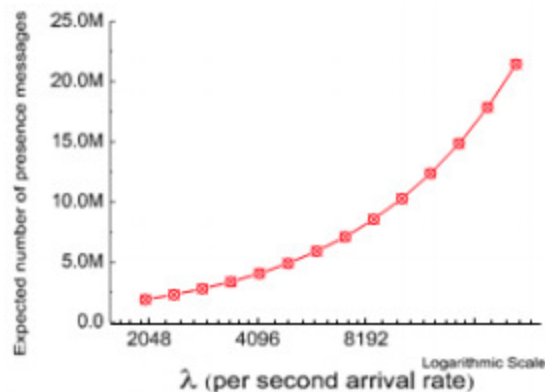


Figure.1: The average arrival rate of mobile users increases from 2000 to 21000 per second in a 1,000 PS nodes mobile presence system

III. RELATED WORK

In this portion, we delineate past investigates on region organizations, and audit the region organization of existing structures. Surely understood business IM structures impact some appearance of united gatherings to give region organizations [7]. Jennings III et al. [7] presented an investigative arrangement of unmistakable characteristics and limits maintained by the three most predominant IM structures, AIM, Microsoft MSN and Yahoo! Banner

conveyor. The inventors similarly gave a survey of the structure architectures and watched that the systems use client server-based architectures. Skype, a predominant voice over IP application, utilizes the Global Index (GI) designing [8] to give a region organization to customers. GI is a multi-layered framework development displaying where each center point keeps up full data of every single open customer. Subsequent to Skype is not an open tradition, it is difficult to choose how GI designing is used exactly. Furthermore, Xiao et al. [9] analyzed the development of MSN and AIM structure. They found that the region information is one of most illuminating action in messaging structures. In [10], makers exhibited that the greatest message development in existing region organizations is buddy NOTIFY messages.

A couple IETF contracts [11]–[13] have tended to almost related topics and various RFC records on messaging and region organizations have been conveyed, e.g.,xmpp [14], SIMPLE [15]. Jibber jabber [16] is an understood association of messaging developments centered around flowed architectures. It gets the scattered auxiliary designing of SMTP traditions. Since Jabber's auxiliary designing is passed on, the outcome is a versatile arrangement of servers that may be scaled much higher than the strong, joined region organizations.

Starting late, there is a fabricate measure of energy toward how to arrange a mutual SIP [17]. P2psip [18] has been proposed to remove the united server, decrease upkeep costs, and balance dissatisfactions in server based SIP course of action. To keep up region information, P2psip clients are sorted out in a DHT structure, instead of in a concentrated server. In any case, the region organization architectures of Jabber and P2psip are appropriated, the mate rundown look issue we described later similarly could impact such dispersed system.

It is noticed that few articles in [19] [21] discuss the versatility issues of the passed on region server basic arranging. Illustration of devotion Andre [19] explores the development delivered as an outcome of region information between customers of between territories that support the XMPP. Houri et al. [20] show that the measure of region development in SIMPLE [13] may be enormously considerable, and they analyze the effect of a sweeping region system on the memory and CPU stacking. Those works in [21], [22] study related issues and making a

starting arrangement of tenets for enhancing between territory region development and present a DHT-based region server basic arranging.

Starting late, region organizations are furthermore joined into convenient organizations. For example, 3gpp has described the compromise of region organization into its point of interest in UMTS. It is engaged around SIP [23] tradition, and utilizations SIMPLE [15] to manage region information. Starting late, some PDAs in like manner help adaptable region organizations. For example, the Instant Messaging and Presence Services (IMPS) was delivered by the Wireless Village consortium and was united into Open Mobile Alliance (OMA) IMPS [24] in 2005. In [25], Chen et al. proposed a desolately unflinching arrangement to diminish the amount of updating messages in compact region organizations of IP Multimedia Subsystem (IMS). Of course, it furthermore perseveres flexibility issue since it uses a central SIP server to perform region redesign of adaptable customers [26]. In [27], makers showed the server flexibility and disseminated administration issues in IMS based vicinity administration.

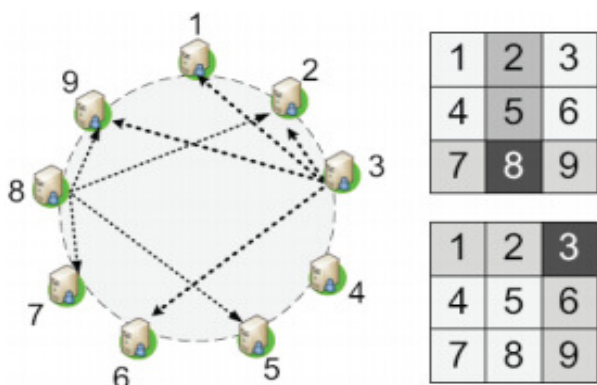


Figure.2: Central SIP Server

IV. DESIGN OF PRESENCECLOUD

Vicinity Cloud is utilized to develop and keep up disseminated server structural planning and can be utilized to effectively question the framework for amigo list looks. Vicinity Cloud comprises of three principle segments that are keep running over an arrangement of vicinity servers. In the configuration of Presence Cloud, we refine the thoughts of P2P frameworks and present a specific outline for versatile vicinity administrations. The three key segments of Presence Cloud are abridged underneath:

A. Presence Cloud Server Overlay

The Presence Cloud server overlay development composes the Presence server hubs into a server-to-server overlay, which gives a decent low-width overlay property as appeared in Fig.3. The low-distance across property ensures that a Presence server hub just needs two jumps to achieve whatever other PS hubs. Our Presence Cloud depends on the idea of framework majority framework, where a PS hub just keeps up an arrangement of PS hubs of size $O(\sqrt{n})$, where n is the quantity of PS hubs in versatile vicinity administrations. In a Presence Cloud framework, every PS hub has an arrangement of PS hubs, called PS list, that developed by utilizing a network majority framework. The extent of a framework majority is $\sqrt{n} \times \sqrt{n}$. At the point when a PS hub joins the server overlay of Presence Cloud, it gets an ID in the network, finds its position in the matrix and gets its PS list by reaching a root server.1 On the $\sqrt{n} \times \sqrt{n}$ framework, a PS hub with a lattice ID can pick one section and one line of passages and these sections will turn into its PS list in a Presence Cloud server overlay. We now demonstrate that every PS hub in a Presence Cloud System just keeps up the PS rundown of $O(\sqrt{n})$, and the development of Presence Cloud utilizing the matrix majority results as a part of every PS hub can achieve any PS hub at most two hops.

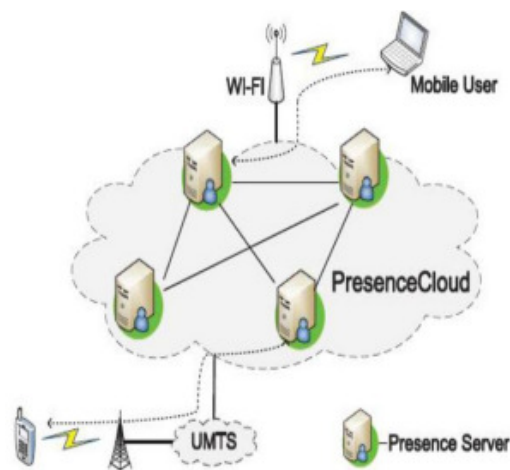


Figure.3: An overview of Presence Cloud.

B. One-Hop Caching Strategy

Vicinity Cloud requires a storing procedure to make a precise of vicinity data of clients to enhance the effectiveness of the hunt operation. With a specific end goal

to adjust to changes in the vicinity of clients, the storing methodology ought to be non concurrent and not require costly systems for conveyed assention. In Presence Cloud, every PS hub keeps up a client rundown of vicinity data of the joined clients, and it is in charge of storing the client rundown of every hub in its PS list, at the end of the day, PS hubs just repeat the client list at most one jump far from itself. The store is redesigned when neighbors build up associations with it, and intermittently upgraded with its neighbors. Along these lines, when a PS hub gets an inquiry, it can react not just with matches from its own client list, additionally give matches from its stores that are the client records offered by the greater part of its neighbors. Our storing system does not require costly overhead for vicinity consistency among PS hubs. At the point when a portable client changes its vicinity data, either in light of the fact that it leaves Presence Cloud, or because of disappointment, the reacted PS hub can disperse its new vicinity to other neighboring PS hubs for getting redesigned rapidly. Hence, this one-bounce reserving technique guarantees that the user's vicinity data could remain for the most part forward and reliable all through the session time of the client. All the more particularly, it ought to be anything but difficult to see that, every PS hub keeps up around $2(\sqrt{n}-1) \times u$ copies of vicinity data, because of every PS hub copies its client list at most one jump far from itself. Here, u is indicated the normal number of versatile clients in a PS node.

C. Directed Buddy Search

We battle that diminishing looking reaction time is critical to portable vicinity administrations. In this way, the pal list looking calculation of Presence Cloud combined with the two-bounce overlay and one-jump reserving procedure guarantees that Presence Cloud can normally give quick reactions to an expansive number of portable clients. To begin with, by sorting out PS hubs in a server-to-server overlay system, we can in this manner utilize one-bounce hunt precisely down questions and along these lines decrease the system movement without critical effect on the query items. Second, by underwriting the one-jump storing that keeps up the client arrangements of its neighbors, we enhance reaction time by expanding the odds of discovering amigos. Unmistakably, this instrument both lessens the system movement and reaction time. Taking into account the system, the number of inhabitants in portable clients can be recovered by a television operation in any PS hub in the

versatile vicinity administration. In addition, the TV message can be piggybacked in a mate hunt message down sparing the expense.

D. Web of Trust

The web-of-trust model varies incredibly from the progressive model. The various leveled model is effectively spoken to with PCs as a tree, yet the web-of-trust all the more nearly identifies with how individuals decide trust in their own particular lives. As individuals experience life and meet new individuals, they look to those they as of now trust to make the determination in the event that they ought to believe these new individuals. In the event that individuals they trust as of now trust this new individual, they will probably do likewise. PGP actualizes this model by permitting individuals to sign one another's keys doling out to each of the keys a level of trust and legitimacy. PGP expect that an authentication ties a key to a man. That individual picks a name to recognize them self, furthermore give an email address as a worldwide identifier. At the point when a client signs another user's key, the marking client is declaring that they have confirmed that the key genuinely has a place with the recorded client and that it is substantial. This strategy for marking keys prompts a specially appointed system of trust. In view of the state of the subsequent diagram, Phil Zimmerman called this framework the "Web of Trust". The framework permits clients to determine the amount of trust to put in a mark by demonstrating what number of autonomous marks must be set on a declaration for it to be viewed as substantia.

E. How PGP Works

PGP consolidates a portion of the best elements of both traditional and open key cryptography. PGP is a half and half cryptosystem. At the point when a client encodes plaintext with PGP, PGP first packs the plaintext. Information pressure spares modem transmission time and plate space and, all the more essentially, reinforces cryptographic security. Most cryptanalysis methods misuse designs found in the plaintext to split the figure. Pressure diminishes these examples in the plaintext; in this manner significantly upgrading imperviousness to cryptanalysis (Files that are too short to pack or which don't pack well aren't compacted). PGP then makes a session key, which is a one-time-just mystery key. This key is an irregular number produced from the arbitrary developments of your mouse and the keystrokes you write. This session key works with

an exceptionally secure, quick routine encryption calculation to encode the plaintext; the outcome is figure content. Once the information is encoded, the session key is then scrambled to the beneficiary's open key. This open key-scrambled session key is transmitted alongside the figure content to the beneficiary. Unscrambling works in the opposite. The beneficiary's duplicate of PGP uses his or her private key to recoup the transitory session key, which PGP then uses to decode the customarily encoded figure content.

The blend of the two encryption systems joins the comfort of open key encryption with the velocity of ordinary encryption. Ordinary encryption is around 1, 000 times quicker than open key encryption. Open key encryption thusly gives an answer for key dissemination and information transmission issues. Utilized together, execution and key circulation are enhanced with no penance in security.

V. CONCLUSIONS

In this paper, we have spoken to Presence Cloud, construction modeling of adaptable server those backings versatile vicinity administrations in substantial scale informal organization administrations. Presence Cloud have low pursuit idleness and enhance the execution of portable vicinity administrations. We talked about in server structural engineering how the adaptable issue emerges and presented the pal list seek issue, this will be an adaptability issue in the conveyed server construction modeling of versatile vicinity administrations. In a basic numerical model, the aggregate number of pal inquiry messages increments essentially with the client landing rate and the quantity of vicinity servers. Vicinity Cloud accomplishes most vital execution picks up regarding the hunt cost and pursuit fulfillment. All in all, Presence Cloud is appeared to be an adaptable versatile vicinity administration in extensive scale interpersonal organization administrations.

VI. REFERENCES

- [1] Facebook, <http://www.facebook.com>.
- [2] Twitter, <http://twitter.com>.
- [3] Foursquare <http://www.foursquare.com>.
- [4] Googlelatitude, <http://www.google.com/intl/enus/latitude/intro.html>.
- [5] Buddycloud, <http://buddycloud.com>.
- [6] Mobile instant messaging, http://en.wikipedia.org/wiki/Mobile_instant_messaging.
- [7] R. B. Jennings, E. M. Nahum, D. P. Olshefski, D. Saha, Z. Y. Shae, and C. Waters, "A study of internet instant messaging and chat protocols," IEEE Network, 2006.
- [8] Goba index, <http://www.skype.com/intl/enus/support/use-r-guides/p2pexplained/>.
- [9] Z. Xiao, L. Guo, and J. Tracey, "Understanding instant messaging traffic characteristics," Proc. of IEEE ICDCS, 2007.
- [10] C. Chi, R. Hao, D. Wang, and Z. Z. Cao, "Ims presence server: Traffic analysis and performance modelling," Proc. of IEEE ICNP, 2008.
- [11] Instant messaging and presence protocol ietf working group <http://www.ietf.org/html.charters/impdp-charter.html>.
- [12] Extensible messaging and presence protocol ietf working group <http://www.ietf.org/html.charters/xmpp-charter.html>.
- [13] Sip for instant messaging and presence leveraging extensions ietf working group. <http://www.ietf.org/html.charters/simple-charter.html>.
- [14] P. Saint-Andre., "Extensible messaging and presence protocol (xmpp): Instant messaging and presence describes instant messaging(im), the most common application of xmpp," RFC 3921, 2004.
- [15] B. Campbell, J. Rosenberg, H. Schulzrinne, C. Huitema, and D. Gurle, "Session initiation protocol (sip) extension for instant messaging," RFC 3428, 2002.
- [16] Jabber, <http://www.jabber.org/>.
- [17] Peer-to-peer session initiation protocol ietf working group, <http://www.ietf.org/html.charters/p2psip-charter.html>.
- [18] K. Singh and H. Schulzrinne, "Peer-to-peer internet telephony using sip," Proc. of ACM NOSSDVA, 2005.
- [19] P. Saint-Andre, "Inter domain presence scaling analysis for the extensible messaging and presence protocol (xmpp)," RFC Internet Draft, 2008.

[20] A. Hourri, T. Rang, and E. Aoki, "Problem statement for sip/simple," RFC Internet-Draft, 2009.

[21] A. Hourri, S. Parameswar, E. Aoki, V. Singh, and H. Schulzrinne, "Scaling requirements for presence in sip/simple," RFC Internet-Draft, 2009.

[22] S. A. Baset, G. Gupta, and H. Schulzrinne, "Openvoip: An open peer-to-peer voip and im system," Proc. of ACM SIGCOMM, 2008.

[23] J. Rosenberg, H. Schulzrinne, G. Camarillo, A. Johnston, J. Peterson, R. Sparks, M. Handley, and E. Schooler, "Sip: Session initiation protocol," RFC 3261, 2002.

[24] Open Mobile Alliance, OMA instant messaging and presence service, 2005.

[25] W. E. Chen, Y. B. Lin, and R. H. Liou, "A weakly consistent scheme for ims presence service," IEEE Transactions on Wireless Communications, 2009.

[26] N. Banerjee, A. Acharya, and S. K. Das, "Seamless sip-based mobility for multimedia applications." IEEE Network, vol. 20, no. 2, pp. 6–13, 2006.

[27] P. Bellavista, A. Corradi, and L. Foschini, "Ims-based presence service with enhanced scalability and guaranteed qos for inter domain enterprise mobility," IEEE Wireless Communications, 2009.

A Proposal towards Effective Image Recovery in Data Hiding Schemes

Y.Rokesh Kumar¹, Vijay Krupa Vatsal K²Assistant Professor, Department of CSE, Malla Reddy Engineering College (A), Telangana, India¹Assistant Professor, Department of CSE, Malla Reddy Engineering College (A), Telangana, India²

ABSTRACT: Reversible data hiding is a significant technique is expansively used in numerous applications, where no distortion of original cover is approved. In practical aspect, numerous techniques of reversible data hiding have come out in recent times. Quite a lot of attempts on reversible data hiding in encrypted images were made. In our work, we propose a novel method for reversible data hiding in encrypted images, in which we do not vacate room following encryption as done but reserve room prior to encryption. Here we firstly empty out room by means of embedding least significant bits of some pixels into other by an established reversible data hiding means and subsequently encrypt the image, so positions of these least significant bits in encrypted image can be employed to embed data. The proposed means can achieve actual reversibility; specifically data extractions as well as image recovery are free of any error and not only does projected method divide data extraction from image decryption but moreover accomplish outstanding performance in different prospects. In the scheme data extraction as well as image recovery is the same to that of framework of vacating room after encryption.

KEYWORDS: Reversible data hiding, Encrypted image, Data extraction, Image decryption, least significant bits.

I. INTRODUCTION

Pertaining to provision of confidentiality for images, encryption is a successful as well as popular means since it converts the original and important content to incomprehensible one. Reversible data hiding in images is a method, by which original cover can be recovered after extraction of embedded message losslessly [1]. Even though few methods of reversible data hiding in encrypted images have been published until now, there are a number of promising applications if reversible data hiding can be functional to encrypted images. A number of attempts on reversible data hiding in encrypted images were made. A more accepted method is on the basis of difference expansion in which difference of each pixel group is extended, and consequently least significant bits of difference are all-zero and can be employed for embedding messages. An additional promising strategy for reversible data hiding is histogram shift in which space is accumulated for data embedding by means of changing bins of histogram. The modern techniques combine difference expansion or histogram shift towards residuals of image, for instance the predicted errors, to attain improved performance. In our work, we suggest a new method for reversible data hiding in encrypted images, in which we do not vacate room following encryption as done but reserve room prior to encryption. In projected method, we initially empty out room by means of embedding least significant bits of some pixels into other by an established reversible data hiding means and subsequently encrypt the image, so positions of these least significant bits in encrypted image can be employed to embed data [2][3]. Previously made methods put into practice reversible data hiding in encrypted images by vacating room following encryption, rather than which we projected by reserving room before encryption. Not only does projected method divide data extraction from image decryption but moreover accomplish outstanding performance in different prospects. Real reversibility is recognized, specifically, data extraction as well as image recovery is free of any error. For specified embedding rates, Peak signal-to-noise ratio of decrypted image enclosing embedded data is considerably enhanced; and for satisfactory Peak signal-to-noise ratio, range of embedding rates is very much enlarged.

International Journal of Innovative Research in Science, Engineering and Technology

(An ISO 3297: 2007 Certified Organization)

Vol. 5, Issue 10, October 2016

II. METHODOLOGY

Reversible data hiding has gained attraction considerably in research interest since it was introduced initially. In realistic aspect, many techniques of reversible data hiding have come out in recent times. Reversible data hiding within encrypted images is a recent subject that has drawn attention due to needs concerning privacy-preserving from managing of cloud data. The entire methods which were introduced earlier embed data by means of reversibly vacating room from encrypted images, which might be subject to a number of errors on data extraction and restoration of image. In our work, we suggest a new method for reversible data hiding in encrypted images, in which we do not vacate room following encryption as done but reserve room prior to encryption and thus it is easy for data hider to embed data reversibly within encrypted image. The proposed means can attain real reversibility; specifically data extractions as well as image recovery are free of any error. Criterion methods of reversible data hiding algorithms are the eventual operator in support of reserving room before encryption and can be simply functional to structure of reserving room before encryption to attain improved performance compared with methods from structure of vacating room after encryption. Earlier methods put into practice reversible data hiding in encrypted images by vacating room following encryption, rather than which we projected by reserving room before encryption [4]. As a result the data hider can advantage from extra space that is emptied out in earlier stage to make data hiding procedure easy. The proposed means can take benefit of all conventional reversible data hiding techniques for plain images and attain excellent performance with no loss of perfect secrecy. This novel method can attain real reversibility, separate data extraction and very much enhancement on quality of marked decrypted images.

III. AN OVER VIEW OF PROPOSED SYSTEM

While losslessly vacating room from encrypted images is comparatively tricky and occasionally ineffective, but passionate for finding of novel reversible data hiding techniques working directly for encrypted did not stop. When we reverse order of encryption as well as vacating room, specifically reserving room earlier to image encryption at content owner side, tasks of reversible data hiding in encrypted images would be more usual and much simple which leads to new framework, reserving room before encryption. The methods that were introduced earlier embed data by means of reversibly vacating room from encrypted images, which might be subject to a number of errors on data extraction and restoration of image. Content owner initially reserves sufficient space on original image and subsequently alter image into its encrypted version by means of the encryption key. The data embed ding procedure in encrypted images is intrinsically reversible for the data hider merely needs to contain data into spare space earlier emptied out. This novel means can accomplish real reversibility, separate data extraction and very much enhancement on quality of marked decrypted images. It can take assistance of the entire conventional reversible data hiding techniques for plain images and attain excellent performance with no loss of perfect privacy. The data extraction as well as image recovery is the same to that of Framework of vacating room after encryption [5]. Standard reversible data hiding algorithms are the ultimate operator in support of reserving room before encryption and can be simply functional to structure of reserving room before encryption to attain improved performance compared with methods from structure of vacating room after encryption. This is since in this new structure, we follow the usual idea that initially losslessly compress redundant image content and subsequently encrypts it regarding protecting privacy. In fact, to construct encrypted image, initial stage is divided into image partition, self reversible embedding and image encryption. In Image Partition, operator here for reserving room earlier than encryption is a criterion reversible data hiding technique, therefore objective of image partition is to build a smoother area on which standard reversible data hiding algorithms such as can achieve improved performance. The objective of self-reversible embedding is to embed least significant bits-planes by employing conventional reversible data hiding algorithms [6]. After image encryption, data hider cannot access content of original image devoid of the encryption key, consequently privacy of content owner being confined.

International Journal of Innovative Research in Science, Engineering and Technology

(An ISO 3297: 2007 Certified Organization)

Vol. 5, Issue 10, October 2016

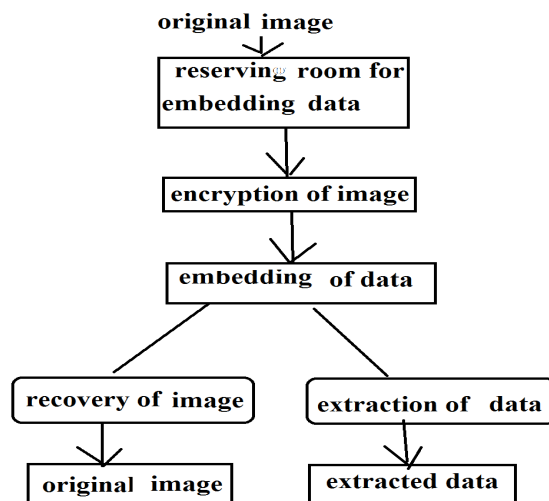


Figure 1: An overview of reserving room before encryption

IV. CONCLUSION

Reversible data hiding within encrypted images is a current subject that has drawn consideration. Although not many methods of reversible data hiding in encrypted images have been published until now, there are a number of promising applications if reversible data hiding can be functional to encrypted images. The modern techniques typically combined difference expansion or histogram shift towards residuals of image, for instance the predicted errors, to attain improved performance. In our work, we recommend a new technique for reversible data hiding in encrypted images, in which we do not vacate room following encryption as done but reserve room prior to encryption. We empty out room initially by embedding least significant bits of some pixels into other by established reversible data hiding means and subsequently encrypt the image, so positions of these least significant bits in encrypted image can be employed to embed data. Projected system screen data extraction from image decryption but moreover accomplishes outstanding performance in different prospects. The system can take advantage of all conventional reversible data hiding techniques for plain images and attain excellent performance with no loss of perfect secrecy.

REFERENCES

- [1] J. Tian, "Reversible data embedding using a difference expansion," IEEE Trans. Circuits Syst. Video Technol., vol. 13, no. 8, pp. 890–896, Aug. 2003.
- [2] Z. Ni, Y. Shi, N. Ansari, and S. Wei, "Reversible data hiding," IEEE Trans. Circuits Syst. Video Technol., vol. 16, no. 3, pp. 354–362, Mar. 2006.
- [3] D.M. Thodi and J. J. Rodriguez, "Expansion embedding techniques for reversible watermarking," IEEE Trans. Image Process., vol. 16, no. 3, pp. 721–730, Mar. 2007.
- [4] W. Liu, W. Zeng, L. Dong, and Q. Yao, "Efficient compression of encrypted grayscale images," IEEE Trans. Image Process., vol. 19, no. 4, pp. 1097–1102, Apr. 2010.
- [5] X. Zhang, "Reversible data hiding in encrypted images," IEEE Signal Process. Lett., vol. 18, no. 4, pp. 255–258, Apr. 2011.
- [6] W. Hong, T. Chen, and H.Wu, "An improved reversible data hiding in encrypted images using side match," IEEE Signal Process. Lett., vol. 19, no. 4, pp. 199–202, Apr. 2012.

**INTERNATIONAL JOURNAL OF ENGINEERING SCIENCES & RESEARCH
TECHNOLOGY****A NOVEL TECHNIQUE FOR SECURE ENCRYPTED MESSAGES IN MOBILE AND
PERVASIVE APPLICATIONS****Mr. P.Venkateshwar Rao*, Mr. G.Vamshi Krishna, Mr. Y. Rokesh Kumar*** Assistant Professor in Computer Science and Engineering, Malla Reddy Engineering College
(Autonomous), Hyderabad, TS.Assistant Professor in Computer Science and Engineering, Malla Reddy Engineering College
(Autonomous), Hyderabad, TS.Assistant Professor in Computer Science and Engineering, Malla Reddy Engineering College
(Autonomous), Hyderabad, TS.**DOI:** 10.5281/zenodo.58633

ABSTRACT

More than applications rely on the existence of small devices that can exchange information and form communication networks. In a significant portion of such applications, the confidentiality and integrity of the communicated messages are of particular interest. In this work, to propose two novel techniques for authenticating short encrypted messages that are directed to meet the requirements of mobile and pervasive applications. By taking advantage of the fact that the message to be authenticated must also be encrypted, to propose provably secure authentication codes that are more efficient than any message authentication code in the literature. The key idea behind the proposed techniques is to utilize the security that the encryption algorithm can provide to design more efficient authentication mechanisms, as opposed to using standalone authentication primitives.

KEYWORDS: Authentication, unconditional security, computational security, universal hash-function families, pervasive computing.

INTRODUCTION

PRESERVING the integrity of messages exchanged over public channels is one of the classic goals in cryptography and the literature is rich with message authentication code (MAC) algorithms that are designed for the sole purpose of preserving message integrity. Based on their security, MACs can be either unconditionally or computationally secure. Unconditionally secure MACs provide message integrity against forgers with unlimited computational power. On the other hand, computationally secure MACs are only secure when forgers have limited computational power. A popular class of unconditionally secure authentication is based on universal hash-function families, pioneered by Carter and Wingman. The study of unconditionally secure message authentication based on universal hash functions has been attracting research attention, both from the design and analysis standpoints. The basic concept allowing for unconditional security is that the authentication key can only be used to authenticate a limited number of exchanged messages. Since the management of onetime keys is considered impractical in many applications, computationally secure MACs have become the method of choice for most real-life applications. In computationally secure MACs, keys can be used to authenticate an arbitrary number of messages. That is, after agreeing on a key, legitimate user can exchange an arbitrary number of authenticated messages with the same key. Depending on the main building block used to construct them, computationally secure MACs can be classified into three main categories: block cipher based, cryptographic hash function based, or universal hash-function family based. The security of different MACs has been exhaustively studied.

The use of one-way cryptographic hash functions for message authentication. The popular example of the use of iterated cryptographic hash functions in the design of message authentication codes is HMAC, which was proposed.

The use of universal hash-function families in the style is not restricted to the design of unconditionally secure authentication. Computationally secure MACs based on universal hash functions can be constructed with two rounds of computations. In the first round, the message to be authenticated is compressed using a universal hash function. Then, in the second round, the compressed image is processed with a cryptographic function. Popular examples of computationally secure universal hashing based MACs include, but are not limited to. Indeed, universal hashing based MACs give better performance when compared to block cipher or cryptographic hashing based MACs. In fact, the fastest MACs. Earlier designs used one-time pad encryption to process the compressed image. However, due to the difficulty to manage such on time keys, recent designs resorted to computationally secure primitives. The main reason behind the performance advantage of universal hashing based MACs is the fact that processing messages block by block using universal hash functions is orders of magnitude faster than processing them block by block using block ciphers or cryptographic hash functions.

One of the main differences between unconditionally secure MACs based on universal hashing and computationally secure MACs based on universal hashing is the requirement to process the compressed image with a cryptographic primitive in the latter class of MACs. This round of computation is necessary to protect the secret key of the universal hash function. There are two important observations to make about existing MAC algorithms. First, they are designed independently of any other operations required to be performed on the message to be authenticated. For instance, if the authenticated message must also be encrypted, existing MACs are not designed to utilize the functionality that can be provided by the underlying encryption algorithm. Second, most existing MACs are designed for the general computer communication systems, independently of the properties that messages can possess. For example, one can find that most existing MACs are inefficient when the messages to be authenticated are short. There is an increasing demand for the deployment of networks consisting of a collection of small devices. In many practical applications, the main purpose of such devices is to communicate short messages. A sensor network, for example, can be deployed to monitor certain events and report some collected data. In many sensor network applications, reported data consist of short confidential measurements. Consider, for instance, a sensor network deployed in a battlefield with the purpose of reporting the existence of moving targets or other temporal activities. In such applications, the confidentiality and integrity of reported events are of critical importance. In another application, consider the increasingly spreading deployment of radio frequency identification (RFID) systems.

The RFID reader must also authenticate the identity of the RFID tag, RFID tags must be equipped with a message authentication mechanism. Another application that is becoming increasingly important is the deployment of body sensor networks. In such applications, small sensors can be embedded in the patient's body to report some vital signs. Again, in some applications the confidentiality and integrity of such reported messages can be important. There have been significant efforts devoted to the design of hardware efficient implementations that suite such small devices. For instance, hardware efficient implementations of block ciphers have been proposed in. Implementations of hardware efficient cryptographic hash functions have also been proposed. In the first technique, to utilize the fact that the message to be authenticated is also encrypted, with any secure encryption algorithm, to append a short random string to be used in the authentication process. Since the random strings used for different operations are independent, the authentication algorithm can benefit from the simplicity of unconditional secure authentication to allow for faster and more efficient authentication, without the difficulty to manage one-time keys. In the second technique, the extra assumption that the used encryption algorithm is block cipher based to further improve the computational efficiency of the first technique. The driving motive behind our investigation is that using a general purpose MAC algorithm to authenticate exchanged messages in such systems might not be the most efficient solution and can lead to waste of resources already available, namely, the security that is provided by the encryption algorithm.

LITERATURE SURVEY & RELATED WORK

The previous approaches for MAC include "A2 – codes from universal hash classes" the purpose of this traditional theory of unconditional authentication (A-Codes) is to protect the transmitter and receiver from deception by an outside opponent. It is assumed that transmitter and receiver trust each other, Simmons extended this model to include protection against certain frauds by transmitter and receiver. This model uses an arbiter, who distributes partial keys to transmitter and receiver and decides in cases of controversy between transmitter and receiver. It is assumed that the arbitrary is trust worthy. The corresponding systems have been termed A2-codes by Simmons.

Another approach “Fast hashing on Pentium” here a cryptographic hash function h maps bit strings of arbitrary finite length into strings of fixed length. Given h and an input x computing $h(x)$ must be easy. A one way hash function must provide both pre-image resistance and second pre-image resistance i.e. it must be computationally infeasible to find respectively, any input which hashes to any pre-specified input. We try to make use of the existing approaches and improve them to utilize their underlying functionality more efficiently. One of the most known block cipher is CBC-Mac based MACs. It is specified in the federal information processing standards publication and ISO. CMAC, a modified version of CBC-MAC is presented in the NIST special publication which was OMAC.

Some other block cipher based MACs include XOR-MAC and PMAC. Can MAC provide full integrity? The answer for this is the two techniques are proposed 1) The message that is authenticated must also be encrypted with any secure encryption algorithm by appending the short random string. Since the random strings used for different operations are independent, the authentication algorithm can benefit from the simplicity of unconditional secure authentication to allow for faster and more efficient authentication. 2) We make extra assumptions that the used encrypted algorithm is a block cipher based to further improve the computational efficiency of the first technique. The general purpose of MAC algorithm that is used to exchange the messages in the system might not be the efficient solution and may lead to the waste of resources. The example for iterated cryptographic hash function in the design of message authentication code is HMAC. It was later adopted as a standard. Another cryptographic hash function based MAC is the MDx-MAC. HMAC and two variants of MDx-MAC are specified in the ISO/IEC.

EXISTING SYSTEM

A popular class of unconditionally secure authentication is based on universal hash-function families, pioneered by Carter and Wingman. Since then, the study of unconditionally secure message authentication based on universal hash functions has been attracting research attention, both from the design and analysis standpoints

DISADVANTAGES:

- Unconditionally secure universal hashing-based MACs are considered impractical in most modern applications, due to the difficulty of managing one-time keys

PROPOSED SYSTEM

- In this paper we propose two new techniques for authenticating short encrypted messages that are more efficient than existing approaches.
- In the first technique, we utilize the fact that the message to be authenticated is also encrypted, with any secure encryption algorithm, to append a short random string to be used in the authentication process. Since the random strings used for different operations are independent, the authentication algorithm can benefit from the simplicity of unconditional secure authentication to allow for faster and more efficient authentication, without the difficulty to manage one-time keys.
- In the second technique, we make the extra assumption that the used encryption algorithm is block cipher based to further improve the computational efficiency of the first technique. The driving motive behind our investigation is that using a general purpose MAC algorithm to authenticate exchanged messages in such systems might not be the most efficient solution and can lead to waste of resources already available, namely, the security that is provided by the encryption algorithm.

ADVANTAGES:

- More efficient than existing approaches.
- The authentication algorithm can benefit from the simplicity of unconditional secure authentication to allow for faster and more efficient authentication, without the difficulty to manage one-time keys.
- The most efficient solution and can lead to waste of resources already available, namely, the security that is provided by the encryption algorithm.

IMPLEMENTATION

Authenticating short encrypted messages:

we describe our first authentication scheme that can be used with any IND-CPA secure encryption algorithm. An important assumption we make is that messages to be authenticated are no longer than a predefined length. This

includes applications in which messages are of fixed length that is known a priori, such as RFID systems in which tags need to authenticate their identifiers, sensor nodes reporting events that belong to certain domain or measurements within a certain range, etc. The novelty of the proposed scheme is to utilize the encryption algorithm to deliver a random string and use it to reach the simplicity and efficiency of one-time pad authentication without the need to manage impractically long keys.

Security Model:

A message authentication scheme consists of a signing algorithm S and a verifying algorithm V . The signing algorithm might be probabilistic, while the verifying one is usually not. Associated with the scheme are parameters κ and N describing the length of the shared key and the resulting authentication tag, respectively.

Security of the Authenticated Encryption Composition:

it defined two notions of integrity for authenticated encryption systems: the first is integrity of plaintext (INT-PTXT) and the second is integrity of cipher text (INT-CTXT). Combined with encryption algorithms that provide indistinguishability under chosen plaintext attacks (IND-CPA), the security of different methods for constructing generic compositions is analyzed. Note that our construction is an instance of the Encrypt-and-Authenticate (E&A) generic composition since the plaintext message goes to the encryption algorithm as an input, and the same plaintext message goes to the authentication algorithm as an input.

Data Privacy:

Recall that two pieces of information are transmitted to the intended receiver (the cipher text and the authentication tag), both of which are functions of the private plaintext message. Now, when it comes to the authentication tag, observe that then once r serves as a one-time key (similar to the role r plays in the construction of Section. The formal analysis that the authentication tag does not compromise message privacy is the same as the one provided. The cipher text of equation, on the other hand, is a standard CBC encryption and its security is well-studied; thus, we give the theorem statement below without a formal proof (interested readers may refer to textbooks in cryptography).

RESULTS

In existing system utilize the fact that the message to be authenticated is also encrypted, with any secure encryption algorithm, to append a short random string to be used in the authentication process. Since the random strings used for different operations are independent, the authentication algorithm can benefit from the simplicity of unconditional secure authentication to allow for faster and more efficient authentication. Use of encryption algorithm is block cipher based to further improve the computational efficiency of the technique. The driving motive behind investigation is that using a general purpose MAC algorithm to authenticate exchanged messages in such systems might not be the most efficient solution and can lead to waste of resources already available, namely, the security that is provided by the encryption algorithm.

In the proposed system have to deliberate the subsequent cryptographic methods that will be realistic in the input that input should be the short message that was called as the Multi-Security technique. Those encryption methods are the data encryption standard and the advanced encryption standard. Then it delivers the password based authentication method in the double encryption technique's cipher text. For significant the order of the operation they have to apply the avalanche effect but to make the method to secure the keys will be transmitted to the user through the mail of the personal contact of the user. In proposed system we have less time complexity, less computational cost, effective integrity, more secure while the transmission, more confidential.

CONCLUSION

With the rapid growth and innovations witnessed in the mobile industry, the communication field has greatly transformed. Continued innovation in the industry, such as mobile Internet and social networking applications has further had a measurable impact in the communication field. In such mobile and pervasive computing where the messages to be authenticated are short we can further improve the present existing Message authentication codes. It has been demonstrated in this paper that authentication tags can be computed with one addition and a one modular multiplication. Given that messages are relatively short, addition and modular Multiplication can be performed faster than existing computationally secure MACs in the literature of cryptography. When devices are equipped with block

ciphers to encrypt messages, a second technique that utilizes the fact that block ciphers can be modeled as strong pseudorandom permutations is proposed to authenticate messages using a single modular addition. Thus the present scheme reduces the energy consumption and running time for computing MAC tags.

FUTURE SCOPE

In the future have to investigate about the further implementation of encryption techniques to enhance the process with the less time complexity and the high integrity in the process. And have to improve the whole performance by implementing the other process oriented to the security of the data in the mobile computing process. And also need to investigate about the other possible ways to improving the data security other than the cryptographic techniques as the additional process to the data security of the data.

REFERENCES

- [1] J. Carter and M. Wegman, "Universal classes of hash functions," in Proceedings of the ninth annual ACM symposium on Theory of computing–STOC'77. ACM, 1977, pp. 106–112.
- [2] M. Wegman and J. Carter, "New classes and applications of hash functions," in 20th Annual Symposium on Foundations of Computer Science–FOCS'79. IEEE, 1979, pp. 175–182.
- [3] L. Carter and M. Wegman, "Universal hash functions," Journal of Computer and System Sciences, vol. 18, no. 2, pp. 143–154, 1979.
- [4] M. Wegman and L. Carter, "New hash functions and their use in authentication and set equality," Journal of Computer and System Sciences, vol. 22, no. 3, pp. 265–279, 1981.
- [5] J. Bierbrauer, "A2-codes from universal hash classes," in Advances in Cryptology–EUROCRYPT'95, vol. 921, Lecture Notes in Computer Science. Springer, 1995, pp. 311–318.
- [6] M. Atici and D. Stinson, "Universal Hashing and Multiple Authentication," in Advances in Cryptology–CRYPTO'96, vol. 96, Lecture Notes in Computer Science. Springer, 1996, pp. 16–30.
- [7] T. Hellesest and T. Johansson, "Universal hash functions from exponential sums over finite fields and Galois rings," in Advances in cryptology– CRYPTO'96, vol. 1109, Lecture Notes in Computer Science. Springer, 1996, pp. 31–44.
- [8] V. Shoup, "On fast and provably secure message authentication based on universal hashing," in Advances in Cryptology–CRYPTO'96, vol. 1109, Lecture Notes in Computer Science. Springer, 1996, pp. 313–328.
- [9] J. Bierbrauer, "Universal hashing and geometric codes," Designs, Codes and Cryptography, vol. 11, no. 3, pp. 207–221, 1997.
- [10] B. Alomair, A. Clark, and R. Poovendran, "The Power of Primes: Security of Authentication Based on a Universal Hash-Function Family," Journal of Mathematical Cryptology, vol. 4, no. 2, 2010.
- [11] B. Alomair and R. Poovendran, "E-MACs: Towards More Secure and More Efficient Constructions of Secure Channels," in the 13th International Conference on Information Security and Cryptology – ICISC'10. Springer, 2010.
- [12] FIPS 113, "Computer Data Authentication," Federal Information Processing Standards Publication, 113, 1985.
- [13] ISO/IEC 9797-1, "Information technology – Security techniques –Message Authentication Codes (MACs) – Part 1: Mechanisms using a block cipher," 1999.
- [14] M. Dworkin, "Recommendation for block cipher modes of operation: The CMAC mode for authentication," 2005.
- [15] T. Iwata and K. Kurosawa, "omac: One-key cbc mac," in Fast Software Encryption–FSE'03, vol. 2887, Lecture notes in computer science. Springer, 2003, pp. 129–153.
- [16] M. Bellare, R. Guerin, and P. Rogaway, "XOR MACs: New methods for message authentication using finite pseudorandom functions," in Advances in Cryptology–CRYPTO'95, vol. 963, Lecture Notes in Computer Science. Springer, 1995, pp. 15–28.

**Department of
Humanities & Sciences**

CREEPING FLOW FROM A CIRCULAR ORIFICE IN A PLANE WALL

P. KALYAN KUMAR*¹

Assistant Professor, Malla Reddy Engineering College, Secunderabad, India.

Dr. SHAHNAZ BATHUL²

Professor (Retd), JNTUH, Kukatpally, Hyderabad, India.

(Received On: 28-11-16; Revised & Accepted On: 18-12-16)

ABSTRACT

Creeping motion of a viscous fluid through a circular hole in a plane when the boundary conditions on the plane are prescribed is studied and integral solution for the problem presented. Infinite series representation and asymptotic expansion are developed to understand the far field behavior of the fluid flow and to facilitate numerical work.

INTRODUCTION

Forste [1], parmet and saibel [2] and viviand and Berger [3] have considered the two-dimensional and axisymmetric creeping motion of a viscous incompressible fluid in the half plane $z > 0$ for an arbitrarily prescribed velocity field in the plane $z = 0$. Integral solutions for asymmetric jet type of flows have been given by vijaya lakshmi [4, 5]. In this paper, integral solution is presented for an axisymmetric flow from a circular hole in the plane wall $z = 0$ when the velocity of flow through the hole is constant. The solution is presented alternatively in the form of an infinite series and asymptotic expansion is also developed to understand the far field behavior of the fluid flow and to facilitate numerical work.

MATHEMATICAL FORMULATION AND SOLUTION

The equations of motion for steady creeping flow are given by Batchelor [6]

$$\text{Equation of momentum: } \nabla^2 \bar{\mu} = \frac{1}{u} \nabla p \quad (1)$$

$$\text{Equation of mass-conservation: } \nabla \cdot \bar{u} = 0 \quad (2)$$

Where ∇^2 is the two-dimensional laplacian, $\bar{\mu}$ is the velocity vector, p the pressure and u the coefficient of viscosity. Let (μ, v, w) be the components of velocity along the directions of the cylindrical polar coordinates (z, p, ϕ) respectively, the plane wall being defined by $z = 0$. Consider the steady flow of a viscous incompressible fluid with a constant velocity μ_0 through a circular orifice $p=a$ in the wall. For an axisymmetric flow we have $\frac{\partial(\cdot)}{\partial \phi} = 0$ and $w = 0$

$$\begin{aligned} \mu &= z \frac{\partial \phi}{\partial z} - \phi \\ v &= z \frac{\partial \phi}{\partial p} \\ w &= 0 \end{aligned} \quad (3)$$

then the eq's (1) and (2) are satisfied, provided that

$$p = p_0 + 2 \mu \frac{\partial \phi}{\partial z} \quad (4)$$

and

$$\nabla^2 \phi = 0, \nabla^2 = \frac{\partial^2}{\partial p^2} + \frac{1}{p} \frac{\partial}{\partial p} + \frac{\partial^2}{\partial z^2} \quad (5)$$

Where p_0 is a constant

Corresponding Author: P. Kalyan Kumar*¹

Assistant Professor, Malla Reddy Engineering College, Secunderabad, India.

The boundary conditions are

$$\left. \begin{aligned} \mu &= \mu_0 \text{ (constant)} & p < a \\ &= 0 & p > a \end{aligned} \right\} \text{ on } z = 0 \quad (6)$$

$$\mu, v \rightarrow 0 \text{ as } z \rightarrow \infty$$

In terms of \emptyset the boundary conditions at $z = 0$ Are

$$\left. \begin{aligned} \emptyset &= -\mu_0 & p < a \\ &= 0 & p > a \end{aligned} \right\} \begin{array}{l} \text{inside the orifice} \\ \text{outside the orifice} \end{array} \quad (7)$$

Now, we have to solve (5) subject to the boundary conditions (7). That is, we have to seek solution for the dirichlet problem for the domain $z > 0$ and the appropriate solution is Lebedev [7]

$$\emptyset(z, p) = -\mu_0 a \int_0^\infty e^{-\lambda z} J_0(\lambda p) J_1(\lambda a) d\lambda \quad (8)$$

We therefore have

$$\mu = \mu_0 a z \int_0^\infty \lambda e^{-\lambda z} J_0(\lambda p) J_1(\lambda a) d\lambda + \mu_0 a \int_0^\infty e^{-\lambda z} J_0(\lambda p) J_1(\lambda a) d\lambda \quad (9)$$

$$v = \mu_0 a \int_0^\infty \lambda e^{-\lambda z} J_1(\lambda p) J_1(\lambda a) d\lambda \quad (10)$$

$$p = p_0 + 2 \mu \mu_0 a \int_0^\infty \lambda e^{-\lambda z} J_0(\lambda p) J_1(\lambda a) d\lambda \quad (11)$$

Here we have used the result Lebedev [7]

$$J_0^1(z) = -J_1(z)$$

We discuss the following cases here:

Case-(1): Putting $\mu = 2q$, $p = x$, $v = 1$, $t = \lambda$ in the formula sneddon [9]

$$\int_0^\infty t^u e^{-pt} J_v(at) dt = \frac{2v\mu_a}{(a^2+p^2)^{\frac{1}{2}\mu+\frac{1}{2}v+\frac{1}{2}}} \frac{\Gamma(\frac{1}{2}\mu+\frac{1}{2}v+\frac{1}{2}) \Gamma(\frac{1}{2}\mu+\frac{1}{2}v+1)}{\Gamma(v+1) \Gamma(\frac{1}{2})} {}_2F_1\left(\frac{1}{2}\mu+\frac{1}{2}v+\frac{1}{2}, \frac{1}{2}v-\frac{1}{2}\mu, 1+v, \frac{a^2}{a^2+p^2}\right) \quad (I.1)$$

$$\text{Where } {}_2F_1(a, b, c, x) = \sum_{r=0}^\infty \frac{(a)_r (b)_r}{(r!) (c)_r} x^r \quad (I.2)$$

With

$(a)_r = a(a+1)(a+2)\dots\dots(a+r-1)$, is the generalized hypergeometric function, and also using the result Lebedev [7]

$$J_m(z) = \sum_{q=0}^\infty \frac{z^{m+2v} (-1)^q}{q! (m+q)!} \quad (I.3)$$

$$\text{In } I_1 = \int_0^\infty e^{-\lambda z} J_0(\lambda p) J_1(\lambda a) d\lambda$$

We obtain

$$\begin{aligned} I_1 &= \int_0^\infty e^{-\lambda z} \sum_{q=0}^\infty \frac{(-1)^q \lambda^{2q} p^{2q}}{2^{2q} (q!)^2} J_1(\lambda a) d\lambda \\ &= \sum_{q=0}^\infty \frac{(-1)^q p^{2q}}{2^{2q} (q!)^2} \int_0^\infty \lambda^{2q} e^{-\lambda z} J_1(\lambda a) d\lambda \\ &= \sum_{q=0}^\infty \frac{(-1)^q (2q+1)! p^{2q}}{(q!)^2} \frac{a}{(z^2+a^2)^{q+1}} F\left(q+1, \frac{1}{2}-q, 2, \frac{a^2}{a^2+z^2}\right) \end{aligned} \quad (I.4)$$

We can derive similarly

$$\begin{aligned} \text{In } I_2 &= \int_0^\infty \lambda e^{-\lambda z} J_0(\lambda p) J_1(\lambda a) d\lambda \\ &= \sum_{q=0}^\infty \frac{(-1)^q p^{2q}}{2^{2q} (q!)^2} \int_0^\infty \lambda^{2q+1} e^{-\lambda z} J_1(\lambda a) d\lambda \\ &= \sum_{q=0}^\infty \frac{(-1)^q (2q+1)! (q+1) p^{2q}}{(q!)^2} \frac{a}{(z^2+a^2)^{q+\frac{3}{2}}} F\left(q+\frac{3}{2}, -q, 2, \frac{a^2}{a^2+z^2}\right) \end{aligned}$$

And

$$\begin{aligned} I_3 &= \int_0^\infty \lambda e^{-\lambda z} J_1(\lambda p) J_1(\lambda a) d\lambda \\ &= \sum_{q=0}^\infty \frac{(-1)^q p^{2q+1}}{2^{2q+1} (q!)^{q+1} (q+1)!} \int_0^\infty \lambda^{2q+2} e^{-\lambda z} J_1(\lambda a) d\lambda \\ &= \sum_{q=0}^\infty \frac{(-1)^q (2q+3)! p^{2q+1}}{(q+1)! q! 2^{2q+2}} \frac{a}{(z^2+a^2)^{2q+2}} F\left(q+2, -q-\frac{1}{2}, 2, \frac{a^2}{a^2+z^2}\right) \end{aligned} \quad (I.6)$$

Case-(2): Laplace transform of Bessel function $J_0(\lambda p)$ is given by Sneddon [9]

$$\begin{aligned} L \{J_0(\lambda p)\} &= \int_0^\infty e^{-\lambda z} J_0(\lambda p) d\lambda \\ &= (z^2 + p^2)^{-\frac{1}{2}} \end{aligned} \quad (\text{II.1})$$

We therefore have on using (I.3)

$$\begin{aligned} I_1 &= L \{J_0(\lambda p)J_1(\lambda a)\} = \int_0^\infty e^{-\lambda z} J_0(\lambda p) J_1(\lambda a) d\lambda \\ &= \int_0^\infty e^{-\lambda z} J_0(\lambda p) \left(\sum_{q=0}^\infty \frac{(-1)^q p^{2q+1} \lambda^{2q+1}}{2^{2q+1} q!(q+1)!} \right) d\lambda \\ &= \sum_{q=0}^\infty \frac{(-1)^q a^{2q+1}}{2^{2q+1} q!(q+1)!} \int_0^\infty \lambda^{2q+1} e^{-\lambda z} J_0(\lambda p) d\lambda, \end{aligned}$$

Interchanging the order of summation and integration,

$$\begin{aligned} I_1 &= \sum_{q=0}^\infty \frac{(-1)^q a^{2q+1}}{2^{2q+1} q!(q+1)!} \frac{\partial^{2q+1}}{\partial z^{2q+1}} ((z^2 + p^2)^{-\frac{1}{2}}) \\ &= \frac{a}{2} \frac{z}{(z^2 + a^2)^{\frac{3}{2}}} + \frac{a^3}{2! 2^3} \left\{ \frac{9z}{(z^2 + a^2)^{\frac{5}{2}}} - \frac{15z^3}{(z^2 + a^2)^{\frac{7}{2}}} \right\} + \dots \end{aligned} \quad (\text{II.2})$$

We also have

$$\begin{aligned} I_2 &= \int_0^\infty \lambda e^{-\lambda z} J_0(\lambda p) J_1(\lambda a) d\lambda \\ &= \sum_{q=0}^\infty \frac{(-1)^q a^{2q+1}}{2^{2q+1} q!(q+1)!} \frac{\partial^{2q+2}}{\partial z^{2q+2}} (z^2 + p^2)^{-\frac{1}{2}} \\ &= \frac{a}{2} \left\{ -\frac{1}{(z^2 + p^2)^{\frac{3}{2}}} + \frac{3z^2}{(z^2 + p^2)^{\frac{5}{2}}} \right\} + \frac{(-1)a^3}{2^3 1! 2!} \left\{ \frac{9}{(z^2 + p^2)^{\frac{5}{2}}} - \frac{90z^2}{(z^2 + p^2)^{\frac{7}{2}}} + \frac{105z^4}{(z^2 + p^2)^{\frac{9}{2}}} \right\} + \dots \end{aligned}$$

And

$$\begin{aligned} I_3 &= \int_0^\infty \lambda e^{-\lambda z} J_1(\lambda p) J_1(\lambda a) d\lambda \\ &= \sum_{q=0}^\infty \frac{(-1)^q a^{2q+1}}{2^{2q+1} q!(q+1)!} \frac{\partial^{2q+2}}{\partial z^{2q+2}} (z^2 + p^2)^{-\frac{1}{2}} \\ &= -\frac{3a}{2} \frac{pz}{(z^2 + p^2)^{\frac{5}{2}}} - \frac{a^3}{2^3 2!} \left\{ \frac{45pz}{(z^2 + p^2)^{\frac{7}{2}}} + \frac{105pz^3}{(z^2 + p^2)^{\frac{9}{2}}} \right\} + \dots \end{aligned} \quad (\text{II.4})$$

Case-(3): We break up the integral I_1 as follows

$$\begin{aligned} I_1 &= \int_0^\infty e^{-\lambda z} J_0(\lambda p) J_1(\lambda a) d\lambda \\ &= \int_0^k e^{-\lambda z} J_0(\lambda p) J_1(\lambda a) d\lambda + \int_k^\infty e^{-\lambda z} J_0(\lambda p) J_1(\lambda a) d\lambda \dots \end{aligned} \quad (\text{III.1})$$

And then estimate the second integral asymptotically for large k. For large z we have Lebedev [7]

$$J_\nu(z) = \left(\frac{2}{\pi z} \right)^{\frac{1}{2}} \cos \left(z - \frac{\nu}{2} \pi - \frac{\pi}{4} \right) \dots \quad (\text{III.2})$$

So that

$$\int_k^\infty e^{-\lambda z} J_0(\lambda p) j_1(\lambda a) d\lambda = -\frac{1}{\pi(ar)^{\frac{1}{2}}} \left[\text{Re} \int_k^\infty \frac{e^{-\lambda[z+i(p+a)]}}{\lambda} d\lambda + \text{Im} \int_k^\infty \frac{e^{-\lambda[z+i(p-a)]}}{\lambda} d\lambda \right] \dots \quad (\text{III.3})$$

Where Re and Im denote the real and imaginary parts respectively. Noticing that each of the above integrals is expressible as the exponential integral Lebedev [7] defined by

$$\text{Ei}(z) = \int_{-\infty}^z \frac{e^t}{t} dt \quad |\arg(-z)| < \pi \dots \quad (\text{III.4})$$

And using the asymptotic representation Lebedev [7]

$$\text{Ei}(z) = \frac{e^z}{z} \sum_{m=0}^n \frac{m!}{z^m} + O(|z|^{-n-1}), \quad |\arg(-z)| < \pi - \delta \dots \quad (\text{III.5})$$

Where δ is an arbitrarily small positive number, we finally obtain, for sufficiently large k

$$\begin{aligned} \int_0^\infty e^{-\lambda z} J_0(\lambda p) J_1(\lambda a) d\lambda &\approx \int_0^k e^{-\lambda z} J_0(\lambda p) J_1(\lambda a) d\lambda - \frac{1}{\pi(ar)^{\frac{1}{2}}} e^{-kz} \\ &\quad \sum_{m=0}^n \frac{m!}{k^{m+1}} \left\{ \frac{\cos[k(p+a) + (m+1)\text{Tan}^{-1}(p+a)/z]}{[z^2 + (p+a)^2]^{m+1/2}} + \frac{\sin[k(p-a) + (m+1)\text{Tan}^{-1}(p-a)/z]}{[z^2 + (p-a)^2]^{m+1/2}} \right\} \dots \end{aligned} \quad (\text{III.6})$$

REFERENCES

1. Forste J: Zamm 43 (1963) 353.
2. Parmet I L & Saibel E, Comm of Pure appl Math XVIII (1965)17.
3. Viviani H a& Berger S A, Journal of Fluid Mech 23 (1965) 417.

4. Vijaya Lakshmi S: Appl. Science Research Journal 17 (1967) 355.
5. Vijaya Lakshmi S: Appl. Science Research Journal 20 (1969) 173.
6. Batchelor G K, An Introduction to Fluid Dynamics, CUP (1977).
7. Lebedev N N, Special functions and their applications, Dover publications.
8. Mc Lachlan N S Bessel functions for engineers, OUP, London 2nd Edition, (1955).
9. Sneddon Ian: The use of integral Transforms, Mc.grawhill edition.
10. Z Dagan: An Infinite-series solution for the creeping motion through an orifice of finite length. Journal of Fluid Mechanics (1982) 505.

Source of support: Nil, Conflict of interest: None Declared

[Copy right © 2016. This is an Open Access article distributed under the terms of the International Journal of Mathematical Archive (IJMA), which permits unrestricted use, distribution, and reproduction in any medium, provided the original work is properly cited.]

Sweep of Sweet Moments:A Retrospection

Nasreen Begum

Assistant Professor in English

Malla Reddy Engineering College (Autonomous)

India

Abstract-

Luscious moments and images will always remain as reminders of the triumph of the human spirit. Glad moments reinvigorate, rejuvenate life. It helps unleash psychological strain and makes the person to be placid. Life seems to be more significant because of the past glory and foreseen gracious moments.

Key words-

Nostalgia: reminiscence of the past, Exuberant: extremely energetic, Overwhelming: irresistibly strong, Drenched: completely wet, Diligent: focus, performing with intense concentration, Endeavour: a sincere attempt, Alleviate: to make less severe.

Looking at your album! What are you reminded about?

If your grandfather tells something about his youth, what is that, he is recalling?

Why do people take snap of sweet moments?

You meet your friend after many years. What is that you are reminding yourself?

Would you rather enjoy today or have great memories tomorrow and forever. Memories underpin meaning. When people often look back on all their experiences, they feel that life seems to be more meaningful. People reveal in the sweep of nostalgia. It makes us feel energetic, enthusiastic and refresh, alleviate one's stress, makes you feel proud of yourself as a personality for the great cause.

You just envisage, a lady really feels elated expecting the future bliss when she is at the threshold of motherhood, presently she enjoys sweet and pleasant moments, expecting a new changes in her near accessible future time, with a blessed sweet doll in her laps which she was yearning for many years. For her life seems to be more significant, where she lives fully in present expecting elegant future.

People tend to move to the peaceful and glorious place during the times of difficulties that would ease the present stress by recalling their blissful moments, that had been red letter moment of their life.

“The past beats inside me like a second heart”¹ said by John Banville. They capture a moment that never comes back. Memories warm you up from the inside, if you could visualize, father is filled with a great pleasure, when his daughter is supposed to get marry in a couple of days, his heart is filled with high spirits, he is full of life at present feeling exuberant, intense happiness of future occasion.

“We all have our time machines, some take us back, and they are called memories. Some take us forward they are called dreams”²---Jeremy Irons. Whether it is a future or past- sweet moments life becomes more worthy and pleasant for a person

Look at the merry in the child just before the day of the festival or his birthday, he is possessed by an overwhelming desire that fills his heart with an intense well-being in the present that makes him to be more lively, smart, and the conscious mind makes him strong. That would become memorable occasion of his life. The sweet moments leads or tends the people to be more aspiring, hopeful and to progress constructively. We all have our time machines where in we build up a positive traits. Cherishing beautiful moments makes a good human being.

Anticipated dreams and cheerful memories make you wonderful and beautify your present. You think and think if it is a rainy day, continuously raining without pause during the journey, if you could see the rain water trickled down from the hillside, from amongst grasses and wild prim roses. It makes you remind of your childhood. Wherein you collected enthusiastically snowballs getting drenched in rain water and ate before it dissolved, smell of wet mud which gives you momentary happiness at present and refresh you from psychological state of being tensed. Life is full of optimistic and sweet surprises which makes our present lively, busy, healthy, visionary intensity of anger in the present takes the shape of comfort when little kid ask father” can you Please tell something about freedom of your youth” as such it is a fact known these days children are much being exposed to the word

¹ John Banville is an Irish novelist adapter of drama sand screen writer

² Jermy Irons is an English actor

freedom through various sources like media and teachers. As it remained a mere term of expression. What would be the best answer to your child? .you would recall and give the best example of your past youth gaining full strength and saying I was a guy never serious about my studies and spent most of the time in wandering among trees ,playing with friends until there was call for mid day meal by mother. Aren't you a resourceful and guide to your child through your thorny sweet past giving him or her live examples to make them overcome all the hurdles and to block an opening to embarrassing fickle mistakes.

'Lucky', this is a term used for many people, if we put a light on this term taking an illustration of professional towering young cognitive guy, who gets appointed for a greater cause in a renowned industry, his heart is a treasure of happiness and little jar of wonderful feelings. He knows the curt truth of being fixed with a suitable designation to discharge a trust in few days. This moment of joy has positive and profound effect on his senses, where in, he recognizes himself to be more , diligent, industrious, despite there is a challenge and hardship ahead, present mellifluous moment would be a candy for him for a short time. Time passes very quickly as it is well said by Jean de Boufflers says "pleasure is the flower that passes; remembrance is the lasting perfume".³

Conclusion:

Therefore the cloying and conjecture moments is a merry in everyone's life, it builds up hope for earnest Endeavour, makes you to be more self assured. Worst times, hurdles, unfavorable moments make you suffused. Swami Vivekananda said "mind is not a dustbin to keep anger, hatred and jealousy, but it is the treasure box to keep love, happiness and sweet memories." ⁴

Notes:

1"sweep of sweet moments" this article makes the reader ponder over precious moments of life which are never retained.

³ French statesman and writer he published complete works in 1803.

⁴Swami Vivekananda was one of the most influential philosophers and social reformers in his contemporary India.

2 John Banville, born on 8dec 1945 has written Book of Evidence ghosts, The untouchable, Eclipse, Shroud, The sea, The Infinities ,Ancient light.

3 Jermy irons born on 19 September 1948,is an English actor .After receiving classical training at Bristol Old Vic Theatre School. Irons began his acting career on stage in 1969.and has since appeared in many West End theatre productions including The Winter's Tale ,Macbeth, Much Ado About nothing and etc. In 1984 he made his Broadway debut in Tom Stoppard's The Real Thing and received a Tony Award.

4 Jean de Boufflers born on May 31, 1736, Nancy—January 1815.A selection of his stories in prose and verse was edited by Eugene Asse in 1878, his poesies by Octave Uzanne in 1886

5 Swami Vivekananda Born on 12,January 1863-4 July 1902.He wrote Raja yoga, Karma Yoga, MY Master and some of his works were published posthumously for example Inspired Talks (1909)



Scholars Research Library

Der Pharmacia Lettre, 2016, 8 (20):14-20
(<http://scholarsresearchlibrary.com/archive.html>)



Synthesis and characterization of 3-arylidenechroman-4-ones and their inhibitory effects on platelet aggregation activity

^{1,2}Mopur Vijaya Bhaskar Reddy, ³Ping-Chung Kuo, ³Hsin-Yi Hung, ⁴Wei-Jern Tsai, and ^{3, 5*}Tian-Shung Wu

¹Department of Chemistry, National Cheng Kung University, Tainan 701, Taiwan, ROC

²Department of Chemistry, Malla Reddy Engineering College (Autonomous), Maisammaguda, Secunderabad 500100, India;

³School of Pharmacy, National Cheng Kung University Hospital, College of Medicine, National Cheng Kung University, Tainan 701, Taiwan, ROC;

⁴National Research Institute of Chinese Medicine, Taipei, Taiwan, ROC;

⁵Department of Pharmacy and Graduate Institute of Pharmaceutical Technology, Tajen University, Pingtung 90741, Taiwan, ROC

ABSTRACT

A series of 3-arylidenechroman-4-one derivatives (1-16) have been synthesized in good yields from chroman-4-one and different substituted aldehydes by the Claisen-Schmidt condensation. All the synthesized compounds were characterized by using spectroscopic analyses including IR, ¹H NMR, ¹³C NMR, EIMS and HREIMS. The synthesized compounds were screened for in vitro inhibitory effects on aggregation of washed rabbit platelets induced by adenosine diphosphate (20 μM) and collagen (10 μg/mL). Compounds **1** (81.3%), **11** (88.7%), and **13** (85.0 %) were showed potent inhibitory effects on ADP-induced aggregation activity, in which their structures possessed 2-thiophene, 3,5-dimethoxybenzene and 2,3-dimethoxybenzene moieties in the B-ring, respectively.

Keywords: 3-arylidenechroman- 4-one derivatives; Claisen-Schmidt condensation; spectroscopic and spectrometric analysis; platelet aggregation activity

INTRODUCTION

Platelet aggregation plays a central role in thrombosis (clot formation). Platelet-mediated thrombus formation in the coronary artery is a primary factor in the development of thrombotic disorders such as unstable angina, myocardial infarction stroke [1-2], and peripheral vascular diseases [3]. Normally, the blood is not aggregated in the blood vessels, but on an occasion of bleeding, blood aggregation is generated as a physiological defense reaction. Platelet aggregation is caused by physiological substances such as thrombin and prostaglandin endoperoxide and can lead an arterial thrombosis [4]. Platelet aggregation is induced by the action of endogenous agonists such as arachidonic acid (AA), adenosine diphosphate (ADP), platelet-activating factor (PAF), thrombin (Thr) and collagen (Col) [5]. The inhibition of platelet function represents a promising approach for the treatment of these diseases. Many antiplatelet drugs have been used clinically, and have certain disadvantages such as notable side effects and inefficient therapy [6-7]. Therefore, searching for more effective and safer antiplatelet agents with fewer side effects is extremely important. Homoisoflavones are a class of naturally occurring oxygen hetero cyclic compounds. It occupied a special place in the field of hetero cycles as this skeleton is an integral part of many natural compounds. It is structurally related to flavonoid consisted a sixteen carbon skeleton, which includes a chromanone or chromane ring system with a benzyl or benzylidene group at C-3 position. Both natural and synthetic chromone derivatives are

known to exhibit numerous biological activities including antifungal, antihistaminic, anti-inflammatory, antioxidant, and antiviral effects [8-17]. Thiochromones and their derivatives are reported to show medicinal properties [18-19]. The current literature shows that there has been a growing trend towards synthesis of heterocyclic containing these two rings [20-21]. As a continuation of our efforts, we synthesized and reported the structures of heterocyclic homoisoflavanones by condensing different substituted aldehydes with 4-chromanone to obtain 3-arylidene chroman-4-one derivatives **1-16** (Scheme1). In the present study, we would report the characterization of 3-arylidene chroman-4-one derivatives and evaluated for their *in vitro* inhibitory effects on aggregation of washed rabbit platelet induced ADP (20 μ M) and Col (10 μ g/mL).

MATERIALS AND METHODS

Chemistry

All the chemicals and reagents were of analytical grade and were used without further purification. All the reaction and purity of synthesized compounds were deduced by thin layer chromatography (TLC) using silica-G plates. The plates were developed by exposing to the iodine vapors. All the synthesized compounds (**1-16**, Scheme-1) were characterized by spectroscopic and spectrometric analyses including IR, ^1H -, ^{13}C -NMR, EIMS and HREIMS techniques to confirm the presence of proposed ring systems. IR spectra were determined on a Shimadzu FT-IR Prestige 21 spectrophotometer. ^1H and ^{13}C NMR spectra were recorded on a Bruker Avance 300 spectrometer, using tetramethylsilane (TMS) as internal standard and all chemical shifts were reported in parts per million (ppm, δ). EIMS and HREIMS spectra were obtained on a VG-70-250S mass spectrometer. Column chromatography was performed on silica gel (70–230 mesh, 230–400 mesh). Purity of the compounds were checked by TLC plates on Pre coated Kieselgel 60 F254 plates (Merck) using *n*-hexane/ethyl acetate as an eluent in the different ratios and the spots were examined under a UV lamp.

Table I. Inhibitory effects of compounds 1-16 on platelet aggregation induced by ADP and Collagen

Compound	Inducer	
	Inhibition percentage (%)	
	ADP	Col
1	81.3	59.9
2	38.0	10.2
3	54.9	73.3
4	60.6	71.7
5	43.3	48.1
6	66.8	32.1
7	31.5	3.9
8	41.5	48.7
9	69.0	69.9
10	54.1	35.4
11	88.7	19.5
12	61.5	0.0
13	85.0	15.0
14	36.4	0.0
15	66.4	55.1
16	47.8	18.9

General procedure for the synthesis of 3-arylidenechroman-4-ones (1-16):

A mixture of chroman-4-one and corresponding aldehydes in methanol (30 mL) then slowly added to the solution 30% KOH (30 mL) were stirred at room temperature for a period of 24 h (monitored by TLC) [22]. After this period, the alcohol was distilled off and the resulting material was treated with water and acidified dil. HCl (30%). The viscous mass was extracted in separating funnel with ethyl acetate (3X50 mL). The ethyl acetate was evaporated under reduced pressure in the rotavapour to obtain residue. This was further purified by over a silica gel chromatography eluted with a mixture of *n*-hexane-EtOAc to obtain compounds **1-16** in good yields.

Spectral data of synthesized isoxazole compounds

(E)-3-(thiophen-2-ylmethylene)chroman-4-one (1). Chroman-4-one (1.48 g, 0.01 moles) and 2-thiophene carboxaldehyde (1.12 g, 0.01 moles) were treated as described above mentioned general method. The crude product was purified by CC eluting *n*-hexane/EtOAc (8:2) yield **1** (pale yellow solid, 2.1 g, 87%). IR (neat) ν_{max} : 3097, 2920, 1662, 1600, 1581, 1469, 1334, 1303, 1211, 1141, 1107, 1041, 983, 948, 856, 829, 752, 713 cm^{-1} . ^1H NMR (300 MHz, CDCl_3): δ 8.01 (2H, d, J = 8.7 Hz), 7.59 (1H, d, J = 5.1 Hz), 7.50 (1H, m), 7.34 (1H, d, J = 2.7 Hz), 7.17 (1H, t, J = 8.7 Hz), 7.06 (1H, t, J = 7.5 Hz), 6.98 (2H, d, J = 8.2 Hz), 5.46 (2H, s). ^{13}C NMR (75 MHz, CDCl_3): δ 181.2, 160.9, 137.6, 135.6, 133.9, 130.9, 128.7, 128.1, 127.8, 127.1 (x2), 121.8, 117.7, 67.7. EIMS m/z (% *rel. int.*): 242 ($[\text{M}]^+$, 100), 241 (14), 213 (26), 181 (3), 134 (8), 122 (37), 121 (72), 120 (5), 96 (7), 92 (9), 57 (10). HREIMS m/z calcd for $\text{C}_{14}\text{H}_{10}\text{O}_2\text{S}$, 242.0402; found, 242.0405.

(E)-3-((3-methylthiophen-2-yl)methylene)chroman-4-one (2). Chroman-4-one (1.48 g, 0.01 moles) and 3-methyl-2-thiophenecarboxaldehyde (1.26 g, 0.01 moles) were treated as described above mentioned general method. The crude product was purified by CC eluting *n*-hexane/EtOAc (8:2) yield **2** (pale yellow solid, 2.1 g, 82%). IR (neat) ν_{\max} : 1654, 1600, 1570, 1465, 1303, 1261, 1211, 1153, 1103, 1041, 983, 948, 744, 605 cm^{-1} . ^1H NMR (300 MHz, CDCl_3): δ 8.08 (1H, br s), 8.02 (1H, dd, $J = 1.8, 7.8$ Hz), 7.50 (2H, m), 7.06 (1H, t, $J = 7.8$ Hz), 6.99 (2H, t, $J = 7.8$ Hz), 5.48 (2H, s), 2.44 (3H, s). ^{13}C NMR (75 MHz, CDCl_3): δ 181.5, 160.9, 144.0, 135.5, 131.2, 130.9, 129.2, 127.7, 127.2, 126.0, 121.9, 121.7, 117.7, 67.7, 14.6. EIMS m/z (% *rel. int.*): 256 ($[\text{M}]^+$, 100), 255 (15), 242 (8), 241 (45), 237 (18), 227 (12), 213 (12), 159 (6), 136 (16), 135 (66), 134 (17), 121 (42), 110 (5), 97 (12), 91 (21), 65 (6). HREIMS m/z calcd for $\text{C}_{15}\text{H}_{12}\text{O}_2\text{S}$, 256.0558; found, 256.0559.

(E)-3-(furan-2-ylmethylene)chroman-4-one (3). Chroman-4-one (1.48 g, 0.01 moles) and 2-furaldehyde (0.96 g, 0.01 moles) were treated as described above mentioned general method. The crude product was purified by CC eluting *n*-hexane/EtOAc (9:1) yield **3** (pale yellow solid, 1.75 g, 77%). IR (neat) ν_{\max} : 1666, 1600, 1469, 1396, 1319, 1257, 1215, 1145, 1026, 918, 883, 833, 752, 601 cm^{-1} . ^1H NMR (300 MHz, CDCl_3): δ 7.99 (1H, d, $J = 1.2$ Hz), 7.61 (1H, s), 7.46 (2H, m), 7.05 (1H, t, $J = 7.2$ Hz), 6.98 (1H, d, $J = 8.4$ Hz), 6.75 (1H, d, $J = 3.3$ Hz), 6.54 (1H, dd, $J = 3.3, 1.2$ Hz), 5.59 (2H, s). ^{13}C NMR (75 MHz, CDCl_3): δ 181.6, 161.3, 151.2, 145.6, 135.6, 127.7, 126.6, 121.9, 121.7, 121.6, 118.5, 117.8, 112.6, 67.9. EIMS m/z (% *rel. int.*): 226 ($[\text{M}]^+$, 100), 225 (14), 197 (44), 169 (15), 141 (8), 121 (20), 120 (12), 106 (14), 105 (12), 92 (9), 78 (19), 65 (4). HREIMS m/z calcd for $\text{C}_{14}\text{H}_{10}\text{O}_3$, 226.0630; found, 226.0630.

(E)-3-((5-metnylfuran-2-yl)methylene)chroman-4-one (4). Chroman-4-one (1.48 g, 0.01 moles) and 5-methyl-2-furaldehyde (1.10 g, 0.01 moles) were treated as described above mentioned general method. The crude product was purified by CC eluting *n*-hexane/ CHCl_3 (1:1) yield **4** (yellow solid, 1.90 g, 79%). IR (neat) ν_{\max} : 2920, 2850, 1666, 1608, 1570, 1516, 1469, 1311, 1261, 1219, 1141, 1026, 956, 756, 721, 601 cm^{-1} . ^1H NMR (300 MHz, CDCl_3): δ 8.00 (1H, dd, $J = 1.8, 8.1$ Hz), 7.47 (2H, m), 7.00 (2H, m), 6.67 (1H, d, $J = 3.0$ Hz), 6.17 (1H, d, $J = 3.0$ Hz), 5.58 (2H, s), 2.40 (3H, s). ^{13}C NMR (75 MHz, CDCl_3): δ 181.7, 161.3, 156.6, 149.9, 135.3, 127.7, 124.9, 122.1, 121.9, 121.6, 120.5, 117.7, 109.3, 68.0, 14.1. EIMS m/z (% *rel. int.*): 240 ($[\text{M}]^+$, 100), 239 (17), 225 (25), 211 (12), 197 (38), 169 (13), 121 (13), 120 (26), 119 (13), 105 (12), 91 (10), 77 (7), 65 (6). HREIMS m/z calcd for $\text{C}_{15}\text{H}_{12}\text{O}_3$, 240.0786; found, 240.0785.

(E)-3-((1-methyl-1H-pyrrol-2-yl)methylene)chroman-4-one (5). Chroman-4-one (1.48 g, 0.01 moles) and N-methylpyrrole-2-carboxaldehyde (1.09 g, 0.01 moles) were treated as described above mentioned general method. The crude product was purified by CC eluting *n*-hexane/EtOAc (8:2) yield **5** (pale yellow solid, 1.70 g, 71%). IR (neat) ν_{\max} : 1647, 1600, 1573, 1473, 1415, 1384, 1323, 1296, 1257, 1172, 1072, 1045, 995, 956, 914, 729, 648 cm^{-1} . ^1H NMR (300 MHz, CDCl_3): δ 7.99 (1H, t, $J = 8.4$ Hz), 7.78 (1H, d, $J = 9.6$ Hz), 7.45 (1H, d, $J = 8.1$ Hz), 6.97 (3H, m), 6.30 (2H, m), 5.39 (2H, s), 3.77 (3H, s). ^{13}C NMR (75 MHz, CDCl_3): δ 181.1, 160.6, 135.3, 128.3, 127.7, 127.5, 124.7, 123.4, 121.9, 121.5, 117.6, 115.8, 109.8, 68.2, 34.5. EIMS m/z (% *rel. int.*): 239 ($[\text{M}]^+$, 100), 238 (23), 210 (19), 121 (19), 119 (32), 118 (69), 117 (9), 104 (8), 94 (5), 91 (6), 77 (4). HREIMS m/z calcd for $\text{C}_{15}\text{H}_{13}\text{O}_2\text{N}$, 239.0946; found, 239.0945.

(E)-3-(4-methoxybenzylidene)chroman-4-one (6). Chroman-4-one (1.48 g, 0.01 moles) and 4-methoxy benzaldehyde (1.36 g, 0.01 moles) were treated as described above mentioned general method. The crude product was purified by CC eluting *n*-hexane/EtOAc (9:1) yield **6** (pale yellow solid, 2.1 g, 79%). IR (neat) ν_{\max} : 2916, 2839, 1666, 1600, 1508, 1465, 1319, 1257, 1211, 1180, 1149, 1111, 1026, 956, 914, 825, 748, 675 cm^{-1} . ^1H NMR (300 MHz, CDCl_3): δ 8.02 (1H, dd, $J = 1.2, 9.0$ Hz), 7.83 (1H, s), 7.46 (1H, m), 7.26 (2H, d, $J = 9.0$ Hz), 7.05 (1H, t, $J = 7.6$ Hz), 6.96 (3H, m), 5.38 (2H, s), 3.85 (3H, s). ^{13}C NMR (75 MHz, CDCl_3): δ 182.1, 160.9, 160.6, 137.2, 135.6, 132.0 (x2), 128.8, 127.8, 126.9, 122.0, 121.7, 117.7, 114.2 (x2), 67.7, 55.3. EIMS m/z (% *rel. int.*): 266 ($[\text{M}]^+$, 100), 265 (39), 256 (7), 251 (14), 237 (12), 235 (8), 223 (6), 146 (29), 145 (14), 131 (17), 121 (44), 103 (17), 92 (7), 77 (11). HREIMS m/z calcd for $\text{C}_{17}\text{H}_{14}\text{O}_3$, 266.0943; found, 266.0943.

(E)-3-(4-(3-methylbut-2-enyloxy)benzylidene)chroman-4-one (7). Chroman-4-one (1.48 g, 0.01 moles) and 4-*O*-prenylbenzaldehyde (1.90 g, 0.01 moles) were treated as described above mentioned general method. The crude product was purified by CC eluting *n*-hexane/EtOAc (8:2) yield **7** (pale yellow solid, 1.92 g, 60%). IR (neat) ν_{\max} : 2962, 2858, 1658, 1585, 1508, 1473, 1423, 1377, 1319, 1257, 1215, 1180, 1149, 1118, 1018, 829, 752, 570 cm^{-1} . ^1H NMR (300 MHz, CDCl_3): δ 8.02 (1H, d, $J = 7.5$ Hz), 7.83 (1H, br s), 7.47 (1H, t, $J = 7.5$ Hz), 7.27 (2H, d, $J = 8.7$ Hz), 7.06 (1H, t, $J = 7.5$ Hz), 6.96 (3H, m), 5.49 (1H, t, $J = 6.6$ Hz), 5.38 (2H, s), 4.56 (2H, d, $J = 6.6$ Hz), 1.81 (3H, s), 1.76 (3H, s). ^{13}C NMR (75 MHz, CDCl_3): δ 182.2, 160.9, 160.0, 138.8, 137.4, 135.6, 132.0 (x2), 128.7, 127.8, 126.9, 122.1, 121.8, 119.1, 117.8, 114.9 (x2), 67.8, 64.9, 25.8, 18.2. EIMS m/z (% *rel. int.*): 320 ($[\text{M}]^+$, 2), 253 (17), 252 (100), 251 (33), 235 (6), 223 (8), 132 (11), 131 (15), 121 (35), 92 (7), 69 (34). HREIMS m/z calcd for $\text{C}_{21}\text{H}_{20}\text{O}_3$, 320.1412; found, 320.1415.

(E)-3-(4-(dimethylamino)benzylidene)chroman-4-one (8). Chroman-4-one (1.48 g, 0.01 moles) and N,N-dimethylbenzaldehyde (1.49 g, 0.01 moles) were treated as described above mentioned general method. The crude product was purified by CC eluting *n*-hexane/EtOAc (8:2) yield **8** (pale yellow solid, 1.89 g, 68%). IR (neat) ν_{\max} : 1654, 1604, 1566, 1523, 1458, 1365, 1319, 1222, 1192, 1141, 1033, 995, 956, 810, 756 cm^{-1} . ^1H NMR (300 MHz, CDCl_3): δ 8.03 (1H, d, $J = 7.5$ Hz), 7.84 (1H, s), 7.47 (1H, d, $J = 6.9$ Hz), 7.28 (2H, d, $J = 9.0$ Hz), 7.06 (1H, t, $J = 7.5$ Hz), 6.97 (1H, d, $J = 8.1$ Hz), 6.74 (2H, d, $J = 9.0$ Hz), 5.45 (2H, s), 3.06 (6H, s). ^{13}C NMR (75 MHz, CDCl_3): δ 182.0, 160.7, 151.1, 138.2, 135.2, 132.5 (x2), 127.7, 126.0, 122.3, 122.2, 121.6, 117.6, 111.7 (x2), 68.1, 40.0 (x2). EIMS m/z (% *rel. int.*): 279 ($[\text{M}]^+$, 100), 278 (30), 250 (14), 159 (30), 158 (47), 144 (6), 143 (5), 139 (6), 115 (14), 92 (5). HREIMS m/z calcd for $\text{C}_{18}\text{H}_{17}\text{O}_2\text{N}$, 279.1259; found, 279.1256.

(E)-3-benzylidenechroman-4-one (9). Chroman-4-one (1.48 g, 0.01 moles) and benzaldehyde (1.06 g, 0.01 moles) were treated as described above mentioned general method. The crude product was purified by CC eluting *n*-hexane/EtOAc (9:1) yield **9** (pale yellow solid, 2.2 g, 93%). IR (neat) ν_{\max} : 3062, 1674, 1604, 1469, 1311, 1265, 1211, 1149, 1107, 1029, 995, 956, 837, 759, 698 cm^{-1} . ^1H NMR (300 MHz, CDCl_3): δ 8.03 (1H, d, $J = 7.5$ Hz), 7.88 (1H, s), 7.46 (4H, m), 7.30 (2H, d, $J = 6.9$ Hz), 7.07 (1H, t, $J = 7.5$ Hz), 6.96 (1H, d, $J = 8.4$ Hz). ^{13}C NMR (75 MHz, CDCl_3): δ 182.1, 161.0, 137.4, 135.8, 134.3, 130.8, 129.9 (x2), 129.4, 128.6 (x2), 127.8, 121.9, 121.8, 117.8, 67.5. EIMS m/z (% *rel. int.*): 236 ($[\text{M}]^+$, 100), 235 (73), 207 (16), 179 (5), 178 (6), 131 (9), 121 (51), 116 (25), 115 (66), 92 (20), 89 (10), 77 (6), 63 (14). HREIMS m/z calcd for $\text{C}_{16}\text{H}_{12}\text{O}_2$, 236.0837; found, 236.0839.

(E)-3-((E)-3-phenylallylidene)chroman-4-one (10). Chroman-4-one (1.48 g, 0.01 moles) and cinnamaldehyde (1.32 g, 0.01 moles) were treated as described above mentioned general method. The crude product was purified by CC eluting *n*-hexane/EtOAc (8:2) yield **10** (pale yellow solid, 2.01 g, 77%). IR (neat) ν_{\max} : 2850, 1662, 1604, 1469, 1392, 1327, 1257, 1215, 1141, 1103, 1018, 92, 829, 752, 690 cm^{-1} . ^1H NMR (300 MHz, CDCl_3): δ 8.01 (1H, d, $J = 6.6$ Hz), 7.49 (4H, d, $J = 9.0$ Hz), 7.37 (3H, d, $J = 6.6$ Hz), 7.03 (3H, d, $J = 16.2$ Hz), 6.98 (1H, s), 5.26 (2H, s). ^{13}C NMR (75 MHz, CDCl_3): δ 181.9, 161.3, 143.3, 135.9 (x2), 135.5, 129.5, 129.0, 128.8 (x2), 127.8, 127.4 (x2), 122.3, 121.8, 121.5, 117.8, 66.9. EIMS m/z (% *rel. int.*): 262 ($[\text{M}]^+$, 100), 261 (45), 247 (6), 185 (16), 171 (27), 142 (21), 141 (48), 131 (14), 128 (7), 121 (56), 115 (31), 105 (10), 92 (13), 77 (14), 63 (9). HREIMS m/z calcd for $\text{C}_{18}\text{H}_{14}\text{O}_2$, 262.0994; found, 262.0992.

(E)-3-(3,5-dimethoxybenzylidene)chroman-4-one (11). Chroman-4-one (1.48 g, 0.01 moles) and 3,5-dimethoxybenzaldehyde (1.66 g, 0.01 moles) were treated as described above mentioned general method. The crude product was purified by CC eluting *n*-hexane/EtOAc (9:1) yield **11** (yellow solid, 2.4 g, 81%). IR (neat) ν_{\max} : 2935, 2839, 1670, 1604, 1469, 1300, 1265, 1203, 1157, 1107, 1064, 1033, 995, 937, 837, 756, 678 cm^{-1} . ^1H NMR (300 MHz, CDCl_3): δ 8.02 (1H, dd, $J = 1.2, 8.1$ Hz), 7.99 (1H, s), 7.50 (1H, m), 7.07 (1H, t, $J = 7.5$ Hz), 6.97 (1H, d, $J = 8.1$ Hz), 6.51 (1H, d, $J = 1.8$ Hz), 6.43 (2H, d, $J = 1.8$ Hz), 5.35 (2H, s), 3.82 (6H, s). ^{13}C NMR (75 MHz, CDCl_3): δ 182.1, 161.1, 160.8 (x2), 137.4, 136.1, 135.8, 131.2, 127.9, 121.9, 121.8, 117.9, 107.8 (x2), 101.3, 67.6, 55.4 (x2). EIMS m/z (% *rel. int.*): 296 ($[\text{M}]^+$, 33), 295 (4), 265 (8), 175 (5), 168 (8), 167 (12), 166 (100), 165 (40), 148 (27), 147 (15), 137 (16), 135 (22), 122 (20), 121 (62), 120 (13), 109 (13), 95 (10), 92 (16), 77 (14), 63 (18), 58 (16). HREIMS m/z calcd for $\text{C}_{18}\text{H}_{16}\text{O}_4$, 296.1049; found, 296.1049.

(E)-3-(benzo[d][1,3]dioxol-5-ylmethylene)chroman-4-one (12). Chroman-4-one (1.48 g, 0.01 moles) and 3,4-methylenedioxybenzaldehyde (1.66 g, 0.01 moles) were treated as described above mentioned general method. The crude product was purified by CC eluting *n*-hexane/EtOAc (9:1) yield **12** (pale yellow solid, 2.2 g, 79%). IR (neat) ν_{\max} : 2897, 1662, 1593, 1477, 1446, 1315, 1261, 1145, 1103, 1033, 918, 867, 813, 756, 721, 671 cm^{-1} . ^1H NMR (300 MHz, CDCl_3): δ 8.00 (1H, d, $J = 9.0$ Hz), 7.77 (1H, s), 7.47 (1H, t, $J = 7.2$ Hz), 7.06 (1H, t, $J = 7.2$ Hz), 6.95 (1H, d, $J = 9.0$ Hz), 6.84 (3H, m), 6.03 (2H, s), 5.35 (2H, s). ^{13}C NMR (75 MHz, CDCl_3): δ 182.0, 160.9, 148.8, 148.0, 137.3, 135.7, 129.3, 128.4, 125.3, 122.0, 121.8, 117.8, 109.8, 108.6, 101.6, 67.7. EIMS m/z (% *rel. int.*): 280 ($[\text{M}]^+$, 100), 279 (28), 251 (9), 221 (8), 160 (35), 159 (20), 130 (6), 121 (71), 102 (31), 76 (11), 75 (6), 63 (8), 57 (7). HREIMS m/z calcd for $\text{C}_{17}\text{H}_{12}\text{O}_4$, 280.0736; found, 280.0735.

(E)-3-(2,3-dimethoxybenzylidene)chroman-4-one (13). Chroman-4-one (1.48 g, 0.01 moles) and 2,3-dimethoxybenzaldehyde (1.66 g, 0.01 moles) were treated as described above mentioned general method. The crude product was purified by CC eluting *n*-hexane/EtOAc (9:1) yield **13** (pale yellow solid, 2.2 g, 74%). IR (neat) ν_{\max} : 2935, 2835, 1670, 1604, 1469, 1311, 1273, 1222, 1149, 1072, 1033, 995, 898, 752, 640 cm^{-1} . ^1H NMR (300 MHz, CDCl_3): δ 8.03 (1H, d, $J = 7.2$ Hz), 7.95 (1H, s), 7.47 (1H, t, $J = 7.2$ Hz), 7.07 (2H, m), 6.73 (1H, d, $J = 7.2$ Hz), 5.18 (2H, s), 3.89 (3H, s), 3.78 (3H, s). ^{13}C NMR (75 MHz, CDCl_3): δ 182.3, 161.3, 152.9, 148.0, 135.7, 133.2, 131.8, 128.7, 127.8, 123.8, 122.0 (x2), 121.7, 117.8, 113.6, 68.2, 61.1, 55.8. EIMS m/z (% *rel. int.*): 296 ($[\text{M}]^+$, 69), 281 (10), 267 (6), 266 (40), 265 (100), 250 (21), 221 (12), 161 (41), 160 (17), 146 (9), 121 (32), 118 (28), 115 (11), 92 (30), 77 (13), 63 (23). HREIMS m/z calcd for $\text{C}_{18}\text{H}_{16}\text{O}_4$, 296.1049; found, 296.1050.

(E)-3-(2,4-dimethoxybenzylidene)chroman-4-one (14). Chroman-4-one (1.48 g, 0.01 moles) and 2,4-dimethoxybenzaldehyde (1.66 g, 0.01 moles) were treated as described above mentioned general method. The crude product was purified by CC eluting *n*-hexane/EtOAc (8:2) yield **14** (pale yellow solid, 2.4 g, 81%). IR (neat) ν_{\max} : 2927, 2843, 1666, 1600, 1500, 1465, 1307, 1269, 1211, 1157, 1114, 1026, 960, 925, 829, 756, 729, 675, 636 cm^{-1} . ^1H NMR (300 MHz, CDCl_3): δ 8.03 (1H, br s), 8.01 (1H, m), 7.47 (1H, m), 7.04 (1H, t, $J = 7.5$ Hz), 6.96 (1H, d, $J = 8.4$ Hz), 6.94 (1H, d, $J = 8.4$ Hz), 6.51 (2H, m), 5.25 (2H, br s), 3.85 (3H, s), 3.84 (3H, s). ^{13}C NMR (75 MHz, CDCl_3): δ 182.4, 162.5, 161.0, 159.7, 135.4, 133.6, 131.4, 128.9, 127.8, 122.2, 121.6, 117.7, 116.5, 104.4, 98.4, 68.2, 55.5, 55.4. EIMS m/z (% *rel. int.*): 296 ($[\text{M}]^+$, 24), 281 (10), 266 (19), 265 (100), 165 (7), 161 (21), 121 (14), 118 (4), 97 (5), 77 (5), 71 (6), 57 (10). HREIMS m/z calcd for $\text{C}_{18}\text{H}_{16}\text{O}_4$, 296.1049; found, 296.1046.

(E)-3-(2,5-dimethoxybenzylidene)chroman-4-one (15). Chroman-4-one (1.48 g, 0.01 moles) and 2,5-dimethoxybenzaldehyde (1.66 g, 0.01 moles) were treated as described above mentioned general method. The crude product was purified by CC eluting *n*-hexane/EtOAc (9:1) yield **15** (pale yellow solid, 2.6 g, 88%). IR (neat) ν_{\max} : 2943, 2835, 1670, 1604, 1469, 1307, 1222, 1149, 1041, 1022, 921, 871, 810, 759, 709, 594 cm^{-1} . ^1H NMR (300 MHz, CDCl_3): δ 8.05 (1H, d, $J = 6.9$ Hz), 7.95 (1H, s), 7.46 (1H, t, $J = 6.9$ Hz), 7.06 (1H, t, $J = 7.2$ Hz), 6.92 (3H, m), 6.65 (1H, d, $J = 6.6$ Hz), 5.22 (2H, s), 3.81 (3H, s), 3.79 (3H, s). ^{13}C NMR (75 MHz, CDCl_3): δ 182.3, 161.2, 153.0, 152.4, 135.6, 133.5, 131.1, 127.8, 124.1, 122.1, 121.7, 117.8, 116.1, 115.6, 111.8, 68.0, 55.9, 55.8. EIMS m/z (% *rel. int.*): 296($[\text{M}]^+$, 16), 266 (19), 265 (100), 161 (13), 121 (6), 118 (7), 92 (4). HREIMS m/z calcd for $\text{C}_{18}\text{H}_{16}\text{O}_4$, 296.1049; found, 296.1050.

(E)-3-(2,3,4-trimethoxybenzylidene)chroman-4-one (16). Chroman-4-one (1.48 g, 0.01 moles) and 2,3,4-trimethoxybenzaldehyde (1.96 g, 0.01 moles) were treated as described above mentioned general method. The crude product was purified by CC eluting *n*-hexane/EtOAc (9:1) yield **16** (pale yellow solid, 2.85 g, 87%). IR (neat) ν_{\max} : 2939, 2839, 1670, 1608, 1589, 1465, 1415, 1300, 1284, 1230, 1145, 1099, 1049, 995, 929, 837, 806, 759, 725, 682 cm^{-1} . ^1H NMR (300 MHz, CDCl_3): δ 8.03 (1H, d, $J = 7.8$ Hz), 7.93 (1H, s), 7.47 (1H, t, $J = 7.2$ Hz), 7.05 (1H, t, $J = 7.2$ Hz), 6.95 (1H, d, $J = 8.1$ Hz), 6.81 (1H, d, $J = 8.1$ Hz), 6.71 (1H, d, $J = 8.7$ Hz), 5.23 (2H, s), 3.93 (3H, s), 3.90 (3H, s), 3.89 (3H, s). ^{13}C NMR (75 MHz, CDCl_3): δ 182.3, 161.1, 155.2, 153.1, 142.3, 135.6, 133.3, 130.0, 127.8, 125.3, 122.1, 121.7, 121.4, 117.7, 106.9, 68.1, 61.4, 60.9, 56.0. EIMS m/z (% *rel. int.*): 326 ($[\text{M}]^+$, 7), 296 (20), 295 (100), 279 (5), 196 (4), 191 (5), 121 (7), 120 (4), 58 (28). HREIMS m/z calcd for $\text{C}_{19}\text{H}_{18}\text{O}_5$, 326.1154; found, 326.1155.

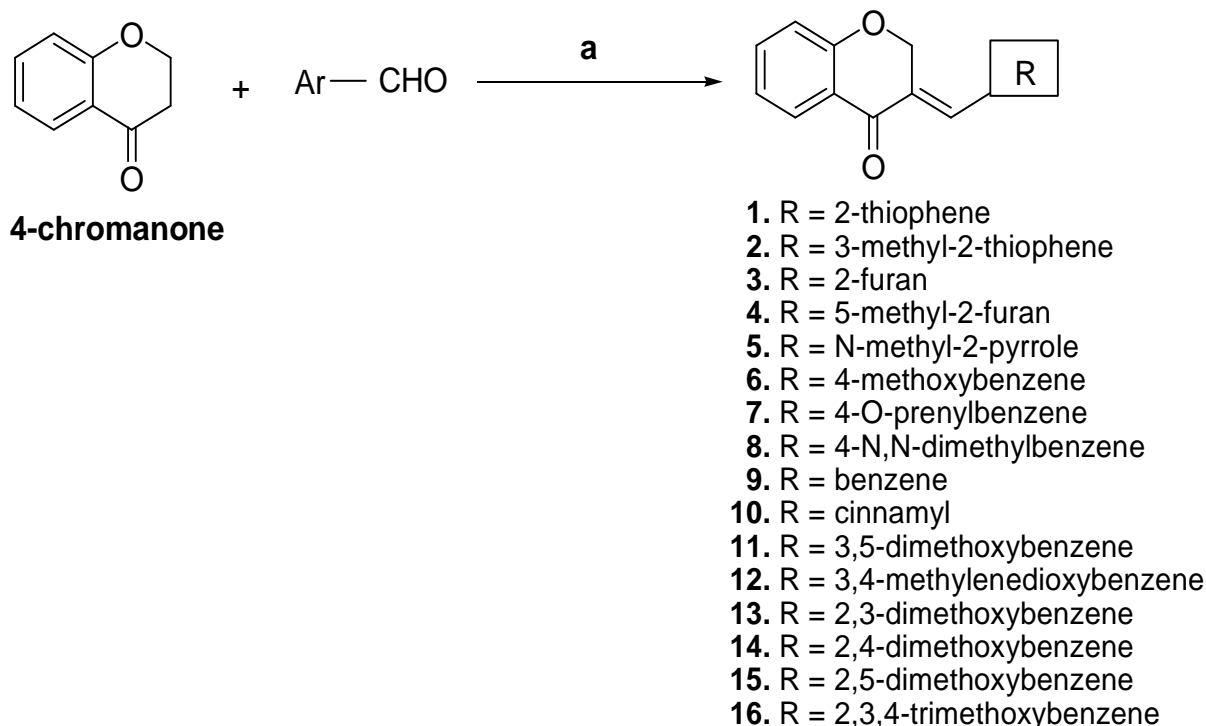
ANTIPLATELET AGGREGATION ACTIVITY

Preparation of the platelet suspension

Washed platelet suspension was prepared as previously described with some modifications [23-25]. In brief, blood was collected from the marginal ear vein of New Zealand White rabbits into tubes containing one-sixth volume of acid-citrate dextrose as anticoagulant. The blood was centrifuged at 1000 g for 8 min. at room temperature. The upper portion was kept as platelet-rich plasma (PRP) after mixing with EDTA to a final concentration of 5mM and re centrifuged at 2000 g for 12 min. The platelet pellet was suspended in modified Ca^{2+} -free Tyrode's buffer (137 mM NaCl, 2.8 mM KCl, 2 mM MgCl_2 , 0.33 mM NaH_2PO_4 , 5 mM glucose, 10 mM HEPES) with 0.35% bovine serum albumin, heparin (50 unit/mL), and apyrase (1unit/mL) and then was incubated at 37 °C for 20 min. After centrifugation at 2000g for 6 min, the washed platelet pellet was re suspended in Tyrode's buffer containing 1 mM Ca^{2+} . For the aggregation test, the platelet numbers were counted by hemacytometer and adjusted to 2.5×10^8 platelets/mL.

Measurement of platelet aggregation

Platelet aggregation was measured turbidimetrically with a light-transmission Platelet Aggregation Chromogenic Kinetic System PACK4 (Helena Laboratories, Beaumont TX) with some modifications [23-25]. The platelet suspension was stirred at 900 rpm and incubated with an appropriate amount of vehicle (dimethyl sulfoxide, DMSO) or various concentrations of test compounds in DMSO at 37 °C for 2 min. Aggregation was induced with ADP (20 μM) or Col (10 $\mu\text{g/mL}$). The transmission of washed platelet suspension was assigned 0% aggregation while transmission through Tyrode's buffer was assigned 100% aggregation. The extent of platelet aggregation was measured as the maximal increase in light transmission within 4 min after the addition of an inducer. To eliminate or minimize any possible effects of the solvent, the final concentration of DMSO in the platelet suspension was fixed at 0.5%. The inhibition percentages of aggregation are presented as mean values ($n \geq 2$).



Scheme 1: (a) 30% KOH solution in methanol stirring at room temperature at 24 hr

RESULTS AND DISCUSSION

The IR spectra of these synthetic compounds exhibited carbonyl absorption bands around 1647-1674 cm^{-1} . In the ^1H -NMR spectra the characteristic resonance signal for H-2 around at δ 5.18- 5.59 and ^{13}C NMR spectrum displayed characteristic signal of C-2 around at δ 68.2- 66.9. The chemical shift for carbonyl carbons (C-4) appeared in the downfield region at δ 182.4- 181.1. We evaluated inhibition effects for **1-16** on ADP and Collagen induced washed platelet aggregation (**Table.1**). Compound **1** showed potent inhibitory effect 81.3% on ADP and 59.9% collagen induced aggregation. While the methyl derivative of **1** decreased inhibitory effects observe on both ADP (38%) and collagen (10.2%)-induced aggregation. Compounds **3** and **4** with furan and 5-methylfuran have ring-B moieties, respectively, showed significant inhibition on ADP (54.9% and 60.6%) and collagen (73.3% and 71.7%) induced aggregation. Compounds **6** and **9** showed significant inhibitory effects on ADP (66.8% and 69.0%)-induced aggregation with benzene and 4-methoxybenzene rings as ring-B moieties. Compounds **11**(88.7%), **13**(85%) and **15** (66.4%) having 3,5-dimethoxy, 2,3-dimethoxy, and 2,5-dimethoxybenzene ring as ring-B moieties, respectively, showed potent inhibition on ADP-induced aggregation. It can be concluded that, all the synthesized 3-arylidenechroman-4-ones (**1-16**) from substituted and heterocyclic aldehydes. Among the **16** compounds screened for *in vitro* inhibitory effects on aggregation of platelets induced ADP and collagen showed potent inhibitory effect on ADP (**1**, **11** and **13**), and collagen (**3**, **4** and **9**) induced aggregation activity. The results indicate that some 3-arylidenechroman-4-ones were relatively significant inhibitors of platelet aggregation.

CONCLUSION

Present study described the synthesis of some 3-arylidene-4-one derivatives. All the synthesized compounds were characterized by IR and ^1H & ^{13}C -NMR and mass spectral analysis and evaluated for antiplatelet aggregation activity. The results indicated that compounds **3**, **4** and **9** were showed potent inhibitory effect on collage and **1**, **11** and **13** were potent on ADP.

Acknowledgements

This study was sponsored by the grant from Ministry of Science and Technology, Taiwan, ROC and grant (No.OUA 95-3-2-021) from National Cheng Kung University, Tainan, Taiwan, ROC awarded to T. S. Wu. Authors were also

thankful for the support in part by Taiwan Department of Health Clinical Trial and Research Center of Excellence (DOH100-TD-B-111-004).

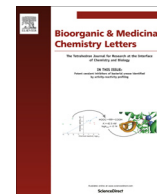
REFERENCES

- [1] M. J Davis, A. C. Thomas, *Br. Heart J.* **1985**, 53, 363-373.
- [2] M. D.Trip, V. M. Cats, F. J. L.Capelle, J.Vreeken, *N. Engl. J. Med.* **1990**, 322, 1549-1554.
- [3] E. Genton, G. P. Clagett, E. W. Salzman, *Chest.* **1986**, 89, 75S-81S.
- [4] V. Fuster, L. Badimon, J. J. Badimon, J. H. Chesebro, *N. Engl. J. Med.* **1992**, 326, 242-250.
- [5] H. Arita, K. Hansaki, *Prog. Lipid Res.* **1989**, 28, 273-301.
- [6] K. Schror, *Drugs.* **1995**, 50, 7-28.
- [7] J. S. Bennett, *Annu. Rev. Med.* **2001**, 52, 161-184.
- [8] M. G. Qualig, N. Desiraj, E. Bossu, R. Sgro, C. Conti, *Chirality.* **1999**, 11, 495-500.
- [9] N. Desiraj, S. Olivieri, M. L. Stein, R. Sgro, N. Orsi, C. Conti, *Antiviral chemistry &chemotherapy.* **1997**, 8, 545-555.
- [10] V. V. R. Siddaiaiah, S. Venkateswarlu, A. V. Krishna Raju, G. V. Subba Raju, *Bioorg.Med.Chem.* **2006**, 14, 2545-2551.
- [11] D. A. Horton, G. T. Bourne, M. L. Symthe, *Chem. Rev.* **2003**, 103, 893-930.
- [12] M. Hadieri, M. Barbier, X. Ronot, A. M. Mariotte, A. Boomendfel, J. Botetonnact, *J. Med.Chem.* **2003**, 46, 2125-2131.
- [13] A. Gupta, A. Dwivedy, G. Keshri, R. Sharma, A. K. Balapure, M. M. Singh, S. Ray, *Bioorg Med Chem Lett.* **2006**, 16, 6006-6012.
- [14] A. Foroumadi, A. Samzadeh- Kermani, S. Emami, G. Dehghan, M. Sorkhi, F. Arabsorkhi, M. R. Heidari, M. Abdollahi, A. Shafiee, *Bioorg Med Chem Lett.* **2007**, 17, 6764-6769.
- [15] J. B. Harborne, C. A. Williams, *Phytochemistry.* **2000**, 55, 481-504.
- [16] G. W. Buston, T. Doba, E. J. Gabe, L. Huges, F. Lee, L. Prasad, K. U. Ingold, *J Am Chem Soc.* **1985**, 107, 7053-7065.
- [17] H. K. Wang, K. F. Bastow, L. M. Cosentino, K. H. Lee, *J Med Chem*, **1996**, 39, 1975-1980.
- [18] Y. Liu, W. Luo, L. Sun, C. Guo, *Drug DiscovTher.* **2008**, 2, 216-218.
- [19] C. K. Ghosh, A. Patra, *J Heterocycle Chem.* **2008**, 45, 1529-1547.
- [20] N. G. Li, Z. H. Shi, Y. P. Tang, H. Y. Ma, J. P. Yang, B. Q. Li, Z. J. Wang, S. L. Song, J. A. Duan, *J.Heterocycl Chem.* **2010**, 47, 785-799.
- [21] W. Wang, H. Li, J. Wang, L. Zu, *J Am Chem.Soc.* **2006**, 128, 10354-10355.
- [22] L. Wu, H. Guo, X. Wang, R. Wu, *Chinese Journal of Organic Chemistry.* **2012**, 32, 608-611.
- [23] W. J. Tsai, H. T. Hsieh, C. C. Chen, Y. C. Kuo, C. F. Chen, *Eur. J. Pharmacol*, **1998**, 346, 103-110.
- [24] C. C. Hung, W. J. Tsai, L. M. Yang, Y. H. Kuo, *Bioorg.Med. Chem.* **2005**, 13, 1791-1797.
- [25] H. C. Hsu, W. C. Yang, W. J. Tsai, C. C. Chen, H. Y. Huang, Y. C. Tsai, *Biochem.Biophys. Res. Commun.* **2006**, 345, 1033-1038.



Contents lists available at ScienceDirect

Bioorganic & Medicinal Chemistry Letters

journal homepage: www.elsevier.com/locate/bmcl

Synthesis and biological evaluation of chalcone, dihydrochalcone, and 1,3-diarylpropane analogs as anti-inflammatory agents

Mopur Vijaya Bhaskar Reddy^{a,1}, Hsin-Yi Hung^{b,1}, Ping-Chung Kuo^{b,1}, Guan-Jhong Huang^c, Yu-Yi Chan^d, Shio-Chyn Huang^e, Shwu-Jen Wu^f, Susan L. Morris-Natschke^g, Kuo-Hsiung Lee^{g,h,*}, Tian-Shung Wu^{b,i,*}

^a Department of Chemistry, National Cheng Kung University, Tainan 701, Taiwan

^b School of Pharmacy, National Cheng Kung University Hospital, College of Medicine, National Cheng Kung University, Tainan 701, Taiwan

^c School of Chinese Pharmaceutical Sciences and Chinese Medicine Resources, College of Pharmacy, China Medical University, Taichung 404, Taiwan

^d Department of Biotechnology, Southern Taiwan University of Science and Technology, Tainan 710, Taiwan

^e Graduate Institute of Pharmaceutical Science, Chia-Nan University of Pharmacy and Science, Tainan 717, Taiwan

^f Department of Medical Technology, Chung Hua University of Medical Technology, Tainan 717, Taiwan

^g Natural Products Research Laboratories, UNC Eshelman School of Pharmacy, University of North Carolina, Chapel Hill, NC 27599, United States

^h Chinese Medicinal Research and Development Center, China Medical University Hospital, China Medical University, Taichung 404, Taiwan

ⁱ Department of Pharmacy, College of Pharmacy and Health Care, Tajen University, Pingtung 907, Taiwan

ARTICLE INFO

Article history:

Received 12 January 2017

Revised 14 February 2017

Accepted 16 February 2017

Available online xxxxx

Keywords:

Chalcones

Dihydrochalcones

1,3-Diarylpropane analogs

Anti-inflammatory agents

ABSTRACT

Twenty-one chalcones were prepared via aldol condensation and subsequent reduction of these compound led to the corresponding dihydrochalcone and 1,3-diphenylpropane derivatives. The synthetic products were examined for their effects on NO inhibition in LPS-activated mouse peritoneal macrophages. Among the tested compounds, a 1,3-diarylpropane analog, 2-(3-(3,4-dimethoxyphenyl)propyl)-5-methoxyphenol (**3p**), displayed the most significant inhibitory effects against NO production. To investigate the mechanism of action, the effects of **3p** on iNOS and COX-2 protein expression were studied by immunoblot. The results concluded that **3p** is capable of inhibiting iNOS expression in LPS-induced RAW264.7 cells via attenuation of NF-κB signaling by ERK, p38, and JNK.

© 2017 Published by Elsevier Ltd.

Flavonoids are a ubiquitous group of polyphenolic substances concentrated in the seeds, fruit skin or peel, bark, and flowers of most plants. Numerous plant medicines contain flavonoids, which have been reported by many authors as having antibacterial, anti-inflammatory, anti-allergic, antimutagenic, antiviral, antineoplastic, and vasodilatory actions. Many studies have shown that some flavonoids are potent antioxidants that are capable of scavenging hydroxyl radicals ($\cdot\text{OH}$), superoxide anions (O_2^-), lipid peroxy radicals, and hydrogen peroxide (H_2O_2). These free radicals have been implicated several disease processes, including asthma,^{1,2} cancer,³ cardiovascular disease,^{4,5} cataracts,^{6,7} diabetes,^{8,9} gastrointestinal inflammatory diseases,^{10,11} liver disease,¹² muscular degeneration,^{13,14} periodontal disease,¹⁵ and other inflammatory processes. In the flavonoid family, chalcones and dihydrochalcones belong to

a major class of bicyclic compounds, which are precursors for flavonoid biosynthesis in plants. The two aromatic rings in these compounds are linked by a three carbon bridge, specifically, propenone in chalcones and propanone in dihydrochalcones. Compounds of both types exert multiple biological activities, including anti-inflammatory, antioxidant and anticancer properties.^{16–21} In addition, viscolin, a 1,3-diarylpropane, displayed potent and selective inhibition on the superoxide anion generation activated by *N*-formyl-methionyl-leucyl-phenylalanine (FMLP) combined with cytochalasin B in human neutrophils, and also exhibited free radical scavenging effects in a 1,1-diphenyl-2-picryl-hydrazyl (DPPH) assay. Both actions could be mediated by viscolin's anti-inflammatory activity.²² Anti-inflammatory and antioxidant therapies are also comprehensive pharmacological approaches in the treatment of inflammatory related disorders.^{23,24}

In the present study, we synthesized three corresponding series of chalcone, dihydrochalcone, and 1,3-diphenylpropane derivatives (Fig. 1, details in [Supplementary Data](#)) and examined the compounds for *in vitro* anti-inflammatory activity using a lipopolysaccharide (LPS)-stimulated RAW264.7 cellular assay. We also evaluated the effect of a selected compound (**3p**) on nuclear factor

* Corresponding authors at: Natural Products Research Laboratories, UNC Eshelman School of Pharmacy, University of North Carolina, Chapel Hill, NC 27599, United States (K.-H. Lee). School of Pharmacy, National Cheng Kung University Hospital, College of Medicine, National Cheng Kung University, Tainan 701, Taiwan (T.-S. Wu).

E-mail addresses: khlee@unc.edu (K.-H. Lee), tswu@mail.ncku.edu.tw (T.-S. Wu).

¹ Authors contributed equally to this work.

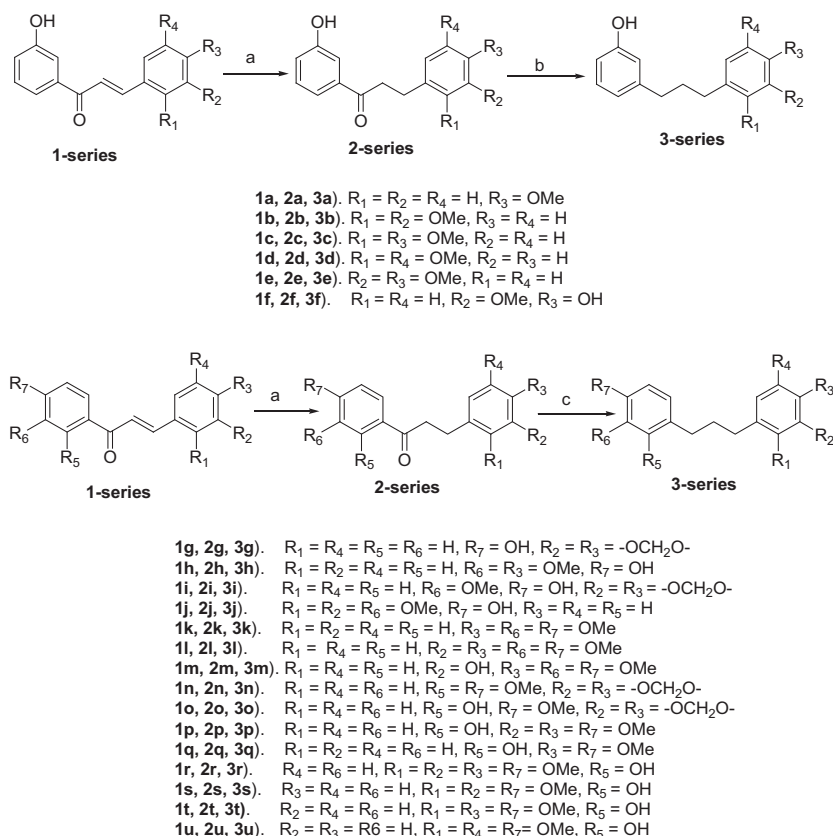


Fig. 1. The chemical structures of the chalcone, dihydrochalcone, and 1,3-diarylpropane analogs. Reagents and conditions: (a) Pd/C, H_2 , EtOAc; (b) Ni–Al alloy (50:50), H_2O , reflux at 110–120 °C for 8–12 h; (c) TFA, $(C_2H_5)_3SiH$, reflux at 50–55 °C for 12 h.

kappa B (NF- κ B) expression and mitogen-activated protein kinase (MAPK) signaling pathways to better understand the molecular mechanism.

Chalcones **1a–1u** were prepared by an aldol condensation of substituted acetophenones and aldehydes in equimolar quantities with KOH as base at room temperature (Fig. 1).²⁵ The stereochemistry of the olefinic carbon–carbon bond of each chalcone was established based on the appropriate 1H NMR coupling constant. Chalcones **1a–1u** then underwent hydrogenation in a H_2 atmosphere with 10% Pd–C as catalyst and EtOAc as solvent for 24–48 h to obtain dihydrochalcones **2a–2u**, respectively, in good yields (Fig. 1).²⁶ To prepare the analogous 1,3-diarylpropanes **3a–3u**, we needed to reduce the carbonyl groups in **2a–2u** to methylene units. To the best of our knowledge, no literature exists on this specific reduction in dihydrochalcones. Also, drawbacks exist to the two common methods used for this conversion: the Wolf–Kishner reaction,²⁷ which cannot be applied to base sensitive substrates, and the Clemmensen reaction, which is not suitable for acid sensitive precursors, often requires harsh conditions and long reaction times, and suffers from poor yields.^{28,29} So herein, we tested two methods for the preparation of 1,3-diphenylpropanes from dihydrochalcones. In method A, dihydrochalcones **2a–2f** and Ni–Al alloy (50:50)³⁰ were combined in H_2O at room temperature and the reaction mixture was stirred vigorously under reflux for 8–12 h giving 1,3-diphenylpropanes **3a–3f**, respectively, in good yields. However, when we applied the same procedure to compounds **2g–2u**, which have oxygenated substituents at C-4, C-2,4, or C-3,4 in ring A, no reaction was observed in most cases, likely due to conjugation and chelation effects. Subsequently, in method B, dihydrochalcones **2g–2u** were stirred with trifluoroacetic acid (TFA) and triethylsilyl hydride $[(C_2H_5)_3SiH]$ ³¹ at 0 °C for 30 min and then at

50–55 °C for 12 h, to provide 1,3-diphenylpropanes **3g–3u**, respectively, in good yields (Fig. 1).

Cell viability and effect of **3p** on LPS-induced NO production in macrophages

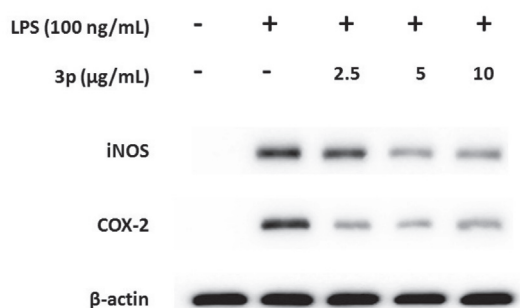
We evaluated the effects of the synthesized chalcones, dihydrochalcones, and 1,3-diphenylpropane derivatives at four concentrations (1.25, 2.5, 5, and 10 μ g/mL) on RAW264.7 cell viability in a MTT assay as well as on NO production by measuring nitrite levels based on the Griess reaction in LPS-activated mouse peritoneal macrophages.¹⁸ NO production was significantly decreased in a dose-dependent manner by the treatment with various compounds from all three series. Compounds **1h**, **1k**, **2e**, **2i**, **2k**, **3a**, **3g**, **3i**, **3m**, **3p**, and **3r** exhibited IC_{50} values in a range of 2.0–9.8 μ g/mL (Tables 1–3, Supplementary Material), without a significant influence on cell viability at that concentration. Thus, the NO inhibitory effects of these compounds were probably not due to cytotoxic effects. Some compounds did affect cell viability, especially at the highest dose level. For example, although **1d** with a 2,5-dimethoxyphenyl ring had a low NO inhibitory IC_{50} value (2.42 μ g/mL), it also reduced cell viability at that concentration (28% reduction at 2.5 μ g/mL). The NO inhibitory ability did not follow similar relationships among the 1-, 2-, 3-compounds, which may suggest different binding modes among these three series. Overall, 1,3-diarylpropane analog **3p** exhibited the best anti-inflammatory activity among the tested compounds. Other biological studies on this compound have not been reported, and the mechanisms underlying the anti-inflammatory activity have not yet been elucidated. Therefore, in the present study, we investi-

gated possible molecular mechanisms of **3p** using LPS-stimulated RAW 264.7 cells *in vitro*.

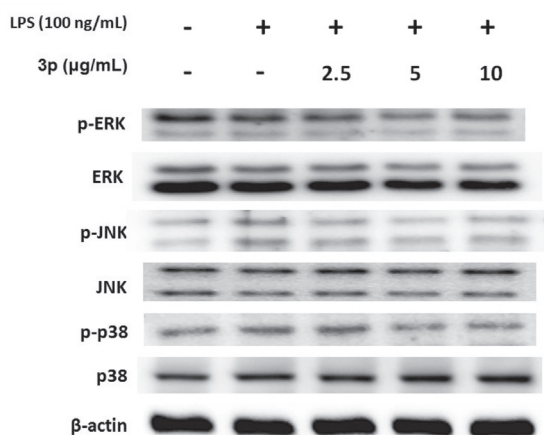
Inhibition of LPS-induced iNOS and COX-2 protein by **3p**

To investigate whether the inhibition of NO production was due to decreased iNOS and COX-2 protein levels, the effect of **3p** on iNOS and COX-2 protein expression was studied by using an immunoblot. Incubation with **3p** (2.5, 5, and 10 $\mu\text{g/mL}$) in the presence of LPS (100 ng/mL) for 24 h inhibited iNOS protein expression

A.



B.



C.

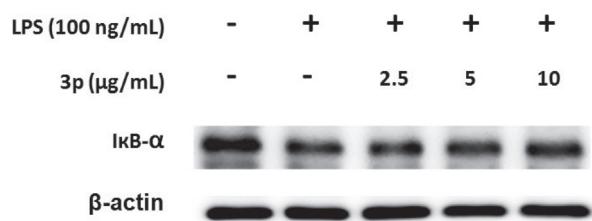


Fig. 2. Inhibition of iNOS, COX-2 (A), MAPK (ERK, JNK, and p38) (B), and NF- κ B (C) protein expression by **3p** in LPS-stimulated RAW264.7 cells. Cells were incubated for 24 h (2A) or 1 h (2B, 2C) with 100 ng/mL of LPS in the absence or presence of **3p** (0, 2.5, 5, and 10 $\mu\text{g/mL}$). Compound **3p** was added 1 h before the incubation with LPS. Lysed cells were then prepared and subjected to Western blotting by using an antibody specific for iNOS, COX-2, MAPK, or NF- κ B. β -Actin was used as an internal control.

in mouse macrophage RAW264.7 cells in a dose-dependent manner (Fig. 2A). The detection of β -actin was also performed in the same blot as an internal control.

Effects of **3p** on the LPS-stimulated activation of MAPKs

MAPKs play critical roles in the regulation of cell growth and differentiation, and control cellular responses to cytokines and stresses. In particular, ERK, p38, and JNK are important for the activation of NF- κ B.^{20,21} To explore whether the inhibition of NF- κ B activation by **3p** is mediated through the MAPK pathway, MAPK phosphorylation was examined by Western blot in RAW 264.7 cells pretreated with **3p** and then with LPS. As shown in Fig. 2B, **3p** suppressed the LPS-induced activation of ERK, JNK, and p38 MAPKs. However, the expression of non-phosphorylated ERK, JNK, and p38 MAPKs was unaffected by LPS or LPS plus **3p**. These results suggest that phosphorylation of MAPKs may be involved in the inhibitory effect of **3p** on LPS-stimulated NF- κ B binding in RAW 264.7 cells.

Inhibition of LPS-induced NF- κ B proteins by **3p**

The effect of NF- κ B expression by **3p** in the presence of LPS for 1 h was assessed by Western blotting. The intensity of protein bands showed an average of 79.2% increase of NF- κ B protein after treatment with **3p** at 2.5, 5, and 10 $\mu\text{g/mL}$ compared with LPS alone (Fig. 2C). Therefore, we concluded that **3p** is capable of inhibiting iNOS expression in LPS induced RAW264.7 cells via attenuation of NF- κ B signaling by ERK, p38, and JNK.

In summary, the synthesized chalcones, dihydrochalcones and 1,3-diarylpropanes were studied for their anti-inflammatory activity *in vitro*. This study suggested that some dihydrochalcones and 1,3-diarylpropanes, especially compound **3p**, may have the potential to be developed as anti-inflammatory agents. However, further studies are necessary to more closely examine the underlying molecular mechanisms and verify direct targets at the transcriptional or post-transcriptional level *in vitro*.

Acknowledgments

This work was supported by a grant (NSC 96-2628-M-006-002) from the National Science Council, Taiwan, and a grant (OUA 95-3-2-021) from National Cheng Kung University, Tainan, Taiwan, awarded to T. S. Wu. This study was also supported in part by the Taiwan Department of Health Clinical Trial and Research Center of Excellence (DOH100-TD-B-111-004).

A. Supplementary material

Supplementary data associated with this article can be found, in the online version, at <http://dx.doi.org/10.1016/j.bmcl.2017.02.038>.

References

- Bast A, Haenen GR, Doelman CJ. *Am J Med.* 1991;91:2S.
- Greene LS. *J Am Coll Nutr.* 1995;14:317.
- Ginter E. *Bratisl Lek Listy.* 1995;96:195.
- Steinberg D, Parthasarathy S, Carew T. *N Engl J Med.* 1989;320:915.
- Hertog MG, Feskens EJ, Hollman PC. *Lancet.* 1993;342:1007.
- Varma SD, Kinoshita JH. *Biochem Pharm.* 1976;25:2505.
- Gerster HZ. *Ernahrungssiss.* 1989;28:56.
- Doly M, Droy-Lefaix MT, Braquet P. *EXS.* 1992;62:299.
- Kahler W, Kuklinski B, Ruhlmann C, Lptoz C. *Z Gesamte Inn Med.* 1993;48:223.
- Smirnov DA. *Khirurgiia.* 1994;3:30.
- Yoshikawa T, Naito Y, Kondo M. *J Nutr Vitaminol.* 1993;39:S35.
- Miguez MP, Anundi I, Sainz-Pardo LA, Lindros KO. *Chem Biol Interact.* 1994;91:51.

13. Lebuissou DA, Leroy L, Rigal G. *Presse Med.* 1986;15:1556.
14. Van der Hagen AM, Yolton DP, Kaminski MS, Yolton RL. *J Am Optom Assoc.* 1993;64:871.
15. Bobyrev VN, Rozkolupa NV, Skripnikova TP. *Stomatologiia.* 1994;73:11.
16. Dicarlo G, Mascolo N, Izzo AA, Capasso F. *Life Sci.* 1999;65:337.
17. Dimmock JR, Elias DW, Beazely MA, Kandepu NM. *Curr Med Chem.* 1999;6:1125.
18. Echeverria C, Santibanez JS, Donoso-Tauda O, Escobar CA, Ramirez-Tagle R. *Int J Mol Sci.* 2009;10:221.
19. Shah A, Khan AM, Qureshi R, Ansari FL, Nazar MF, Shah SS. *Int J Mol Sci.* 2008;9:1424.
20. Katsori AM, Hadjipavlou-Latina D. *Curr Med Chem.* 2009;16:1062.
21. Vogel S, Barbic M, Jurgentliemk G, Heilmann J. *Eur J Med Chem.* 2010;45:2206.
22. Hwang TL, Leu YL, Kao SH, Tang MC, Chang HL. *Free Radic Biol Med.* 2006;41:1433.
23. Cuzzocrea S, Riley DP, Caputi AP, Salvemini D. *Pharmacol Rev.* 2001;53:135.
24. Middleton E, Kandaswami C, Theoharides TC. *Pharmacol Rev.* 2000;52:673.
25. (a) Cabrera M, Simoens M, Falchi G, et al. *Bioorg Med Chem.* 2007;15:3356;
(b) Won SJ, Liu CT, Tsao LT, et al. *Eur J Med Chem.* 2005;40:103;
(c) Xia Y, Yang Z, Xia P, Bastow KF, Nakanishi Y, Lee KH. *Bioorg Med Chem Lett.* 2000;10:6991;
(d) Vijaya Bhaskar Reddy M, Su CH, Chiou WF, et al. *Bioorg Med Chem.* 2008;16:7358.
26. Chantrapromma K, Rattapa Y, Karalai C, Lojanapiwatana V, Seechamnaturakit V. *Phytochemistry.* 2000;53:511.
27. Jain AS. *Synlett.* 2004;13:2445.
28. Schwartz MA, Rose FF, Holton RA, Scott SW, Vishnuvajjala B. *J Am Chem Soc.* 1977;99:2571.
29. Iinuma M, Matoba Y, Tanaka T, Mizuno M. *Chem Pharm Bull.* 1986;34:1656.
30. Ishimoto K, Mitoma Y, Nagashima S, et al. *Chem Comm.* 2003;4:514.
31. West CT, Stephen J, Donnelly DA, Doyle MP. *J Org Chem.* 1973;38:2675.



Scholars Research Library

Der Pharmacia Lettre, 2016, 8 (20):172-176
(<http://scholarsresearchlibrary.com/archive.html>)



Inhibitory effects of Bichalcone derivatives on Superoxide anion generation ($O_2^{\bullet-}$) and elastase release by activated human neutrophils in response to FMLP/CB

Mopur Vijaya Bhaskar Reddy,^{1,2} Tsong-Long Hwang³ and Tian-Shung Wu^{1*}

¹Department of chemistry, National Cheng Kung University, Tainan 701, Taiwan.

²Malla Reddy Engineering College (Autonomous), Maisammaguda, Secunderabad 500100, India

³Graduate Institute of Natural Products, College of Medicine, Chang Gung University, 259, Taoyan, Taiwan 701

ABSTRACT

Chalcones have a distinctive 1,3-diaryl propenone skeleton and exert numerous biological effects. Previously we synthesized (**1a-23**) bichalcones through the piperazine Mannich base linkage with different substitution on the both ring-B of the chalcone moieties. These compounds were subjected into the inhibitory effects on Formyl-Met-Leu-Phe (FMLP) and cytochalasin B (CB) stimulated $O_2^{\bullet-}$ generation and elastase release in human neutrophils. Among the tested compounds, **3-23** were exhibited potent elastase release inhibitory effects in activated human neutrophils with the IC_{50} values ranges from 4.98 μ M to 50.87 μ M

Keywords: Mannich base linked bichalcones, superoxide generation ($O_2^{\bullet-}$) and elastase release.

INTRODUCTION

Chalcones possess a 1,3-diphenyl-2-propen-1-one basic skeleton in which two aromatic rings are connected by a three carbon α , β -unsaturated carbonyl system. They are intermediates in the biosynthesis of flavonoids, which are substances widespread in plants and with an array of biological activities; however, their structure differs considerably from the other members of the flavonoids family [1]. Chalcones are reported with diverse biological activities including antihyperglycemic, [2] antibacterial, [3] antiplatelet, [4] antiulcerative, [5] antimalarial, [6] antiviral, [7] antileishmanial, [8] antioxidant, [9] antitubercular, [10] tyrosinase inhibiting, [11] anti-inflammatory, [12] and analgesic activities [13].

Neutrophils play a pivotal role in the defense of the human body against infections. However, overwhelming activation of neutrophils is known to elicit tissue damage. Human neutrophils are known to play important roles in the pathogenesis of various diseases, such as ischemic heart disease, acute myocardial infarction, sepsis, and atherogenesis [14–17]. In response to diverse stimuli, activated neutrophils secrete a series of cytotoxins, such as the superoxide anion ($O_2^{\bullet-}$), a precursor of other ROS, granule proteases, and bioactive lipids [18-19]. $O_2^{\bullet-}$ production is linked to the killing of invading microorganisms, but it can also directly or indirectly cause damage by destroying surrounding tissues. Neutrophil granules contain many antimicrobial and potentially cytotoxic substances. Neutrophil elastase is a major secreted product of stimulated neutrophils and a major contributor to the destruction

of tissue in chronic inflammatory disease [20]. Therefore, it is crucial to restrain respiratory burst and degranulation in physiological conditions while potentiating these functions in infected tissues and organs. Previously we synthesized [21] a series of bichalcone analogs through the piperazine Mannich base linkage with different substitutions on the ring-B of the chalcone moiety (**1a-23**) (Figure 1) were displayed potent activity against four human cancer cell lines including KB, A549, HCT-8 and DU145 and mechanism action of compound **23** in the HT-29 human colon adenocarcinoma cell line. In addition to this, compounds **3-23** were tested for the inhibition of nitric oxide (NO) production in murine microglial cells, **4** (IC₅₀ 0.34 μ M) and **11** (IC₅₀ 0.5 μ M) were exhibited more potent than a specific NOS inhibitor L-NAME (L-nitroarginine methyl ester) (IC₅₀ 18.9 μ M) [21]. Considering the pharmacological importance of bichalcone analogs (**1a-23**) through the piperazine Mannich base linkage with different substitution pattern in the ring-B, herein we describe the respiratory burst and degranulation caused by the inhibitory effects of superoxide anion generation ($O_2^{\cdot-}$) and elastase release in response to Fmlp/CB induced human neutrophils (Table 1). In this study we found that Mannich base linked bichalcones analogs were significantly inhibited in superoxide anion generation ($O_2^{\cdot-}$) and potent inhibition was observed in elastase release.

MATERIALS AND METHODS

Materials Bichalcone derivatives were synthesized (published results) [21] and dissolved in dimethyl sulfoxide (DMSO) to make stock solutions. Aprotinin, *N*-(2-((*p*-bromocinnamyl)amino)ethyl)-5-isoquinolinesulfonamide (H89), KT5720 (9*S*,10*S*,12*R*-2,3,9,10,11,12-hexahydro-10-hydroxy-9-methyl-1-oxo-9,12-epoxy-1*H*-diindolo(1,2,3-*fg*:3',2',1'-*kl*)pyrrolo(3,4-*i*)(1,6)benzodiazocine-10-carboxylic acid hexyl ester), leupeptin, phenylmethylsulfonyl fluoride (PMSF), 3-(1-(3-(amidinothio)propyl-1*H*-indol-3-yl))-3-(1-methyl-1*H*-indol-3-yl)maleimide (Ro318220), rolipram, and zaprinast were obtained from Calbiochem (La Jolla, CA, U.S.A.). Fluo-3 AM was purchased from Molecular Probes (Eugene, OR, U.S.A.). 2-(4-iodophenyl)-3-(4-nitrophenyl)-5-(2,4-disulfophenyl)-2*H*-tetrazolium monosodium salt (WST-1) was purchased from Dojindo Laboratories (Kumamoto, Japan). All other chemicals were obtained from Sigma (St Louis, MO, U.S.A.). When drugs were dissolved in DMSO, the final concentration of DMSO in cell experiments did not exceed 0.5% and did not affect the parameters measured.

Preparation of human neutrophils:

Blood was taken from healthy human donors (20~32 years old) by venipuncture, using a protocol approved by the institutional review board at Chang Gung Memorial Hospital. Neutrophils were isolated with a standard method of dextran sedimentation prior to centrifugation in a Ficoll Hypaque gradient and hypotonic lysis of erythrocytes [22-23]. Purified neutrophils that contained > 98% viable cells, as determined by the trypan blue exclusion method, were resuspended in a calcium (Ca^{2+})-free HBSS buffer at pH 7.4, and were maintained at 4 °C before use.

Measurement of $O_2^{\cdot-}$ generation:

The assay of $O_2^{\cdot-}$ generation was based on the SOD-inhibitable reduction of ferricytochrome *c* [24]. In brief, after supplementation with 0.5 mg/ml ferricytochrome *c* and 1 mM Ca^{2+} , neutrophils were equilibrated at 37 °C for 2 min and incubated with drugs for 5 min. Cells were activated with 100 Nm fMLP for 10 min. When fMLP was used as a stimulant, CB (1 μ g/ml) was incubated for 3 min before activation by the peptide (fMLP/CB). Changes in absorbance with the reduction of ferricytochrome *c* at 550 nm were continuously monitored in a double-beam, six-cell positioner spectrophotometer with constant stirring (Hitachi U-3010, Tokyo, Japan). Calculations were based on differences in the reactions with and without SOD (100 U/ml) divided by the extinction coefficient for the reduction of ferricytochrome *c* ($\epsilon = 21.1$ /mM/10 mm).

Measurement of elastase release:

Degranulation of azurophilic granules was determined by elastase release as described previously [22]. Experiments were performed using MeO-Suc-Ala-Ala-Pro-Val-p-nitroanilide as the elastase substrate. Briefly, after supplementation with MeO-Suc-Ala-Ala-Pro-Val-p-nitroanilide (100 μ M), neutrophils (5×10^5 /ml) were equilibrated at 37 °C for 2 min and incubated with drugs for 5 min. Cells were activated by 100 Nm fMLP and 0.5 μ g/ml CB, and changes in absorbance at 405 nm were continuously monitored to assay elastase release. The results are expressed as the percent of the initial rate of elastase release in the fMLP/CB-activated, drug-free control system.

RESULTS AND DISCUSSION

We examined the inhibitory effects on Formyl-Met-Leu-Phe (fMLP) and cytochalasin B (CB) stimulated $O_2^{\cdot-}$ generation and elastase release in human neutrophils. Compounds **5** and **8** are 2-furan and 5-methyl-2-furan groups

in ring-B, respectively. Among these, **5** exhibited potent inhibitory effects on both superoxide generation ($O_2^{\cdot-}$) and elastase release in FMLP/CB induced human neutrophils. Compound **3** (IC_{50} 19.73 μ M) was more potent than **20** (IC_{50} 35.36 μ M), in elastase release inhibition, and they have only one structural difference. Both compounds possess a 2-pyridyl group as ring-B, but an additional methoxy group at C-3 position in **20** was responsible for decrease the elastase release inhibition. Compound **6** (IC_{50} 11.87 μ M) was more potent than **7** (IC_{50} 35.67 μ M) in elastase release inhibition, and the corresponding methoxy derivative **15** (IC_{50} 28.60 μ M) exhibited less elastase inhibition observed in human neutrophils. These results indicate that methyl group on thiophene ring and methoxy group on benzene ring caused for the decrease elastase inhibition observed in compounds **7** and **15**. Compounds **10** (IC_{50} 3.46 μ M), **11** (IC_{50} 6.20 μ M) and **12** (IC_{50} 3.52 μ M) having phenyl, 4-methoxyphenyl and 3,4-methylenedioxy benzene groups in ring-B, respectively, were exhibited more potent inhibition observed in Fmlp/CB induced in superoxide anion generation ($O_2^{\cdot-}$). Compound **7** (IC_{50} 0.08 μ M) is more potent than the corresponding methoxy derivative **16** (IC_{50} 2.92 μ M) in superoxide anion generation, indicating that methoxy functionality was responsible for decrease the of superoxide anion generation inhibition in Fmlp/CB induced human neutrophils. Compounds **21** (IC_{50} 19.35 μ M) and **22** (IC_{50} 4.98 μ M) are having pyrrole and N-methylpyrrole moieties in ring-B. These results clearly indicate methyl group play a major role for enhance the inhibition of elastase release in human neutrophils but compound **22** (IC_{50} 4.98 μ M) was more potent elastase release inhibition observed than the corresponding bichalcone derivative **9** (IC_{50} 23.05 μ M) in human neutrophils. Compound **23** (IC_{50} 6.67 μ M) exhibited more potent inhibition observed in superoxide anion generation than **4** (IC_{50} 26.08 μ M). Compound **19** having 2-chlorobenzene as ring-B of both chalcone moieties, which was potently inhibited Fmlp/CB induced superoxide anion generation in human neutrophils.

Based on the *in vitro* preliminary results observed for compounds **1a-23** in FMLP/CB stimulated elastase release in human neutrophils with IC_{50} values ranging from 4.98 μ M to 50.87 μ M compared to control PMSF (IC_{50} 95.0 μ M). These data could be provided as the bichalcones linked with the Mannich base group for further design and development of anti-inflammatory agents.

Table 1 Effects of compounds (**1a-23**) on superoxide anion generation and elastase release by human neutrophils in response to fMLP/CB.

Compound	Superoxide anion IC_{50} (μ M) ^a or (Inh %)	Elastase IC_{50} (μ M) ^a or (Inh %)
1a	(15.33 \pm 2.29)**	(-2.65 \pm 4.43)
2a	(15.46 \pm 2.76)**	(-4.90 \pm 3.20)
3	(22.24 \pm 3.46)**	(19.73 \pm 6.01)*
4	(26.08 \pm 3.78)**	(21.43 \pm 3.11)**
5	(13.34 \pm 3.16)*	(7.88 \pm 2.45)*
6	(-1.29 \pm 1.97)	(11.87 \pm 3.26)*
7	(0.08 \pm 0.79)	(35.67 \pm 7.16)**
8	(26.68 \pm 1.80)***	(14.47 \pm 7.44)
9	(-0.73 \pm 1.90)	(23.05 \pm 4.07)**
10	(3.46 \pm 3.09)	(18.74 \pm 7.64)
11	(6.20 \pm 2.56)	(36.95 \pm 2.00)***
12	(3.52 \pm 2.26)	(50.87 \pm 7.22)**
13	(-2.31 \pm 1.40)	(23.08 \pm 2.04)***
14	(10.20 \pm 3.76)	(20.24 \pm 2.24)***
15	(-1.40 \pm 2.69)	(28.60 \pm 2.24)***
16	(2.92 \pm 2.97)	(26.30 \pm 1.70)***
17	(-0.06 \pm 2.71)	(23.71 \pm 3.21)**
18	(5.32 \pm 0.94)**	(33.32 \pm 2.27)***
19	(4.72 \pm 1.77)	(31.55 \pm 5.58)**
20	(27.27 \pm 6.27)*	(35.36 \pm 7.54)**
21	(10.37 \pm 6.39)	(19.35 \pm 5.52)*
22	(-2.97 \pm 6.58)	(4.98 \pm 5.28)
23	(6.67 \pm 1.18)	(27.95 \pm 2.34)***
DPI ^b	1.02 \pm 0.35	N
PMSF ^b	N	95.0 \pm 25

Percentage of inhibition (Inh %) at 30 μ M concentration. Results are presented as mean \pm S.E.M. (n = 3). *P<0.05, **P<0.01, ***P<0.001 compared with the control value.

^aConcentration necessary for 50% inhibition (IC_{50}).

^bDiphenyleneiodonium (DPI, a NADPH oxidase inhibitor) and phenylmethylsulfonyl fluoride (PMSF, a serine protease inhibitor) were used as the positive controls in the generation of superoxide anion and elastase release, respectively.

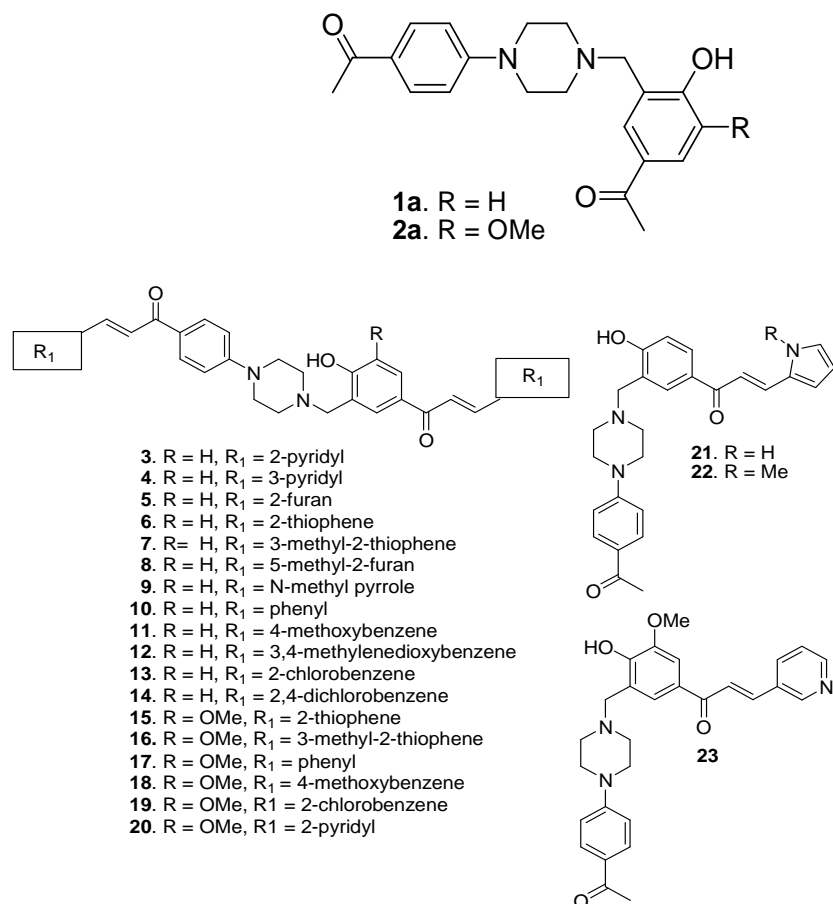


Figure 1: Bichalcone analogs 3-23

CONCLUSION

Present study described the inhibitory effects on Formyl-Met-Leu-Phe (FMLP) and cytochalasin B (CB) stimulated $O_2^{\bullet-}$ generation and elastase release in human neutrophils and the most active compounds with the IC_{50} values **5** (IC_{50} 7.88 μ M), **6** (IC_{50} 11.87 μ M), **21** (IC_{50} 19.35 μ M) and **22** (IC_{50} 4.98 μ M), respectively, against the inhibition of elastase release in activated human neutrophils.

Acknowledgments

This work was supported by a grant of National Science Council, Taiwan, Republic of China, and Grant No.(OUA 95-3-2-021) from the National Cheng Kung University, Tainan, Taiwan R.O.C awarded to T. S. Wu. This study is supported in part by Taiwan Department of Health Clinical Trial and Research Center of Excellence (DOH100-TD-B-111-004).

REFERENCES

- [1] J.B. Harborne, "The Flavonoids—Advances in Research since 1986." Chapman and Hall, London, **1994**.
- [2] M. Satyanarayana, P. Tiwari, B.K. Tripathi, A.K. Srivastava, R. Pratap R. *Bioorg. Med. Chem.*, **2004**, 12, 883.
- [3] X.F. Liu, C.J. Zheng, L.P. Sun, X.K. Liu, H.R. Piao, *Eur. J. Med. Chem.* **2011**, 46, 3469.
- [4] L.M. Zhao, H.S. Jin, L.P. Sun, H.R. Piao, Z.S. Quan, *Bioorg. Med. Chem. Lett.*, **2005**, 15, 5027.
- [5] S. Mukarami, M. Muramatsu, H. Aihara, S. Otomo, *Biochem. Pharmacol.*, **1991**, 42, 1447.
- [6] M. Liu, P. Wilairat, M.L. Go, *J. Med. Chem.*, **2001**, 44, 4443.

-
- [7] J.C. Onyilagna, B. Malhotra, M. Elder, G.H.N. Towers, *Can. J. PlantPathol.*, **1997**, 19, 133.
- [8] S.F. Nielsen, M. Chen, T.G. Theander, A. Kharazmi, S. Christensen, *Bioorg. Med. Chem. Lett.*, **1995**, 5, 449.
- [9] C.L. Miranda, J.F. Stevens, V. Ivanov, M. McCall, B. Frei, M.L. Deinzer, D.R. Buhler, *J. Agric. Food Chem.*, **2000**, 48, 3876.
- [10] P.M. Sivakumar, S.K. GeethaBabu, D. Mukesh, *Chem. Pharm. Bull.*, **2007**, 55, 44.
- [11] S. Khatib, O. Nerya, R. Musa, M. Shmuel, S. Tamir, J. Vaya, *Bioorg.Med. Chem.*, **2005**, 13, 433.
- [12] H.K. Hsieh, L.T. Tsao, J.P. Wang, C.N. Lin, *J. Pharm. Pharmacol.*, **2000**, 52, 163.
- [13] G.S. Viana, M.A. Bandeira, F.J. Matos, *Phytomedicine*, **2003**, 10, 189.
- [14] K.A. Brown, S. D. Brain, J. D. Pearson, J. D. Edgeworth, S. M. Lewis, D. F. Treacher. *Lancet*, **2006**, 368, 157.
- [15] O. Gach, M. Nys, G. Deby-Dupont, J. P. Chapelle, M. Lamy, L. A. Pierard, V. Legrand. *Int. J. Cardiol.* **2006**, 112, 59.
- [16] H.A. Lehr, M. D. Menger K. Messmer. *J. Lab. Clin. Med.* **1993**, 121: 539.
- [17] B.J. Evans, D. O. Haskard, J. R. Finch, I. R. Hambleton, R. C. Landis, K. M. Taylor. *J. Thorac. Cardiovasc. Surg.* **2008**, 135: 999.
- [18] C. Nathan. *Nat. Rev. Immunol.* **2006**, 6: 173.
- [19] P. Lacy, G. Eitzen. *Front. Biosci.* **2008**, 13: 5559.
- [20] C.T. Pham. *Nat. Rev. Immunol.* **2006**, 6: 541.
- [21] M.Vijaya Bhaksar Reddy, Y.C. Chen, J.S. Yang, T.L. Hwang, K.F. Bastow, K. Qian, K.H. Lee, T.S. Wu. *Bioorg.Med. Chem.*, **2011**, 19, 1895.
- [22] T.L. Hwang, G.L. Li, Y.H. Lan, Y.C. Chia, P.W. Hsieh, Y.H. Wu, Y.C. Wu. *Free Radic. Biol.Med.* **2009**, 15, 520.
- [23] A. Boyum, D. Lovhaug, L. Tresland, E.M. Nordlie. *Scand. J. Immunol.* **1991**, 34, 697.
- [24] B.M. Babior, R.S. Kipnes, J. Curnutte. *J. Clin.Invest.* **1973**, 52, 741.